Dissertation
zur Erlangung des akademischen Grades eines Doktors der Naturwissenschaften in der Fakultät Physik der Technischen Universität Dortmund

Investigation of radiation damage in n^+-in-n planar pixel sensors for future ATLAS pixel detector upgrades

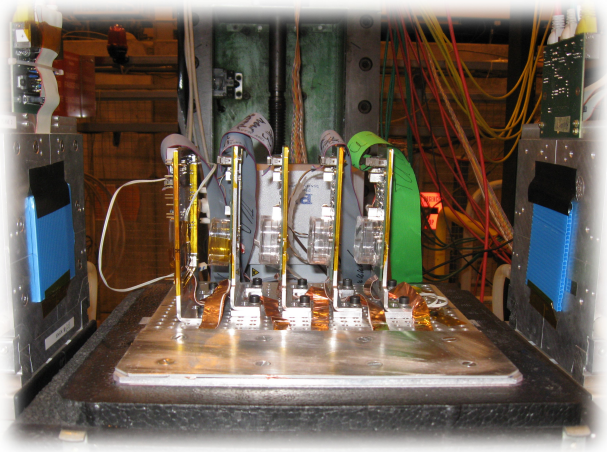

vorgelegt von
Dipl.-Phys. André Rummler

Dortmund, April 2014

Lehrstuhl für Experimentelle Physik IV
Fakultät für Physik
Technische Universität Dortmund

Dissertation
zur Erlangung des akademischen Grades
eines Doktors der Naturwissenschaften
in der Fakultät Physik
der Technischen Universität Dortmund

Investigation of radiation damage in n^+-in-n planar pixel sensors for future ATLAS pixel detector upgrades

vorgelegt von Dipl.-Phys. André Rummler
Lehrstuhl für Experimentelle Physik IV
Fakultät für Physik
Technische Universität Dortmund
Dortmund, April 2014

Gutachter:	Prof. Dr. C. Gößling, TU Dortmund
Zweitgutachter:	Priv.-Doz. Dr. R. Klingenberg, TU Dortmund
Beisitzer:	Dr. B. Siegmann, TU Dortmund
Termin der mündlichen Prüfung:	16.5.2014

Contents

CHAPTER 1

Introduction

The ongoing effort to understand the subatomic world requires the advance to always higher and higher energies as well as an increase in the collected statistics. The LHC[1] located at CERN[2] in Geneva is currently the largest particle accelerator in the world. Its design centre-of-mass energy of 14 TeV and luminosity of $1 \times 10^{34}\,\mathrm{cm}^{-2}\mathrm{s}^{-1}$ will allow to explore very rare high-energy processes. One of the two large multi-purpose detectors at the LHC is ATLAS[3]. It was built for tasks like the search for the Higgs-Boson. The current assumption is that ATLAS and CMS[4] have already succeeded in finding it using the data gained during the first two years of LHC operation. Now ATLAS is going to measure its properties while continuing to look for new physics such as super symmetry.

The ATLAS detector consists of several sub-detectors which are arranged concentrically. The inner-most detector is the pixel detector which is extremely important for track reconstruction and thus allows the identification of secondary vertices. The active part of the pixel detector are hybrid modules where a planar n^+-in-n silicon pixel sensor is connected by bump bonds to separate readout chips, which are made in CMOS[5] technology. The planar pixel sensor is structured into individual pixel cells. When a charged particle traverses the depleted bulk of a pixel, electron-hole pairs are created and the mirror charge is registered in the corresponding cell of the readout chip.

Due to the vicinity of the interaction point the whole pixel detector is exposed to an extremely high radiation background which is without precedence for segmented particle detector. This is especially pronounced for the inner-most layer — the b-layer. The radiation causes changes in the silicon crystal lattice and leads to several macroscopic effects, such as an increase in the leakage current and a degradation of its charge collection efficiency leading on its part to a decrease of

1 **L**arge **H**adron **C**ollider
2 **C**onseil **E**uropéen pour la **R**echerche **N**ucléaire
3 **A** **T**oroidal **L**HC **A**pparatu**S**
4 **C**ompact **M**uon **S**olenoid
5 **C**omplementary **M**etal **O**xide **S**emiconductor

the overall hit efficiency. Before the currently installed pixel detector was built, the radiation hardness of in n^+-in-n planar silicon sensors had been only demonstrated up to a fluence of $2 \times 10^{15} n_{eq.}\, cm^{-2}$.

This thesis extends this limit to fluences of $5 \times 10^{15} n_{eq.}\, cm^{-2}$ to $2 \times 10^{16} n_{eq.}\, cm^{-2}$. The fluence of $5 \times 10^{15} n_{eq.}\, cm^{-2}$ was set initially as the required end-of-life fluence of the currently built first upgrade of the pixel detector – the IBL[1]. This is an additional (fourth) pixel layer which will serve to mitigate the damage of the current inner-most layer. The results demonstrated that requirements will be met and resulted in building 75% of the IBL sensor area in n^+-in-n technology.

After having been operated for a couple of years, it is foreseen to ramp the LHC luminosity up to $5 \times 10^{35}\, cm^{-2} s^{-1}$ by upgrading it to the HL-LHC[2]. In preparation for that ATLAS will replace the whole, by-then thoroughly degraded, pixel detector with a new one. This new pixel detector will be part of a new full silicon inner detector, where the new strip detector will extend outwards including the space currently occupied by the TRT[3]. The TRT will not be able to cope with the increased occupancy. Taking into account the planned run time, the new pixel detector will require the inner-most pixel sensors to be qualified for a fluence of up to $2 \times 10^{16} n_{eq.}\, cm^{-2}$. The operability of such highly irradiated n^+-in-n silicon pixel sensors is demonstrated in this thesis as well. For this purpose both measurements in the lab using radioactive sources as well as test beam measurements at the test beam facilities located at CERN-SPS[4] and DESY[5] were conducted. The phase 2 upgrade of the pixel detector has different requirements for the sensors depending on the layer: The inner-most layer has to be able to withstand a very high fluence and has to cope with a significant increase in occupancy. Layers positioned further away from the interaction point do not require such radiation hardness, but are on the other hand more cost sensitive due to their large area.

The main challenge was posed by the fact that at the time when this study was started no readout chip qualified to withstand the required ionising dose was available. Now (in 2014) this condition has partially changed as in the course of the R&D for the IBL the FE-I4 became available. Nevertheless, sufficient radiation hard frontend chips for the phase 2 (HL-LHC) are still under development. In order to disentangle the effects of the radiation damage of the sensor and of the readout chip several methods were employed.

The simple approach to irradiate a sufficient number of assemblies and subsequently to select those where the readout electronics still was working properly, yielded already quite good results, although it proved to be a quite tedious process.

1 **I**nsertable **B**-**L**ayer
2 **H**igh **L**uminosity - LHC
3 **T**ransition **R**adiation **T**racker
4 **S**uper **P**roton **S**ynchrotron
5 **D**eutsches **E**lektronen **SY**nchrotron

Unfortunately, the performance of the frontend chip might be also affected by the irradiation, leading to a degraded measured sensor performance as well.

An alternative approach is to use another bump bonding technology with indium stubs. The flip chip mating with indium requires comparatively low temperatures. This fact makes it possible to irradiate the sensors first and to mate them afterwards with an unirradiated readout electronics. This attempt succeded in cross-checking of the results.

Finally, a completely disjunct readout method was developed using a so-called fanout chip. This is a chip that was designed to be connected to a FE-I3 single chip sensor instead of a FE-I3. In contrast to the FE-I3 it is completely passive and thus it is inherently radiation hard. It is composed of aluminium traces processed on a electronics grade silicon wafer. Those traces lead the signal from single pixels or combined groups of pixels to wirebond pads located on the circumferential balcony. These wirebond pads allow to evaluate the charge signals using discrete readout electronics which can be connected and removed several times as wirebond connections are used. This feature makes it possible to keep the readout electronics unirradiated as well as to intercalibrate it with other assemblies. A similar approach is routinely used when measuring strip sensors.

Chapter 2 first gives a short overview of the LHC and the ATLAS detector including their physics goals. Afterwards, a more detailed description of the currently existing inner detector and especially of the pixel detector is given.

In chapter 3 a short summary of the semiconductor physics necessary for understanding the basic properties and function of the silicon sensor is presented. A focus is put on the interaction between high energy particles and the sensor.

The diverse microscopic effects and resulting changes in macroscopic properties of the silicon sensor caused by prolonged irradiation are explained in chapter 4.

Chapter 5 takes a detailed look at the ATLAS upgrade plans, especially those parts dealing with the pixel detector. On the one hand these are the plans for the IBL detector which is currently under construction and on the other hand the preliminary options for the full silicon pixel detector to be realized after 2021/2022.

Chapter 6 explains the different samples used in the analysis. Their properties like bulk thickness, design, irradiation and flip-chip technology are demonstrated. Some details regarding the irradiation facilities are presented as well.

The chapter 7 deals with the fanout readout system, particularly with its design and qualification. A setup for the quick evaluation of fanout structures is presented together with a system for measuring irradiated fanout assemblies.

Chapter 8 illustrates the methods used for measuring frontend based assemblies

in the lab and in the test beam environment, describing among other things the telescope, readout system, cooling, environmental monitoring and the software used for data analysis.

In chapter 9 an overview is given of the results gained with frontend based assemblies. Both lab measurements as well as test beam data are considered.

Finally, in chapter 10 a summary of the observations and an outlook on further possible measurements are given.

Schematical drawings of the wafer layouts presented in appendix A show the origin of the sensors used in this investigation.

The mounting and cooling connection of each DUT[1] is depicted in appendix B for documentation purposes.

Detailed descriptions and result plots giving an idea of the data quality for all test beam measurements are shown in appendix C.

The list in appendix D includes all publications available up to now, which contain results from this thesis.

1 **D**evice **U**nder **T**est

CHAPTER 2

The ATLAS Detector at LHC

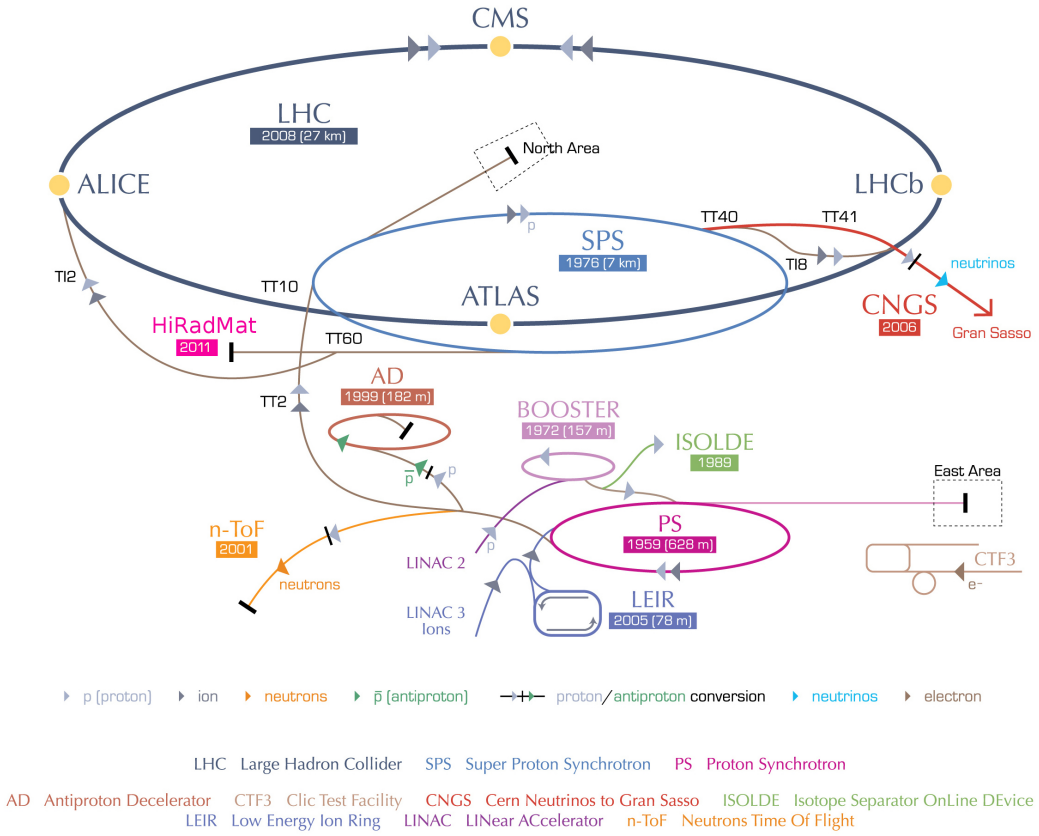

Figure 2.1: Overview of the LHC accelerator complex. Taken from [Lef08] and modified according to [LIU13].

2.1 LHC

The LHC[1] is a synchrotron at CERN[2] with a target centre-of-mass energy of 14 TeV and a luminosity of $1 \times 10^{34}\,\mathrm{cm}^{-2}\mathrm{s}^{-1}$. It occupies the same tunnel as its predecessor the electron-positron collider LEP[3] and its circumference is roughly 27 km. It is the last part of the accelerator chain which starts with the LINAC2[4] in case of protons and LINAC3[5] in case of lead ions. In the beginning of the LINAC2 the hydrogen molecules are ionised and then accelerated to an energy of 50 MeV. Then they are filled into the PSB[6], which they leave at an energy of 1.4 GeV. The PS[7] and SPS[8] increase the energy to 26 GeV and 450 GeV respectively. Through the transfer tunnels TI2 and TI8 the protons are injected in opposite directions into the LHC where they are brought into collision at four interaction points. At those four interaction points the major detectors of the LHC are located: ATLAS[9], CMS[10], LHCb[11] and ALICE[12]. In case of lead ions the LINAC3 is used to accelerate them to an energy of 4.2 MeV before they are brought to an energy of 14.8 MeV by the LEIR[13] and subsequently fed into the PS as well.

2.2 Physics at LHC

Elementary particles and their interaction are described by the standard model. Matter is made of fermions which follow the Fermi-Dirac statistic. There are 6 quarks, 6 leptons and their anti-particles. Those are subdivided into three generations. The first generation consists of the up- and down-quark, the electron and the electron-neutrino as well as their anti-particles. The second generation is made of the strange- and charm quark, the muon and muon-neutrino and their anti-particles. Finally, the third generation is built of the bottom- and top quark, the tau and tau-neutrino, accompanied by their anti-particles as well. All stable matter is made of particles belonging to the first and lightest generation as members of the second and third generation decay into members of the first generation. Of the known four forces only three are described by the standard model – gravitation is not covered. Interaction between particles is described as the exchange of force carriers, the so-called gauge bosons. The fundamental particles of the standard model are summarized in fig. 2.2.

1 **L**arge **H**adron **C**ollider
2 **C**onseil **E**uropéen pour la **R**echerche **N**ucléaire
3 **L**arge **E**lectron-**P**ositron Collider
4 **LIN**ear **AC**celerator **2** - accelerator at CERN
5 **LIN**ear **AC**celerator **3** - accelerator at CERN
6 **P**roton **S**ynchrotron **B**ooster - accelerator at CERN
7 **P**roton **S**ynchrotron - accelerator at CERN
8 **S**uper **P**roton **S**ynchrotron
9 **A** **T**oroidal **L**HC **A**pparatu**S**
10 **C**ompact **M**uon **S**olenoid
11 **LHC**-**b**eauty
12 **A** **L**arge **I**on **C**ollider **E**xperiment
13 **L**ow **E**nergy **I**on **R**ing

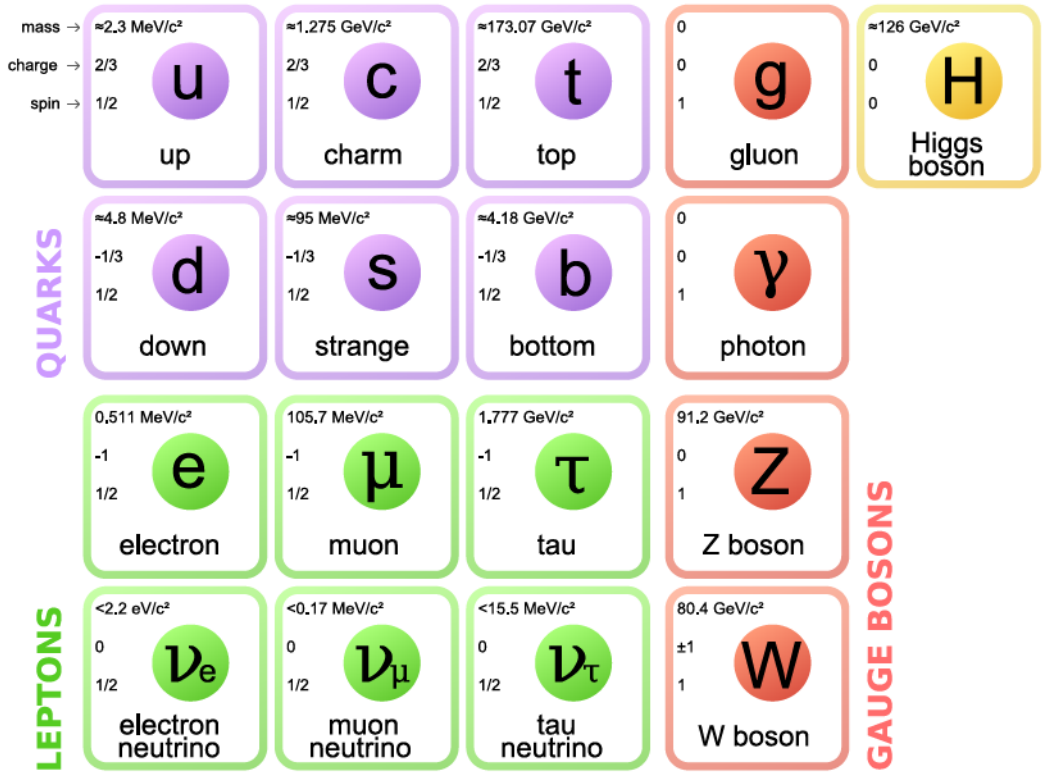

Figure 2.2: The standard model of particle physics. [Mis13]

2.3 ATLAS

2.3.1 Overview

ATLAS is, along with CMS, one of the two multi-purpose detectors at LHC. Its design goal was to maximize the number of measurable physics signatures in order to be able to cover the broadest possible range of physics. The detector has a diameter of 22 m, a length of 44 m and a mass of 7000 t (see fig. 2.3). Like most particle detectors at ring colliders, it consists of a series of subdetectors, which are concentrically arranged around the interaction region where the beams from the LHC collide, thus covering almost 4π solid angle. It can be divided into four major parts: the inner detector, the calorimeters, the muon spectrometer and the magnet systems. Each of these is in turn made of multiple layers. The detectors deliver complementary data. The inner detector tracks particles precisely and measures their momentum by utilizing the particle track bending effect of the magnetic field. The calorimeters measure the energy of all particles, except for muons whose momentum is recorded in the muon system.

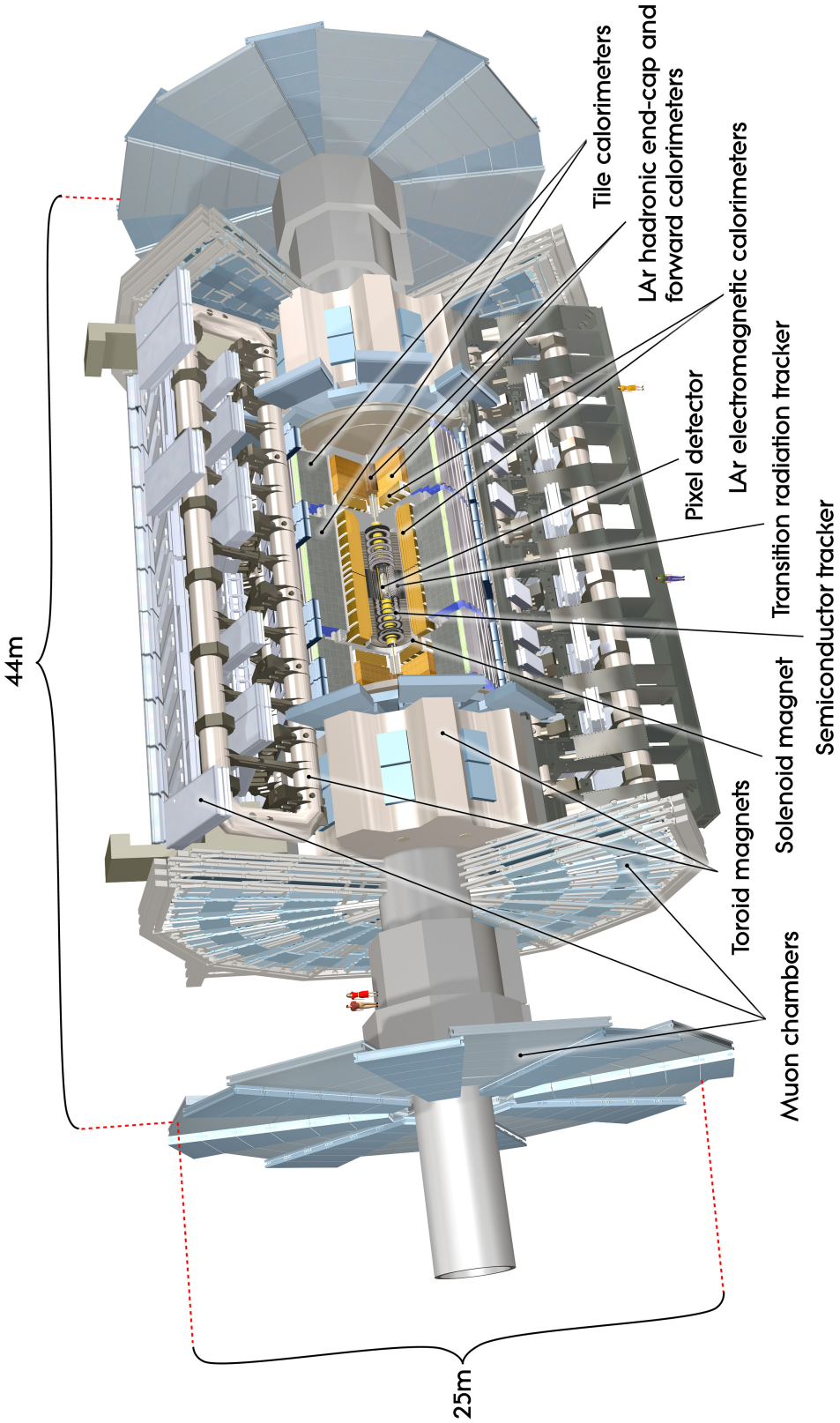

Figure 2.3: Complete layout of the ATLAS detector. Taken from "The ATLAS experiment at CERN, `http://atlas.ch`, image 0803012_01".

2.3.2 Calorimeters

There are two different types of calorimeter located between the solenoid magnet and the muon spectrometer. More inwards this is the EMCAL[1] (electromagnetic calorimeter) which is surrounded by the hadronic calorimeter HCAL[2]. Both of them are so-called sampling calorimeters, that means that they use different materials for interacting with the particles and measurement of the resulting showers. The passive absorber material and the active detector material are arranged in form of alternating layers. The EMCAL uses liquid argon as a sampling material, whereas the absorber is made of lead and steel. The HCAL consists (mostly) of steel and scintillator material which is read out using PMTs[3]. [ATL96a; ATL96b; ATL+08]

2.3.3 Muon Spectrometer

The muon spectrometer is the outer-most subdetector which starts at a radius of approximately 5 m and extends to the full radius of ATLAS. As it is located outside the calorimeters one can be sure that only muons (besides the neutrinos which are not detectable with ATLAS) reach the muon spectrometer. It is situated within the solenoid magnetic field (peak 3.9 T) which is generated by the air coil magnetic system, thus making it possible to determine the momentum of the muons by recording the bending radius. [ATL97b; ATL97a; ATL+08]

2.3.4 Inner Detector

The inner detector (see fig. 2.4) is the tracker of ATLAS and makes it possible to reconstruct the tracks of charged particles. Due to the solenoid magnetic field in which it is situated, it also measures the charge and momentum of the traversing particles. Its high spatial resolution, next to the interaction point, allows to resolve primary and secondary vertices. It consists of the pixel detector, the semiconductor tracker and the transition radiation tracker and has a length of about 7 m and an outer radius of roughly 1.15 m. The number of layers, their allocation and the composition of the sub detectors is due to a compromise between several competing factors: Near the interaction point, the granularity has to be higher in order to achieve a good resolution and to achieve a good track differentiation, although the occupancy is high. The amount of gained information, especially granularity, opposes the radiation length, which is particularly critical as the inner detector is located at the centre of ATLAS. Each additional layer, together with the necessary services, adds to the material budget and so leads to additional multiple scattering.

1 **E**lectro**M**agnetic **CAL**orimeter
2 **H**adronic **CAL**orimeter
3 **P**hoto **M**ultiplier **T**ubes

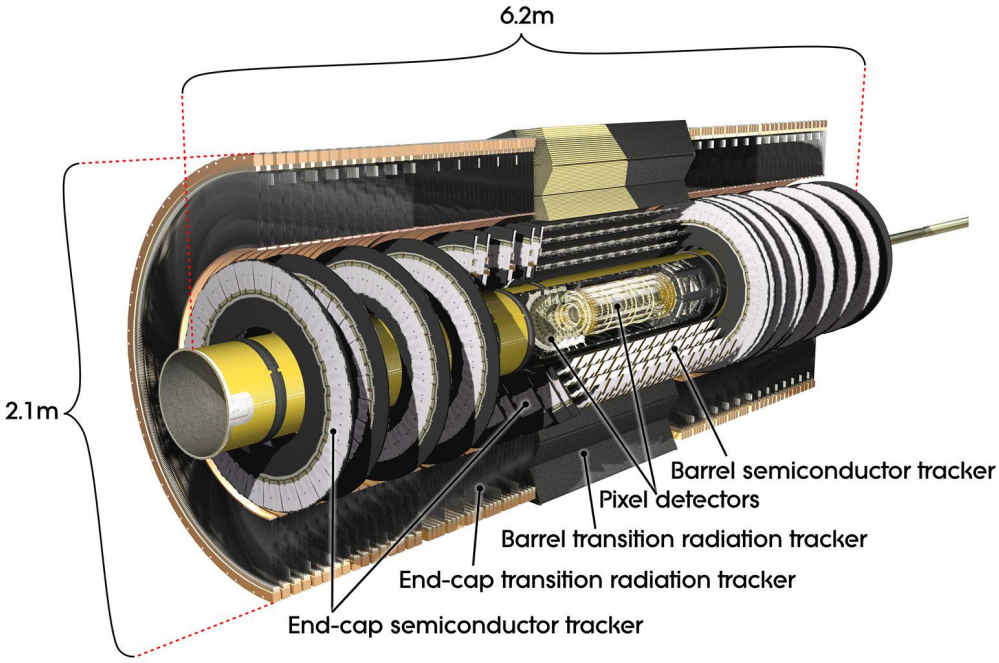

Figure 2.4: The ATLAS inner detector. Taken from "The ATLAS experiment at CERN, `http://atlas.ch`, image 0803014_01".

2.3.4.1 Transition Radiation Detector

The TRT[1] is a combined straw tracker and transition radiation detector. It is the outermost part of the inner detector with a length of 5.4 m (including endcaps) and a radius of 1.06 m. Its volume is composed of tubes with a diameter of 4 mm that are filled with a gas mixture consisting mostly of xenon and it is designed to operate at room temperature. Each of the tubes contains a wire in its centre which has high voltage applied to it and which collects the charge produced either by charged particles that cause ionisation while traversing the gas volume or by transition radiation photons. The transition radiation is caused by ultra relativistic particles — in this case mostly electrons — traversing materials with differing indices of refraction. These materials are positioned between the tubes. Two different charge thresholds help to differentiate between the two mechanisms and thus also between different particles. The TRT has a spatial resolution of 170 µm per straw and a typical track will trigger 36 hits on average.[ATL+08; ATL13b]

2.3.4.2 Semiconductor Tracker

The SCT[2] is made of p-in-n silicon microstrip modules. To enable the measurement of a z-position, each of the four layers is built as a double layer with crossed strips

1 **T**ransition **R**adiation **T**racker
2 **S**emi**C**onductor **T**racker

which are rotated 40 mrad with respect to each other. The layers are located at 30 cm, 37.3 cm, 44.7 cm and 52 cm. The SCT has 6.2 million channels enabling a spatial resolution of $R\phi = 16\,\mu m$ and $z = 580\,\mu m$ and covers unfurled $63\,m^2$ of silicon. Each strip sensor has 786 strips with a pitch of 80 µm, produced in a one sided process and it is connected to another sensor using wirebonds on order to create 12.8 cm long strips. At one end of this pair of sensors the readout electronics is located and connected to the sensor through wirebonds as well. In the SCT layers located inwards to the interaction point the radiation hardness as well as the ability to cope with a higher occupancy had to be taken into account.[ATL+08; ATL13a]

2.3.4.3 Pixel Detector

The pixel detector is the inner-most subdetector of the inner detector. It consists of three barrel layers and three disks on each side. The barrel layers are located at a distance of 5.05 cm (b-layer), 8.85 cm (layer 1) and 12.25 cm from the interaction point. The three disks are mounted on both sides at distances of 49.5 cm, 58.0 cm and 65.0 cm. The pixel detector delivers at least three high resolution track points per track with $|\eta| < 2.5$ and has an intrinsic resolution of at least $\sigma_{r\phi} = 12\,\mu m$ and $\sigma_z = 115\,\mu m$. Each layer consists of staves which are rotated 20° along the long axis in order to overlap slightly the next stave and so avoiding gaps in the detector. This is called roofing. The smallest unit is a stave which is the support structure for the mechanical fixing and the cooling for 13 pixel modules. Several staves form together a half-shell and each layer consists of two half-shells. Each stave is populated with 13 modules which are on their part slightly inclined orthogonal to the long axis and are overlapping each other. This is called shingling and can be seen in fig. 2.5. The middle module of each stave is horizontally aligned and the neighbouring modules are tilted by 1.1° to it. Each module is oriented with its long side along the z-direction. A stave is made of a part called TMT2 (consisting of carbon fibre) and an aluminium cooling pipe. As each module produces 5 W heat loss, a good cooling system is necessary to keep the modules at their working temperature of −10 °C. Evaporating C_3F_8 (octafluorpropan) is currently used as a cooling agent. New detector parts installed during phase 0 and phase 2 upgrades will use CO_2 as a freezing agent due to its superb performance and reliability.

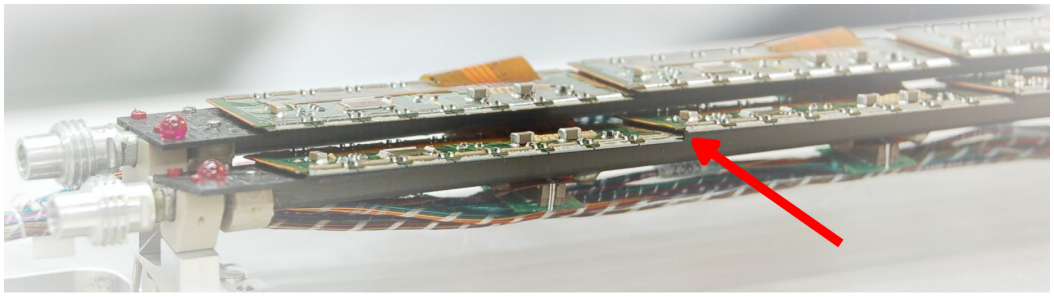

Figure 2.5: The photo shows a part of a stave and illustrates the overlap of the modules called shingling (see arrow). [Tro12]

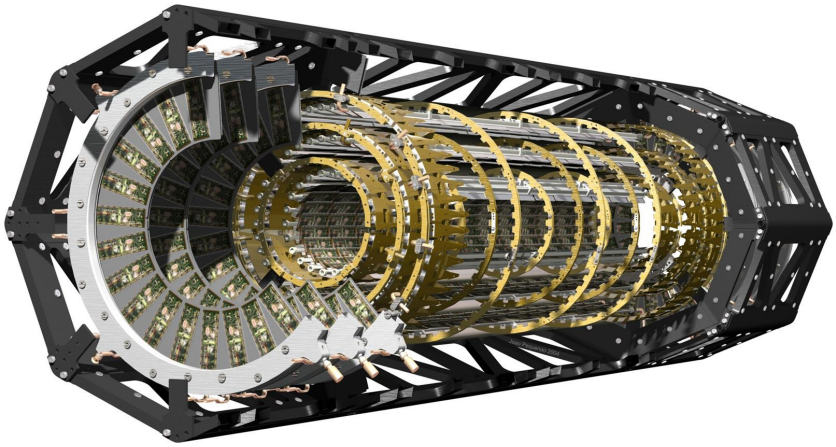

Figure 2.6: ATLAS pixel detector. Taken from "The ATLAS experiment at CERN, `http://atlas.ch`".

2.3.4.4 Modules

Adding up the modules of all three layers and all six disks, the inner detector consists of 1744 modules. The heart of each module is the sensor which is also called tile. It is bump bonded to 16 frontend chips of the type FE-I3. They are wirebonded on their outer rim to the flex hybrid which is glued to the opposite side (p-side) of the sensor tile. The flex hybrid is a so-called FCB[1] made of 50 µm thick Kapton substrate with copper circuit paths on both sides. It carries several passive SMD[2] components like resistors and capacitors, an NTC[3] ceramic thermistor for temperature control and the "brain" of the module, the MCC[4], responsible for data processing and communication with the outer detector electronics. The frontend chips are the first link in the long chain of processing electronics. Each pixel cell on the sensor is connected by a bump bond (PbSn or indium) with a readout cell on a frontend chip. It contains a charge sensitive amplifier followed by a 8 bit analogue-digital converter, a small memory, several regulators and two capacitors (see fig. 2.8). The capacitor C_{inj} makes it possible to inject a defined amount of charge and to adjust the response with the regulators during the tuning process. The other capacitor C_{fb} is charged by the signal entering the readout cell through the bump bond and discharged by the so-called feedback current. The discriminator digitalizes that signal and measures the charge in terms of ToT[5]. This is the time with the signal above the pre-adjusted threshold (see fig. 2.9). Usually, this is set to 3200 electrons.

1 **F**lexible **C**ircuit **B**oard
2 **S**urface **M**ounted **D**evice
3 **N**egative **T**emperature **C**oefficient thermistor
4 **M**odule **C**ontrol **C**hip
5 **T**ime **O**ver **T**hreshold

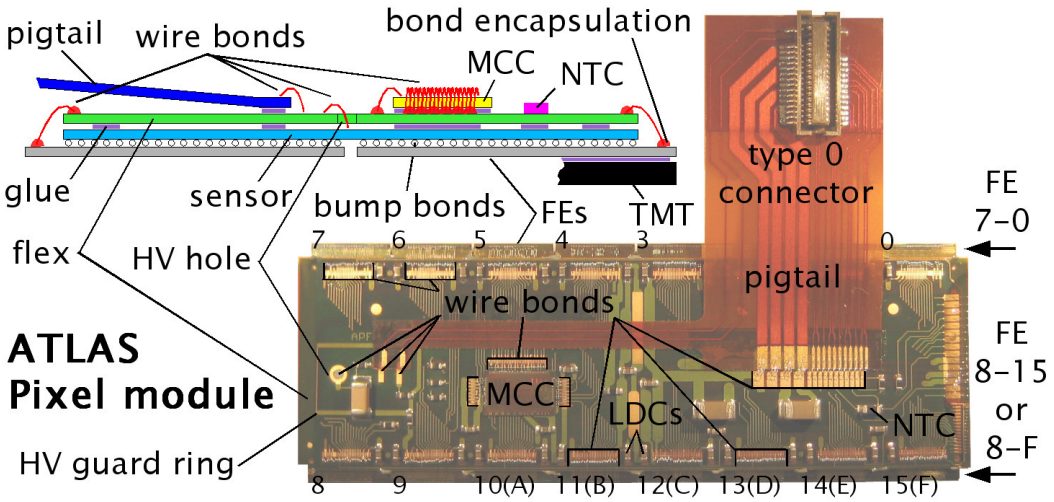

Figure 2.7: Basic layout of the ATLAS Pixel module. [Dob04]

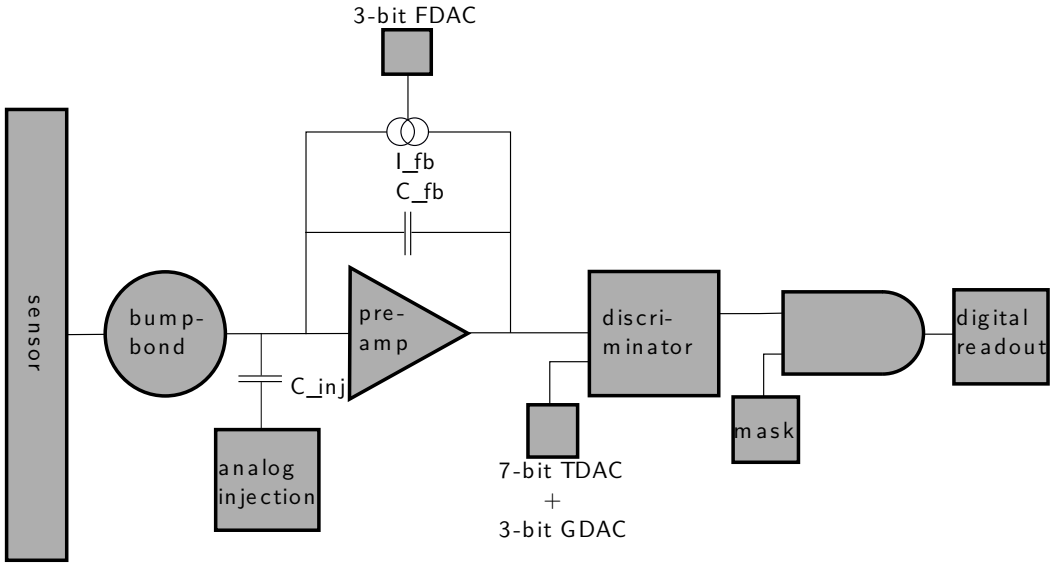

Figure 2.8: Schematic of the analogue part of a FE-I3 readout cell. [Rei06]

2.3.4.5 Sensors

The sensor is made of floatzone silicon with a crystal orientation of $\langle 1\,1\,1 \rangle$ and a n-type base doping. The n-side is segmented into a pixel cell array by the n^+-implantations which have an outline of $30\,\mu m \times 380\,\mu m$. Due to a distance of $20\,\mu m$ between two pixels the final pixel size is $50\,\mu m \times 400\,\mu m$. On the inner border, where two or four FE[1]s are butted at the edges with a margin of $200\,\mu m$, there are long pixels, ganged pixels and combinations of them (see fig. 2.10) to avoid insensitive

1 **F**ront**E**nd Electronic

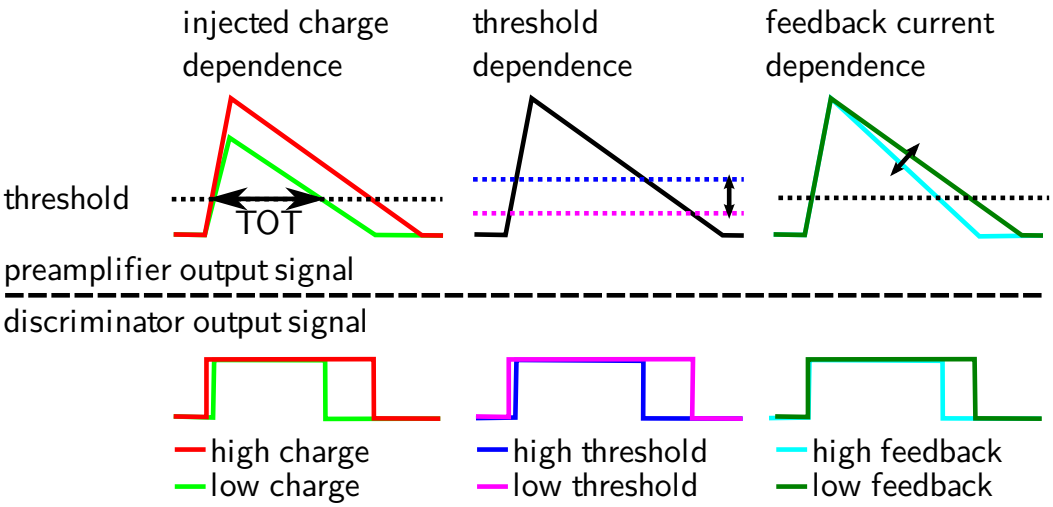

Figure 2.9: Injected charge, threshold and feedback current dependency of the ToT signal in the preamplifier and the discriminator. [Dob04]

areas as much as possible. As the sensor consists of n-type silicon, the depletion zone starts from the n-side. Therefore, it can be only operated fully depleted.

Irradiation leads to type inversion and afterwards the depletion zone growth starts on the p-side, so maintaining functionality in the non fully depleted mode. The implant zones are covered by a structured metal layer which is passivated for protection. There are openings in the passivation layer for the bump bonds. The pixel cells are isolated from each other by a method called moderated p-spray [Hüg01]. It is more tolerant against mask shift than p-stop and more effective than simple p-spray.

The punch through effect enables testing during the production and avoids a negative effect of potentially existing floating pixels during operation. It works by employing the lateral depletion zone which connects two pixels, if a voltage difference of $U_{PT} = 0.7\,\mathrm{V}$, the punch-through voltage, is exceeded (see fig. 2.11). During operation the bias grid is pulled to ground by two bump bond contacts (fig. 2.12) on the n-side [Hüg01]. This will be later important for some of the measurements discussed in this work.

Furthermore, it can be seen in fig. 2.13 that the sensors have a multiple guard ring structure on their p-side. It is necessary to isolate the conducting dicing edge from the depletion zone in order to avoid breakthrough.

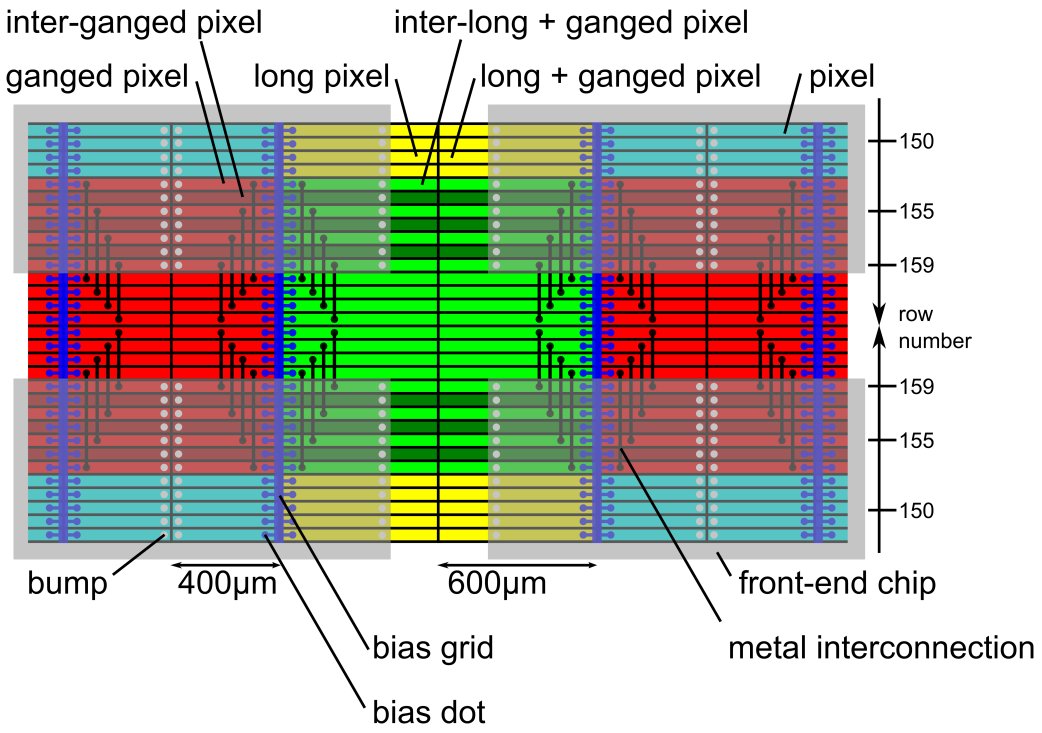

Figure 2.10: Layout of the ATLAS Pixel Sensor in the interchip region. [Dob04]

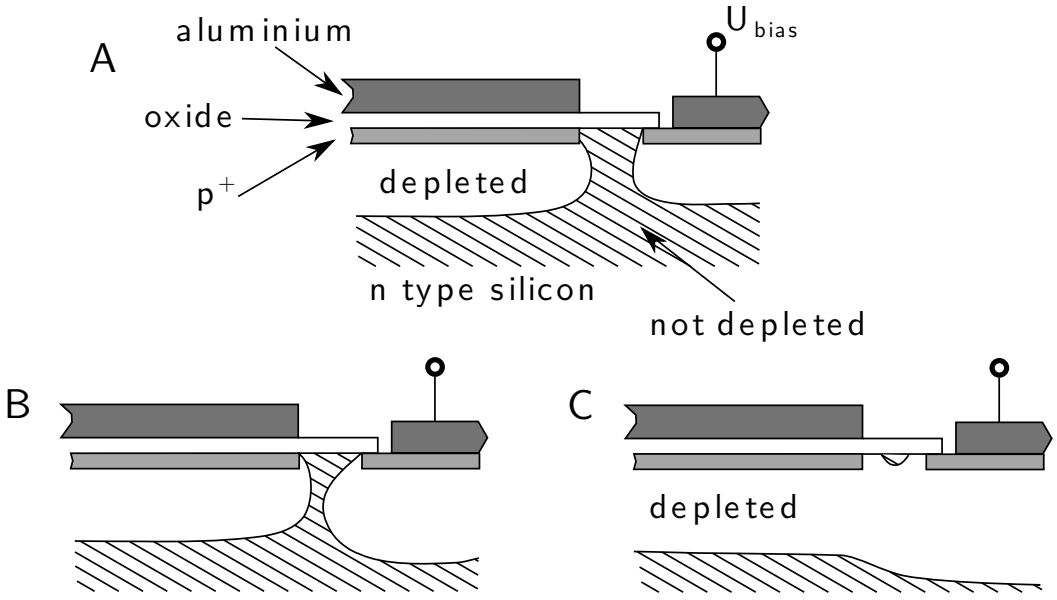

Figure 2.11: Illustration of the Punch-Through Effect. A: sensor without any bias voltage; B: Bias voltage reaches the punch through voltage U_{pt}; C: Bias voltage is larger than the punch through voltage. [Web04]

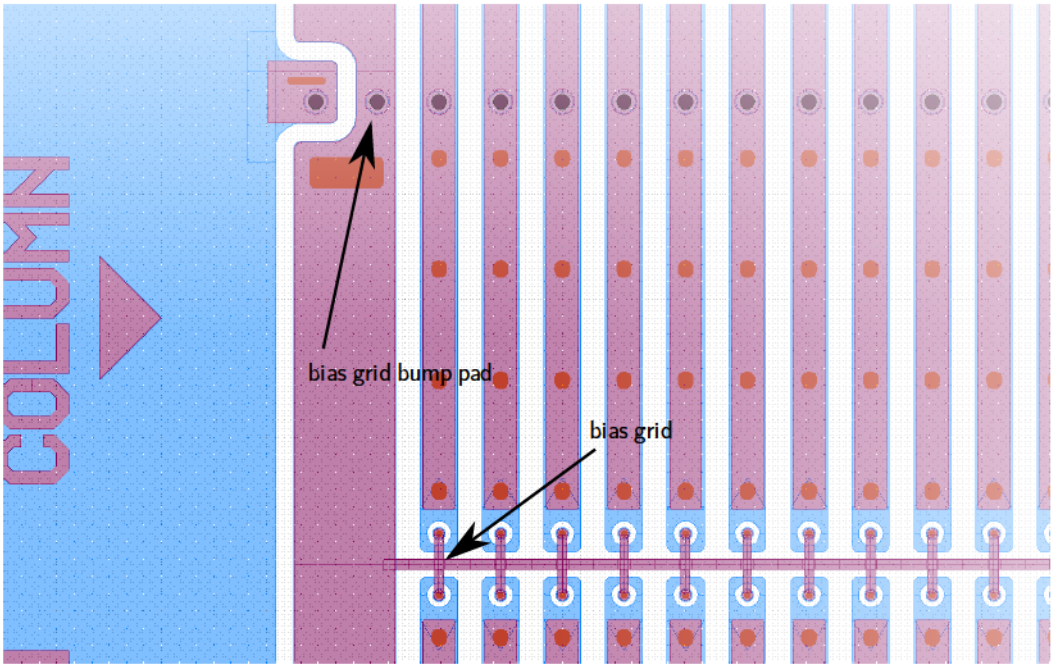

Figure 2.12: Bump pad for ground connection and metal layer connection to outer guard ring on an ATLAS Single Chip.

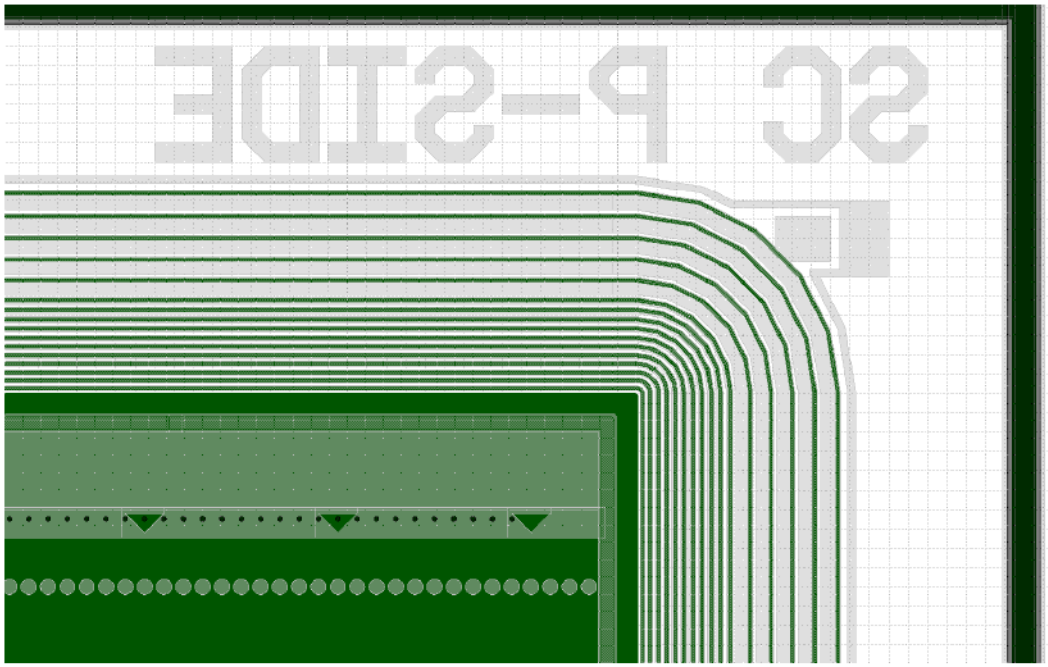

Figure 2.13: Multiple guard ring structure.

CHAPTER 3

Planar Silicon Pixel Detectors

This chapter gives a short introduction into the basic properties and working principles of silicon semiconductor detectors. It is valid for unirradiated sensors while the changes caused by radiation damage are covered in chapter 4. [Spi06; Rum09]

3.1 Ionising Energy Loss in Matter

Ionising radiation passing through silicon creates free charge carriers. These are electrons and holes which can be collected by electrodes and detected as a signal. The formation of those free charge carriers is reversible and does not damage the crystal. The non ionising charge deposition leads to crystal damage, which is discussed in chapter 4. The energy loss of photons and charged particles in matter is caused by different processes.

3.1.1 Photons

There are three different effects caused by the interaction between photons and matter. The photoelectric effect dominates at low energies. Between 30 keV and 5 MeV the Compton-Effect is most important and at higher energies most photons cause pair production.

3.1.1.1 Photoelectric Effect

The term photoelectric effect describes the process of the absorption of an incoming photon by a bound electron which can leave the atom, if the absorbed energy surpasses the binding energy of the electron

$$\gamma + \text{nucleus} \rightarrow e^- + \text{nucleus}^+ \,. \tag{3.1}$$

The electron carries away the energy difference as kinetic energy

$$E^e_{\text{kin}} = E_\gamma - E_B \,. \tag{3.2}$$

By impacts with other bound electrons the energy E^e_{kin} is dispensed to them. The recoil momentum is taken by the involved atomic nuclei. The cross-section can be

solved analytically and has to be modelled using simplified assumptions

$$\sigma_{pe} = \frac{8\pi}{3} r_e^2 \alpha^3 Z^5 \left(\frac{mc^2}{E_\gamma}\right)^\delta \tag{3.3}$$

in which

$$\delta = \begin{cases} 3.5 & \text{if } E_\gamma \ll mc^2 \\ 1 & \text{if } E_\gamma \gg E_{\text{Ion}} \,. \end{cases} \tag{3.4}$$

In silicon the absorbed energy has to exceed the band gap energy of 1.21 eV [Chi13]. Therefore, only photons with a wavelength smaller than 1100 nm can be detected. At higher energies the additional constraint of momentum conservation and the ionisation energy $E = 3.6\,\text{eV}$ have to be taken into account. Low energy gamma-photons deposit a localized charge cloud, as the photoelectric effect dominates and the extent of the cloud is determined by the range of the ejected photo electron. The photoelectric effect dominates below an energy of approximately 30 keV.

3.1.1.2 Compton Scattering

The compton scattering describes the inelastic interaction of a photon with a free electron on condition that the relativistic four-momentum is conserved. A bound electron can be treated as approximately free in case of high photon energies $E_\gamma = h\nu$, with respect to the binding energy E_B, which is in the order of the Rydberg energy ($E_{\text{Ryd}} = 13.6\,\text{eV}$). During the scattering the initial photon is absorbed and a new one with a different energy $E_\gamma^{'}$ as well as momentum is emitted with an angle Θ with respect to the initial photon direction

$$E_\gamma^{'} = \frac{E_\gamma}{1 + \frac{E_\gamma}{m_e c^2}\left(1 - \cos\Theta\right)} \,, \tag{3.5}$$

where m_e is the electron mass and c the speed of light. The differential cross section is described by the Klein-Nishina formula

$$\frac{d\sigma}{d\Omega} = \frac{1}{2} r_0^2 \left(\frac{E_\gamma^{'}}{E_\gamma} + \frac{E_\gamma}{E_\gamma^{'}} - \sin^2\Theta\right) \,, \tag{3.6}$$

where $r_0 = \frac{e_0^2}{m_e c^2} = 2.8 \times 10^{-13}\,\text{cm}$ is the classical electron radius. After the scattering the final electron has a kinetic energy of $E_\gamma - E_\gamma^{'}$ and leaves the atom which is ionised. The sensor has to be thick enough to cover the maximal length of the Compton cascade.

3.1.1.3 Electron-Positron Pair Production

If the incoming photons surpass the necessary energy threshold

$$E_\gamma^{\min} = 2 \cdot m_P + 2\frac{m_P}{m_R} \,, \tag{3.7}$$

the conversion of a photon into a electron-positron pair becomes possible.

3.1.2 Energy Loss of Charged Particles in Matter

For a charged particle there are several ways for interaction besides ionisation. One of them is bremsstrahlung

$$-\left(\frac{dE}{dx}\right)_{\text{rad}} = \frac{E_\gamma}{X_0} \propto \frac{1}{m^2}\,, \tag{3.8}$$

where E_γ is the bremsstrahlung energy spectrum and X_0 the radiation length

$$X_0 = \left(\frac{4Z^2 N_A \rho \alpha r_e^2}{A} \ln \frac{183}{Z^{\frac{1}{3}}}\right). \tag{3.9}$$

For heavier charged particles the energy loss by elastic and inelastic scattering as well as Čerenkov radiation is quantified by the Bethe-Bloch equation

$$-\frac{dE}{dx} = 2\pi N_A r_e^2 m_e c^2 \rho \frac{Z}{A}\frac{z}{\beta}\left[\ln\left(\frac{2m_e\gamma^2\nu^2 E_{\max}}{I^2}\right) - 2\beta^2 - \delta - \frac{C}{Z}\right] \tag{3.10}$$

where:

N_A Avogadros' constant

r_0 classical electron radius

m_e electron mass (511 keV)

c speed of light

ρ density of the medium ($\rho = 2.33\,\text{g cm}^{-3}$ for silicon)

z charge of the traversing particle in units of e_0

Z atomic number of the medium ($Z = 14$ for silicon)

A atomic weight of the medium ($A = 28.09$ for silicon)

β velocity ν of the traversing particle in units of speed of light

$\gamma = \frac{1}{\sqrt{1-\beta^2}}$

I effective ionisation potential of the medium ($I = 137\,\text{eV}$ for silicon)

δ density correction

C shell correction

$E_{max} \approx 2m_e c^2 \beta^2 \gamma^2$, if $M \gg m_e$, maximum energy transfer in a single collision

M mass of the traversing particle.

3.1.2.1 Alpha-Particles

Alpha-particles traversing matter lose their kinetic energy by ionisation. Their differential energy loss along their path is described by the Bethe-Bloch formula for heavy particles. Alpha-particles are stopped in silicon after a relatively short track due to their charge $z = 2$. As an example α-particles from a $^{241}_{95}$Am source with kinetic energies of 5.486 MeV and 5.443 MeV have a mean penetration depth of $28.06 \pm 0.31\,\mu$m.

3.1.2.2 MIPs and Electrons

Particles in the region of the minimum of differential energy loss are called minimum ionising particles. They deposit their energy evenly along their track in form of a charge carrier tube. The differential energy loss in silicon is

$$\left.\frac{dE}{dx}\right|_{\text{min}} = 3.8\,\text{MeV}\,\text{cm}^{-1}\,. \tag{3.11}$$

MIPs[1] are measured by the pixel detector in ATLAS[2], specifically pions and protons. Unfortunately, it is not possible to get those for laboratory tests. Therefore, as a MIP approximation $^{90}_{38}$Sr electrons are used. This isotope makes a β-decay into $^{90}_{39}$Y. The maximum energy of the emitted electrons is 0.5 MeV. $^{90}_{39}$Y converts into the stable $^{90}_{40}$Zr isotope by a secondary β-decay with a maximum energy of 2.3 MeV. The half lives of the two subsequent decays are 28.64 a and 61.1 h [NIS13]. For thick absorbers the mean and most probable values are identical and can be calculated by Bethe-Bloch resulting in a Gauss distribution. For thin absorbers, such as the detectors examined here, there is additionally the rarely occurring process of high energy electron creation during the ionisation processes. Those electrons are called δ-electrons and they can ionise further atoms. This leads to an asymmetry in the energy spectrum called Landau distribution (fig. 3.1). In 250 μm thick silicon, this results in a mean energy loss of 97.5 keV (27000 electrons) and in a most probable energy loss of 70 keV (19400 electrons).

1 **M**inimal **I**onising **P**articles
2 **A** **T**oroidal **L**HC **A**pparatu**S**

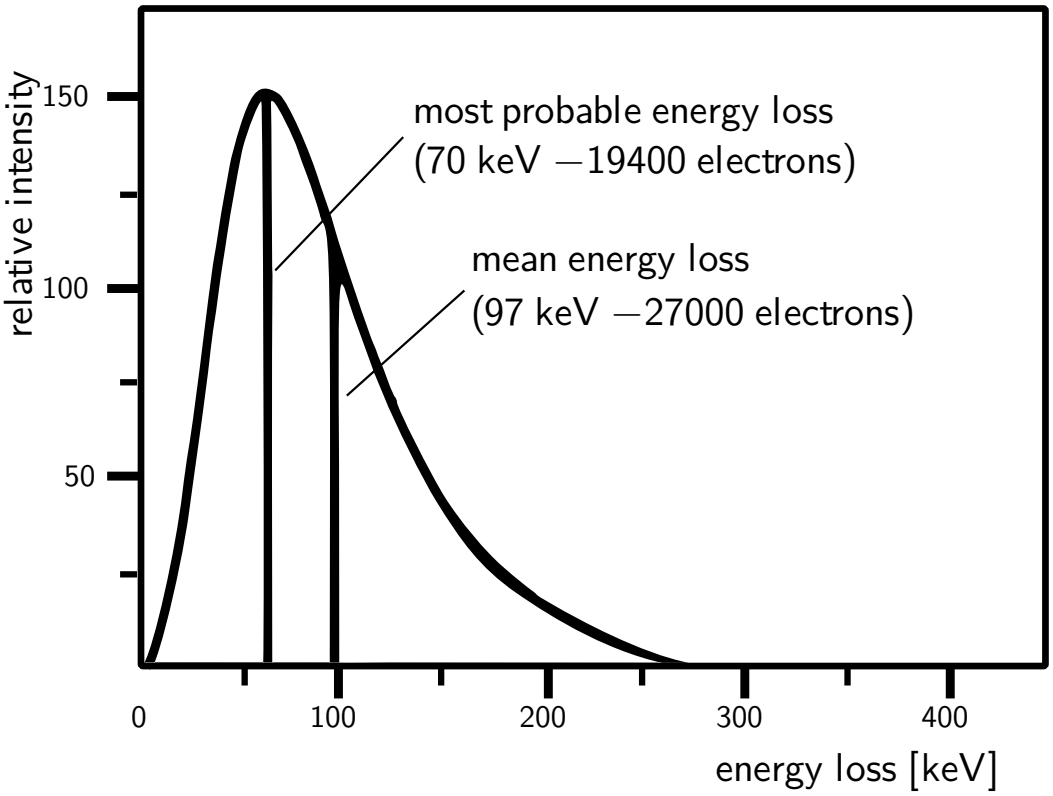

Figure 3.1: The Landau distribution as the energy spectrum of charged MIPs in a 250 µm thick silicon sensor. Taken from [Koh02] and modified.

3.2 Semiconductors

Silicon is a fourth main group element in the periodic table of elements and forms a diamond-like crystal lattice. This kind of lattice can be represented as two fcc-lattices shifted by 1/4 along the diagonal. It is a semiconductor and its electrical properties can be described by band gap theory. All electron states belong either to the valence band or to the conduction band. The highest energy in the valence band is E_V, the lowest in the conduction band is E_C. Straightforward the band gap energy [Chi13] between them is

$$E_G = E_C - E_V \tag{3.12}$$
$$= 1.21\,\text{eV}\,(\text{for silicon})\,. \tag{3.13}$$

At low temperatures only the valence band is filled. Higher temperatures lead according to the Fermi-Dirac statistics to a population of the conduction band. Each electron which moves from the valence band to the conductive band leaves a hole, acting as a free charge carrier as well. The semiconductor becomes conductive.

3.2.1 Intrinsic Semiconductors

In an idealised situation an intrinsic semiconductor does not have any impurities. All free electrons and holes are just thermally excited and their number in equilibrium is given by the Fermi-Dirac distribution

$$F(E) = \frac{1}{1 + \exp\left(\frac{E-E_F}{k_B T}\right)}, \tag{3.14}$$

where E_F is the Fermi energy with an occupation probability of 0.5 and T is the absolute temperature in Kelvin. For a Fermi energy within the band gap which is not too close to E_V and E_C, this equation can be split into separate parts for electrons (n) and holes (p)

$$F_n(E) \simeq \exp\left(\frac{E - E_F}{k_B T}\right) \tag{3.15}$$

and

$$F_p(E) = 1 - F_n(E) \simeq \exp\left(\frac{E_F - E}{k_B T}\right). \tag{3.16}$$

The density of state of electrons with an energy E_{kin} is

$$N(E_{\text{kin}})dE_{\text{kin}} = 4\pi \cdot \left(\frac{2m_i}{h^2}\right)^{\frac{3}{2}} E_{\text{kin}}^{\frac{1}{2}} dE_{\text{kin}}\,, \tag{3.17}$$

where m_i is the effective energy of the electrons (i=n) and holes (i=p). The kinetic energy of the electrons is determined by their distance to the lower end of the conductive band and for the holes by the distance to the upper end of the valence band. By integration of the charge carrier density and the occupation probability one receives the density of free electrons

$$n = 2\left(\frac{2\pi m_n k_B T}{h^2}\right)^{\frac{3}{2}} \cdot e^{\left(\frac{E_C - E_F}{k_B T}\right)} = N_C \cdot e^{\left(\frac{E_C - E_F}{k_B T}\right)} \tag{3.18}$$

and the density of holes

$$p = 2\left(\frac{2\pi m_p k_B T}{h^2}\right)^{\frac{3}{2}} \cdot e^{\left(\frac{E_F - E_V}{k_B T}\right)} = N_V \cdot e^{\left(\frac{E_F - E_V}{k_B T}\right)}. \tag{3.19}$$

N_C and N_V are the density of state of the conductive and valence band. The product

$$n_e \cdot n_h = N_C N_V e^{\left(-\frac{E_C - E_V}{k_B T}\right)} = N_C N_V e^{\left(-\frac{E_G}{k_B T}\right)} \tag{3.20}$$

is independent of the Fermi energy E_F. Another condition is that the number of electrons equals the number of holes as there is charge conservation. This results

in

$$E_i = \frac{E_C + E_V}{2} + \frac{3k_B T}{4} \ln\left(\frac{m_p}{m_n}\right), \tag{3.21}$$

where E_i is the Fermi level for intrinsic semiconductors. The Fermi energy E_F is close to the centre of the band gap, the deviation is caused by the effective masses of the charge carriers. The intrinsic energy level E_i, defined by eq. (3.21), is also important for the extrinsic semiconductors described in the next section. Equation (3.18) and eq. (3.19) can be transformed to

$$n = n_I \cdot \exp\left(\frac{E_F - E_i}{k_B T}\right) \tag{3.22}$$

and

$$p = n_I \cdot \exp\left(\frac{E_i - E_F}{k_B T}\right). \tag{3.23}$$

3.2.2 Extrinsic Semiconductors

Extrinsic semiconductors are intrinsic semiconductors which are doped, that means impurities are added by purpose. This can be done during the crystal growth resulting in a base doping for the whole ingot or later during the production on the surface of a wafer. A doping with an element of the fifth main group, such as arsenic or phosphorus, leads to a surplus of electrons as these elements have five valence electrons and silicon has only four electrons. As a consequence of this the material is called n-type. The usage of third main group elements, prominently boron, produces a surplus of holes. This material is called p-doped. The doping leads to a creation of a new energy level within the energy gap. With n-doping this new energy state E_D lies shortly below the conductive band. According to the Fermi-Dirac statistics electrons can be already promoted into this higher energy state at low energies. For p-doped material there is a new energy state E_V near the valence band, which accepts electrons and leaves mobile holes in the valence band. These additional energy states lead to a shift of the Fermi energy E_F. In the case of the n-doping, E_F is shifted more in direction of the conductive band, and vice versa. On condition that the electron concentration of the conductive band is as large as the donor concentration, the Fermi energy E_F of highly n-doped semiconductors can be calculated according to

$$E_C - E_F = k_B T \ln \frac{N_C}{N_D}. \tag{3.24}$$

For p-doped semiconductors the Fermi energy is

$$E_F - E_V = k_B T \ln \frac{N_V}{N_A}. \tag{3.25}$$

In n-type semiconductors electrons are the majority charge carrier and a smaller number of holes form the minority charge carrier. For p-doped semiconductors the

circumstances are reversed.

3.2.3 Charge Carrier Transport

Mobile charge carriers can move by diffusion or by drift within the crystal. While drift occurs when an electric field is present, diffusion is always possible. The charge carriers have an energy of $\frac{3}{2}k_BT$ with a mean velocity of $1 \times 10^7\,\mathrm{cm\,s^{-1}}$. The mean free pathlength is $1 \times 10^{-5}\,\mathrm{cm}$. Diffusion is proportional to the charge carrier density gradient.

$$\vec{F_e} = -D_e \cdot \vec{\nabla} n_e \tag{3.26}$$

$$\vec{F_h} = -D_h \cdot \vec{\nabla} n_h \tag{3.27}$$

$\vec{F_e}$ and $\vec{F_h}$ are electron and hole fluxes. The diffusion depends on the diffusion constants D_e and D_h. In an electrical field the charge carriers start to drift. The drift velocity is influenced by field strength and the effective mass

$$\vec{v}_{\mathrm{dr,e}} = -\frac{e_0 \cdot \tau_f}{m_e}\vec{E} = -\mu_e \vec{E} \tag{3.28}$$

$$\vec{v}_{\mathrm{dr,h}} = \frac{e_0 \cdot \tau_f}{m_h}\vec{E} \quad = \mu_h \vec{E}\,. \tag{3.29}$$

μ_i is the charge carrier mobility. The current consists of diffusion and in case of an external electrical field of drift

$$\vec{J_e} = e_0 \mu_e n_e \vec{E} + e_0 D_e \vec{\nabla} n_e \tag{3.30}$$

$$\vec{J_h} = e_0 \mu_h n_h \vec{E} + e_0 D_h \vec{\nabla} n_h\,. \tag{3.31}$$

Mobility and diffusion constants are connected by the Einstein equation

$$D_e = \frac{k_B T}{e_0}\mu_e \tag{3.32}$$

$$D_h = \frac{k_B T}{e_0}\mu_h\,. \tag{3.33}$$

3.2.4 P-N-Junction

A pn-junction develops where the surface of a p-doped and an n-doped semiconductor come into contact with each other. Due to the concentration gradient, electrons from the n-side diffuse to the p-side and recombine with holes. The holes from the p-side diffuse to the n-side and recombine with electrons. In this way the volume around the boundary layer becomes depleted. The charge carrier migration causes an electric field antagonizing the migration process. Thus the size of the depletion zone is limited. In the energy band model the pn-junction leads to a bending of the bands as the Fermi energy has to be identical in the two differently doped areas at the same temperature. That yields the in-build-voltage B_{bi}, which raises the energy level in the p-zone and decreases it in the n-zone. The concentration of the majority

charge carriers can be calculated by combining the term eq. (3.18) and eq. (3.19), resulting in

$$\left.\begin{aligned} n_e = N_D = n_i e^{\left(\frac{E_F - E_i^n}{k_B T}\right)} \\ n_h = N_A = n_i e^{\left(\frac{E_i^p - E_F}{k_B T}\right)} \end{aligned}\right\} \Rightarrow N_A \cdot N_D = n_i^2 e^{\left(\frac{E_i^p - E_i^n}{k_B T}\right)}, \tag{3.34}$$

where N_A is the acceptor concentration in the p-doped region and N_D is the donor concentration in the n-doped region. Hence the voltage V_{bi} is

$$V_{\mathrm{bi}} = \frac{1}{e_0}\left(E_i^p - E_i^n\right) = \frac{k_B T}{e_0} \ln\left(\frac{N_A N_D}{n_i^2}\right). \tag{3.35}$$

The electrical field has to vanish at the boundary surface of the depleted volume

$$N_D d_n = N_A d_P\,, \tag{3.36}$$

d_n and d_p are the depths of the depleted volume in the n-doped zone and in the p-doped zone. The Gaussian law helps to calculate the strength of the electrical field at the pn-junction as an integral over the charge density ρ. For the field $E_{\max}$ follows

$$E_{\max} = \frac{1}{\varepsilon\varepsilon_0} e_0 N_D d_n = \frac{1}{\varepsilon\varepsilon_0} e_0 N_A d_p\,. \tag{3.37}$$

The voltage built by the electrical field drops to zero at the borders of the depleted zone. Under the assumption that the voltage between them equals exactly V_{bi}, the thickness of the depleted zone is

$$d = \sqrt{\frac{2\varepsilon\varepsilon_0(N_A + N_D)}{\varepsilon_0 N_A N_D} V_{\mathrm{bi}}}\,. \tag{3.38}$$

For an assymetric doping profile the approximation results in

$$d \approx \sqrt{\frac{2\varepsilon\varepsilon_0}{\varepsilon_0 N_D} V_{\mathrm{bi}}} \tag{3.39}$$

and

$$E_{\max} \approx \sqrt{\frac{2\,\mathrm{e}_0}{\varepsilon\varepsilon_0} N_D V_{\mathrm{bi}}}\,. \tag{3.40}$$

This is interesting for the ATLAS pixel sensors, as a strongly doped p^+ layer is placed on a weakly doped (just the base doping) n layer. When an external voltage is applied against the doping concentration, the depletion zone grows. In case of the ATLAS pixel sensors the bias voltage has to be negative. The voltage which leads

to a depletion of the whole sensor volume is called depletion voltage

$$V_{\mathrm{dep}} = \frac{e_0 N_D}{\varepsilon\varepsilon_0}\frac{d^2}{2}\,. \tag{3.41}$$

As the depletion voltage is much higher than the built-in-voltage V_{bi}, it is reasonable to neglect it and so the thickness of the depleted zone results in

$$x = \sqrt{\frac{2\varepsilon\varepsilon_0}{eN_D}} \cdot \sqrt{U}. \tag{3.42}$$

3.2.5 Charge Generation and Collection

When an ionising particle traverses the detector charge is generated according to the processes described in section 3.1. The created electron-hole-pairs have to be separated as soon as possible, otherwise they recombine immediately. The depletion zone has to be as large as possible as it is the sensitive part of the bulk. In order to separate the electrons and holes an external electric field is used. This results in movement of the electrons and holes to their respective electrode, where the signal is coupled out by metal layers. The length of the signal depends on the velocity v of the charge carriers, which depends on the reverse voltage and the mobility (position and temperature). The collected charge is induced in the electrodes by the moving generated charge and can be explained generally by the mirror charge concept. It is described specifically by the Ramo theorem

$$dQ = q\vec{E}_R(\vec{r}) \cdot \vec{v}_{\mathrm{dr}}(\vec{r})dt\,. \tag{3.43}$$

$\vec{E}_R$ is the so-called Ramo field describing the coupling between the drifting charge and the electrode. The Ramo or weighing field is described by the weighing potential Φ_R

$$\vec{E}_R = -\vec{\nabla}\Phi_R\,. \tag{3.44}$$

The weighing field depends only on geometry and determines how charge motion couples to an electrode.

CHAPTER 4

Radiation Damage

The total leakage current of a silicon sensor consists of the surface current and the bulk current. The bulk current is composed of the diffusion current and the generation current. Diffusion current is caused by charge carrier drift in the non-depleted part of the sensor, the generation current by electron-hole generation in the space charge area. The main part of leakage current in radiation damaged sensors as well as in most non-irradiated devices is caused by the generation current which is dependant on the volume and the generation rate of electron-hole pairs [Spi06; Lut99; Rum09].

4.1 Crystal Defect Types and Formation

Traversing the crystal, the particles can deposit energy by several means. As already described in section 3.1, this can happen in form of ionisation. This kind of energy deposition keeps the crystal intact as it reverts into its prior state. Non-ionising interaction with the crystal leads to permanent crystal damage. The most important processes are:

- Removal of a silicon atom from its place in the crystal lattice leads to interstitials and vacancies. These are so-called point defects.
- The interaction between the traversing particle and nuclei leads to nuclear conversion.
- If enough energy is transferred to an atom knocked out of the lattice, it can cause further damage leading to defect clusters.

In order to remove an atom from the lattice, a minimal energy transfer of 15 keV is necessary. The hit atom is called PKA[1]. As the effects of different particles (such as hadrons, electrons, pions) vary, it is suitable to scale them to a quantity called standard irradiation. According to the NIEL[2] thesis only the non ionising energy

1 **P**rimary **K**nock-on **A**tom
2 **N**on **I**onising **E**nergy **L**oss

loss has to be taken into account and only the interaction with the PKA depends on the kind of radiation. All further damage is caused by the PKA. The non-ionising energy loss is converted to the energy loss caused by fictional neutrons with the energy of 1 MeV. That is why all fluences are usually expressed in form of $n_{\mathrm{eq}}\mathrm{cm}^{-2}$. At room temperature the point defects can move in the crystal lattice. On the one side this can lead to annealing (see section 4.5). On the other side the defects can combine with each other or with inherent impurities to form more complex defects [Wun92]. A schematic visualisation of selected defect types is shown in fig. 4.1. The so-called hardness factor κ is unique for each irradiation facility and its knowledge enables to convert irradiation fluences into equivalent fluences

$$\Phi_{\mathrm{eq}} = \kappa \cdot \Phi_{\mathrm{irr}} \,, \tag{4.1}$$

where Φ_{irr} is the fluence. The irradiation leads in principle to three macroscopic effects that are described in the following.

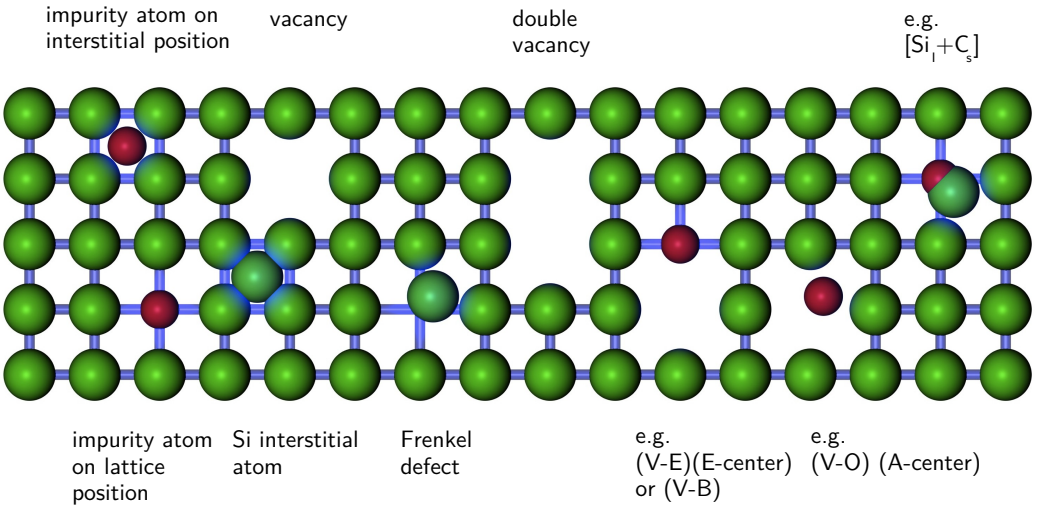

Figure 4.1: Schematic illustration showing different crystal defects. Original taken from [Wun92] and modified in [Tro12].

4.2 Leakage Current

The defects caused by radiation can lead to the creation of mid-gap states [Spi06] causing an increase of the reverse bias current. The increase of current can be described in good approximation for nearly all materials and investigated fluences

by the equation

$$I_{\text{leak}} = \alpha \cdot \Phi_{\text{eq}} \cdot V \,, \tag{4.2}$$

where the factor α is the current related damage rate and its value is [Mol99]

$$\alpha\,(80\,\text{min},60\,^{\circ}\text{C}) = (3.99 \pm 0.03) \cdot 10^{-17}\,\text{Acm}^{-1}\,, \tag{4.3}$$

which is valid after a heat treatment for 80 min at 60 °C.

4.3 Effective Doping Concentration and Type Inversion

With irradiation the effective doping

$$N_{\text{eff}} = N_D - N_A \tag{4.4}$$

of the n-type material seems to decrease until it appears undoped and with continued irradiation it begins to behave p-type like. There are several factors, donor removal by crystal lattice defects is one of them. More important is the fact that displacement damage acts as an acceptor-like state which is populated by electrons from the bulk and results in an increasingly negative space charge. After enough irradiation this leads to type inversion. The change in the effective doping concentration changes the depletion voltage

$$V_{\text{dep}} = \frac{e_0 |N_{\text{eff}}|}{\varepsilon\varepsilon_0} \frac{d^2}{2} \,. \tag{4.5}$$

The development of N_{eff} is improved by using DOFZ[1] base material instead of the standard float-zone material. There are several mechanisms on the microscopic scale, one of the effects of oxygen dimers is the creation of shallow thermal donors.

4.4 Trapping

Even more important for the operation of highly irradiated silicon sensors, than the fact that due to high leakage current the sensors can be only operated under depleted, is trapping. This means that electrons and holes moving to their respective electrode are captured by defects and that they are released too late for contributing to the charge signal. The inverse trapping time can be described by the equations

$$\frac{1}{\tau_0} = \beta \cdot \Phi_{\text{eq}} \tag{4.6}$$

$$\beta = \left(\sum_i g_i f_i(t)(1 - P_i)\sigma_t \right) \nu_{\text{th}} \,, \tag{4.7}$$

1 **D**iffusion **O**xygenated **F**loat**Z**one

where g_i is the introduction rate, P_i is the occupation probability of traps with the cross section σ_t and ν_{th}.

4.5 Annealing

As already mentioned donor removal as well as build-up of stable charge are permanent and do not show time dependant behaviour. This is called stable damage:

$$N_c = N_{c0}(1 - e^{(-c\Phi_{\mathrm{eq}})}) + g_c\Phi_{\mathrm{eq}}\,. \tag{4.8}$$

Furthermore, there is beneficial annealing, which describes a temperature dependant recovery from the change in space charge

$$N_a = g_a\Phi_{\mathrm{eq}}e^{(-t/\tau_a)}\,. \tag{4.9}$$

Beneficial annealing can decrease the depletion voltage after type conversion. The effect of reverse annealing works against it and leads to a further reduction of the effective charge concentration and to an increase of the depletion voltage. As the usable voltage is limited by the current services (cables, high voltage supplies), it is planned to run the detector shortly at a higher temperature and afterwards to cool it continuously. Generally, temperature management of the sensors is a necessity while planned and unplanned maintenance periods have to be taken into account. Reverse annealing can be described by the equation

$$N_y = N_{y0} \cdot \left(1 - e^{(-t/\tau_y)}\right)\,. \tag{4.10}$$

4.6 Charge Amplification

Results gained first with strip sensors and then with pixel sensors of different layouts and technologies show that for high bias voltages more charge is collected than expected from the trapping model [Cas+10; Man+11; Mil+12; Kra+02; Kra+10; Kra+09; Ere+11]. This effect is called charge multiplication and it is assumed to be caused by impact ionisation. This should occur along steep electric field zones at the implant borders and is expected to show an exponential behaviour. The collected charge calculated with the simple trapping model is summarized in table 4.1.

Φ_{eq}	$1 \cdot 10^{15}\,\mathrm{n_{eq}\,cm^{-2}}$	$5 \cdot 10^{15}\,\mathrm{n_{eq}\,cm^{-2}}$	$1 \cdot 10^{16}\,\mathrm{n_{eq}\,cm^{-2}}$	$2 \cdot 10^{16}\,\mathrm{n_{eq}\,cm^{-2}}$
λ_{av}	$240\,\mu\mathrm{m}$	$50\,\mu\mathrm{m}$	$25\,\mu\mathrm{m}$	$12\,\mu\mathrm{m}$
$\varepsilon_{\mathrm{hit}}$	$19\,\mathrm{ke^-}$	$< 4\,\mathrm{ke^-}$	$< 1.3\,\mathrm{ke^-}$	$< 1\,\mathrm{ke^-}$

Table 4.1: The collection distance at the saturation velocity λ_{av} and the resulting effective charge at different fluences [Mik+11].

CHAPTER 5

Upgrade Plans

In this chapter a short overview of the planned operation parameters for the LHC[1] is given. Based on those the possible upgrade scenarios of ATLAS[2] are described. A summary of the performance during the last two years of successful operation before the first long shutdown and a sketch of the planned changes is given in [Roz13].

5.1 LHC Upgrade

With the shutdown of the LHC in the beginning of 2013 the phase 0 of the upgrade has started. It is foreseen to last for two years and during this time the accelerator will be prepared to run at its design energy of 14 TeV. Until 2021/2022 the necessary preparations for an increase of the luminosity up to $5 \cdot 10^{34}\,\mathrm{cm}^{-2}\mathrm{s}^{-1}$ should be concluded. The currently foreseen global schedule is shown in fig. 5.1. [HL-13]

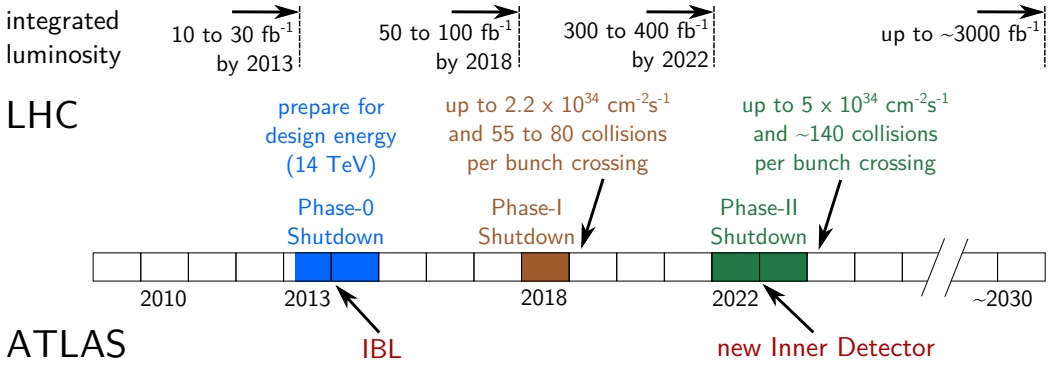

Figure 5.1: General overview of the time schedule for the upgrades of LHC and ATLAS [Wit13], based on information from [ATL12b].

1 **L**arge **H**adron **C**ollider
2 **A** **T**oroidal **L**HC **A**pparatu**S**

5.2 ATLAS Upgrade

5.2.1 ATLAS Phase 0

On the part of the ATLAS pixel detector a major goal for the ongoing shutdown phase 0 is the introduction of a fourth pixel layer called IBL[1]. An representation of the layout is shown in fig. 5.2. The IBL has been already constructed, integrated with the new service quarter panels and its installation is just now (mid of 2014) being finalized. The new service quarter panels were originally motivated by the rapid off-detector VCSEL[2] mortality, which was finally attributed to humidity and the VCSEL type used in the off-detector boards. Nevertheless, as "most of the on-detector failures are probably related to the optoboards (cold soldering, broken wire-bonds, VCSEL failure, capacitors defects, etc.)"[Roz13], it is expected to recover about 80% of the currently 88 disabled modules by their installation. [Cap+10; ATL12a]

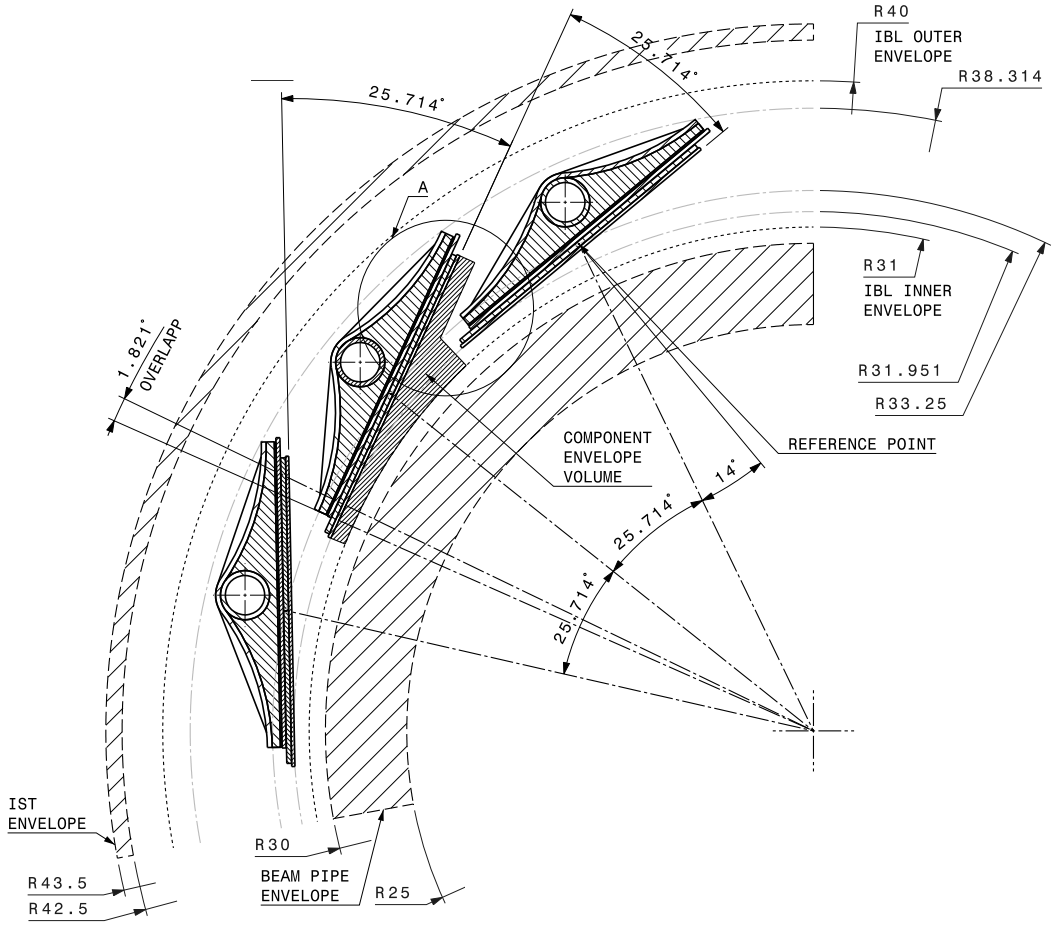

Figure 5.2: Cross section through the $r\phi$-plane of the IBL. [Cap+10]

1 **I**nsertable **B**-**L**ayer
2 **V**ertical-**C**avity **S**urface-**E**mitting **L**aser

5.2.2 ATLAS Phase 2

Basically the phase 2 upgrade calls for a complete replacement of the inner detector. As the TRT[1] will not be able to cope with the multiplicity, it is foreseen to fill the volume currently used by the TRT with silicon strips. On the part of the pixel detector it is supposed to spread out to huger radii by introducing more layers. Currently there are five of them foreseen.

There are several possible scenarios mentioned in [ATL12b] which are under investigation. Different technologies like Gossip, 3D, diamond, HVCMOS[2] [Per+13] and variations of them like 3D diamond are possible candidates for the different layers. Cheaper alternatives for the bump bonding like TSV[3], but also bumpless technologies like HVCMOS [Per09], are investigated as well.

Depending on the radius there are different requirements for each layer. For the innermost layer the radiation hardness will be the most critical point. Simulations predict an accumulated end-of-life fluence (including safety factors) of roughly $2 \times 10^{16} \mathrm{n_{eq.}}\,\mathrm{cm}^{-2}$ (see fig. 5.3). Furthermore, it should be able to process the data at the expected high occupancy and the radiation length should be as low as possible.

On the one hand the outermost layer will only receive a fluence of $1 \times 10^{15} \mathrm{n_{eq.}}\,\mathrm{cm}^{-2}$, thus making radiation hardness a secondary problem, when comparing the situation to e.g. the currently existing b-layer. On the other hand cost-efficiency becomes

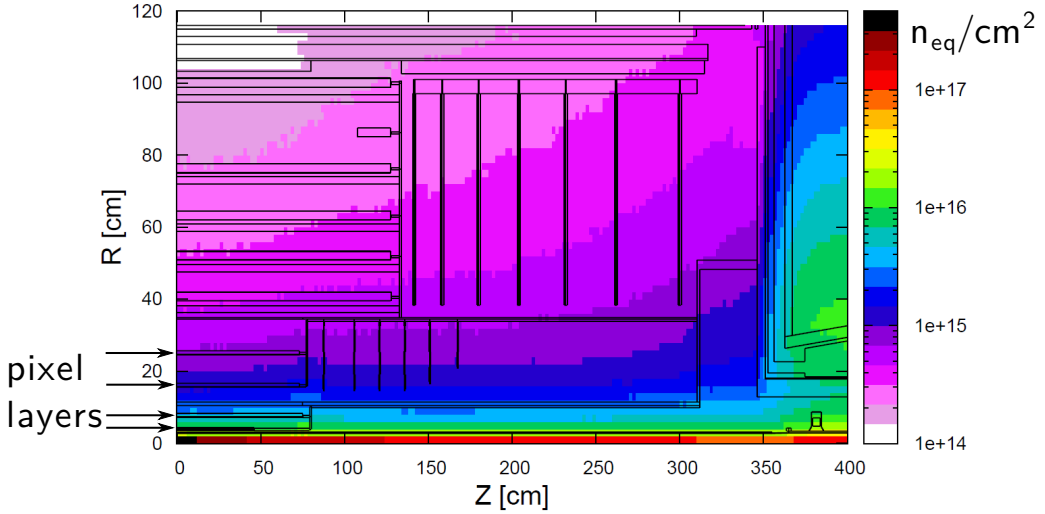

Figure 5.3: Simulation of an rz-map of the neutron equivalent fluence, expected for the ATLAS Inner Tracker region, normalised to $3000\,\mathrm{fb}^{-1}$ of 14 TeV minimum b ias events. Taken from [ATL12b] and modified.

1 **T**ransition **R**adiation **T**racker
2 **H**igh **V**oltage**C**omplementary **M**etal **O**xide **S**emiconductor
3 **T**hrough **S**ilicon **V**ia(s)

an issue when going to larger radii. The currently planned outer-most layer alone needs about $20\,\mathrm{m}^2$ of silicon. Compared to the current $2\,\mathrm{m}^2$ of the pixel detector this is a completely new dimension.

For the inter-mediate layers 2 and 3, MCz[1] as a sensor material is under consideration. Its property, where equal doses of charged and uncharged particles cancel out their respective radiation damage, makes it attractive for a region having such a radiation background.

In the outermost layer 4-chip modules are foreseen as a measure to decrease the cost. [ATL13c] The new cooling system will be much more powerful and reliable as it will be based on CO_2 as a freezing agent.

1 **M**agnetic **Cz**ochralski

CHAPTER 6

Samples

In the beginning of this chapter a short overview of the assemblies used in this thesis is given. Afterwards their general properties are discussed, the evolution of the carrier PCBs[1] is presented and the pecularities of the irradiation facilities are summarized.

6.1 DUT Description

Most of the sensors used in this study are a byproduct of the original ATLAS[2] sensor production and therefore they had to fulfil the ATLAS quality assurance criteria. The structures were located at the edge of the wafer, as can be seen in the wafer maps in appendix A. They were originally intended for production accompanying tests as well as R&D. They are produced on 250 µm thick DOFZ[3] silicon material with a crystal orientation of $\langle 1\,1\,1 \rangle$. DOFZ means that the silicon is oxygen enriched which drastically improves its radiation hardness as demonstrated by the ROSE[4] collaboration[5]. For this purpose the wafers are exposed for 24 h to an oxygen atmosphere at high temperatures. This leads to diffusion of oxygen into the silicon bulk. Afterwards, the resulting silicon oxide layer is stripped off. A couple of sensors were taken from experimental productions in 2009 and 2010. While the design of other test structures located on those wafers was modified, the layout of the sensors used here, remained the same. This means that they have 50 µm × 400 µm long standard pixels and 16 guard rings. The only exception is the assembly DO-46 which has the pixel shifted stepwise guard ring design used for the study of the edge region. A more detailed explanation of this design, its intended purpose and the results may be found in [Wit13]. Otherwise, the change in the 2009 and 2010 productions was a variation of the bulk thickness which is expected to have an influence on the charge collection behaviour due to the changed electric field within the depleted sensor.

1 **P**rinted **C**ircuit **B**oards
2 **A** **T**oroidal **L**HC **A**pparatu**S**
3 **D**iffusion **O**xygenated **F**loat**Z**one
4 **R**esearch and development **O**n Silicon for future **E**xperiments
5 `http://rd48.web.cern.ch/RD48/`

Three of the sensors DO-34, DO-36 and DO-38 were produced on MCz[1]-Material. This differs from the conventional float zone material by using a magnetic field during the crystal growth. It has peculiar properties and is supposed to show better radiation hardness when exposed to mixed field irradiation.

Another important distinction, which is independent from the inherent sensor properties, is the connection technology. The standard connection technology in this thesis are PbSn bump balls. This flip-chip technology requires a quite high temperature (see fig. 6.1) during the final connection of frontend and sensor. The flip-chip mating has to be finalized prior to the irradiation as the exposure to such a high temperature is detrimental to irradiated sensors. For making the study of sensors with undamaged readout electronics possible, also the alternative indium bump bonding is employed. There the required temperature during the connection step is much lower, thus allowing flip-chip mating after the irradiation of the sensors. All assemblies used are FE-I3 based single chip assemblies. The only exception is the FE-I4A based SCC-31 which is used as a reference plane during certain testbeam runs.

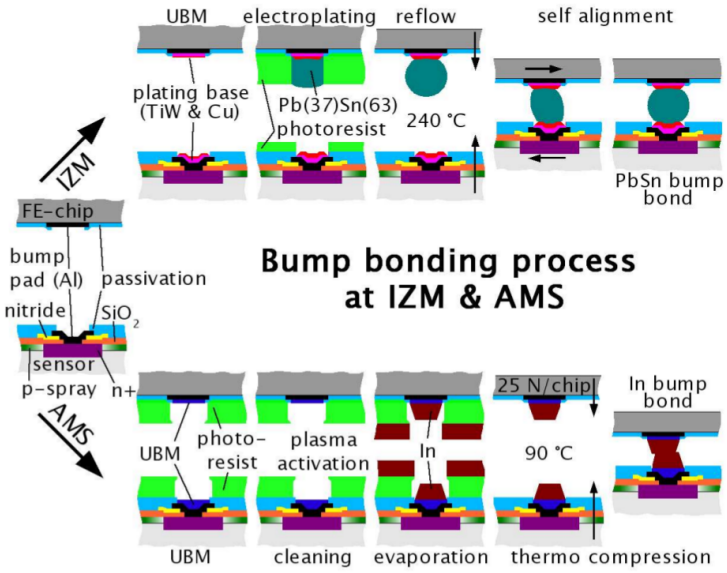

Figure 6.1: Schematic comparison between the PbSn and indium bump bonding processes.[Dob04]

1 **M**agnetic **Cz**ochralski

assembly name	*sensor ID*	*bulk thickness [μm]*	*sensor material*	*sensor production*	*frontend ID*	*bumbond type*	*bias resistor [Ω]*	*fluence [$n_{eq}cm^{-2}$]*	*particle type*	*irradiation site*
DO-1	unknown	250	DOFz	original	10-5A	PbSn	10000	-	-	-
SCC-31	301061-07-03	250	DOFz	IBL[1]	ASN6QHH(23)	AgSn	10000	-	-	-
DO-36	292100-02-21	285	MCz	CiS 2010	2-4B	PbSn	10000	$5.05 \cdot 10^{14} \pm 4.14 \cdot 10^{13}$	p	PS
DO-38	292100-03-07	285	MCz	CiS 2010	3-4A	PbSn	10000	$9.98 \cdot 10^{14} \pm 7.58 \cdot 10^{13}$	p	PS
DO-I-13	8296-31-07	250	DOFz	original	29112092	In	9380	$1.00 \cdot 10^{15} \pm 7.00 \cdot 10^{13}$	p	ICK
DO-7	7971-16-06	250	DOFz	original	7-6B	PbSn	941000	$1.00 \cdot 10^{15} \pm 7.00 \cdot 10^{13}$	p	ICK
DO-8	6968-22-04	250	DOFz	original	-	PbSn	10000	$1.00 \cdot 10^{15} \pm 7.00 \cdot 10^{13}$	p	ICK
DO-34	292100-03-12	285	MCz	CiS 2010	3-4B	PbSn	10000	$1.89 \cdot 10^{15} \pm 1.40 \cdot 10^{14}$	p	PS
DO-I-7	6134-11-04	250	DOFz	original	30612091	In	9380	$2.20 \cdot 10^{15} \pm 1.54 \cdot 10^{14}$	p	ICK
DO-47	301068-03-17	150	DOFz	CiS 2011[2]	9-3A	PbSn	9380	$5.00 \cdot 10^{15} \pm 3.50 \cdot 10^{14}$	n	JSI
DO-9	6968-24-06	250	DOFz	original	5-6B	PbSn	9370	$5.00 \cdot 10^{15} \pm 3.50 \cdot 10^{14}$	n	JSI
DO-13	291921-05-10	285	DOFz	CiS 2009[2]	6-11A	PbSn	9360	$5.00 \cdot 10^{15} \pm 3.50 \cdot 10^{14}$	n	JSI
DO-I-11	6139-06-04	250	DOFz	original	30610142	In	9380	$1.00 \cdot 10^{16} \pm 7.00 \cdot 10^{14}$	p	ICK
DO-I-12	8283-21-09	250	DOFz	original	Z1005B	In	9370	$1.40 \cdot 10^{16} \pm 9.80 \cdot 10^{14}$	p	ICK
DO-I-5	3633-03-04	250	DOFz	original	29108151	In	9380	$1.40 \cdot 10^{16} \pm 9.80 \cdot 10^{14}$	p	ICK
DO-10	6146-02-06	250	DOFz	original	4-6A	PbSn	9999	$2.00 \cdot 10^{16} \pm 2.00 \cdot 10^{15}$	n	JSI
DO-24	291921-04-04	285	DOFz	CiS 2009[3]	3-11B2	PbSn	9350	$2.00 \cdot 10^{16} \pm 2.00 \cdot 10^{15}$	n	JSI

Table 6.1: List of all DUTs and their properties which were used successfully in lab and testbeam measurements. (ICK: Irradiation Center Karlsruhe, PS: CERN-PS, JSI: Jožef Stefan Institute in Ljubljana)

1 Slim edge design read out by a FE-I4.
2 Pixel shifted stepwise design at the edge.
3 Pixel implants are divided into four parts for all pixels in the grid between column 10-14 and row 25-64.

6.2 Irradiation Facilities

6.2.1 CERN-PS at Geneve

The proton irradiations were conducted at CERN[1]-PS[2]. It is a source of 24 GeV protons, which are provided in form of a beam with a diameter of 2 cm. Taking the Gaussian profile into account an area of roughly 0.7 cm × 0.7 cm can be homogeneously irradiated, which covers the active area of SingleChips. Among the several CERN-PS beam lines Irrad-1, Irrad-3 and Irrad-5 are those relevant for pure proton irradiations. Irrad-3 and Irrad-5 have restricted access and they are equipped for irradiation of larger objects, also in scan mode.

Irrad-1 is adequate for objects with a maximum size of approximately 1.5 cm × 1.5 cm and it has the advantage of having an easier access. All samples to be irradiated in Irrad-1 are inserted into cutouts (on each side 1 mm larger than the sample) in the middle of cardboards (fig. 6.3), fastened on both sides with a piece of Kapton tape. Usually "normal" scotch tape is sufficient, but at very high fluences it is not durable enough. Exactly cut out pieces of lens cleaning tissue are used to isolate several (up to 3) samples against each other, as they are inserted together into one piece of card board and further to prevent contact between the adhesive side of the Kapton tape and the samples. The cardboard cards are piled in a slot on a shuttle (fig. 6.2) which can be driven remotely through a labyrinth into the beam and after irradiation back to the measuring hut without the need for a beam shutdown. The samples in the middle of each card should not bulge, as the pile of cards is pressed together and might damage the samples. This determines together

Figure 6.2: The left picture shows the shuttle (picture taken from [CER]) at PS Irrad-1 which brings the samples remotely into the beam and back, the four brackets hold the sample cardboard cards. In the right picture the shuttle is shown with the cold box installed, which enables irradiations at 0 °C and below. One part of the samples was irradiated cold, the rest at room temperature (28 °C), as the cold box broke down due to irradiation damage of the peltier elements.

1 **C**onseil **E**uropéen pour la **R**echerche **N**ucléaire
2 **P**roton **S**ynchrotron - accelerator at CERN

with the absorption of the samples the limit to the number of samples per card. Dosimetry of the samples is done by measuring the activation of aluminium foils, which are irradiated together with the samples. Aluminium is transformed by the nuclear reactions to sodium isotopes:

$$^{27}_{13}\mathrm{Al} + p \longrightarrow {}^{24}_{11}\mathrm{Na} + 3p + n \tag{6.1}$$

$$^{27}_{13}\mathrm{Al} + p \longrightarrow {}^{22}_{11}\mathrm{Na} + 3p + 3n\,. \tag{6.2}$$

$^{24}_{11}$Na emits after a β^--decay photons with an energy of 1369 keV and $^{22}_{11}$Na sends out photons after a β^+-decay with an energy of 1275 keV. Those are measured with a Ge spectrometer. The hardness factor of the protons is 0.62 [Mol99]. The transport from Geneva to Dortmund was kept below 0 °C with cooling packs in the box shown in fig. 6.4.

6.2.2 JSI-Triga at Ljubljana

Neutron irradiations are carried out at the Jožef Stefan Institute at Ljubljana using the TRIGA[1] Mark II nuclear reactor with a peak power of 250 kW. The samples are sealed in small fused fitting polyethylene bags, for each fluence one of them is used. Within these bags the samples are separated and protected from scratching with the same lens cleaning tissue which is wrapped around them. At the reactor site the samples are placed in plastic cylinders and inserted into the reactor core through a tube which leads through the shielding water. The reactors' hardness factor is 0.90 ± 0.05. The received fluence at the reactor is calculated from the reactor power and irradiation time. Regular calibrations and cross-checks of this relation (also spatially within irradiation container $2R = 2.5$ cm, $H = 10$ cm) are

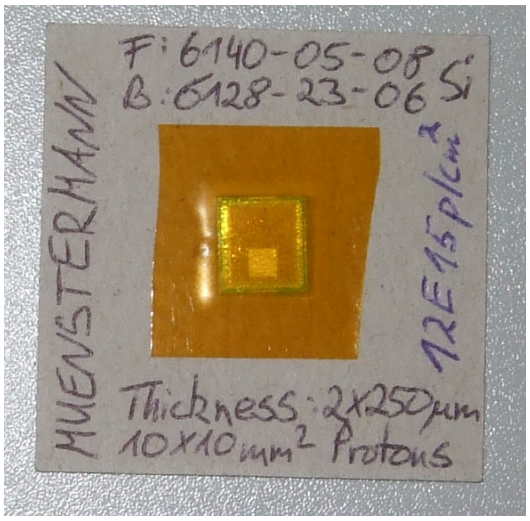

Figure 6.3: A typical cardboard card package prepared for CERN-PS.

1 **T**raining, **R**esearch, **I**sotopes, **G**eneral **A**tomic

Figure 6.4: The left picture shows the transport box used for the cold transport of the irradiated samples back from CERN (provided by the irradiation facility) and the right image depicts the corresponding cryostat.

performed [Kra09]. Therefore, the uncertainty of the fluence is estimated to be less than 10%. During the transport of the samples to Dortmund they are kept cold as well.

6.2.3 Irradiation Center Karlsruhe

At the irradiation centre Karlsruhe the samples can be irradiated with a high intensity 24 MeV beam of protons used in scanning mode. During the irradiation the samples are cooled with refrigerated nitrogen. For the irradiation they are fastened with tape on a carrier plate and placed within the irradiation box. Due to the low energy of the particles, the ionising dose deposited in the assemblies is very high and FE-I3 assemblies irradiated above $2 \times 10^{15} \mathrm{n_{eq.}\ cm^{-2}}$ stop working. In case of irradiating mounted single chip assemblies, a cover plate is used to protect the LVDS[1] driver ICs. This safety cover is shown in fig. 6.5 together with four mounted assemblies for demonstration purposes.

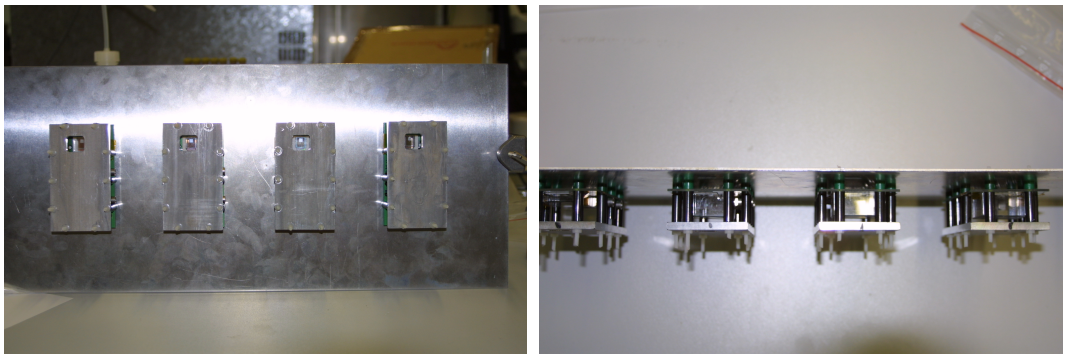

(a) SCA carrier for irradiations in Karlsruhe – front view.

(b) SCA carrier for irradiations in Karlsruhe – top view.

Figure 6.5: SCA carrier for irradiations in Karlsruhe. The cover plate (5 mm thick aluminium) protects the rest of the PCB and especially the LVDS driver ICs from the the radiation.

CHAPTER 7

Fanout

The fanout is a readout device which makes it possible to measure FE-I3 sized single chip sensors without a permanently bonded active readout electronics. This is useful for disentangling the effects of irradiated sensors and irradiated readout electronics. Furthermore, this enables the cross calibration of charge collection measurements by exchanging the readout electronics between different samples repeatedly as it is usually done with strip sensors. First, a motivation for this approach is given and a preparatory study using probe needles for contacting is presented. Afterwards, the fanout chip is described in more details and the first fanout readout setup is demonstrated together with results from an unirradiated frontend assembly. A setup for the automatized full characterization of a fanout assembly is introduced, followed by an outlook on further studies and developments planned with the fanout structure.

7.1 Motivation

The basic challenge of measuring irradiated and especially highly irradiated hybrid sensors is that usually both the sensor and the readout electronics have to be irradiated simultaneously. The final flip-chip step is a high temperature step, which has to occur before the irradiation in order to avoid potentially fatal annealing damage to the irradiated sensor (compare chapter 6 for details of the flip-chip connection process). The targeted fluences in this thesis require an irradiation of the readout electronics FE-I3 beyond its specifications, thus causing partially complete failure or erratic behaviour. Further details of the observed failure

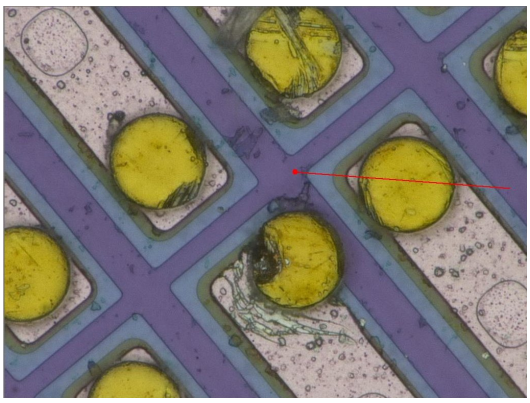

Figure 7.1: Picture showing part of a single chip sensor where the (slightly battered) bump bond pads (yellow circles) can be seen.

modes and an alternative method to avoid those difficulties are described in section 9.1. In [Rum09] a first attempt was made to contact individual bump bond pads (see fig. 7.1) on an unflipped sensor with a needle prober. A minimum of three simultaneous set needles was deemed to be necessary in order to contact the bias grid, outer guard ring and one pixel. The mechanical stability necessary to conduct this exercise reliably, was partially gained by employing a wafer probe station, which is equipped with air filled vibration absorbers.

In fig. 7.2 the setup used for the needle contacting is shown, its main feature is the probe station with a customized vacuum holder for the sensors and a cover for cooled measurements. A scintillator is mounted below an opening under the sensor for externally triggered source measurements. The use of an external trigger reduces the noise drastically. There is a separate needle for the bias voltage supply from the bottom. The readout was realized with a Cremat[1] CR-110 charge sensitive preamplifier mounted on a commercially available evaluation board. The voltage signal from the preamplifier was amplified and fed into a computer controlled oscilloscope.

Figure 7.3 shows the actual contacting of two bump bond pads (diameter about 13 µm). It could be demonstrated that an analogue readout using a charge sensitive preamplifier is feasible, although needle contacts are not the best method. The stability of the achievable contacting was an issue as the contacting quality deteriorated over time. Furthermore, the UBM[2] did not take kindly to repeated contacting trials. The small signals were mixed with noise through EMI[3], which made it evident that a better shielding was necessary.

1 `http://www.cremat.com/`
2 **U**nder **B**ond **M**etallization
3 **E**lectro**m**agnetic **I**nterferences

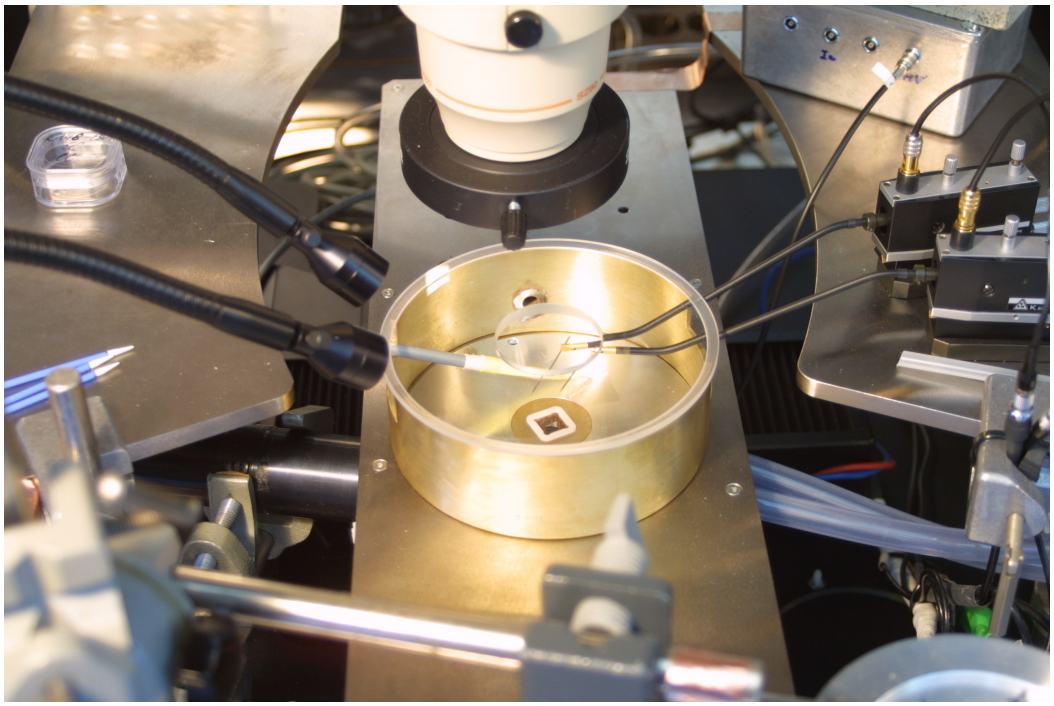

Figure 7.2: Overview of the setup for needle prober based readout of a FE-I3 sized single chip sensor. The central sample carrier is in the middle and on the right the preamplifier box with two needle probes can be seen. [Rum09]

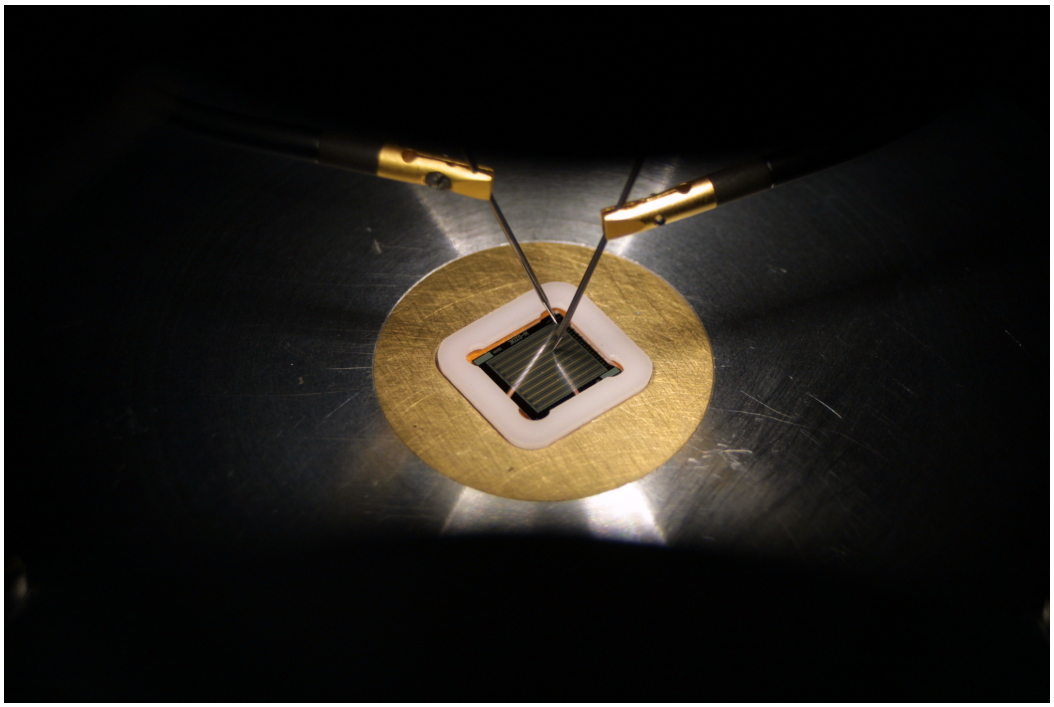

Figure 7.3: Closeup view of a FE-I3 sized single chip sensor where an individual pixel and the bias grid are contacted with PH100 needle probers. [Rum09]

7.2 Description

The fanout is a simple (electronically) passive silicon chip which can be flip chipped to a sensor prior to irradiation. Although emulating mechanically a FE-I3 readout chip, it does not contain anything vulnerable to radiation damage. Instead of active electronics the fanout chip only has passivated aluminium traces processed on electronics grade silicon wafers, which lead the unconditioned charge signal from each bump ball to wirebond pads. This is realized for a number of individual pixels as well as pixel groups. The signal of pixels that belong to groups — emulating strips or pad diodes — is in each case brought together at one wirebond pad.

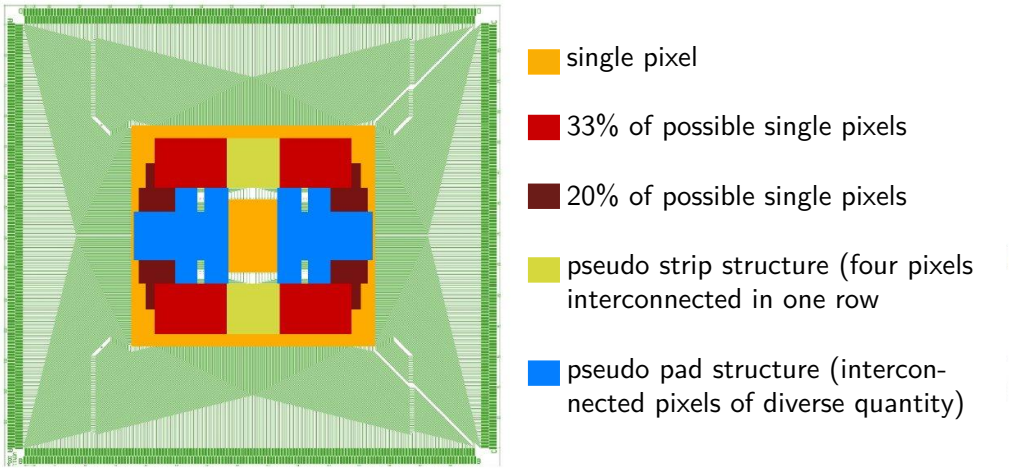

Figure 7.4: Schematic of fanout chip with markings showing the differently read-out pixels. [Tro12]

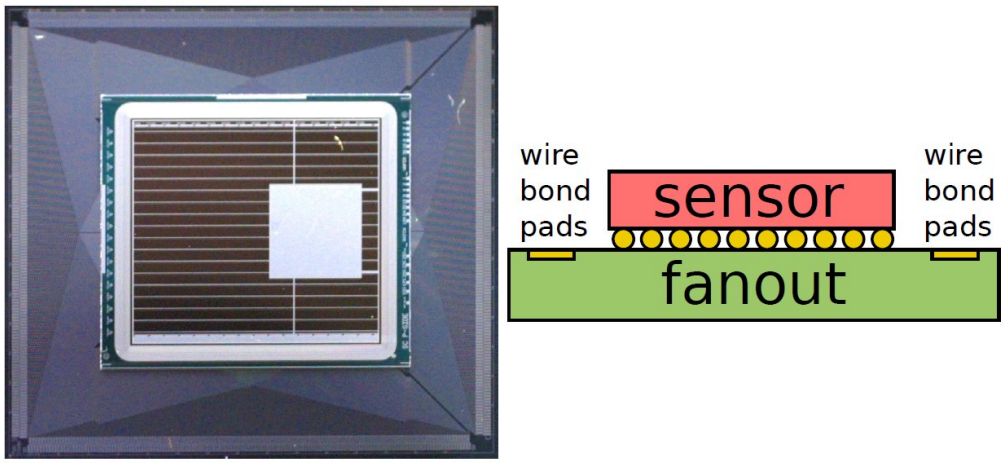

Figure 7.5: Photo of an unmounted fanout assembly where the pixel sensor can been seen in the middle of the circumferential fanout balcony with the wirebond pads. [Plü12]

The location of the differently connected pixels is shown in fig. 7.4. The pixels,

which can be contacted individually, are arranged in a way which makes it possible to connect several pixels lying beside each other in order to study charge sharing. The wirebonds pads, about 1150 in total, are accessible after the conclusion of the flip-chip process, as they are located on a balcony which extends from beneath the sensor on all four sides (see fig. 7.5). The bump bond pads were treated with the appropriate UBM for the PbSn flip-chip process.

7.3 Setup

The readout of the fanout is realized in a similar way as in the preliminary study. The mechanical issues are omitted by avoiding the needle contacting. The whole setup is enclosed in a shield enclosure targeting the EMI observed previously. A test cell of the type $5230-30$, produced by ETS-Lindgren[1], depicted in fig. 7.6, is used for this purpose. The design of its feedthrough plate and the design of the grounding scheme are of utmost importance to ensure the test cell's effectivity.

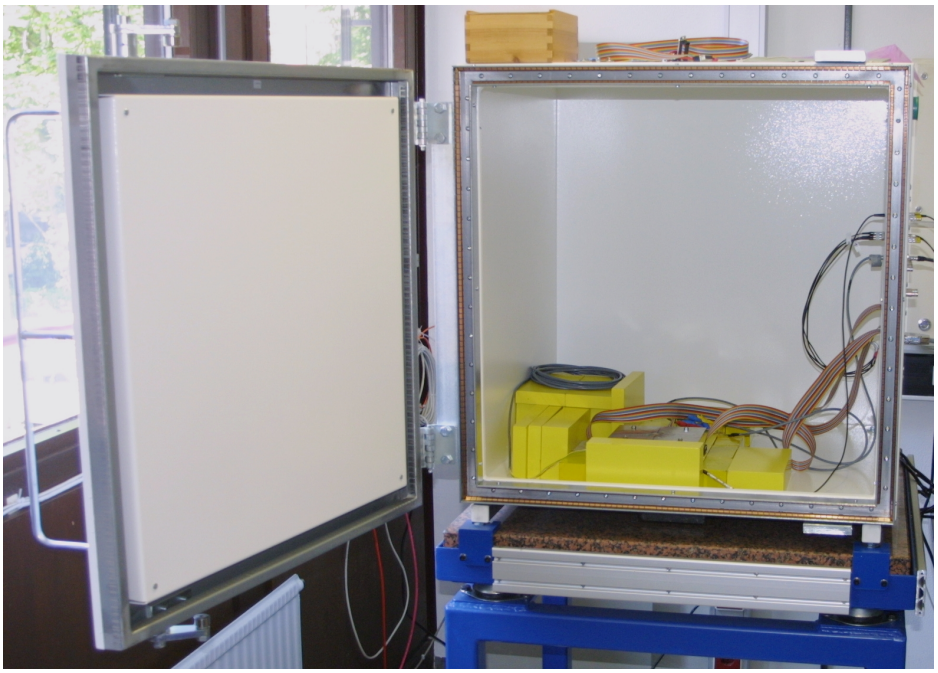

Figure 7.6: The test enclosure used for reduction of EMI in the fanout system. The cables on the right side are plugged into the feedthrough plate. Important for the function of the test enclosure is the material of the box, the double folded door edge with beryllium copper springs and the conductive mesh between the box and the feedthrough plate. [Rie14]

Commercially available feedthrough couplers are used for populating the feedthrough plate. Some of them, especially the sub-d connectors, are equipped with ferrite rings around the signal lines. In order to minimize openings, the holes for those couplers

1 http://www.ets-lindgren.com/

are milled into the feedthrough plate (see fig. 7.7) and are bolstered with conductive mesh.[Plü12] The schematic of the readout is shown in fig. 7.8.

A Cremat[1] CR-110 charge sensitive preamplifier, mounted on the CR-150 evaluation board, is used to convert the charge into voltage signals. The voltage signals are fed into a main amplifier. The re-conditioned signal is acquired using an oscilloscope. The trigger signal of the scintillator is digitalized as well and can be applied afterwards in the analysis software. The oscilloscope is read out using a GPIB[2]-LAN[3] interface. A new mechanics which provides an improved cooling option is currently under development. The data acquisition has been altered as well, using a self-made successor to the CR-150 board. The new board converts the signal from single ended to differential, before sending it out of its box. Instead of an oscilloscope a VME[4] based flash ADC[5] is used for digitalization [Rie14]. Examples of the data gained with the first setup and an unirradiated fanout assembly are given in fig. 7.9, fig. 7.10 and fig. 7.11. The fanout assembly has been equipped with a 250 µm thick DOFZ[6] n^+-in-n pixel sensor. The IV-curve in fig. 7.9 shows a dip around −40 V which indicates the depletion voltage. The position of the 59.5 keV photo peak in fig. 7.10 is used to calibrate the energy axis of the $^{90}_{38}$Sr spectrum in fig. 7.11.

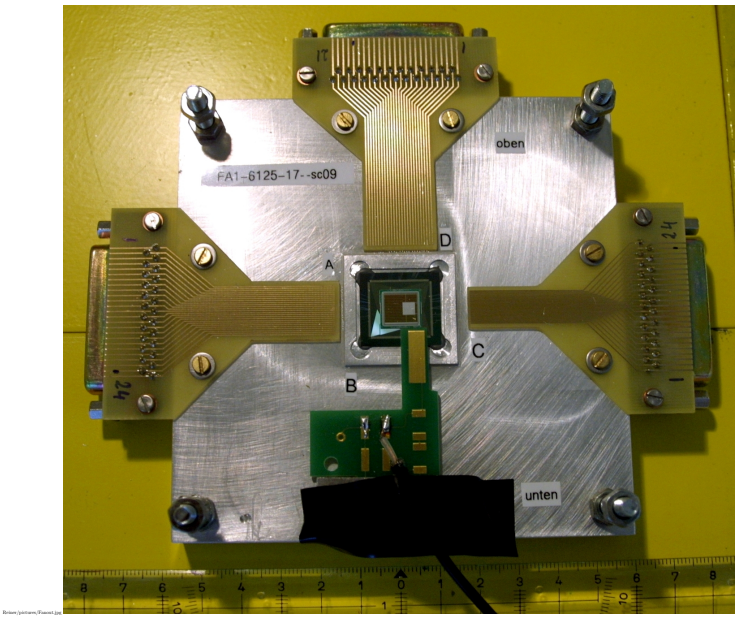

Figure 7.7: First design for a fanout mounting. [Plü12]

1 http://www.cremat.com/
2 **G**eneral **P**urpose **I**nstrument **B**us
3 **L**ocal **A**rea **N**etwork
4 **V**ersa **M**odule **E**urocard
5 **A**nalog **D**igital **C**onverter
6 **D**iffusion **O**xygenated **F**loat**Z**one

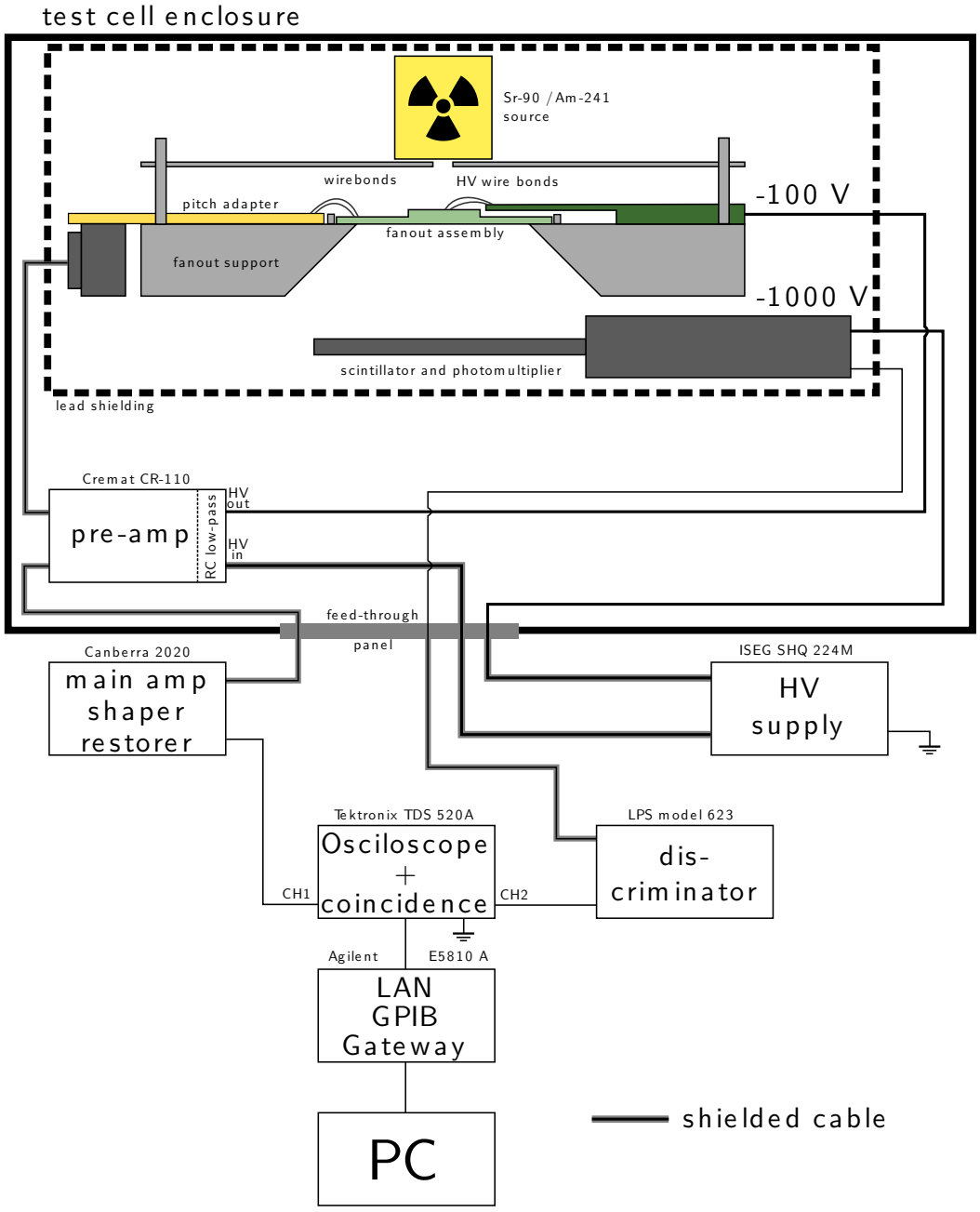

Figure 7.8: First design for a fanout mounting consisting of a thick aluminium carrier where a conical shaped opening is milled under the position foreseen for the fanout assembly. A slight recess makes it easier to position the fanout and it is glued on the thin remaining strip of aluminium. On four sides PCBs are attached which lead the signal of selected fanout wirebond pads through wirebonds onto SUB-D connectors with 25 poles each. Through the green PCB on the bottom the bias voltage is supplied to the high voltage pad on the sensor surface. [Plü12]

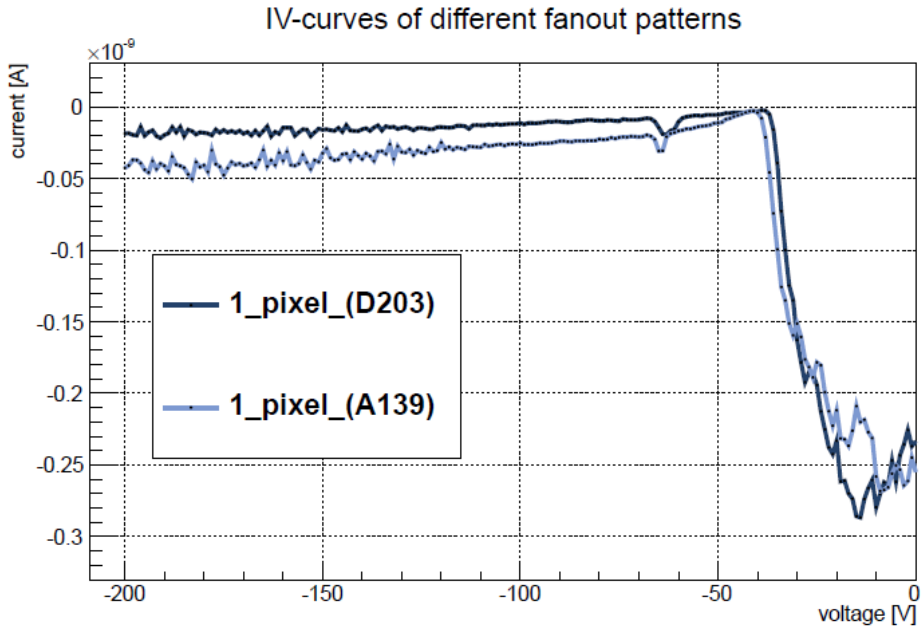

Figure 7.9: IV-curve of a single pixel measured through a fanout. [Plü12]

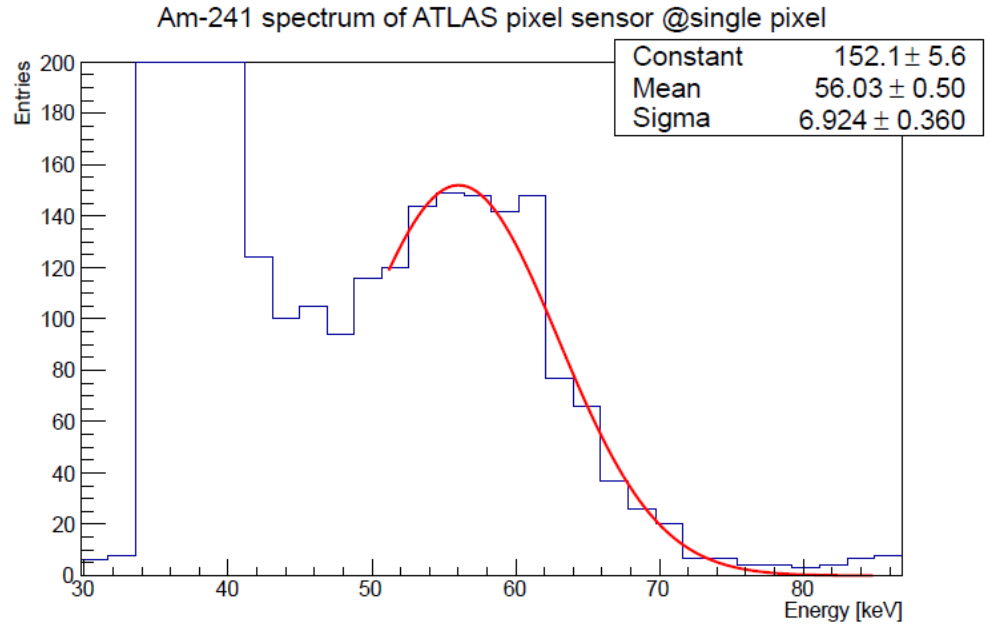

Figure 7.10: Signal of a single pixel readout through a fanout when illuminated with a $^{241}_{95}Am$ source. The fit is Gaussian and only meant to guide the eye. [Plü12]

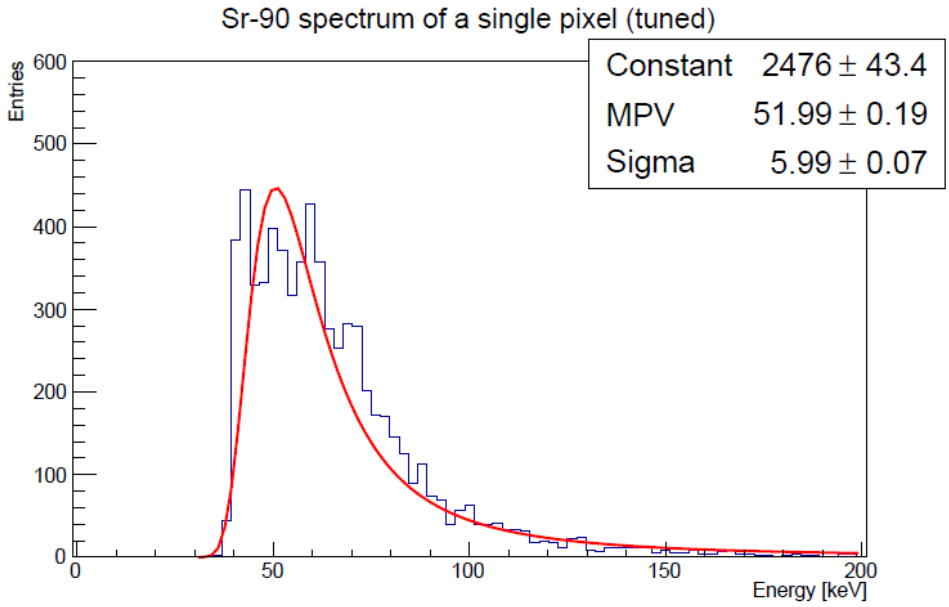

Figure 7.11: Signal of a single read out through a fanout when illuminated with a ${}^{90}_{38}Sr$ source. The output has been energy calibrated using the photo peak in fig. 7.10. The fit function is a landau distribution and only meant to guide the eye. [Plü12]

7.4 Automatised Characterization

The first measurements were done by switching manually pin by pin of the sub-d connector. Although the currently existing setups impose a limit on the number of connected wirebonds pads, this is extremely time consuming.

In order to identify properly working pixels, it is useful to make an IV-scan of each pixel or pixel equivalent (group). To simplify this process an automatized readout system was developed [Abt13]. Its schematic is shown in fig. 7.12. It is built around a Keithley[1] 7002 multiplexer which selects the currently read out pixel. This signal is measured by the Keithley 487 pico ampere meter, whereas the bias grid and outer guard currents are measured by their own dedicated Keithley 487 devices. This enables the simultaneous measurement of the pixel current, bias grid current and outer guard ring current, together with the temperature. The temperature is recorded through a Keithley 196.

All those devices are controlled through their GPIB connection. A computer connected to an Agilent GPIB-LAN interface acts as bus master. The software is realized in form of a compiled ACLiC[2]/ROOT[2] script which uses the e4meas library [Kle11]. This library was extended in order to include the multiplexer, as well as the external

1 `http://www.keithley.com/`
2 **A**utomatic **C**ompiler of **Li**braries for CINT[3]

triggering capability of the measurement devices. This external triggering helps to synchronize the measurements as far as possible.

The IO-port of the Keithley 7002 generates a TTL[1]-pulse which is fed into the external trigger input of the other measurement devices. Before triggering, the measurement devices Keithley 487 and Keithley 196 are programmed to take a couple of measurements which are written into their inbuilt memory. The data is read out after the conclusion of this measurement cycle in order to save time. While the data is being transferred over the GPIB bus, the bias voltage is already changed to a new value. The number of data points taken by the devices can be adjusted in the control script, it is usually set to 100 consecutive measurements in order to reduce noise by calculating a mean value for the current.

2 `http://root.cern.ch`

1 **T**ransistor **T**ransistor **L**ogic

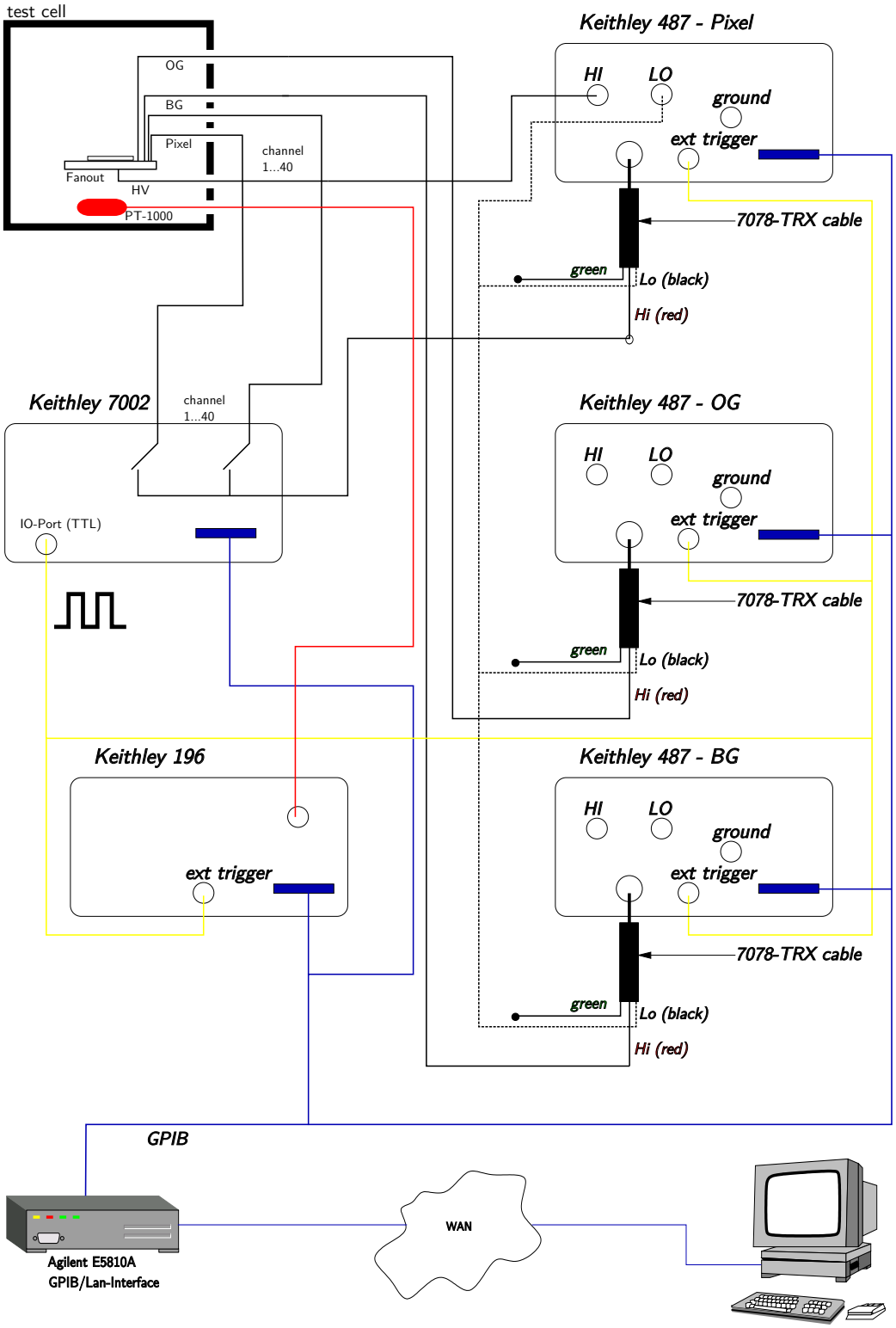

Figure 7.12: Overview of the automatized characterization system for fanout assemblies.

CHAPTER 8

Methods of Lab and Test Beam Measurements

8.1 Measurement of the IV-Characteristics

All sensors were characterized prior to the flip-chip mating by measuring the current at different applied bias voltages. Henceforward it will be called an IV-measurement and the resulting plot IV-curve. This is the slightly imprecise but commonly used designation. In case of sensors prepared for indium bump bonding, this measurement was repeated before and after irradiation. Sensors prepared to be flip-chipped with PbSn bump bonds were only characterized in the unirradiated state. The measurements were conducted on a modified vacuum chuck mounted on a probe station in a class 1000 clean room.

The chuck consists of a plastic disc where a stripe of copper tape is glued over a hole in the disc. On the bottom there is a nipple screwed in the threaded hole which makes it possible to attach a vacuum pump. The bias voltage was applied through a PH100 needle prober by Süss[1].

The cooling of the irradiated sensors was achieved by placing small chunks of dry ice next to the sensor. The dry ice cools down the metal surface where the sensor rests on. Condensation was avoided by covering the whole chuck with a transparent lid and flushing the interior with dry nitrogen.

For the measurement itself a K487 pico ampere meter was employed as a voltage source as well as an ampere meter (see fig. 8.1). The device was computer controlled through a GPIB[2]-LAN[3] interface that was operated by a script based on the e4meas library [Kle11]. Only sensors fulfilling the ATLAS[4] quality assurance criteria [KL04] were used and only those performing best were selected. Criteria were the absolute current (below 2 µA) and the slope of the IV-curve. The latter criterium was a fairly

1 `http://www.suss.com/`
2 **G**eneral **P**urpose **I**nstrument **B**us
3 **L**ocal **A**rea **N**etwork
4 **A** **T**oroidal **L**HC **A**pparatu**S**

soft one. Special attention was paid to the existence of a flat platform before a clearly pronounced bend followed by an exponential development. As the exponential trend indicates a speedy breakdown, the bend has to be well above the depletion voltage.

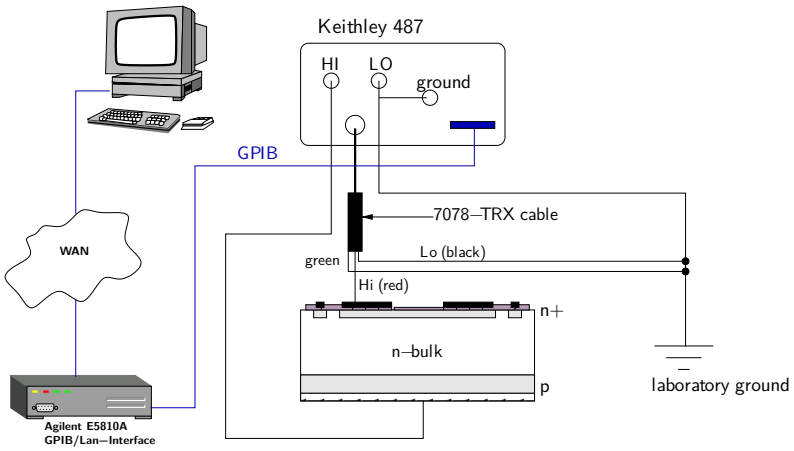

Figure 8.1: Setup for measuring IV-curve of unflipped structures. The drawing is taken from [Raj03] and modified.

8.2 Pre-testing of the FE-I3 Chips

The FE-I3 chips with indium stubs originated from a wafer left-over during the production for the currently installed pixel detector. This wafer was fully qualified until it was damaged during the first cut along a dicing street due to a disintegrating diamond dicing blade (shown in fig. 8.2). The old bare module test setup [Dob04] was used to verify that the chips were still operational.

Its central part is a probe card with a needle comb which allows to contact all FE-I3 wirebond pads at the same time. This card was redesigned (see fig. 8.3), as the previous one was controlled by a VME[1] card, which was no longer functional. The probe card is mechanically fastened (its inclination in two axes is manually adjustable using micrometer screws), while the assembly (or in this case the bare frontend) is located on a linear table movable in three axes. The table's step motors are computer controlled and there are end switches which stop the movement as soon as the needle comb touches down evenly with sufficient force.

The probe card is connected by a flat ribbon cable to the USBpix system (see section 8.3.2) and basically emulates a single chip card. Successful digital and analogue scans were required for declaring a frontend qualified. Additionally to these scans, a visual inspection was conducted, which revealed that only the chips along the first cut were damaged. Those were subsequently discarded.

1 **V**ersa **M**odule **E**urocard

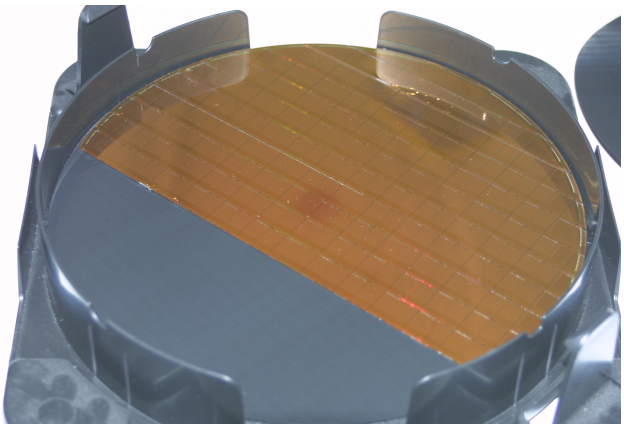

Figure 8.2: Indium FE-I3 wafer with the breaking edge visible.

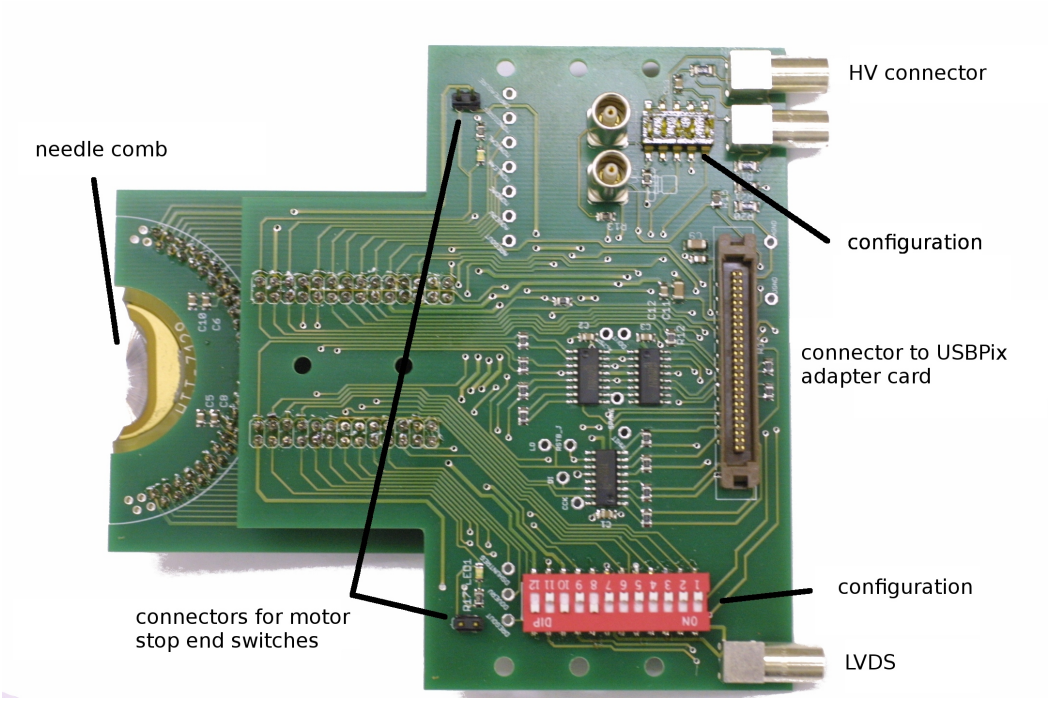

Figure 8.3: New bare module test card for FE-I3 chips and FE-I3 based assemblies. Taken from [Lap12] and modified.

8.3 Operation of the FE-I3 ATLAS Readout Chip

8.3.1 TurboDAQ

The TurboDAQ system was used in the beginning of this thesis both for laboratory tests and for the test beam readout of FE-I3 assemblies.

It makes the readout of ATLAS pixel modules possible, where the data and control information of 16 frontend chips are merged by a MCC[1]. Single chip assemblies can be alternatively connected to a TPCC[2] as shown in fig. 8.4. This device allows to switch between up to four assemblies, but does not provide simultaneous readout.

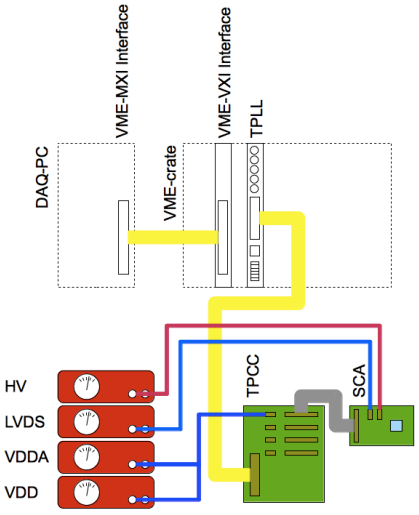

Figure 8.4: Schematic of TurboDAQ setup used for laboratory tests.[Tro12]

Furthermore, the TPCC contains the drivers necessary for the LVDS[3] signal. The TPCC is coupled to the TPLL[4] which is constructed as a VME card. The TPLL can be controlled through the VME back plane and a VME-MXI[5] module enables the computer control of the whole system.

The software used on the computer is called TurboDAQ, too. A more detailed description of the TurboDAQ system may be found in [Dob04] and the test beam extensions are documented in [Tro12]. It was phased out in favour of the USBpix system due to the discontinuation of its development. Furthermore, it does not support the FE-I4. There were also problems with the TurboDAQ setup when used for test beam measurements, which manifested in desynchronisation of events and in strange interferences between DUTs[6] [Tro12].

8.3.2 USBPix

The USBpix system was used for the majority of measurements. It was developed as the successor of the TurboDAQ system and is based on the so-called MultiIO-board, which is connected by USB[7] directly to a computer. Its heart is a XILINX[8] Virtex

1 **M**odule **C**ontrol **C**hip
2 **T**urbo **P**ixel **C**ontrol **C**ard
3 **L**ow **V**oltage **D**ifferential **S**ignal
4 **T**urbo **P**ixel **L**ow **L**evel
5 **M**ultisystem E**X**tension **I**nterface
6 **D**evice **U**nder **T**ests
7 **U**niversal **S**erial **B**us
8 `http://www.xilinx.com/`

3 FPGA[1] coupled to 2 MB SRAM[2] and a micro controller that handles the USB communication. There are different adapter boards available, the basic ones are for FE-I3 and FE-I4 single chip assemblies. An external trigger input is available and expects TTL[3] signals. For a detailed description see [Bon14a]. A USBpix system equipped with a FE-I3 single chip readout card is shown in fig. 8.5, whereas the same system together with a FE-I4 adapter card can be seen in fig. 8.6.

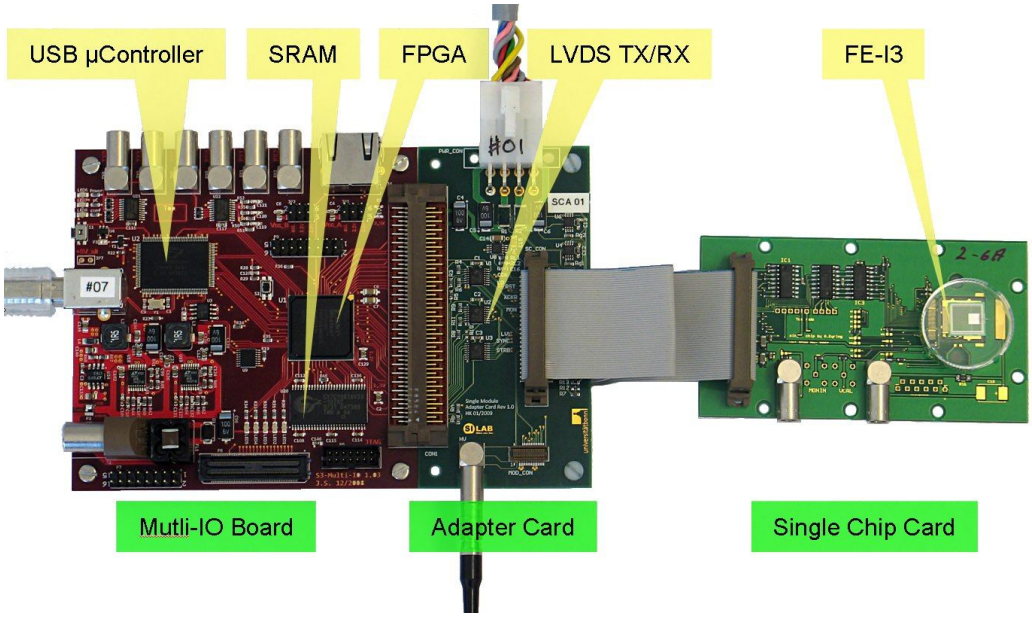

Figure 8.5: Overview of the central components of an USBPix system equipped for a FE-I3 based Single-Chip assembly including an original "Bonn" style SCA card. [Wei13]

8.3.3 Calibration Procedure – Tuning

All used readout systems offer similar scans and tuning procedures (tunes). Tunes are scans which result in setting certain parameters in the readout chips. The tunes presented here are provided by the FE-I3 version of the STcontrol (control program for the USBpix system). Their description is taken from [Bon14b]. Section 2.3.4.5 explains the basic configuration options of each FE-I3 cell which control the threshold and the feedback current. It is necessary to repeat the tunes several times as the settings for the threshold and feedback current influence each other to a certain degree. The general goal is to achieve a homogeneous threshold distribution over all pixels and a ToT[4] response, which utilises as much as possible of the available

1 **F**ield **P**rogrammable **G**ata **Array**
2 **S**tatic **R**andom **A**ccess **M**emory
3 **T**ransistor **T**ransistor **L**ogic
4 **T**ime **O**ver **T**hreshold

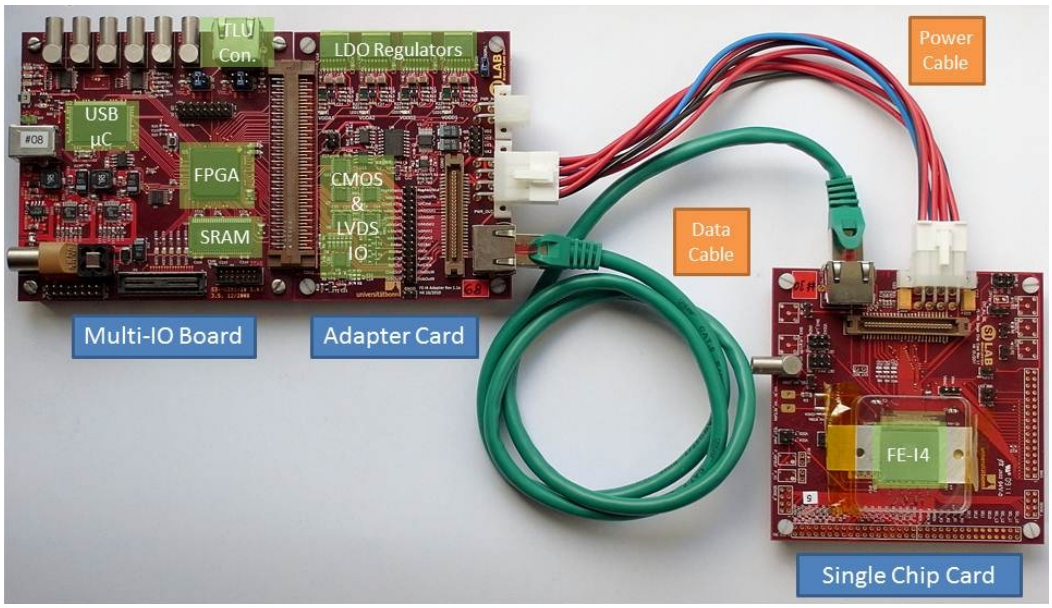

Figure 8.6: Overview of the central components of an USBPix system equipped for a FE-I4A based Single-Chip assembly including a V1.0 FE-I4A SCA card. [Bon14a]

ToT range. Usually, first the GDAC[1] and IF[2] are set, what can be done manually or using the designated tunes. Afterwards, the tunes are executed in the order: TDAC[3], FDAC[4] and TDAC. At last, a threshold and ToT verify scan confirm that the tune was successful. A ToT-Calib scan completes the tuning and creates the data necessary later on for the ToT to charge conversion.

8.3.3.1 Digital Scan

A basic scan which sends 200 times the strobe signal to the frontend discriminator with a fixed length. The same number of hits should be recognized, if everything works well.

8.3.3.2 Analogue Scan

The analogue scan sends the strobe signal 200 times to the frontend preamplifier with a fixed charge and expects 200 hits back.

8.3.3.3 Threshold Scan

The threshold scan injects a varied amount of charge and measures the number of hits. For each pixel this results in a distribution which is fitted with a s-curve (error

1 **G**lobal Threshold **D**igital to**A**nalog **C**onverter
2 IFeedback
3 **T**hreshold **D**igital to **A**nalog **C**onverter
4 **F**eedback-current **D**igital to **A**nalog **C**onverter

function) and yields the threshold (inflexion point) and noise (distance between 30% and 70%) as fitting parameters.

8.3.3.4 GDAC Tune

The GDAC tune varies the GDAC, which determines the global threshold for all pixel cells and does a quick threshold scan for each of them. It attempts to set the GDAC in a way, that the threshold scan approaches the target threshold as close as possible. The target threshold is usually set to 3200 electrons.

8.3.3.5 IF Tune

The IF tune injects about 20000 electrons into the pixel cell preamplifier and measures the ToT response while changing the IF setting with the goal to achieve the preset ToT. The target is normally a response of 60 ToT at 20000 electrons.

8.3.3.6 TDAC Tune

Similar to the GDAC tune the TDAC tune attempts to set a target threshold. The difference is that each pixel cell is tuned individually using its TDAC register.

8.3.3.7 FDAC Tune

A fixed charge is injected and the FDAC of each pixel cell is varied until its ToT response approaches the target value.

8.3.3.8 ToT Verify Scan

Similar to the IF and FDAC tunes a fixed charge of 20000 electrons is injected and the ToT response is measured. The settings derived during the previous tunes are applied.

8.3.3.9 ToT Calib Scan

For each pixel different charges are injected and the ToT response is recorded in each case. The resulting ToT against injected charge curves are fitted and three calibration values are calculated (the fitting constants). These values are necessary in order to calculate the charge from measured ToTs. These data are read directly from the resulting ROOT file (in the rootDB[1] file format) by the ClusterAnalysis program when analysing data taken in the lab.

For the test beam analysis the scan results are extracted from the ROOT file using a patched ClusterAnalysis version (prepared for this thesis), which writes them out into a plain ASCII[2] file. This file is then read by TbMon. The TurboDAQ

1 `https://twiki.cern.ch/twiki/bin/view/Atlas/STControlDocPage`
2 **A**merican **S**tandard **C**ode for **I**nformation **I**nterchange

and the USBpix systems use two different fit functions. The conversion from ToT to electrons for results gained with the TurboDAQ system is done according to the equation

$$q = \frac{B}{\mathrm{ToT} - A} - C \tag{8.1}$$

and for the USBpix system with the equation

$$q = \frac{\mathrm{ToT}}{A} \cdot C - \frac{B}{1 - \frac{\mathrm{ToT}}{A}} \,. \tag{8.2}$$

8.3.3.10 Source Scan

A source scan puts an assembly into the data taking mode where real hit information generated in the attached sensor is recorded. An external trigger source can be provided, e.g. a photo multiplier attached to a scintillator. A TTL signal is expected. Otherwise, the internal triggering mode is used, that triggers on the global hit bus of the frontend.

8.3.4 ClusterAnalysis

Irrespectively of the used readout system, source scans result in so-called raw-files. They contain raw hit data in slightly different data formats depending on the data taking system, which all describe raw hit data and are to a large extent compatible. All those data can be analysed using a program which is called "ClusterAnalysis" and which provides the capability to deal with all these different data formats. The data is first loaded into the program together with the calibration file if available. Then the data is clustered and in the third step analysed. The program also offers options to do a deep inspection of trigger events.

8.4 Single Chip Carrrier PCBs

The PCB[1] for the FE-I3 single chip assembly underwent several iterations. In its original version the assembly was glued on an area of the PCB, which is fitted with thermal vias. After measuring the heat resistance using heating foil, it was recognized that the heat conductivity is insufficient. Subsequently, this part was removed and replaced by an aluminium carrier. This aluminium carrier is fitted on its backside with a stripe of copper tape leading to the cold mass. The heat sink is either provided by a piece of dry ice or by the heat exchanger when using a chiller.

This aluminium carrier is constructed as thin as possible in order to reduce mass when measuring the samples in the test beam, so avoiding unnecessary multiple

1 **P**rinted **C**ircuit **B**oard

scattering.

It was observed that the original single chip cards are not able to withstand more than 700 V bias voltage before sparking occurs and the voltage shortens out. This is due to an insufficient distance between the high voltage line and the ground plane on the PCB. The first workaround applied to a couple of samples at that time is exemplary shown in fig. 8.7. There the bias voltage supply circuit, integrated in the PCB, was bypassed by attaching a separate piece of PCB material with a copper trace, which was connected to a free flying cable. From this copper trace a wirebond connection to the HV[1] pad on the sensor was realised. After this approach turned out usable, this construction was made more reliable and solid by creating a small daughter board, which is glued on the single chip PCB and covers the original HV wirebond pad completely (see fig. 8.8 and fig. 8.9). This daughter board includes a LEMO[2] 0S connector and the necessary bias resistor(s) and capacitor.

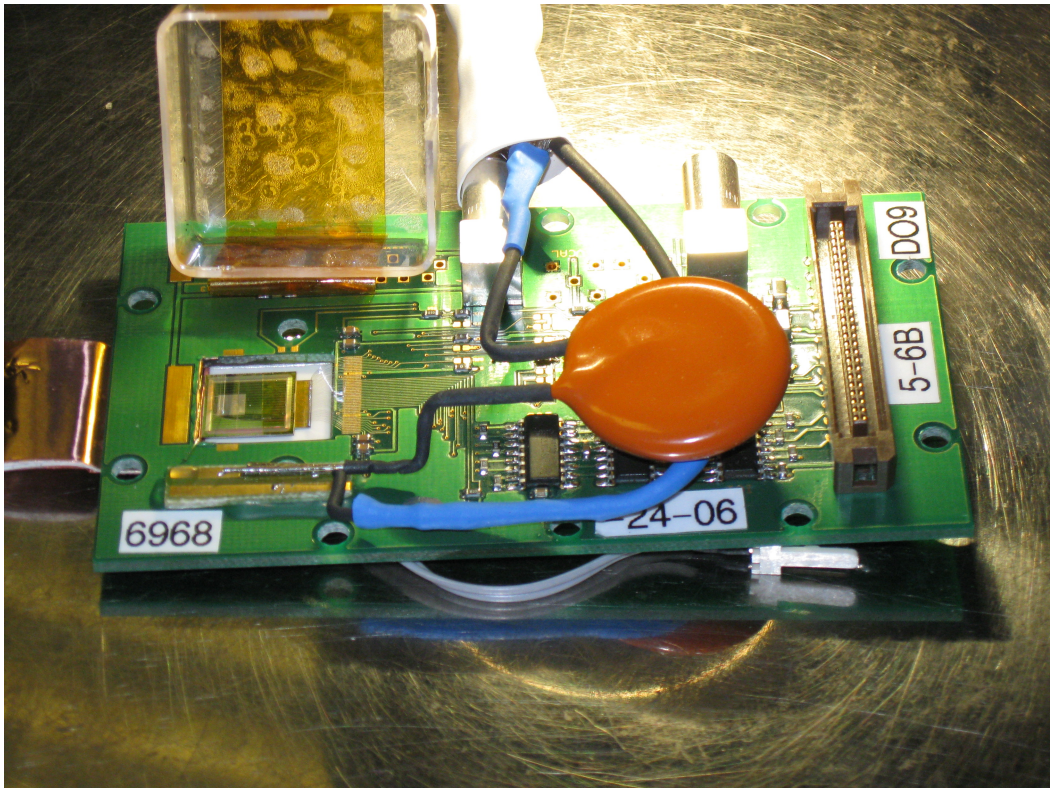

Figure 8.7: Assembly DO-9 mounted on SCC card demonstrating improvised workaround for the sparking problem. The bias resistor is hidden as it is covered by shrink tube.

There are two versions differing slightly in the foot print of the used bias resistor.

1 **H**igh **V**oltage
2 `http://www.lemo.com`

The connection to the ground of the main PCB is realised by soldiering a piece of wire through the appropriate test pad. The final iteration is a completely new version of the single chip card as shown in fig. 8.10. It incorporates the design of the HV daughter board with generous distances between the HV trace and everything else. The middle pin of the LEMO 0S connector has to be attached to a trace on the bottom side of the double sided PCB, as otherwise there is a risk of sparking. The new PCB design also features a connector for a permanently fastened PT1000.

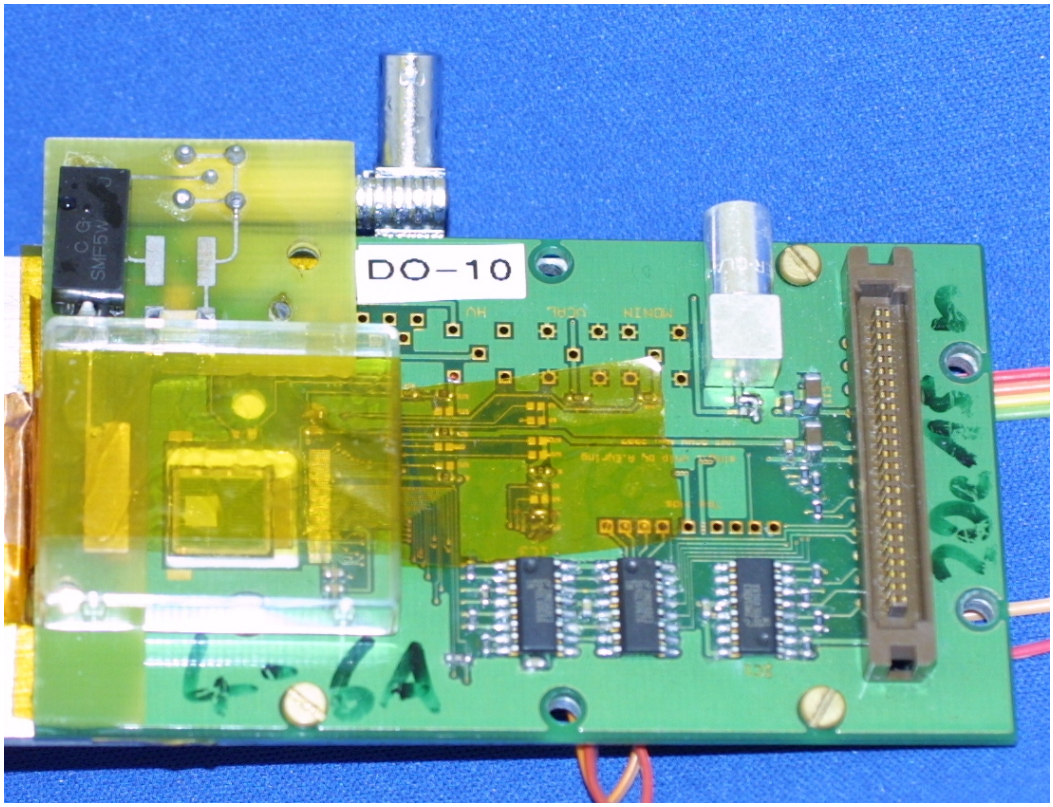

Figure 8.8: Assembly DO-10 mounted on SCC card demonstrating first HV daughter card version.

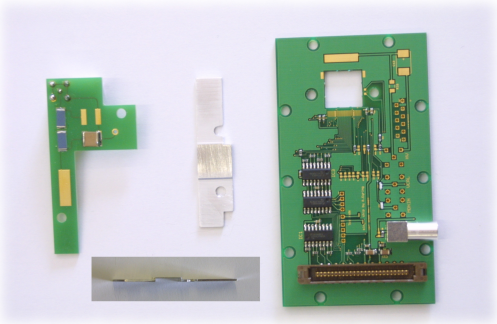

(a) From left to right: HV daughter board, aluminium carrier in piston design (below sid view) and new Bonn single chip card.

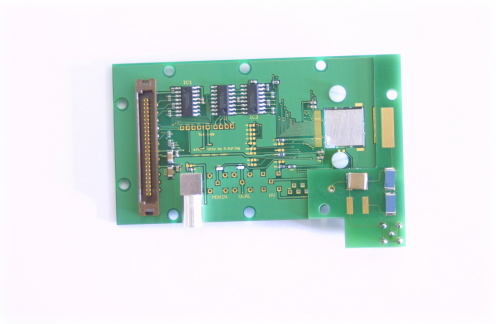

(b) All parts put together - the daughter card as well as the carrier were glued with epoxy on the single chip card.

Figure 8.9: Third iteration of the FE-I3 single chip assembly mounting.

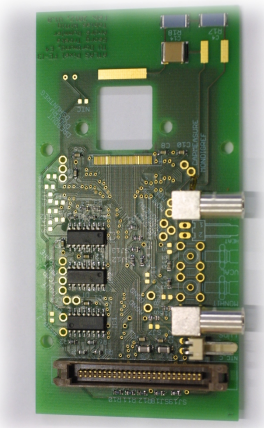

(a) Newly designed single chip card with improved HV capability and PT1000 connectors.

(b) New aluminium carrier.

(c) All parts put together.

Figure 8.10: Fourth iteration of the FE-I3 single chip assembly mounting.

8.5 Lab Setup for Measuring Assemblies

In the laboratory the setup shown in fig. 8.11a was used for the source scan measurements. The whole setup is enclosed in an isolated box made of polypropylene which can be flushed with dry nitrogen. There are two different cooling options: Either several large blocks of dry ice are placed on the base plate or a chiller cools down the heat exchanger which forms the base plate. The PCB of the assembly is fixed with screws on a holder (fig. 8.11b), where its assembly is automatically aligned with the scintillator below it and the source sitting on a separate holder above it. The scintillator is used for triggering the readout of the USBpix-System.

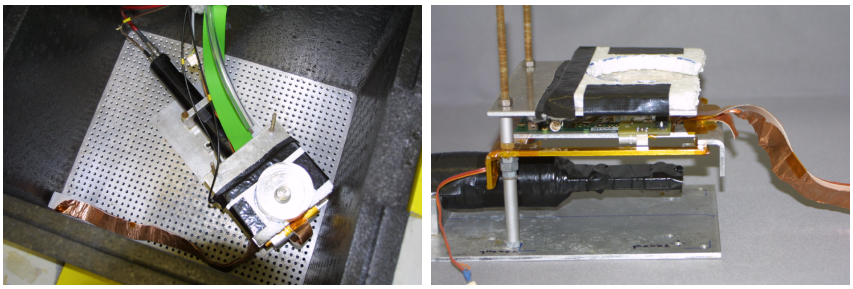

(a) Look inside the isolation box containing the lab setup for measuring irradiated assemblies. The DUT is mounted on a frame above a scintillator which is connected through a light duct to a photomultiplier (black tube). In this picture the dry ice option is shown, where the cooling is realised by placing two or three blocks of dry ice on top of the base plate. The heat is partially conducted through the copper stripe attached to the backside of the assembly and partially through the cold carbon dioxide which evaporates, when the dry ice sublimates. Photo by [Wiz13].

(b) Detailed photo of the holder used for measurements of irradiated und unirradited FE-I3 based assemblies in the laboratory. On the bottom there is the photomultiplier tube where the small extending on the side contains the scintillator (1 cm × 1 cm) attached through a light guide. The holder aligns the PCB automatically in a way that the assembly is positioned directly above the small scintillator plate. Another holder above the PCB offers an enclosure which aligns the radioactive source with the assembly and the scintillator quickly without a lot of manual intervention. Photo by [Wiz13].

Figure 8.11: Photos showing details of the lab setup with dry ice cooling.

8.6 Test Beam

Test beam measurements using high-energy particle beams and a telescope are the best test for high-energy particle detectors as they emulate the application in the real detector system as closely as possible. The particles constituting the beam are similar to the ones measured in the real experiment - minimum ionising particles. The telescope allows to quantify the performance of the DUT. More about the measurable quantities and how they are calculated can be found in chapter section 8.6.4.

8.6.1 Beamlines

The tests were conducted at two different beam lines, one located at the CERN[1]-SPS[2] and the other one at DESY II[3]. The beam provided at CERN-SPS area H6 benefits from the fact that the behaviour of the 120 GeV to 180 GeV pions is more realistic than the 4 GeV to 6 GeV positrons at the DESY II accelerator. Especially, the multiple scattering is much more pronounced at the lower energies, making it unfeasible to operate more than two DUTs at the same time and decreasing the spatial resolution as well. Nevertheless, many basic measurements are also possible at DESY II and for the time of the shutdown at CERN it is the only easily available test beam facility.

8.6.1.1 CERN-SPS

CERN-SPS is part of the main accelerator chain at CERN as described in chapter 2. 400 GeV protons are ejected (see fig. 8.12) and shot into the target T4 (see fig. 8.13), where they are converted into $\pi^{\pm}$. A spectrometer magnet, which can be controlled by the user, selects a certain energy and a couple of focusing and bending magnets create a beam with a diameter of roughly 1 cm. As the SPS supplies several experiments, the beam is not continuously supplied but follows a cycle. This cycle can vary due to the number of currently supplied experiments, but it is typically 42 s long and the extraction lasts 9.6 s. More information about the SPS, the beamline H6 and its associated beam test area H6B may be found in [Tro12].

8.6.1.2 DESY

The accelerator chain (see fig. 8.14) at DESY[4] consists of the LINAC II[5] and the storage ring PIA[6] which accelerate electrons/positrons up to 450 MeV. Afterwards, the particles are accelerated further up to an energy of 6 GeV in the synchrotron DESY II. After ejection the particles hit a target producing photons, which are used

1 **C**onseil **E**uropéen pour la **R**echerche **N**ucléaire
2 **S**uper **P**roton **S**ynchrotron
3 **D**eutsches **E**lektronen **SY**nchrotron II - accelerator at DESY
4 **D**eutsches **E**lektronen **SY**nchrotron
5 **LIN**ear **AC**celerator **II** - accelerator at DESY
6 **P**ositron **I**ntensity **A**ccumulator - accelerator at DESY

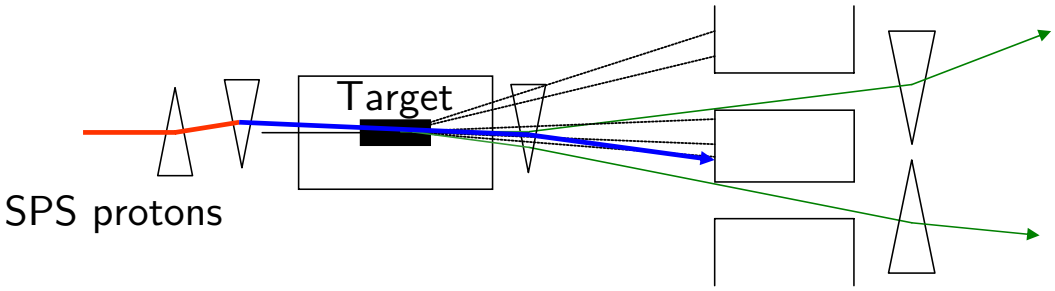

Figure 8.12: Schematic drawing of the SPS target area. The primary beam, coming from left passes to dipole magnets to change incident angle into the target (wobbling), the secondary particles are generated in the target, passing a spectrometer magnet, are collimated and guided to two beamlines. [Tro12]

afterwards for production of electrons and positrons by pair production through a secondary target. The downstream magnet helps to select the particle type and energy.

8.6.2 EUDET-Telescope

Most of the time the EUDET[1] telescope (or its sibling/successor the ACONITE[2]) was used to measure the trajectories of the beam particles. It was moved between DESY and CERN depending on where the next test beam period was ready to commence. The telescope consists of two arms which are mounted on a rigid mechanical support structure consisting of an aluminium frame. Between the two telescope arms there is space enough for the box containing the DUTs. Each of the two arms consists for its part of three telescope planes.

The telescope planes use Mimosa26 MAPS[3] (integrated) sensors with an active area of 21.2 mm × 10.6 mm and square pixels with a size of 18.4 µm × 18.4 µm. The Mimosa26 sensors employ a rolling shutter system with an accumulated integration time of 112 µs. It is impossible to determine in which order the hits during one readout cycle, corresponding to one event, were registered, as the hits are not time stamped. This lack of information introduces an uncertainty between the mapping of the tracks registered during one event and the hits registered in the DUT. Furthermore, the discrepancy between the data taking time of 112 µs of the Mimosa26 planes and the much shorter 400 ns recording time of the FE-I3/FE-I4 DUTs means that there are a lot of tracks registered by the telescope, which cannot be registered by the DUTs, as they are not in the right time window (out-of-time tracks).

The calculation of the hit efficiency requires that a track is only accepted as valid, if it shows a corresponding hit in at least one reference plane. Without this

1 **DET**ector-project supported by the **E**uropean **U**nion
2 ATLAS copy of the MIMOSA-NI telescope
3 **M**onolythic **A**ctive **P**ixel **S**ensors

Figure 8.13: CERN SPS target area. [Cer]

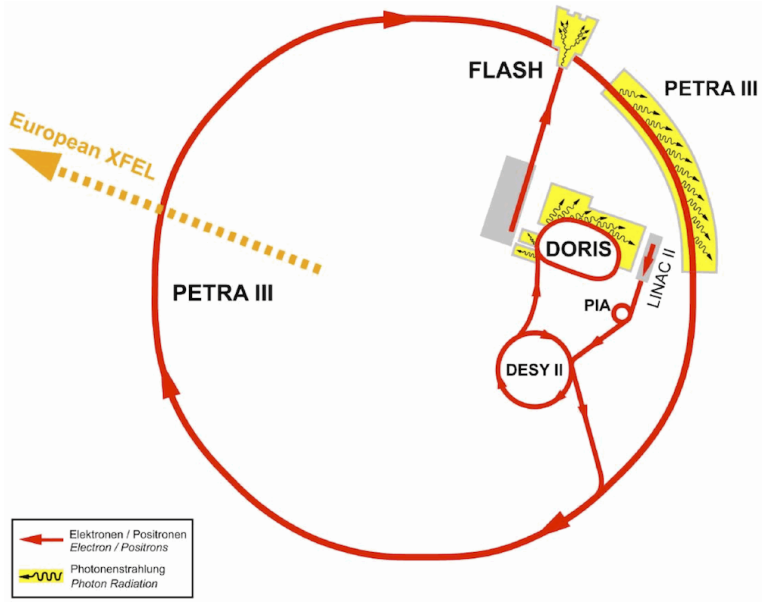

Figure 8.14: The accelerator complex at DESY. [DES12]

requirement the hit efficiency would be artificially decreased. Reference planes should be well understood FE-I3/FE-I4 assemblies, which have a minimal number of dead pixels (decreasing the overall efficiency as they are taking out wrongly tracks) and a minimal number of hot pixels (decreasing the measured DUT efficiency as out-of-time tracks are falsely declared as in-time-tracks). The readout of an event is triggered by two pairs of crossed scintillators, which are read out by photomultipliers. One pair is mounted upstream of the telescope, the other one downstream. The scintillators cover an area of $2\,\text{cm} \times 1\,\text{cm}$. They are usually operated in coincidence mode, that means that an event is triggered, if all of them register a particle passing. The trigger signal is processed and distributed by the so-called TLU[1].

8.6.3 DUT Setup

The DUTs are placed in the DOBOX[2] between the two telescope arms. The box sits on a x-y-table which helps to position it correctly in the beam. This can be done remotely while watching the correlation plots in the online monitor. For details of the mechanics refer to [Tro12].

8.6.3.1 DUT Enclosure and Mechanics

The DUTs are mounted on angled aluminium frames which are adapted precisely to the size of the PCBs. The frames are fastened with machine screws on a base plate which features a grid of threads. Alternatively, there is a number of spacers, wedges and rotation blocks available which can be mounted between the base plate and the frame in order to turn the DUT in η or ϕ direction. A simultaneous rotation both in η and ϕ is possible by combining certain elements. The whole construction set is designed with a focus on keeping the sensors in the beam axis. The spacers help to keep the sensors at the same height, if there are DUTs mounted in a different way.

The assemblies are cooled through stripes of copper tape, which are attached on one end to the backside of the carrier PCB. This is done by folding the end of the copper tape, thus creating kind of a spring. A typical mounting situation is shown in fig. 8.15 and fig. 8.16. A very small amount of thermal grease is applied afterwards and the copper tape is pressed on by Kapton tape. The other end of each copper stripe lies flat on the ground plate and is pressed against it with a spacer plate. The dry ice placed on the spacer plate cools the bottom plate. The heat is transferred from the assemblies through the copper stripes and the air. The cover of the enclosure is divided into two parts making it possible to keep the DUTs covered while placing dry ice during the initial cooling down or while replacing dry ice during long measurement campaigns. While the secondary compartment is opened, the DUT compartment is flushed with dry nitrogen. This serves to avoid condensation on the DUTs. After closing the box the flushing can be stopped, as the evaporating carbon dioxide blocks out the wet outside air. For safety reasons

1 **T**rigger **L**ogic **U**nit
2 **DO**rtmund testbeam **BOX**

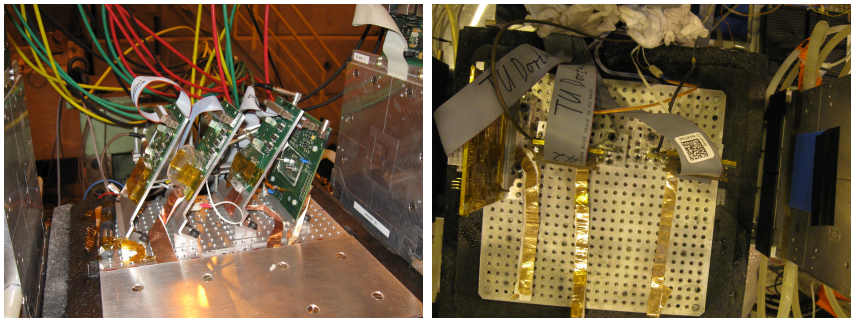

Figure 8.15: Examples for mounting of DUTs in the DOBOX with an inclination to the beam (in ϕ in the left and in η on the right).

Figure 8.16: DOBOX where only the DUT compartment is closed allowing a look into the opened dry ice compartment.

the bias voltage is usually switched off during this operation, although the DUTs remain protected from light.

8.6.3.2 DCS Monitoring

A monitoring software called "testbeamDCS" [Lap12] has been developed with the primary intention to be used during test beams for recording and controlling the environmental sensors of the DUTs. Later on, it has been also used for lab measurements. It can control up to two ISEG[4] power supplies which have both two independent channels. Their voltage may be set while the currently applied (bias) voltage and current is read out regularly for each channel. A Keithley 2000 fitted out with a 10 channel multi switch card is read out as well. This means that each temperature is read every second and the time stamp is maximum 10/11 s off. The software has a receiver component for the EUDET run control signals, which transmits the current run number and start/stop messages. It is implemented as a separate script in order to make it more stable. This script registers as a receiver with the run control on start up and writes the messages into a file which is read by the main program. Since 2012 a PVSS[5] based solution using a CAN[1] bus controlled ISEG crate and ELMB[2] was used.

8.6.3.3 DAQ

During the first test beam periods in 2009 and 2010 the TurboDAQ system was used (for details of the system see section 8.3.1). A detailed description of the parts necessary for the test beam integration is given in [Tro12]. Since 2011 only the USBpix system was used as it has a couple of advantages: better stability and less hardware overhead.

8.6.4 Reconstruction and Analysis

The telescope produces raw data which are afterwards reconstructed using the EUTelescope[8] software that is implemented as a processor within the MARLIN[39] framework. EUTelescope consists of several specialised sub-processors which are called consecutively. First, the raw data is converted into the lcio file format. Then the hit information is clustered and noisy pixels are removed. The main steps consist of the hit making, aligning and track fitting. Finally, a ROOT file in the so-called tbtrack file format is generated.

---

1 **C**ontroller **A**rea **N**etwork
2 **E**mbedded **L**ocal **M**onitor **B**oard
4 `http://www.iseg-hv.com/`
5 A SCADA[6] system by ETM[7] which has been renamed to WinCC-OA.
6 **S**upervisory **C**ontrol **a**nd **D**ata **A**cquisition
7 `http://www.pvss.com/`
8 `http://eutelescope.web.cern.ch/`
9 `http://ilcsoft.desy.de/portal/software_packages/marlin/index_eng.html`
3 **M**odular **A**nalysis & **R**econstruction for the **LIN**ear Collider

The analysis of the test beam data was done with the revamped TbMon-Framework (version 1.99). It reads in tbtrack files which were generated by the reconstruction software, reclusters the hit information, searches for hotpixels in the DUTs, applies cuts and data corrections, checks every track for existing reference hits, matches tracks to clusters and fills finally the histograms.

8.6.4.1 Checkalign

The alignment done in the reconstruction is not always perfect and it is easier to correct for global shifts afterwards within TbMon. Furthermore, EUTelescope is not equipped to deal with time dependant shifts, a feature that is useful for this setup as the weight of the dry ice changes with time and thus the torque acting on the x-y-table changes as well. In fig. 8.17 an example from the May 2012 test beam is shown. The top plot shows the residual distribution as is comes directly from the reconstructed data and the bottom plot shows the same distribution after the output of the checkalign processor has been applied.

8.6.4.2 Hotpixelfinder

Pixels giving a signal above threshold more often than expected or even permanently are so-called "hot" pixels. Their signal should not be included in the evaluated collected charge distribution and hit efficiency, as they result from noise and not from a particle passing through the bulk. The same is true for pixels that do not show any signal at all for some reason. Those pixels are called "dead" pixels. Both groups are flagged appropriately during the first TBmon pass over the data. In order to eliminate the hot pixels the ratio of hits within the acceptable level 1 timing window and hits outside of this window is calculated. A cut criterion of $0.5 \cdot 10^{-3}$ is usually applied on this value. "Dead" pixels can be recognized simply by looking for pixels that do not fire at all. After having been flagged, both types of pixels are excluded from the analysis during the second TBmon pass.

8.6.4.3 Referencing

The Mimosa26 planes used in the telescope are a rolling shutter system which takes data for about 112 µs after a trigger signal has been received. During this time usually more than 100 hits are registered in a telescope plane. The order in which they are registered is unknown as they are not time stamped. By comparison the readout time of the DUTs is much shorter: 16×25 ns. There are many tracks registered in the telescope planes, which even the best working DUTs has no chance to register, as it is not active for the whole time. If this issue is not treated, the calculated hit efficiency of the DUTs gets decreased. This is solved using referencing. Each track has to match a hit in at least one DUT different from that which is currently evaluated. Otherwise, it is not regarded as a valid track.

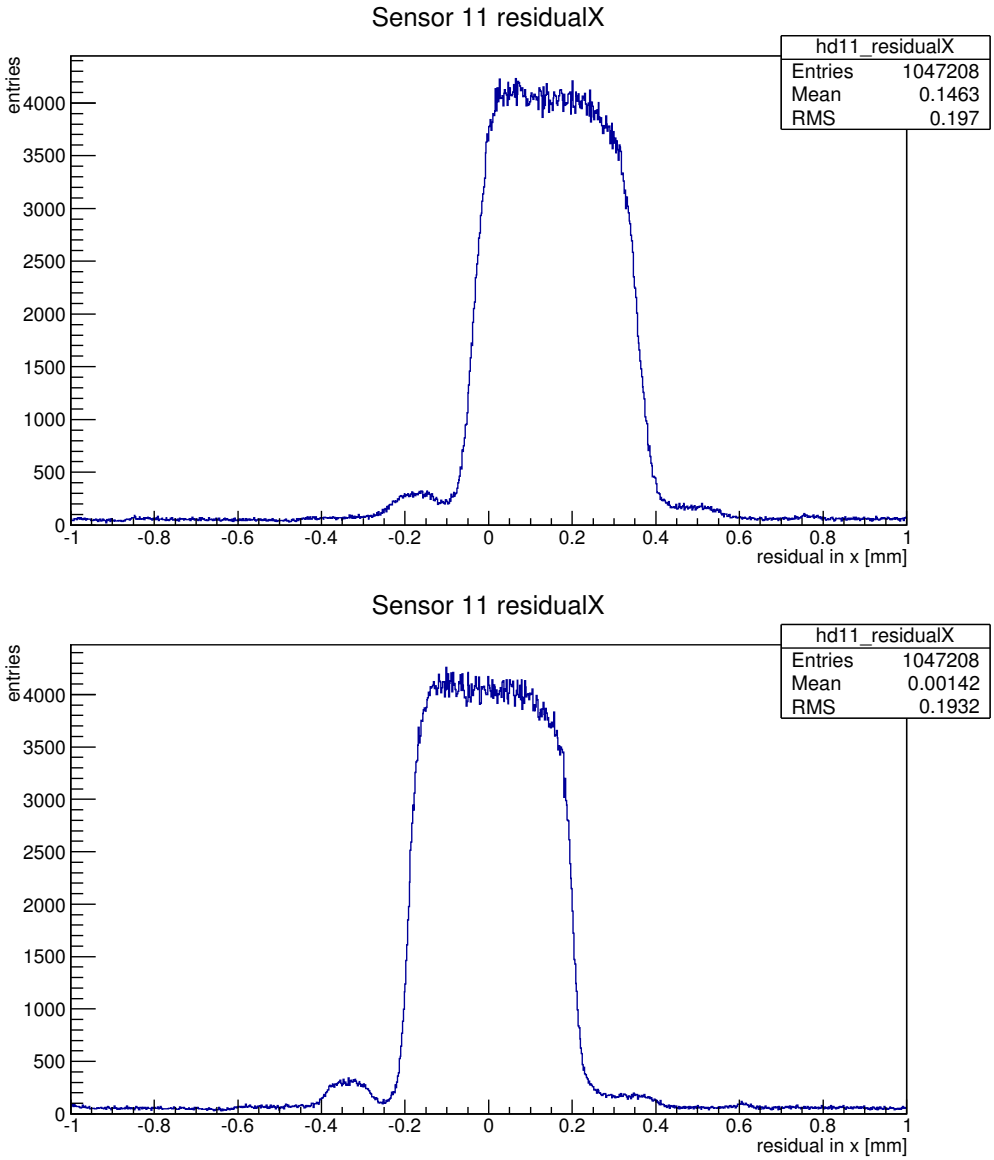

Figure 8.17: Residual distribution in x of the DUT DO-10 in the run range 767-795 recorded during the May 2012 test beam campaign at CERN SPS before and after the TBmon checkalign processor has been applied.

8.6.4.4 Matching

Matching means the assignment of a cluster to a track. A cluster is assumed to have been caused by a track if the distance between the cluster and the track is no more than 1.5 times the pitch. There are different possibilities to estimate the position of the cluster, such as the geometrical mean and more advanced cluster centre finding algorithms, but usually for this purpose the distance is calculated just by looking at each individual pixel constituting the cluster.

8.6.4.5 Efficiency

The hit efficiency is defined as

$$\varepsilon_{\text{hit}} = \frac{\text{number of matched tracks in DUT}}{\text{number of referenced tracks in DUT}} \,. \tag{8.3}$$

In the global hit efficiency value, which is calculated in this analysis processor and shown in chapter 9, hot and dead pixels are excluded as well as edge regions. The error given by this processor is the simple statistical error. The evaluation of the test beam results shows that this error underestimates the real error.

8.6.4.6 Qefficiency Analysis

The qefficiency analysis works with charge values calculated from the measured ToT values with help of the charge calibration. The charge is histogrammed either in total or separated according to cluster sizes. Furthermore, the space resolved mean charge deposition is plotted as well.

CHAPTER 9

Results of Lab and Test Beam Measurements

This chapter summarizes the results gained from measurements on irradiated single chip assemblies either using a radioactive source in the lab or accelerator particles at test beam sites. The details of the procedures are explained in chapter 8. The test beam data are limited to those taken at perpendicular incidence or relatively low angles. There are several effects which have an impact on those measurement results.

A particularly severe influence is the radiation damage of the readout sensor in case of assemblies which were irradiated entirely. In order to assess the reliability of the sensor related values, a study focused on the frontend related changes was done. After the assessment of the error limits the charge collection and efficiency results are shown and their evolution is discussed. Space resolved measurement results enabled by the test beam measurements are helpful in this endeavour. Another effect — annealing — is of high interest both for the measurements presented here as well as for the real life operation of the pixel detector. Therefore, the results of a study of the impact of voluntary annealing on the frontend as well as the sensor are shown.

9.1 Impact of Irradiated FE-I3 Readout Electronics

Usually, the study of the effects of radiation damage in the pixel sensor requires the joint irradiation of the sensor and the frontend electronics as they are connected irreversibly by bump bonds. The distinction between frontend and sensor related irradiation effects becomes thus more complicated. Furthermore, out of necessity the FE-I3 is operated here outside of its design limits. The maximum ionising dose is the relevant quantity as surface damage is more important for CMOS[1] electronics than silicon sensors.

The hit map shown in fig. 9.1 is a good example for one of the effects that may occur. It was taken using a $^{90}_{38}$Sr source (see section 8.3.3.10) and clearly shows a

1 **C**omplementary **M**etal **O**xide **S**emiconductor

periodic pattern which can be only explained by digital effects in the frontend. Although basic digital communication with the FE-I3 always works, erratic behaviour can be observed.

Some assemblies stop working completely after irradiation. Basic functionality shall be here defined as yielding a reasonable digital and analogue scan. Other assemblies show infrequently strange behaviour like an increase in noise, empty events or patterns during source scans. By simply thawing the malfunctioning assembly at room temperature and refreezing it afterwards, such temporary problems can be mitigated. Primarily this applies to assemblies irradiated either with neutrons or high energy protons. In contrast assemblies irradiated with low energy protons at Karlsruhe stopped working (actually no digital scan possible anymore) above a fluence of $1 \times 10^{15} \mathrm{n_{eq.}\ cm^{-2}}$ due to the extremely high ionising dose. The systematic measurements of frontend behaviour in the following sections employ a chiller based cooling system (see fig. 9.2) in order to vary the temperature reliably.

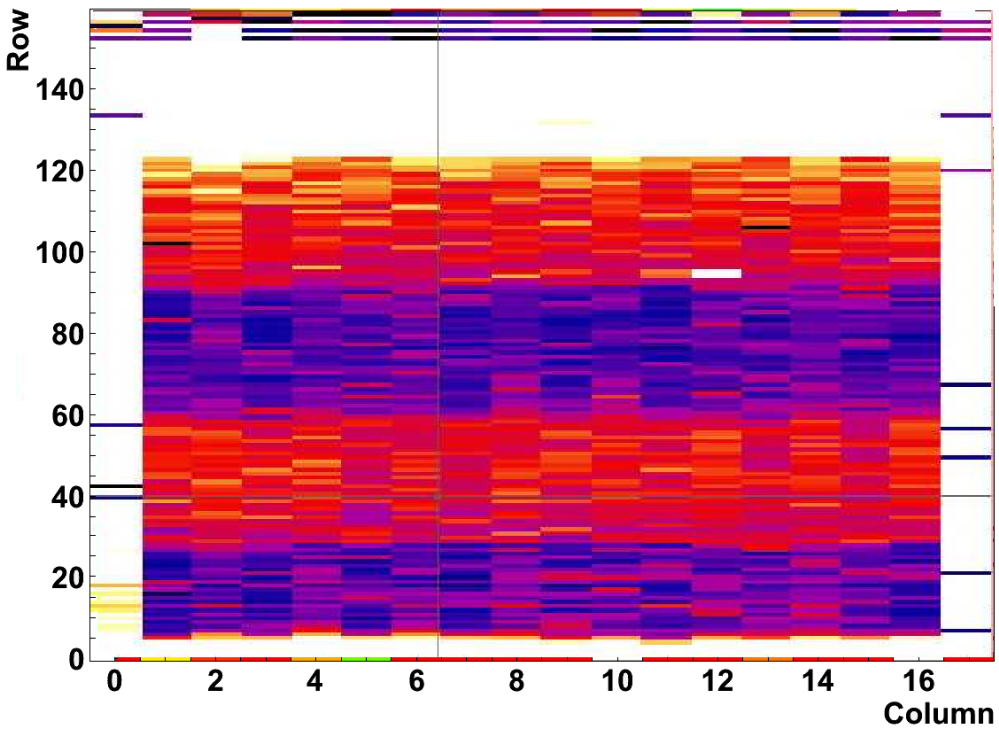

Figure 9.1: Hit map of a moderately irradiated assembly in which a digital structure is clearly visible. The darker stripes indicate a lower hit count than the light red areas. It illustrates the problems which may occur with irradiated frontends.

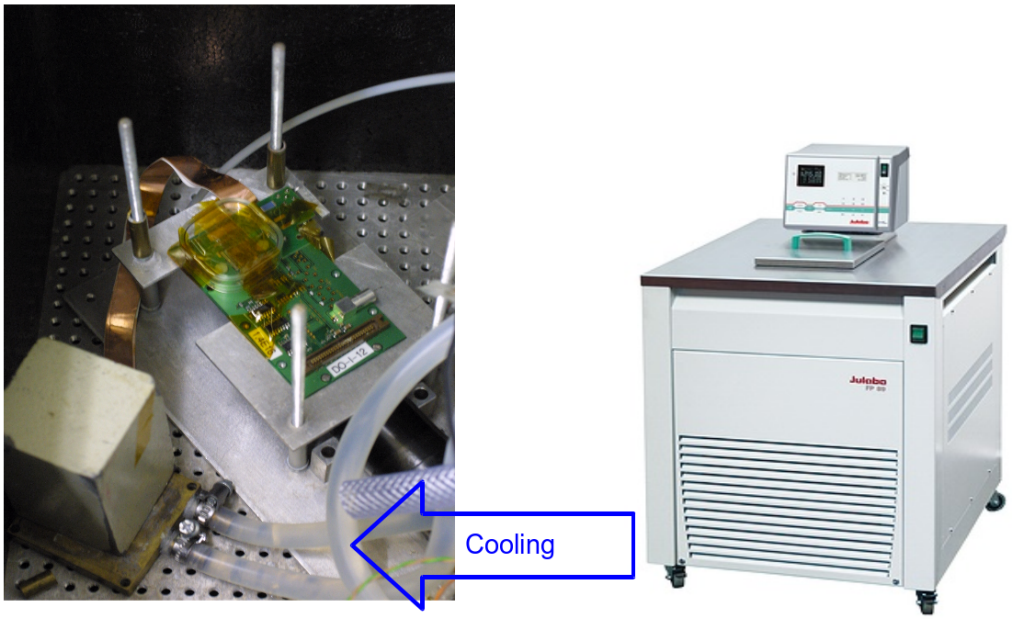

Figure 9.2: Setup used for the temperature dependant measurements on DO-9. On the left side the sample box is shown where the heat exchanger (below the block) is pressed on the copper striper which is attached to the backside of the assembly. The chiller and the heat exchanger, depicted on the right side, are connected through triple isolated hoses.

Most of those systematic studies use the assembly DO-9, which has an $250\mu m$ thick DOFZ[1] sensor and has been irradiated at Ljubljana with neutrons to a fluence of $5 \times 10^{15} \mathrm{n_{eq.}\,cm^{-2}}$. The assembly was read out by a USBpix system.

9.1.1 Influence of the Bias Voltage

In order to isolate the influence of the bias voltage on the frontend calibration, the temperature influence is excluded by keeping the assembly at a constant temperature of $-15\,°\mathrm{C}$. The temperature is continuously monitored with a PT100 temperature sensor (NTC[2]) positioned directly behind the aluminium carrier sheet (see section 8.4). This temperature sensor is connected directly to the chiller and used internally to regulate the temperature of the external cooling circuit. After cooling down a sufficiently long time has to pass until the temperature is settled. The voltage was varied in $100\,V$ steps and after each increase a ToT[3] calibration scan and threshold scan were done. During the ToT scan 20000 electrons are injected repeatedly into each pixel cell by the calibrations circuit and the response ToT is recorded. Histogramming the mean response values for each pixel cell individually,

1 **D**iffusion **O**xygenated **F**loat**Z**one
2 **N**egative **T**emperature **C**oefficient thermistor
3 **T**ime **O**ver **T**hreshold

results in Gaussian shaped ToT distributions for all pixels. The MPV[1] of those ToT distributions are plotted in fig. 9.3. It can be clearly observed that the bias voltage applied to the sensor has an impact on the ToT calibration of the frontend. According to the plot in fig. 9.4 the bias voltage seems to have little impact on the threshold distribution.

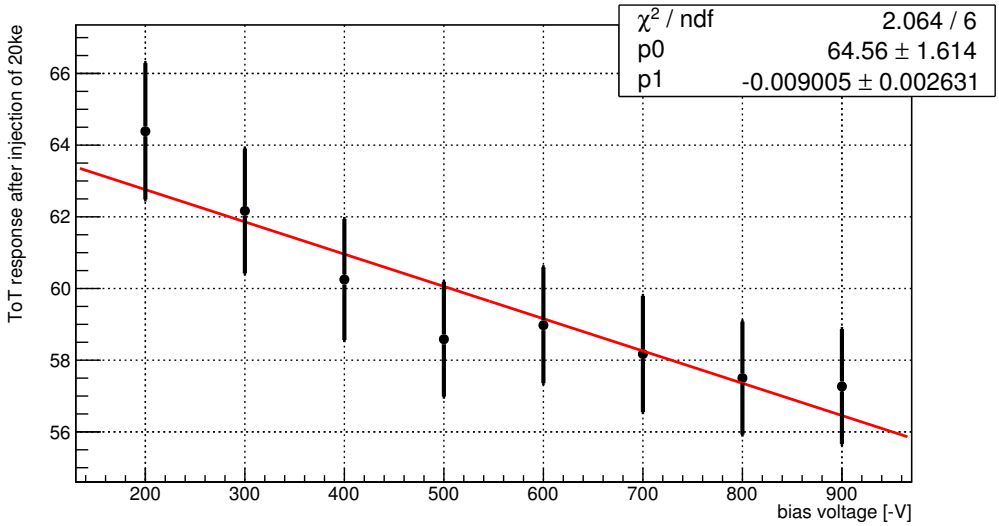

Figure 9.3: ToT values registered by assembly DO-9 after 20000 electrons have been injected using the calibration functionality at different bias voltages. Based on data by [Lap12].

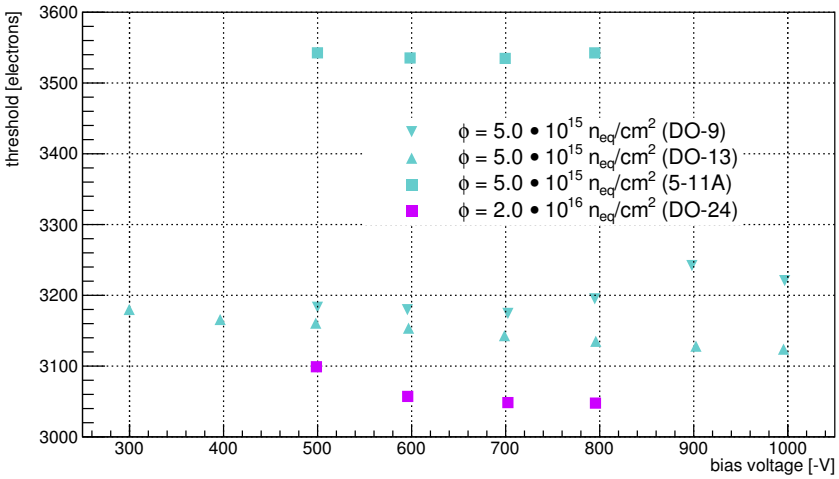

Figure 9.4: Threshold plotted against the bias voltage. Based on data by [Lap12].

1 **M**ost **P**robable **V**alue

9.1.2 Temperature Dependence

In order to measure the temperature dependence of various frontend parameters the bias voltage was set and kept at a constant value of −700 V. Figure 9.5 shows that the ToT value for a certain amount of injected electrons is proportional to the temperature. Its impact is rather severe.

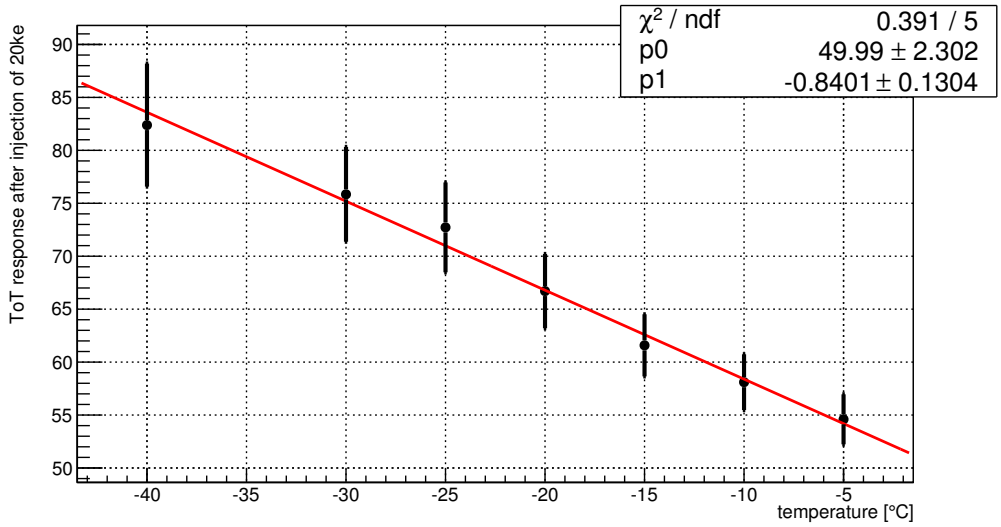

Figure 9.5: ToT values registered by assembly DO-9 after 20000 electrons have been injected using the calibration functionality at different ambient temperatures. Based on data by [Lap12].

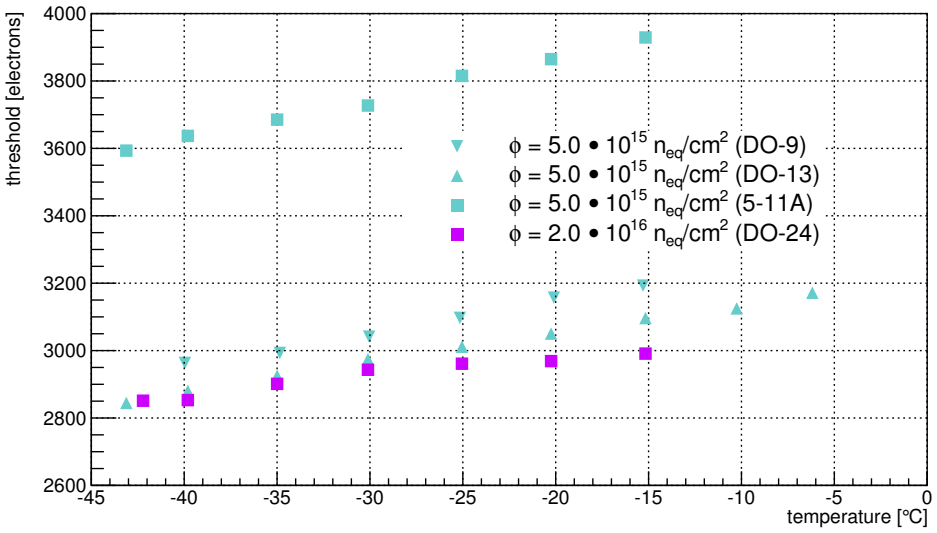

Figure 9.6: Threshold plotted against the temperature. Based on data by [Lap12].

There is also a slight increase of the threshold when the temperature rises, which

can seen in fig. 9.6.

9.1.3 Position of the Radioactive Source

In order to check whether the exact positioning of the $^{90}_{38}$Sr source during lab measurements is relevant, the radioactive source was deliberately set at different — partially misaligned — positions. All other parameters, including the temperature and the bias voltage, as well as the calibration of the assembly, were kept the same during the measurement. The beam spot visible in the hit map in fig. 9.7 clearly reveals the position of the source.

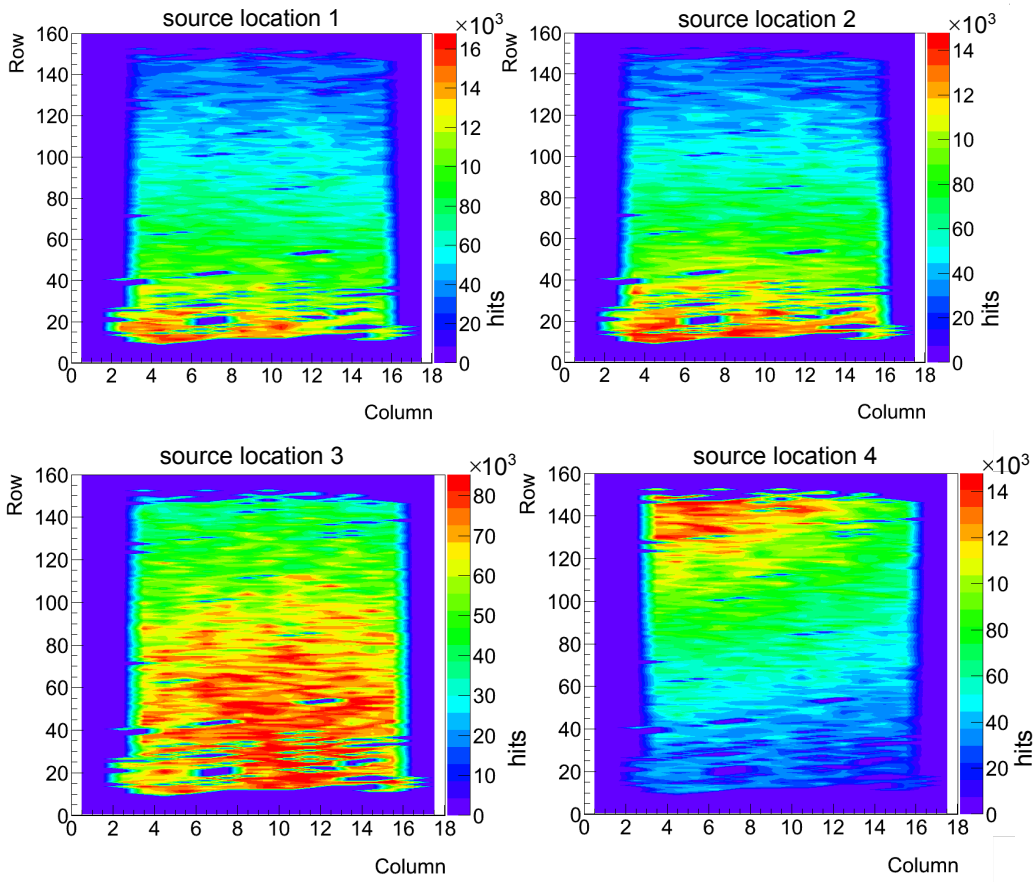

Figure 9.7: Hit maps showing the different positions of the radioactive source. [Lap12]

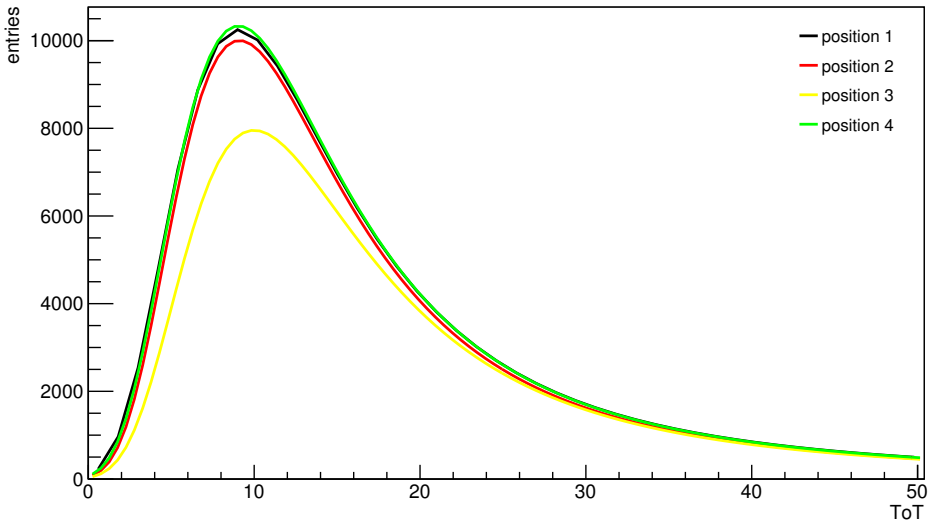

Figure 9.8: Overlay of ToT distributions taken with the assembly DO-9 where the $^{90}_{38}$Sr source was set at different positions. [Lap12]

Figure 9.8 shows the charge distribution for those four positions visible in the hit maps. There is no influence on the total collected charge, but the hit rate differs.

9.1.4 Annealing

Annealing caused by deliberate or involuntary heating is important for the operation of irradiated sensors. The impact on the charge collection, with a focus on the changes in the frontend, is shown in the following. The assembly DO-10 is used for this purpose. A tuning at a fixed bias voltage of $-2000\,\mathrm{V}$ was created. After each variation of the bias voltage a threshold and bias scan were performed. The plots in fig. 9.9 and fig. 9.10 do not show any clear influence of the bias voltage, except for the ToT which slightly fluctuates.

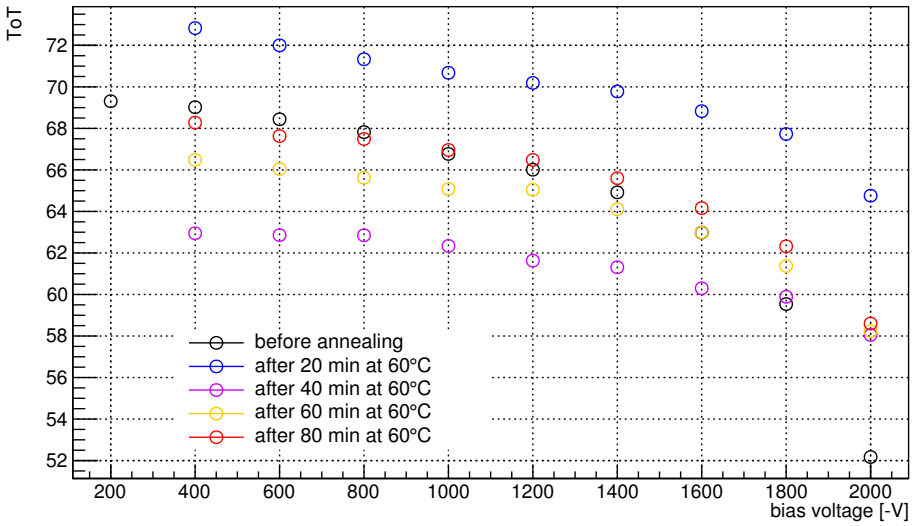

Figure 9.9: ToT shift after annealing steps. Based on data by [Wiz13].

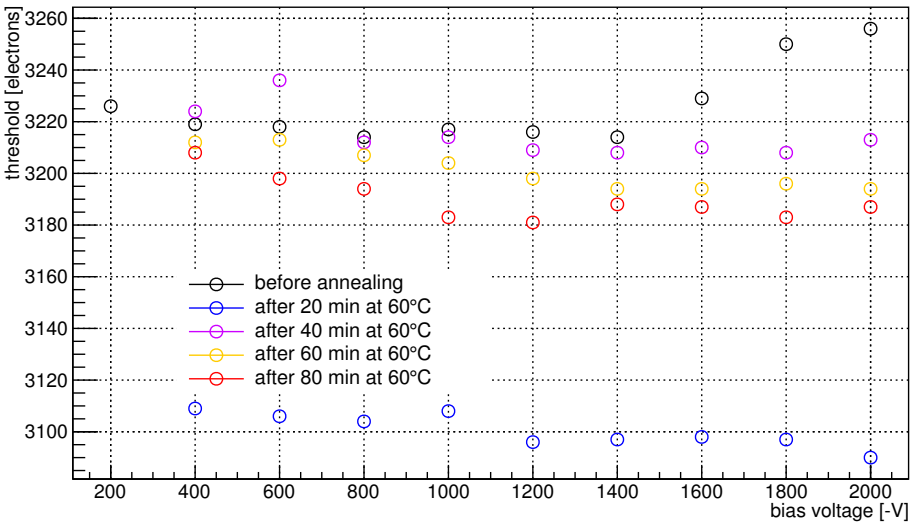

Figure 9.10: Threshold shift after annealing steps. Based on data by [Wiz13].

9.2 Calculation of Error Limits for Test Beam Measurements

9.2.1 Uncertainty of the Charge Calculation

As mentioned in the previous chapter, the ToT to charge conversion uncertainty is mainly based on the temperature drift. In order to make an estimation of this error the fit values gained with the assembly DO-9 were used, with the simplification that a linear ToT/charge relation was assumed

$$\Delta q[\text{electrons}] = \gamma_{\text{temp}} \cdot \Delta\vartheta[\text{K}]\,, \tag{9.1}$$

where

$$\gamma_{\text{temp}} = 279\,\text{electrons/K} \tag{9.2}$$

was derived from the fit in fig. 9.5. For the purposes of the test beam analyses, the environmental data from the DCS[1] monitoring were used to calculate the maximum temperature difference within a run range as a worst case estimation. Additionally, the bias voltage demonstrated an influence on the ToT as well

$$\Delta q[\text{electrons}] = \gamma_{\text{volt}} \cdot \Delta U[\text{V}]\,, \tag{9.3}$$

where the fit yields

$$\gamma_{\text{volt}} = 3\,\text{electrons/V}\,. \tag{9.4}$$

Only when a proper charge calibration is not available, and a calibration taken at a different bias voltage has to be applied, this becomes relevant. In a few cases the calibration scans taken during the test beam proved later on to be corrupted.

9.2.2 Uncertainty of the Bias Voltage

The uncertainty on the bias voltage results from the voltage drop over the bias resistor on the PCB[2]. The resistor of each assembly was individually measured and for each run range the maximum current was extracted from the environmental log files (see section 8.6.3.2 for details on the environmental monitoring system). The bias resistance and maximum bias current were used for the calculation of the maximum reducing voltage of each run range

$$\Delta U[\text{V}] = R_{\text{bias}}[\Omega] \cdot I_{\text{max}}[\text{A}]\,. \tag{9.5}$$

9.2.3 Uncertainty of the Fluence

The actually delivered fluence, as explained in section 6.2, is partially assessed by measuring the activation of aluminium foil. The radiation background, e.g. in the

1 **D**etector **C**ontrol **S**ystem
2 **P**rinted **C**ircuit **B**oard

JSI[1] reactor, is often so well known, due to regular measurements and simulations, that a very good estimate can be calculated using the irradiation position and time. If the irradiation facility specifies an uncertainty on the fluence, it is marked down respectively in the overview table and the plots. If no uncertainty is given, a blanket uncertainty of 10% is assumed for the purposes of this study.

9.2.4 Uncertainty of the Annealing

The annealing, i.e. the changes in the irradiated crystal lattice induced by heat, is relevant for the bias current and charge collection as examined in section 4.5. All DUTs[2] used were not deliberately annealed but kept cold as thoroughly as possible. The only exempt is the assembly DO-10 during the annealing test presented in section 9.4. This test was done after the test beam and lab measurements with this assembly had been concluded.

The annealing was limited by means of storage at temperatures below −20 °C, either in a freezer in the lab or at test beam sites. During transports this was achieved by using an isolated box filled with dry ice or cool packs. While using the assemblies actively, they had to be kept at very low temperatures anyhow. A temperature logger was included in each parcel when transporting the assemblies by shipment. Nevertheless, it is necessary to thaw the sensors from time to time in order to mount or dismount them in an experimental setup or for wirebonding them. Such operations cannot be reasonably executed in the cold state due to condensation leading to glazed frost.

The amount of time the assemblies had to spent unthawed differs, but it can be assumed that a maximum of 24 h at room temperature 20 °C is not exceeded. The annealing received through these operations can be neglected.

9.2.5 Uncertainty of the Hit Efficiency

The hit efficiency strongly depends on the cuts that are used and also on the definition of the hit efficiency which is applied. One of the major parameters is to decide whether dead or hot pixels are hold against the efficiency. In the real detector it is naturally necessary to include all factors which decrease the operation efficiency as one is only interested in the overall functionality.

Major contributions to the pixel detector's inefficiency during its first years of running, that are non-sensor related, are mechanical or connection failures. However, in the context of studying the sensors it is reasonable to omit such effects that are probably caused by the insufficiently radiation hard readout electronics.

Another value which has a huge impact on the resulting hit efficiency is the level 1 timing cut which is used for noise reduction. Furthermore, the number of required reference hits, decreasing the overall number of hits but improving the data quality

1 **J**ožef **S**tefan **I**nstitute in Ljubljana
2 **D**evice **U**nder **T**ests

at the same time, is relevant. The quality of the reference planes influences the hit efficiency as well, as they represent the base line of what one expects to see in the DUT.

It is reasonable to assume that the uncertainty increases in those cases where due to a lack of DUT slots no properly understood, unirradiated, reference plane was available but another, probably irradiated, DUT had to serve in this role. Sometimes, single failing pixels cause a significant decrease of the global hit efficiency as well. All these qualifications show that the hit efficiency is a quantity which strongly depends on its definition and has to be carefully considered for all practical purposes.

9.3 Behaviour of Irradiated and Unirradiated Assemblies

A detailed description of the samples measured is given in table 6.1. All samples belong to two major groups: Those that were irradiated after making the flip-chip connection and those where only the sensor was irradiated. They had to undergo both externally triggered source scans at the laboratory using a $^{90}_{38}$Sr radioactive source and test beam measurements. The test beam data used here, were taken during six test beam campaigns, four of them located at CERN[1]-SPS[2] and two at DESY[3].

The basic difference between the CERN-SPS and the DESY test beam site is that at CERN 120 GeV to 180 GeV pions are used, whereas at DESY 4 GeV electrons are available. More details of the test beam sites can be found in section 8.6. The intrinsic resolution of the telescope is decreased through the significant multiple scattering stimulated by the low energy of the particles provided at DESY. Partially, this is mitigated by measuring only two assemblies simultaneously, instead of 4 assemblies (or even 8, which was possible as long as the TurboDAQ setup was used) at CERN. In this way the radiation length of the material in the beam was decreased.

An summarized overview of the test beam results is given in table 9.1. More details regarding the composition of the batches — those are the groups of assemblies measured together at one time — and the chronological order are presented in table C.1. All runs were analysed using hotpixel masking and running residual adjustment. The minimum number of reference DUTs was set to one. In some cases it was necessary to increase the hot pixel cut criterion as otherwise (almost) the whole sensor would have been masked due to noise.

Detailed result plots for each run range are printed in appendix C (only available in the electronics version of this thesis), where for each DUT a number of standard plots is made available. Some of those plots will be explained in the following on the basis of selected example plots.

1 **C**onseil **E**uropéen pour la **R**echerche **N**ucléaire
2 **S**uper **P**roton **S**ynchrotron
3 **D**eutsches **E**lektronen **SY**nchrotron

9.3.1 Test Beam Control and Results Plots

The plot in fig. 9.11b shows the evolution of the temperature against the time during the run range. These data points, just as those of the other environmental plots, come from the environmental log files created by the testbeamDCS software (compare section 8.6.3.2). The measurement is taken once per second for each temperature sensor positioned behind the respective DUT.

These plots are tagged with run numbers. They are written above the horizontal lines representing the time interval for each run. Their colour indicates whether a run was valid and used (blue) or discarded (red). Sometimes, there are also time intervals which seemingly do not belong to a run. This mostly occurred when the run control was stopped during the ongoing run range or when for a couple of invalid runs the start and stop times were not known due to a rare hang up of the system. This happened once or twice while the system was running unsupervised during an unstaffed night shift.

The run numbers and their start and stop times are mostly extracted by a self-written combination of a bash script and ROOT[1] macro from the eudaq runcontrol logs and checked for basic sanity, such as causality. In some cases missing times — the run control terminated in an uncontrolled way — were supplemented in the interactive mode of this script by using entries from the manual log spread sheet. In the newer test beam campaigns this process got easier as soon as a new feature of the testbeamDCS software made it possible to receive messages from the runcontrol program. This enabled it to write a separate environmental file for each run number automatically.

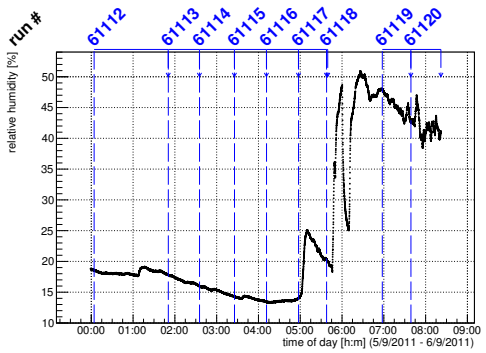

(a) Example of a humidity against time plot. This one is taken from the range 61112-61120 during the September 2011 test beam at CERN. All runs here are valid which is indicated by the blue colour.

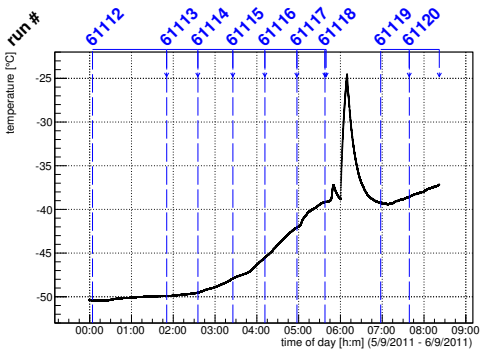

(b) Example of a temperature against time plot. This one is for DO-I-5, taken from the range 61112-61120 during the September 2011 test beam at CERN. All runs here are valid which is indicated by the blue colour.

Figure 9.11: Example environmental test beam plots.

1 `http://root.cern.ch`

This also applies to other environmental values, such as the currently applied bias voltage, which is measured by the ISEG (see fig. 9.12a) together with the bias current (see fig. 9.12b). During some run ranges also a humidity measurement was provided for the whole DOBOX[1]. In these cases a plot of the humidity against time is available similar to the one in fig. 9.11a. The general trend in the humidity plot shown here is certainly reasonable, but otherwise there is a huge systematic error on these values as it is difficult to measure humiditiy reliably at such low temperatures. The Honeywell HIH4000[2] sensor was operated below its minimum operation temperature as specified in its spec sheet.

The hot pixel mask in fig. 9.13b is created during the first analysis pass. In some cases when only very few pixels remained unmasked, the hit occupancy criterion was increased. This is regarded as justifiable when the level 1 timing plot looks sufficiently good. In case of a very flat level 1 timing distribution the run range is often discarded for that particular DUT or the obtained values are at least regarded as unreliable.

The indium flipped assemblies (see fig. 9.13a) show a lot of dead spots in this plot, especially around the corners. These unresponsive corners and edges are a typical syndrome of unconnected bump bonds. The lacking bump bond quality identified in this cases is caused by the fact that the frontends were stored for an unusually long time (several years as they were produced during the original ATLAS[3] production). As in the case of the PbSn flipped assemblies, the frontends carry the prepared

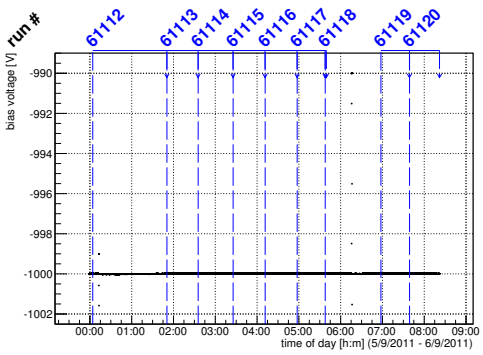

(a) Example of a bias voltage against time plot. This one is for DO-I-5, taken from the range 61112-61120 during the September 2011 test beam at CERN. All runs here are valid which is indicated by the blue colour.

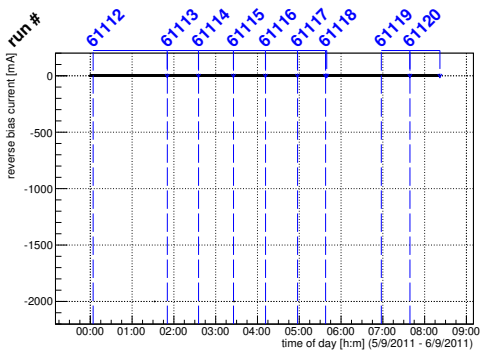

(b) Example of a bias current against time plot. This one is for DO-I-5, taken from the range 61112-61120 during the September 2011 test beam at CERN. All runs here are valid which is indicated by the blue colour.

Figure 9.12: Example environmental test beam plots.

1 **DO**rtmund testbeam **BOX**
2 `http://nearsys.com/catalog/sensor/hih4000.pdf`
3 **A** **T**oroidal **L**HC **A**pparatu**S**

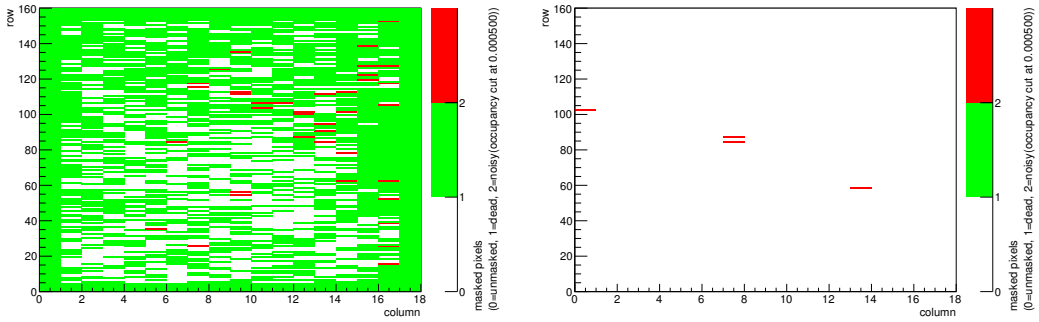

(a) Example of a really bad mask map (DUT DO-I-5). The green colour indicates that a lot of pixels do not fire at all. The bad quality in this case was caused by bump bond difficulties which were evocated by overlain photo resist.

(b) Example of a good mask map (of DUT DO-10). Almost all pixels show signal and almost none are masked out.

Figure 9.13: Example test beam plots (mask maps).

bump ball stubs.

In order to protect those bump balls before the flip-chip mating, they are covered with a photo resin. This resin is intended to be removed shortly before flip-chipping. The resin seems to have hardened provoked by the long storage, making its removal not completely successful, which led on its part to warping. Those pixels which were connected successfully, worked quite well. The other troubles occuring with irradiated frontends were naturally absent from the indium flipped assemblies.

The level 1 timing distribution in fig. 9.14 is useful for evaluation of the DUT's behaviour with regard to proper calibration settings. A sharp peak, covering one or two bins, is expected, as the timing between the trigger provided through the telescope scintillators and the recording of the signal in the particular DUT should always stay the same. If there is a flat distribution in the surrounding level 1 timing bins, a lot of noise exists and has to be repaired by the hotpixel removal in the TbMon analysis. If there is no clear peak visible, this usually means that something strange happened during operation and that the data are not really usable for that particular DUT.

The plots in fig. 9.15a and fig. 9.15b show the calibration constants A and B (C looks very similar and is thus ommitted here) for each pixel in form of a sensor map. Those constants are necessary for the conversion of the ToT values into charge. On their own they are not very informative, although one can see whether there is a slight variation in the values. If a map looks too homogenous, this hints on a problem with the scan. For a more detailed assessment of the calibration scan a closer look at the scan file itself is necessary.

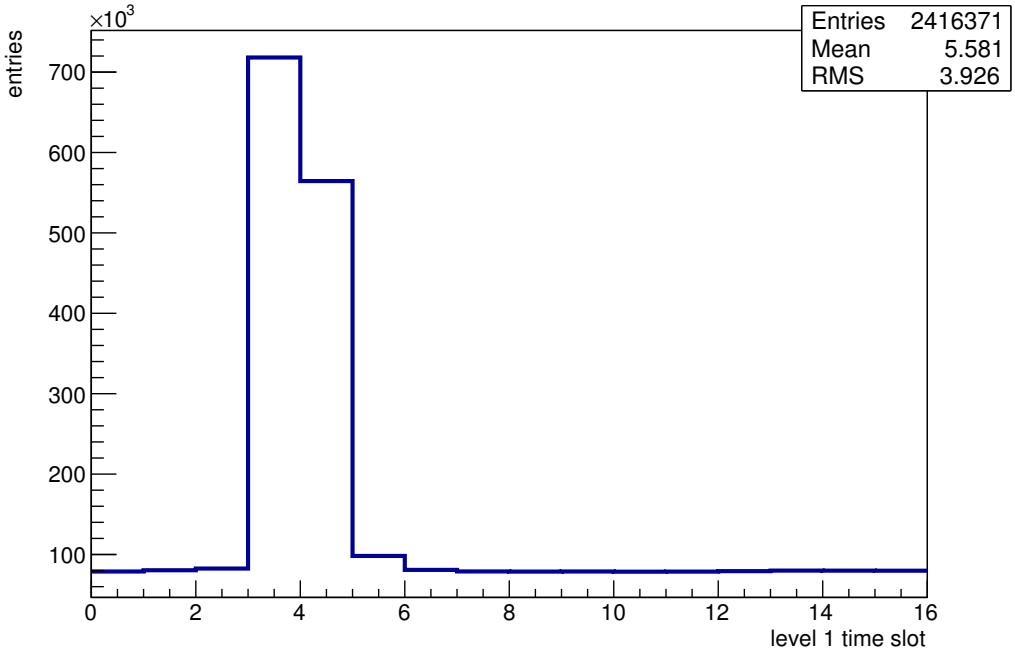

Figure 9.14: Example timing distribution of DUT DO-10. It is important that there is sharp peak visible, that's typically two bins wide. If there is a rather high and flat distribution around a apeak, this indicates a lot of noise and the noise occupancy should be tightened a bit by way of trial. When the level 1 timing distribution is completely irregular this usually means that either the frontend is in a bad operation mode and needs a reset or that it is broken.

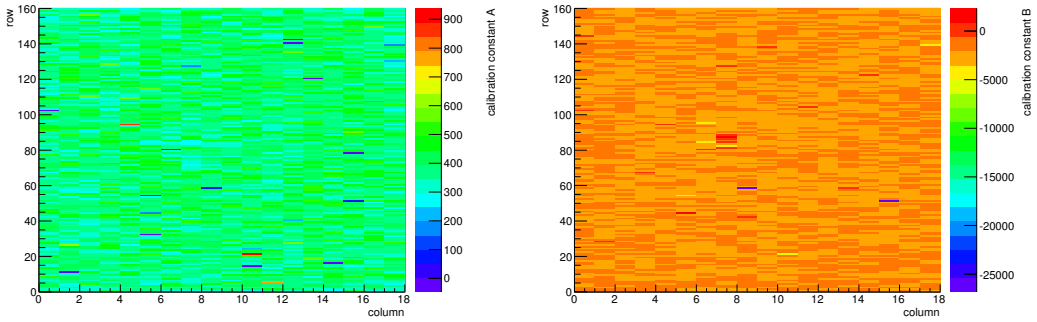

(a) Example of a calibration map (A) by DUT DO-10.

(b) Example of a calibration map (B) by DUT DO-10.

Figure 9.15: Example test beam plots (calibration maps).

Plots showing the quality of the reconstruction (both influenced by the data taking and cuts applied later on and also mirroring the care taken during shift correction) are the residuals in X and Y shown in fig. 9.16a and fig. 9.16b. They indicate good data quality when they are centred around the position 0 and have a width equivalent to the pixel pitch. The residual is the difference between the track position estimated by the telescope and the position calculated from the hit cluster in the DUT.

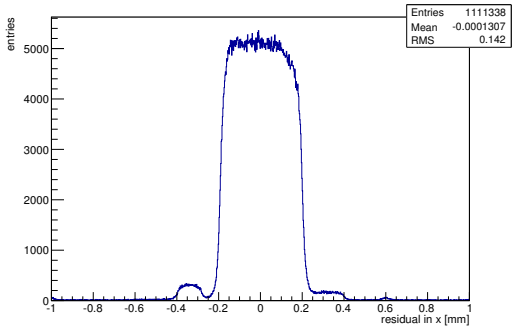

(a) Example of a (rather good) residual distribution in X (DUT DO-10).

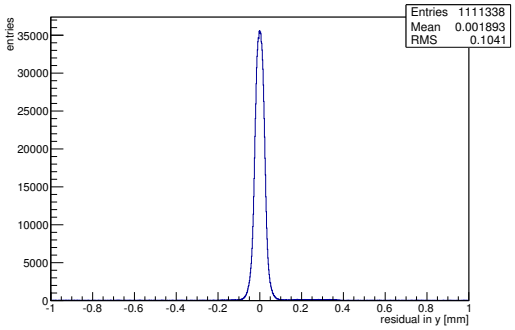

(b) Example of a (rather good) residual distribution in Y (DUT DO-10).

Figure 9.16: Example test beam plots (residual distributions).

Figure 9.17a shows the hit efficiency map, that means the efficiency for each pixel. It is useful to recognize particularly less efficient areas. Sometimes the overwhole hit efficiency can be drastically increased by masking out just a couple of pixels standing out in this plot. The complementary plot in fig. 9.17b shows the hit inefficiency map of the whole sensor. This quantity is especially useful when dealing with small differences of high hit efficiencies.

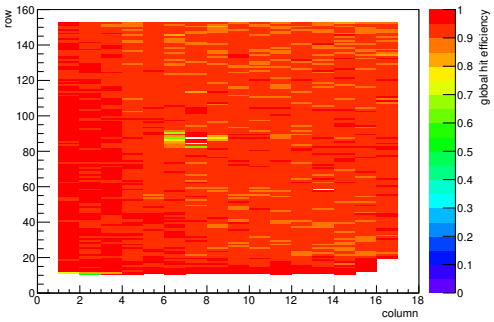

(a) Global sensor efficiency map for DUT DO-10.

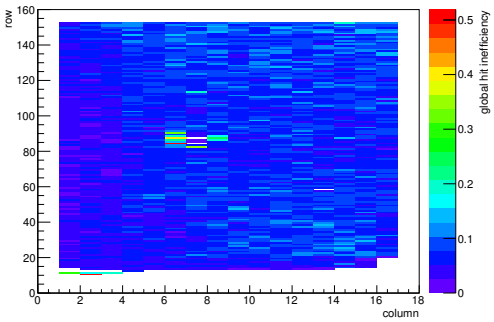

(b) Complementary global sensor inefficiency map for DUT DO-10.

Figure 9.17: Example test beam plots (sensor efficiency maps).

The collected charge distribution is shown as a sum of all cluster sizes and individually for different cluster sizes in figures such as fig. 9.18. According to the theory, the resulting charge distribution should follow a Landau-Vavilov distribution. For the source measurements in the lab this function was fitted to the distributions and the most probable value derived as a fitting parameter. This has been omitted for the test beam measurements as the fitting does not work very well for those data sets. The charge values shown in the table and plotted in the appropriate plots are simply the bin with the highest entry.

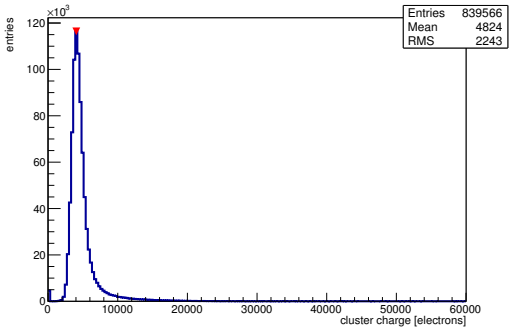

Figure 9.18: Total charge distribution of DUT DO-10.

The cluster size distribution in fig. 9.19a typically shows that the majority of clusters are formed of 1 and 2 hit clusters, when the sensor is operated at perpendicular incidence. The time dependant hit efficiency plots, such as the one in fig. 9.19b, also give a good overview of the data quality. The trend should be rather constant.

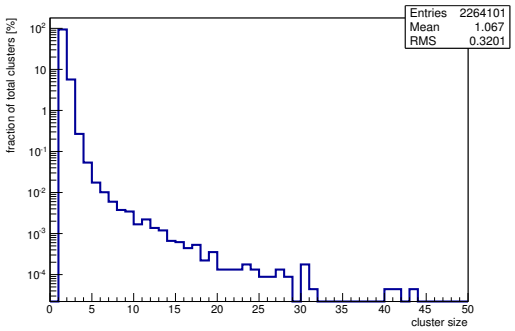

(a) Clustersize distribution for DUT DO-10.

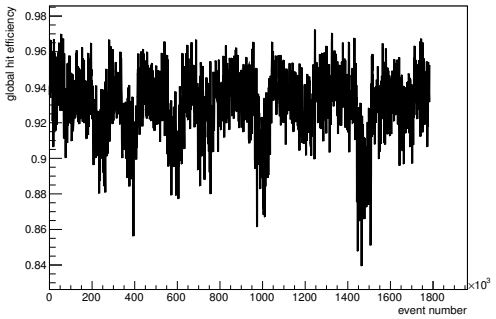

(b) Time dependant hit efficiency for DUT DO-10.

Figure 9.19: Example cluster size distribution and time dependant hit efficiency for DUT DO-10.

For the plots in fig. 9.20a and in fig. 9.20b the available telescope resolution was used for mapping the hit efficiency and mean cluster charge on the surface of one pixel. The results show the possible influence of the different substructures within a pixel layout on the efficiency of the pixel.

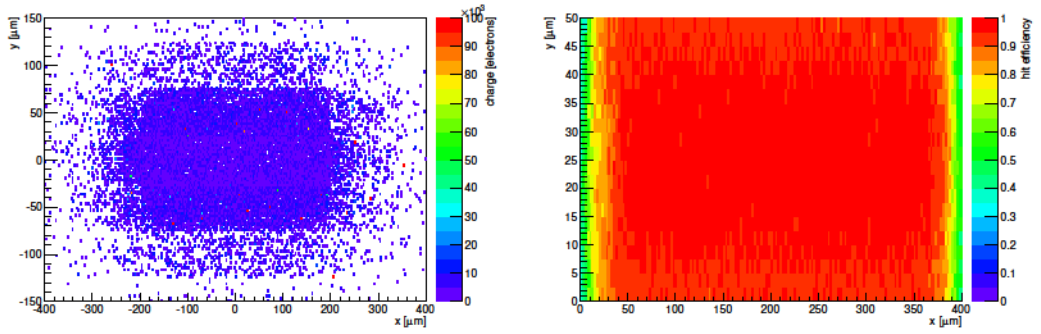

(a) Example sub pixel resolved mean charge distribution for DUT DO-10.

(b) Example sub pixel resolved hit efficiency distribution for DUT DO-10.

Figure 9.20: Example sub pixel resolved plots for DUT DO-10.

9.3.2 General Results

The collected charge for all cluster sizes is plotted against the bias voltage in fig. 9.25. For the lower irradiated assemblies it can be observed that there are two sections where the charge development behaves differently. Therefore, two different cases have to be distinguished here. The relationship between the collected charge and the applied bias voltage seems to be linear above a certain voltage threshold. The amount of charge increases with the growth of the charge collection zone which equals the depletion width below the depletion voltage. This means that the sensor is operated under-depleted. According to eq. (3.42) the depletion width is proportional to $\sqrt{U_{\text{bias}}}$. When the sensor is operated over-depleted, the charge either stagnates or

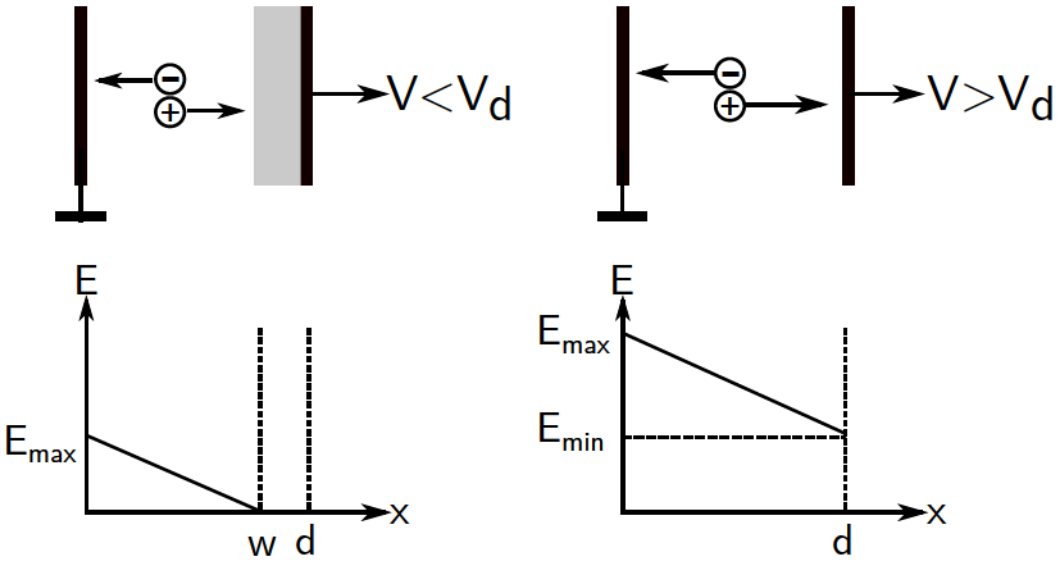

Figure 9.21: Theoretical electric field in a sensor in the underdepleted (on the left) and overdepleted state (on the right). According to [Spi06].

grows linearly with the bias voltage. The schematic drawing of the sensor's interior in the right portion in fig. 9.21 shows that in this situation the eletric field strength increases. This leads to a decrease in the charge collection time and thus in the impact of trapping. The clearly visible bend in the curves of the lowly irradiated assemblies indicates the passing of the depletion voltage.

For highly irradiated assemblies above $5 \times 10^{15} \mathrm{n_{eq.}\,cm^{-2}}$ this behaviour is no longer valid. Either the under depleted zone is no longer existing in the previous form or the threshold is too high and makes it impossible to observe the lower part of the curve. Especially, the lab data show a steeper slope for low bias voltages. Comparing the values for the expected charge values in table 4.1 with those values actually gained with the $5 \times 10^{15} \mathrm{n_{eq.}\,cm^{-2}}$ irradiated assembly DO-9 and even more with those gained with the $2 \times 10^{16} \mathrm{n_{eq.}\,cm^{-2}}$ irradiated assembly DO-10, it becomes clear that much more charge is registered, than expected from a naive trapping model.

Although, the amount of charge is compatible with the assumption that charge amplification occurs, the exponential charge development expected from impact ionisation is not observed. The slope becomes flat and seems to satiate. If impact ionisation is indeed responsible for the huge charge surplus, then there has to be a limiting mechanism. Test beam pions show a bit more charge than lab electrons. For the majority of clusters, which are formed of one and two hit clusters, the total summed charge lies between the charge calculated for one and two hit clusters individually. External triggering improves the signal quality of source measurements in the lab by reducing the noise. Looking at the development of the cluster size fractions in fig. 9.22, fig. 9.23 and fig. 9.24 three phenomena can be observed:

- One hit clusters are dominant.
- The amount of one hit clusters decreases in favour of two hit clusters with an increased bias voltage. This is due to neighbouring pixels passing the threshold. This is more pronounced than the counter effect that the lateral dispersion of the charge cloud decreases and thus the charge sharing is reduced.
- An increase of the received fluence shifts the ration in favor of smaller clusters.

Comparing the charge collection plot and the hit efficiency plot the impact of the set threshold is clearly visible. Under a certain charge region the hit efficiency drops quickly. This can be also seen in fig. 9.30 and fig. 9.29 where hit inefficiency, respectively hit efficiency, is plotted against the collected charge. Below the usual threshold of 3000-4000 electrons the hit efficiency drops below 50%. Afterwards, it shows an asymptotic behaviour which is probably dominated by single inefficient pixels and statistical fluctuations.

Even at very high fluences, such as $2 \times 10^{16} \mathrm{n_{eq.}\,cm^{-2}}$ which is expected as the

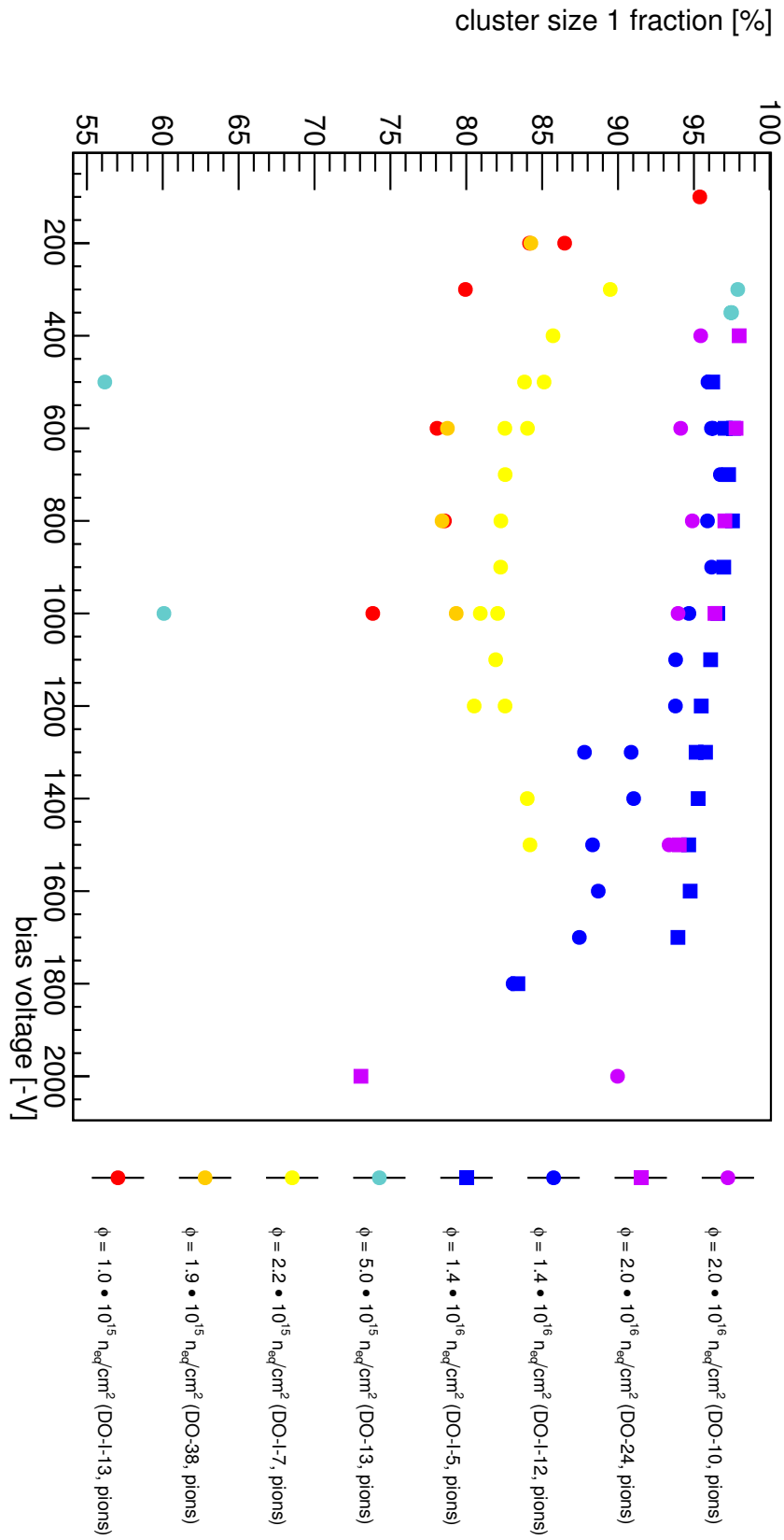

Figure 9.22: Fraction of clusters with one hit plotted against the bias voltage.

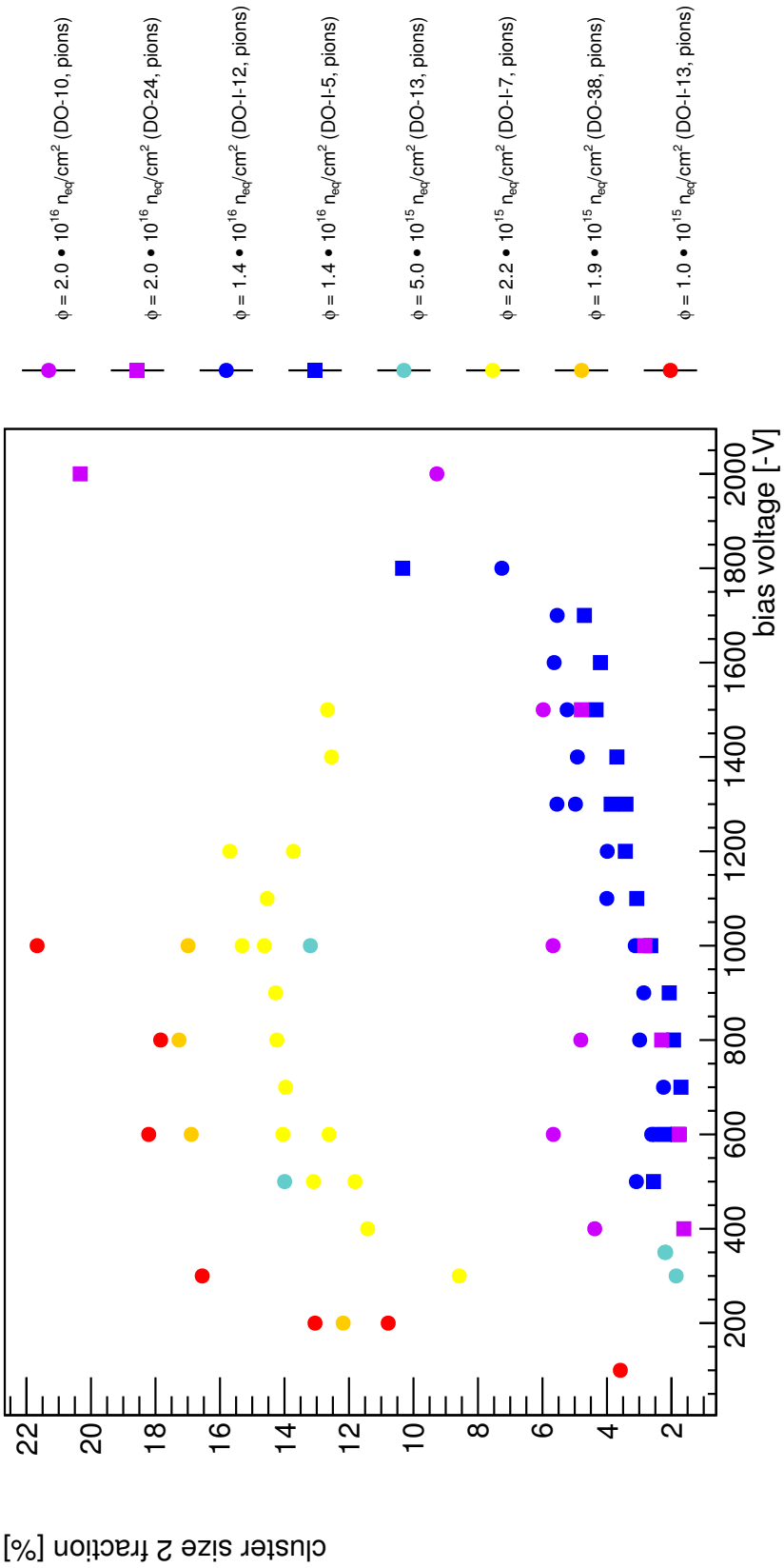

Figure 9.23: Fraction of clusters with two hits plotted against the bias voltage.

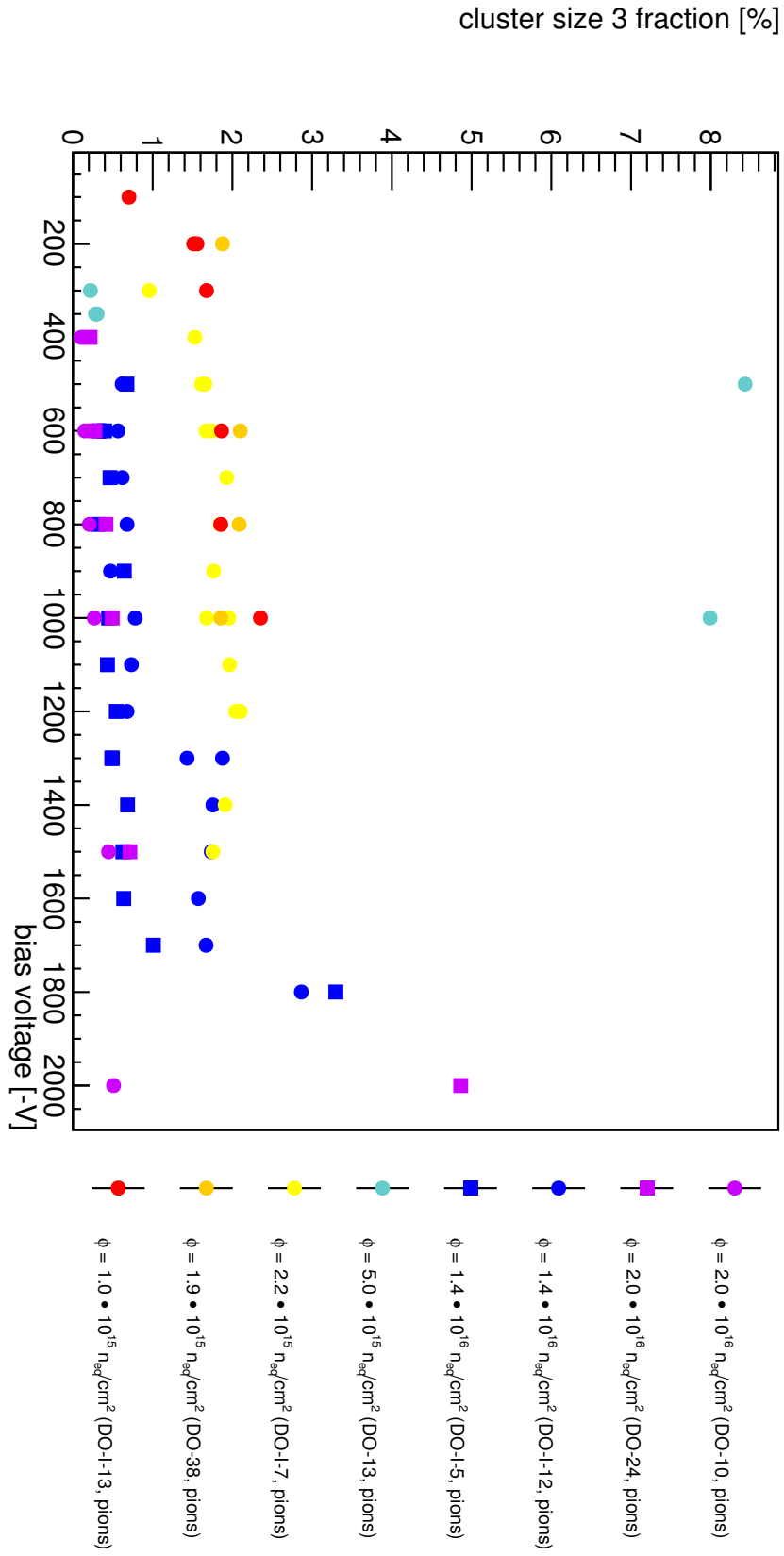

Figure 9.24: Fraction of clusters with three hits plotted against the bias voltage.

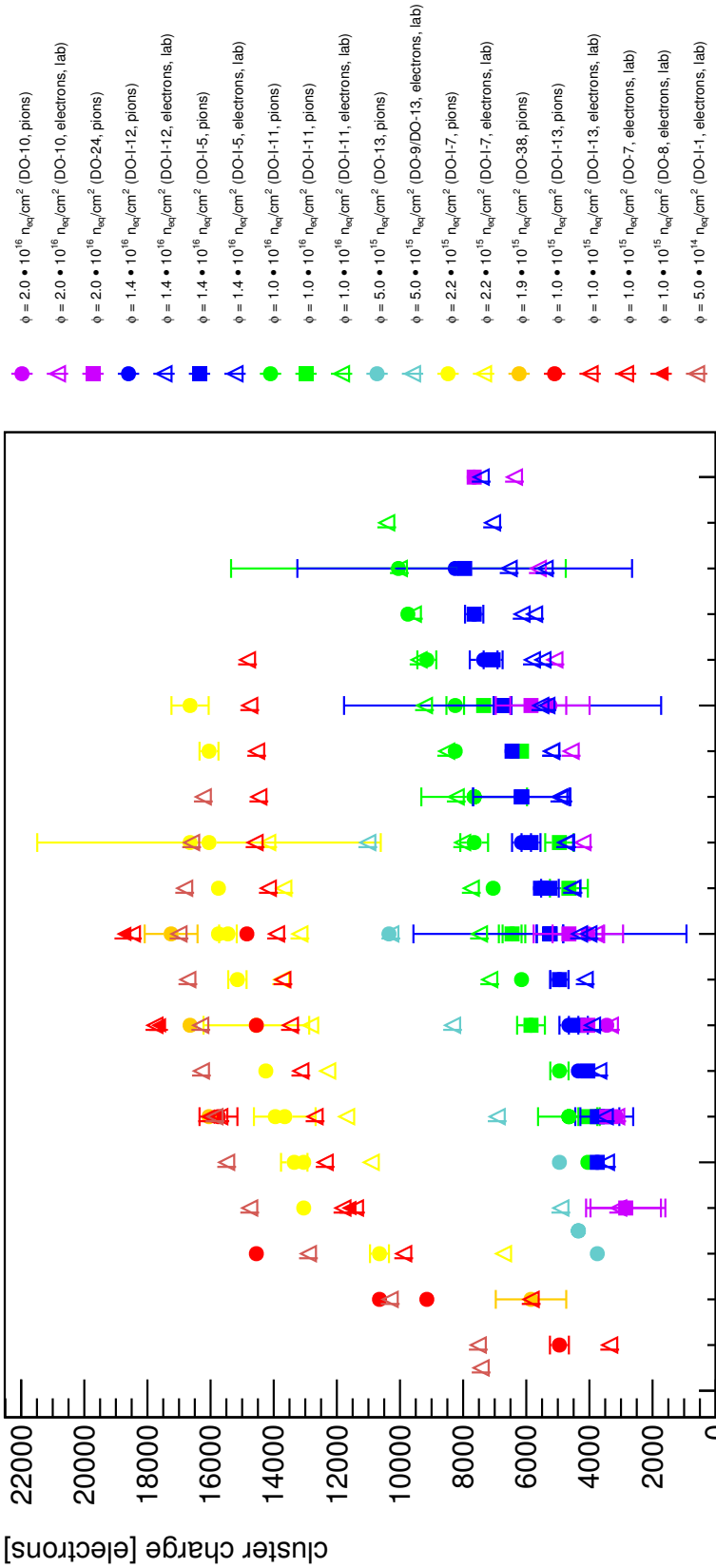

Figure 9.25: Total cluster charge plotted against the bias voltage.

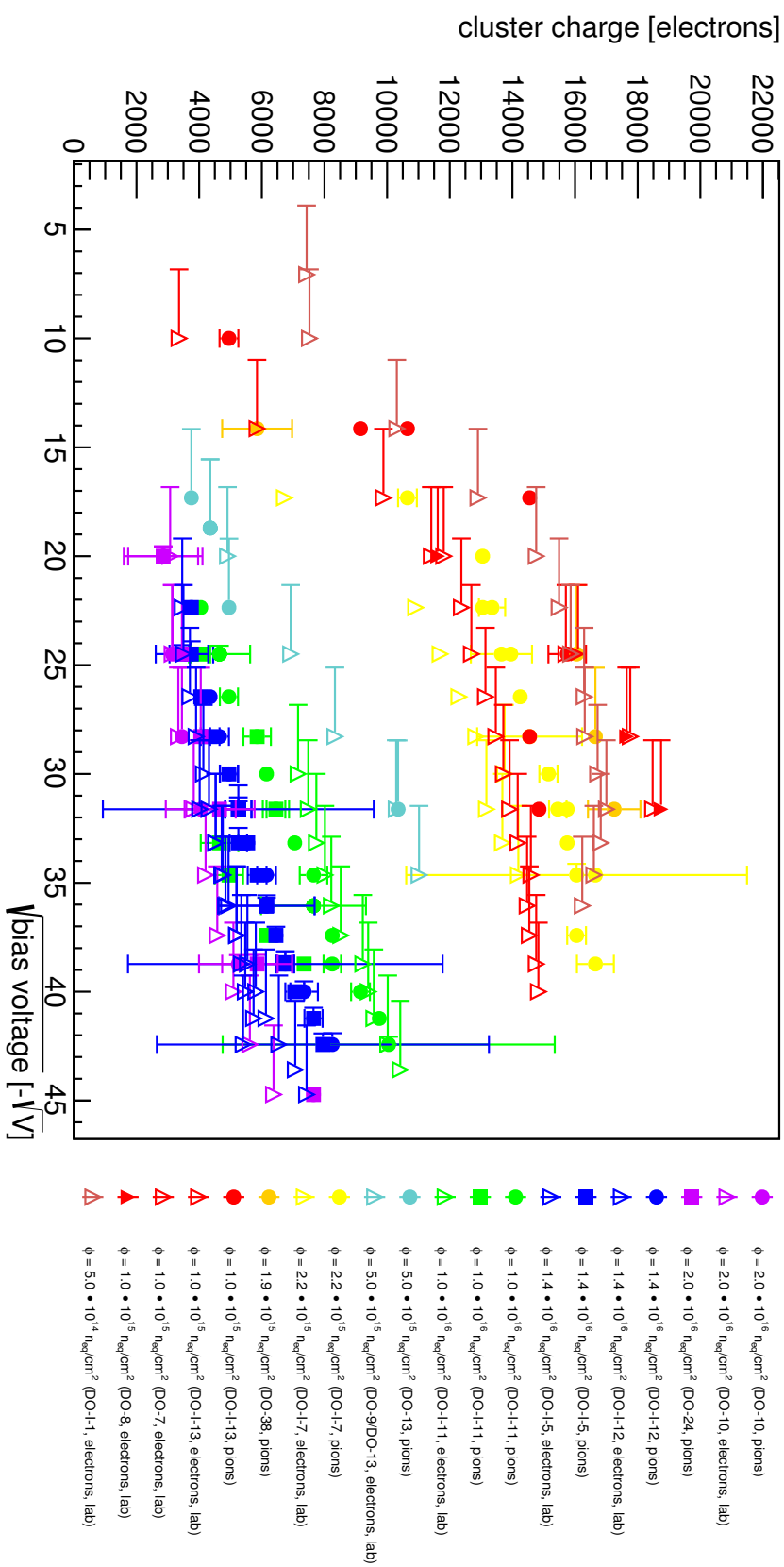

Figure 9.26: Total cluster charge vs bias voltage.

end-of-life fluence for the new b-layer of the HL-LHC[1] (including safety factors), a more than sufficient hit efficiency can be achieved with planar silicon sensor using a moderate bias voltage of 1500 V. The highest irradiated assemblies, whether they were PbSn (DO-10 and DO-24) or indium bump bonded (DO-I-5 and DO-I-12), worked reliably and performed exceptionally well. In fig. 9.29 the hit efficiency is plotted against the voltage. In order to get a clearer picture, as the values get quite small, the hit inefficiency is plotted in fig. 9.30. In both cases a logarithmic scale is applied to the y-axis resulting in a mostly linear hit inefficiency depending on the bias voltage. 100% efficiency is approached asymptotically.

This development of the hit efficiency in dependence of the cluster charge (see fig. 9.31) can be interpreted, assuming a simple model where only single pixels are considered and cluster effects disregarded. In this model a hit in a pixel produces either enough charge to be above the threshold or it does not respond at all. The threshold distribution in a well working assembly is Gaussian, as can be seen in fig. 9.27 using the example of the assembly DO-10, and thus the hit efficiency (as defined in section 8.6.4.5) is basically the integral from $-\infty$ to the charge q produced by the currently set bias voltage as demonstrated in eq. (9.6) through eq. (9.8).

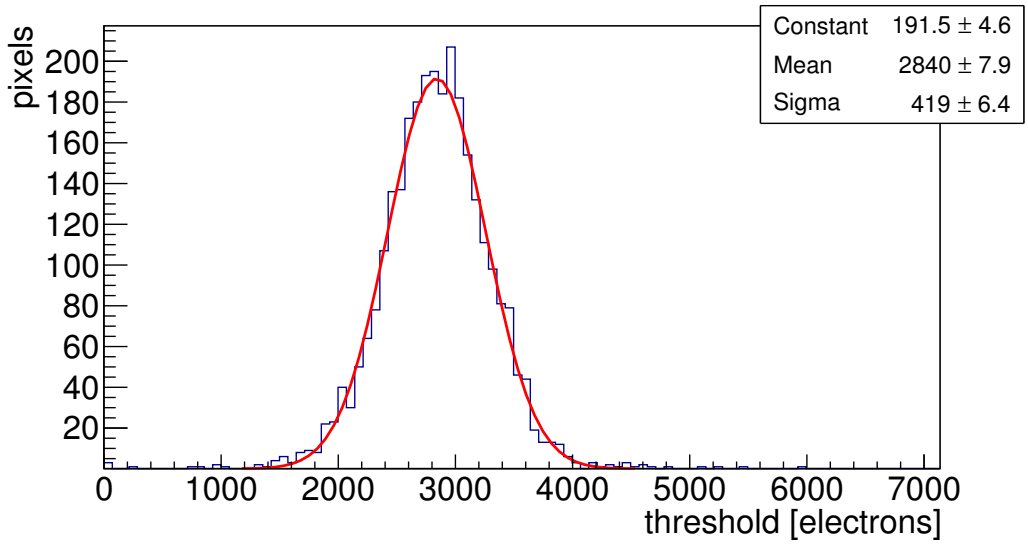

Figure 9.27: Threshold distribution of the assembly DO-10 after tuning. It was taken after the run 945 while being operated at a bias voltage of 1500 V. It shows the typical Gaussian shape.

1 **H**igh **L**uminosity - LHC

$$\varepsilon_{\text{hit}} \approx \int_{-\infty}^{q} \frac{1}{a\sqrt{2\cdot\pi}} \cdot \exp\left(\frac{-(x-b)^2}{2\cdot a^2}\right) dx = \left[-\frac{1}{2}\cdot \text{erf}\left(\frac{b-x}{\sqrt{2}\cdot a}\right)\right]_{-\infty}^{q} \tag{9.6}$$

$$= \frac{1}{2}\cdot \text{erf}\left(\frac{q-b}{\sqrt{2}\cdot a}\right) + \frac{1}{2} \tag{9.7}$$

$$\text{using } \lim_{x\to\infty} \text{erf}\,(x) = 1 \tag{9.8}$$

The error of the hit efficiency estimated from the simple statistical error as explained in section 8.6.4.5 appears too small, when comparing e.g. the results of the DUTs DO-10 and DO-24. Both of them have the same layout, received the same fluence and were tuned to almost the same threshold. Nevertheless, there is a significant deviation in the measured hit efficiency when the same bias voltage is applied. From this difference an error of 10% is estimated and applied on all hit efficiency values. In fig. 9.32 the data points for the assembly DO-10 were fitted using this function. The same function plotted exemplary for various typical threshold and width combinations is shown in fig. 9.28. It seems that there are further effects disturbing the curve. One of them might be cluster effects, where the cluster position moves out of the matching radius, when pixels belonging to the cluster move below or above the threshold.

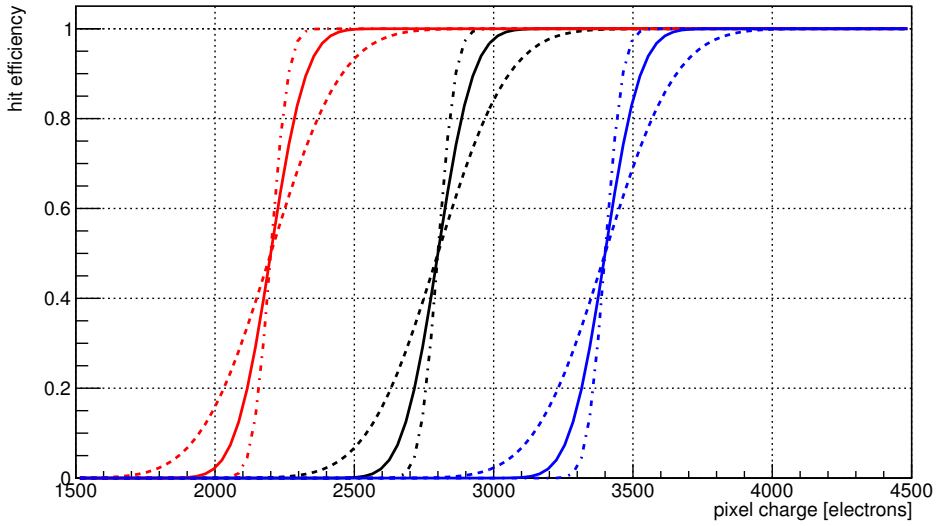

Figure 9.28: Fit function eq. (9.6) for hit efficiency in dependence of the bias voltage plotted for different exemplary sets of parameters a (width of threshold distribution) and b (mean of threshold distribution). The threshold parameters are $b = 2200$ (red curves), $b = 2800$ (black curves) and $b = 3400$ (blue curves). The widths used for each set of plots are $a = 50$, $a = 100$ and $a = 200$ (from left to right).

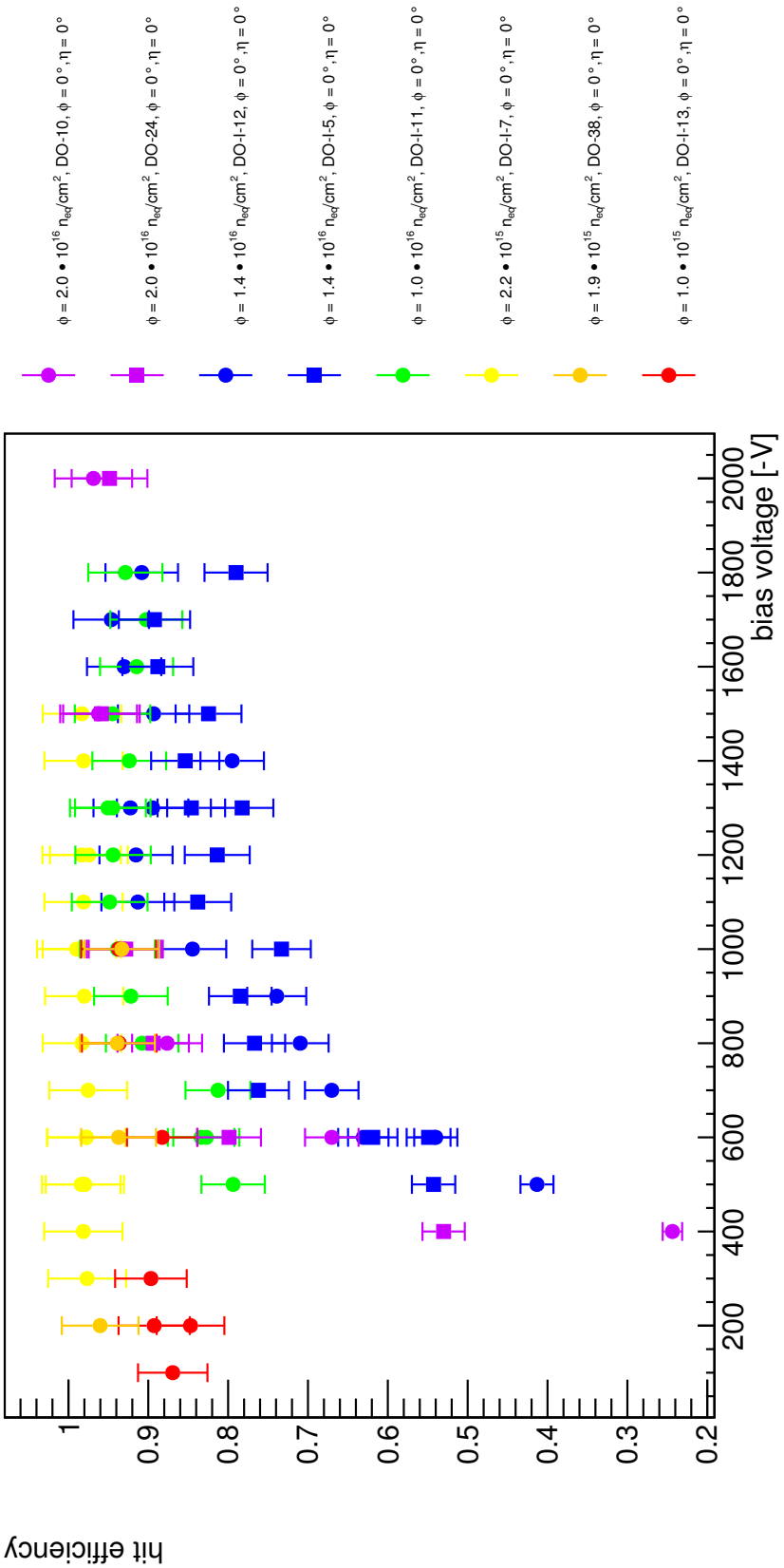

Figure 9.29: Hit efficiency plotted against the bias voltage.

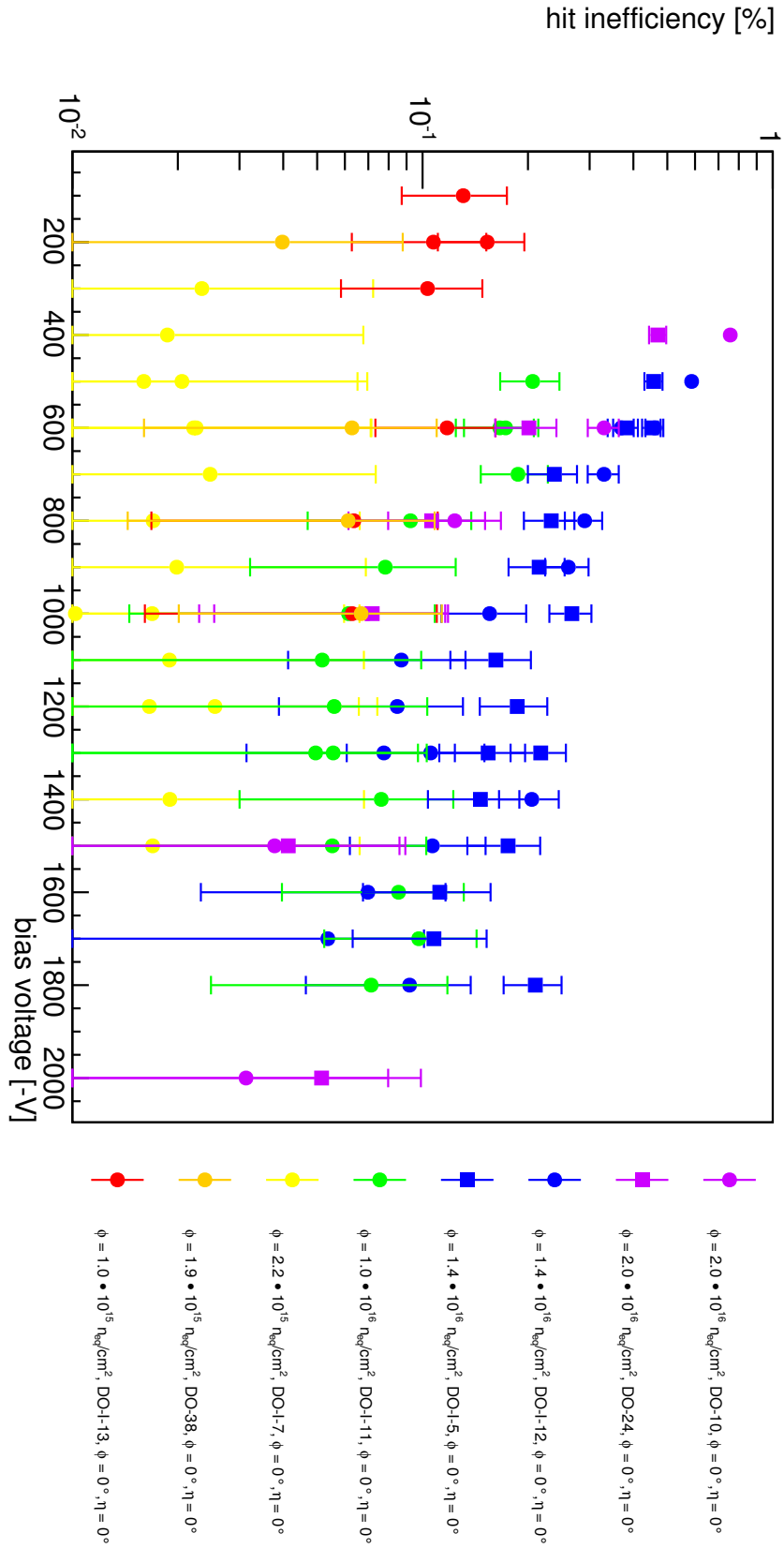

Figure 9.30: Hit inefficiency plotted against the bias voltage with fits.

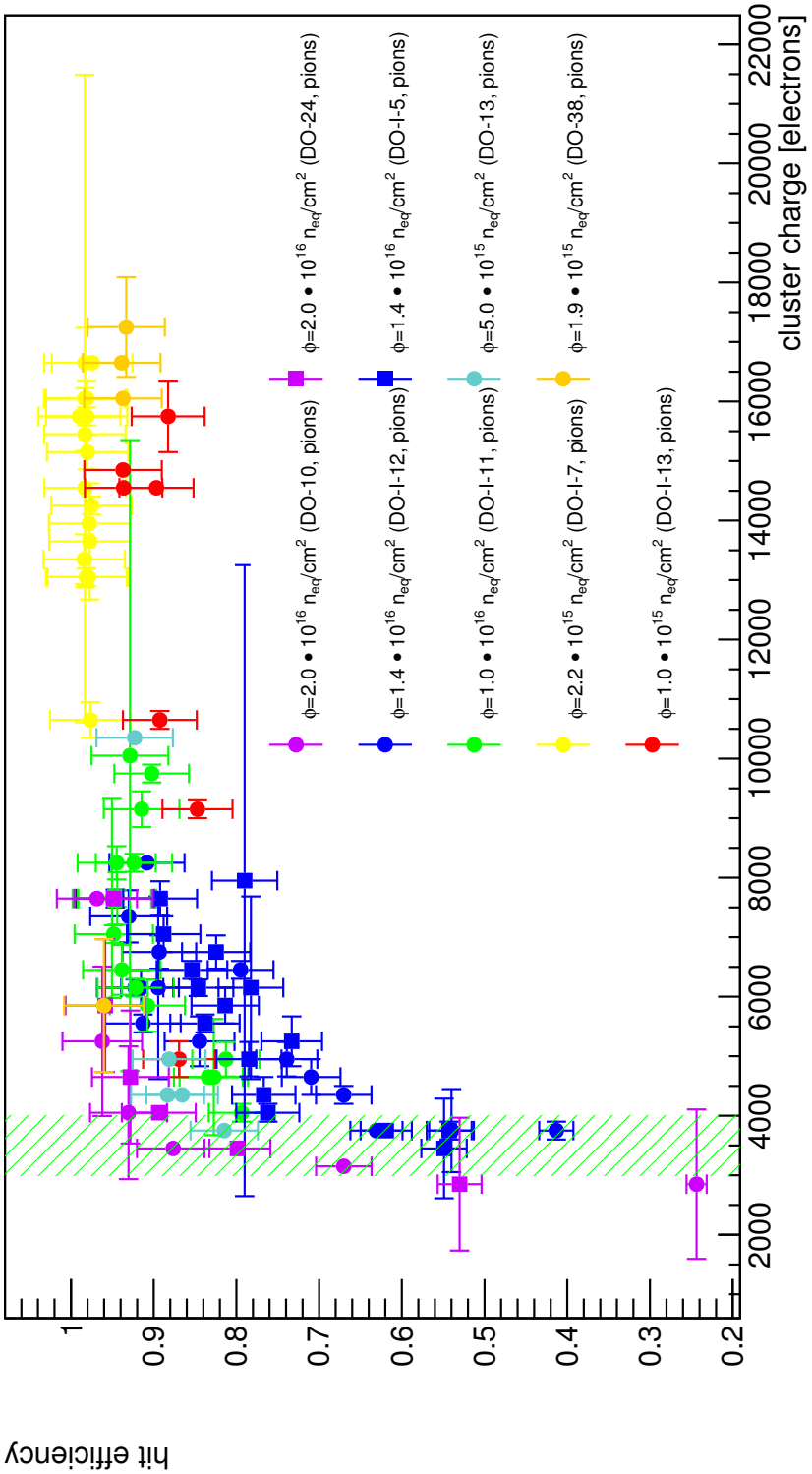

Figure 9.31: This plot shows the hit efficiency plotted against the total cluster charge. The data were taken during different test beam periods in 2011 through 2013. After the cluster charge has reached the level of the mean threshold (indicated by the hatched area) it stays quite stable. Below that value the hit efficiency decreases rapidly. The gradual change in the hit efficiency is due to the fact that the threshold follows a Gaussian distribution.

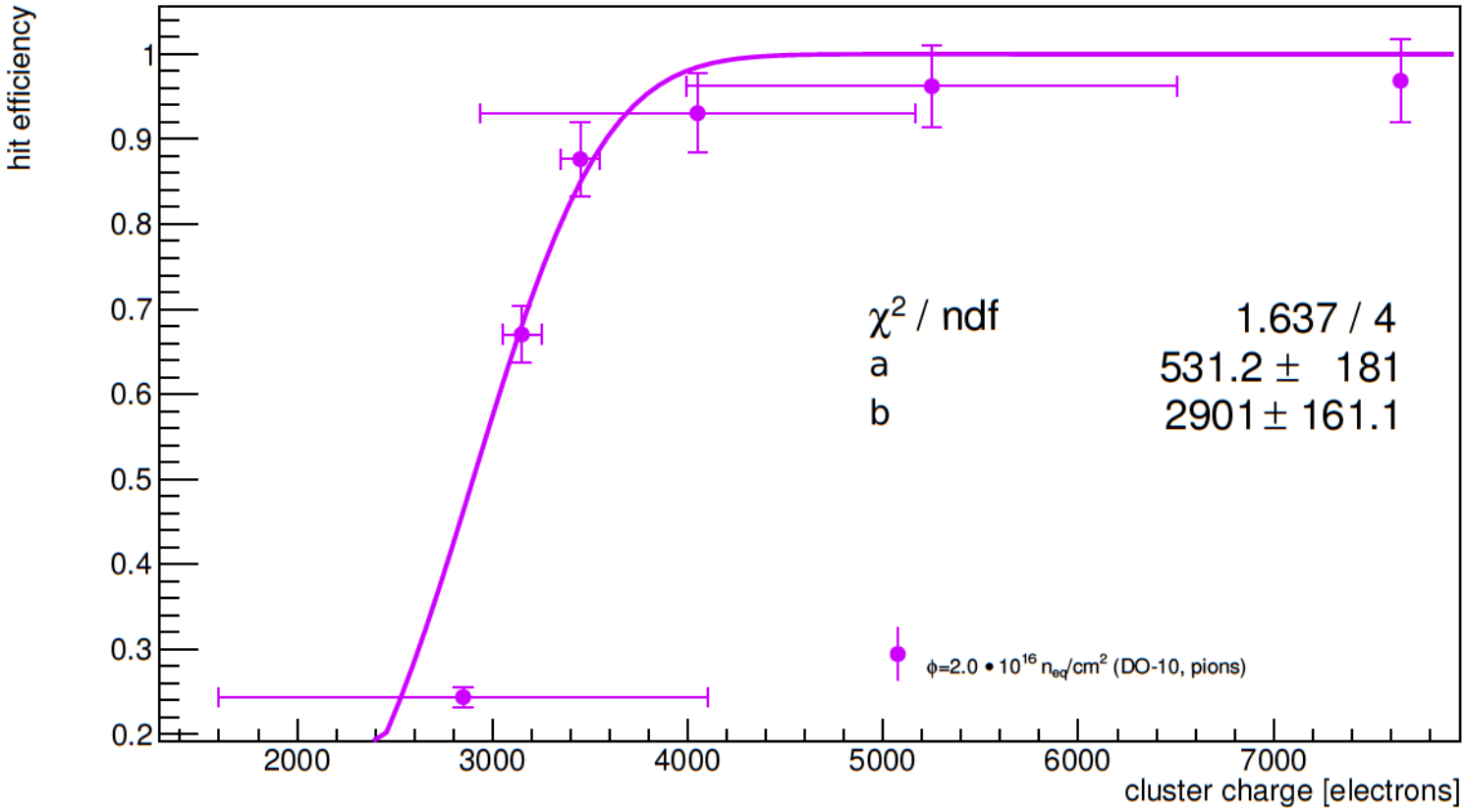

Figure 9.32: This plot shows the hit efficiency plotted against the total cluster charge for the assembly DO-10. After the cluster charge has reached the level of the mean threshold it stays quite stable. This is indicated by the hatched area similar to the plot in fig. 9.31. By comparison the the width of the area is smaller as it was calculated by looking up the maximum and minimum threshold for the assembly DO-10 in table 9.1. Below that value the hit efficiency decreases rapidly. The gradual change in the hit efficiency is due to the fact that the threshold follows a Gaussian distribution. The fit is based on the function eq. (9.7): $\varepsilon_{\text{hit}} = \frac{1}{2} \cdot \text{erf}\left(\frac{q-b}{\sqrt{2}\cdot a}\right) + \frac{1}{2}$. It is obvious that the general trend is covered, but there are also additional parameters. In this case the fit works exceptionally well and the value obtained for the parameter b agrees very well with the mean of the measured thresholds.

U [V]	DUT	Threshold [electrons]	Testbeam	Run range	Charge [electrons]	Hit efficiency [%]	CS1 [%]	CS2 [%]	CS3 [%]
$\psi = 1 \times 10^{15} n_{eq.}\,cm^{-2}$ (24 MeV protons at Karlsruhe)									
100	DO-I-13	2426	July 2011	50586−50586	4950±300	86.9345±0.3893	95.39	3.59	0.70
200	DO-I-13	2678	July 2011	50598−50599	9150±150	84.7078±0.1010	84.17	13.05	1.51
200	DO-I-13	2426	July 2011	50585−50585	10650±150	89.2569±0.3502	86.48	10.78	1.56
300	DO-I-13	2426	July 2011	50584−50584	14550±0	89.6682±0.3472	79.94	16.55	1.68
600	DO-I-13	2426	July 2011	50587−50587	15750±600	88.2541±0.3882	78.07	18.21	1.86
800	DO-I-13	2828	July 2011	50578−50582	14550±0	93.6371±0.0587	78.56	17.84	1.85
1000	DO-I-13	2426	July 2011	50588−50597	14850±0	93.7044±0.0336	73.84	21.67	2.35
$\psi = 1.9 \times 10^{15} n_{eq.}\,cm^{-2}$ (24 MeV protons at Karlsruhe)									
200	DO-38	3263	May 2012	883−907	5850±1116	96.0241±0.0293	84.26	12.18	1.88
600	DO-38	3250	May 2012	767−795	16050±100	93.7131±0.0295	78.76	16.89	2.10
800	DO-38	3245	May 2012	797−833	16650±100	93.8681±0.0299	78.40	17.27	2.08
1000	DO-38	3238	May 2012	835−882	17250±837	93.3214±0.0240	79.34	16.99	1.86
$\psi = 2.2 \times 10^{15} n_{eq.}\,cm^{-2}$ (24 MeV protons at Karlsruhe)									
300	DO-I-7	3162	Sep 2011	61249−61249	10650±300	97.6575±0.2691	89.49	8.58	0.96
400	DO-I-7	3162	Sep 2011	61250−61251	13050±150	98.1329±0.1850	85.71	11.42	1.53
500	DO-I-7	3246	Sep 2011	61281−61289	13350±418	98.4010±0.0315	83.84	13.10	1.61
500	DO-I-7	3162	Sep 2011	61252−61252	13050±0	97.9449±0.2967	85.13	11.81	1.65
600	DO-I-7	3162	Sep 2011	61253−61253	13950±0	97.7808±0.2438	84.03	12.62	1.67
600	DO-I-7	3209	Sep 2011	61298−61303	13650±976	97.7432±0.0421	82.54	14.05	1.74
700	DO-I-7	3162	Sep 2011	61254−61254	14250±150	97.5264±0.2493	82.56	13.96	1.93
800	DO-I-7	3162	Sep 2011	61264−61273	14550±1674	98.2999±0.0266	82.28	14.24	1.85
900	DO-I-7	3162	Sep 2011	61256−61256	15150±290	98.0145±0.2171	82.26	14.27	1.76

Table 9.1: Overview of testbeam results for DUTs at $\eta = 0$ and $\phi = 0$.

U [V]	DUT	Threshold [electrons]	Testbeam	Run range	Charge [electrons]	Hit efficiency [%]	CS1 [%]	CS2 [%]	CS3 [%]
1000	DO-I-7	3241	Sep 2011	61290−61296	15450±279	98.3107±0.0284	80.92	15.31	1.96
1000	DO-I-7	3162	Sep 2011	61257−61257	15750±0	98.9806±0.1584	82.06	14.62	1.68
1100	DO-I-7	3162	Sep 2011	61258−61259	15750±150	98.1071±0.1210	81.94	14.54	1.96
1200	DO-I-7	3162	Sep 2011	61260−61260	16650±0	97.4465±0.2533	82.56	13.73	2.10
1200	DO-I-7	3190	Sep 2011	61304−61315	16050±5440	98.3414±0.0284	80.52	15.69	2.04
1400	DO-I-7	3162	Sep 2011	61262−61262	16050±300	98.1018±0.1909	84.02	12.54	1.91
1500	DO-I-7	3162	Sep 2011	61263−61263	16650±590	98.3047±0.1834	84.20	12.66	1.75
$\psi = 5.0 \times 10^{15} \mathrm{n_{eq.}}\,\mathrm{cm}^{-2}$ (Reactor neutrons at Ljubljana)									
300	DO-13	3820	Feb 2011	31066−31069	3750±100	81.4758±0.0944	97.89	1.86	0.22
350	DO-13	3820	Feb 2011	31140−31165	4350±100	88.3203±0.0338	97.43	2.21	0.30
350	DO-13	3820	Feb 2011	31071−31082	4350±100	86.5586±0.0560	97.48	2.18	0.28
500	DO-13	3820	Feb 2011	31037−31064	4950±100	88.1423±2.0325	56.18	14.00	8.43
1000	DO-13	3820	Feb 2011	30684−30715	10350±100	92.3011±0.0253	60.08	13.20	7.99
$\psi = 1 \times 10^{16} \mathrm{n_{eq.}}\,\mathrm{cm}^{-2}$ (24 MeV protons at Karlsruhe)									
500	DO-I-11	3154	Sep 2011	61249−61249	4050±150	79.3718±0.6807	97.52	1.80	0.30
600	DO-I-11	2158	July 2011	50584−50584	4050±300	93.3333±4.5542	67.60	11.27	5.76
600	DO-I-11	3154	Sep 2011	61250−61251	4650±0	83.3860±0.4933	92.43	3.71	1.09
600	DO-I-11	3202	Sep 2011	61298−61303	4650±976	82.7320±0.1033	91.27	3.91	1.50
700	DO-I-11	3154	Sep 2011	61252−61252	4950±290	81.2728±0.7855	84.42	6.24	2.37
800	DO-I-11	3068	July 2011	50578−50582	5850±0	71.7320±1.8202	70.14	10.33	5.57
800	DO-I-11	3154	Sep 2011	61253−61253	5850±440	90.7643±0.4717	82.15	6.95	3.24
900	DO-I-11	3154	Sep 2011	61254−61254	6150±150	92.1746±0.4316	84.94	5.94	2.85
1000	DO-I-11	2346	July 2011	50598−50599	6450±300	66.4619±0.1309	53.31	14.69	8.17
1000	DO-I-11	3222	Sep 2011	61281−61289	6450±418	93.8536±0.0611	82.90	7.11	2.91

Table 9.1: Overview of testbeam results for DUTs at $\eta = 0$ and $\phi = 0$.

U [V]	DUT	Threshold [electrons]	Testbeam	Run range	Charge [electrons]	Hit efficiency [%]	CS1 [%]	CS2 [%]	CS3 [%]
1100	DO-I-11	3154	Sep 2011	61256−61256	7050±150	94.8319±0.3507	72.15	10.03	5.18
1100	DO-I-11	2158	July 2011	50585−50585	4650±600	83.7724±0.4169	66.07	11.95	6.12
1200	DO-I-11	3154	Sep 2011	61257−61257	7650±440	94.4072±0.3689	65.98	11.70	6.03
1200	DO-I-11	2158	July 2011	50586−50586	4950±450	82.7901±0.4345	64.79	12.50	6.20
1300	DO-I-11	3154	Sep 2011	61264−61273	7650±1674	95.0503±0.0460	67.63	11.63	5.58
1300	DO-I-11	3154	Sep 2011	61258−61259	7650±140	94.4444±0.2097	64.40	12.02	6.21
1400	DO-I-11	2158	July 2011	50587−50587	6150±150	100.0000±0.0000	62.67	13.69	6.68
1400	DO-I-11	3154	Sep 2011	61260−61260	8250±150	92.3794±0.4393	58.76	13.68	7.09
1500	DO-I-11	3205	Sep 2011	61290−61296	8250±279	94.4777±0.0515	60.33	13.81	6.93
1500	DO-I-11	2158	July 2011	50588−50597	7350±0	82.0626±0.0518	57.94	15.73	7.22
1600	DO-I-11	3154	Sep 2011	61262−61262	9150±300	91.4606±0.4028	55.65	14.66	7.90
1700	DO-I-11	3154	Sep 2011	61263−61263	9750±150	90.2491±0.4347	53.81	15.06	7.98
1800	DO-I-11	3187	Sep 2011	61304−61315	10050±5301	92.8693±0.0589	55.77	14.90	7.74
$\psi = 1.4 \times 10^{16} n_{eq.}\,cm^{-2}$ (24 MeV protons at Karlsruhe)									
500	DO-I-12	3959	Sep 2011	61249−61249	3750±150	41.3223±1.1558	95.92	3.09	0.62
500	DO-I-5	3616	Sep 2011	61249−61249	3750±150	54.2710±1.2625	96.24	2.56	0.68
600	DO-I-12	3959	Sep 2011	61250−61251	3750±0	63.0697±0.8276	96.27	2.61	0.37
600	DO-I-12	4026	Sep 2011	61298−61303	3750±698	53.9958±0.1746	96.15	2.52	0.56
600	DO-I-5	3616	Sep 2011	61250−61251	3750±0	61.8885±0.9458	97.06	2.23	0.40
600	DO-I-5	3675	Sep 2011	61298−61303	3450±837	54.8949±0.1817	97.61	1.80	0.32
700	DO-I-12	3959	Sep 2011	61252−61252	4350±150	67.0251±1.2587	96.74	2.25	0.62
700	DO-I-5	3616	Sep 2011	61252−61252	4050±150	76.2030±1.2596	97.28	1.71	0.47
800	DO-I-12	3959	Sep 2011	61253−61253	4650±300	70.9649±0.9506	95.89	2.99	0.68
800	DO-I-5	3616	Sep 2011	61253−61253	4350±300	76.6935±1.0130	97.54	1.94	0.31
900	DO-I-12	3959	Sep 2011	61254−61254	4950±290	73.9112±0.8986	96.17	2.86	0.47

Table 9.1: Overview of testbeam results for DUTs at $\eta = 0$ and $\phi = 0$.

U [V]	DUT	Threshold [electrons]	Testbeam	Run range	Charge [electrons]	Hit efficiency [%]	CS1 [%]	CS2 [%]	CS3 [%]
900	DO-I-5	3616	Sep 2011	61254−61254	4950±290	78.4734±0.9632	96.96	2.07	0.64
1000	DO-I-5	3701	Sep 2011	61281−61289	5250±418	73.3123±0.1462	96.57	2.64	0.45
1000	DO-I-5	3372	Sep 2011	61112−61120	5250±4324	74.8445±0.1343	97.23	2.22	0.33
1000	DO-I-12	4060	Sep 2011	61281−61289	5250±418	84.4567±0.1144	94.67	3.12	0.78
1100	DO-I-5	3616	Sep 2011	61256−61256	5550±150	83.8032±0.8662	96.10	3.08	0.43
1100	DO-I-5	3372	Sep 2011	61124−61128	5250±279	74.8445±0.0000	97.23	2.22	0.33
1100	DO-I-12	3959	Sep 2011	61256−61256	5550±150	91.3043±0.5602	93.79	4.01	0.73
1200	DO-I-12	3959	Sep 2011	61257−61257	6150±300	91.5346±0.5684	93.78	3.99	0.68
1200	DO-I-5	3616	Sep 2011	61257−61257	5850±300	81.3622±0.8948	95.48	3.43	0.54
1300	DO-I-12	3959	Sep 2011	61264−61273	6150±1534	89.4540±0.0872	87.79	5.55	1.88
1300	DO-I-12	3959	Sep 2011	61258−61259	6150±140	92.2462±0.3114	90.86	4.98	1.43
1300	DO-I-5	3616	Sep 2011	61258−61259	6150±140	84.6068±0.4558	95.14	3.87	0.49
1300	DO-I-5	3616	Sep 2011	61264−61273	6150±1534	78.2479±0.1152	95.76	3.41	0.50
1400	DO-I-12	3959	Sep 2011	61260−61260	6450±150	79.4906±0.8535	91.03	4.92	1.75
1400	DO-I-5	3616	Sep 2011	61260−61260	6450±150	85.3726±0.8334	95.28	3.69	0.69
1500	DO-I-5	3950	Sep 2011	61130−61146	6750±5022	76.4642±0.1307	96.94	2.46	0.40
1500	DO-I-12	4050	Sep 2011	61290−61296	6750±279	89.3333±0.1206	88.32	5.24	1.73
1500	DO-I-5	3701	Sep 2011	61290−61296	6750±279	82.4525±0.1136	94.66	4.34	0.63
1600	DO-I-5	3616	Sep 2011	61262−61262	7050±300	88.8009±0.6273	94.75	4.20	0.64
1600	DO-I-12	3959	Sep 2011	61262−61262	7350±440	93.0217±0.4724	88.70	5.64	1.57
1700	DO-I-5	3616	Sep 2011	61263−61263	7650±290	89.2238±0.6301	93.95	4.70	1.01
1700	DO-I-12	3959	Sep 2011	61263−61263	7650±150	94.6379±0.4203	87.45	5.54	1.67
1800	DO-I-5	3669	Sep 2011	61304−61315	7950±5301	79.0082±0.1379	83.40	10.34	3.30
1800	DO-I-12	4023	Sep 2011	61304−61315	8250±0	90.8174±0.1291	83.08	7.26	2.86

Table 9.1: Overview of testbeam results for DUTs at $\eta = 0$ and $\phi = 0$.

U [V]	DUT	Threshold [electrons]	Testbeam	Run range	Charge [electrons]	Hit efficiency [%]	CS1 [%]	CS2 [%]	CS3 [%]
$\psi = 2 \times 10^{16} n_{eq.}$ cm^{-2}(Reactor neutrons at Ljubljana)									
400	DO-10	2964	May 2012	883−907	2850±1256	24.3603±0.0541	95.45	4.38	0.10
400	DO-24	2877	May 2012	883−907	2850±1116	53.0121±0.0709	97.98	1.62	0.21
600	DO-10	2942	May 2012	767−795	3150±100	67.0165±0.0488	94.13	5.66	0.15
600	DO-24	2854	May 2012	767−795	3450±100	79.8805±0.0485	97.77	1.75	0.28
800	DO-10	2944	May 2012	797−833	3450±100	87.6424±0.0358	94.89	4.81	0.21
800	DO-24	2846	May 2012	797−833	4050±100	89.3866±0.0381	97.04	2.30	0.41
1000	DO-24	2837	May 2012	739−765	4650±1116	92.8186±0.0327	96.39	2.83	0.49
1000	DO-10	2934	May 2012	739−765	4050±1116	93.0467±0.0276	93.95	5.67	0.27
1500	DO-24	2840	May 2012	835−882	5850±1116	95.8649±0.0193	94.03	4.79	0.71
1500	DO-10	2939	May 2012	835−882	5250±1256	96.2197±0.0157	93.36	5.98	0.45
2000	DO-10	3461	Aug 2012	71579−71628	7650±0	96.8684±0.0306	89.97	9.27	0.51
2000	DO-24	2707	Aug 2012	71579−71628	7650±0	94.8522±0.0373	73.06	20.33	4.86

Table 9.1: Overview of testbeam results for DUTs at $\eta = 0$ and $\phi = 0$.

9.3.3 Sub Pixel Resolved Results

One main advantage of test beam measurements is that the hit information can be gained with a higher resolution when built into the DUT, due to the telescope tracking. There is a particularly interesting representation, which projects the sub pixel resolved physical values, such as the hit efficiency or mean charge, on the area of one virtual pixel. In fig. 9.34 such hit efficiency plots are shown for the DUT DO-I-11 (proton irradiated to a fluence of $1.0 \times 10^{16} \mathrm{n_{eq.}\ cm^{-2}}$) at different bias voltages.

In this case the aspect ratio was corrected to the values of a real standard pixel, in order to make it easier comparable to the cell layout. The schematic of a pixel cell, generated directly from the GDS-II[1] design file, is shown as well. In general, it shows a high hit efficiency which is homogenously distributed. The rapid decline around the edges is noticeable. This is mostly due to charge sharing among adjacent

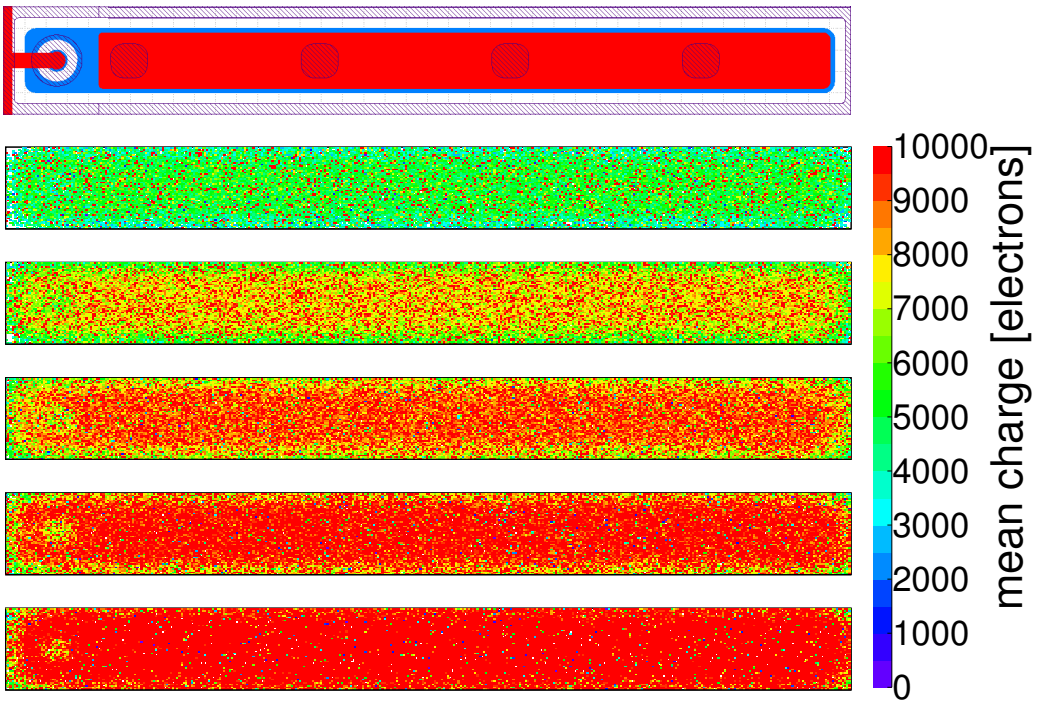

Figure 9.33: Sub pixel resolved mean charge for DO-I-11 assembly. The area represents one virtual pixel where all hits are projected on. The shown plots are generated from run ranges taken during the September 2011 test beam campaign at CERN SPS. During each run range the DUT was operated with a different bias voltage, from top to bottom these are: 600 V, 1000 V, 1300 V, 1500 V and 1800 V. When comparing the results with the layout schematic on the top one can observe that the mean charge is decreased around the edges and particularly in the bias dot region. This effect is less pronounced than in the correspnding hit efficiency plot.

1 **G**raphic **D**atabase **S**ystem - II

pixels and can be also observed at lower fluences. More striking is the pronounced circle at the left short side, which also demonstrates a low hit efficiency. It directly correlates with the drop of the mean charge, what can be seen in fig. 9.33. At this point the so-called bias dot is located. This is a separate implant zone connected to the metal layer of the bias grid. Obviously, due to this layout feature, charge gets lost und decreases the hit efficiency.

Due to the huge impact on the global hit efficiency, it is under consideration how this might be avoided. One idea is to omit the bias grid completely, but that makes testing at an unflipped state almost impossible. Other options are a temporary metal layer to be removed after testing or a change of the bias grid layout resulting in less charge collection loss.

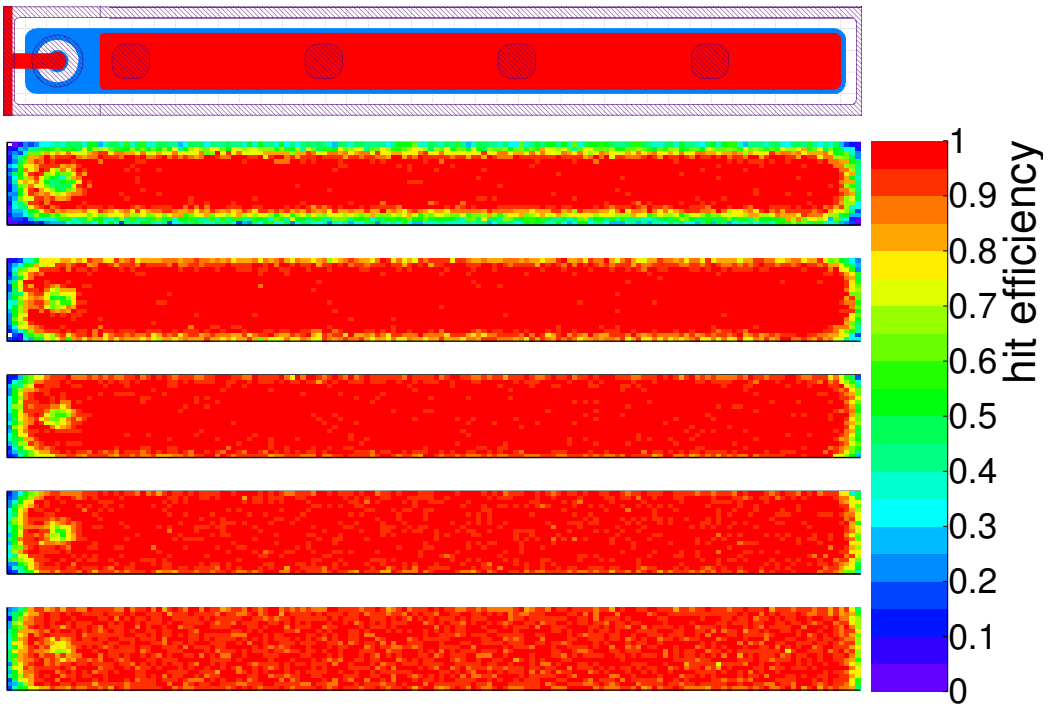

Figure 9.34: Sub pixel resolved hit efficiency for the DO-I-11 assembly. The area represents one virtual pixel where all hits are projected on. The shown plots are generated from run ranges taken during the September 2011 test beam campaign at CERN SPS. During each run range the DUT was operated with a different bias voltage, from top to bottom these are: 600 V, 1000 V, 1300 V, 1500 V and 1800 V. When comparing the results with the layout schematic on the top, it becomes obvious that most of the hit efficiency gets lost around the edges and particularly in the bias dot region.

9.4 Annealing Studies

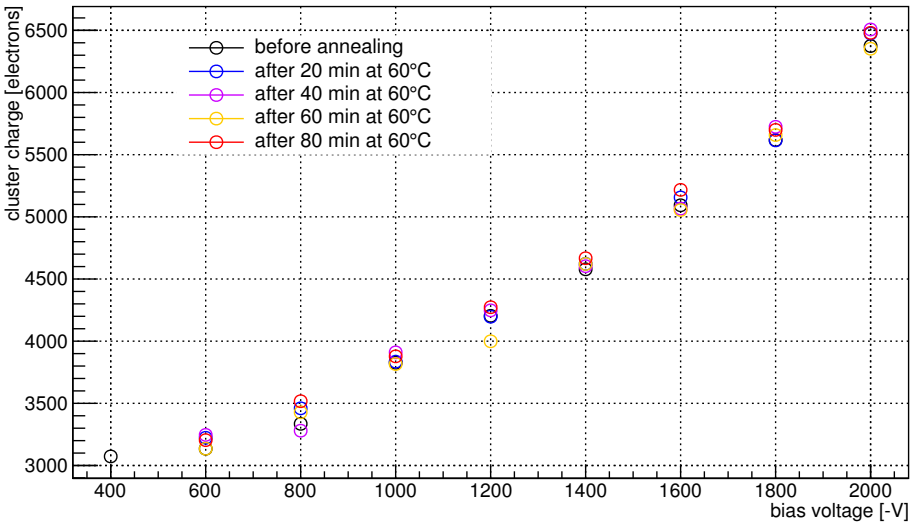

Figure 9.35: Cluster charge plotted against the bias voltage for different annealing steps (assembly DO-10). Based on data by [Wiz13].

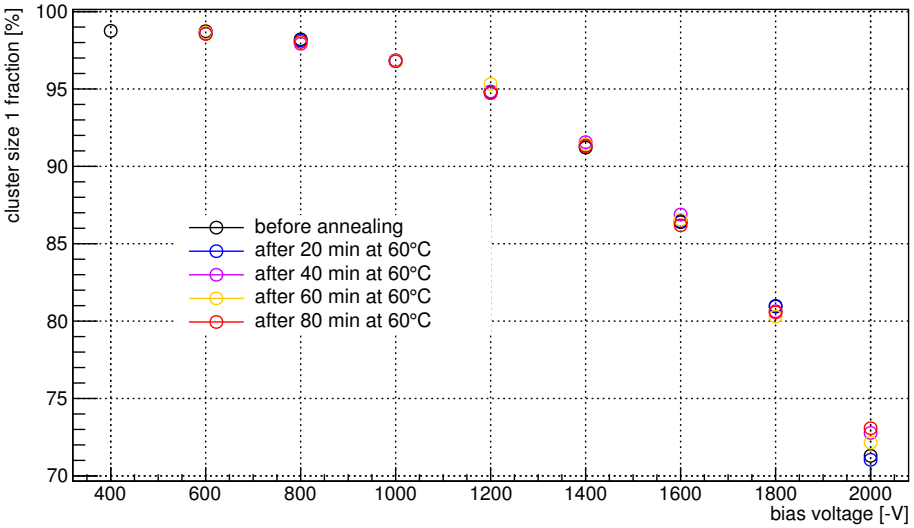

Figure 9.36: Fraction of clusters with the size of 1 hit plotted against the bias voltage for different annealing steps (assembly DO-10). Based on data by [Wiz13].

It is important to study the annealing behaviour of the sensors as the real detector will receive deliberate (in order to minimize the leakage current, see section 4.5),

planned (shutdown of cooling plant for maintenance) and probably involuntary (due to cooling failure) annealing.

For this purpose, in collaboration with [Wiz13] (see appendix D), the assembly DO-10 was heated four times at 60 °C in an oven for 20 minutes at a time. During the annealing the assembly was unpowered and disconnected from the readout system. After each annealing step, source scans with a $^{90}_{38}$Sr source were taken for several bias voltages. This was done in the course of the same study as in section 9.1.4. The same DUT was employed but a new ToT calibration was created after each annealing step and bias voltage variation. In fig. 9.35 the charge is plotted against the bias voltage. There is no obvious change in the collected charge after 80 min of annealing. This is in contrast with certain results where charge amplification was observed.

There are indications that especially long term annealing might increase that effect. As shown in section 9.3 some kind of charge amplification effect has to be active in the higher irradiated n^+-in-n assemblies, because there has been more charge observed than expected from the trapping model. At the same time the satiation towards higher bias voltages is atypical. Therefore, either the annealing behaviour is atypical as well or there might be some effect after longer annealing times. This has to be investigated in further studies. Figure 9.36 shows the influence of the bias voltage on the cluster size distribution. After the annealing the fraction of larger clusters at high bias voltages seems to have increased slightly.

CHAPTER 10

Conclusions and Outlook

The ATLAS[1] detector at the LHC[2] accelerator, located at CERN[3], Geneva, currently undergoes its first planned long shutdown, after having taken successfully data for three years. The analysis of the existing data has already confirmed the existence of the long sought Higgs-boson, which completes the particle zoo of the standard model. Now it is pending, among other things, to measure its properties and to continue the search for new physics.

Within ATLAS the installation of a fourth pixel layer, called IBL[4], is currently ongoing. This fourth pixel layer will help the pixel detector to balance out the loss of efficiency caused by radiation damage particularly in the inner-most layer. Around 2021/2022 it is foreseen to replace the whole inner tracker of ATLAS with a new full silicon tracker. This will be necessary due to the radiation damage accumulated by then and in order to prepare ATLAS for the conditions expected after the phase 2 upgrade of the LHC, which entails an increase in luminosity and thus in occupancy.

In this thesis sensors from the original ATLAS production, as well as from dedicated R&D wafer productions, were used to create assemblies read out by the FE-I3 readout electronics. They were irradiated with reactor neutrons at Ljubljana, high energy protons at CERN-PS[5] and low energy protons in Karlsruhe. The most strongly irradiated assemblies were exposed to a fluence of $2 \times 10^{16} \mathrm{n_{eq.}}\,\mathrm{cm}^{-2}$.

For the operation of the sensors a higher bias voltage had to be applied than previously used, going up to $-2000\,\mathrm{V}$. In order to achieve this, the carrier PCB[6] had to be modified, as the already existing PCB was not able to withstand such a high voltage. Furthermore, a solution for the necessary cooling had to be found.

1 **A** **T**oroidal **L**HC **A**pparatu**S**
2 **L**arge **H**adron **C**ollider
3 **C**onseil **E**uropéen pour la **R**echerche **N**ucléaire
4 **I**nsertable **B**-**L**ayer
5 **P**roton **S**ynchrotron - accelerator at CERN
6 **P**rinted **C**ircuit **B**oard

One option used for the cooling employs dry ice. This proved to be a very robust solution as it works without any moveable parts and complicated electronics. Its disadvantage is that on its own it is not controllable. An attempt to circumvent this limitation by using counter heating proved successful.

Another cooling system implemented in this thesis uses a deep temperature chiller with an external cooling circuit and an attached heat exchanger. This allows both an inherent control of the temperature and running for a basically unlimited time without the necessity for replacing regularly dry ice blocks. Its disadvantage is a certain vulnerability of the chiller and that rapid changes in the temperature are not possible.

Special attention was paid to the transfer of the heat from the assembly to the heat sink. This is particularly difficult due to the fact that the heat produced in the sensor has to pass through several layers of material (bump bonds, frontend, glue and PCB) with a low thermal conductivity. After preliminary studies a low-tech solution using copper tape was identified as adequate.

This thesis demonstrates for the first time, that highly irradiated planar silicon pixel sensors can be operated successfully and reliably after having been irradiated to a fluence of $2 \times 10^{16} \mathrm{n_{eq.}\,cm^{-2}}$. This was done with a focus on the charge collection efficiency using radioactive sources in the lab as well as particle beams at test beam facilities. Using those six test beam campaigns at DESY[1] and CERN-SPS[2] an absolute hit efficiency could be derived. The hit efficiency demonstrated by highly irradiated assemblies at moderate bias voltages of $-1000\,\mathrm{V}$ to $-1500\,\mathrm{V}$ was in a fully satisfactory zone of above 95%.

A model for the observed dependency between the collected charge and the hit efficiency was created and tested. It is based on the threshold dispersion. The test beam measurements offer a sufficiently high resolution for estimating the charge collection and hit efficiency in sub-pixel resolution. The drop in hit efficiency could be thus attributed to a layout feature of the pixel sensor — the bias dot. This is a part of the so-called bias grid, which is necessary for testing the sensor.

In future studies new ways to get rid off this source of inefficiency will be studied (no bias grid, temporary metal layer, different bias grid layouts). Furthermore, when the sensors are mounted at (more realistic) steeper angles, the hit efficiency will increase even more. This shows that planar $\mathrm{n^+}$-in-n sensors could be able to cope with the conditions in the b-layer of the phase 2 pixel detector replacement towards its projected end-of-life fluence of $2 \times 10^{16} \mathrm{n_{eq.}\,cm^{-2}}$.

The results obtained with assemblies irradiated to fluences ranging from moder-

1 **D**eutsches **E**lektronen **SY**nchrotron
2 **S**uper **P**roton **S**ynchrotron

ate $5 \times 10^{15} \mathrm{n_{eq.}}\,\mathrm{cm}^{-2}$ to very high $2 \times 10^{16} \mathrm{n_{eq.}}\,\mathrm{cm}^{-2}$ show that much more charge is collected than expected from the trapping model. The correlation between the applied bias voltage and the collected charge is linear for the highest irradiated assemblies, what is compatible with the usual electric field model of a sensor which is over-depleted. Naturally, these highly irradiated sensors cannot be depleted at such low voltages, so that this model cannot be correct. The surplus of charge must be explained by charge amplification, similar to the effect observed previously in strip detectors.

In contrast to many of the alternative observations, explained by impact ionisation, no exponential behaviour was observed and the charge satiated. This indicates some kind of limiting mechanism. In order to illuminate the exact activity inside the sensor, certain test beam runs taken during this work might prove helpful in the future as well. These are measurements at very steep angles which make it possible to excite the sensor at defined depths. The evaluation of these data is technically very challenging.

The main challenge has been to disentangle the effects of irradiated sensors and irradiated readout electronics. The latter poses a special difficulty, as no sufficiently radiation hard readout electronics was available at the time of the studies. The successor of the used FE-I3, the FE-I4, only became available later on. Nevertheless, using a sufficiently high variety of assemblies yielded enough working modules after irradiation. Alternatively, a low temperature flip-chip process with indium bumps was employed and worked very well. The cross-check between the assemblies with irradiated and unirradiated frontends did not show any huge difference in the results.

In order to improve the understanding of the FE-I3, dedicated studies on its behaviour depending on temperature, bias voltage and annealing were conducted. In particular, the temperature and bias voltage have a huge impact on the calculated (not real) charge and threshold. The conclusion is that for precise measurements, especially of the charge, it is important to keep the conditions as stable as possible and to retune the assembly promptly.

One of the highest irradiated assemblies was used for a limited annealing study. Up to an annealing time of 80 min at 60 °C, which should keep the sensor well in the zone of beneficial annealing, no significant influence on the charge collection was observed. This program will be continued in order to investigate long term annealing.

For the control and monitoring of the conditions during the lab and test beam measurements a control system called testbeamDCS was developed.

An additional method for avoiding the use of irradiated frontends is the fanout, a new tool for the study of irradiated pixel sensors. The intention behind its development is to disentangle completely the effects on the frontend and sensor by using a discrete readout electronics. It even allows to replace the electronics several times, thus making inter-calibration examinations similar to strip sensors possible. The

main complication was the high sensitivity to electromagnetic interference (causing noise), which became manageable by using a shielding box and proper grounding.

A system for the quick IV-characterization of a fanout, using a limited number of picoamperemeters, was developed as well. This is useful to determine good pixel channels. Those studies should be continued by using already irradiated fanout assemblies (up to a fluence of $5 \times 10^{16} \mathrm{n_{eq.}\,cm^{-2}}$), much more than possible with available frontend chips) and systematically studying them, including bias scans, annealing and other sensor materials such as MCz[1]. Sensors from MCz require mixed irradiation.

Moreover, it might be possible to read out more channels using a strip readout system (like the Beetle[2]-chip for the LHCb[3] strip detector). In this way the fanout system might even become test beam capable.

Another avenue might be the combination of the fanout readout system with a laser injected TCT[4] setup. The capacitance of even highly irradiated pixel cells should be small enough for usable TCT signals, in contrast to pad diodes that can no longer be successfully characterized above a certain fluence. Finally, a fanout chip compatible with the FE-I4 could be designed and fabricated.

1 **M**agnetic **Cz**ochralski
2 http://www.kip.uni-heidelberg.de/lhcb/
3 **LHC-b**eauty
4 **T**ransient **C**urrent **T**echnique

Bibliography

[Abt13] Mona Abt. 'Aufbau eines Messplatzes zur automatischen IV-Charakterisierung von Fanout-basierten n^+-in-n planaren Siliziumpixelsensoren'. Bachelor thesis. TU Dortmund, Sept. 2013 (cit. on p. 49).

[Bon14a] Universität Bonn. *Description of the USBpix-system*. 2014. URL: `http://icwiki.physik.uni-bonn.de/twiki/bin/view/Systems/UsbPix` (visited on 03/16/2014) (cit. on pp. 57, 58).

[Bon14b] Universität Bonn. *STcontrol user manual – FE-I3 version*. 2014. URL: `http://icwiki.physik.uni-bonn.de/twiki/bin/view/Systems/STcontrolUserGuide` (visited on 03/16/2014) (cit. on p. 57).

[Cap+10] Mar Capeans et al. *ATLAS insertable b-layer technical design report*. Tech. rep. CERN-LHCC-2010-013. ATLAS-TDR-19. Geneva: CERN, Sept. 2010 (cit. on p. 32).

[Cas+10] Gianluigi Casse et al. 'Enhanced efficiency of segmented silicon detectors of different thicknesses after proton irradiations up to $1 \times 10^{16}\,n_{eq}cm^{-2}$'. In: *Nuclear Instruments and Methods in Physics Research Section A: Accelerators, Spectrometers, Detectors and Associated Equipment* 624.2 (Dec. 2010), pp. 401–404. ISSN: 0168-9002. URL: `http://www.sciencedirect.com/science/article/pii/S0168900210003906` (cit. on p. 30).

[Cer] 'TCC2, the target hall of the SPS North Area'. CERN-PHOTO-7801703X. Jan. 1978. URL: `http://cds.cern.ch/record/917351?ln=en` (cit. on p. 67).

[Chi13] Alexander Chilingarov. 'Temperature dependence of the current generated in Si bulk'. In: *Journal of Instrumentation* 8.10 (2013), P10003. URL: `http://stacks.iop.org/1748-0221/8/i=10/a=P10003` (cit. on pp. 18, 21).

[DES12] DESY. *Overview accelerator chain at DESY*. 2012. URL: `http://hasylab.desy.de/images/content/e81/e83/imageobject147/DESY-Beschleuniger_ger.jpg` (visited on 05/12/2012) (cit. on p. 67).

[Dob04] Daniel Adam Dobos. 'Production accompanying testing of the ATLAS Pixel module'. CERN-THESIS-2007-016. Diploma thesis. Universität Dortmund, 2004 (cit. on pp. 13–15, 36, 54, 56).

[Ere+11] Vladimir Eremin et al. 'Avalanche effect in Si heavily irradiated detectors: Physical model and perspectives for application'. In: *Nuclear Instruments and Methods in Physics Research Section A: Accelerators, Spectrometers, Detectors and Associated Equipment* 658.1 (Dec. 2011), pp. 145–151. ISSN: 0168-9002. URL: http://www.sciencedirect.com/science/article/pii/S0168900211008461 (cit. on p. 30).

[Hüg01] Fabian Georg Hügging. 'Der ATLAS Pixelsensor – Der state-of-the-art Pixelsensor für teilchenphysikalische Anwendungen mit extrem hohen Strahlungsfeldern'. PhD thesis. Universität Dortmund, 2001 (cit. on p. 14).

[KL04] Jonas M. Klaiber-Lodewigs. *Pixel Sensor Quality Assurance Plan*. ATLAS Project Document ATL-IP-QP-0001. ATLAS, Apr. 2004 (cit. on p. 53).

[Kle11] Stephan von Kleist. 'Charakterisierungsmessungen von ATLAS-Pixel-Teststrukturen mit verschiedenen automatisierten Messverfahren'. Bachelor thesis. TU Dortmund, Mar. 2011 (cit. on pp. 49, 53).

[Koh02] Robert Kohrs. 'Charakterisierung von ATLAS-Pixelmodulen im Laserstrahl und hinsichtlich der 'bump'- und 'flip-chip'-Technologie'. BONN-IB-2002-15. Diploma thesis. Universität Bonn, 2002 (cit. on p. 21).

[Kra09] Gregor Kramberger. *personal communication*. The received fluence at the reactor is calculated from the reactor power and irradiation time. Regular calibrations and cross-checks of this relation (also spatially within irradiation container 2R=2.5, H=10 cm) are performed. Therefore the uncertainty in fluence is known to be less than 10%. 2009 (cit. on p. 40).

[Kra+02] Gregor Kramberger et al. 'Determination of effective trapping times for electrons and holes in irradiated silicon'. In: *Nuclear Instruments and Methods in Physics Research Section A: Accelerators, Spectrometers, Detectors and Associated Equipment* 476.3 (2002), pp. 645–651. ISSN: 0168-9002. DOI: 10.1016/S0168-9002(01)01653-9. URL: http://www.sciencedirect.com/science/article/B6TJM-44T1BJN-H/2/7094ace5d2a864587bad6e934b1533af (cit. on p. 30).

[Kra+09] Gregor Kramberger et al. 'Investigation of electric field and charge multiplication in silicon detectors by Edge-TCT'. In: *Nuclear Science Symposium Conference Record (NSS/MIC), 2009 IEEE*. 2009, pp. 1740–1748. DOI: 10.1109/NSSMIC.2009.5402213 (cit. on p. 30).

[Kra+10] Gregor Kramberger et al. 'Investigation of Irradiated Silicon Detectors by Edge-TCT'. In: *Nuclear Science, IEEE Transactions on* 57.4 (2010), pp. 2294–2302. ISSN: 0018-9499. DOI: 10.1109/TNS.2010.2051957 (cit. on p. 30).

[Lap12] Tobias Lapsien. 'Messungen an hochbestrahlten ATLAS Silizium Pixel Sensoren mit unbestrahlter Ausleseelektronik'. Diploma thesis. TU Dortmund, 2012. URL: http://www.e4.physik.tu-dortmund.de/twiki/pub/E4/Diplomarbeiten/tlapsien_diplomarbeit.pdf (cit. on pp. 55, 70, 78–81).

[Lef08] Christiane Lefèvre. 'The CERN accelerator complex. Complexe des accélérateurs du CERN'. CERN-DI-0812015. Dec. 2008. URL: http://cds.cern.ch/record/1260465?ln=en (cit. on p. 5).

[Lut99] Gerhard Lutz. *Semiconductor Radiation Detectors*. Springer, 1999. URL: http://lmu.web.psi.ch/psd/lutz_sc_rad_detect.pdf (cit. on p. 27).

[Man+11] Igor Mandić et al. 'Annealing effects in n^+-p strip detectors irradiated with high neutron fluences'. In: *Nuclear Instruments and Methods in Physics Research Section A: Accelerators, Spectrometers, Detectors and Associated Equipment* 629.1 (Feb. 2011), pp. 101–105. ISSN: 0168-9002. URL: http://www.sciencedirect.com/science/article/pii/S0168900210025209 (cit. on p. 30).

[Mik+11] Marko Mikuž et al. 'Study of anomalous charge collection efficiency in heavily irradiated silicon strip detectors'. In: *Nuclear Instruments and Methods in Physics Research Section A: Accelerators, Spectrometers, Detectors and Associated Equipment* 636.1, Supplement (Apr. 2011), S50–S55. ISSN: 0168-9002. URL: http://www.sciencedirect.com/science/article/pii/S0168900210009381 (cit. on p. 30).

[Mil+12] Marko Milovanović et al. 'Effects of accelerated long term annealing in highly irradiated n^+-p strip detector examined by Edge-TCT'. In: *Journal of Instrumentation* 7.06 (2012), P06007. URL: http://stacks.iop.org/1748-0221/7/i=06/a=P06007 (cit. on p. 30).

[Mol99] Michael Moll. 'Radiation Damage in Silicon Particle Detectors'. DESY-THESIS-1999-040. PhD thesis. DESY, 1999. URL: http://mmoll.web.cern.ch/mmoll/thesis/ (cit. on pp. 29, 39).

[NIS13] NIST. *XCOM*. 2013. URL: http://physics.nist.gov/PhysRefData/Xcom/Text/XCOM.html (cit. on p. 20).

[Per09] Ivan Perić. 'Hybrid Pixel Particle-Detector Without Bump Interconnection'. In: *Nuclear Science, IEEE Transactions on* 56.2 (2009), pp. 519–528. ISSN: 0018-9499. DOI: 10.1109/TNS.2009.2014951 (cit. on p. 33).

[Per+13] Ivan Perić et al. 'High-voltage pixel detectors in commercial CMOS technologies for ATLAS, CLIC and Mu3e experiments'. In: *Nuclear Instruments and Methods in Physics Research Section A: Accelerators, Spectrometers, Detectors and Associated Equipment* 0 (2013), pp. –. ISSN: 0168-9002. DOI: http://dx.doi.org/10.1016/j.nima.2013.05.006. URL: http://www.sciencedirect.com/science/article/pii/S0168900213005263 (cit. on p. 33).

[Plü12] Till Plümer. 'Fanout enabled charge collection measurements of planar n^+-in-n ATLAS silicon pixel sensors'. Diploma thesis. TU Dortmund, 2012. URL: http://www.e4.physik.tu-dortmund.de/twiki/pub/E4/Diplomarbeiten/final-diploma-thesis-pluemer.pdf (cit. on pp. 44, 46–49).

[Raj03] Silke Rajek. 'Charakterisierung des Ladungssammlungsverhaltens von strahlungsgeschädigten Silizumsensoren für Teilchenphysikalische Anwendungen am LHC'. Diploma thesis. Universität Dortmund, 2003 (cit. on p. 54).

[Rei06] Ingo Reisinger. 'Spatial and vertex resolution studies on the ATLAS Pixel Detector based on Combined Testbeam 2004 data'. Diploma thesis. Universität Dortmund, 2006 (cit. on p. 13).

[Rie14] Julia Rietenbach. 'Further Development on a read-out system for the Fanout'. Master thesis. TU Dortmund, 2014 (cit. on pp. 45, 46).

[Roz13] Alexandre Rozanov. 'Status and future of the ATLAS Pixel Detector at the LHC'. In: *Nuclear Instruments and Methods in Physics Research Section A: Accelerators, Spectrometers, Detectors and Associated Equipment* 0 (2013). ISSN: 0168-9002. DOI: http://dx.doi.org/10.1016/j.nima.2013.05.190. URL: http://www.sciencedirect.com/science/article/pii/S0168900213008164 (cit. on pp. 31, 32).

[Rum09] André Rummler. 'Design and Commissioning of a Setup for Charge Collection Efficiency Measurements of Highly Irradiated ATLAS Pixel Sensors'. Diploma thesis. TU Dortmund, 2009 (cit. on pp. 17, 27, 42, 43).

[Spi06] Helmuth Spieler. *Semiconductor Detector Systems*. 3rd ed. Series on Semiconductor Science and Technology. editors: R.J. Nicholas, H. Kamimura. Oxford science publications, 2006 (cit. on pp. 17, 27, 28, 92).

[Tro12] Georg Troska. 'Development and operation of a testbeam setup for qualification studies of ATLAS pixel sensors'. PhD thesis. TU Dortmund, 2012. URL: http://hdl.handle.net/2003/29351 (cit. on pp. 11, 28, 44, 56, 65, 66, 68, 70).

[Web04] Jens Weber. 'Production Accompanying Measurements on the ATLAS Pixel Sensor'. Diploma thesis. Universität Dortmund, 2004 (cit. on p. 15).

[Wei13] Philipp Weigell. 'Investigation of Properties of Novel Silicon Pixel Assemblies Employing Thin n-in-p Sensors and 3D-Integration'. PhD thesis. Technische Universität München, 2013. URL: http://publications.mppmu.mpg.de/2013/MPP-2013-5/FullText.pdf (cit. on p. 57).

[Wit13] Tobias Wittig. 'Slim edge studies, design and quality control of planar ATLAS IBL pixel sensors'. PhD thesis. TU Dortmund, June 2013. URL: http://hdl.handle.net/2003/30362 (cit. on pp. 31, 35).

[Wiz13] Felix Wizemann. 'Annealing abhängige Messungen an einem hochbestrahlten planaren n^+-in-n Silizium-Pixelsensor-FE-I3-Assembly'. Bachelor thesis. TU Dortmund, July 2013 (cit. on pp. 64, 82, 112, 113).

[Wun92] Renate Wunstorf. 'Systematische Untersuchungen zur Strahlenresistenz von Silizium-Detektoren für die Verwendung in Hochenergiephysik-Experimenten'. PhD thesis. Universität Hamburg, 1992. URL: http://www-library.desy.de/preparch/desy/int_rep/fh1k-92-01.pdf (cit. on p. 28).

[ATL12a] ATLAS Collaboration. *ATLAS Insertable B-Layer Technical Design Report Addendum*. Tech. rep. CERN-LHCC-2012-009. ATLAS-TDR-19-ADD-1. Addendum to CERN-LHCC-2010-013, ATLAS-TDR-019. Geneva: CERN, May 2012 (cit. on p. 32).

[ATL12b] ATLAS Collaboration. *Letter of Intent for the Phase-II Upgrade of the ATLAS Experiment*. Tech. rep. CERN-LHCC-2012-022. LHCC-I-023. Geneva: CERN, Dec. 2012. URL: http://cds.cern.ch/record/1502664/?ln=de (cit. on pp. 31, 33).

[ATL13a] ATLAS Collaboration. *Short description of the ATLAS SCT detector*. 2013. URL: http://atlas.ch/sct.html (visited on 04/06/2013) (cit. on p. 11).

[ATL13b] ATLAS Collaboration. *Short description of the ATLAS TRT detector*. 2013. URL: http://atlas.ch/trt.html (visited on 04/06/2013) (cit. on p. 10).

[ATL13c] ATLAS Upgrade Steering Committee. *ATLAS Upgrade Steering Committee webpage*. 2013. URL: https://atlas.web.cern.ch/Atlas/Upgrade/ (visited on 04/12/2013) (cit. on p. 34).

[ATL96a] ATLAS Collaboration. *ATLAS Liquid Argon Calorimeter : Technical Design Report*. Tech. rep. CERN/LHCC/96-41. CERN, 1996 (cit. on p. 9).

[ATL96b] ATLAS Collaboration. *ATLAS Tile Calorimeter : Technical Design Report*. Tech. rep. CERN/LHCC/96-42. CERN, 1996 (cit. on p. 9).

[ATL97a] ATLAS Collaboration. *ATLAS Barrel Toroid : Technical Design Report*. Tech. rep. CERN/LHCC/97-019. ATLAS-TDR-7. CERN, 1997 (cit. on p. 9).

[ATL97b] ATLAS Collaboration. *ATLAS End-Cap Toroids : Technical Design Report*. Tech. rep. ATLAS-TDR-8; CERN-LHCC-97-020. CERN, 1997. URL: http://cds.cern.ch/record/331066?ln=de (cit. on p. 9).

[ATL+08] ATLAS Collaboration with Aad, G et al. 'The ATLAS Experiment at the CERN Large Hadron Collider'. In: *Journal of Instrumentation* 3.08 (2008), S08003. URL: http://stacks.iop.org/1748-0221/3/i=08/a=S08003 (cit. on pp. 9–11).

[CER] CERN-PS irradiation facility. URL: https://irradiation.web.cern.ch/irradiation/Photo_irrad1.htm (cit. on p. 38).

[HL-13] HL-LHC Project. *The HL-LHC Project webpage*. 2013. URL: http://hilumilhc.web.cern.ch/hilumilhc/index.html (visited on 04/12/2013) (cit. on p. 31).

[LIU13] LIU Project. *LHC Injectors Upgrade Project website*. 2013. URL: https://espace.cern.ch/liu-project/default.aspx (visited on 04/01/2013) (cit. on p. 5).

[Mis13] MissMJ. *Standard model of elementary particles*. 2013. URL: http://upload.wikimedia.org/wikipedia/commons/0/00/Standard_Model_of_Elementary_Particles.svg (visited on 12/31/2013) (cit. on p. 7).

List of Figures

List of Tables

List of Acronyms

ACLiC **A**utomatic **C**ompiler of **Li**braries for CINT[1] 49
ADC **A**nalog **D**igital **C**onverter 46
ALICE **A** **L**arge **I**on **C**ollider **E**xperiment 6
ASCII **A**merican **S**tandard **C**ode for **I**nformation **I**nterchange 59
ATLAS **A** **T**oroidal **L**HC **A**pparatu**S** 115
CAN **C**ontroller **A**rea **N**etwork 70
CERN **C**onseil **E**uropéen pour la **R**echerche **N**ucléaire 115
CINT **C** and C++ **INT**erpreter 149
CMOS **C**omplementary **M**etal **O**xide **S**emiconductor 75
CMS **C**ompact **M**uon **S**olenoid 6
DCS **D**etector **C**ontrol **S**ystem 83
DESY II **D**eutsches **E**lektronen **SY**nchrotron II - accelerator at DESY 65
DESY **D**eutsches **E**lektronen **SY**nchrotron 116
DUT **D**evice **U**nder **T**est 165
DOBOX **DO**rtmund testbeam **BOX** 87
DOFZ **D**iffusion **O**xygenated **F**loat**Z**one 77
DUT **D**evice **U**nder **T**est 165
ELMB **E**mbedded **L**ocal **M**onitor **B**oard 70
EMCAL **E**lectro**M**agnetic **CAL**orimeter 9
EMI **E**lectro**m**agnetic **I**nterferences 42
EUDET **DET**ector-project supported by the **E**uropean **U**nion 66
FCB **F**lexible **C**ircuit **B**oard 12
FDAC **F**eedback-current **D**igital to **A**nalog **C**onverter 58
FE **F**ront**E**nd Electronic 13
FPGA **F**ield **P**rogrammable **G**ata **Array** 57

1 **C** and C++ **INT**erpreter

Index

APPENDIX A

Wafer Maps

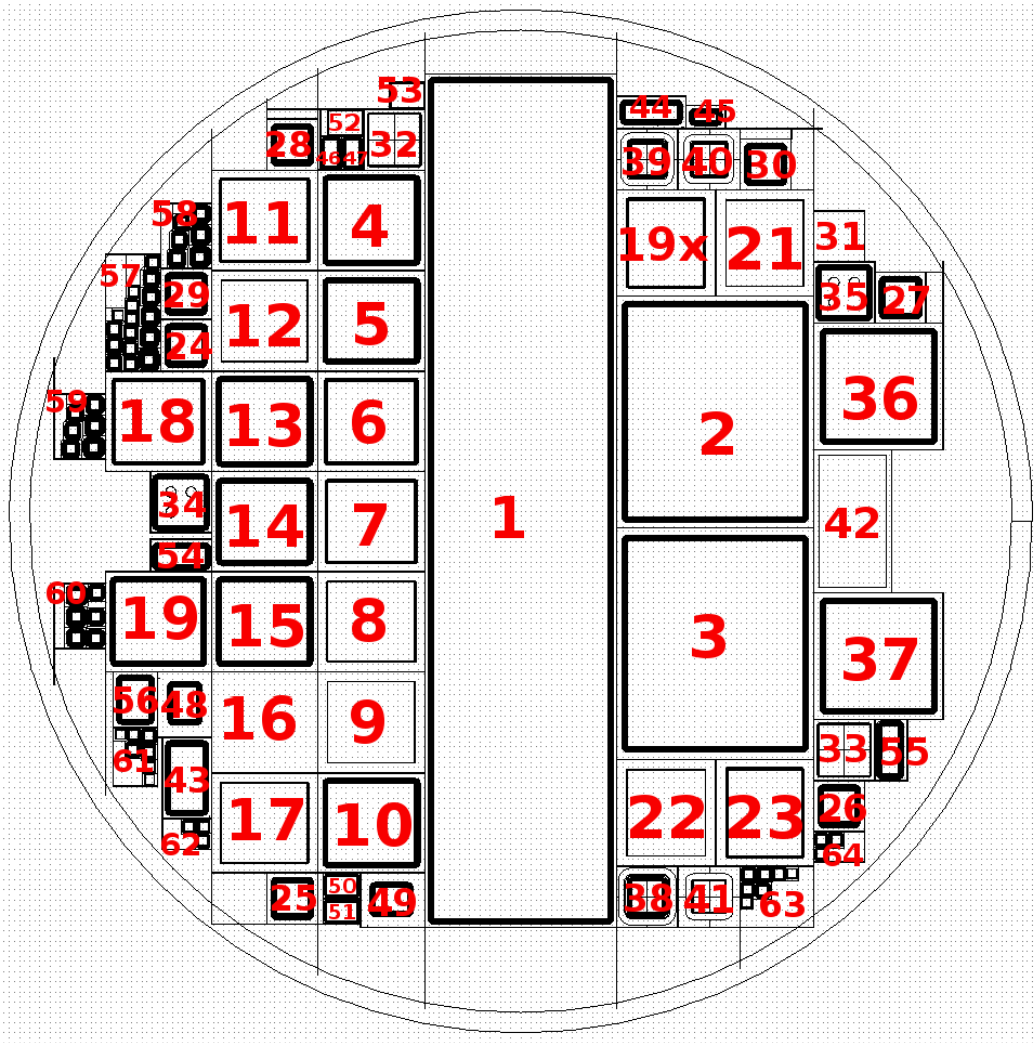

Figure A.1: Wafer map of the 2009 CiS production.

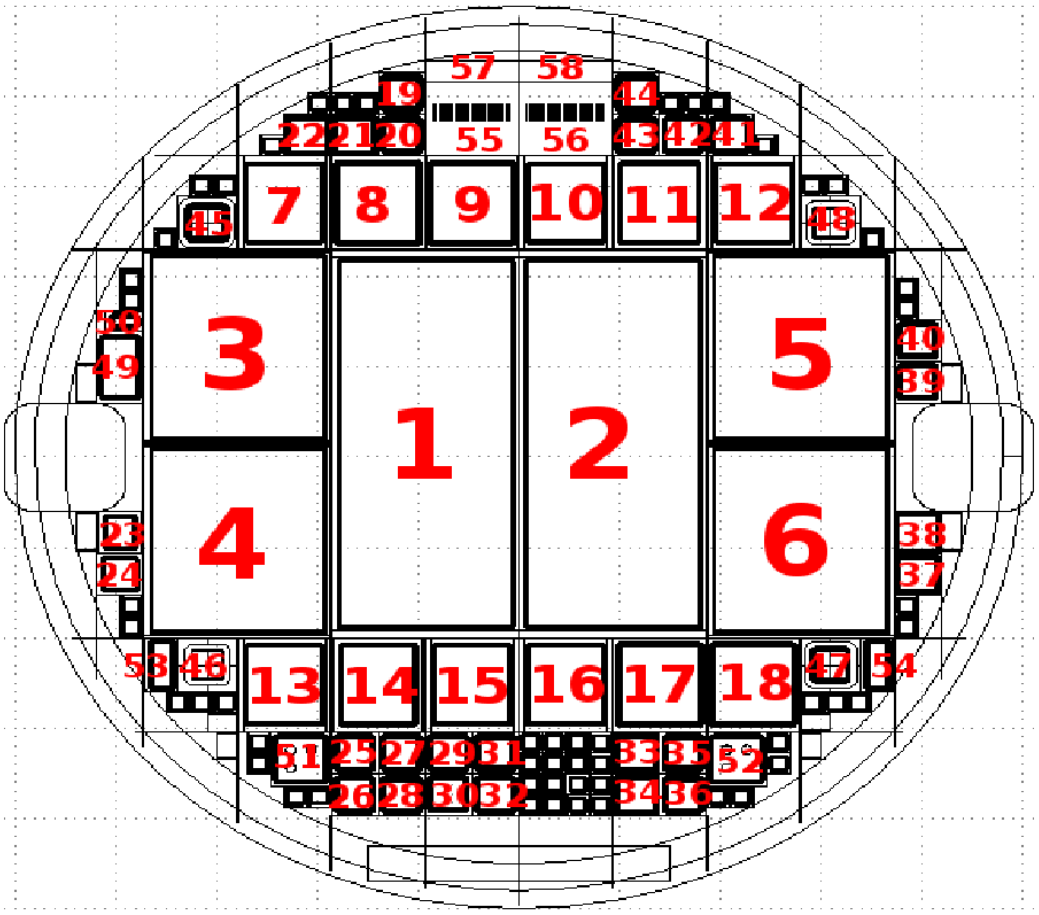

Figure A.2: Wafer map of the 2010 CiS production.

Dicing plan n-side

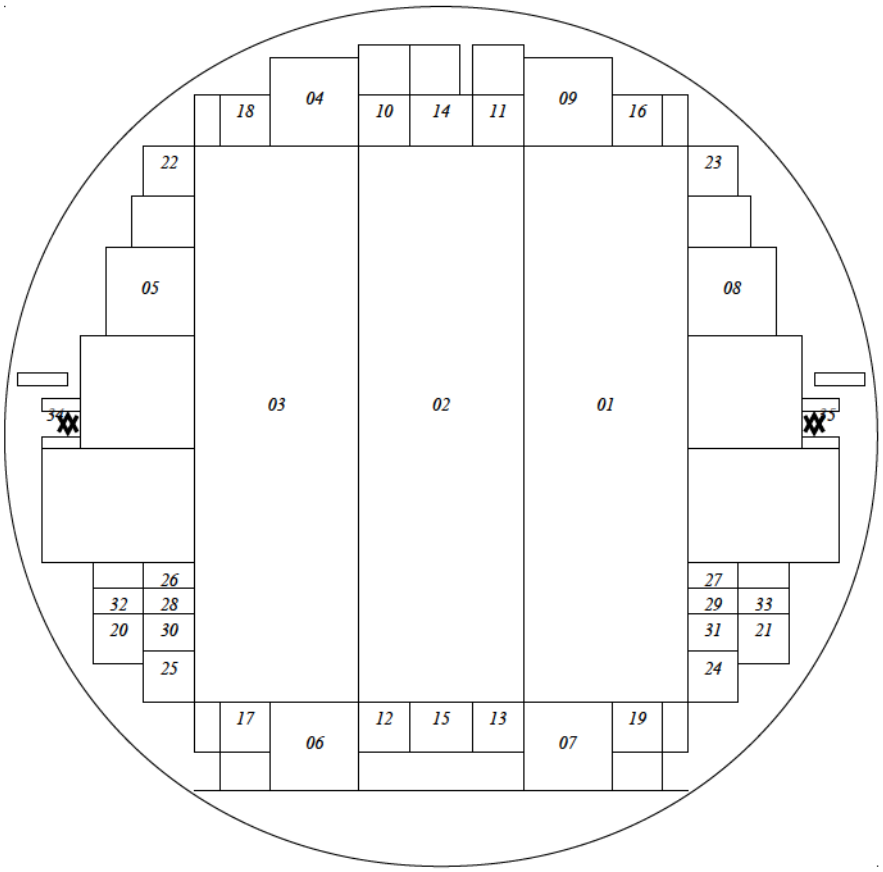

n-side wafer map

Numbered ATLAS structures:

01-03: sensor tiles
04-09: single chip sensors
10-13: mini chip sensors
14-15: inter pixel test structures
16-17: diodes with guard ring
18-21: ROSE type diodes
22-25: oxide test fields
26-27: n-side test structures
28-29: p-side test structures
30-31: breakdown monitors
32-33: p-side MOS arrays
34-35: mask alignment structures

Figure A.3: Wafer map of original ATLAS pixel production.

APPENDIX B

Photos of Assemblies

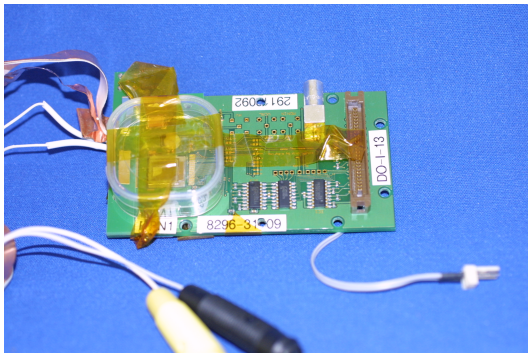

(a) Front side DO-I-13

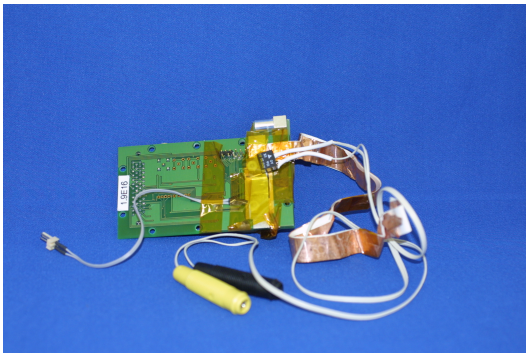

(b) Back side DO-I-13

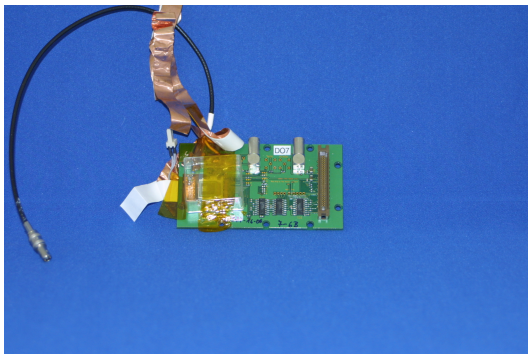

(c) Front side DO-7

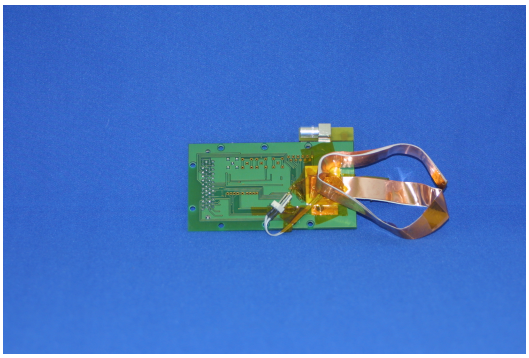

(d) Back side DO-7

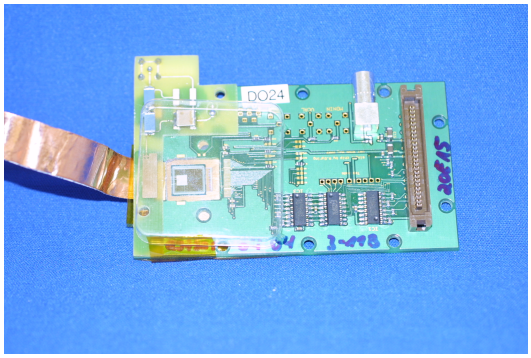

(e) Front side DO-24

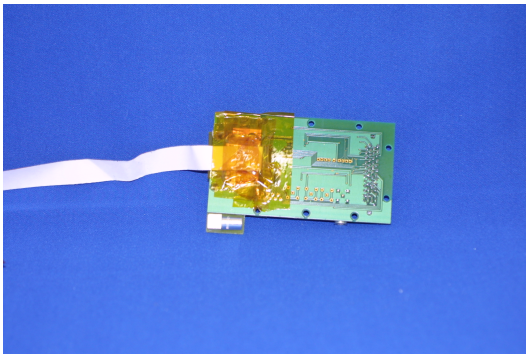

(f) Back side DO-24

Figure B.1: Photos of DUTs, showing modifications and cooling.

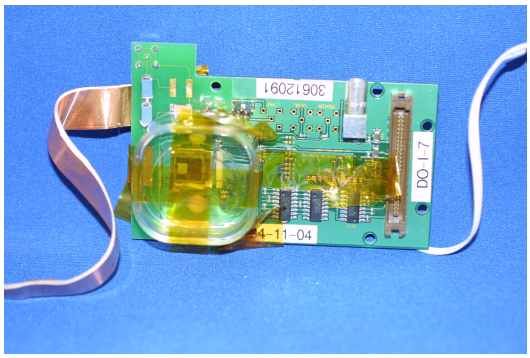

(a) Front side DO-I-7

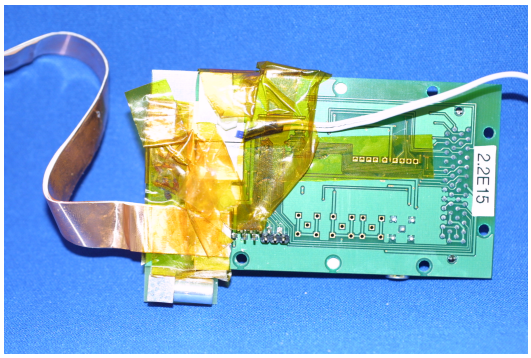

(b) Back side DO-I-7

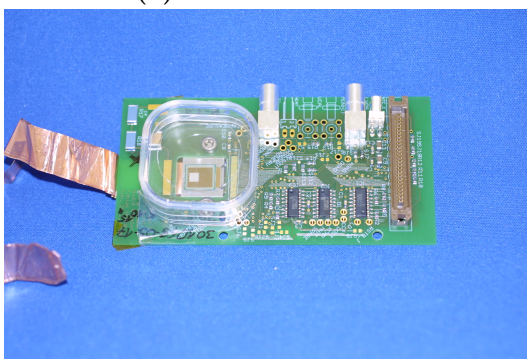

(c) Front side DO-47

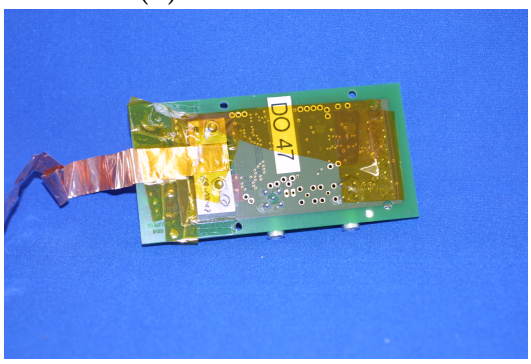

(d) Back side DO-47

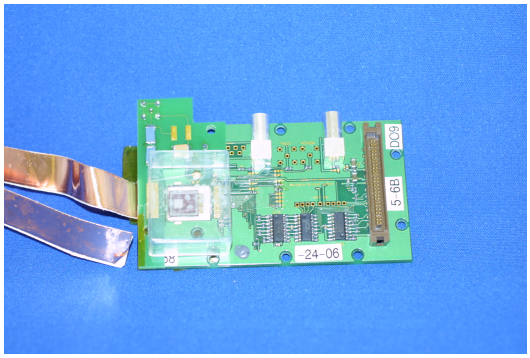

(e) Front side DO-9

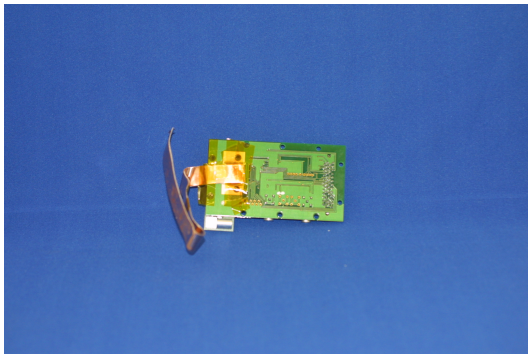

(f) Back side DO-9

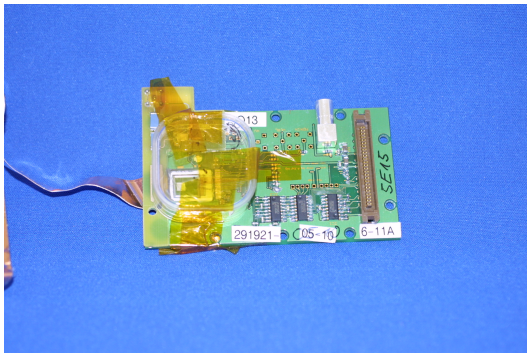

(g) Front side DO-13

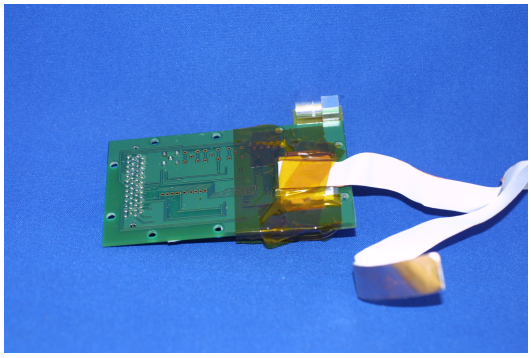

(h) Back side DO-13

Figure B.2: Photos of DUTs, showing modifications and cooling. (cont.)

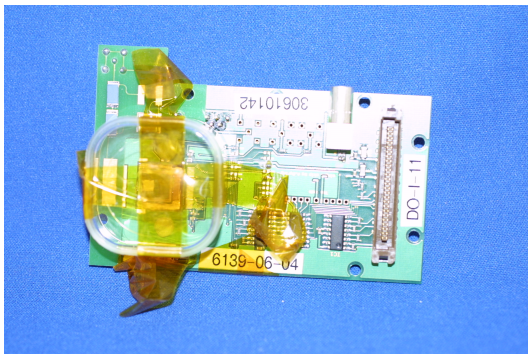

(a) Front side DO-I-11

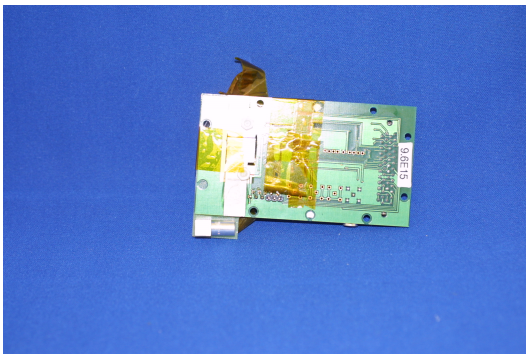

(b) Back side DO-I-11

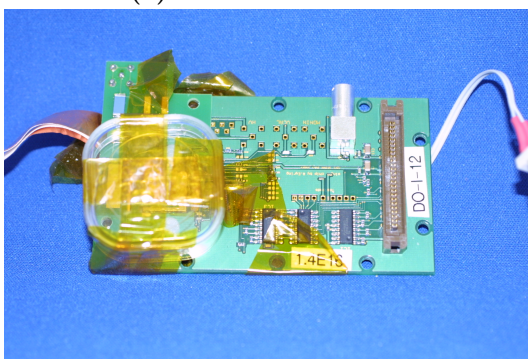

(c) Front side DO-I-12

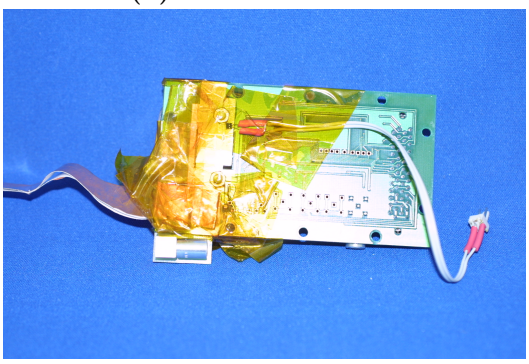

(d) Back side DO-I-12

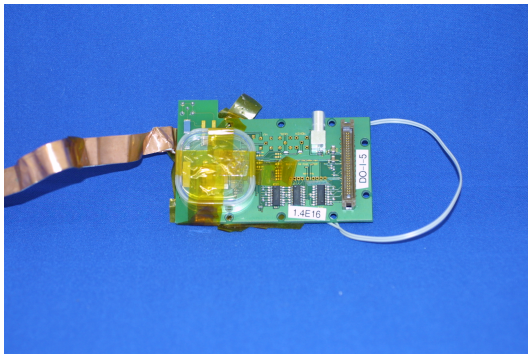

(e) Front side DO-I-5

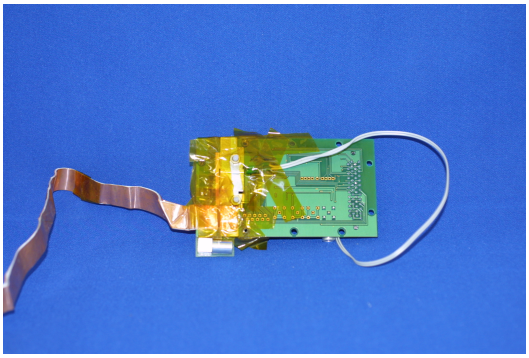

(f) Back side DO-I-5

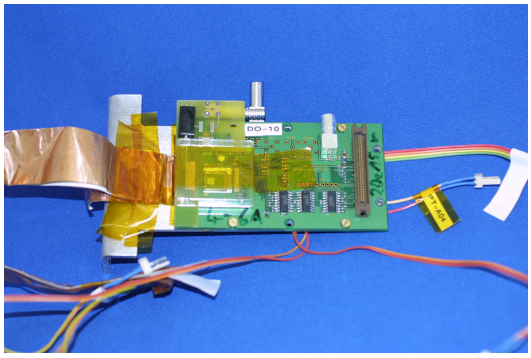

(g) Front side DO-10

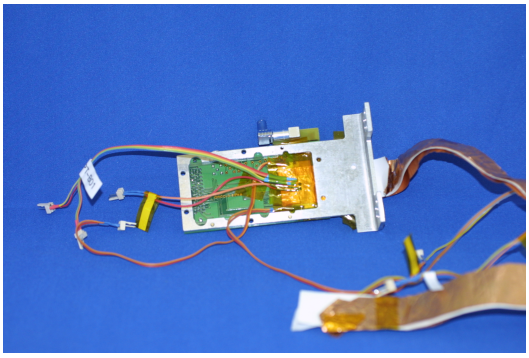

(h) Back side DO-10

Figure B.3: Photos of DUTs, showing modifications and cooling. (cont.)

APPENDIX C

Details of all Test Beam Measurements

Plots (a) through (c) show the development of the set bias voltage, bias current and temperature over time. Those data is taken from the environmental log files (compare section 8.6.3.2) and tagged with run numbers using the runcontrol log information.

Partially interesting is the hot pixel mask in (d) which is created during the first analysis pass. There the indium flipped assemblies show a lot of dead spots and missing corners. This is due to unconnected bump bonds, especially the missing corners and edges are a typical syndrome. The cause for this lacking bump bond quality was that the frontends were stored for an unusually long time (several years as they were produced during the original ATLAS production). The frontends carry the prepared bump ball stubs similar to the frontends in the case of the PbSn flipped assemblies. In order to protect those before flip-chipping they were covered with photo resin. This resin is intended to be removed shortly before the final flip-chip mating. Unfortunately, due to the long storage the resin hardened and its removal was not completely successful leading to warping. Nevertheless, those pixels which were connected successfully worked quite well. All troubles occuring specifically with irradiated frontends were absent from the indium flipped assemblies.

The level 1 timing distribution in figures (e) is useful to evaluate the behaviour of the DUT[1] with regard to proper calibration settings. A sharp peak covering one or two bins is expected as the timing between the trigger through the telescope scintillators and the recording of the signal in the particular DUT should always stay the same. If there is a flat background in the surrounding level 1 bins this indicates a lot of noise and can be partially mitigated by the hotpixel removal in the TbMon analysis. If there is no clear peak visible this usually means that something strange happened during operation and that the data are not really usable for that DUT.

Plots showing the quality of the reconstruction (both influenced by the data taking and cuts applied later on and also mirroring the care taken during shift

1 **D**evice **U**nder **T**est

correction) are the residuals in X and Y shown in figures (i) and (j). They indicate good data quality when they are centred around 0 and have a width equivalent to the pixel pitch. The residual is the difference between the track position estimated by the telescope and the position calculated from the hit cluster in the DUT.

The collected charge distribution is shown as a sum and individually for different cluster sizes in figures (m) through (q). This distribution usually follows a Landau-Vavilov function. For the source measurements in the laboratory, such a function is fitted to the distributions and the most probable value is derived as a fitting parameter. This is omitted for the test beam measurements as the fit does not work very well for this data. The charge values shown in the table and plotted in the appropriate plots are simply the bin with the highest entry.

The time dependent hit efficiency plots (r) also give a good indication of the data quality.

For plots (s) through (u) the available telescope resolution was used to map the hit efficiency and mean cluster charge on the surface of one pixel. This gives an idea of the impact of the different substructures within a pixel layout on the efficiency.

#	DUT name	run period	bias [V]	η	ϕ	run range	details
0	DO-1	IBL Feb. 2011 DESY	150	0	0	30684−30715	fig. C.1 on page 175
1	DO-13	IBL Feb. 2011 DESY	1000	0	0	30684−30715	fig. C.2 on page 179
0	DO-1	IBL Feb. 2011 DESY	150	0	0	31037−31064	fig. C.3 on page 182
1	DO-13	IBL Feb. 2011 DESY	500	0	0	31037−31064	fig. C.4 on page 185
0	DO-1	IBL Feb. 2011 DESY	150	0	0	31066−31069	fig. C.5 on page 188
1	DO-13	IBL Feb. 2011 DESY	300	0	0	31066−31069	fig. C.6 on page 191
0	DO-1	IBL Feb. 2011 DESY	150	0	0	31071−31082	fig. C.7 on page 194
1	DO-13	IBL Feb. 2011 DESY	350	0	0	31071−31082	fig. C.8 on page 197
0	DO-1	IBL Feb. 2011 DESY	150	0	0	31140−31165	fig. C.9 on page 200
1	DO-13	IBL Feb. 2011 DESY	350	0	0	31140−31165	fig. C.10 on page 203
0	KEK1R	PPS Jul. 2011 CERN	200	0	0	50578−50582	fig. C.11 on page 207
1	KEK2R	PPS Jul. 2011 CERN	200	0	0	50578−50582	fig. C.12 on page 210
2	DO-I-11	PPS Jul. 2011 CERN	800	0	0	50578−50582	fig. C.13 on page 213
3	DO-I-13	PPS Jul. 2011 CERN	800	0	0	50578−50582	fig. C.14 on page 216
0	KEK1R	PPS Jul. 2011 CERN	200	0	0	50584−50584	fig. C.15 on page 219
1	KEK2R	PPS Jul. 2011 CERN	200	0	0	50584−50584	fig. C.16 on page 222
2	DO-I-11	PPS Jul. 2011 CERN	600	0	0	50584−50584	fig. C.17 on page 225
3	DO-I-13	PPS Jul. 2011 CERN	300	0	0	50584−50584	fig. C.18 on page 228
0	KEK1R	PPS Jul. 2011 CERN	200	0	0	50585−50585	fig. C.19 on page 231
1	KEK2R	PPS Jul. 2011 CERN	200	0	0	50585−50585	fig. C.20 on page 234
2	DO-I-11	PPS Jul. 2011 CERN	1100	0	0	50585−50585	fig. C.21 on page 237
3	DO-I-13	PPS Jul. 2011 CERN	200	0	0	50585−50585	fig. C.22 on page 240
0	KEK1R	PPS Jul. 2011 CERN	200	0	0	50586−50586	fig. C.23 on page 243
1	KEK2R	PPS Jul. 2011 CERN	200	0	0	50586−50586	fig. C.24 on page 246

#	DUT name	run period	bias [V]	η	ϕ	run range	details
2	DO-I-11	PPS Jul. 2011 CERN	1200	0	0	50586−50586	fig. C.25 on page 249
3	DO-I-13	PPS Jul. 2011 CERN	100	0	0	50586−50586	fig. C.26 on page 252
0	KEK1R	PPS Jul. 2011 CERN	200	0	0	50587−50587	fig. C.27 on page 255
1	KEK2R	PPS Jul. 2011 CERN	200	0	0	50587−50587	fig. C.28 on page 258
2	DO-I-11	PPS Jul. 2011 CERN	1400	0	0	50587−50587	fig. C.29 on page 261
3	DO-I-13	PPS Jul. 2011 CERN	600	0	0	50587−50587	fig. C.30 on page 264
0	KEK1R	PPS Jul. 2011 CERN	200	0	0	50588−50597	fig. C.31 on page 267
1	KEK2R	PPS Jul. 2011 CERN	200	0	0	50588−50597	fig. C.32 on page 270
2	DO-I-11	PPS Jul. 2011 CERN	1500	0	0	50588−50597	fig. C.33 on page 273
3	DO-I-13	PPS Jul. 2011 CERN	1000	0	0	50588−50597	fig. C.34 on page 276
0	KEK1R	PPS Jul. 2011 CERN	200	0	0	50598−50599	fig. C.35 on page 279
1	KEK2R	PPS Jul. 2011 CERN	200	0	0	50598−50599	fig. C.36 on page 282
2	DO-I-11	PPS Jul. 2011 CERN	1000	0	0	50598−50599	fig. C.37 on page 285
3	DO-I-13	PPS Jul. 2011 CERN	200	0	0	50598−50599	fig. C.38 on page 288
0	KEK1R	PPS Jul. 2011 CERN	200	0	15	50600−50603	fig. C.39 on page 291
1	KEK2R	PPS Jul. 2011 CERN	200	0	15	50600−50603	fig. C.40 on page 294
2	DO-I-11	PPS Jul. 2011 CERN	1500	0	15	50600−50603	fig. C.41 on page 297
3	DO-I-13	PPS Jul. 2011 CERN	200	0	15	50600−50603	fig. C.42 on page 300
0	SLID10	PPS Sep. 2011 CERN	100	0	0	61112−61120	fig. C.43 on page 303
1	SLID09	PPS Sep. 2011 CERN	300	0	0	61112−61120	fig. C.44 on page 306
2	CiS5e15	PPS Sep. 2011 CERN	600	0	0	61112−61120	fig. C.45 on page 309
3	DO-I-5	PPS Sep. 2011 CERN	1000	0	0	61112−61120	fig. C.46 on page 312
0	SLID10	PPS Sep. 2011 CERN	100	0	0	61124−61128	fig. C.47 on page 315
1	SLID09	PPS Sep. 2011 CERN	350	0	0	61124−61128	fig. C.48 on page 318
2	CiS5e15	PPS Sep. 2011 CERN	800	0	0	61124−61128	fig. C.49 on page 321

#	DUT name	run period	bias [V]	η	ϕ	run range	details
3	DO-I-5	PPS Sep. 2011 CERN	1100	0	0	61124−61128	fig. C.50 on page 324
0	SLID10	PPS Sep. 2011 CERN	100	0	0	61130−61146	fig. C.51 on page 327
1	SLID09	PPS Sep. 2011 CERN	350	0	0	61130−61146	fig. C.52 on page 330
2	CiS5e15	PPS Sep. 2011 CERN	700	0	0	61130−61146	fig. C.53 on page 333
3	DO-I-5	PPS Sep. 2011 CERN	1500	0	0	61130−61146	fig. C.54 on page 336
0	DO-I-7	PPS Sep. 2011 CERN	300	0	0	61249−61249	fig. C.55 on page 339
1	DO-I-11	PPS Sep. 2011 CERN	500	0	0	61249−61249	fig. C.56 on page 342
2	DO-I-5	PPS Sep. 2011 CERN	500	0	0	61249−61249	fig. C.57 on page 345
3	DO-I-12	PPS Sep. 2011 CERN	500	0	0	61249−61249	fig. C.58 on page 348
0	DO-I-7	PPS Sep. 2011 CERN	400	0	0	61250−61251	fig. C.59 on page 351
1	DO-I-11	PPS Sep. 2011 CERN	600	0	0	61250−61251	fig. C.60 on page 354
2	DO-I-5	PPS Sep. 2011 CERN	600	0	0	61250−61251	fig. C.61 on page 357
3	DO-I-12	PPS Sep. 2011 CERN	600	0	0	61250−61251	fig. C.62 on page 360
0	DO-I-7	PPS Sep. 2011 CERN	500	0	0	61252−61252	fig. C.63 on page 363
1	DO-I-11	PPS Sep. 2011 CERN	700	0	0	61252−61252	fig. C.64 on page 366
2	DO-I-5	PPS Sep. 2011 CERN	700	0	0	61252−61252	fig. C.65 on page 369
3	DO-I-12	PPS Sep. 2011 CERN	700	0	0	61252−61252	fig. C.66 on page 372
0	DO-I-7	PPS Sep. 2011 CERN	600	0	0	61253−61253	fig. C.67 on page 375
1	DO-I-11	PPS Sep. 2011 CERN	800	0	0	61253−61253	fig. C.68 on page 378
2	DO-I-5	PPS Sep. 2011 CERN	800	0	0	61253−61253	fig. C.69 on page 381
3	DO-I-12	PPS Sep. 2011 CERN	800	0	0	61253−61253	fig. C.70 on page 384
0	DO-I-7	PPS Sep. 2011 CERN	700	0	0	61254−61254	fig. C.71 on page 387
1	DO-I-11	PPS Sep. 2011 CERN	900	0	0	61254−61254	fig. C.72 on page 390
2	DO-I-5	PPS Sep. 2011 CERN	900	0	0	61254−61254	fig. C.73 on page 393
3	DO-I-12	PPS Sep. 2011 CERN	900	0	0	61254−61254	fig. C.74 on page 396

#	DUT name	run period	bias [V]	η	ϕ	run range	details
0	DO-I-7	PPS Sep. 2011 CERN	800	0	0	61255−61255	fig. C.75 on page 399
1	DO-I-11	PPS Sep. 2011 CERN	1000	0	0	61255−61255	fig. C.76 on page 402
2	DO-I-5	PPS Sep. 2011 CERN	1000	0	0	61255−61255	fig. C.77 on page 405
3	DO-I-12	PPS Sep. 2011 CERN	1000	0	0	61255−61255	fig. C.78 on page 408
0	DO-I-7	PPS Sep. 2011 CERN	900	0	0	61256−61256	fig. C.79 on page 411
1	DO-I-11	PPS Sep. 2011 CERN	1100	0	0	61256−61256	fig. C.80 on page 414
2	DO-I-5	PPS Sep. 2011 CERN	1100	0	0	61256−61256	fig. C.81 on page 417
3	DO-I-12	PPS Sep. 2011 CERN	1100	0	0	61256−61256	fig. C.82 on page 420
0	DO-I-7	PPS Sep. 2011 CERN	1000	0	0	61257−61257	fig. C.83 on page 423
1	DO-I-11	PPS Sep. 2011 CERN	1200	0	0	61257−61257	fig. C.84 on page 426
2	DO-I-5	PPS Sep. 2011 CERN	1200	0	0	61257−61257	fig. C.85 on page 429
3	DO-I-12	PPS Sep. 2011 CERN	1200	0	0	61257−61257	fig. C.86 on page 432
0	DO-I-7	PPS Sep. 2011 CERN	1100	0	0	61258−61259	fig. C.87 on page 435
1	DO-I-11	PPS Sep. 2011 CERN	1300	0	0	61258−61259	fig. C.88 on page 438
2	DO-I-5	PPS Sep. 2011 CERN	1300	0	0	61258−61259	fig. C.89 on page 441
3	DO-I-12	PPS Sep. 2011 CERN	1300	0	0	61258−61259	fig. C.90 on page 444
0	DO-I-7	PPS Sep. 2011 CERN	1200	0	0	61260−61260	fig. C.91 on page 447
1	DO-I-11	PPS Sep. 2011 CERN	1400	0	0	61260−61260	fig. C.92 on page 450
2	DO-I-5	PPS Sep. 2011 CERN	1400	0	0	61260−61260	fig. C.93 on page 453
3	DO-I-12	PPS Sep. 2011 CERN	1400	0	0	61260−61260	fig. C.94 on page 456
0	DO-I-7	PPS Sep. 2011 CERN	1300	0	0	61261−61261	fig. C.95 on page 459
1	DO-I-11	PPS Sep. 2011 CERN	1500	0	0	61261−61261	fig. C.96 on page 462
2	DO-I-5	PPS Sep. 2011 CERN	1500	0	0	61261−61261	fig. C.97 on page 465
3	DO-I-12	PPS Sep. 2011 CERN	1500	0	0	61261−61261	fig. C.98 on page 468
0	DO-I-7	PPS Sep. 2011 CERN	1400	0	0	61262−61262	fig. C.99 on page 471

#	DUT name	run period	bias [V]	η	ϕ	run range	details
1	DO-I-11	PPS Sep. 2011 CERN	1600	0	0	61262−61262	fig. C.100 on page 474
2	DO-I-5	PPS Sep. 2011 CERN	1600	0	0	61262−61262	fig. C.101 on page 477
3	DO-I-12	PPS Sep. 2011 CERN	1600	0	0	61262−61262	fig. C.102 on page 480
0	DO-I-7	PPS Sep. 2011 CERN	1500	0	0	61263−61263	fig. C.103 on page 483
1	DO-I-11	PPS Sep. 2011 CERN	1700	0	0	61263−61263	fig. C.104 on page 486
2	DO-I-5	PPS Sep. 2011 CERN	1700	0	0	61263−61263	fig. C.105 on page 489
3	DO-I-12	PPS Sep. 2011 CERN	1700	0	0	61263−61263	fig. C.106 on page 492
0	DO-I-7	PPS Sep. 2011 CERN	800	0	0	61264−61273	fig. C.107 on page 495
1	DO-I-11	PPS Sep. 2011 CERN	1300	0	0	61264−61273	fig. C.108 on page 498
2	DO-I-5	PPS Sep. 2011 CERN	1300	0	0	61264−61273	fig. C.109 on page 501
3	DO-I-12	PPS Sep. 2011 CERN	1300	0	0	61264−61273	fig. C.110 on page 504
0	DO-I-7	PPS Sep. 2011 CERN	500	0	0	61281−61289	fig. C.111 on page 507
1	DO-I-11	PPS Sep. 2011 CERN	1000	0	0	61281−61289	fig. C.112 on page 510
2	DO-I-5	PPS Sep. 2011 CERN	1000	0	0	61281−61289	fig. C.113 on page 513
3	DO-I-12	PPS Sep. 2011 CERN	1000	0	0	61281−61289	fig. C.114 on page 516
0	DO-I-7	PPS Sep. 2011 CERN	1000	0	0	61290−61296	fig. C.115 on page 519
1	DO-I-11	PPS Sep. 2011 CERN	1500	0	0	61290−61296	fig. C.116 on page 522
2	DO-I-5	PPS Sep. 2011 CERN	1500	0	0	61290−61296	fig. C.117 on page 525
3	DO-I-12	PPS Sep. 2011 CERN	1500	0	0	61290−61296	fig. C.118 on page 528
0	DO-I-7	PPS Sep. 2011 CERN	600	0	0	61298−61303	fig. C.119 on page 531
1	DO-I-11	PPS Sep. 2011 CERN	600	0	0	61298−61303	fig. C.120 on page 534
2	DO-I-5	PPS Sep. 2011 CERN	600	0	0	61298−61303	fig. C.121 on page 537
3	DO-I-12	PPS Sep. 2011 CERN	600	0	0	61298−61303	fig. C.122 on page 540
0	DO-I-7	PPS Sep. 2011 CERN	1200	0	0	61304−61315	fig. C.123 on page 543
1	DO-I-11	PPS Sep. 2011 CERN	1800	0	0	61304−61315	fig. C.124 on page 546

#	DUT name	run period	bias [V]	η	ϕ	run range	details
2	DO-I-5	PPS Sep. 2011 CERN	1800	0	0	61304−61315	fig. C.125 on page 549
3	DO-I-12	PPS Sep. 2011 CERN	1800	0	0	61304−61315	fig. C.126 on page 552
0	DO-1	PPS Mar. 2012 DESY	150	0	0	125−129	fig. C.127 on page 555
1	DO-36	PPS Mar. 2012 DESY	600	0	0	125−129	fig. C.128 on page 558
0	DO-1	PPS Mar. 2012 DESY	150	0	0	130−135	fig. C.129 on page 561
1	DO-36	PPS Mar. 2012 DESY	1000	0	0	130−135	fig. C.130 on page 564
0	DO-1	PPS Mar. 2012 DESY	150	0	0	143−147	fig. C.131 on page 567
1	DO-36	PPS Mar. 2012 DESY	800	0	0	143−147	fig. C.132 on page 570
0	DO-1	PPS Mar. 2012 DESY	150	0	0	149−154	fig. C.133 on page 573
1	DO-36	PPS Mar. 2012 DESY	600	0	0	149−154	fig. C.134 on page 576
0	DO-1	PPS Mar. 2012 DESY	150	0	0	160−165	fig. C.135 on page 579
1	DO-36	PPS Mar. 2012 DESY	400	0	0	160−165	fig. C.136 on page 582
0	DO-1	PPS Mar. 2012 DESY	150	0	0	166−172	fig. C.137 on page 585
1	DO-36	PPS Mar. 2012 DESY	200	0	0	166−172	fig. C.138 on page 588
0	DO-1	PPS Mar. 2012 DESY	150	0	0	210−249	fig. C.139 on page 591
1	DO-36	PPS Mar. 2012 DESY	1000	0	0	210−249	fig. C.140 on page 594
0	DO-1	PPS Mar. 2012 DESY	150	0	0	251−303	fig. C.141 on page 597
1	DO-36	PPS Mar. 2012 DESY	800	0	0	251−303	fig. C.142 on page 600
0	DO-1	PPS Mar. 2012 DESY	150	0	0	305−356	fig. C.143 on page 603
1	DO-36	PPS Mar. 2012 DESY	600	0	0	305−356	fig. C.144 on page 606
0	DO-1	PPS Mar. 2012 DESY	150	0	0	358−405	fig. C.145 on page 609
1	DO-36	PPS Mar. 2012 DESY	400	0	0	358−405	fig. C.146 on page 612
0	DO-1	PPS Mar. 2012 DESY	150	0	0	408−452	fig. C.147 on page 615

#	DUT name	run period	bias [V]	η	ϕ	run range	details
1	DO-36	PPS Mar. 2012 DESY	200	0	0	408−452	fig. C.148 on page 618
0	DO-1	PPS May 2012 CERN	150	0	0	739−765	fig. C.155 on page 639
1	DO-10	PPS May 2012 CERN	1000	0	0	739−765	fig. C.156 on page 641
2	DO-24	PPS May 2012 CERN	1000	0	0	739−765	fig. C.157 on page 644
3	DO-38	PPS May 2012 CERN	1000	0	0	739−765	fig. C.158 on page 647
0	DO-1	PPS May 2012 CERN	150	0	0	767−795	fig. C.159 on page 650
1	DO-10	PPS May 2012 CERN	600	0	0	767−795	fig. C.160 on page 653
2	DO-24	PPS May 2012 CERN	600	0	0	767−795	fig. C.161 on page 656
3	DO-38	PPS May 2012 CERN	600	0	0	767−795	fig. C.162 on page 659
0	DO-1	PPS May 2012 CERN	150	0	0	797−833	fig. C.163 on page 662
1	DO-10	PPS May 2012 CERN	800	0	0	797−833	fig. C.164 on page 665
2	DO-24	PPS May 2012 CERN	800	0	0	797−833	fig. C.165 on page 668
3	DO-38	PPS May 2012 CERN	800	0	0	797−833	fig. C.166 on page 671
0	DO-1	PPS May 2012 CERN	150	0	0	835−882	fig. C.167 on page 674
1	DO-10	PPS May 2012 CERN	1500	0	0	835−882	fig. C.168 on page 677
2	DO-24	PPS May 2012 CERN	1500	0	0	835−882	fig. C.169 on page 680
3	DO-38	PPS May 2012 CERN	1000	0	0	835−882	fig. C.170 on page 683
0	DO-1	PPS May 2012 CERN	150	0	0	883−907	fig. C.171 on page 686
1	DO-10	PPS May 2012 CERN	400	0	0	883−907	fig. C.172 on page 689
2	DO-24	PPS May 2012 CERN	400	0	0	883−907	fig. C.173 on page 692
3	DO-38	PPS May 2012 CERN	200	0	0	883−907	fig. C.174 on page 695
0	DO-1	PPS May 2012 CERN	150	0	0	918−945	fig. C.175 on page 698
1	DO-10	PPS May 2012 CERN	1500	15	0	918−945	fig. C.176 on page 701
2	DO-24	PPS May 2012 CERN	1500	15	0	918−945	fig. C.177 on page 704
3	DO-38	PPS May 2012 CERN	1000	15	0	918−945	fig. C.178 on page 707

#	DUT name	run period	bias [V]	η	ϕ	run range	details
0	DO-1	PPS May 2012 CERN	150	15	0	947−980	fig. C.179 on page 710
1	DO-10	PPS May 2012 CERN	1000	15	0	947−980	fig. C.180 on page 713
2	DO-24	PPS May 2012 CERN	1000	15	0	947−980	fig. C.181 on page 716
3	DO-38	PPS May 2012 CERN	600	15	0	947−980	fig. C.182 on page 719
0	DO-1	PPS Aug. 2012 CERN	150	0	0	71579−71628	fig. C.183 on page 722
1	DO-10	PPS Aug. 2012 CERN	2000	0	0	71579−71628	fig. C.184 on page 725
2	DO-24	PPS Aug. 2012 CERN	2000	0	0	71579−71628	fig. C.185 on page 728
3	DO23	PPS Aug. 2012 CERN	1000	0	0	71579−71628	fig. C.186 on page 731

Table C.1: Overview of all runs.

C.1 DESY February 2011

C.1.1 Runs 30684-30715

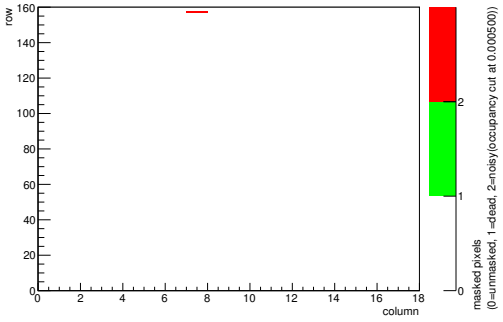

(a) Map of masked pixels.

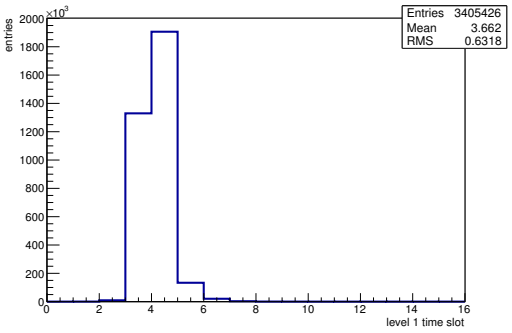

(b) Lvl1 distribution.

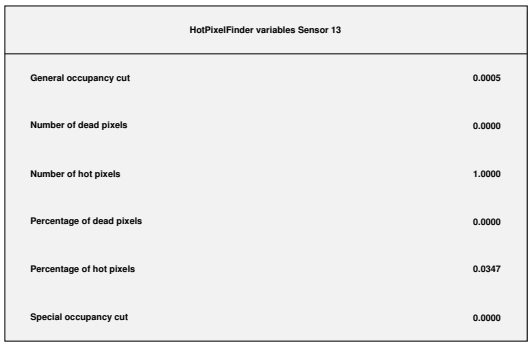

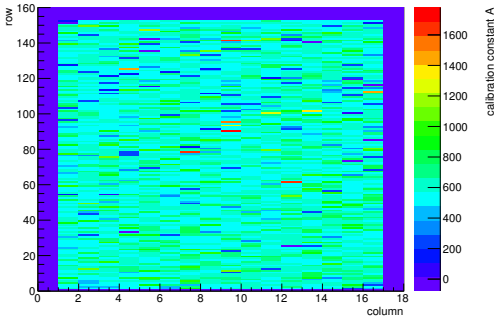

(c) Calibration constant A.

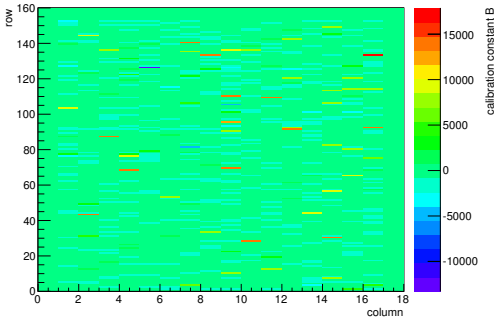

(d) Calibration constant B.

Figure C.1: Detailed plots for test beam measurement of DO-1 (description see section 6.1) sample (running as DUT0) during runs 30684-30715 in the February 2011 test beam period at DESY. Summary of the data in chapter 9. *(cont.)*

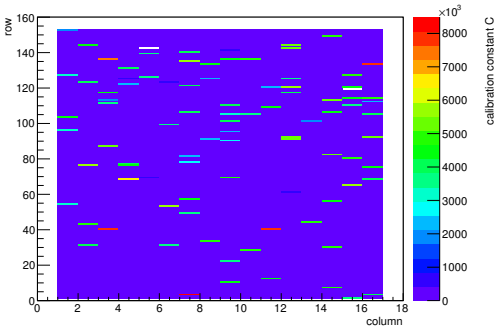

(e) Calibration constant C.

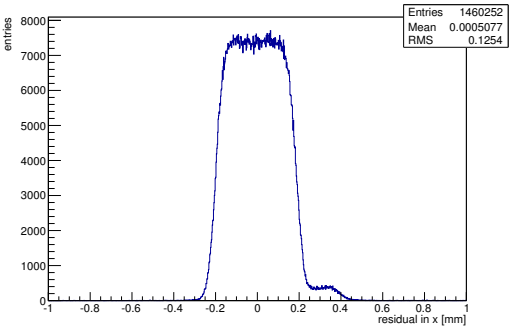

(f) Track residual in x.

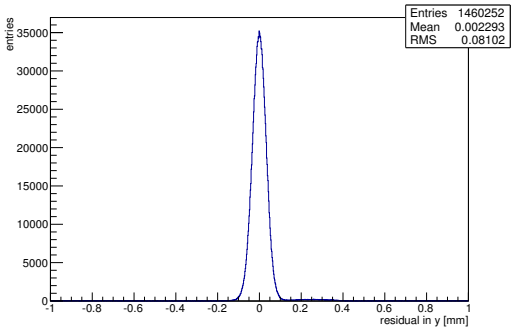

(g) Track residual in y.

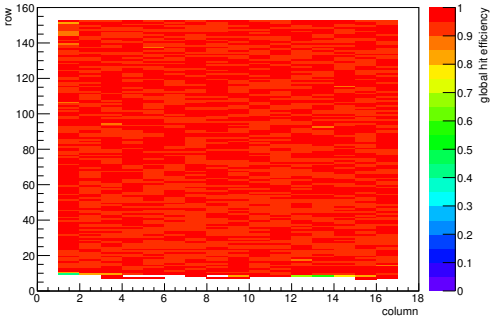

(h) Hit efficiency map.

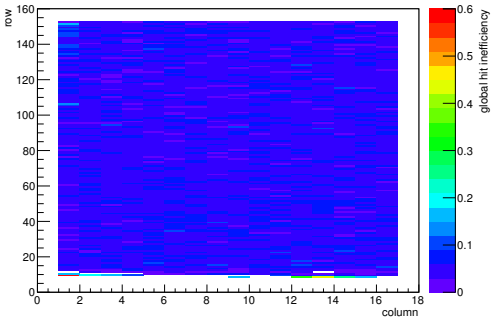

(i) Hit inefficiency map.

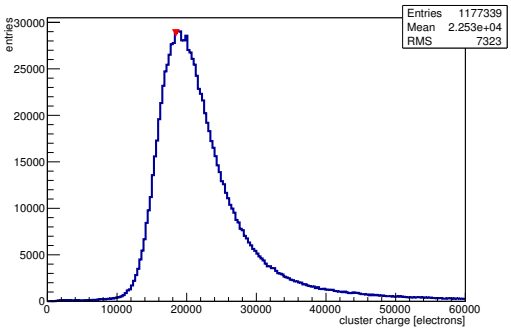

(j) Charge distribution (all cluster sizes included).

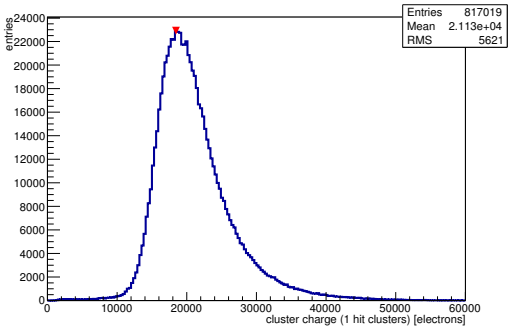

(k) Charge distribution (1 hit cluster).

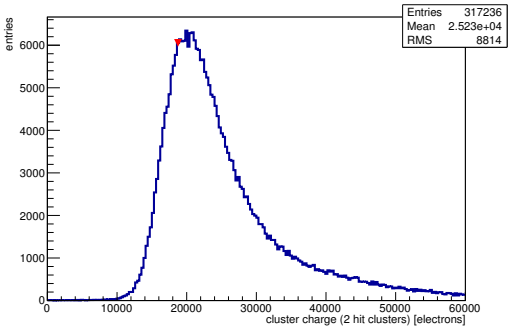

(l) Charge distribution (2 hit cluster).

Figure C.1: Detailed plots for test beam measurement of DO-1 (description see section 6.1) sample (running as DUT0) during runs 30684-30715 in the February 2011 test beam period at DESY. Summary of the data in chapter 9. *(cont.)*

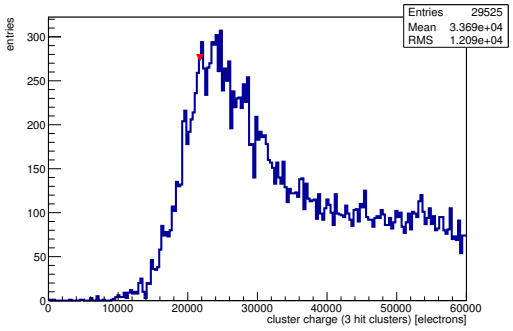

(m) Charge distribution (3 hit cluster).

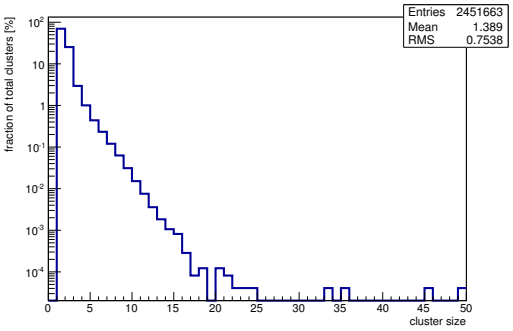

(n) Cluster size distribution.

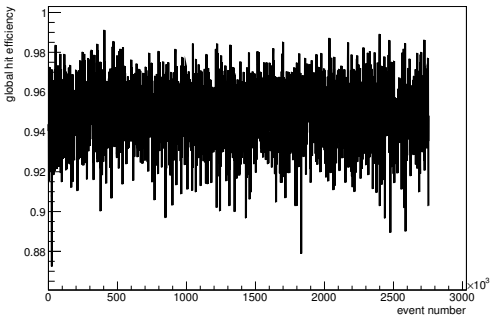

(o) Hit efficiency vs event number.

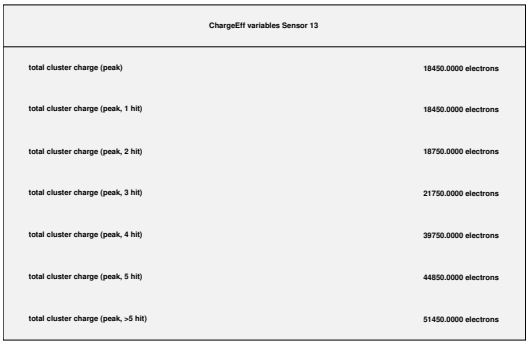

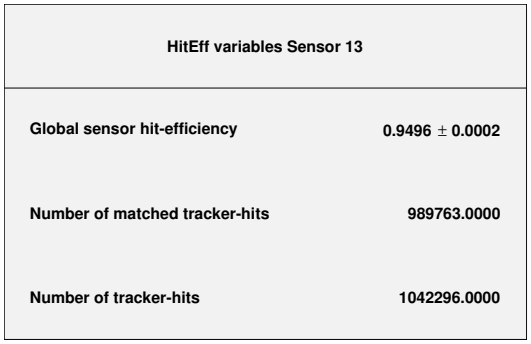

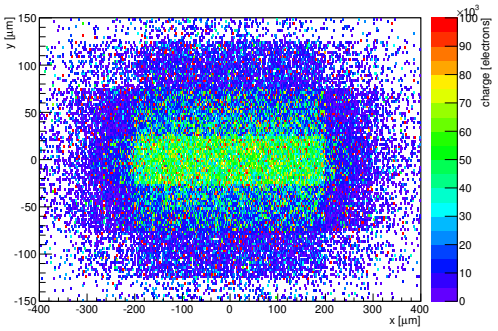

(p) Single pixel mean charge.

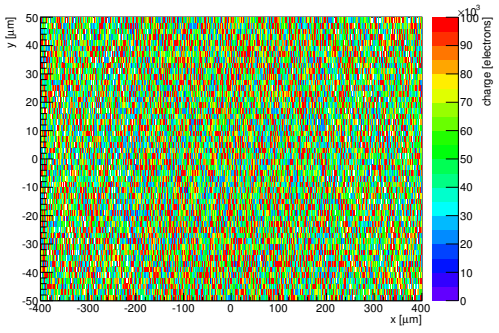

(q) Single pixel mean charge.

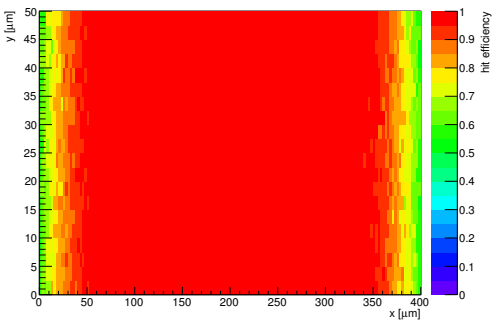

(r) Single pixel hit efficiency.

Figure C.1: Detailed plots for test beam measurement of DO-1 (description see section 6.1) sample (running as DUT0) during runs 30684-30715 in the February 2011 test beam period at DESY. Summary of the data in chapter 9.

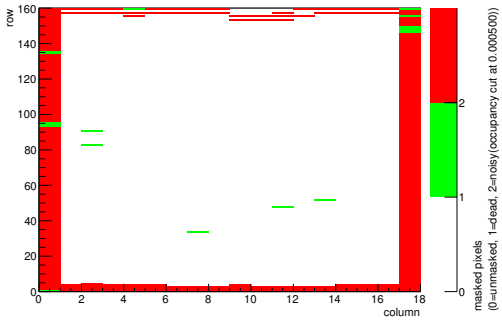

(a) Map of masked pixels.

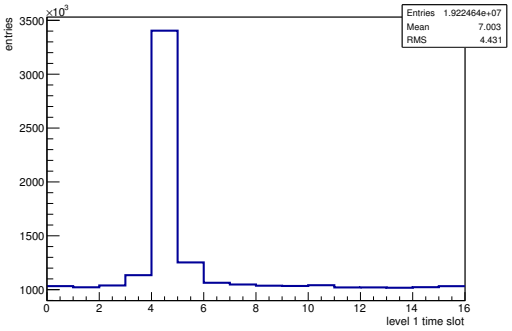

(b) Lvl1 distribution.

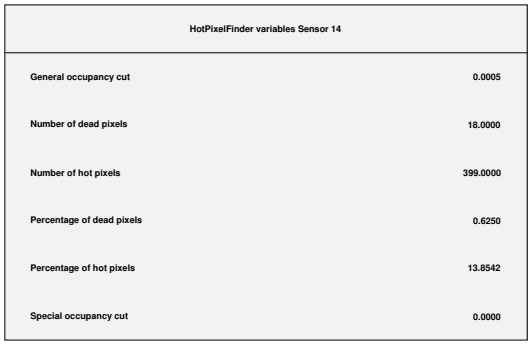

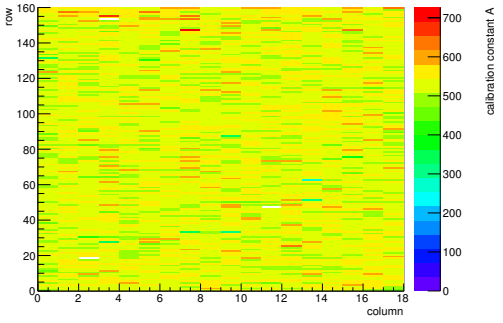

(c) Calibration constant A.

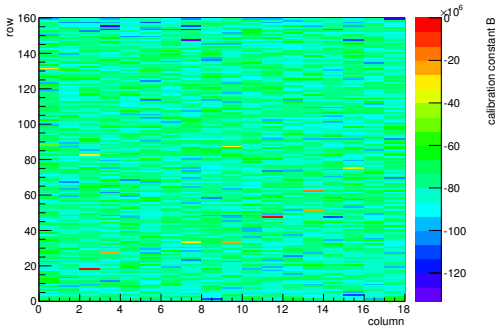

(d) Calibration constant B.

Figure C.2: Detailed plots for test beam measurement of DO-13 (description see section 6.1) sample (running as DUT1) during runs 30684-30715 in the February 2011 test beam period at DESY. Summary of the data in chapter 9. *(cont.)*

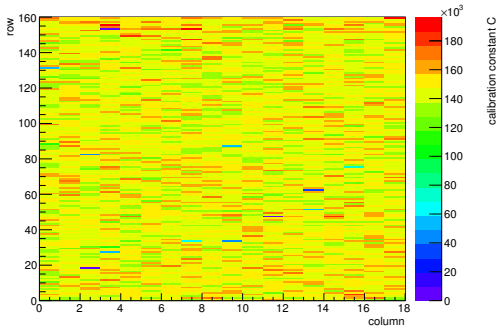

(e) Calibration constant C.

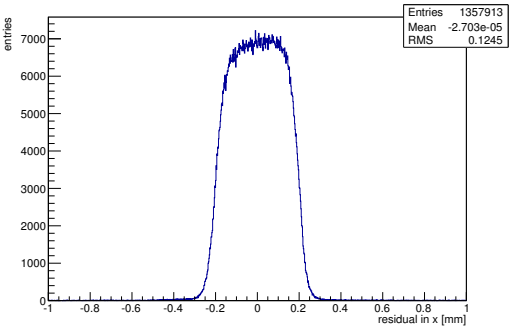

(f) Track residual in x.

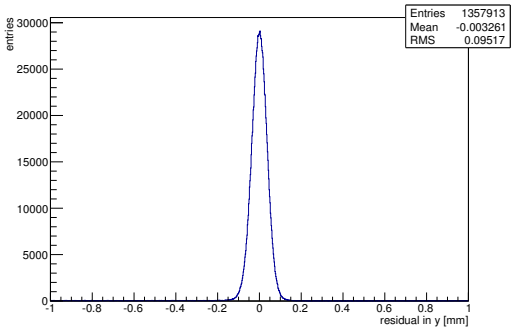

(g) Track residual in y.

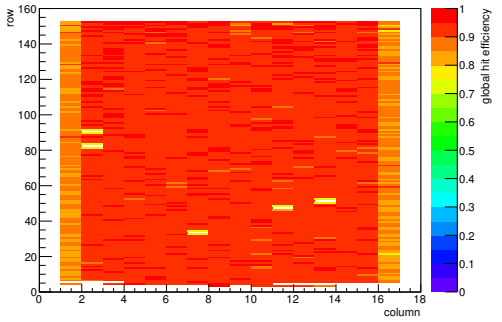

(h) Hit efficiency map.

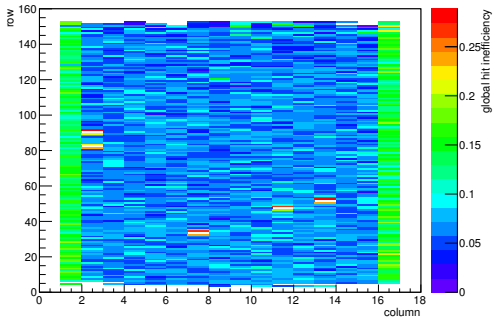

(i) Hit inefficiency map.

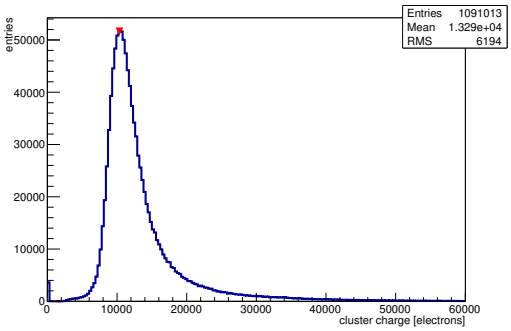

(j) Charge distribution (all cluster sizes included).

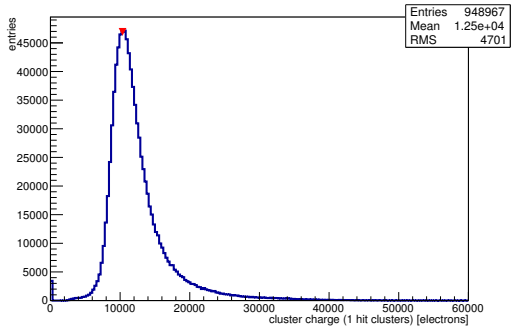

(k) Charge distribution (1 hit cluster).

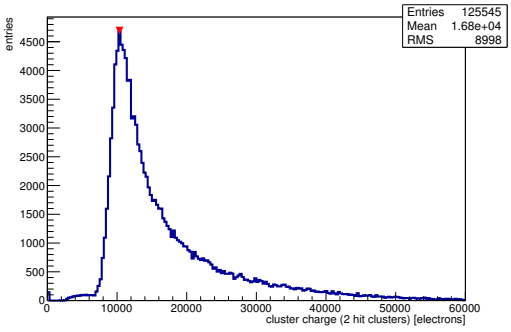

(l) Charge distribution (2 hit cluster).

Figure C.2: Detailed plots for test beam measurement of DO-13 (description see section 6.1) sample (running as DUT1) during runs 30684-30715 in the February 2011 test beam period at DESY. Summary of the data in chapter 9. *(cont.)*

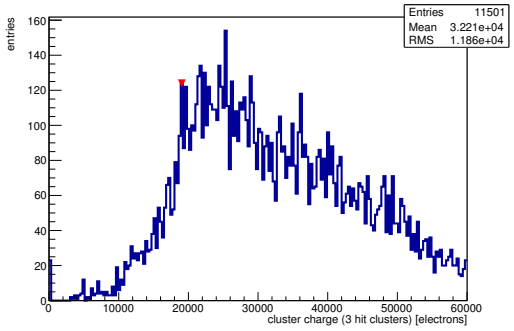

(m) Charge distribution (3 hit cluster).

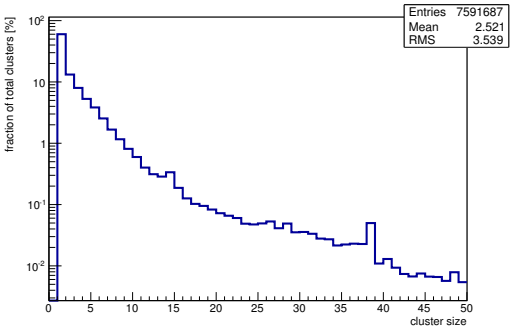

(n) Cluster size distribution.

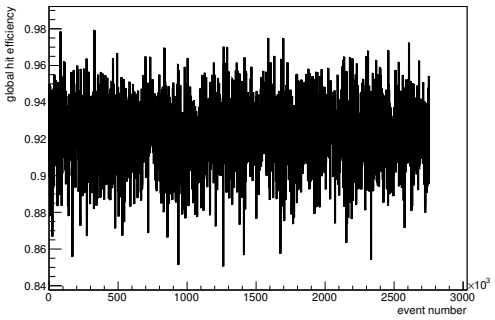

(o) Hit efficiency vs event number.

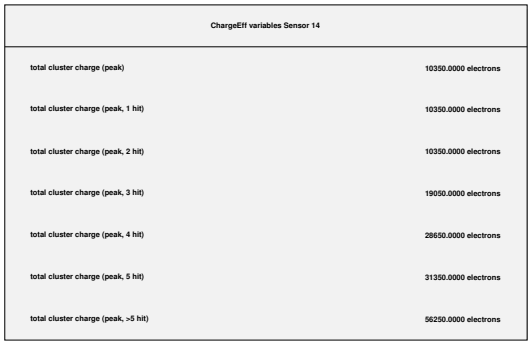

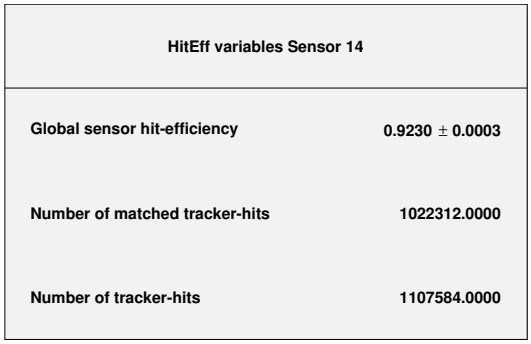

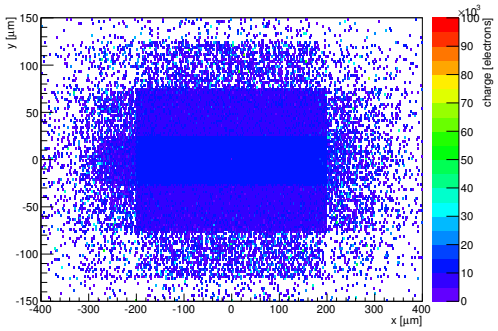

(p) Single pixel mean charge.

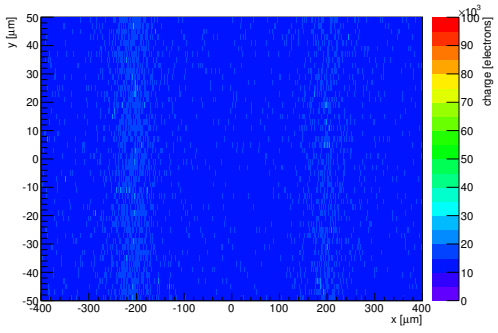

(q) Single pixel mean charge.

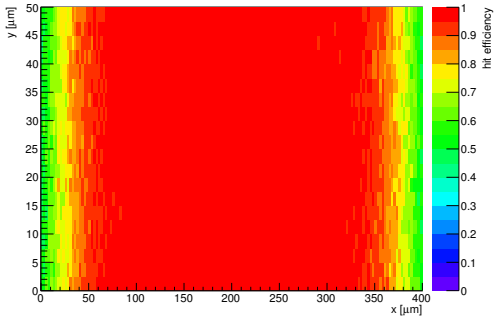

(r) Single pixel hit efficiency.

Figure C.2: Detailed plots for test beam measurement of DO-13 (description see section 6.1) sample (running as DUT1) during runs 30684-30715 in the February 2011 test beam period at DESY. Summary of the data in chapter 9.

C.1.2 Runs 31037-31064

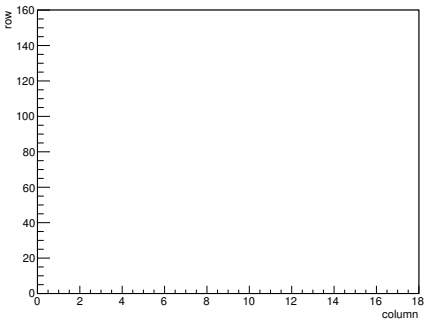

(a) Map of masked pixels.

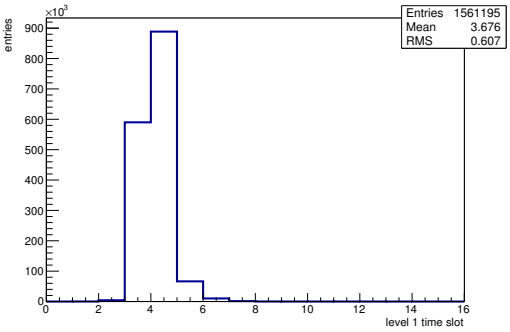

(b) Lvl1 distribution.

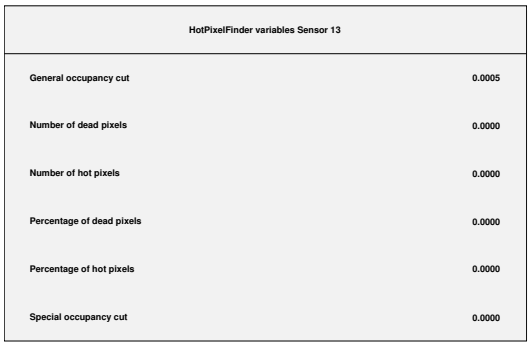

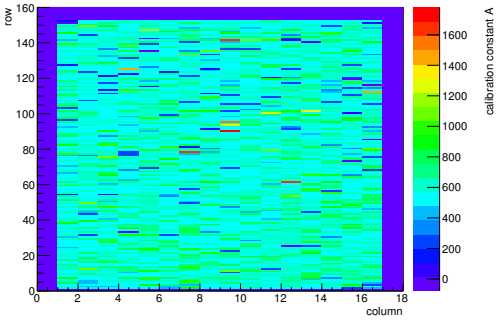

(c) Calibration constant A.

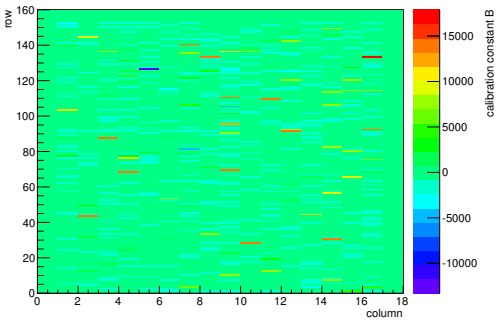

(d) Calibration constant B.

Figure C.3: Detailed plots for test beam measurement of DO-1 (description see section 6.1) sample (running as DUT0) during runs 31037-31064 in the February 2011 test beam period at DESY. Summary of the data in chapter 9. *(cont.)*

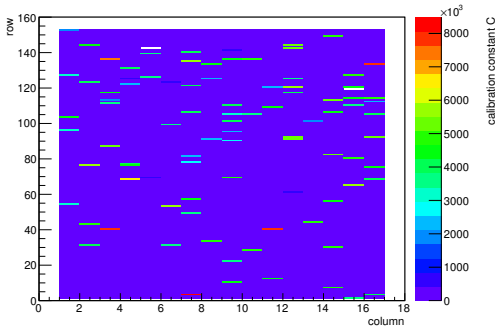

(e) Calibration constant C.

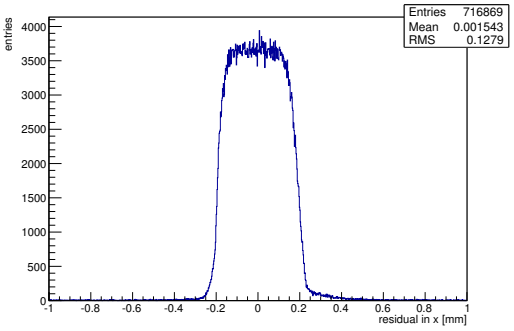

(f) Track residual in x.

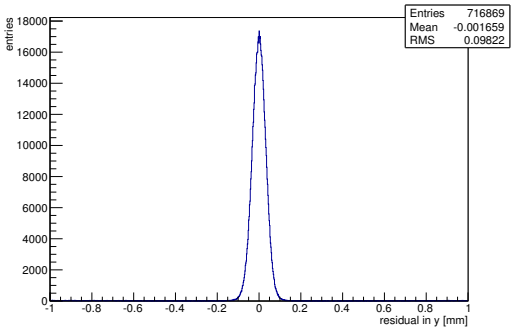

(g) Track residual in y.

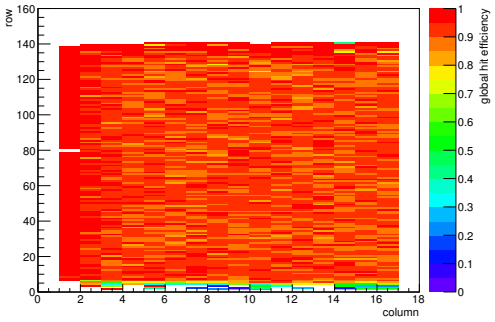

(h) Hit efficiency map.

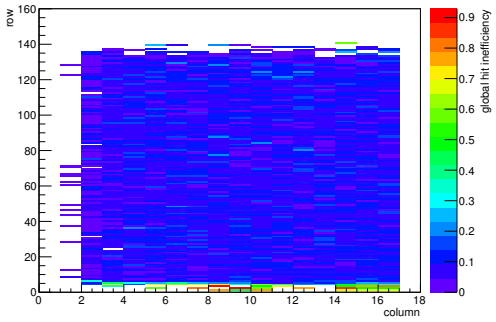

(i) Hit inefficiency map.

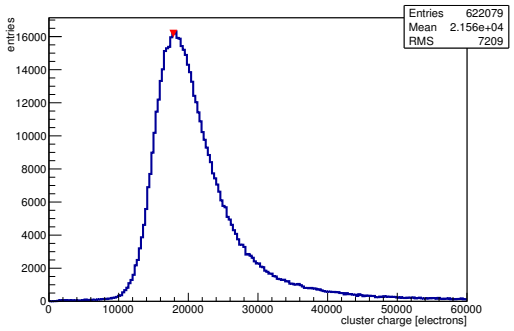

(j) Charge distribution (all cluster sizes included).

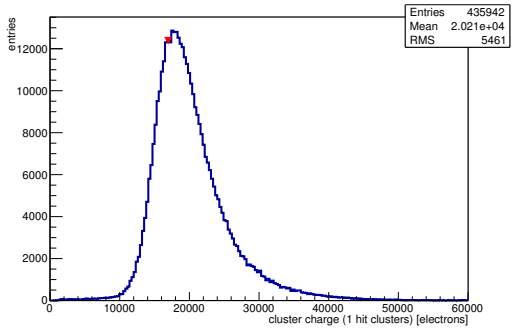

(k) Charge distribution (1 hit cluster).

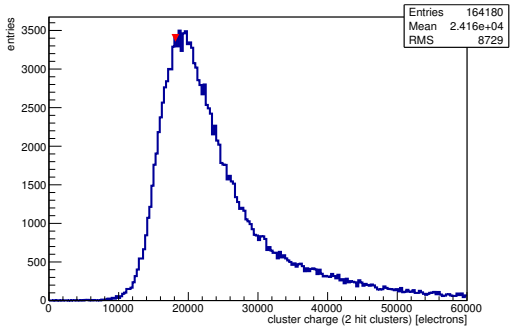

(l) Charge distribution (2 hit cluster).

Figure C.3: Detailed plots for test beam measurement of DO-1 (description see section 6.1) sample (running as DUT0) during runs 31037-31064 in the February 2011 test beam period at DESY. Summary of the data in chapter 9. *(cont.)*

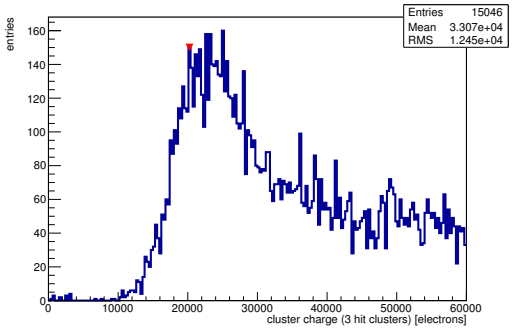

(m) Charge distribution (3 hit cluster).

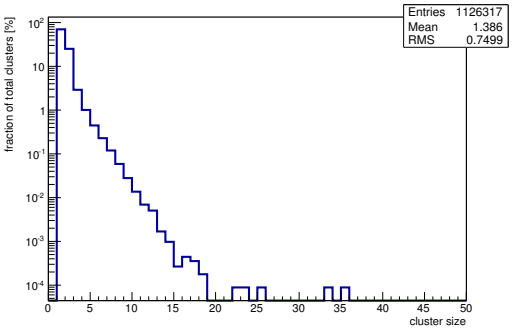

(n) Cluster size distribution.

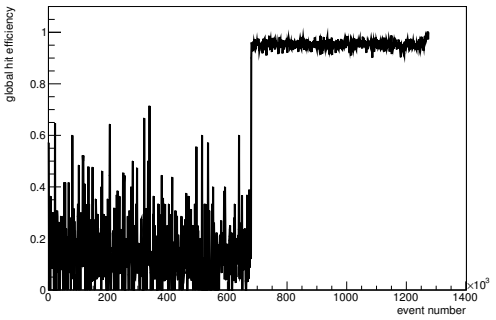

(o) Hit efficiency vs event number.

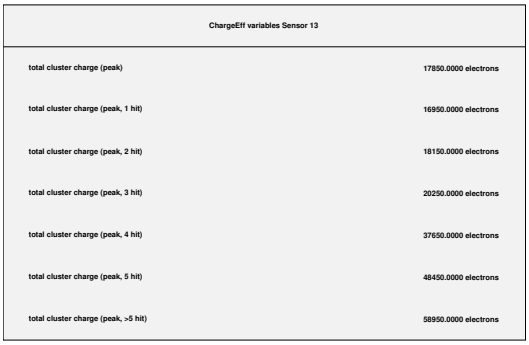

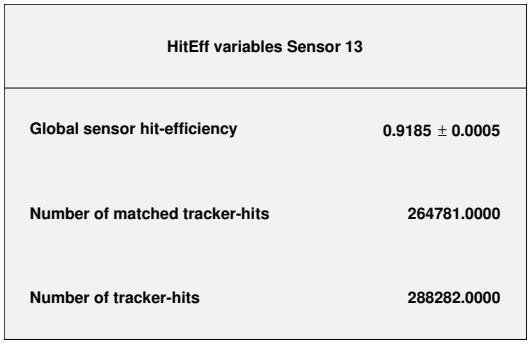

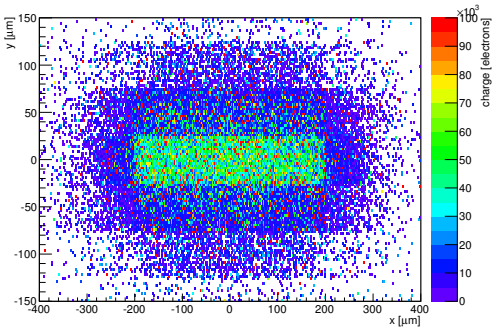

(p) Single pixel mean charge.

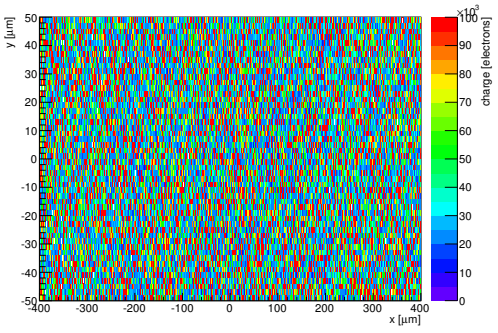

(q) Single pixel mean charge.

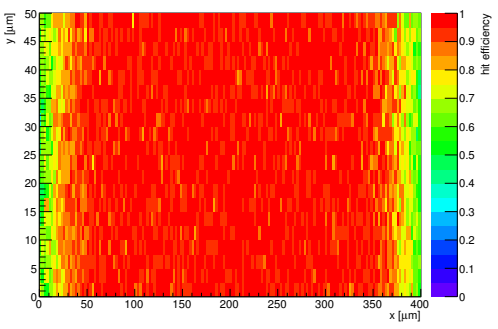

(r) Single pixel hit efficiency.

Figure C.3: Detailed plots for test beam measurement of DO-1 (description see section 6.1) sample (running as DUT0) during runs 31037-31064 in the February 2011 test beam period at DESY. Summary of the data in chapter 9.

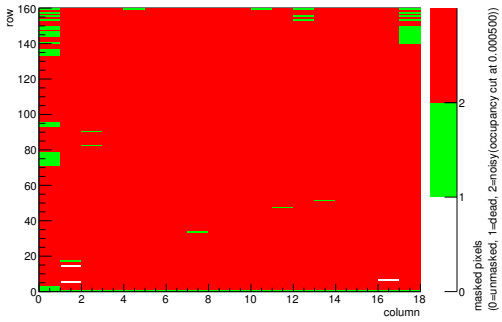

(a) Map of masked pixels.

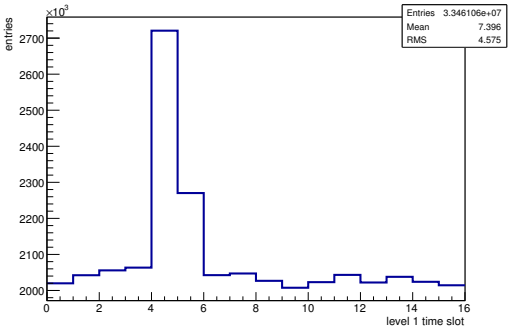

(b) Lvl1 distribution.

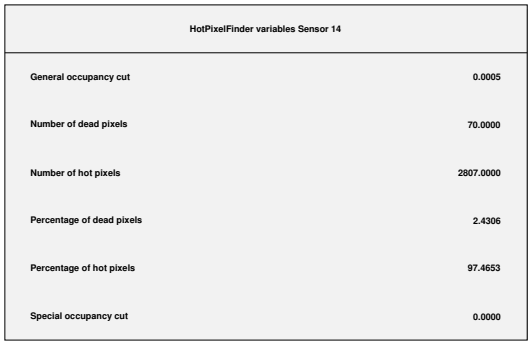

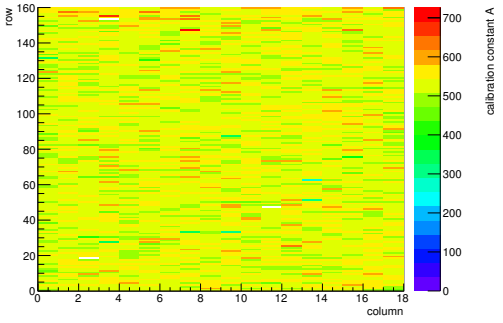

(c) Calibration constant A.

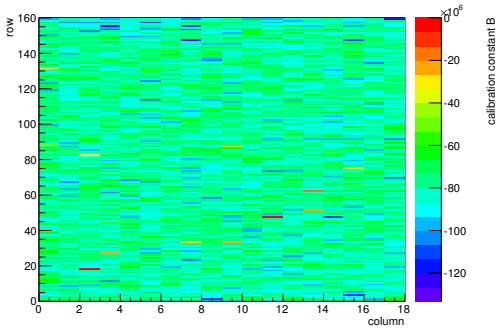

(d) Calibration constant B.

Figure C.4: Detailed plots for test beam measurement of DO-13 (description see section 6.1) sample (running as DUT1) during runs 31037-31064 in the February 2011 test beam period at DESY. Summary of the data in chapter 9. *(cont.)*

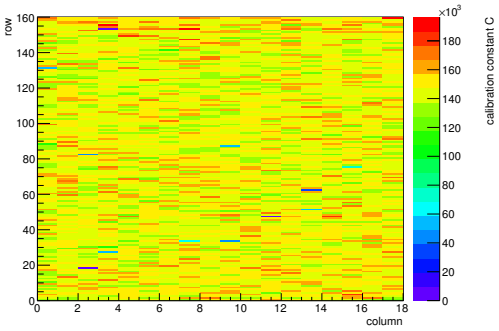

(e) Calibration constant C.

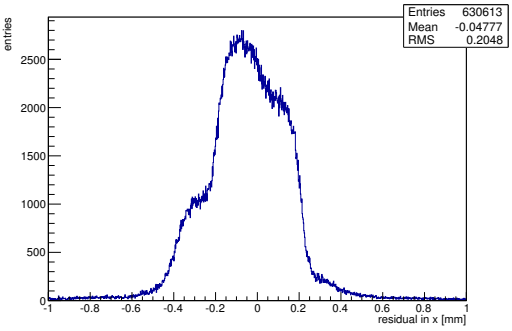

(f) Track residual in x.

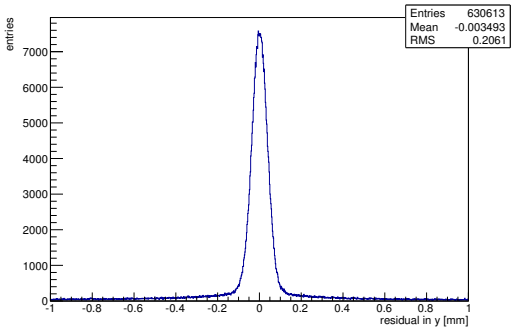

(g) Track residual in y.

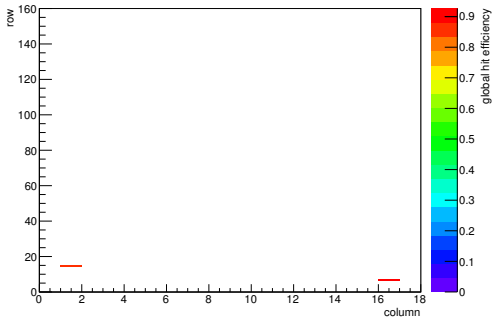

(h) Hit efficiency map.

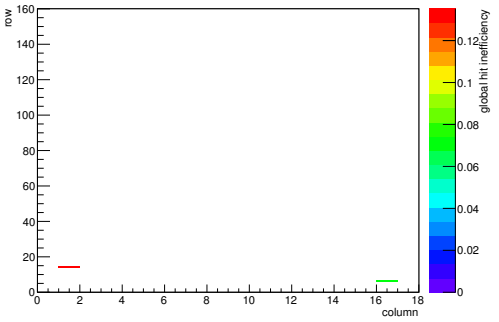

(i) Hit inefficiency map.

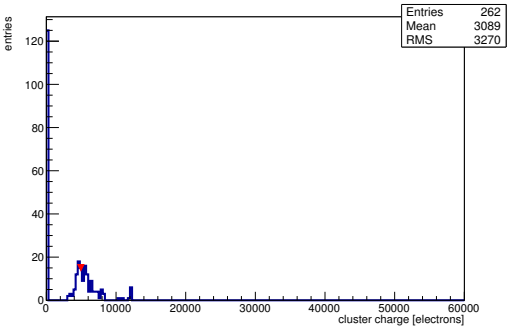

(j) Charge distribution (all cluster sizes included).

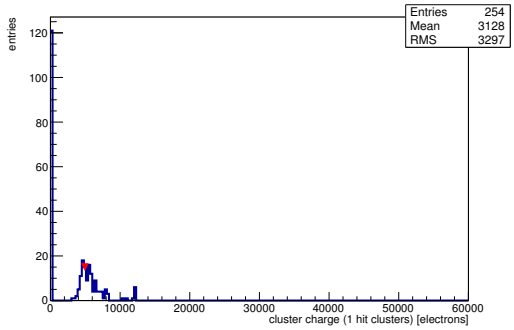

(k) Charge distribution (1 hit cluster).

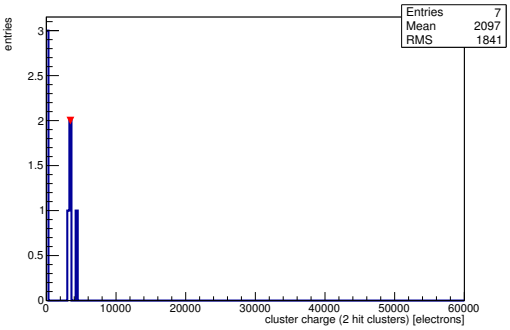

(l) Charge distribution (2 hit cluster).

Figure C.4: Detailed plots for test beam measurement of DO-13 (description see section 6.1) sample (running as DUT1) during runs 31037-31064 in the February 2011 test beam period at DESY. Summary of the data in chapter 9. *(cont.)*

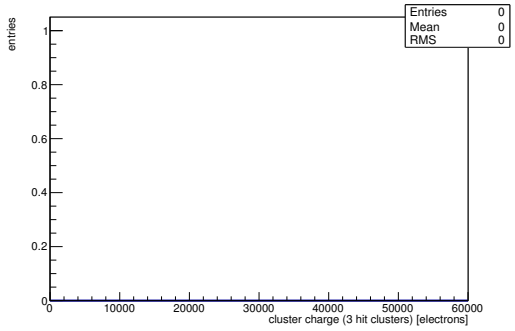

(m) Charge distribution (3 hit cluster).

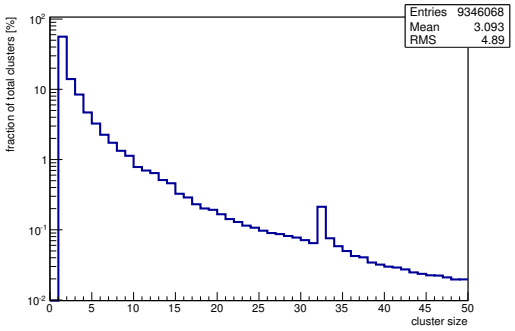

(n) Cluster size distribution.

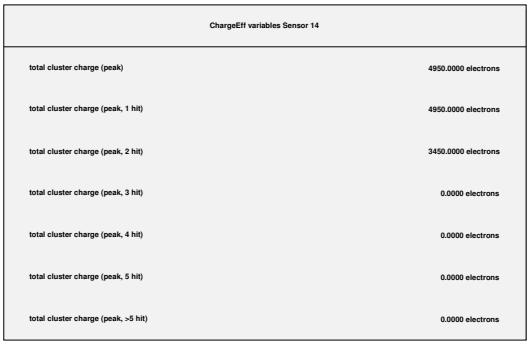

(o) Hit efficiency vs event number.

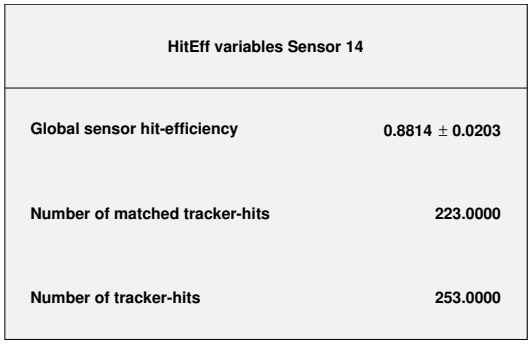

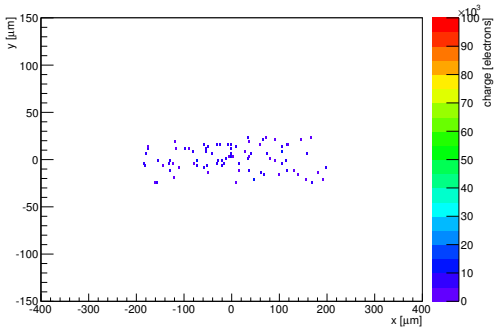

(p) Single pixel mean charge.

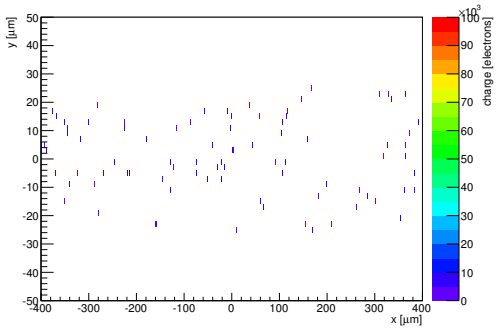

(q) Single pixel mean charge.

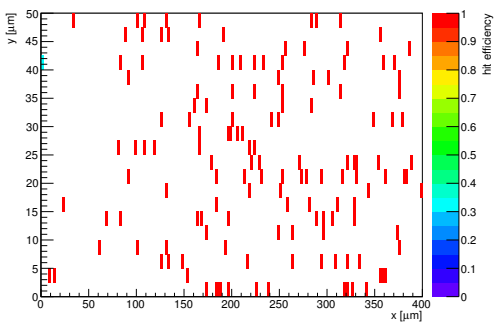

(r) Single pixel hit efficiency.

Figure C.4: Detailed plots for test beam measurement of DO-13 (description see section 6.1) sample (running as DUT1) during runs 31037-31064 in the February 2011 test beam period at DESY. Summary of the data in chapter 9.

C.1.3 Runs 31066-31069

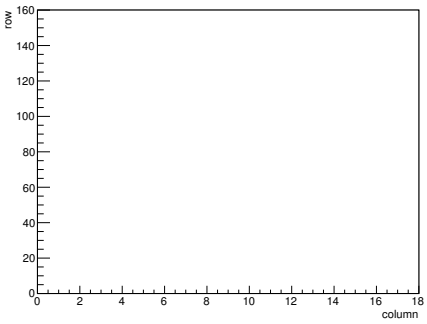

(a) Map of masked pixels.

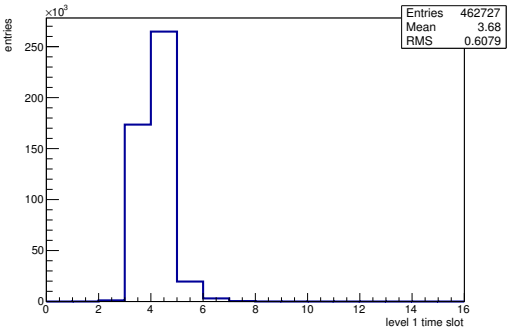

(b) Lvl1 distribution.

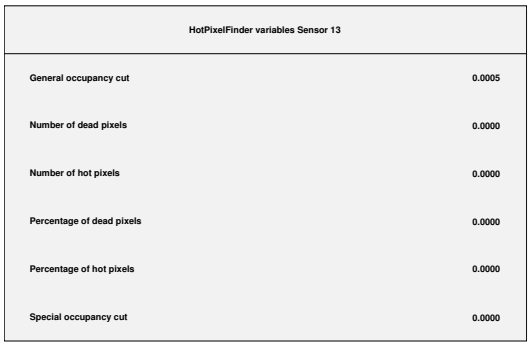

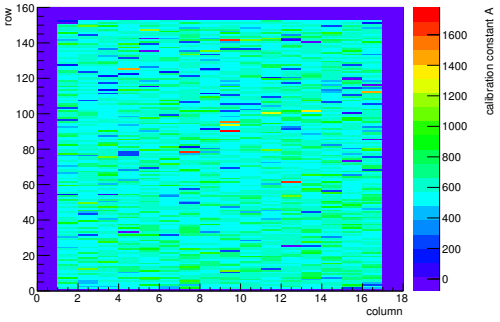

(c) Calibration constant A.

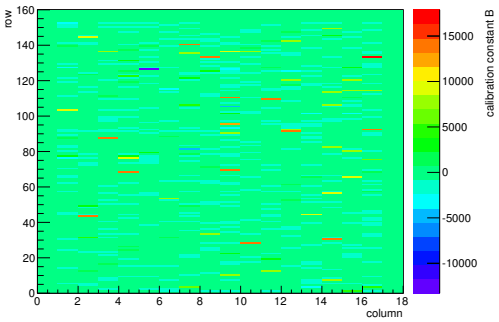

(d) Calibration constant B.

Figure C.5: Detailed plots for test beam measurement of DO-1 (description see section 6.1) sample (running as DUT0) during runs 31066-31069 in the February 2011 test beam period at DESY. Summary of the data in chapter 9. *(cont.)*

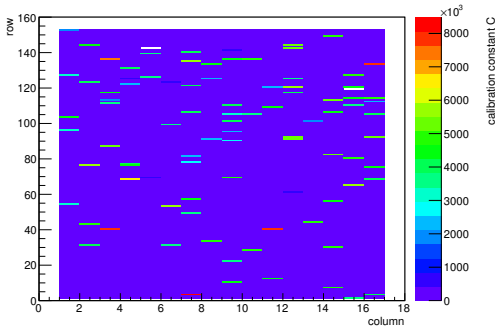

(e) Calibration constant C.

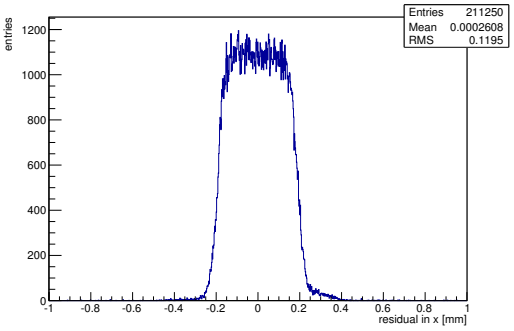

(f) Track residual in x.

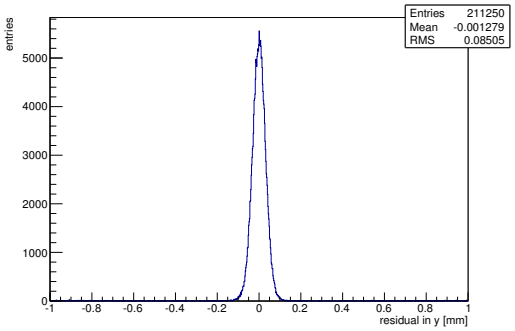

(g) Track residual in y.

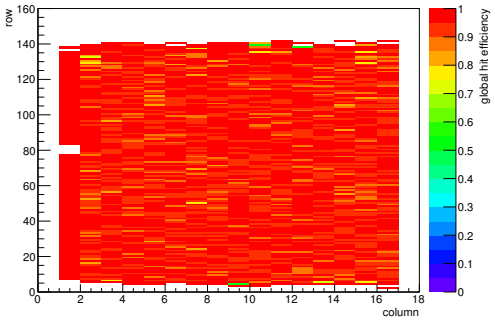

(h) Hit efficiency map.

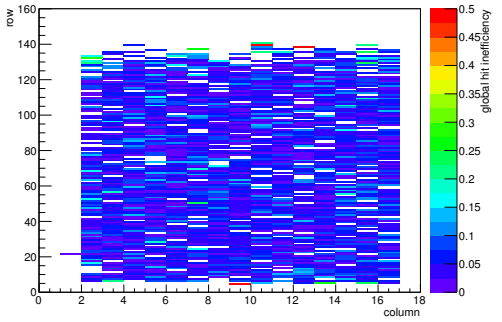

(i) Hit inefficiency map.

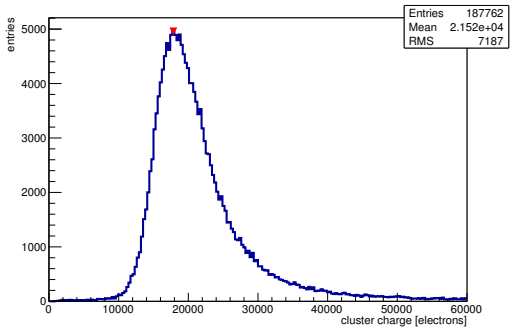

(j) Charge distribution (all cluster sizes included).

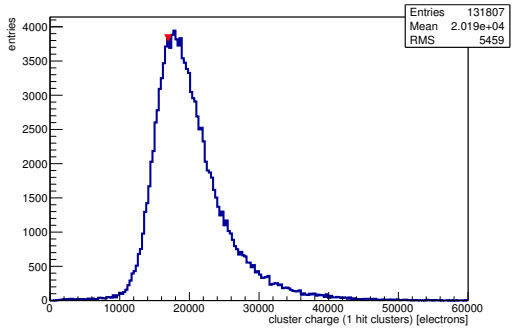

(k) Charge distribution (1 hit cluster).

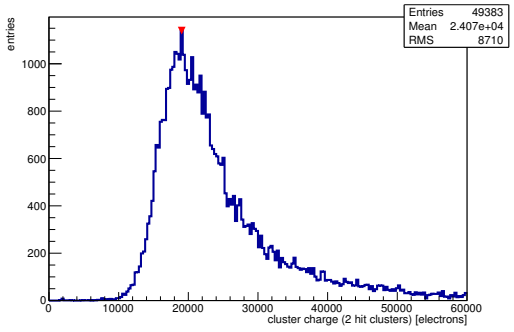

(l) Charge distribution (2 hit cluster).

Figure C.5: Detailed plots for test beam measurement of DO-1 (description see section 6.1) sample (running as DUT0) during runs 31066-31069 in the February 2011 test beam period at DESY. Summary of the data in chapter 9. *(cont.)*

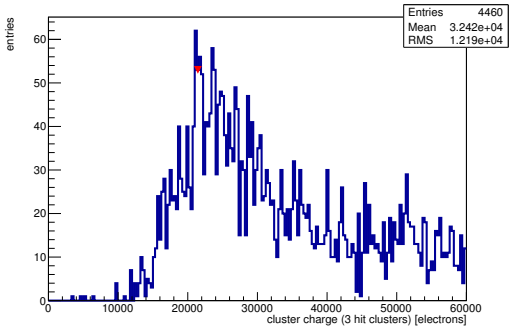

(m) Charge distribution (3 hit cluster).

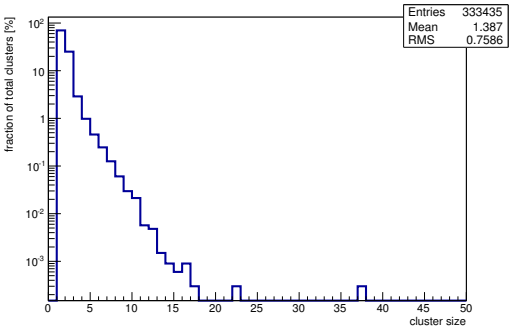

(n) Cluster size distribution.

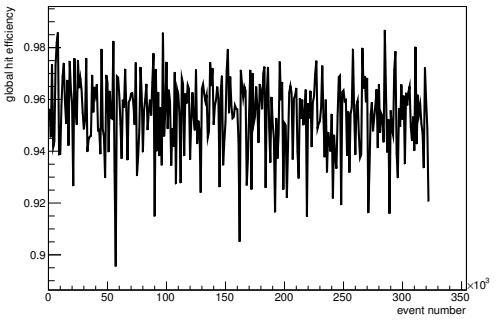

(o) Hit efficiency vs event number.

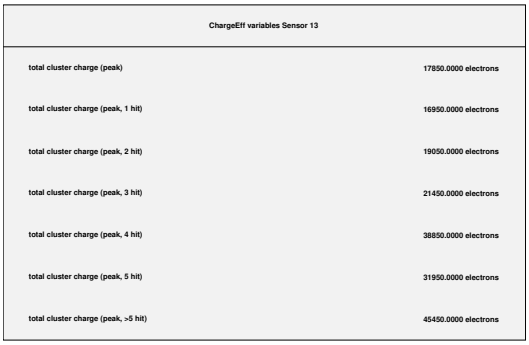

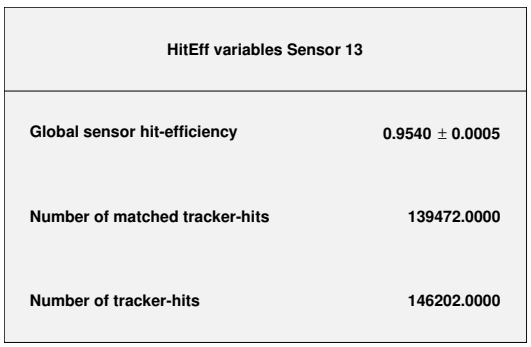

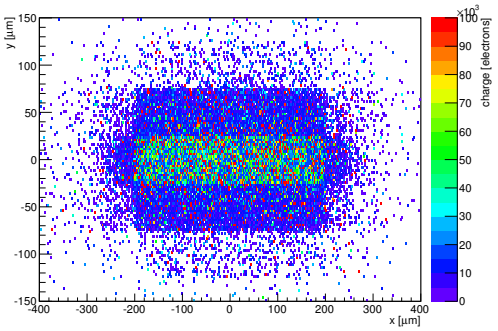

(p) Single pixel mean charge.

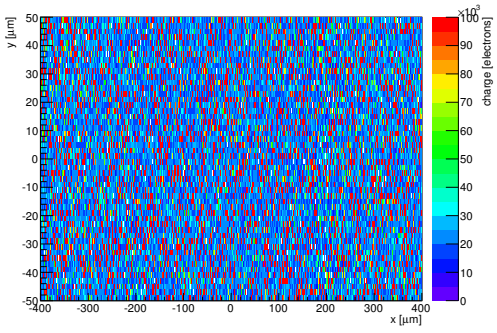

(q) Single pixel mean charge.

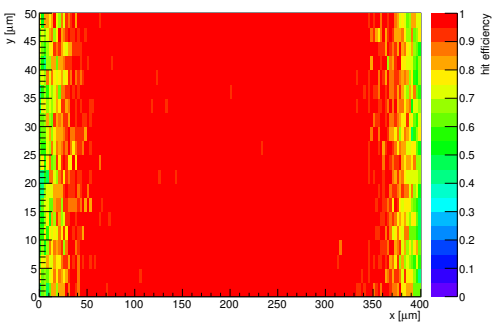

(r) Single pixel hit efficiency.

Figure C.5: Detailed plots for test beam measurement of DO-1 (description see section 6.1) sample (running as DUT0) during runs 31066-31069 in the February 2011 test beam period at DESY. Summary of the data in chapter 9.

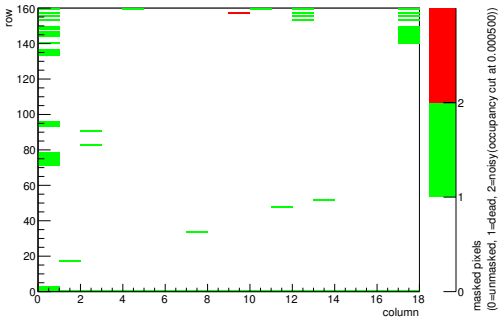

(a) Map of masked pixels.

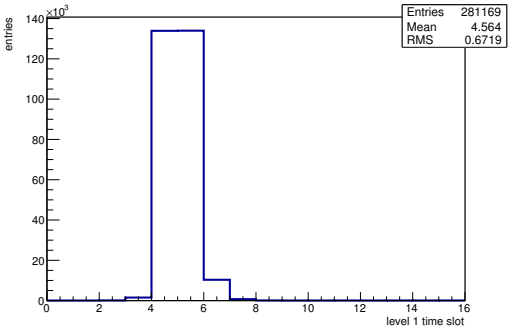

(b) Lvl1 distribution.

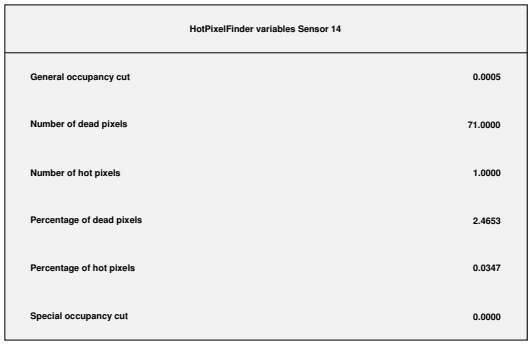

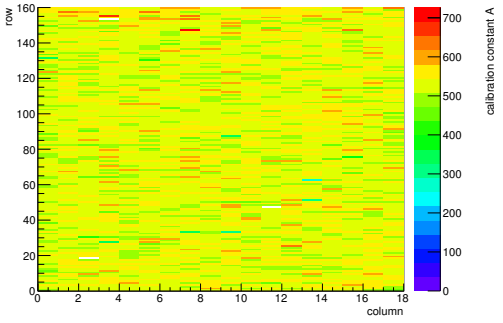

(c) Calibration constant A.

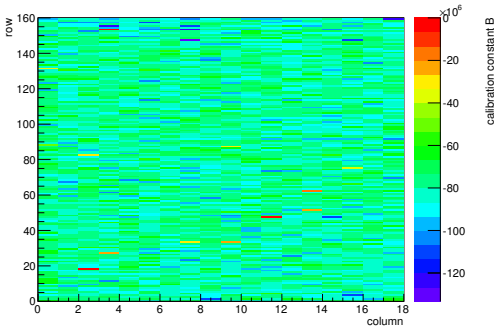

(d) Calibration constant B.

Figure C.6: Detailed plots for test beam measurement of DO-13 (description see section 6.1) sample (running as DUT1) during runs 31066-31069 in the February 2011 test beam period at DESY. Summary of the data in chapter 9. *(cont.)*

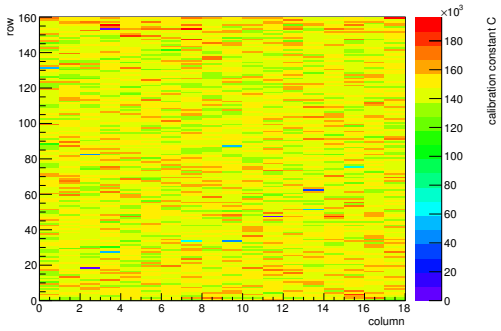

(e) Calibration constant C.

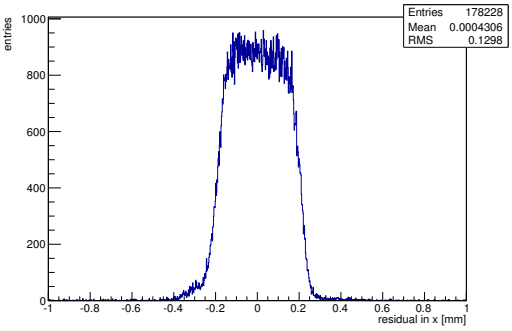

(f) Track residual in x.

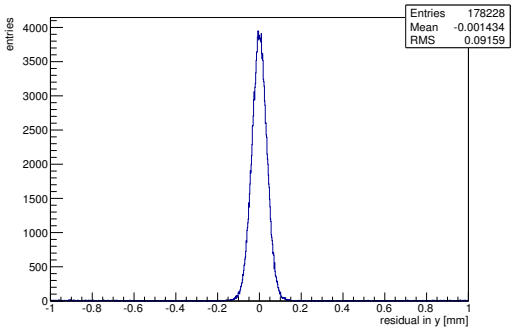

(g) Track residual in y.

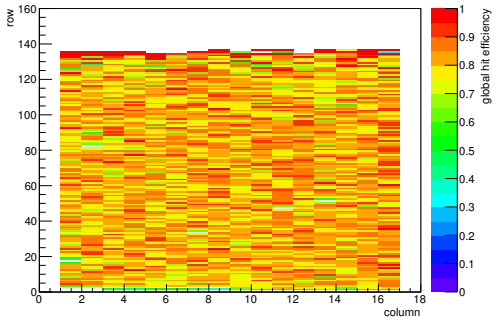

(h) Hit efficiency map.

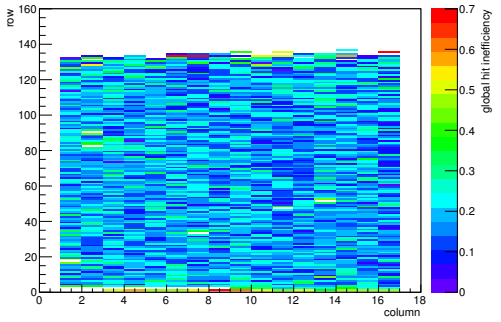

(i) Hit inefficiency map.

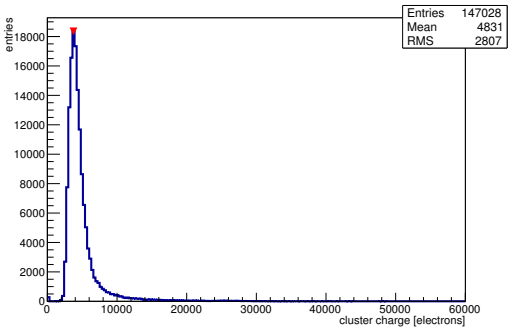

(j) Charge distribution (all cluster sizes included).

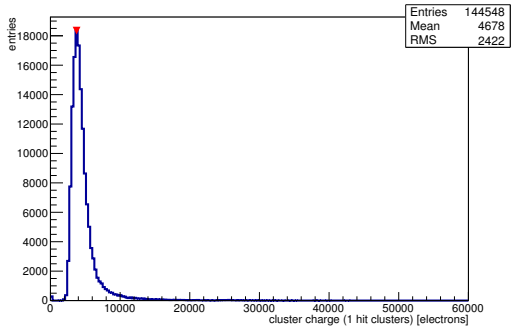

(k) Charge distribution (1 hit cluster).

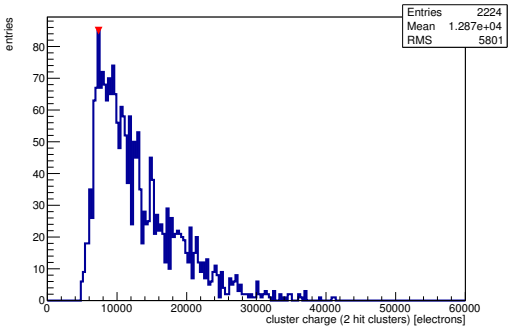

(l) Charge distribution (2 hit cluster).

Figure C.6: Detailed plots for test beam measurement of DO-13 (description see section 6.1) sample (running as DUT1) during runs 31066-31069 in the February 2011 test beam period at DESY. Summary of the data in chapter 9. *(cont.)*

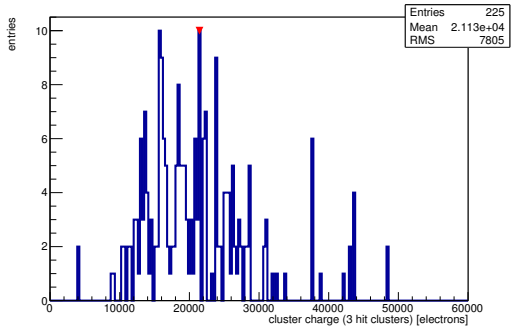

(m) Charge distribution (3 hit cluster).

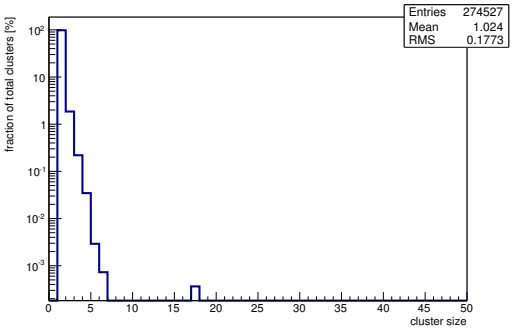

(n) Cluster size distribution.

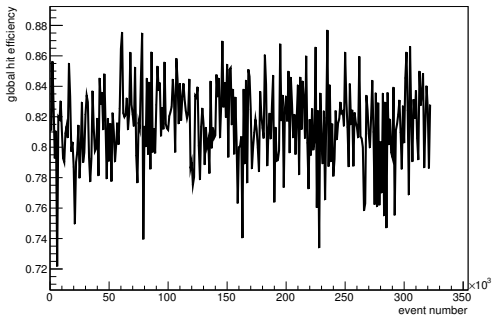

(o) Hit efficiency vs event number.

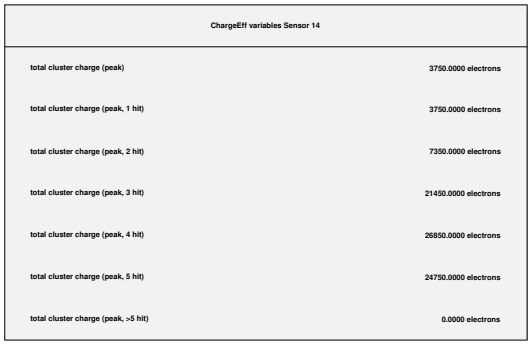

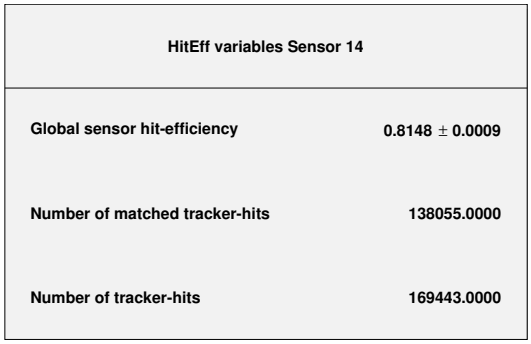

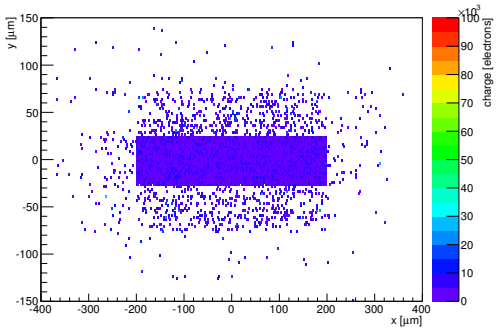

(p) Single pixel mean charge.

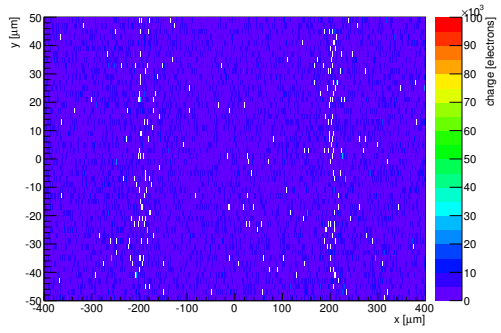

(q) Single pixel mean charge.

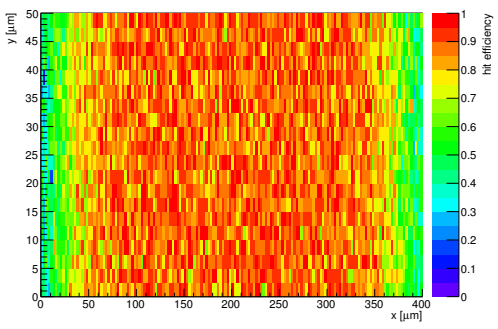

(r) Single pixel hit efficiency.

Figure C.6: Detailed plots for test beam measurement of DO-13 (description see section 6.1) sample (running as DUT1) during runs 31066-31069 in the February 2011 test beam period at DESY. Summary of the data in chapter 9.

C.1.4 Runs 31071-31082

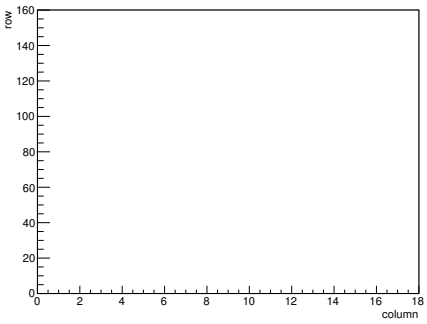

(a) Map of masked pixels.

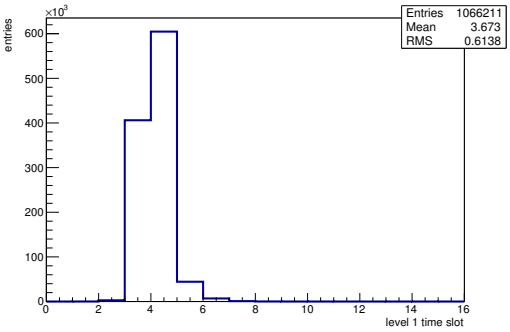

(b) Lvl1 distribution.

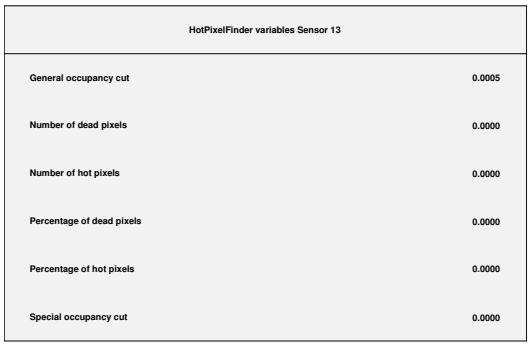

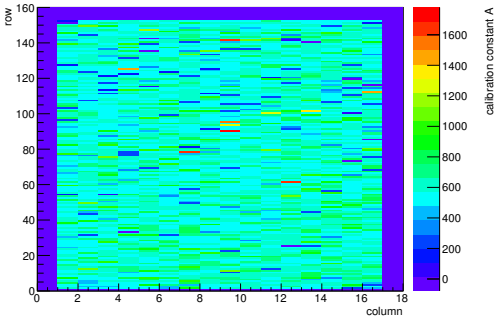

(c) Calibration constant A.

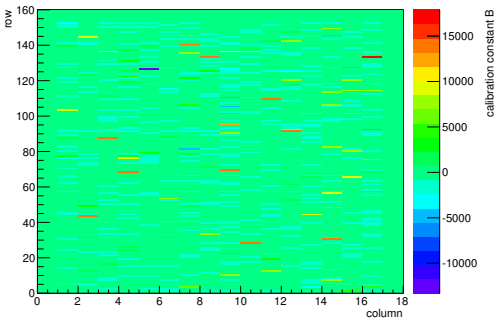

(d) Calibration constant B.

Figure C.7: Detailed plots for test beam measurement of DO-1 (description see section 6.1) sample (running as DUT0) during runs 31071-31082 in the February 2011 test beam period at DESY. Summary of the data in chapter 9. *(cont.)*

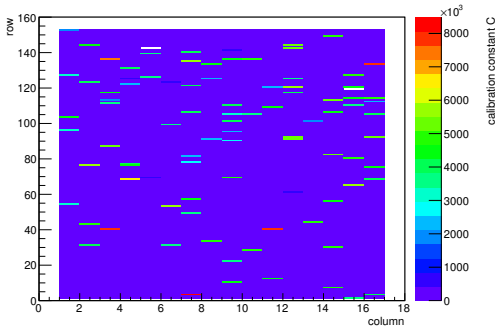

(e) Calibration constant C.

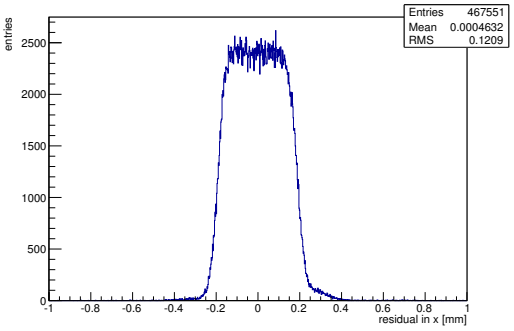

(f) Track residual in x.

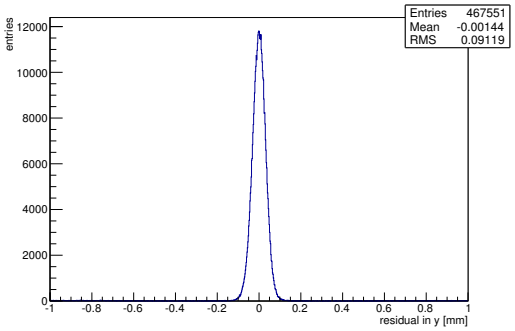

(g) Track residual in y.

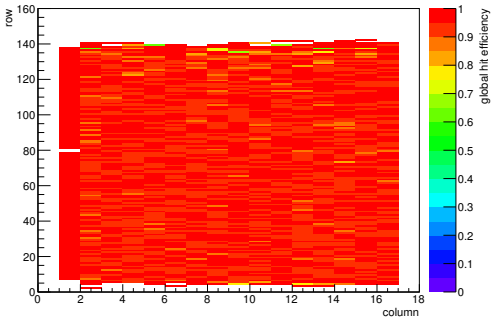

(h) Hit efficiency map.

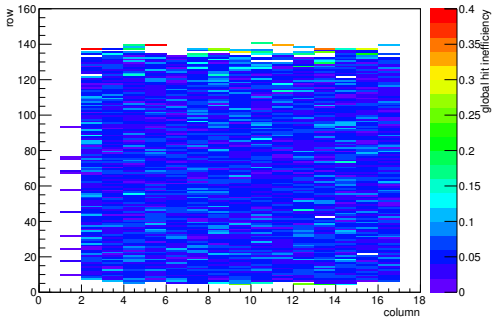

(i) Hit inefficiency map.

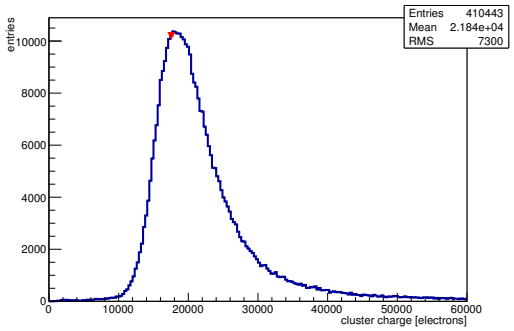

(j) Charge distribution (all cluster sizes included).

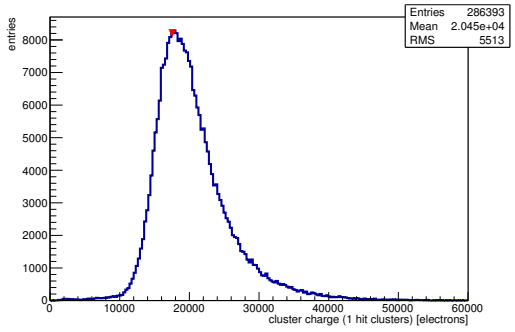

(k) Charge distribution (1 hit cluster).

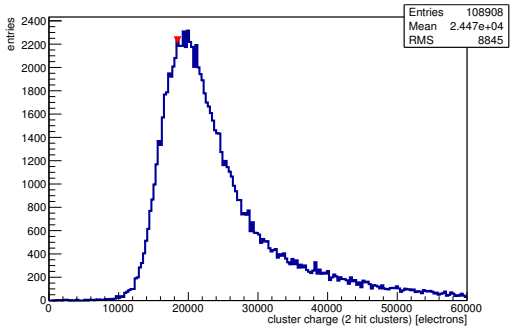

(l) Charge distribution (2 hit cluster).

Figure C.7: Detailed plots for test beam measurement of DO-1 (description see section 6.1) sample (running as DUT0) during runs 31071-31082 in the February 2011 test beam period at DESY. Summary of the data in chapter 9. *(cont.)*

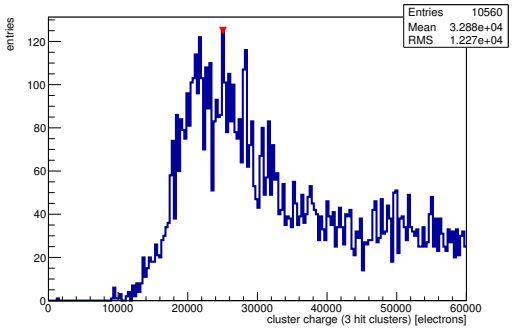

(m) Charge distribution (3 hit cluster).

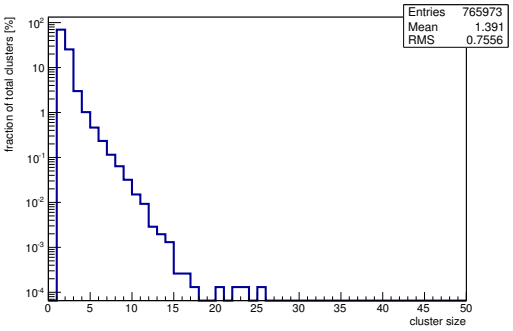

(n) Cluster size distribution.

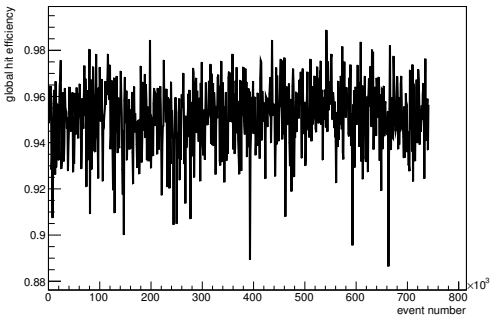

(o) Hit efficiency vs event number.

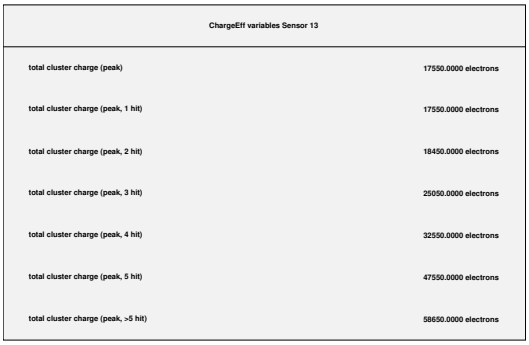

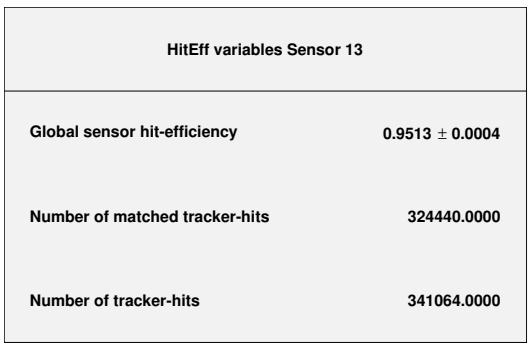

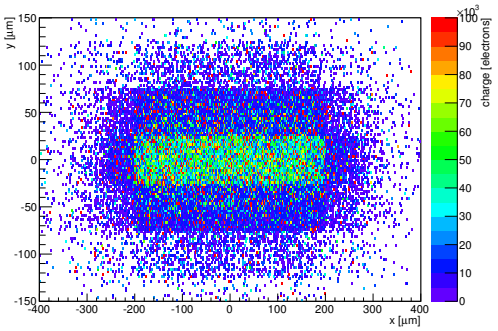

(p) Single pixel mean charge.

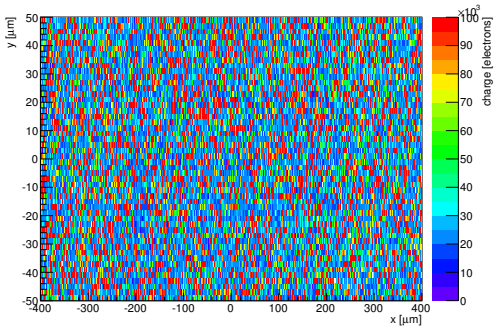

(q) Single pixel mean charge.

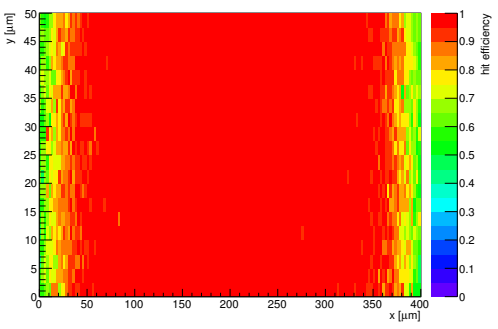

(r) Single pixel hit efficiency.

Figure C.7: Detailed plots for test beam measurement of DO-1 (description see section 6.1) sample (running as DUT0) during runs 31071-31082 in the February 2011 test beam period at DESY. Summary of the data in chapter 9.

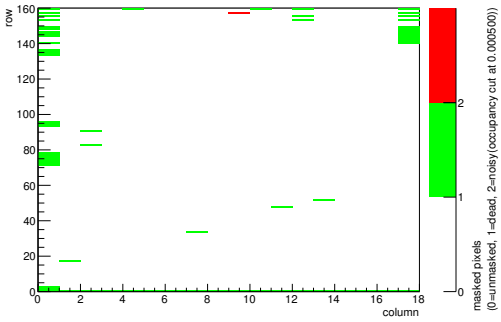

(a) Map of masked pixels.

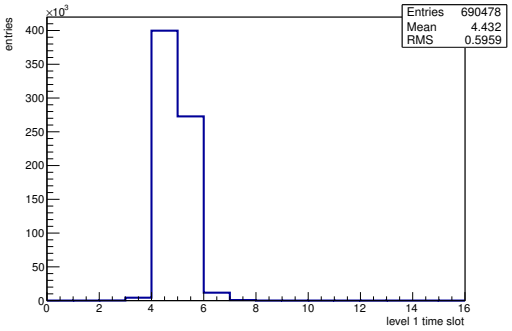

(b) Lvl1 distribution.

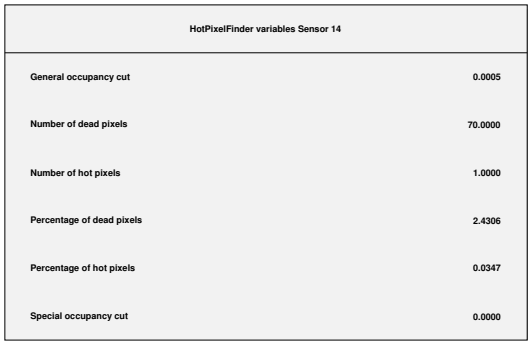

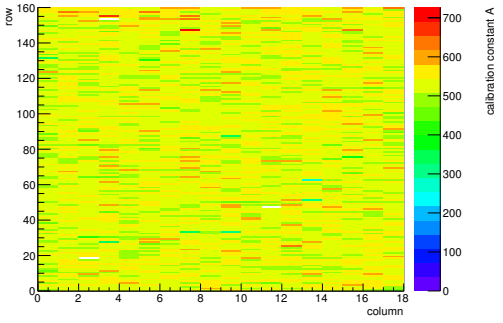

(c) Calibration constant A.

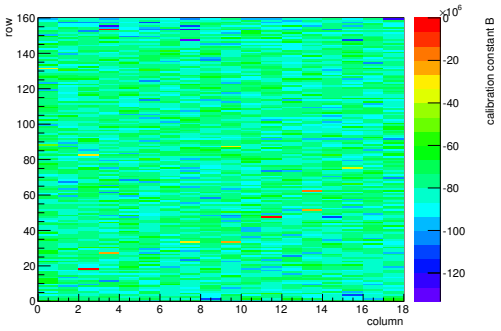

(d) Calibration constant B.

Figure C.8: Detailed plots for test beam measurement of DO-13 (description see section 6.1) sample (running as DUT1) during runs 31071-31082 in the February 2011 test beam period at DESY. Summary of the data in chapter 9. *(cont.)*

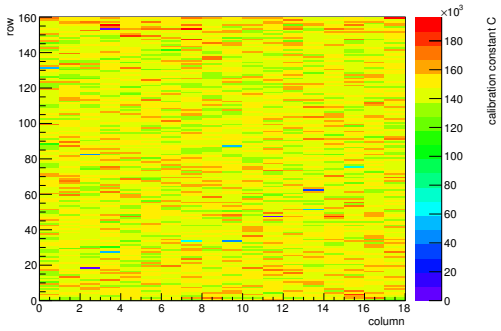

(e) Calibration constant C.

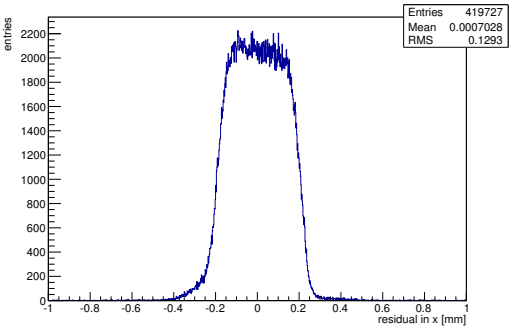

(f) Track residual in x.

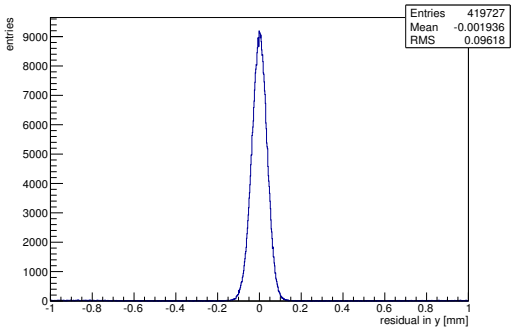

(g) Track residual in y.

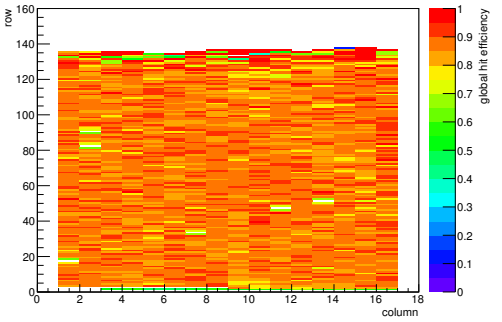

(h) Hit efficiency map.

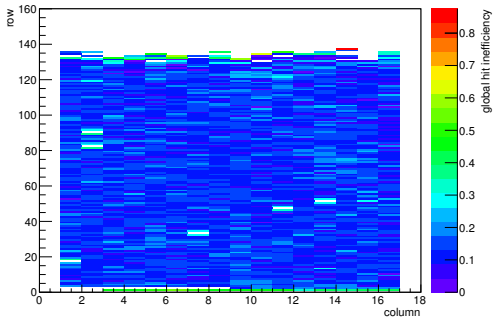

(i) Hit inefficiency map.

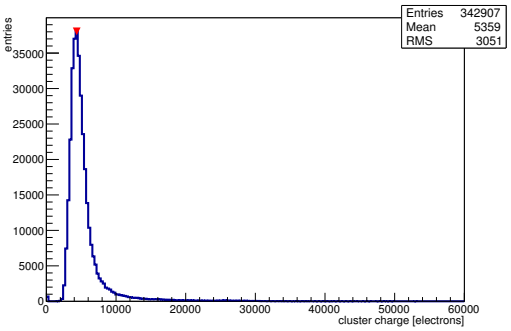

(j) Charge distribution (all cluster sizes included).

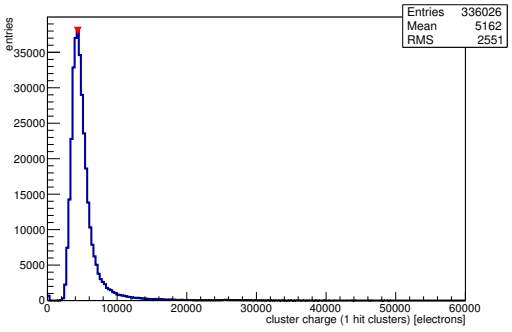

(k) Charge distribution (1 hit cluster).

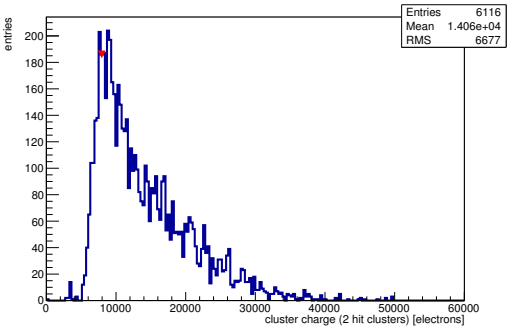

(l) Charge distribution (2 hit cluster).

Figure C.8: Detailed plots for test beam measurement of DO-13 (description see section 6.1) sample (running as DUT1) during runs 31071-31082 in the February 2011 test beam period at DESY. Summary of the data in chapter 9. *(cont.)*

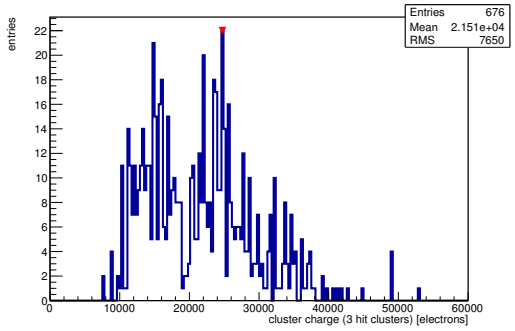

(m) Charge distribution (3 hit cluster).

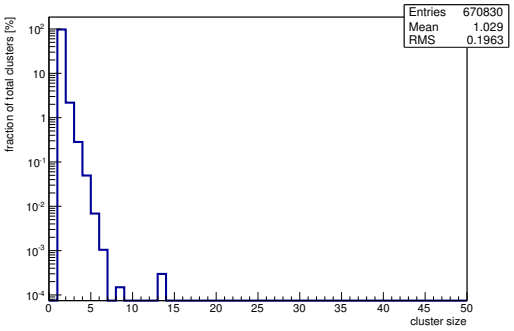

(n) Cluster size distribution.

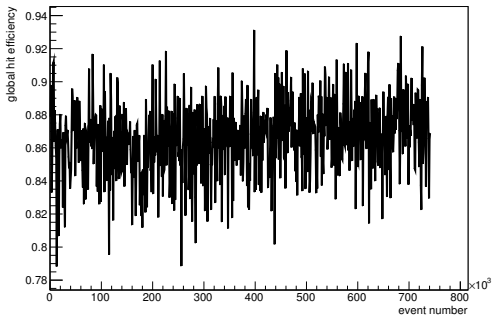

(o) Hit efficiency vs event number.

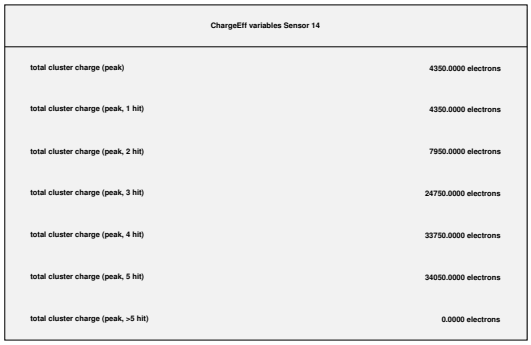

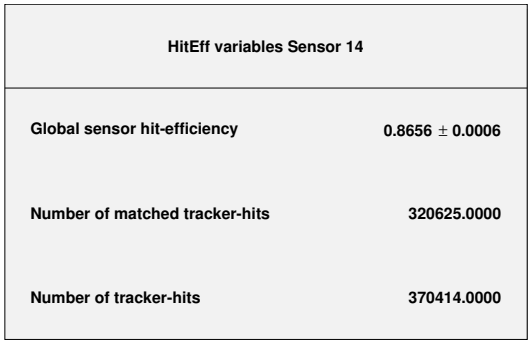

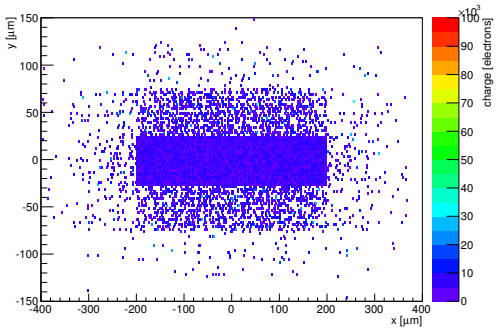

(p) Single pixel mean charge.

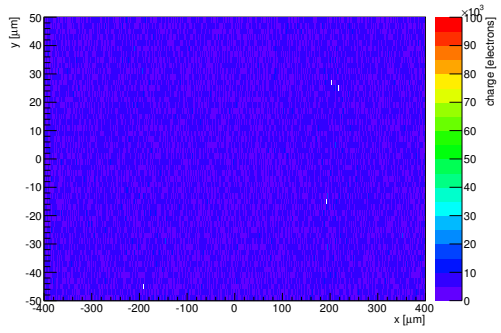

(q) Single pixel mean charge.

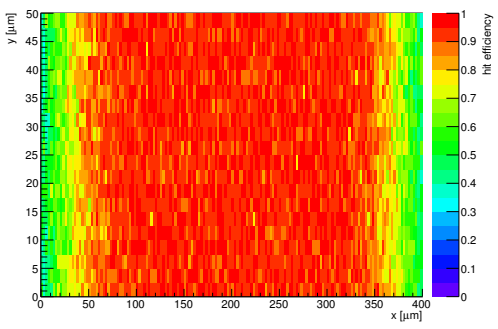

(r) Single pixel hit efficiency.

Figure C.8: Detailed plots for test beam measurement of DO-13 (description see section 6.1) sample (running as DUT1) during runs 31071-31082 in the February 2011 test beam period at DESY. Summary of the data in chapter 9.

C.1.5 Runs 31140-31165

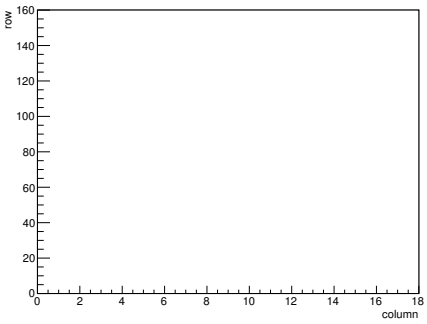

(a) Map of masked pixels.

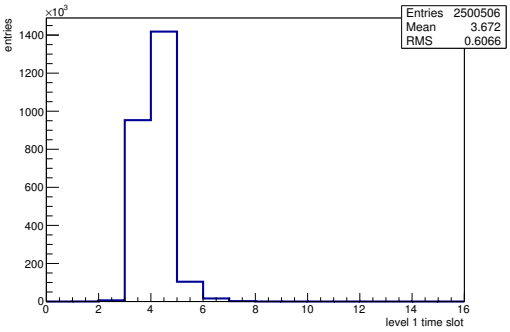

(b) Lvl1 distribution.

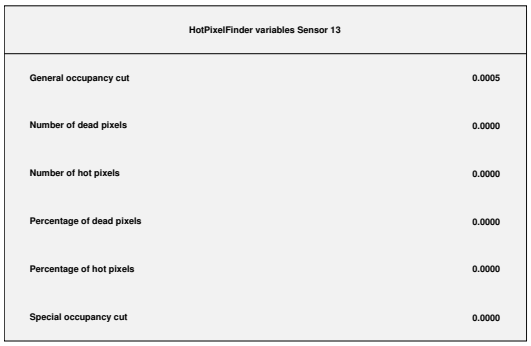

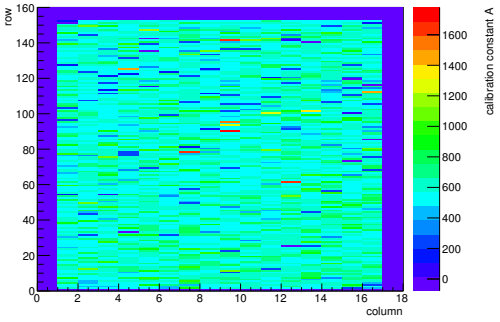

(c) Calibration constant A.

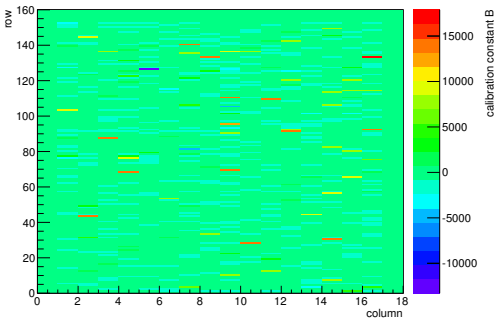

(d) Calibration constant B.

Figure C.9: Detailed plots for test beam measurement of DO-1 (description see section 6.1) sample (running as DUT0) during runs 31140-31165 in the February 2011 test beam period at DESY. Summary of the data in chapter 9. *(cont.)*

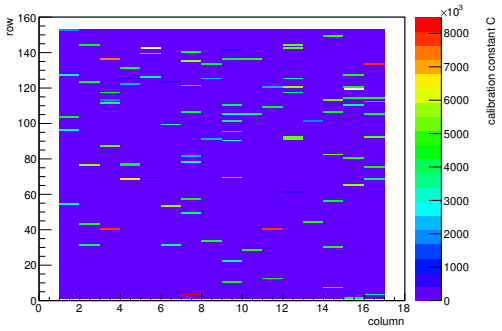

(e) Calibration constant C.

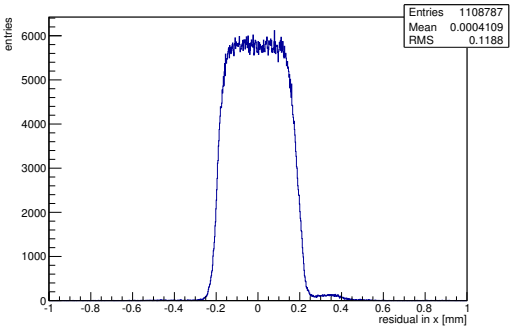

(f) Track residual in x.

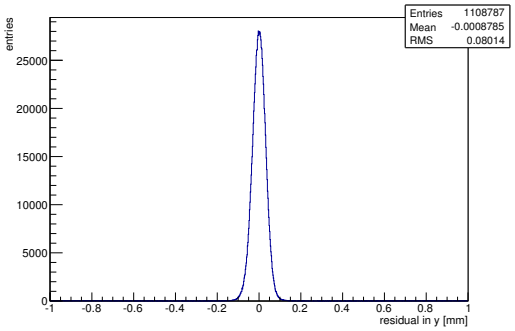

(g) Track residual in y.

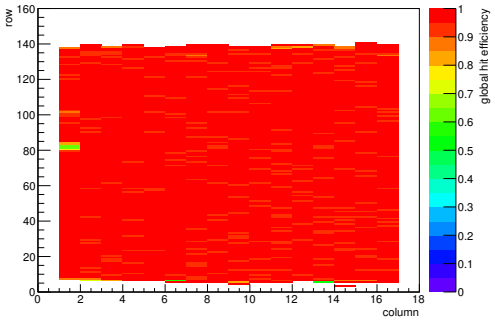

(h) Hit efficiency map.

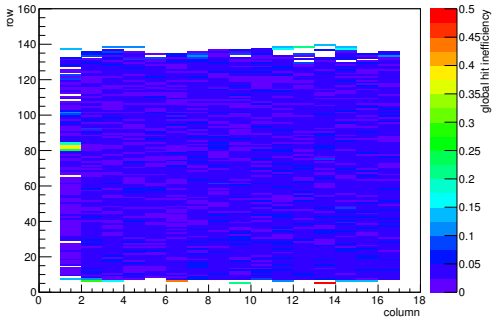

(i) Hit inefficiency map.

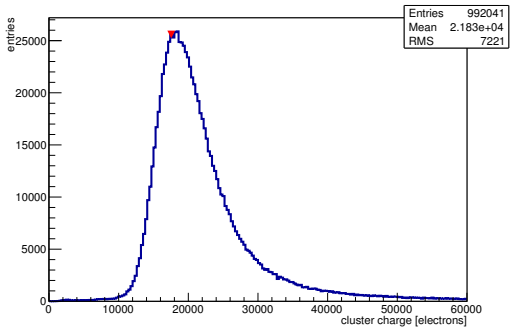

(j) Charge distribution (all cluster sizes included).

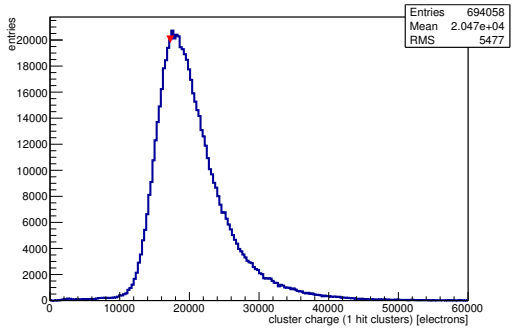

(k) Charge distribution (1 hit cluster).

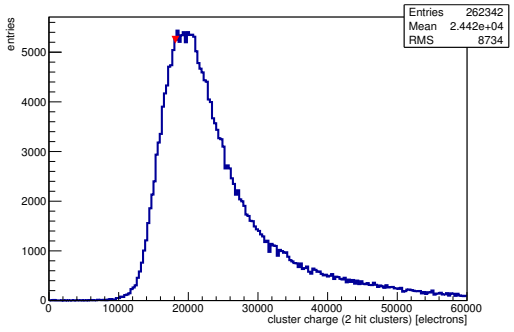

(l) Charge distribution (2 hit cluster).

Figure C.9: Detailed plots for test beam measurement of DO-1 (description see section 6.1) sample (running as DUT0) during runs 31140-31165 in the February 2011 test beam period at DESY. Summary of the data in chapter 9. *(cont.)*

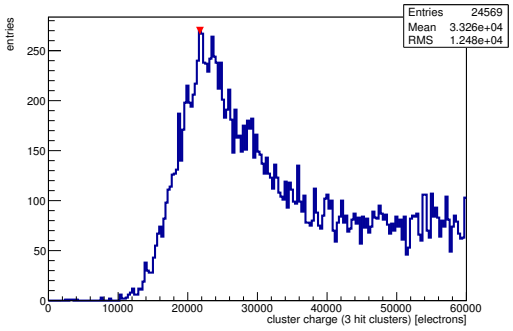

(m) Charge distribution (3 hit cluster).

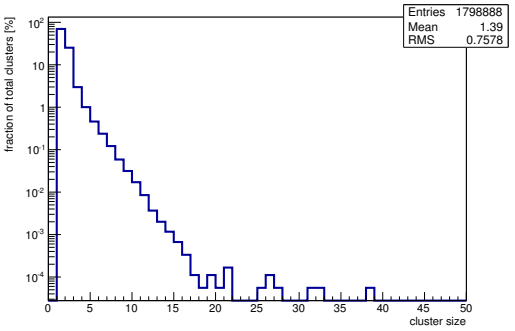

(n) Cluster size distribution.

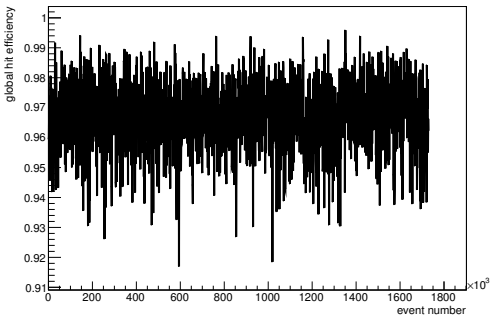

(o) Hit efficiency vs event number.

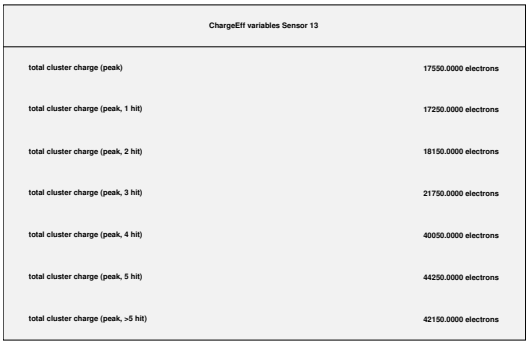

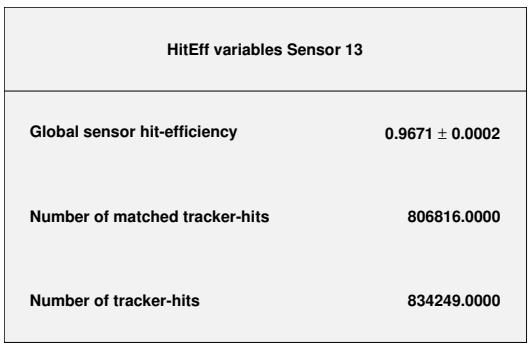

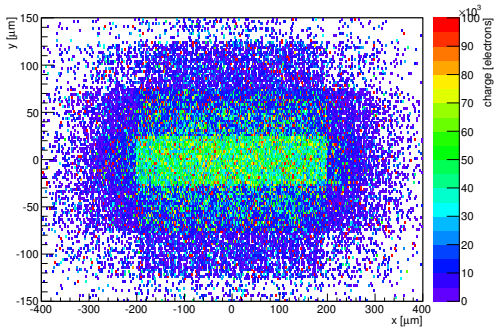

(p) Single pixel mean charge.

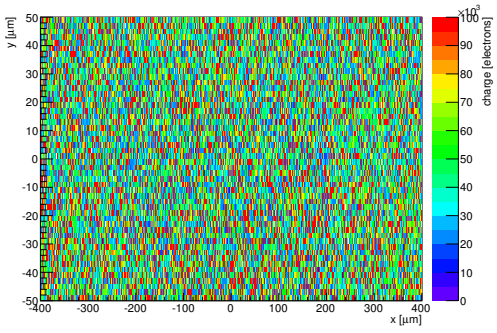

(q) Single pixel mean charge.

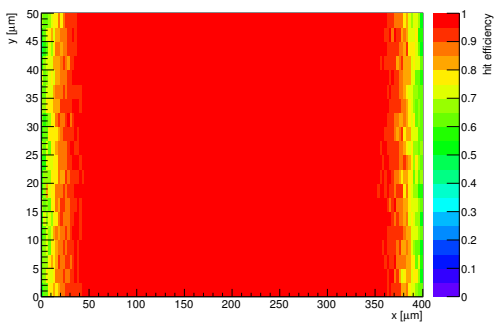

(r) Single pixel hit efficiency.

Figure C.9: Detailed plots for test beam measurement of DO-1 (description see section 6.1) sample (running as DUT0) during runs 31140-31165 in the February 2011 test beam period at DESY. Summary of the data in chapter 9.

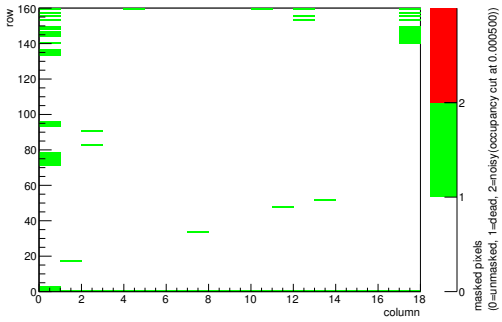

(a) Map of masked pixels.

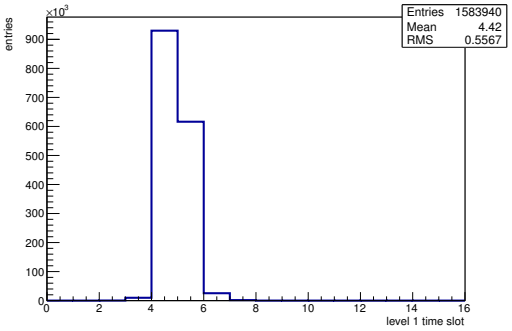

(b) Lvl1 distribution.

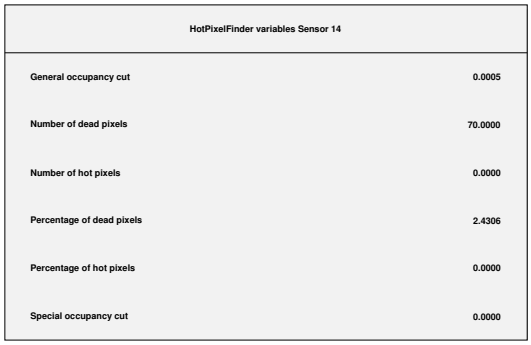

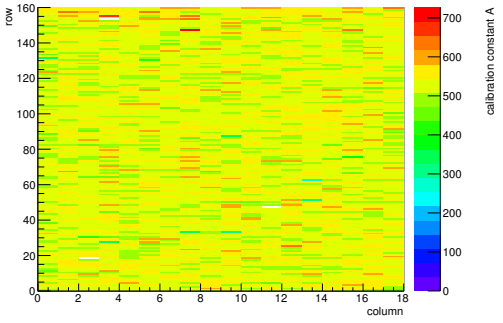

(c) Calibration constant A.

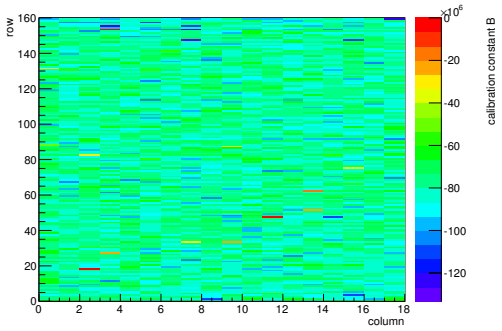

(d) Calibration constant B.

Figure C.10: Detailed plots for test beam measurement of DO-13 (description see section 6.1) sample (running as DUT1) during runs 31140-31165 in the February 2011 test beam period at DESY. Summary of the data in chapter 9. *(cont.)*

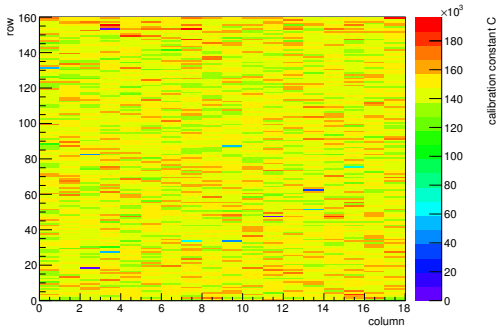

(e) Calibration constant C.

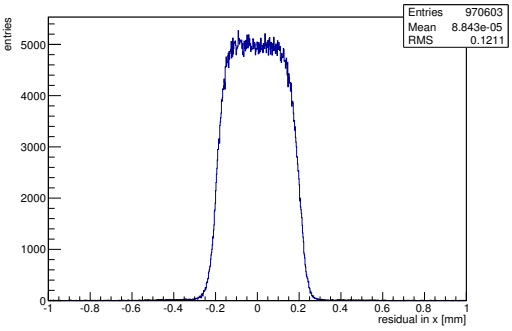

(f) Track residual in x.

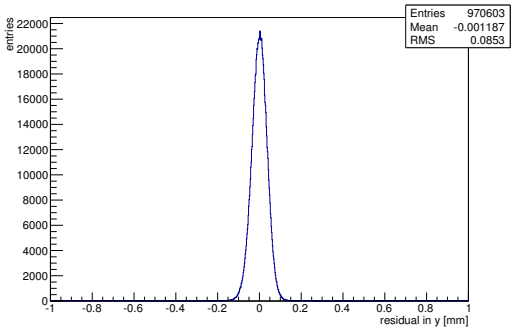

(g) Track residual in y.

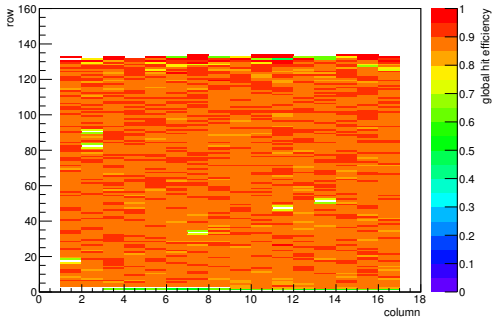

(h) Hit efficiency map.

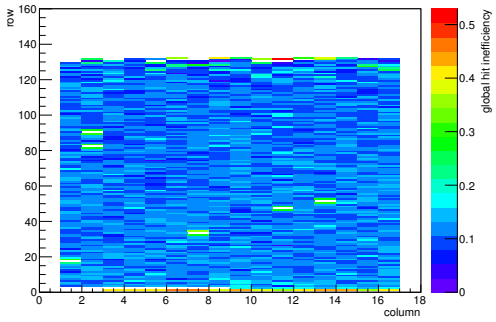

(i) Hit inefficiency map.

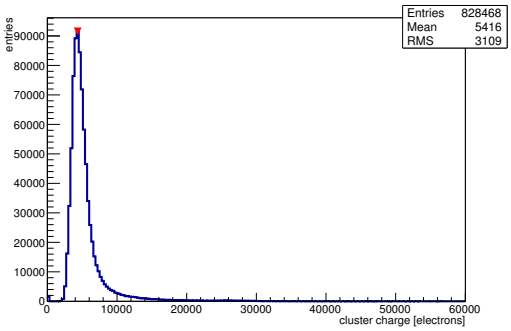

(j) Charge distribution (all cluster sizes included).

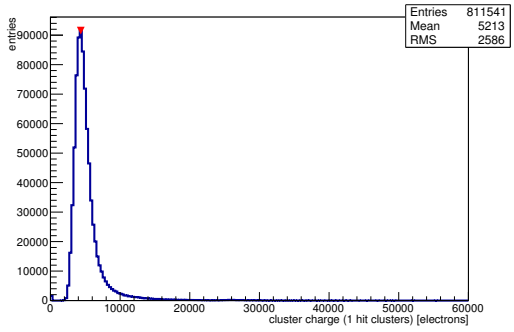

(k) Charge distribution (1 hit cluster).

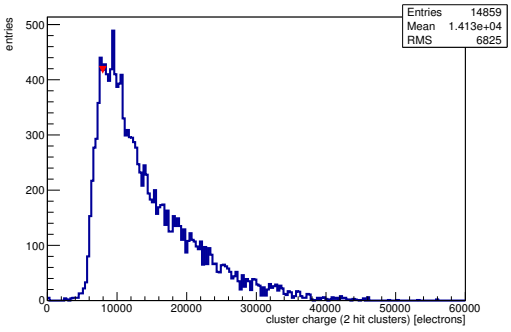

(l) Charge distribution (2 hit cluster).

Figure C.10: Detailed plots for test beam measurement of DO-13 (description see section 6.1) sample (running as DUT1) during runs 31140-31165 in the February 2011 test beam period at DESY. Summary of the data in chapter 9. *(cont.)*

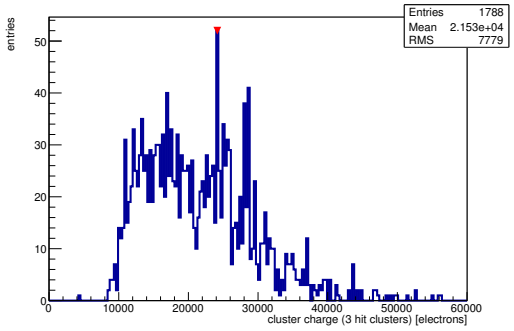

(m) Charge distribution (3 hit cluster).

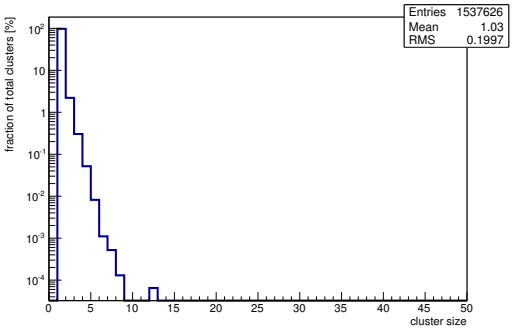

(n) Cluster size distribution.

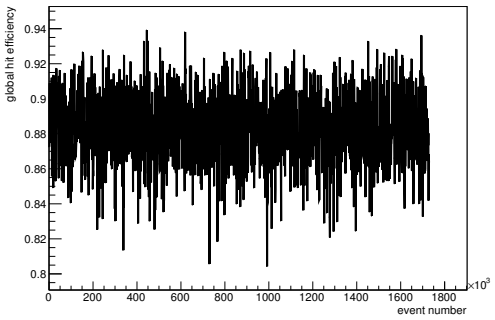

(o) Hit efficiency vs event number.

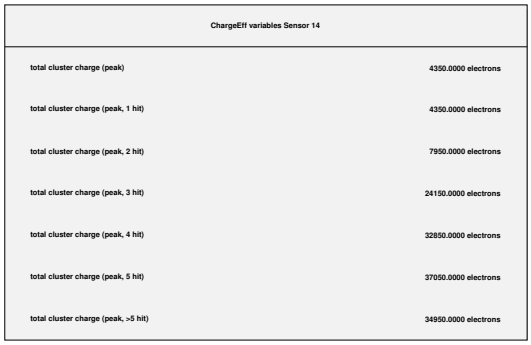

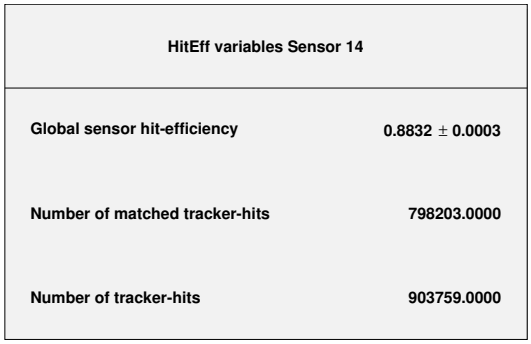

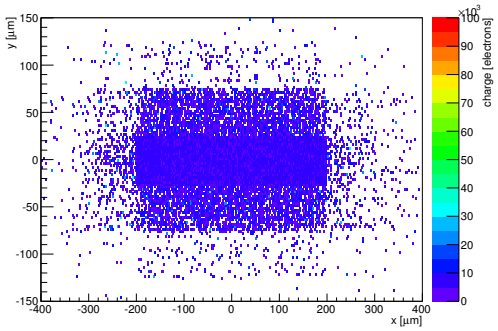

(p) Single pixel mean charge.

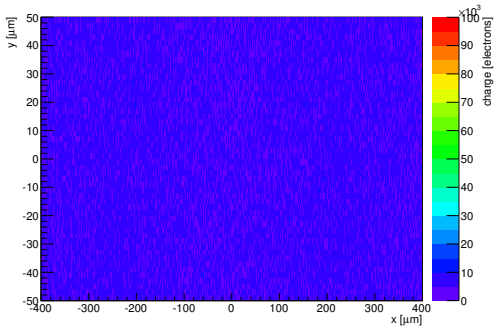

(q) Single pixel mean charge.

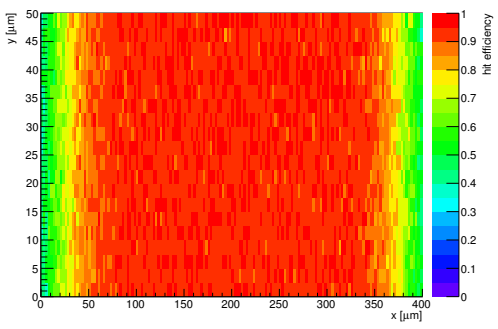

(r) Single pixel hit efficiency.

Figure C.10: Detailed plots for test beam measurement of DO-13 (description see section 6.1) sample (running as DUT1) during runs 31140-31165 in the February 2011 test beam period at DESY. Summary of the data in chapter 9.

C.2 CERN SPS July 2011

C.2.1 Runs 50578-50582

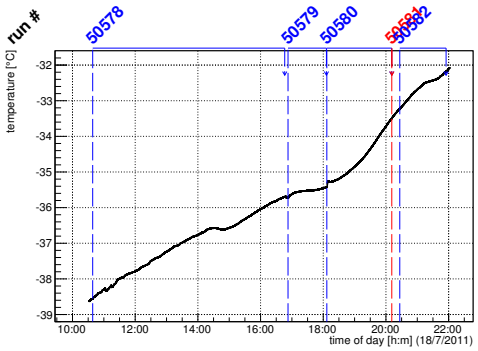

(a) Temperature vs time.

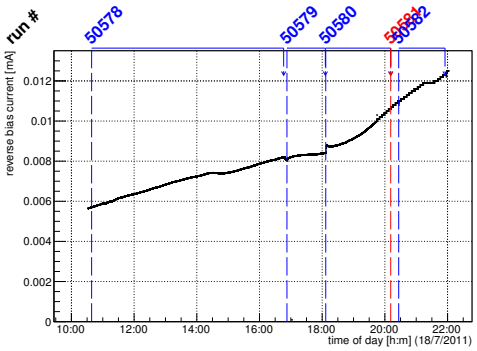

(b) Bias current vs time.

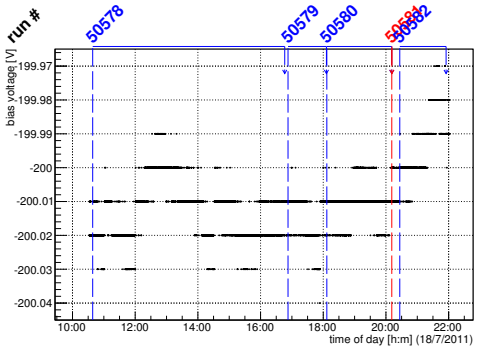

(c) Currently applied bias voltage vs time.

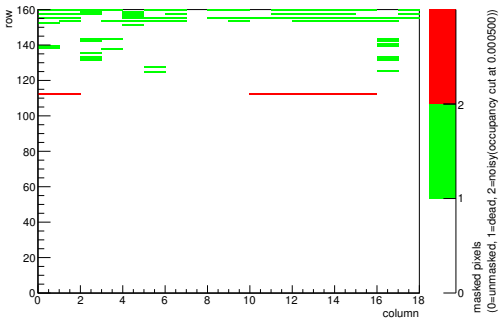

(d) Map of masked pixels.

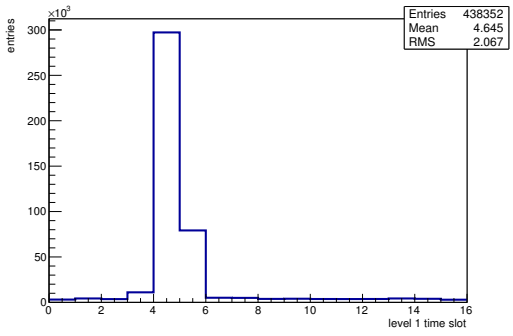

(e) Lvl1 distribution.

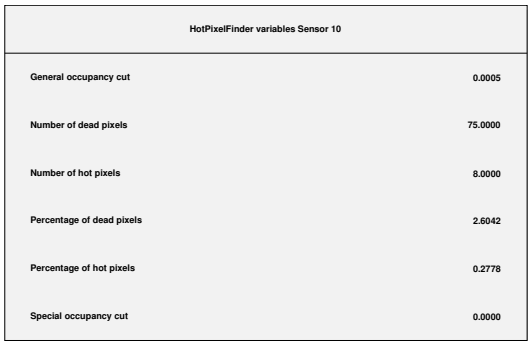

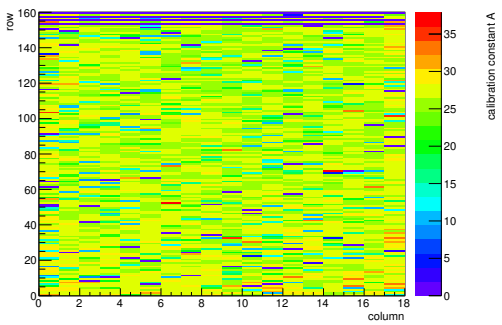

(f) Calibration constant A.

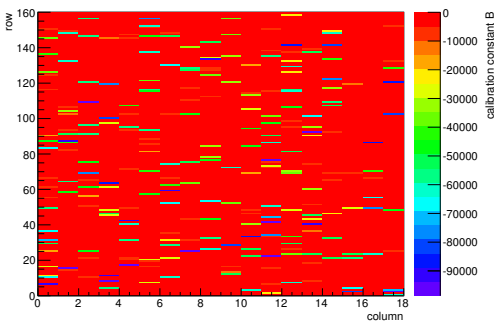

(g) Calibration constant B.

Figure C.11: Detailed plots for test beam measurement of KEK1R (description see section 6.1) sample (running as DUT0) during runs 50578-50582 in the July 2011 test beam period at CERN SPS in area H6B. Summary of the data in chapter 9. *(cont.)*

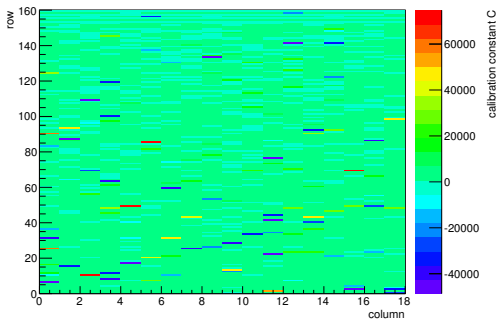

(h) Calibration constant C.

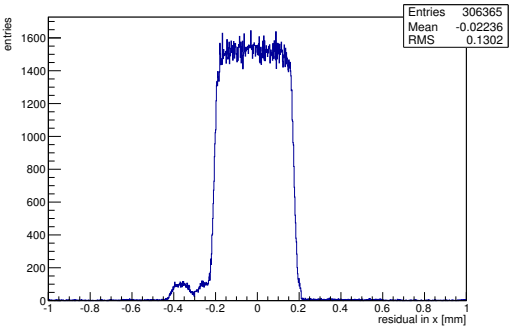

(i) Track residual in x.

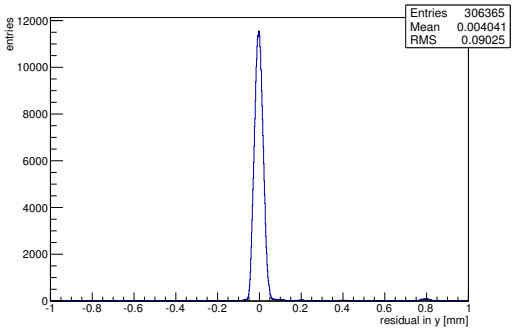

(j) Track residual in y.

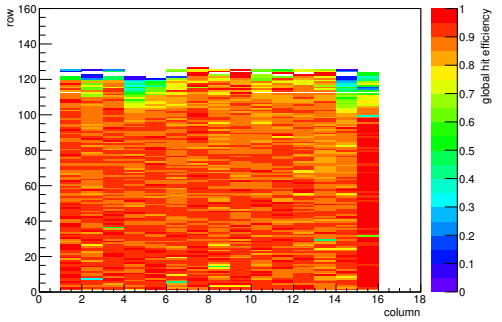

(k) Hit efficiency map.

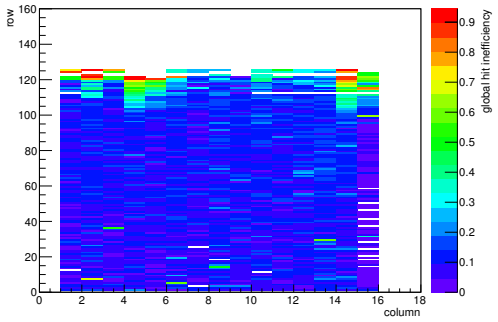

(l) Hit inefficiency map.

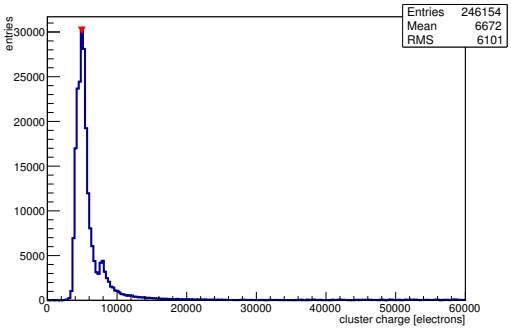

(m) Charge distribution (all cluster sizes included).

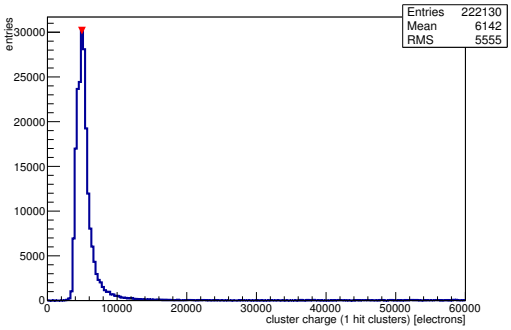

(n) Charge distribution (1 hit cluster).

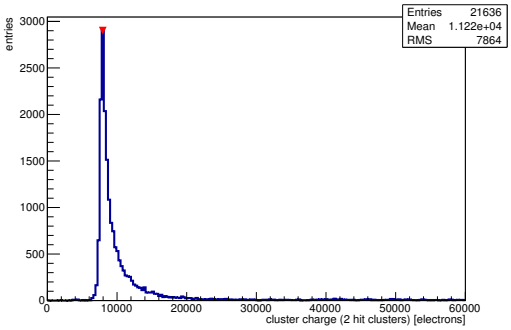

(o) Charge distribution (2 hit cluster).

Figure C.11: Detailed plots for test beam measurement of KEK1R (description see section 6.1) sample (running as DUT0) during runs 50578-50582 in the July 2011 test beam period at CERN SPS in area H6B. Summary of the data in chapter 9. *(cont.)*

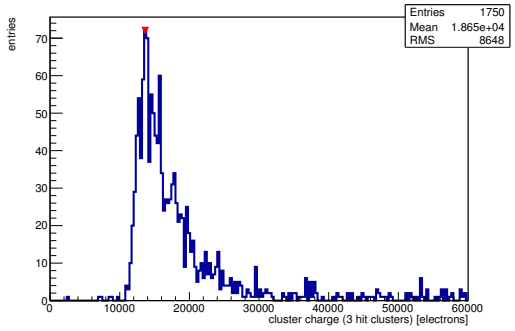

(p) Charge distribution (3 hit cluster).

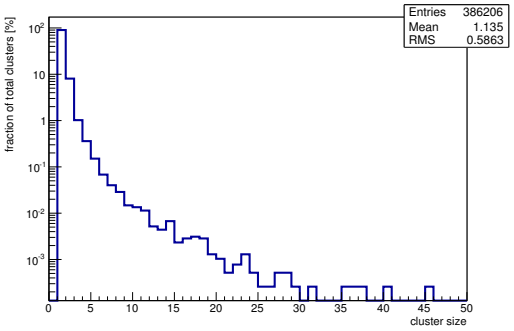

(q) Cluster size distribution.

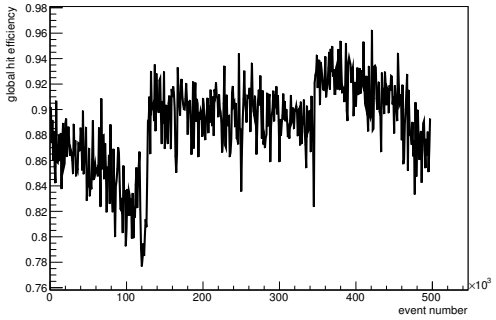

(r) Hit efficiency vs event number.

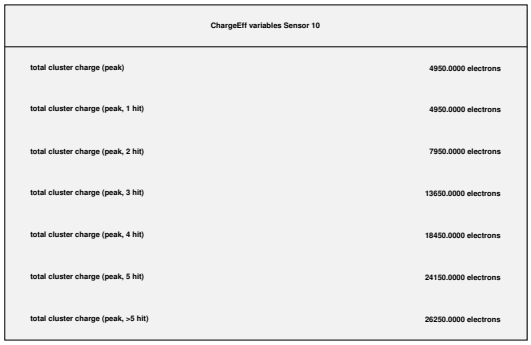

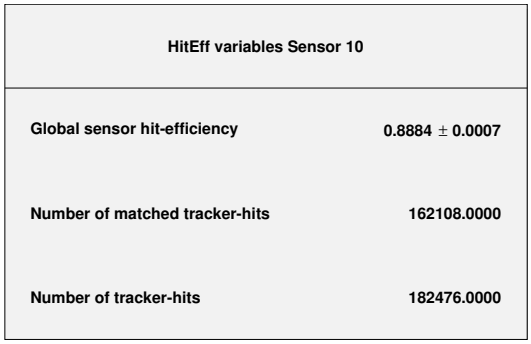

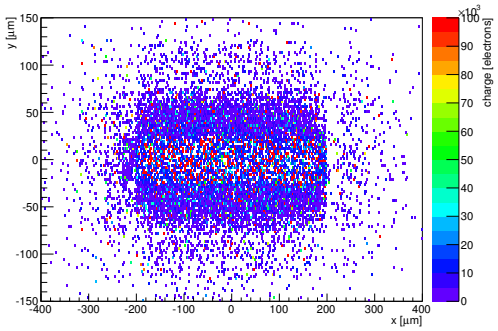

(s) Single pixel mean charge.

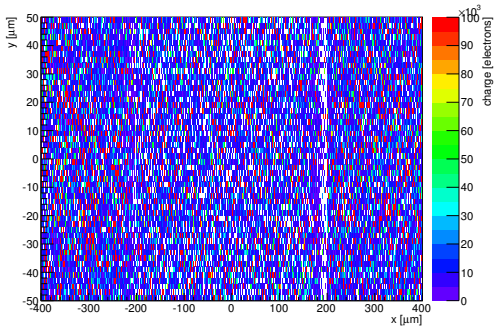

(t) Single pixel mean charge.

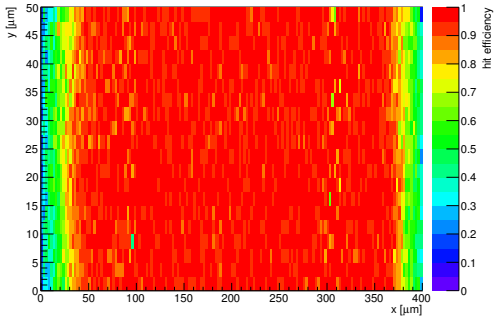

(u) Single pixel hit efficiency.

Figure C.11: Detailed plots for test beam measurement of KEK1R (description see section 6.1) sample (running as DUT0) during runs 50578-50582 in the July 2011 test beam period at CERN SPS in area H6B. Summary of the data in chapter 9.

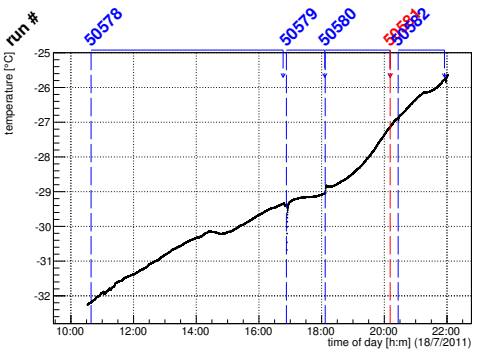

(a) Temperature vs time.

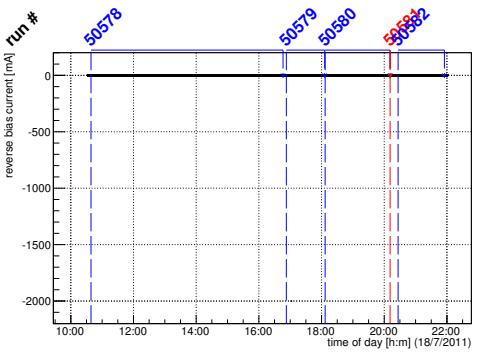

(b) Bias current vs time.

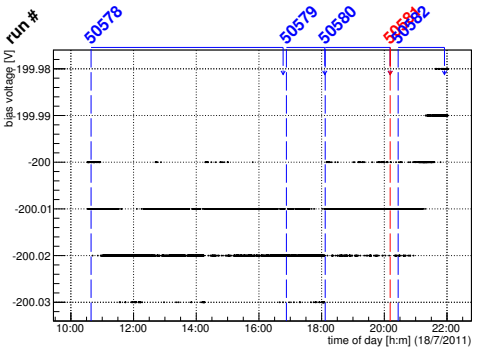

(c) Currently applied bias voltage vs time.

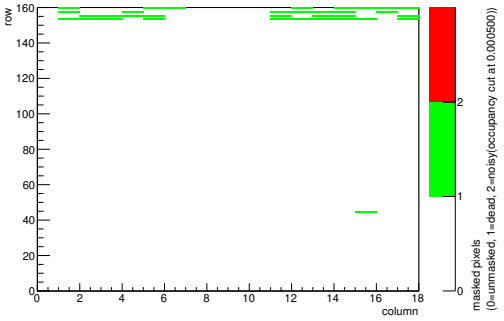

(d) Map of masked pixels.

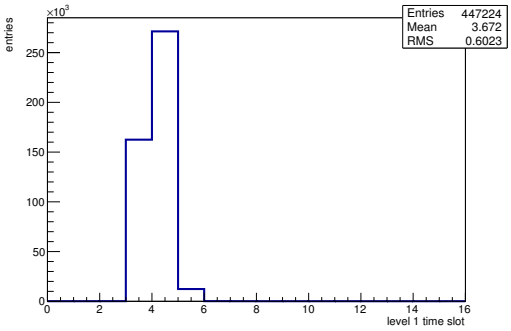

(e) Lvl1 distribution.

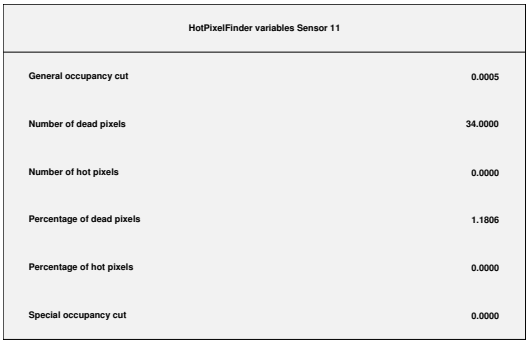

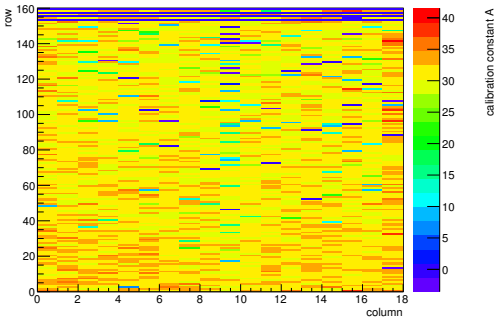

(f) Calibration constant A.

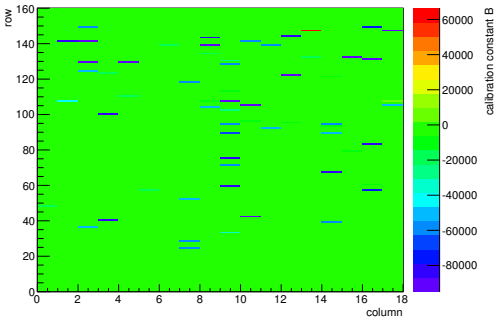

(g) Calibration constant B.

Figure C.12: Detailed plots for test beam measurement of KEK2R (description see section 6.1) sample (running as DUT1) during runs 50578-50582 in the July 2011 test beam period at CERN SPS in area H6B. Summary of the data in chapter 9. *(cont.)*

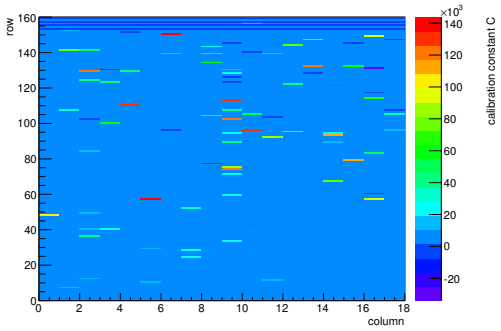

(h) Calibration constant C.

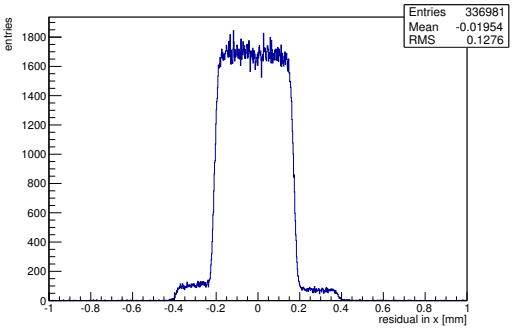

(i) Track residual in x.

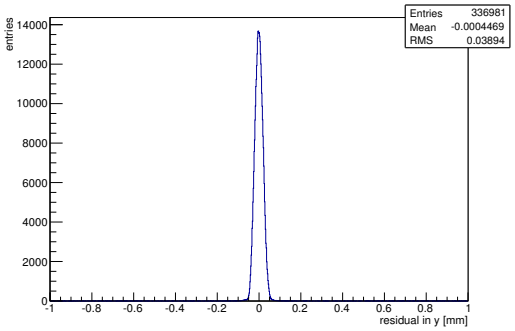

(j) Track residual in y.

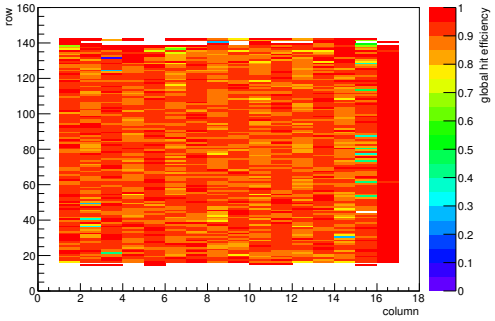

(k) Hit efficiency map.

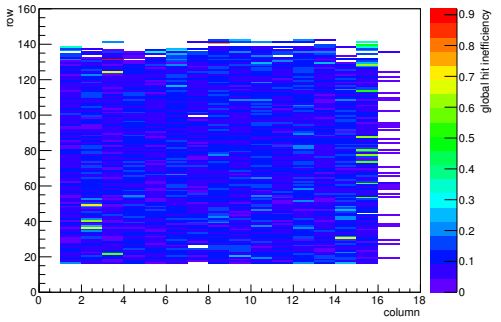

(l) Hit inefficiency map.

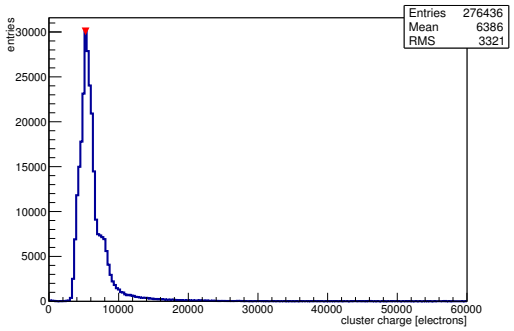

(m) Charge distribution (all cluster sizes included).

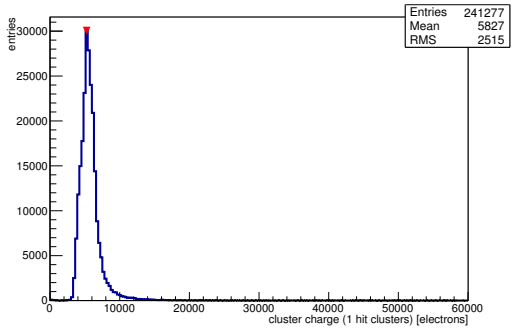

(n) Charge distribution (1 hit cluster).

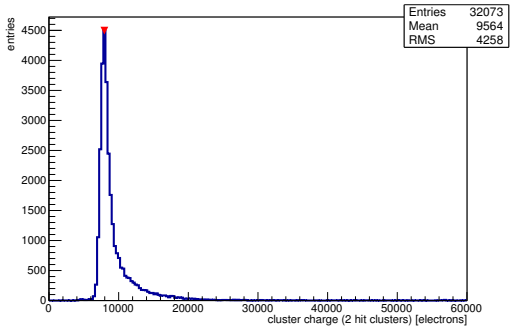

(o) Charge distribution (2 hit cluster).

Figure C.12: Detailed plots for test beam measurement of KEK2R (description see section 6.1) sample (running as DUT1) during runs 50578-50582 in the July 2011 test beam period at CERN SPS in area H6B. Summary of the data in chapter 9. *(cont.)*

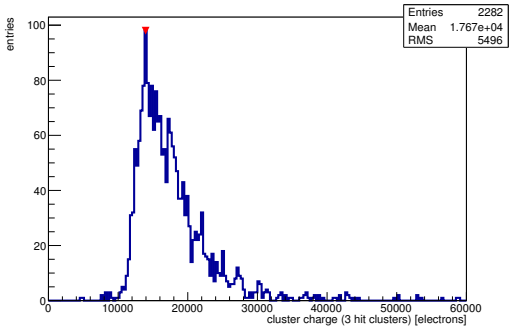

(p) Charge distribution (3 hit cluster).

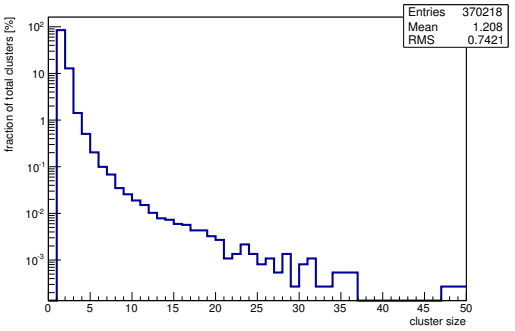

(q) Cluster size distribution.

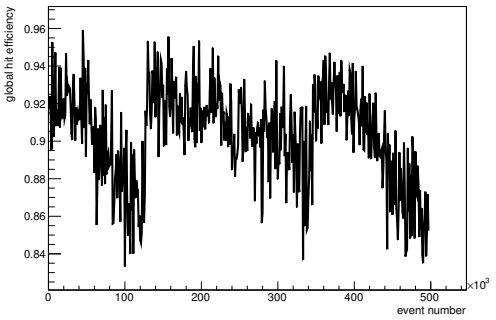

(r) Hit efficiency vs event number.

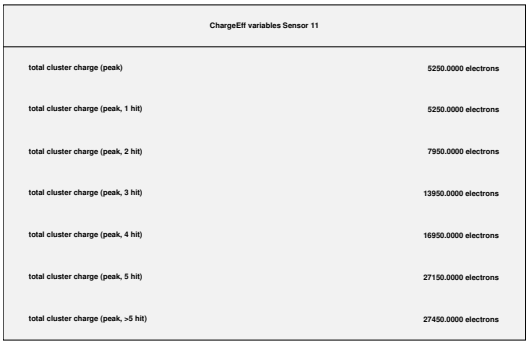

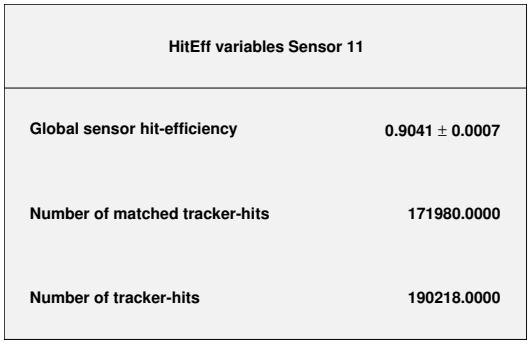

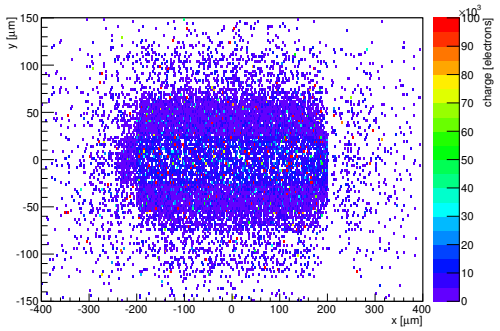

(s) Single pixel mean charge.

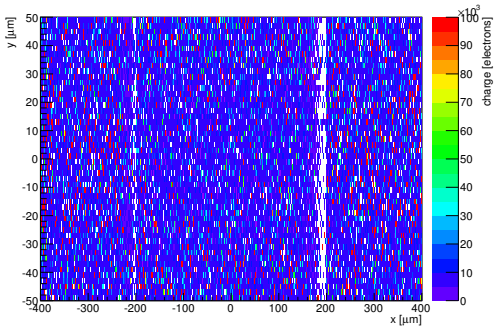

(t) Single pixel mean charge.

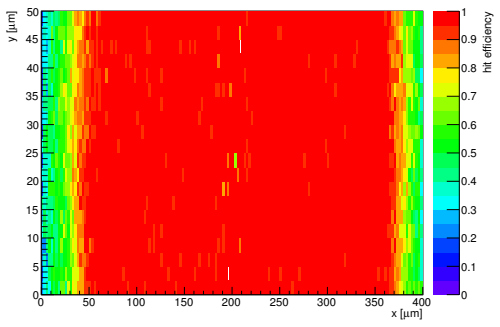

(u) Single pixel hit efficiency.

Figure C.12: Detailed plots for test beam measurement of KEK2R (description see section 6.1) sample (running as DUT1) during runs 50578-50582 in the July 2011 test beam period at CERN SPS in area H6B. Summary of the data in chapter 9.

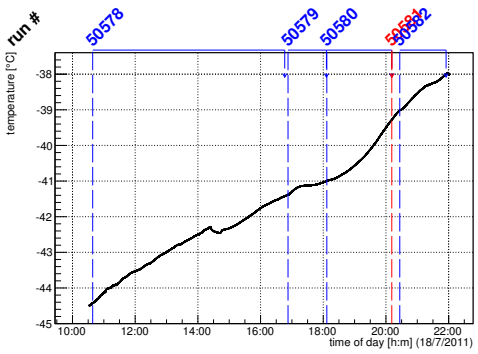

(a) Temperature vs time.

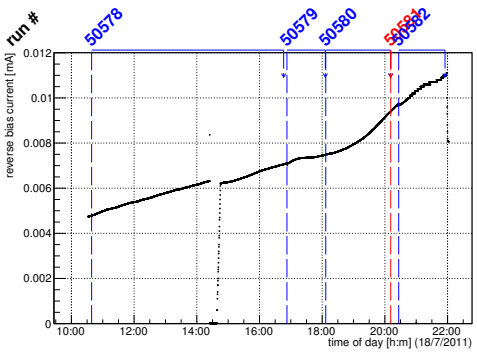

(b) Bias current vs time.

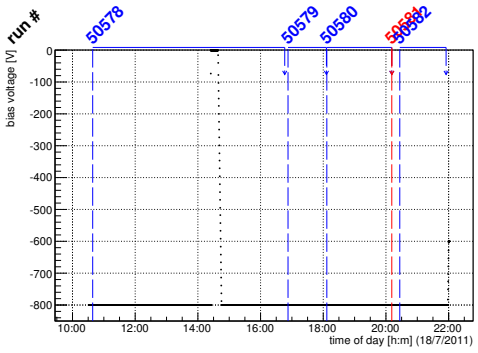

(c) Currently applied bias voltage vs time.

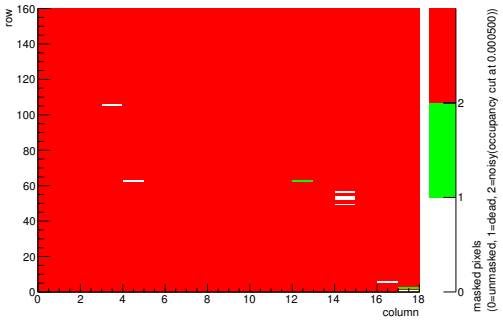

(d) Map of masked pixels.

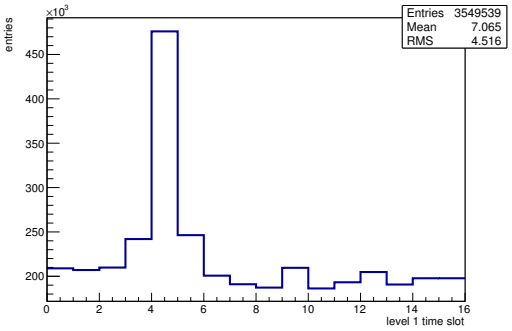

(e) Lvl1 distribution.

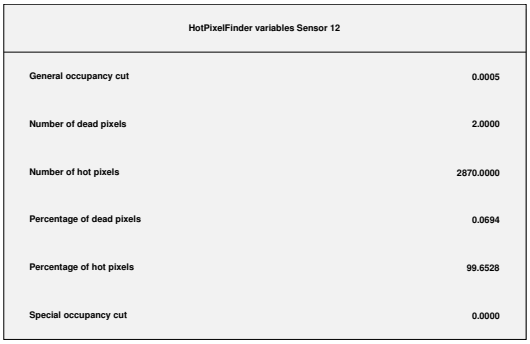

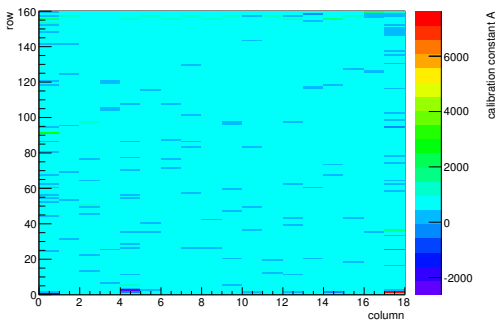

(f) Calibration constant A.

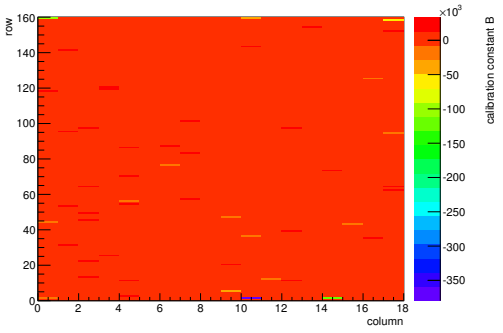

(g) Calibration constant B.

Figure C.13: Detailed plots for test beam measurement of DO-I-11 (description see section 6.1) sample (running as DUT2) during runs 50578-50582 in the July 2011 test beam period at CERN SPS in area H6B. Summary of the data in chapter 9. *(cont.)*

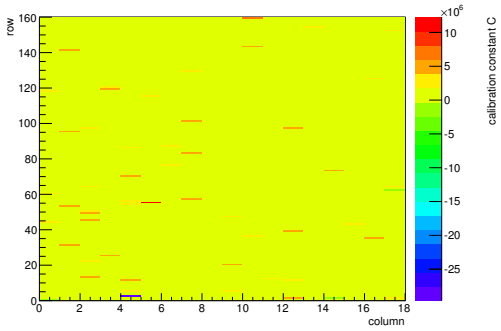

(h) Calibration constant C.

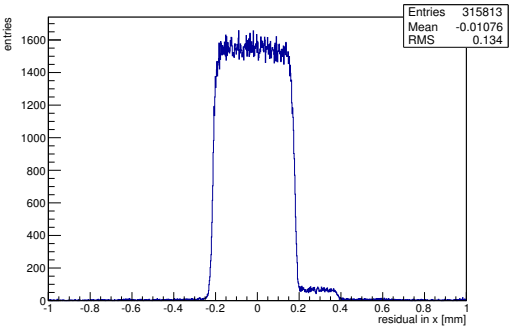

(i) Track residual in x.

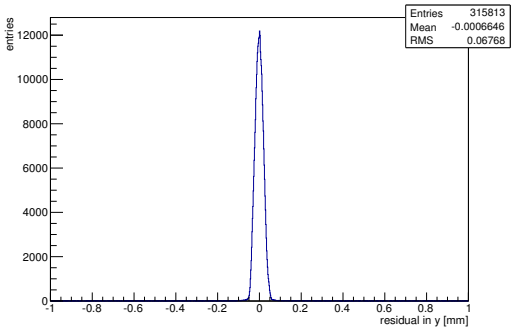

(j) Track residual in y.

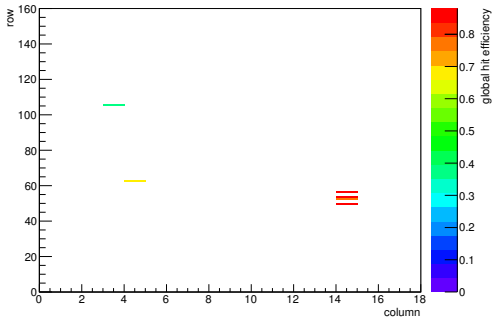

(k) Hit efficiency map.

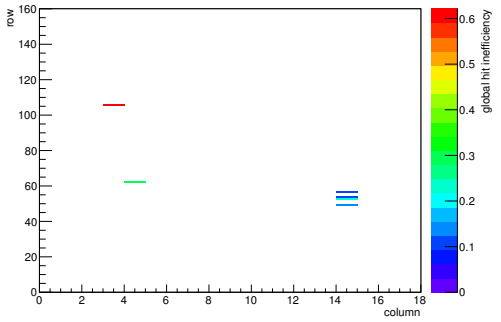

(l) Hit inefficiency map.

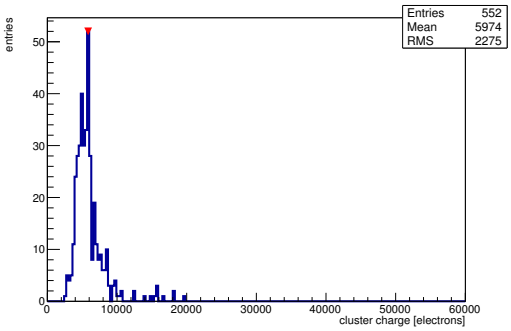

(m) Charge distribution (all cluster sizes included).

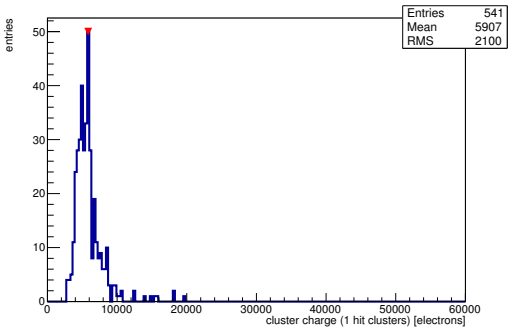

(n) Charge distribution (1 hit cluster).

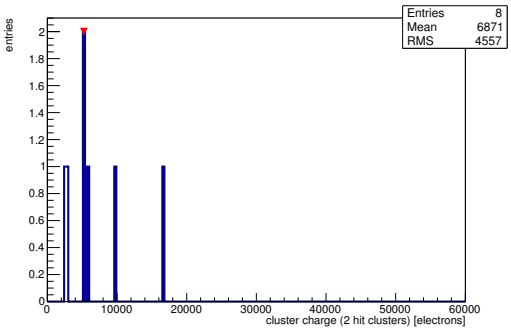

(o) Charge distribution (2 hit cluster).

Figure C.13: Detailed plots for test beam measurement of DO-I-11 (description see section 6.1) sample (running as DUT2) during runs 50578-50582 in the July 2011 test beam period at CERN SPS in area H6B. Summary of the data in chapter 9. *(cont.)*

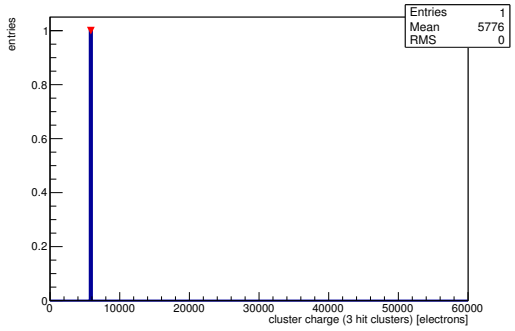

(p) Charge distribution (3 hit cluster).

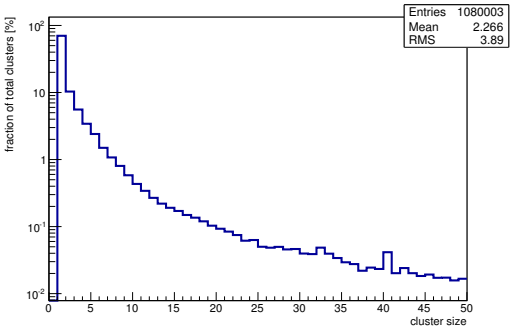

(q) Cluster size distribution.

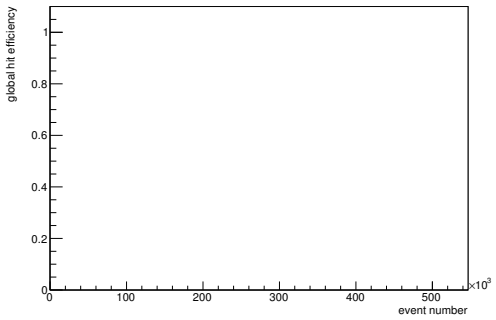

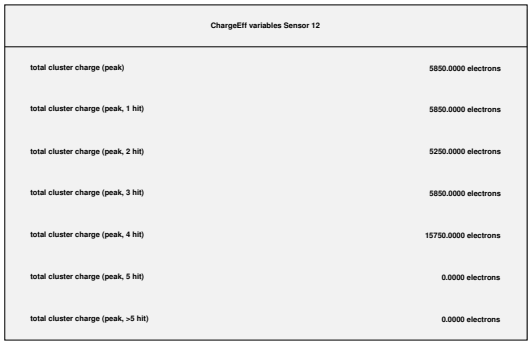

(r) Hit efficiency vs event number.

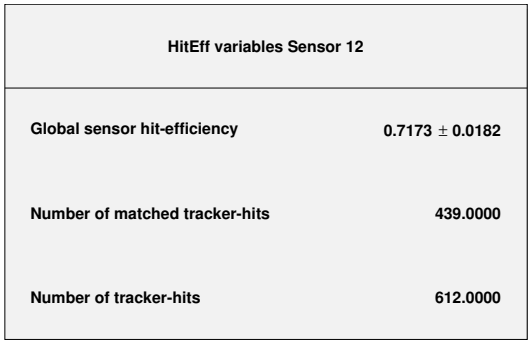

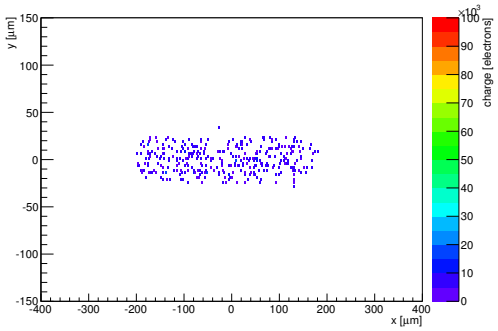

(s) Single pixel mean charge.

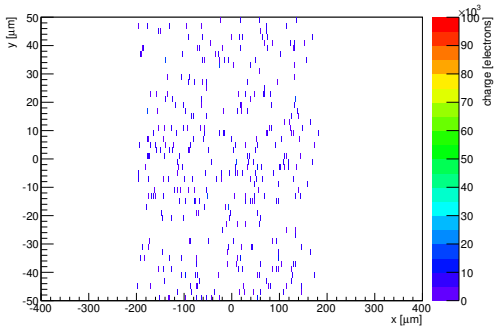

(t) Single pixel mean charge.

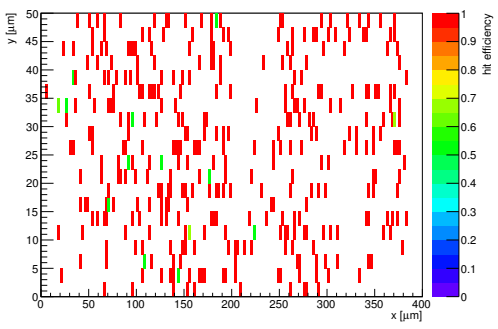

(u) Single pixel hit efficiency.

Figure C.13: Detailed plots for test beam measurement of DO-I-11 (description see section 6.1) sample (running as DUT2) during runs 50578-50582 in the July 2011 test beam period at CERN SPS in area H6B. Summary of the data in chapter 9.

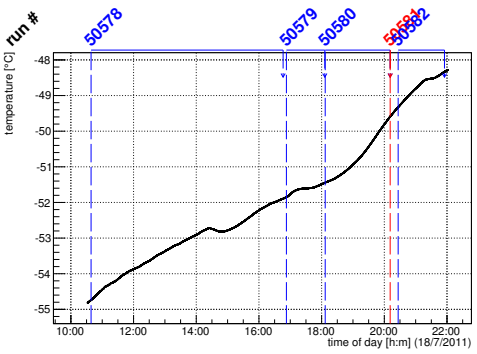

(a) Temperature vs time.

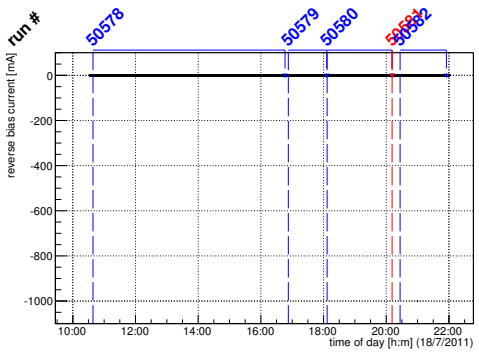

(b) Bias current vs time.

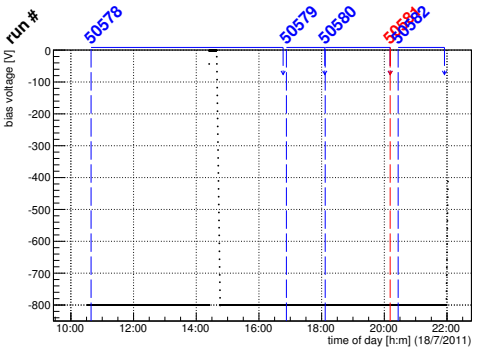

(c) Currently applied bias voltage vs time.

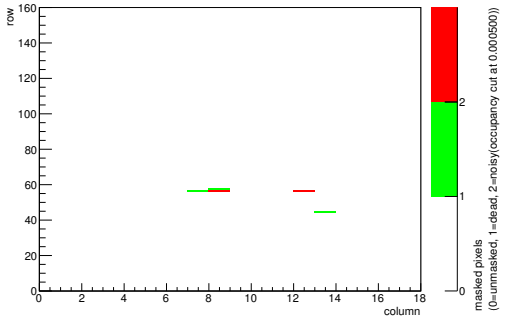

(d) Map of masked pixels.

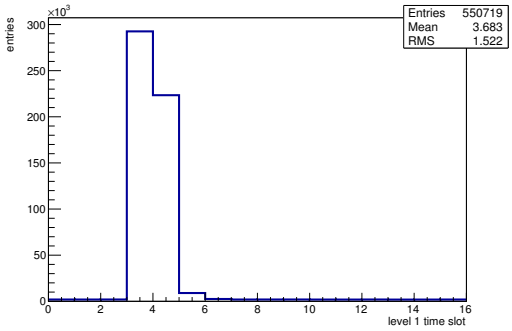

(e) Lvl1 distribution.

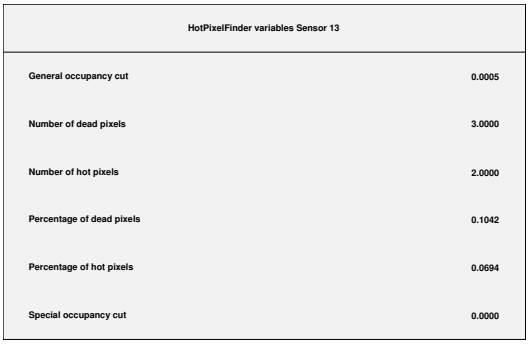

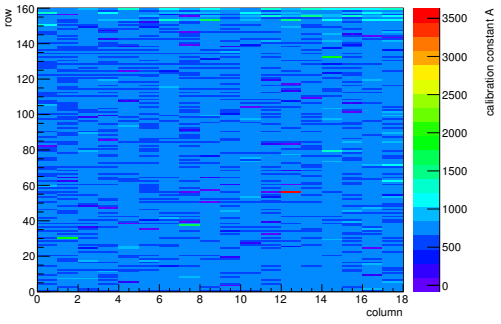

(f) Calibration constant A.

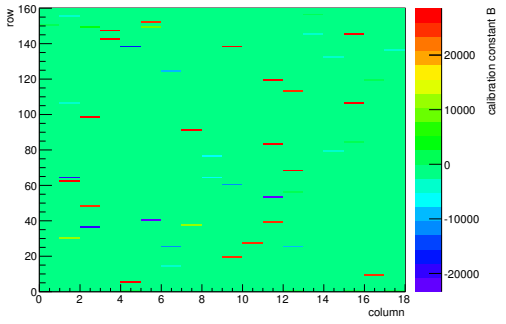

(g) Calibration constant B.

Figure C.14: Detailed plots for test beam measurement of DO-I-13 (description see section 6.1) sample (running as DUT3) during runs 50578-50582 in the July 2011 test beam period at CERN SPS in area H6B. Summary of the data in chapter 9. *(cont.)*

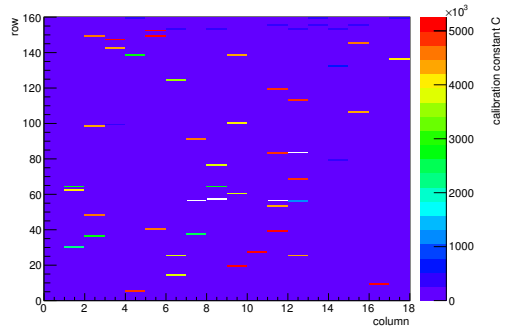

(h) Calibration constant C.

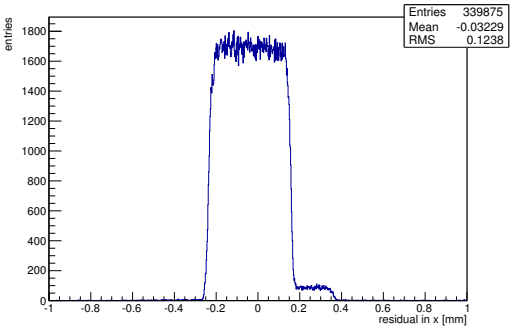

(i) Track residual in x.

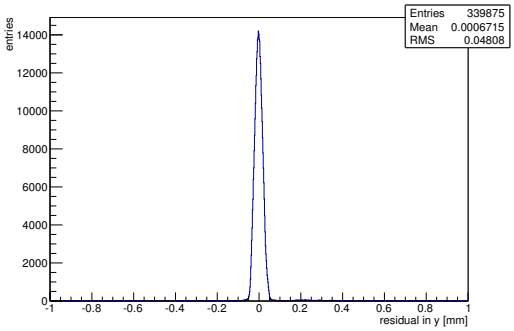

(j) Track residual in y.

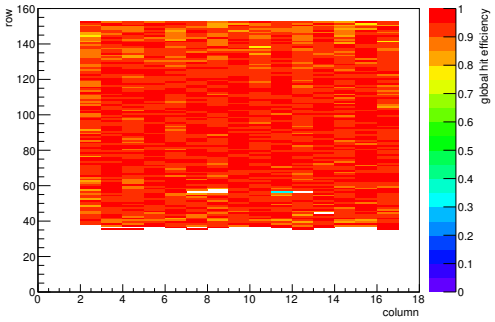

(k) Hit efficiency map.

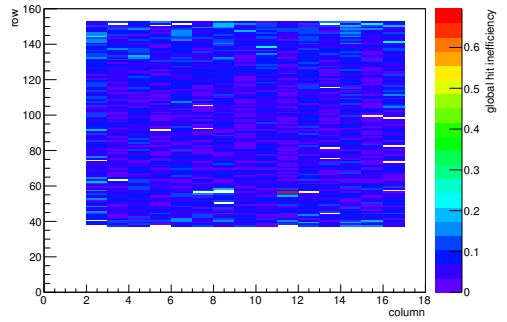

(l) Hit inefficiency map.

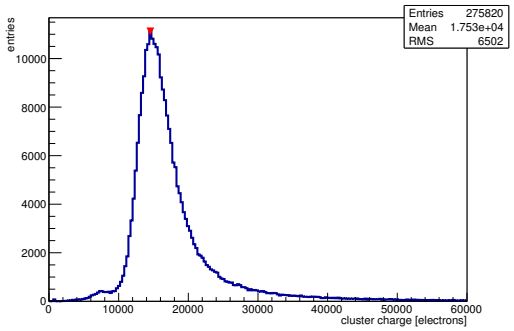

(m) Charge distribution (all cluster sizes included).

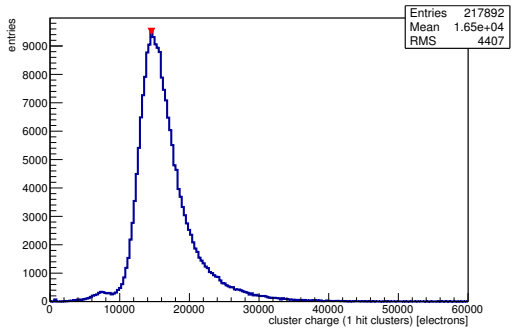

(n) Charge distribution (1 hit cluster).

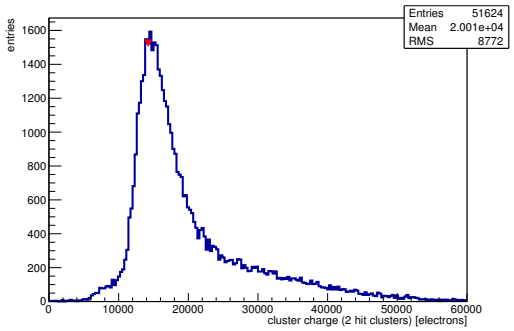

(o) Charge distribution (2 hit cluster).

Figure C.14: Detailed plots for test beam measurement of DO-I-13 (description see section 6.1) sample (running as DUT3) during runs 50578-50582 in the July 2011 test beam period at CERN SPS in area H6B. Summary of the data in chapter 9. *(cont.)*

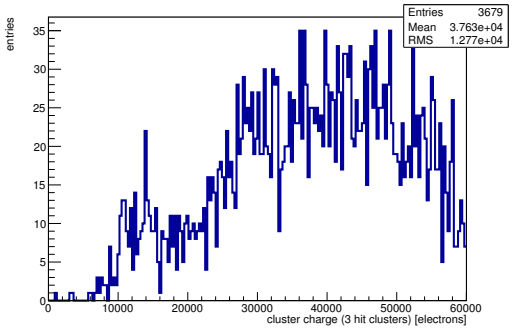

(p) Charge distribution (3 hit cluster).

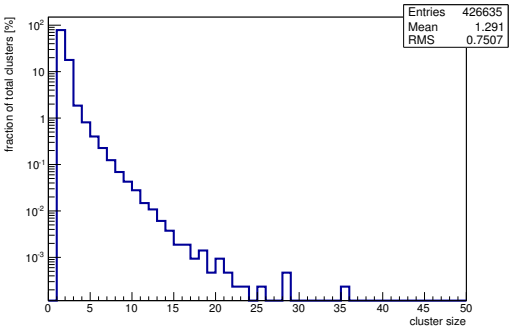

(q) Cluster size distribution.

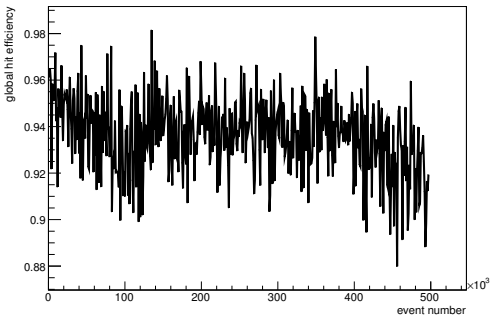

(r) Hit efficiency vs event number.

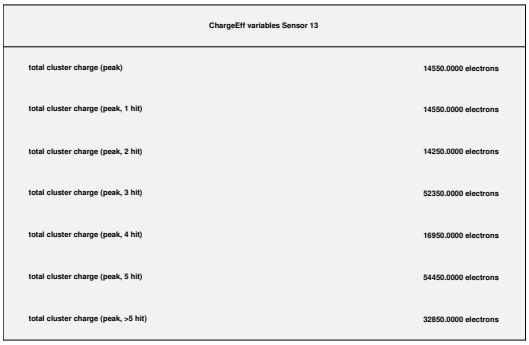

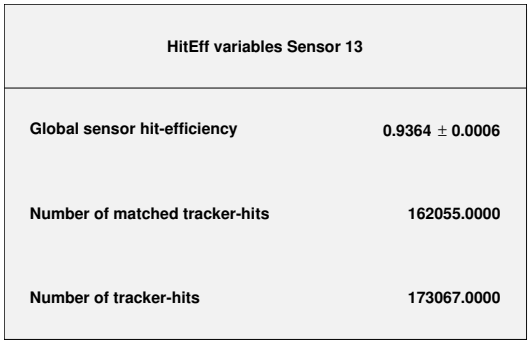

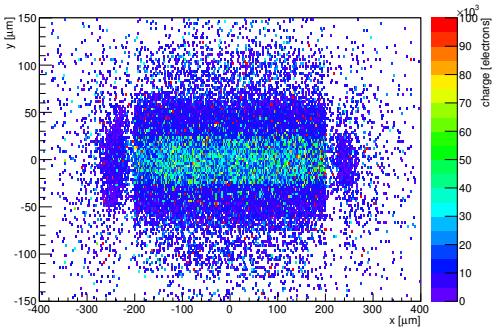

(s) Single pixel mean charge.

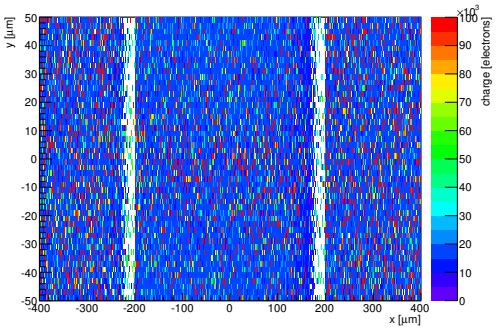

(t) Single pixel mean charge.

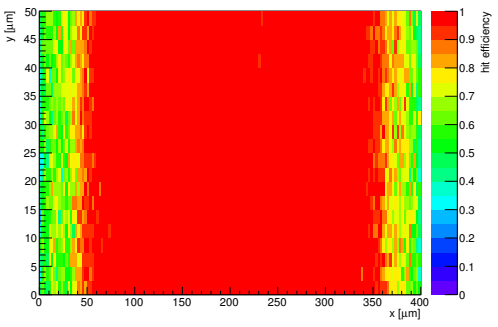

(u) Single pixel hit efficiency.

Figure C.14: Detailed plots for test beam measurement of DO-I-13 (description see section 6.1) sample (running as DUT3) during runs 50578-50582 in the July 2011 test beam period at CERN SPS in area H6B. Summary of the data in chapter 9.

C.2.2 Run 50584

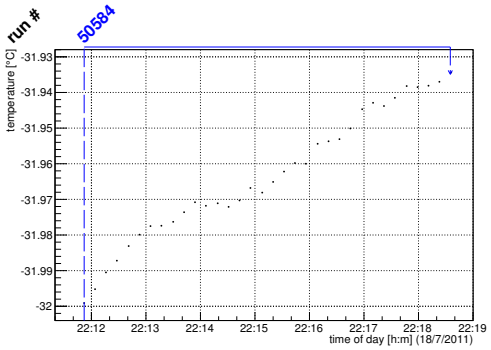

(a) Temperature vs time.

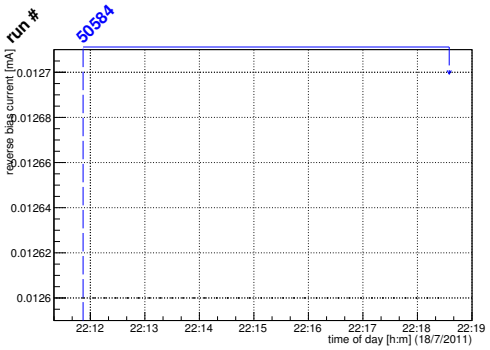

(b) Bias current vs time.

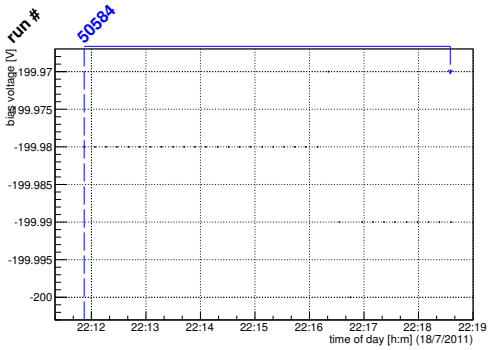

(c) Currently applied bias voltage vs time.

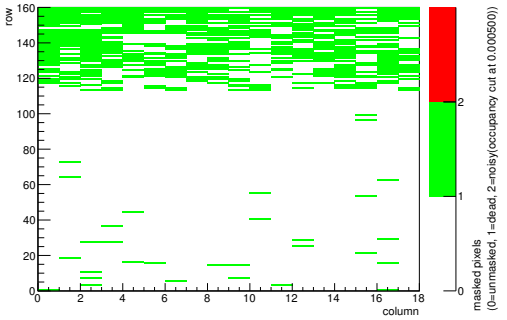

(d) Map of masked pixels.

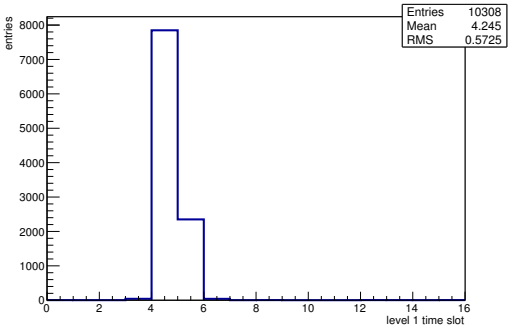

(e) Lvl1 distribution.

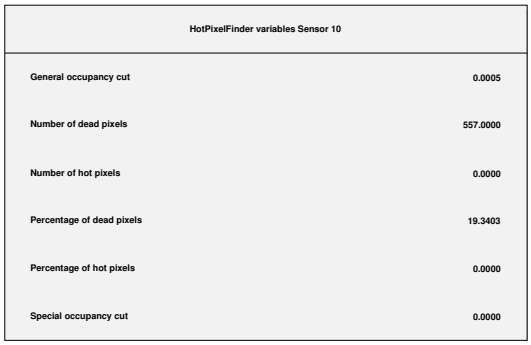

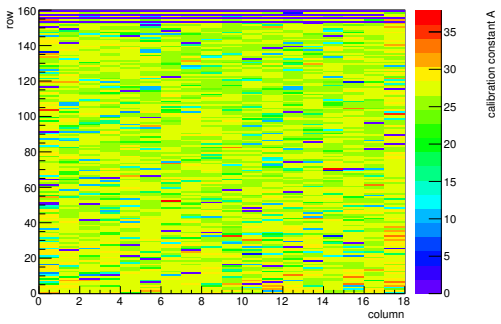

(f) Calibration constant A.

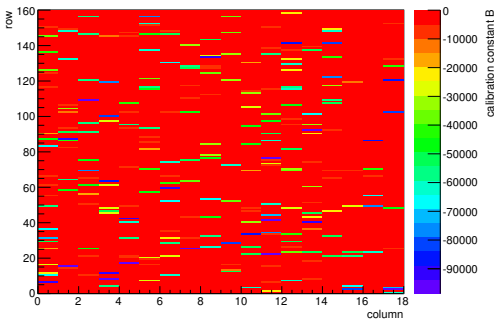

(g) Calibration constant B.

Figure C.15: Detailed plots for test beam measurement of KEK1R (description see section 6.1) sample (running as DUT0) during runs 50584 in the July 2011 test beam period at CERN SPS in area H6B. Summary of the data in chapter 9. *(cont.)*

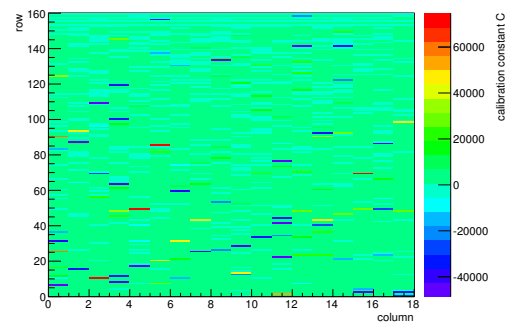

(h) Calibration constant C.

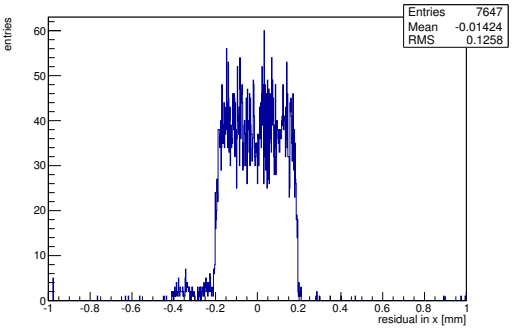

(i) Track residual in x.

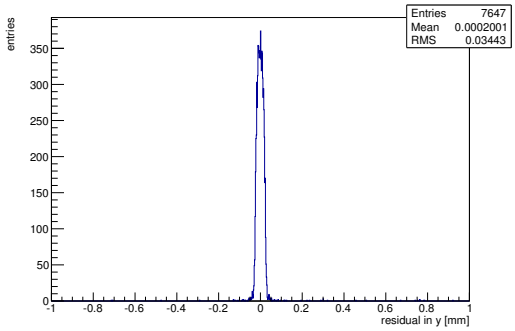

(j) Track residual in y.

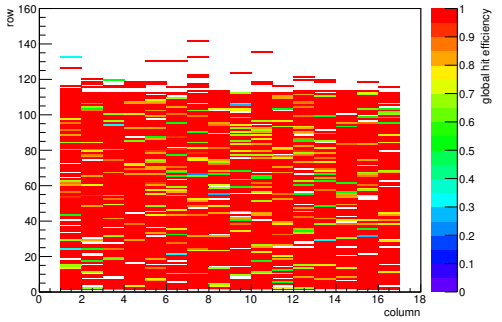

(k) Hit efficiency map.

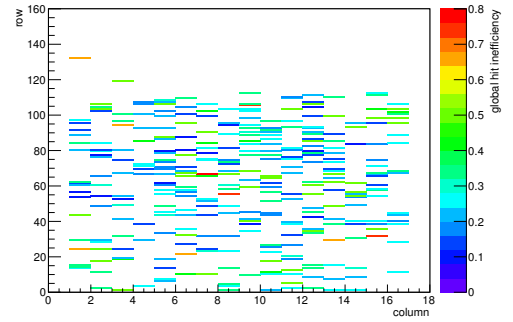

(l) Hit inefficiency map.

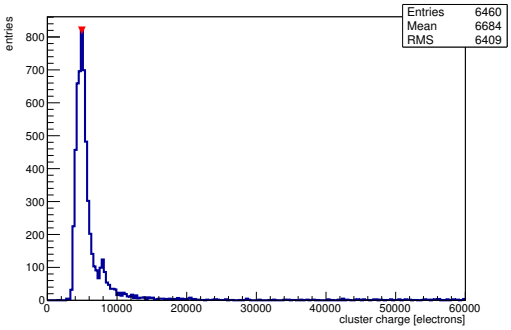

(m) Charge distribution (all cluster sizes included).

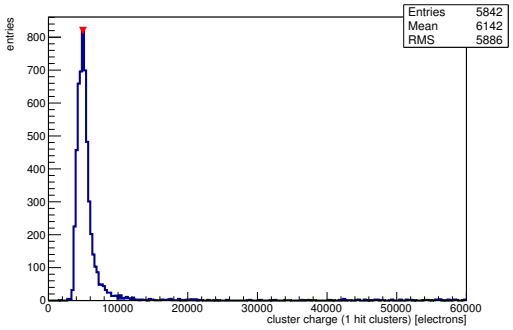

(n) Charge distribution (1 hit cluster).

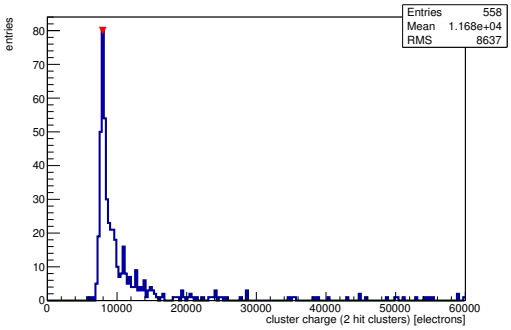

(o) Charge distribution (2 hit cluster).

Figure C.15: Detailed plots for test beam measurement of KEK1R (description see section 6.1) sample (running as DUT0) during runs 50584 in the July 2011 test beam period at CERN SPS in area H6B. Summary of the data in chapter 9. *(cont.)*

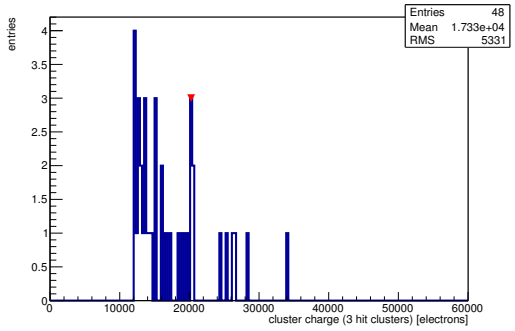

(p) Charge distribution (3 hit cluster).

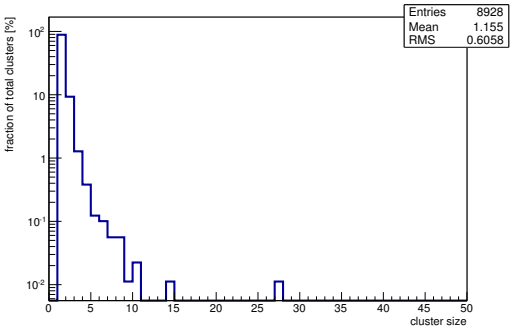

(q) Cluster size distribution.

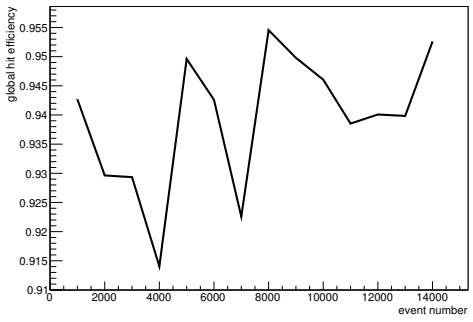

(r) Hit efficiency vs event number.

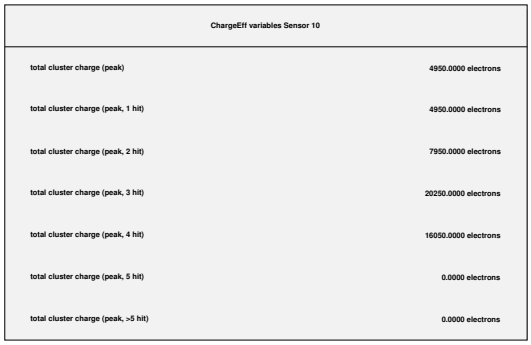

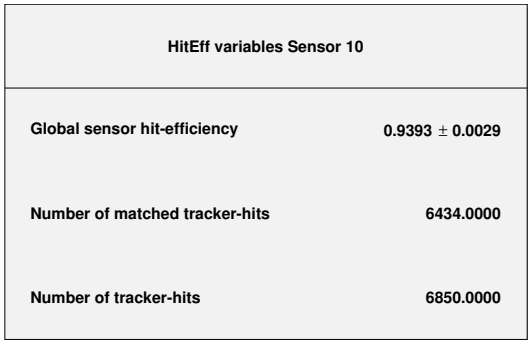

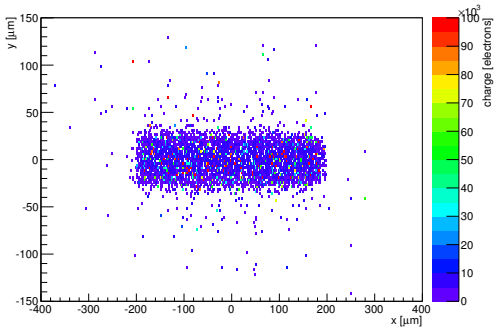

(s) Single pixel mean charge.

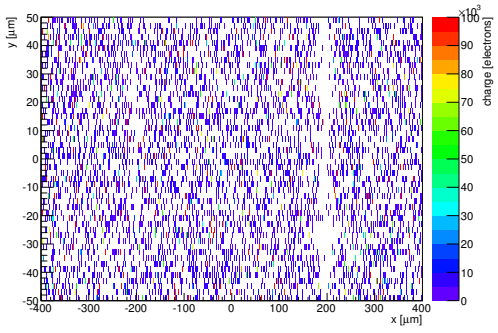

(t) Single pixel mean charge.

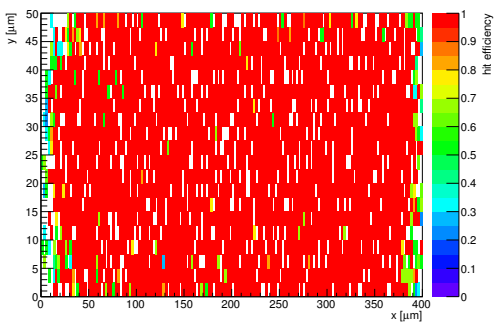

(u) Single pixel hit efficiency.

Figure C.15: Detailed plots for test beam measurement of KEK1R (description see section 6.1) sample (running as DUT0) during runs 50584 in the July 2011 test beam period at CERN SPS in area H6B. Summary of the data in chapter 9.

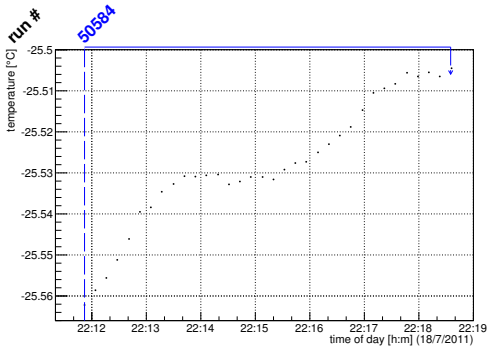

(a) Temperature vs time.

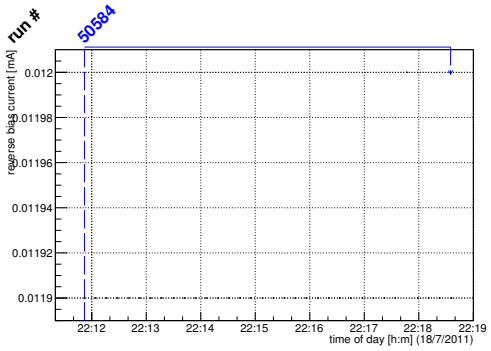

(b) Bias current vs time.

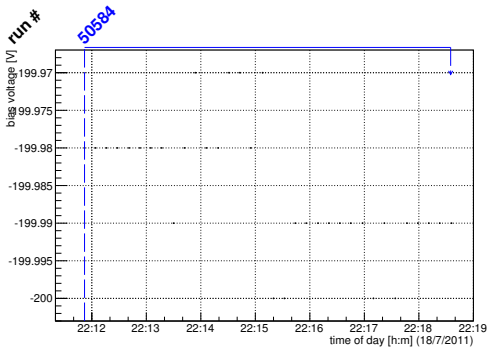

(c) Currently applied bias voltage vs time.

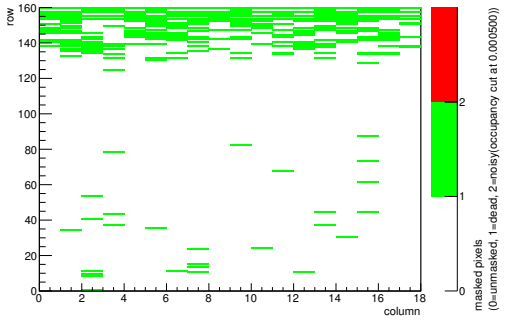

(d) Map of masked pixels.

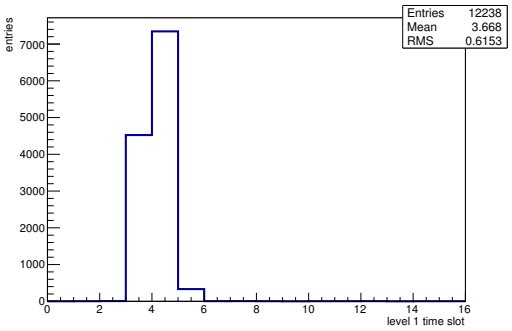

(e) Lvl1 distribution.

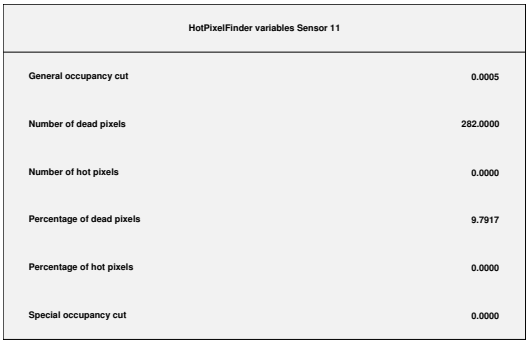

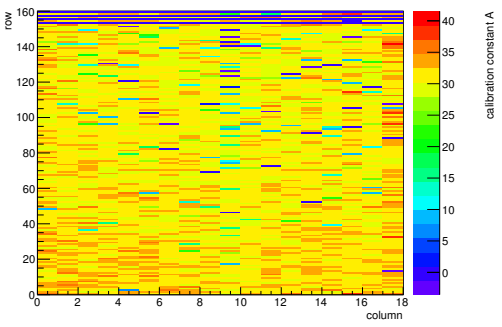

(f) Calibration constant A.

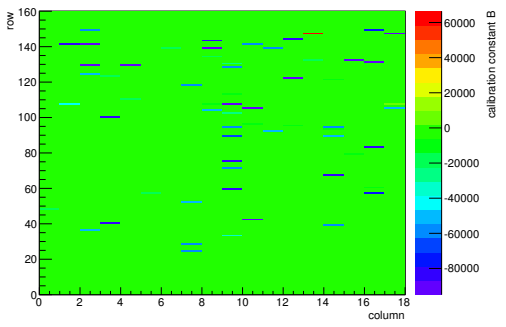

(g) Calibration constant B.

Figure C.16: Detailed plots for test beam measurement of KEK2R (description see section 6.1) sample (running as DUT1) during runs 50584 in the July 2011 test beam period at CERN SPS in area H6B. Summary of the data in chapter 9. *(cont.)*

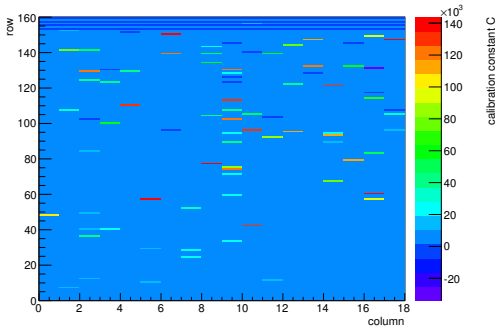

(h) Calibration constant C.

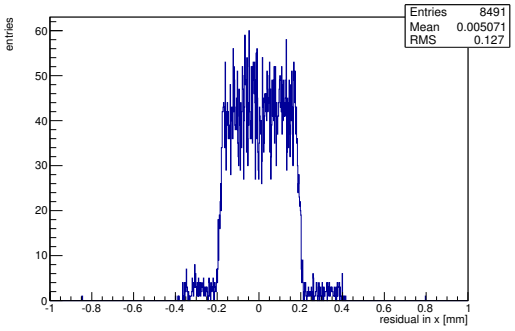

(i) Track residual in x.

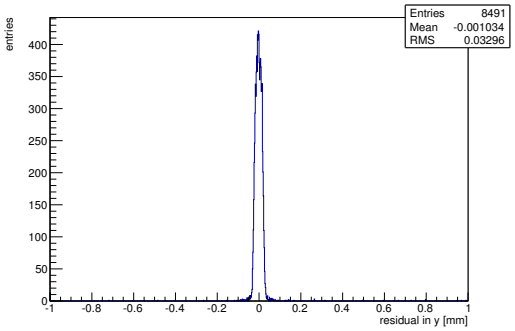

(j) Track residual in y.

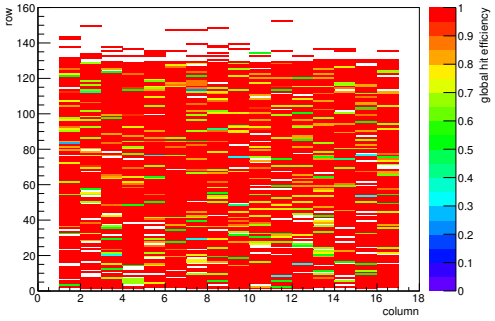

(k) Hit efficiency map.

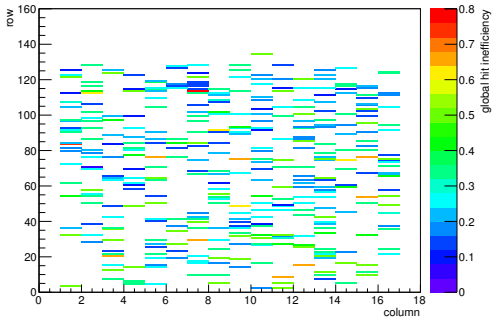

(l) Hit inefficiency map.

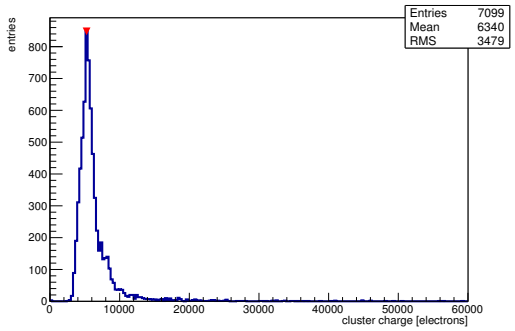

(m) Charge distribution (all cluster sizes included).

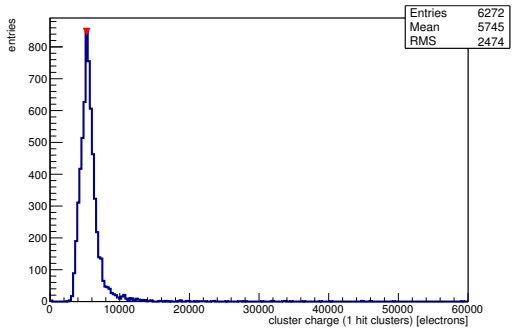

(n) Charge distribution (1 hit cluster).

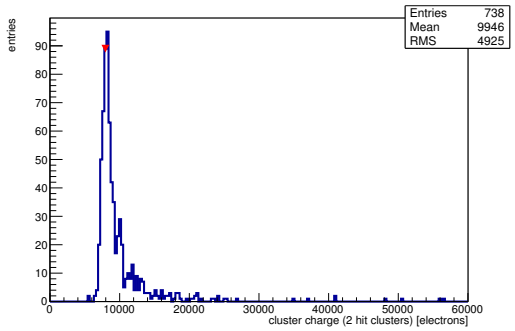

(o) Charge distribution (2 hit cluster).

Figure C.16: Detailed plots for test beam measurement of KEK2R (description see section 6.1) sample (running as DUT1) during runs 50584 in the July 2011 test beam period at CERN SPS in area H6B. Summary of the data in chapter 9. *(cont.)*

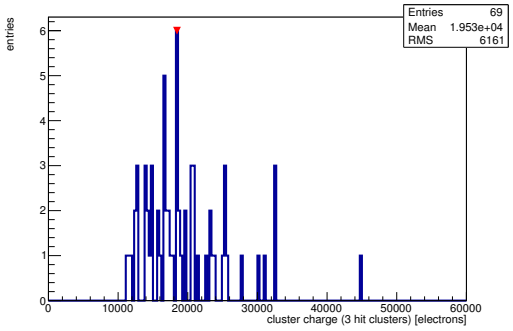

(p) Charge distribution (3 hit cluster).

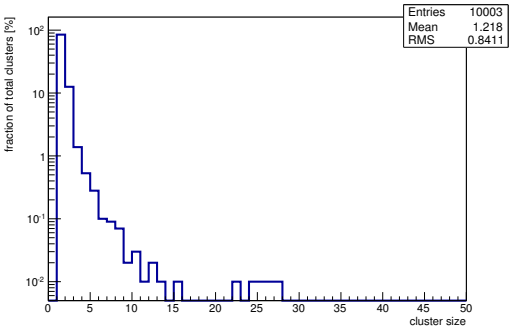

(q) Cluster size distribution.

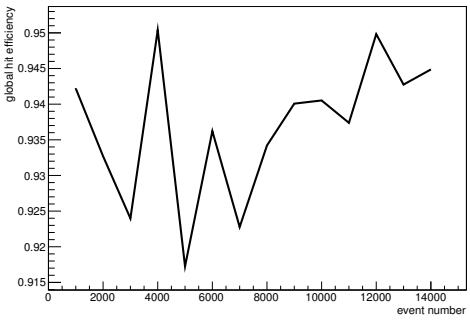

(r) Hit efficiency vs event number.

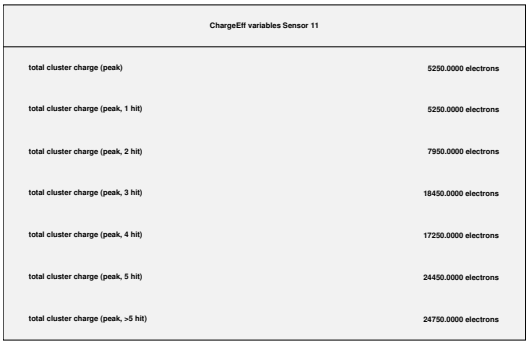

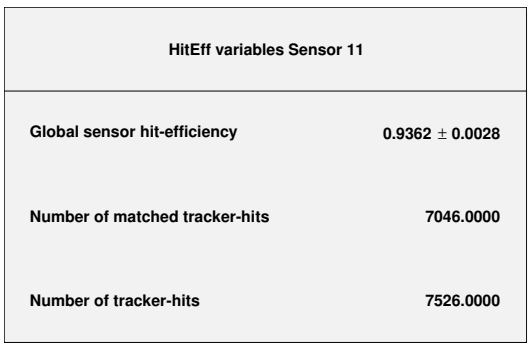

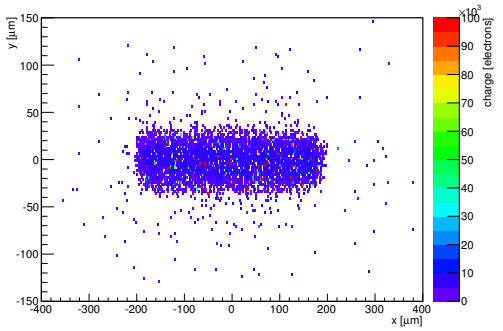

(s) Single pixel mean charge.

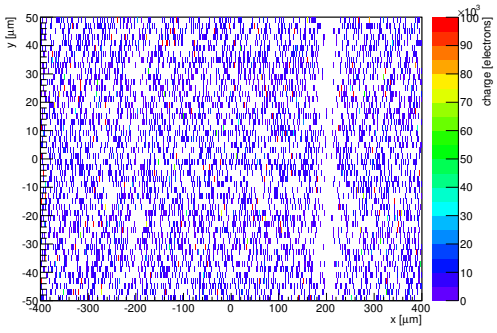

(t) Single pixel mean charge.

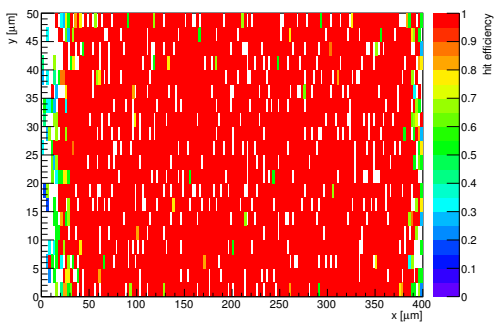

(u) Single pixel hit efficiency.

Figure C.16: Detailed plots for test beam measurement of KEK2R (description see section 6.1) sample (running as DUT1) during runs 50584 in the July 2011 test beam period at CERN SPS in area H6B. Summary of the data in chapter 9.

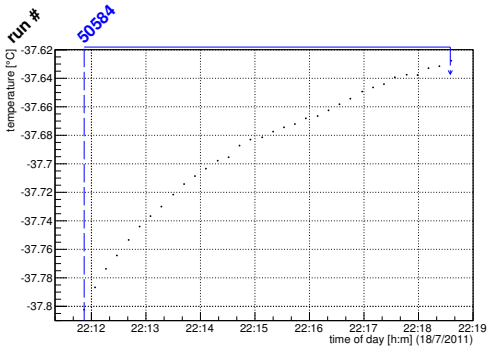

(a) Temperature vs time.

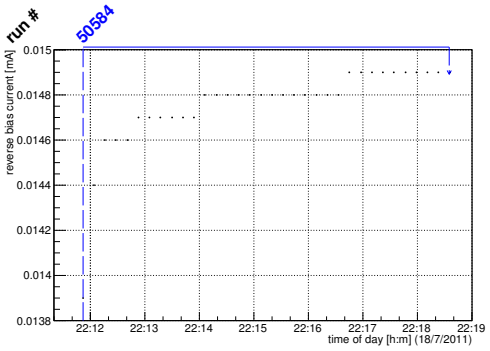

(b) Bias current vs time.

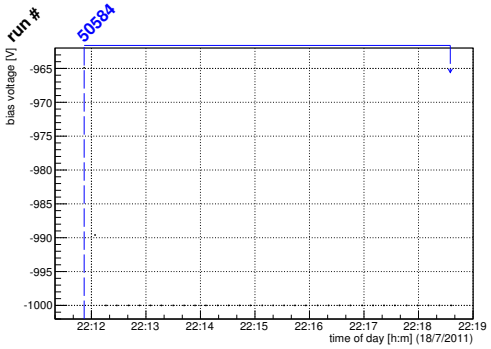

(c) Currently applied bias voltage vs time.

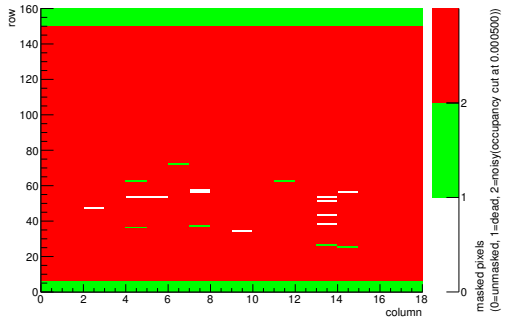

(d) Map of masked pixels.

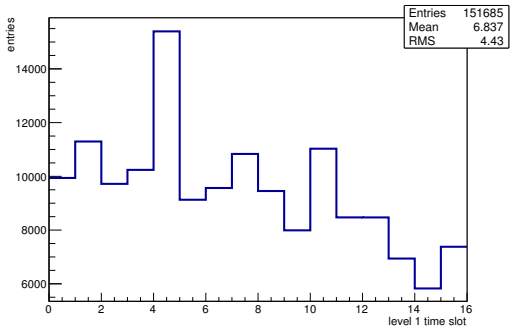

(e) Lvl1 distribution.

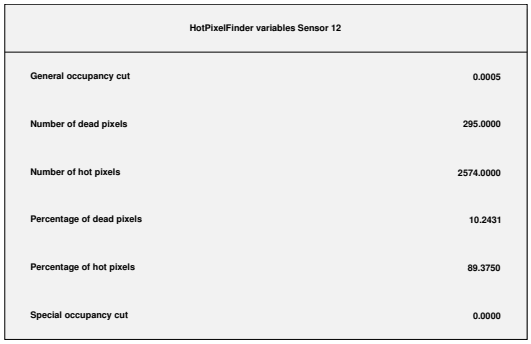

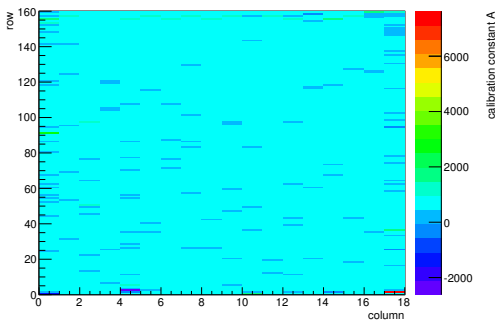

(f) Calibration constant A.

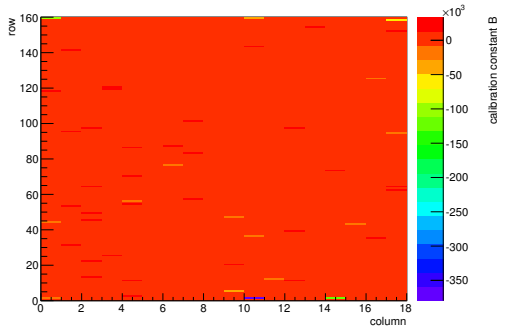

(g) Calibration constant B.

Figure C.17: Detailed plots for test beam measurement of DO-I-11 (description see section 6.1) sample (running as DUT2) during runs 50584 in the July 2011 test beam period at CERN SPS in area H6B. Summary of the data in chapter 9. *(cont.)*

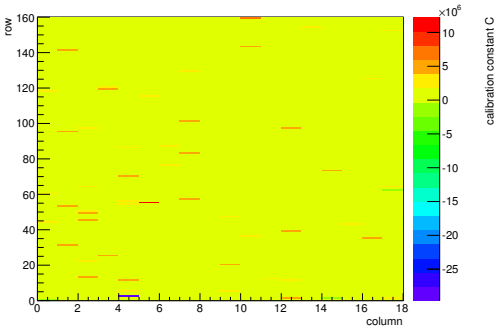

(h) Calibration constant C.

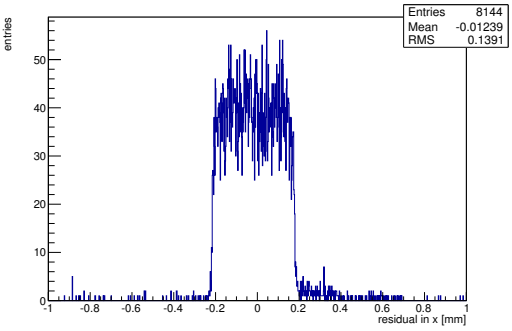

(i) Track residual in x.

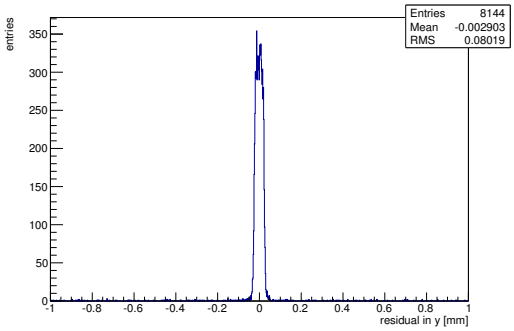

(j) Track residual in y.

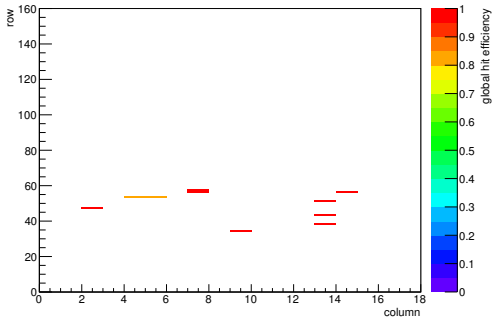

(k) Hit efficiency map.

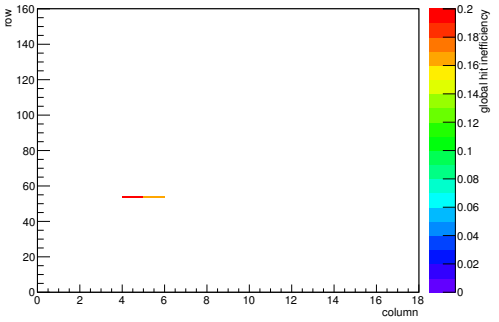

(l) Hit inefficiency map.

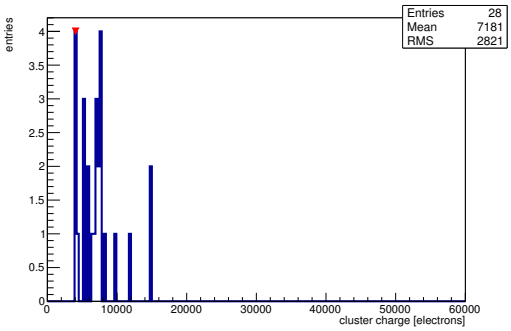

(m) Charge distribution (all cluster sizes included).

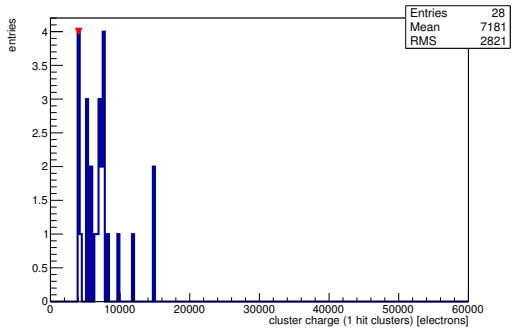

(n) Charge distribution (1 hit cluster).

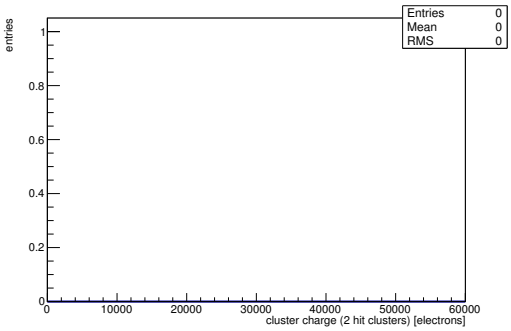

(o) Charge distribution (2 hit cluster).

Figure C.17: Detailed plots for test beam measurement of DO-I-11 (description see section 6.1) sample (running as DUT2) during runs 50584 in the July 2011 test beam period at CERN SPS in area H6B. Summary of the data in chapter 9. *(cont.)*

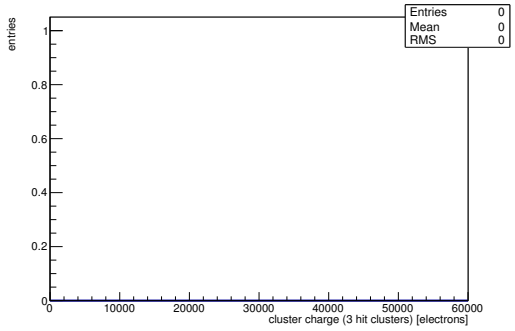

(p) Charge distribution (3 hit cluster).

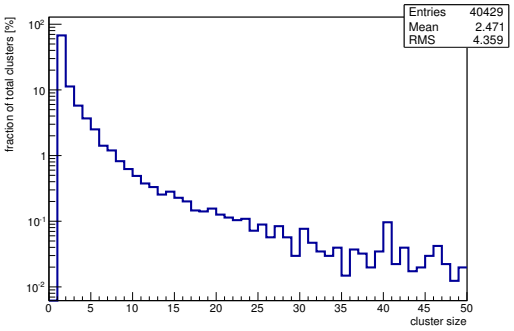

(q) Cluster size distribution.

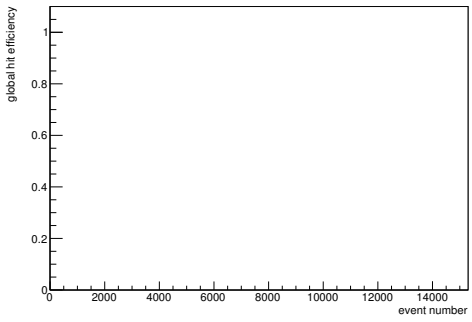

(r) Hit efficiency vs event number.

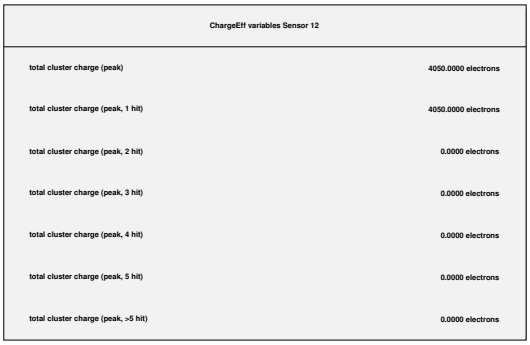

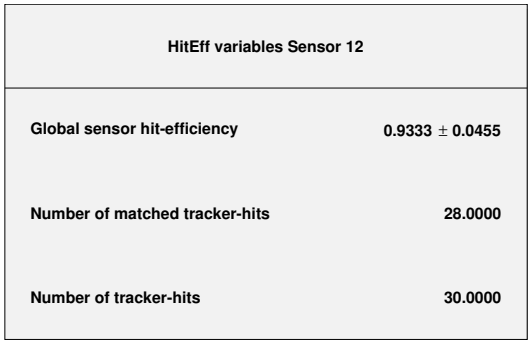

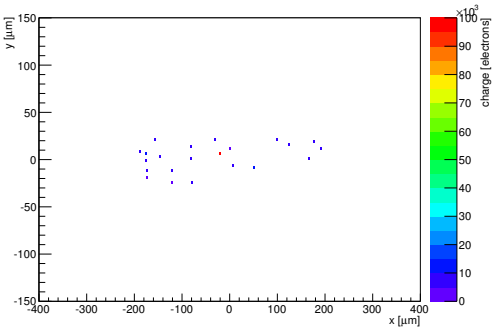

(s) Single pixel mean charge.

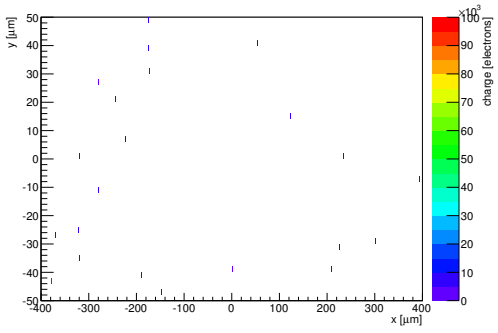

(t) Single pixel mean charge.

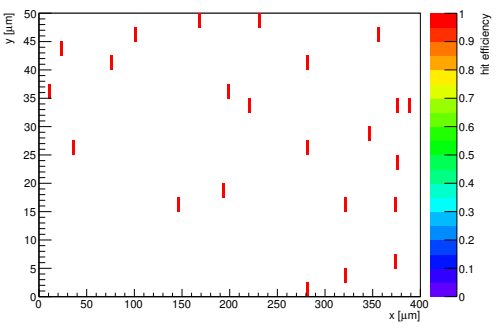

(u) Single pixel hit efficiency.

Figure C.17: Detailed plots for test beam measurement of DO-I-11 (description see section 6.1) sample (running as DUT2) during runs 50584 in the July 2011 test beam period at CERN SPS in area H6B. Summary of the data in chapter 9.

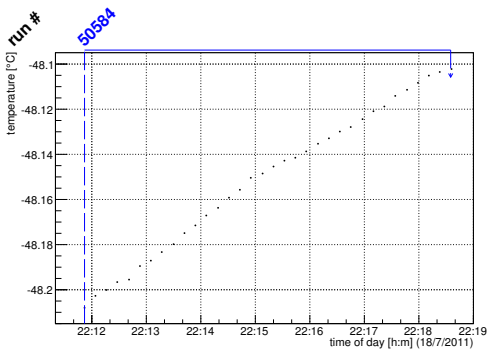

(a) Temperature vs time.

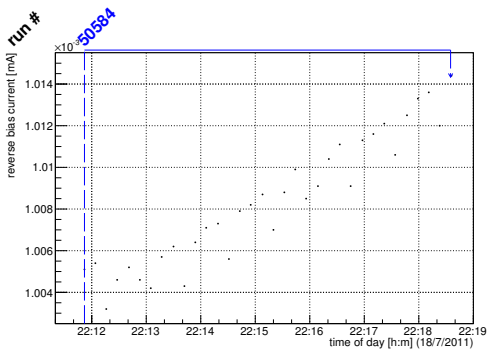

(b) Bias current vs time.

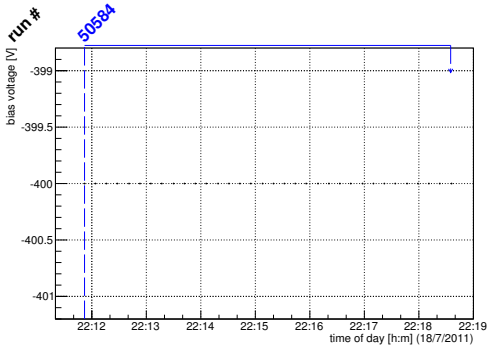

(c) Currently applied bias voltage vs time.

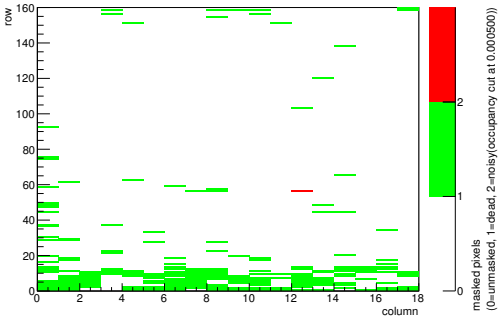

(d) Map of masked pixels.

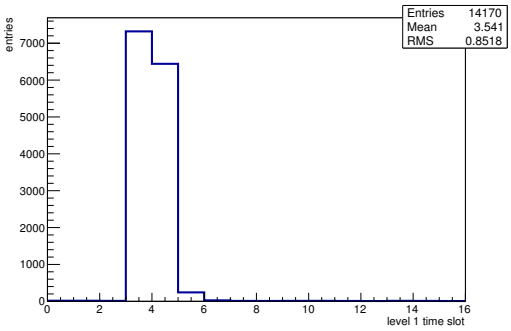

(e) Lvl1 distribution.

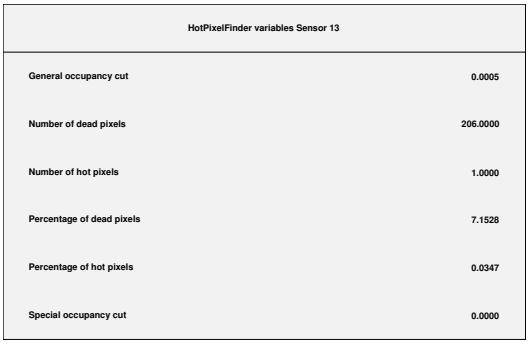

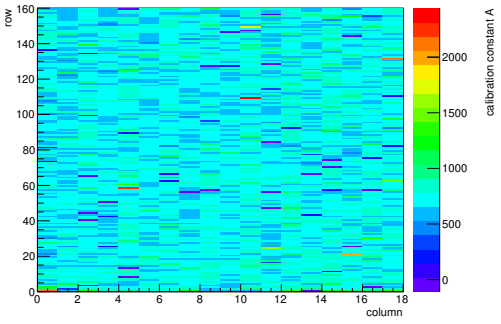

(f) Calibration constant A.

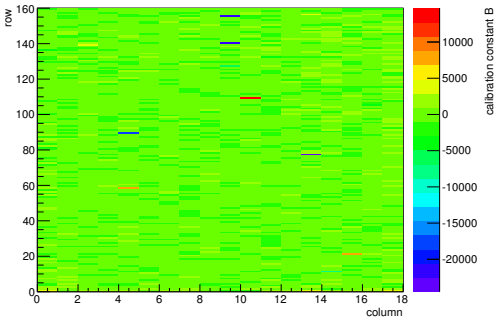

(g) Calibration constant B.

Figure C.18: Detailed plots for test beam measurement of DO-I-13 (description see section 6.1) sample (running as DUT3) during runs 50584 in the July 2011 test beam period at CERN SPS in area H6B. Summary of the data in chapter 9. *(cont.)*

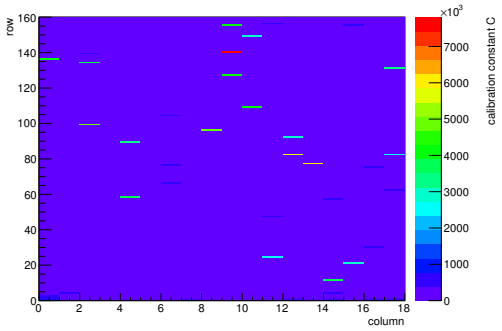

(h) Calibration constant C.

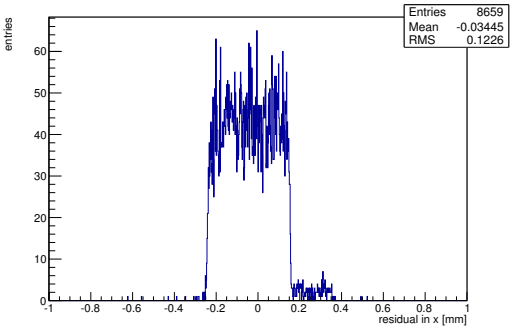

(i) Track residual in x.

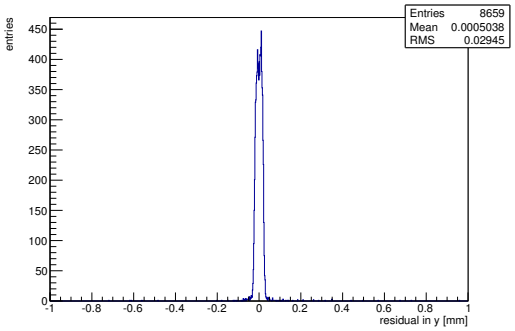

(j) Track residual in y.

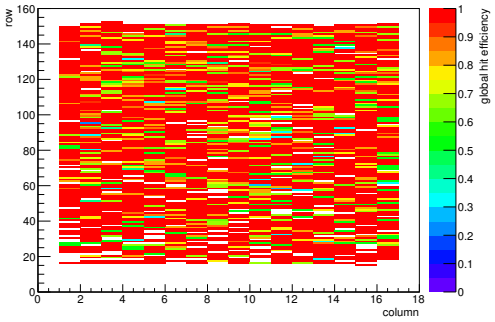

(k) Hit efficiency map.

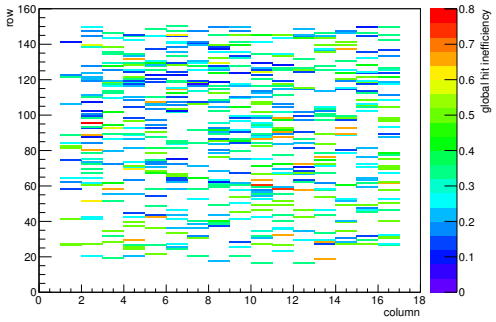

(l) Hit inefficiency map.

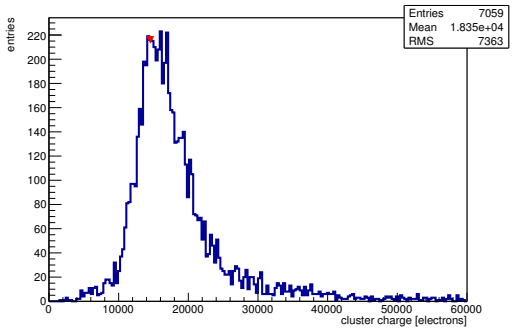

(m) Charge distribution (all cluster sizes included).

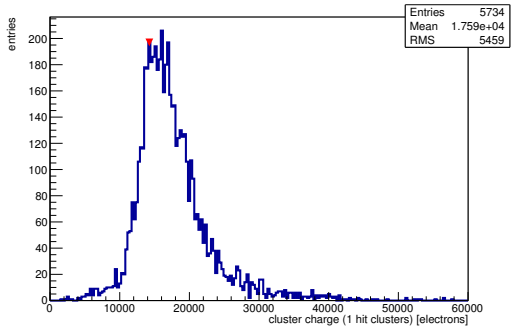

(n) Charge distribution (1 hit cluster).

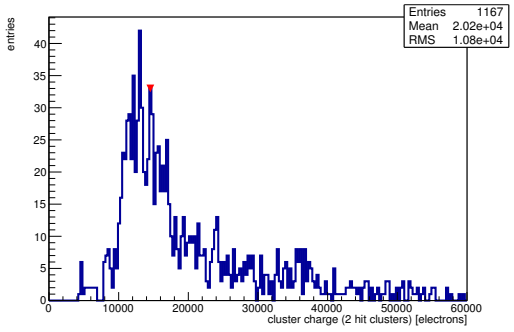

(o) Charge distribution (2 hit cluster).

Figure C.18: Detailed plots for test beam measurement of DO-I-13 (description see section 6.1) sample (running as DUT3) during runs 50584 in the July 2011 test beam period at CERN SPS in area H6B. Summary of the data in chapter 9. *(cont.)*

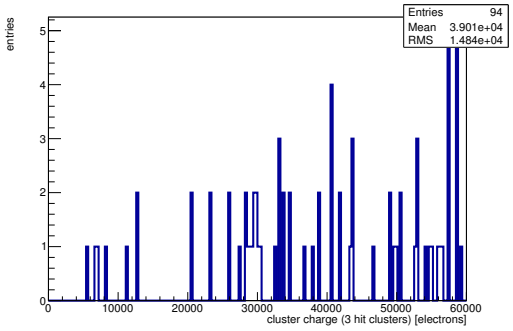

(p) Charge distribution (3 hit cluster).

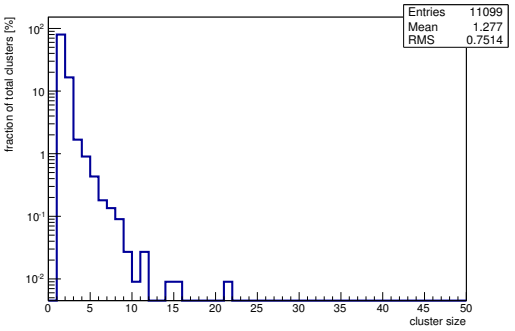

(q) Cluster size distribution.

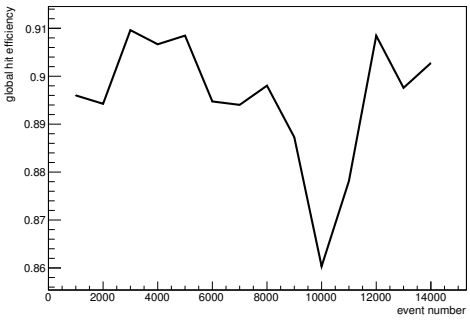

(r) Hit efficiency vs event number.

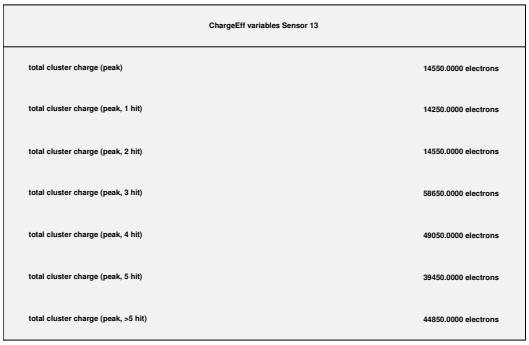

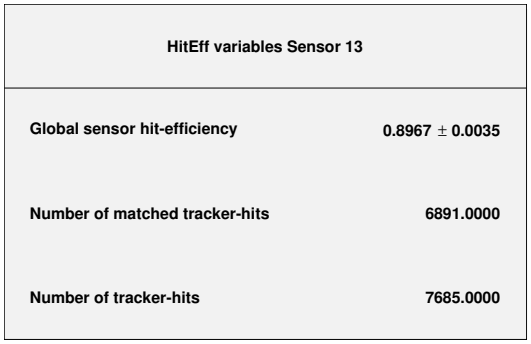

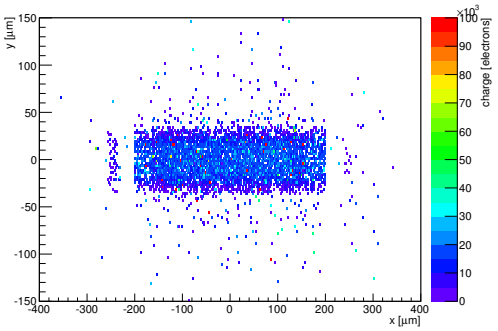

(s) Single pixel mean charge.

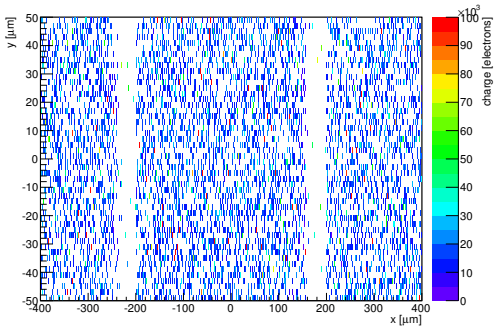

(t) Single pixel mean charge.

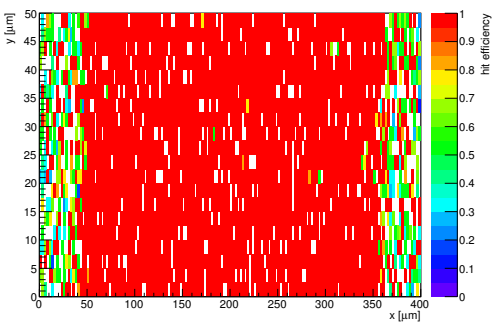

(u) Single pixel hit efficiency.

Figure C.18: Detailed plots for test beam measurement of DO-I-13 (description see section 6.1) sample (running as DUT3) during runs 50584 in the July 2011 test beam period at CERN SPS in area H6B. Summary of the data in chapter 9.

C.2.3 Run 50585

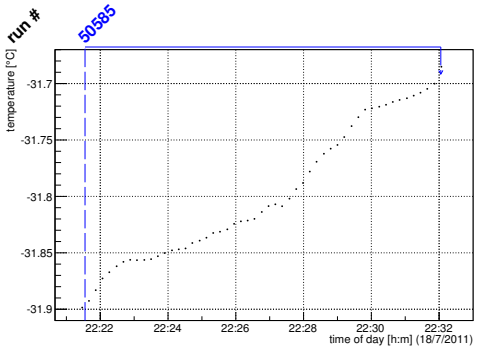

(a) Temperature vs time.

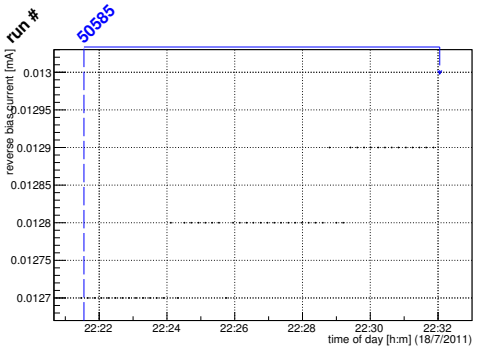

(b) Bias current vs time.

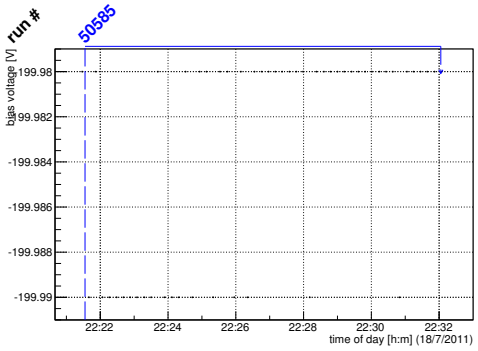

(c) Currently applied bias voltage vs time.

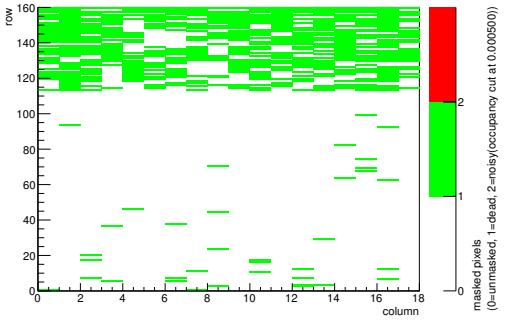

(d) Map of masked pixels.

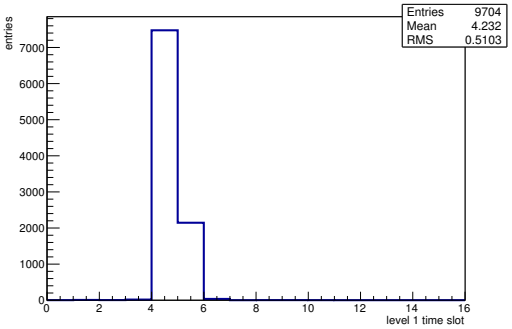

(e) Lvl1 distribution.

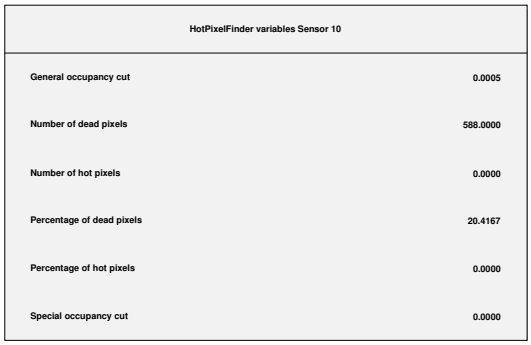

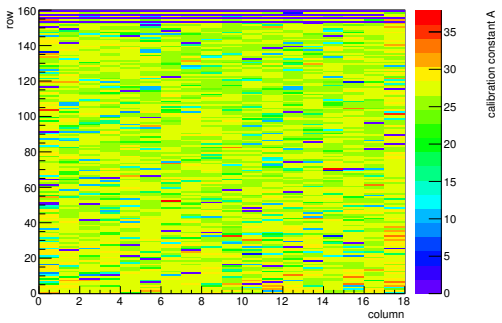

(f) Calibration constant A.

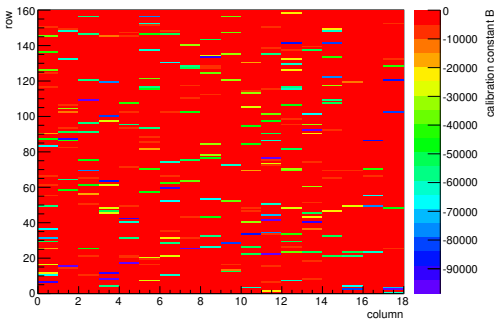

(g) Calibration constant B.

Figure C.19: Detailed plots for test beam measurement of KEK1R (description see section 6.1) sample (running as DUT0) during runs 50585 in the July 2011 test beam period at CERN SPS in area H6B. Summary of the data in chapter 9. *(cont.)*

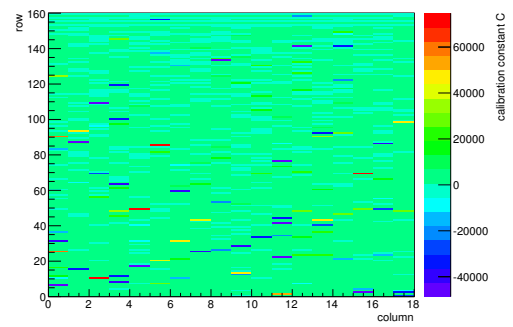

(h) Calibration constant C.

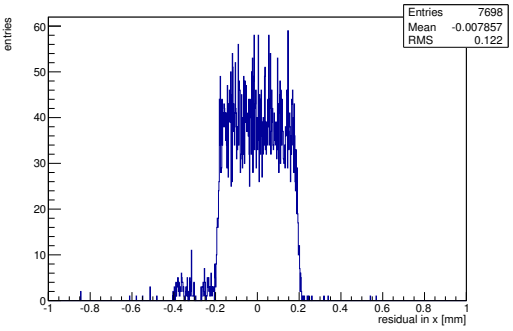

(i) Track residual in x.

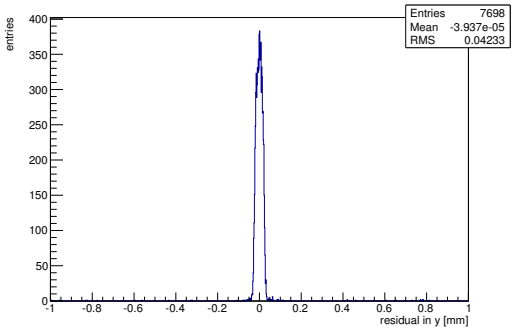

(j) Track residual in y.

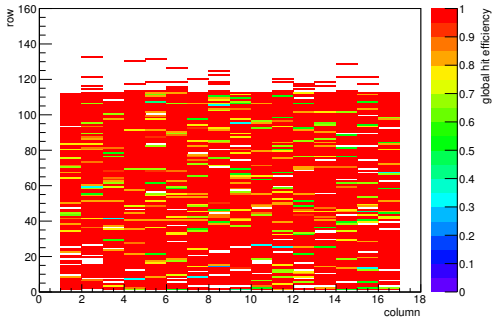

(k) Hit efficiency map.

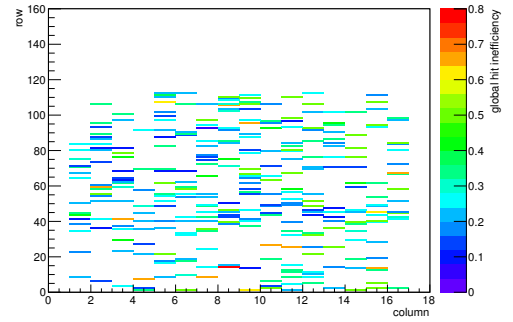

(l) Hit inefficiency map.

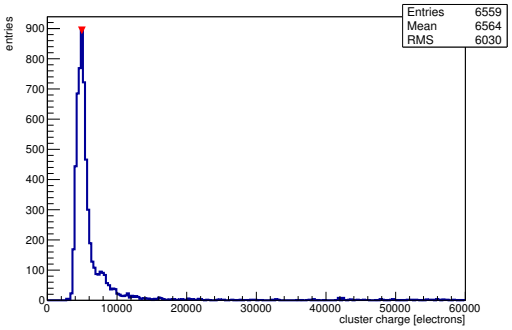

(m) Charge distribution (all cluster sizes included).

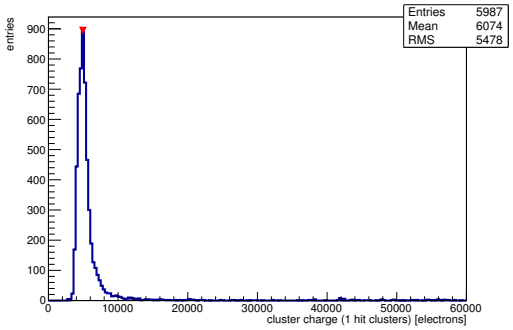

(n) Charge distribution (1 hit cluster).

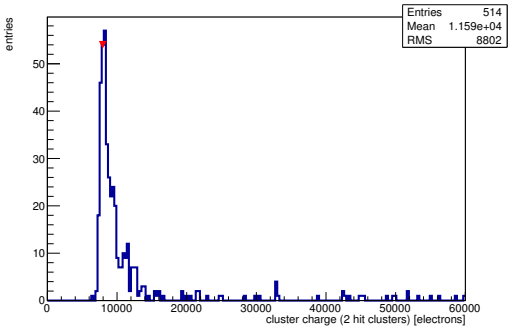

(o) Charge distribution (2 hit cluster).

Figure C.19: Detailed plots for test beam measurement of KEK1R (description see section 6.1) sample (running as DUT0) during runs 50585 in the July 2011 test beam period at CERN SPS in area H6B. Summary of the data in chapter 9. *(cont.)*

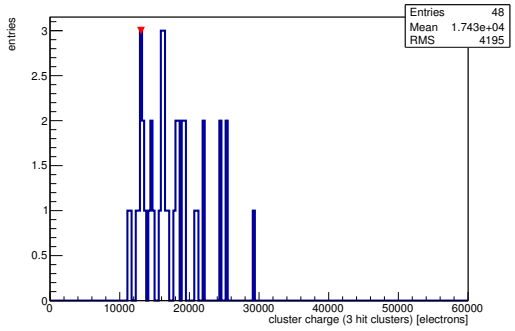

(p) Charge distribution (3 hit cluster).

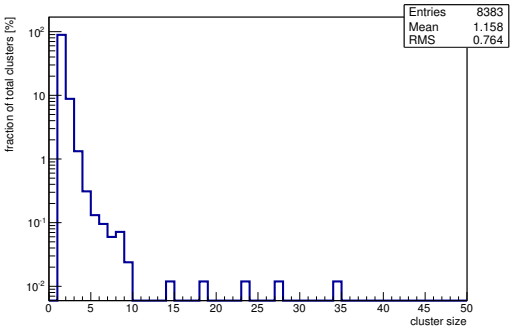

(q) Cluster size distribution.

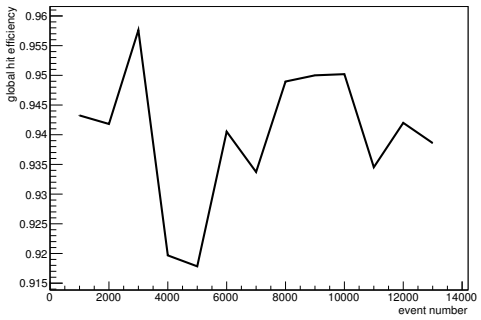

(r) Hit efficiency vs event number.

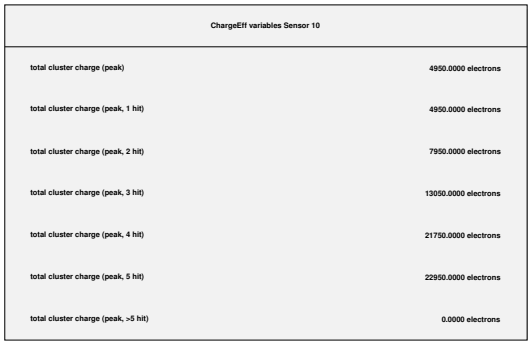

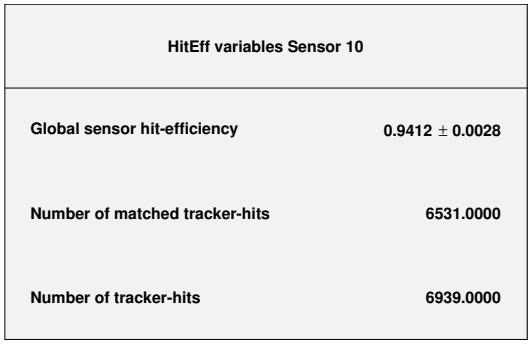

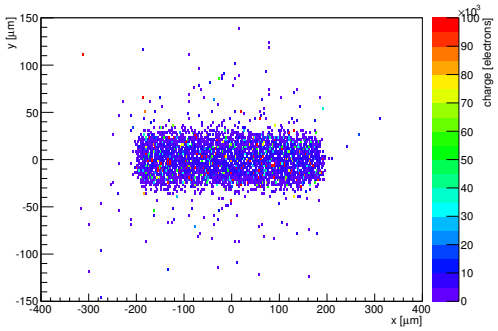

(s) Single pixel mean charge.

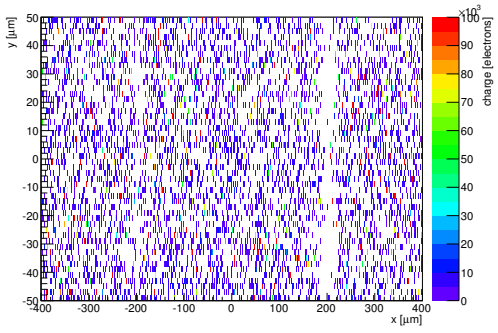

(t) Single pixel mean charge.

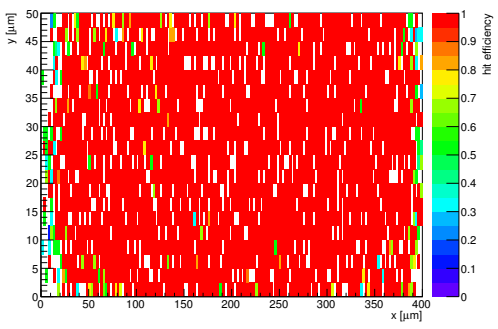

(u) Single pixel hit efficiency.

Figure C.19: Detailed plots for test beam measurement of KEK1R (description see section 6.1) sample (running as DUT0) during runs 50585 in the July 2011 test beam period at CERN SPS in area H6B. Summary of the data in chapter 9.

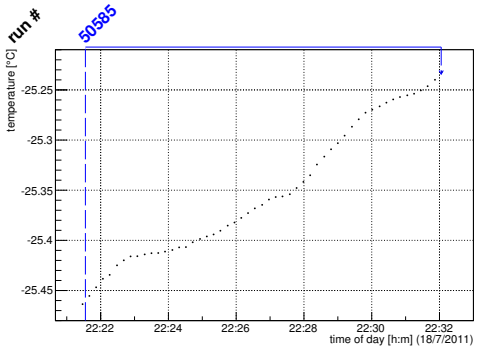

(a) Temperature vs time.

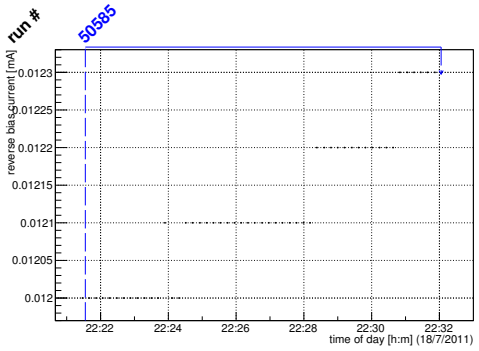

(b) Bias current vs time.

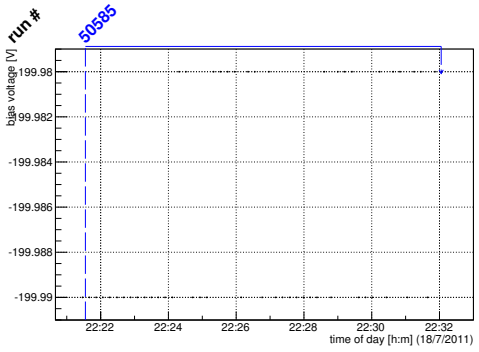

(c) Currently applied bias voltage vs time.

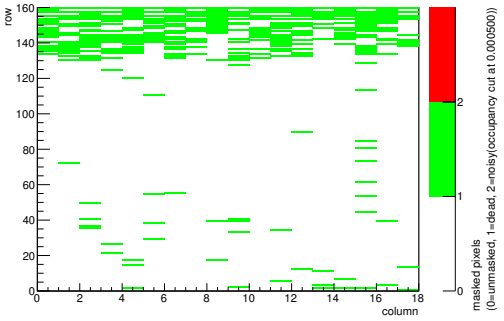

(d) Map of masked pixels.

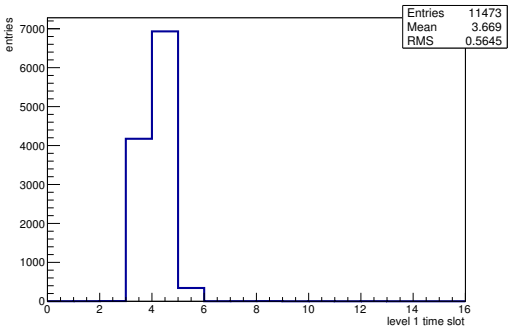

(e) Lvl1 distribution.

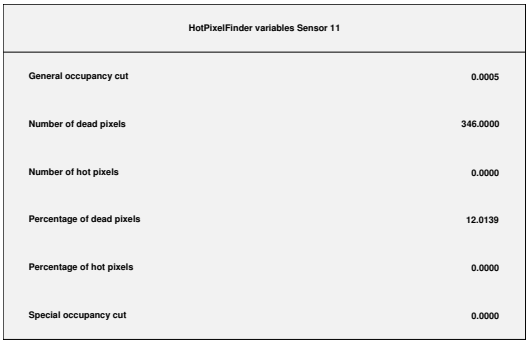

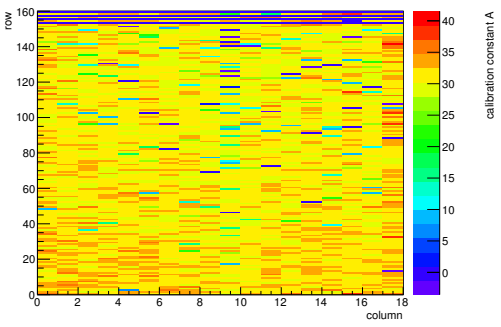

(f) Calibration constant A.

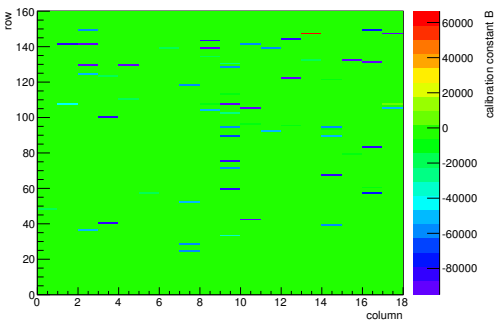

(g) Calibration constant B.

Figure C.20: Detailed plots for test beam measurement of KEK2R (description see section 6.1) sample (running as DUT1) during runs 50585 in the July 2011 test beam period at CERN SPS in area H6B. Summary of the data in chapter 9. *(cont.)*

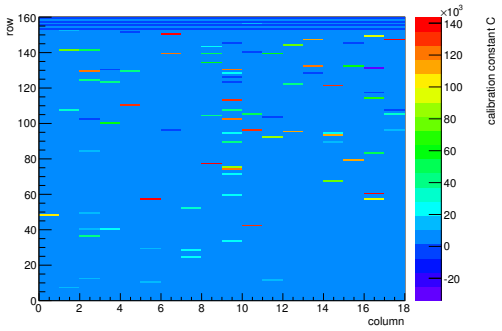

(h) Calibration constant C.

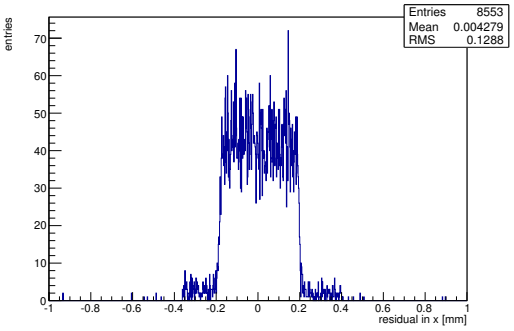

(i) Track residual in x.

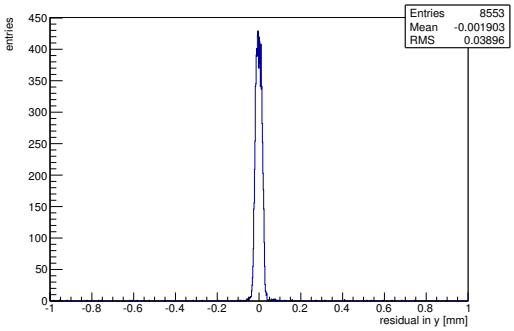

(j) Track residual in y.

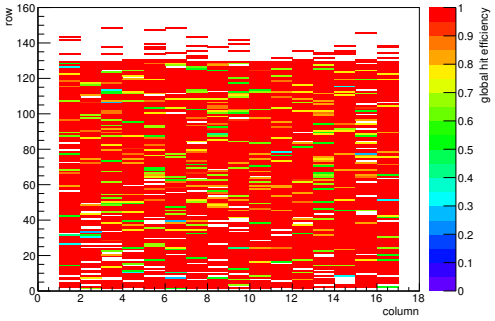

(k) Hit efficiency map.

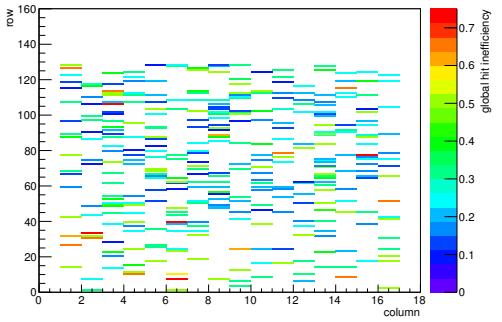

(l) Hit inefficiency map.

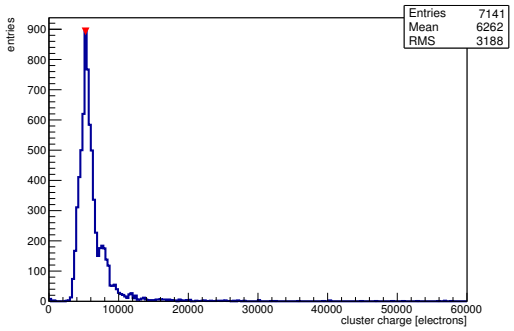

(m) Charge distribution (all cluster sizes included).

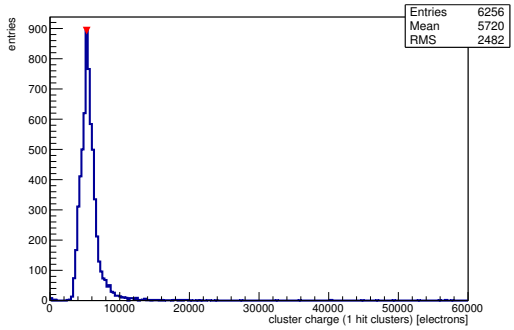

(n) Charge distribution (1 hit cluster).

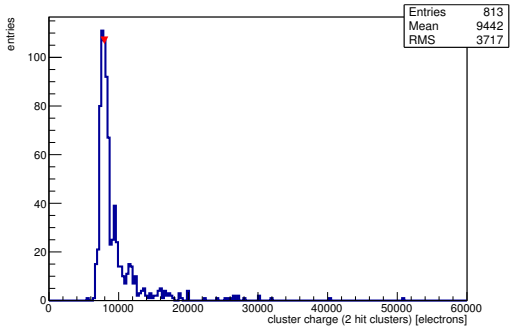

(o) Charge distribution (2 hit cluster).

Figure C.20: Detailed plots for test beam measurement of KEK2R (description see section 6.1) sample (running as DUT1) during runs 50585 in the July 2011 test beam period at CERN SPS in area H6B. Summary of the data in chapter 9. *(cont.)*

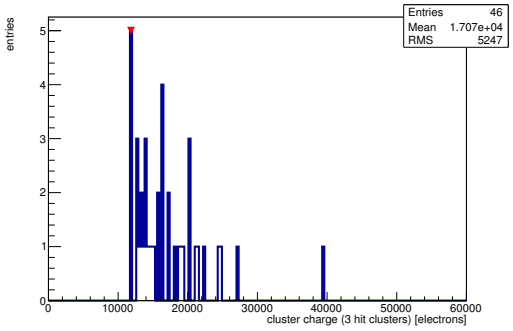

(p) Charge distribution (3 hit cluster).

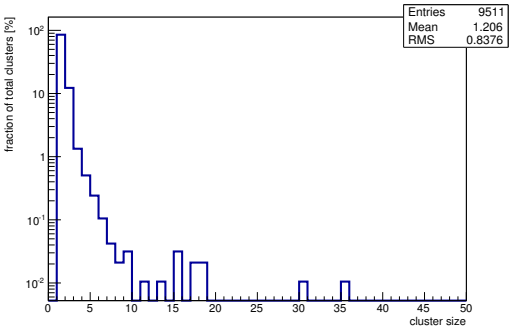

(q) Cluster size distribution.

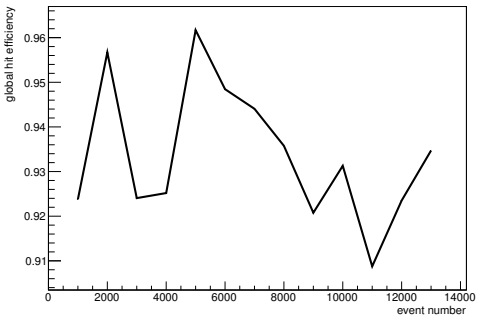

(r) Hit efficiency vs event number.

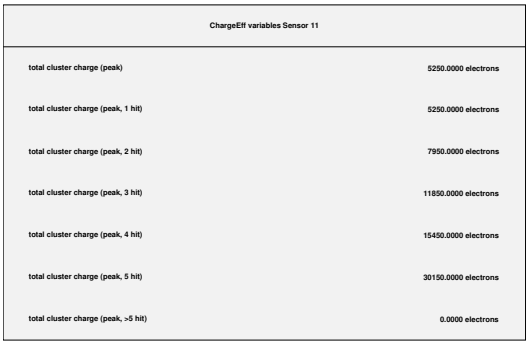

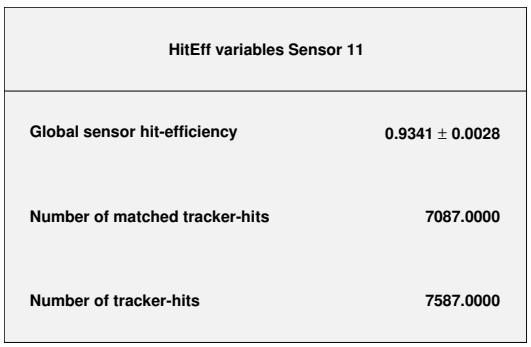

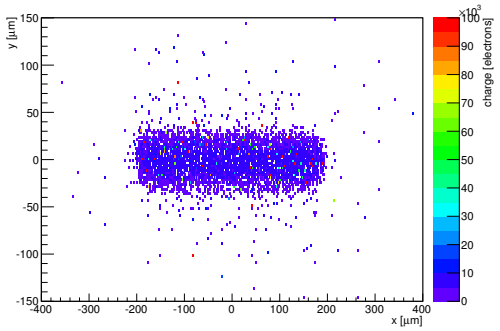

(s) Single pixel mean charge.

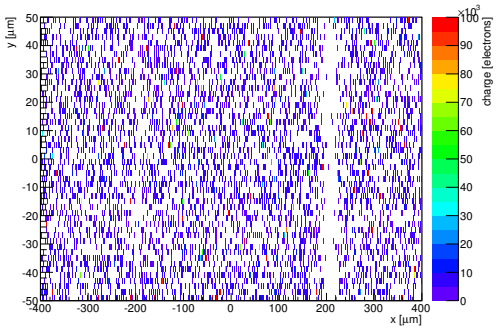

(t) Single pixel mean charge.

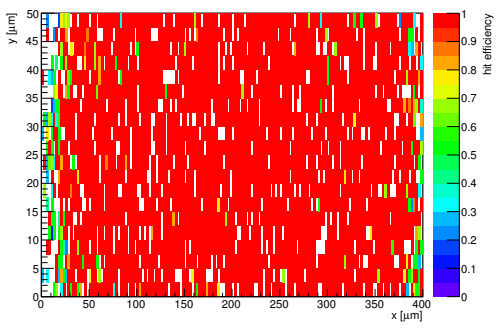

(u) Single pixel hit efficiency.

Figure C.20: Detailed plots for test beam measurement of KEK2R (description see section 6.1) sample (running as DUT1) during runs 50585 in the July 2011 test beam period at CERN SPS in area H6B. Summary of the data in chapter 9.

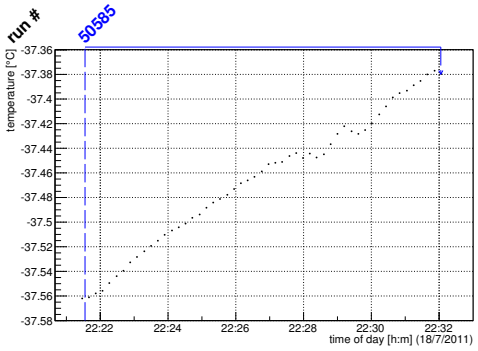

(a) Temperature vs time.

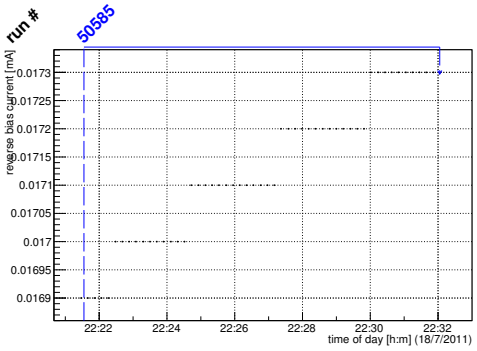

(b) Bias current vs time.

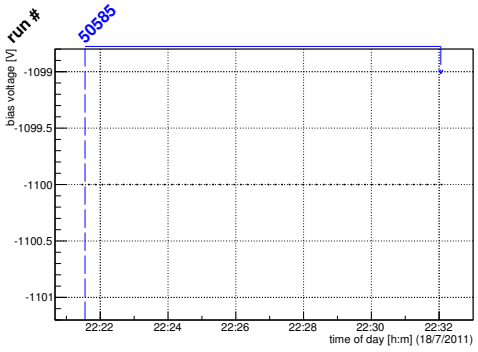

(c) Currently applied bias voltage vs time.

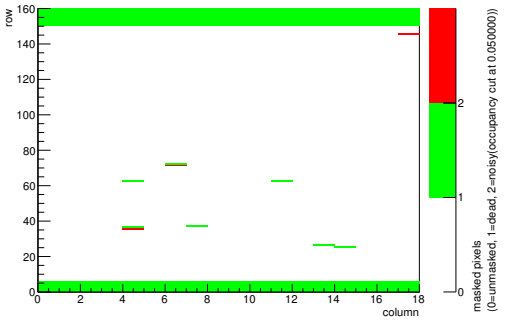

(d) Map of masked pixels.

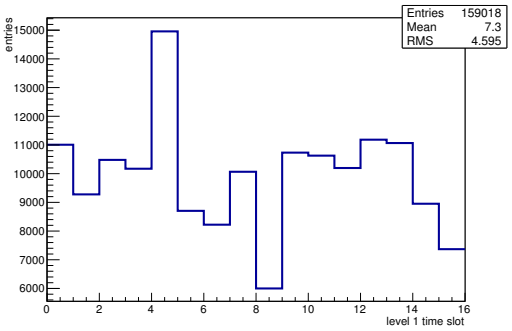

(e) Lvl1 distribution.

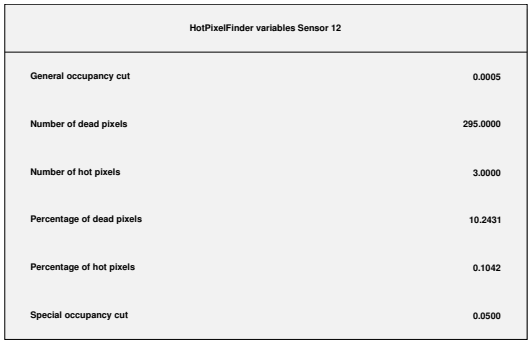

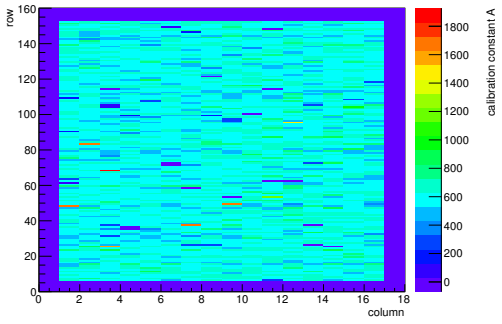

(f) Calibration constant A.

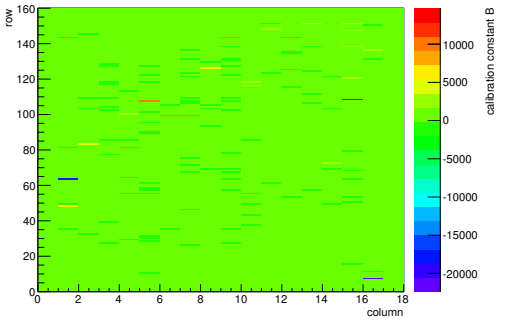

(g) Calibration constant B.

Figure C.21: Detailed plots for test beam measurement of DO-I-11 (description see section 6.1) sample (running as DUT2) during runs 50585 in the July 2011 test beam period at CERN SPS in area H6B. Summary of the data in chapter 9. *(cont.)*

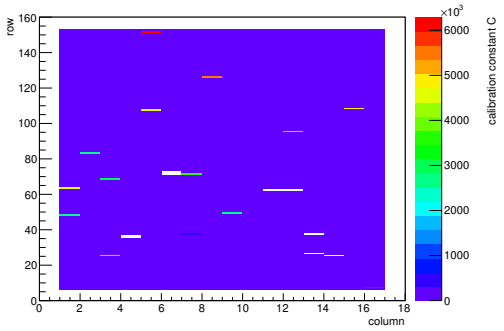

(h) Calibration constant C.

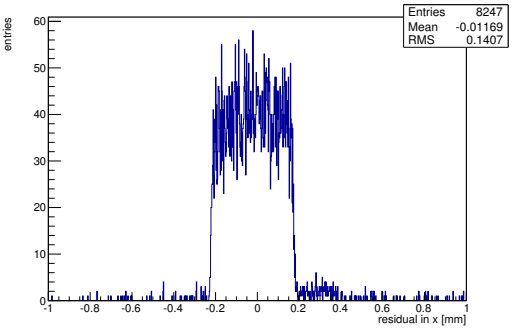

(i) Track residual in x.

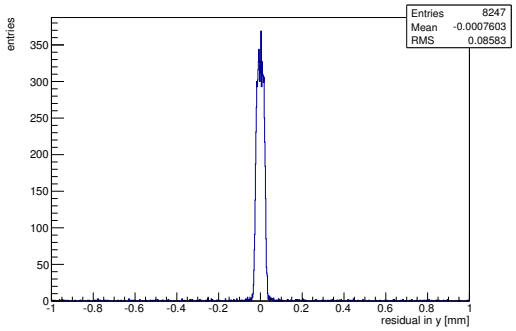

(j) Track residual in y.

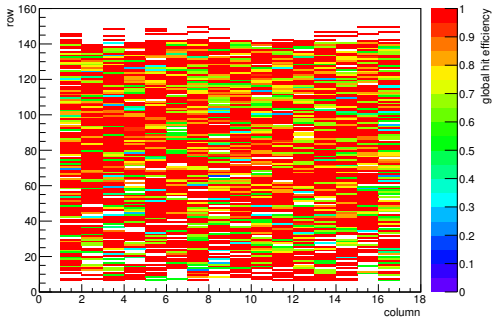

(k) Hit efficiency map.

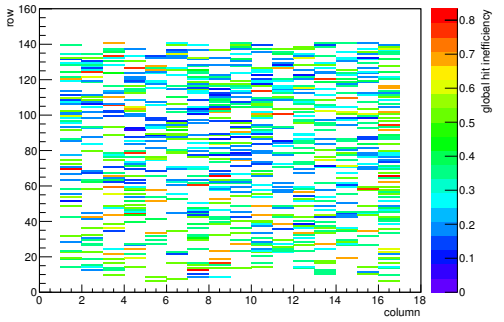

(l) Hit inefficiency map.

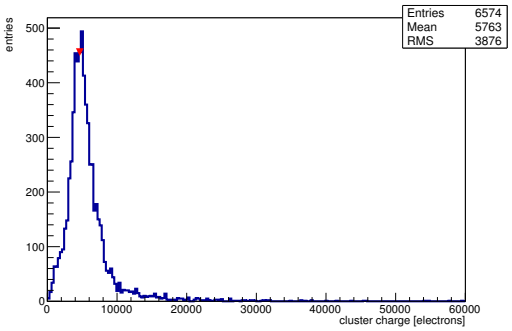

(m) Charge distribution (all cluster sizes included).

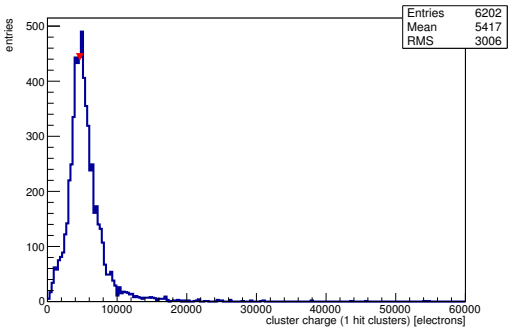

(n) Charge distribution (1 hit cluster).

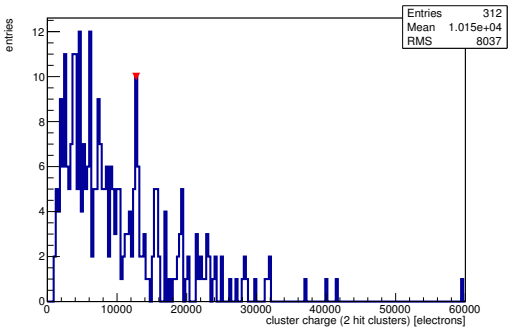

(o) Charge distribution (2 hit cluster).

Figure C.21: Detailed plots for test beam measurement of DO-I-11 (description see section 6.1) sample (running as DUT2) during runs 50585 in the July 2011 test beam period at CERN SPS in area H6B. Summary of the data in chapter 9. *(cont.)*

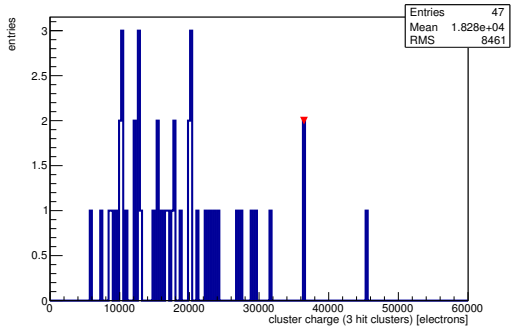

(p) Charge distribution (3 hit cluster).

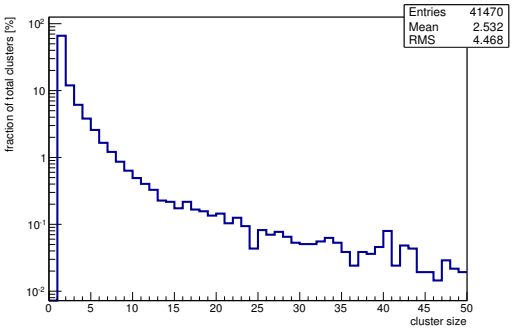

(q) Cluster size distribution.

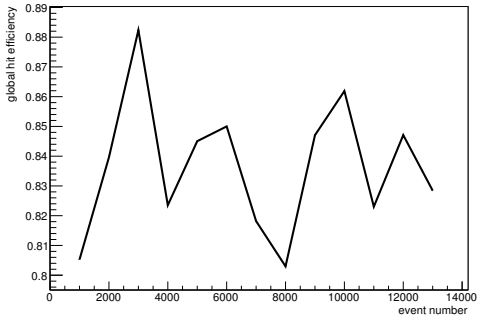

(r) Hit efficiency vs event number.

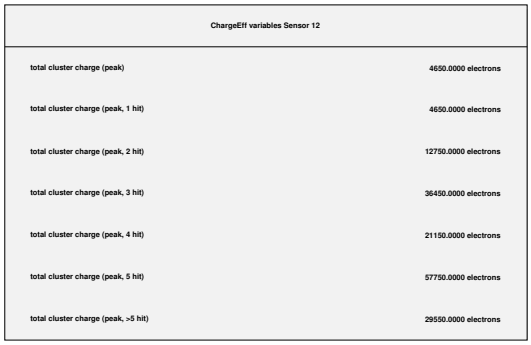

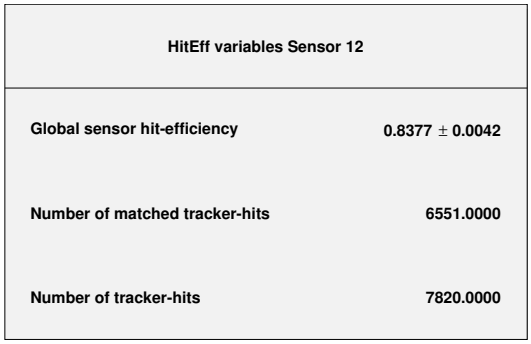

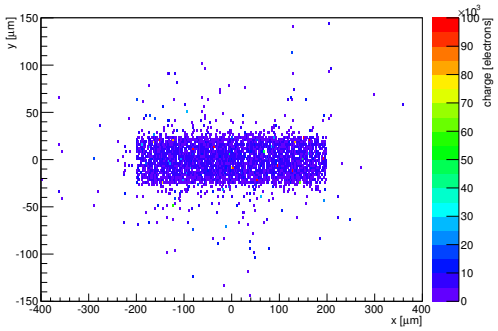

(s) Single pixel mean charge.

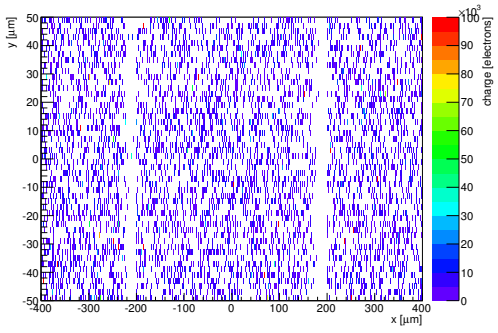

(t) Single pixel mean charge.

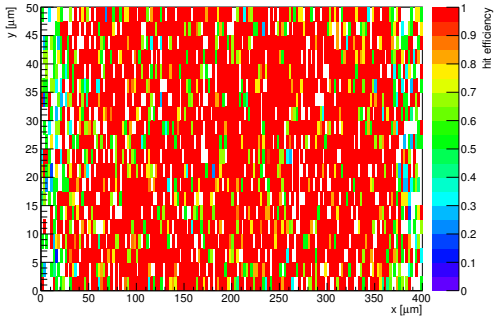

(u) Single pixel hit efficiency.

Figure C.21: Detailed plots for test beam measurement of DO-I-11 (description see section 6.1) sample (running as DUT2) during runs 50585 in the July 2011 test beam period at CERN SPS in area H6B. Summary of the data in chapter 9.

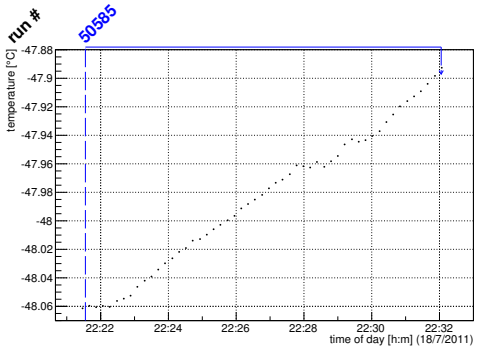

(a) Temperature vs time.

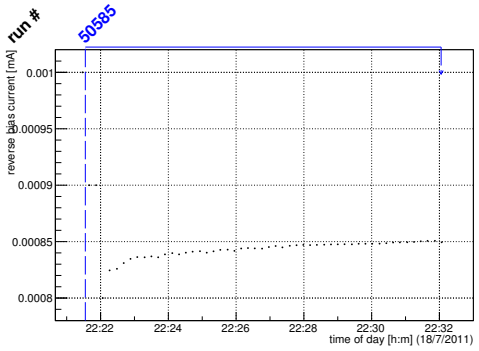

(b) Bias current vs time.

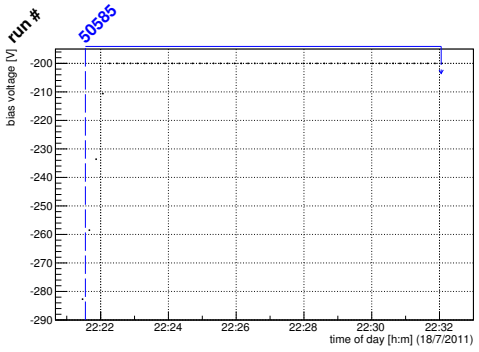

(c) Currently applied bias voltage vs time.

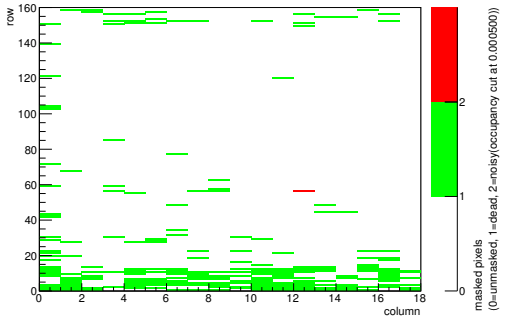

(d) Map of masked pixels.

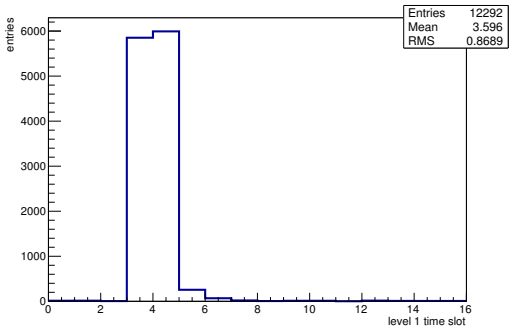

(e) Lvl1 distribution.

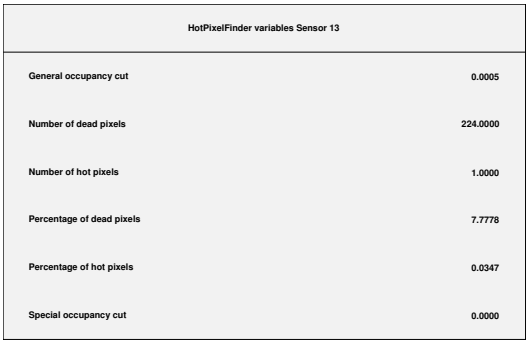

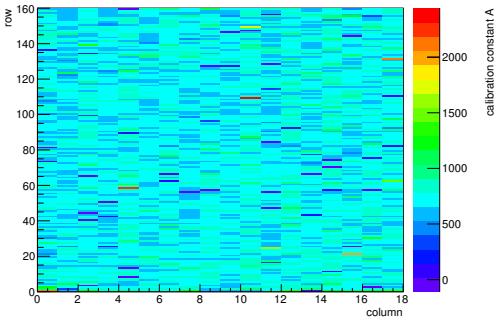

(f) Calibration constant A.

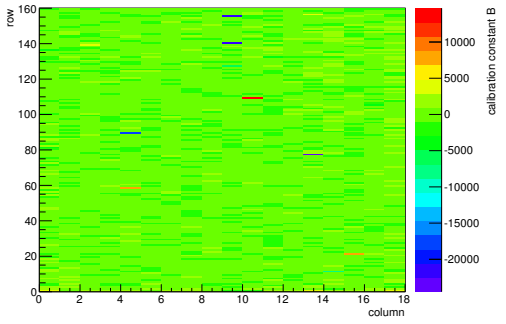

(g) Calibration constant B.

Figure C.22: Detailed plots for test beam measurement of DO-I-13 (description see section 6.1) sample (running as DUT3) during runs 50585 in the July 2011 test beam period at CERN SPS in area H6B. Summary of the data in chapter 9. *(cont.)*

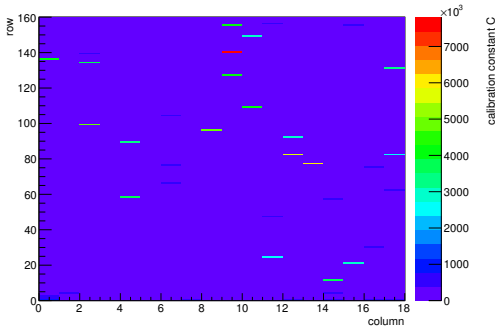

(h) Calibration constant C.

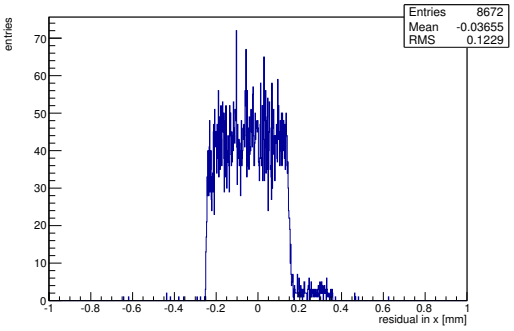

(i) Track residual in x.

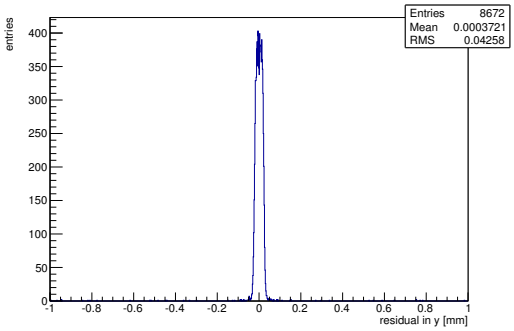

(j) Track residual in y.

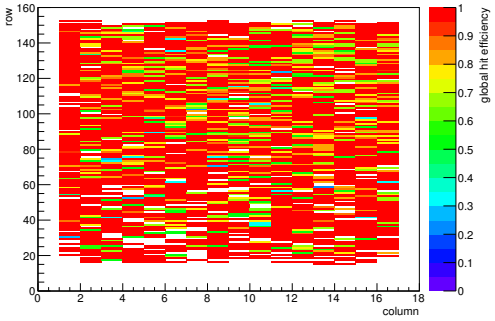

(k) Hit efficiency map.

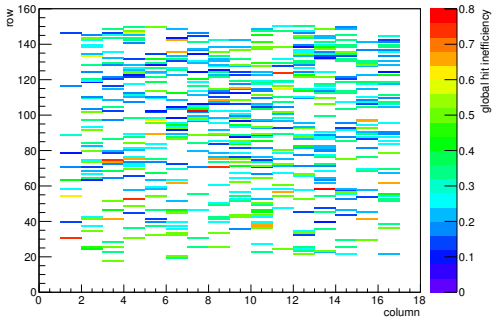

(l) Hit inefficiency map.

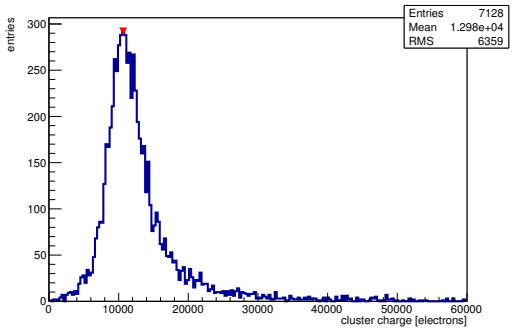

(m) Charge distribution (all cluster sizes included).

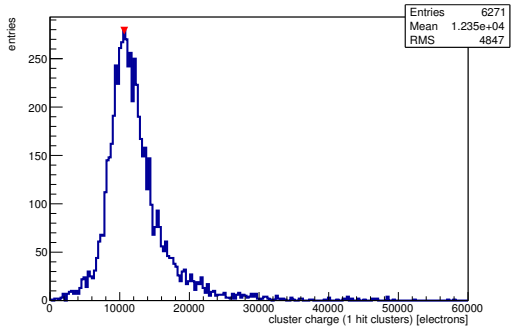

(n) Charge distribution (1 hit cluster).

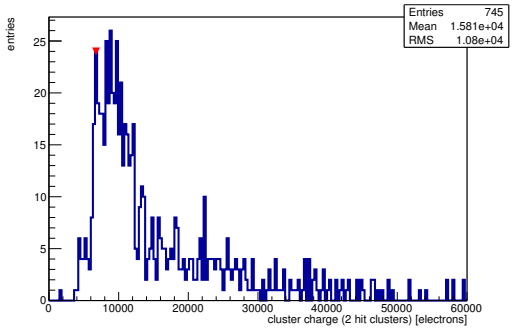

(o) Charge distribution (2 hit cluster).

Figure C.22: Detailed plots for test beam measurement of DO-I-13 (description see section 6.1) sample (running as DUT3) during runs 50585 in the July 2011 test beam period at CERN SPS in area H6B. Summary of the data in chapter 9. *(cont.)*

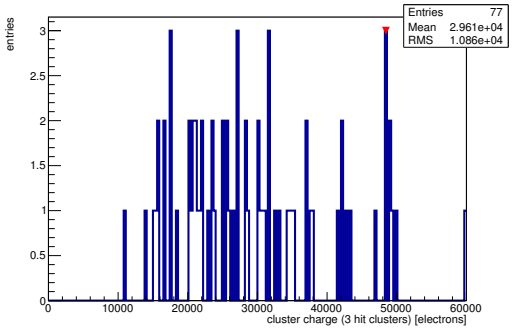

(p) Charge distribution (3 hit cluster).

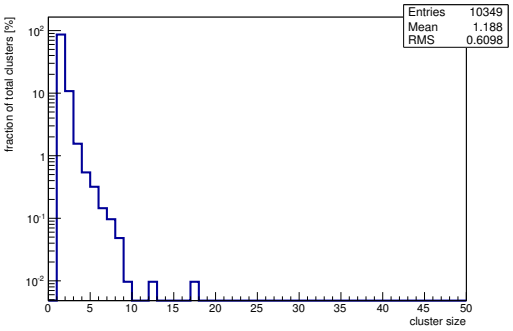

(q) Cluster size distribution.

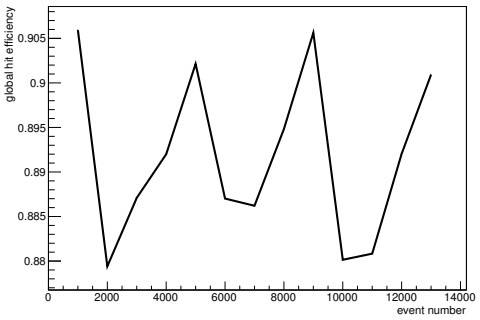

(r) Hit efficiency vs event number.

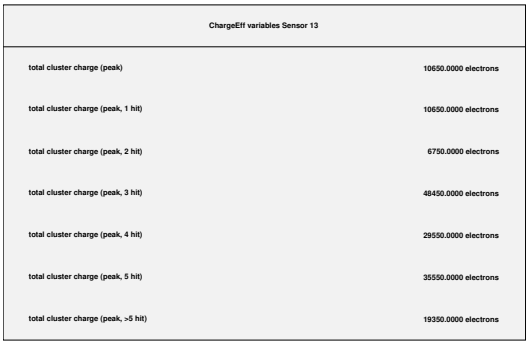

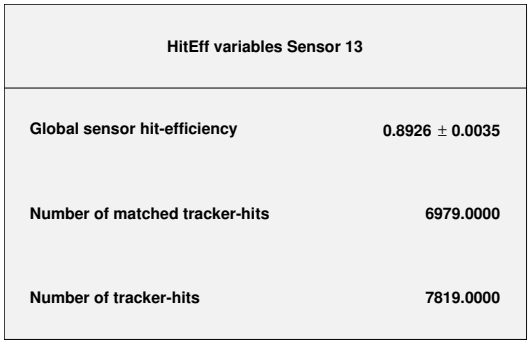

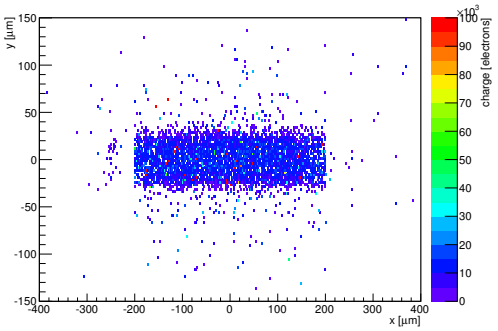

(s) Single pixel mean charge.

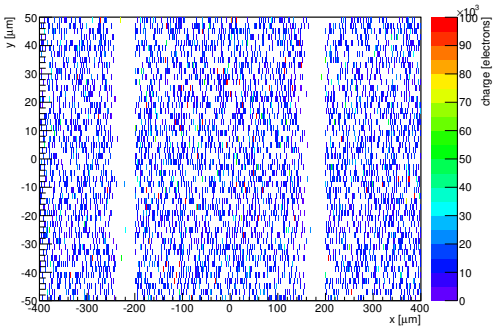

(t) Single pixel mean charge.

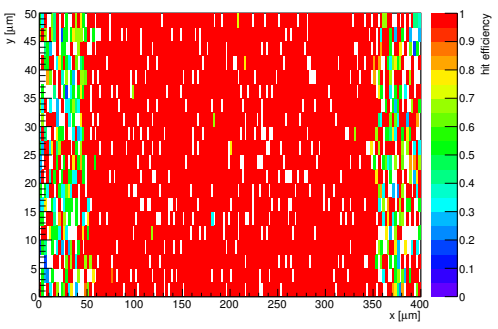

(u) Single pixel hit efficiency.

Figure C.22: Detailed plots for test beam measurement of DO-I-13 (description see section 6.1) sample (running as DUT3) during runs 50585 in the July 2011 test beam period at CERN SPS in area H6B. Summary of the data in chapter 9.

C.2.4 Run 50586

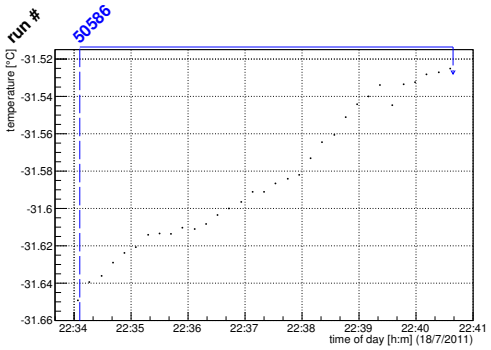

(a) Temperature vs time.

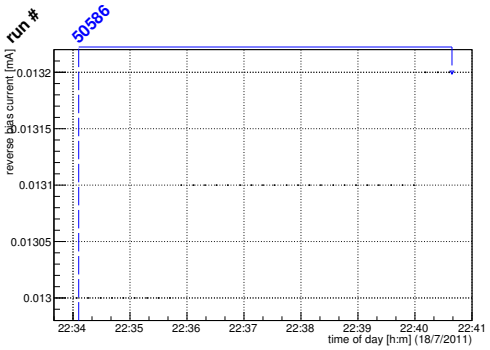

(b) Bias current vs time.

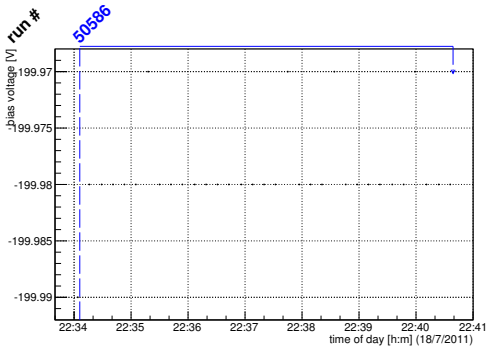

(c) Currently applied bias voltage vs time.

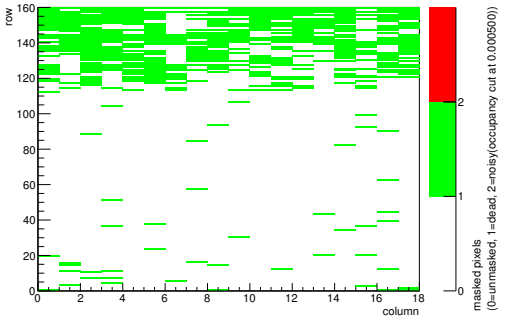

(d) Map of masked pixels.

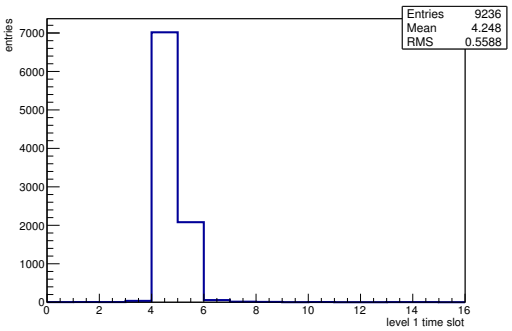

(e) Lvl1 distribution.

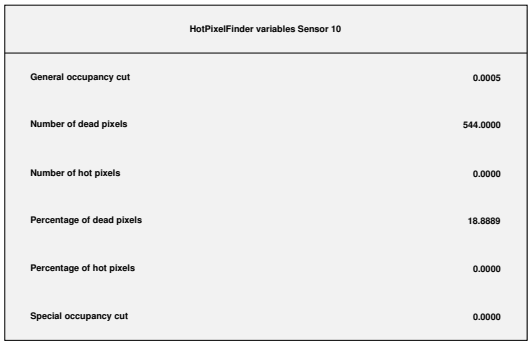

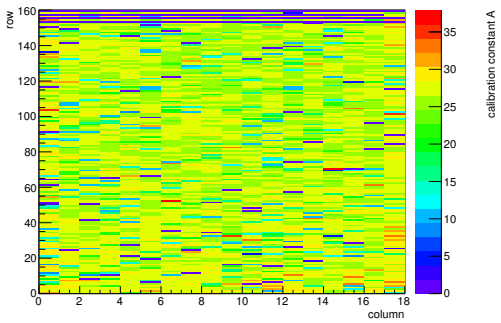

(f) Calibration constant A.

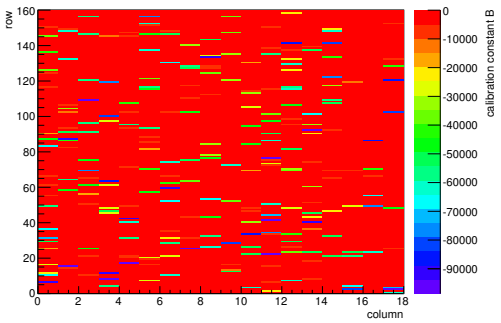

(g) Calibration constant B.

Figure C.23: Detailed plots for test beam measurement of KEK1R (description see section 6.1) sample (running as DUT0) during runs 50586 in the July 2011 test beam period at CERN SPS in area H6B. Summary of the data in chapter 9. *(cont.)*

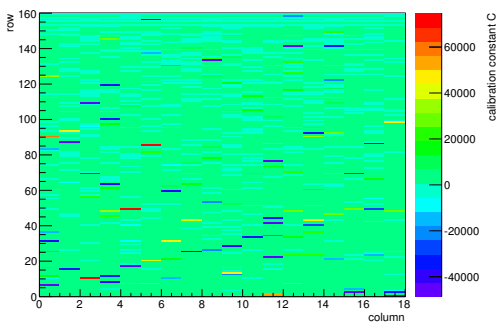

(h) Calibration constant C.

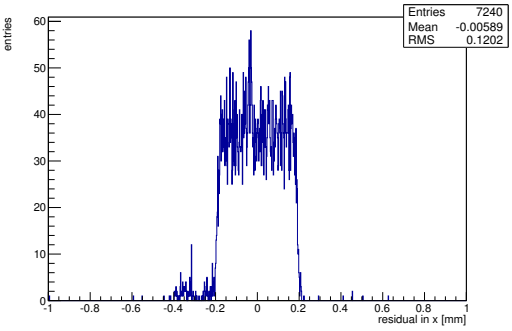

(i) Track residual in x.

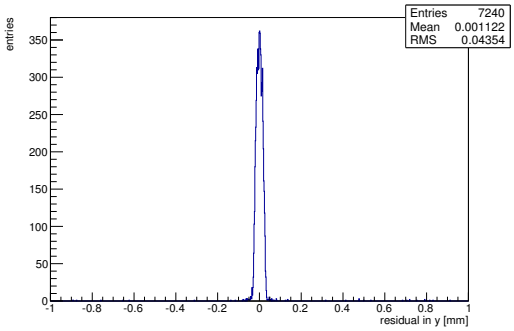

(j) Track residual in y.

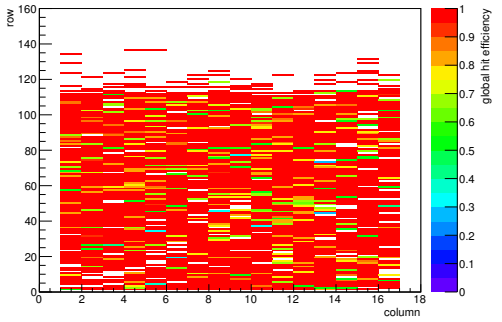

(k) Hit efficiency map.

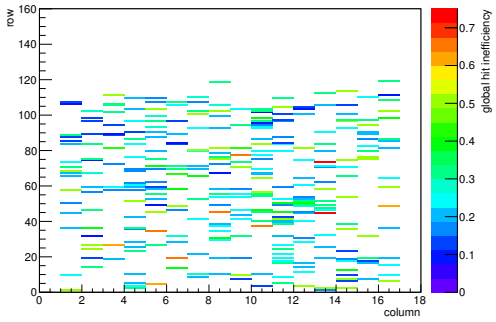

(l) Hit inefficiency map.

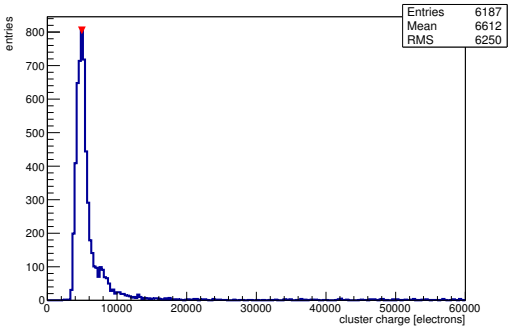

(m) Charge distribution (all cluster sizes included).

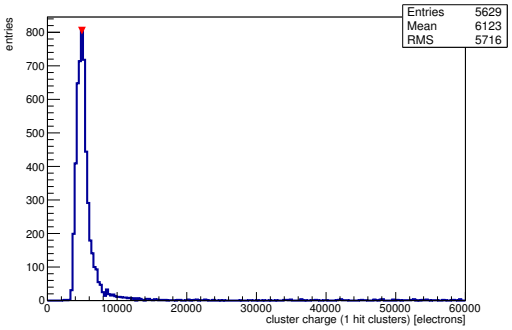

(n) Charge distribution (1 hit cluster).

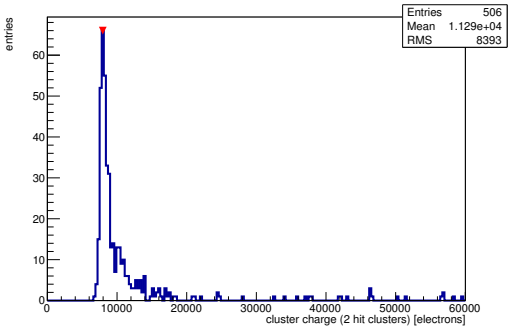

(o) Charge distribution (2 hit cluster).

Figure C.23: Detailed plots for test beam measurement of KEK1R (description see section 6.1) sample (running as DUT0) during runs 50586 in the July 2011 test beam period at CERN SPS in area H6B. Summary of the data in chapter 9. *(cont.)*

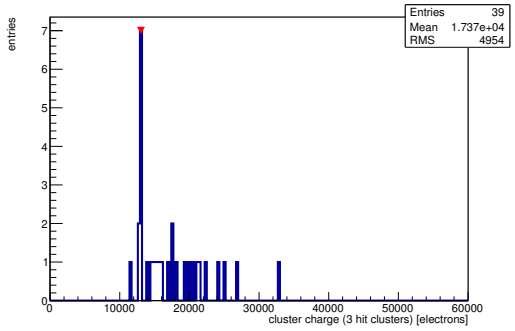

(p) Charge distribution (3 hit cluster).

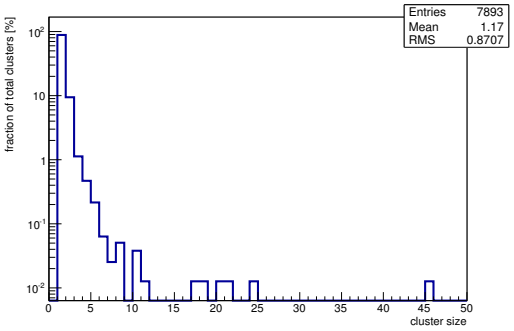

(q) Cluster size distribution.

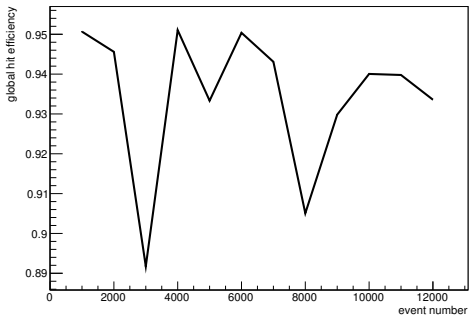

(r) Hit efficiency vs event number.

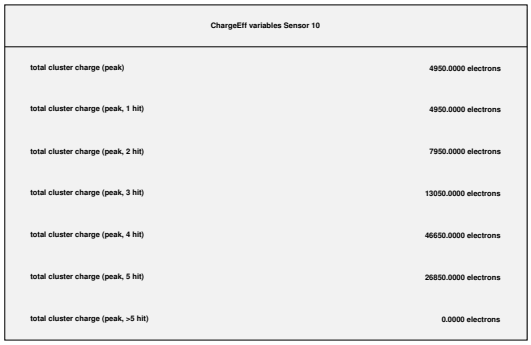

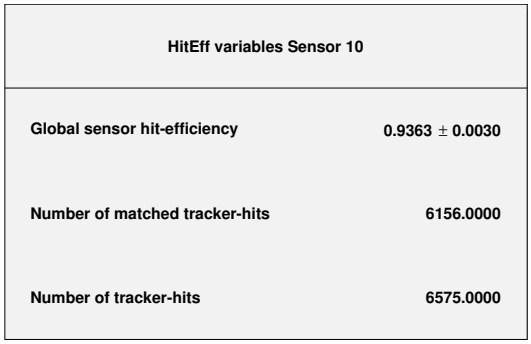

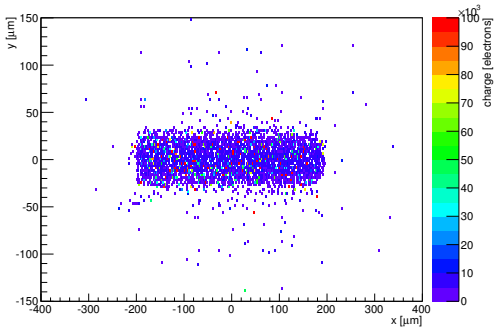

(s) Single pixel mean charge.

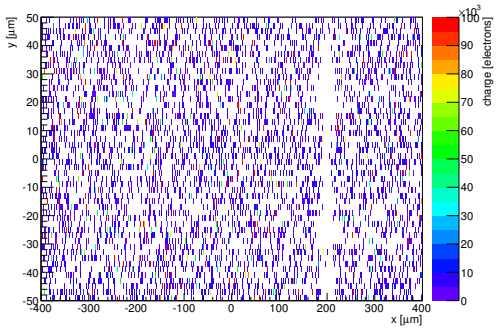

(t) Single pixel mean charge.

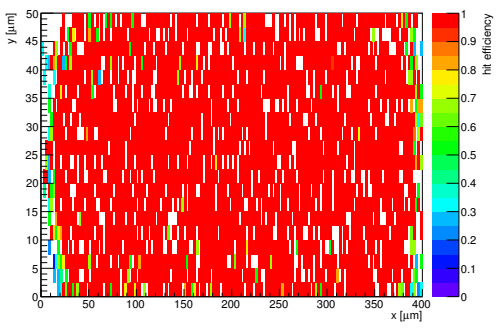

(u) Single pixel hit efficiency.

Figure C.23: Detailed plots for test beam measurement of KEK1R (description see section 6.1) sample (running as DUT0) during runs 50586 in the July 2011 test beam period at CERN SPS in area H6B. Summary of the data in chapter 9.

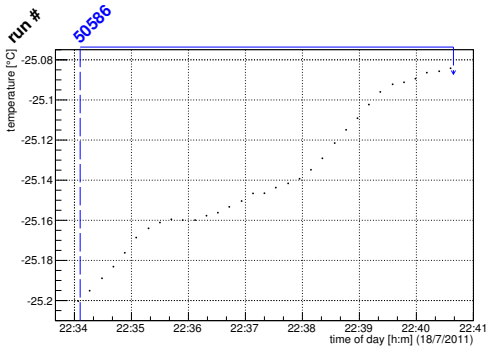

(a) Temperature vs time.

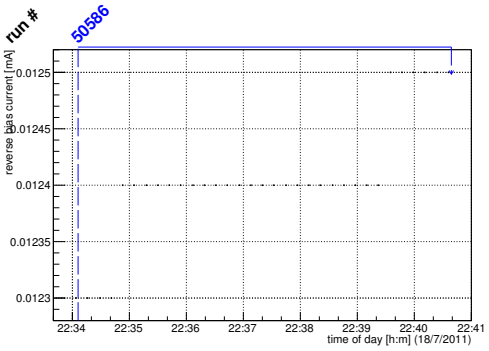

(b) Bias current vs time.

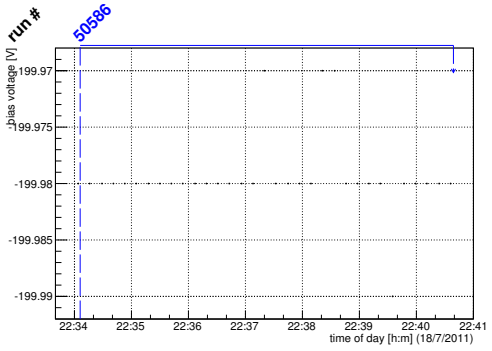

(c) Currently applied bias voltage vs time.

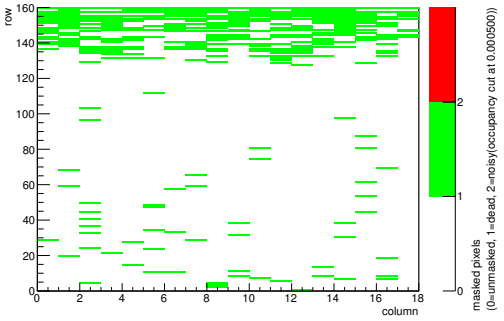

(d) Map of masked pixels.

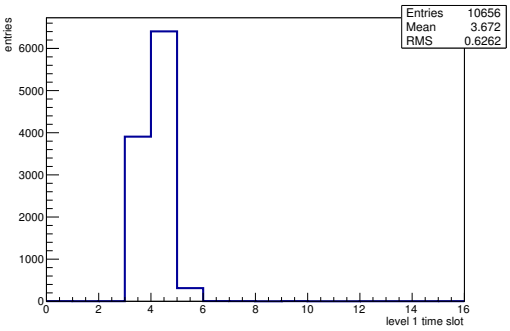

(e) Lvl1 distribution.

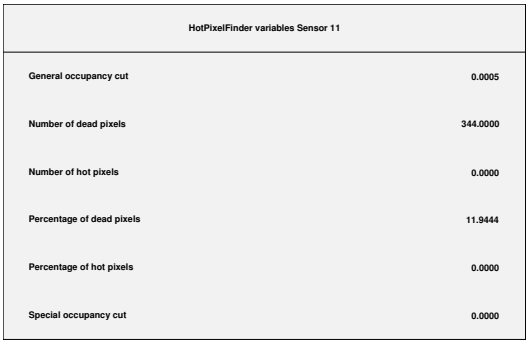

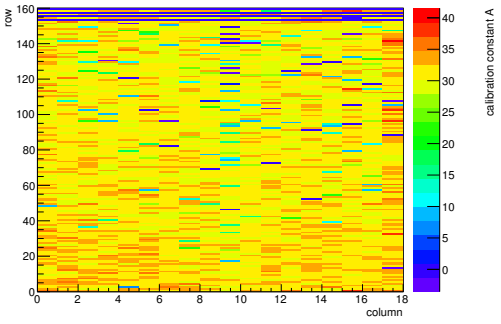

(f) Calibration constant A.

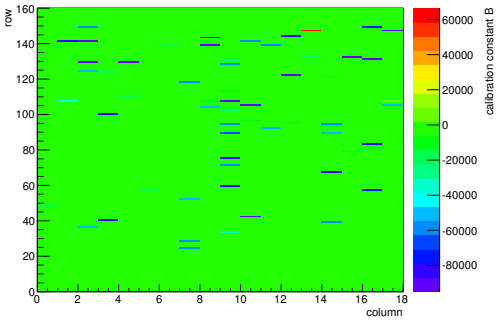

(g) Calibration constant B.

Figure C.24: Detailed plots for test beam measurement of KEK2R (description see section 6.1) sample (running as DUT1) during runs 50586 in the July 2011 test beam period at CERN SPS in area H6B. Summary of the data in chapter 9. *(cont.)*

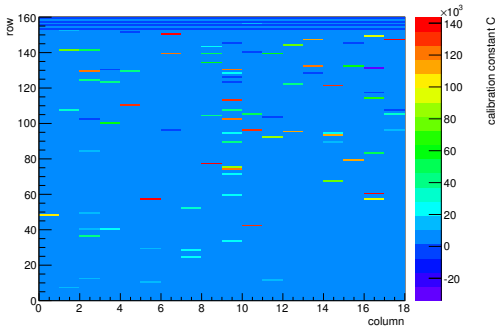

(h) Calibration constant C.

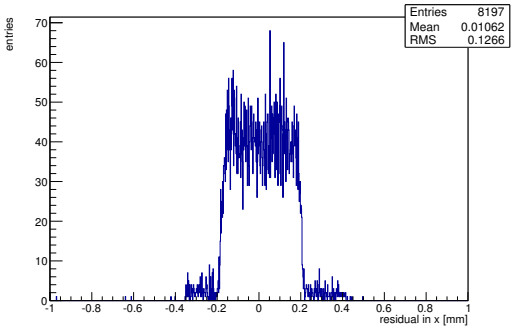

(i) Track residual in x.

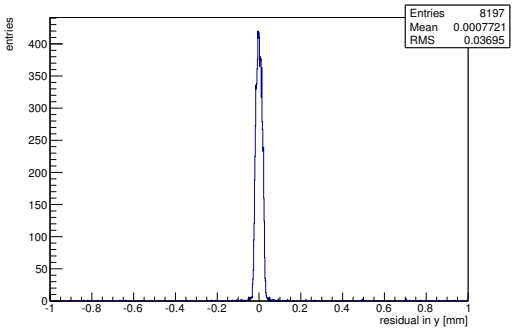

(j) Track residual in y.

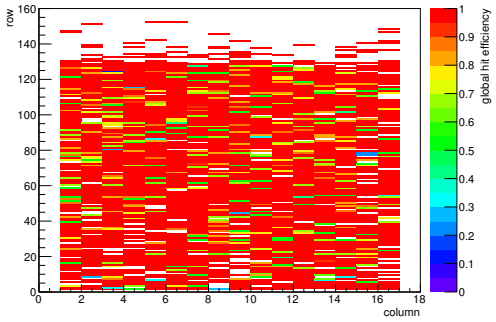

(k) Hit efficiency map.

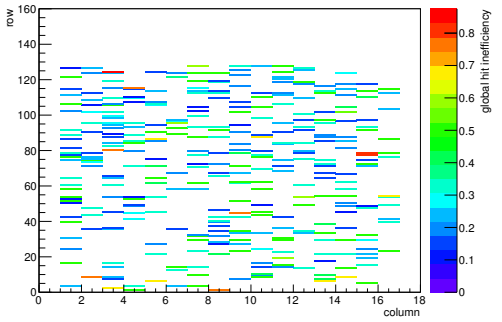

(l) Hit inefficiency map.

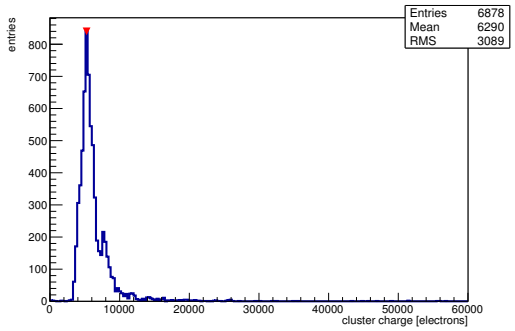

(m) Charge distribution (all cluster sizes included).

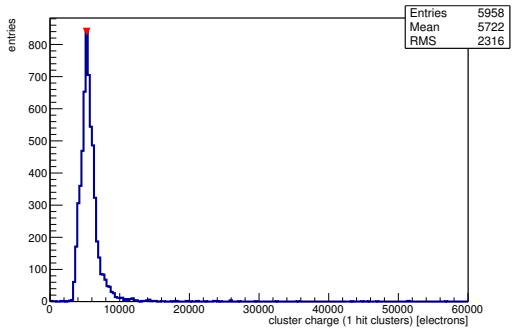

(n) Charge distribution (1 hit cluster).

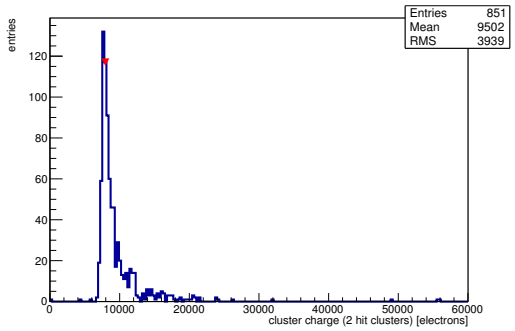

(o) Charge distribution (2 hit cluster).

Figure C.24: Detailed plots for test beam measurement of KEK2R (description see section 6.1) sample (running as DUT1) during runs 50586 in the July 2011 test beam period at CERN SPS in area H6B. Summary of the data in chapter 9. *(cont.)*

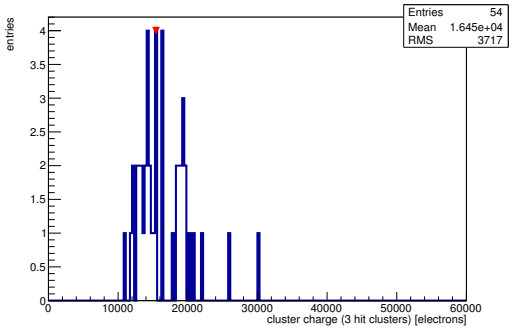

(p) Charge distribution (3 hit cluster).

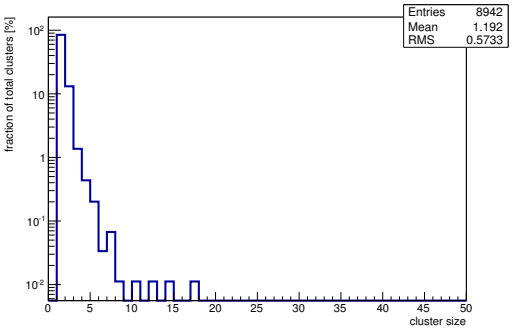

(q) Cluster size distribution.

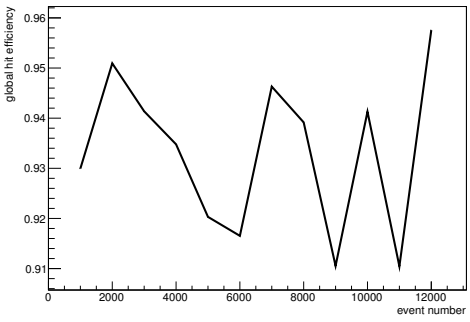

(r) Hit efficiency vs event number.

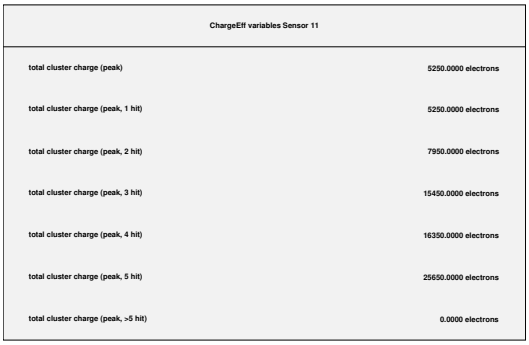

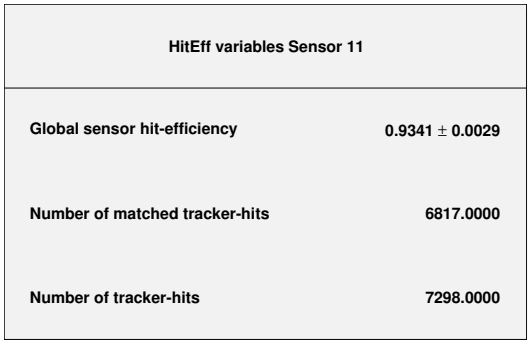

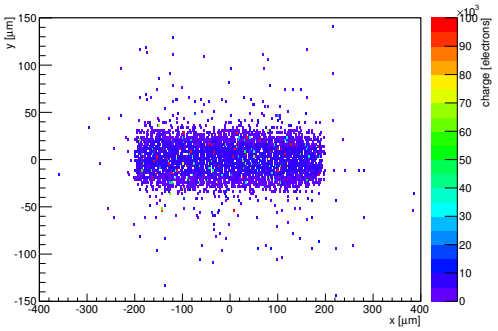

(s) Single pixel mean charge.

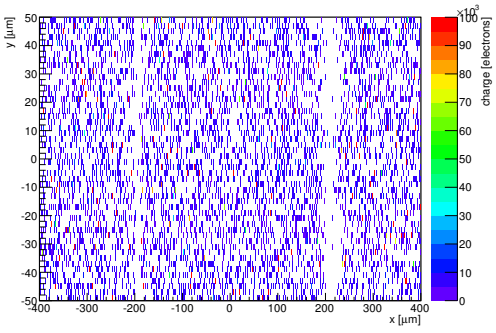

(t) Single pixel mean charge.

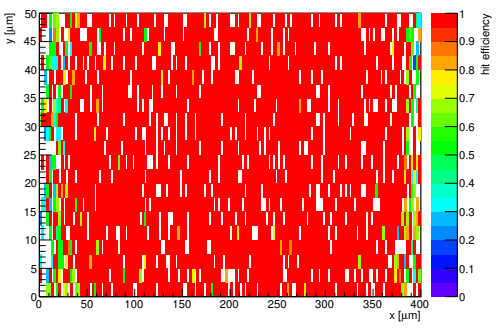

(u) Single pixel hit efficiency.

Figure C.24: Detailed plots for test beam measurement of KEK2R (description see section 6.1) sample (running as DUT1) during runs 50586 in the July 2011 test beam period at CERN SPS in area H6B. Summary of the data in chapter 9.

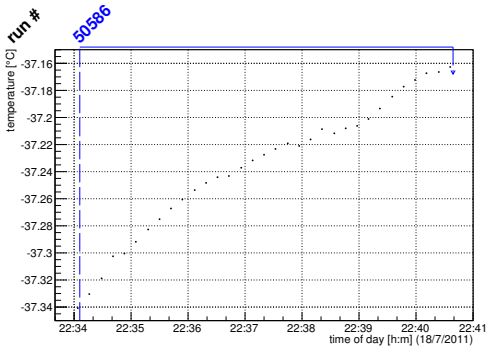

(a) Temperature vs time.

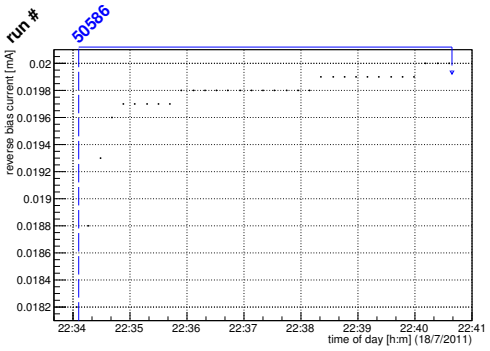

(b) Bias current vs time.

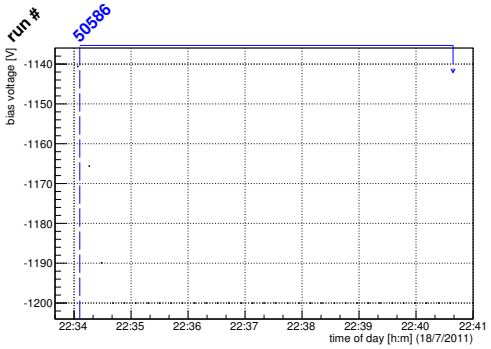

(c) Currently applied bias voltage vs time.

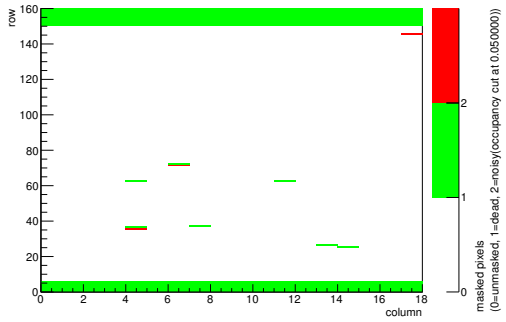

(d) Map of masked pixels.

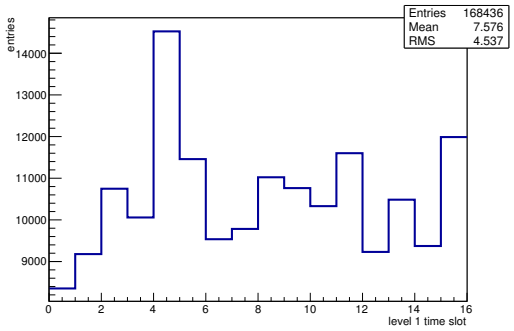

(e) Lvl1 distribution.

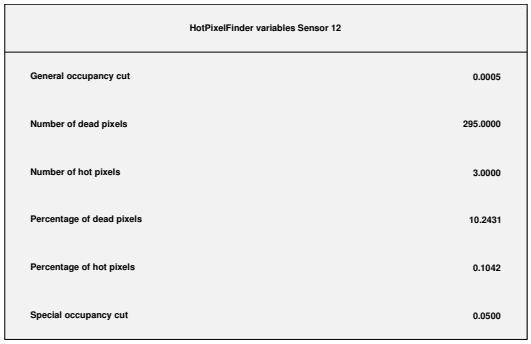

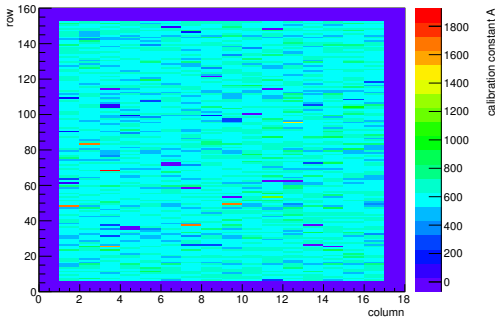

(f) Calibration constant A.

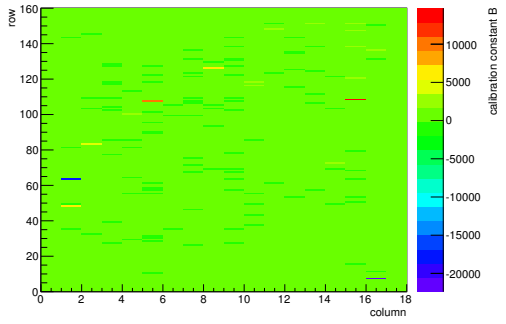

(g) Calibration constant B.

Figure C.25: Detailed plots for test beam measurement of DO-I-11 (description see section 6.1) sample (running as DUT2) during runs 50586 in the July 2011 test beam period at CERN SPS in area H6B. Summary of the data in chapter 9. *(cont.)*

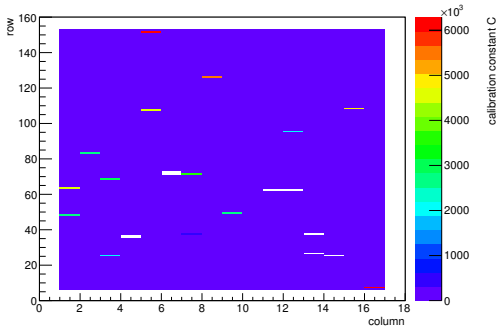

(h) Calibration constant C.

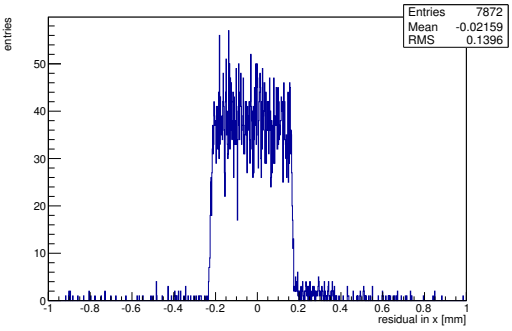

(i) Track residual in x.

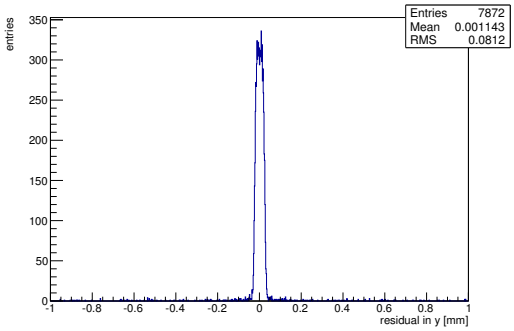

(j) Track residual in y.

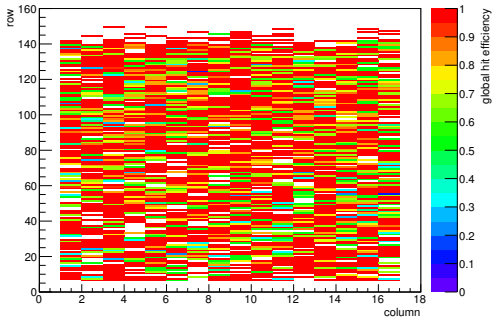

(k) Hit efficiency map.

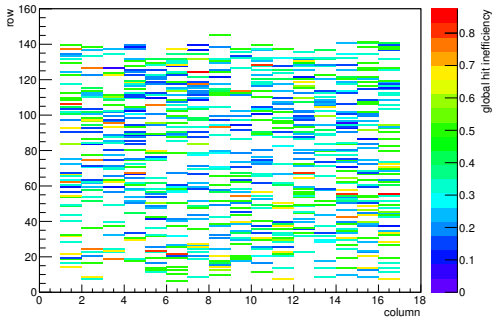

(l) Hit inefficiency map.

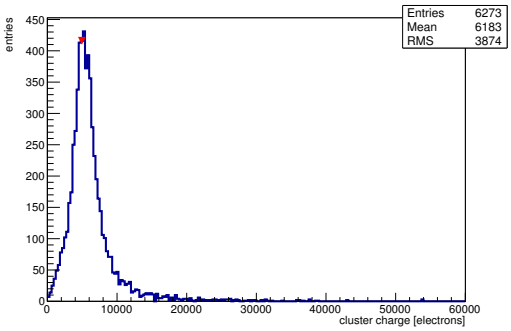

(m) Charge distribution (all cluster sizes included).

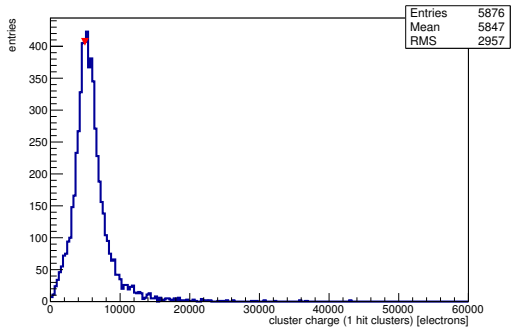

(n) Charge distribution (1 hit cluster).

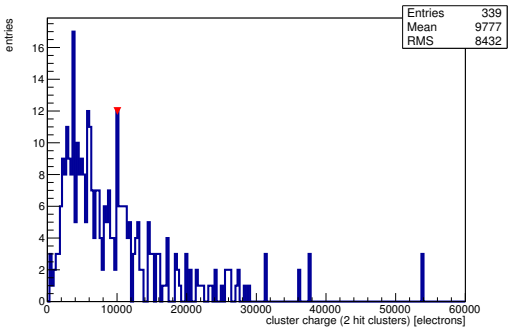

(o) Charge distribution (2 hit cluster).

Figure C.25: Detailed plots for test beam measurement of DO-I-11 (description see section 6.1) sample (running as DUT2) during runs 50586 in the July 2011 test beam period at CERN SPS in area H6B. Summary of the data in chapter 9. *(cont.)*

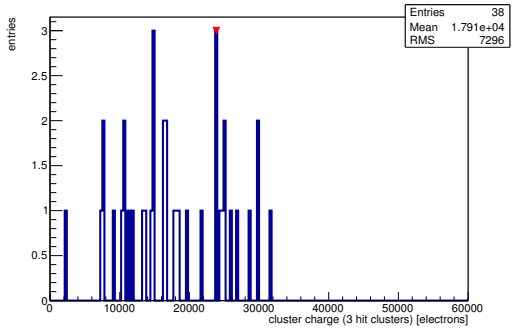

(p) Charge distribution (3 hit cluster).

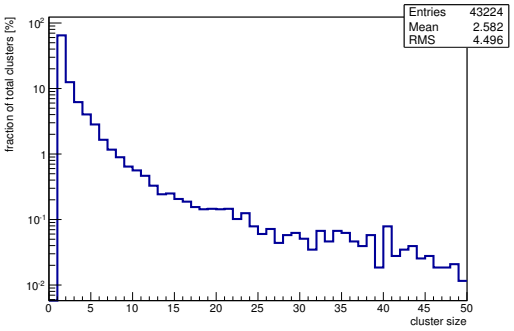

(q) Cluster size distribution.

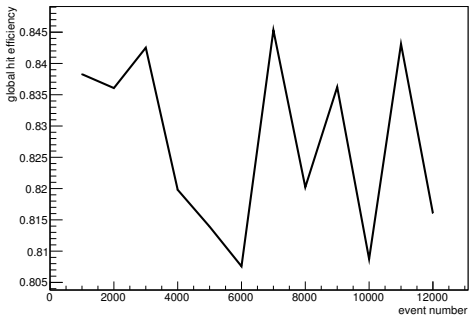

(r) Hit efficiency vs event number.

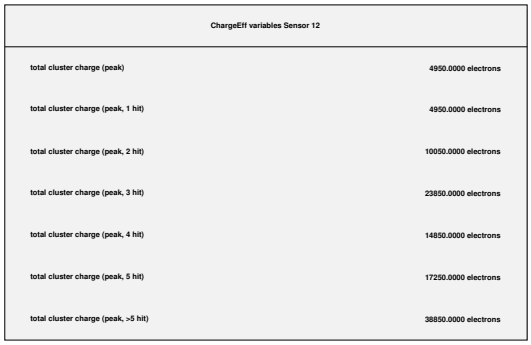

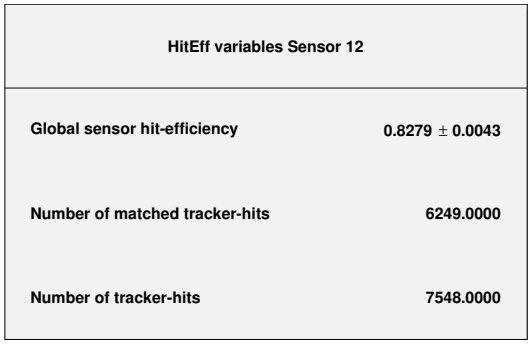

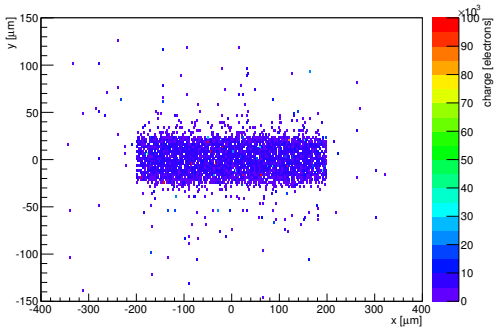

(s) Single pixel mean charge.

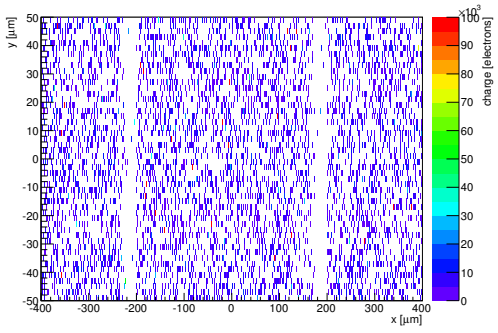

(t) Single pixel mean charge.

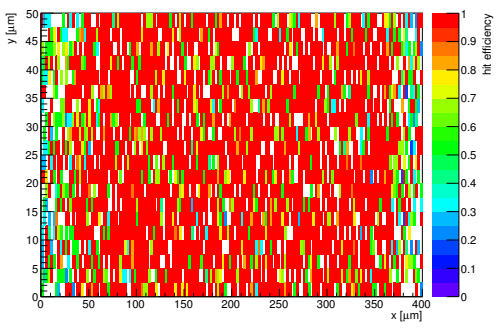

(u) Single pixel hit efficiency.

Figure C.25: Detailed plots for test beam measurement of DO-I-11 (description see section 6.1) sample (running as DUT2) during runs 50586 in the July 2011 test beam period at CERN SPS in area H6B. Summary of the data in chapter 9.

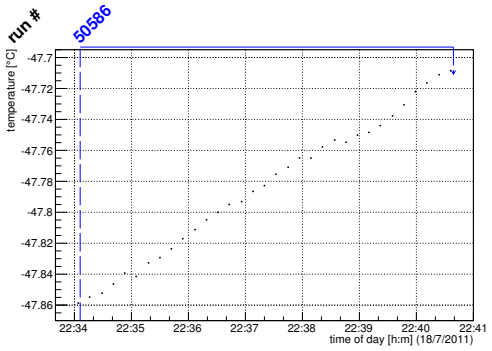

(a) Temperature vs time.

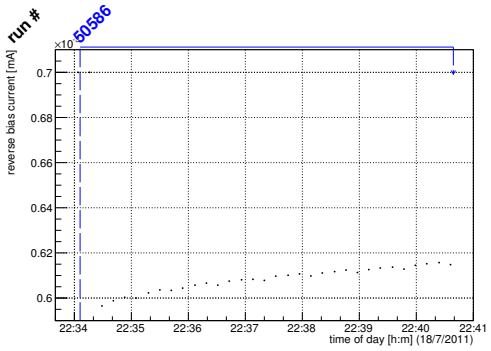

(b) Bias current vs time.

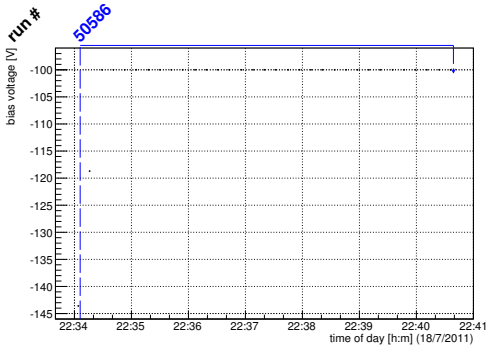

(c) Currently applied bias voltage vs time.

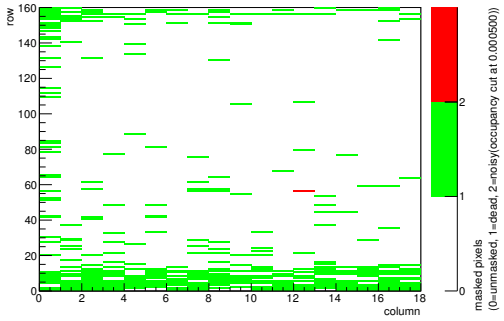

(d) Map of masked pixels.

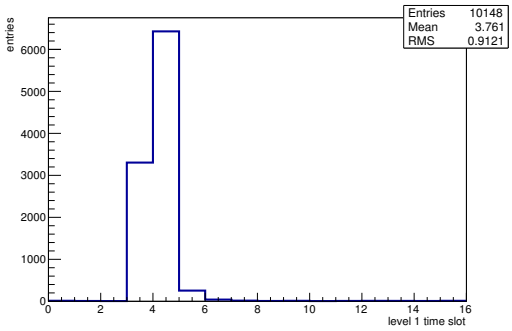

(e) Lvl1 distribution.

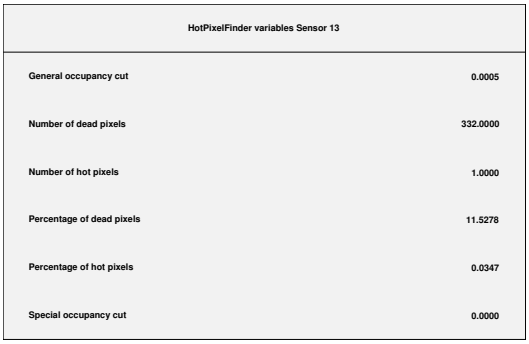

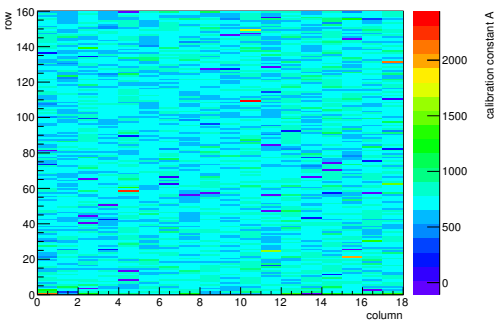

(f) Calibration constant A.

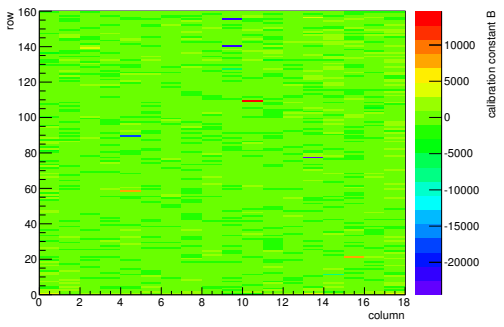

(g) Calibration constant B.

Figure C.26: Detailed plots for test beam measurement of DO-I-13 (description see section 6.1) sample (running as DUT3) during runs 50586 in the July 2011 test beam period at CERN SPS in area H6B. Summary of the data in chapter 9. *(cont.)*

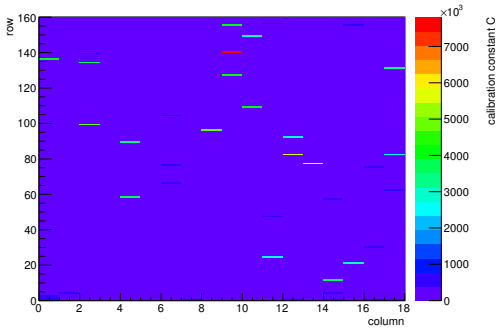

(h) Calibration constant C.

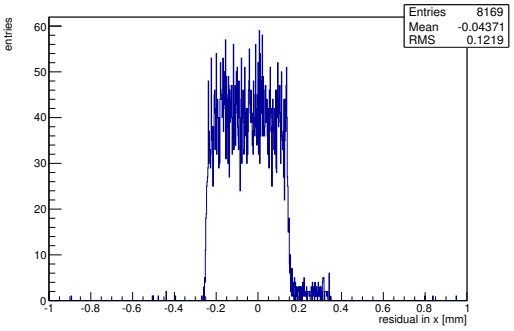

(i) Track residual in x.

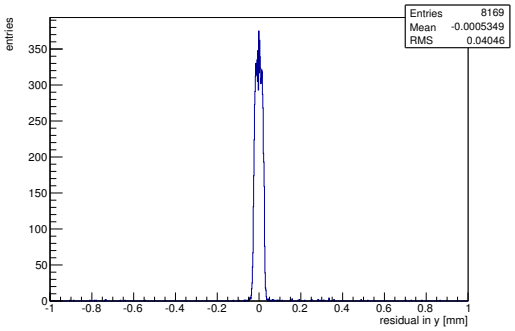

(j) Track residual in y.

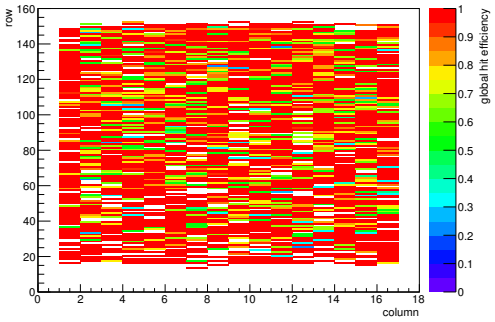

(k) Hit efficiency map.

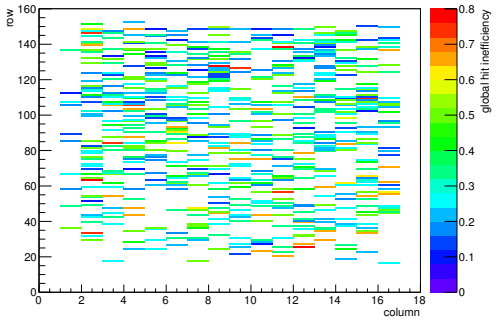

(l) Hit inefficiency map.

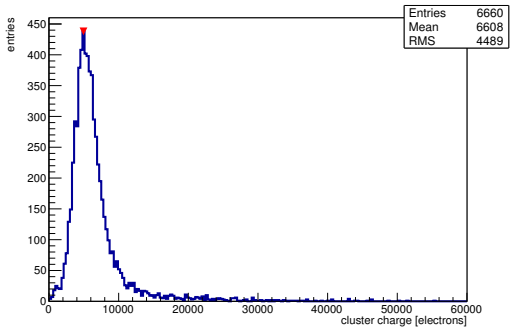

(m) Charge distribution (all cluster sizes included).

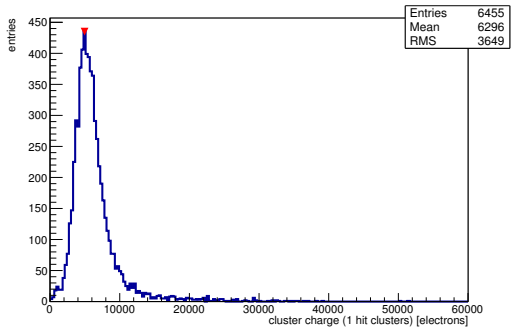

(n) Charge distribution (1 hit cluster).

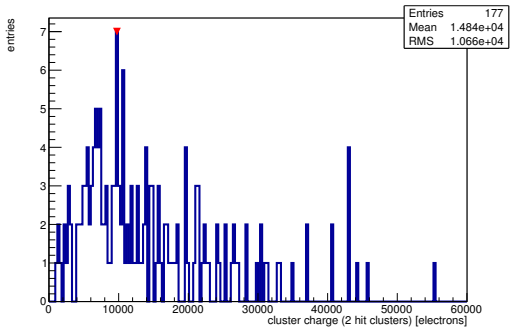

(o) Charge distribution (2 hit cluster).

Figure C.26: Detailed plots for test beam measurement of DO-I-13 (description see section 6.1) sample (running as DUT3) during runs 50586 in the July 2011 test beam period at CERN SPS in area H6B. Summary of the data in chapter 9. *(cont.)*

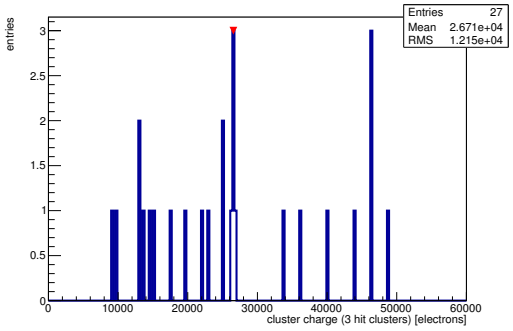

(p) Charge distribution (3 hit cluster).

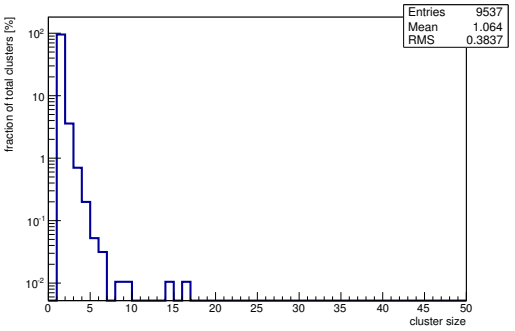

(q) Cluster size distribution.

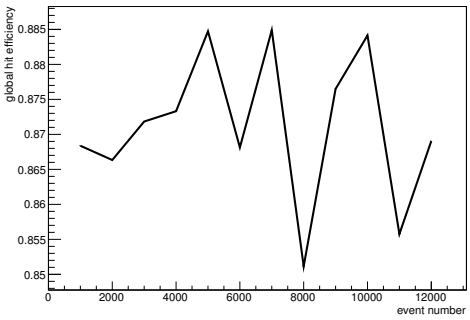

(r) Hit efficiency vs event number.

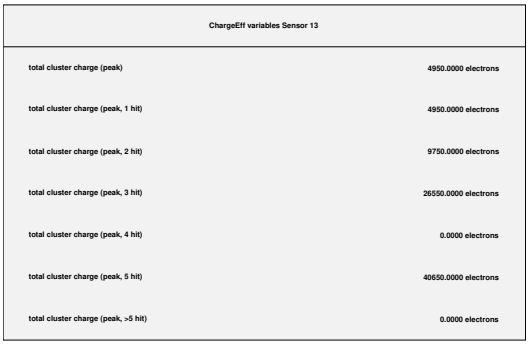

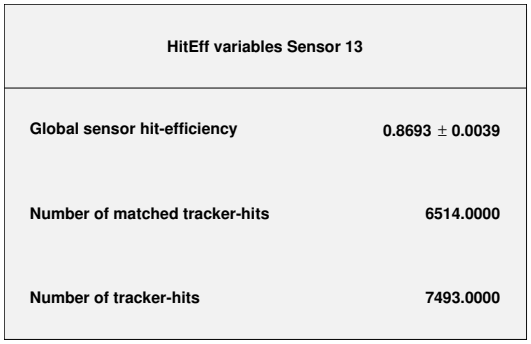

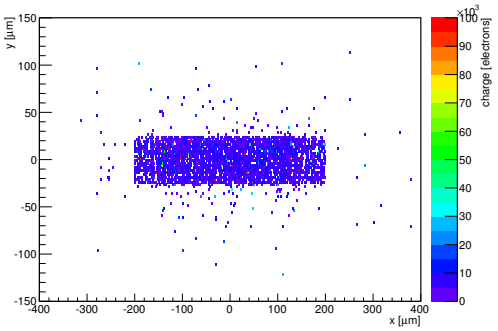

(s) Single pixel mean charge.

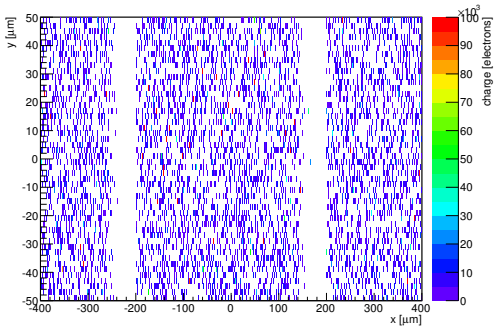

(t) Single pixel mean charge.

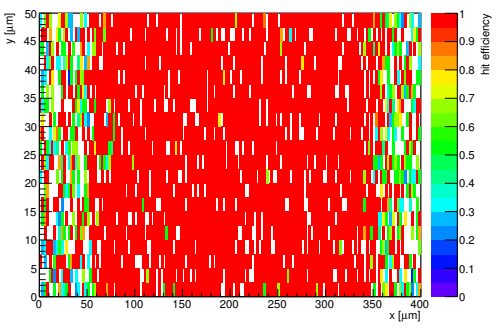

(u) Single pixel hit efficiency.

Figure C.26: Detailed plots for test beam measurement of DO-I-13 (description see section 6.1) sample (running as DUT3) during runs 50586 in the July 2011 test beam period at CERN SPS in area H6B. Summary of the data in chapter 9.

C.2.5 Run 50587

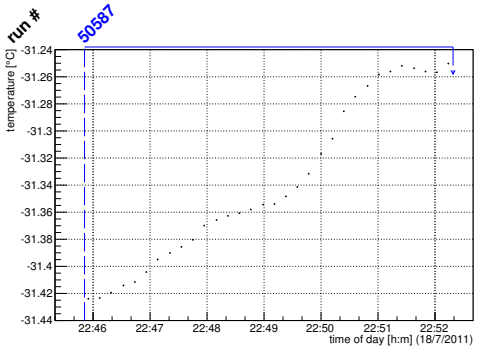

(a) Temperature vs time.

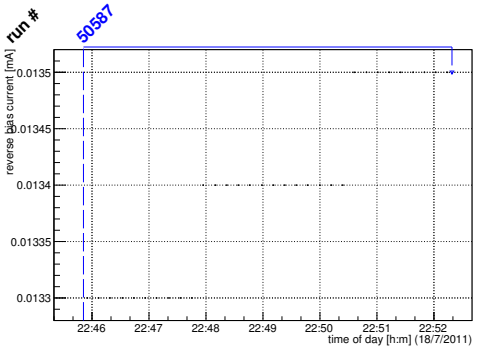

(b) Bias current vs time.

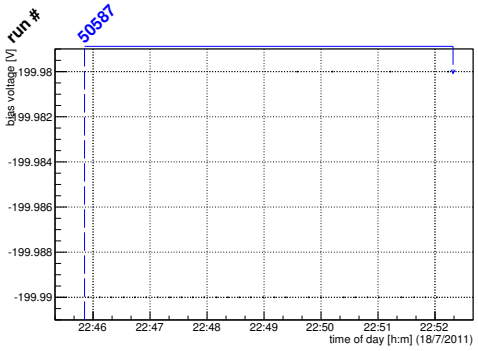

(c) Currently applied bias voltage vs time.

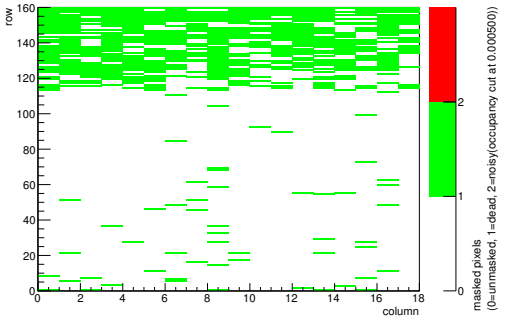

(d) Map of masked pixels.

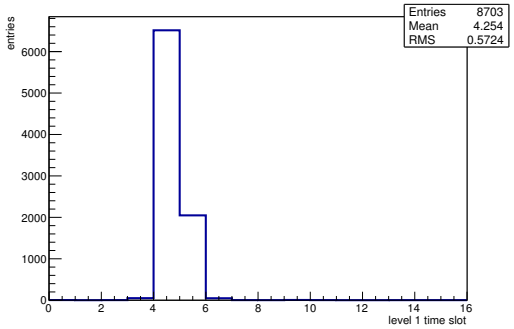

(e) Lvl1 distribution.

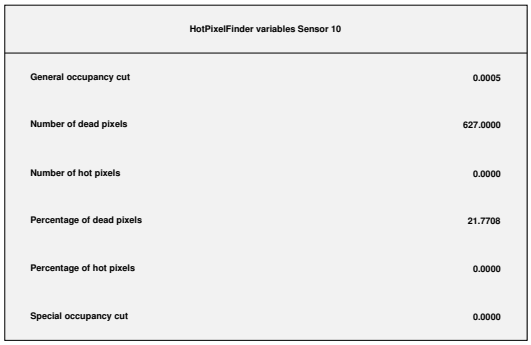

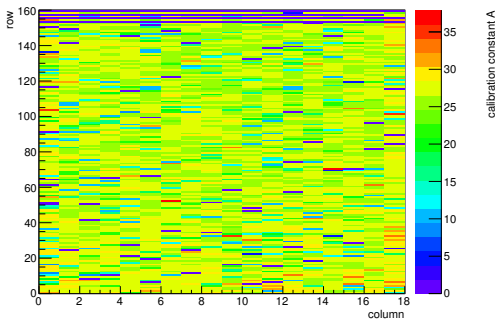

(f) Calibration constant A.

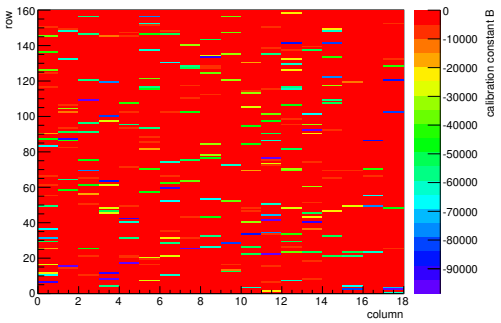

(g) Calibration constant B.

Figure C.27: Detailed plots for test beam measurement of KEK1R (description see section 6.1) sample (running as DUT0) during runs 50587 in the July 2011 test beam period at CERN SPS in area H6B. Summary of the data in chapter 9. *(cont.)*

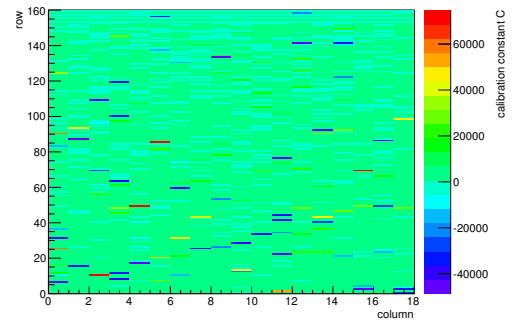

(h) Calibration constant C.

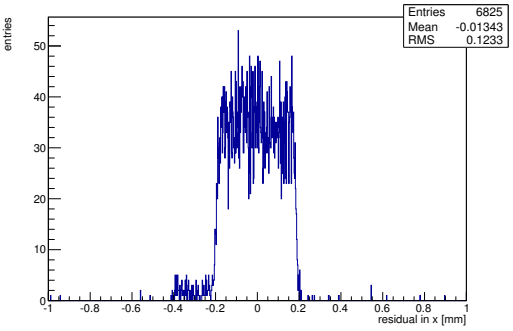

(i) Track residual in x.

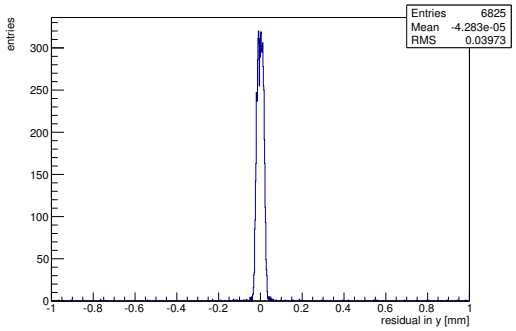

(j) Track residual in y.

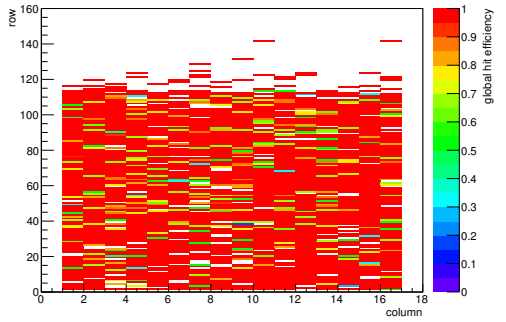

(k) Hit efficiency map.

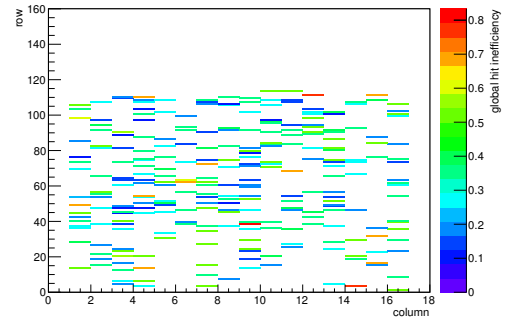

(l) Hit inefficiency map.

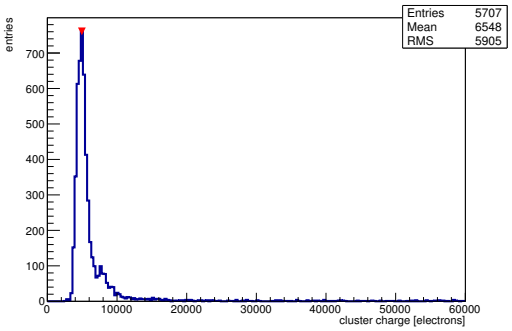

(m) Charge distribution (all cluster sizes included).

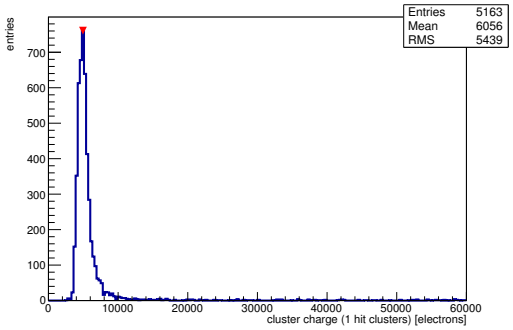

(n) Charge distribution (1 hit cluster).

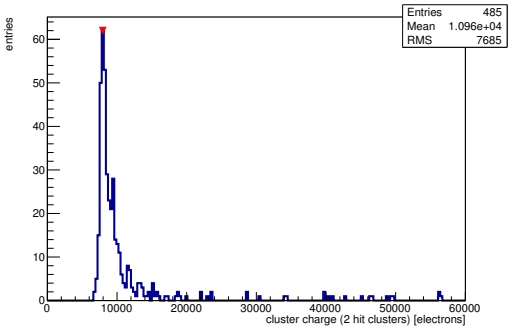

(o) Charge distribution (2 hit cluster).

Figure C.27: Detailed plots for test beam measurement of KEK1R (description see section 6.1) sample (running as DUT0) during runs 50587 in the July 2011 test beam period at CERN SPS in area H6B. Summary of the data in chapter 9. *(cont.)*

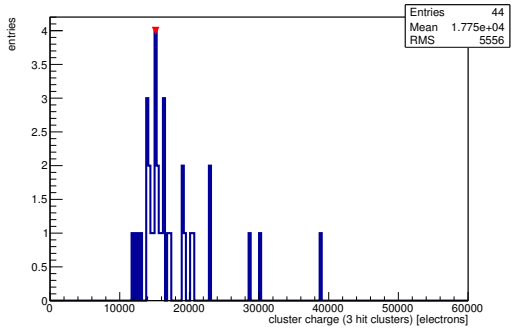

(p) Charge distribution (3 hit cluster).

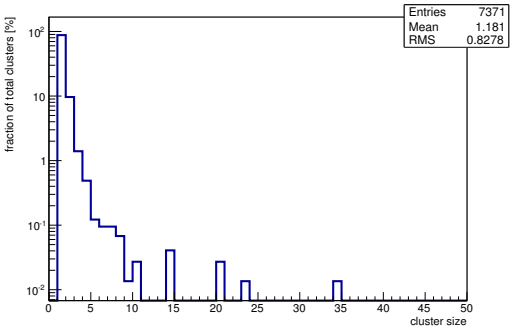

(q) Cluster size distribution.

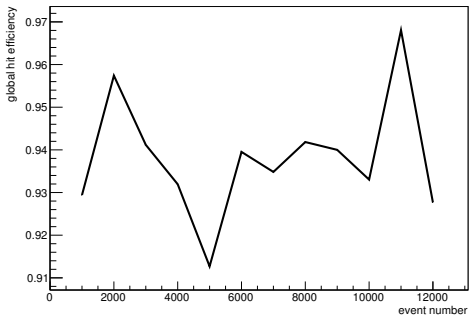

(r) Hit efficiency vs event number.

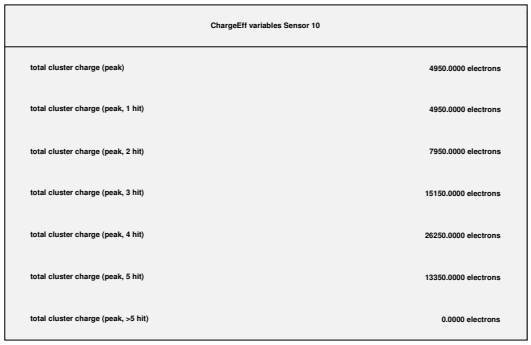

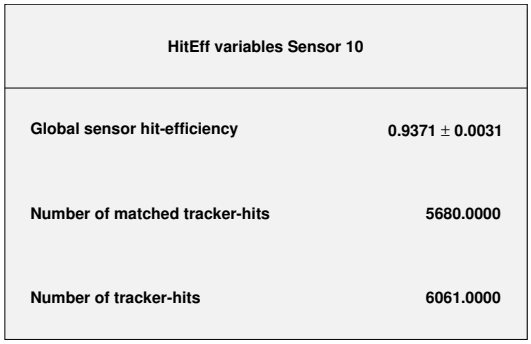

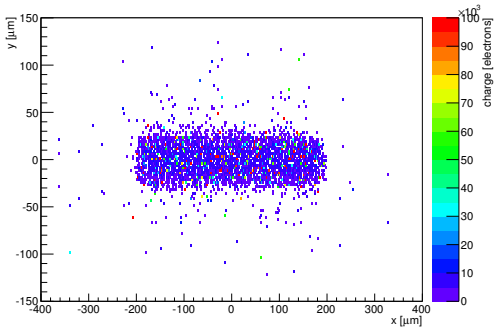

(s) Single pixel mean charge.

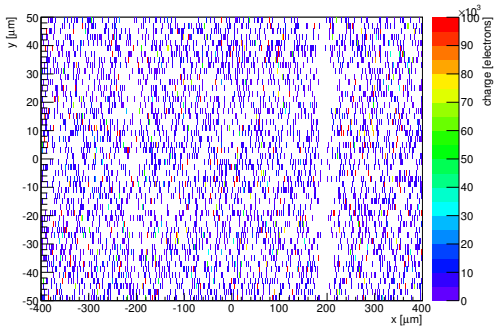

(t) Single pixel mean charge.

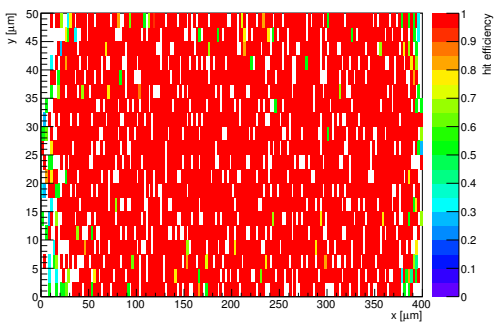

(u) Single pixel hit efficiency.

Figure C.27: Detailed plots for test beam measurement of KEK1R (description see section 6.1) sample (running as DUT0) during runs 50587 in the July 2011 test beam period at CERN SPS in area H6B. Summary of the data in chapter 9.

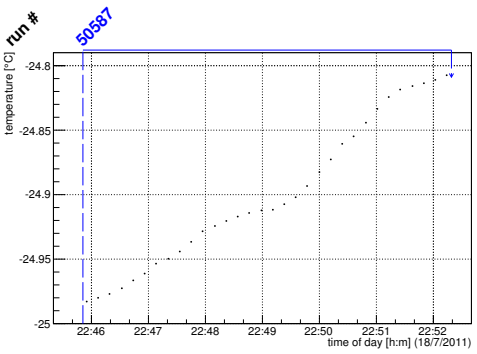

(a) Temperature vs time.

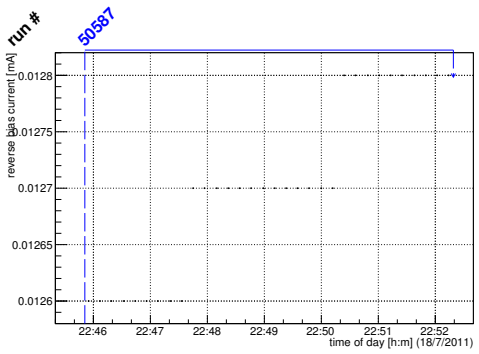

(b) Bias current vs time.

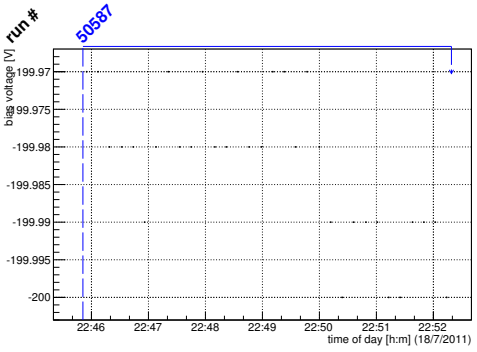

(c) Currently applied bias voltage vs time.

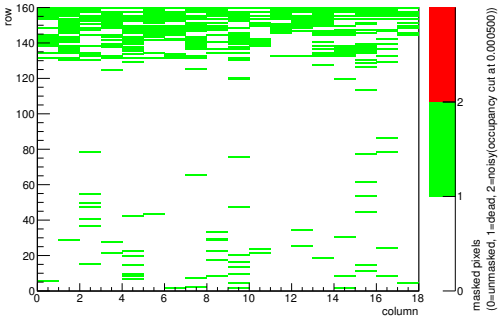

(d) Map of masked pixels.

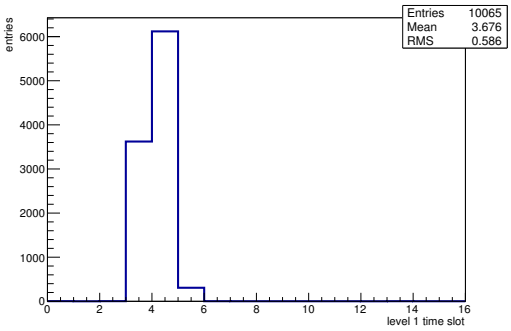

(e) Lvl1 distribution.

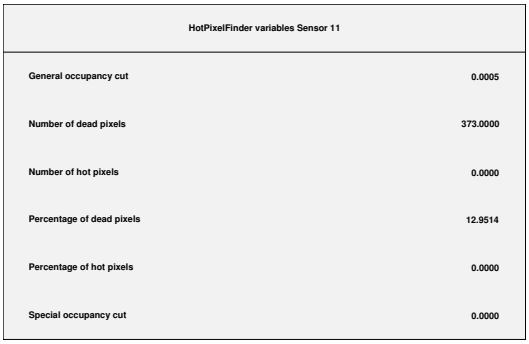

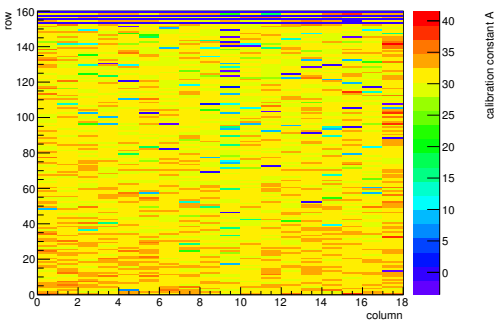

(f) Calibration constant A.

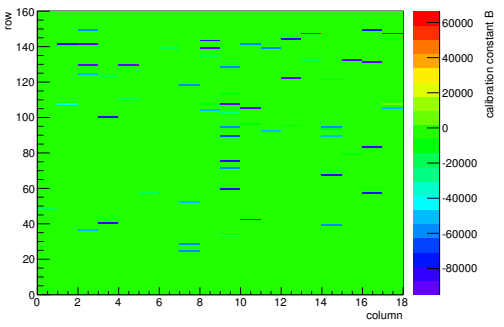

(g) Calibration constant B.

Figure C.28: Detailed plots for test beam measurement of KEK2R (description see section 6.1) sample (running as DUT1) during runs 50587 in the July 2011 test beam period at CERN SPS in area H6B. Summary of the data in chapter 9. *(cont.)*

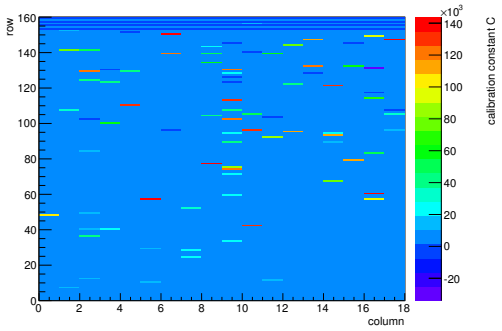

(h) Calibration constant C.

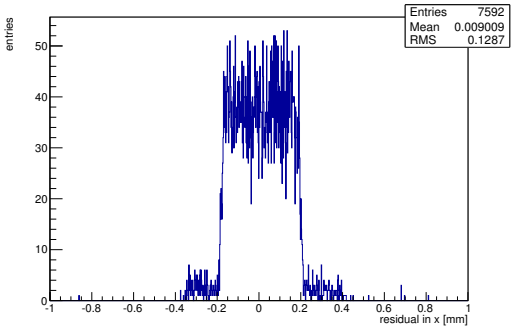

(i) Track residual in x.

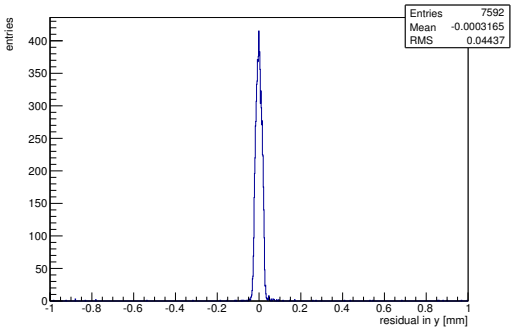

(j) Track residual in y.

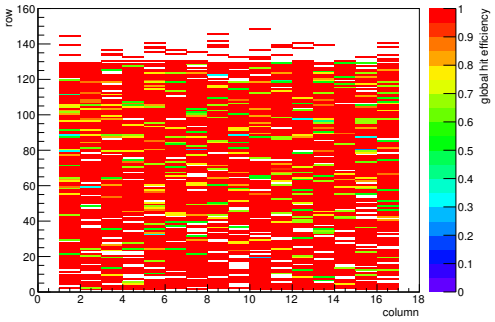

(k) Hit efficiency map.

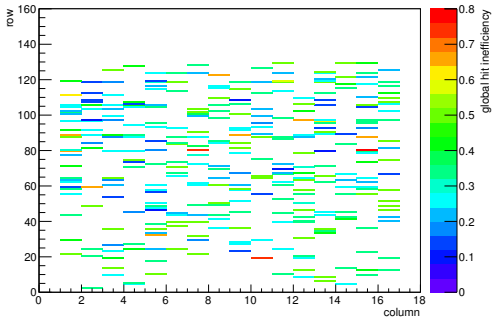

(l) Hit inefficiency map.

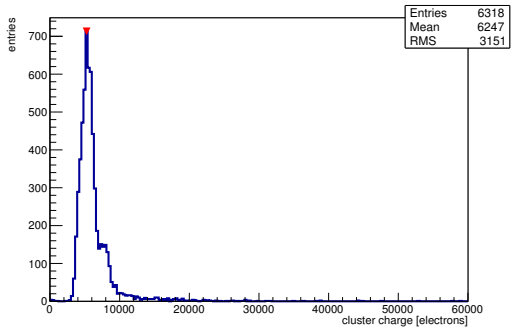

(m) Charge distribution (all cluster sizes included).

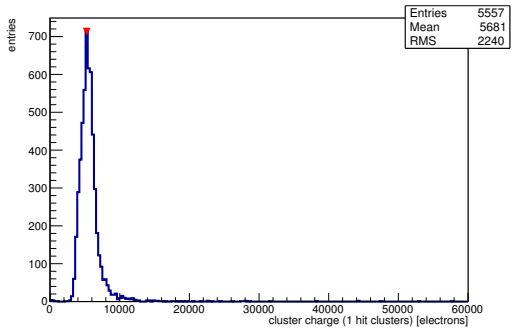

(n) Charge distribution (1 hit cluster).

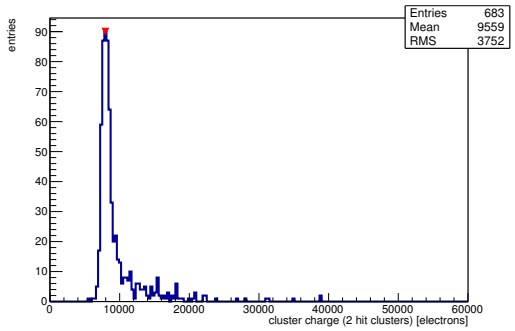

(o) Charge distribution (2 hit cluster).

Figure C.28: Detailed plots for test beam measurement of KEK2R (description see section 6.1) sample (running as DUT1) during runs 50587 in the July 2011 test beam period at CERN SPS in area H6B. Summary of the data in chapter 9. *(cont.)*

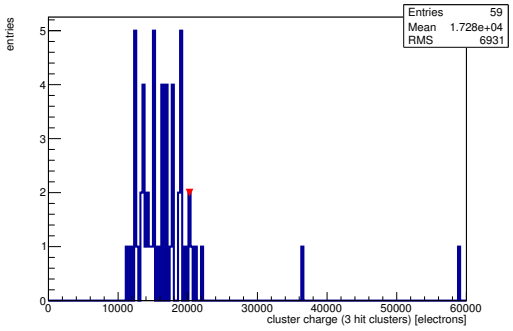

(p) Charge distribution (3 hit cluster).

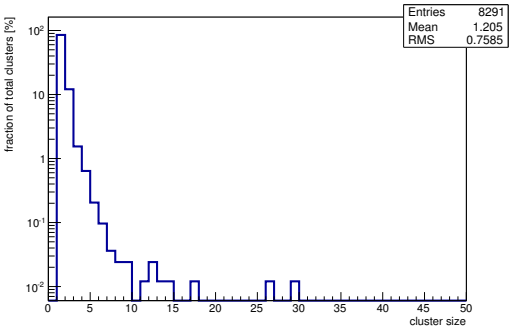

(q) Cluster size distribution.

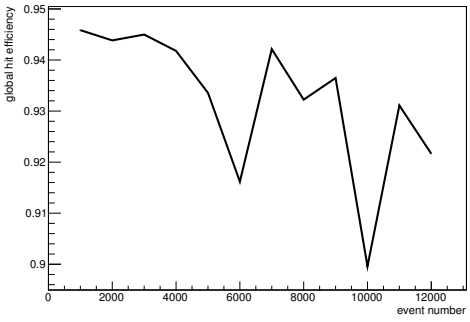

(r) Hit efficiency vs event number.

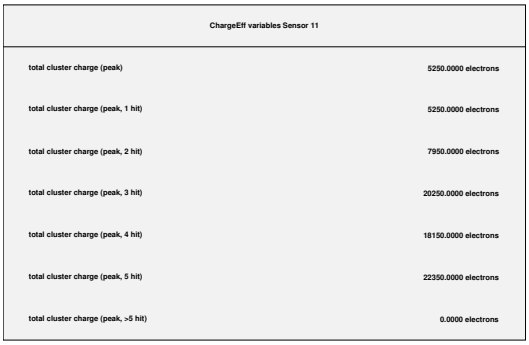

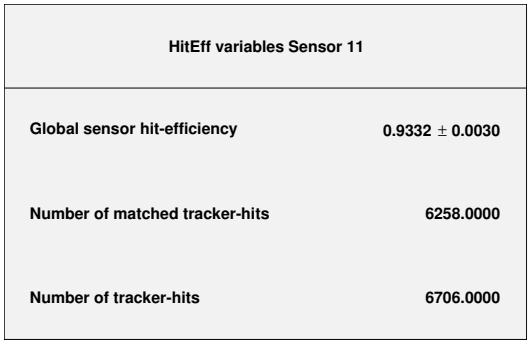

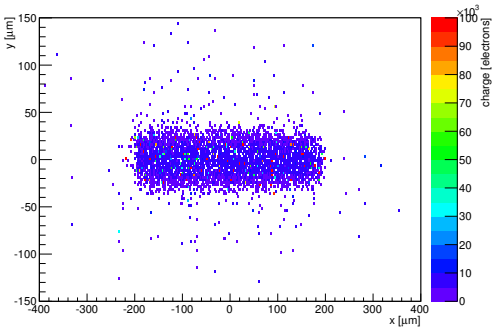

(s) Single pixel mean charge.

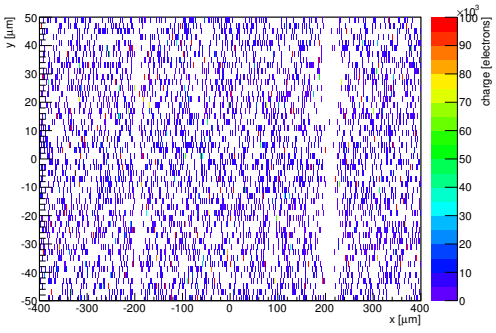

(t) Single pixel mean charge.

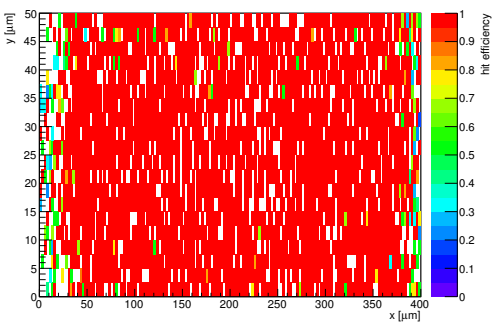

(u) Single pixel hit efficiency.

Figure C.28: Detailed plots for test beam measurement of KEK2R (description see section 6.1) sample (running as DUT1) during runs 50587 in the July 2011 test beam period at CERN SPS in area H6B. Summary of the data in chapter 9.

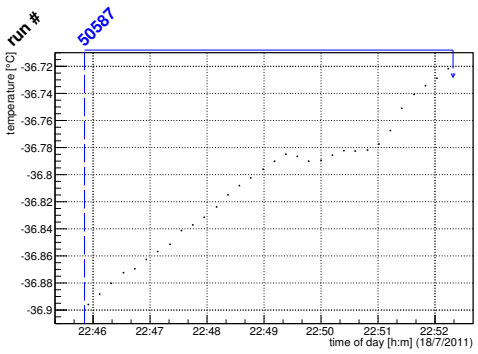

(a) Temperature vs time.

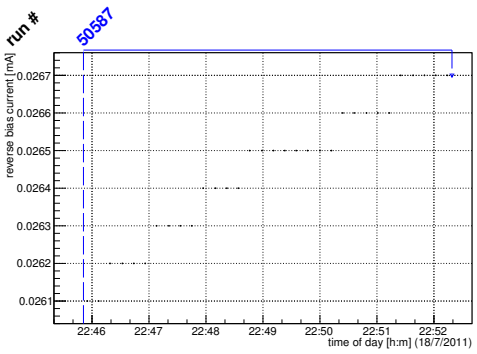

(b) Bias current vs time.

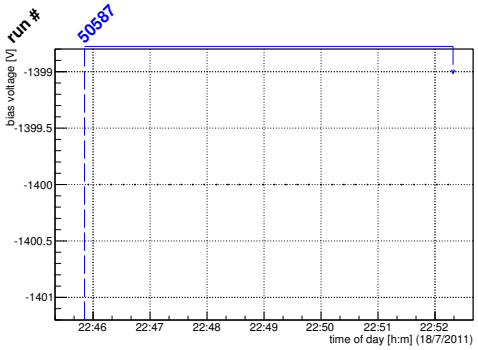

(c) Currently applied bias voltage vs time.

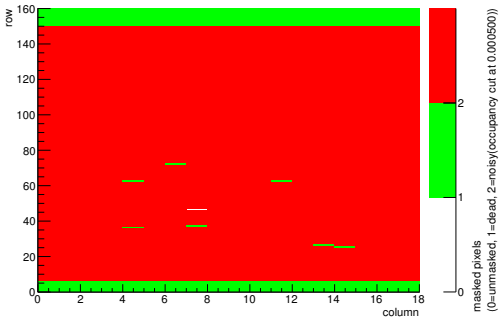

(d) Map of masked pixels.

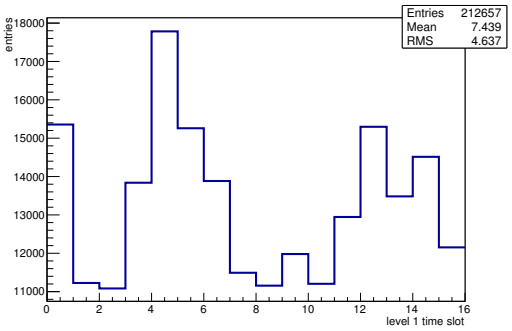

(e) Lvl1 distribution.

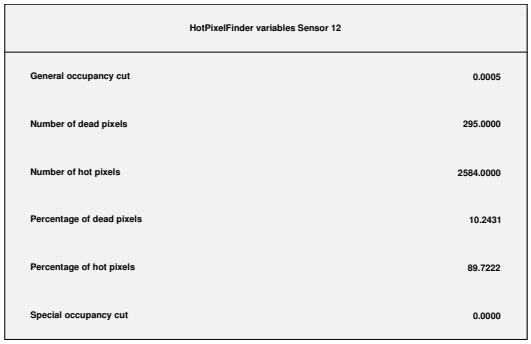

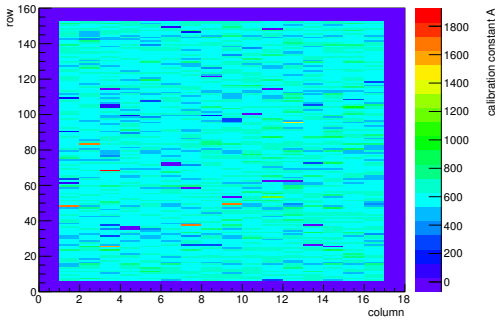

(f) Calibration constant A.

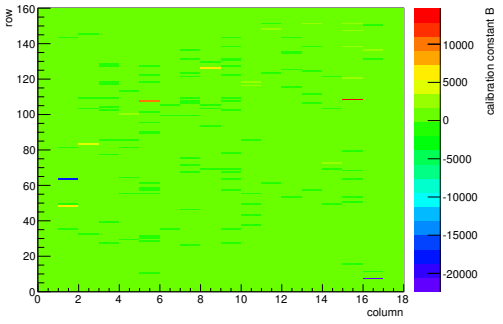

(g) Calibration constant B.

Figure C.29: Detailed plots for test beam measurement of DO-I-11 (description see section 6.1) sample (running as DUT2) during runs 50587 in the July 2011 test beam period at CERN SPS in area H6B. Summary of the data in chapter 9. *(cont.)*

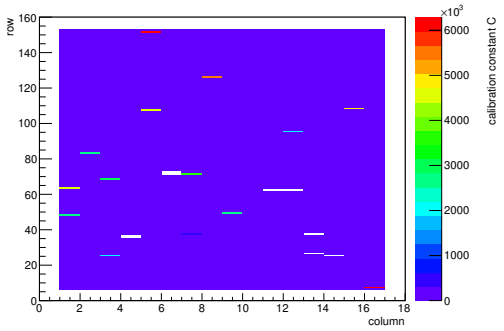

(h) Calibration constant C.

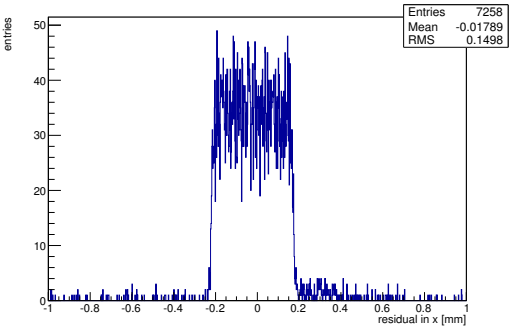

(i) Track residual in x.

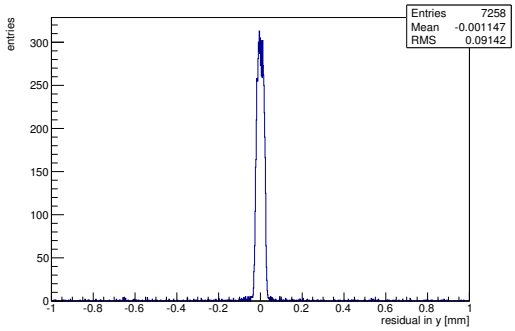

(j) Track residual in y.

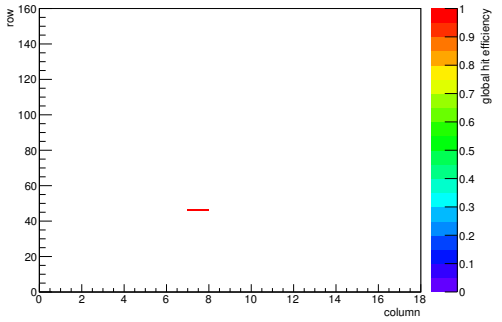

(k) Hit efficiency map.

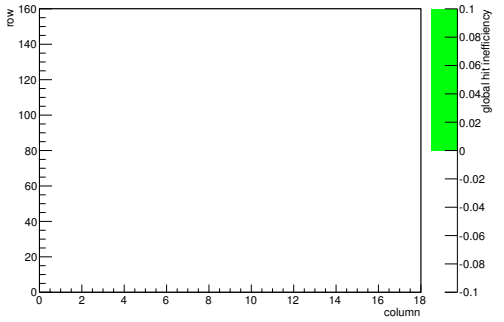

(l) Hit inefficiency map.

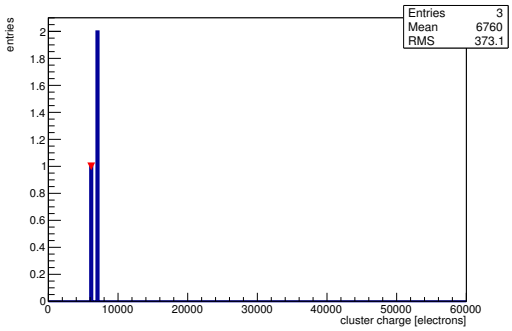

(m) Charge distribution (all cluster sizes included).

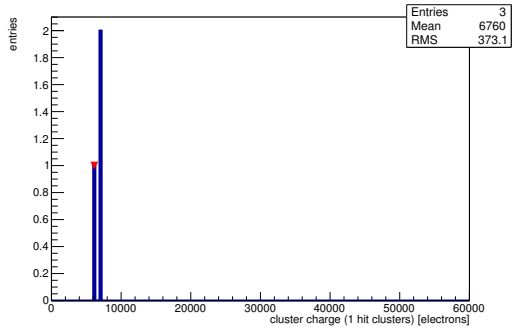

(n) Charge distribution (1 hit cluster).

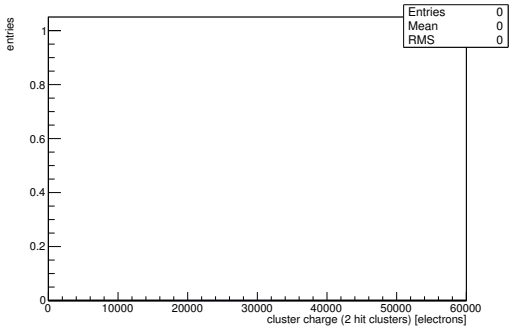

(o) Charge distribution (2 hit cluster).

Figure C.29: Detailed plots for test beam measurement of DO-I-11 (description see section 6.1) sample (running as DUT2) during runs 50587 in the July 2011 test beam period at CERN SPS in area H6B. Summary of the data in chapter 9. *(cont.)*

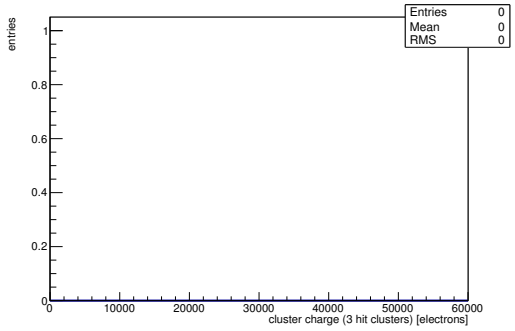

(p) Charge distribution (3 hit cluster).

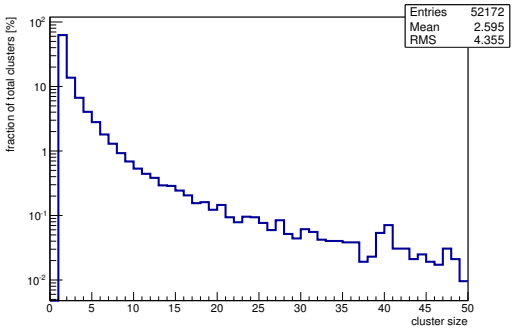

(q) Cluster size distribution.

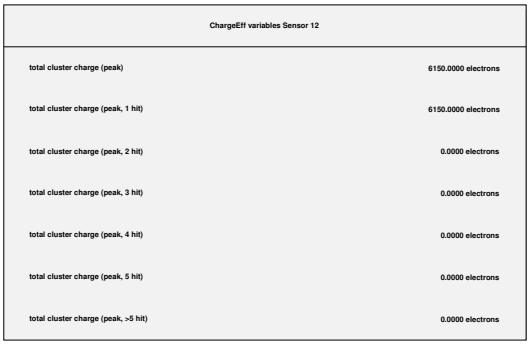

(r) Hit efficiency vs event number.

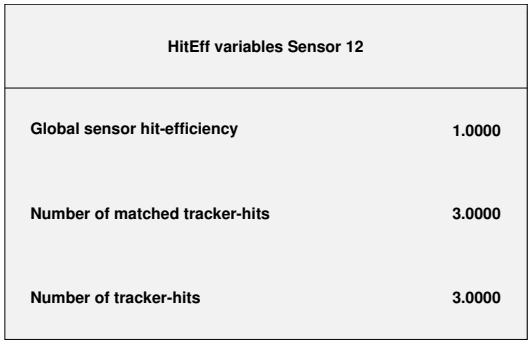

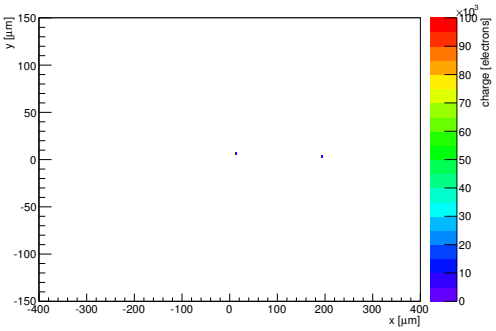

(s) Single pixel mean charge.

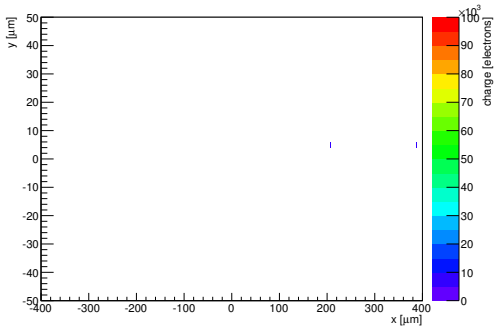

(t) Single pixel mean charge.

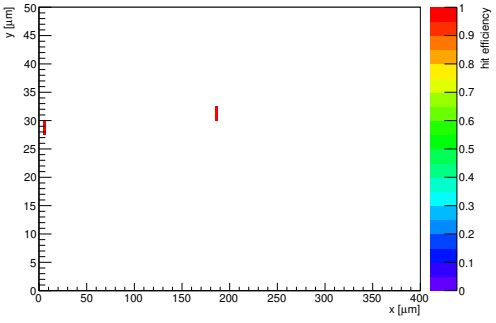

(u) Single pixel hit efficiency.

Figure C.29: Detailed plots for test beam measurement of DO-I-11 (description see section 6.1) sample (running as DUT2) during runs 50587 in the July 2011 test beam period at CERN SPS in area H6B. Summary of the data in chapter 9.

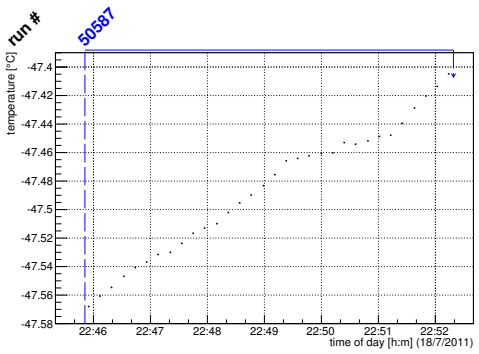

(a) Temperature vs time.

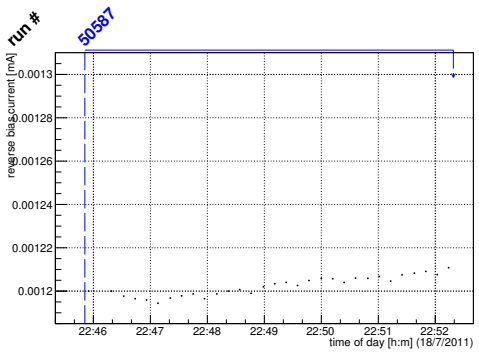

(b) Bias current vs time.

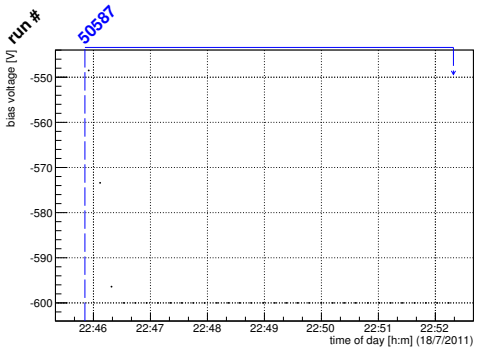

(c) Currently applied bias voltage vs time.

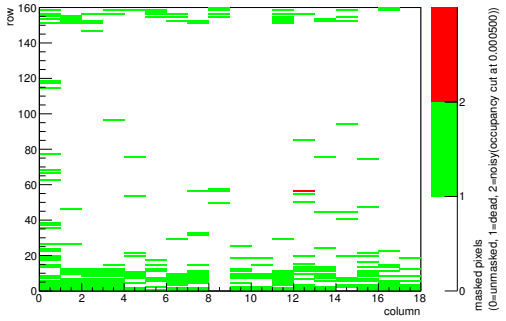

(d) Map of masked pixels.

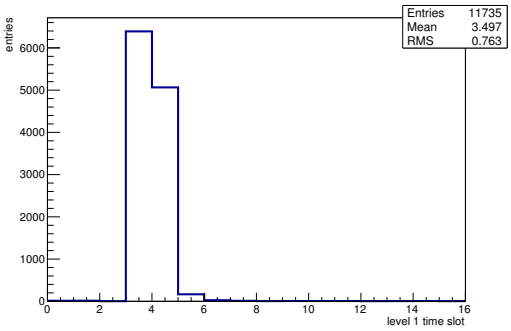

(e) Lvl1 distribution.

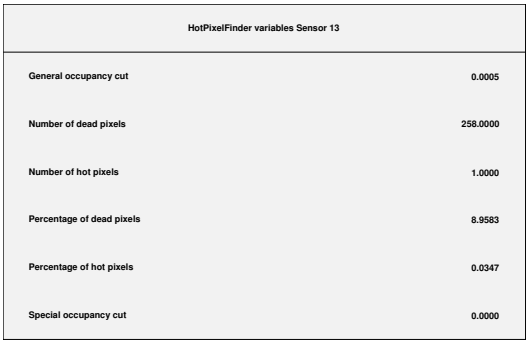

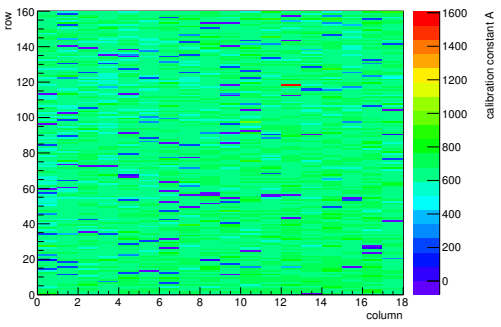

(f) Calibration constant A.

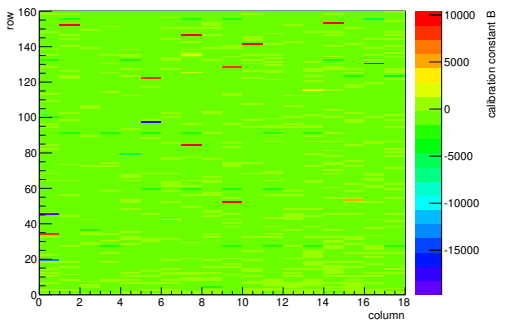

(g) Calibration constant B.

Figure C.30: Detailed plots for test beam measurement of DO-I-13 (description see section 6.1) sample (running as DUT3) during runs 50587 in the July 2011 test beam period at CERN SPS in area H6B. Summary of the data in chapter 9. *(cont.)*

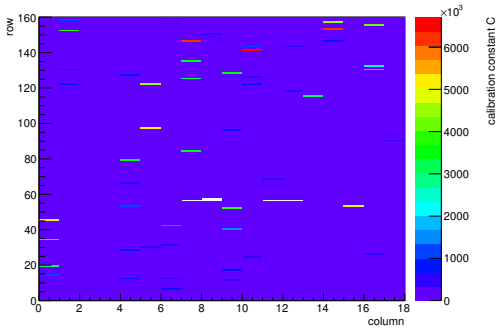

(h) Calibration constant C.

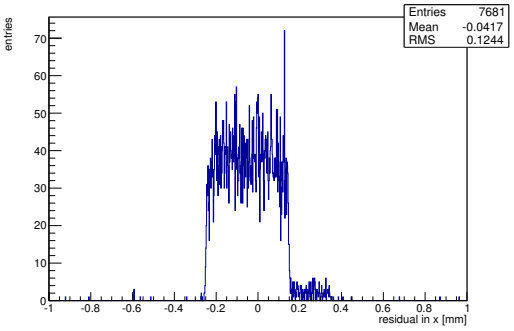

(i) Track residual in x.

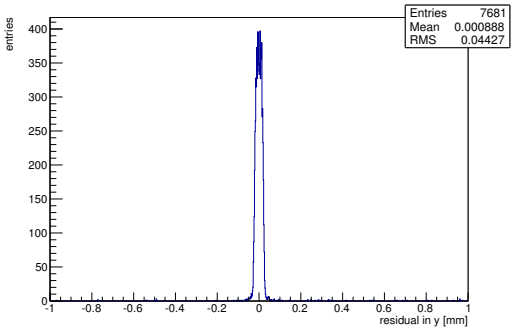

(j) Track residual in y.

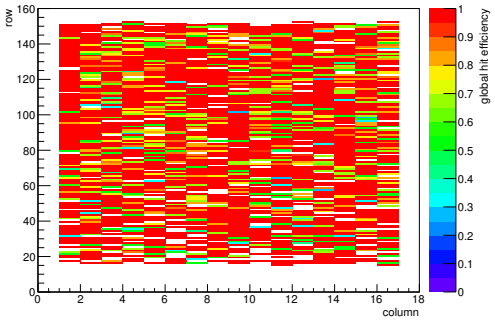

(k) Hit efficiency map.

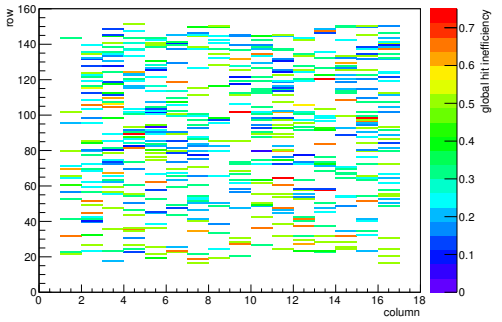

(l) Hit inefficiency map.

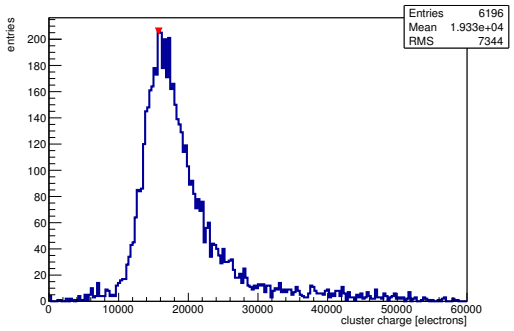

(m) Charge distribution (all cluster sizes included).

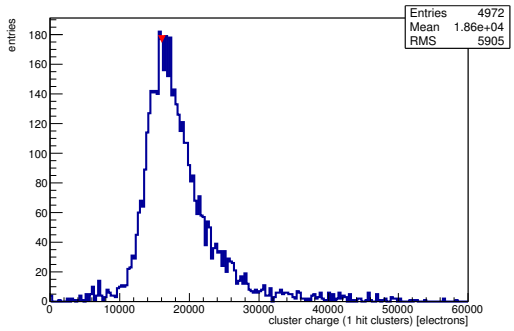

(n) Charge distribution (1 hit cluster).

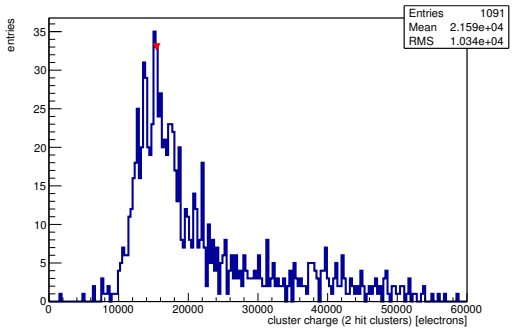

(o) Charge distribution (2 hit cluster).

Figure C.30: Detailed plots for test beam measurement of DO-I-13 (description see section 6.1) sample (running as DUT3) during runs 50587 in the July 2011 test beam period at CERN SPS in area H6B. Summary of the data in chapter 9. *(cont.)*

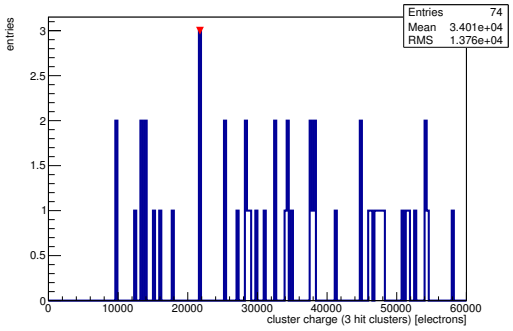

(p) Charge distribution (3 hit cluster).

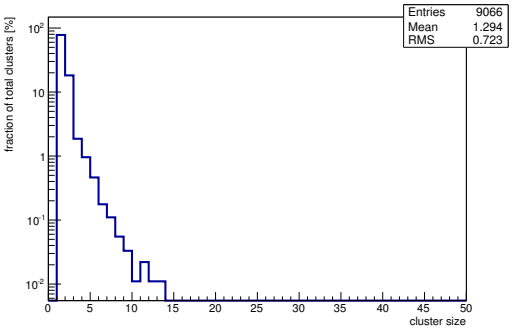

(q) Cluster size distribution.

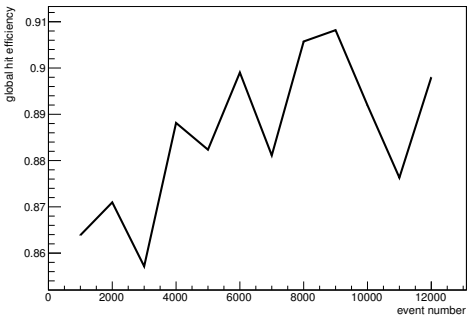

(r) Hit efficiency vs event number.

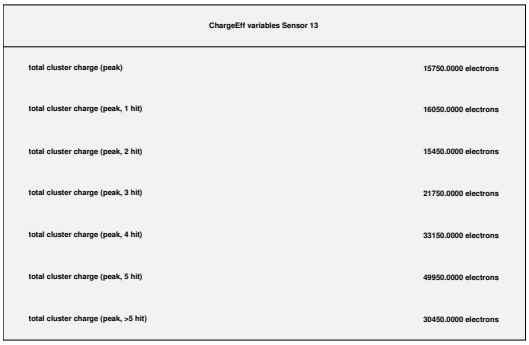

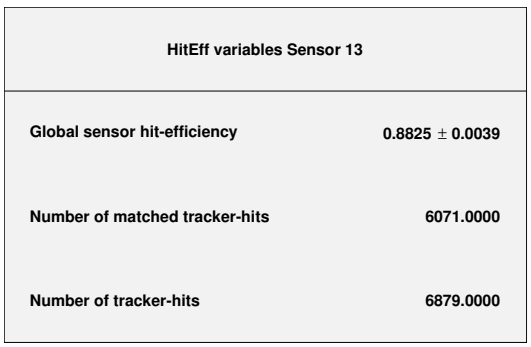

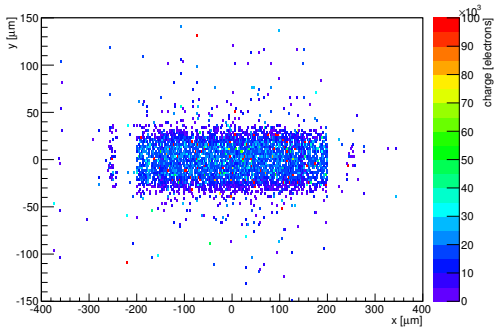

(s) Single pixel mean charge.

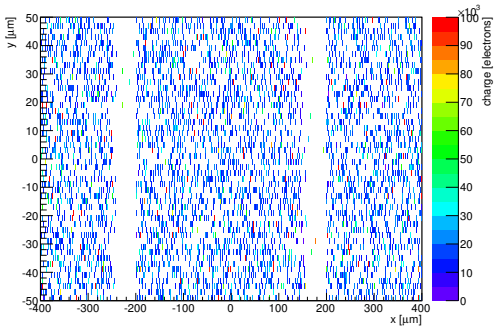

(t) Single pixel mean charge.

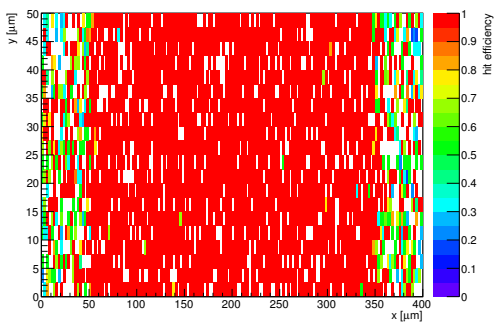

(u) Single pixel hit efficiency.

Figure C.30: Detailed plots for test beam measurement of DO-I-13 (description see section 6.1) sample (running as DUT3) during runs 50587 in the July 2011 test beam period at CERN SPS in area H6B. Summary of the data in chapter 9.

C.2.6 Runs 50588-50597

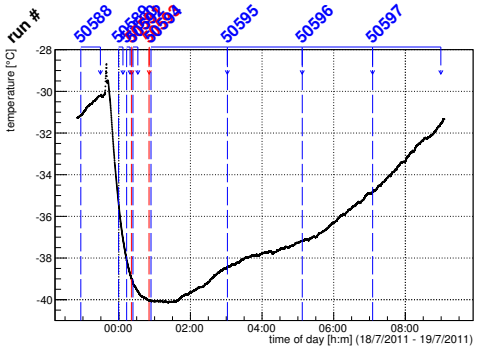

(a) Temperature vs time.

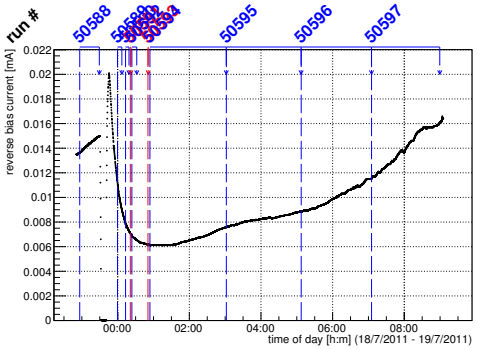

(b) Bias current vs time.

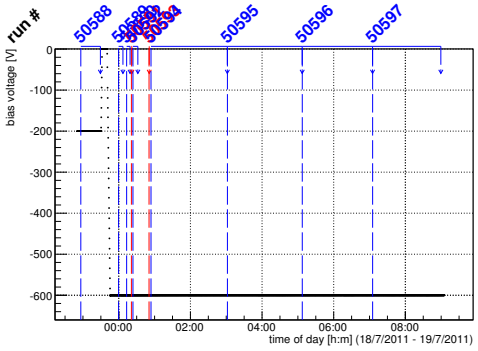

(c) Currently applied bias voltage vs time.

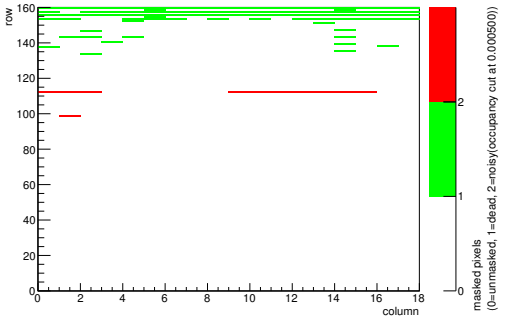

(d) Map of masked pixels.

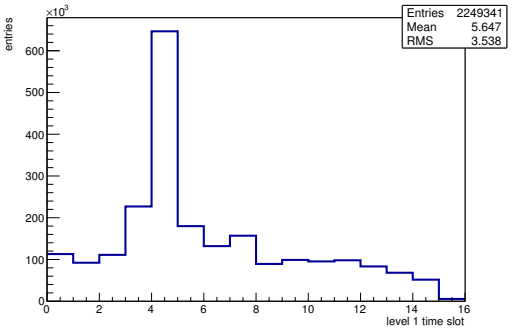

(e) Lvl1 distribution.

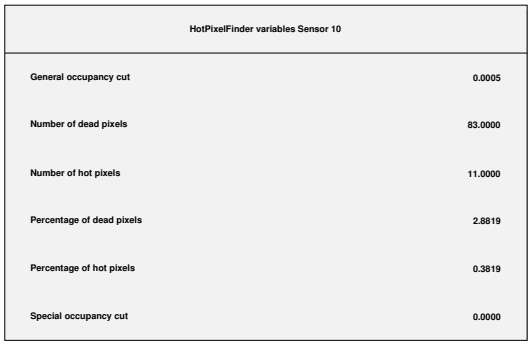

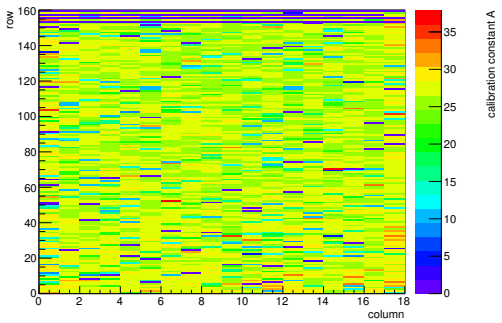

(f) Calibration constant A.

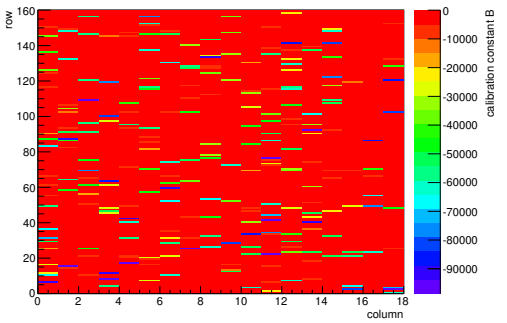

(g) Calibration constant B.

Figure C.31: Detailed plots for test beam measurement of KEK1R (description see section 6.1) sample (running as DUT0) during runs 50588-50597 in the July 2011 test beam period at CERN SPS in area H6B. Summary of the data in chapter 9. *(cont.)*

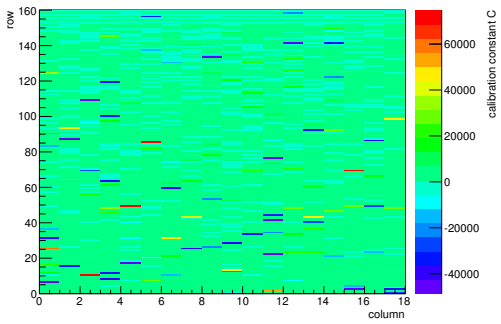

(h) Calibration constant C.

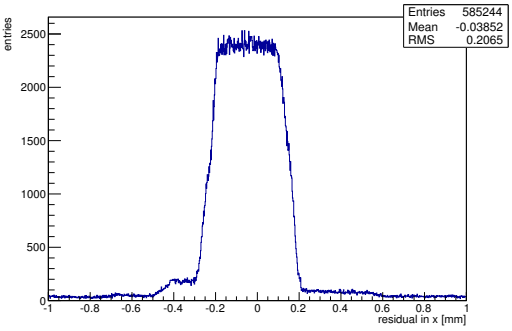

(i) Track residual in x.

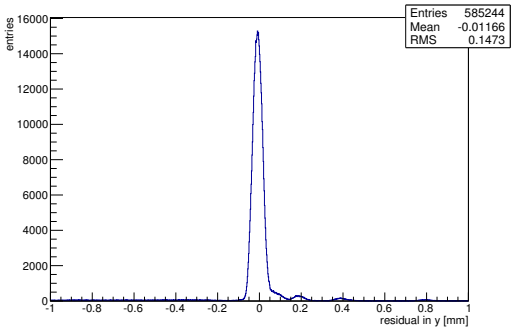

(j) Track residual in y.

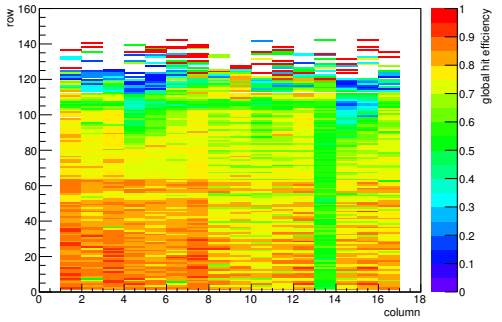

(k) Hit efficiency map.

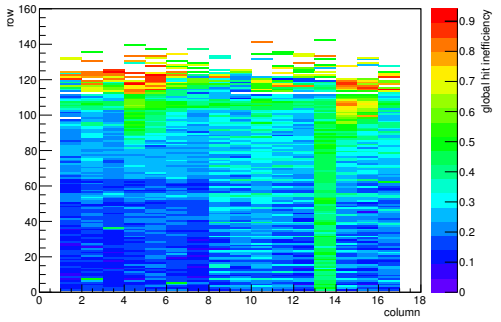

(l) Hit inefficiency map.

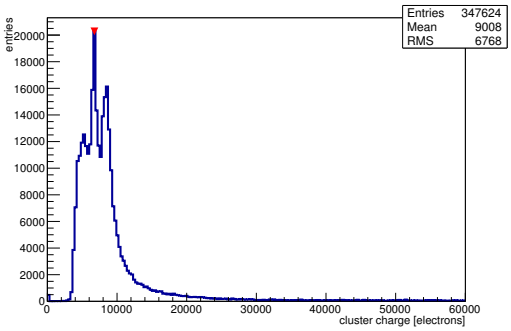

(m) Charge distribution (all cluster sizes included).

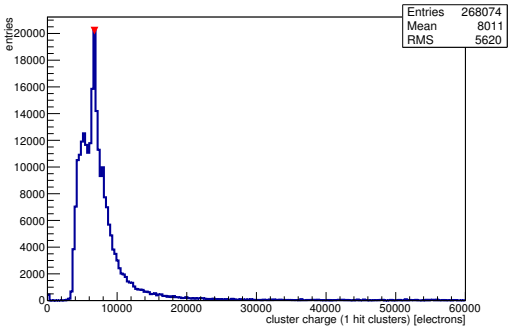

(n) Charge distribution (1 hit cluster).

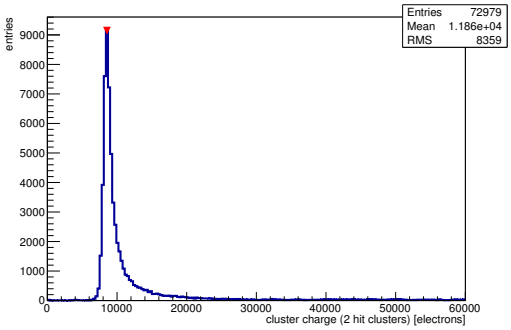

(o) Charge distribution (2 hit cluster).

Figure C.31: Detailed plots for test beam measurement of KEK1R (description see section 6.1) sample (running as DUT0) during runs 50588-50597 in the July 2011 test beam period at CERN SPS in area H6B. Summary of the data in chapter 9. *(cont.)*

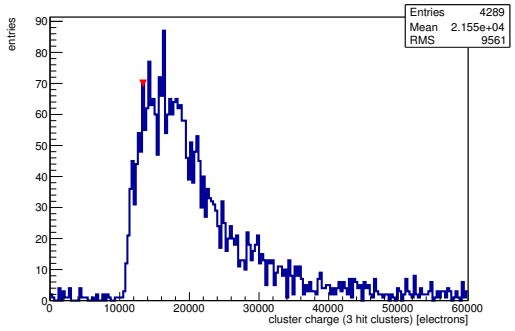

(p) Charge distribution (3 hit cluster).

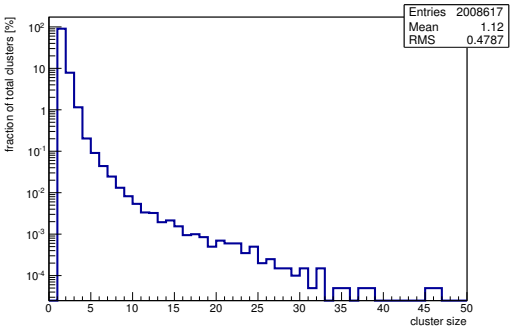

(q) Cluster size distribution.

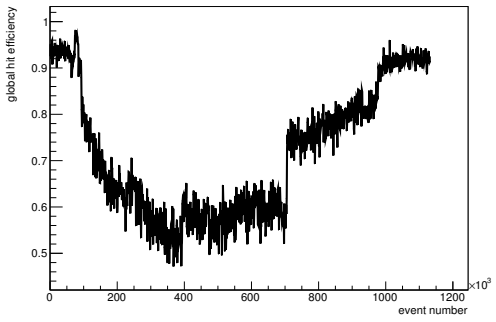

(r) Hit efficiency vs event number.

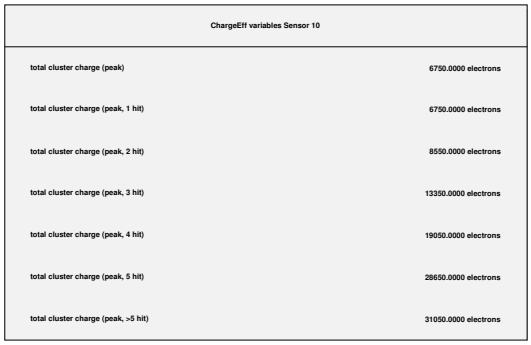

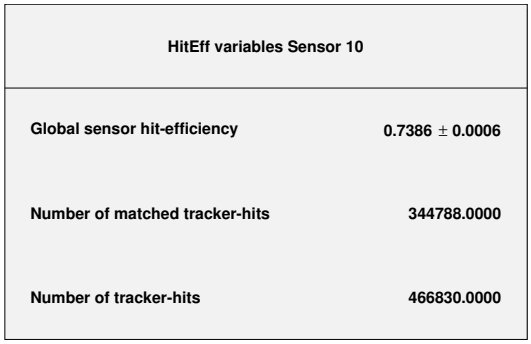

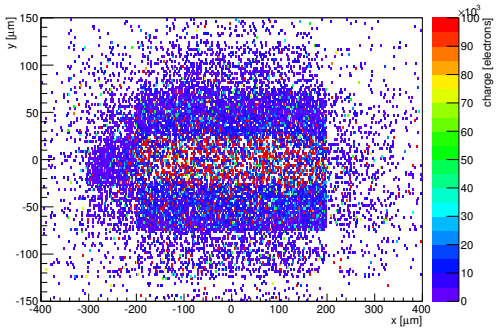

(s) Single pixel mean charge.

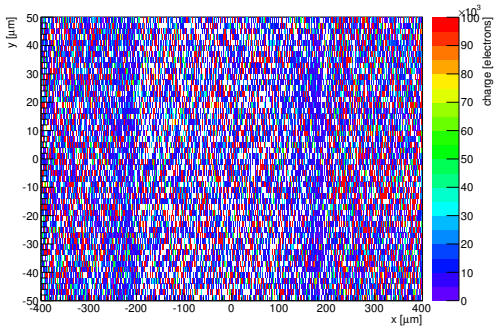

(t) Single pixel mean charge.

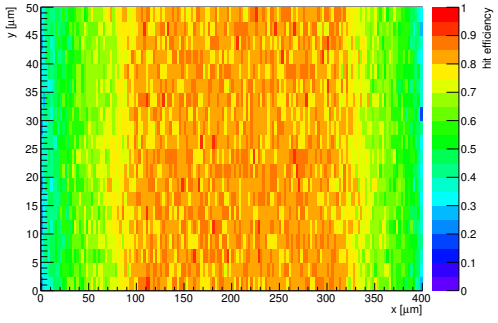

(u) Single pixel hit efficiency.

Figure C.31: Detailed plots for test beam measurement of KEK1R (description see section 6.1) sample (running as DUT0) during runs 50588-50597 in the July 2011 test beam period at CERN SPS in area H6B. Summary of the data in chapter 9.

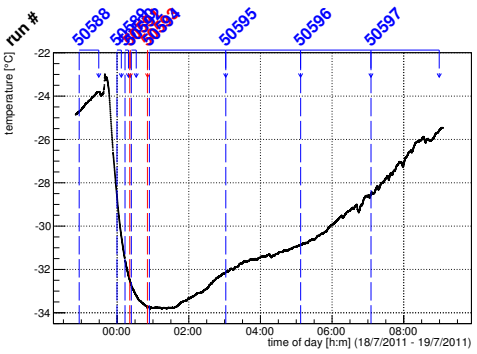

(a) Temperature vs time.

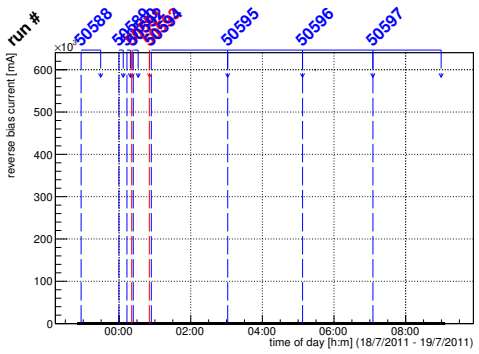

(b) Bias current vs time.

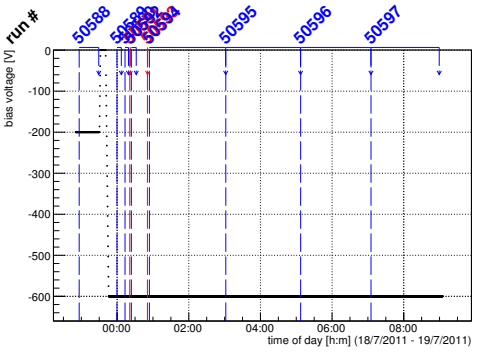

(c) Currently applied bias voltage vs time.

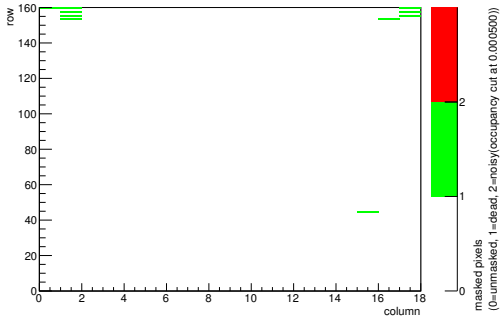

(d) Map of masked pixels.

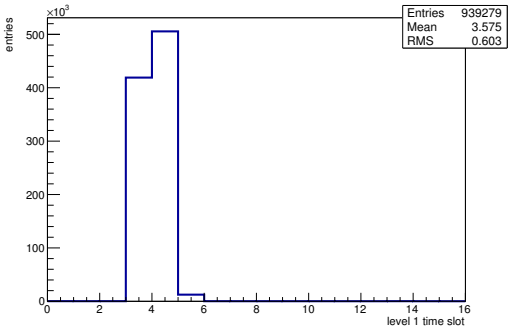

(e) Lvl1 distribution.

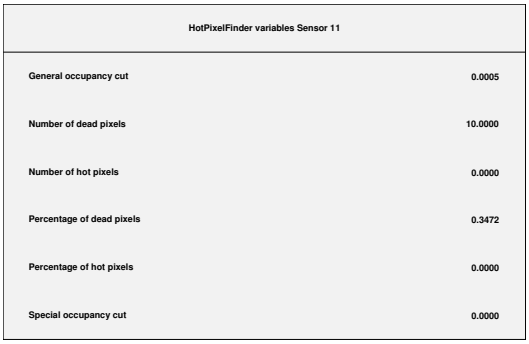

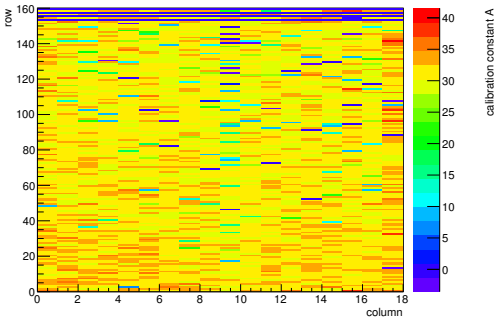

(f) Calibration constant A.

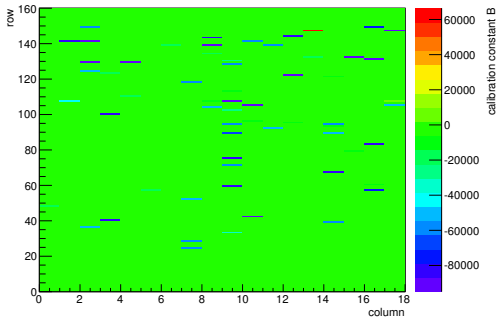

(g) Calibration constant B.

Figure C.32: Detailed plots for test beam measurement of KEK2R (description see section 6.1) sample (running as DUT1) during runs 50588-50597 in the July 2011 test beam period at CERN SPS in area H6B. Summary of the data in chapter 9. *(cont.)*

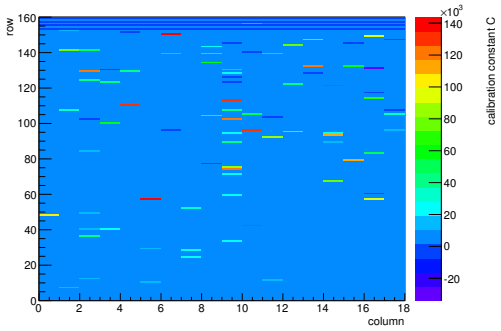

(h) Calibration constant C.

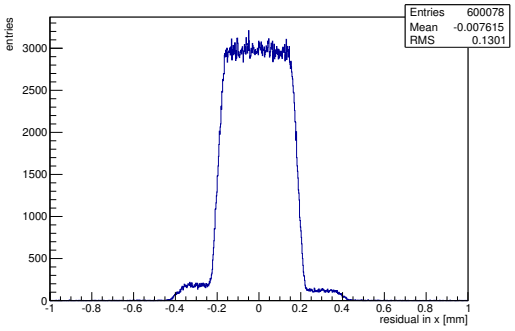

(i) Track residual in x.

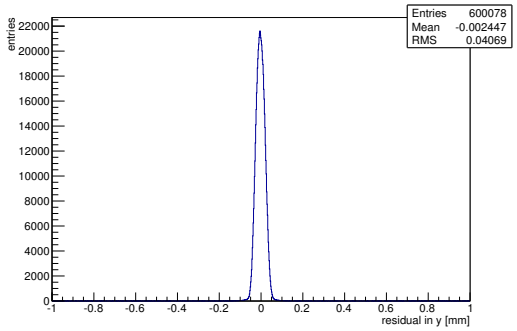

(j) Track residual in y.

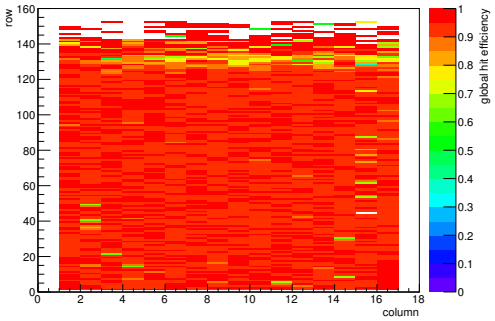

(k) Hit efficiency map.

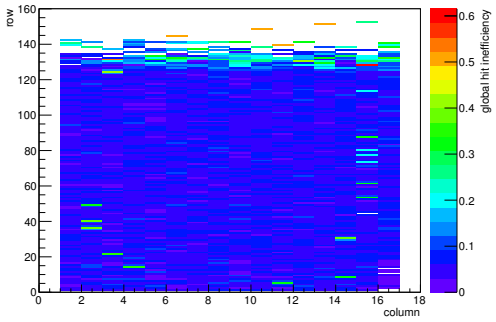

(l) Hit inefficiency map.

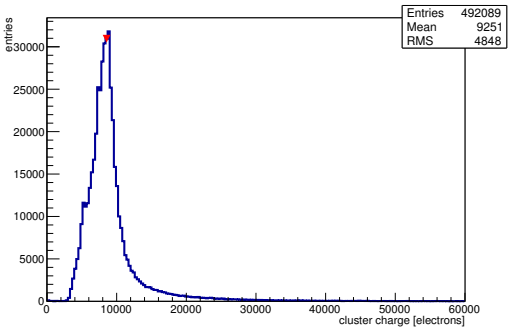

(m) Charge distribution (all cluster sizes included).

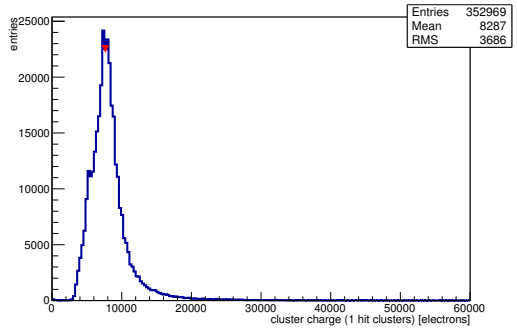

(n) Charge distribution (1 hit cluster).

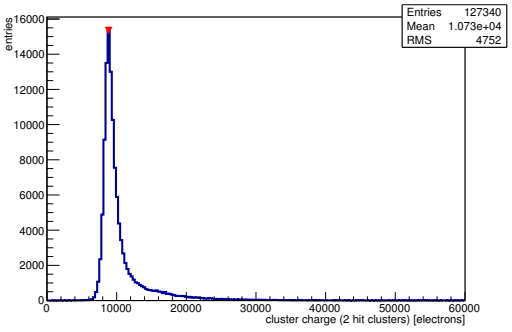

(o) Charge distribution (2 hit cluster).

Figure C.32: Detailed plots for test beam measurement of KEK2R (description see section 6.1) sample (running as DUT1) during runs 50588-50597 in the July 2011 test beam period at CERN SPS in area H6B. Summary of the data in chapter 9. *(cont.)*

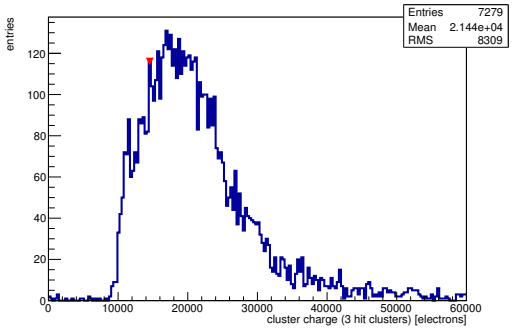

(p) Charge distribution (3 hit cluster).

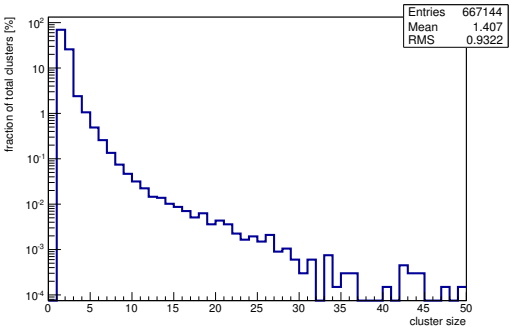

(q) Cluster size distribution.

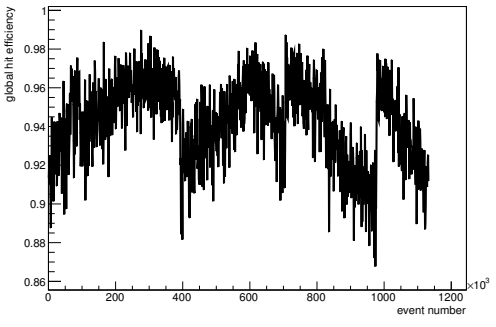

(r) Hit efficiency vs event number.

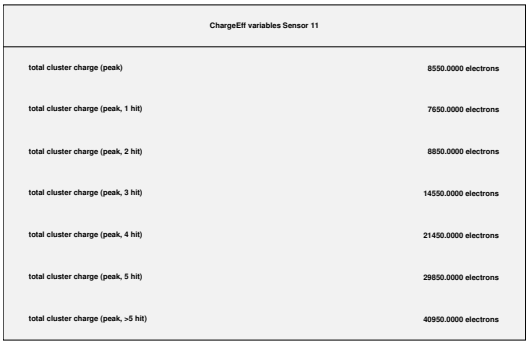

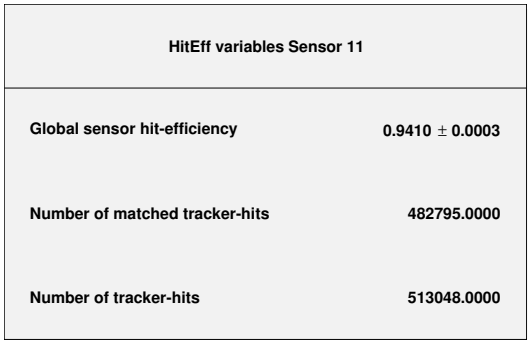

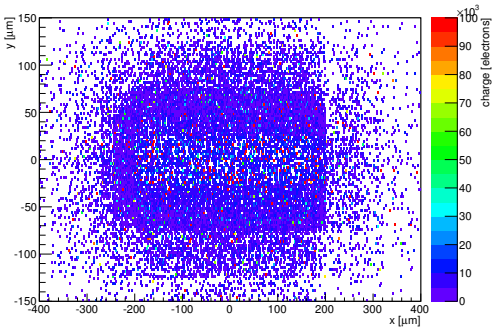

(s) Single pixel mean charge.

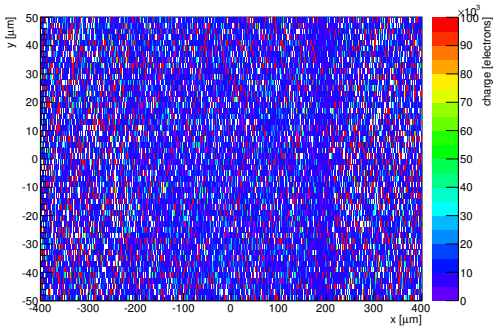

(t) Single pixel mean charge.

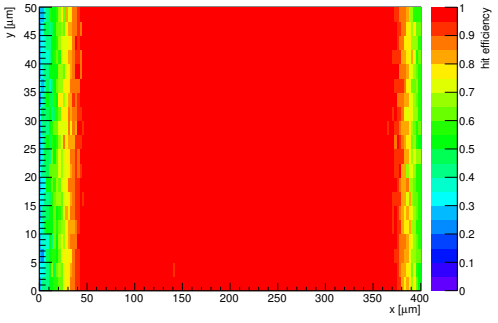

(u) Single pixel hit efficiency.

Figure C.32: Detailed plots for test beam measurement of KEK2R (description see section 6.1) sample (running as DUT1) during runs 50588-50597 in the July 2011 test beam period at CERN SPS in area H6B. Summary of the data in chapter 9.

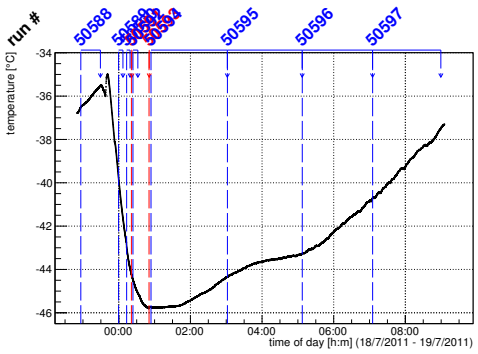

(a) Temperature vs time.

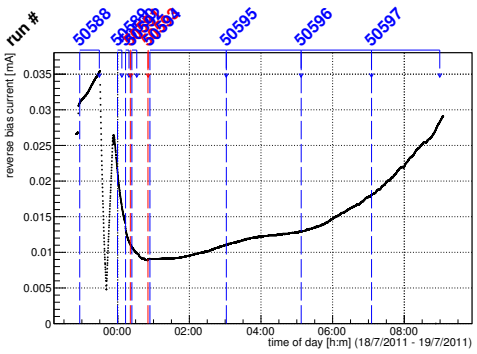

(b) Bias current vs time.

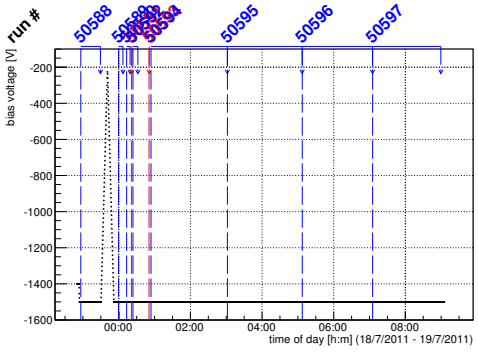

(c) Currently applied bias voltage vs time.

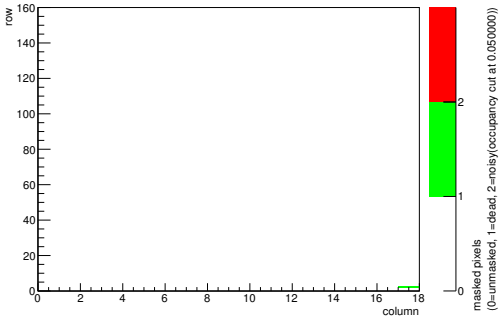

(d) Map of masked pixels.

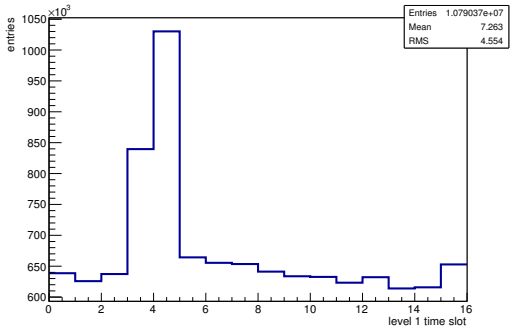

(e) Lvl1 distribution.

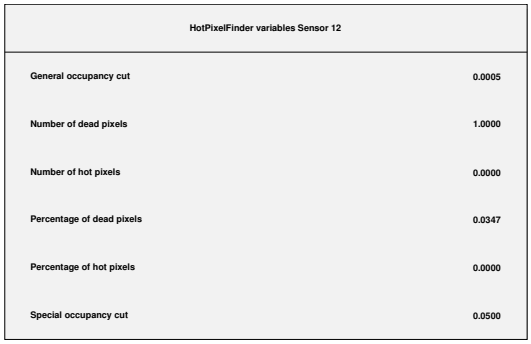

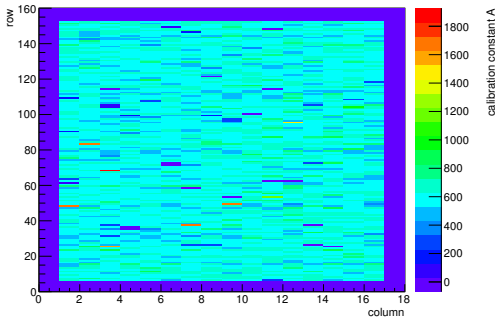

(f) Calibration constant A.

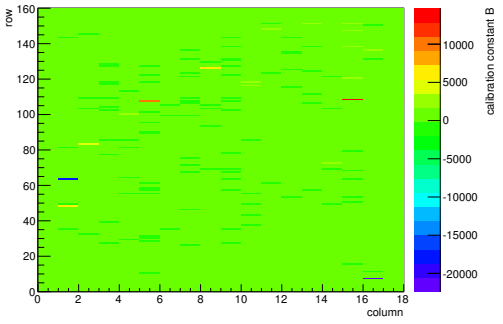

(g) Calibration constant B.

Figure C.33: Detailed plots for test beam measurement of DO-I-11 (description see section 6.1) sample (running as DUT2) during runs 50588-50597 in the July 2011 test beam period at CERN SPS in area H6B. Summary of the data in chapter 9. *(cont.)*

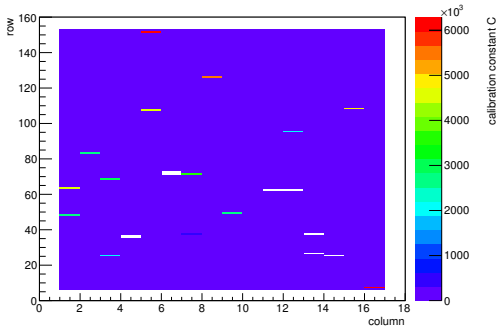

(h) Calibration constant C.

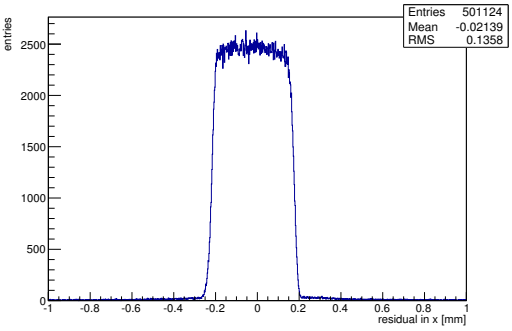

(i) Track residual in x.

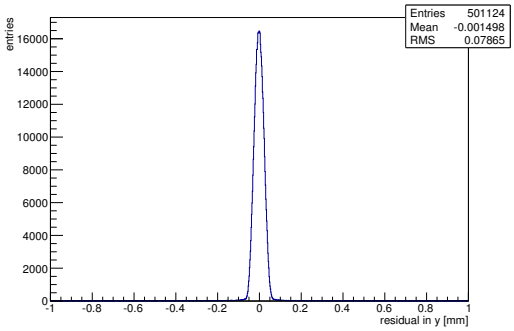

(j) Track residual in y.

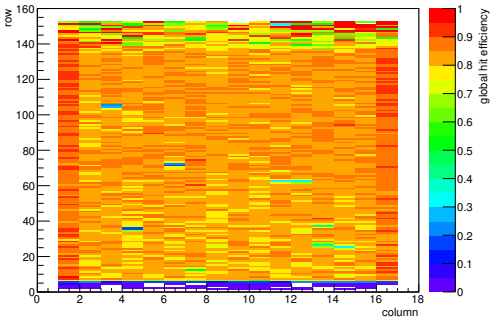

(k) Hit efficiency map.

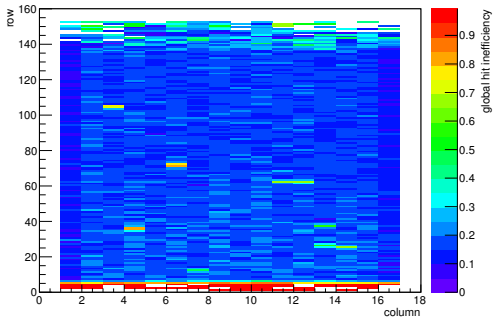

(l) Hit inefficiency map.

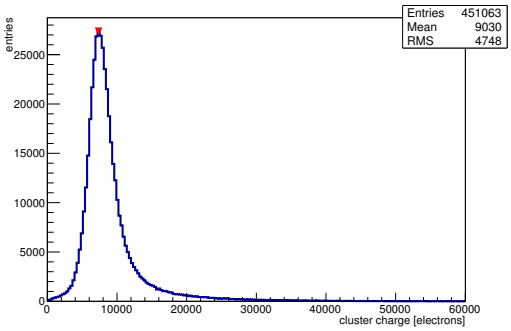

(m) Charge distribution (all cluster sizes included).

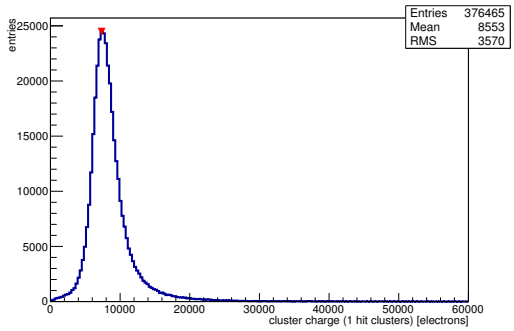

(n) Charge distribution (1 hit cluster).

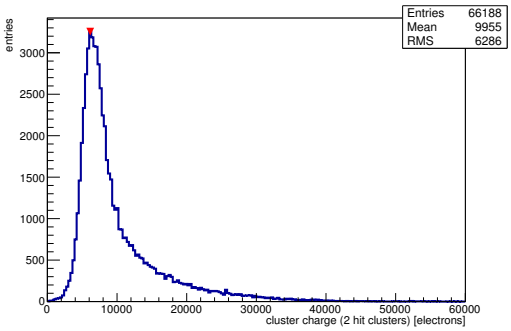

(o) Charge distribution (2 hit cluster).

Figure C.33: Detailed plots for test beam measurement of DO-I-11 (description see section 6.1) sample (running as DUT2) during runs 50588-50597 in the July 2011 test beam period at CERN SPS in area H6B. Summary of the data in chapter 9. *(cont.)*

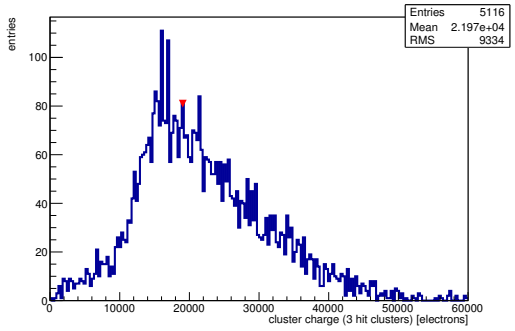

(p) Charge distribution (3 hit cluster).

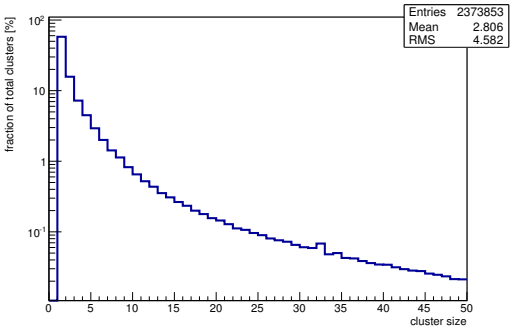

(q) Cluster size distribution.

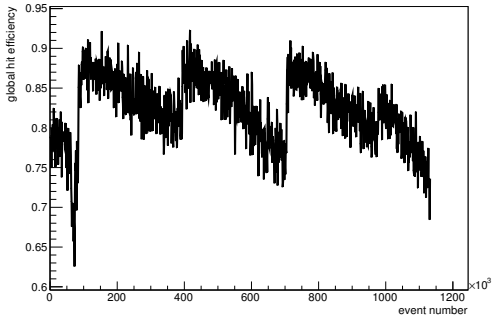

(r) Hit efficiency vs event number.

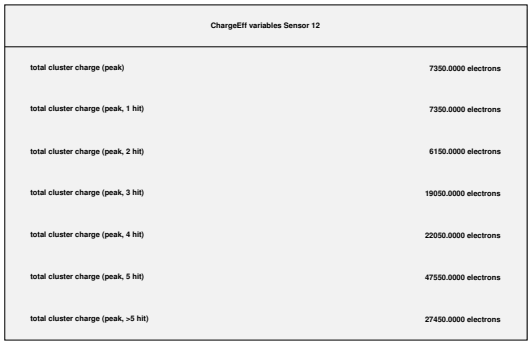

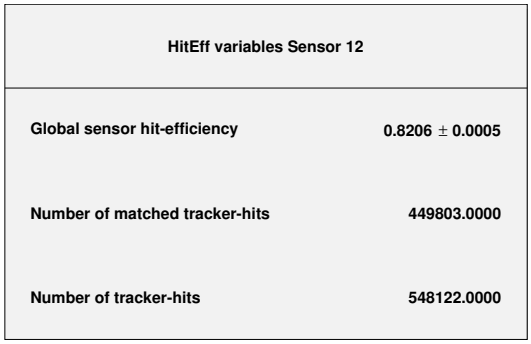

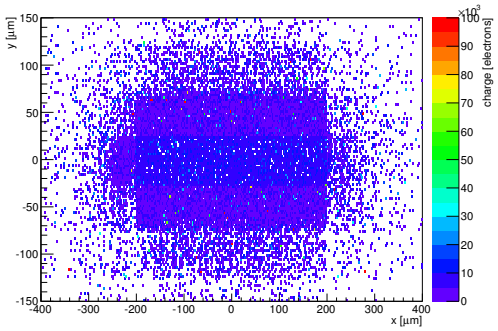

(s) Single pixel mean charge.

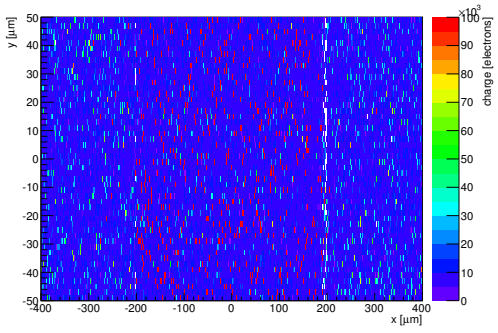

(t) Single pixel mean charge.

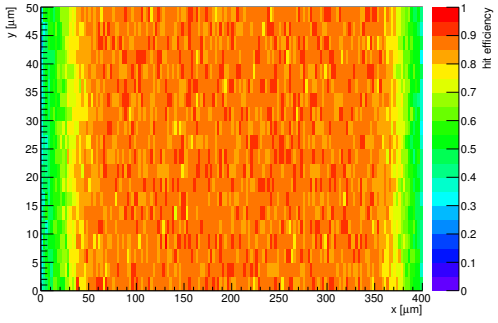

(u) Single pixel hit efficiency.

Figure C.33: Detailed plots for test beam measurement of DO-I-11 (description see section 6.1) sample (running as DUT2) during runs 50588-50597 in the July 2011 test beam period at CERN SPS in area H6B. Summary of the data in chapter 9.

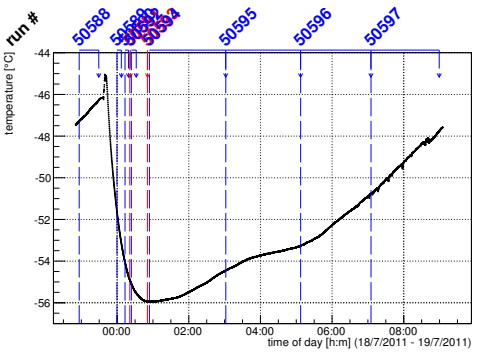

(a) Temperature vs time.

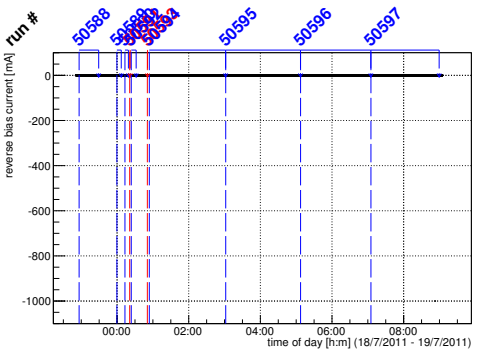

(b) Bias current vs time.

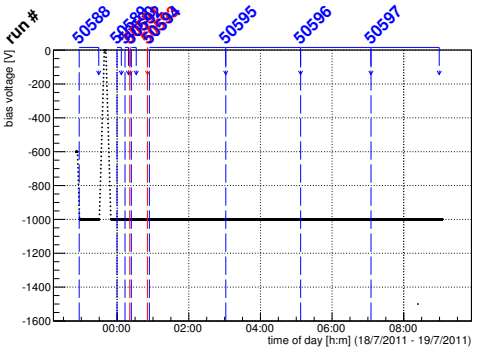

(c) Currently applied bias voltage vs time.

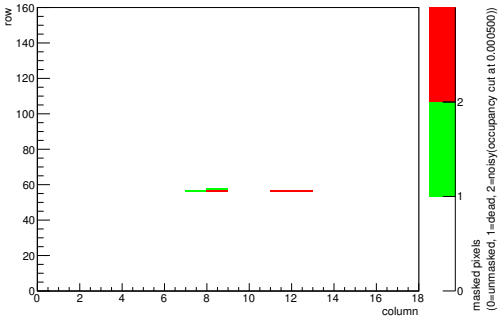

(d) Map of masked pixels.

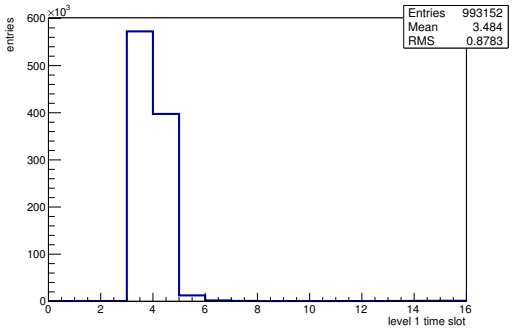

(e) Lvl1 distribution.

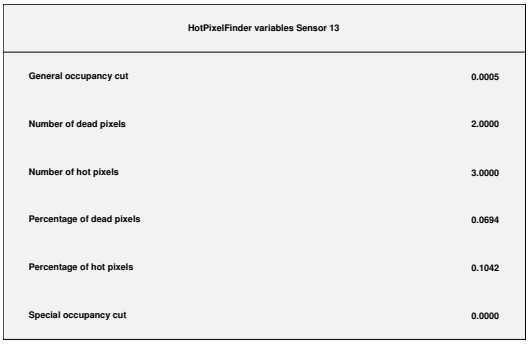

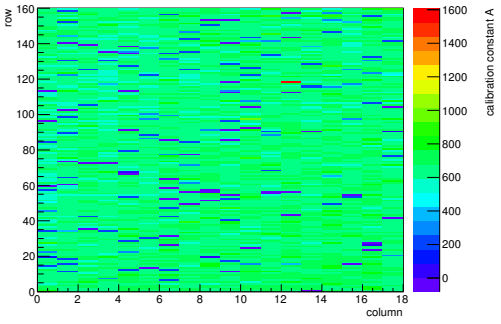

(f) Calibration constant A.

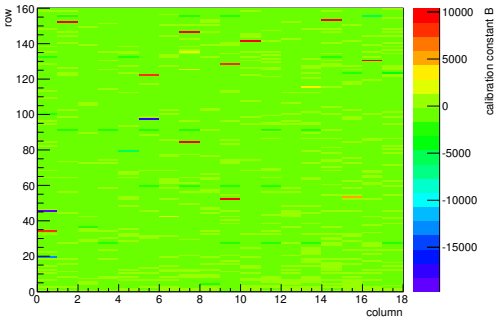

(g) Calibration constant B.

Figure C.34: Detailed plots for test beam measurement of DO-I-13 (description see section 6.1) sample (running as DUT3) during runs 50588-50597 in the July 2011 test beam period at CERN SPS in area H6B. Summary of the data in chapter 9. *(cont.)*

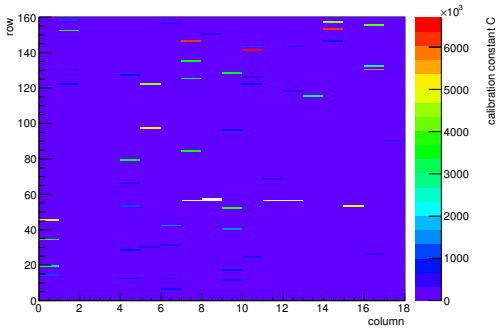

(h) Calibration constant C.

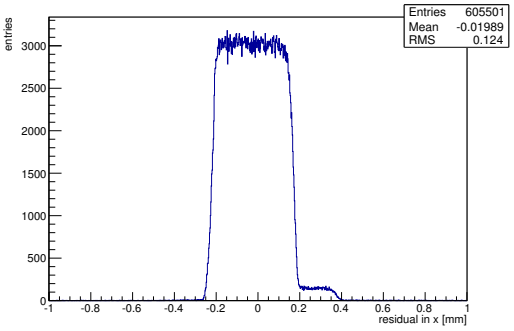

(i) Track residual in x.

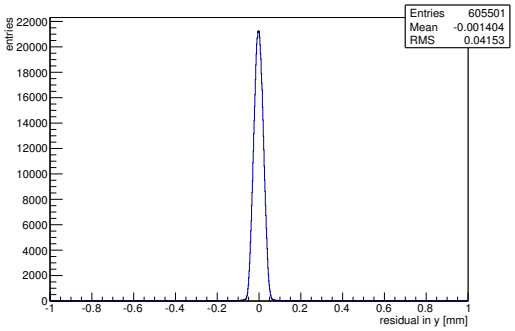

(j) Track residual in y.

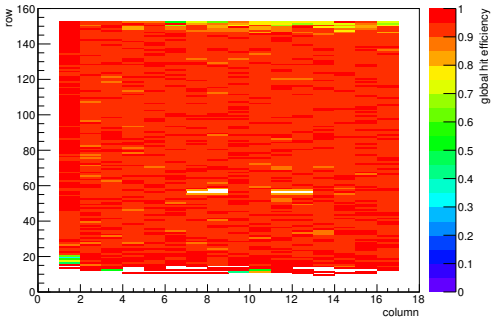

(k) Hit efficiency map.

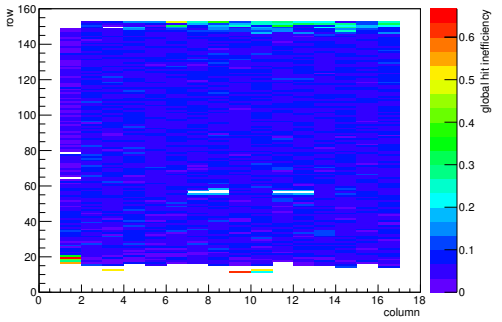

(l) Hit inefficiency map.

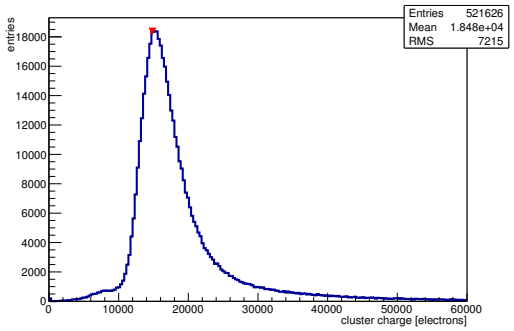

(m) Charge distribution (all cluster sizes included).

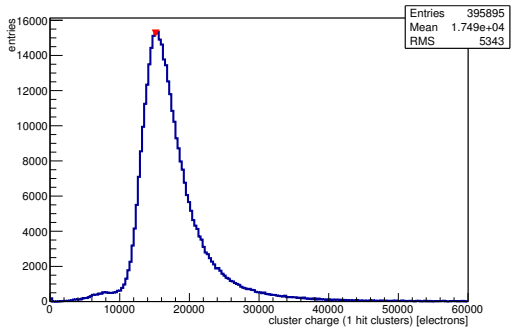

(n) Charge distribution (1 hit cluster).

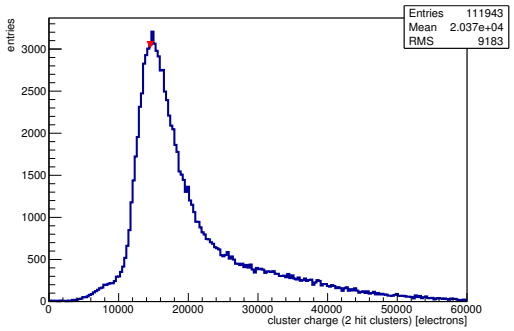

(o) Charge distribution (2 hit cluster).

Figure C.34: Detailed plots for test beam measurement of DO-I-13 (description see section 6.1) sample (running as DUT3) during runs 50588-50597 in the July 2011 test beam period at CERN SPS in area H6B. Summary of the data in chapter 9. *(cont.)*

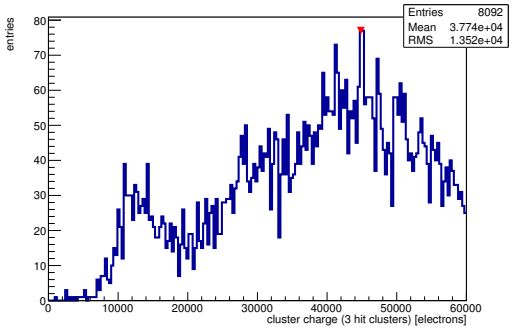

(p) Charge distribution (3 hit cluster).

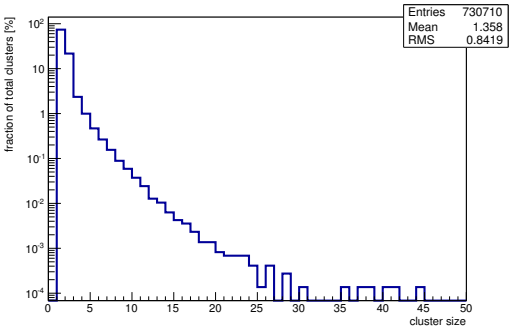

(q) Cluster size distribution.

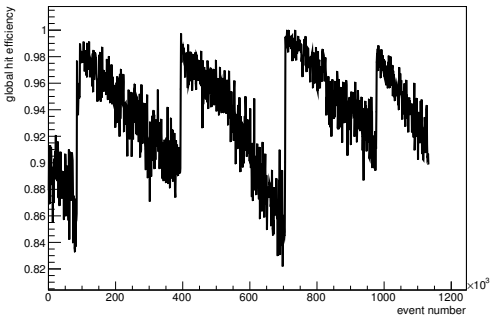

(r) Hit efficiency vs event number.

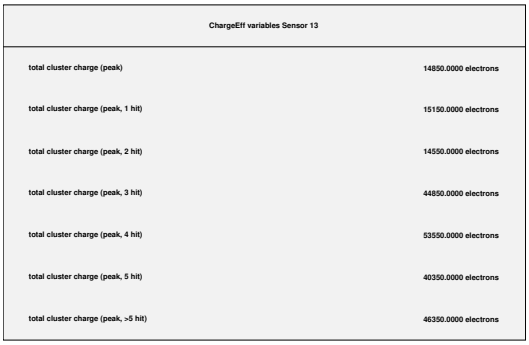

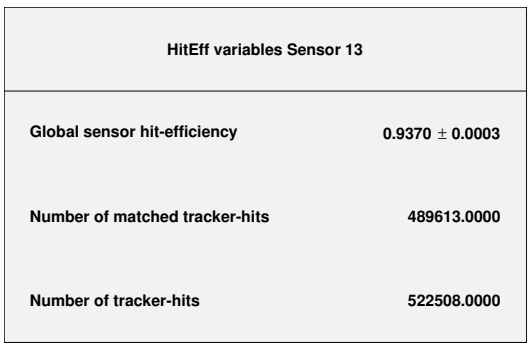

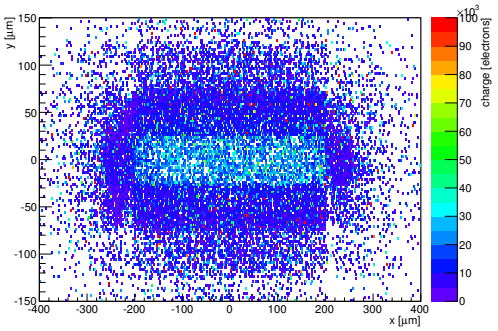

(s) Single pixel mean charge.

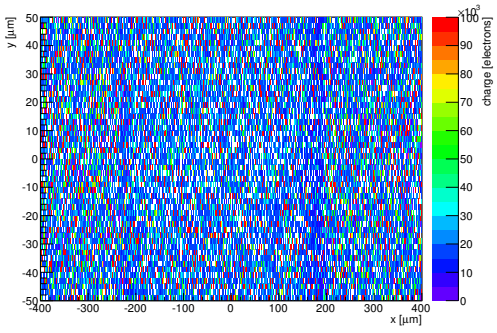

(t) Single pixel mean charge.

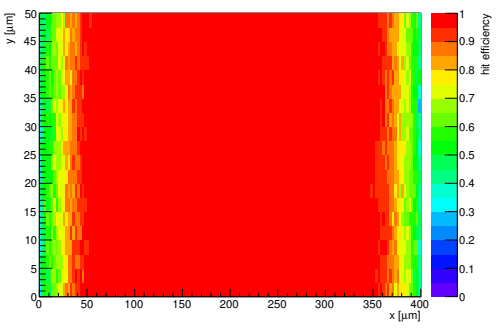

(u) Single pixel hit efficiency.

Figure C.34: Detailed plots for test beam measurement of DO-I-13 (description see section 6.1) sample (running as DUT3) during runs 50588-50597 in the July 2011 test beam period at CERN SPS in area H6B. Summary of the data in chapter 9.

C.2.7 Runs 50598-50599

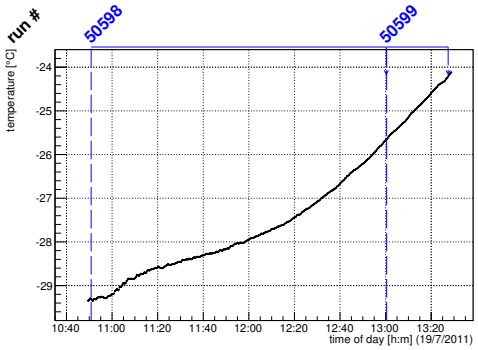

(a) Temperature vs time.

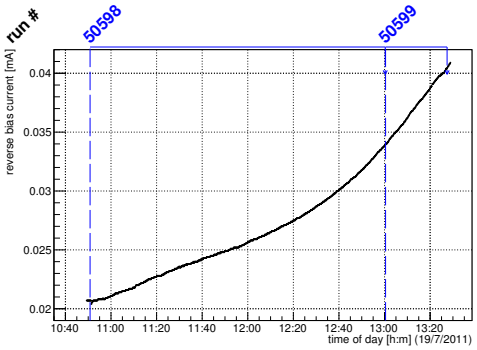

(b) Bias current vs time.

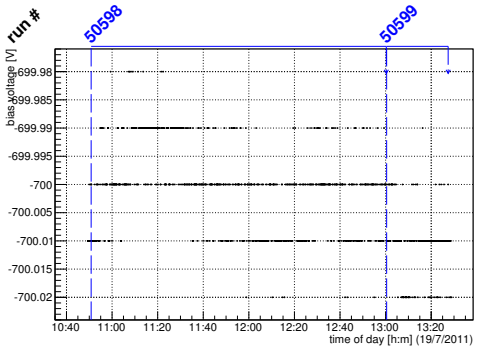

(c) Currently applied bias voltage vs time.

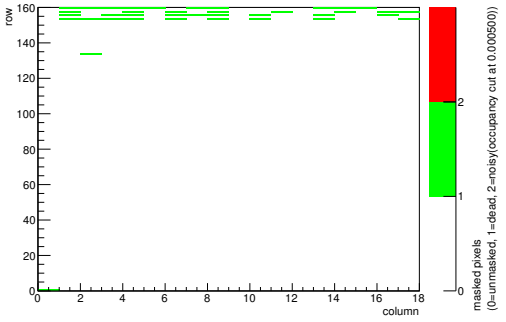

(d) Map of masked pixels.

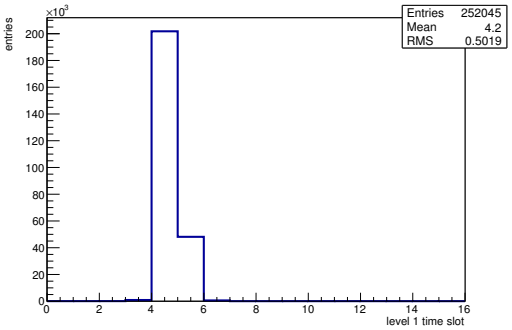

(e) Lvl1 distribution.

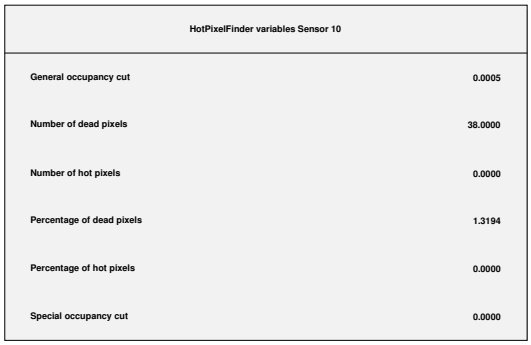

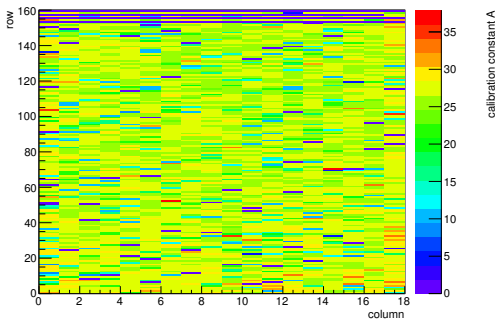

(f) Calibration constant A.

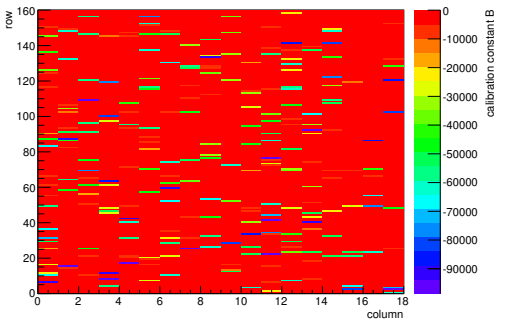

(g) Calibration constant B.

Figure C.35: Detailed plots for test beam measurement of KEK1R (description see section 6.1) sample (running as DUT0) during runs 50598-50599 in the July 2011 test beam period at CERN SPS in area H6B. Summary of the data in chapter 9. *(cont.)*

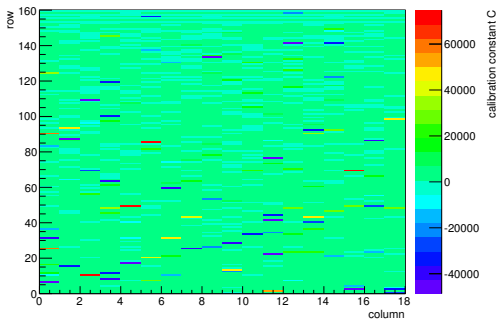

(h) Calibration constant C.

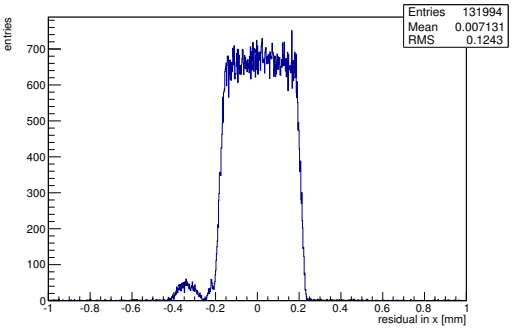

(i) Track residual in x.

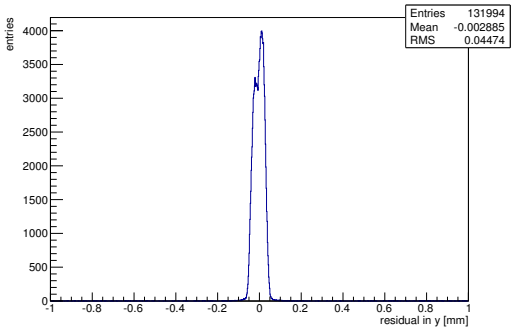

(j) Track residual in y.

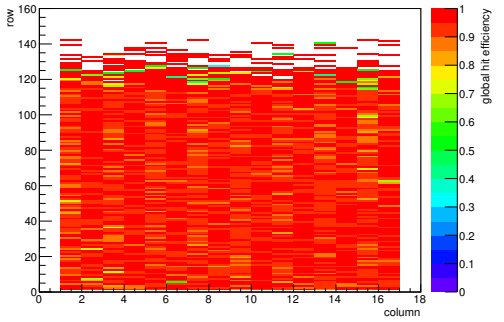

(k) Hit efficiency map.

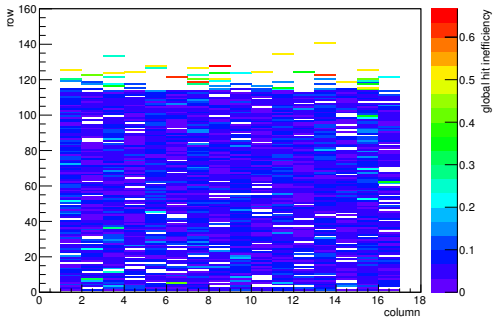

(l) Hit inefficiency map.

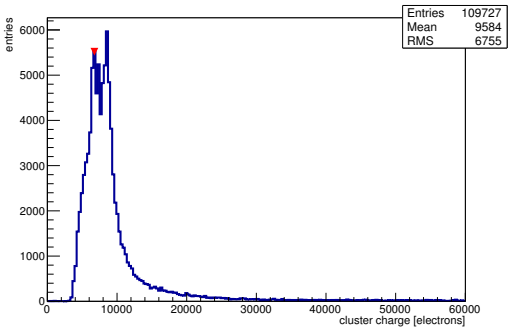

(m) Charge distribution (all cluster sizes included).

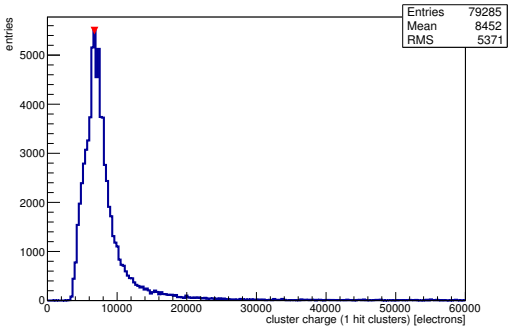

(n) Charge distribution (1 hit cluster).

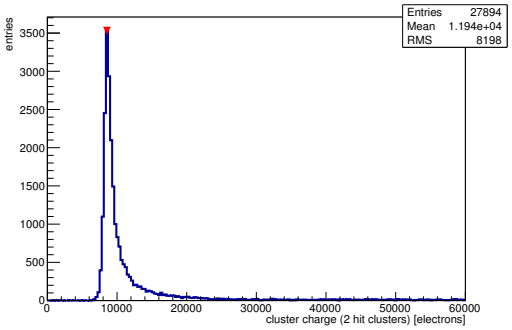

(o) Charge distribution (2 hit cluster).

Figure C.35: Detailed plots for test beam measurement of KEK1R (description see section 6.1) sample (running as DUT0) during runs 50598-50599 in the July 2011 test beam period at CERN SPS in area H6B. Summary of the data in chapter 9. *(cont.)*

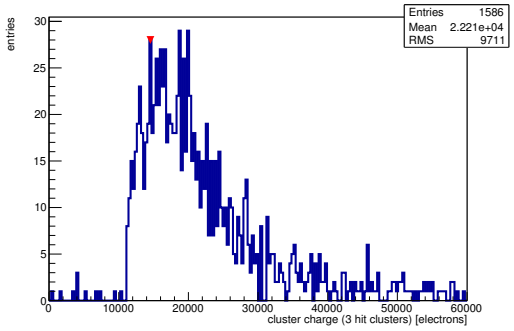

(p) Charge distribution (3 hit cluster).

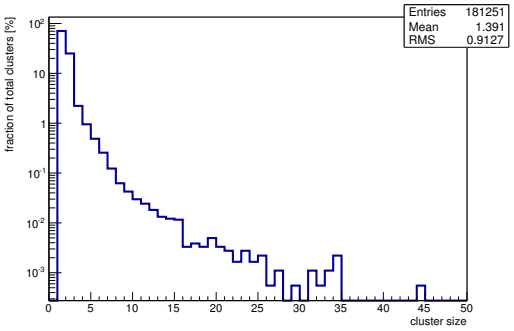

(q) Cluster size distribution.

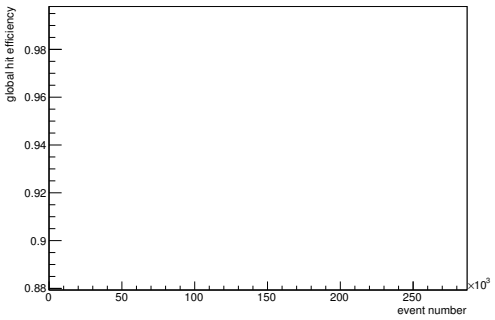

(r) Hit efficiency vs event number.

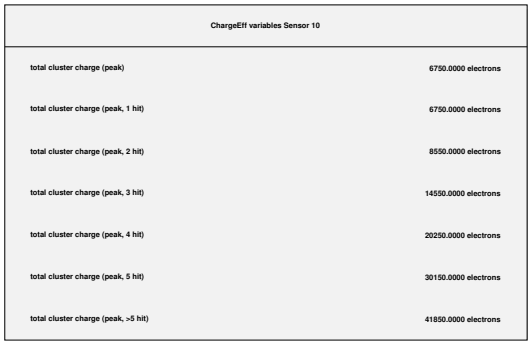

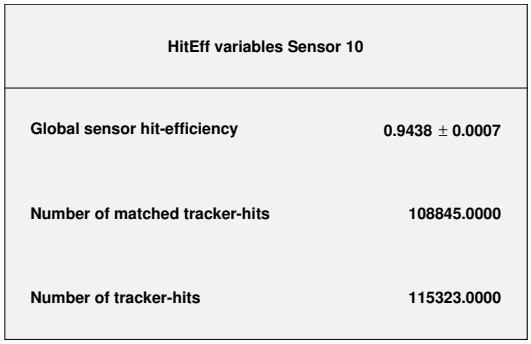

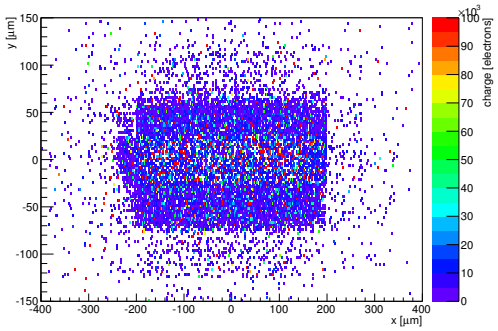

(s) Single pixel mean charge.

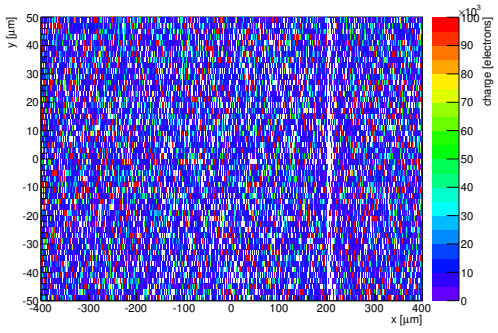

(t) Single pixel mean charge.

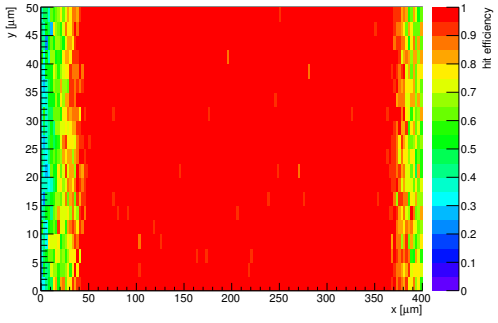

(u) Single pixel hit efficiency.

Figure C.35: Detailed plots for test beam measurement of KEK1R (description see section 6.1) sample (running as DUT0) during runs 50598-50599 in the July 2011 test beam period at CERN SPS in area H6B. Summary of the data in chapter 9.

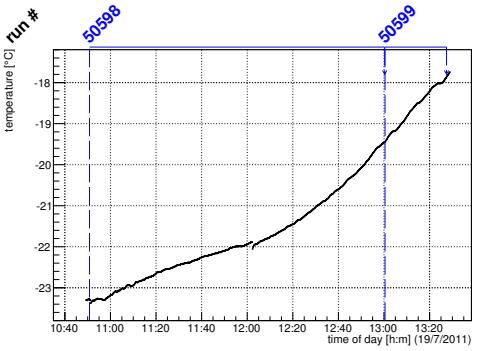

(a) Temperature vs time.

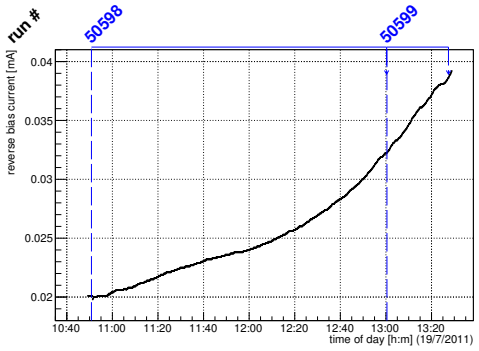

(b) Bias current vs time.

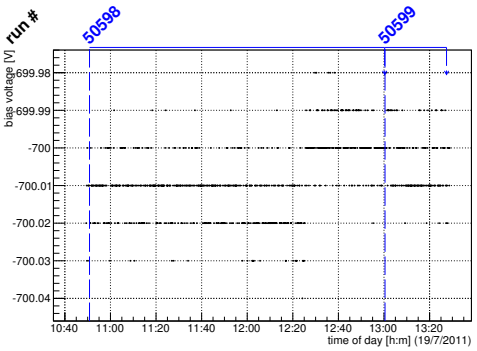

(c) Currently applied bias voltage vs time.

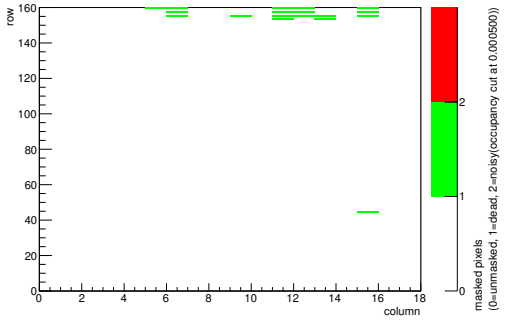

(d) Map of masked pixels.

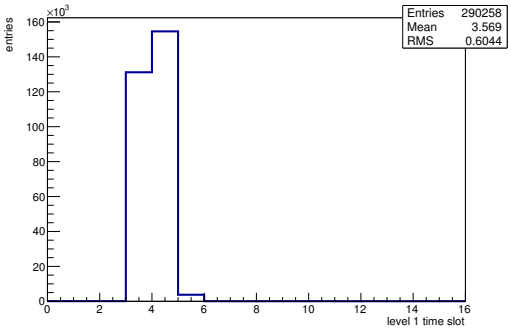

(e) Lvl1 distribution.

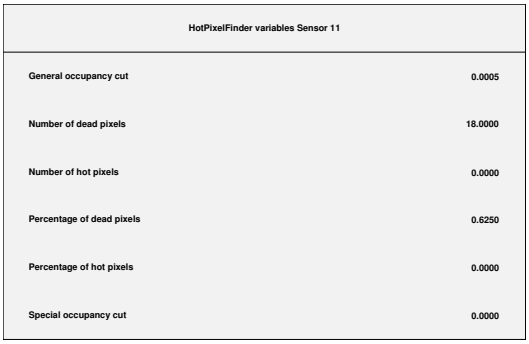

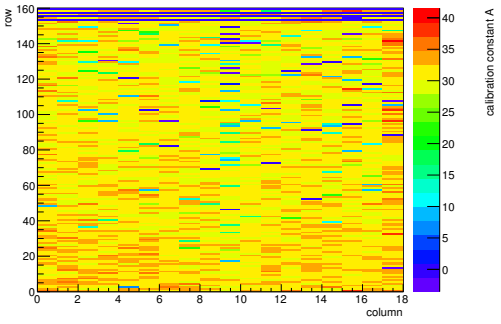

(f) Calibration constant A.

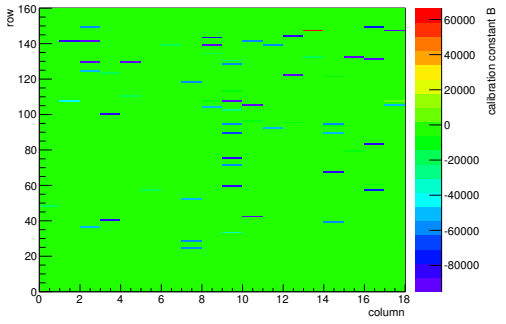

(g) Calibration constant B.

Figure C.36: Detailed plots for test beam measurement of KEK2R (description see section 6.1) sample (running as DUT1) during runs 50598-50599 in the July 2011 test beam period at CERN SPS in area H6B. Summary of the data in chapter 9. *(cont.)*

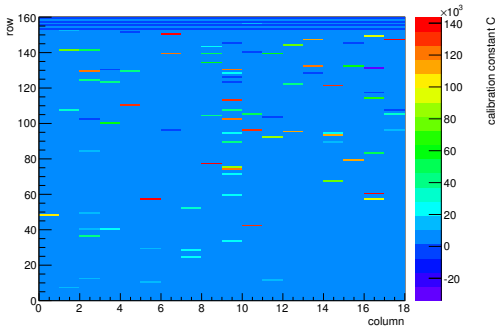

(h) Calibration constant C.

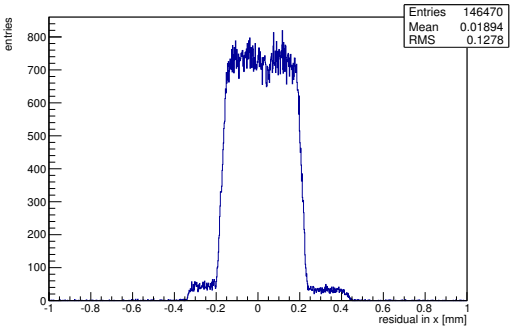

(i) Track residual in x.

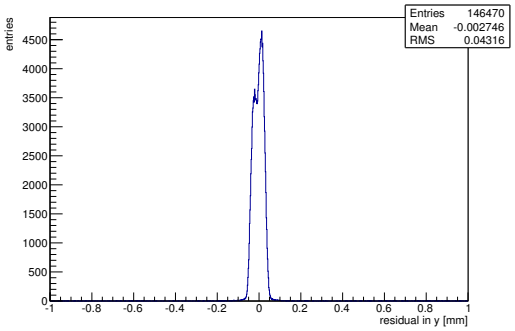

(j) Track residual in y.

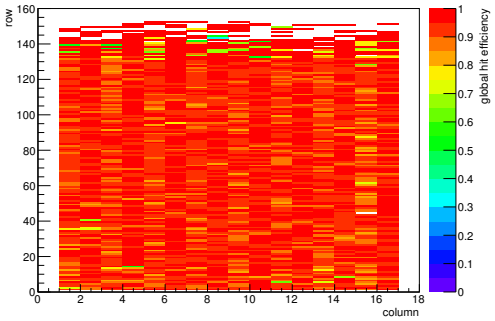

(k) Hit efficiency map.

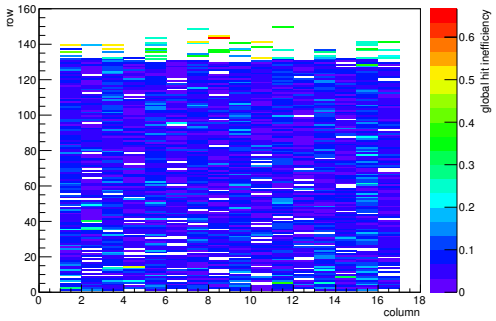

(l) Hit inefficiency map.

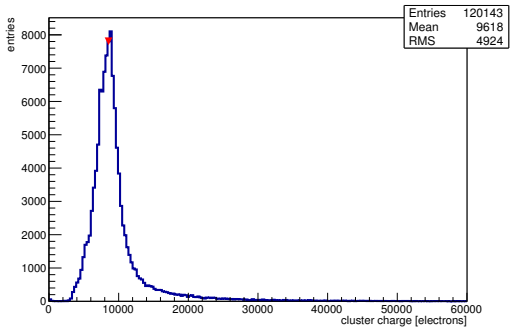

(m) Charge distribution (all cluster sizes included).

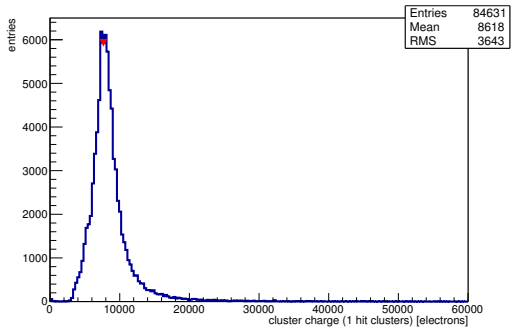

(n) Charge distribution (1 hit cluster).

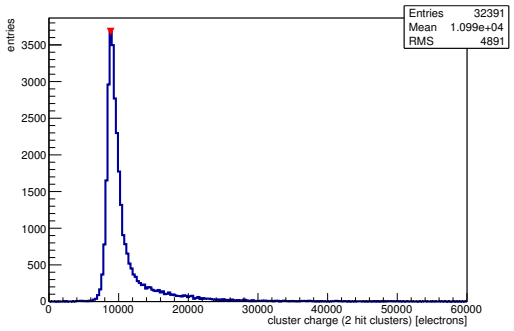

(o) Charge distribution (2 hit cluster).

Figure C.36: Detailed plots for test beam measurement of KEK2R (description see section 6.1) sample (running as DUT1) during runs 50598-50599 in the July 2011 test beam period at CERN SPS in area H6B. Summary of the data in chapter 9. *(cont.)*

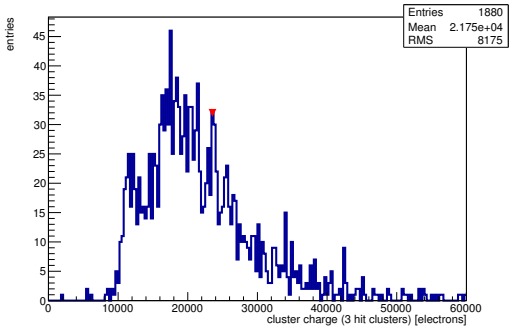

(p) Charge distribution (3 hit cluster).

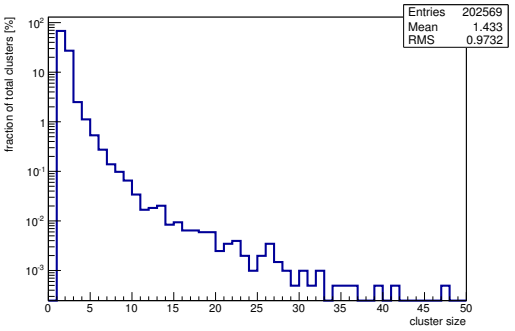

(q) Cluster size distribution.

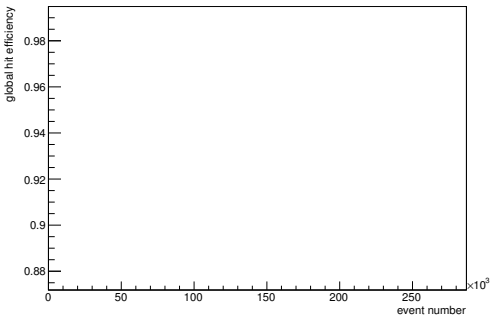

(r) Hit efficiency vs event number.

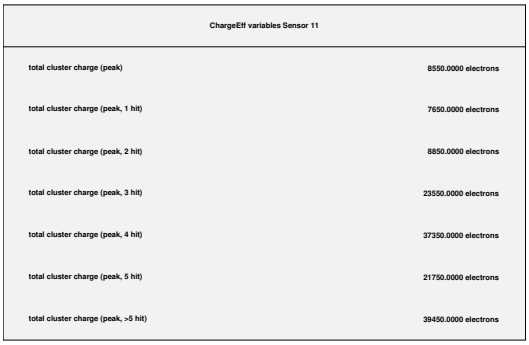

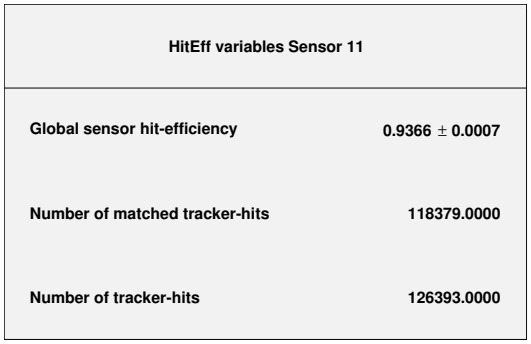

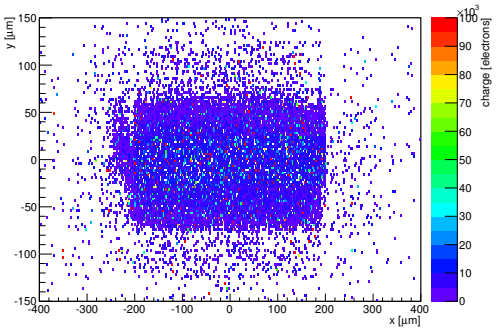

(s) Single pixel mean charge.

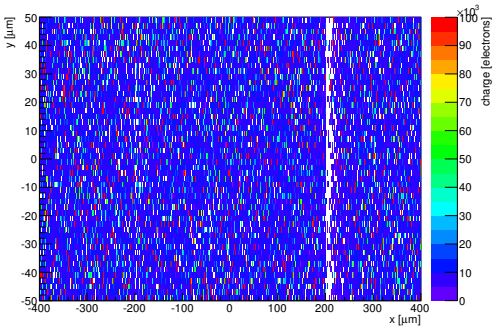

(t) Single pixel mean charge.

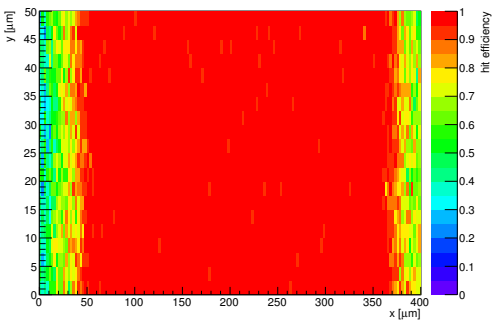

(u) Single pixel hit efficiency.

Figure C.36: Detailed plots for test beam measurement of KEK2R (description see section 6.1) sample (running as DUT1) during runs 50598-50599 in the July 2011 test beam period at CERN SPS in area H6B. Summary of the data in chapter 9.

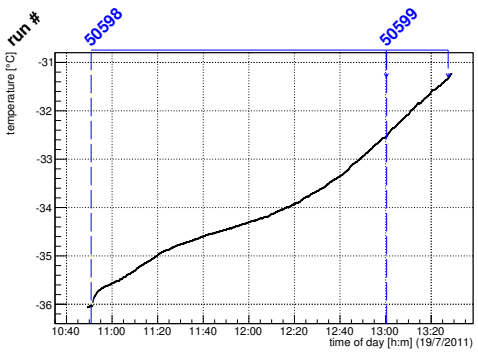

(a) Temperature vs time.

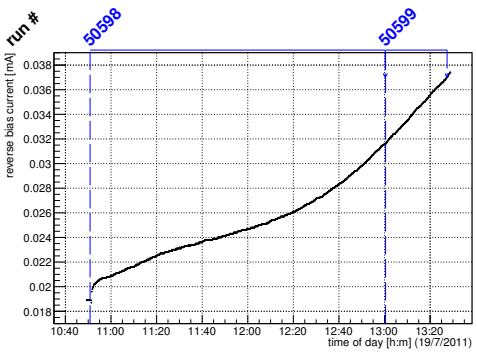

(b) Bias current vs time.

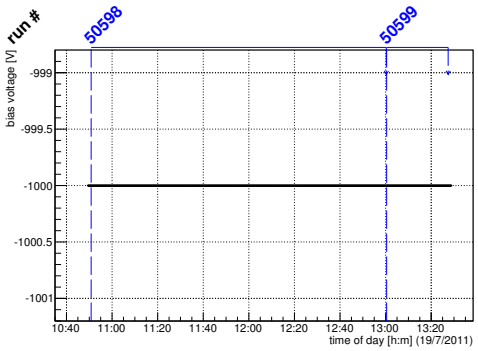

(c) Currently applied bias voltage vs time.

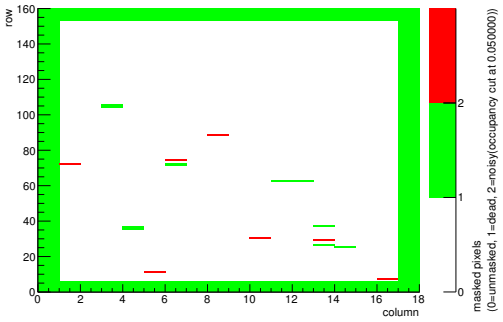

(d) Map of masked pixels.

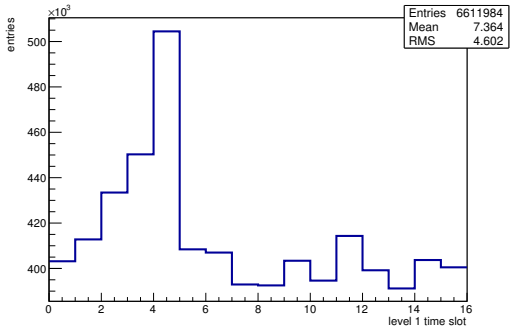

(e) Lvl1 distribution.

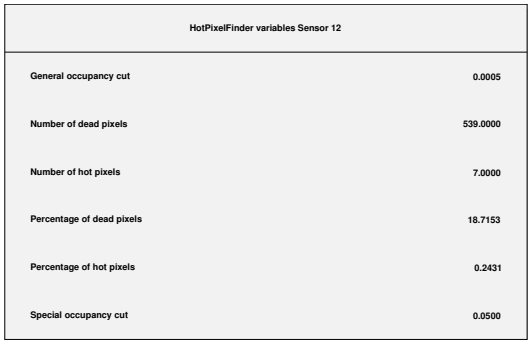

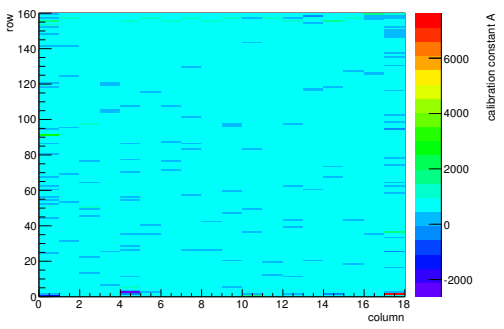

(f) Calibration constant A.

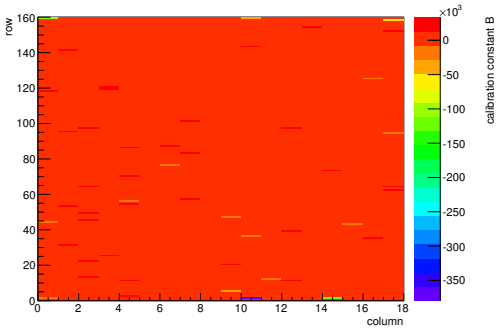

(g) Calibration constant B.

Figure C.37: Detailed plots for test beam measurement of DO-I-11 (description see section 6.1) sample (running as DUT2) during runs 50598-50599 in the July 2011 test beam period at CERN SPS in area H6B. Summary of the data in chapter 9. *(cont.)*

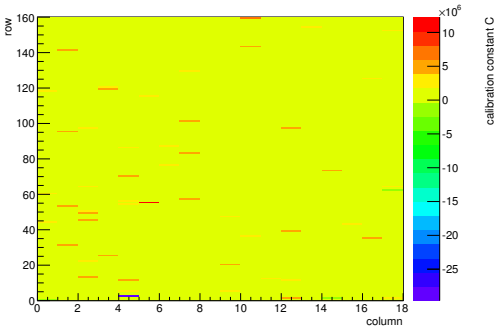

(h) Calibration constant C.

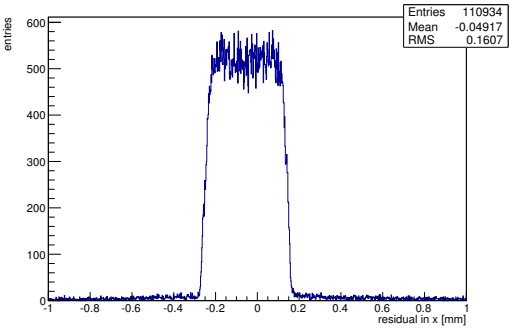

(i) Track residual in x.

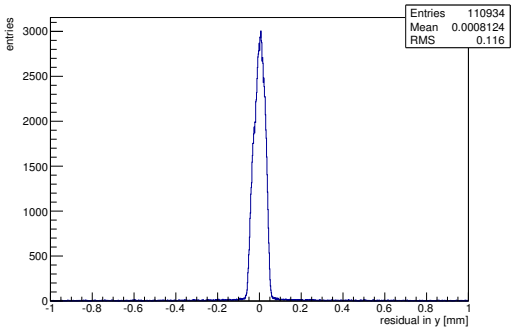

(j) Track residual in y.

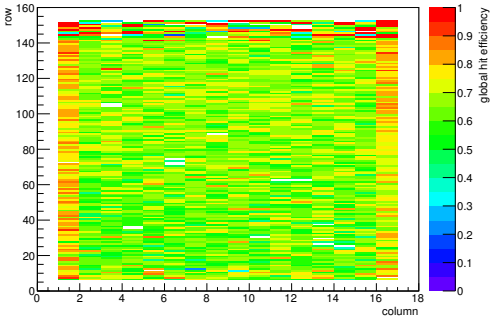

(k) Hit efficiency map.

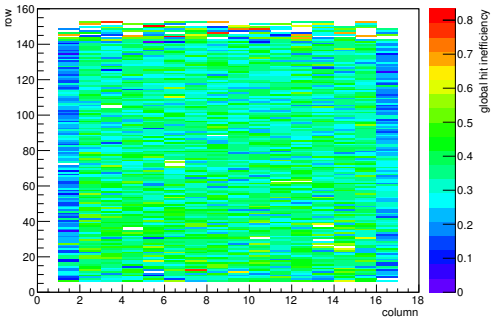

(l) Hit inefficiency map.

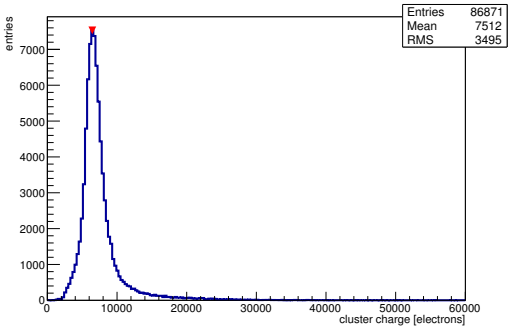

(m) Charge distribution (all cluster sizes included).

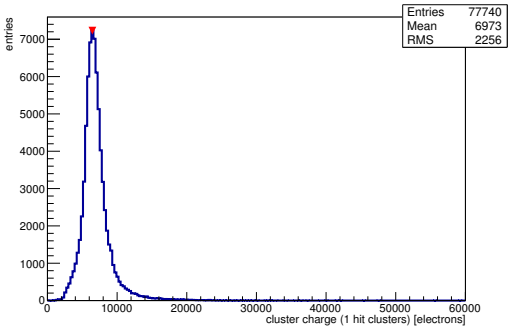

(n) Charge distribution (1 hit cluster).

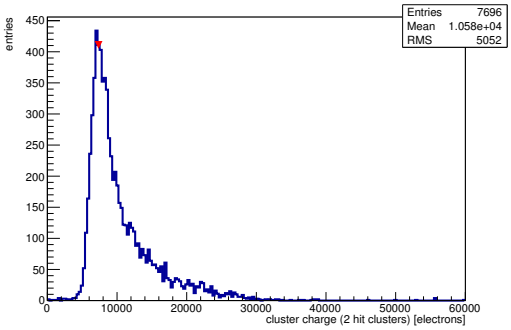

(o) Charge distribution (2 hit cluster).

Figure C.37: Detailed plots for test beam measurement of DO-I-11 (description see section 6.1) sample (running as DUT2) during runs 50598-50599 in the July 2011 test beam period at CERN SPS in area H6B. Summary of the data in chapter 9. *(cont.)*

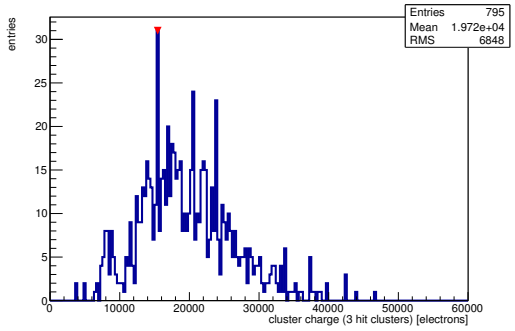

(p) Charge distribution (3 hit cluster).

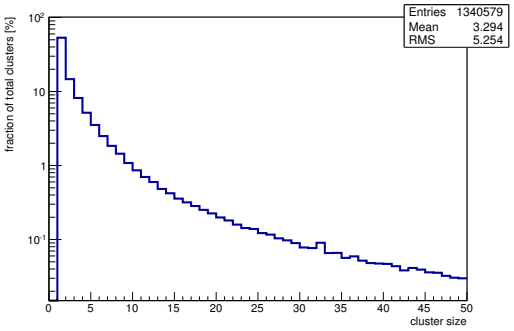

(q) Cluster size distribution.

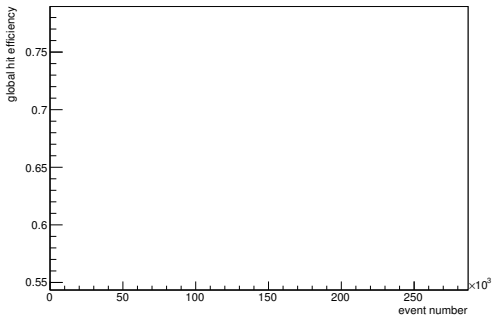

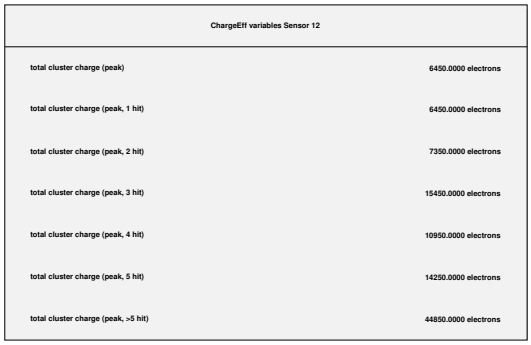

(r) Hit efficiency vs event number.

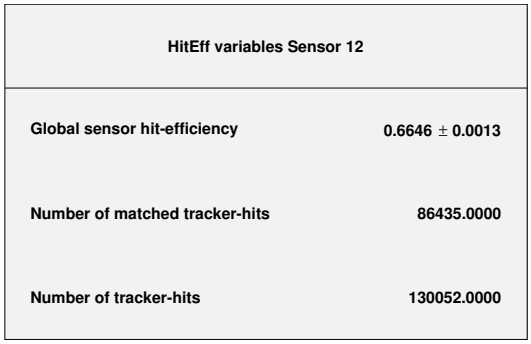

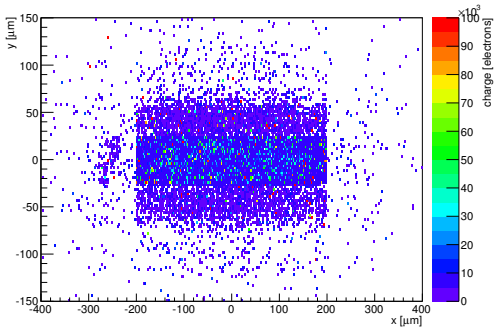

(s) Single pixel mean charge.

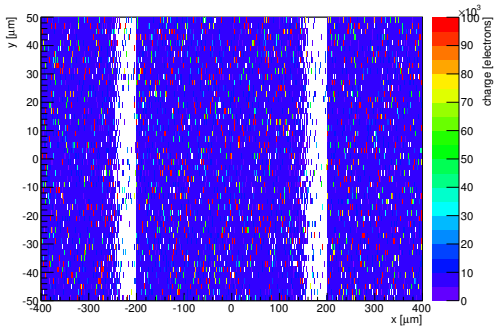

(t) Single pixel mean charge.

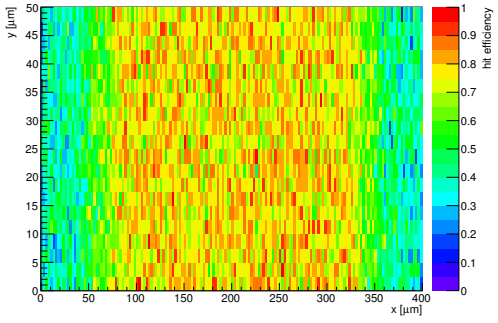

(u) Single pixel hit efficiency.

Figure C.37: Detailed plots for test beam measurement of DO-I-11 (description see section 6.1) sample (running as DUT2) during runs 50598-50599 in the July 2011 test beam period at CERN SPS in area H6B. Summary of the data in chapter 9.

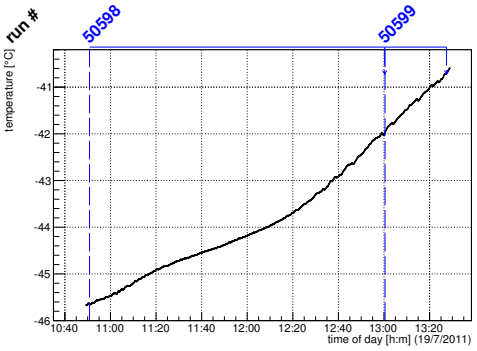

(a) Temperature vs time.

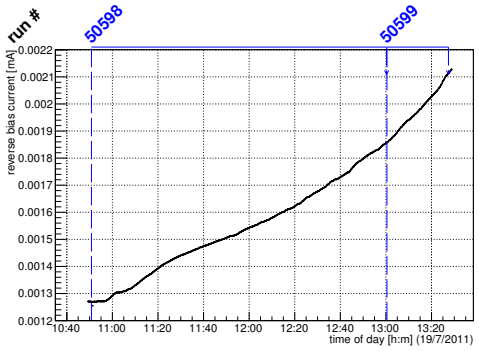

(b) Bias current vs time.

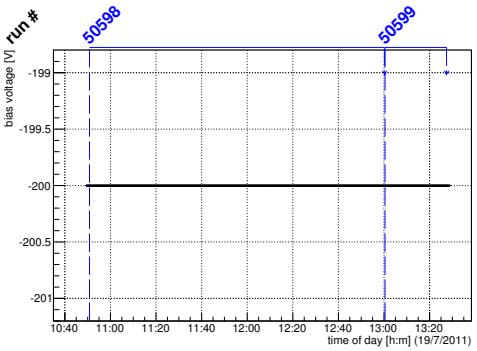

(c) Currently applied bias voltage vs time.

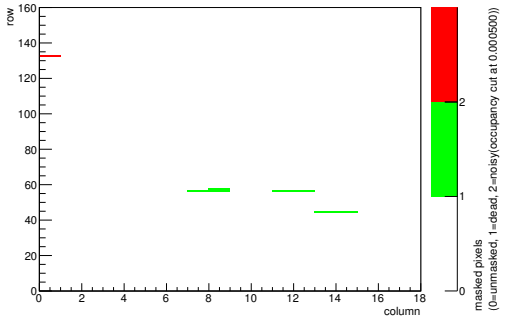

(d) Map of masked pixels.

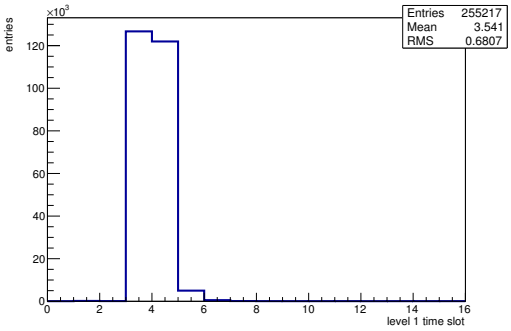

(e) Lvl1 distribution.

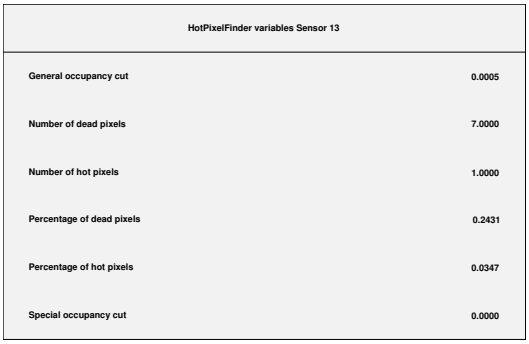

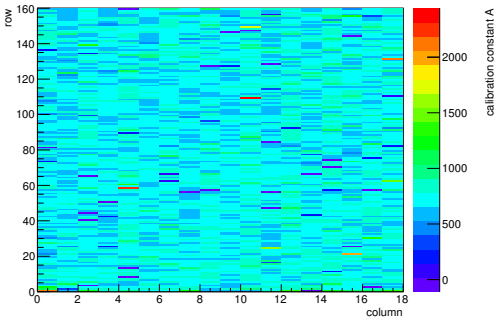

(f) Calibration constant A.

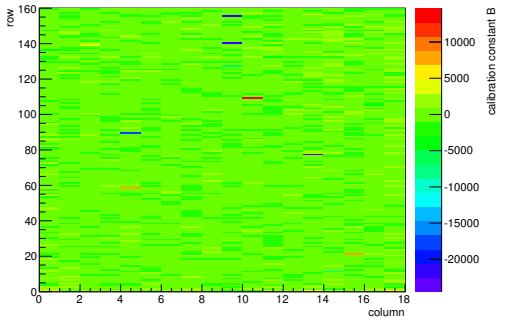

(g) Calibration constant B.

Figure C.38: Detailed plots for test beam measurement of DO-I-13 (description see section 6.1) sample (running as DUT3) during runs 50598-50599 in the July 2011 test beam period at CERN SPS in area H6B. Summary of the data in chapter 9. *(cont.)*

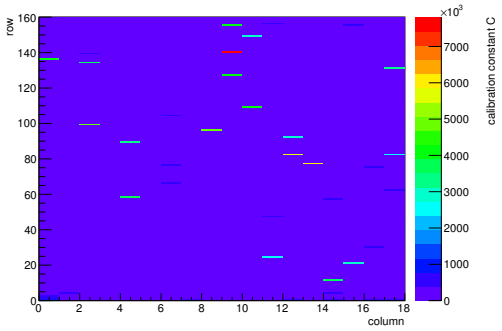

(h) Calibration constant C.

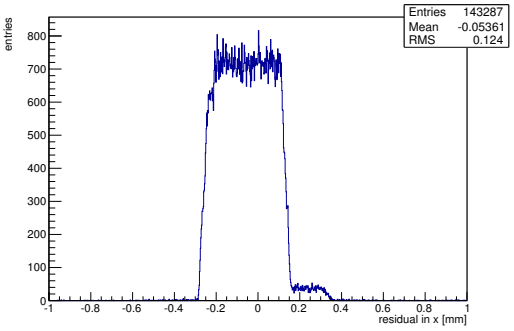

(i) Track residual in x.

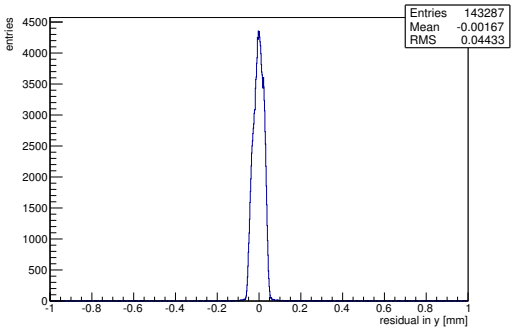

(j) Track residual in y.

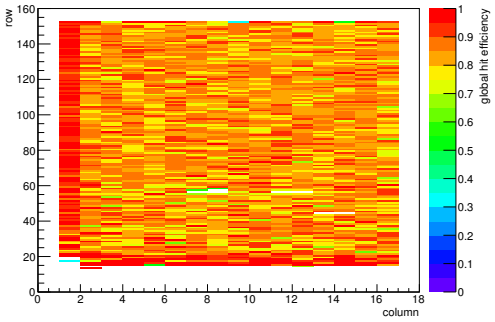

(k) Hit efficiency map.

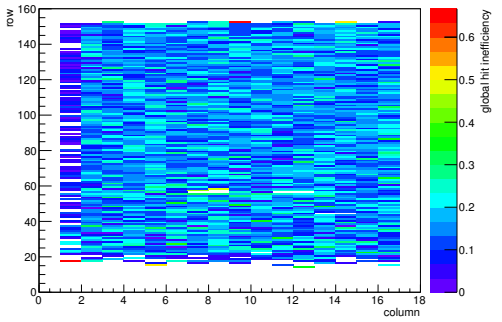

(l) Hit inefficiency map.

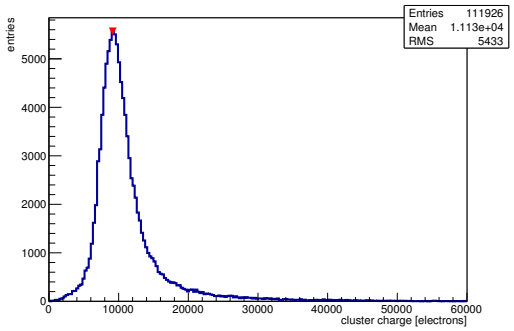

(m) Charge distribution (all cluster sizes included).

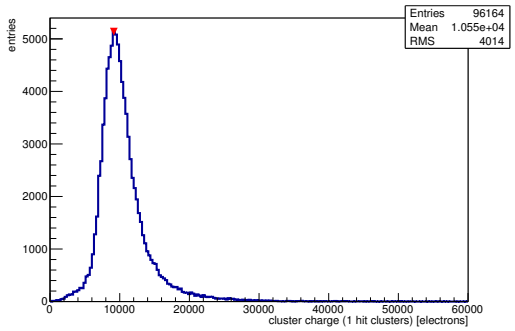

(n) Charge distribution (1 hit cluster).

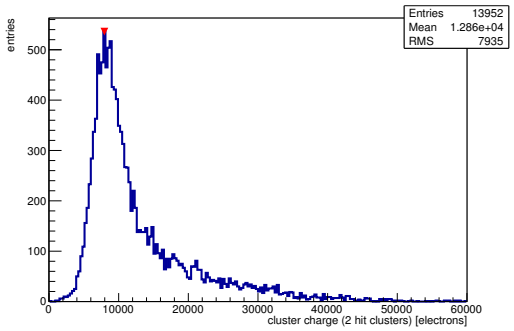

(o) Charge distribution (2 hit cluster).

Figure C.38: Detailed plots for test beam measurement of DO-I-13 (description see section 6.1) sample (running as DUT3) during runs 50598-50599 in the July 2011 test beam period at CERN SPS in area H6B. Summary of the data in chapter 9. *(cont.)*

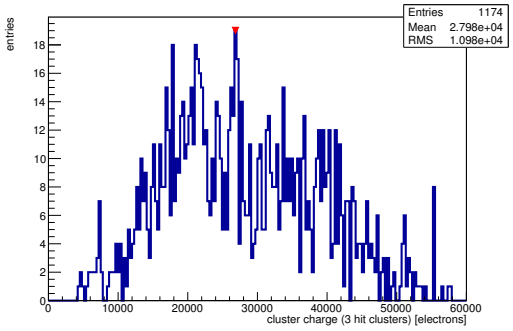

(p) Charge distribution (3 hit cluster).

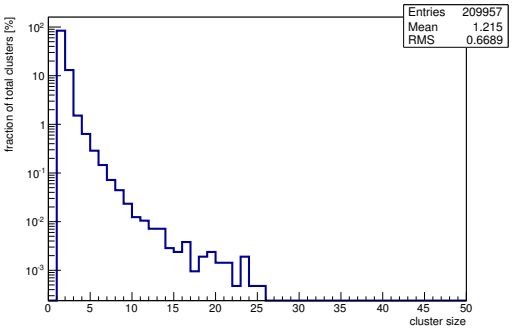

(q) Cluster size distribution.

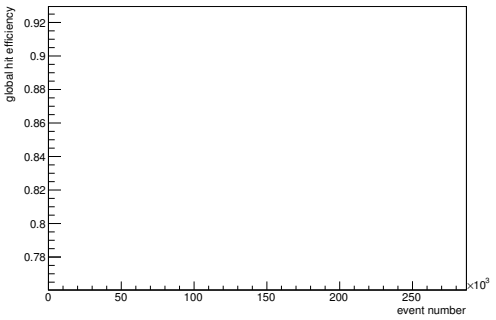

(r) Hit efficiency vs event number.

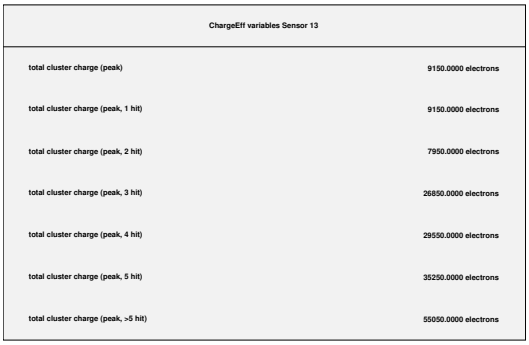

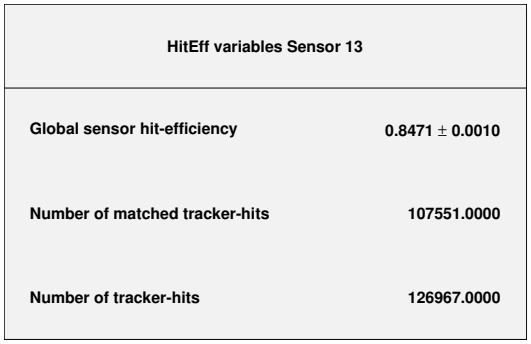

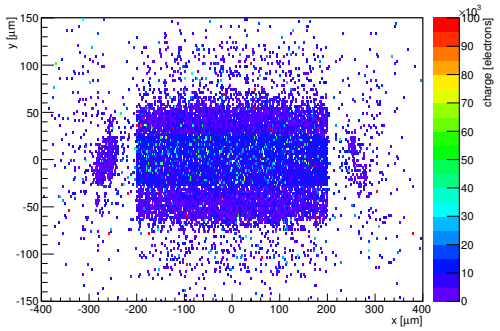

(s) Single pixel mean charge.

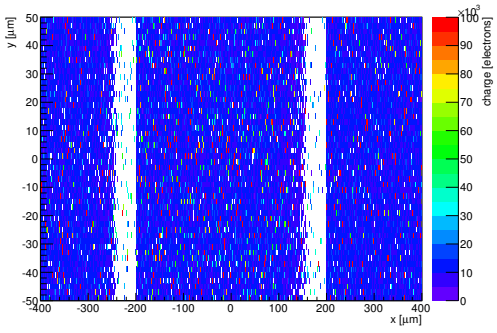

(t) Single pixel mean charge.

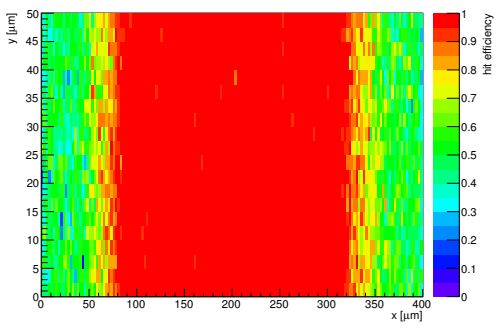

(u) Single pixel hit efficiency.

Figure C.38: Detailed plots for test beam measurement of DO-I-13 (description see section 6.1) sample (running as DUT3) during runs 50598-50599 in the July 2011 test beam period at CERN SPS in area H6B. Summary of the data in chapter 9.

C.2.8 Runs 50600-50603

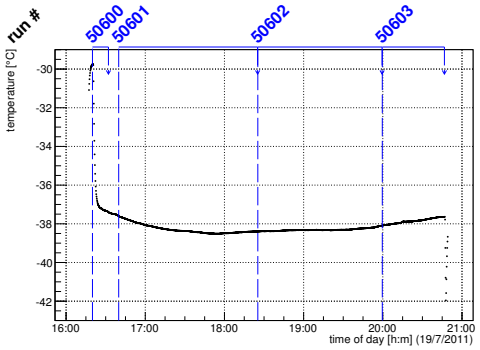

(a) Temperature vs time.

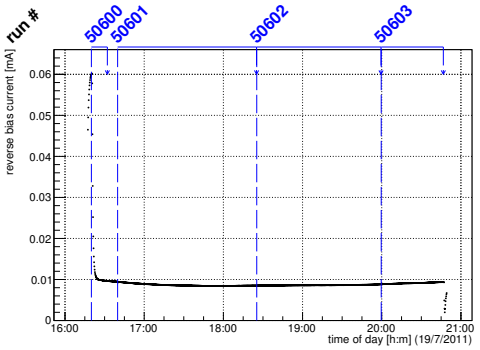

(b) Bias current vs time.

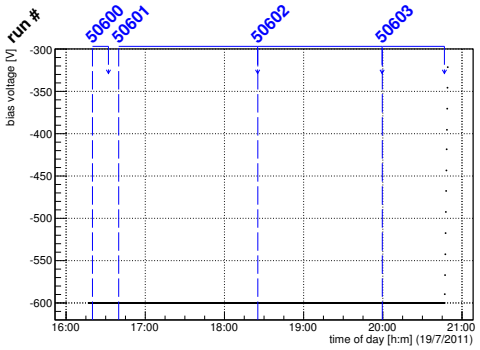

(c) Currently applied bias voltage vs time.

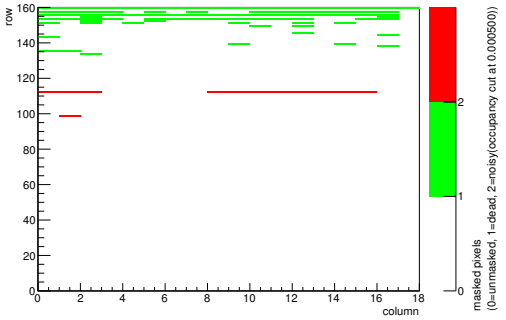

(d) Map of masked pixels.

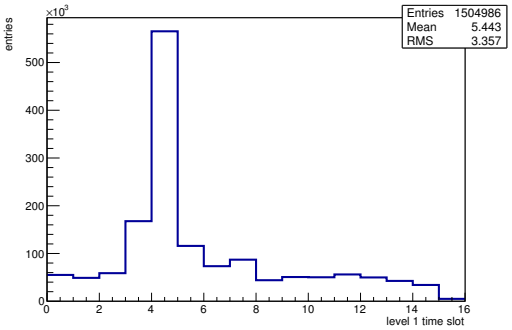

(e) Lvl1 distribution.

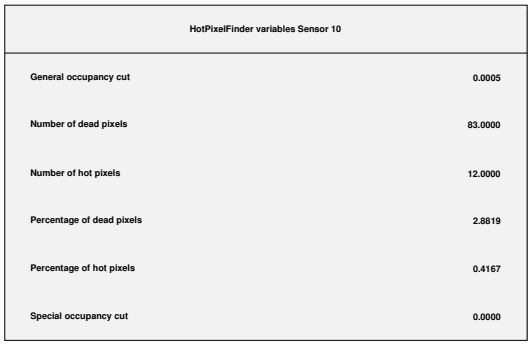

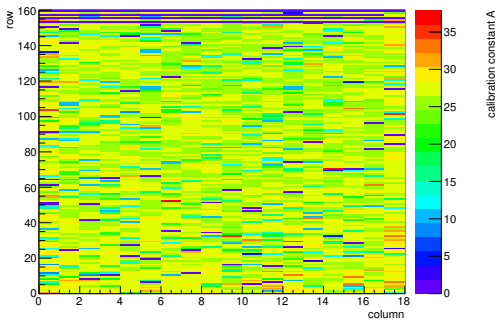

(f) Calibration constant A.

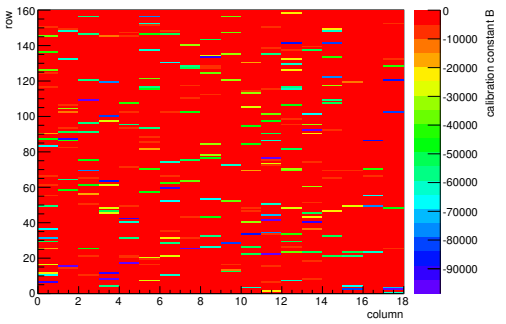

(g) Calibration constant B.

Figure C.39: Detailed plots for test beam measurement of KEK1R (description see section 6.1) sample (running as DUT0) during runs 50600-50603 in the July 2011 test beam period at CERN SPS in area H6B. Summary of the data in chapter 9. *(cont.)*

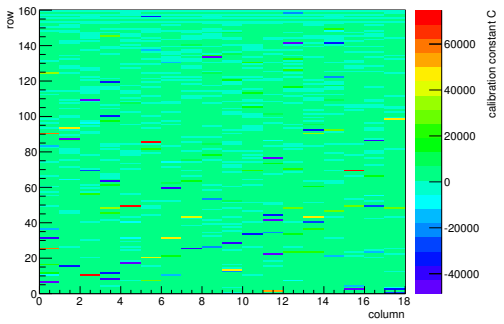

(h) Calibration constant C.

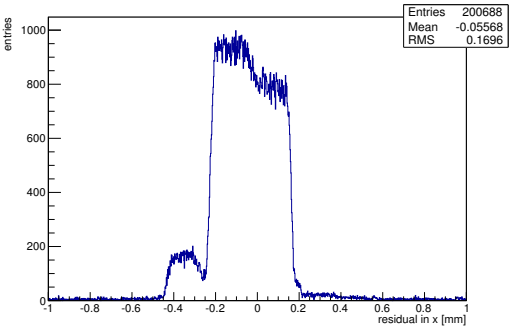

(i) Track residual in x.

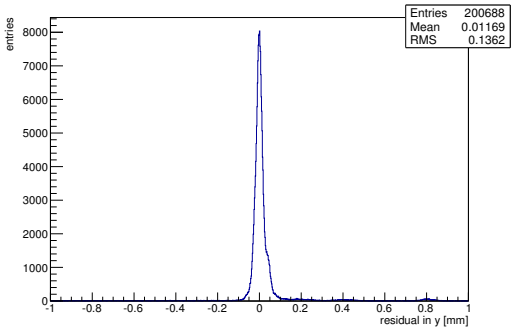

(j) Track residual in y.

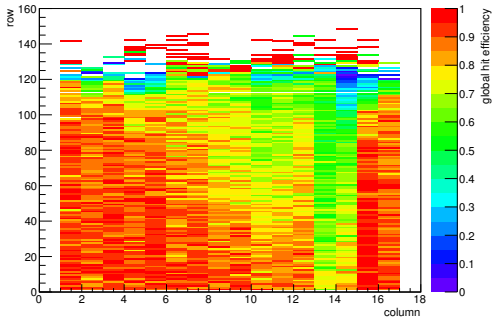

(k) Hit efficiency map.

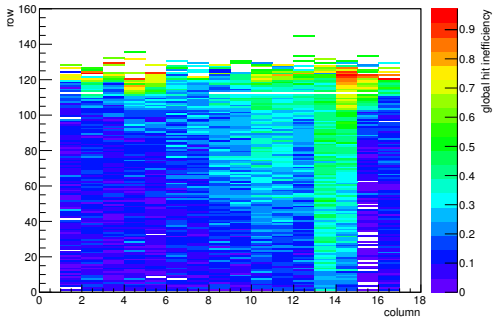

(l) Hit inefficiency map.

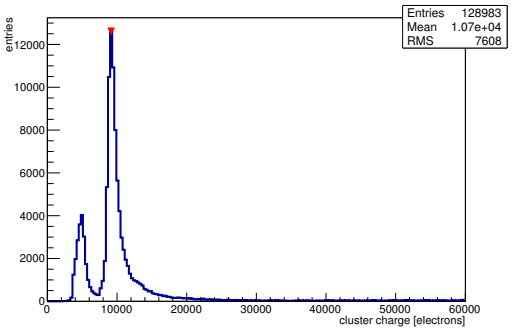

(m) Charge distribution (all cluster sizes included).

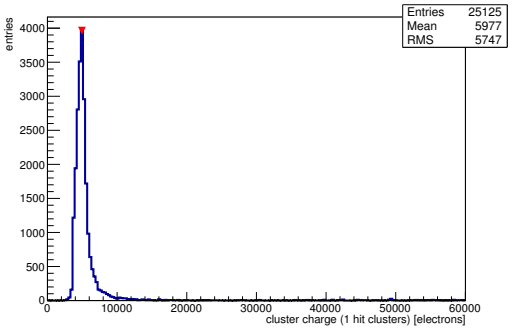

(n) Charge distribution (1 hit cluster).

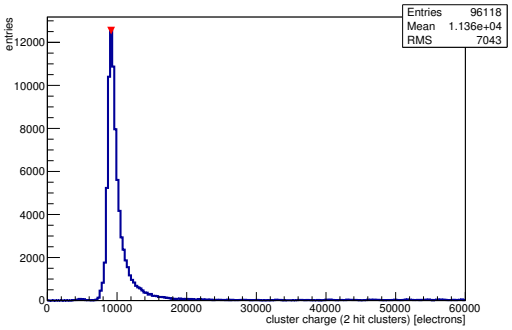

(o) Charge distribution (2 hit cluster).

Figure C.39: Detailed plots for test beam measurement of KEK1R (description see section 6.1) sample (running as DUT0) during runs 50600-50603 in the July 2011 test beam period at CERN SPS in area H6B. Summary of the data in chapter 9. *(cont.)*

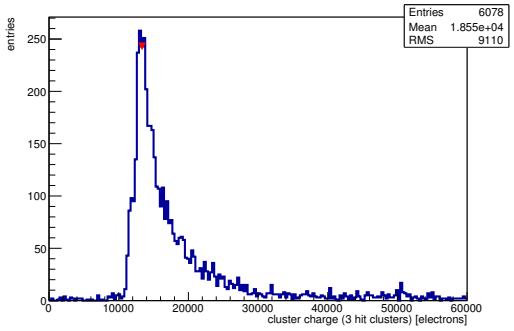

(p) Charge distribution (3 hit cluster).

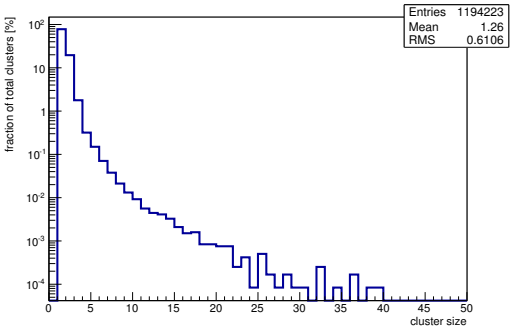

(q) Cluster size distribution.

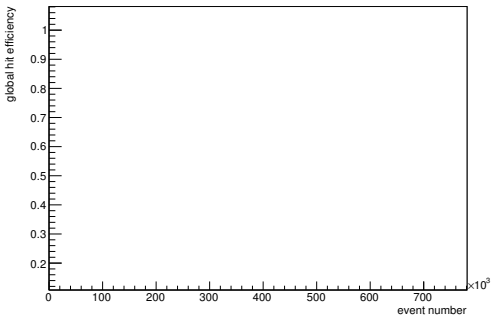

(r) Hit efficiency vs event number.

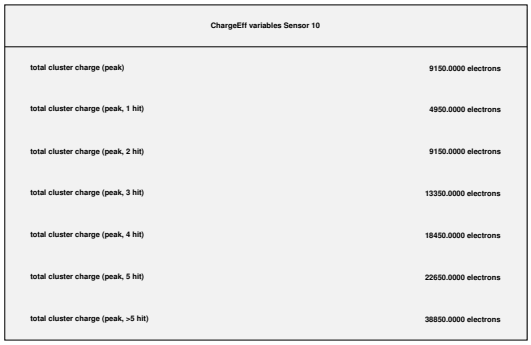

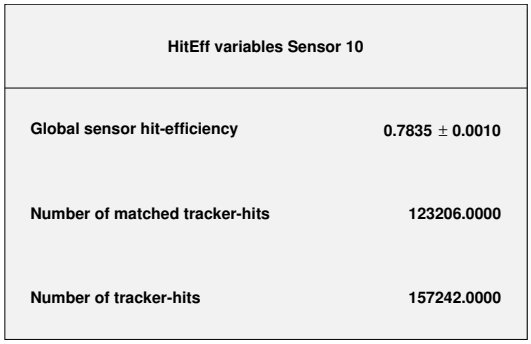

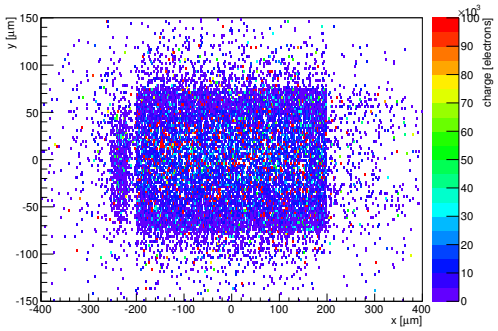

(s) Single pixel mean charge.

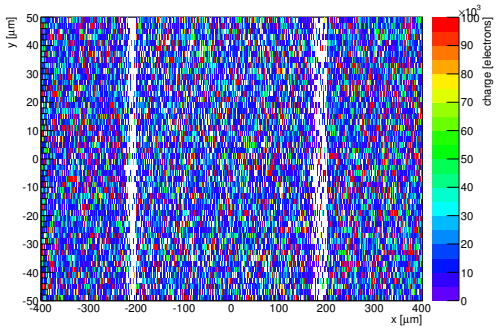

(t) Single pixel mean charge.

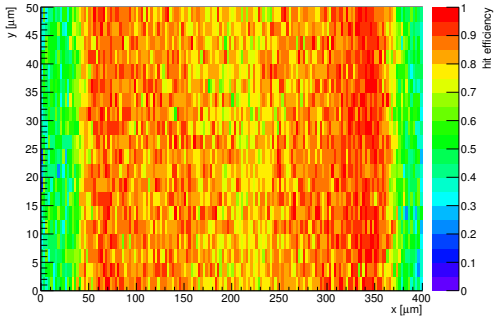

(u) Single pixel hit efficiency.

Figure C.39: Detailed plots for test beam measurement of KEK1R (description see section 6.1) sample (running as DUT0) during runs 50600-50603 in the July 2011 test beam period at CERN SPS in area H6B. Summary of the data in chapter 9.

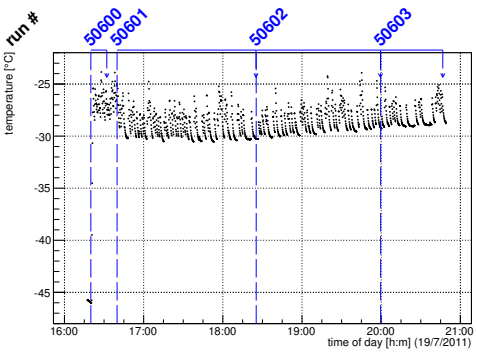

(a) Temperature vs time.

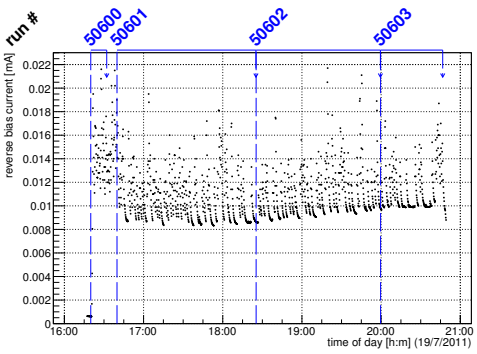

(b) Bias current vs time.

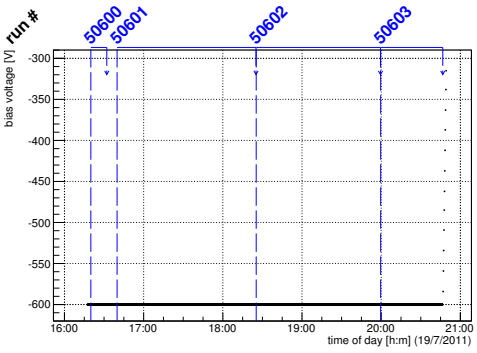

(c) Currently applied bias voltage vs time.

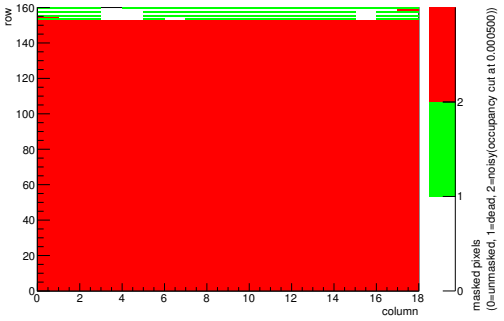

(d) Map of masked pixels.

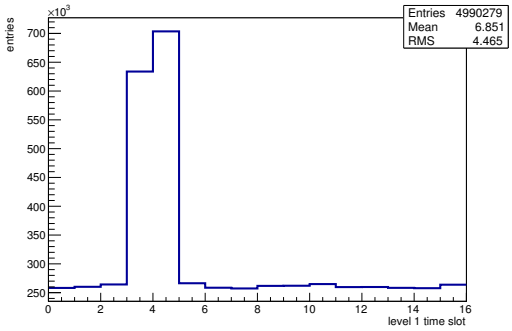

(e) Lvl1 distribution.

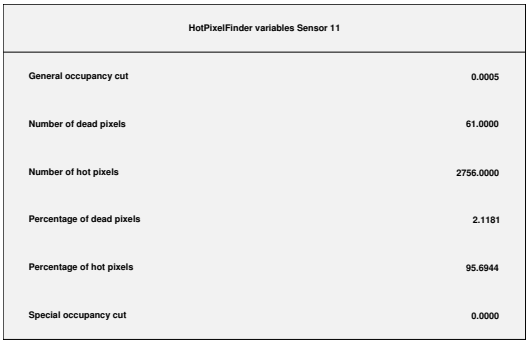

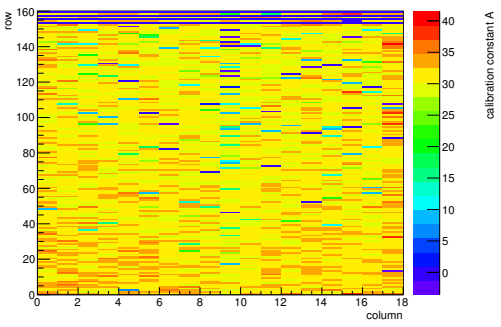

(f) Calibration constant A.

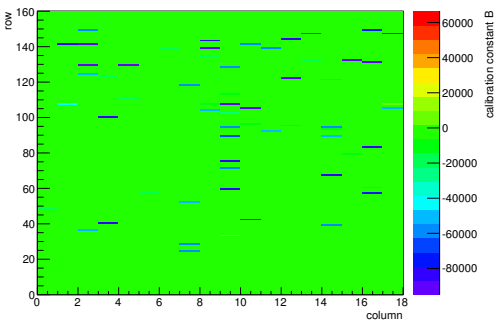

(g) Calibration constant B.

Figure C.40: Detailed plots for test beam measurement of KEK2R (description see section 6.1) sample (running as DUT1) during runs 50600-50603 in the July 2011 test beam period at CERN SPS in area H6B. Summary of the data in chapter 9. *(cont.)*

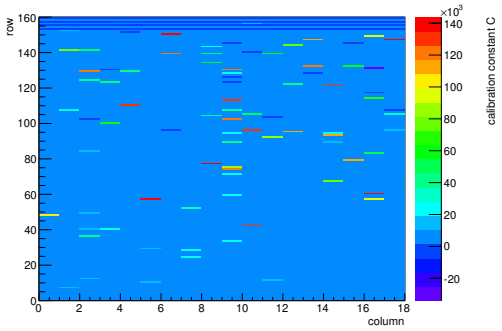

(h) Calibration constant C.

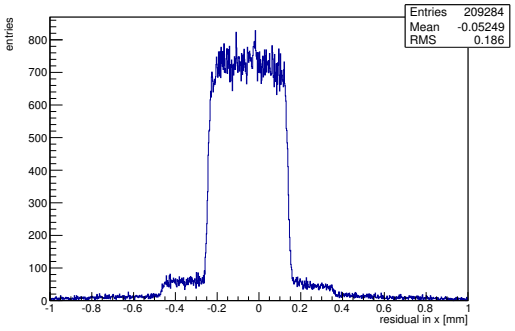

(i) Track residual in x.

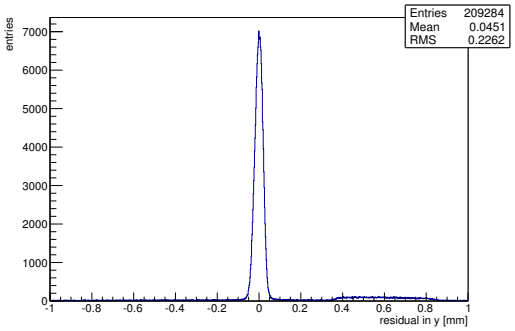

(j) Track residual in y.

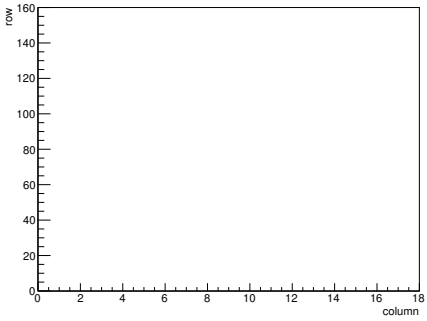

(k) Hit efficiency map.

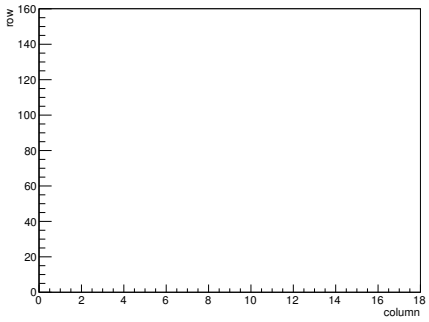

(l) Hit inefficiency map.

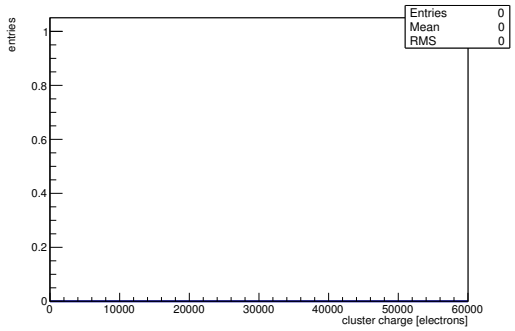

(m) Charge distribution (all cluster sizes included).

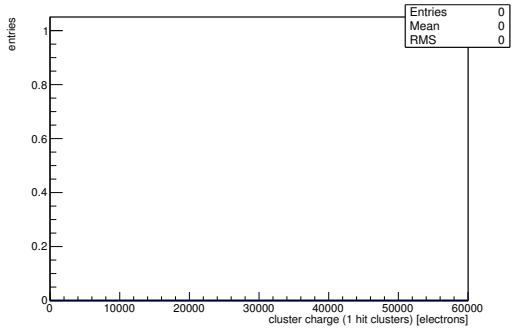

(n) Charge distribution (1 hit cluster).

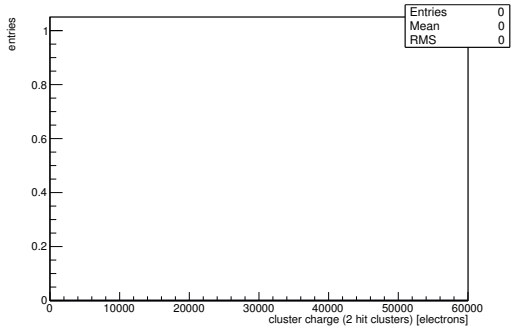

(o) Charge distribution (2 hit cluster).

Figure C.40: Detailed plots for test beam measurement of KEK2R (description see section 6.1) sample (running as DUT1) during runs 50600-50603 in the July 2011 test beam period at CERN SPS in area H6B. Summary of the data in chapter 9. *(cont.)*

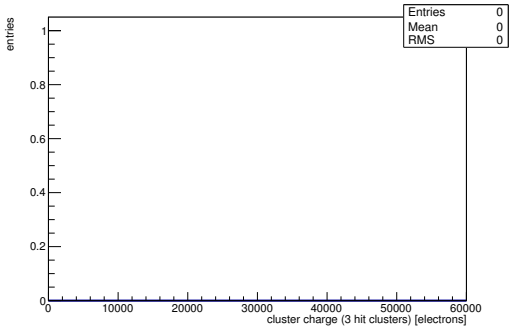

(p) Charge distribution (3 hit cluster).

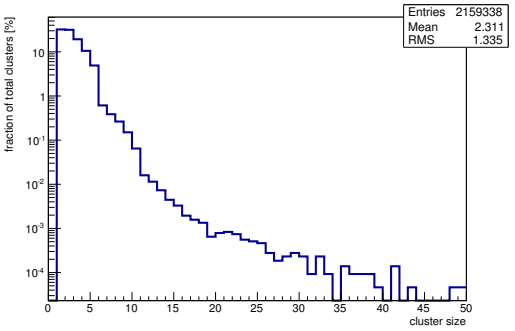

(q) Cluster size distribution.

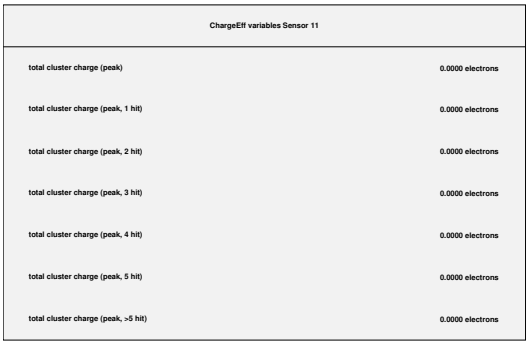

(r) Hit efficiency vs event number.

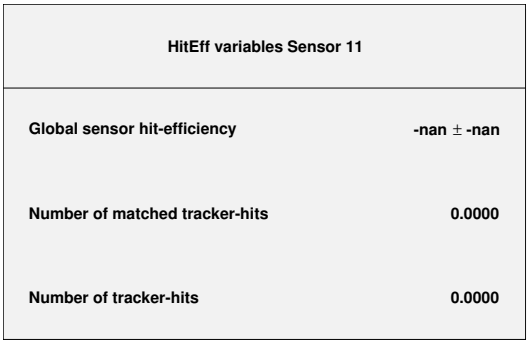

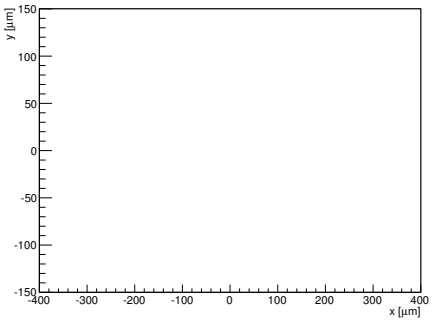

(s) Single pixel mean charge.

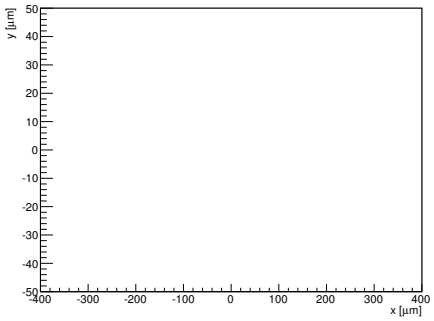

(t) Single pixel mean charge.

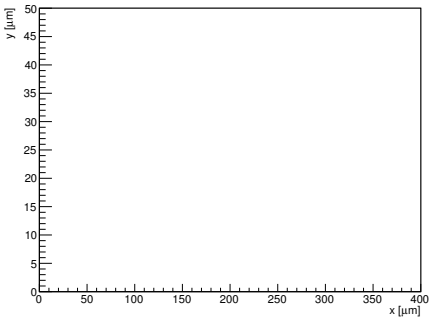

(u) Single pixel hit efficiency.

Figure C.40: Detailed plots for test beam measurement of KEK2R (description see section 6.1) sample (running as DUT1) during runs 50600-50603 in the July 2011 test beam period at CERN SPS in area H6B. Summary of the data in chapter 9.

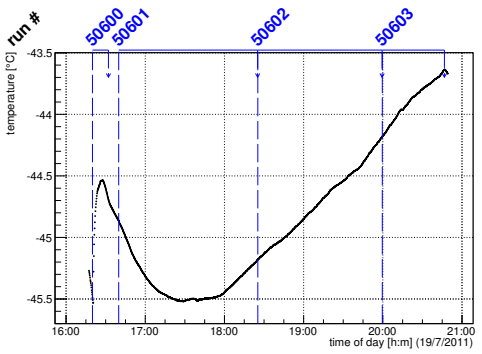

(a) Temperature vs time.

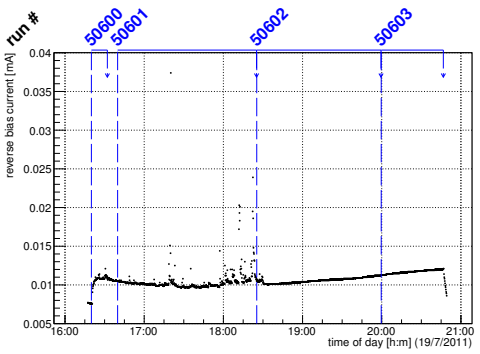

(b) Bias current vs time.

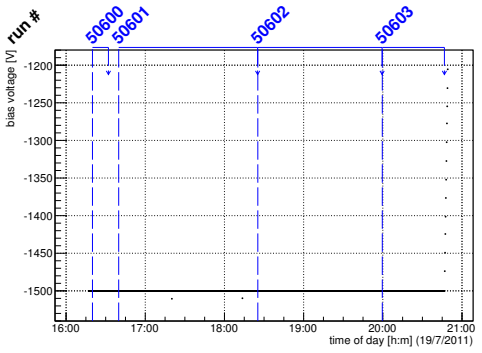

(c) Currently applied bias voltage vs time.

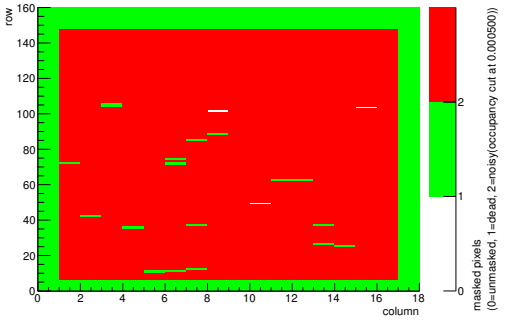

(d) Map of masked pixels.

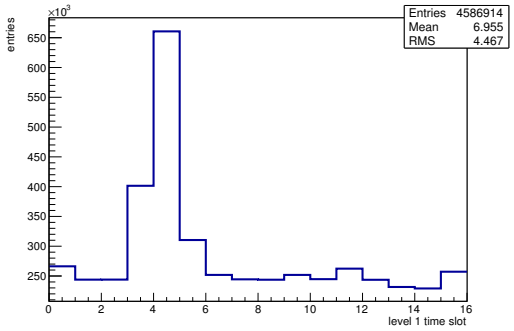

(e) Lvl1 distribution.

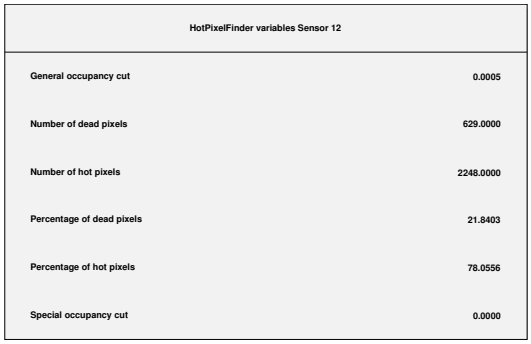

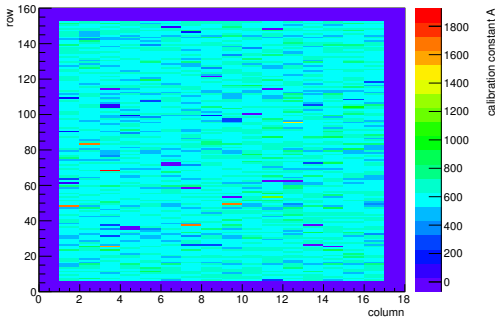

(f) Calibration constant A.

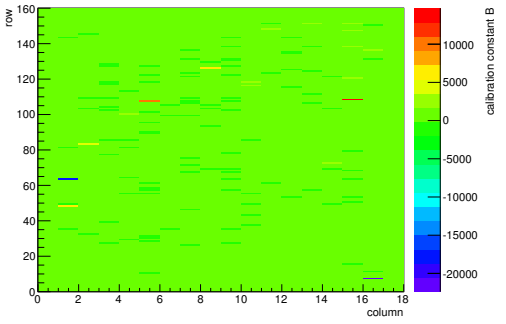

(g) Calibration constant B.

Figure C.41: Detailed plots for test beam measurement of DO-I-11 (description see section 6.1) sample (running as DUT2) during runs 50600-50603 in the July 2011 test beam period at CERN SPS in area H6B. Summary of the data in chapter 9. *(cont.)*

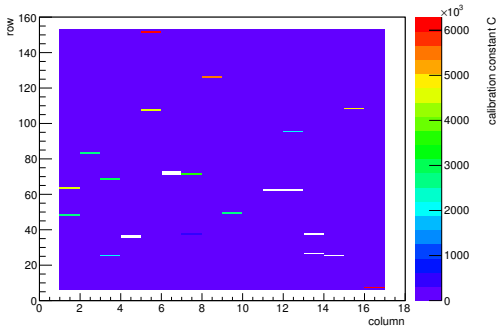

(h) Calibration constant C.

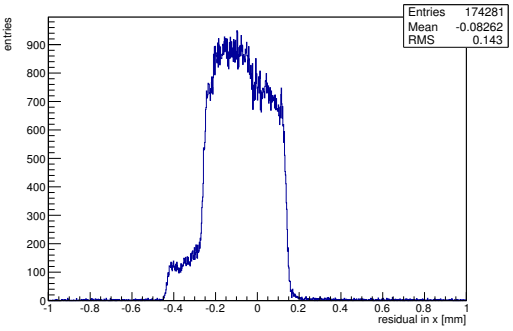

(i) Track residual in x.

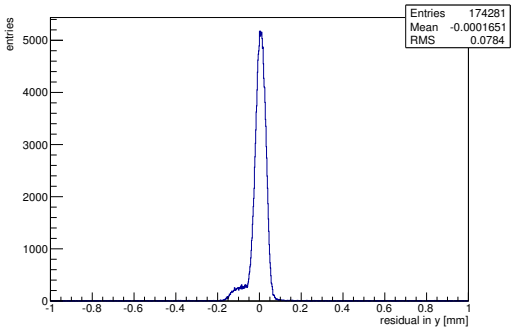

(j) Track residual in y.

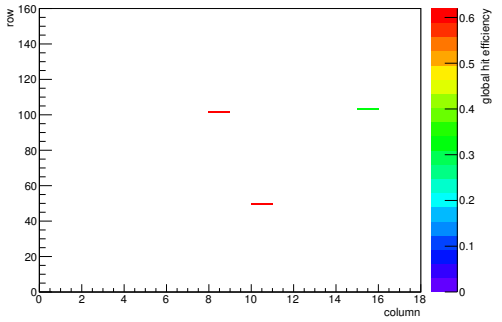

(k) Hit efficiency map.

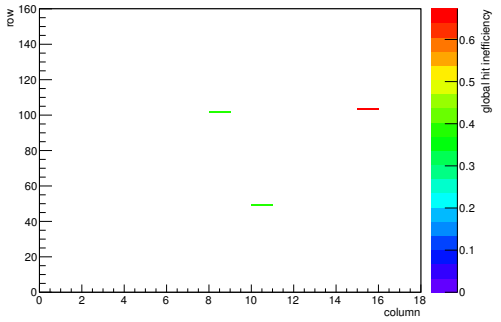

(l) Hit inefficiency map.

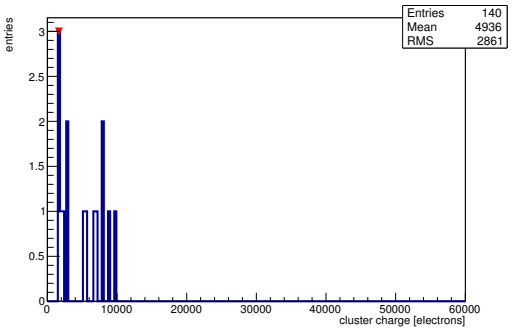

(m) Charge distribution (all cluster sizes included).

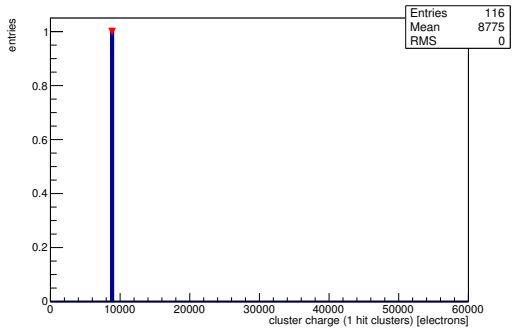

(n) Charge distribution (1 hit cluster).

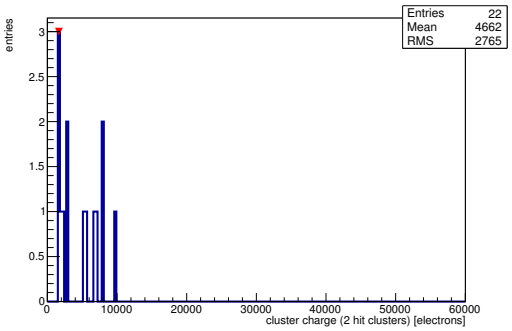

(o) Charge distribution (2 hit cluster).

Figure C.41: Detailed plots for test beam measurement of DO-I-11 (description see section 6.1) sample (running as DUT2) during runs 50600-50603 in the July 2011 test beam period at CERN SPS in area H6B. Summary of the data in chapter 9. *(cont.)*

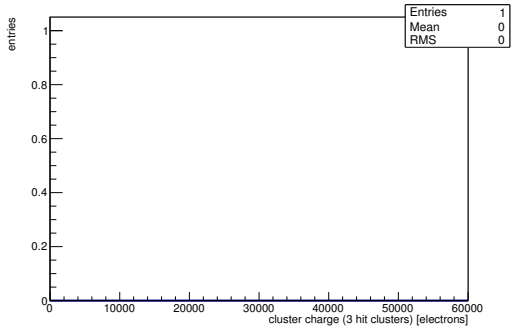

(p) Charge distribution (3 hit cluster).

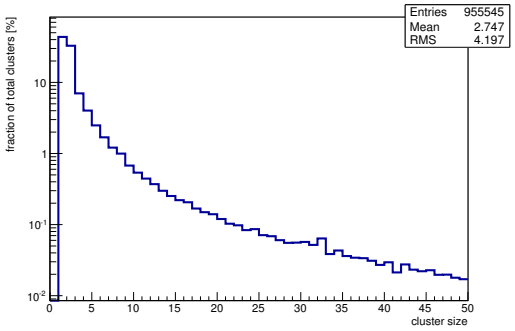

(q) Cluster size distribution.

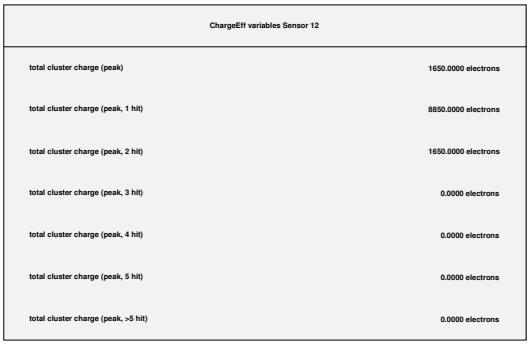

(r) Hit efficiency vs event number.

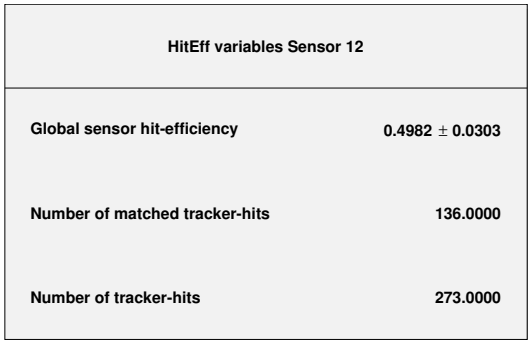

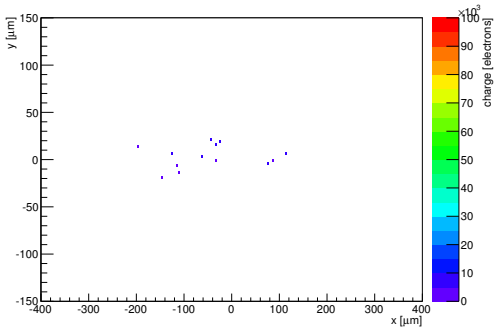

(s) Single pixel mean charge.

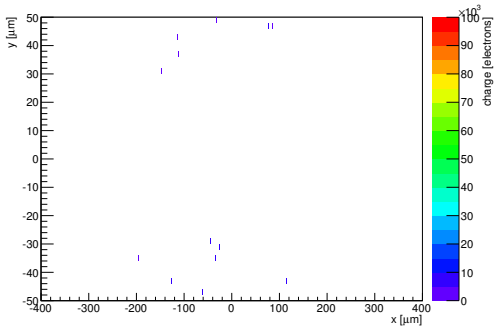

(t) Single pixel mean charge.

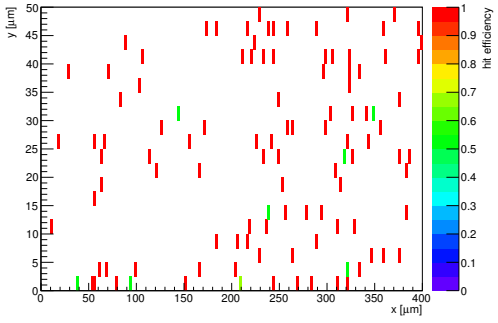

(u) Single pixel hit efficiency.

Figure C.41: Detailed plots for test beam measurement of DO-I-11 (description see section 6.1) sample (running as DUT2) during runs 50600-50603 in the July 2011 test beam period at CERN SPS in area H6B. Summary of the data in chapter 9.

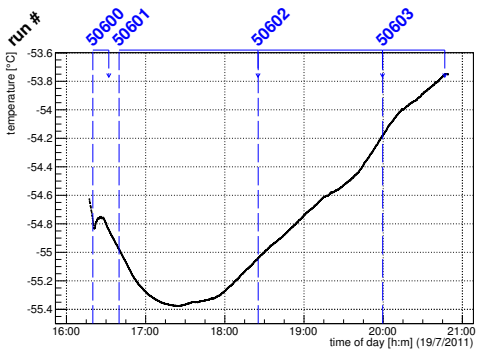

(a) Temperature vs time.

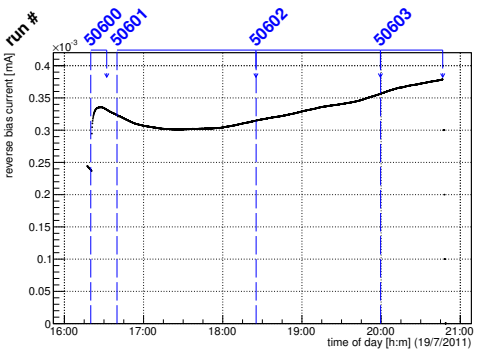

(b) Bias current vs time.

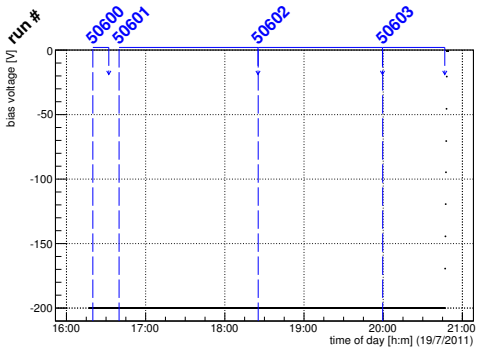

(c) Currently applied bias voltage vs time.

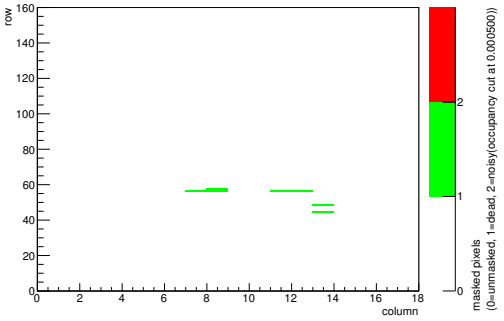

(d) Map of masked pixels.

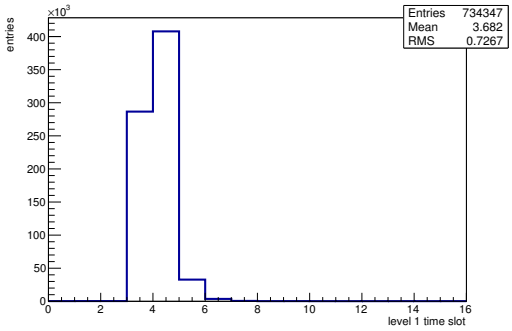

(e) Lvl1 distribution.

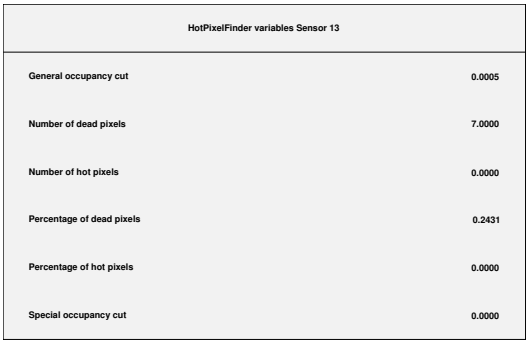

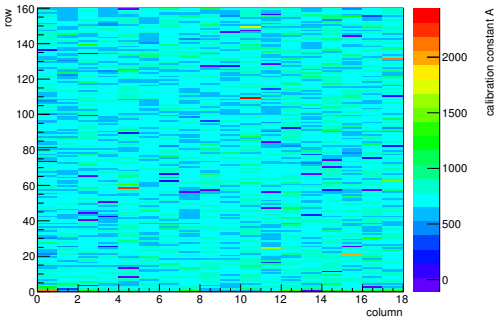

(f) Calibration constant A.

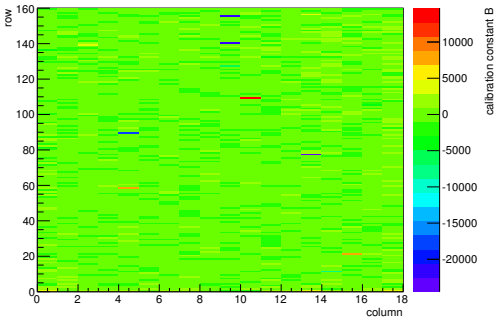

(g) Calibration constant B.

Figure C.42: Detailed plots for test beam measurement of DO-I-13 (description see section 6.1) sample (running as DUT3) during runs 50600-50603 in the July 2011 test beam period at CERN SPS in area H6B. Summary of the data in chapter 9. *(cont.)*

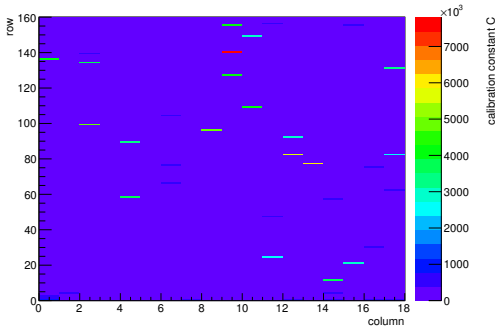

(h) Calibration constant C.

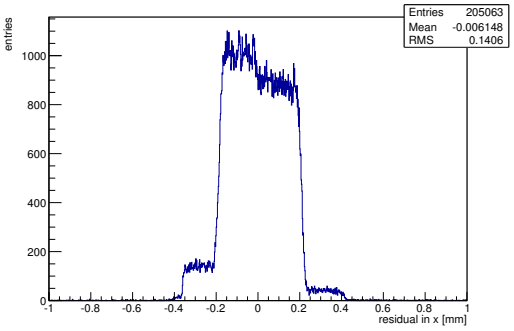

(i) Track residual in x.

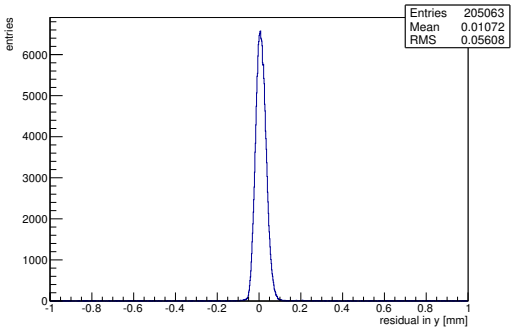

(j) Track residual in y.

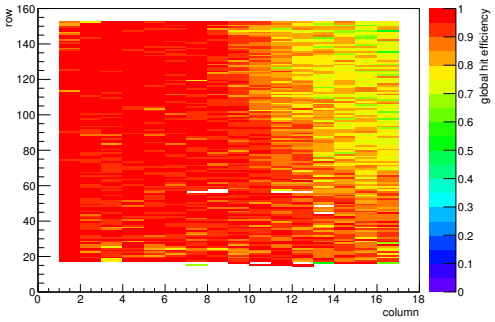

(k) Hit efficiency map.

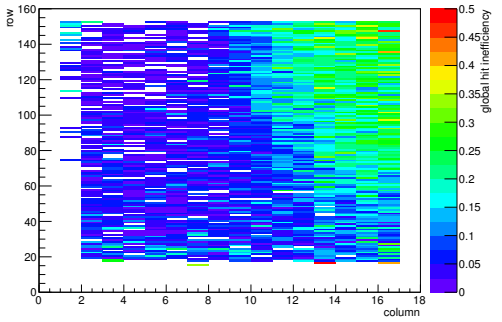

(l) Hit inefficiency map.

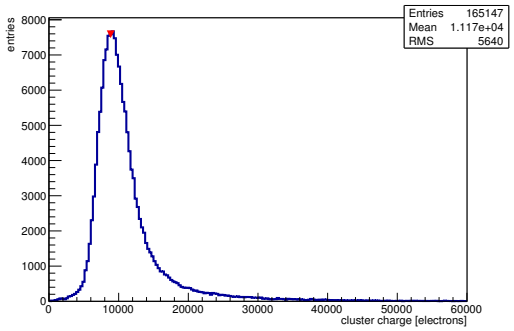

(m) Charge distribution (all cluster sizes included).

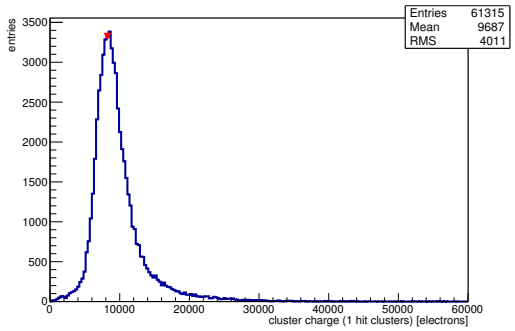

(n) Charge distribution (1 hit cluster).

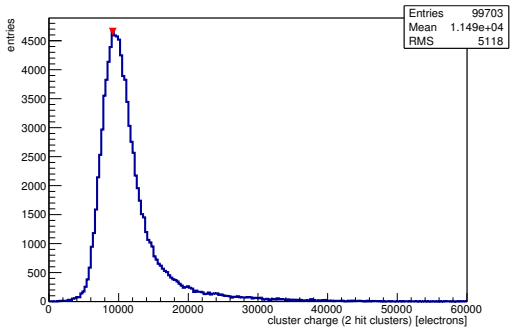

(o) Charge distribution (2 hit cluster).

Figure C.42: Detailed plots for test beam measurement of DO-I-13 (description see section 6.1) sample (running as DUT3) during runs 50600-50603 in the July 2011 test beam period at CERN SPS in area H6B. Summary of the data in chapter 9. *(cont.)*

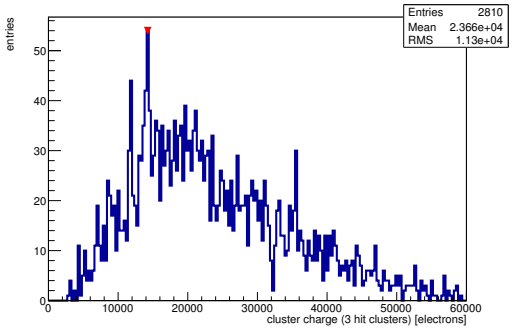

(p) Charge distribution (3 hit cluster).

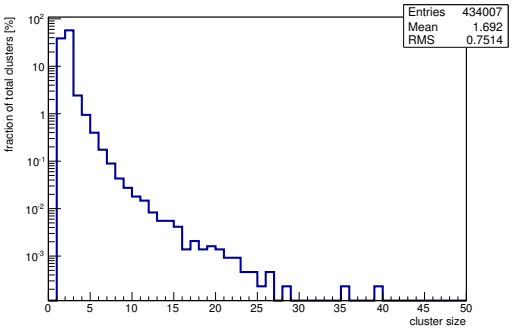

(q) Cluster size distribution.

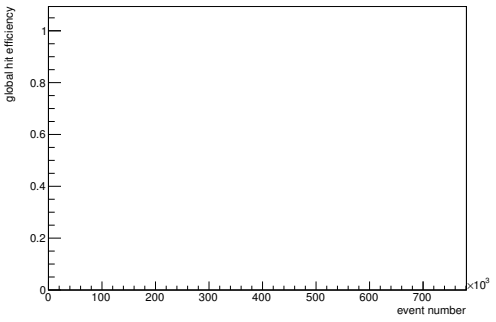

(r) Hit efficiency vs event number.

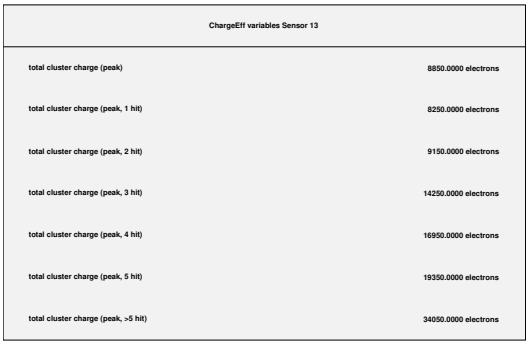

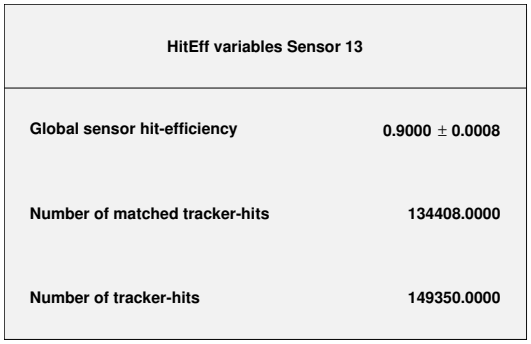

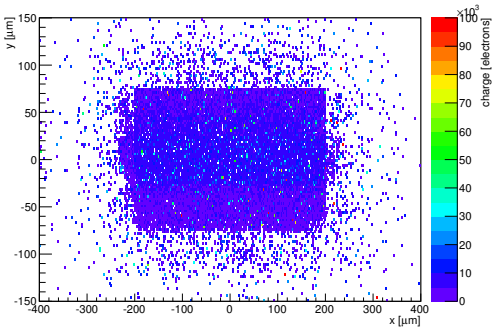

(s) Single pixel mean charge.

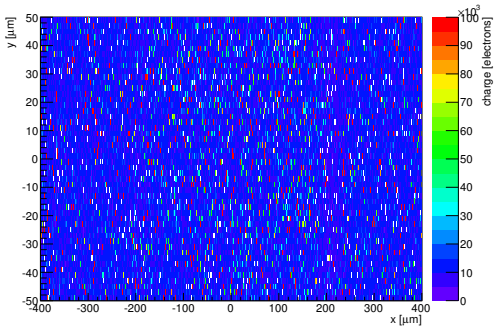

(t) Single pixel mean charge.

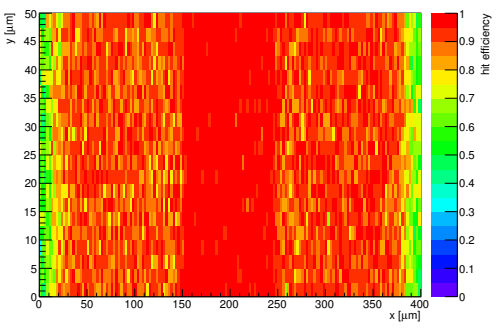

(u) Single pixel hit efficiency.

Figure C.42: Detailed plots for test beam measurement of DO-I-13 (description see section 6.1) sample (running as DUT3) during runs 50600-50603 in the July 2011 test beam period at CERN SPS in area H6B. Summary of the data in chapter 9.

C.3 CERN SPS September 2011

C.3.1 Runs 61112-61120

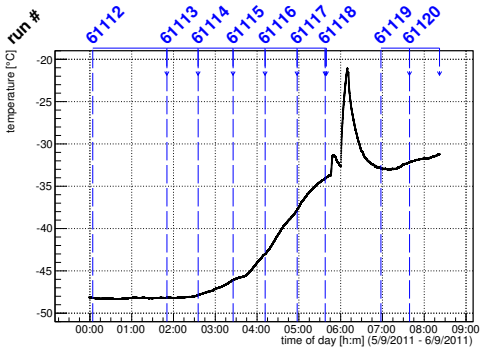

(a) Temperature vs time.

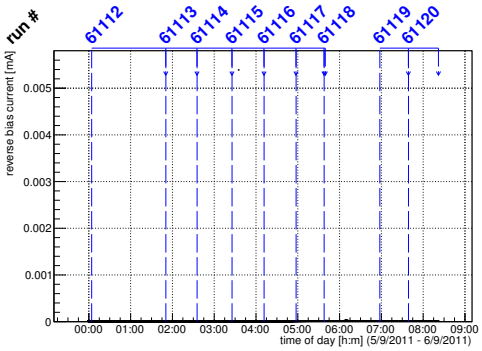

(b) Bias current vs time.

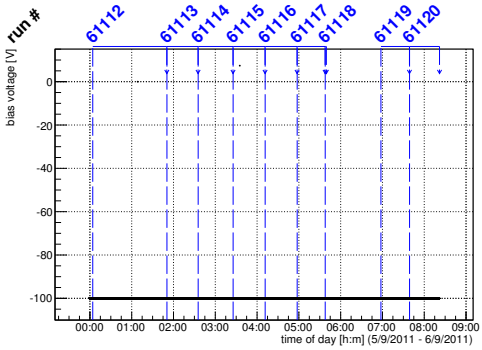

(c) Currently applied bias voltage vs time.

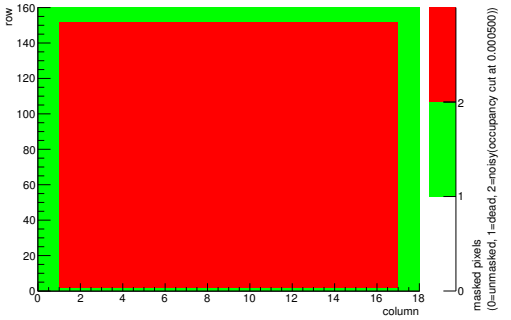

(d) Map of masked pixels.

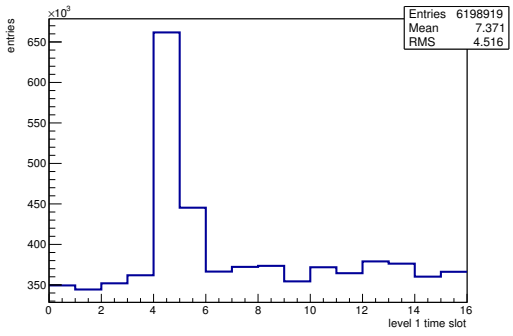

(e) Lvl1 distribution.

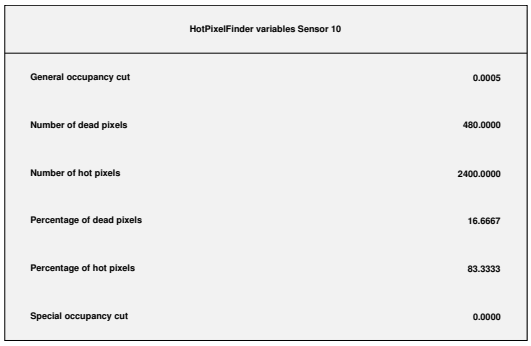

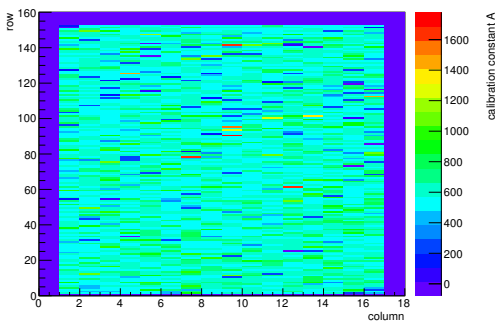

(f) Calibration constant A.

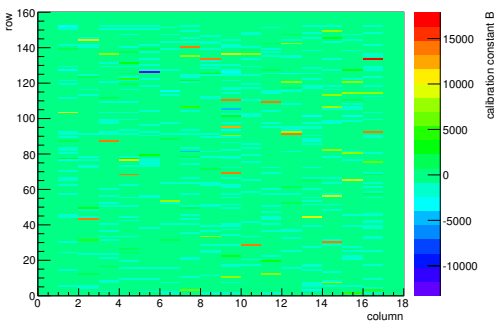

(g) Calibration constant B.

Figure C.43: Detailed plots for test beam measurement of SLID10 (description see section 6.1) sample (running as DUT0) during runs 61112-61120 in the September 2011 test beam period at CERN SPS in area H6B. Summary of the data in chapter 9. *(cont.)*

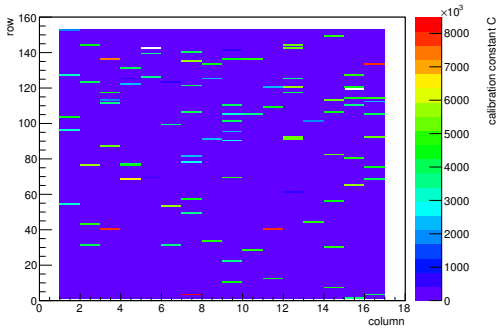

(h) Calibration constant C.

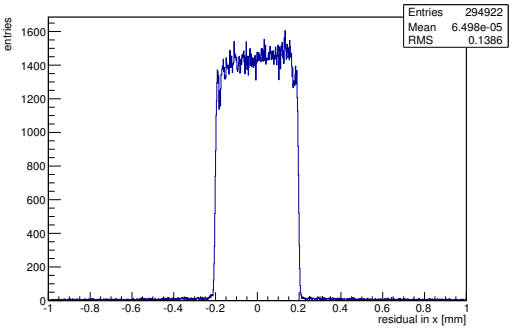

(i) Track residual in x.

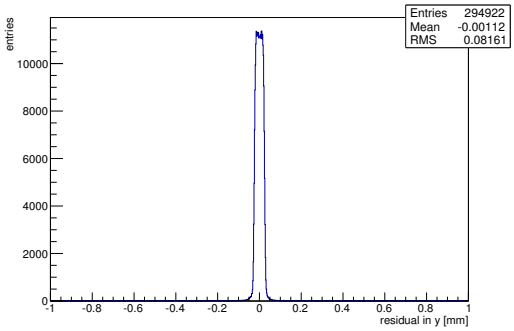

(j) Track residual in y.

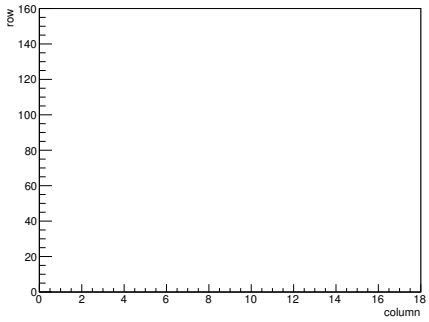

(k) Hit efficiency map.

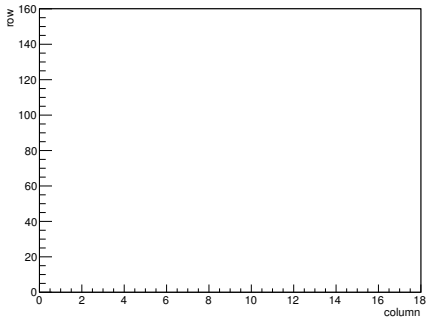

(l) Hit inefficiency map.

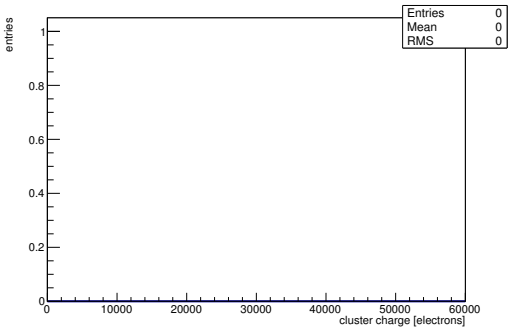

(m) Charge distribution (all cluster sizes included).

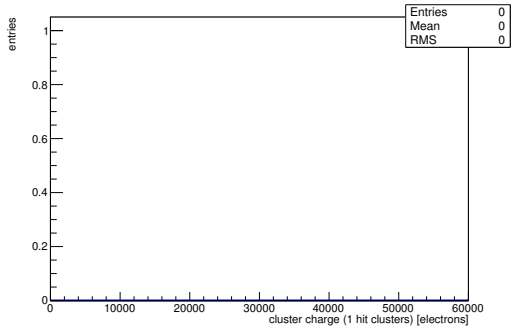

(n) Charge distribution (1 hit cluster).

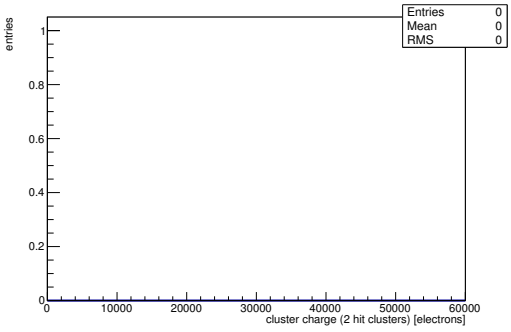

(o) Charge distribution (2 hit cluster).

Figure C.43: Detailed plots for test beam measurement of SLID10 (description see section 6.1) sample (running as DUT0) during runs 61112-61120 in the September 2011 test beam period at CERN SPS in area H6B. Summary of the data in chapter 9. *(cont.)*

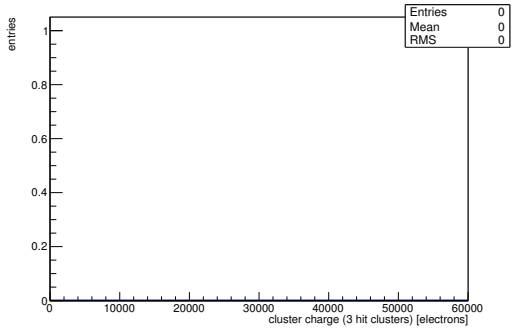

(p) Charge distribution (3 hit cluster).

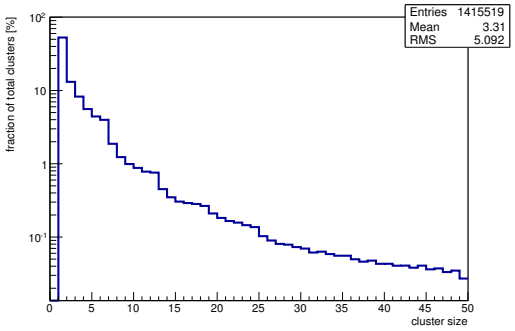

(q) Cluster size distribution.

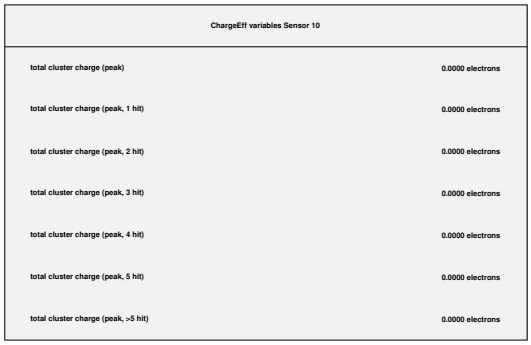

(r) Hit efficiency vs event number.

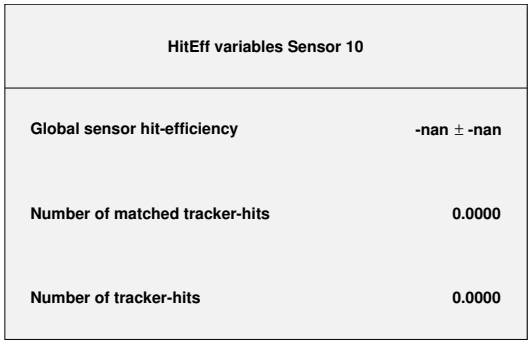

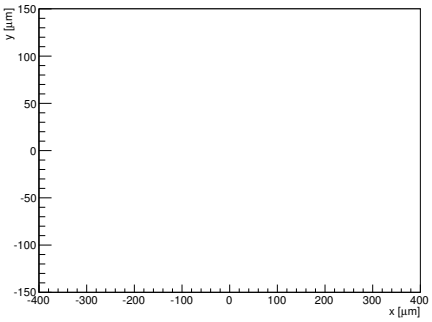

(s) Single pixel mean charge.

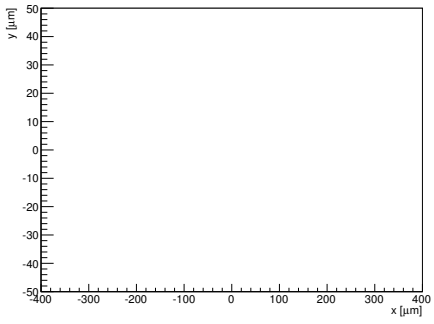

(t) Single pixel mean charge.

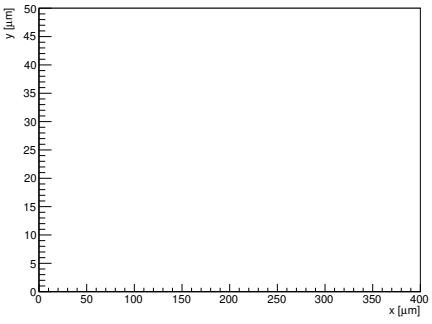

(u) Single pixel hit efficiency.

Figure C.43: Detailed plots for test beam measurement of SLID10 (description see section 6.1) sample (running as DUT0) during runs 61112-61120 in the September 2011 test beam period at CERN SPS in area H6B. Summary of the data in chapter 9.

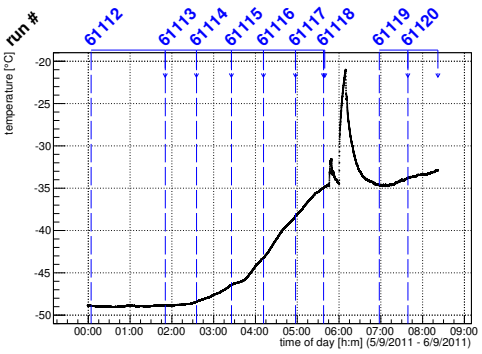

(a) Temperature vs time.

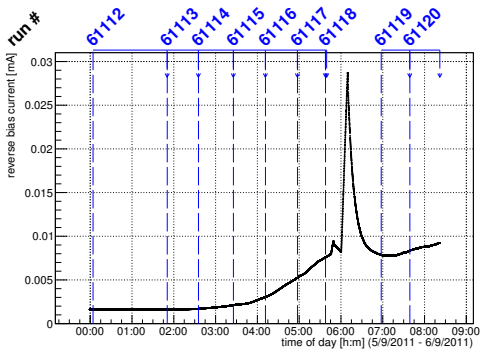

(b) Bias current vs time.

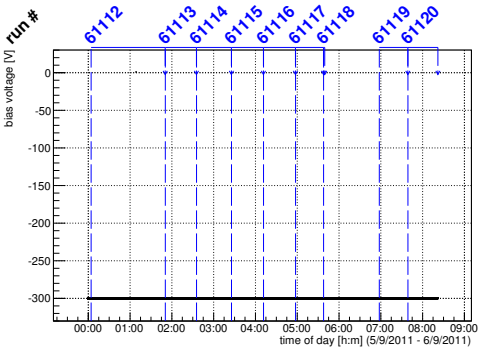

(c) Currently applied bias voltage vs time.

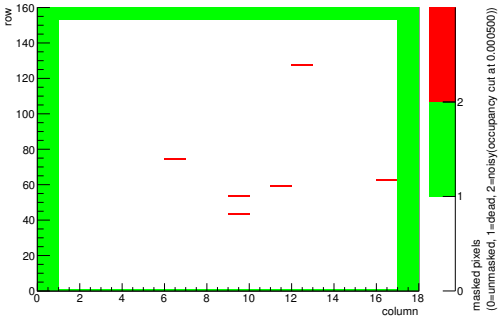

(d) Map of masked pixels.

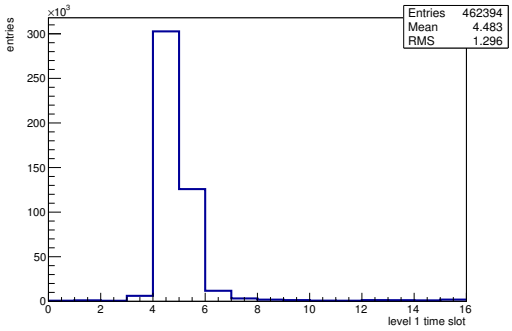

(e) Lvl1 distribution.

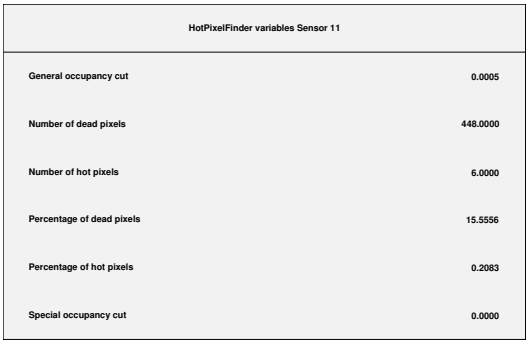

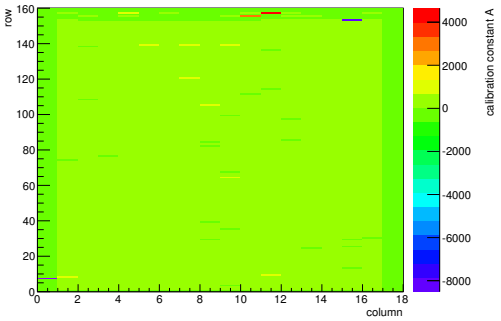

(f) Calibration constant A.

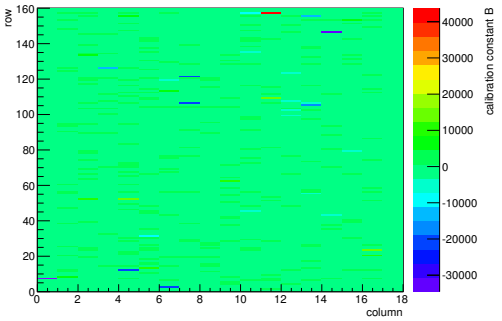

(g) Calibration constant B.

Figure C.44: Detailed plots for test beam measurement of SLID09 (description see section 6.1) sample (running as DUT1) during runs 61112-61120 in the September 2011 test beam period at CERN SPS in area H6B. Summary of the data in chapter 9. *(cont.)*

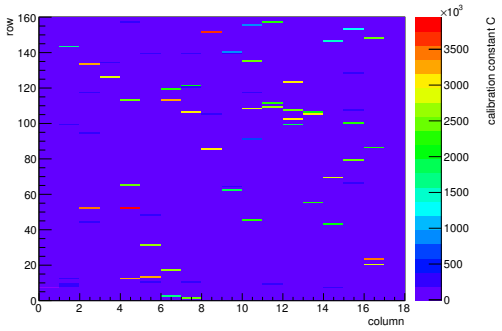

(h) Calibration constant C.

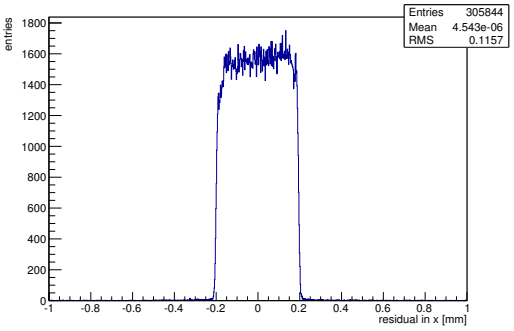

(i) Track residual in x.

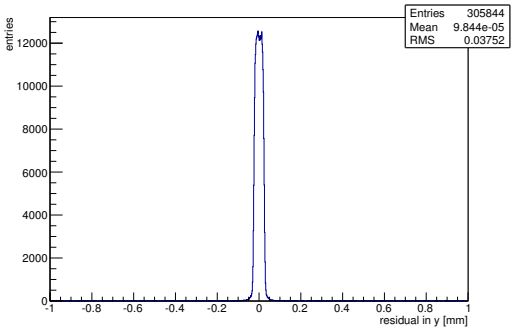

(j) Track residual in y.

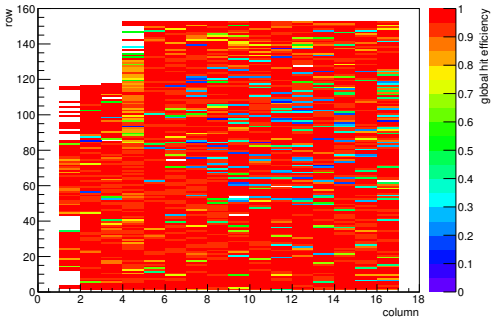

(k) Hit efficiency map.

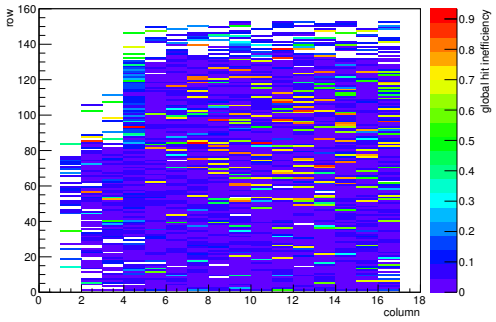

(l) Hit inefficiency map.

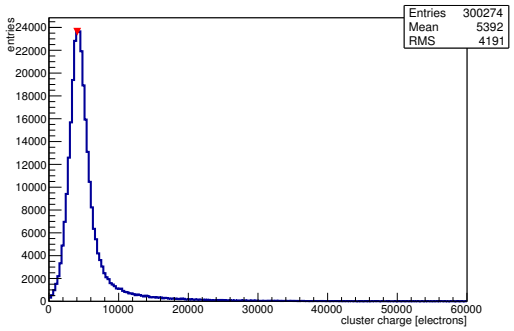

(m) Charge distribution (all cluster sizes included).

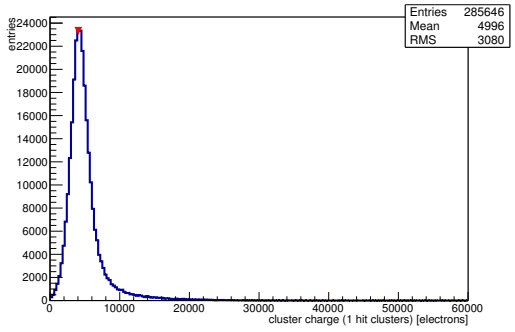

(n) Charge distribution (1 hit cluster).

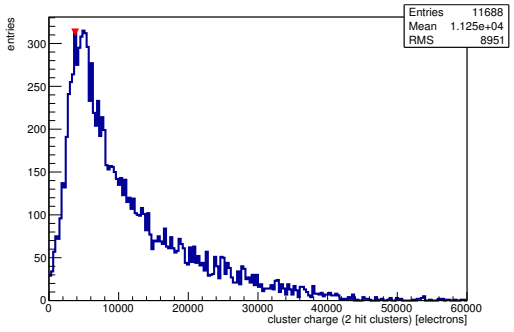

(o) Charge distribution (2 hit cluster).

Figure C.44: Detailed plots for test beam measurement of SLID09 (description see section 6.1) sample (running as DUT1) during runs 61112-61120 in the September 2011 test beam period at CERN SPS in area H6B. Summary of the data in chapter 9. *(cont.)*

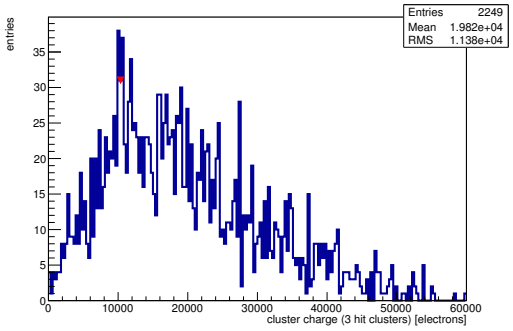

(p) Charge distribution (3 hit cluster).

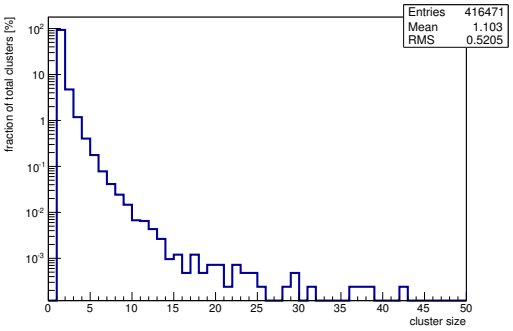

(q) Cluster size distribution.

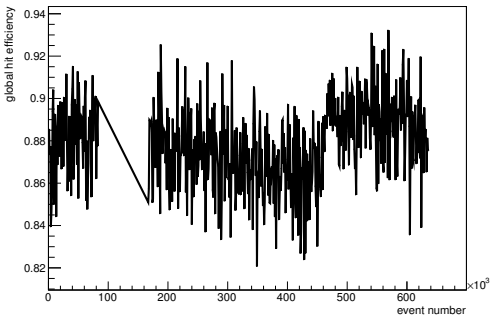

(r) Hit efficiency vs event number.

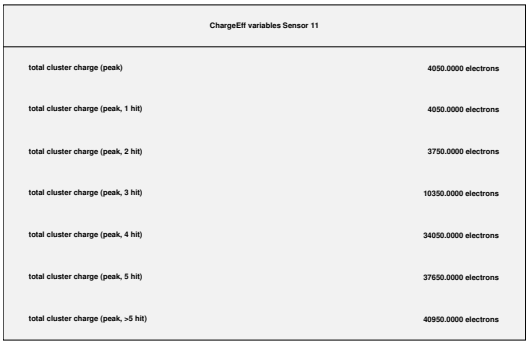

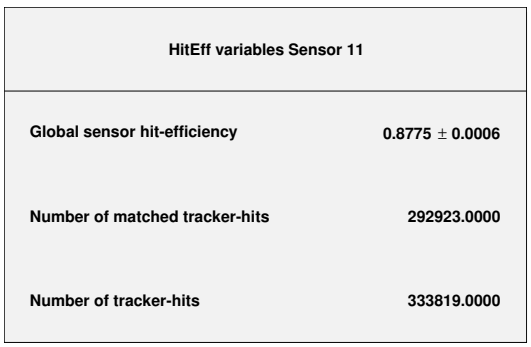

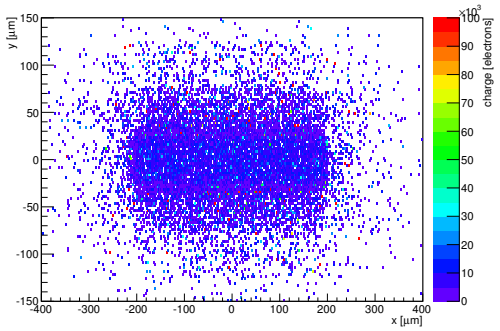

(s) Single pixel mean charge.

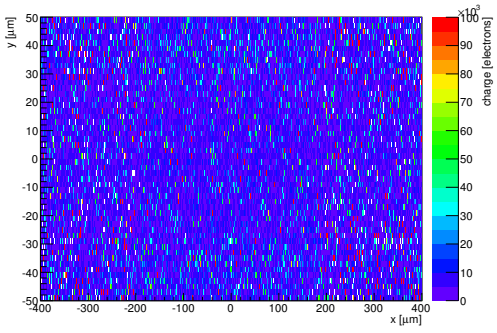

(t) Single pixel mean charge.

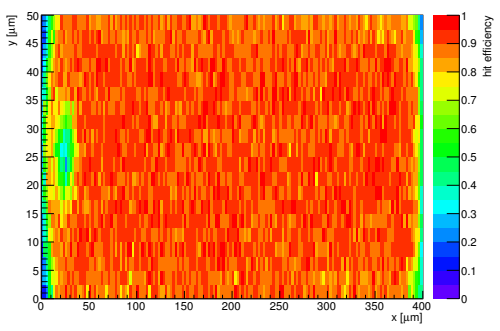

(u) Single pixel hit efficiency.

Figure C.44: Detailed plots for test beam measurement of SLID09 (description see section 6.1) sample (running as DUT1) during runs 61112-61120 in the September 2011 test beam period at CERN SPS in area H6B. Summary of the data in chapter 9.

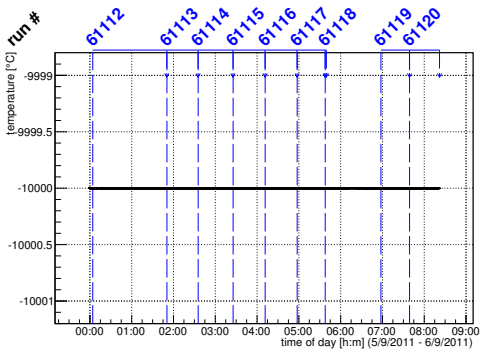

(a) Temperature vs time.

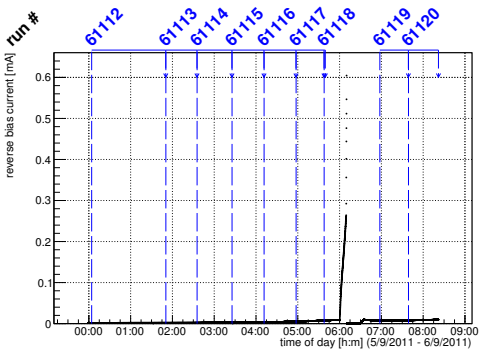

(b) Bias current vs time.

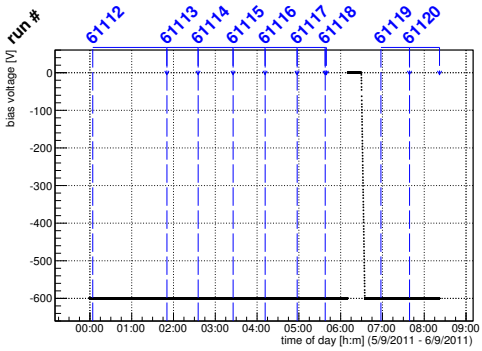

(c) Currently applied bias voltage vs time.

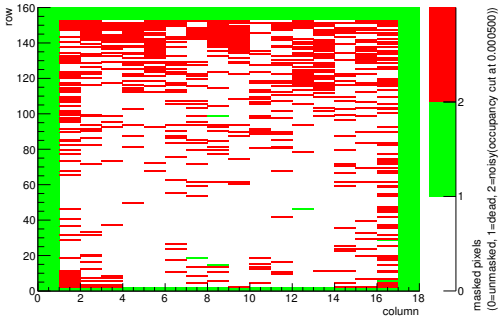

(d) Map of masked pixels.

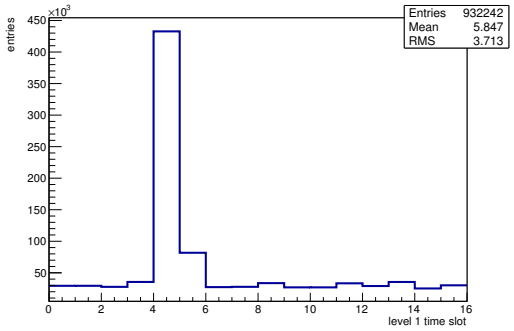

(e) Lvl1 distribution.

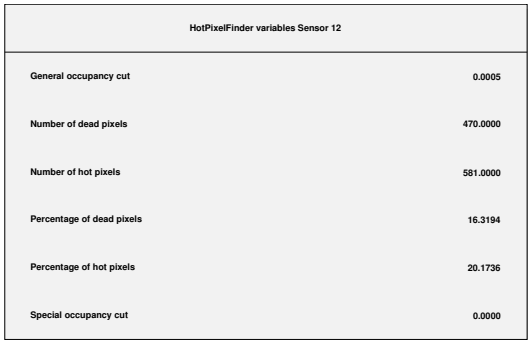

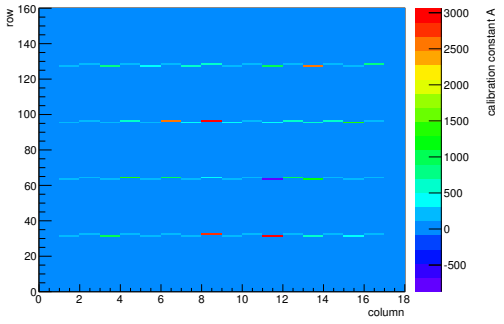

(f) Calibration constant A.

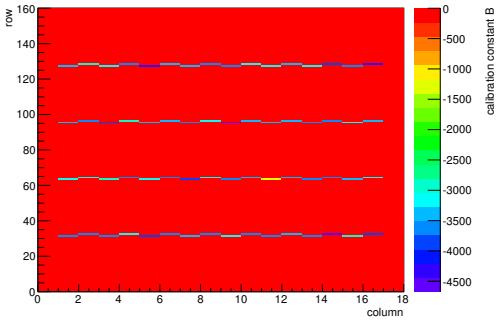

(g) Calibration constant B.

Figure C.45: Detailed plots for test beam measurement of CiS5e15 (description see section 6.1) sample (running as DUT2) during runs 61112-61120 in the September 2011 test beam period at CERN SPS in area H6B. Summary of the data in chapter 9. *(cont.)*

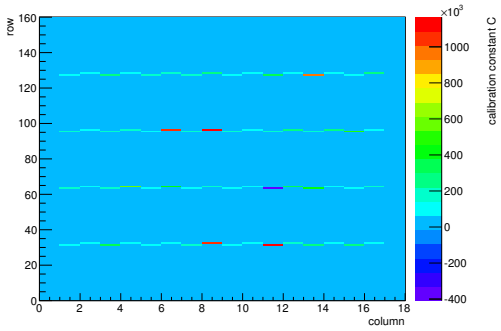

(h) Calibration constant C.

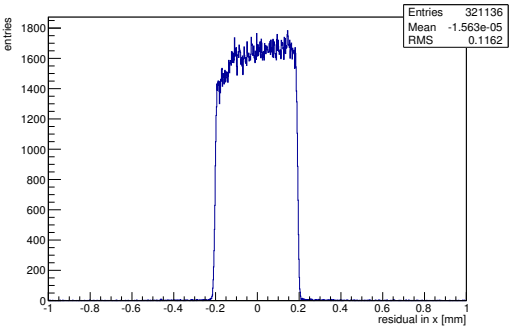

(i) Track residual in x.

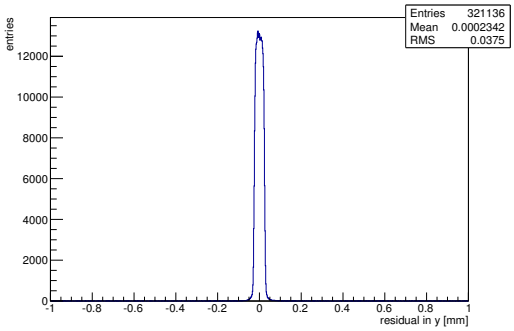

(j) Track residual in y.

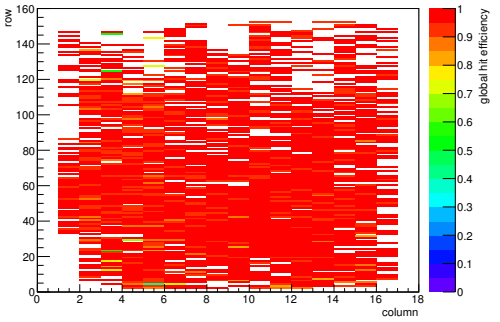

(k) Hit efficiency map.

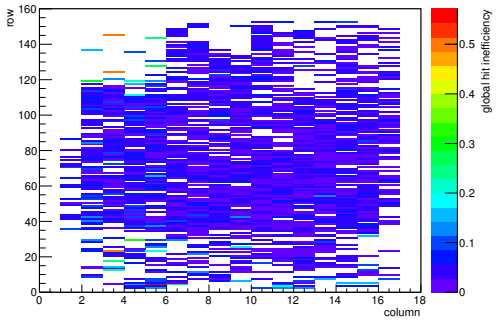

(l) Hit inefficiency map.

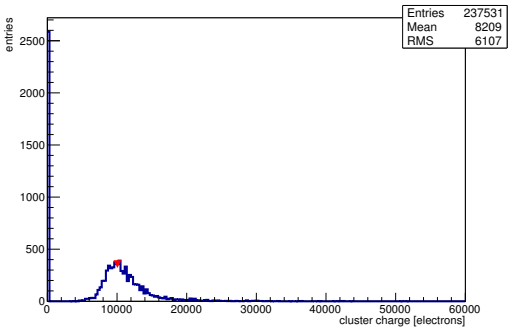

(m) Charge distribution (all cluster sizes included).

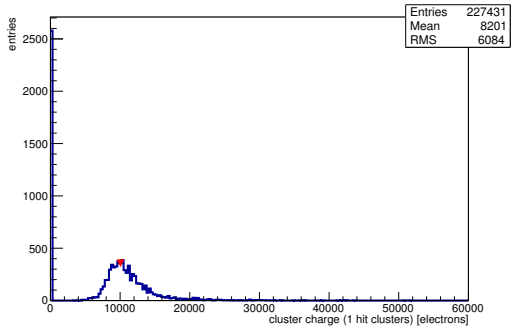

(n) Charge distribution (1 hit cluster).

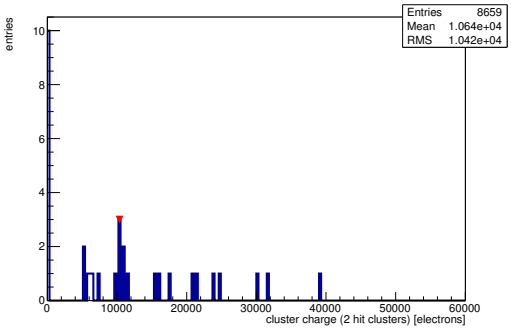

(o) Charge distribution (2 hit cluster).

Figure C.45: Detailed plots for test beam measurement of CiS5e15 (description see section 6.1) sample (running as DUT2) during runs 61112-61120 in the September 2011 test beam period at CERN SPS in area H6B. Summary of the data in chapter 9. *(cont.)*

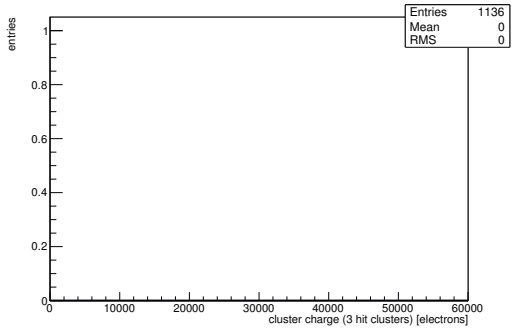

(p) Charge distribution (3 hit cluster).

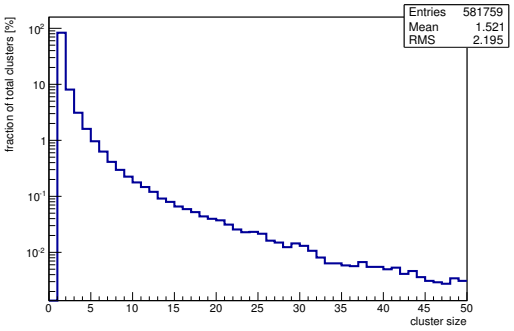

(q) Cluster size distribution.

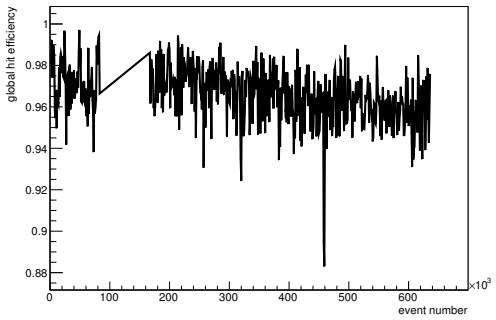

(r) Hit efficiency vs event number.

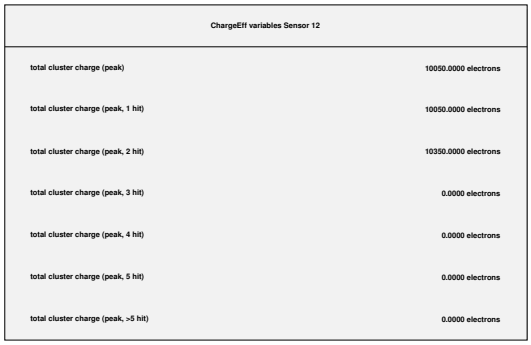

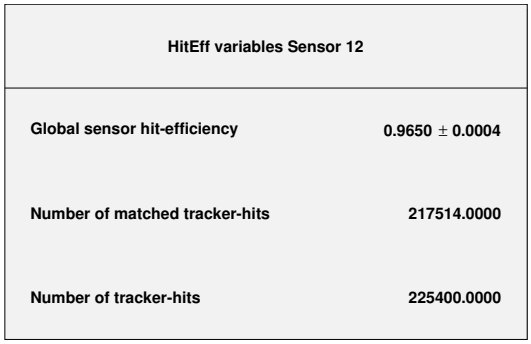

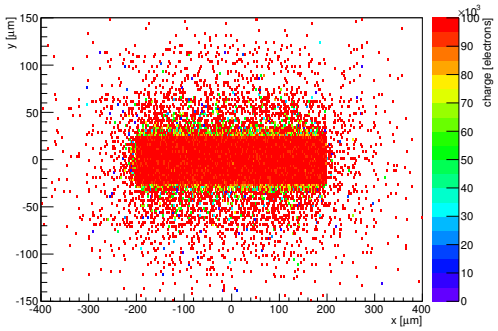

(s) Single pixel mean charge.

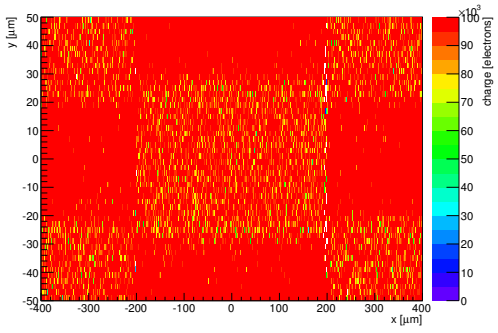

(t) Single pixel mean charge.

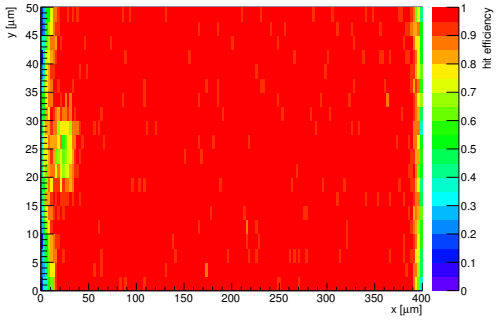

(u) Single pixel hit efficiency.

Figure C.45: Detailed plots for test beam measurement of CiS5e15 (description see section 6.1) sample (running as DUT2) during runs 61112-61120 in the September 2011 test beam period at CERN SPS in area H6B. Summary of the data in chapter 9.

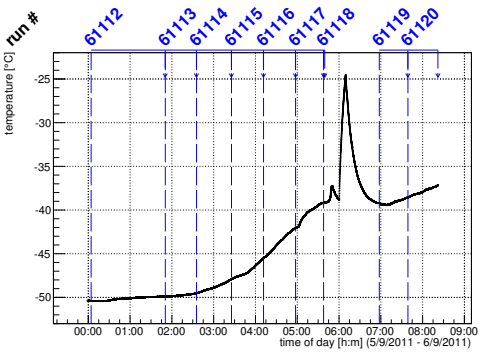

(a) Temperature vs time.

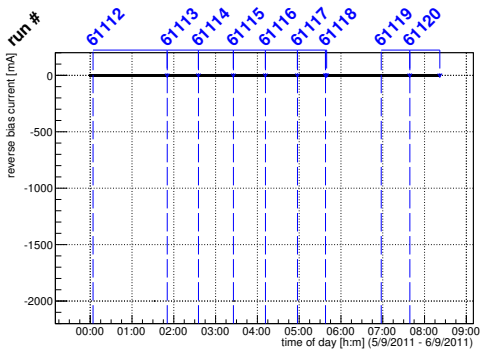

(b) Bias current vs time.

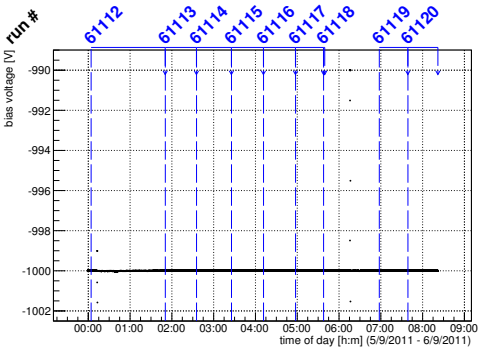

(c) Currently applied bias voltage vs time.

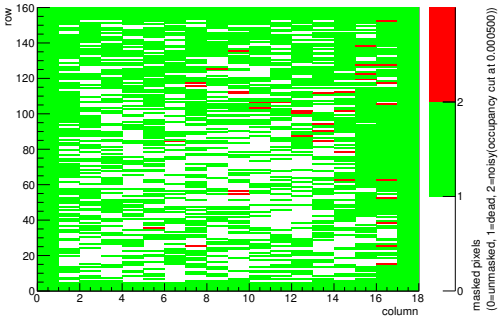

(d) Map of masked pixels.

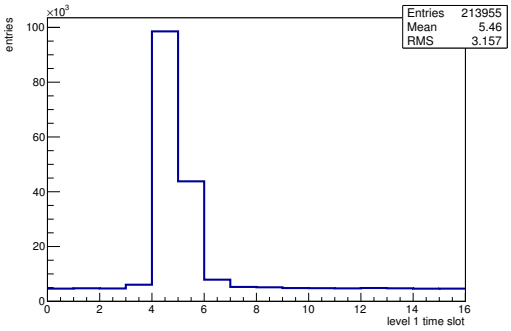

(e) Lvl1 distribution.

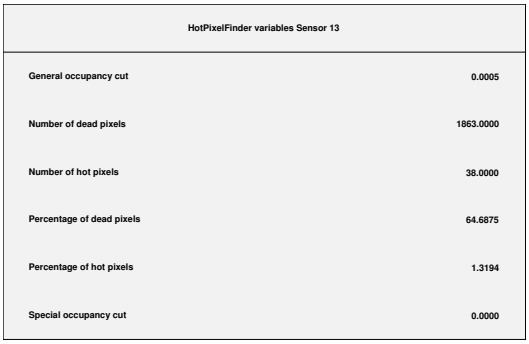

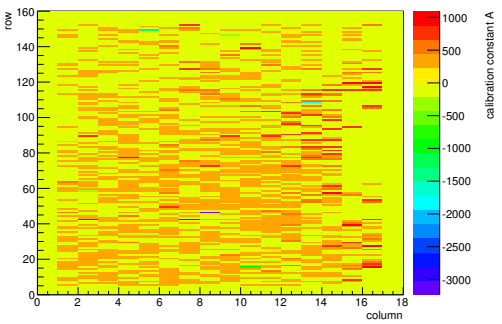

(f) Calibration constant A.

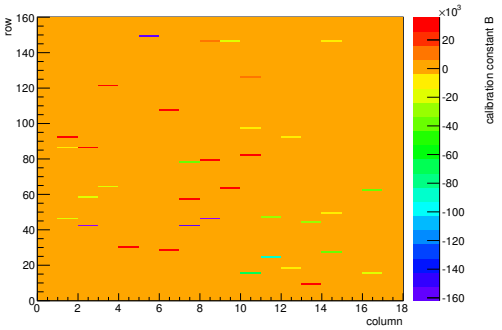

(g) Calibration constant B.

Figure C.46: Detailed plots for test beam measurement of DO-I-5 (description see section 6.1) sample (running as DUT3) during runs 61112-61120 in the September 2011 test beam period at CERN SPS in area H6B. Summary of the data in chapter 9. *(cont.)*

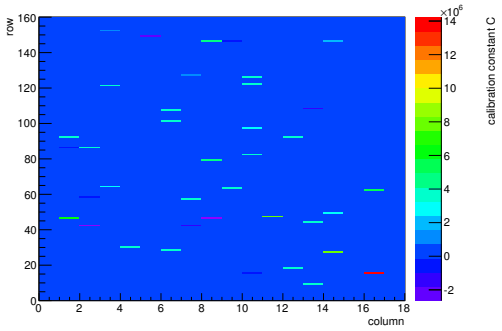

(h) Calibration constant C.

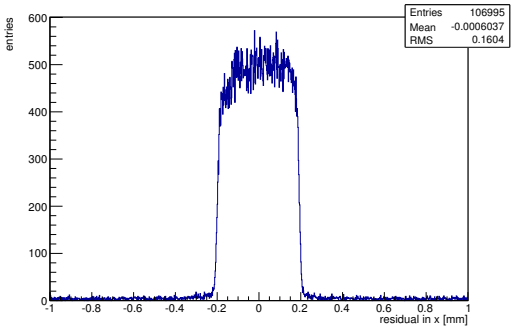

(i) Track residual in x.

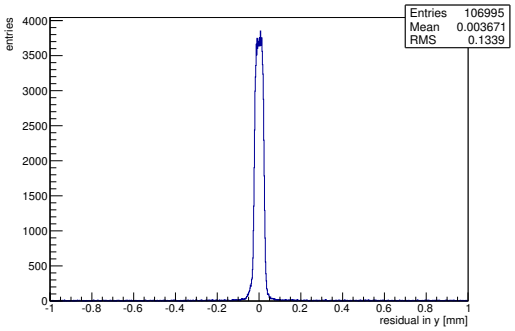

(j) Track residual in y.

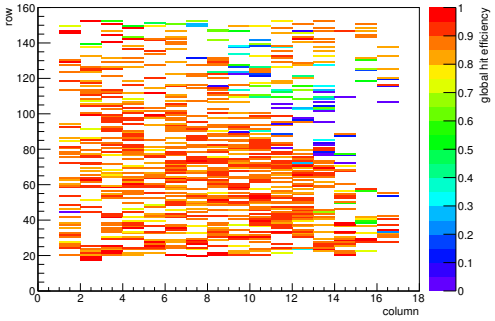

(k) Hit efficiency map.

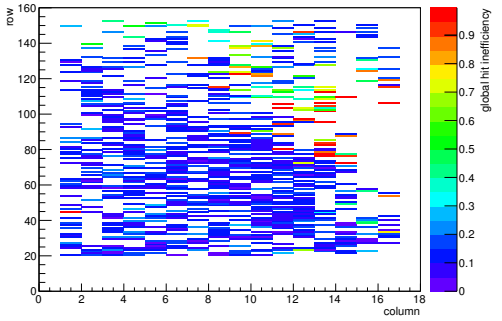

(l) Hit inefficiency map.

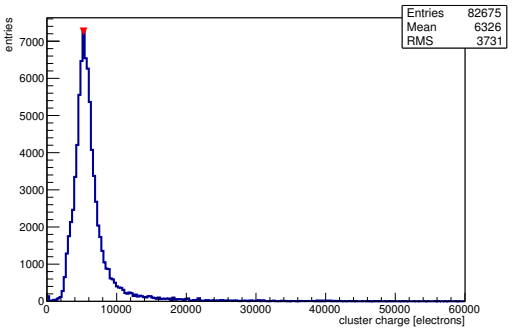

(m) Charge distribution (all cluster sizes included).

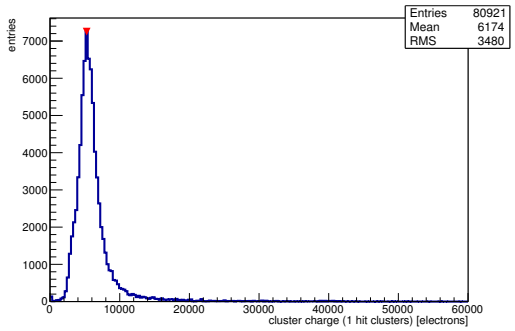

(n) Charge distribution (1 hit cluster).

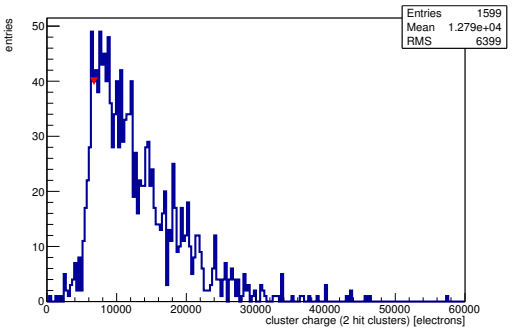

(o) Charge distribution (2 hit cluster).

Figure C.46: Detailed plots for test beam measurement of DO-I-5 (description see section 6.1) sample (running as DUT3) during runs 61112-61120 in the September 2011 test beam period at CERN SPS in area H6B. Summary of the data in chapter 9. *(cont.)*

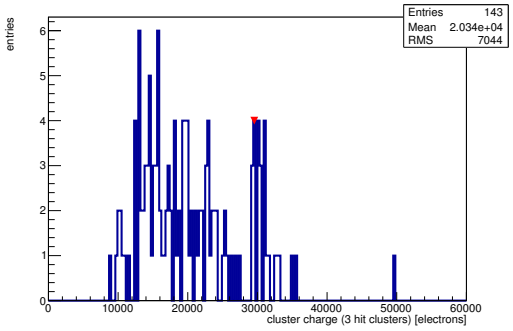

(p) Charge distribution (3 hit cluster).

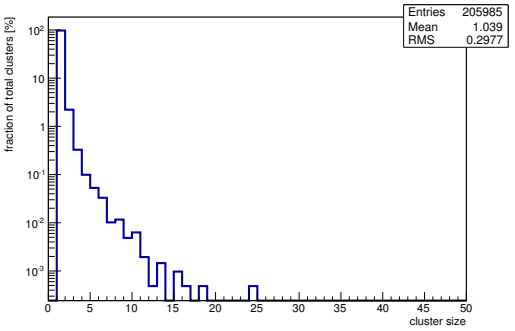

(q) Cluster size distribution.

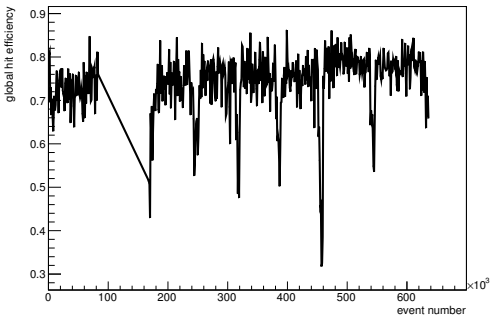

(r) Hit efficiency vs event number.

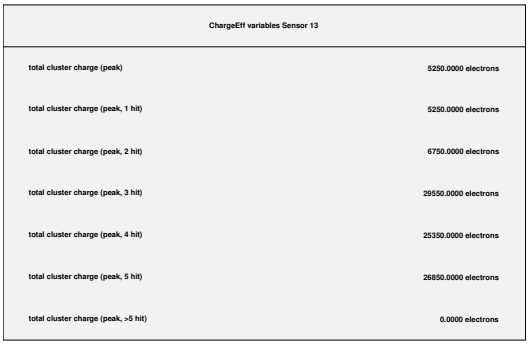

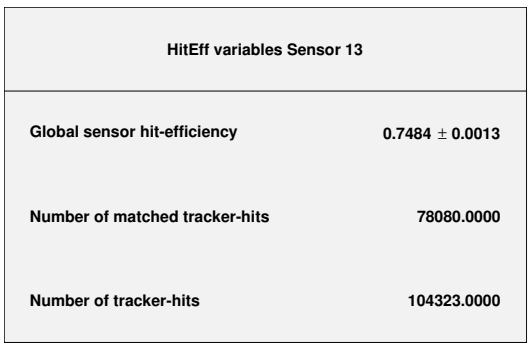

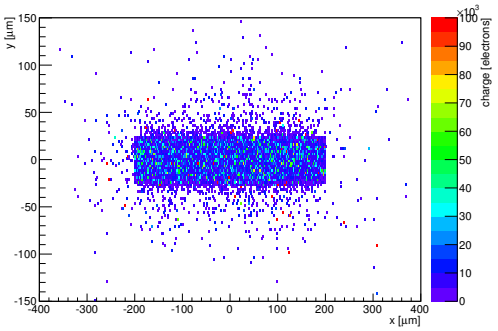

(s) Single pixel mean charge.

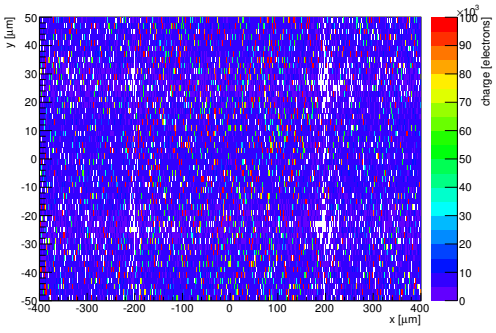

(t) Single pixel mean charge.

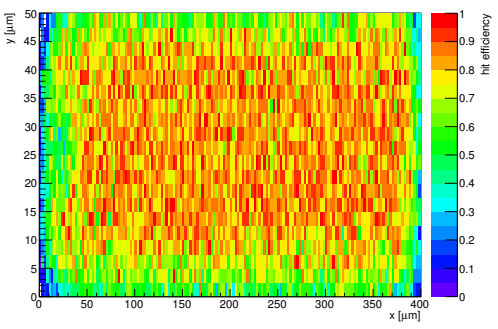

(u) Single pixel hit efficiency.

Figure C.46: Detailed plots for test beam measurement of DO-I-5 (description see section 6.1) sample (running as DUT3) during runs 61112-61120 in the September 2011 test beam period at CERN SPS in area H6B. Summary of the data in chapter 9.

C.3.2 Runs 61124-61128

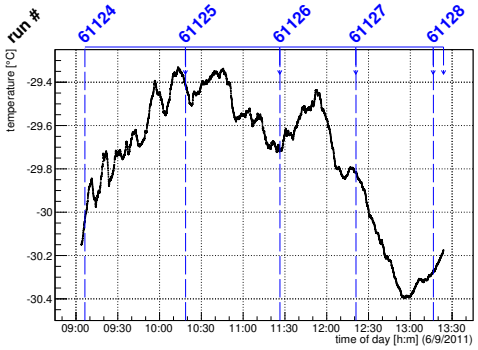

(a) Temperature vs time.

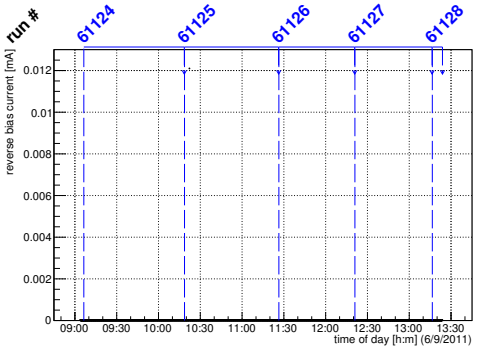

(b) Bias current vs time.

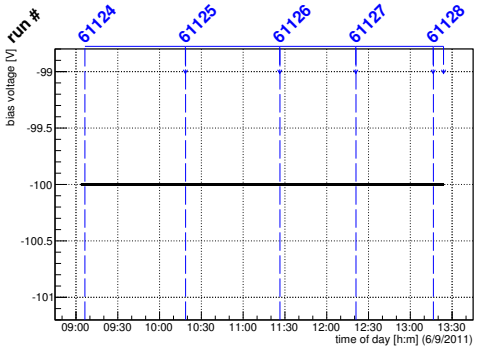

(c) Currently applied bias voltage vs time.

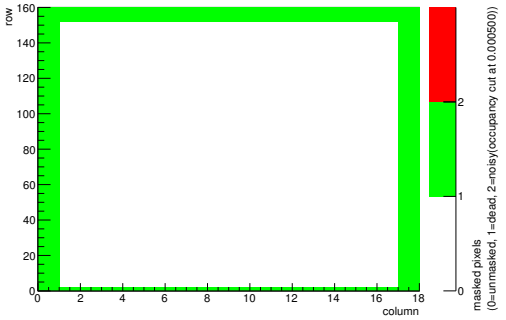

(d) Map of masked pixels.

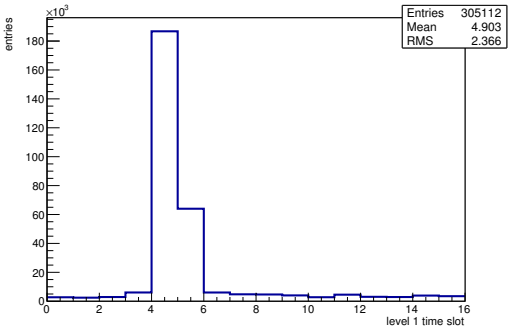

(e) Lvl1 distribution.

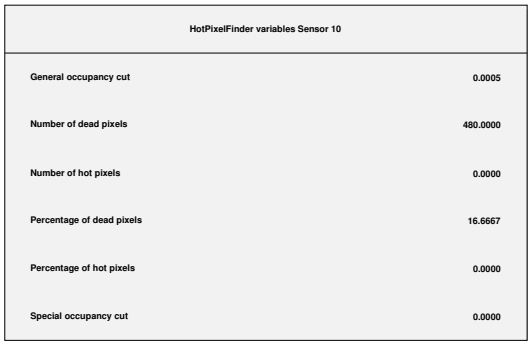

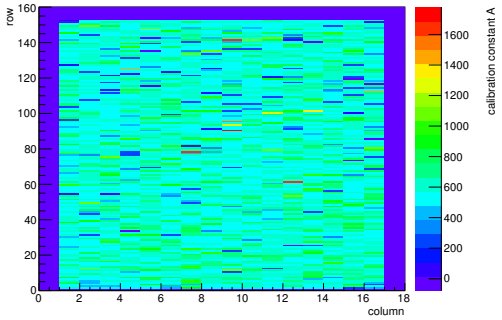

(f) Calibration constant A.

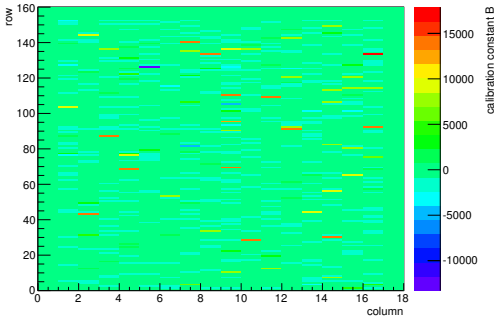

(g) Calibration constant B.

Figure C.47: Detailed plots for test beam measurement of SLID10 (description see section 6.1) sample (running as DUT0) during runs 61124-61128 in the September 2011 test beam period at CERN SPS in area H6B. Summary of the data in chapter 9. *(cont.)*

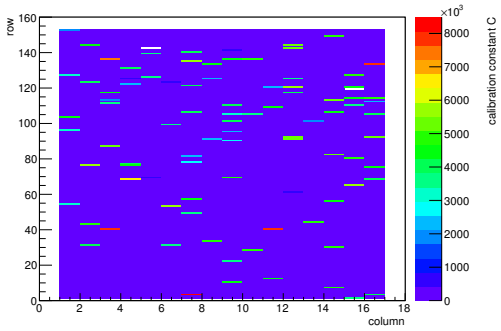

(h) Calibration constant C.

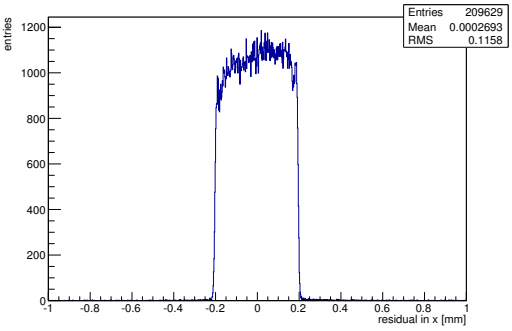

(i) Track residual in x.

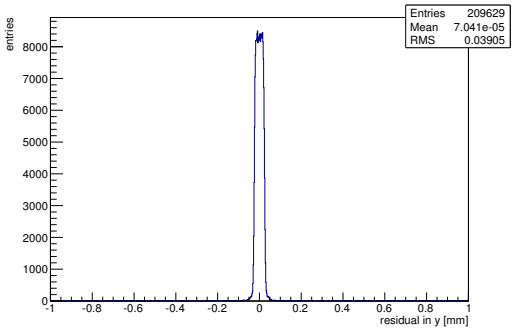

(j) Track residual in y.

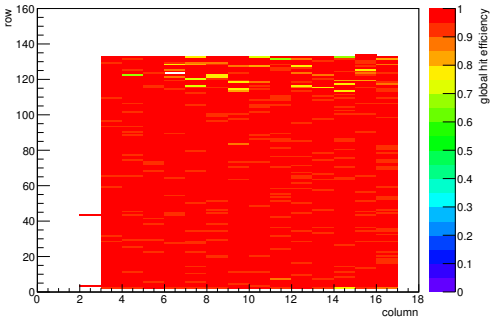

(k) Hit efficiency map.

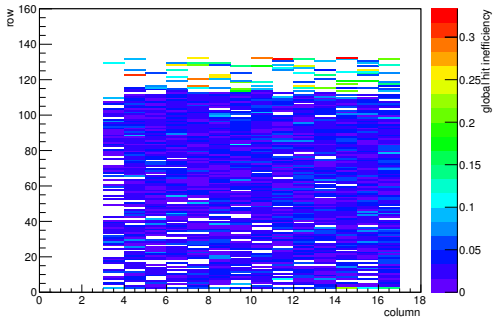

(l) Hit inefficiency map.

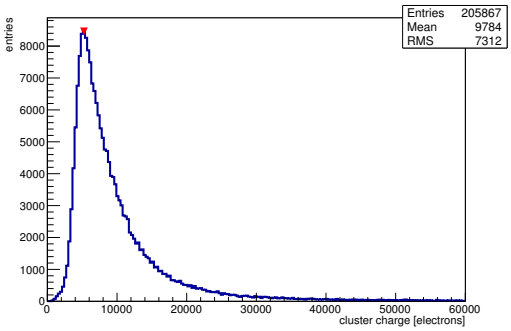

(m) Charge distribution (all cluster sizes included).

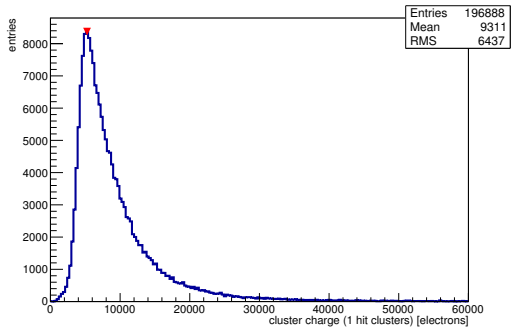

(n) Charge distribution (1 hit cluster).

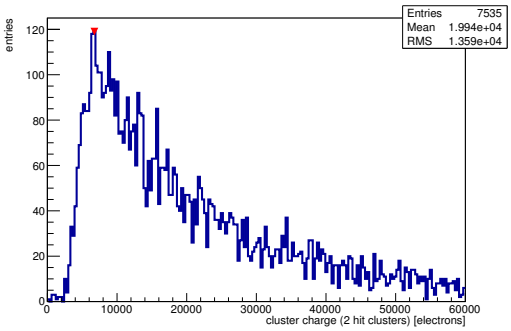

(o) Charge distribution (2 hit cluster).

Figure C.47: Detailed plots for test beam measurement of SLID10 (description see section 6.1) sample (running as DUT0) during runs 61124-61128 in the September 2011 test beam period at CERN SPS in area H6B. Summary of the data in chapter 9. *(cont.)*

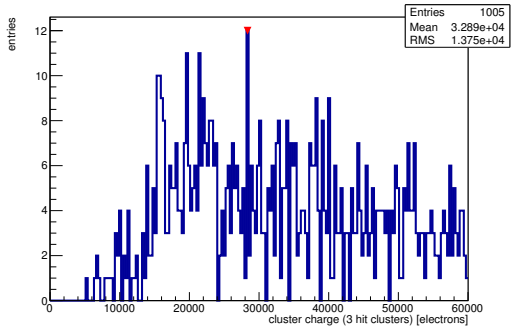

(p) Charge distribution (3 hit cluster).

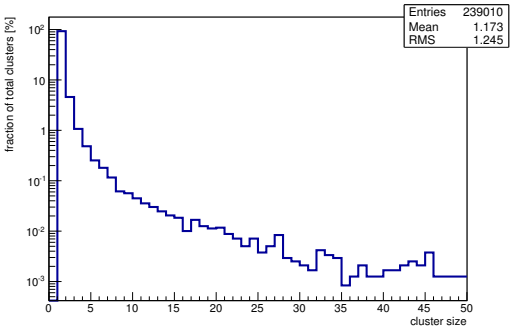

(q) Cluster size distribution.

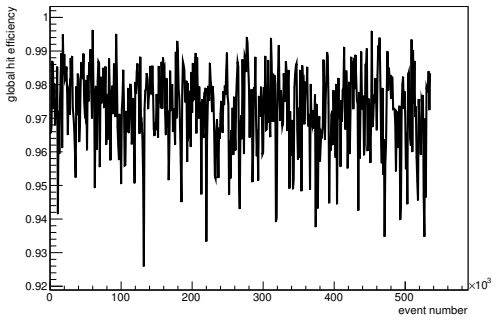

(r) Hit efficiency vs event number.

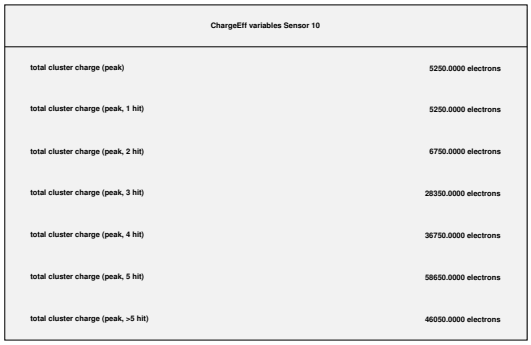

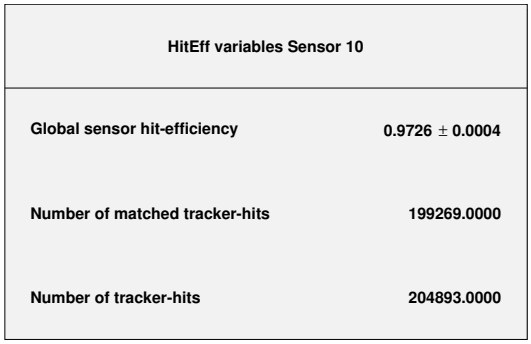

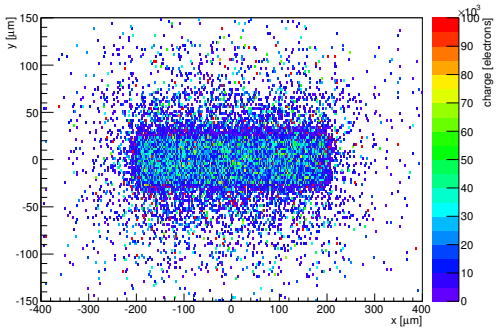

(s) Single pixel mean charge.

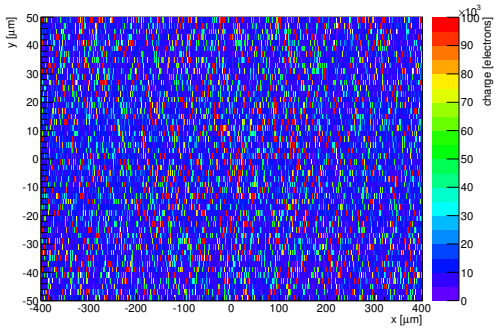

(t) Single pixel mean charge.

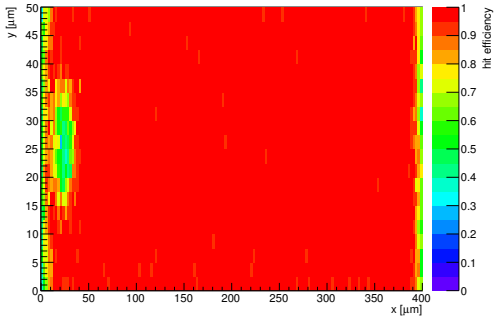

(u) Single pixel hit efficiency.

Figure C.47: Detailed plots for test beam measurement of SLID10 (description see section 6.1) sample (running as DUT0) during runs 61124-61128 in the September 2011 test beam period at CERN SPS in area H6B. Summary of the data in chapter 9.

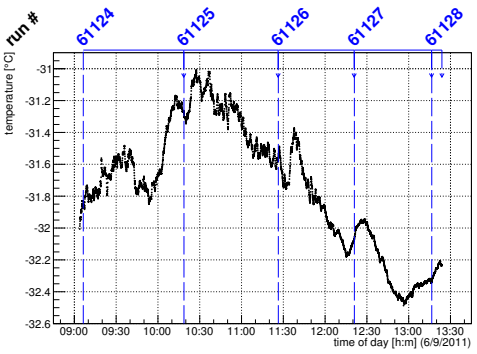

(a) Temperature vs time.

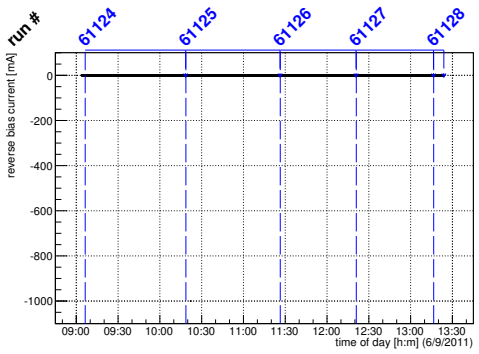

(b) Bias current vs time.

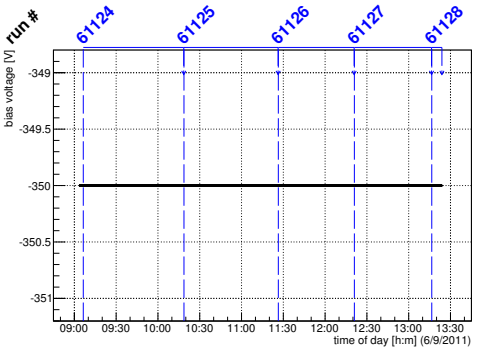

(c) Currently applied bias voltage vs time.

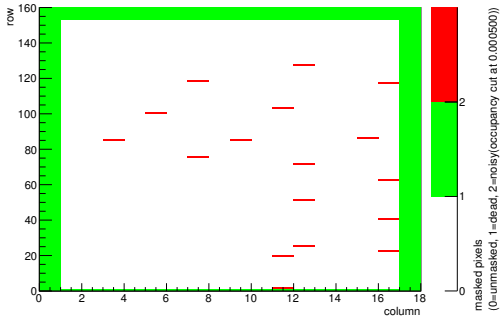

(d) Map of masked pixels.

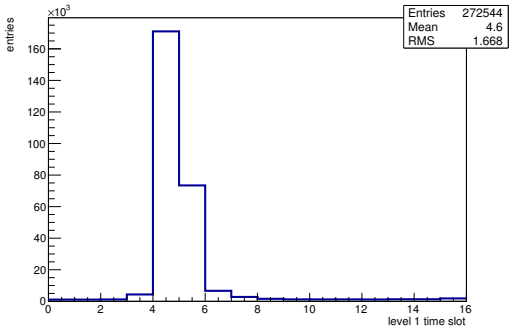

(e) Lvl1 distribution.

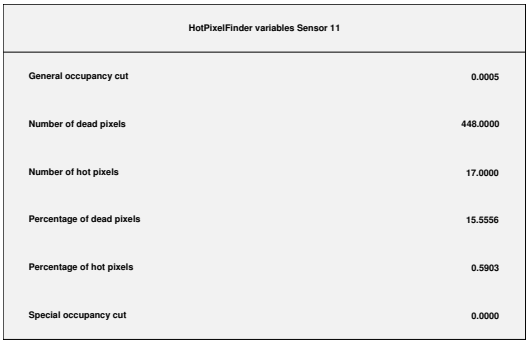

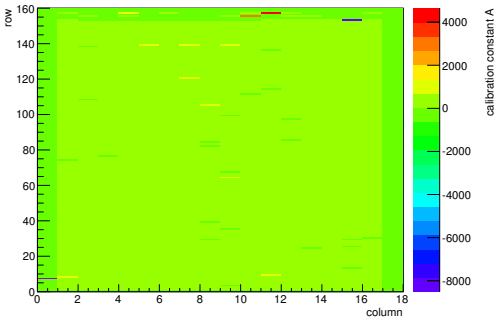

(f) Calibration constant A.

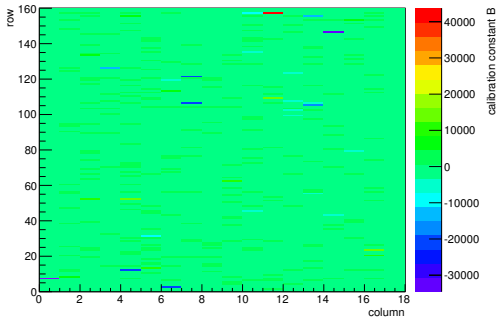

(g) Calibration constant B.

Figure C.48: Detailed plots for test beam measurement of SLID09 (description see section 6.1) sample (running as DUT1) during runs 61124-61128 in the September 2011 test beam period at CERN SPS in area H6B. Summary of the data in chapter 9. *(cont.)*

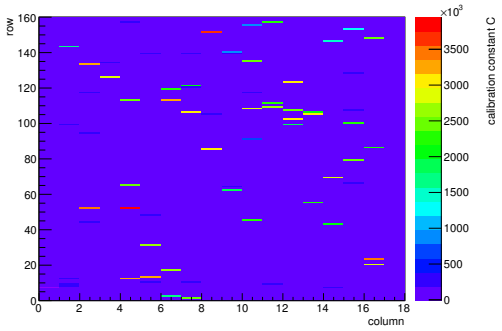

(h) Calibration constant C.

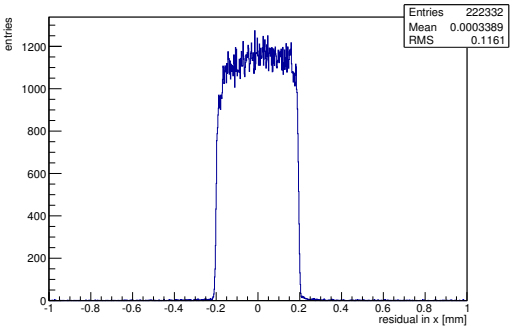

(i) Track residual in x.

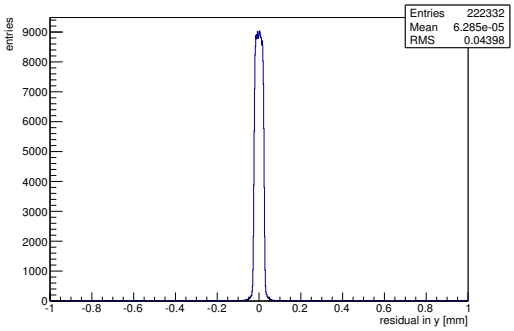

(j) Track residual in y.

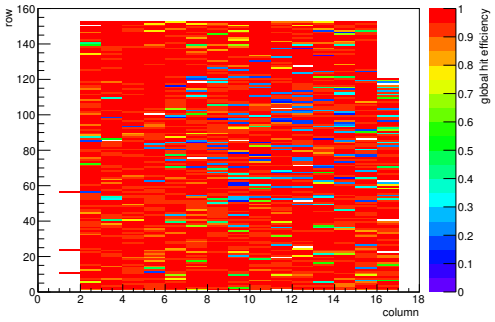

(k) Hit efficiency map.

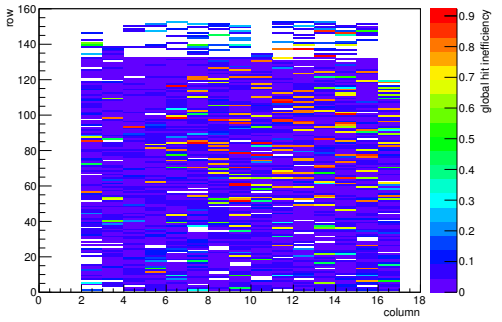

(l) Hit inefficiency map.

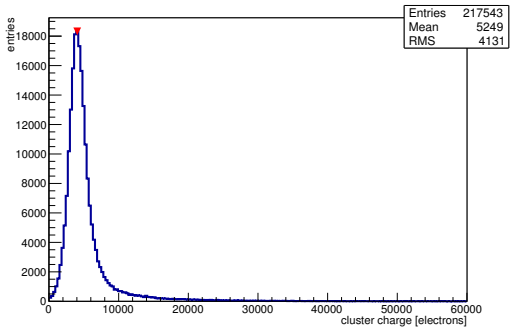

(m) Charge distribution (all cluster sizes included).

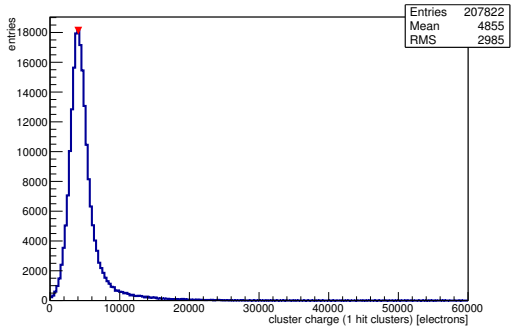

(n) Charge distribution (1 hit cluster).

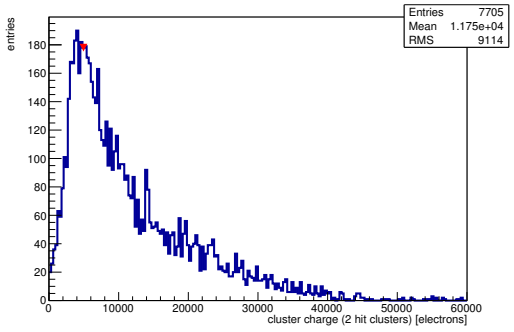

(o) Charge distribution (2 hit cluster).

Figure C.48: Detailed plots for test beam measurement of SLID09 (description see section 6.1) sample (running as DUT1) during runs 61124-61128 in the September 2011 test beam period at CERN SPS in area H6B. Summary of the data in chapter 9. *(cont.)*

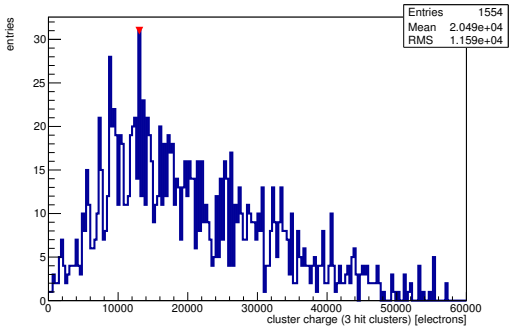

(p) Charge distribution (3 hit cluster).

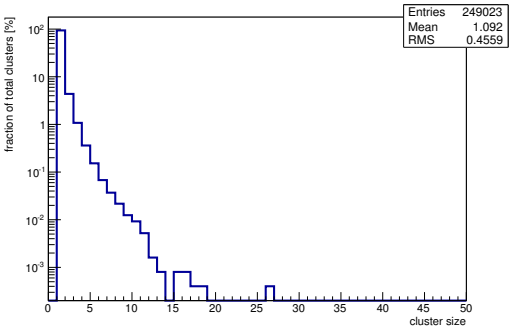

(q) Cluster size distribution.

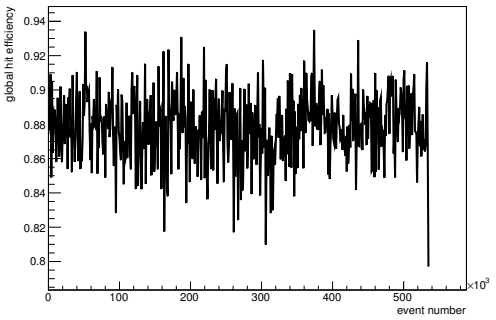

(r) Hit efficiency vs event number.

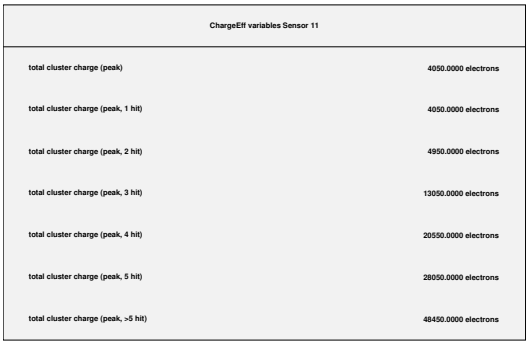

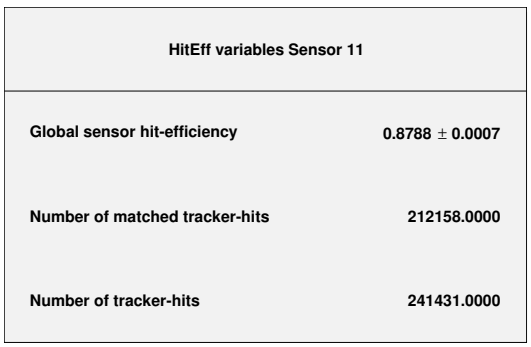

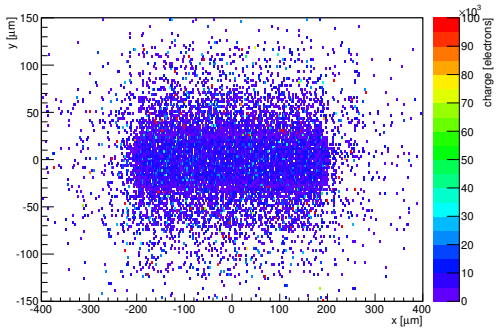

(s) Single pixel mean charge.

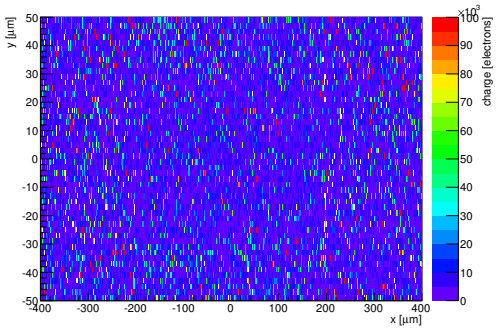

(t) Single pixel mean charge.

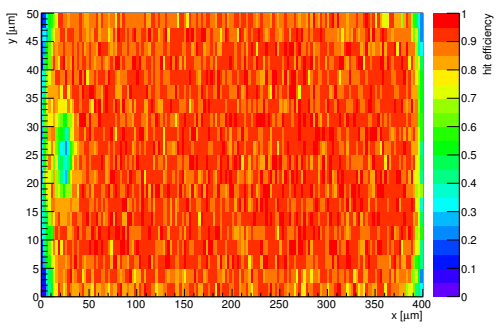

(u) Single pixel hit efficiency.

Figure C.48: Detailed plots for test beam measurement of SLID09 (description see section 6.1) sample (running as DUT1) during runs 61124-61128 in the September 2011 test beam period at CERN SPS in area H6B. Summary of the data in chapter 9.

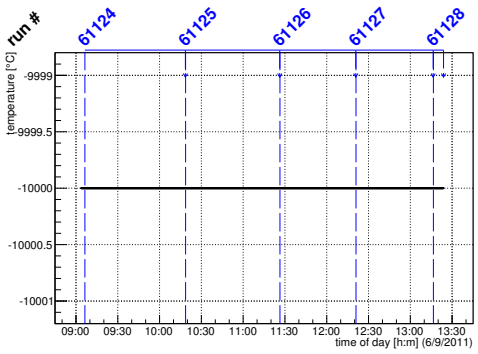

(a) Temperature vs time.

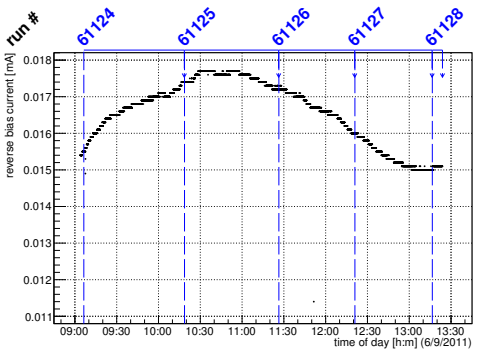

(b) Bias current vs time.

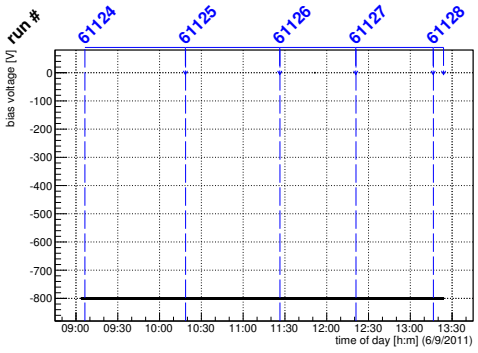

(c) Currently applied bias voltage vs time.

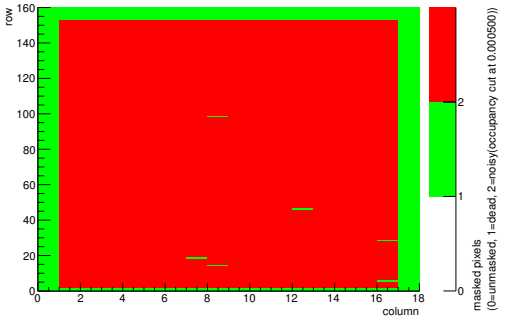

(d) Map of masked pixels.

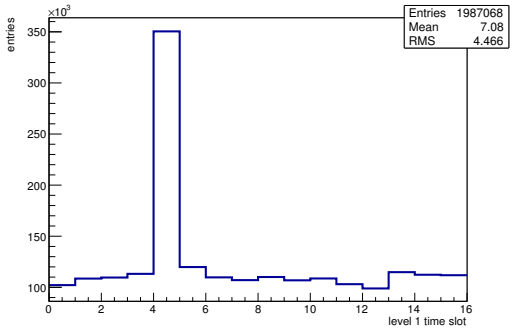

(e) Lvl1 distribution.

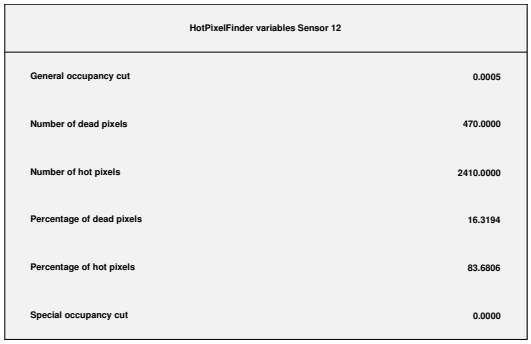

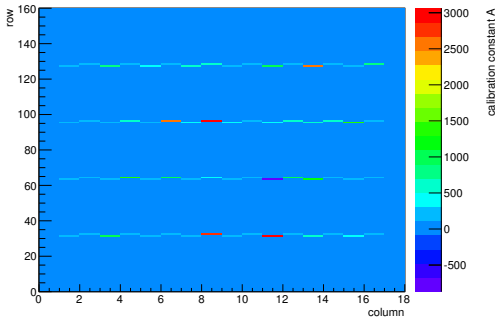

(f) Calibration constant A.

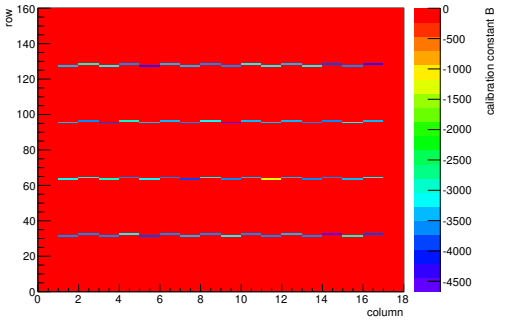

(g) Calibration constant B.

Figure C.49: Detailed plots for test beam measurement of CiS5e15 (description see section 6.1) sample (running as DUT2) during runs 61124-61128 in the September 2011 test beam period at CERN SPS in area H6B. Summary of the data in chapter 9. *(cont.)*

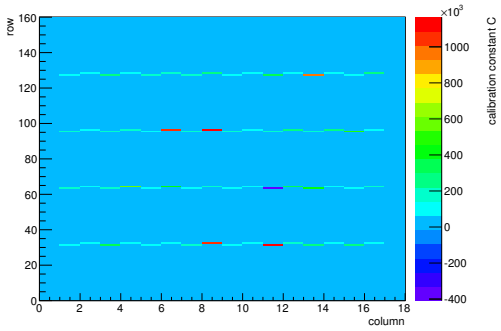

(h) Calibration constant C.

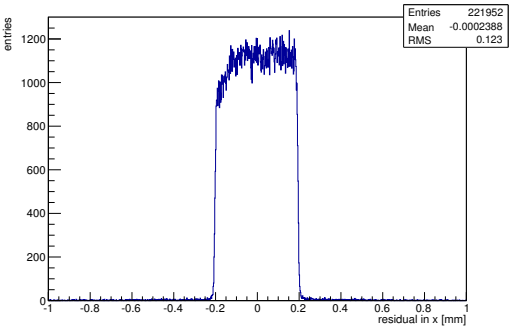

(i) Track residual in x.

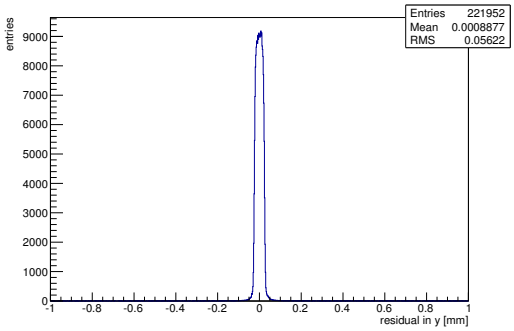

(j) Track residual in y.

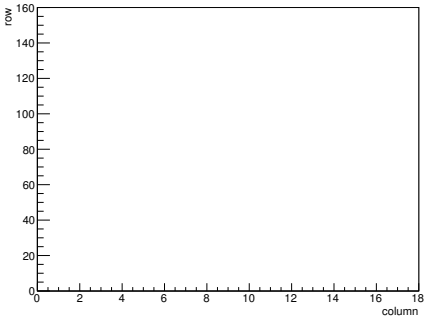

(k) Hit efficiency map.

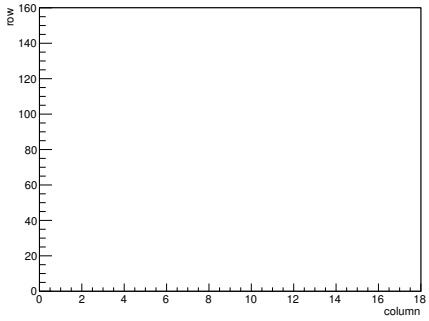

(l) Hit inefficiency map.

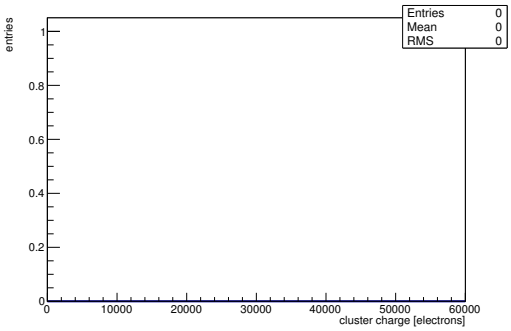

(m) Charge distribution (all cluster sizes included).

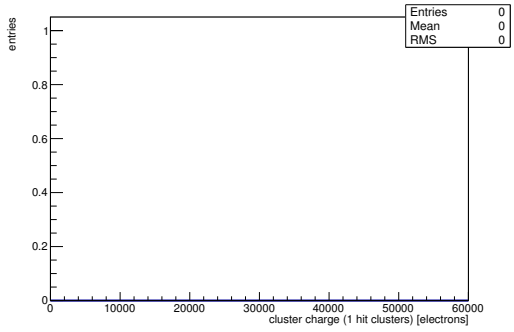

(n) Charge distribution (1 hit cluster).

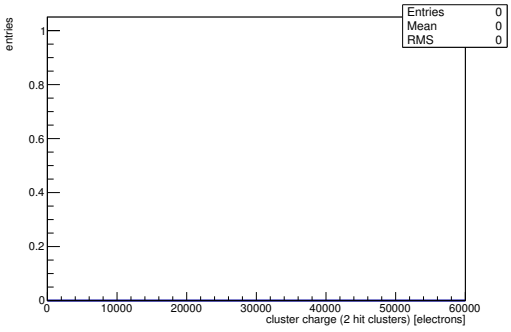

(o) Charge distribution (2 hit cluster).

Figure C.49: Detailed plots for test beam measurement of CiS5e15 (description see section 6.1) sample (running as DUT2) during runs 61124-61128 in the September 2011 test beam period at CERN SPS in area H6B. Summary of the data in chapter 9. *(cont.)*

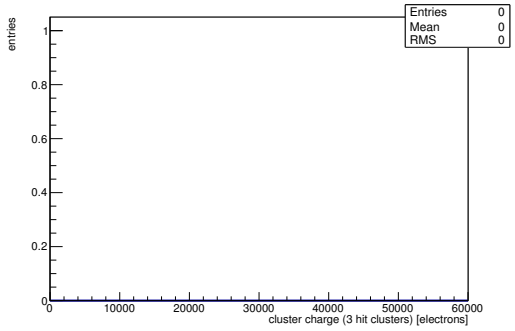

(p) Charge distribution (3 hit cluster).

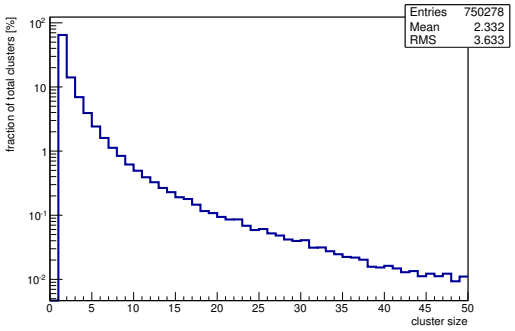

(q) Cluster size distribution.

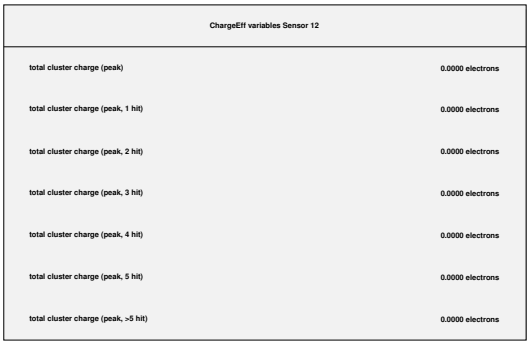

(r) Hit efficiency vs event number.

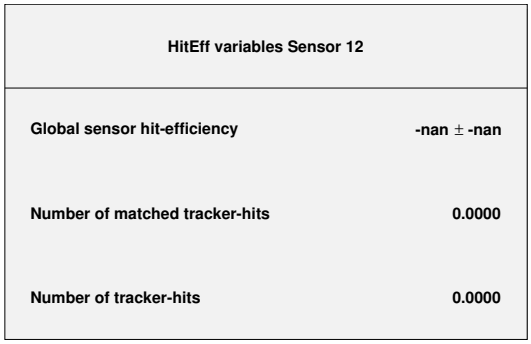

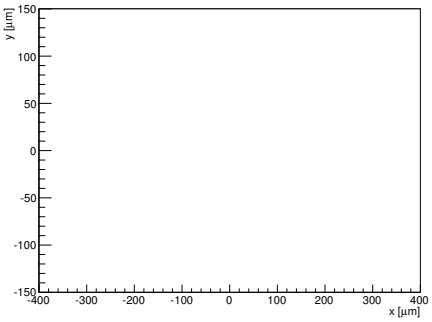

(s) Single pixel mean charge.

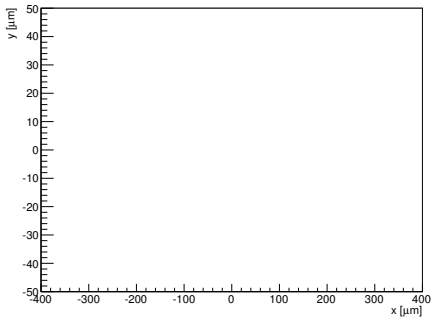

(t) Single pixel mean charge.

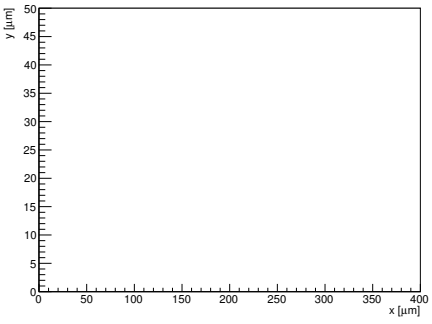

(u) Single pixel hit efficiency.

Figure C.49: Detailed plots for test beam measurement of CiS5e15 (description see section 6.1) sample (running as DUT2) during runs 61124-61128 in the September 2011 test beam period at CERN SPS in area H6B. Summary of the data in chapter 9.

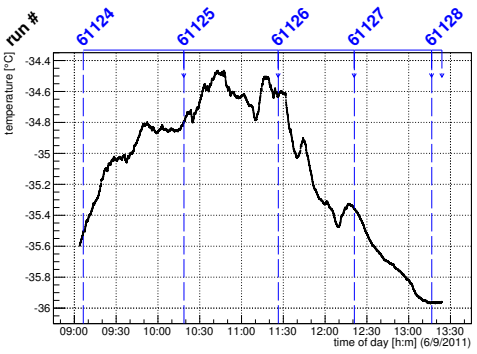

(a) Temperature vs time.

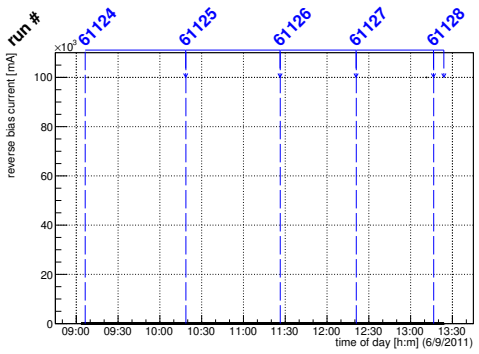

(b) Bias current vs time.

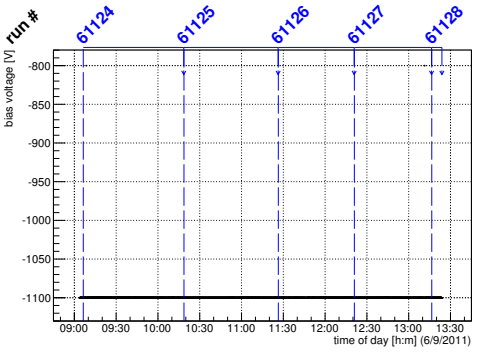

(c) Currently applied bias voltage vs time.

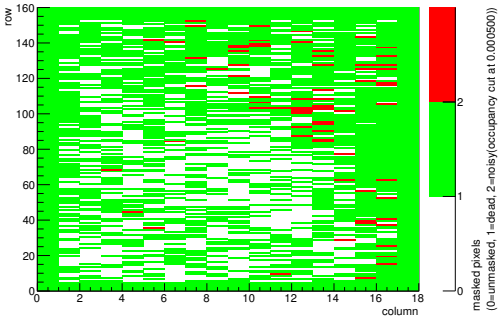

(d) Map of masked pixels.

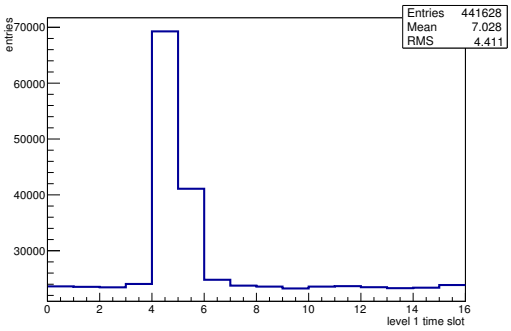

(e) Lvl1 distribution.

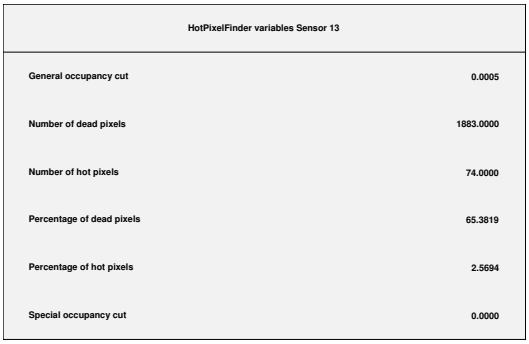

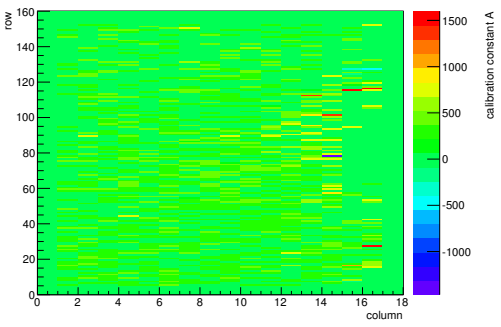

(f) Calibration constant A.

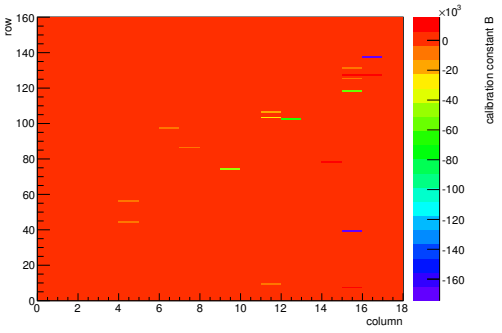

(g) Calibration constant B.

Figure C.50: Detailed plots for test beam measurement of DO-I-5 (description see section 6.1) sample (running as DUT3) during runs 61124-61128 in the September 2011 test beam period at CERN SPS in area H6B. Summary of the data in chapter 9. *(cont.)*

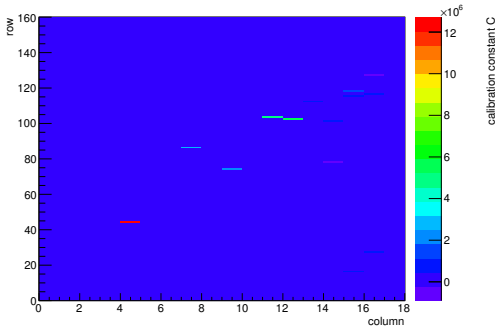

(h) Calibration constant C.

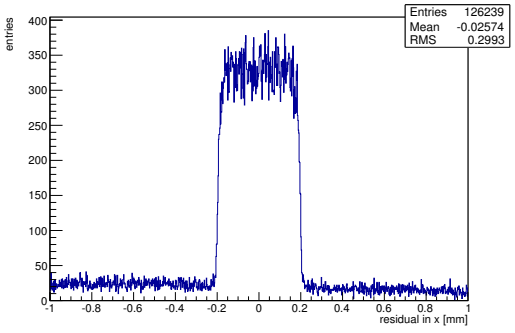

(i) Track residual in x.

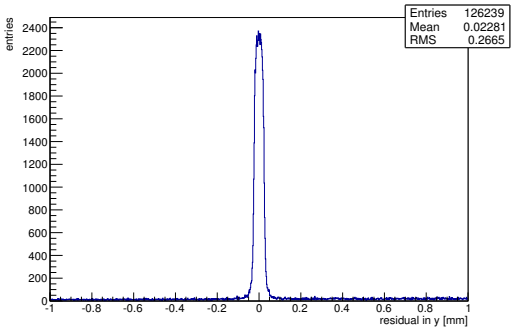

(j) Track residual in y.

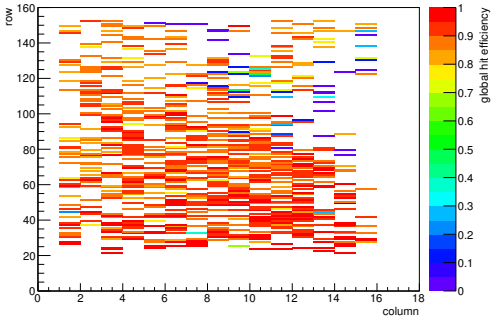

(k) Hit efficiency map.

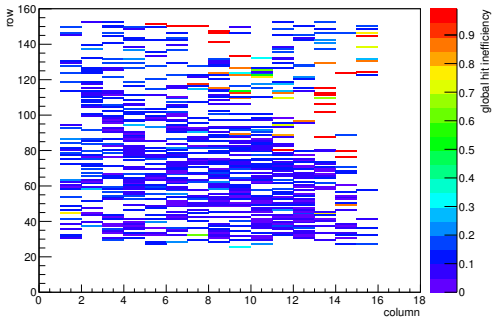

(l) Hit inefficiency map.

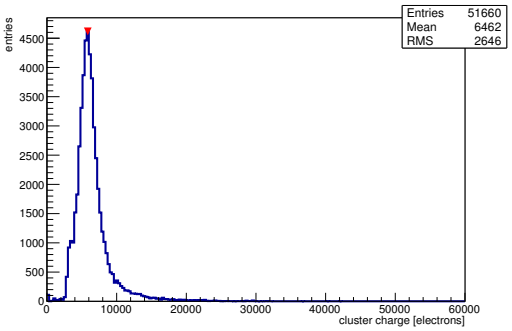

(m) Charge distribution (all cluster sizes included).

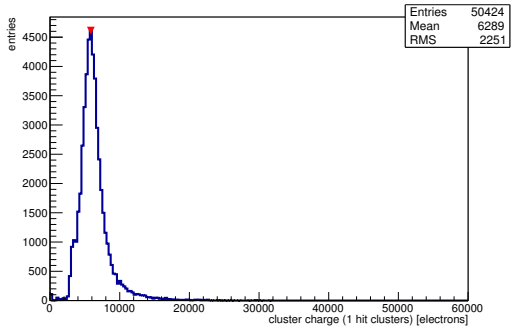

(n) Charge distribution (1 hit cluster).

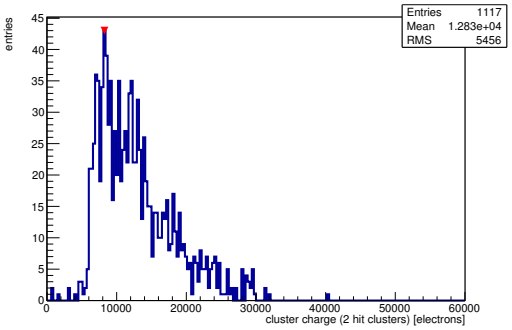

(o) Charge distribution (2 hit cluster).

Figure C.50: Detailed plots for test beam measurement of DO-I-5 (description see section 6.1) sample (running as DUT3) during runs 61124-61128 in the September 2011 test beam period at CERN SPS in area H6B. Summary of the data in chapter 9. *(cont.)*

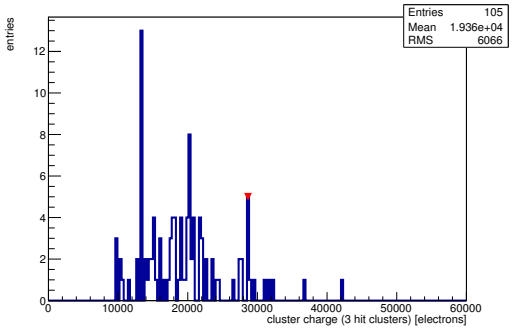

(p) Charge distribution (3 hit cluster).

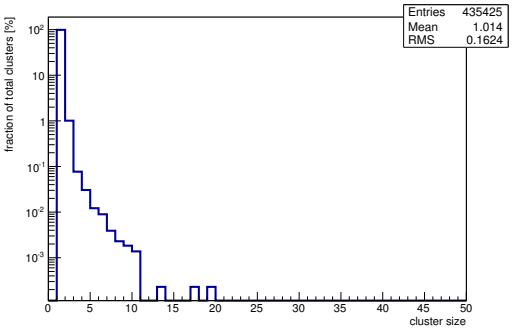

(q) Cluster size distribution.

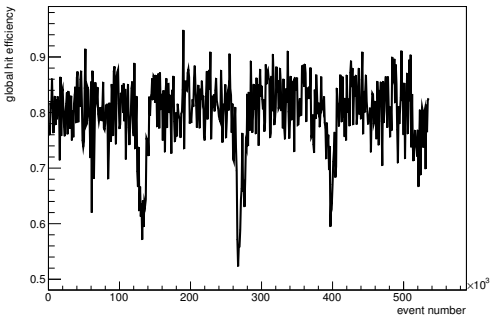

(r) Hit efficiency vs event number.

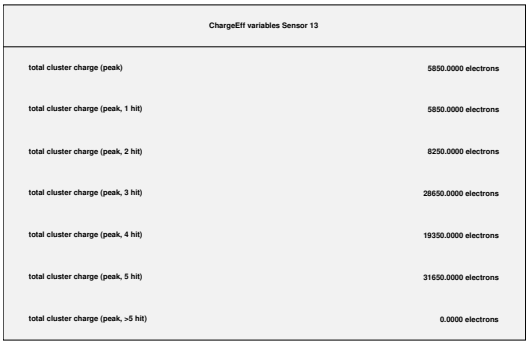

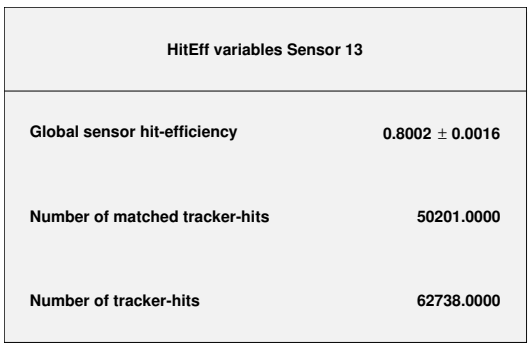

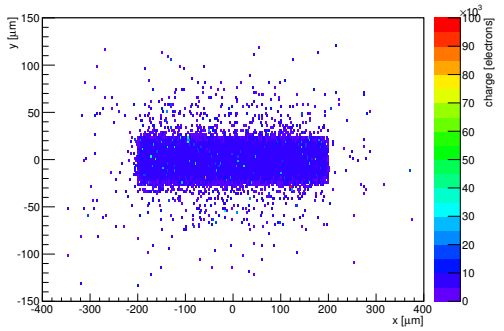

(s) Single pixel mean charge.

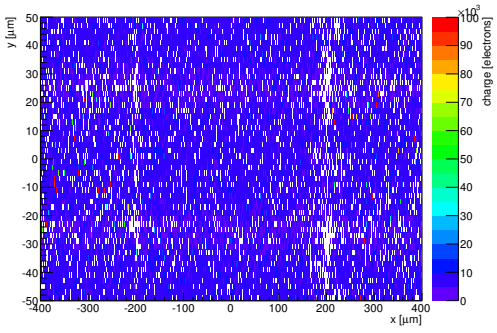

(t) Single pixel mean charge.

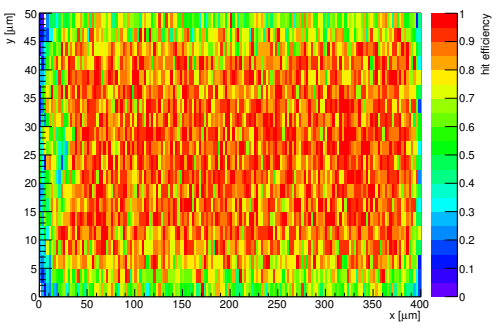

(u) Single pixel hit efficiency.

Figure C.50: Detailed plots for test beam measurement of DO-I-5 (description see section 6.1) sample (running as DUT3) during runs 61124-61128 in the September 2011 test beam period at CERN SPS in area H6B. Summary of the data in chapter 9.

C.3.3 Runs 61130-61146

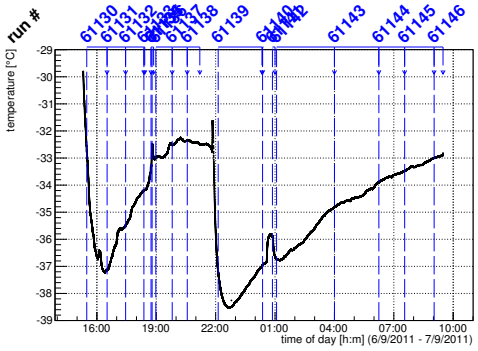

(a) Temperature vs time.

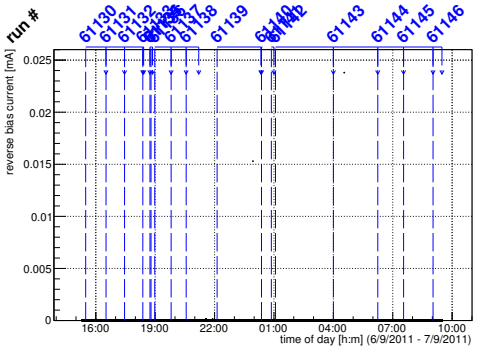

(b) Bias current vs time.

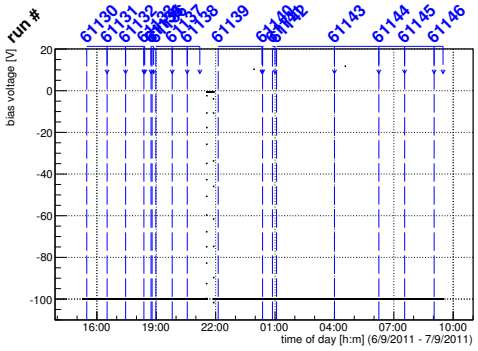

(c) Currently applied bias voltage vs time.

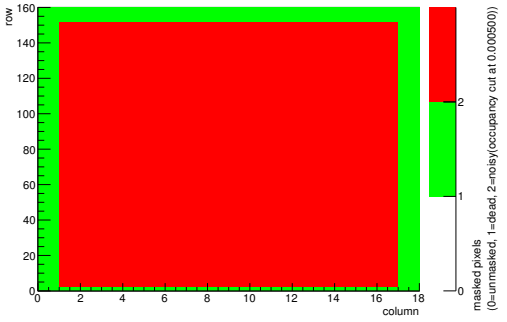

(d) Map of masked pixels.

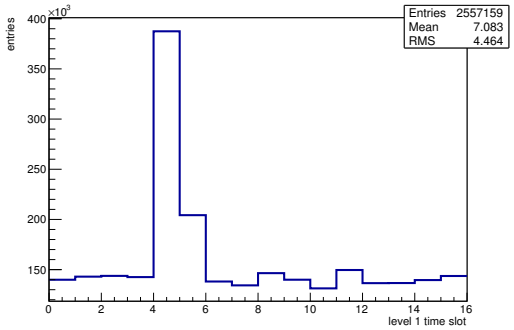

(e) Lvl1 distribution.

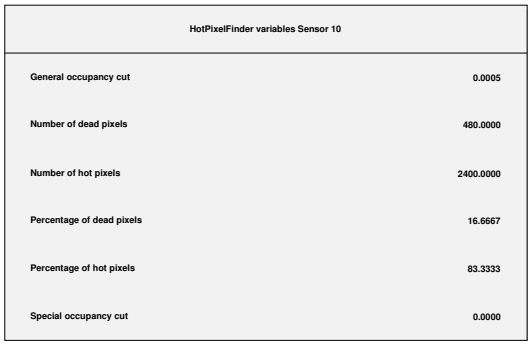

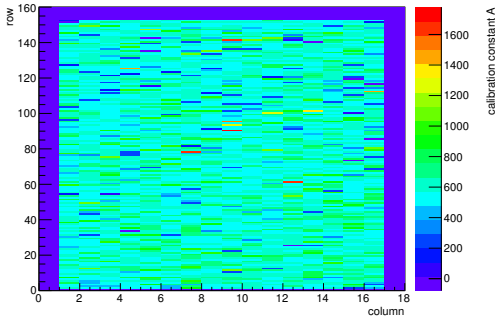

(f) Calibration constant A.

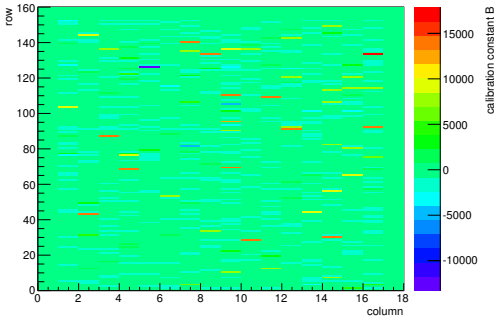

(g) Calibration constant B.

Figure C.51: Detailed plots for test beam measurement of SLID10 (description see section 6.1) sample (running as DUT0) during runs 61130-61146 in the September 2011 test beam period at CERN SPS in area H6B. Summary of the data in chapter 9. *(cont.)*

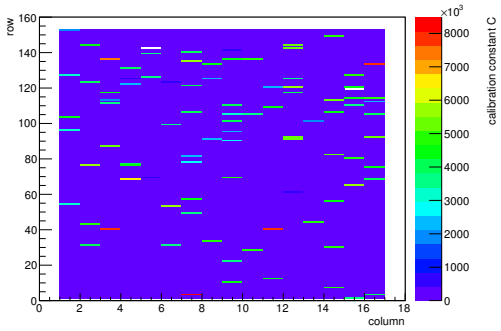

(h) Calibration constant C.

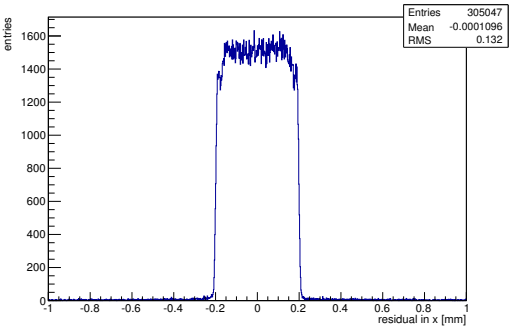

(i) Track residual in x.

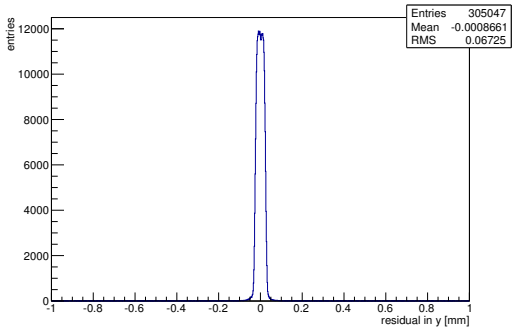

(j) Track residual in y.

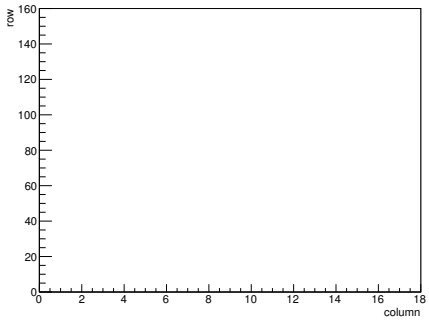

(k) Hit efficiency map.

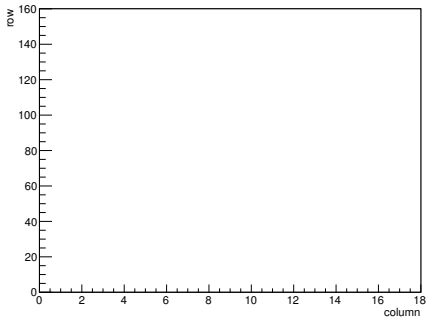

(l) Hit inefficiency map.

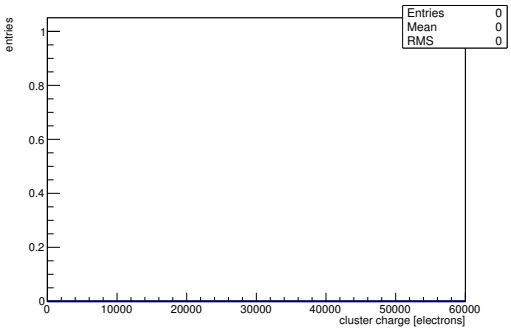

(m) Charge distribution (all cluster sizes included).

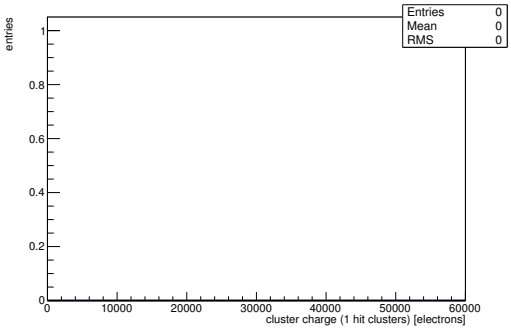

(n) Charge distribution (1 hit cluster).

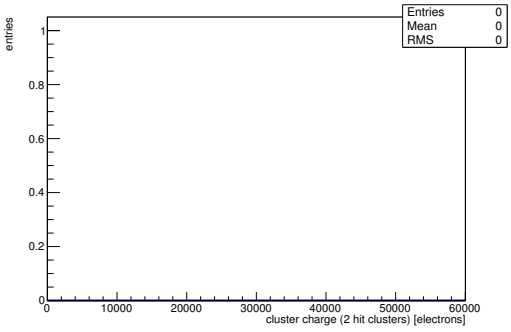

(o) Charge distribution (2 hit cluster).

Figure C.51: Detailed plots for test beam measurement of SLID10 (description see section 6.1) sample (running as DUT0) during runs 61130-61146 in the September 2011 test beam period at CERN SPS in area H6B. Summary of the data in chapter 9. *(cont.)*

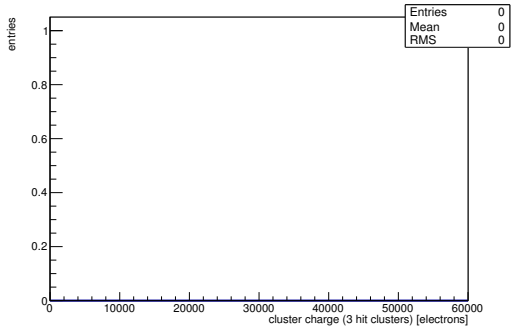

(p) Charge distribution (3 hit cluster).

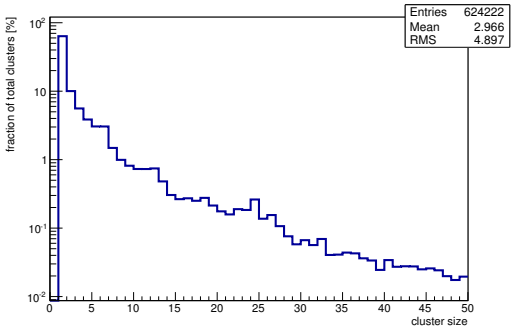

(q) Cluster size distribution.

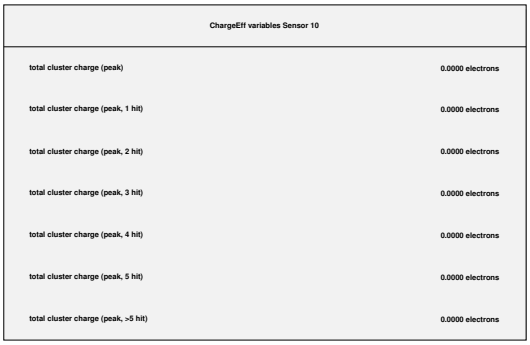

(r) Hit efficiency vs event number.

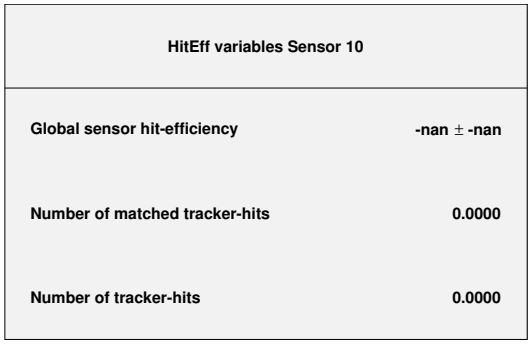

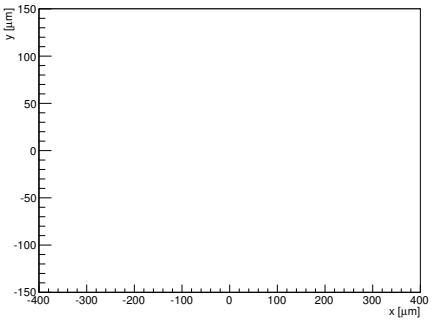

(s) Single pixel mean charge.

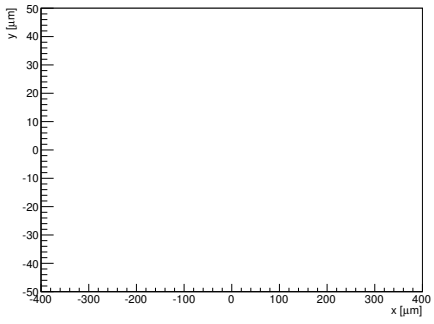

(t) Single pixel mean charge.

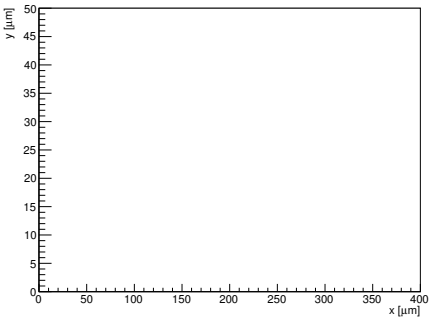

(u) Single pixel hit efficiency.

Figure C.51: Detailed plots for test beam measurement of SLID10 (description see section 6.1) sample (running as DUT0) during runs 61130-61146 in the September 2011 test beam period at CERN SPS in area H6B. Summary of the data in chapter 9.

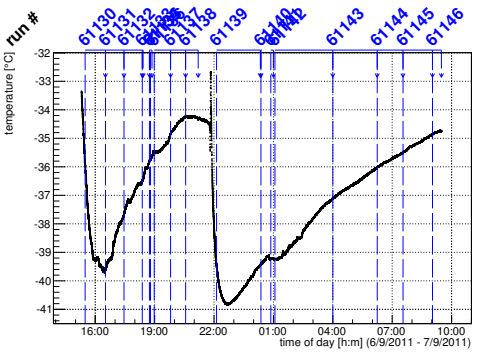

(a) Temperature vs time.

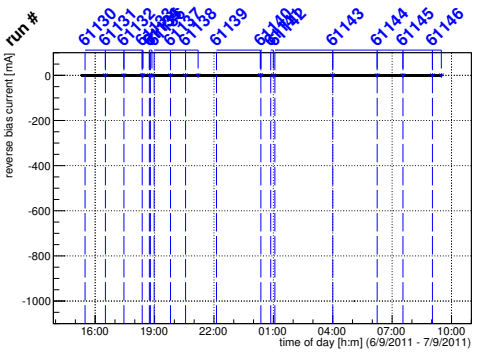

(b) Bias current vs time.

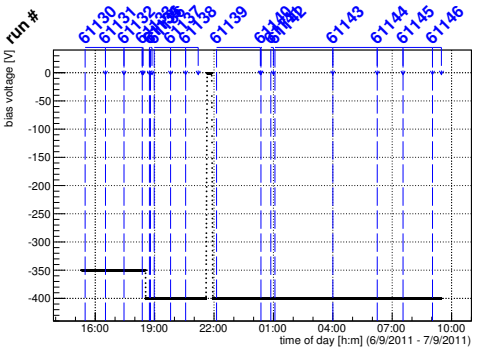

(c) Currently applied bias voltage vs time.

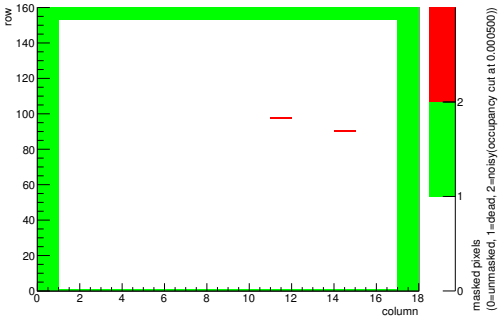

(d) Map of masked pixels.

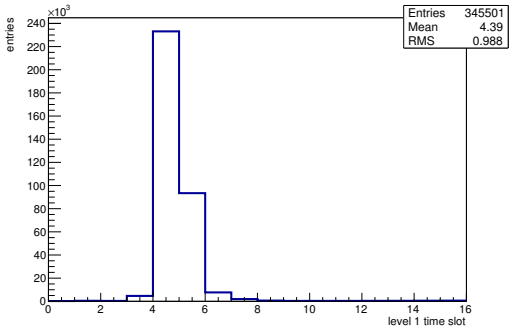

(e) Lvl1 distribution.

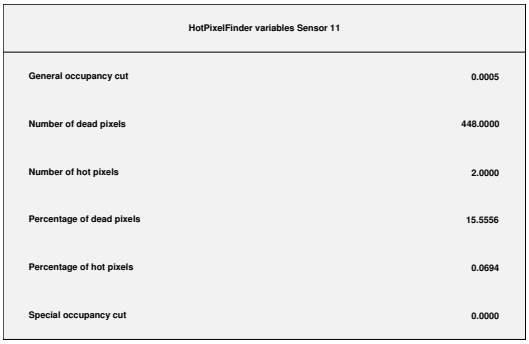

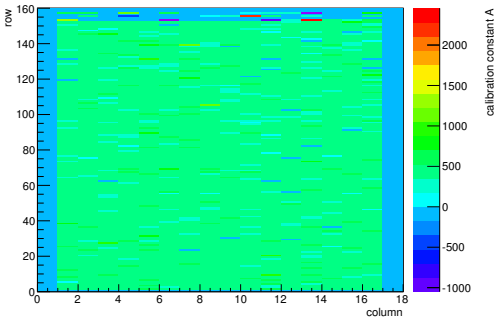

(f) Calibration constant A.

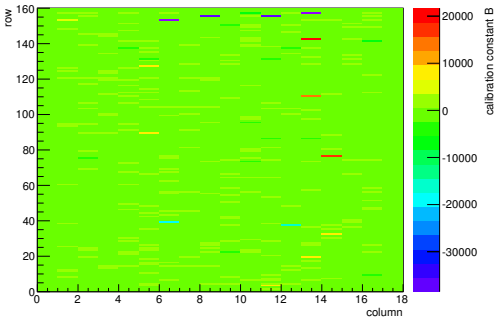

(g) Calibration constant B.

Figure C.52: Detailed plots for test beam measurement of SLID09 (description see section 6.1) sample (running as DUT1) during runs 61130-61146 in the September 2011 test beam period at CERN SPS in area H6B. Summary of the data in chapter 9. *(cont.)*

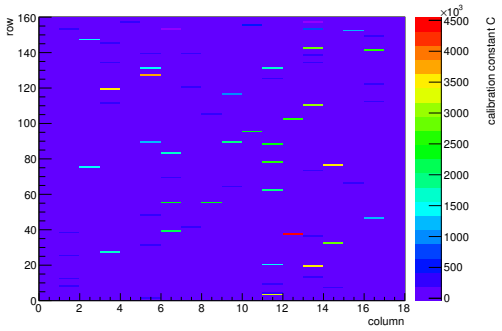

(h) Calibration constant C.

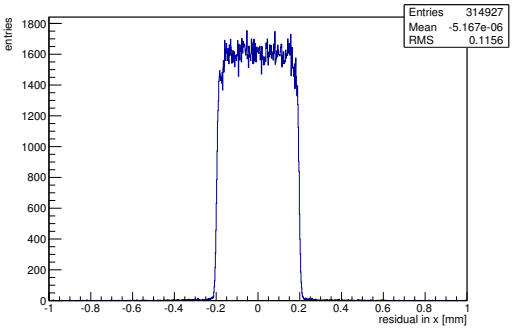

(i) Track residual in x.

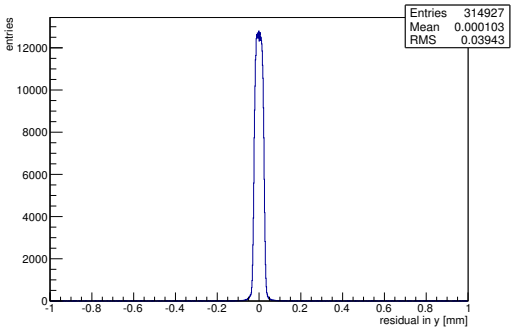

(j) Track residual in y.

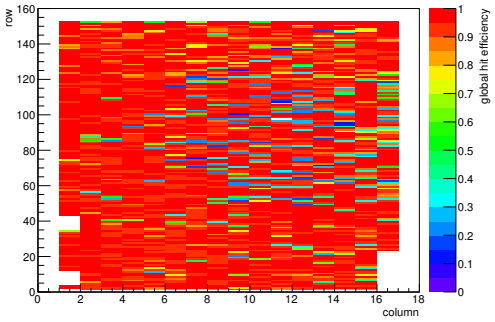

(k) Hit efficiency map.

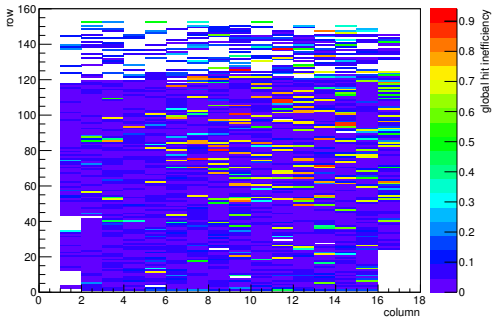

(l) Hit inefficiency map.

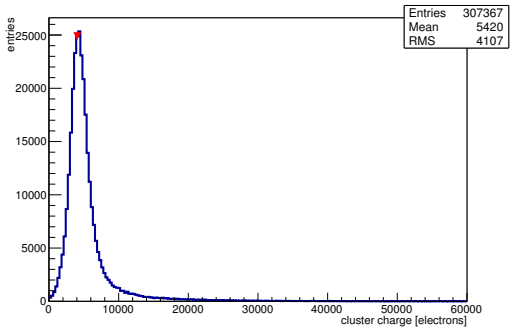

(m) Charge distribution (all cluster sizes included).

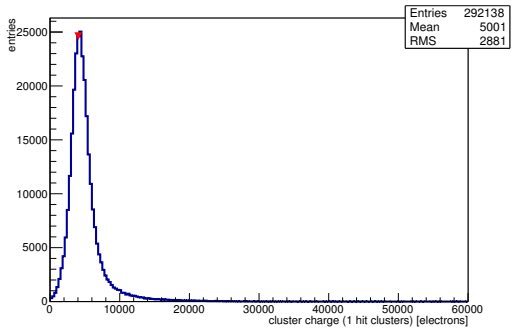

(n) Charge distribution (1 hit cluster).

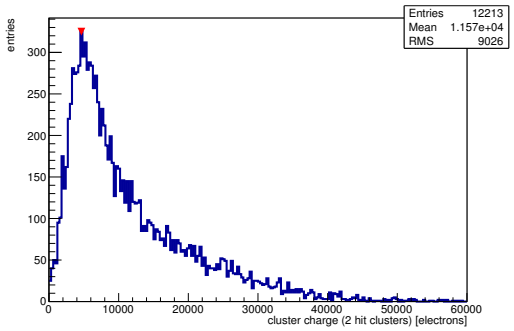

(o) Charge distribution (2 hit cluster).

Figure C.52: Detailed plots for test beam measurement of SLID09 (description see section 6.1) sample (running as DUT1) during runs 61130-61146 in the September 2011 test beam period at CERN SPS in area H6B. Summary of the data in chapter 9. *(cont.)*

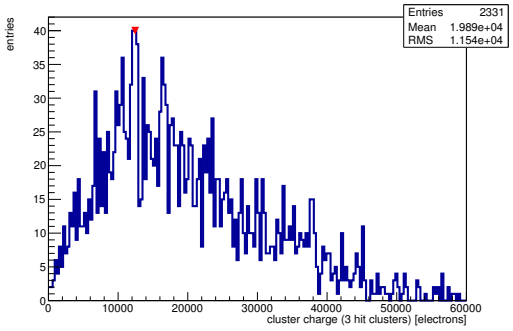

(p) Charge distribution (3 hit cluster).

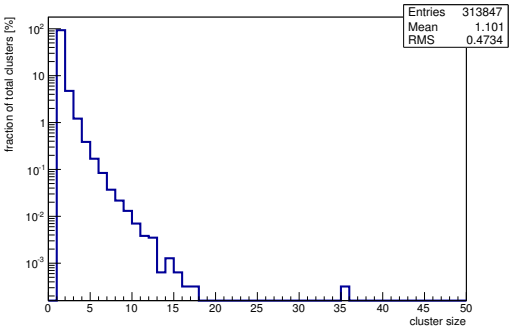

(q) Cluster size distribution.

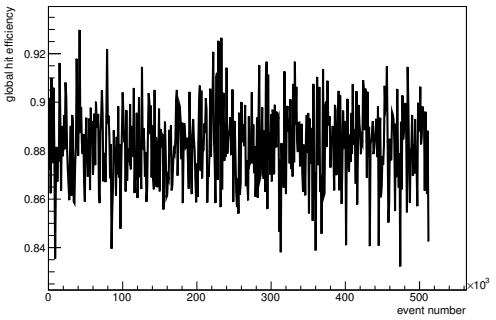

(r) Hit efficiency vs event number.

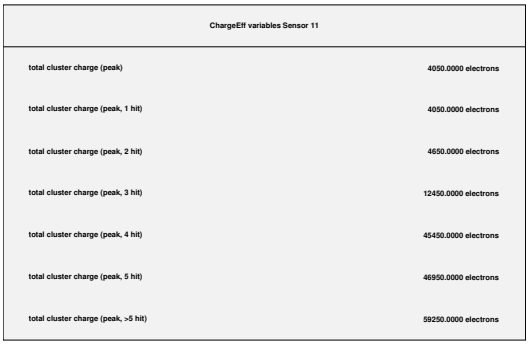

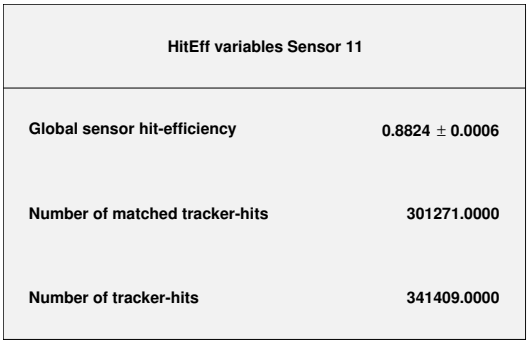

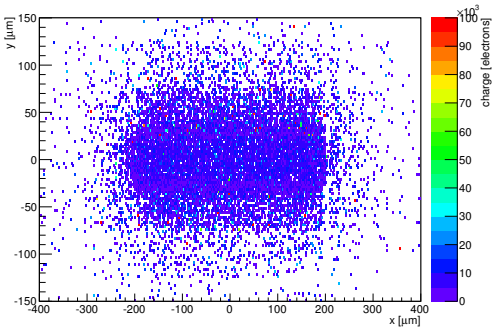

(s) Single pixel mean charge.

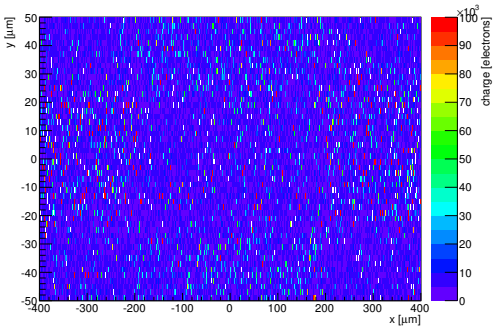

(t) Single pixel mean charge.

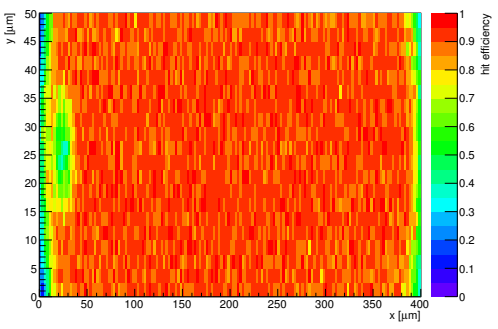

(u) Single pixel hit efficiency.

Figure C.52: Detailed plots for test beam measurement of SLID09 (description see section 6.1) sample (running as DUT1) during runs 61130-61146 in the September 2011 test beam period at CERN SPS in area H6B. Summary of the data in chapter 9.

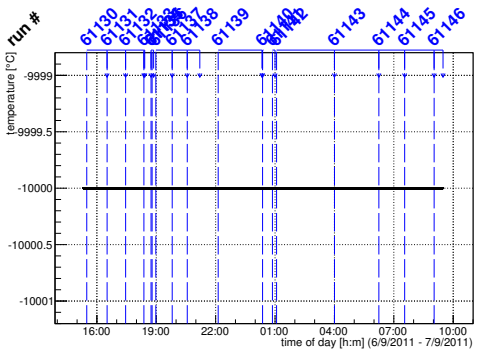

(a) Temperature vs time.

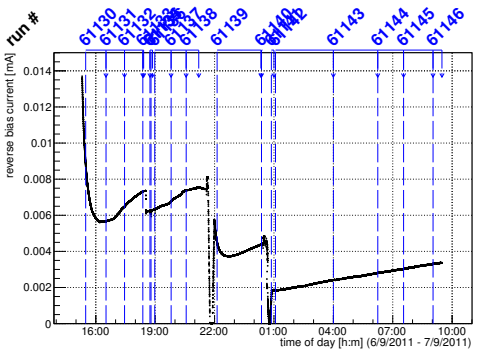

(b) Bias current vs time.

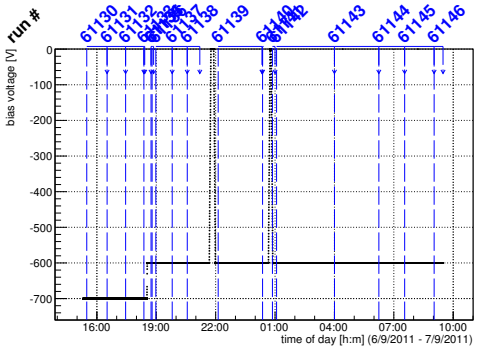

(c) Currently applied bias voltage vs time.

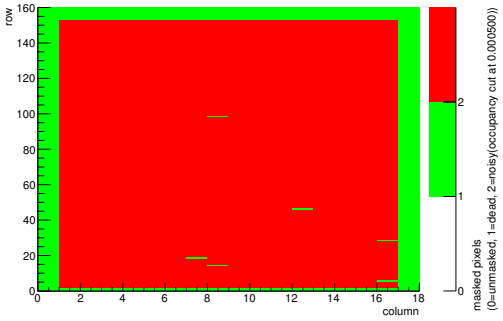

(d) Map of masked pixels.

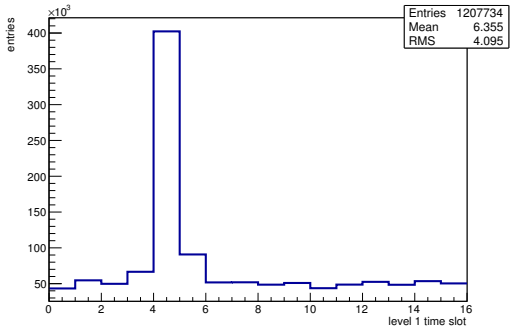

(e) Lvl1 distribution.

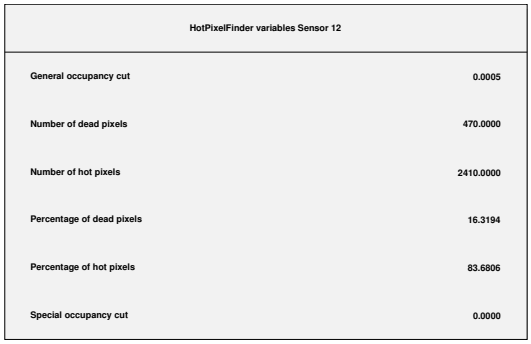

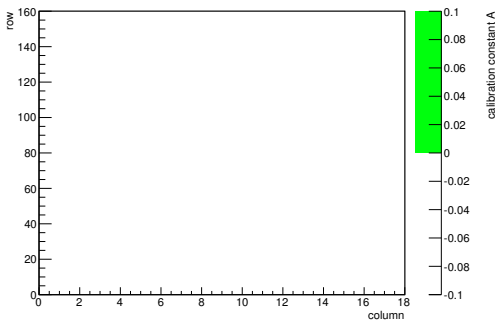

(f) Calibration constant A.

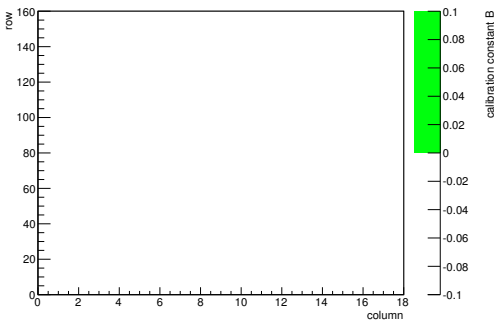

(g) Calibration constant B.

Figure C.53: Detailed plots for test beam measurement of CiS5e15 (description see section 6.1) sample (running as DUT2) during runs 61130-61146 in the September 2011 test beam period at CERN SPS in area H6B. Summary of the data in chapter 9. *(cont.)*

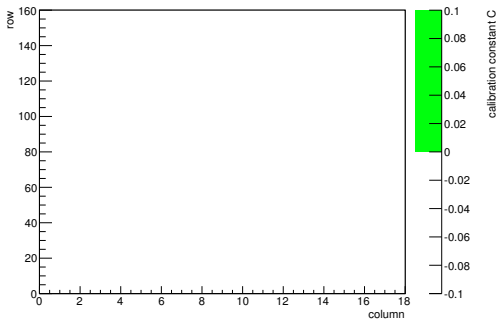

(h) Calibration constant C.

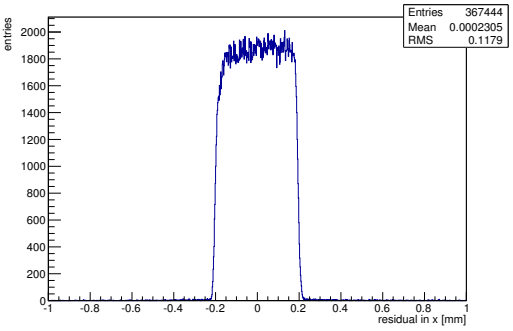

(i) Track residual in x.

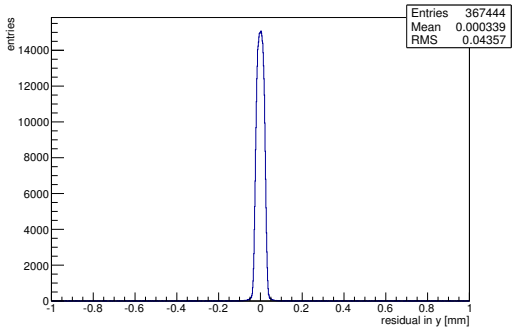

(j) Track residual in y.

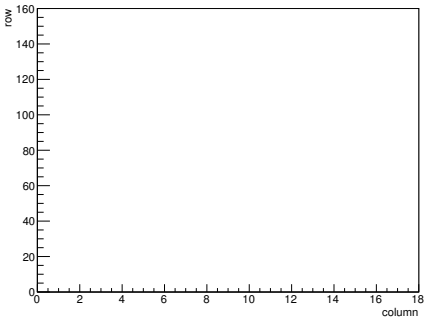

(k) Hit efficiency map.

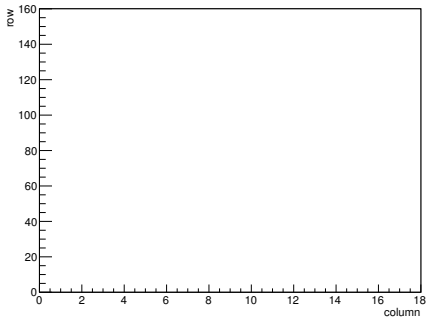

(l) Hit inefficiency map.

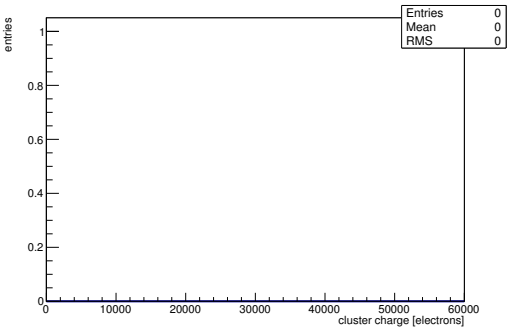

(m) Charge distribution (all cluster sizes included).

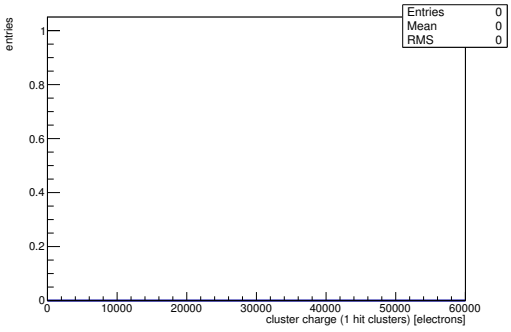

(n) Charge distribution (1 hit cluster).

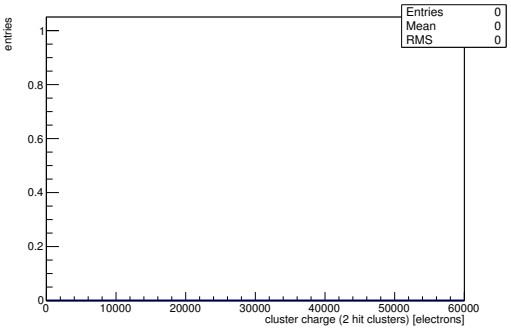

(o) Charge distribution (2 hit cluster).

Figure C.53: Detailed plots for test beam measurement of CiS5e15 (description see section 6.1) sample (running as DUT2) during runs 61130-61146 in the September 2011 test beam period at CERN SPS in area H6B. Summary of the data in chapter 9. *(cont.)*

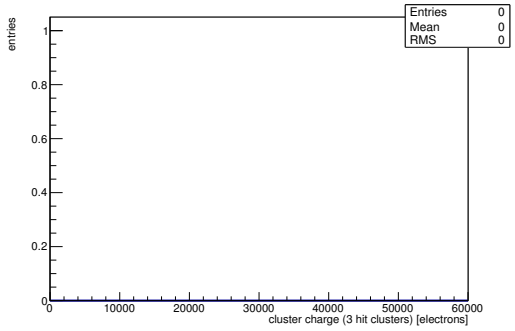

(p) Charge distribution (3 hit cluster).

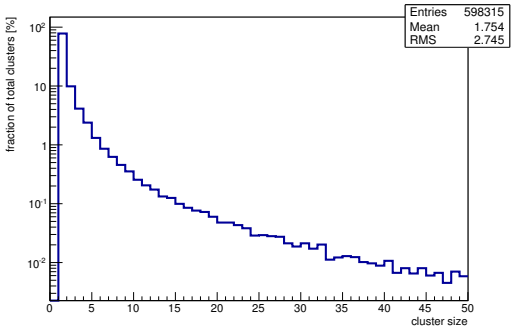

(q) Cluster size distribution.

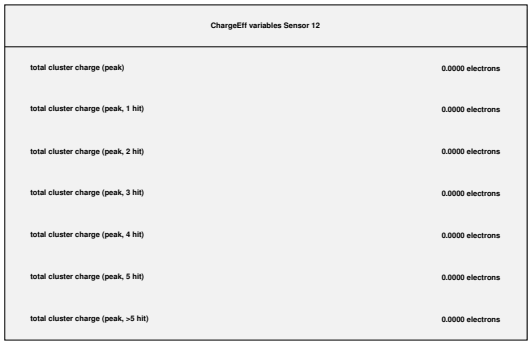

(r) Hit efficiency vs event number.

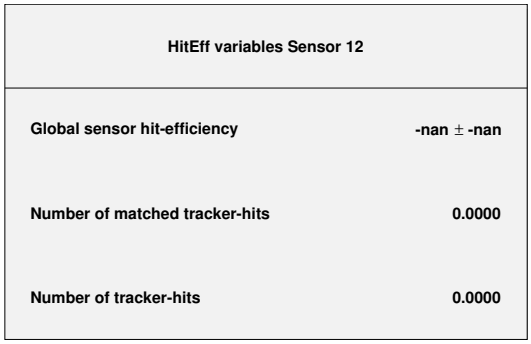

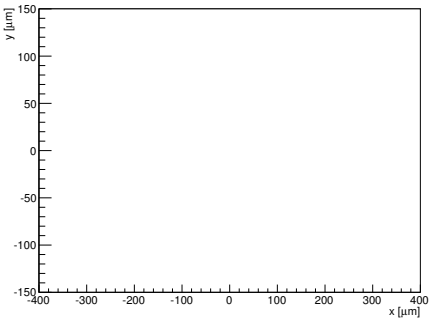

(s) Single pixel mean charge.

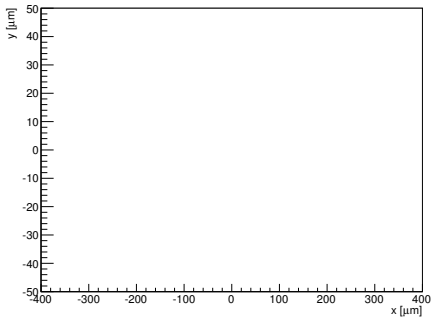

(t) Single pixel mean charge.

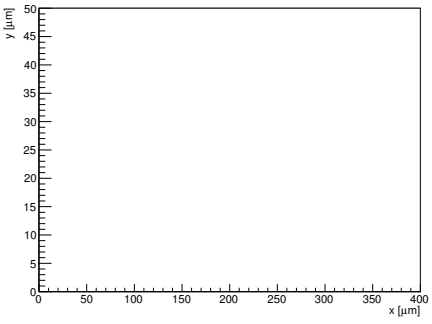

(u) Single pixel hit efficiency.

Figure C.53: Detailed plots for test beam measurement of CiS5e15 (description see section 6.1) sample (running as DUT2) during runs 61130-61146 in the September 2011 test beam period at CERN SPS in area H6B. Summary of the data in chapter 9.

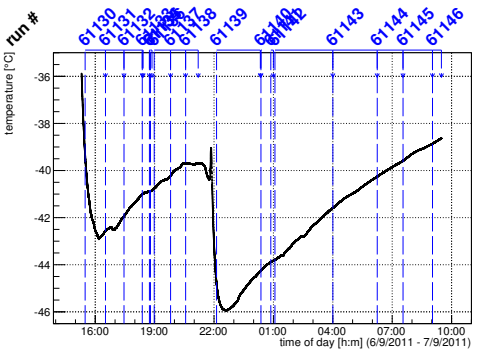

(a) Temperature vs time.

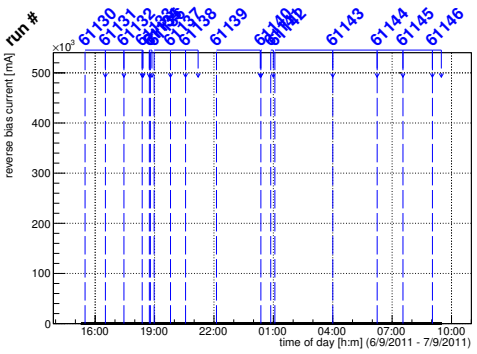

(b) Bias current vs time.

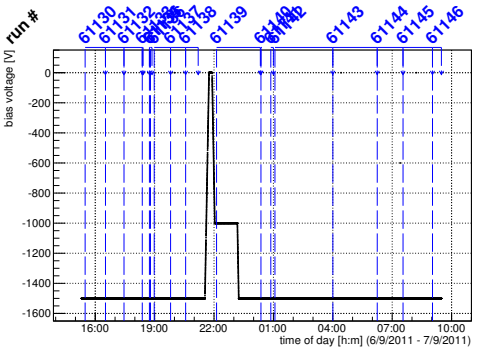

(c) Currently applied bias voltage vs time.

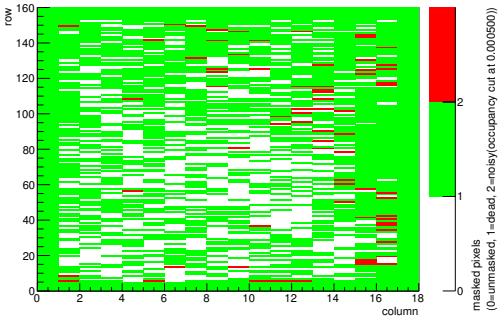

(d) Map of masked pixels.

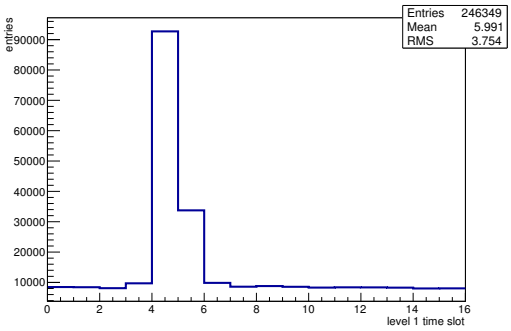

(e) Lvl1 distribution.

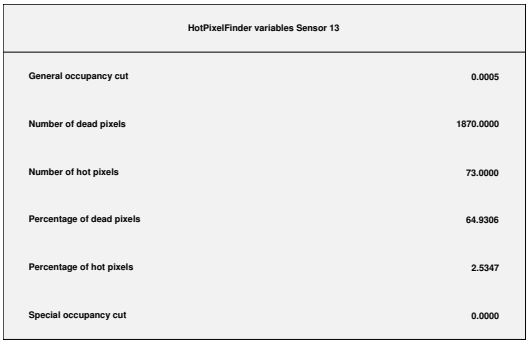

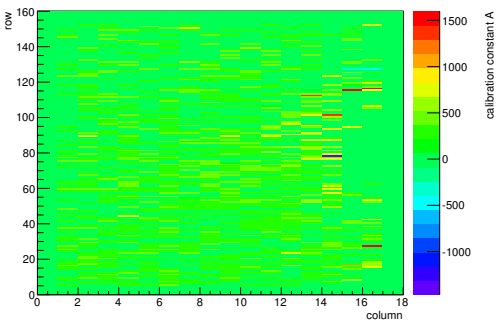

(f) Calibration constant A.

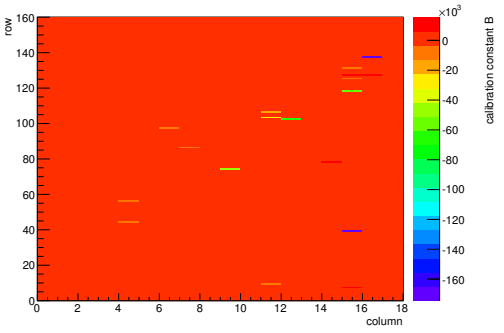

(g) Calibration constant B.

Figure C.54: Detailed plots for test beam measurement of DO-I-5 (description see section 6.1) sample (running as DUT3) during runs 61130-61146 in the September 2011 test beam period at CERN SPS in area H6B. Summary of the data in chapter 9. *(cont.)*

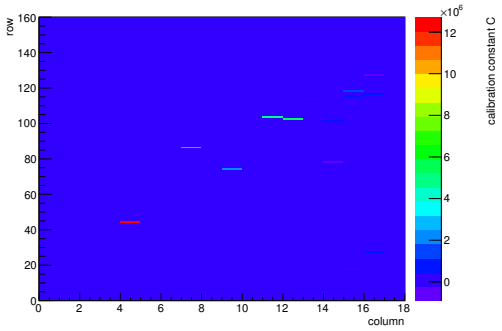

(h) Calibration constant C.

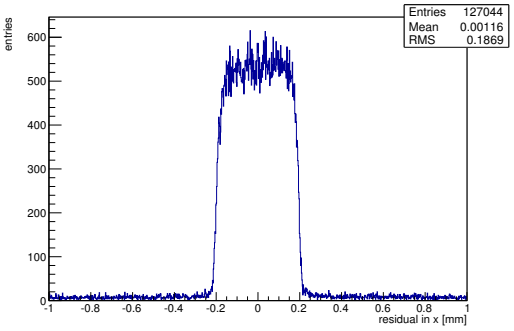

(i) Track residual in x.

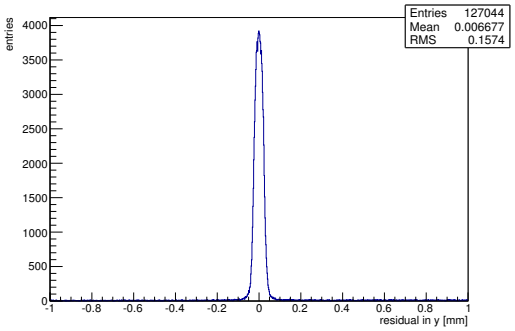

(j) Track residual in y.

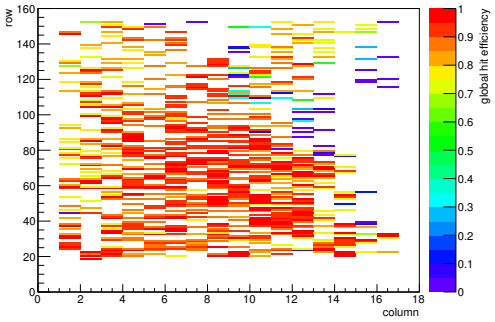

(k) Hit efficiency map.

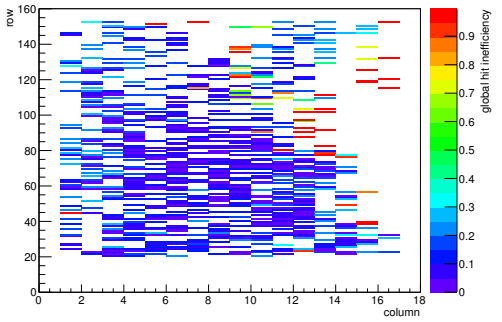

(l) Hit inefficiency map.

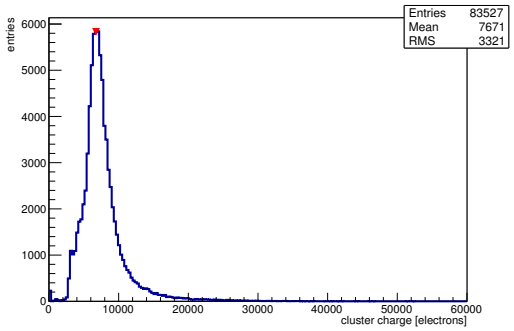

(m) Charge distribution (all cluster sizes included).

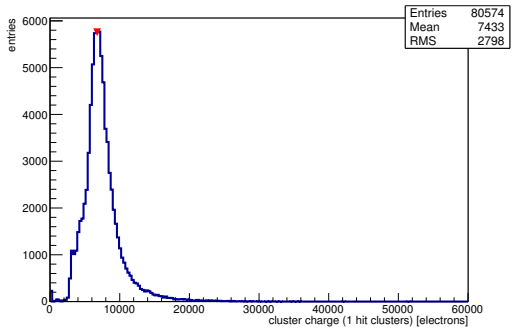

(n) Charge distribution (1 hit cluster).

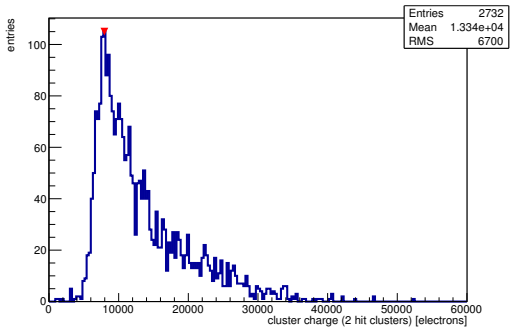

(o) Charge distribution (2 hit cluster).

Figure C.54: Detailed plots for test beam measurement of DO-I-5 (description see section 6.1) sample (running as DUT3) during runs 61130-61146 in the September 2011 test beam period at CERN SPS in area H6B. Summary of the data in chapter 9. *(cont.)*

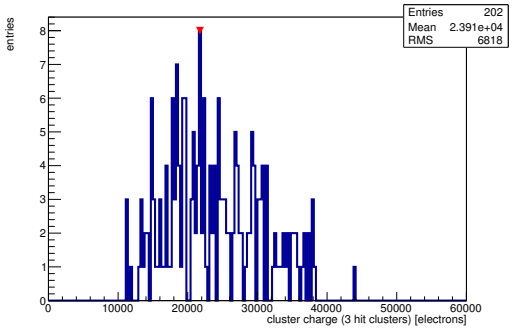

(p) Charge distribution (3 hit cluster).

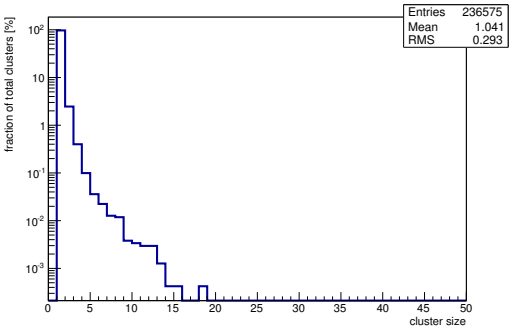

(q) Cluster size distribution.

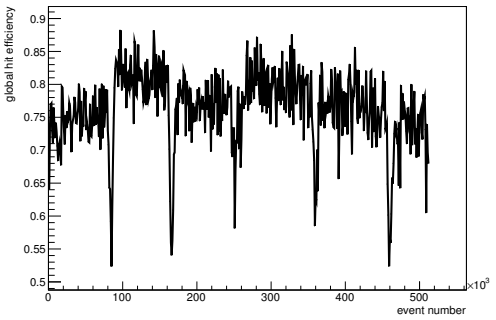

(r) Hit efficiency vs event number.

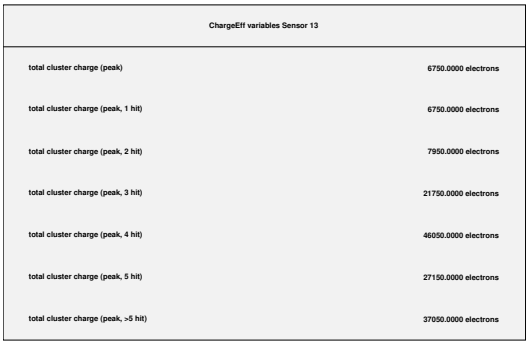

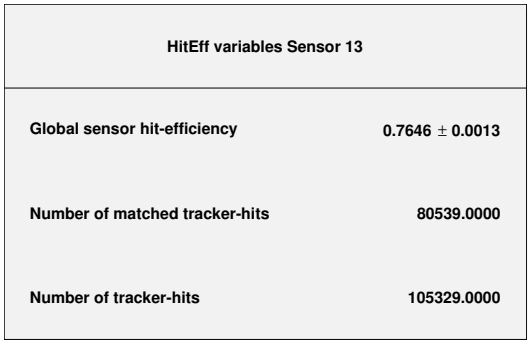

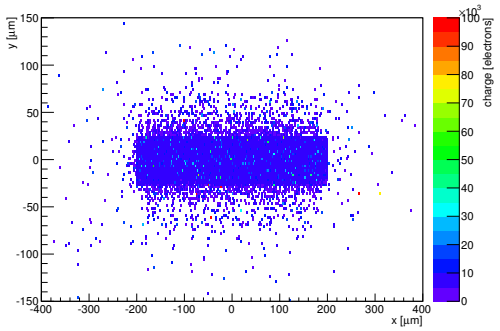

(s) Single pixel mean charge.

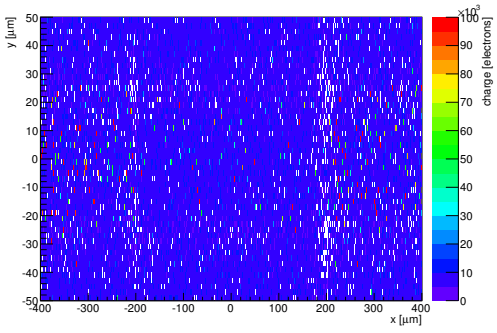

(t) Single pixel mean charge.

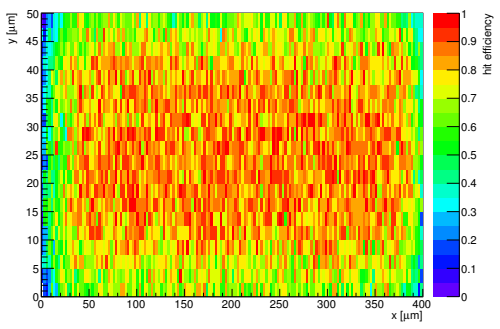

(u) Single pixel hit efficiency.

Figure C.54: Detailed plots for test beam measurement of DO-I-5 (description see section 6.1) sample (running as DUT3) during runs 61130-61146 in the September 2011 test beam period at CERN SPS in area H6B. Summary of the data in chapter 9.

C.3.4 Run 61249

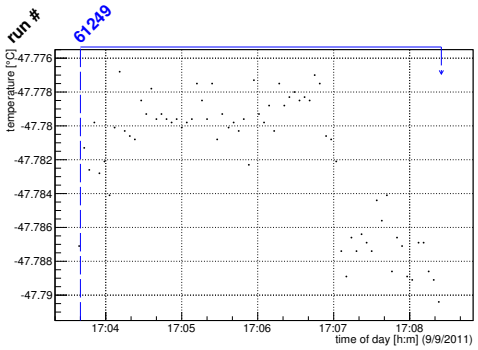

(a) Temperature vs time.

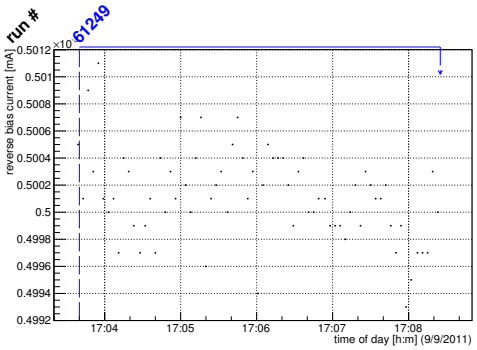

(b) Bias current vs time.

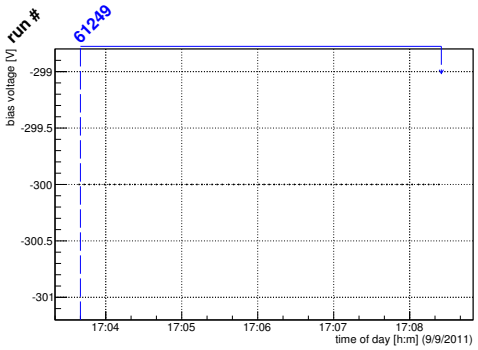

(c) Currently applied bias voltage vs time.

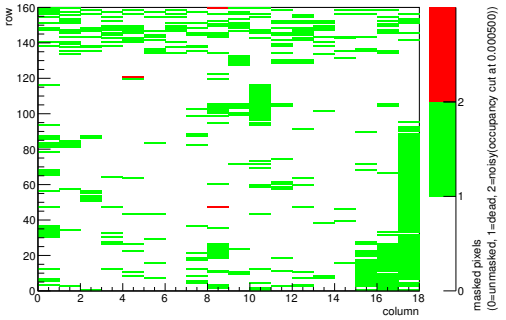

(d) Map of masked pixels.

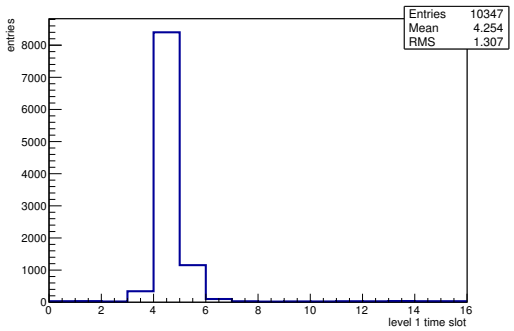

(e) Lvl1 distribution.

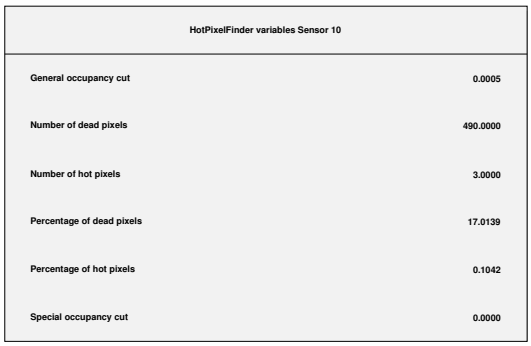

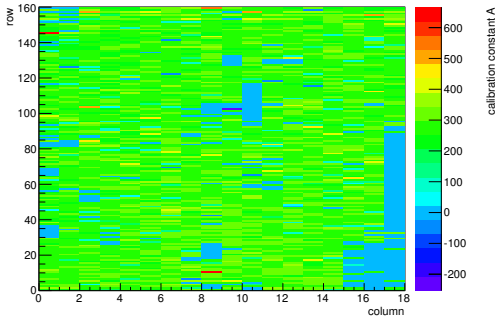

(f) Calibration constant A.

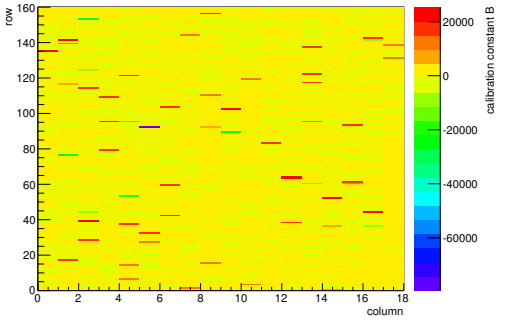

(g) Calibration constant B.

Figure C.55: Detailed plots for test beam measurement of DO-I-7 (description see section 6.1) sample (running as DUT0) during runs 61249 in the September 2011 test beam period at CERN SPS in area H6B. Summary of the data in chapter 9. *(cont.)*

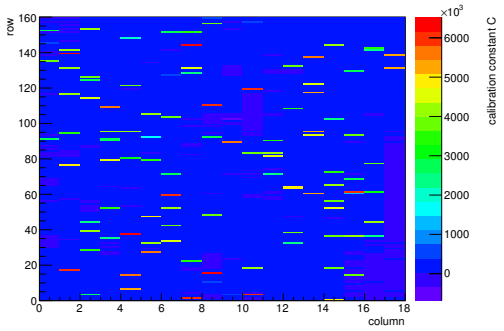

(h) Calibration constant C.

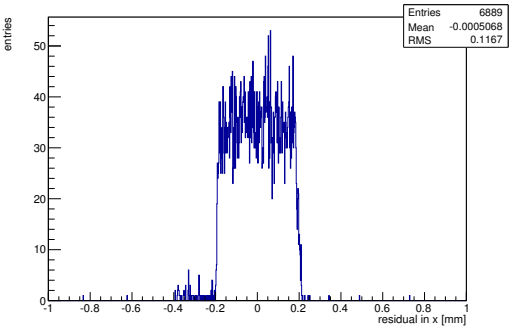

(i) Track residual in x.

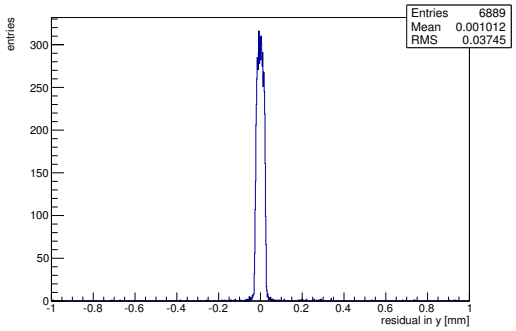

(j) Track residual in y.

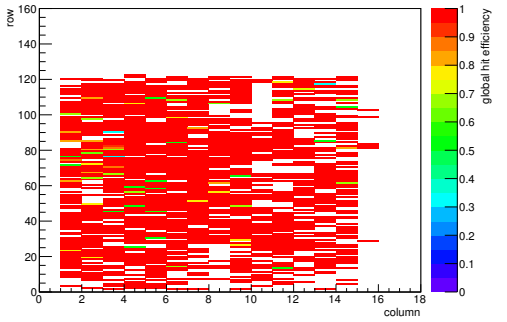

(k) Hit efficiency map.

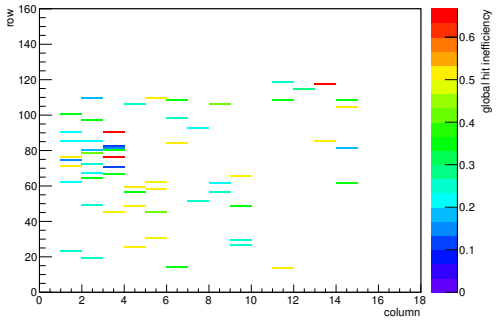

(l) Hit inefficiency map.

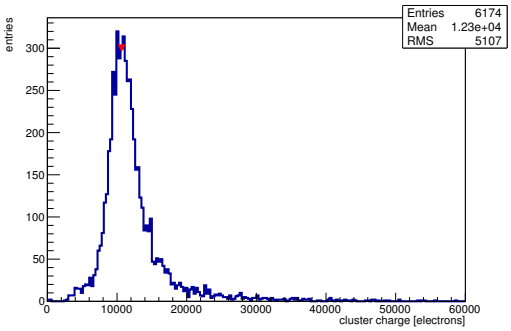

(m) Charge distribution (all cluster sizes included).

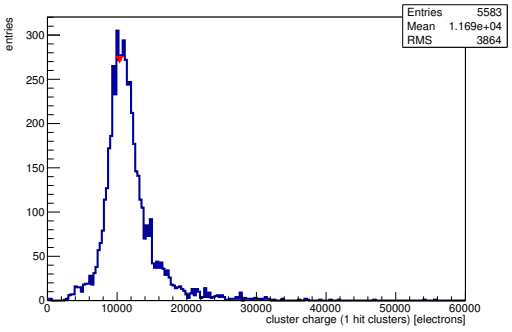

(n) Charge distribution (1 hit cluster).

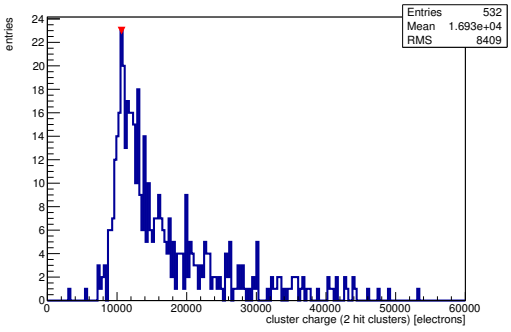

(o) Charge distribution (2 hit cluster).

Figure C.55: Detailed plots for test beam measurement of DO-I-7 (description see section 6.1) sample (running as DUT0) during runs 61249 in the September 2011 test beam period at CERN SPS in area H6B. Summary of the data in chapter 9. *(cont.)*

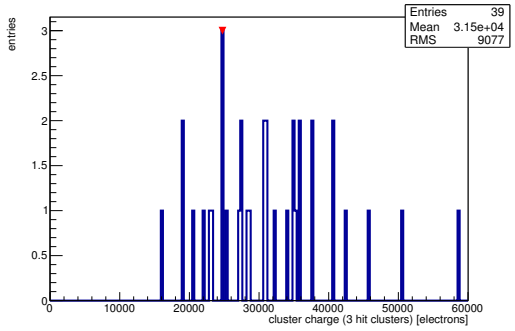

(p) Charge distribution (3 hit cluster).

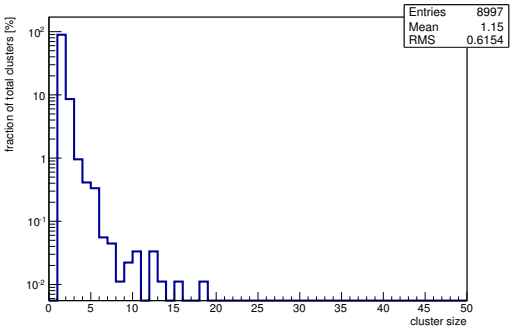

(q) Cluster size distribution.

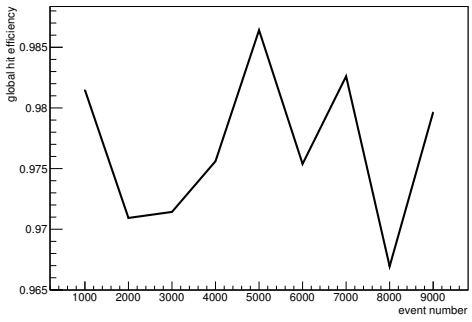

(r) Hit efficiency vs event number.

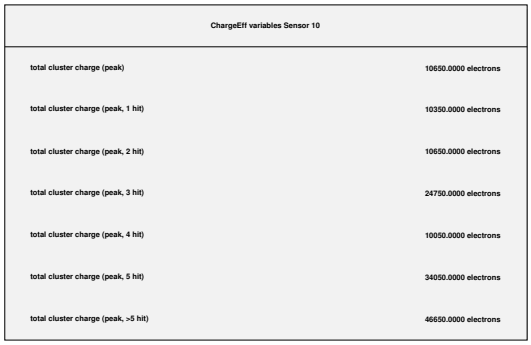

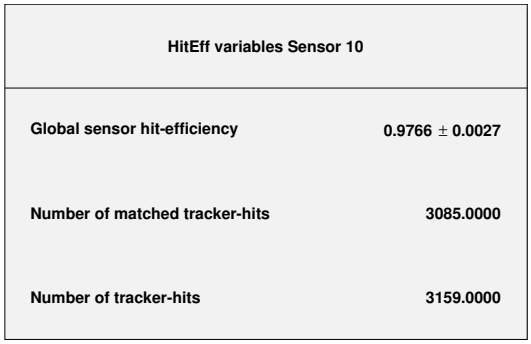

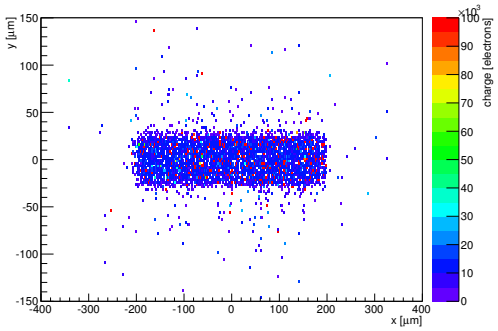

(s) Single pixel mean charge.

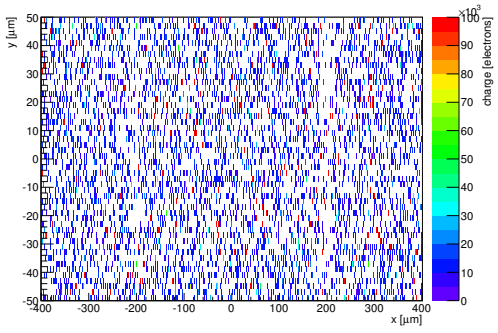

(t) Single pixel mean charge.

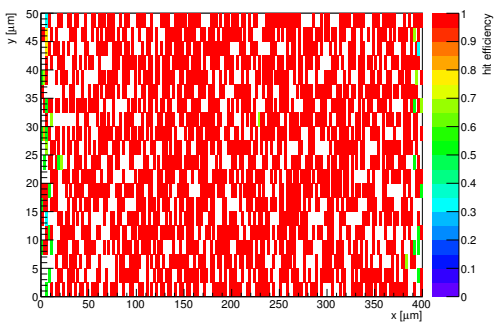

(u) Single pixel hit efficiency.

Figure C.55: Detailed plots for test beam measurement of DO-I-7 (description see section 6.1) sample (running as DUT0) during runs 61249 in the September 2011 test beam period at CERN SPS in area H6B. Summary of the data in chapter 9.

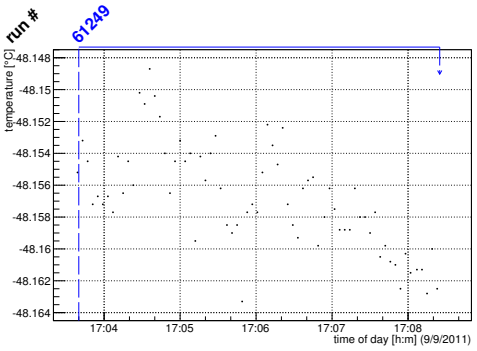

(a) Temperature vs time.

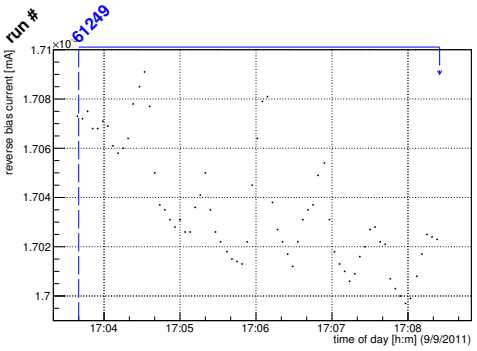

(b) Bias current vs time.

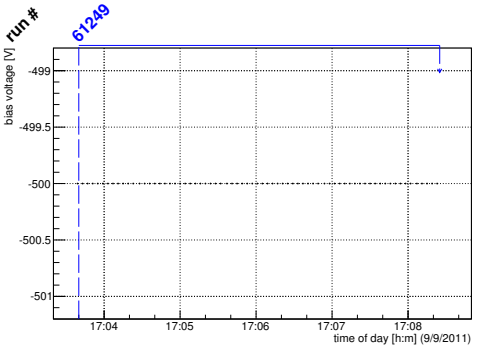

(c) Currently applied bias voltage vs time.

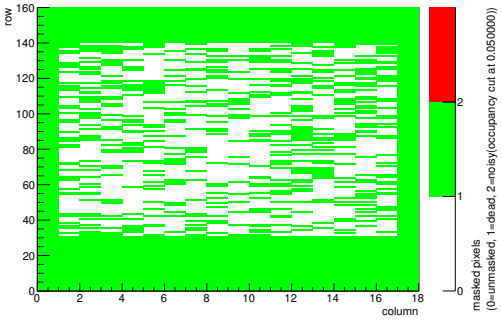

(d) Map of masked pixels.

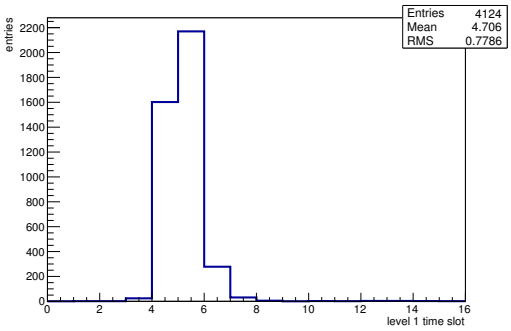

(e) Lvl1 distribution.

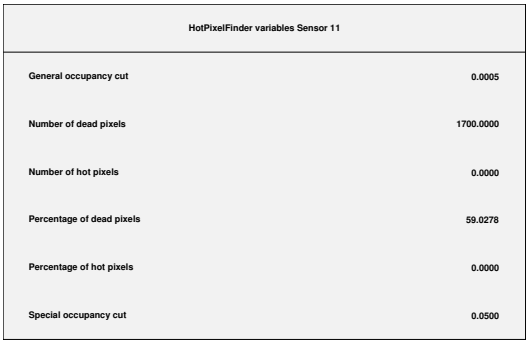

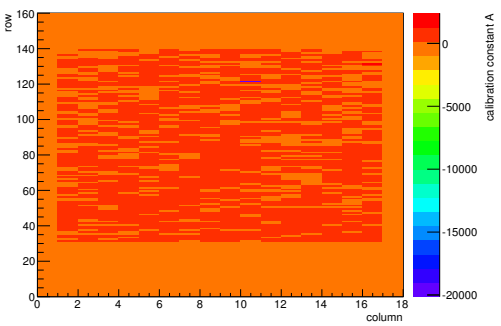

(f) Calibration constant A.

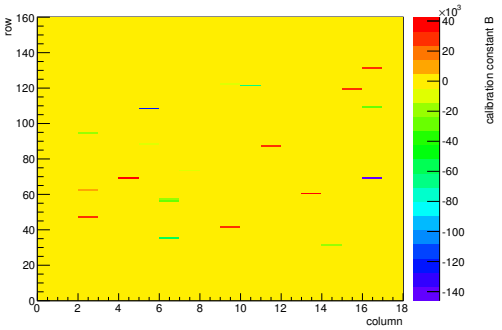

(g) Calibration constant B.

Figure C.56: Detailed plots for test beam measurement of DO-I-11 (description see section 6.1) sample (running as DUT1) during runs 61249 in the September 2011 test beam period at CERN SPS in area H6B. Summary of the data in chapter 9. *(cont.)*

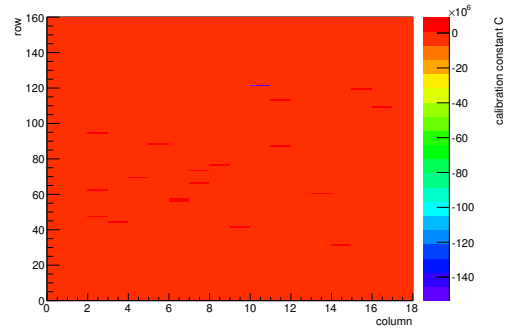

(h) Calibration constant C.

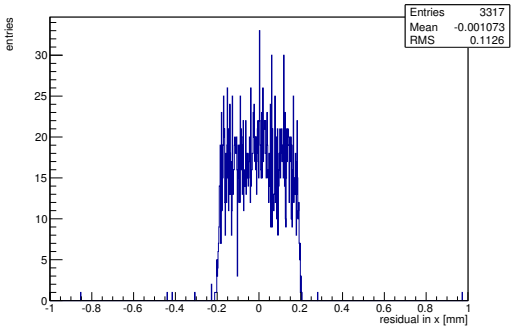

(i) Track residual in x.

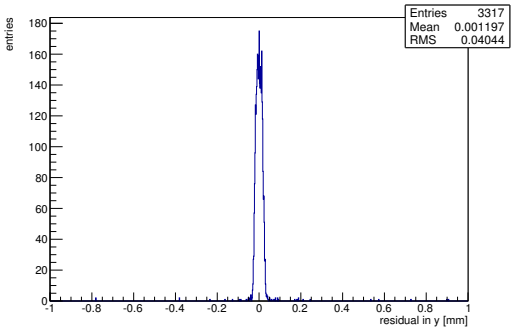

(j) Track residual in y.

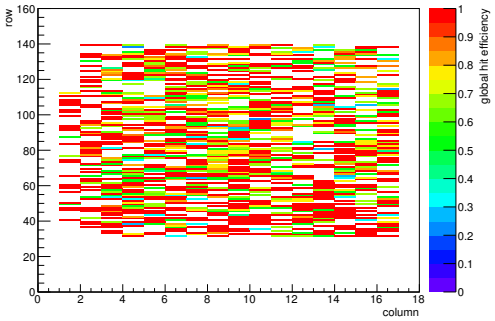

(k) Hit efficiency map.

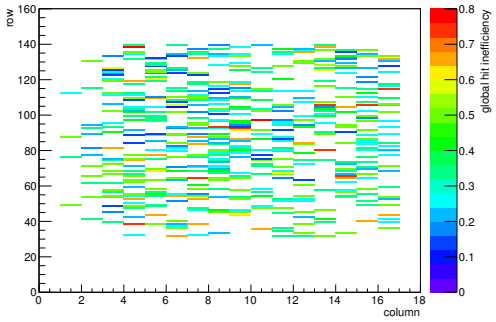

(l) Hit inefficiency map.

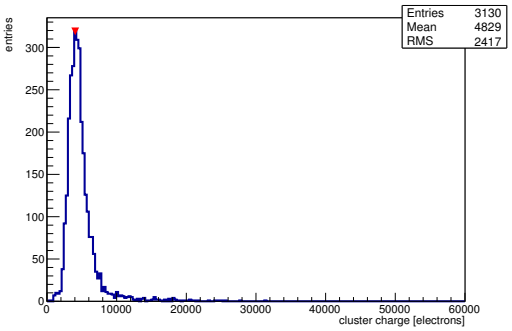

(m) Charge distribution (all cluster sizes included).

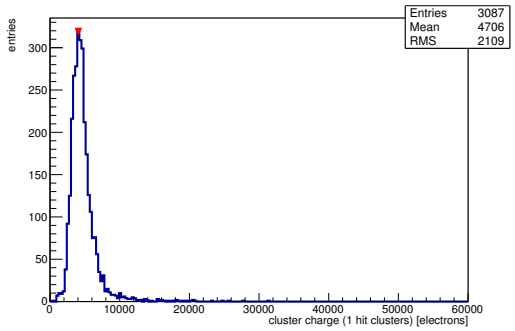

(n) Charge distribution (1 hit cluster).

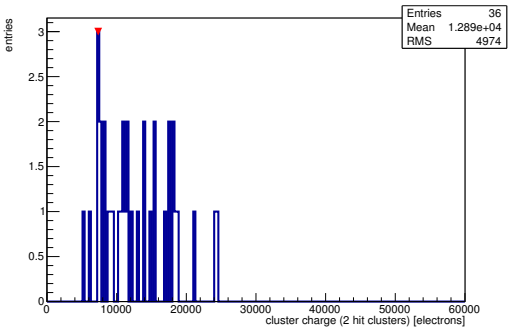

(o) Charge distribution (2 hit cluster).

Figure C.56: Detailed plots for test beam measurement of DO-I-11 (description see section 6.1) sample (running as DUT1) during runs 61249 in the September 2011 test beam period at CERN SPS in area H6B. Summary of the data in chapter 9. *(cont.)*

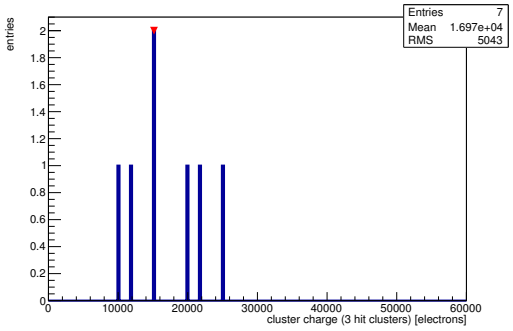

(p) Charge distribution (3 hit cluster).

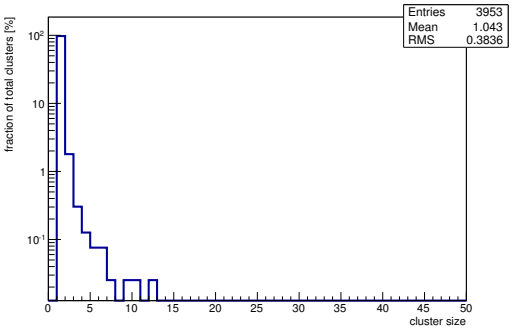

(q) Cluster size distribution.

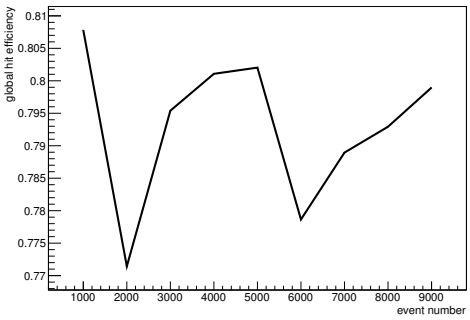

(r) Hit efficiency vs event number.

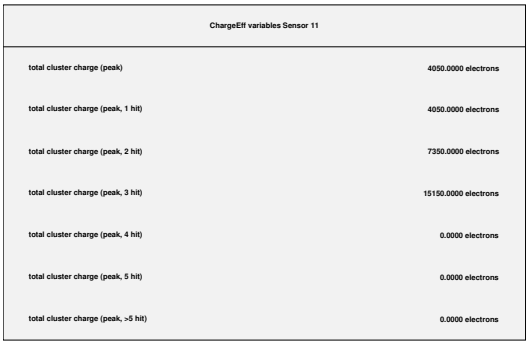

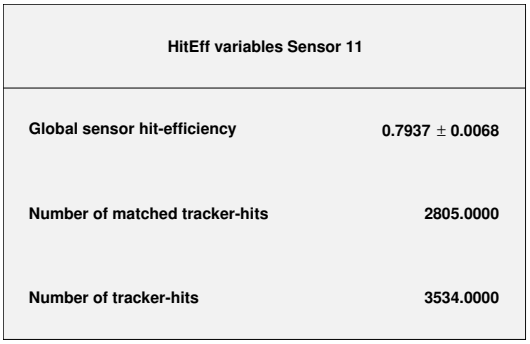

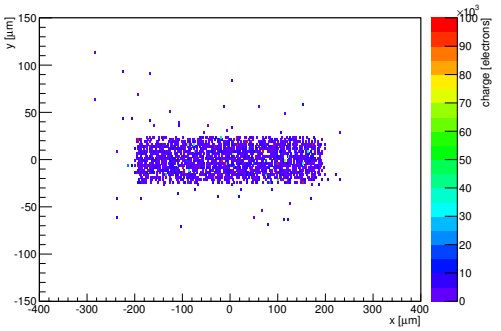

(s) Single pixel mean charge.

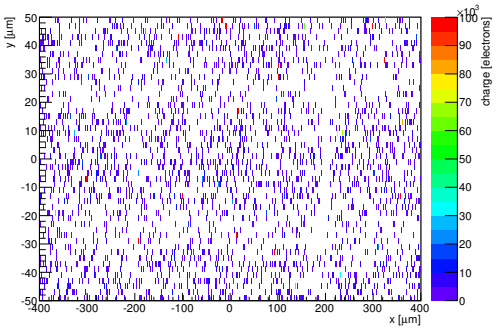

(t) Single pixel mean charge.

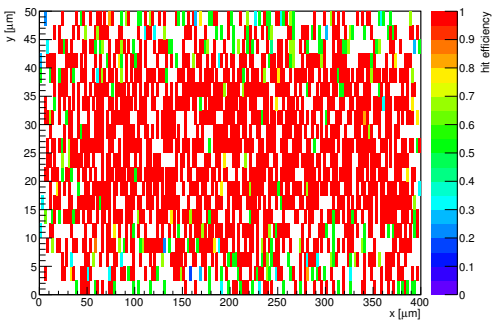

(u) Single pixel hit efficiency.

Figure C.56: Detailed plots for test beam measurement of DO-I-11 (description see section 6.1) sample (running as DUT1) during runs 61249 in the September 2011 test beam period at CERN SPS in area H6B. Summary of the data in chapter 9.

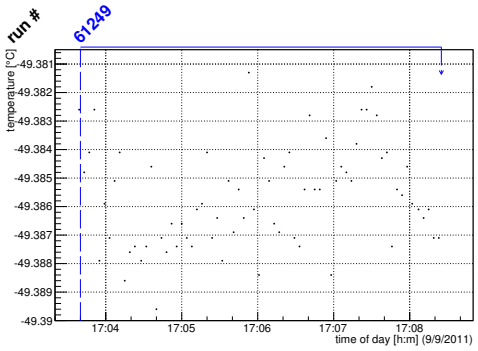

(a) Temperature vs time.

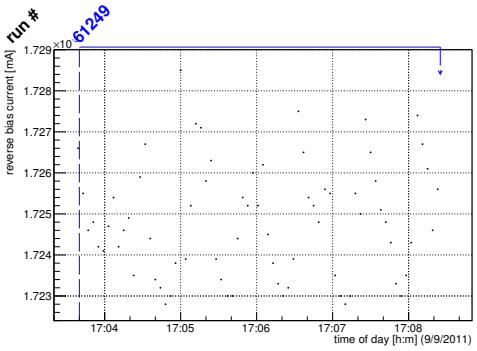

(b) Bias current vs time.

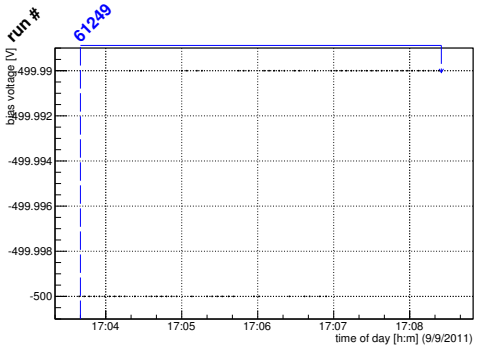

(c) Currently applied bias voltage vs time.

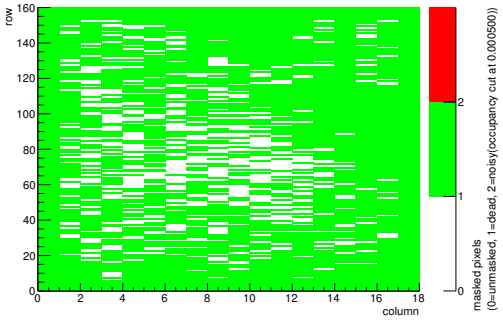

(d) Map of masked pixels.

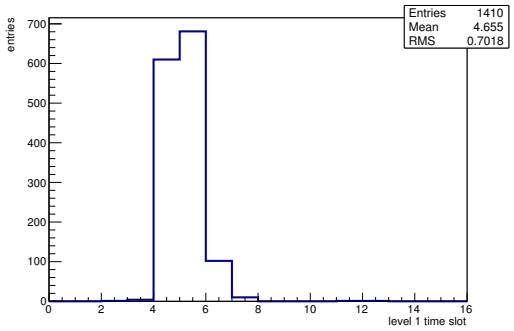

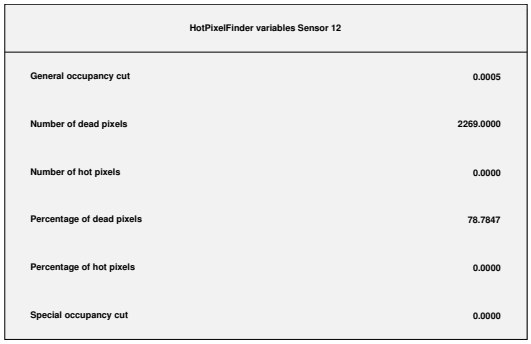

(e) Lvl1 distribution.

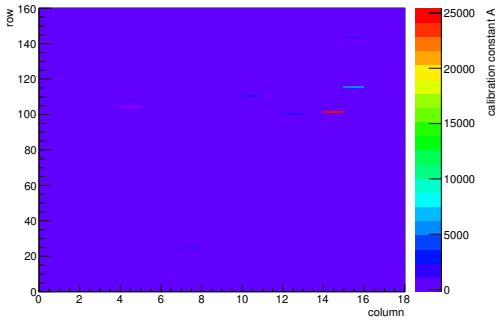

(f) Calibration constant A.

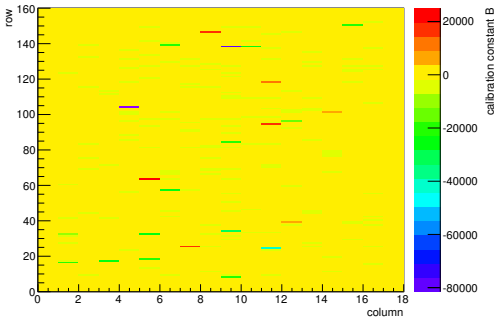

(g) Calibration constant B.

Figure C.57: Detailed plots for test beam measurement of DO-I-5 (description see section 6.1) sample (running as DUT2) during runs 61249 in the September 2011 test beam period at CERN SPS in area H6B. Summary of the data in chapter 9. *(cont.)*

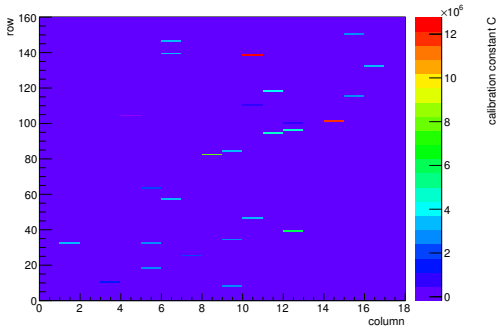

(h) Calibration constant C.

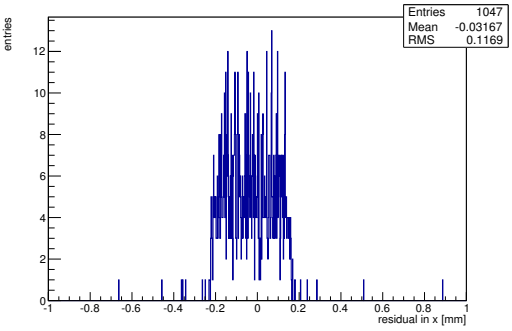

(i) Track residual in x.

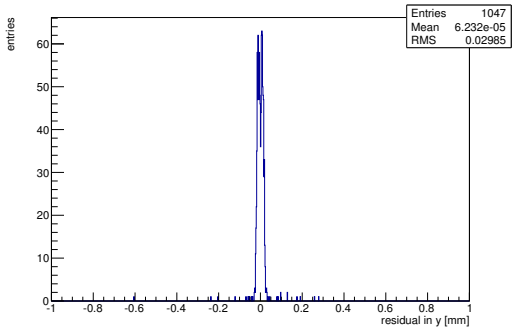

(j) Track residual in y.

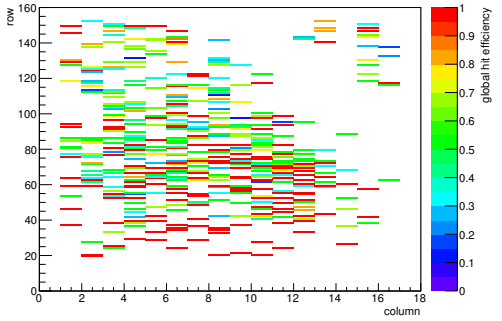

(k) Hit efficiency map.

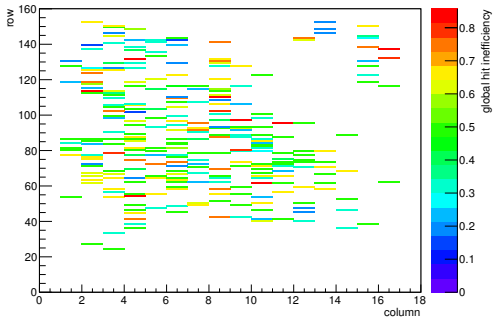

(l) Hit inefficiency map.

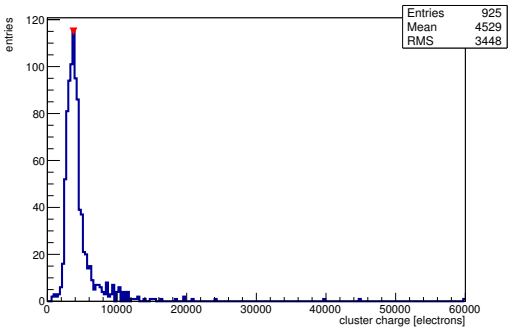

(m) Charge distribution (all cluster sizes included).

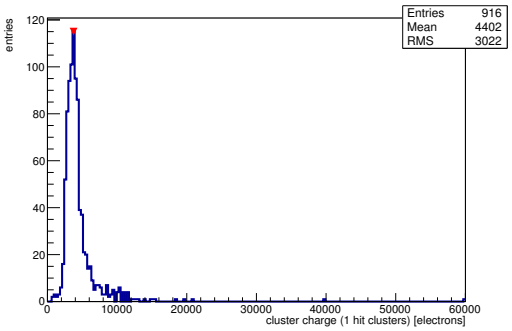

(n) Charge distribution (1 hit cluster).

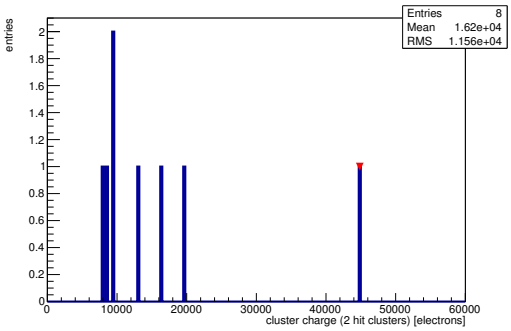

(o) Charge distribution (2 hit cluster).

Figure C.57: Detailed plots for test beam measurement of DO-I-5 (description see section 6.1) sample (running as DUT2) during runs 61249 in the September 2011 test beam period at CERN SPS in area H6B. Summary of the data in chapter 9. *(cont.)*

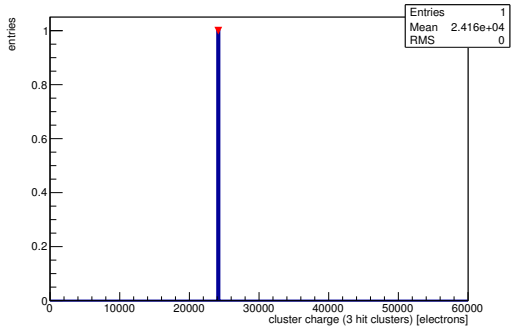

(p) Charge distribution (3 hit cluster).

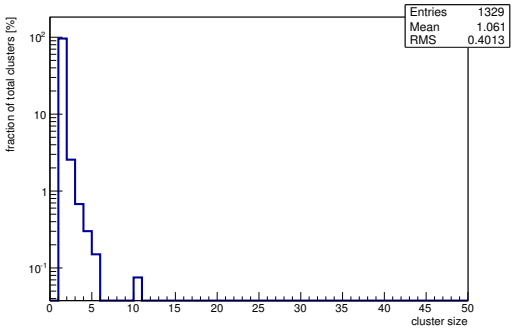

(q) Cluster size distribution.

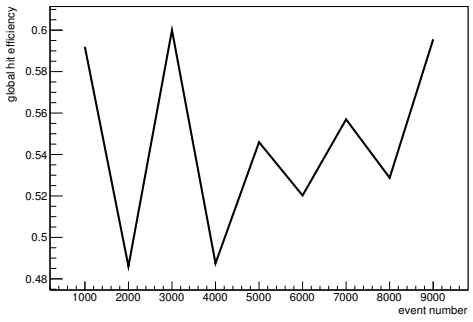

(r) Hit efficiency vs event number.

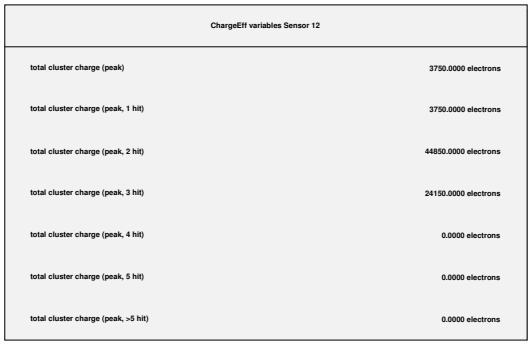

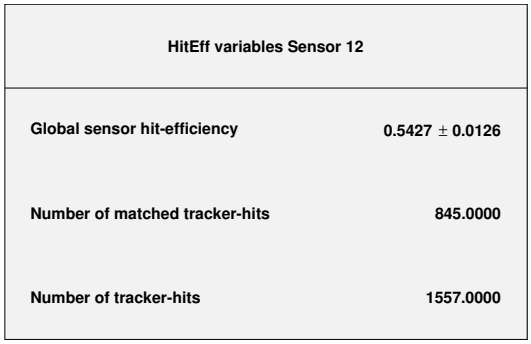

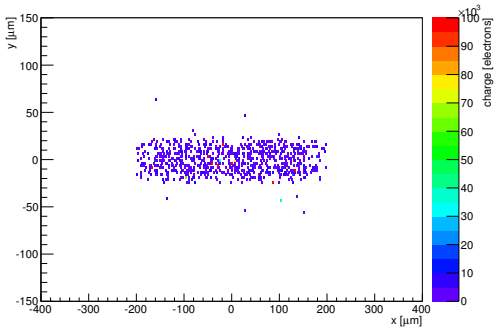

(s) Single pixel mean charge.

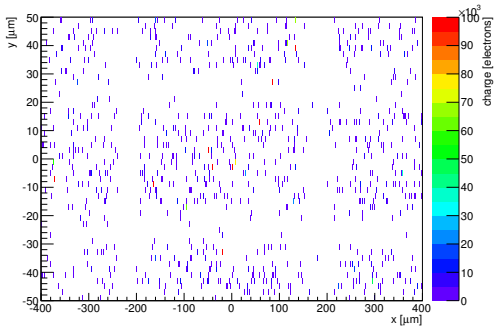

(t) Single pixel mean charge.

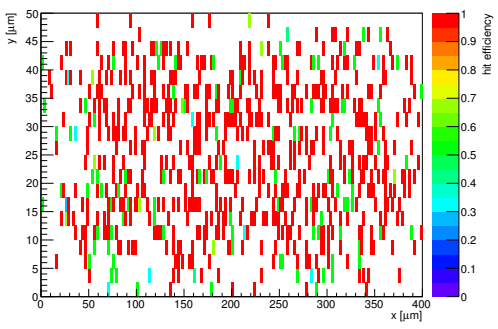

(u) Single pixel hit efficiency.

Figure C.57: Detailed plots for test beam measurement of DO-I-5 (description see section 6.1) sample (running as DUT2) during runs 61249 in the September 2011 test beam period at CERN SPS in area H6B. Summary of the data in chapter 9.

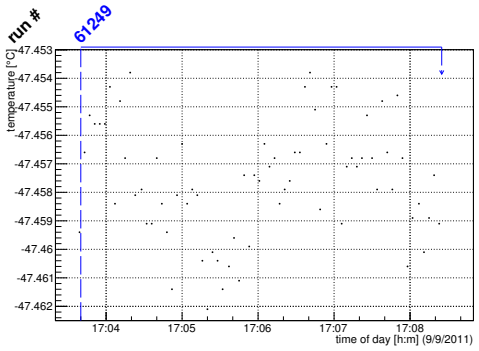

(a) Temperature vs time.

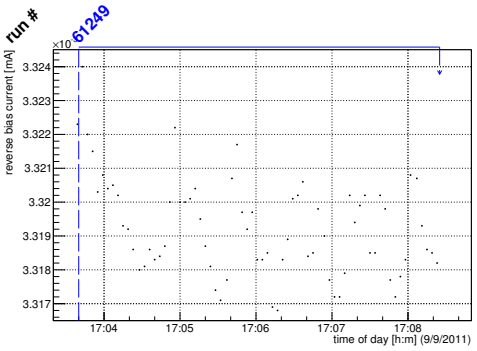

(b) Bias current vs time.

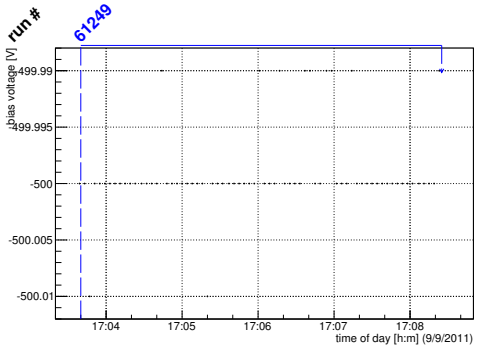

(c) Currently applied bias voltage vs time.

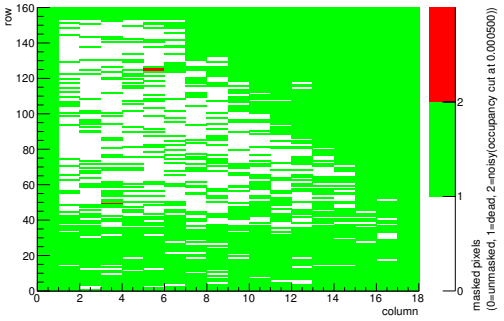

(d) Map of masked pixels.

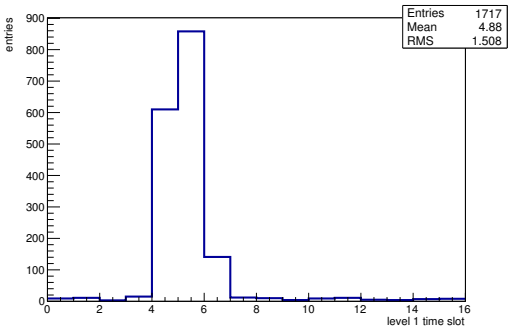

(e) Lvl1 distribution.

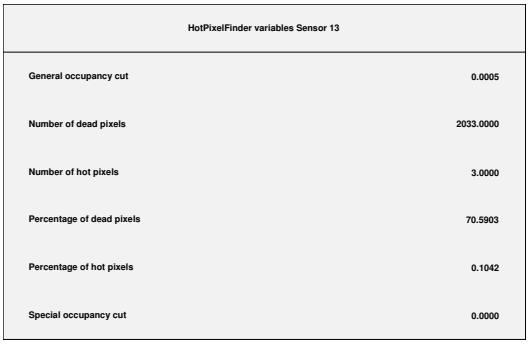

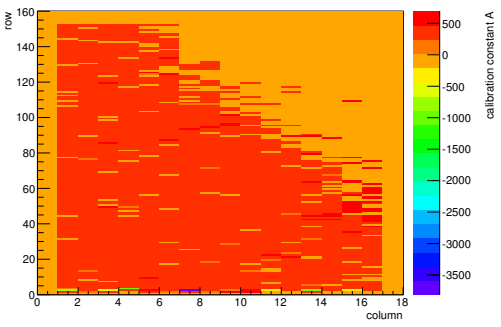

(f) Calibration constant A.

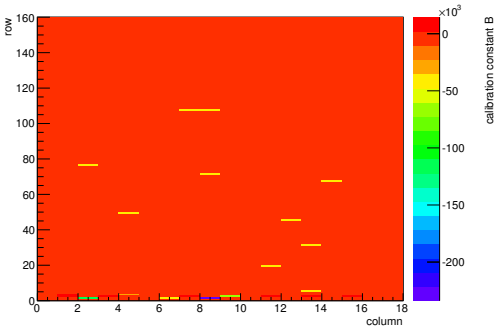

(g) Calibration constant B.

Figure C.58: Detailed plots for test beam measurement of DO-I-12 (description see section 6.1) sample (running as DUT3) during runs 61249 in the September 2011 test beam period at CERN SPS in area H6B. Summary of the data in chapter 9. *(cont.)*

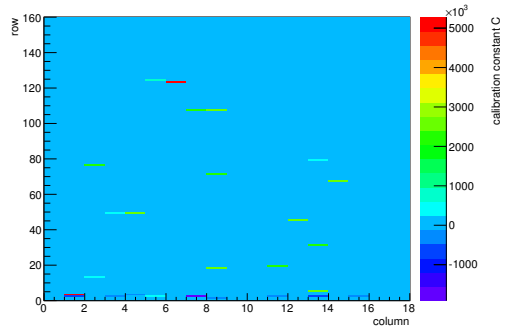

(h) Calibration constant C.

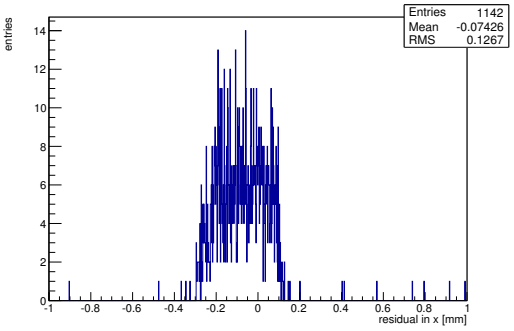

(i) Track residual in x.

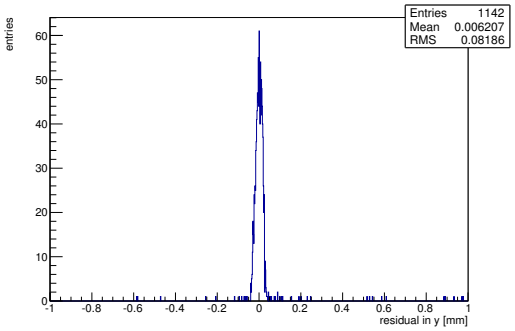

(j) Track residual in y.

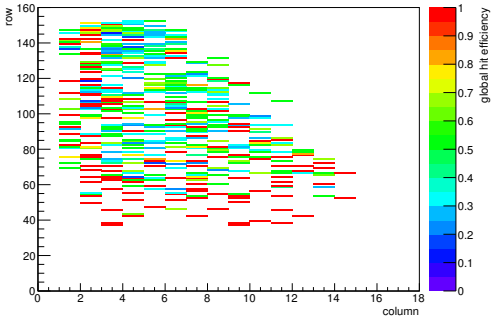

(k) Hit efficiency map.

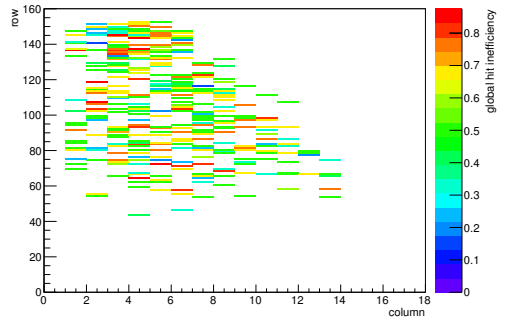

(l) Hit inefficiency map.

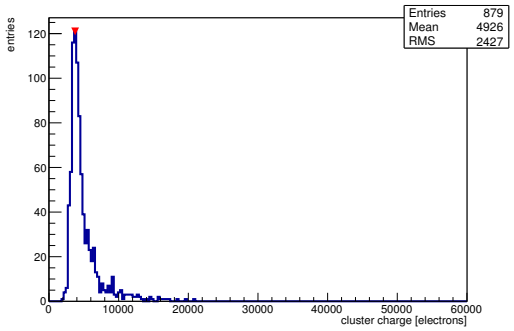

(m) Charge distribution (all cluster sizes included).

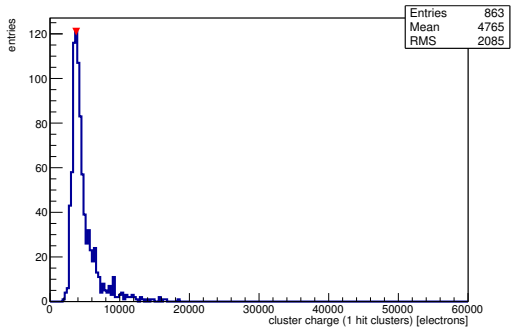

(n) Charge distribution (1 hit cluster).

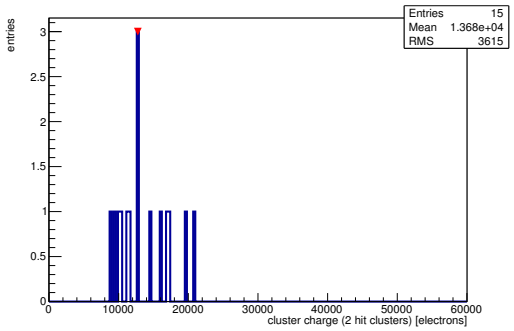

(o) Charge distribution (2 hit cluster).

Figure C.58: Detailed plots for test beam measurement of DO-I-12 (description see section 6.1) sample (running as DUT3) during runs 61249 in the September 2011 test beam period at CERN SPS in area H6B. Summary of the data in chapter 9. *(cont.)*

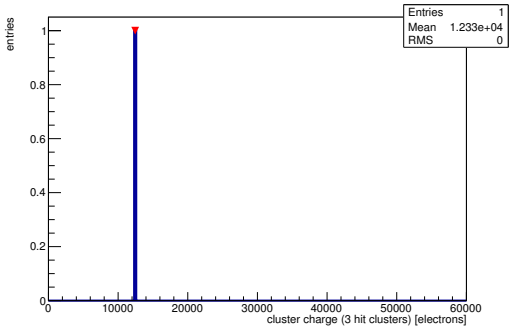

(p) Charge distribution (3 hit cluster).

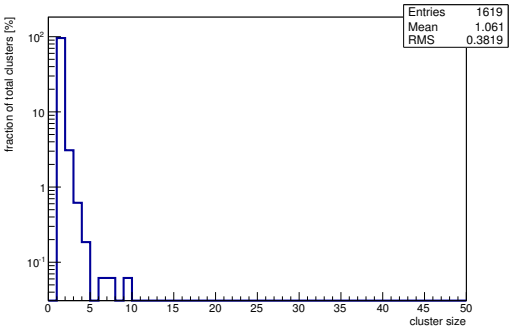

(q) Cluster size distribution.

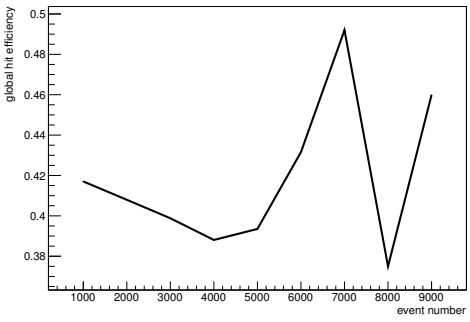

(r) Hit efficiency vs event number.

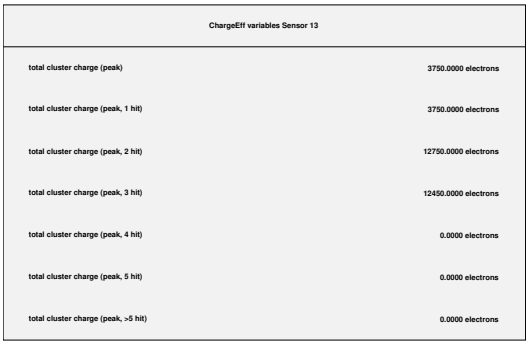

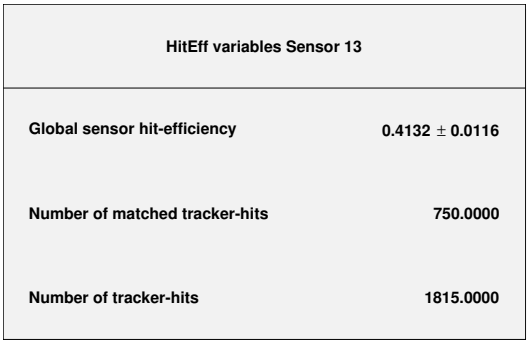

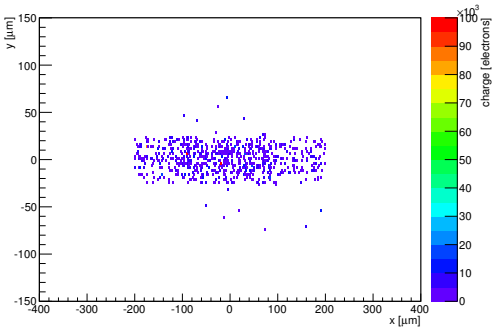

(s) Single pixel mean charge.

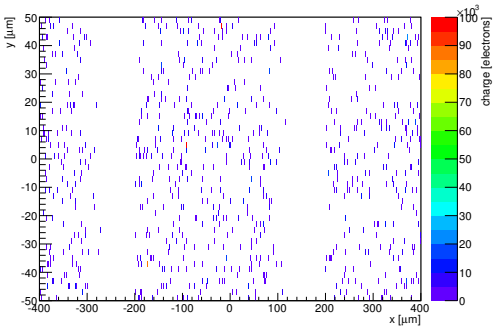

(t) Single pixel mean charge.

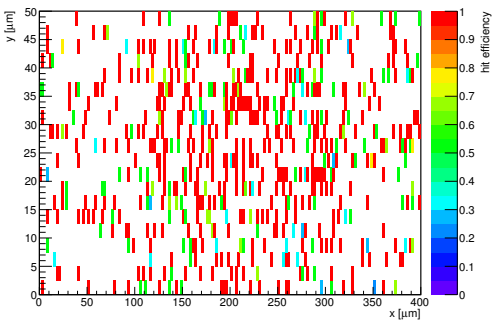

(u) Single pixel hit efficiency.

Figure C.58: Detailed plots for test beam measurement of DO-I-12 (description see section 6.1) sample (running as DUT3) during runs 61249 in the September 2011 test beam period at CERN SPS in area H6B. Summary of the data in chapter 9.

C.3.5 Runs 61250-61251

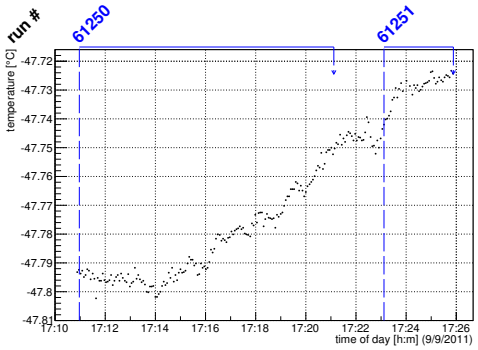

(a) Temperature vs time.

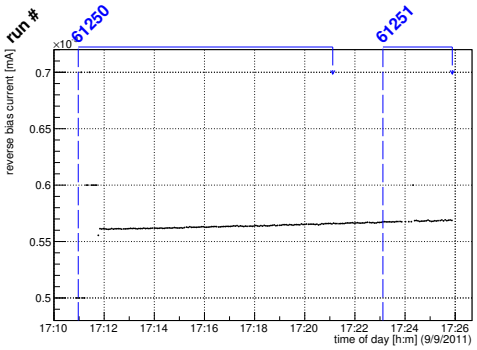

(b) Bias current vs time.

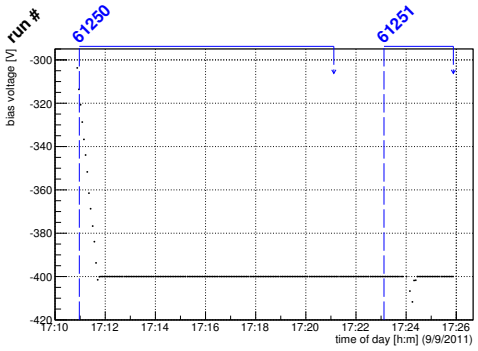

(c) Currently applied bias voltage vs time.

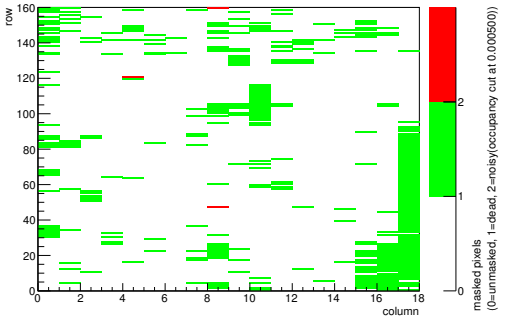

(d) Map of masked pixels.

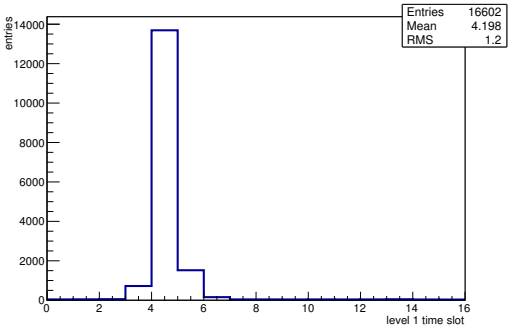

(e) Lvl1 distribution.

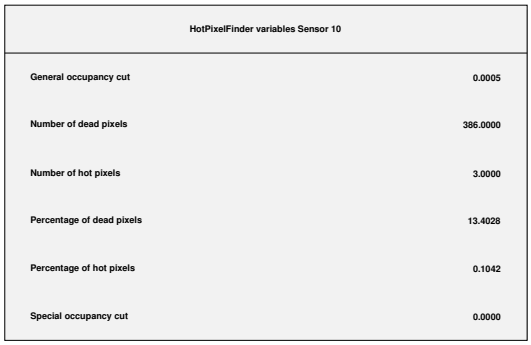

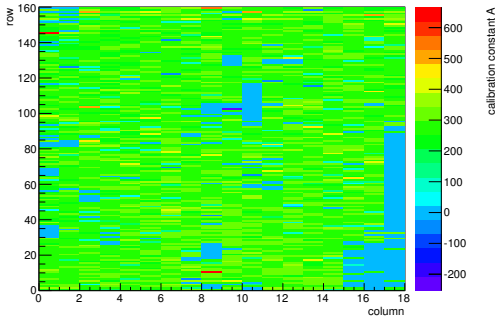

(f) Calibration constant A.

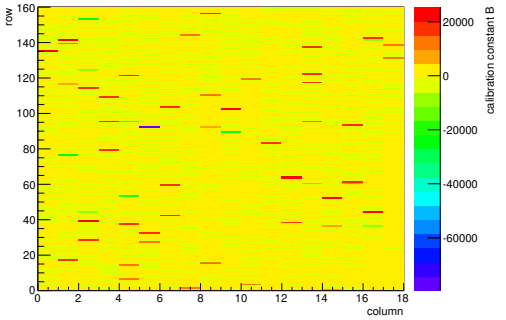

(g) Calibration constant B.

Figure C.59: Detailed plots for test beam measurement of DO-I-7 (description see section 6.1) sample (running as DUT0) during runs 61250-61251 in the September 2011 test beam period at CERN SPS in area H6B. Summary of the data in chapter 9. *(cont.)*

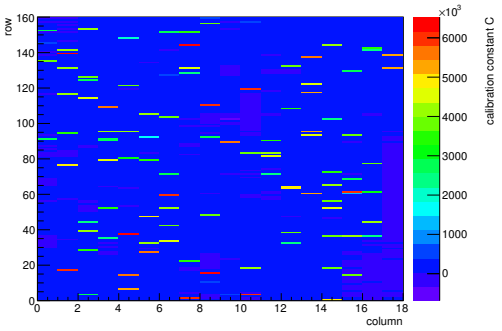

(h) Calibration constant C.

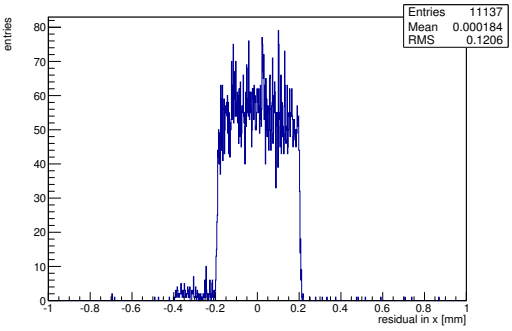

(i) Track residual in x.

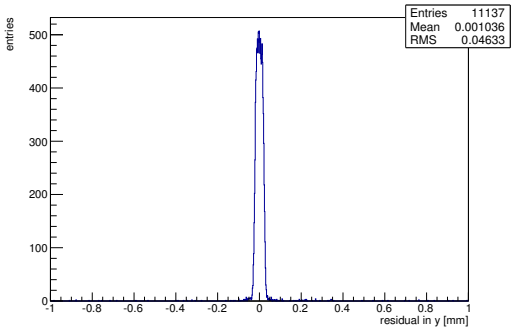

(j) Track residual in y.

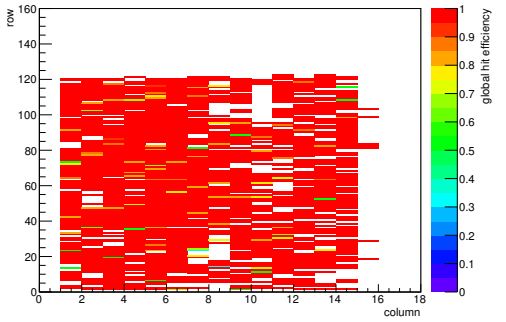

(k) Hit efficiency map.

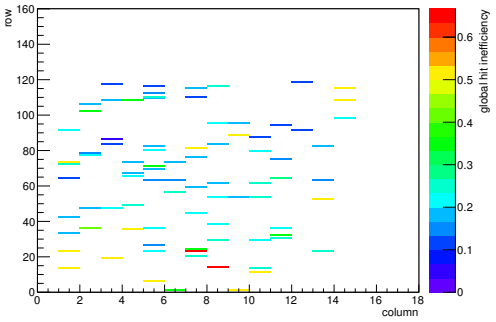

(l) Hit inefficiency map.

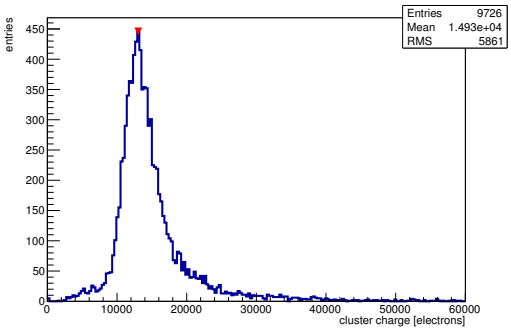

(m) Charge distribution (all cluster sizes included).

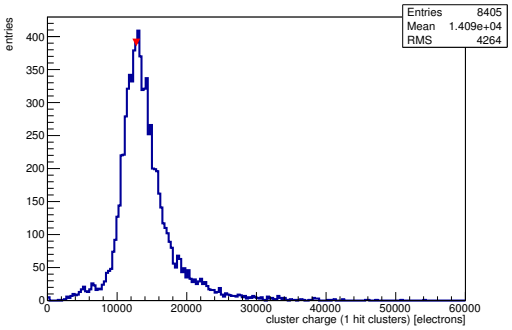

(n) Charge distribution (1 hit cluster).

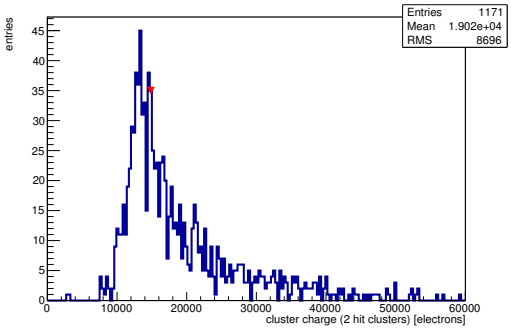

(o) Charge distribution (2 hit cluster).

Figure C.59: Detailed plots for test beam measurement of DO-I-7 (description see section 6.1) sample (running as DUT0) during runs 61250-61251 in the September 2011 test beam period at CERN SPS in area H6B. Summary of the data in chapter 9. *(cont.)*

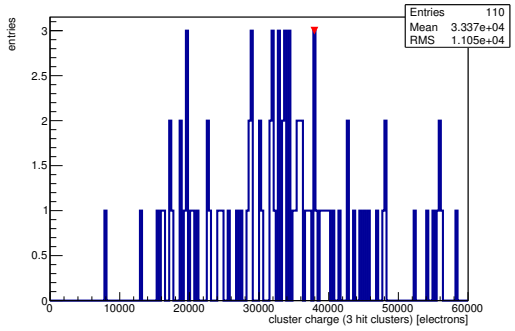

(p) Charge distribution (3 hit cluster).

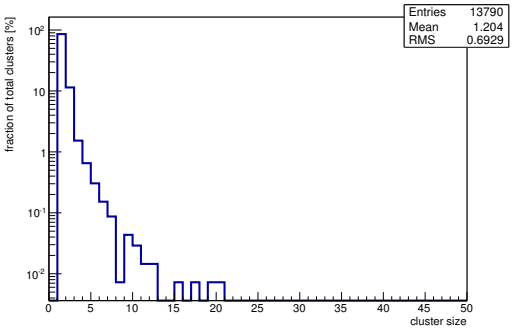

(q) Cluster size distribution.

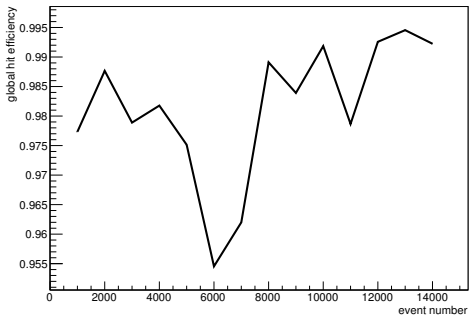

(r) Hit efficiency vs event number.

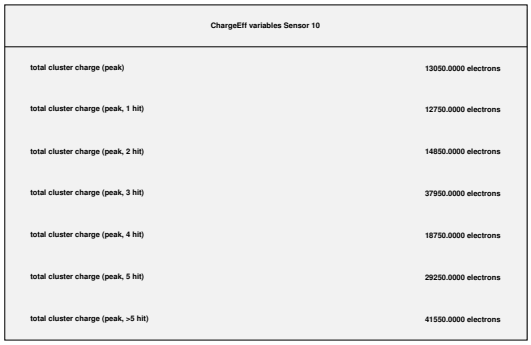

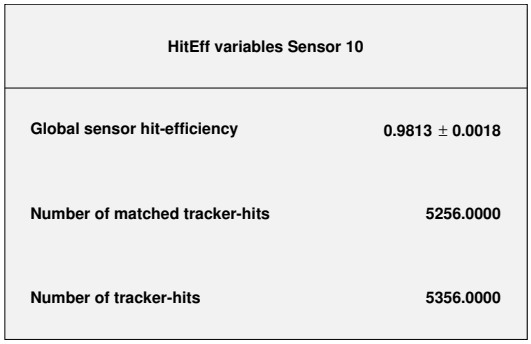

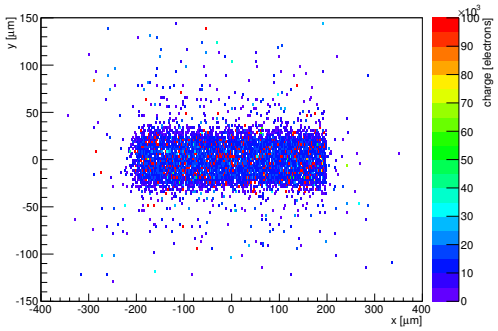

(s) Single pixel mean charge.

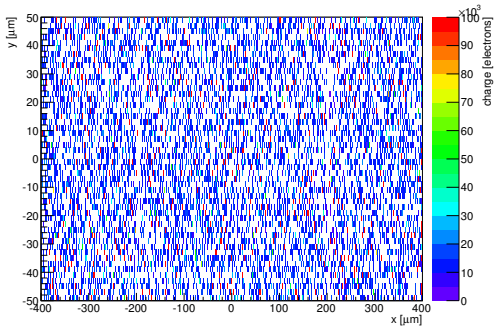

(t) Single pixel mean charge.

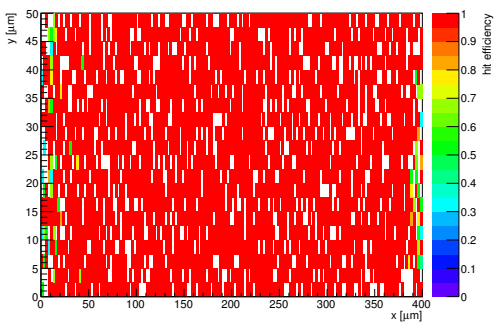

(u) Single pixel hit efficiency.

Figure C.59: Detailed plots for test beam measurement of DO-I-7 (description see section 6.1) sample (running as DUT0) during runs 61250-61251 in the September 2011 test beam period at CERN SPS in area H6B. Summary of the data in chapter 9.

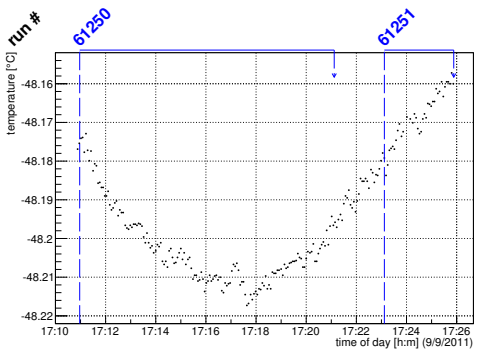

(a) Temperature vs time.

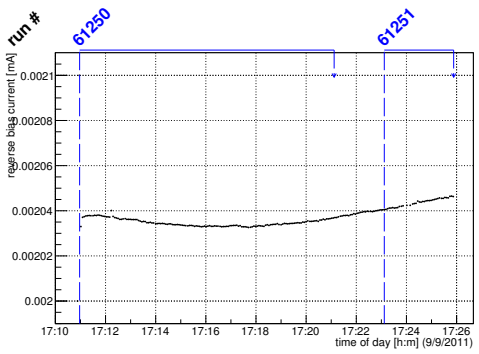

(b) Bias current vs time.

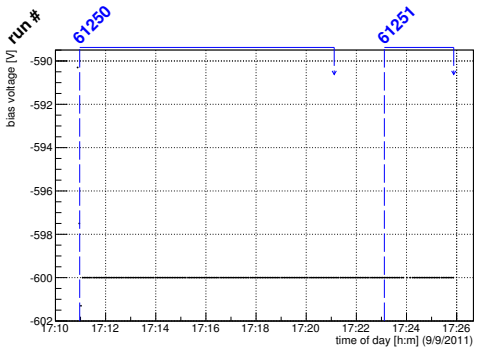

(c) Currently applied bias voltage vs time.

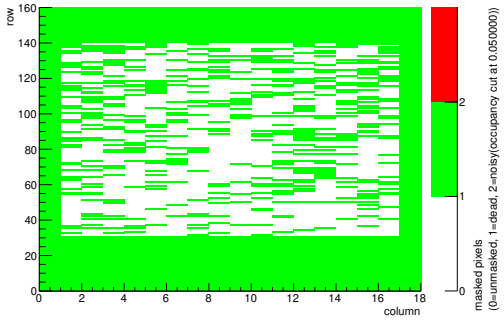

(d) Map of masked pixels.

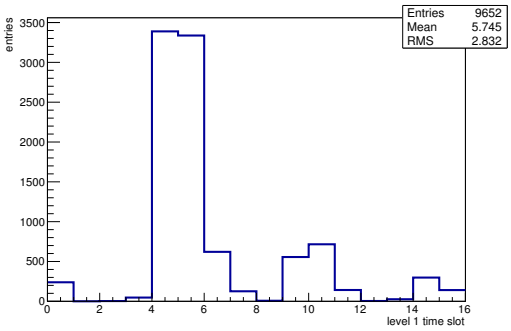

(e) Lvl1 distribution.

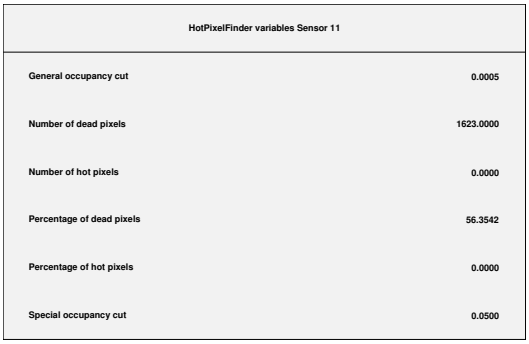

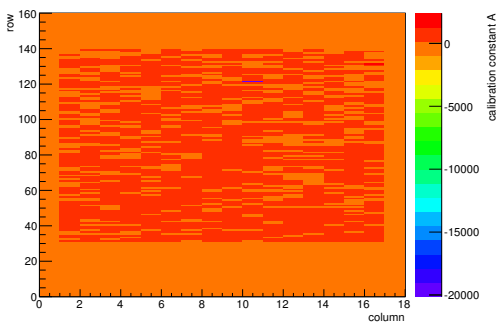

(f) Calibration constant A.

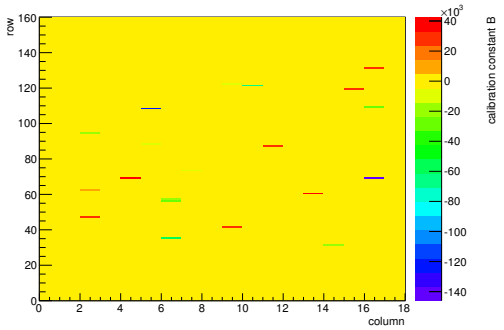

(g) Calibration constant B.

Figure C.60: Detailed plots for test beam measurement of DO-I-11 (description see section 6.1) sample (running as DUT1) during runs 61250-61251 in the September 2011 test beam period at CERN SPS in area H6B. Summary of the data in chapter 9. *(cont.)*

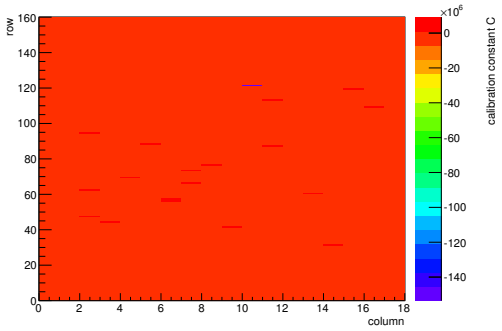

(h) Calibration constant C.

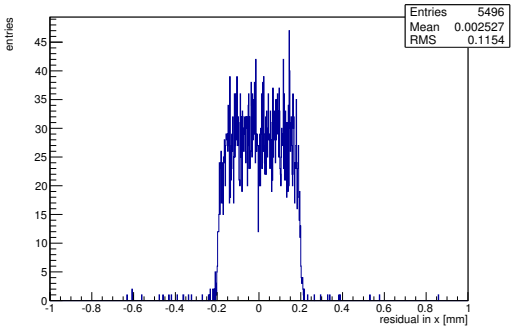

(i) Track residual in x.

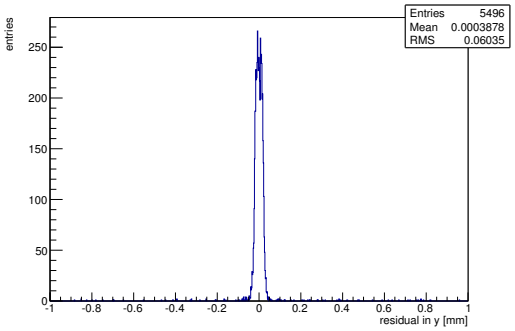

(j) Track residual in y.

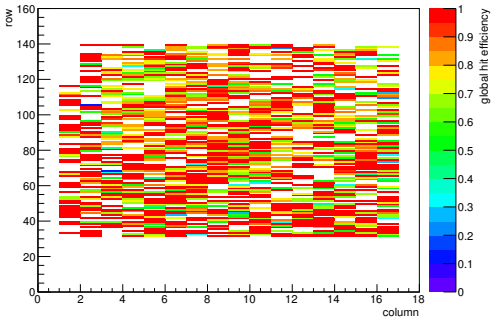

(k) Hit efficiency map.

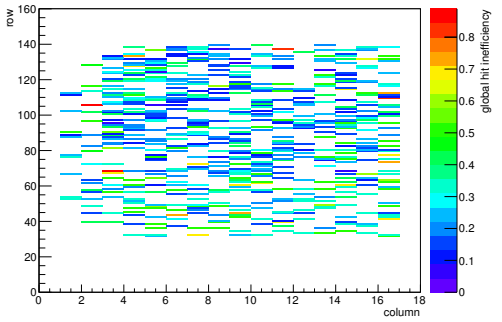

(l) Hit inefficiency map.

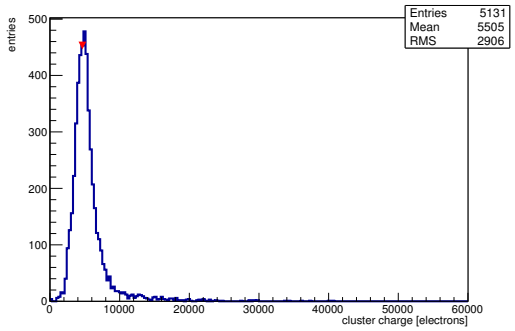

(m) Charge distribution (all cluster sizes included).

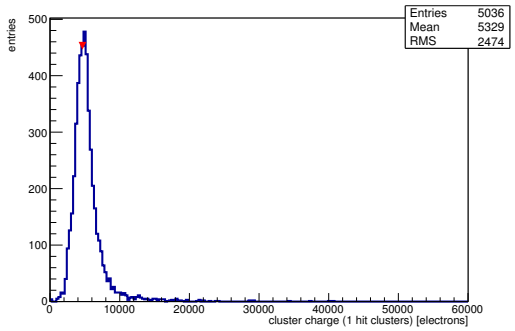

(n) Charge distribution (1 hit cluster).

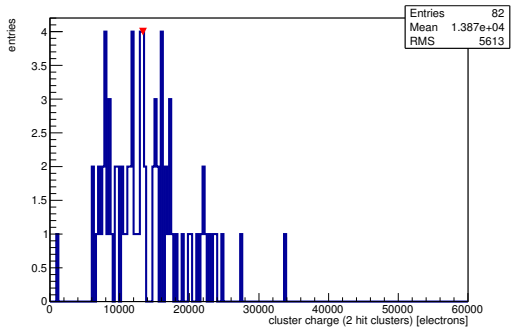

(o) Charge distribution (2 hit cluster).

Figure C.60: Detailed plots for test beam measurement of DO-I-11 (description see section 6.1) sample (running as DUT1) during runs 61250-61251 in the September 2011 test beam period at CERN SPS in area H6B. Summary of the data in chapter 9. *(cont.)*

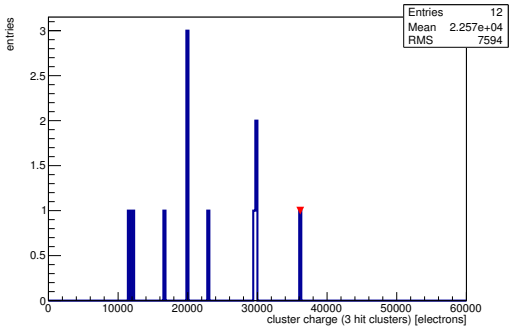

(p) Charge distribution (3 hit cluster).

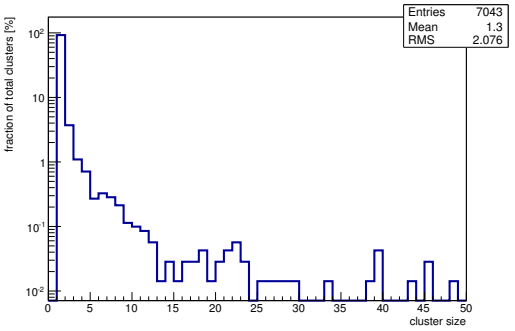

(q) Cluster size distribution.

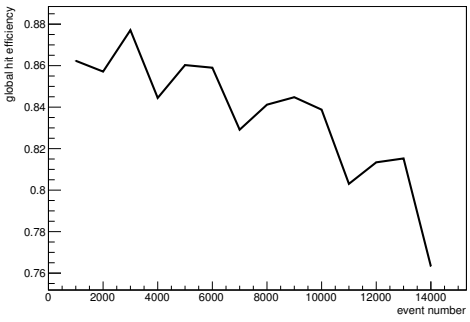

(r) Hit efficiency vs event number.

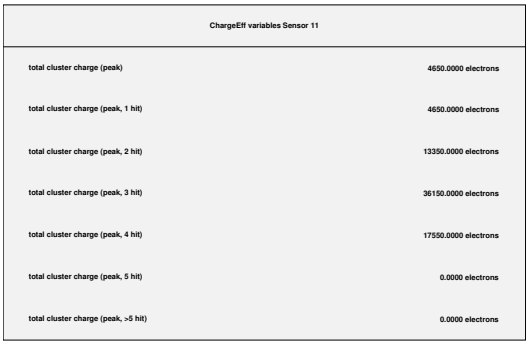

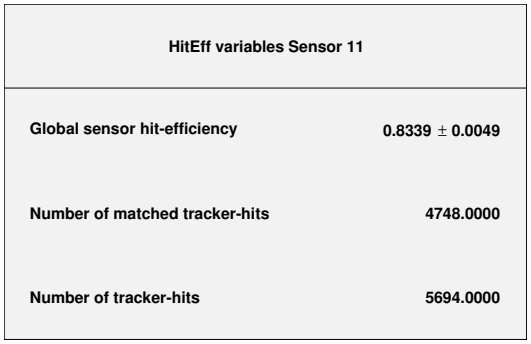

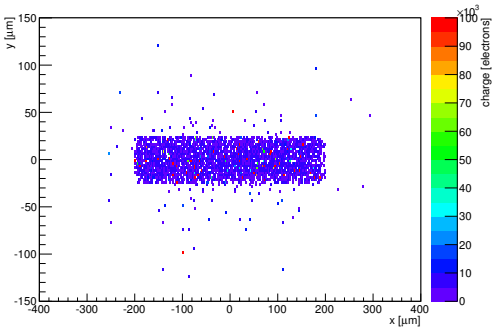

(s) Single pixel mean charge.

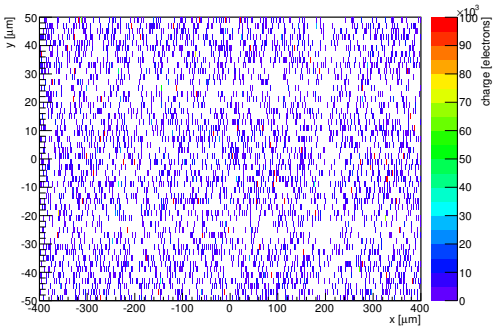

(t) Single pixel mean charge.

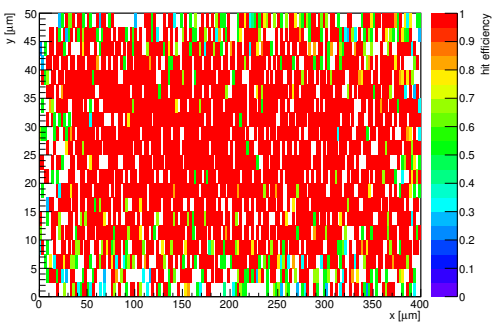

(u) Single pixel hit efficiency.

Figure C.60: Detailed plots for test beam measurement of DO-I-11 (description see section 6.1) sample (running as DUT1) during runs 61250-61251 in the September 2011 test beam period at CERN SPS in area H6B. Summary of the data in chapter 9.

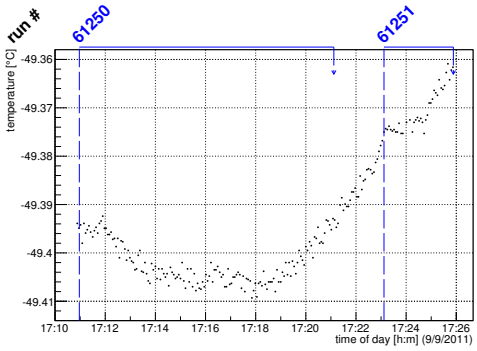

(a) Temperature vs time.

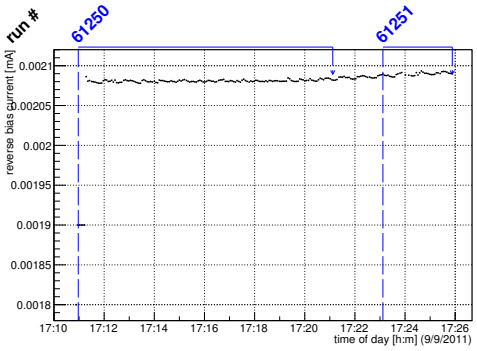

(b) Bias current vs time.

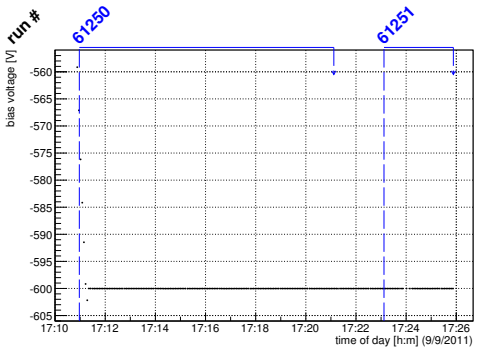

(c) Currently applied bias voltage vs time.

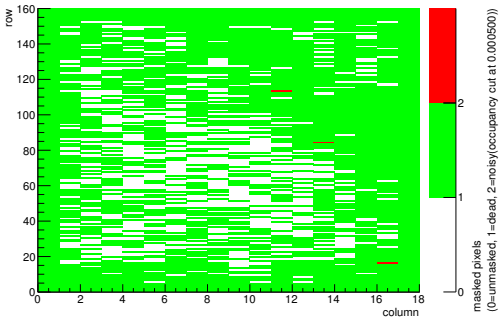

(d) Map of masked pixels.

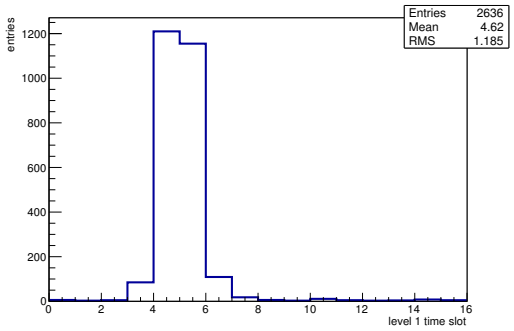

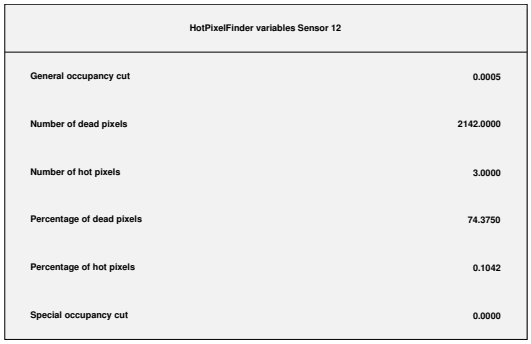

(e) Lvl1 distribution.

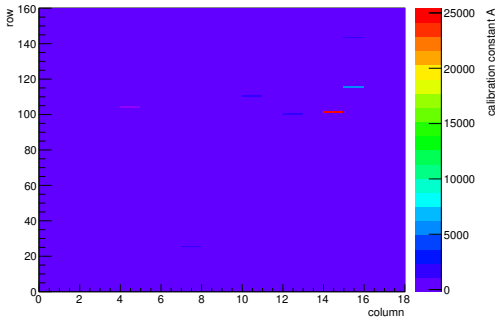

(f) Calibration constant A.

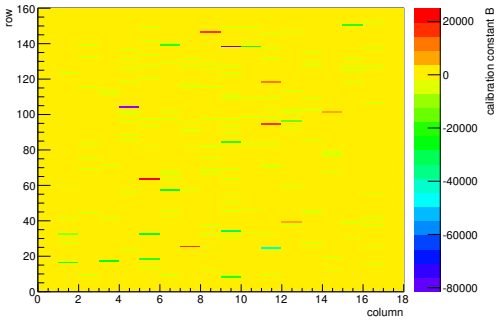

(g) Calibration constant B.

Figure C.61: Detailed plots for test beam measurement of DO-I-5 (description see section 6.1) sample (running as DUT2) during runs 61250-61251 in the September 2011 test beam period at CERN SPS in area H6B. Summary of the data in chapter 9. *(cont.)*

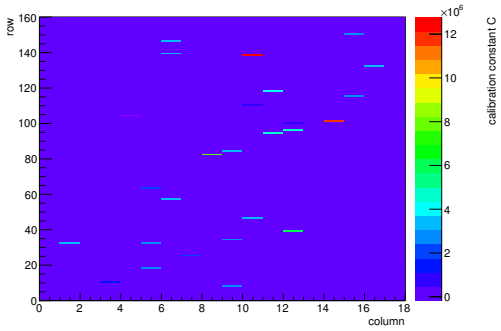

(h) Calibration constant C.

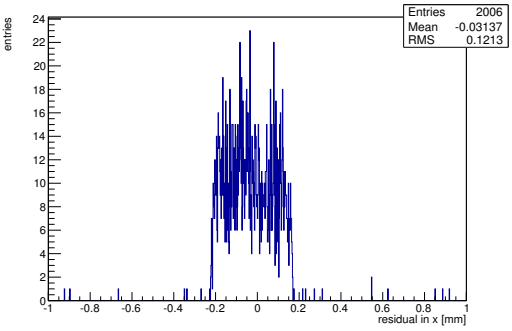

(i) Track residual in x.

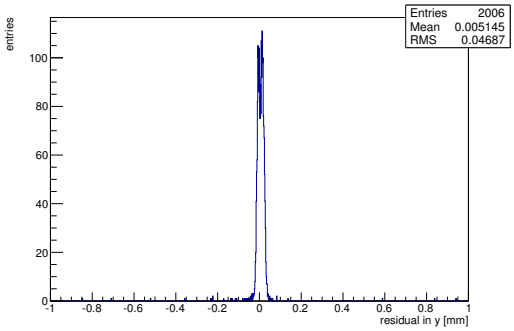

(j) Track residual in y.

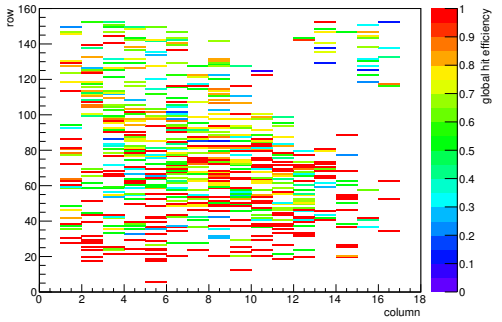

(k) Hit efficiency map.

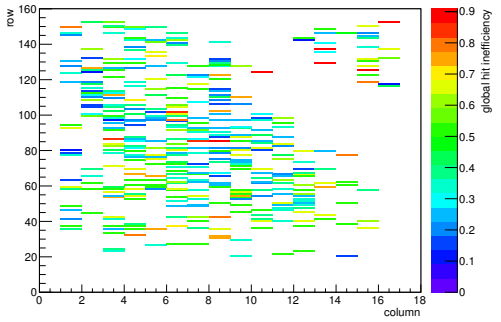

(l) Hit inefficiency map.

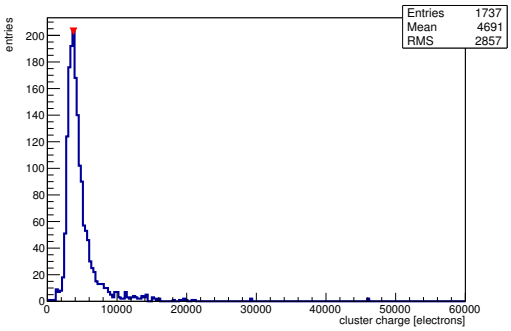

(m) Charge distribution (all cluster sizes included).

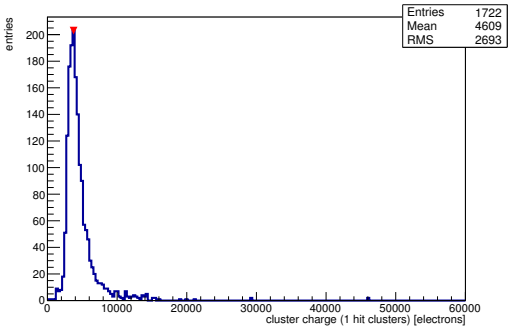

(n) Charge distribution (1 hit cluster).

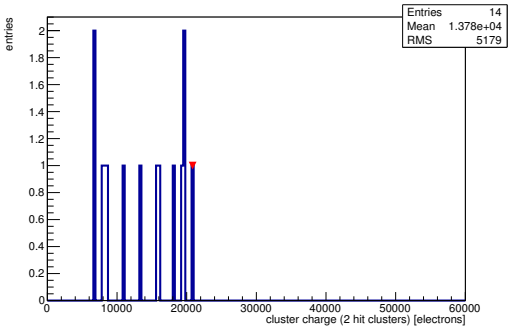

(o) Charge distribution (2 hit cluster).

Figure C.61: Detailed plots for test beam measurement of DO-I-5 (description see section 6.1) sample (running as DUT2) during runs 61250-61251 in the September 2011 test beam period at CERN SPS in area H6B. Summary of the data in chapter 9. *(cont.)*

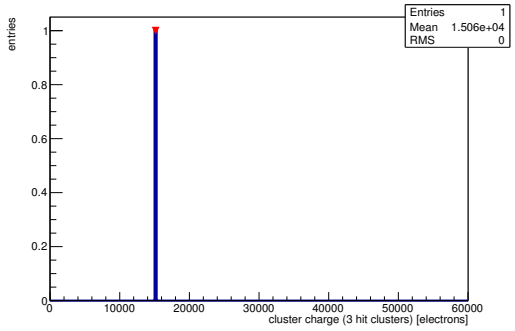

(p) Charge distribution (3 hit cluster).

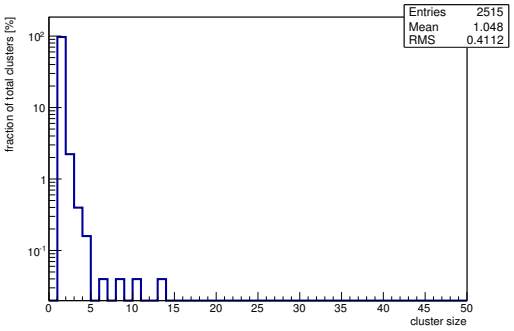

(q) Cluster size distribution.

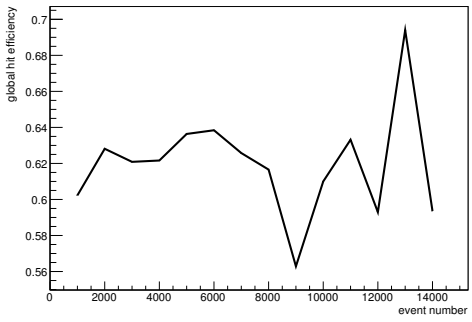

(r) Hit efficiency vs event number.

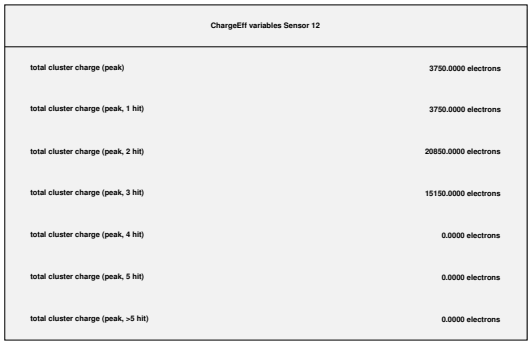

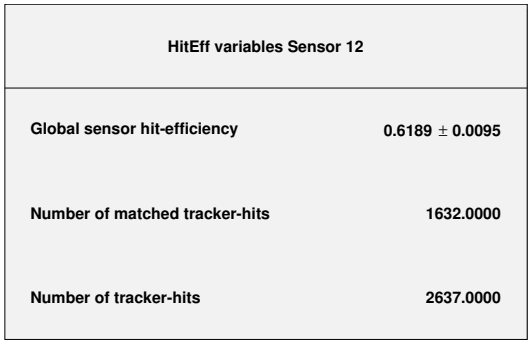

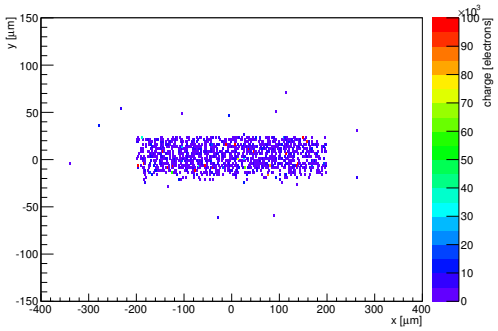

(s) Single pixel mean charge.

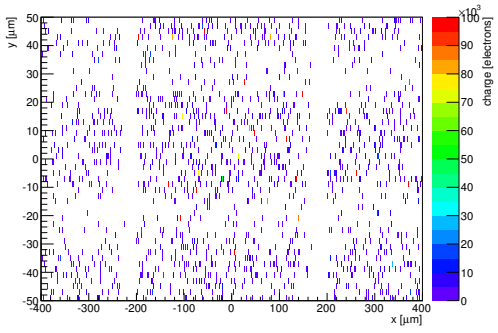

(t) Single pixel mean charge.

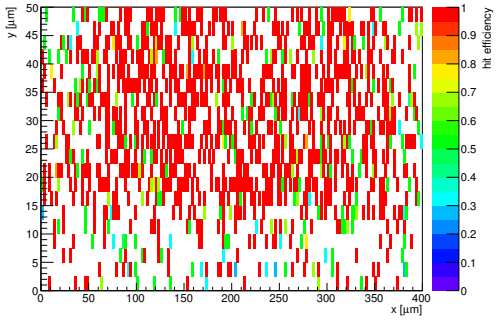

(u) Single pixel hit efficiency.

Figure C.61: Detailed plots for test beam measurement of DO-I-5 (description see section 6.1) sample (running as DUT2) during runs 61250-61251 in the September 2011 test beam period at CERN SPS in area H6B. Summary of the data in chapter 9.

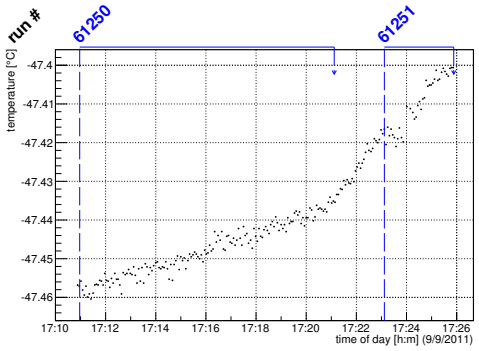

(a) Temperature vs time.

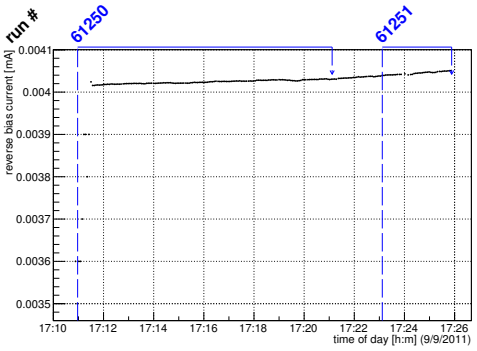

(b) Bias current vs time.

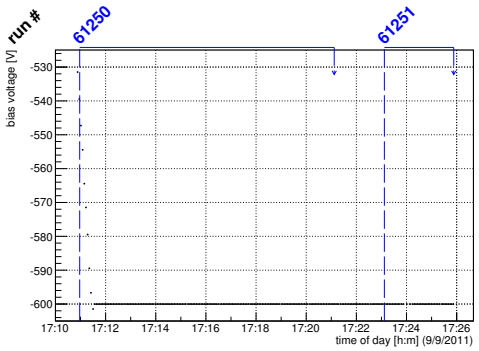

(c) Currently applied bias voltage vs time.

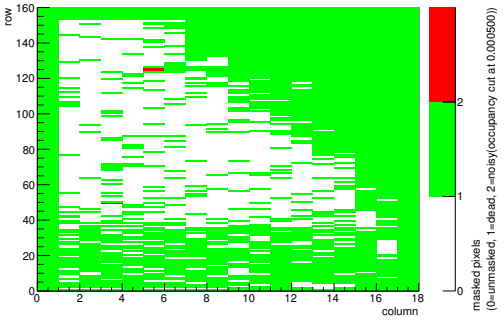

(d) Map of masked pixels.

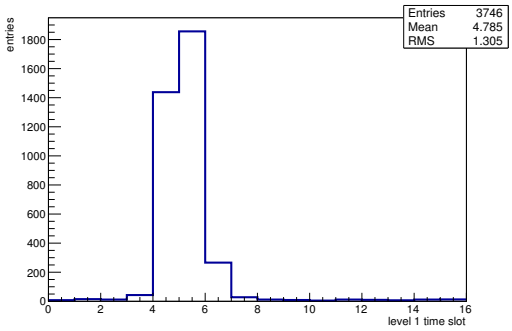

(e) Lvl1 distribution.

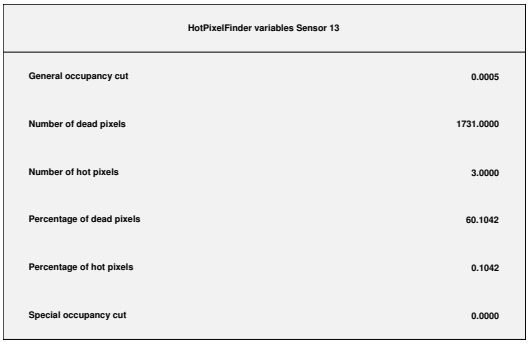

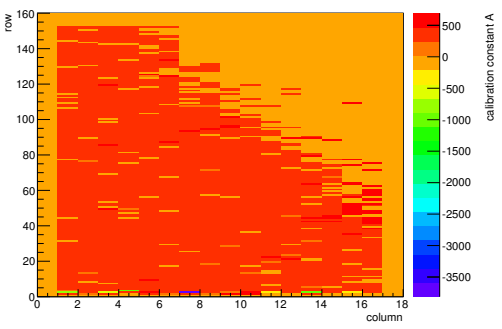

(f) Calibration constant A.

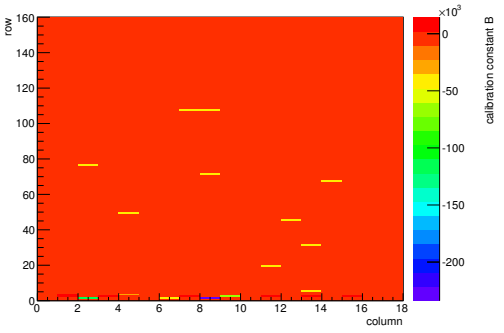

(g) Calibration constant B.

Figure C.62: Detailed plots for test beam measurement of DO-I-12 (description see section 6.1) sample (running as DUT3) during runs 61250-61251 in the September 2011 test beam period at CERN SPS in area H6B. Summary of the data in chapter 9. *(cont.)*

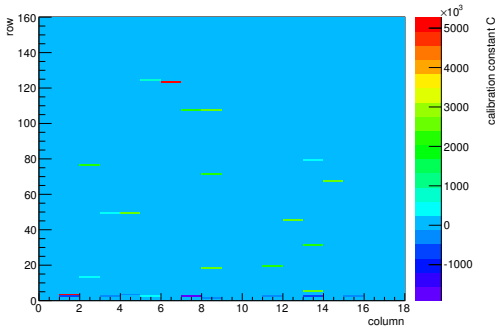

(h) Calibration constant C.

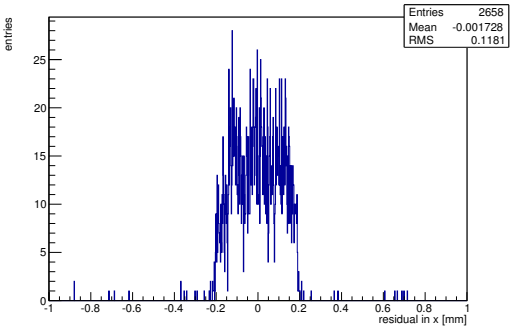

(i) Track residual in x.

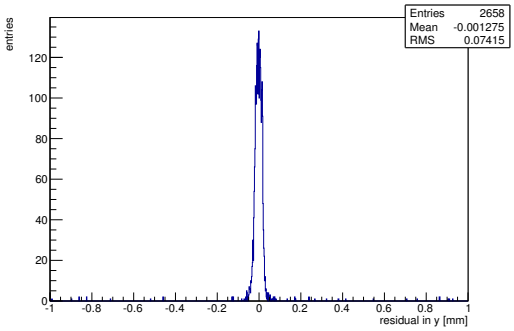

(j) Track residual in y.

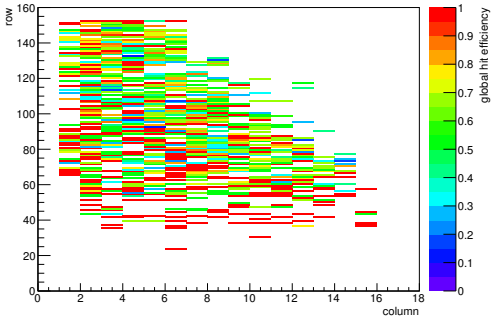

(k) Hit efficiency map.

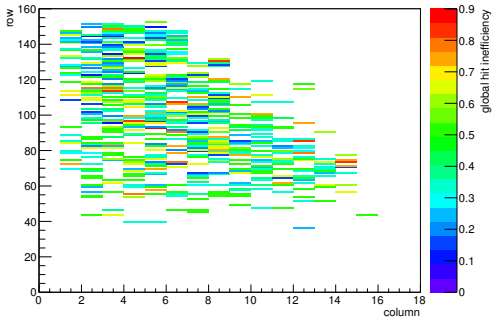

(l) Hit inefficiency map.

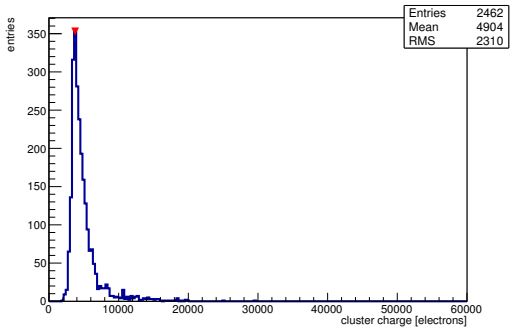

(m) Charge distribution (all cluster sizes included).

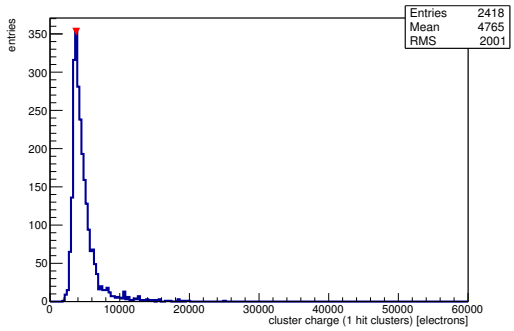

(n) Charge distribution (1 hit cluster).

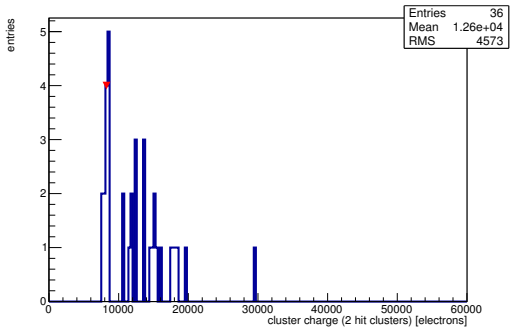

(o) Charge distribution (2 hit cluster).

Figure C.62: Detailed plots for test beam measurement of DO-I-12 (description see section 6.1) sample (running as DUT3) during runs 61250-61251 in the September 2011 test beam period at CERN SPS in area H6B. Summary of the data in chapter 9. *(cont.)*

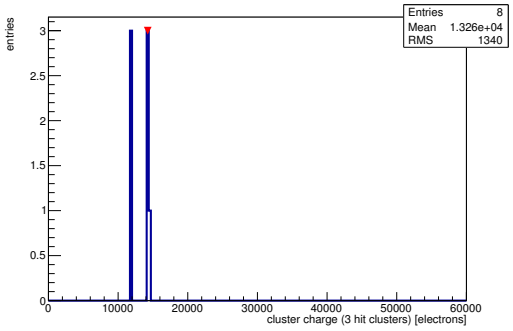

(p) Charge distribution (3 hit cluster).

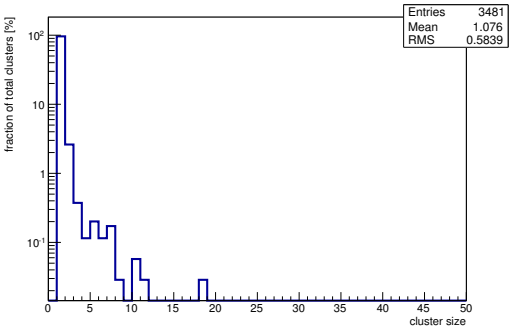

(q) Cluster size distribution.

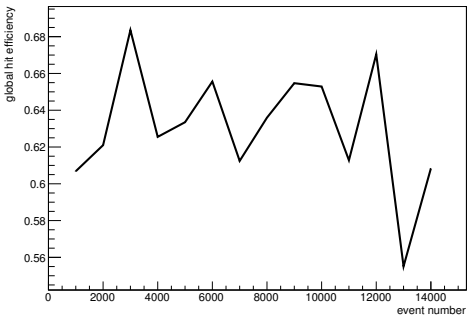

(r) Hit efficiency vs event number.

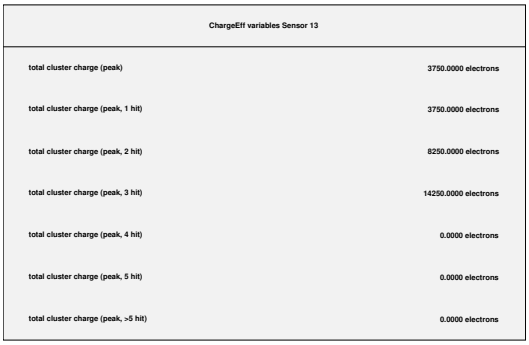

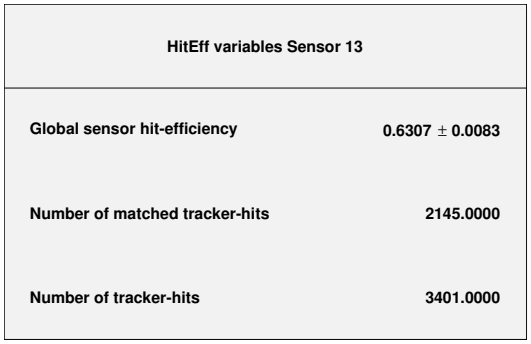

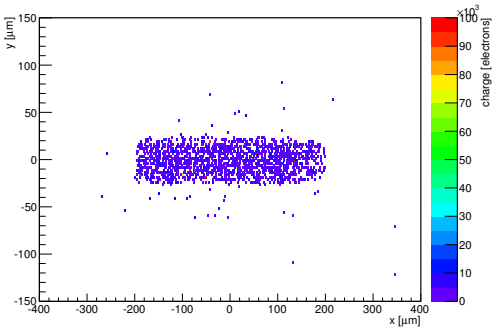

(s) Single pixel mean charge.

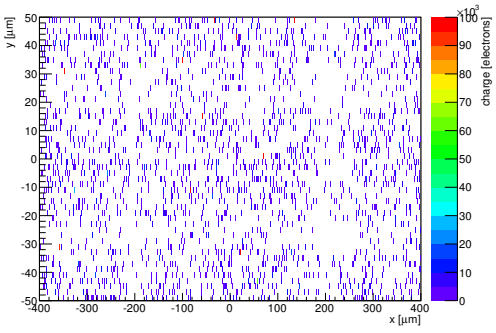

(t) Single pixel mean charge.

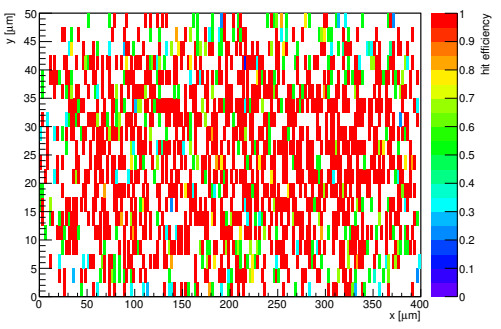

(u) Single pixel hit efficiency.

Figure C.62: Detailed plots for test beam measurement of DO-I-12 (description see section 6.1) sample (running as DUT3) during runs 61250-61251 in the September 2011 test beam period at CERN SPS in area H6B. Summary of the data in chapter 9.

C.3.6 Run 61252

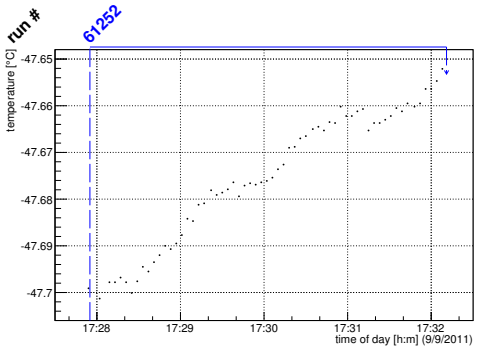

(a) Temperature vs time.

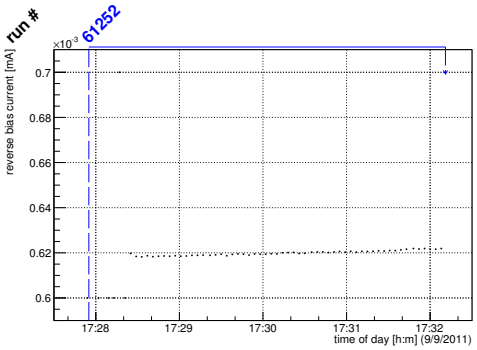

(b) Bias current vs time.

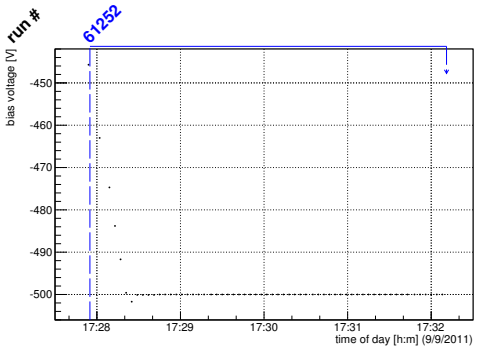

(c) Currently applied bias voltage vs time.

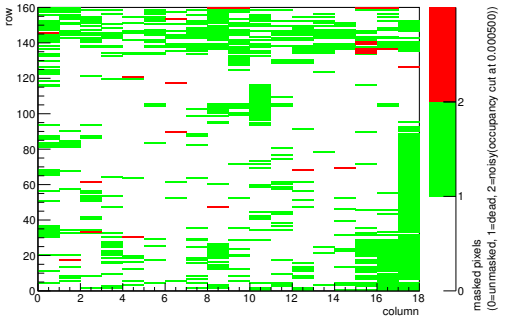

(d) Map of masked pixels.

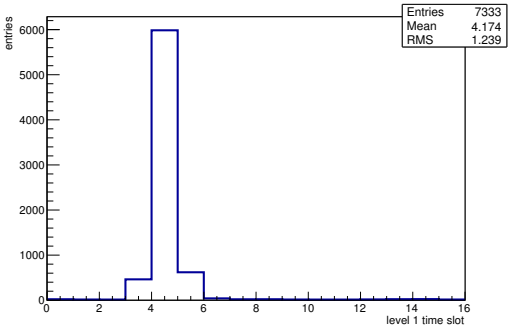

(e) Lvl1 distribution.

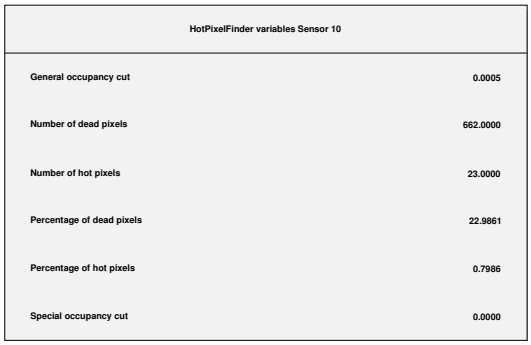

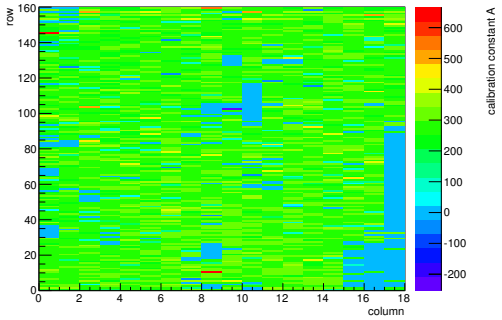

(f) Calibration constant A.

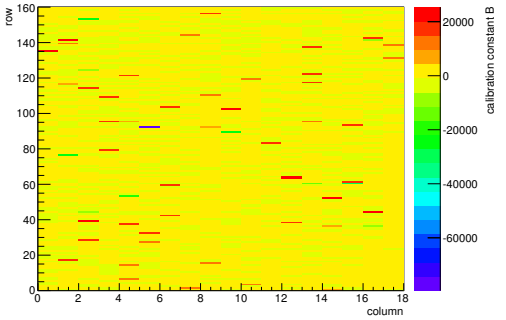

(g) Calibration constant B.

Figure C.63: Detailed plots for test beam measurement of DO-I-7 (description see section 6.1) sample (running as DUT0) during runs 61252 in the September 2011 test beam period at CERN SPS in area H6B. Summary of the data in chapter 9. *(cont.)*

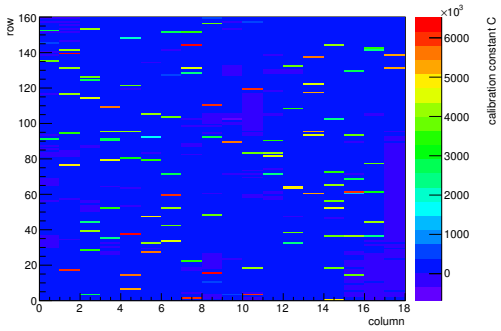

(h) Calibration constant C.

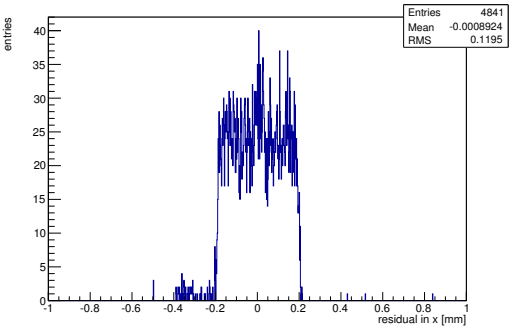

(i) Track residual in x.

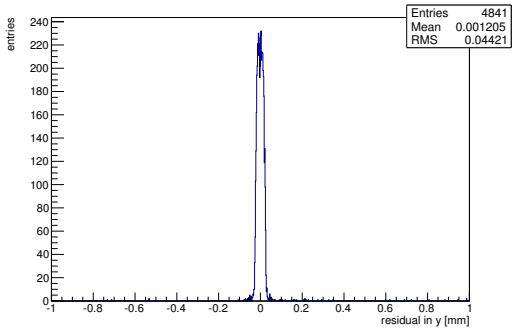

(j) Track residual in y.

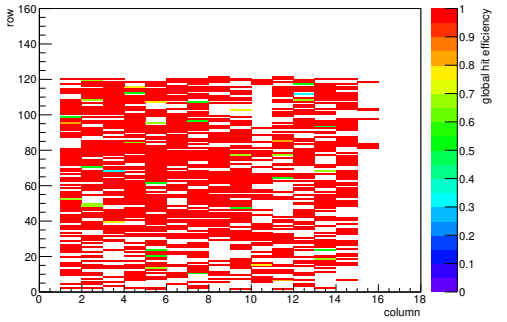

(k) Hit efficiency map.

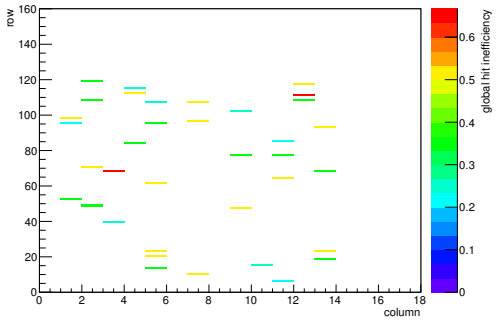

(l) Hit inefficiency map.

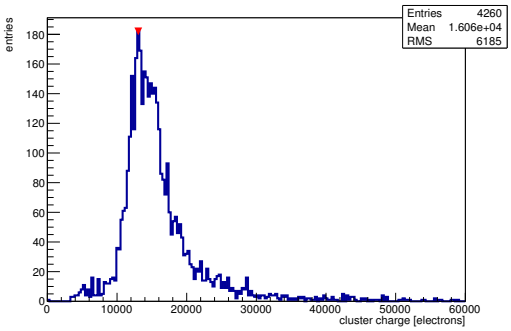

(m) Charge distribution (all cluster sizes included).

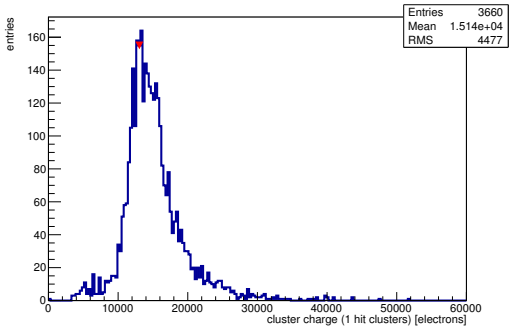

(n) Charge distribution (1 hit cluster).

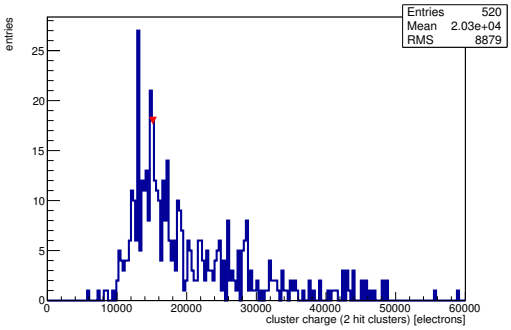

(o) Charge distribution (2 hit cluster).

Figure C.63: Detailed plots for test beam measurement of DO-I-7 (description see section 6.1) sample (running as DUT0) during runs 61252 in the September 2011 test beam period at CERN SPS in area H6B. Summary of the data in chapter 9. *(cont.)*

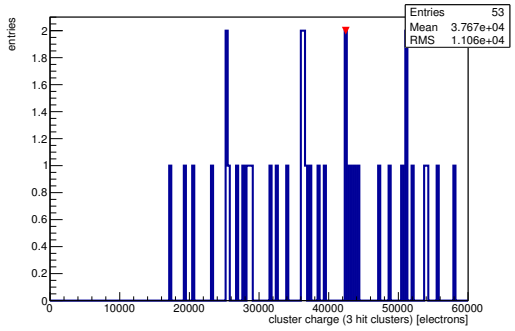

(p) Charge distribution (3 hit cluster).

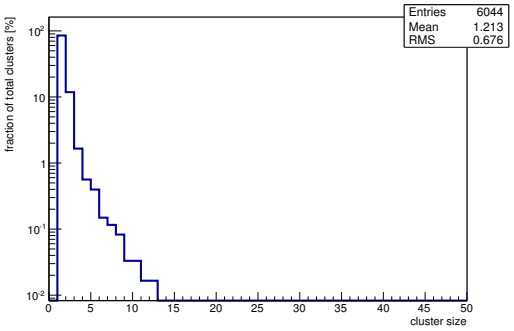

(q) Cluster size distribution.

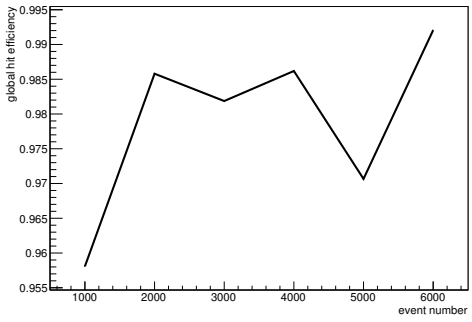

(r) Hit efficiency vs event number.

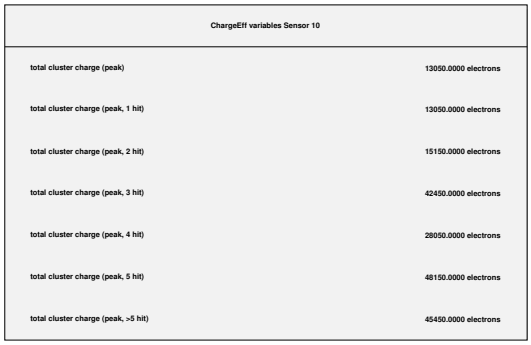

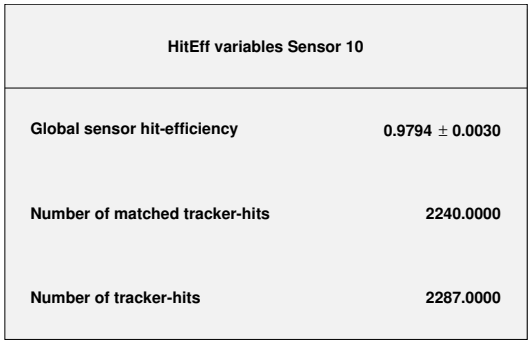

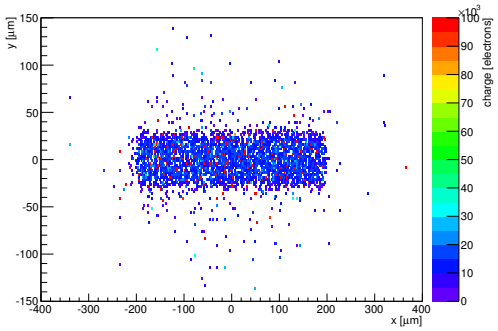

(s) Single pixel mean charge.

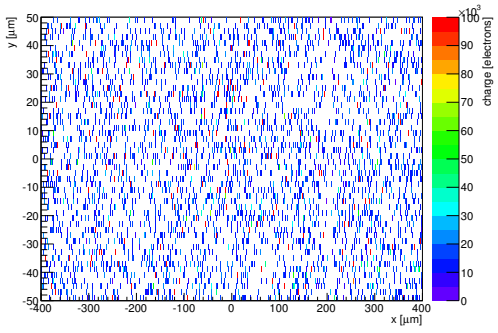

(t) Single pixel mean charge.

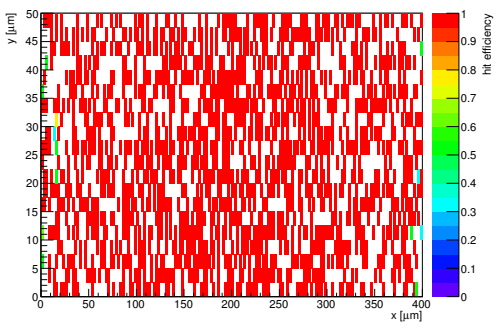

(u) Single pixel hit efficiency.

Figure C.63: Detailed plots for test beam measurement of DO-I-7 (description see section 6.1) sample (running as DUT0) during runs 61252 in the September 2011 test beam period at CERN SPS in area H6B. Summary of the data in chapter 9.

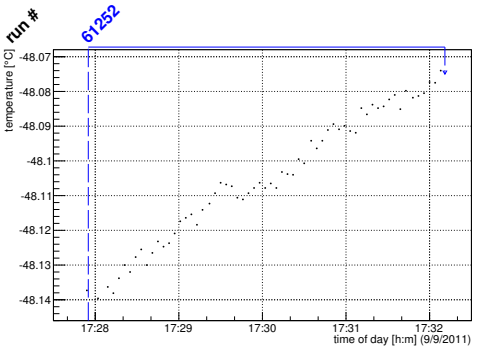

(a) Temperature vs time.

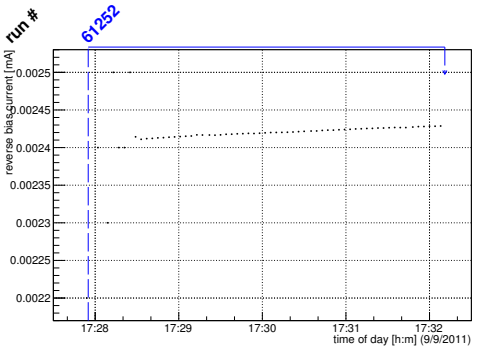

(b) Bias current vs time.

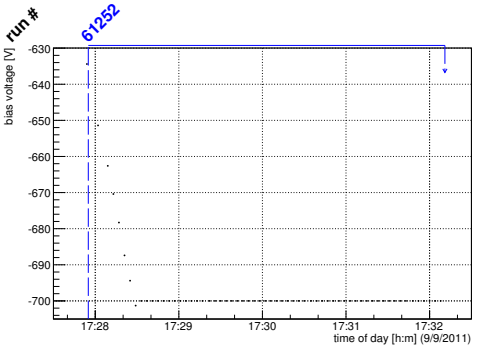

(c) Currently applied bias voltage vs time.

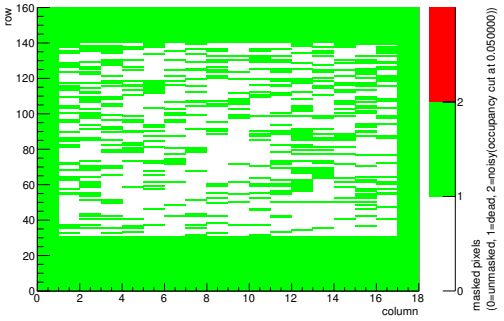

(d) Map of masked pixels.

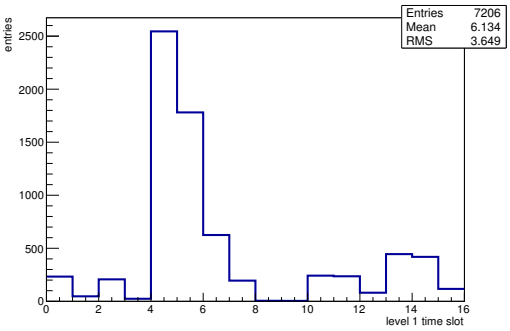

(e) Lvl1 distribution.

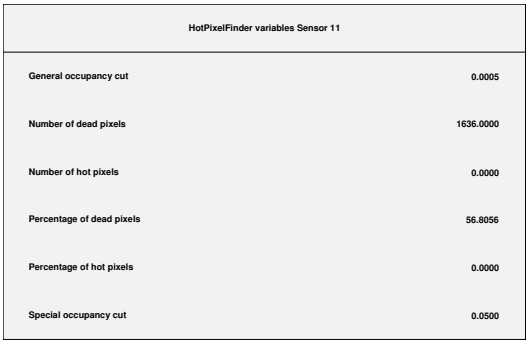

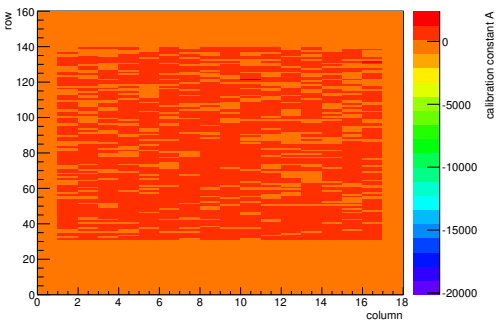

(f) Calibration constant A.

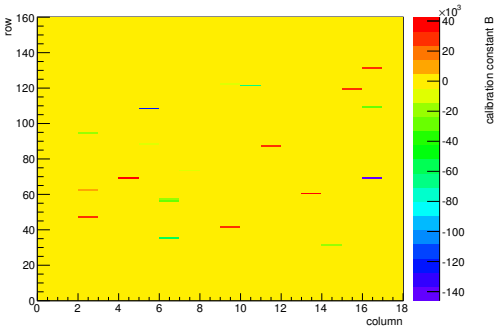

(g) Calibration constant B.

Figure C.64: Detailed plots for test beam measurement of DO-I-11 (description see section 6.1) sample (running as DUT1) during runs 61252 in the September 2011 test beam period at CERN SPS in area H6B. Summary of the data in chapter 9. *(cont.)*

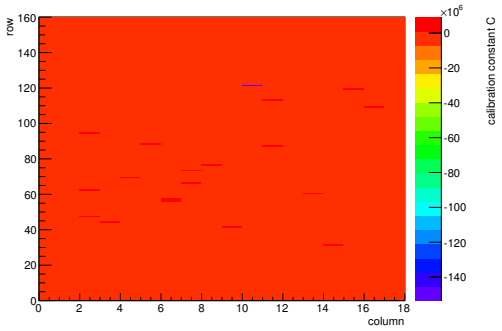

(h) Calibration constant C.

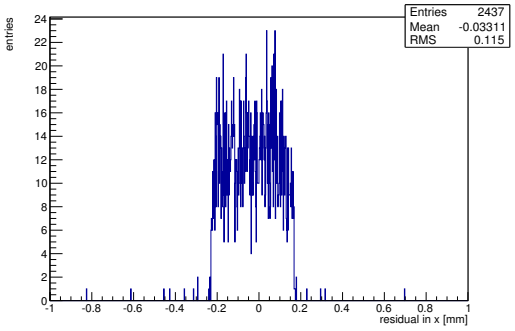

(i) Track residual in x.

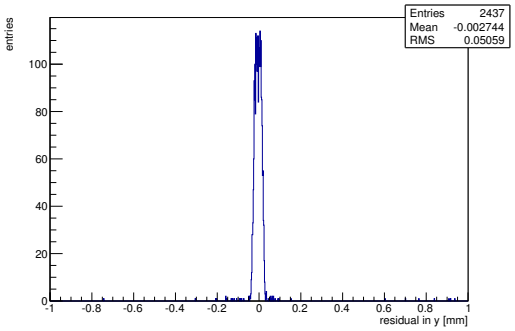

(j) Track residual in y.

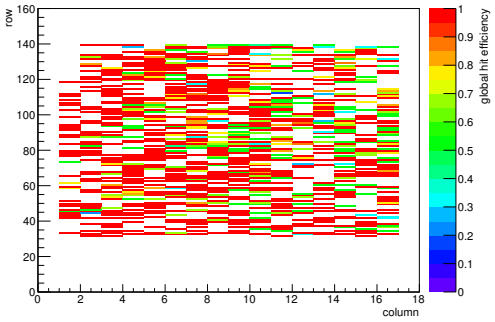

(k) Hit efficiency map.

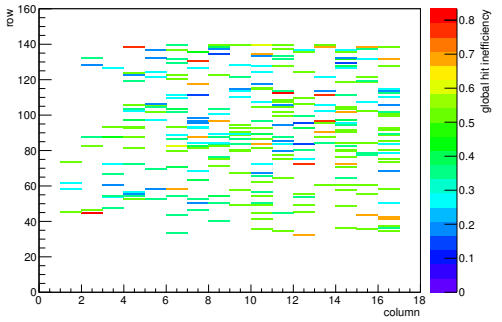

(l) Hit inefficiency map.

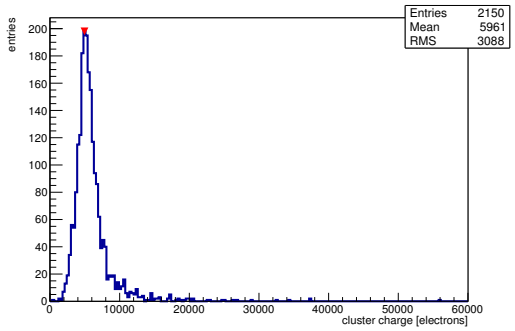

(m) Charge distribution (all cluster sizes included).

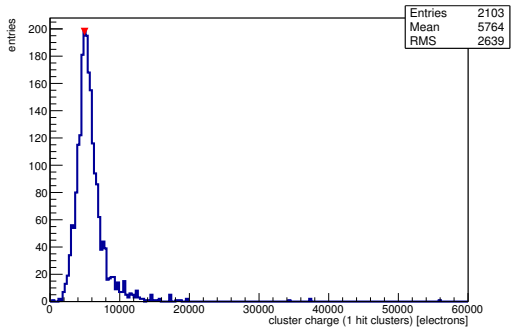

(n) Charge distribution (1 hit cluster).

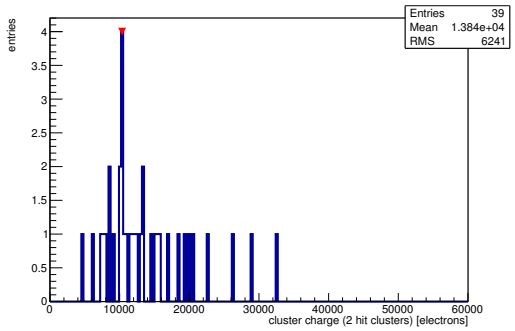

(o) Charge distribution (2 hit cluster).

Figure C.64: Detailed plots for test beam measurement of DO-I-11 (description see section 6.1) sample (running as DUT1) during runs 61252 in the September 2011 test beam period at CERN SPS in area H6B. Summary of the data in chapter 9. *(cont.)*

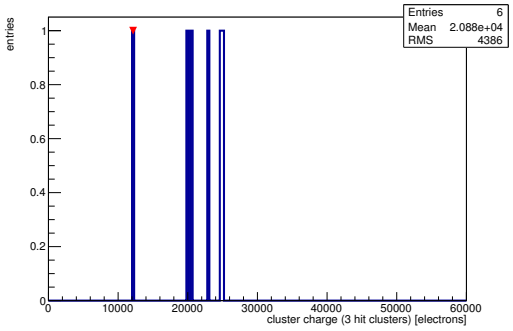

(p) Charge distribution (3 hit cluster).

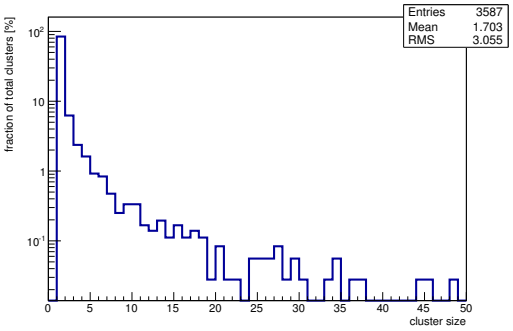

(q) Cluster size distribution.

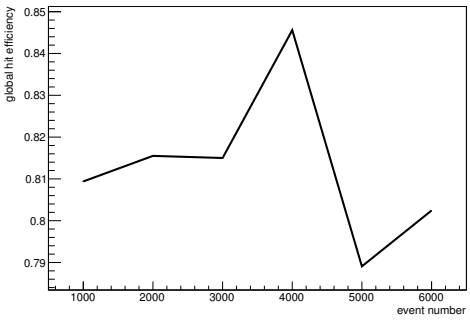

(r) Hit efficiency vs event number.

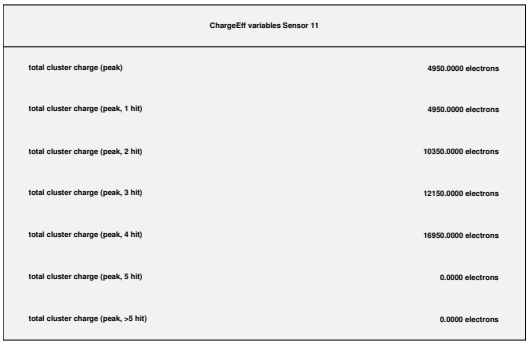

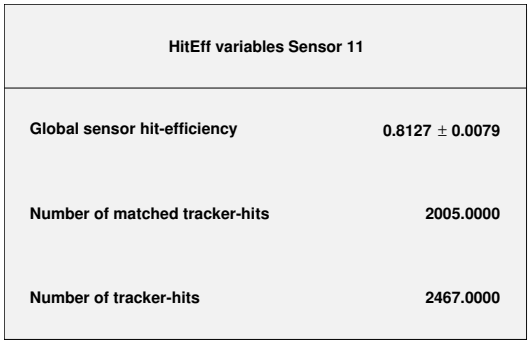

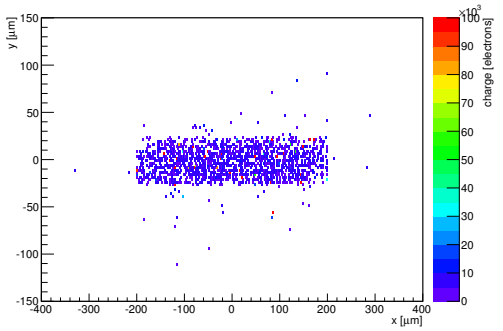

(s) Single pixel mean charge.

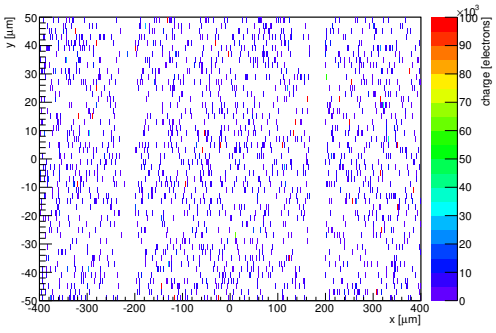

(t) Single pixel mean charge.

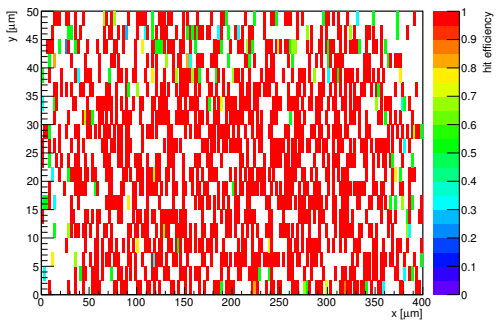

(u) Single pixel hit efficiency.

Figure C.64: Detailed plots for test beam measurement of DO-I-11 (description see section 6.1) sample (running as DUT1) during runs 61252 in the September 2011 test beam period at CERN SPS in area H6B. Summary of the data in chapter 9.

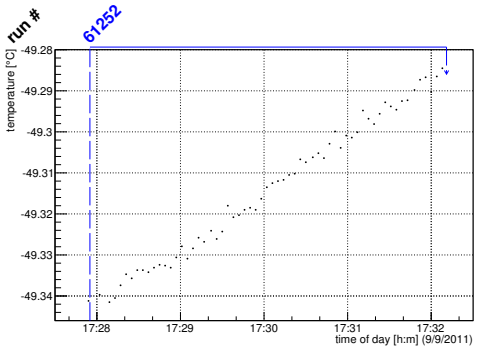

(a) Temperature vs time.

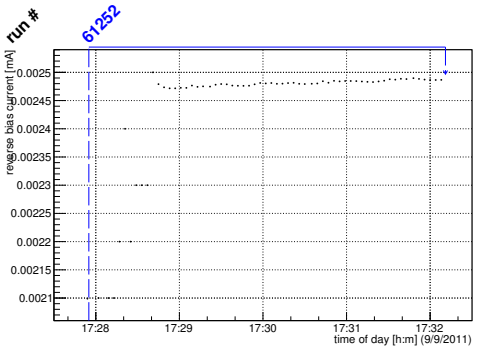

(b) Bias current vs time.

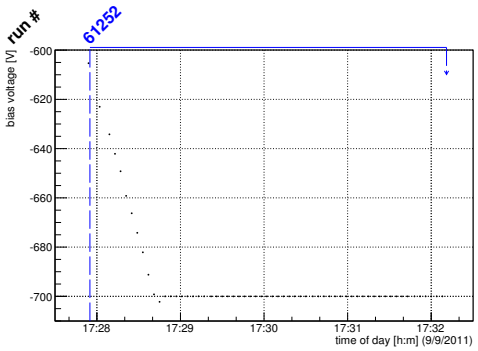

(c) Currently applied bias voltage vs time.

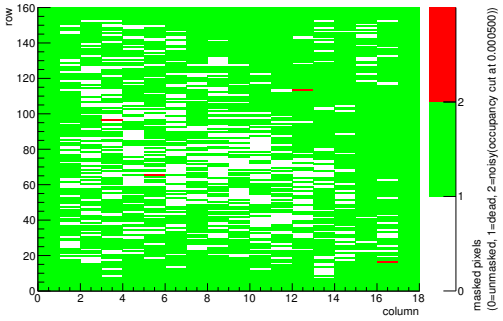

(d) Map of masked pixels.

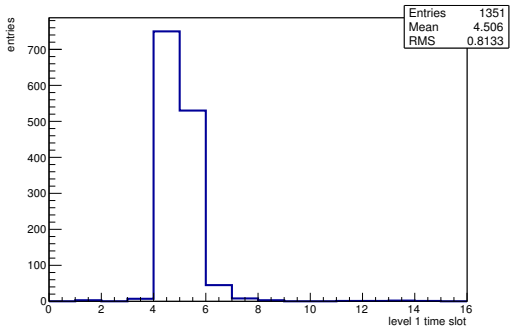

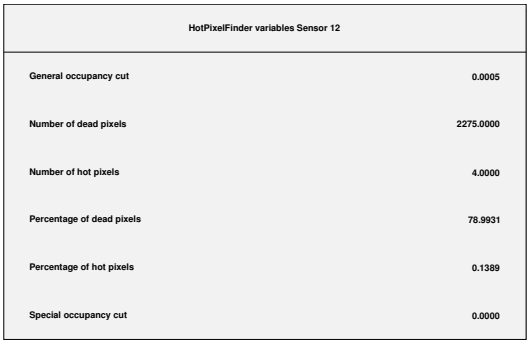

(e) Lvl1 distribution.

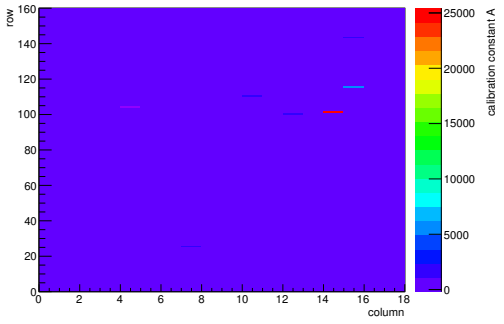

(f) Calibration constant A.

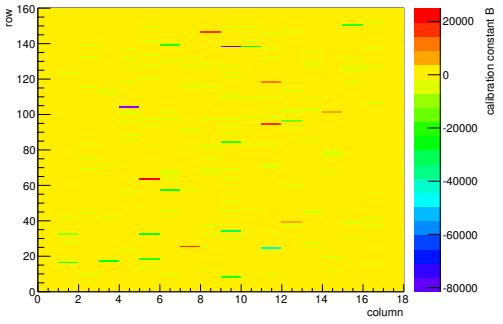

(g) Calibration constant B.

Figure C.65: Detailed plots for test beam measurement of DO-I-5 (description see section 6.1) sample (running as DUT2) during runs 61252 in the September 2011 test beam period at CERN SPS in area H6B. Summary of the data in chapter 9. *(cont.)*

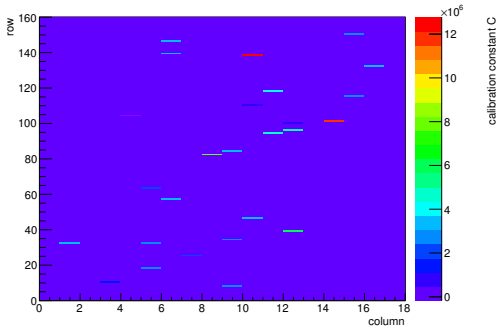

(h) Calibration constant C.

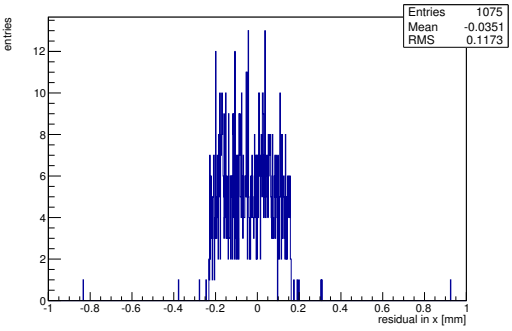

(i) Track residual in x.

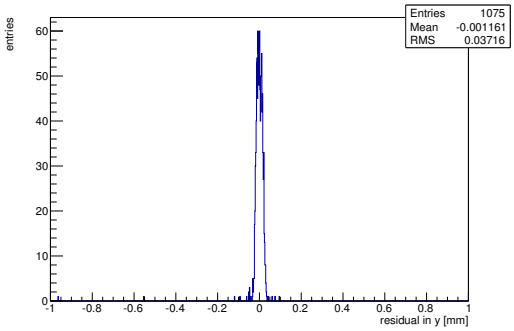

(j) Track residual in y.

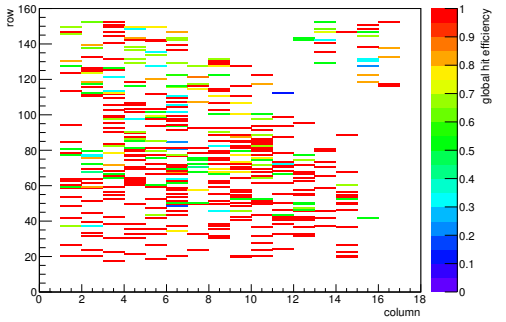

(k) Hit efficiency map.

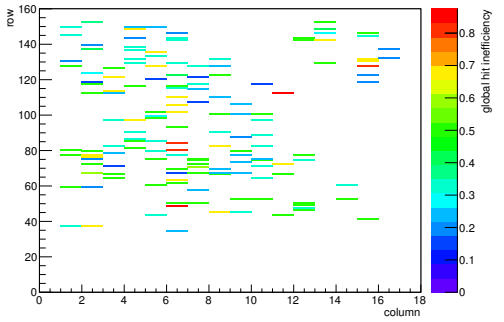

(l) Hit inefficiency map.

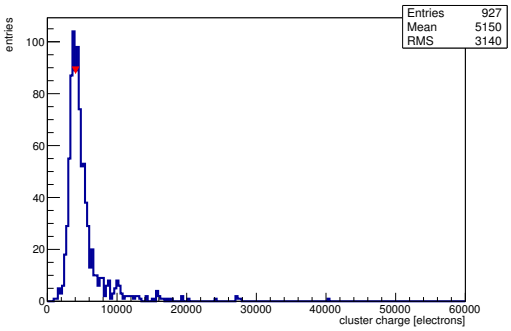

(m) Charge distribution (all cluster sizes included).

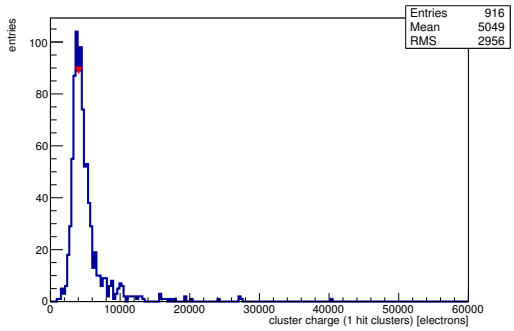

(n) Charge distribution (1 hit cluster).

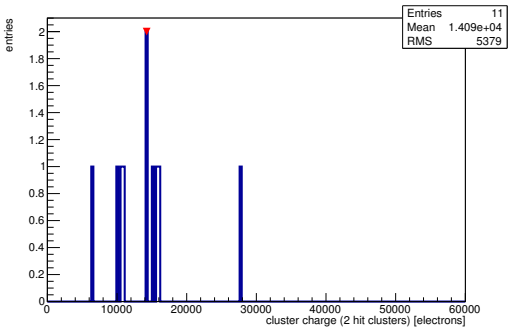

(o) Charge distribution (2 hit cluster).

Figure C.65: Detailed plots for test beam measurement of DO-I-5 (description see section 6.1) sample (running as DUT2) during runs 61252 in the September 2011 test beam period at CERN SPS in area H6B. Summary of the data in chapter 9. *(cont.)*

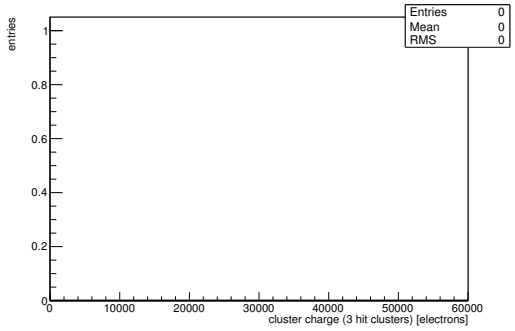

(p) Charge distribution (3 hit cluster).

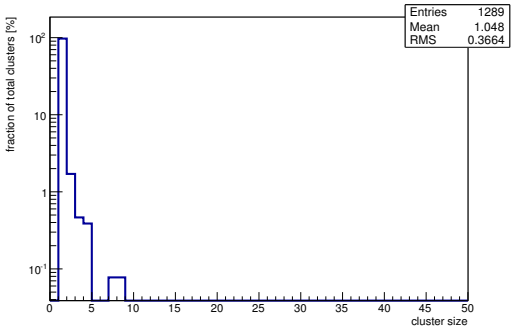

(q) Cluster size distribution.

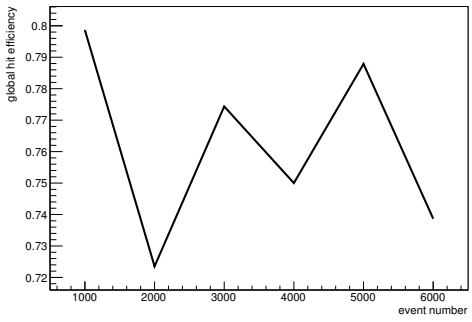

(r) Hit efficiency vs event number.

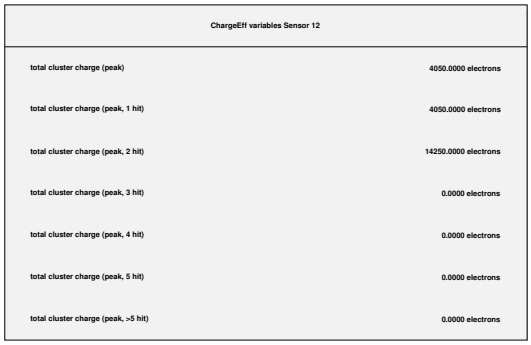

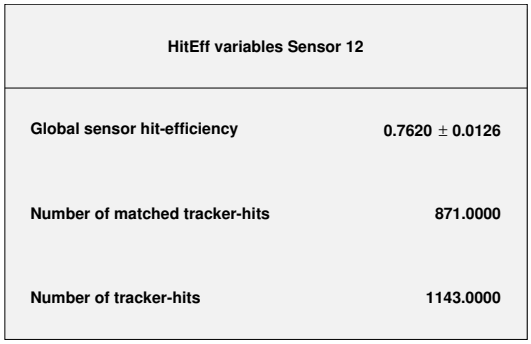

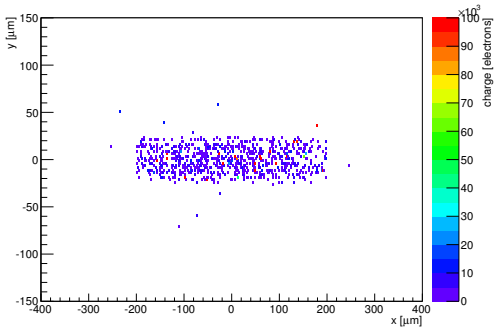

(s) Single pixel mean charge.

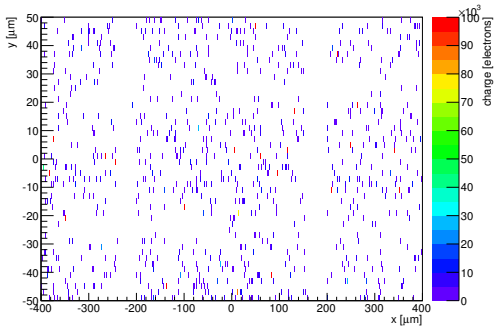

(t) Single pixel mean charge.

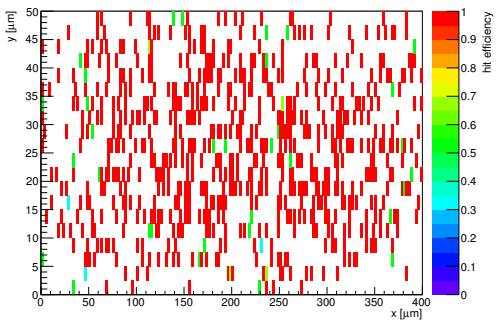

(u) Single pixel hit efficiency.

Figure C.65: Detailed plots for test beam measurement of DO-I-5 (description see section 6.1) sample (running as DUT2) during runs 61252 in the September 2011 test beam period at CERN SPS in area H6B. Summary of the data in chapter 9.

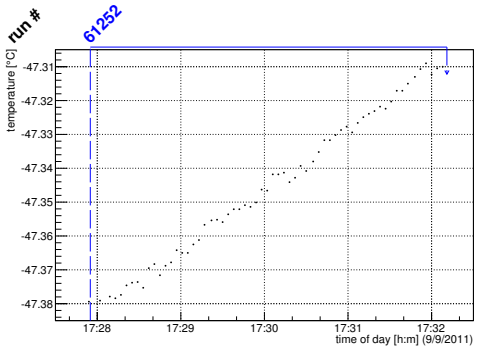

(a) Temperature vs time.

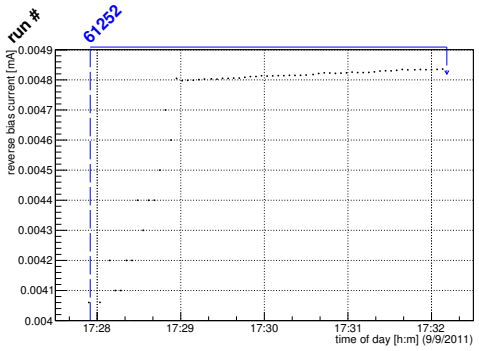

(b) Bias current vs time.

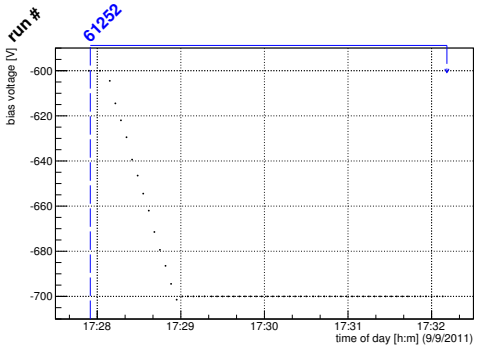

(c) Currently applied bias voltage vs time.

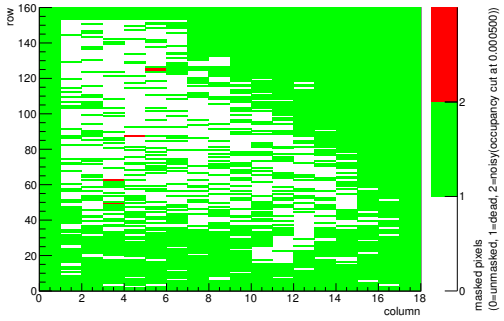

(d) Map of masked pixels.

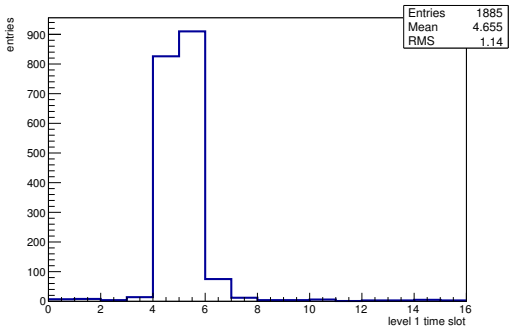

(e) Lvl1 distribution.

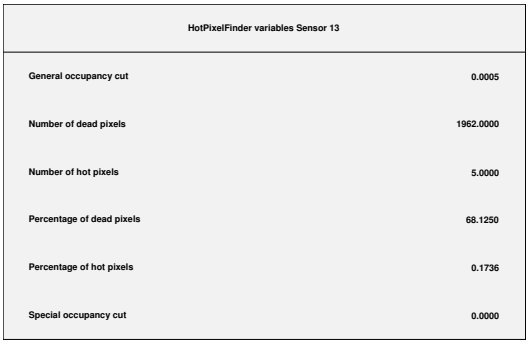

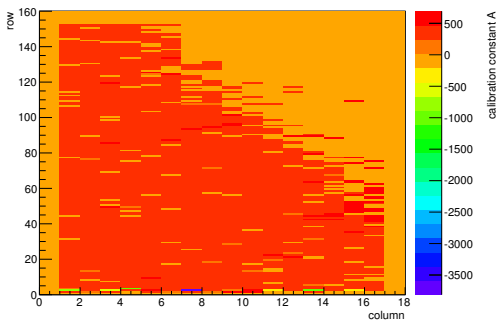

(f) Calibration constant A.

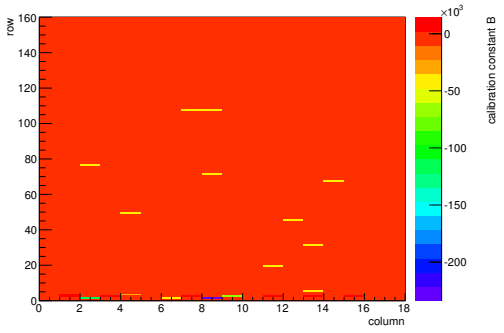

(g) Calibration constant B.

Figure C.66: Detailed plots for test beam measurement of DO-I-12 (description see section 6.1) sample (running as DUT3) during runs 61252 in the September 2011 test beam period at CERN SPS in area H6B. Summary of the data in chapter 9. *(cont.)*

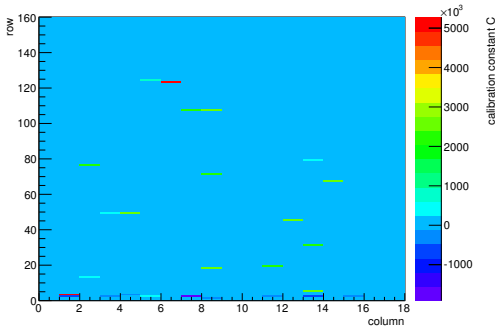

(h) Calibration constant C.

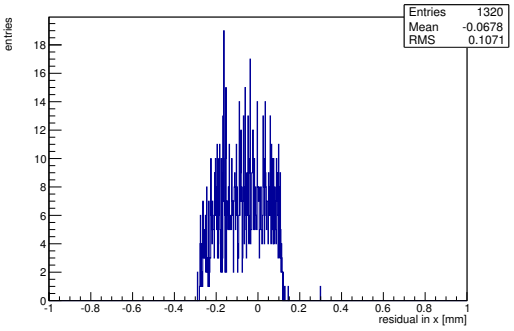

(i) Track residual in x.

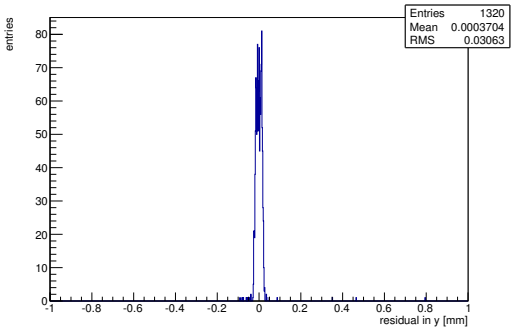

(j) Track residual in y.

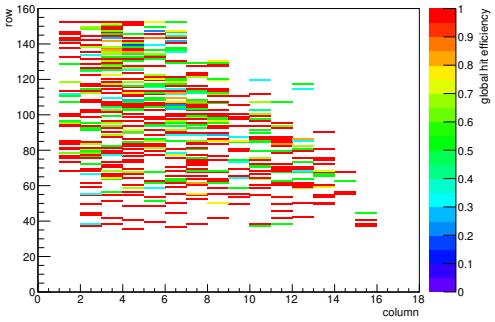

(k) Hit efficiency map.

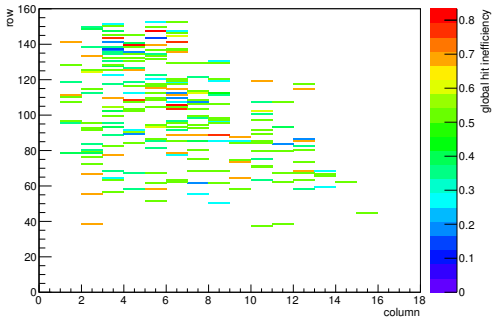

(l) Hit inefficiency map.

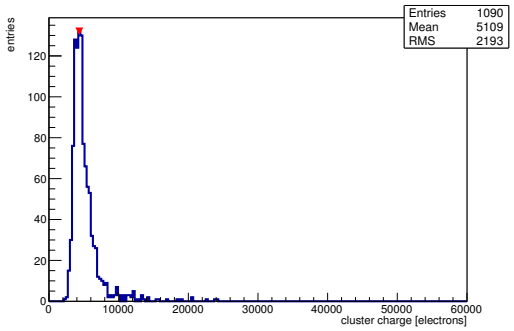

(m) Charge distribution (all cluster sizes included).

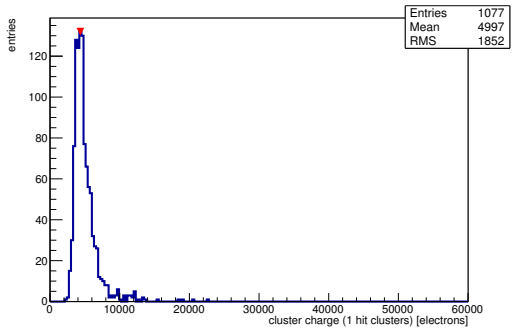

(n) Charge distribution (1 hit cluster).

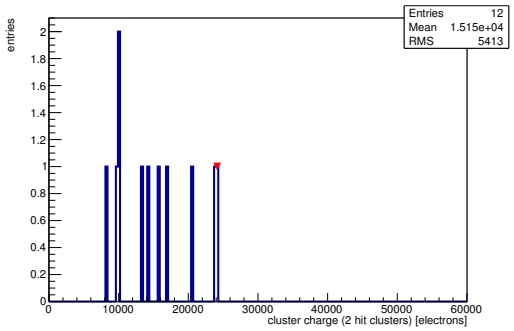

(o) Charge distribution (2 hit cluster).

Figure C.66: Detailed plots for test beam measurement of DO-I-12 (description see section 6.1) sample (running as DUT3) during runs 61252 in the September 2011 test beam period at CERN SPS in area H6B. Summary of the data in chapter 9. *(cont.)*

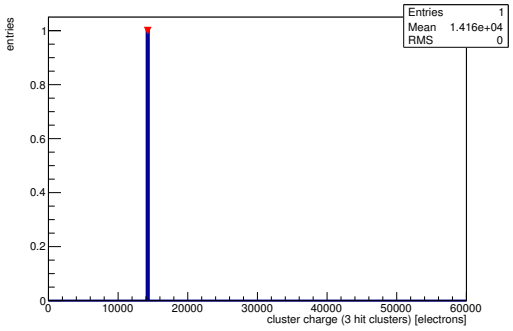

(p) Charge distribution (3 hit cluster).

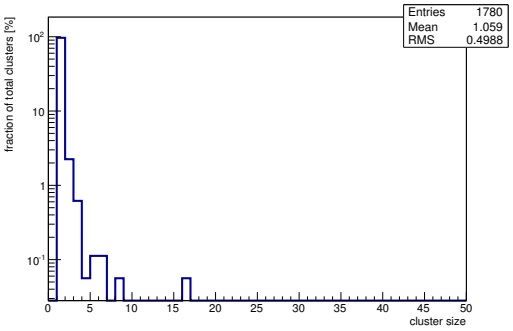

(q) Cluster size distribution.

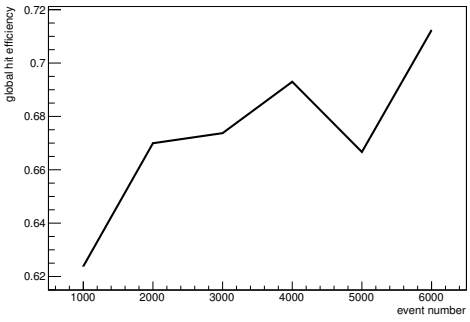

(r) Hit efficiency vs event number.

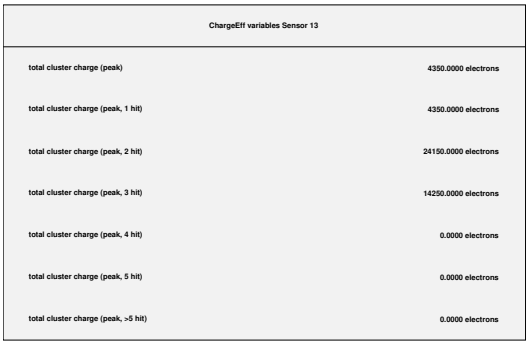

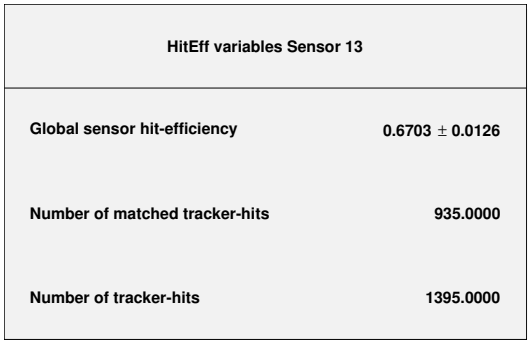

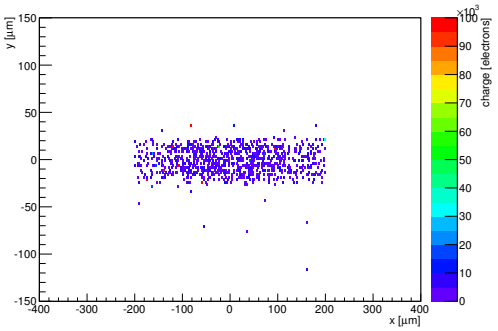

(s) Single pixel mean charge.

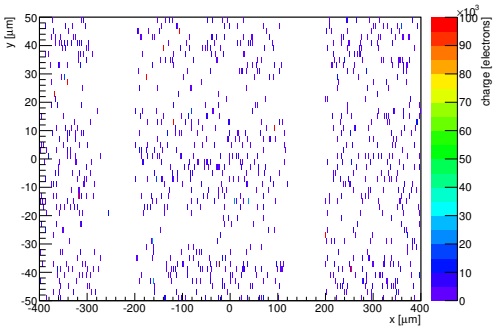

(t) Single pixel mean charge.

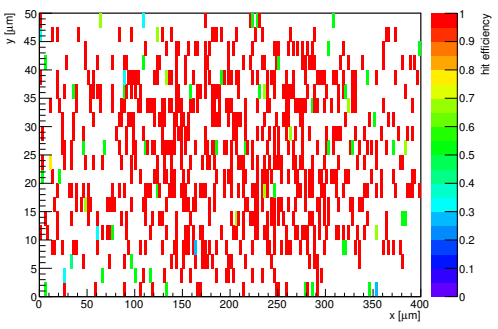

(u) Single pixel hit efficiency.

Figure C.66: Detailed plots for test beam measurement of DO-I-12 (description see section 6.1) sample (running as DUT3) during runs 61252 in the September 2011 test beam period at CERN SPS in area H6B. Summary of the data in chapter 9.

C.3.7 Run 61253

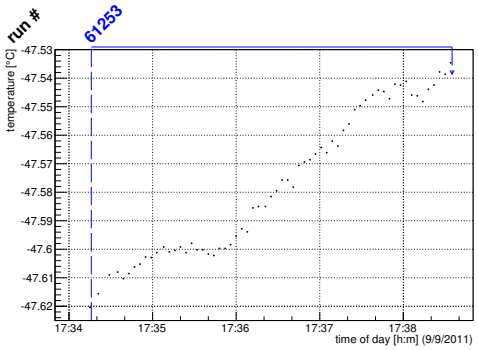

(a) Temperature vs time.

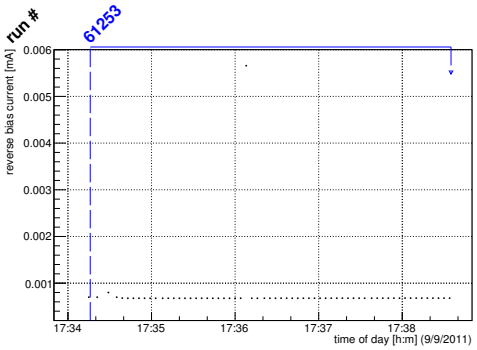

(b) Bias current vs time.

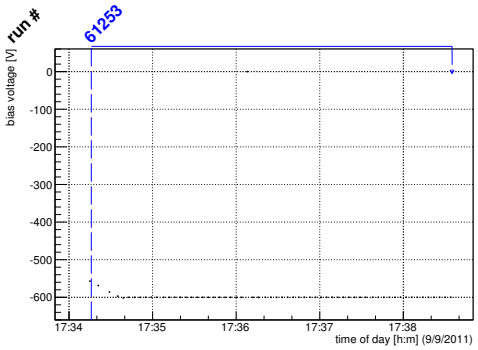

(c) Currently applied bias voltage vs time.

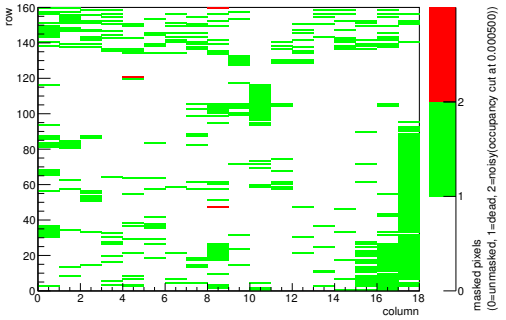

(d) Map of masked pixels.

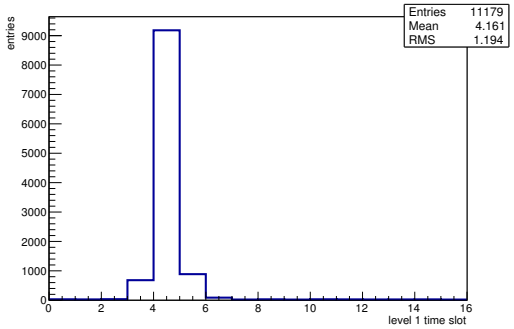

(e) Lvl1 distribution.

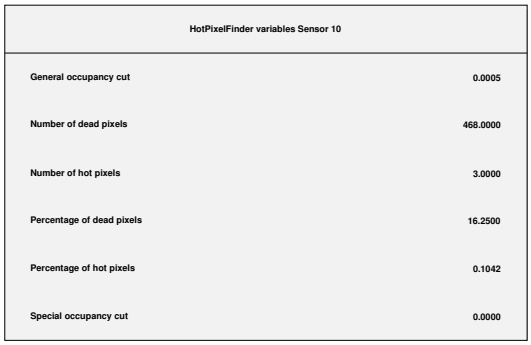

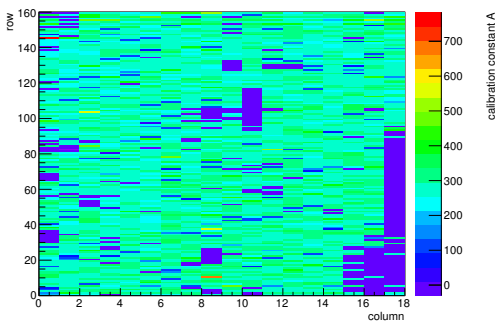

(f) Calibration constant A.

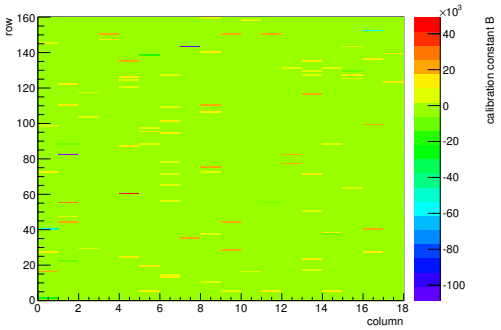

(g) Calibration constant B.

Figure C.67: Detailed plots for test beam measurement of DO-I-7 (description see section 6.1) sample (running as DUT0) during runs 61253 in the September 2011 test beam period at CERN SPS in area H6B. Summary of the data in chapter 9. *(cont.)*

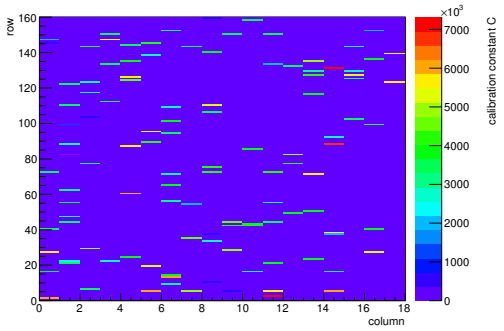

(h) Calibration constant C.

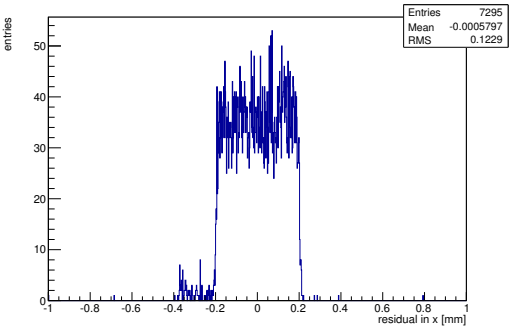

(i) Track residual in x.

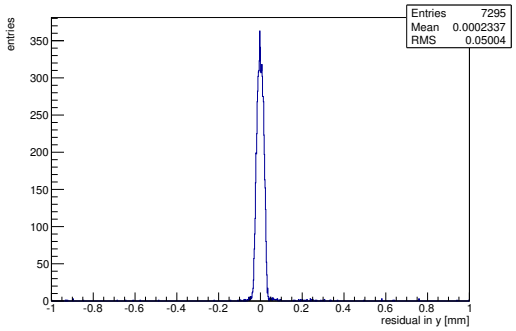

(j) Track residual in y.

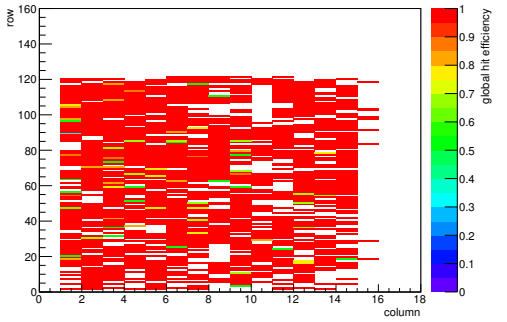

(k) Hit efficiency map.

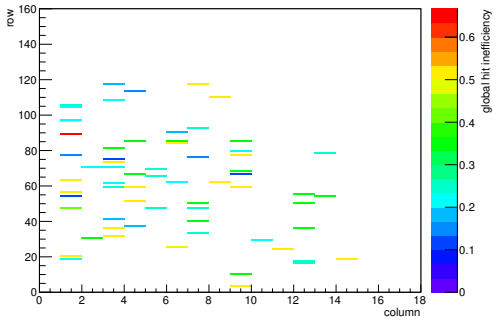

(l) Hit inefficiency map.

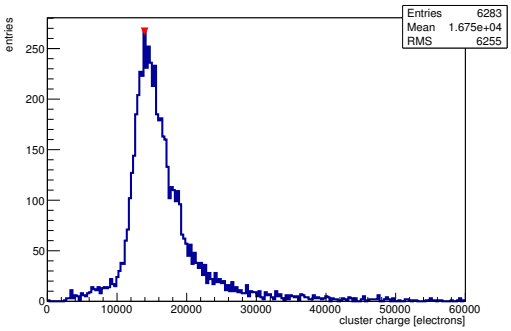

(m) Charge distribution (all cluster sizes included).

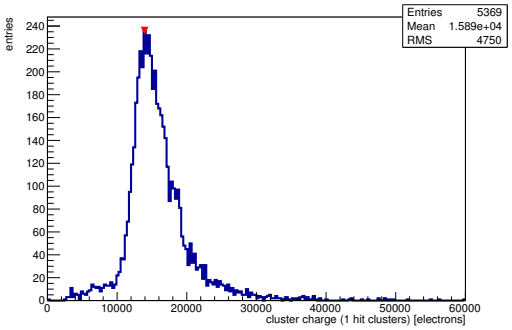

(n) Charge distribution (1 hit cluster).

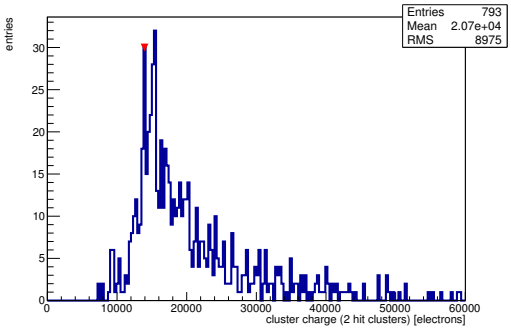

(o) Charge distribution (2 hit cluster).

Figure C.67: Detailed plots for test beam measurement of DO-I-7 (description see section 6.1) sample (running as DUT0) during runs 61253 in the September 2011 test beam period at CERN SPS in area H6B. Summary of the data in chapter 9. *(cont.)*

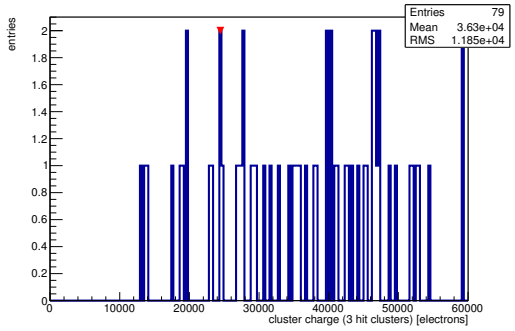

(p) Charge distribution (3 hit cluster).

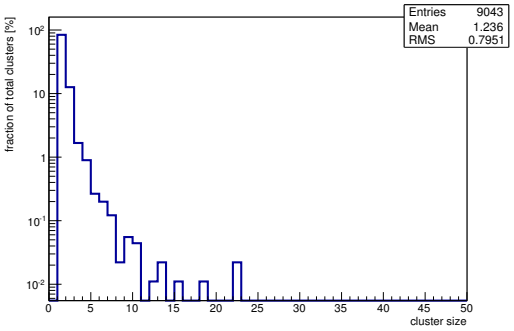

(q) Cluster size distribution.

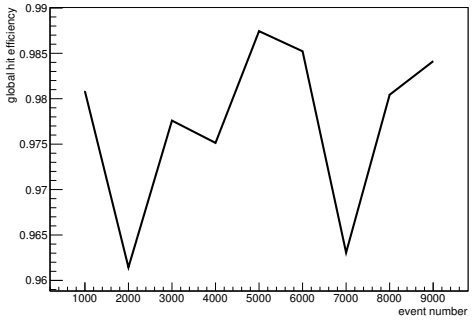

(r) Hit efficiency vs event number.

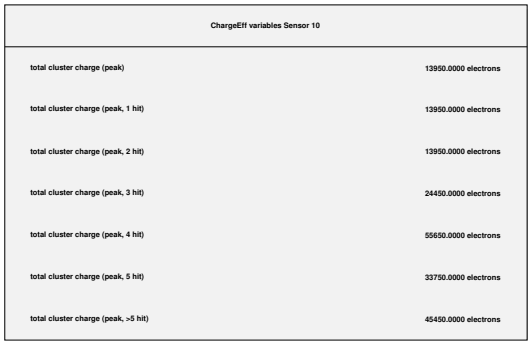

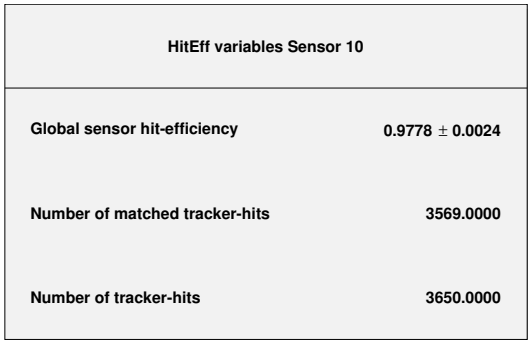

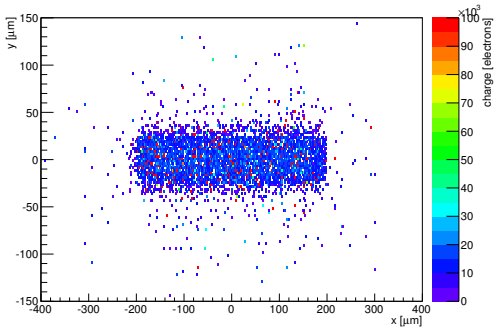

(s) Single pixel mean charge.

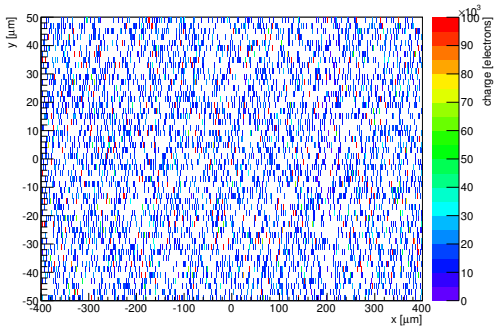

(t) Single pixel mean charge.

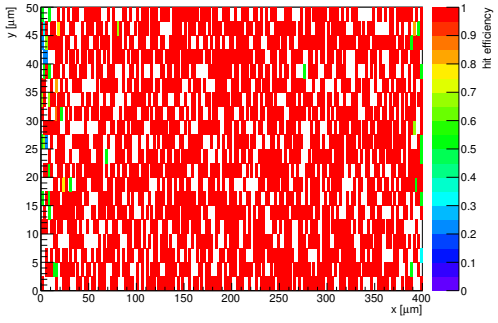

(u) Single pixel hit efficiency.

Figure C.67: Detailed plots for test beam measurement of DO-I-7 (description see section 6.1) sample (running as DUT0) during runs 61253 in the September 2011 test beam period at CERN SPS in area H6B. Summary of the data in chapter 9.

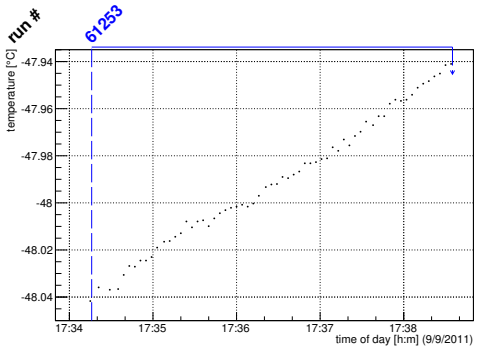

(a) Temperature vs time.

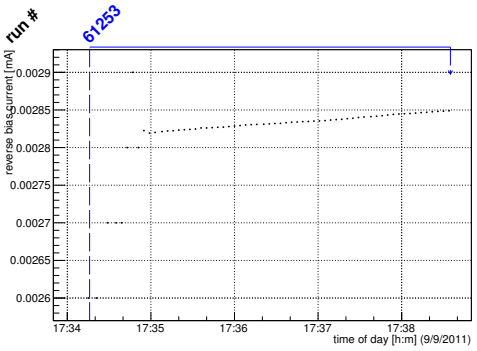

(b) Bias current vs time.

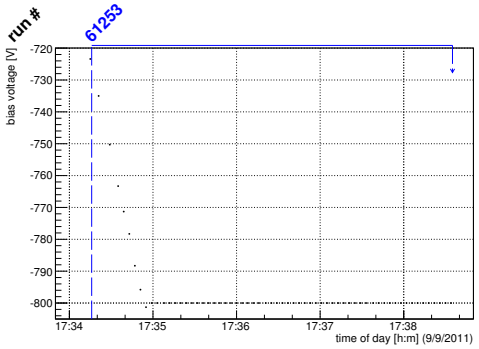

(c) Currently applied bias voltage vs time.

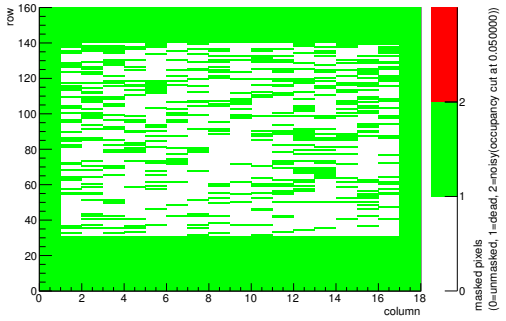

(d) Map of masked pixels.

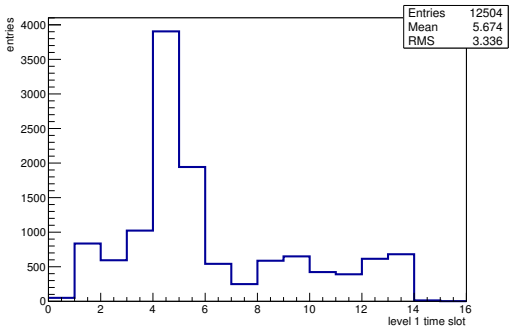

(e) Lvl1 distribution.

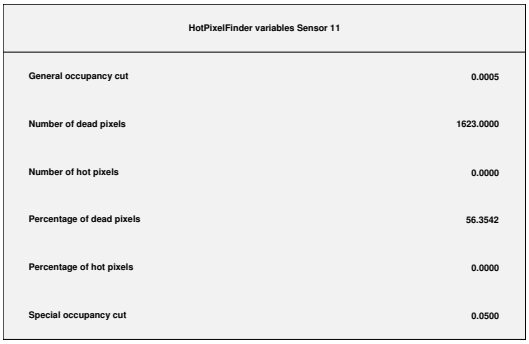

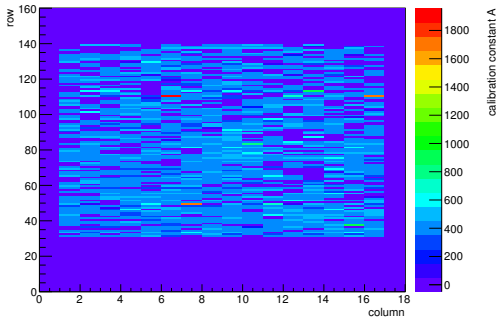

(f) Calibration constant A.

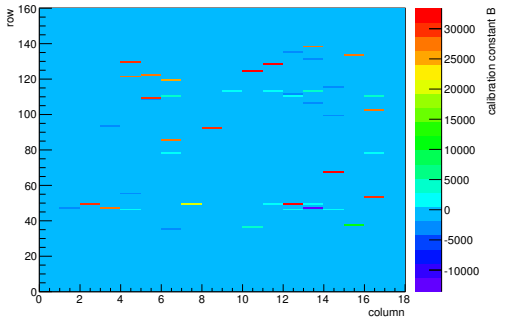

(g) Calibration constant B.

Figure C.68: Detailed plots for test beam measurement of DO-I-11 (description see section 6.1) sample (running as DUT1) during runs 61253 in the September 2011 test beam period at CERN SPS in area H6B. Summary of the data in chapter 9. *(cont.)*

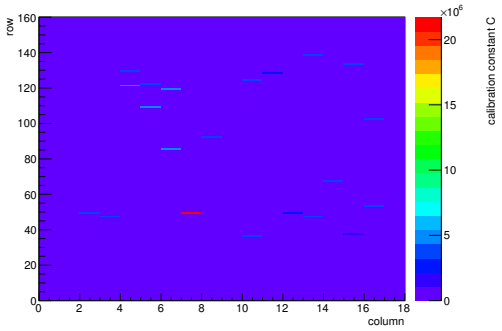

(h) Calibration constant C.

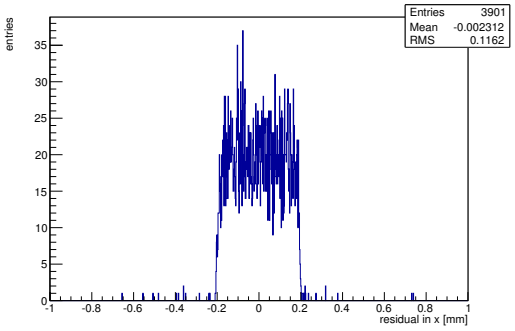

(i) Track residual in x.

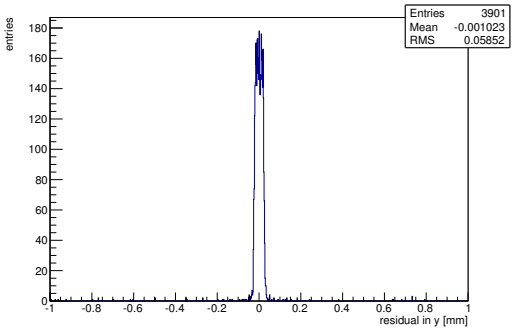

(j) Track residual in y.

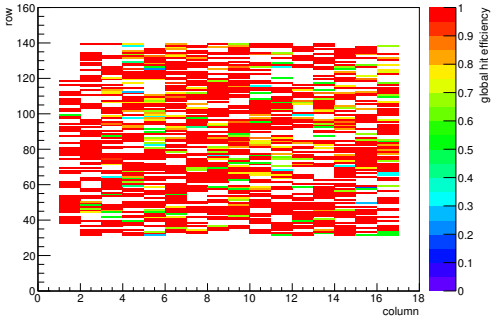

(k) Hit efficiency map.

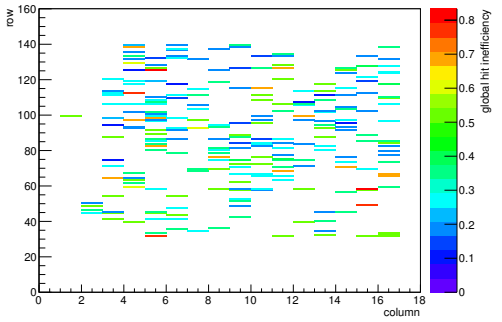

(l) Hit inefficiency map.

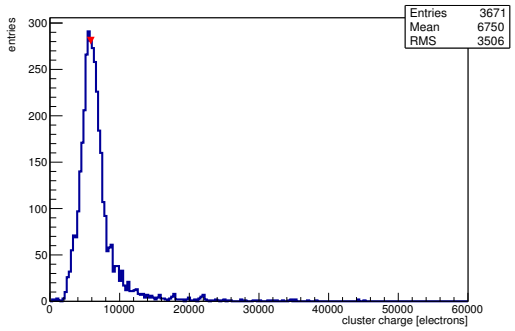

(m) Charge distribution (all cluster sizes included).

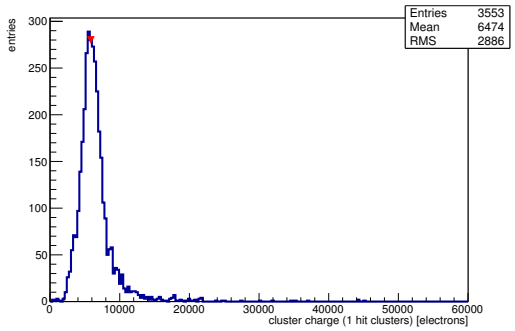

(n) Charge distribution (1 hit cluster).

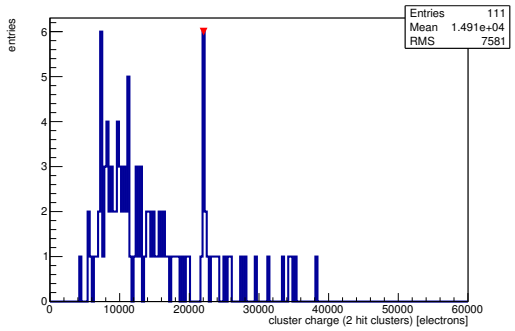

(o) Charge distribution (2 hit cluster).

Figure C.68: Detailed plots for test beam measurement of DO-I-11 (description see section 6.1) sample (running as DUT1) during runs 61253 in the September 2011 test beam period at CERN SPS in area H6B. Summary of the data in chapter 9. *(cont.)*

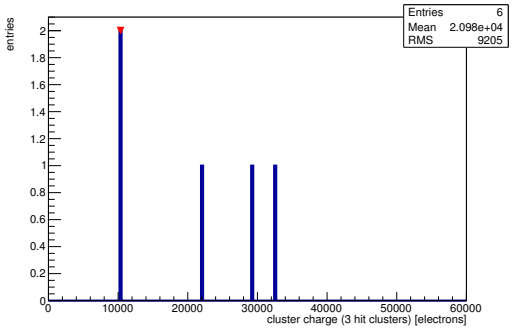

(p) Charge distribution (3 hit cluster).

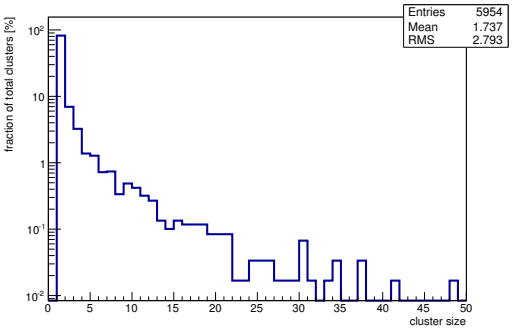

(q) Cluster size distribution.

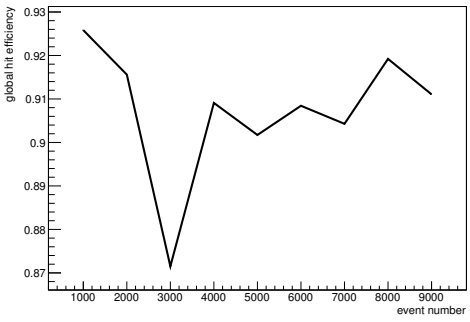

(r) Hit efficiency vs event number.

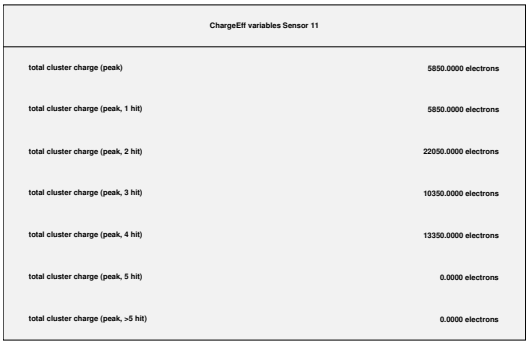

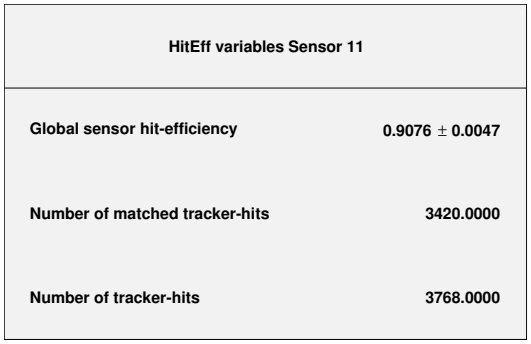

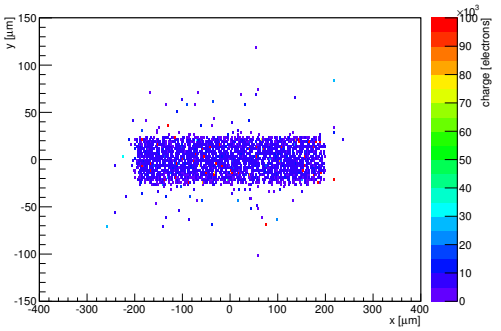

(s) Single pixel mean charge.

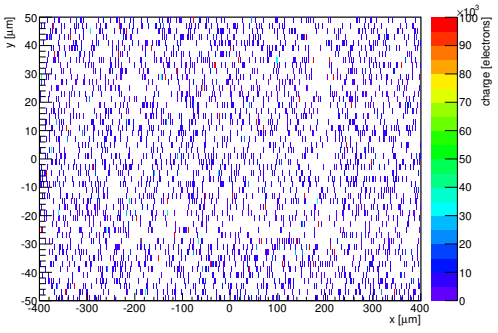

(t) Single pixel mean charge.

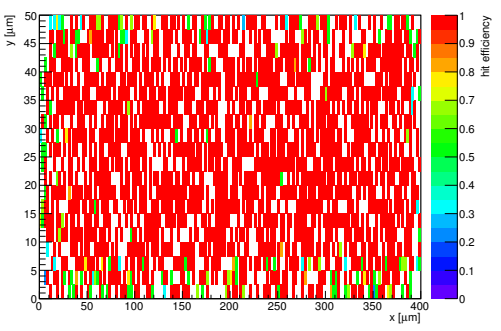

(u) Single pixel hit efficiency.

Figure C.68: Detailed plots for test beam measurement of DO-I-11 (description see section 6.1) sample (running as DUT1) during runs 61253 in the September 2011 test beam period at CERN SPS in area H6B. Summary of the data in chapter 9.

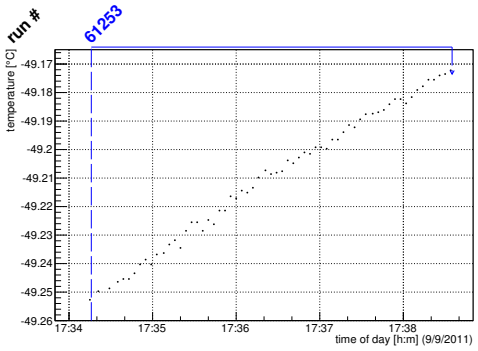

(a) Temperature vs time.

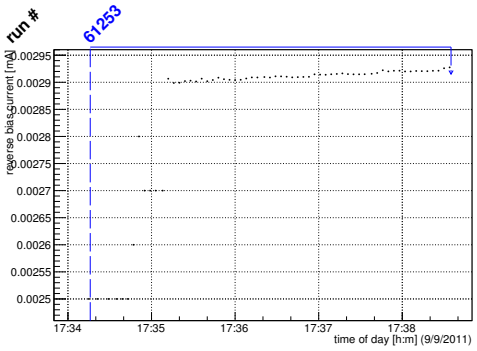

(b) Bias current vs time.

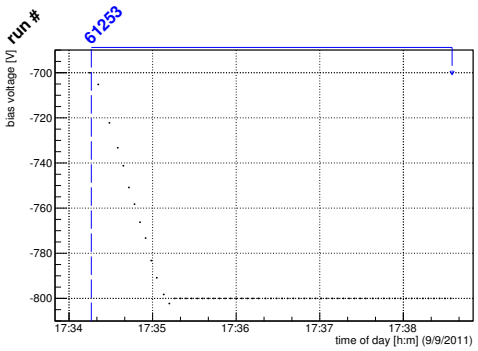

(c) Currently applied bias voltage vs time.

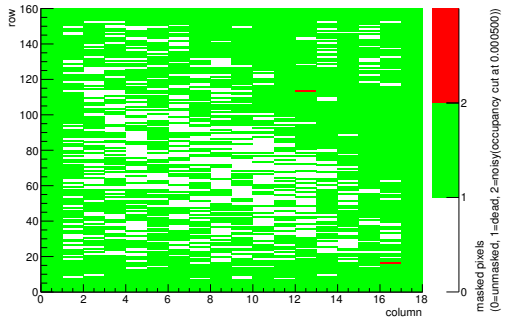

(d) Map of masked pixels.

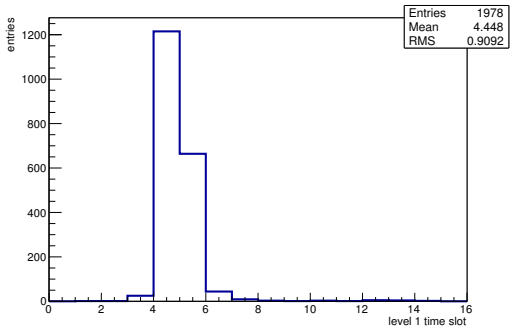

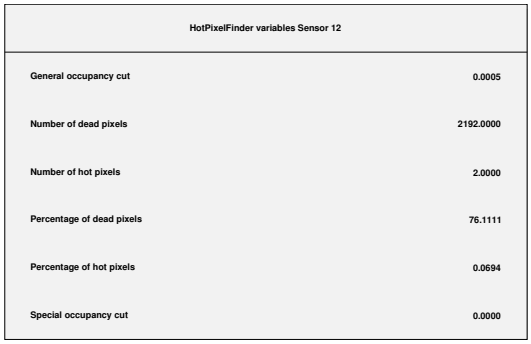

(e) Lvl1 distribution.

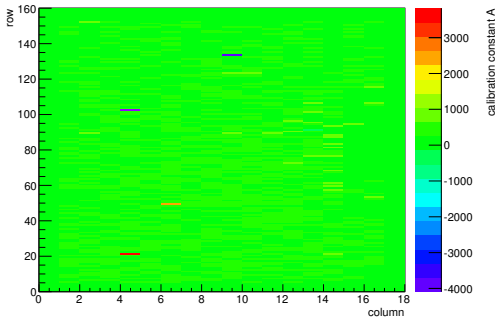

(f) Calibration constant A.

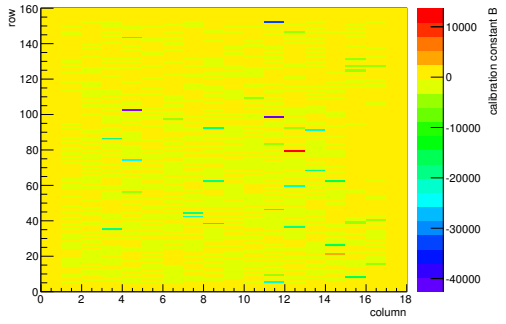

(g) Calibration constant B.

Figure C.69: Detailed plots for test beam measurement of DO-I-5 (description see section 6.1) sample (running as DUT2) during runs 61253 in the September 2011 test beam period at CERN SPS in area H6B. Summary of the data in chapter 9. *(cont.)*

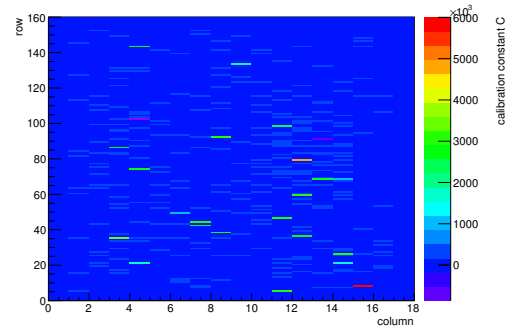

(h) Calibration constant C.

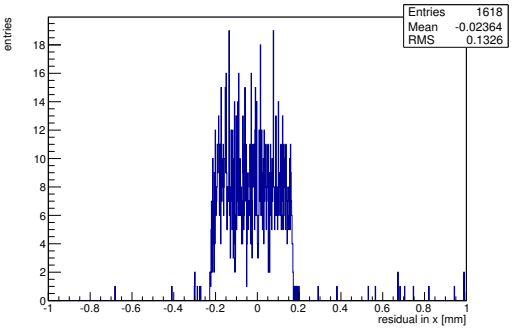

(i) Track residual in x.

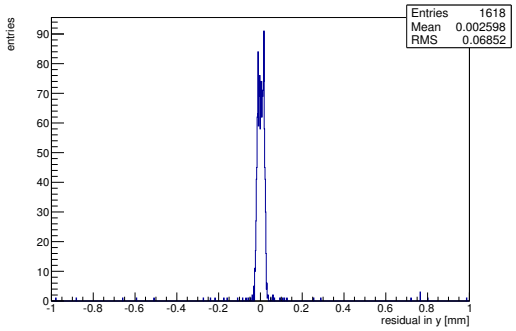

(j) Track residual in y.

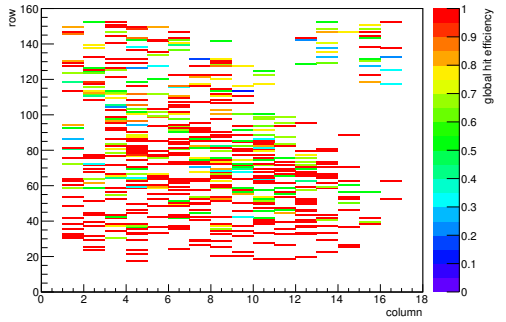

(k) Hit efficiency map.

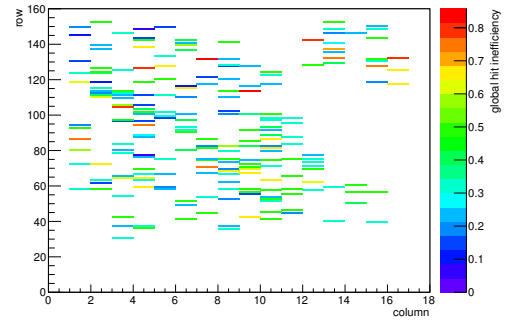

(l) Hit inefficiency map.

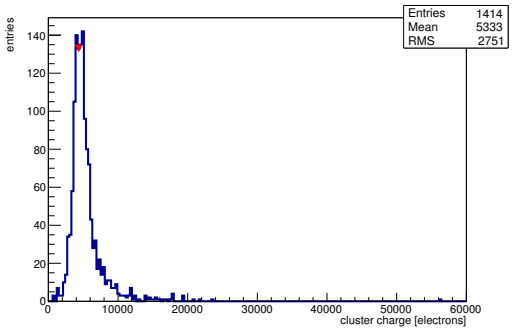

(m) Charge distribution (all cluster sizes included).

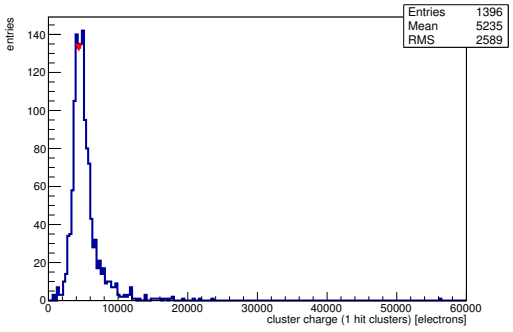

(n) Charge distribution (1 hit cluster).

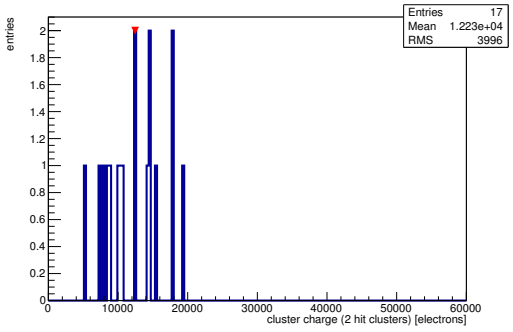

(o) Charge distribution (2 hit cluster).

Figure C.69: Detailed plots for test beam measurement of DO-I-5 (description see section 6.1) sample (running as DUT2) during runs 61253 in the September 2011 test beam period at CERN SPS in area H6B. Summary of the data in chapter 9. *(cont.)*

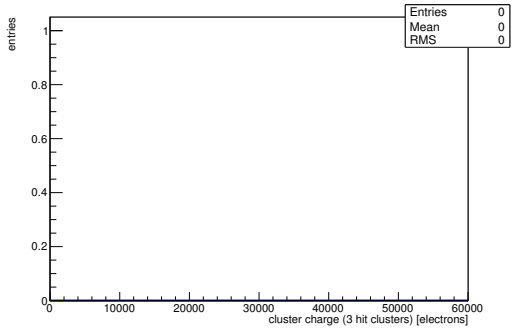

(p) Charge distribution (3 hit cluster).

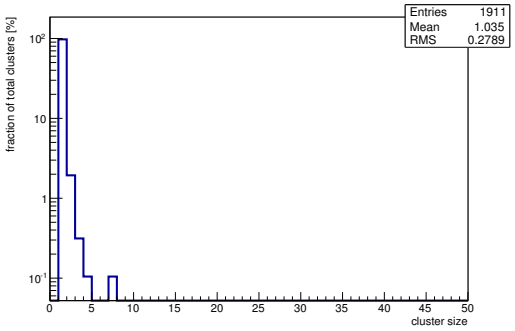

(q) Cluster size distribution.

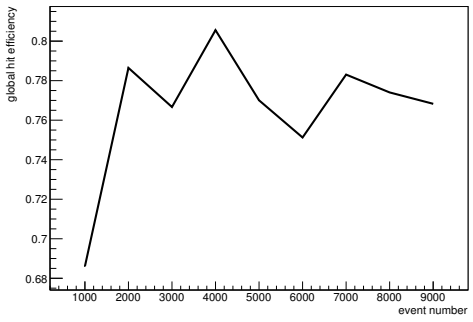

(r) Hit efficiency vs event number.

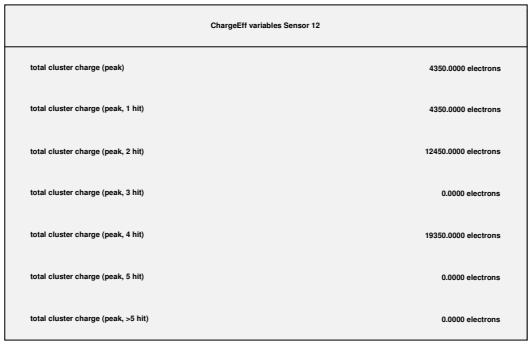

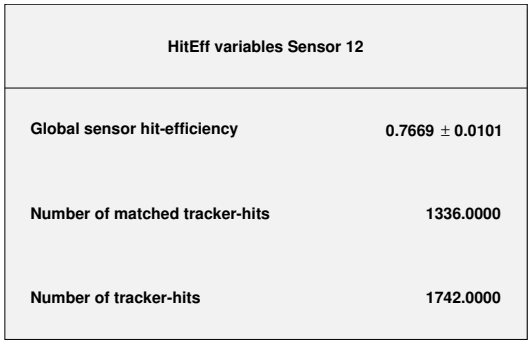

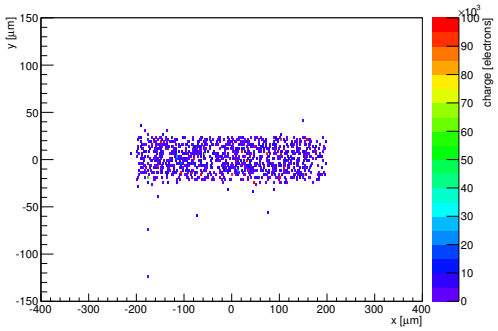

(s) Single pixel mean charge.

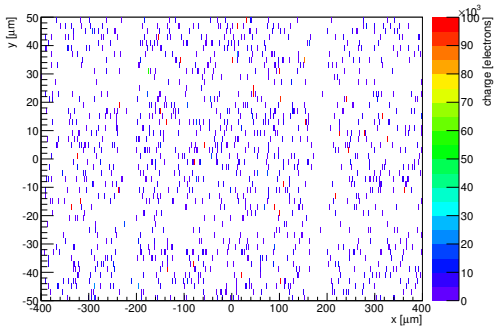

(t) Single pixel mean charge.

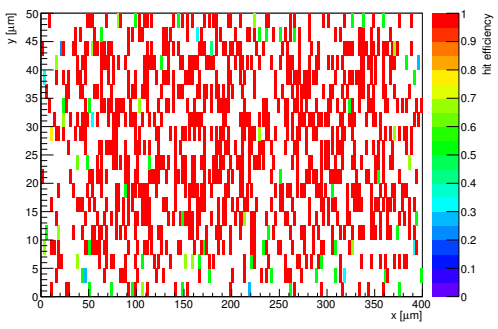

(u) Single pixel hit efficiency.

Figure C.69: Detailed plots for test beam measurement of DO-I-5 (description see section 6.1) sample (running as DUT2) during runs 61253 in the September 2011 test beam period at CERN SPS in area H6B. Summary of the data in chapter 9.

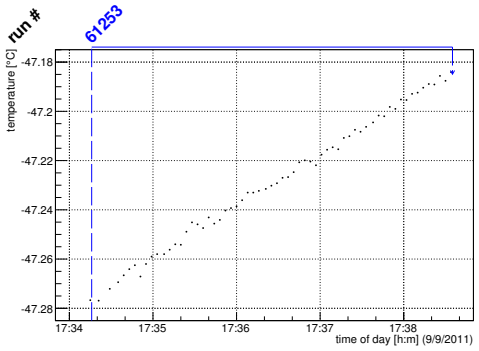

(a) Temperature vs time.

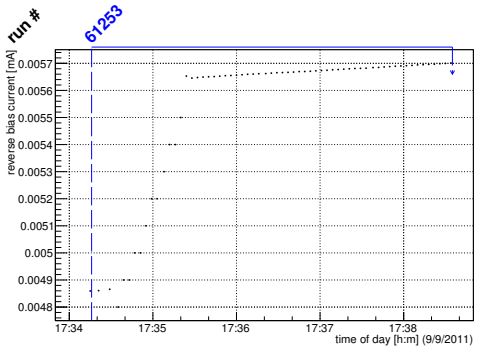

(b) Bias current vs time.

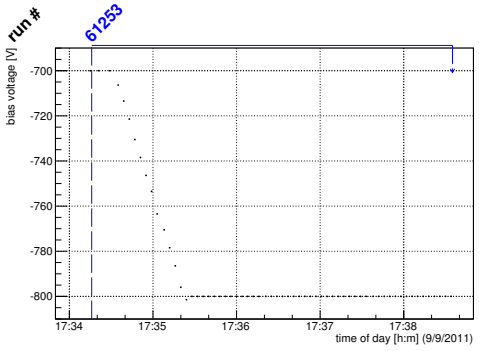

(c) Currently applied bias voltage vs time.

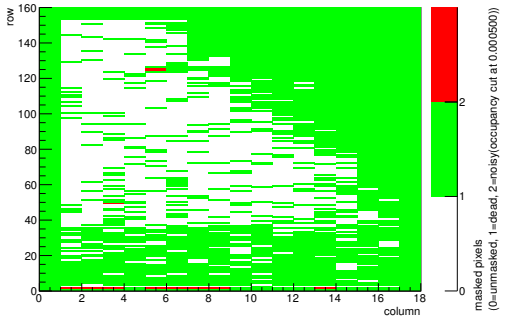

(d) Map of masked pixels.

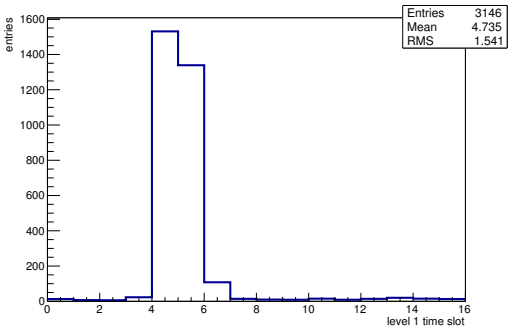

(e) Lvl1 distribution.

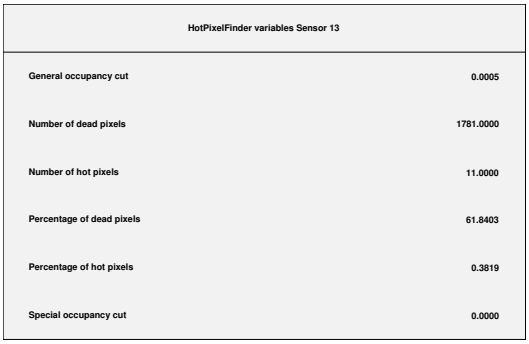

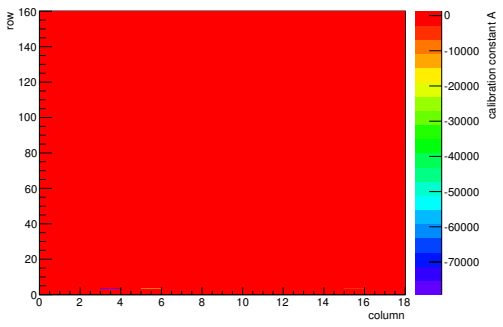

(f) Calibration constant A.

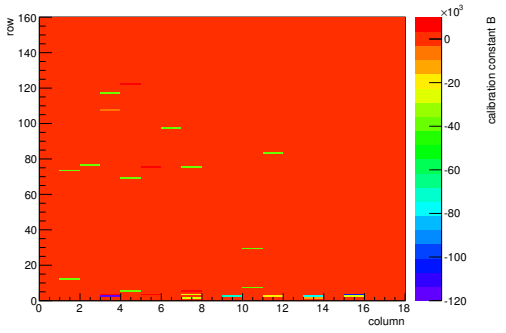

(g) Calibration constant B.

Figure C.70: Detailed plots for test beam measurement of DO-I-12 (description see section 6.1) sample (running as DUT3) during runs 61253 in the September 2011 test beam period at CERN SPS in area H6B. Summary of the data in chapter 9. *(cont.)*

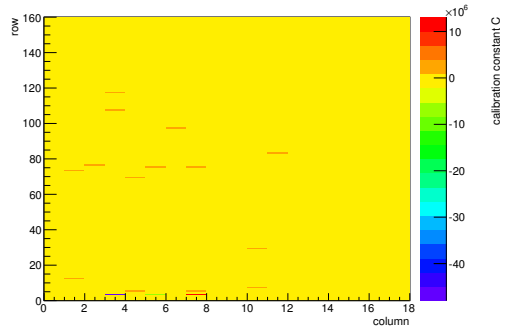

(h) Calibration constant C.

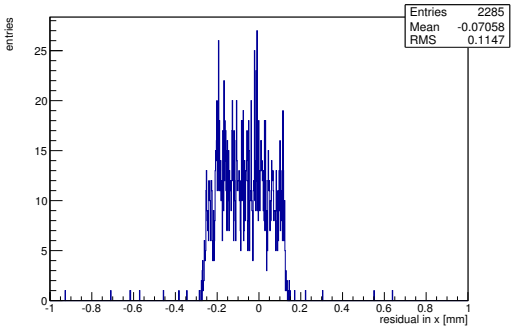

(i) Track residual in x.

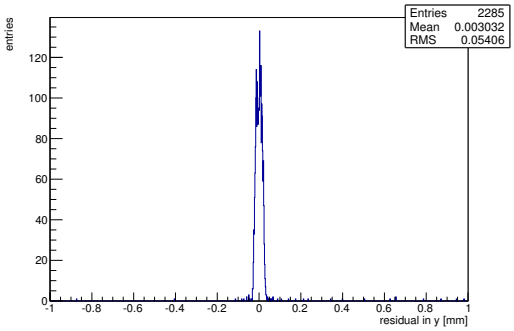

(j) Track residual in y.

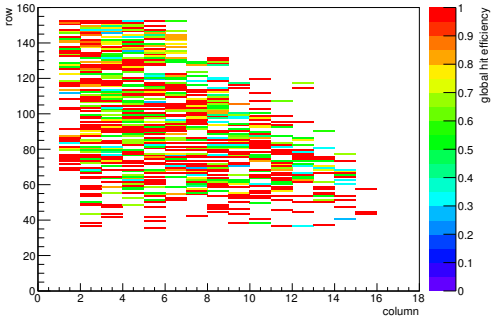

(k) Hit efficiency map.

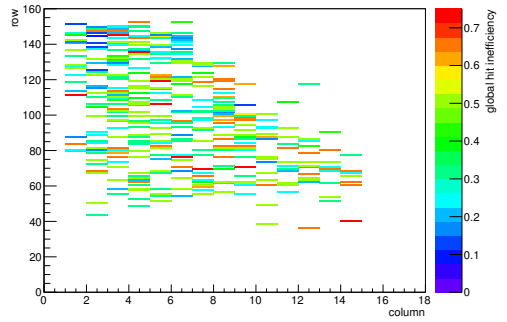

(l) Hit inefficiency map.

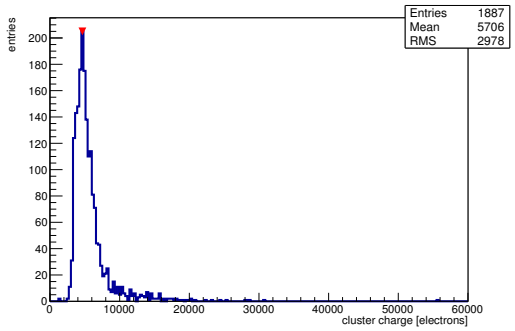

(m) Charge distribution (all cluster sizes included).

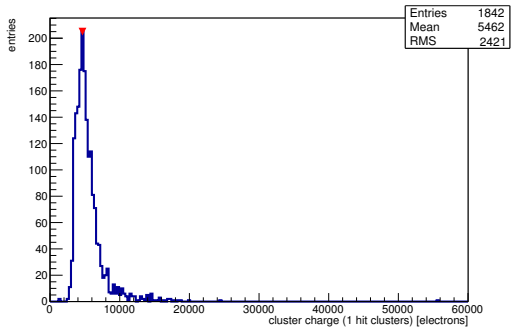

(n) Charge distribution (1 hit cluster).

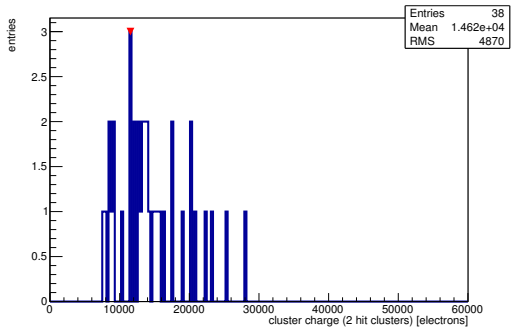

(o) Charge distribution (2 hit cluster).

Figure C.70: Detailed plots for test beam measurement of DO-I-12 (description see section 6.1) sample (running as DUT3) during runs 61253 in the September 2011 test beam period at CERN SPS in area H6B. Summary of the data in chapter 9. *(cont.)*

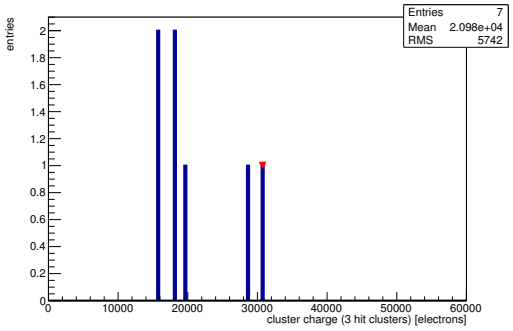

(p) Charge distribution (3 hit cluster).

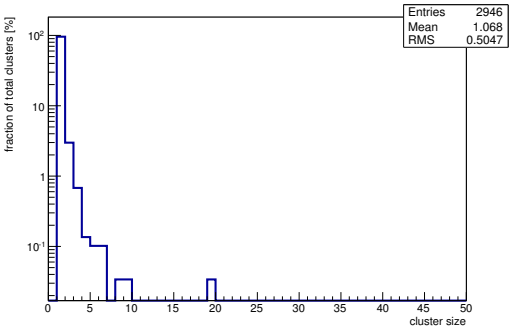

(q) Cluster size distribution.

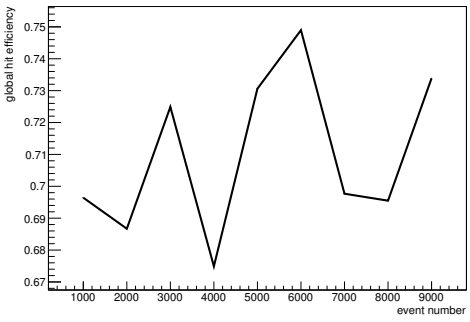

(r) Hit efficiency vs event number.

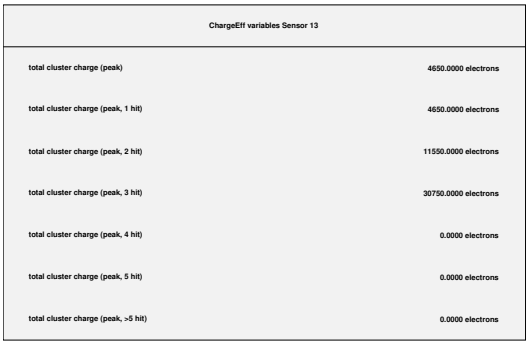

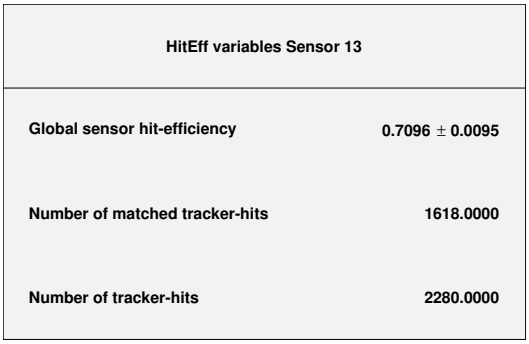

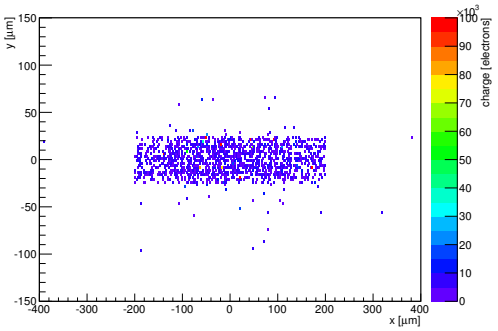

(s) Single pixel mean charge.

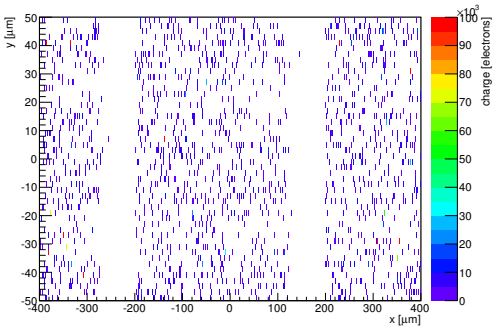

(t) Single pixel mean charge.

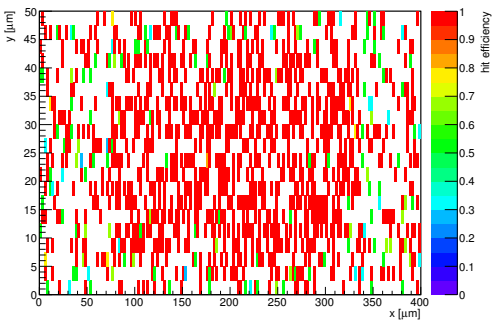

(u) Single pixel hit efficiency.

Figure C.70: Detailed plots for test beam measurement of DO-I-12 (description see section 6.1) sample (running as DUT3) during runs 61253 in the September 2011 test beam period at CERN SPS in area H6B. Summary of the data in chapter 9.

C.3.8 Run 61254

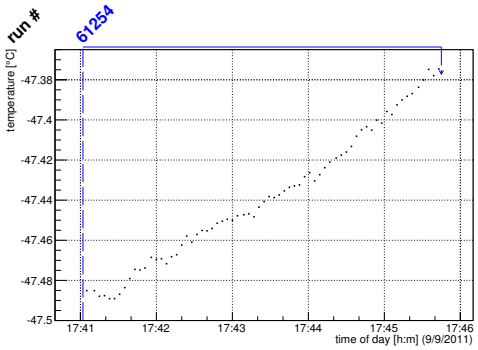

(a) Temperature vs time.

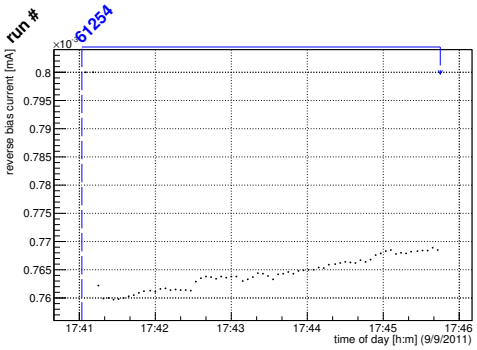

(b) Bias current vs time.

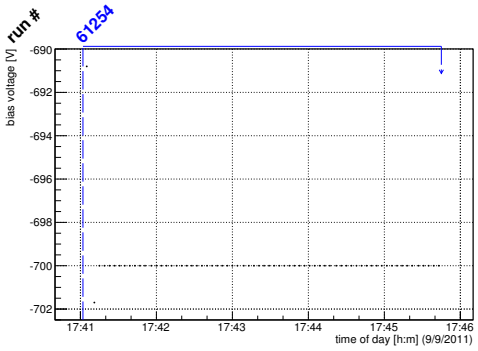

(c) Currently applied bias voltage vs time.

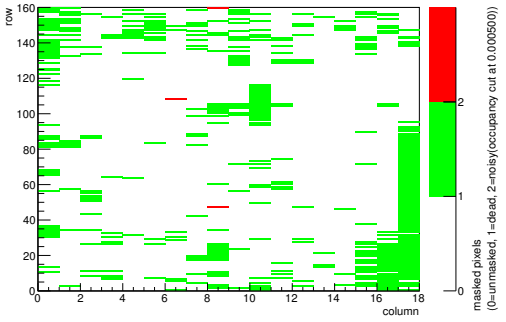

(d) Map of masked pixels.

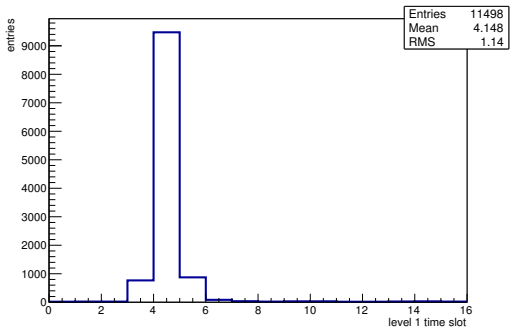

(e) Lvl1 distribution.

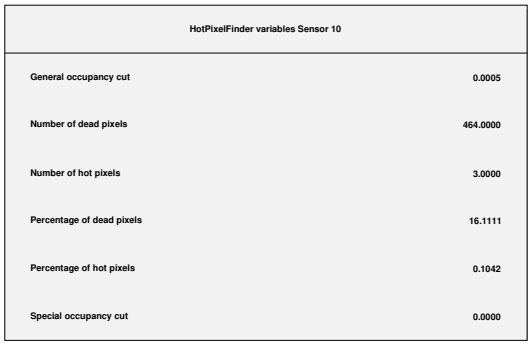

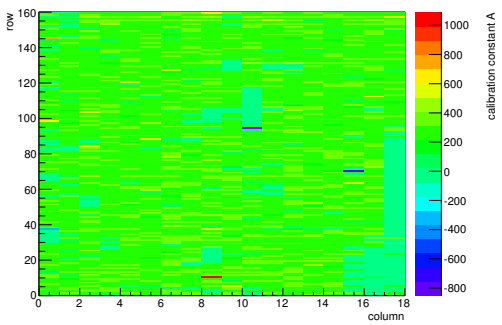

(f) Calibration constant A.

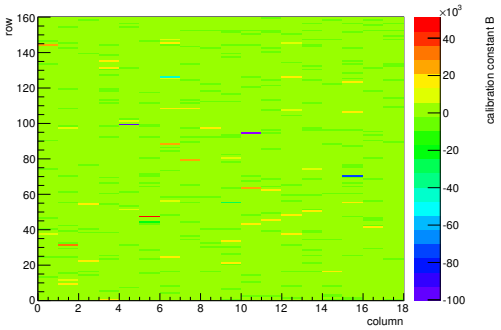

(g) Calibration constant B.

Figure C.71: Detailed plots for test beam measurement of DO-I-7 (description see section 6.1) sample (running as DUT0) during runs 61254 in the September 2011 test beam period at CERN SPS in area H6B. Summary of the data in chapter 9. *(cont.)*

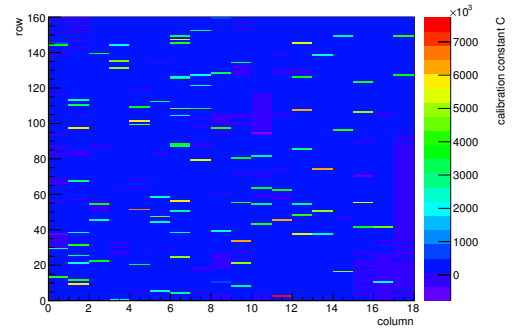

(h) Calibration constant C.

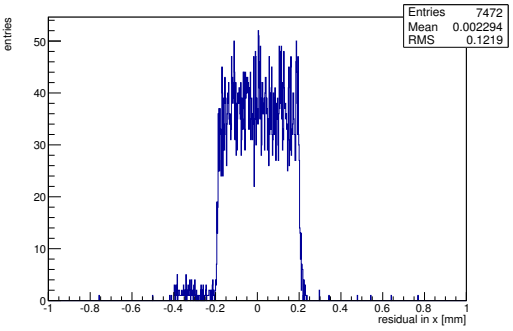

(i) Track residual in x.

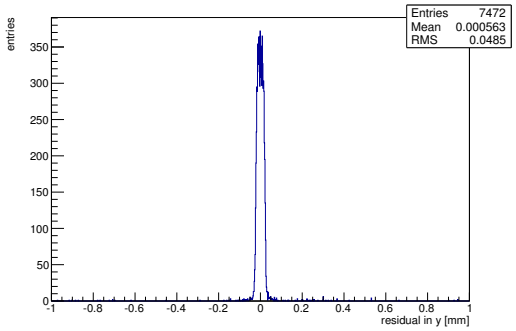

(j) Track residual in y.

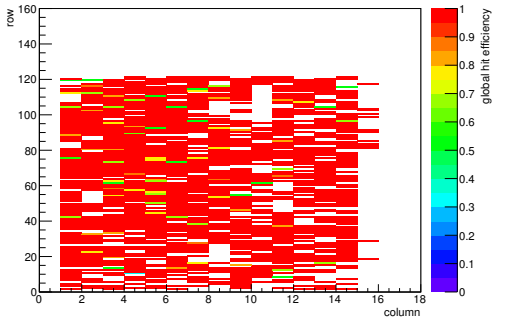

(k) Hit efficiency map.

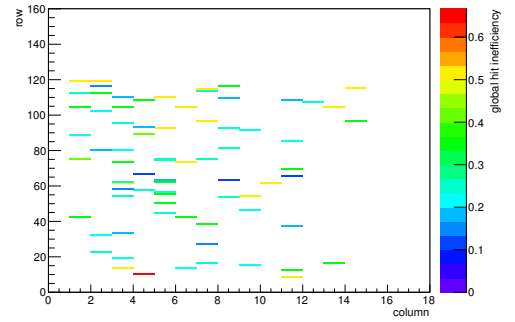

(l) Hit inefficiency map.

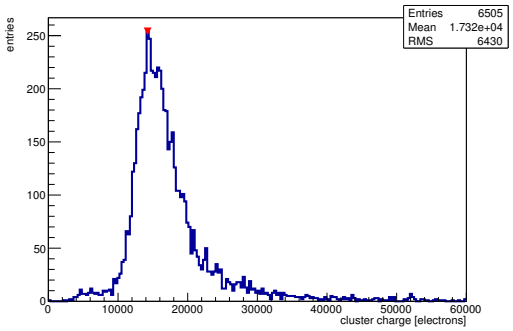

(m) Charge distribution (all cluster sizes included).

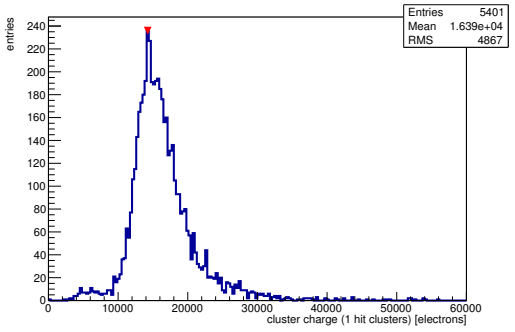

(n) Charge distribution (1 hit cluster).

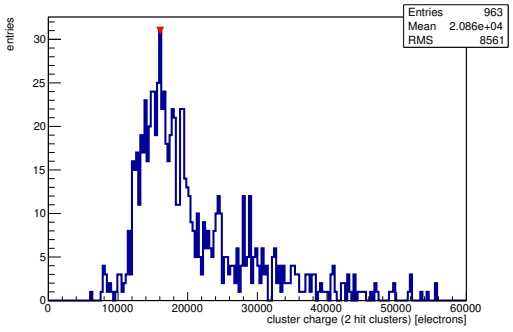

(o) Charge distribution (2 hit cluster).

Figure C.71: Detailed plots for test beam measurement of DO-I-7 (description see section 6.1) sample (running as DUT0) during runs 61254 in the September 2011 test beam period at CERN SPS in area H6B. Summary of the data in chapter 9. *(cont.)*

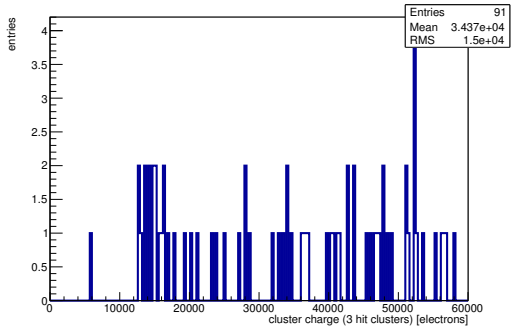

(p) Charge distribution (3 hit cluster).

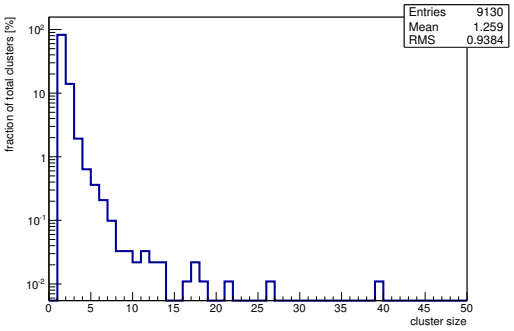

(q) Cluster size distribution.

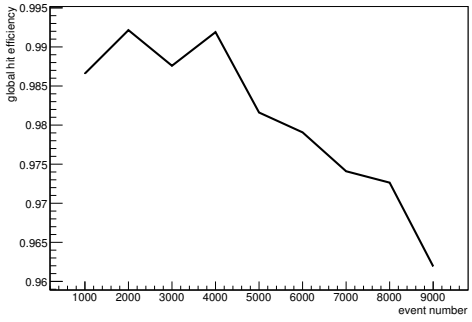

(r) Hit efficiency vs event number.

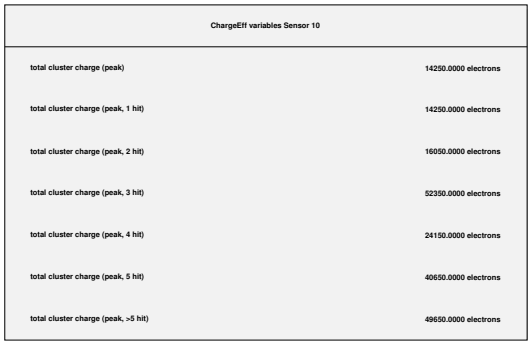

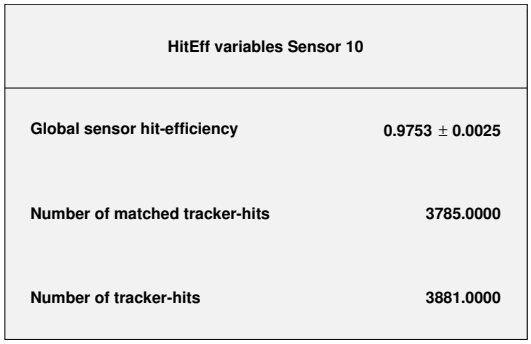

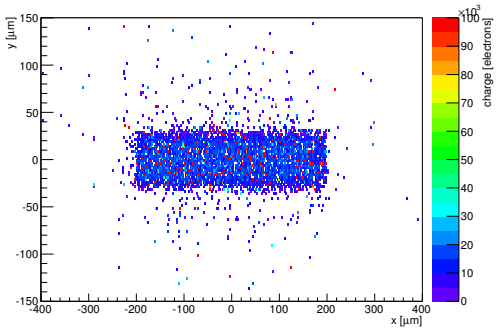

(s) Single pixel mean charge.

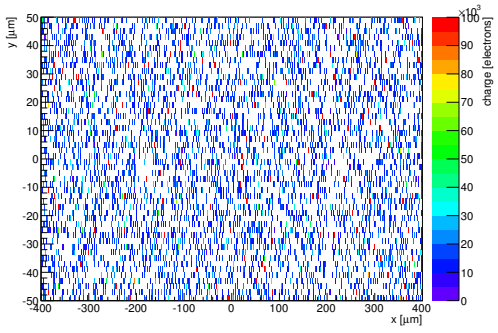

(t) Single pixel mean charge.

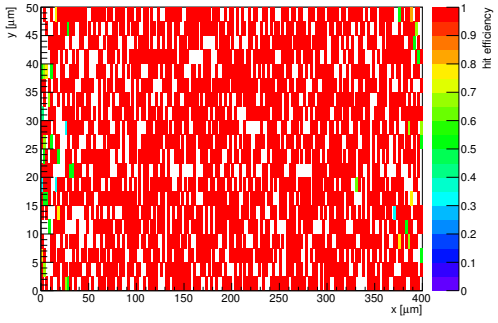

(u) Single pixel hit efficiency.

Figure C.71: Detailed plots for test beam measurement of DO-I-7 (description see section 6.1) sample (running as DUT0) during runs 61254 in the September 2011 test beam period at CERN SPS in area H6B. Summary of the data in chapter 9.

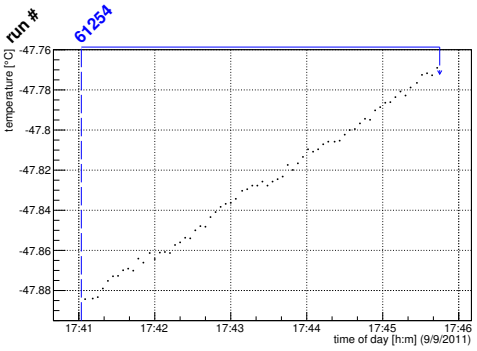

(a) Temperature vs time.

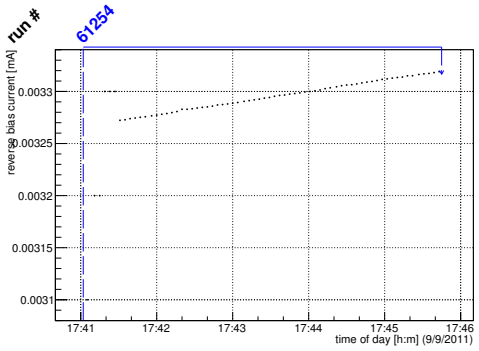

(b) Bias current vs time.

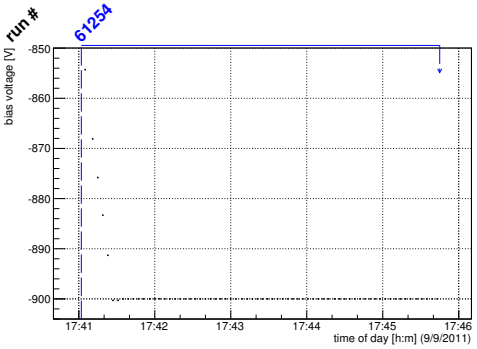

(c) Currently applied bias voltage vs time.

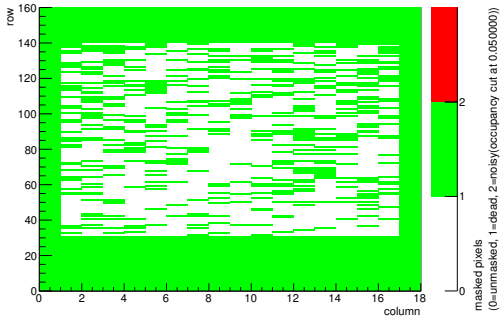

(d) Map of masked pixels.

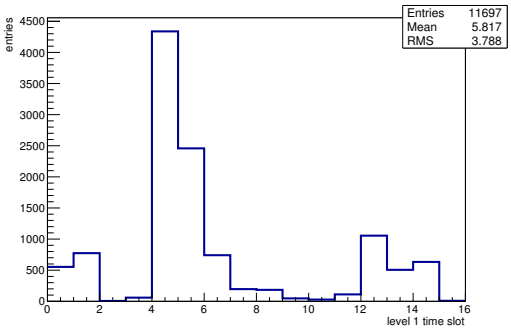

(e) Lvl1 distribution.

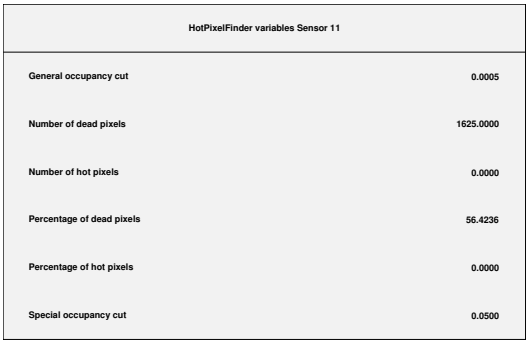

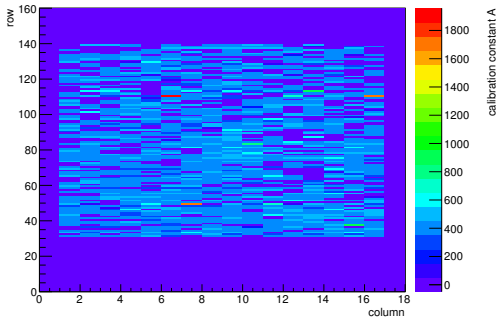

(f) Calibration constant A.

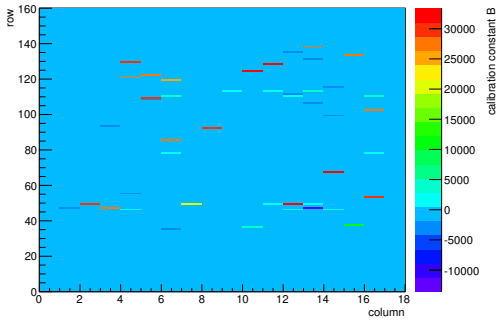

(g) Calibration constant B.

Figure C.72: Detailed plots for test beam measurement of DO-I-11 (description see section 6.1) sample (running as DUT1) during runs 61254 in the September 2011 test beam period at CERN SPS in area H6B. Summary of the data in chapter 9. *(cont.)*

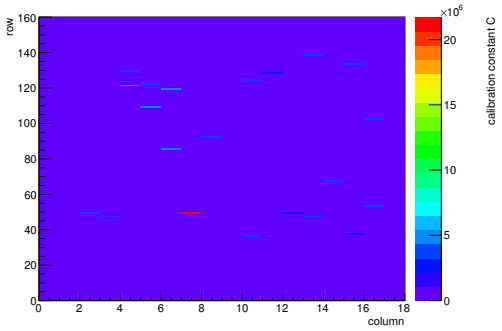

(h) Calibration constant C.

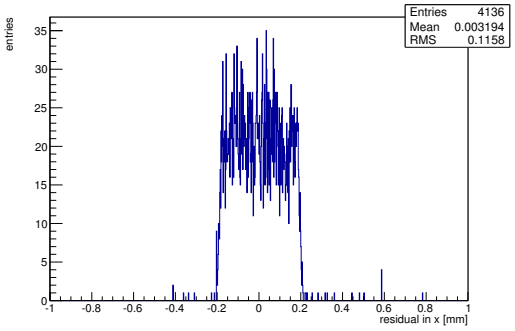

(i) Track residual in x.

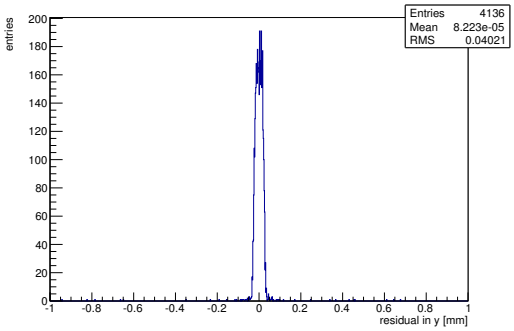

(j) Track residual in y.

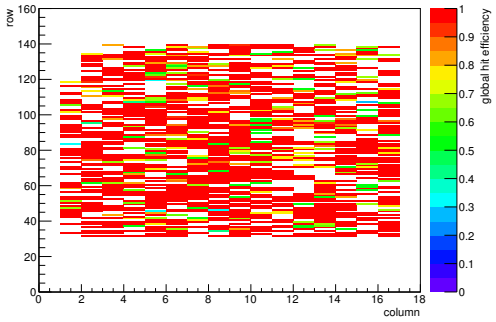

(k) Hit efficiency map.

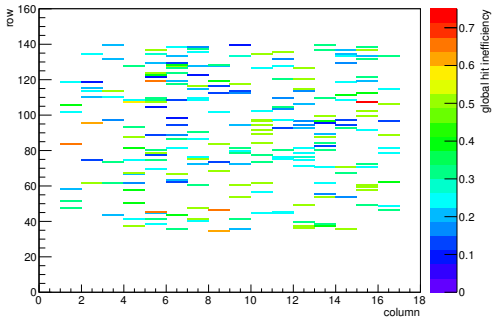

(l) Hit inefficiency map.

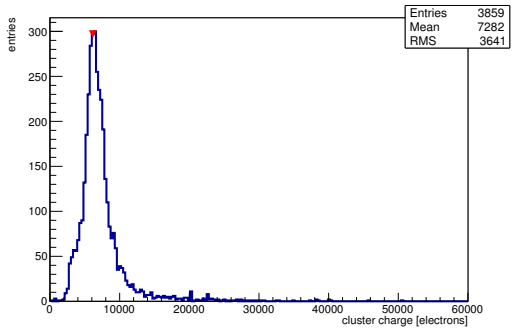

(m) Charge distribution (all cluster sizes included).

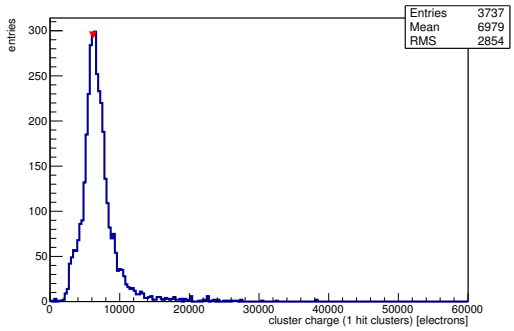

(n) Charge distribution (1 hit cluster).

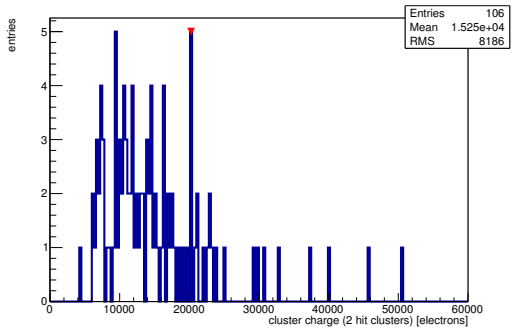

(o) Charge distribution (2 hit cluster).

Figure C.72: Detailed plots for test beam measurement of DO-I-11 (description see section 6.1) sample (running as DUT1) during runs 61254 in the September 2011 test beam period at CERN SPS in area H6B. Summary of the data in chapter 9. *(cont.)*

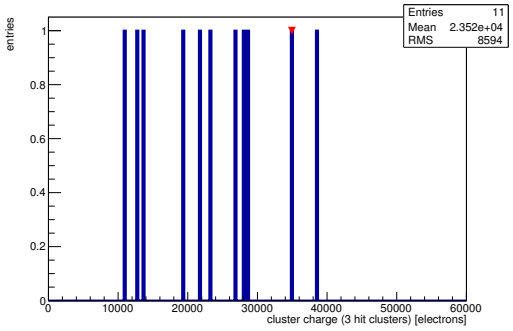

(p) Charge distribution (3 hit cluster).

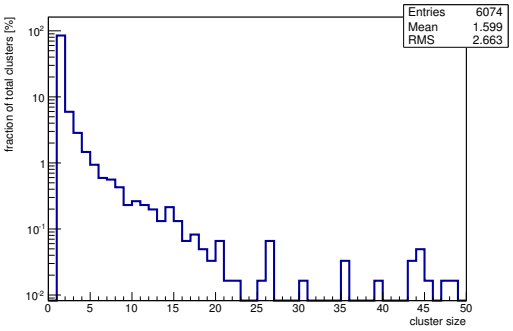

(q) Cluster size distribution.

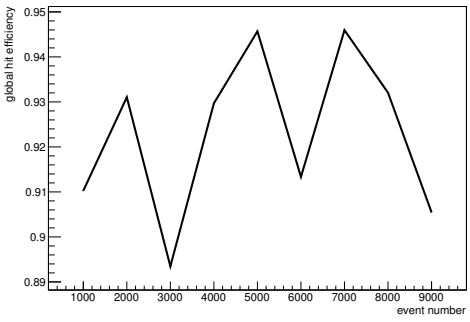

(r) Hit efficiency vs event number.

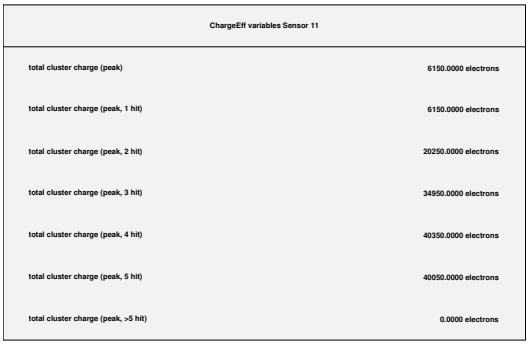

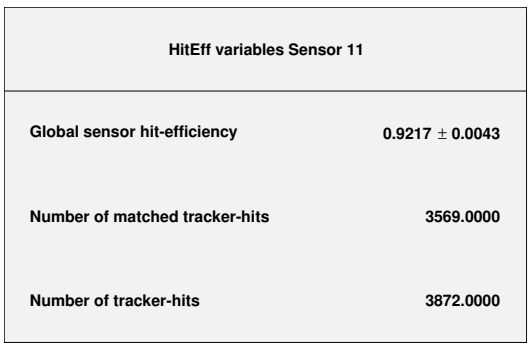

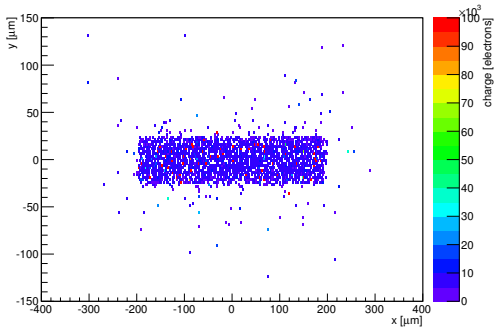

(s) Single pixel mean charge.

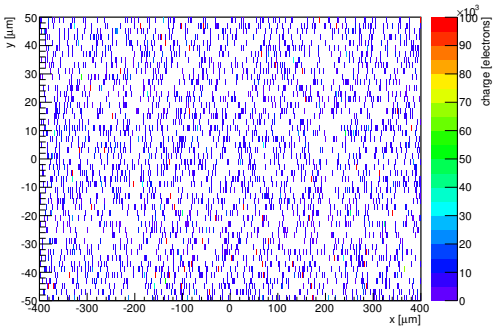

(t) Single pixel mean charge.

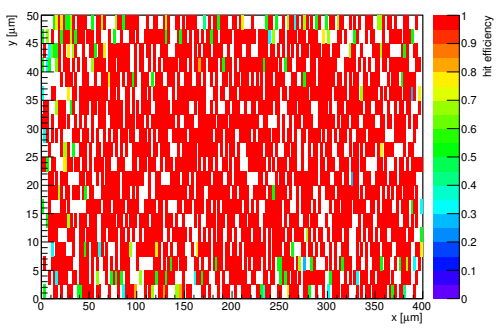

(u) Single pixel hit efficiency.

Figure C.72: Detailed plots for test beam measurement of DO-I-11 (description see section 6.1) sample (running as DUT1) during runs 61254 in the September 2011 test beam period at CERN SPS in area H6B. Summary of the data in chapter 9.

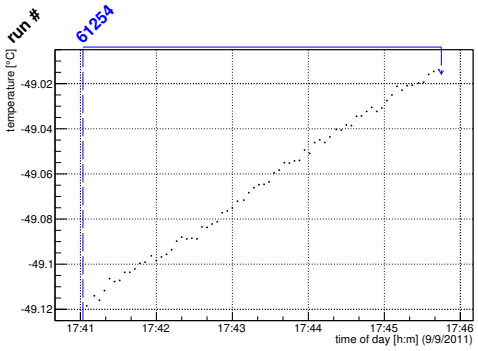

(a) Temperature vs time.

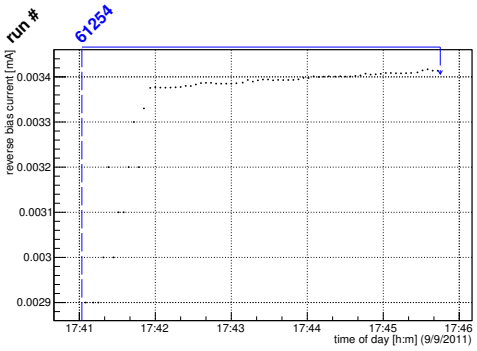

(b) Bias current vs time.

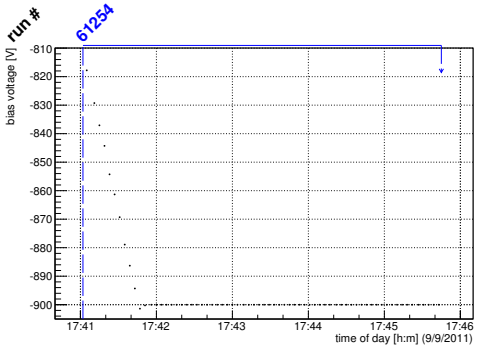

(c) Currently applied bias voltage vs time.

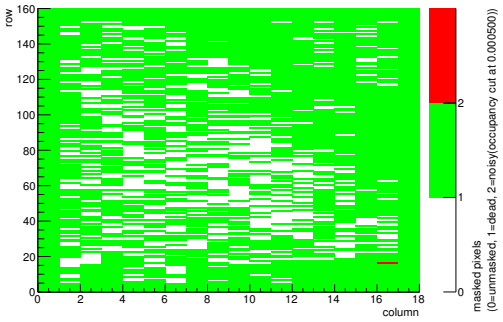

(d) Map of masked pixels.

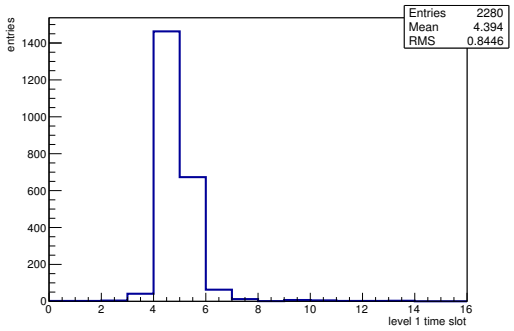

(e) Lvl1 distribution.

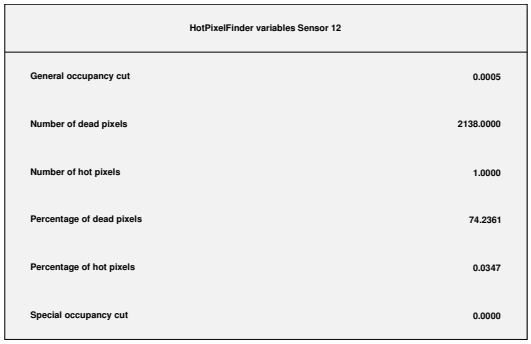

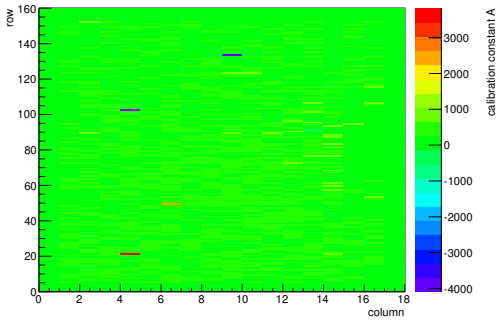

(f) Calibration constant A.

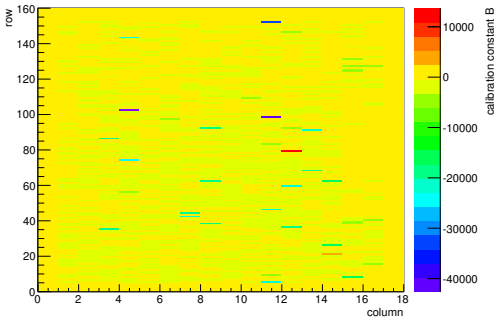

(g) Calibration constant B.

Figure C.73: Detailed plots for test beam measurement of DO-I-5 (description see section 6.1) sample (running as DUT2) during runs 61254 in the September 2011 test beam period at CERN SPS in area H6B. Summary of the data in chapter 9. *(cont.)*

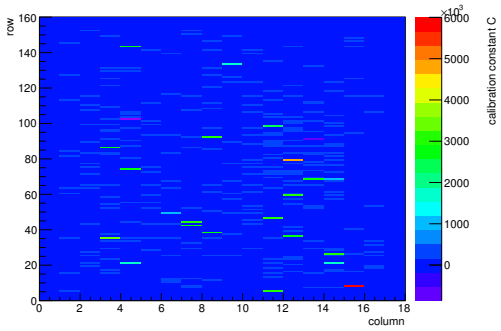

(h) Calibration constant C.

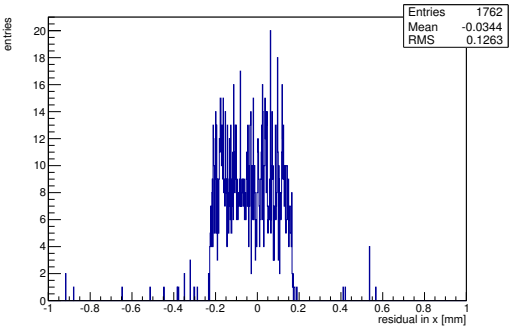

(i) Track residual in x.

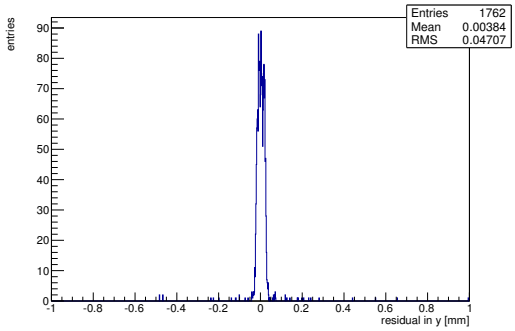

(j) Track residual in y.

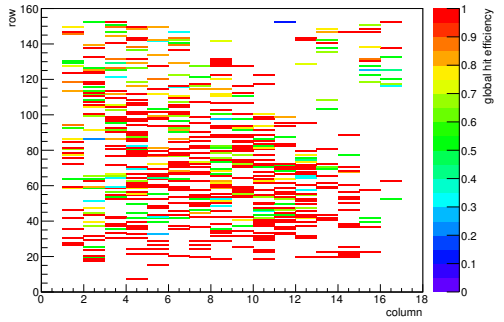

(k) Hit efficiency map.

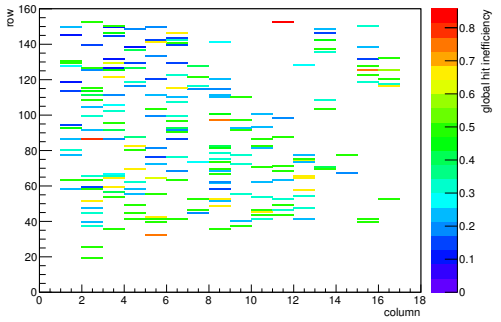

(l) Hit inefficiency map.

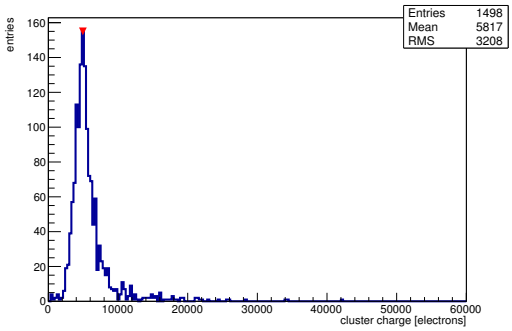

(m) Charge distribution (all cluster sizes included).

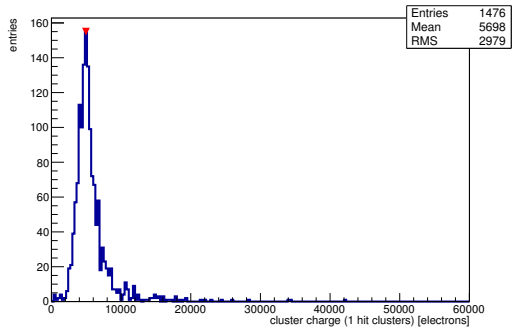

(n) Charge distribution (1 hit cluster).

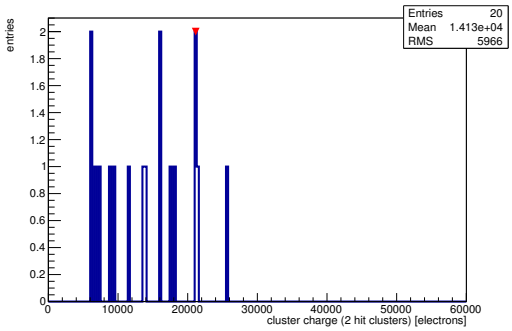

(o) Charge distribution (2 hit cluster).

Figure C.73: Detailed plots for test beam measurement of DO-I-5 (description see section 6.1) sample (running as DUT2) during runs 61254 in the September 2011 test beam period at CERN SPS in area H6B. Summary of the data in chapter 9. *(cont.)*

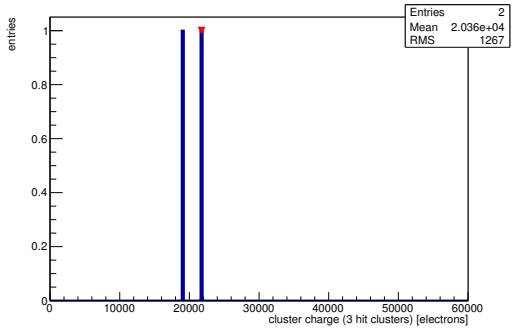

(p) Charge distribution (3 hit cluster).

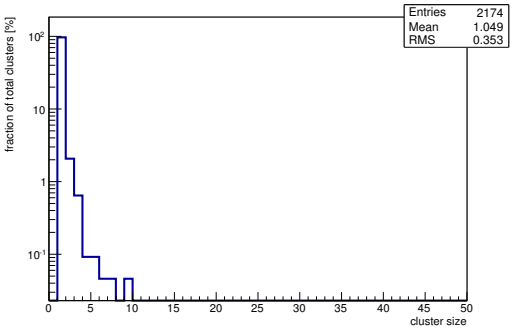

(q) Cluster size distribution.

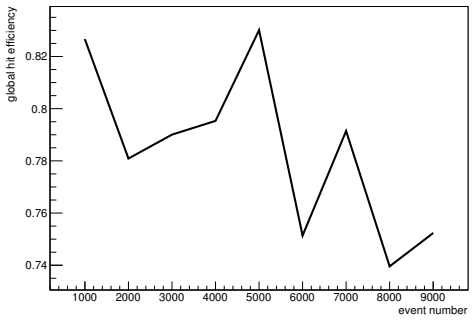

(r) Hit efficiency vs event number.

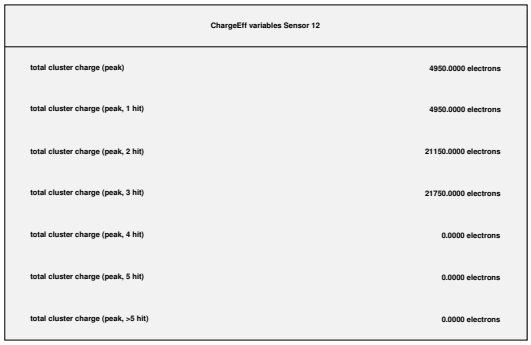

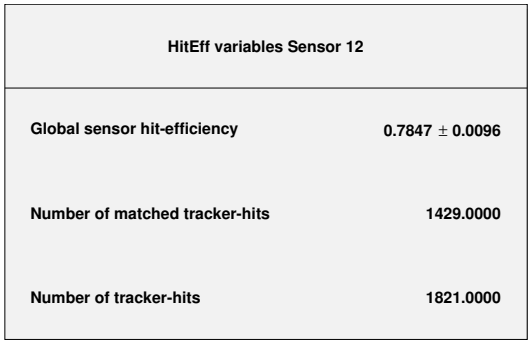

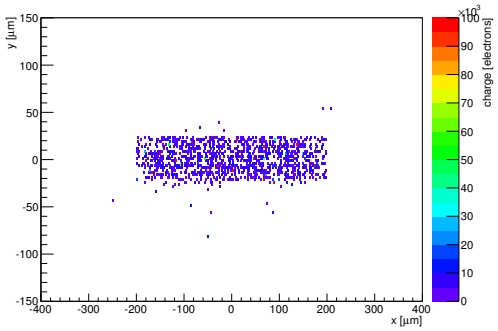

(s) Single pixel mean charge.

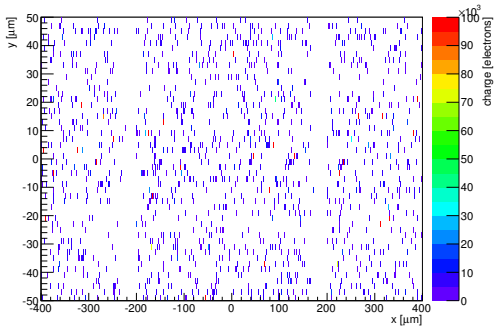

(t) Single pixel mean charge.

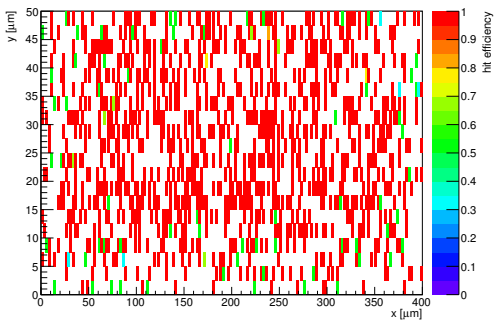

(u) Single pixel hit efficiency.

Figure C.73: Detailed plots for test beam measurement of DO-I-5 (description see section 6.1) sample (running as DUT2) during runs 61254 in the September 2011 test beam period at CERN SPS in area H6B. Summary of the data in chapter 9.

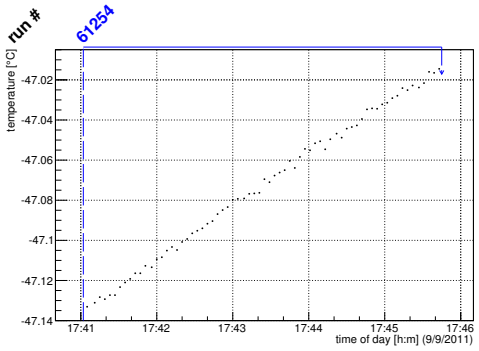

(a) Temperature vs time.

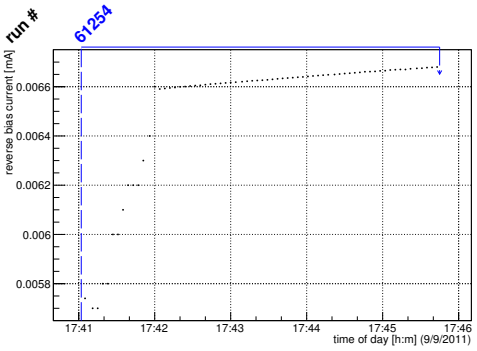

(b) Bias current vs time.

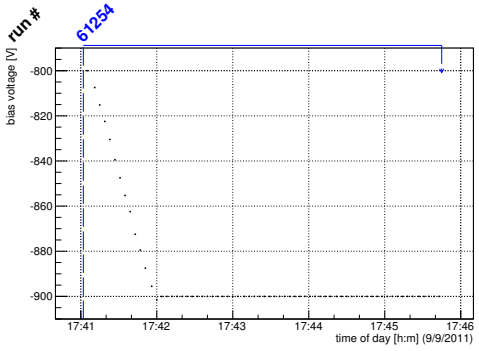

(c) Currently applied bias voltage vs time.

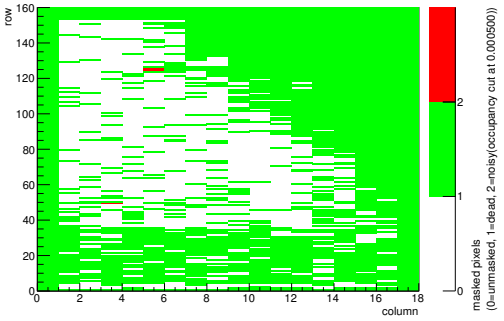

(d) Map of masked pixels.

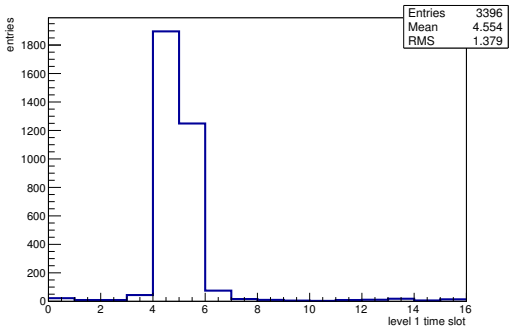

(e) Lvl1 distribution.

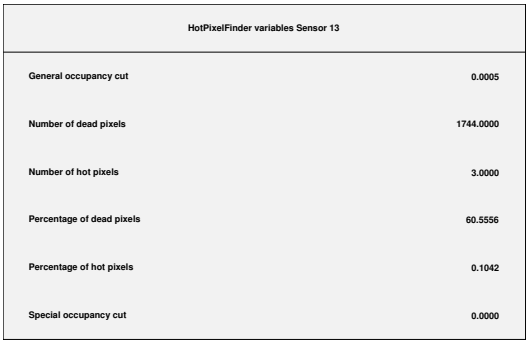

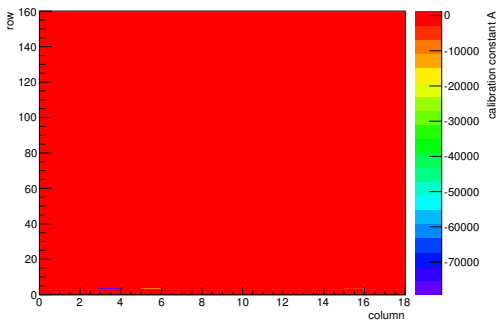

(f) Calibration constant A.

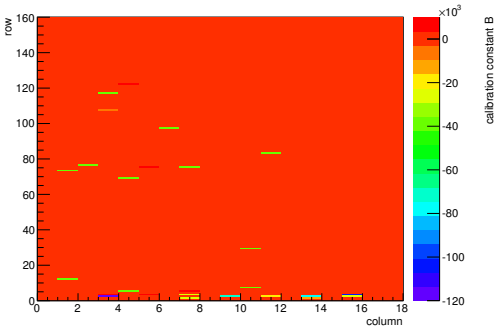

(g) Calibration constant B.

Figure C.74: Detailed plots for test beam measurement of DO-I-12 (description see section 6.1) sample (running as DUT3) during runs 61254 in the September 2011 test beam period at CERN SPS in area H6B. Summary of the data in chapter 9. *(cont.)*

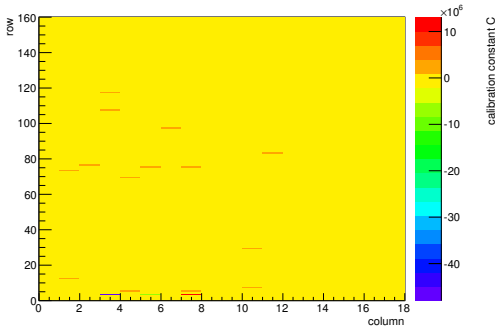

(h) Calibration constant C.

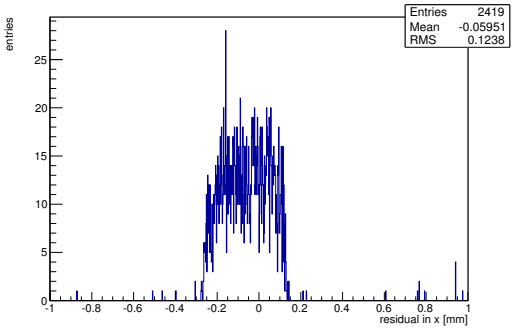

(i) Track residual in x.

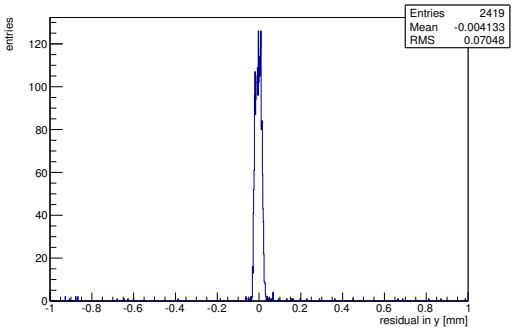

(j) Track residual in y.

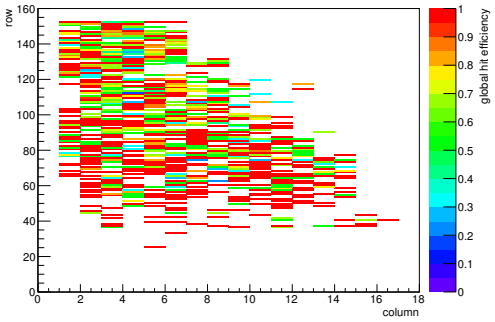

(k) Hit efficiency map.

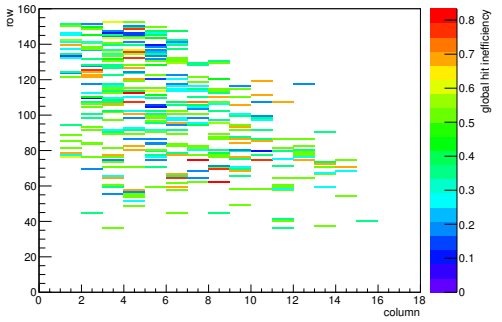

(l) Hit inefficiency map.

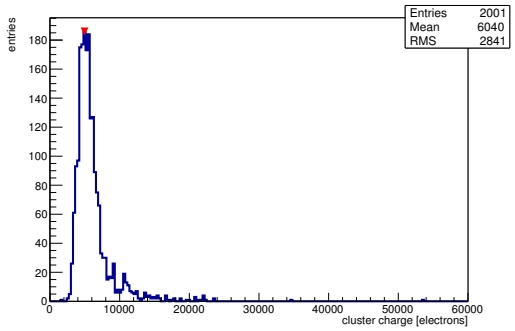

(m) Charge distribution (all cluster sizes included).

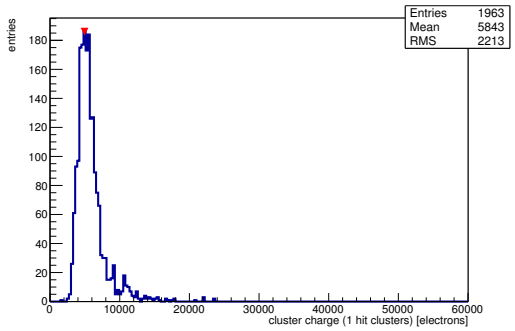

(n) Charge distribution (1 hit cluster).

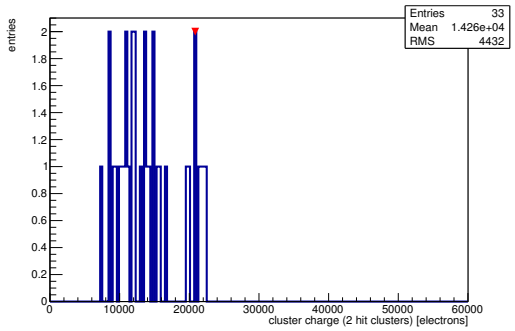

(o) Charge distribution (2 hit cluster).

Figure C.74: Detailed plots for test beam measurement of DO-I-12 (description see section 6.1) sample (running as DUT3) during runs 61254 in the September 2011 test beam period at CERN SPS in area H6B. Summary of the data in chapter 9. *(cont.)*

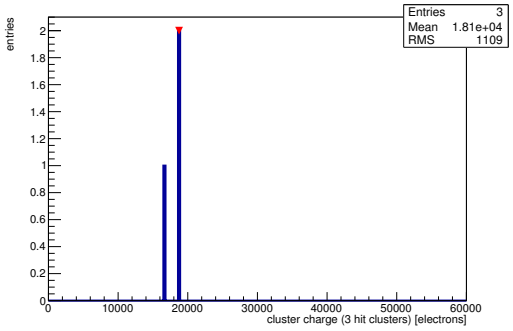

(p) Charge distribution (3 hit cluster).

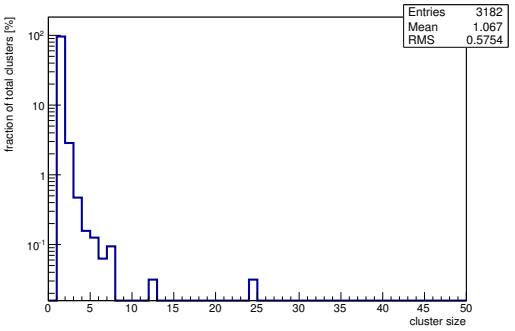

(q) Cluster size distribution.

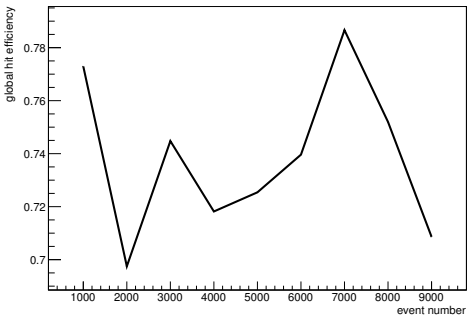

(r) Hit efficiency vs event number.

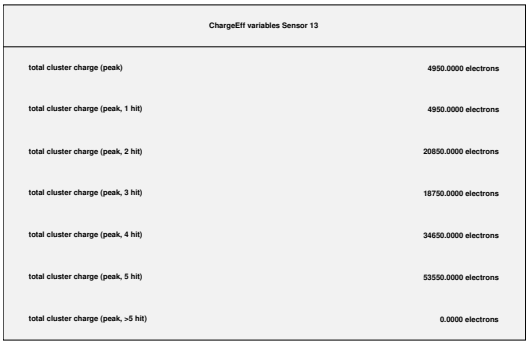

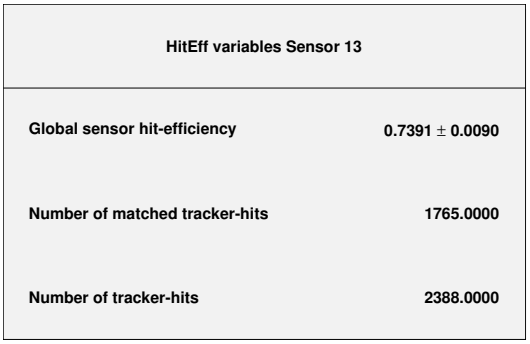

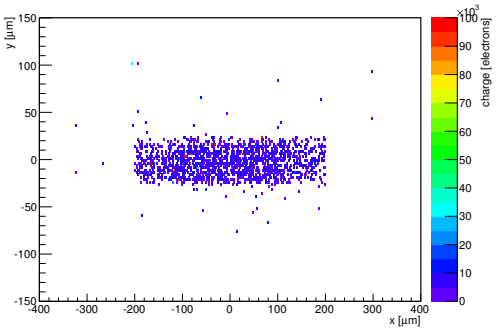

(s) Single pixel mean charge.

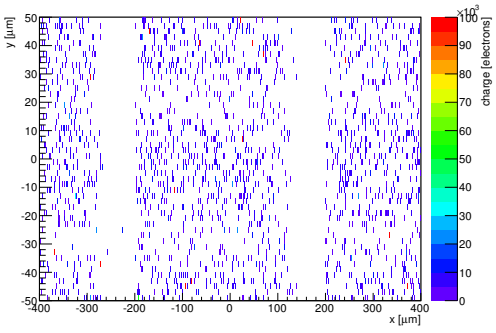

(t) Single pixel mean charge.

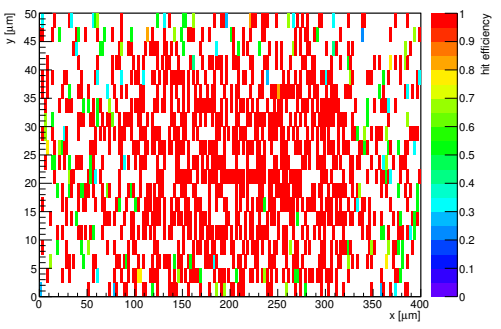

(u) Single pixel hit efficiency.

Figure C.74: Detailed plots for test beam measurement of DO-I-12 (description see section 6.1) sample (running as DUT3) during runs 61254 in the September 2011 test beam period at CERN SPS in area H6B. Summary of the data in chapter 9.

C.3.9 Run 61255

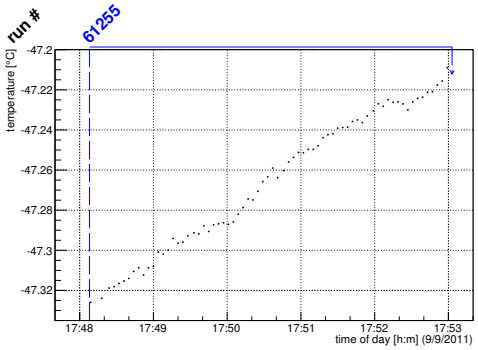

(a) Temperature vs time.

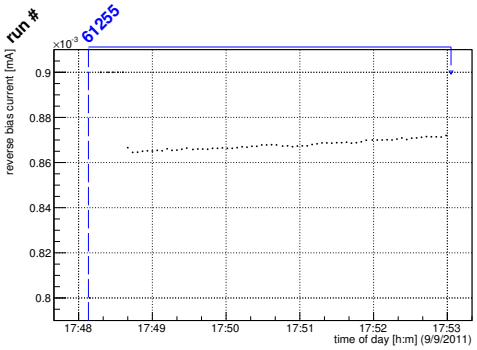

(b) Bias current vs time.

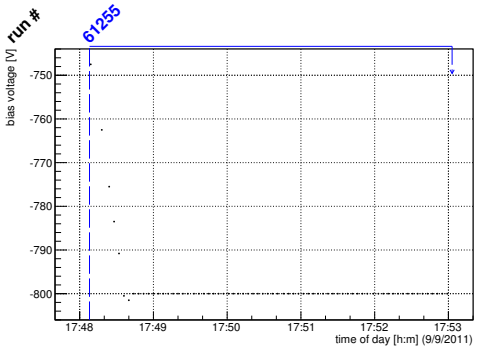

(c) Currently applied bias voltage vs time.

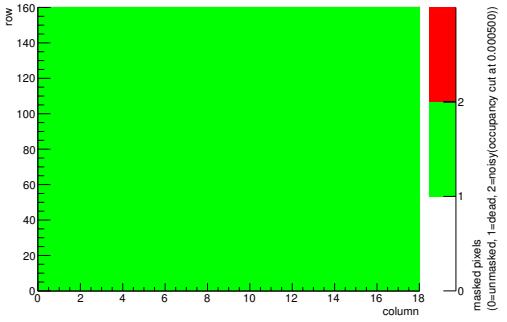

(d) Map of masked pixels.

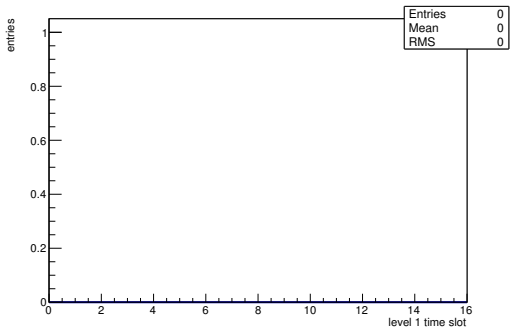

(e) Lvl1 distribution.

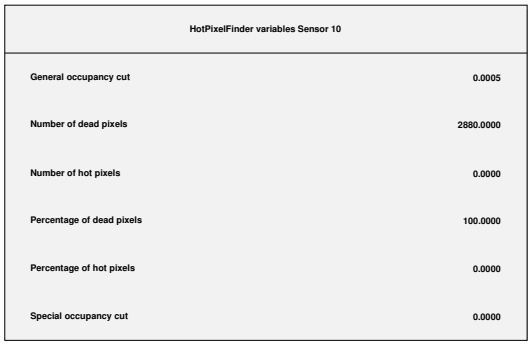

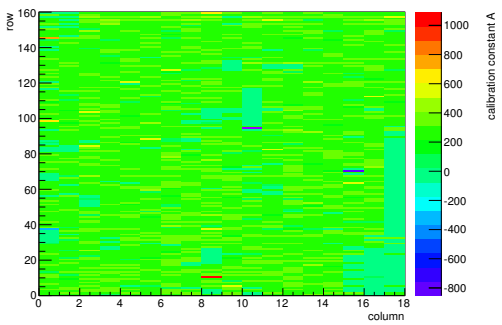

(f) Calibration constant A.

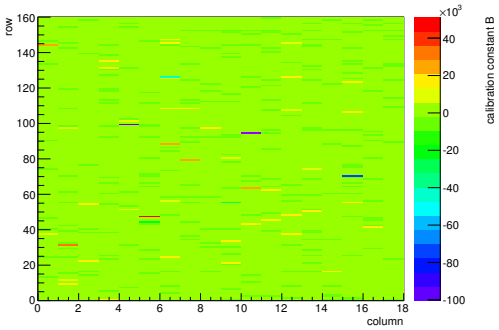

(g) Calibration constant B.

Figure C.75: Detailed plots for test beam measurement of DO-I-7 (description see section 6.1) sample (running as DUT0) during runs 61255 in the September 2011 test beam period at CERN SPS in area H6B. Summary of the data in chapter 9. *(cont.)*

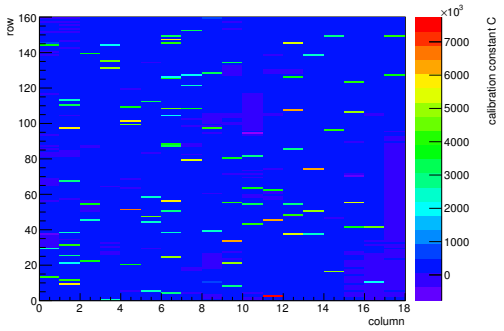

(h) Calibration constant C.

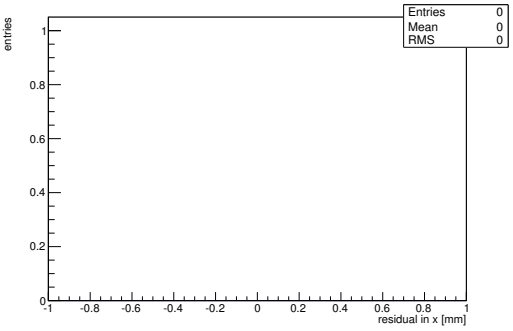

(i) Track residual in x.

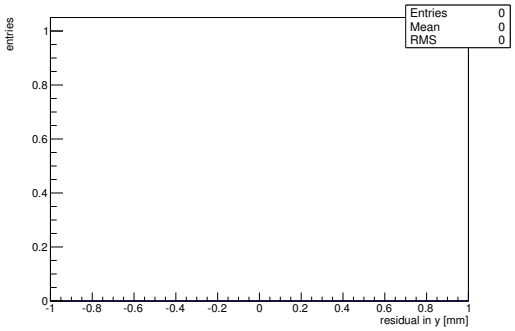

(j) Track residual in y.

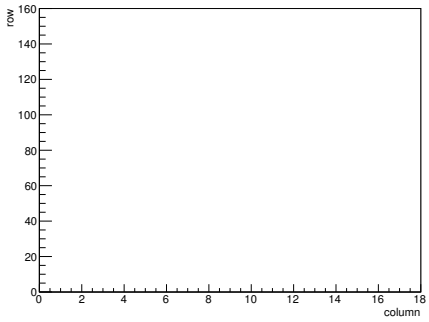

(k) Hit efficiency map.

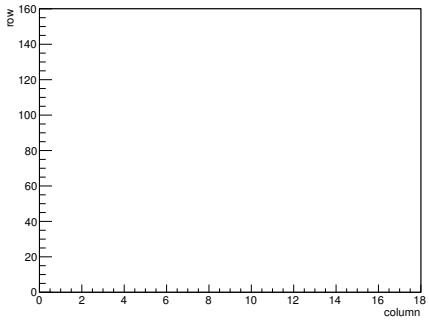

(l) Hit inefficiency map.

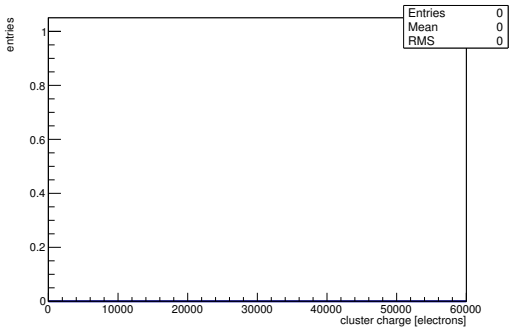

(m) Charge distribution (all cluster sizes included).

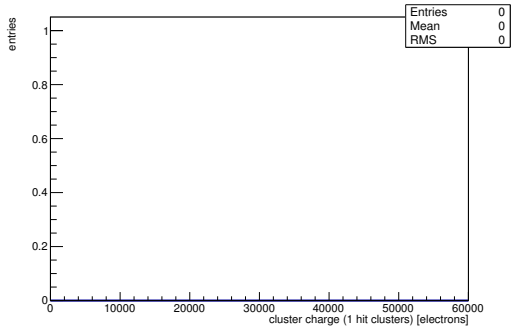

(n) Charge distribution (1 hit cluster).

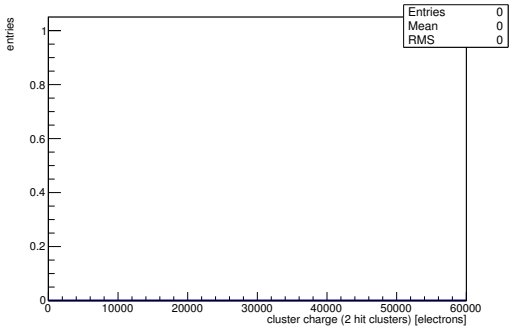

(o) Charge distribution (2 hit cluster).

Figure C.75: Detailed plots for test beam measurement of DO-I-7 (description see section 6.1) sample (running as DUT0) during runs 61255 in the September 2011 test beam period at CERN SPS in area H6B. Summary of the data in chapter 9. *(cont.)*

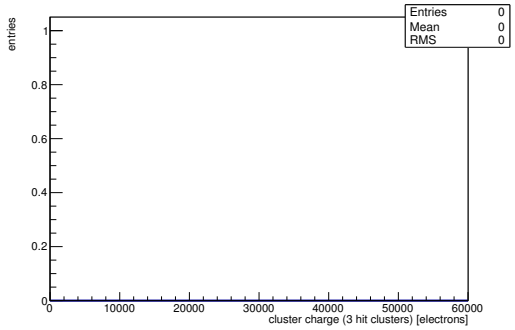

(p) Charge distribution (3 hit cluster).

(q) Cluster size distribution.

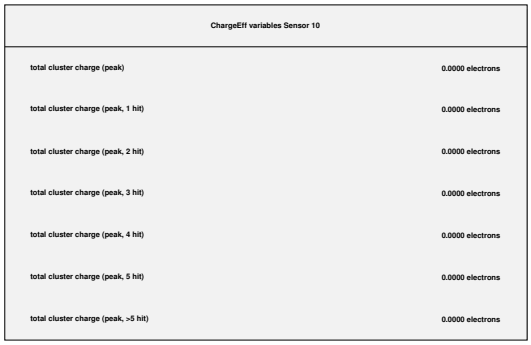

(r) Hit efficiency vs event number.

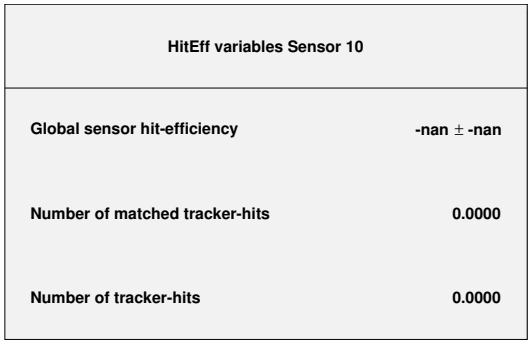

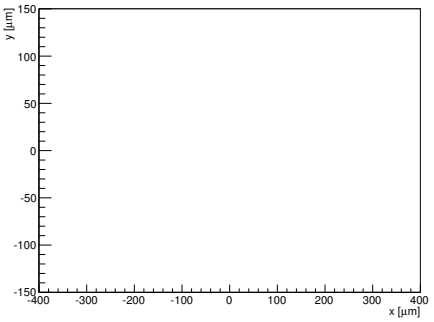

(s) Single pixel mean charge.

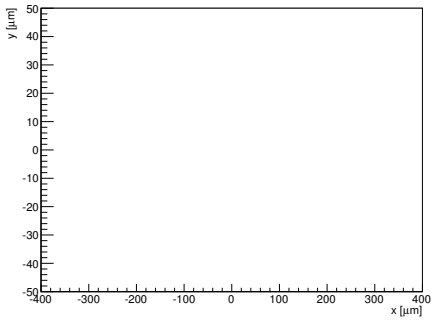

(t) Single pixel mean charge.

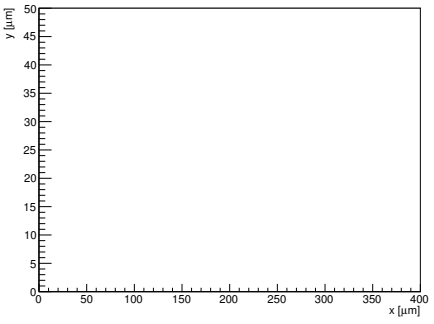

(u) Single pixel hit efficiency.

Figure C.75: Detailed plots for test beam measurement of DO-I-7 (description see section 6.1) sample (running as DUT0) during runs 61255 in the September 2011 test beam period at CERN SPS in area H6B. Summary of the data in chapter 9.

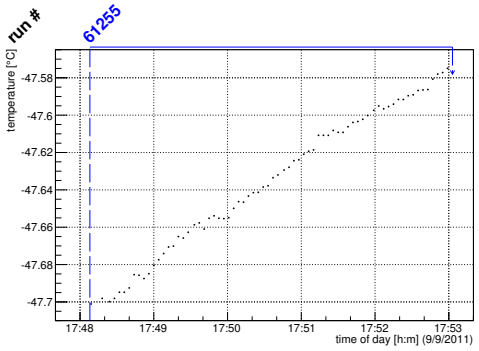

(a) Temperature vs time.

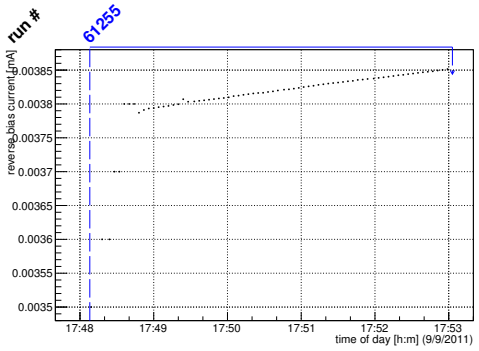

(b) Bias current vs time.

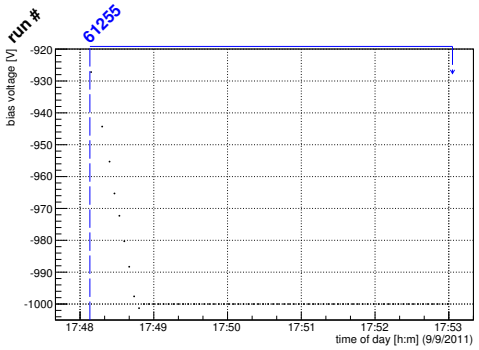

(c) Currently applied bias voltage vs time.

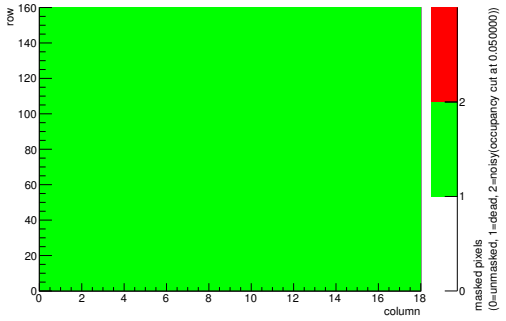

(d) Map of masked pixels.

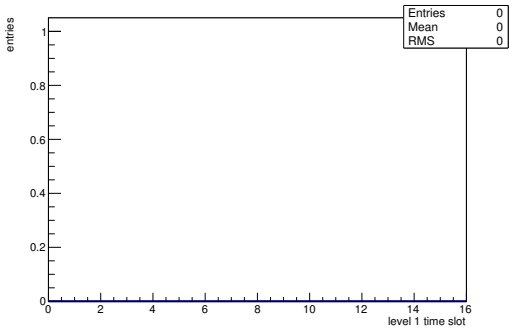

(e) Lvl1 distribution.

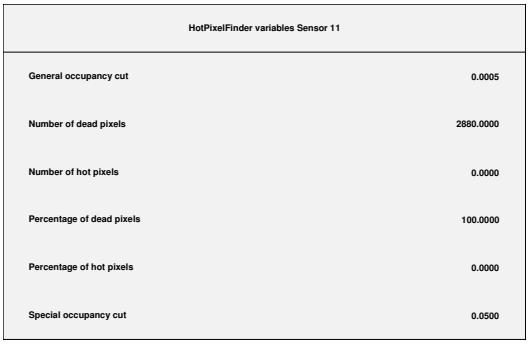

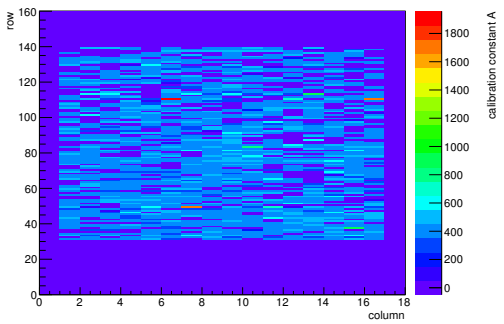

(f) Calibration constant A.

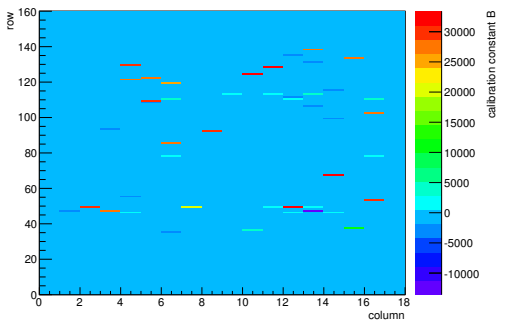

(g) Calibration constant B.

Figure C.76: Detailed plots for test beam measurement of DO-I-11 (description see section 6.1) sample (running as DUT1) during runs 61255 in the September 2011 test beam period at CERN SPS in area H6B. Summary of the data in chapter 9. *(cont.)*

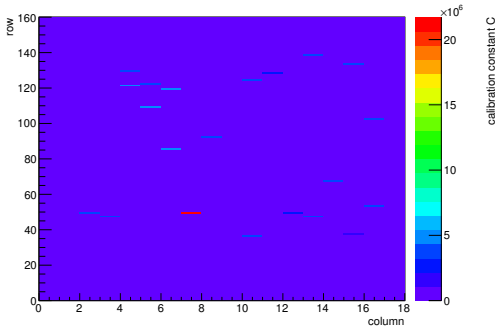

(h) Calibration constant C.

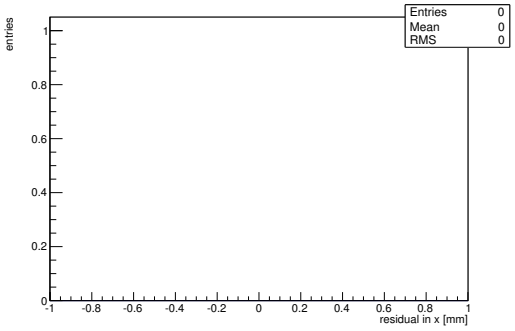

(i) Track residual in x.

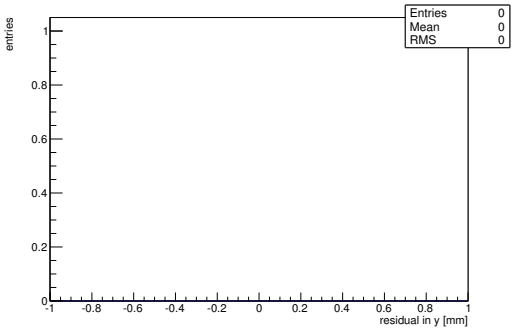

(j) Track residual in y.

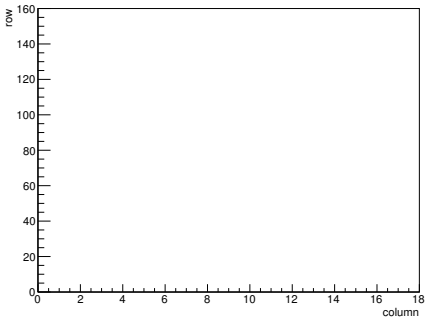

(k) Hit efficiency map.

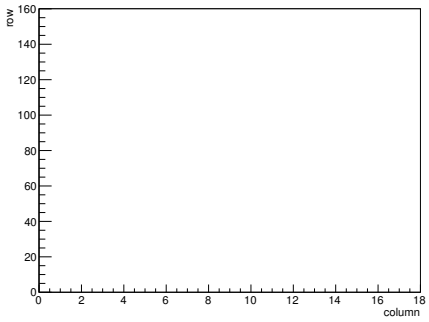

(l) Hit inefficiency map.

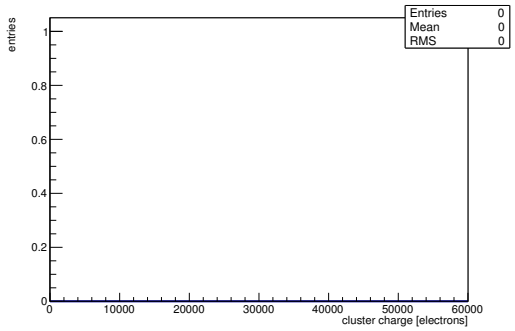

(m) Charge distribution (all cluster sizes included).

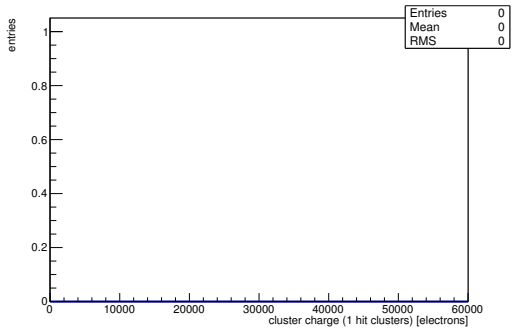

(n) Charge distribution (1 hit cluster).

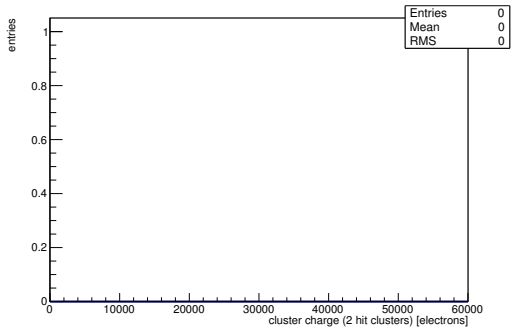

(o) Charge distribution (2 hit cluster).

Figure C.76: Detailed plots for test beam measurement of DO-I-11 (description see section 6.1) sample (running as DUT1) during runs 61255 in the September 2011 test beam period at CERN SPS in area H6B. Summary of the data in chapter 9. *(cont.)*

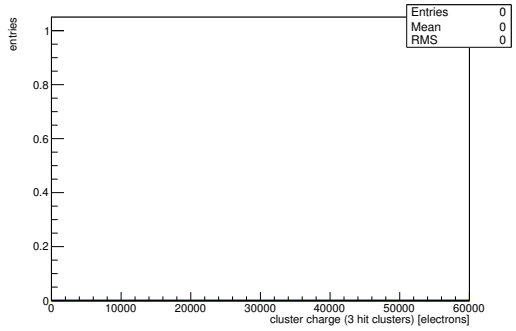

(p) Charge distribution (3 hit cluster).

(q) Cluster size distribution.

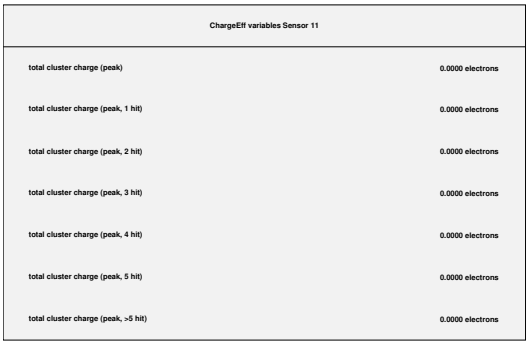

(r) Hit efficiency vs event number.

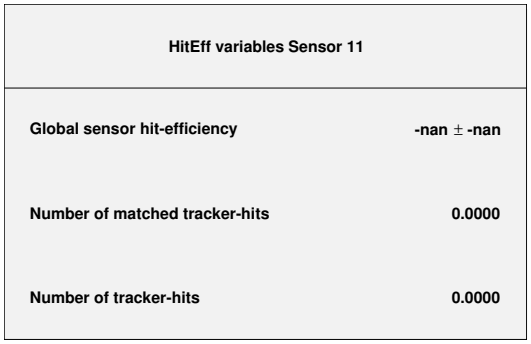

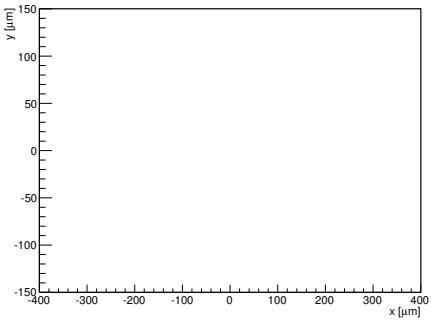

(s) Single pixel mean charge.

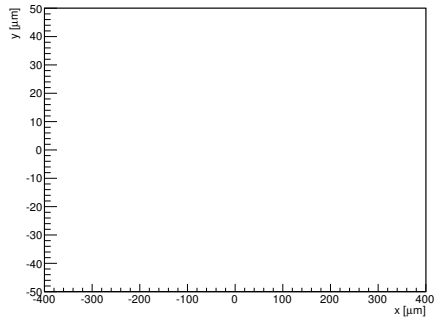

(t) Single pixel mean charge.

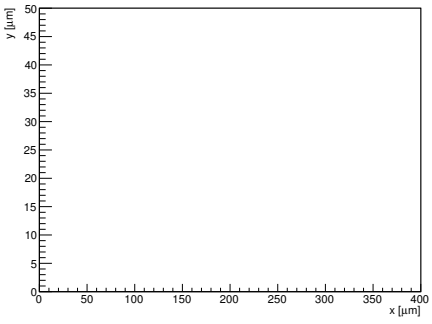

(u) Single pixel hit efficiency.

Figure C.76: Detailed plots for test beam measurement of DO-I-11 (description see section 6.1) sample (running as DUT1) during runs 61255 in the September 2011 test beam period at CERN SPS in area H6B. Summary of the data in chapter 9.

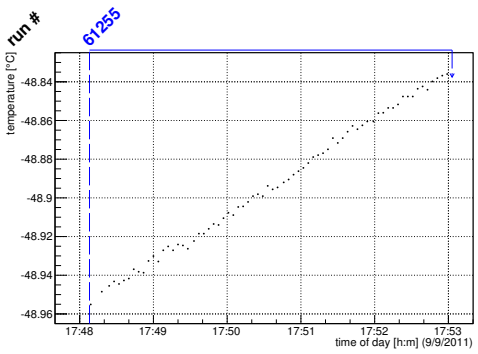

(a) Temperature vs time.

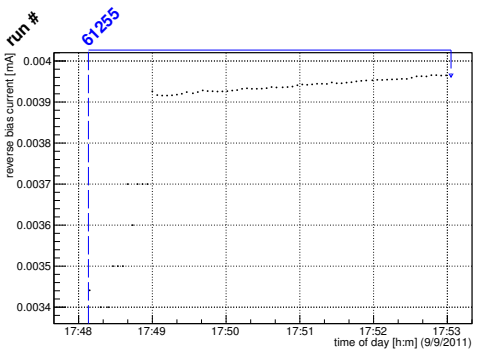

(b) Bias current vs time.

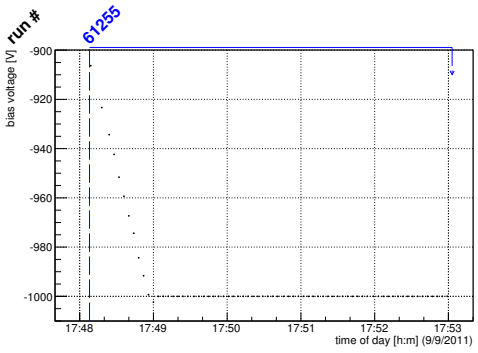

(c) Currently applied bias voltage vs time.

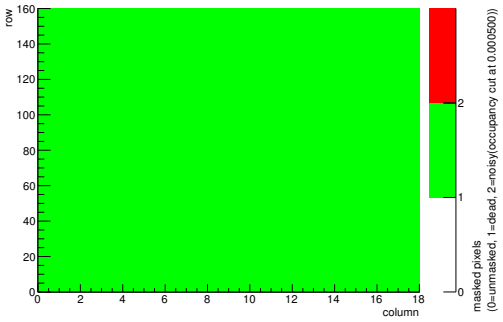

(d) Map of masked pixels.

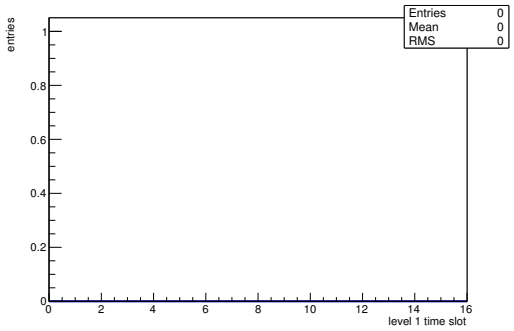

(e) Lvl1 distribution.

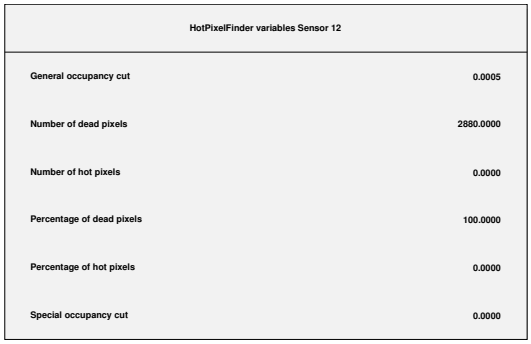

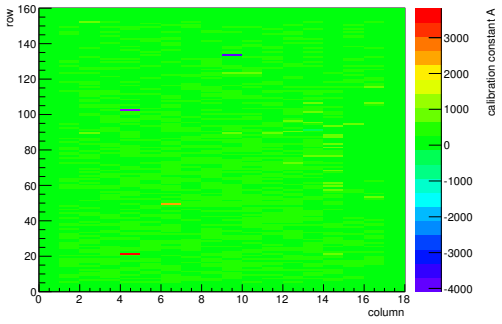

(f) Calibration constant A.

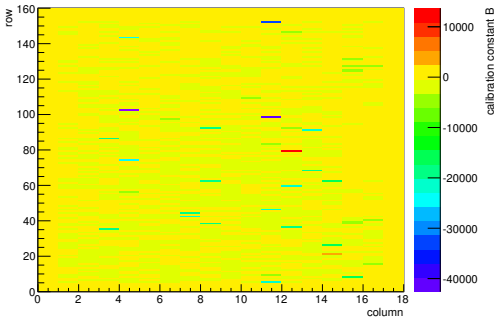

(g) Calibration constant B.

Figure C.77: Detailed plots for test beam measurement of DO-I-5 (description see section 6.1) sample (running as DUT2) during runs 61255 in the September 2011 test beam period at CERN SPS in area H6B. Summary of the data in chapter 9. *(cont.)*

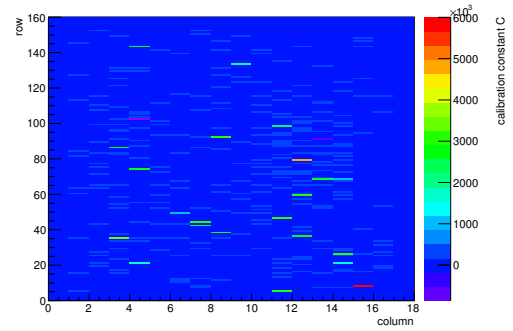

(h) Calibration constant C.

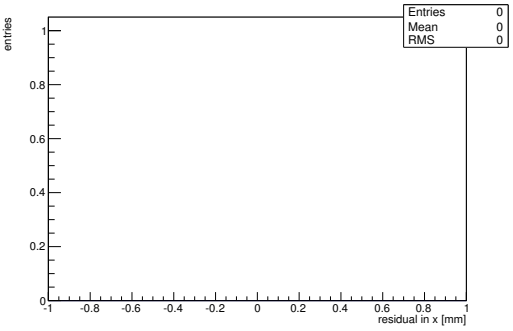

(i) Track residual in x.

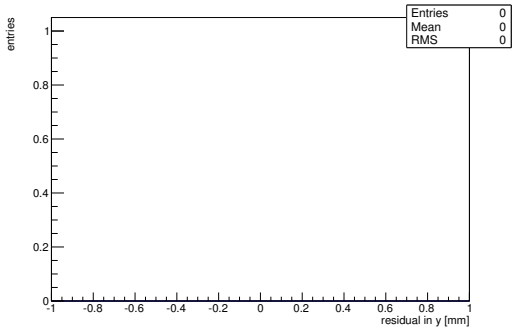

(j) Track residual in y.

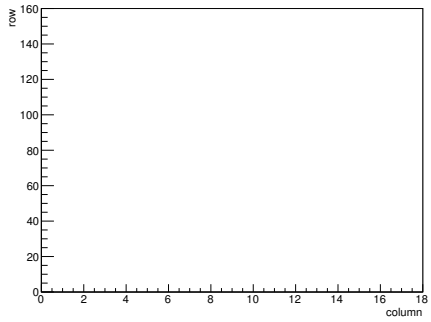

(k) Hit efficiency map.

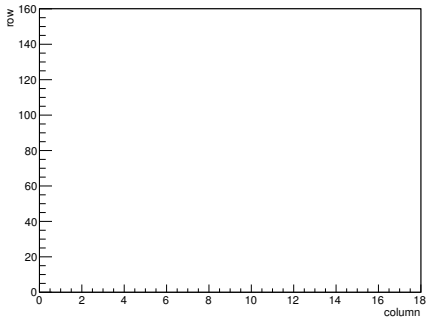

(l) Hit inefficiency map.

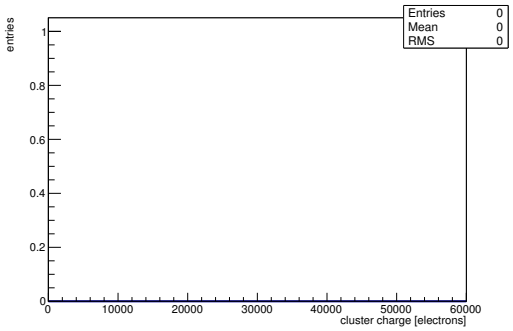

(m) Charge distribution (all cluster sizes included).

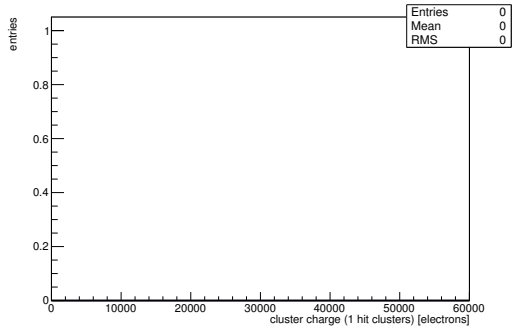

(n) Charge distribution (1 hit cluster).

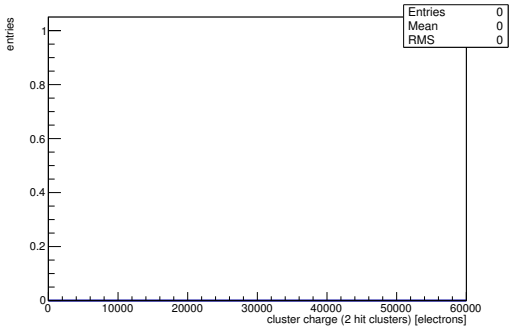

(o) Charge distribution (2 hit cluster).

Figure C.77: Detailed plots for test beam measurement of DO-I-5 (description see section 6.1) sample (running as DUT2) during runs 61255 in the September 2011 test beam period at CERN SPS in area H6B. Summary of the data in chapter 9. *(cont.)*

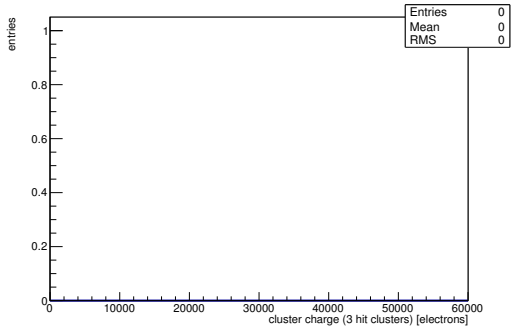

(p) Charge distribution (3 hit cluster).

(q) Cluster size distribution.

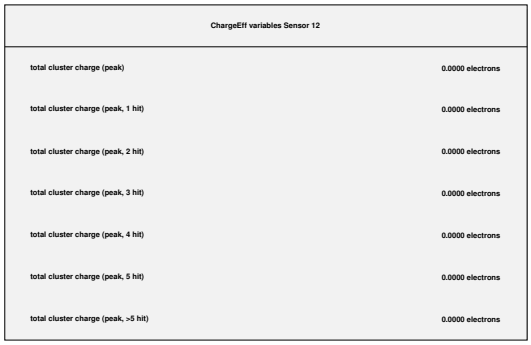

(r) Hit efficiency vs event number.

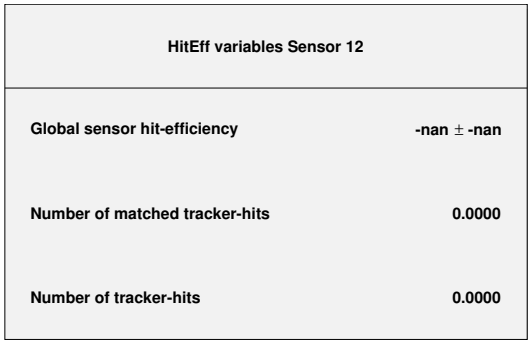

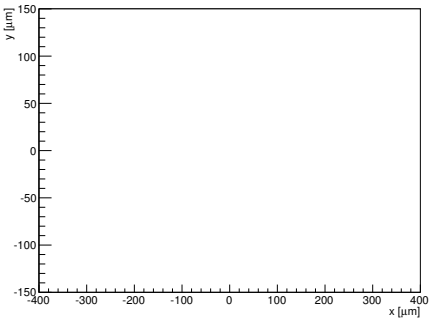

(s) Single pixel mean charge.

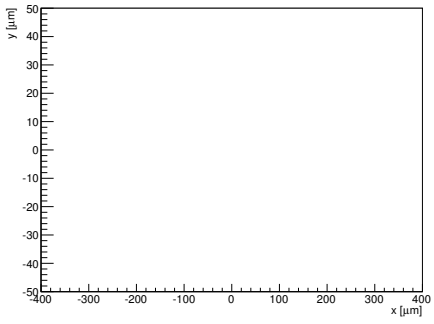

(t) Single pixel mean charge.

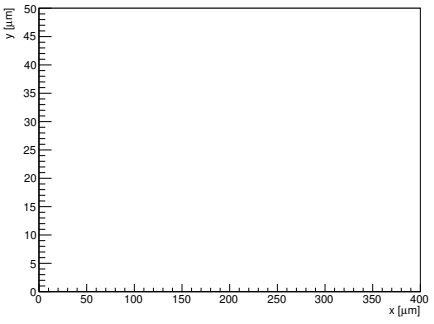

(u) Single pixel hit efficiency.

Figure C.77: Detailed plots for test beam measurement of DO-I-5 (description see section 6.1) sample (running as DUT2) during runs 61255 in the September 2011 test beam period at CERN SPS in area H6B. Summary of the data in chapter 9.

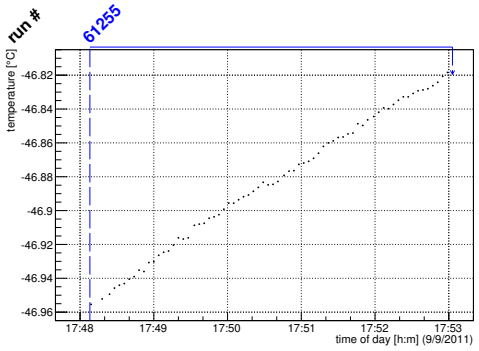

(a) Temperature vs time.

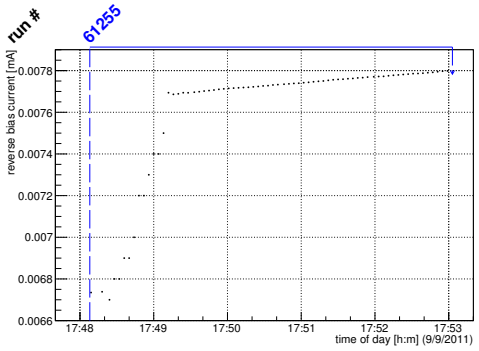

(b) Bias current vs time.

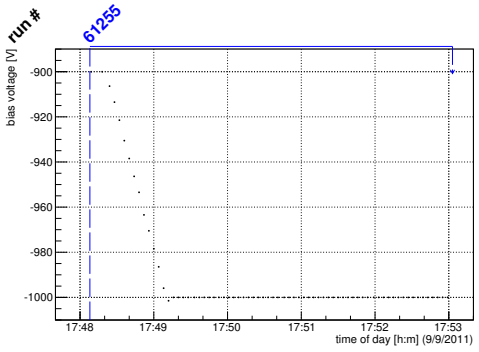

(c) Currently applied bias voltage vs time.

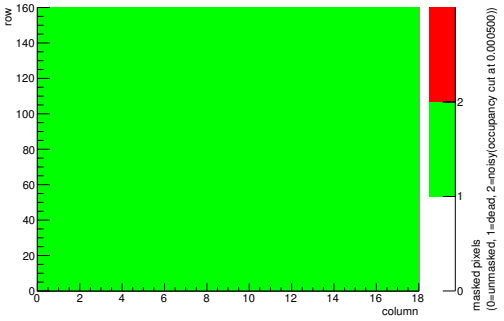

(d) Map of masked pixels.

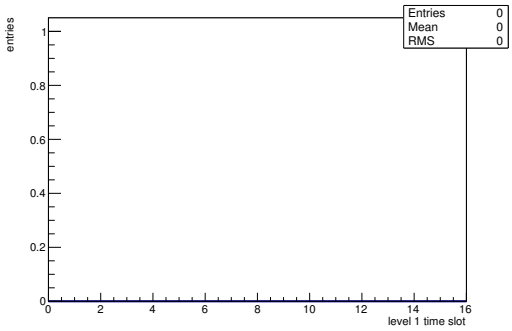

(e) Lvl1 distribution.

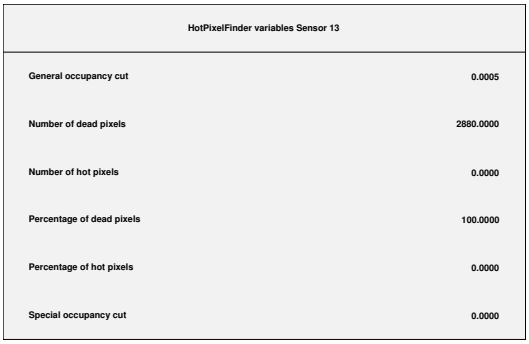

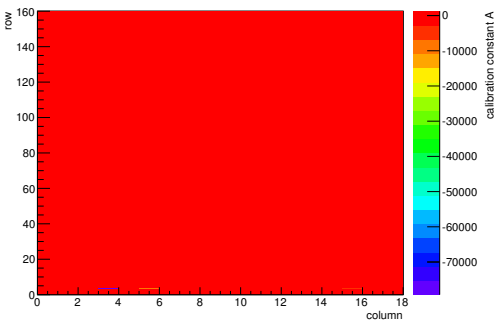

(f) Calibration constant A.

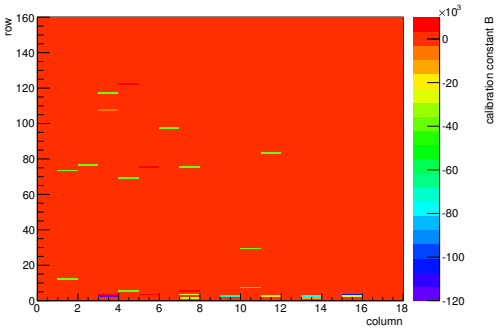

(g) Calibration constant B.

Figure C.78: Detailed plots for test beam measurement of DO-I-12 (description see section 6.1) sample (running as DUT3) during runs 61255 in the September 2011 test beam period at CERN SPS in area H6B. Summary of the data in chapter 9. *(cont.)*

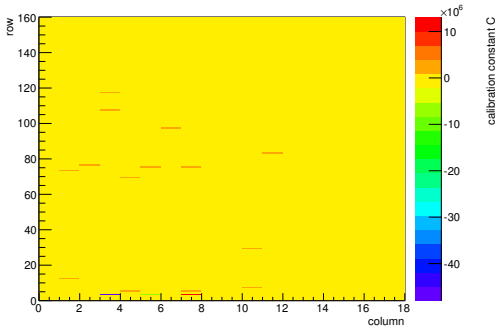

(h) Calibration constant C.

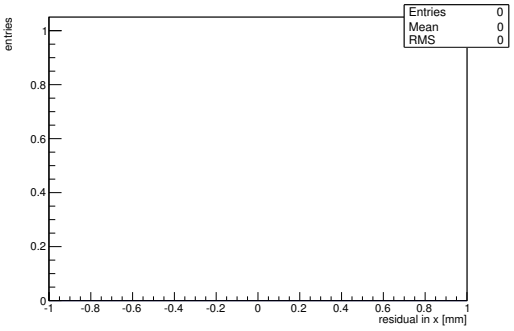

(i) Track residual in x.

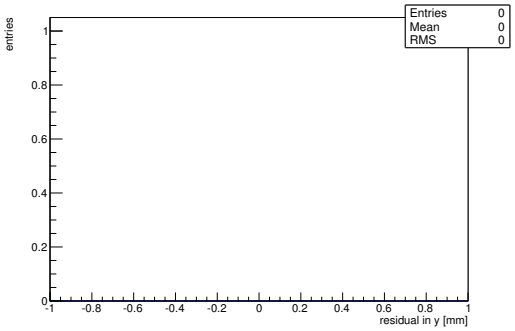

(j) Track residual in y.

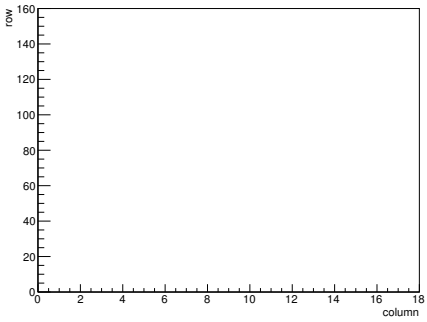

(k) Hit efficiency map.

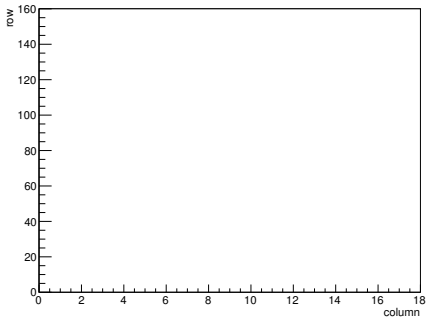

(l) Hit inefficiency map.

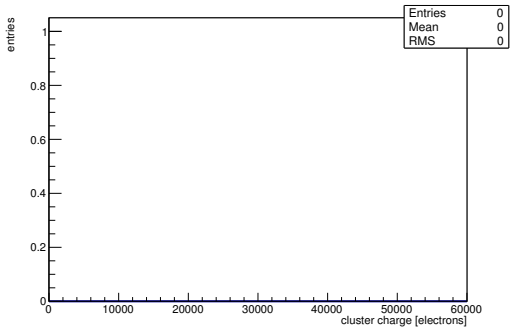

(m) Charge distribution (all cluster sizes included).

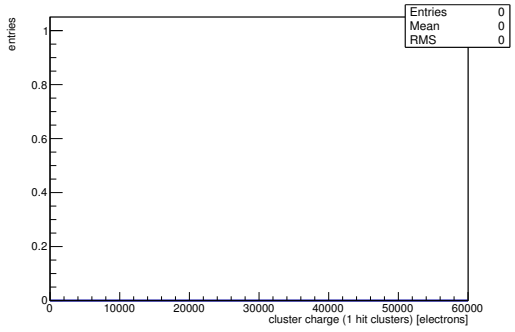

(n) Charge distribution (1 hit cluster).

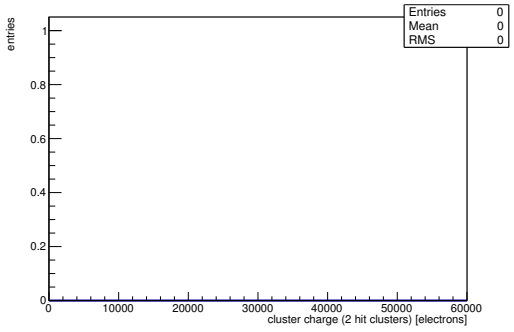

(o) Charge distribution (2 hit cluster).

Figure C.78: Detailed plots for test beam measurement of DO-I-12 (description see section 6.1) sample (running as DUT3) during runs 61255 in the September 2011 test beam period at CERN SPS in area H6B. Summary of the data in chapter 9. *(cont.)*

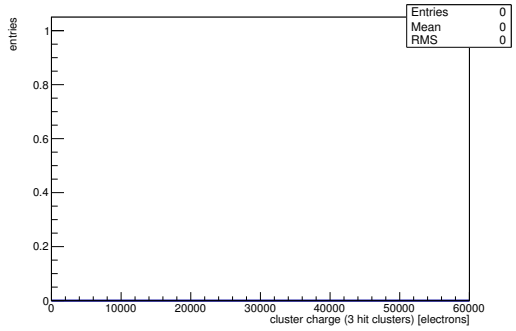

(p) Charge distribution (3 hit cluster).

(q) Cluster size distribution.

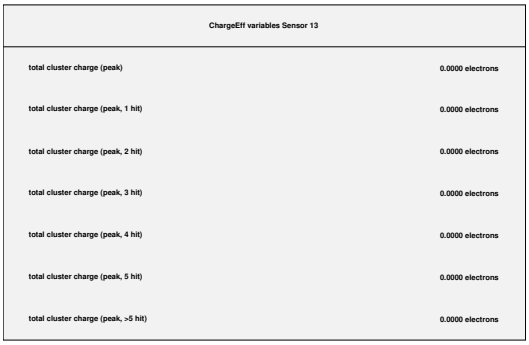

(r) Hit efficiency vs event number.

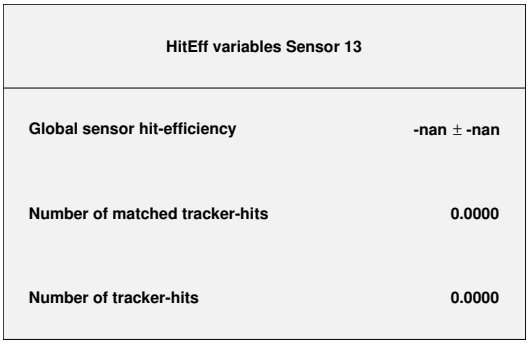

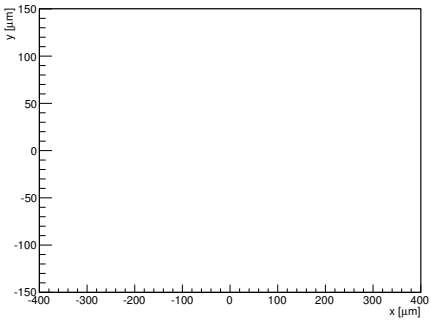

(s) Single pixel mean charge.

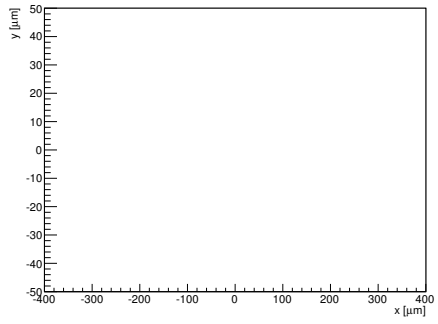

(t) Single pixel mean charge.

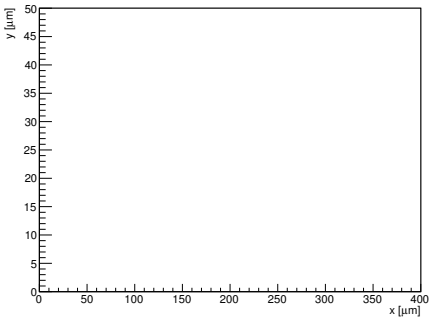

(u) Single pixel hit efficiency.

Figure C.78: Detailed plots for test beam measurement of DO-I-12 (description see section 6.1) sample (running as DUT3) during runs 61255 in the September 2011 test beam period at CERN SPS in area H6B. Summary of the data in chapter 9.

C.3.10 Run 61256

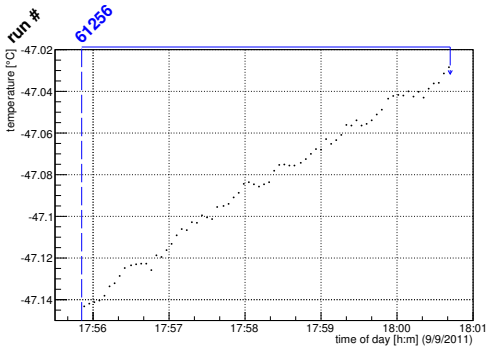

(a) Temperature vs time.

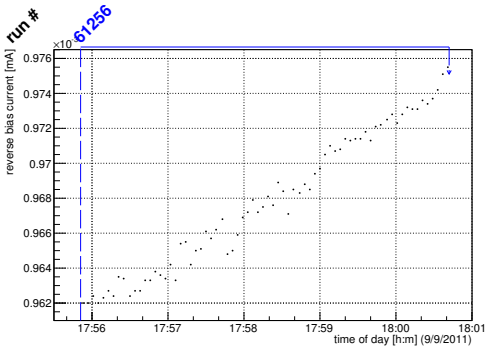

(b) Bias current vs time.

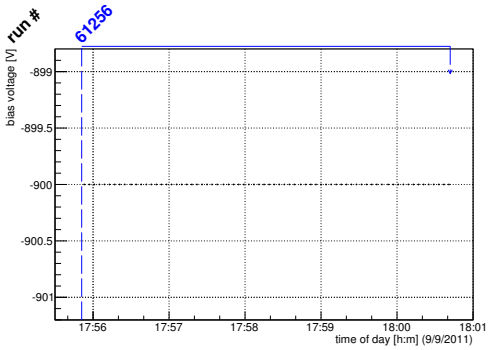

(c) Currently applied bias voltage vs time.

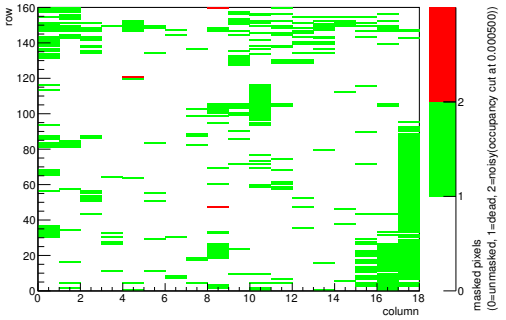

(d) Map of masked pixels.

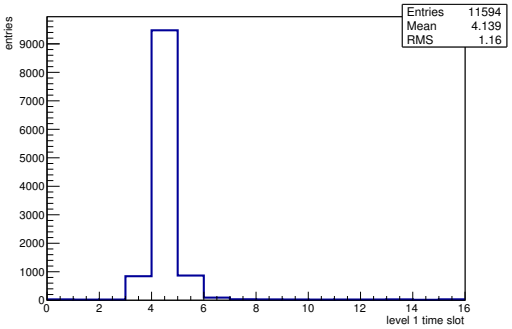

(e) Lvl1 distribution.

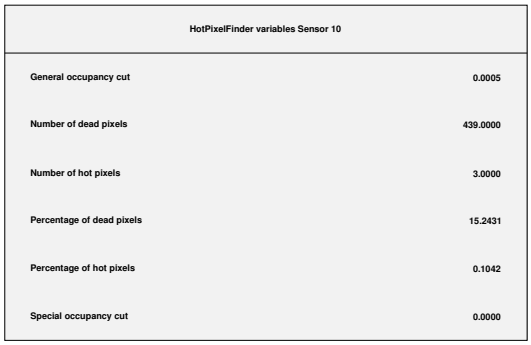

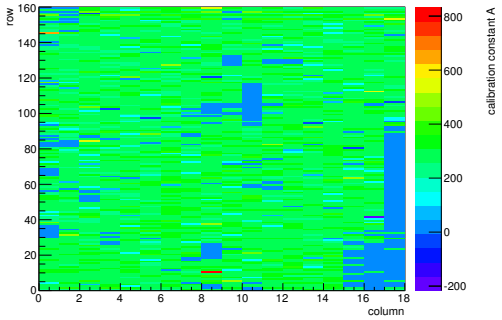

(f) Calibration constant A.

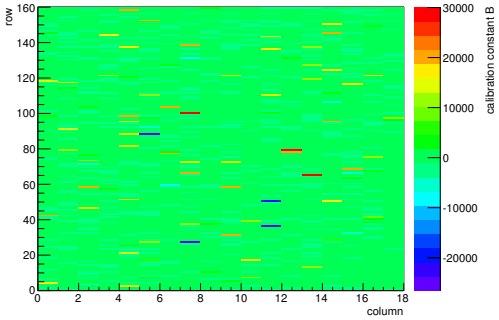

(g) Calibration constant B.

Figure C.79: Detailed plots for test beam measurement of DO-I-7 (description see section 6.1) sample (running as DUT0) during runs 61256 in the September 2011 test beam period at CERN SPS in area H6B. Summary of the data in chapter 9. *(cont.)*

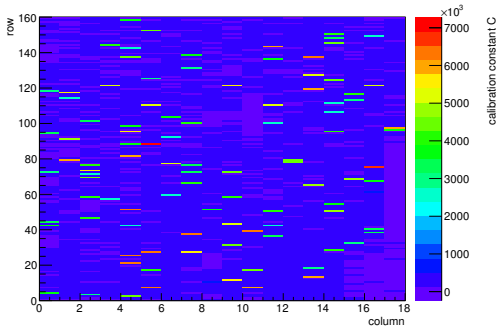

(h) Calibration constant C.

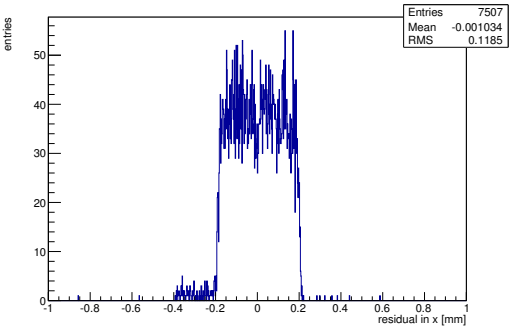

(i) Track residual in x.

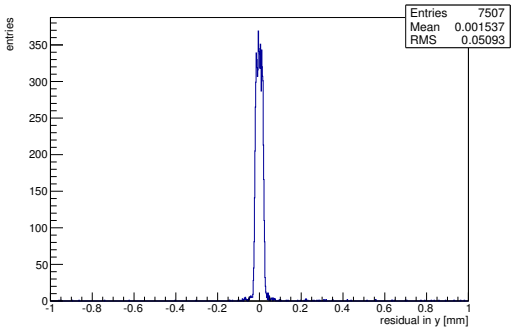

(j) Track residual in y.

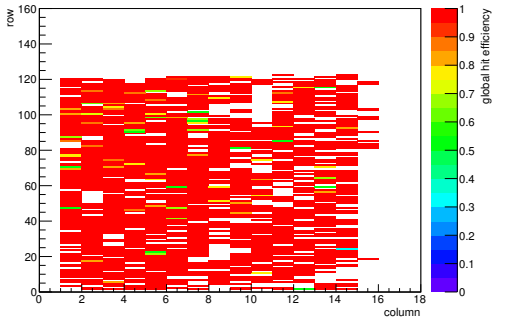

(k) Hit efficiency map.

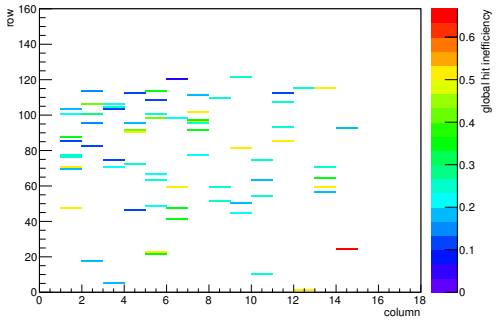

(l) Hit inefficiency map.

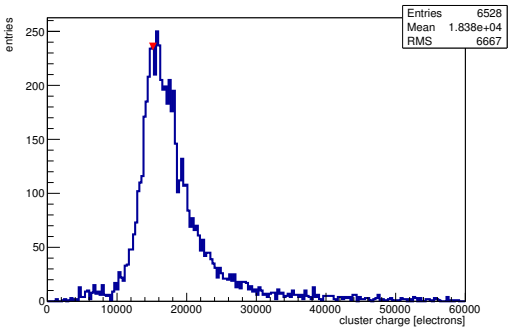

(m) Charge distribution (all cluster sizes included).

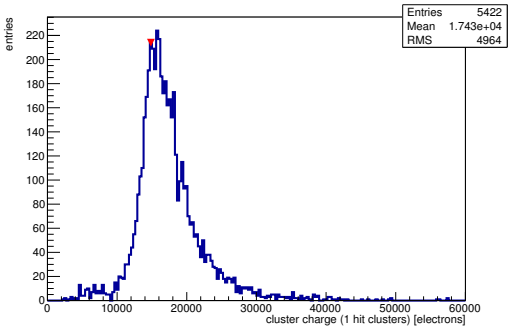

(n) Charge distribution (1 hit cluster).

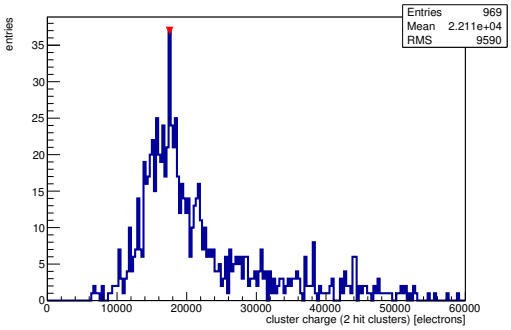

(o) Charge distribution (2 hit cluster).

Figure C.79: Detailed plots for test beam measurement of DO-I-7 (description see section 6.1) sample (running as DUT0) during runs 61256 in the September 2011 test beam period at CERN SPS in area H6B. Summary of the data in chapter 9. *(cont.)*

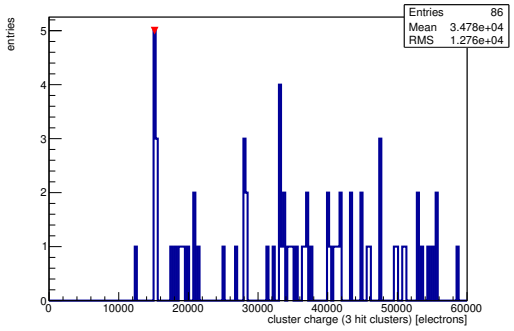

(p) Charge distribution (3 hit cluster).

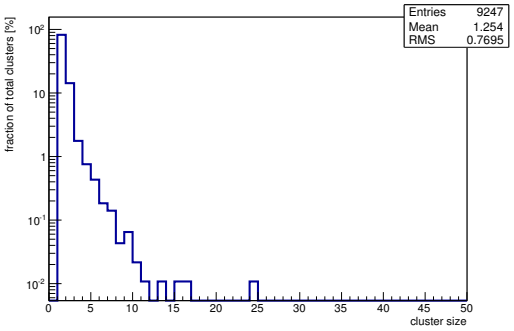

(q) Cluster size distribution.

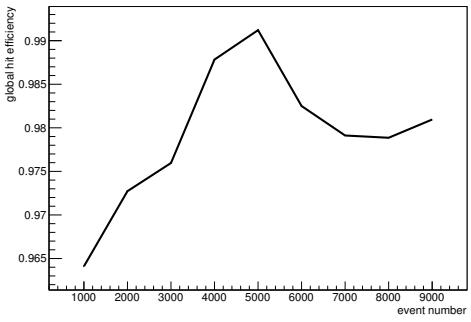

(r) Hit efficiency vs event number.

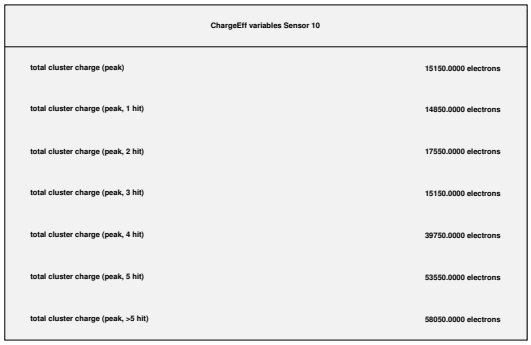

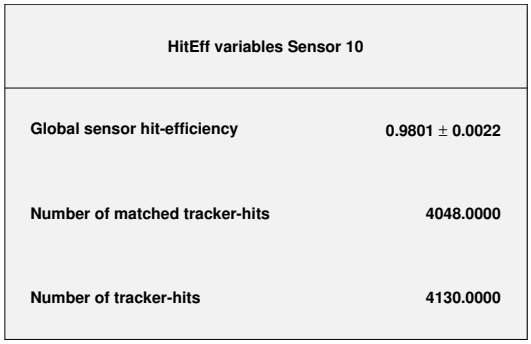

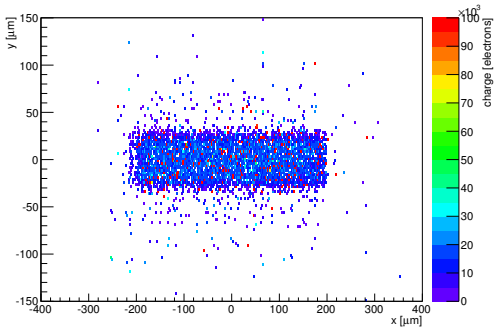

(s) Single pixel mean charge.

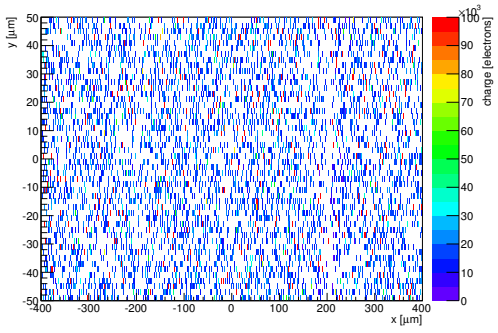

(t) Single pixel mean charge.

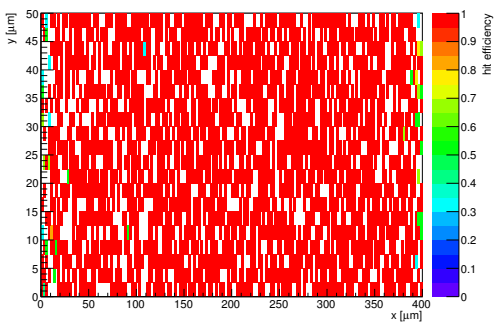

(u) Single pixel hit efficiency.

Figure C.79: Detailed plots for test beam measurement of DO-I-7 (description see section 6.1) sample (running as DUT0) during runs 61256 in the September 2011 test beam period at CERN SPS in area H6B. Summary of the data in chapter 9.

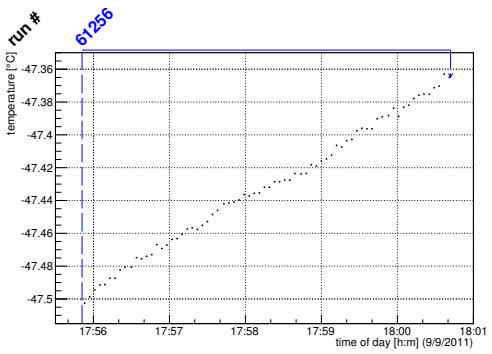

(a) Temperature vs time.

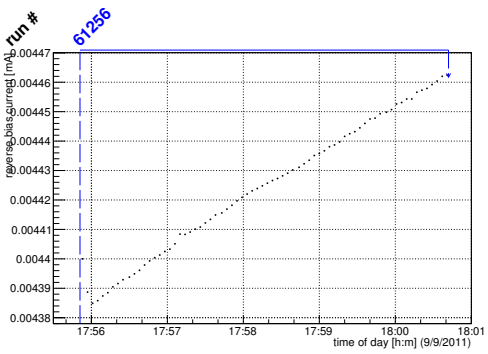

(b) Bias current vs time.

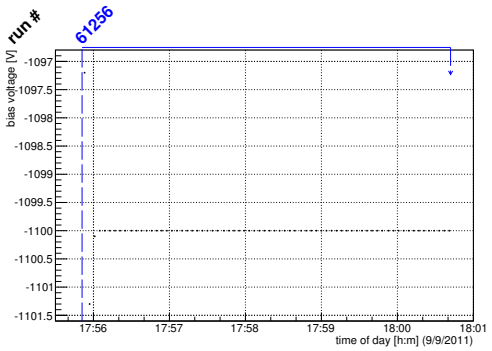

(c) Currently applied bias voltage vs time.

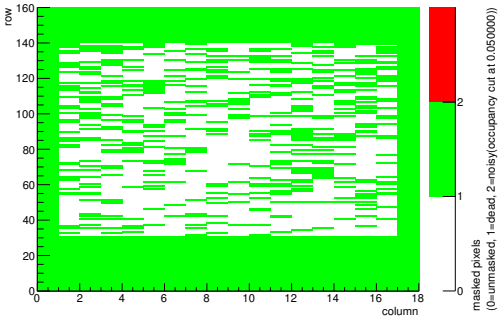

(d) Map of masked pixels.

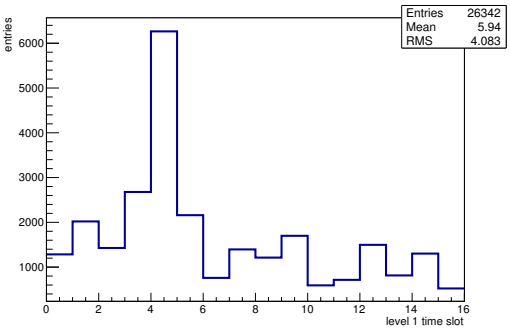

(e) Lvl1 distribution.

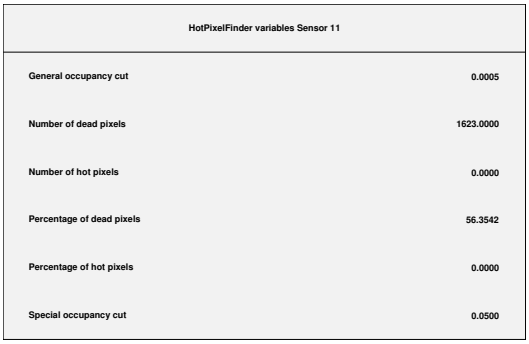

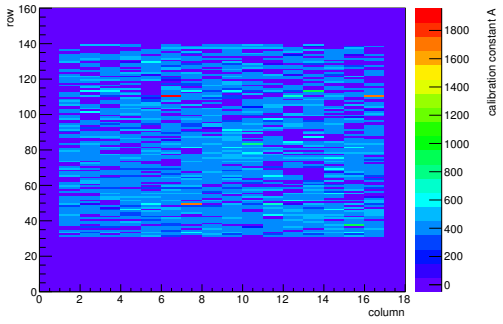

(f) Calibration constant A.

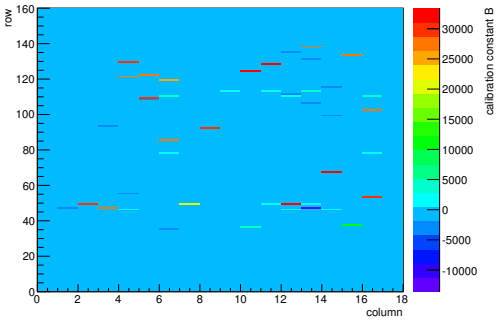

(g) Calibration constant B.

Figure C.80: Detailed plots for test beam measurement of DO-I-11 (description see section 6.1) sample (running as DUT1) during runs 61256 in the September 2011 test beam period at CERN SPS in area H6B. Summary of the data in chapter 9. *(cont.)*

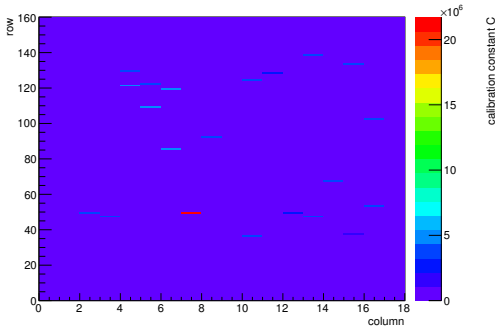

(h) Calibration constant C.

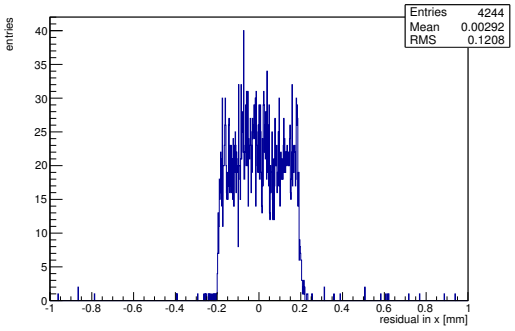

(i) Track residual in x.

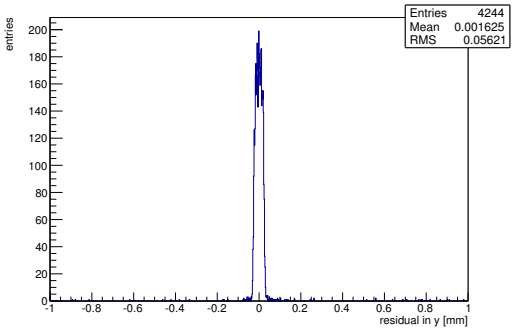

(j) Track residual in y.

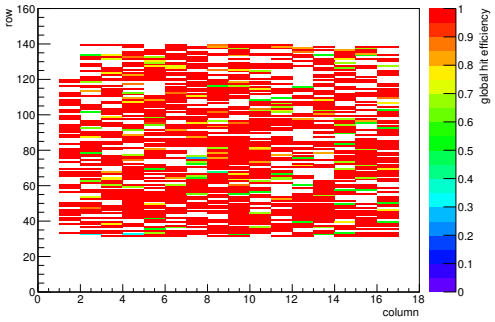

(k) Hit efficiency map.

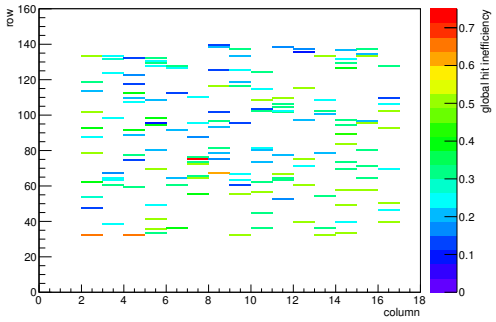

(l) Hit inefficiency map.

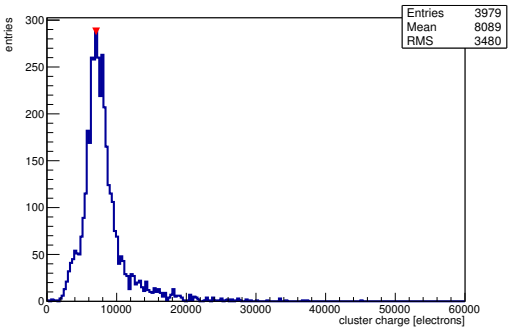

(m) Charge distribution (all cluster sizes included).

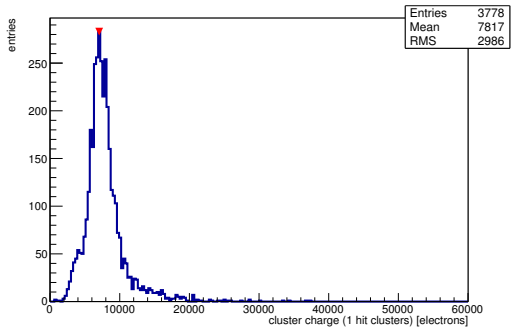

(n) Charge distribution (1 hit cluster).

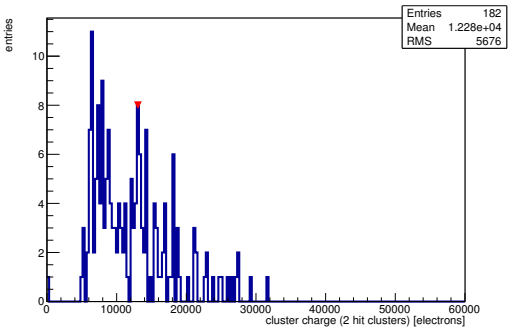

(o) Charge distribution (2 hit cluster).

Figure C.80: Detailed plots for test beam measurement of DO-I-11 (description see section 6.1) sample (running as DUT1) during runs 61256 in the September 2011 test beam period at CERN SPS in area H6B. Summary of the data in chapter 9. *(cont.)*

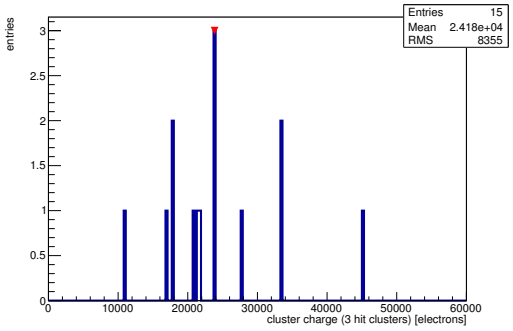

(p) Charge distribution (3 hit cluster).

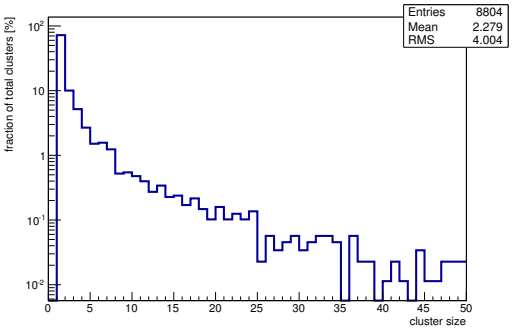

(q) Cluster size distribution.

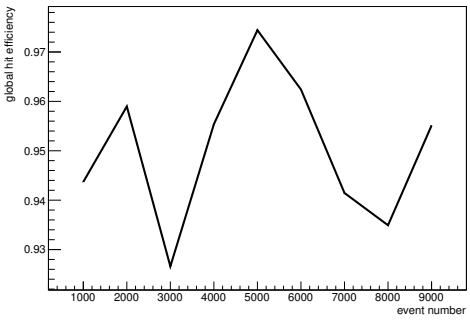

(r) Hit efficiency vs event number.

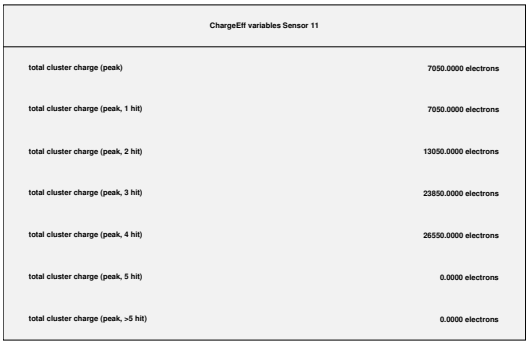

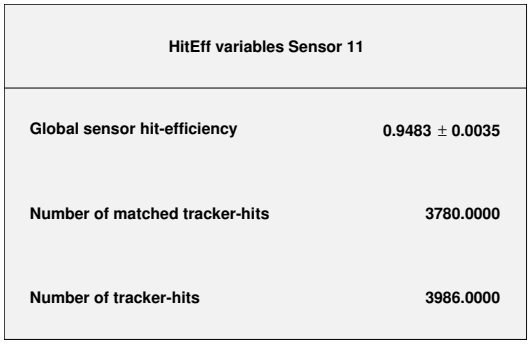

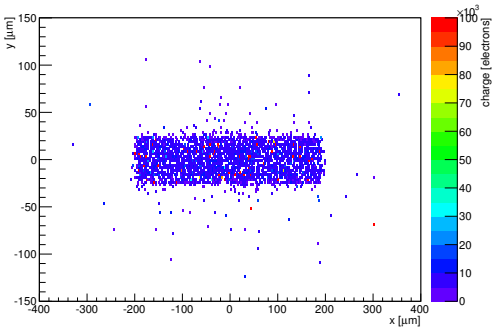

(s) Single pixel mean charge.

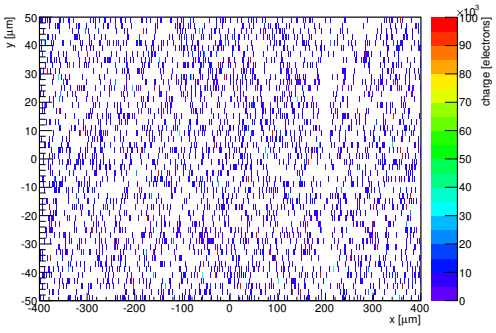

(t) Single pixel mean charge.

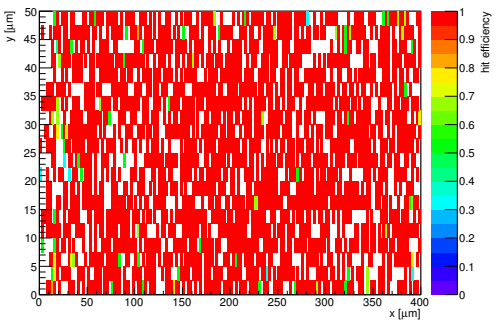

(u) Single pixel hit efficiency.

Figure C.80: Detailed plots for test beam measurement of DO-I-11 (description see section 6.1) sample (running as DUT1) during runs 61256 in the September 2011 test beam period at CERN SPS in area H6B. Summary of the data in chapter 9.

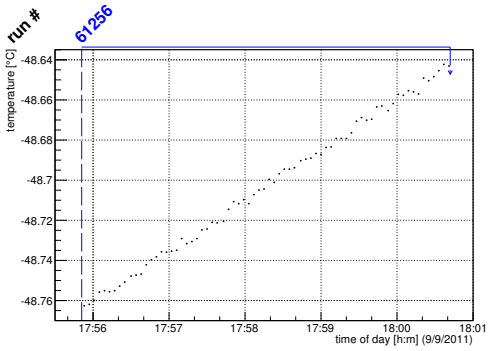

(a) Temperature vs time.

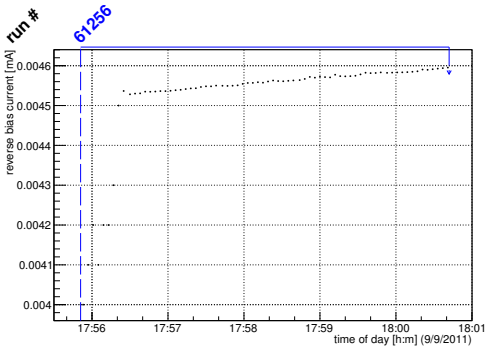

(b) Bias current vs time.

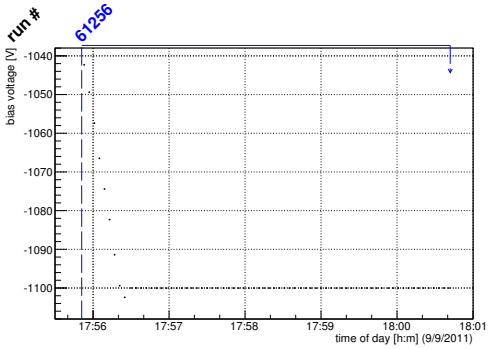

(c) Currently applied bias voltage vs time.

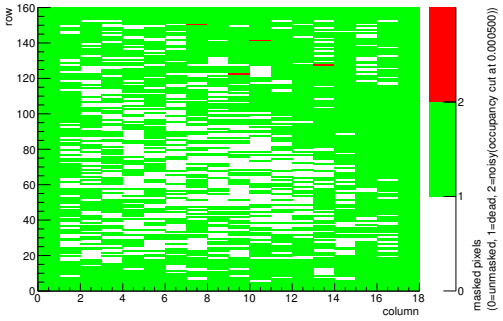

(d) Map of masked pixels.

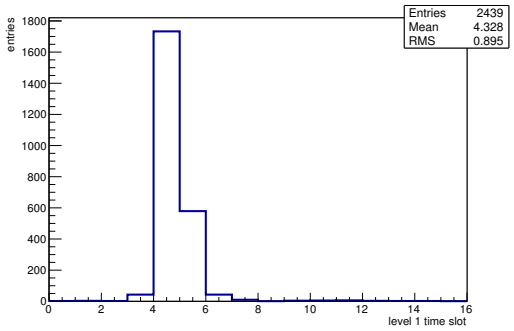

(e) Lvl1 distribution.

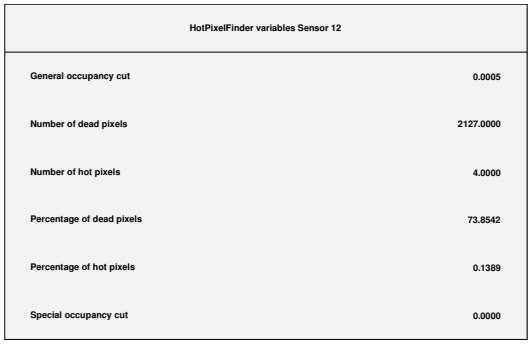

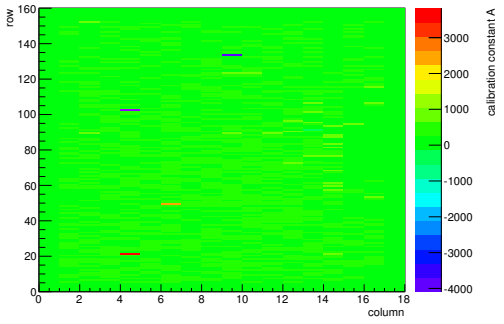

(f) Calibration constant A.

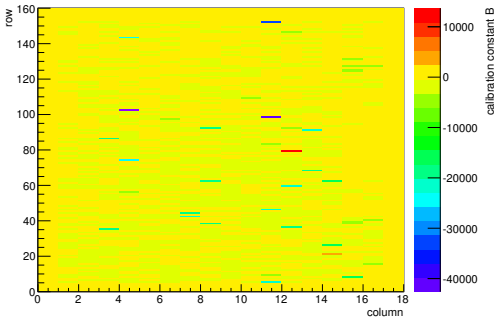

(g) Calibration constant B.

Figure C.81: Detailed plots for test beam measurement of DO-I-5 (description see section 6.1) sample (running as DUT2) during runs 61256 in the September 2011 test beam period at CERN SPS in area H6B. Summary of the data in chapter 9. *(cont.)*

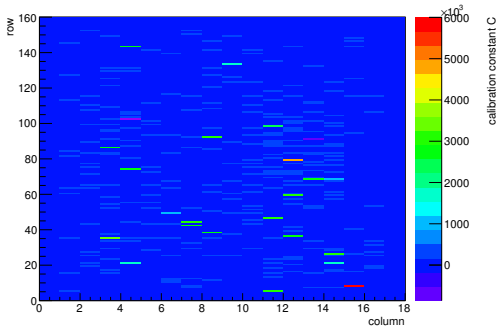

(h) Calibration constant C.

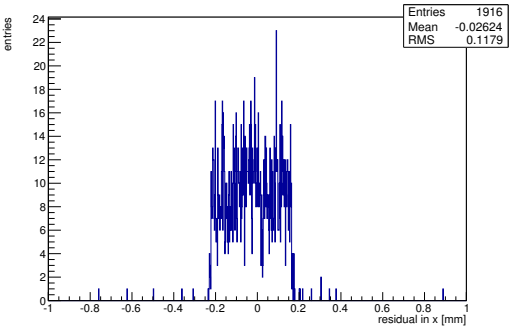

(i) Track residual in x.

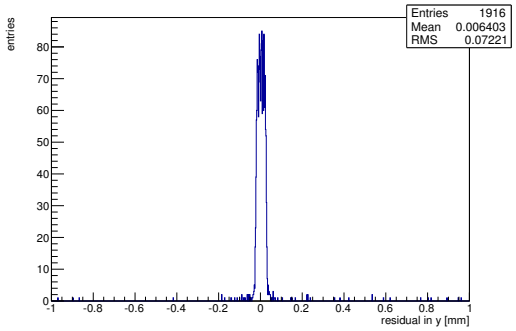

(j) Track residual in y.

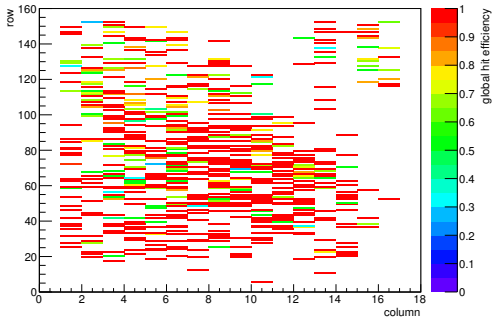

(k) Hit efficiency map.

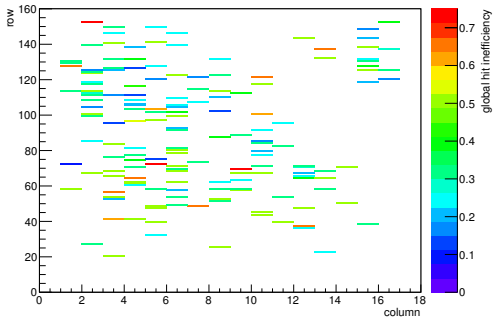

(l) Hit inefficiency map.

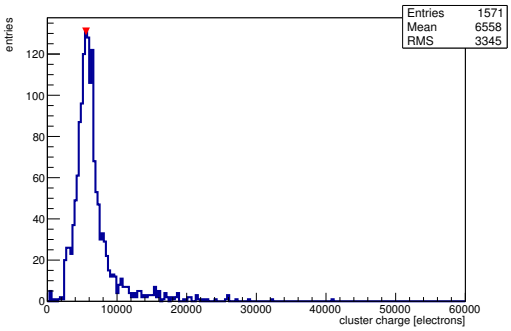

(m) Charge distribution (all cluster sizes included).

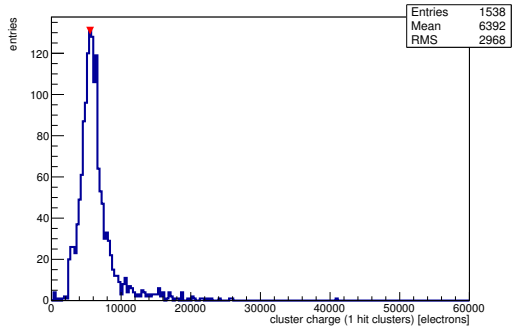

(n) Charge distribution (1 hit cluster).

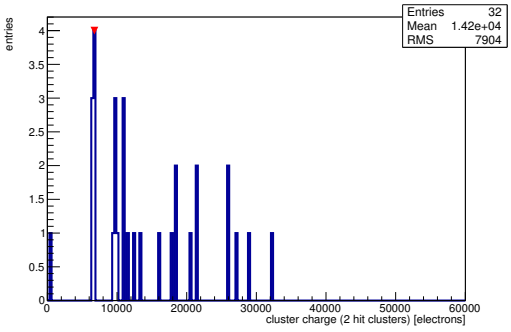

(o) Charge distribution (2 hit cluster).

Figure C.81: Detailed plots for test beam measurement of DO-I-5 (description see section 6.1) sample (running as DUT2) during runs 61256 in the September 2011 test beam period at CERN SPS in area H6B. Summary of the data in chapter 9. *(cont.)*

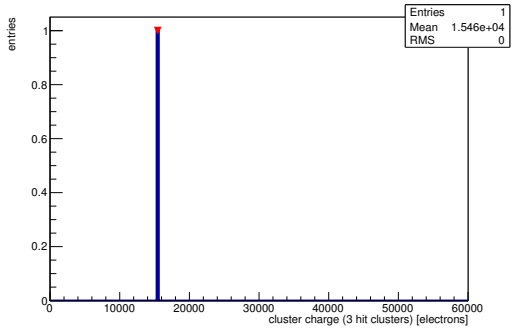

(p) Charge distribution (3 hit cluster).

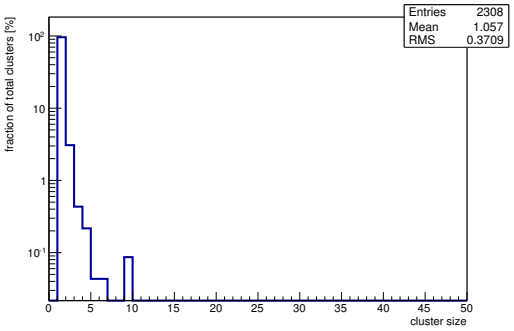

(q) Cluster size distribution.

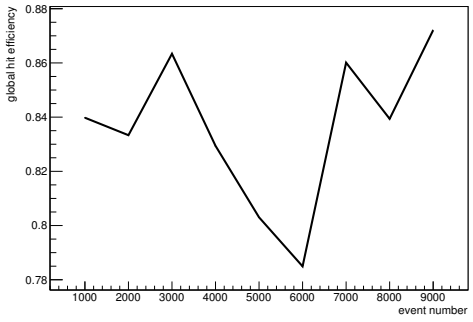

(r) Hit efficiency vs event number.

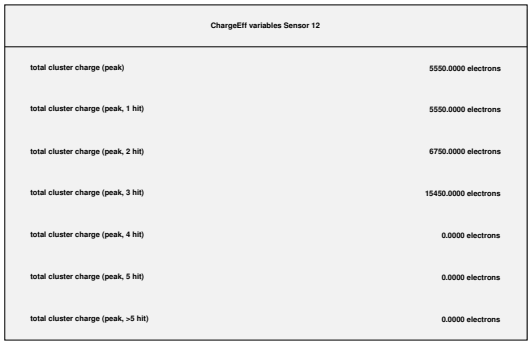

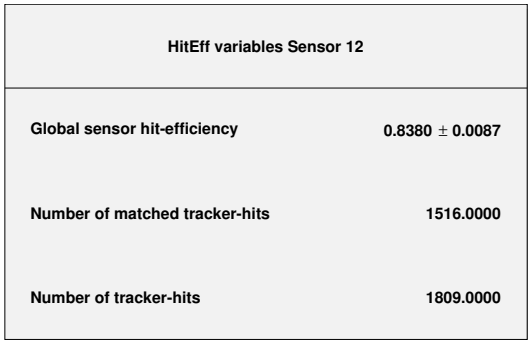

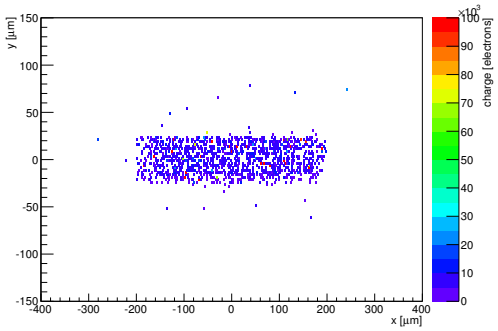

(s) Single pixel mean charge.

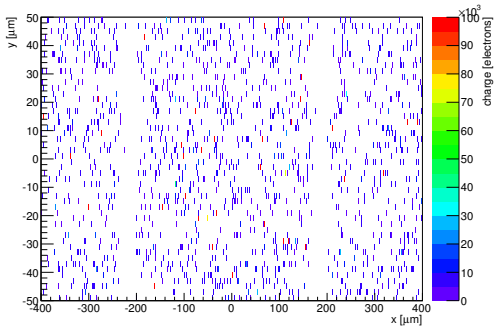

(t) Single pixel mean charge.

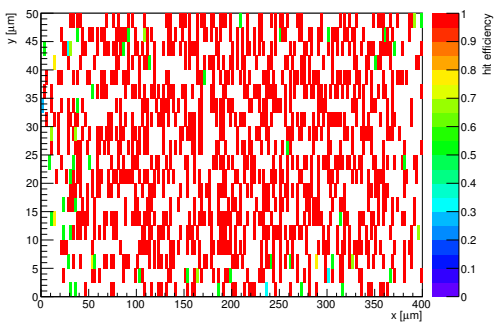

(u) Single pixel hit efficiency.

Figure C.81: Detailed plots for test beam measurement of DO-I-5 (description see section 6.1) sample (running as DUT2) during runs 61256 in the September 2011 test beam period at CERN SPS in area H6B. Summary of the data in chapter 9.

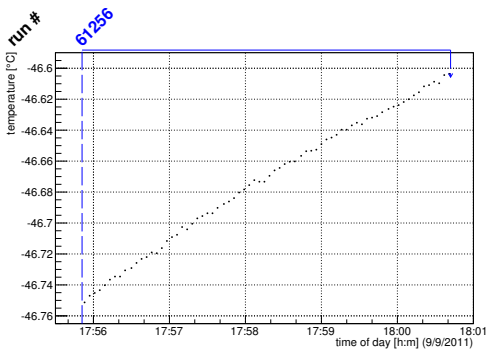

(a) Temperature vs time.

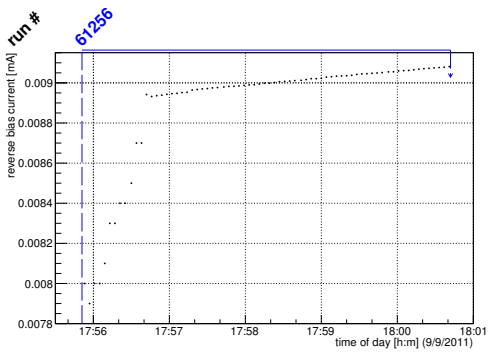

(b) Bias current vs time.

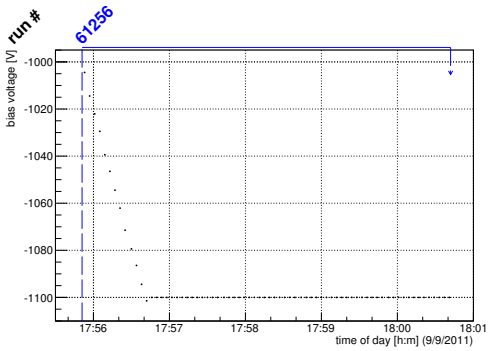

(c) Currently applied bias voltage vs time.

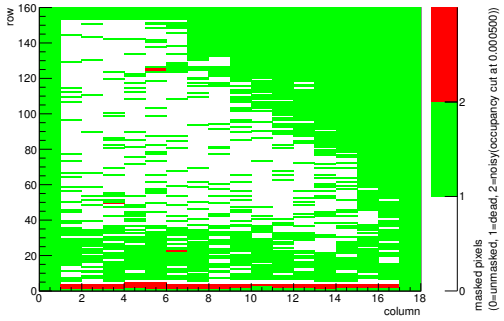

(d) Map of masked pixels.

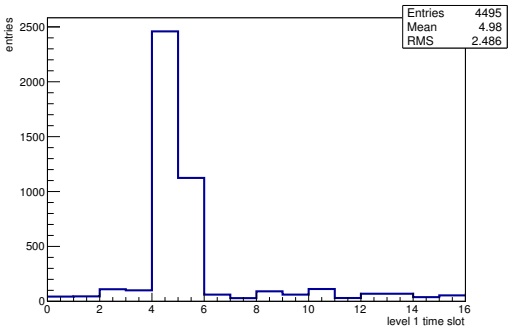

(e) Lvl1 distribution.

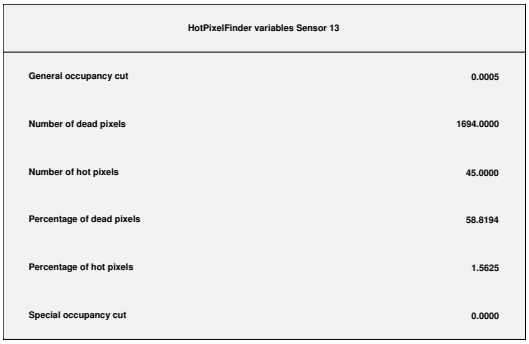

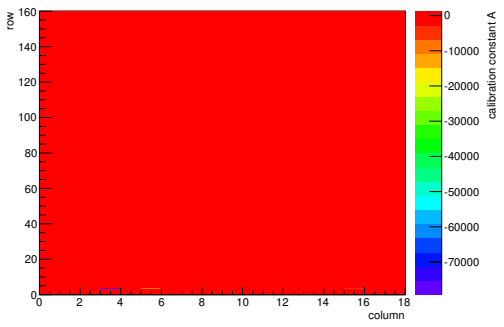

(f) Calibration constant A.

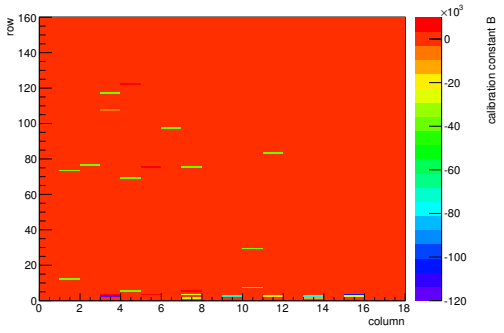

(g) Calibration constant B.

Figure C.82: Detailed plots for test beam measurement of DO-I-12 (description see section 6.1) sample (running as DUT3) during runs 61256 in the September 2011 test beam period at CERN SPS in area H6B. Summary of the data in chapter 9. *(cont.)*

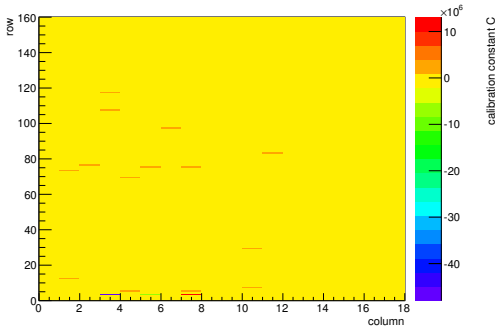

(h) Calibration constant C.

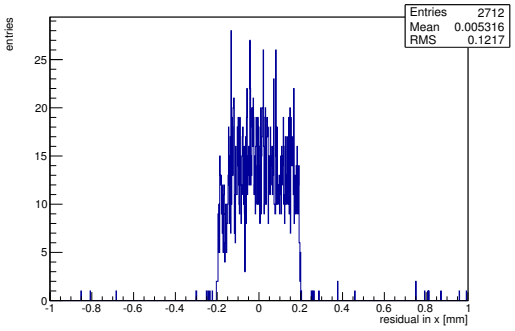

(i) Track residual in x.

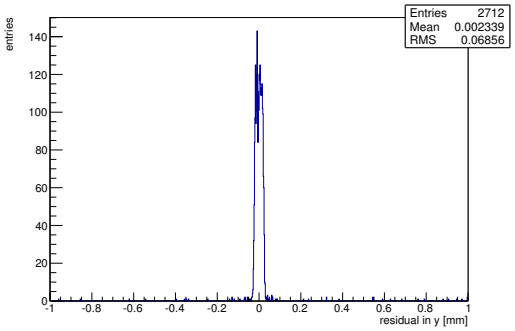

(j) Track residual in y.

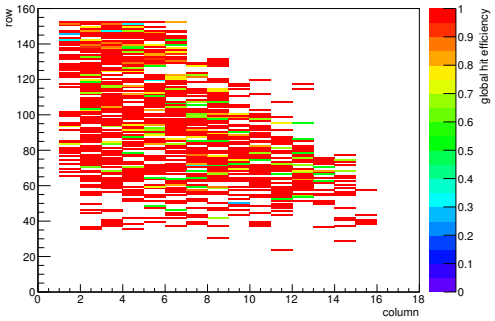

(k) Hit efficiency map.

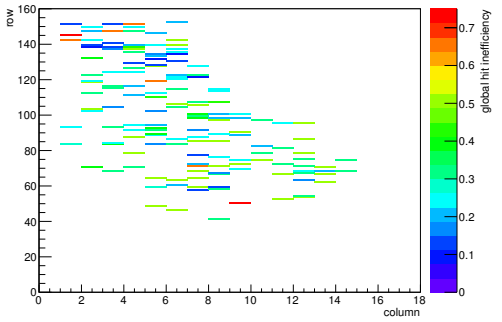

(l) Hit inefficiency map.

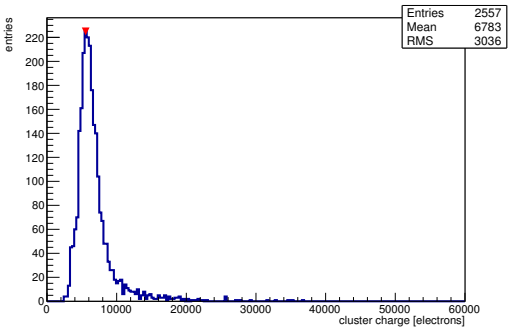

(m) Charge distribution (all cluster sizes included).

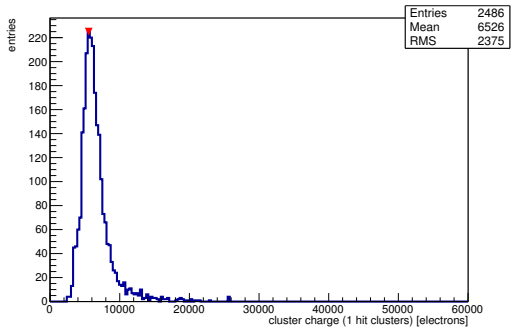

(n) Charge distribution (1 hit cluster).

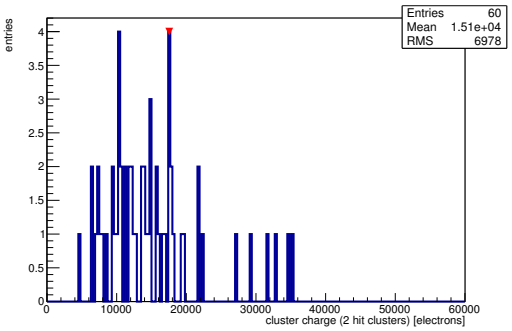

(o) Charge distribution (2 hit cluster).

Figure C.82: Detailed plots for test beam measurement of DO-I-12 (description see section 6.1) sample (running as DUT3) during runs 61256 in the September 2011 test beam period at CERN SPS in area H6B. Summary of the data in chapter 9. *(cont.)*

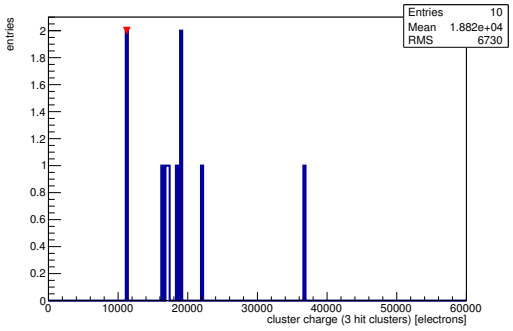

(p) Charge distribution (3 hit cluster).

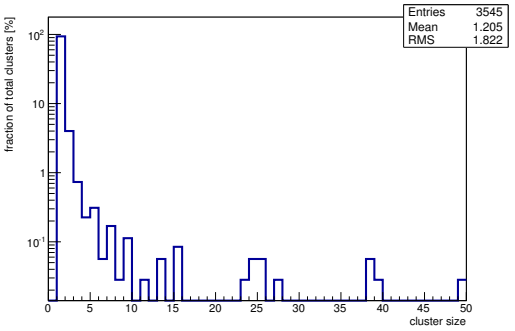

(q) Cluster size distribution.

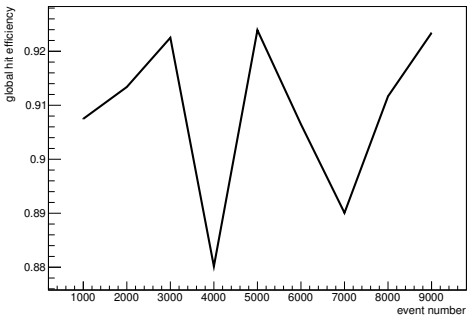

(r) Hit efficiency vs event number.

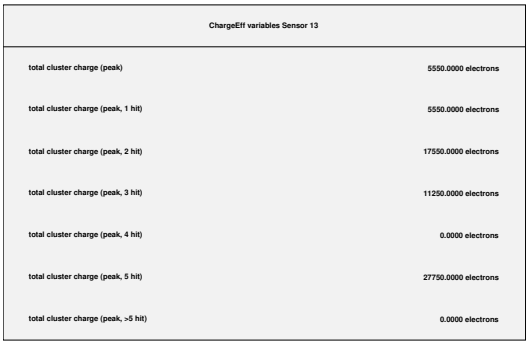

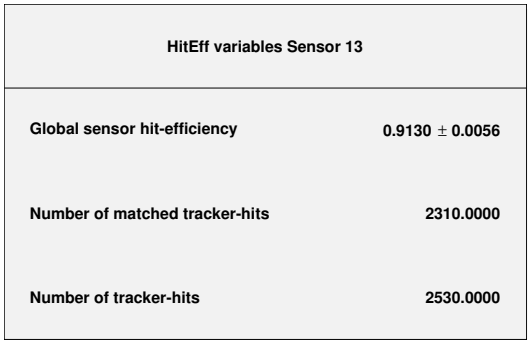

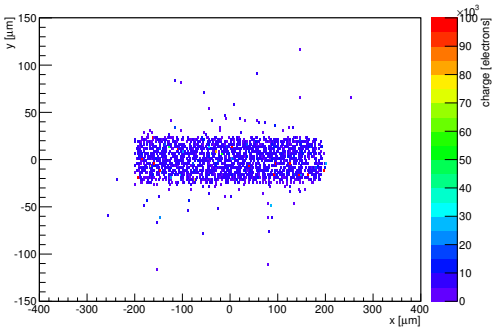

(s) Single pixel mean charge.

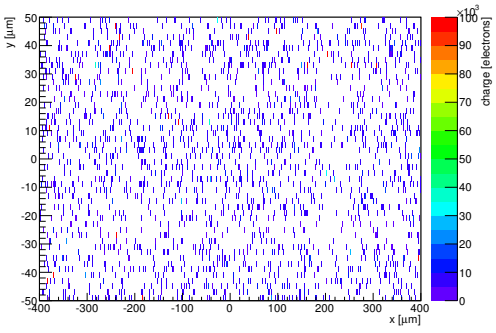

(t) Single pixel mean charge.

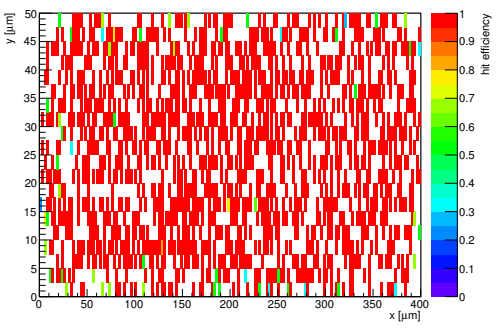

(u) Single pixel hit efficiency.

Figure C.82: Detailed plots for test beam measurement of DO-I-12 (description see section 6.1) sample (running as DUT3) during runs 61256 in the September 2011 test beam period at CERN SPS in area H6B. Summary of the data in chapter 9.

C.3.11 Run 61257

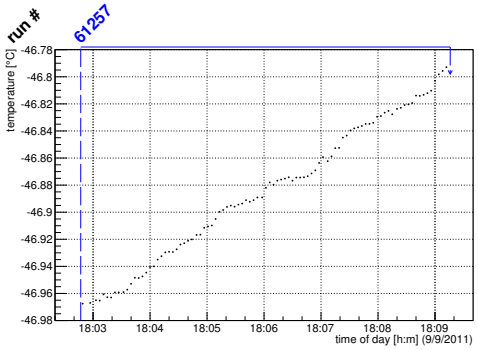

(a) Temperature vs time.

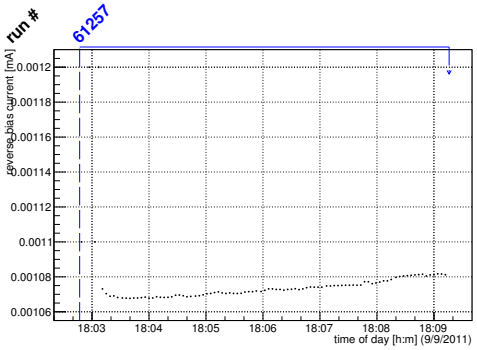

(b) Bias current vs time.

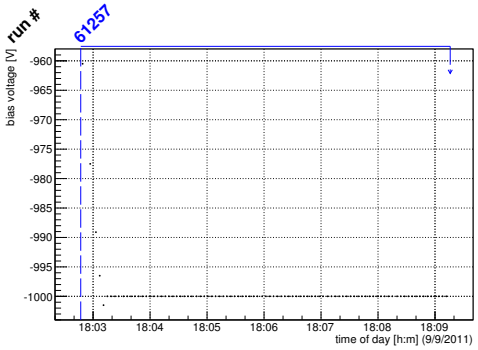

(c) Currently applied bias voltage vs time.

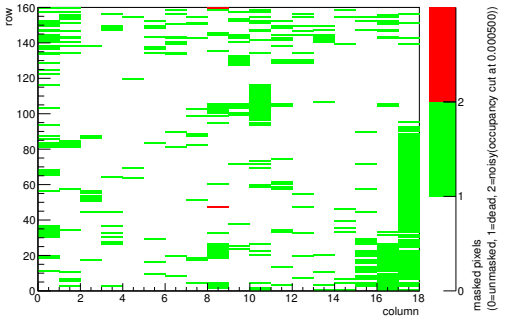

(d) Map of masked pixels.

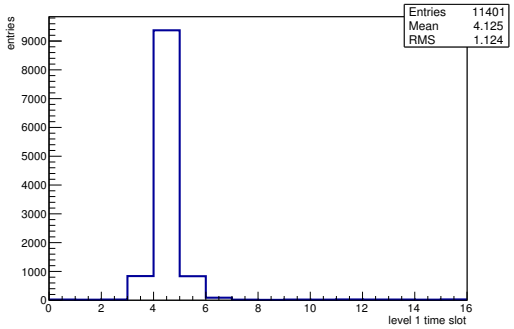

(e) Lvl1 distribution.

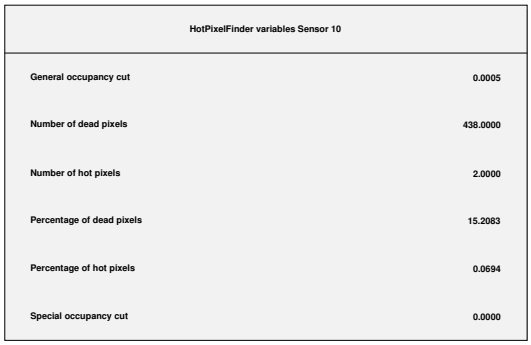

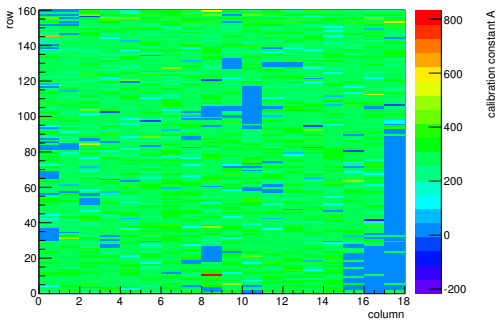

(f) Calibration constant A.

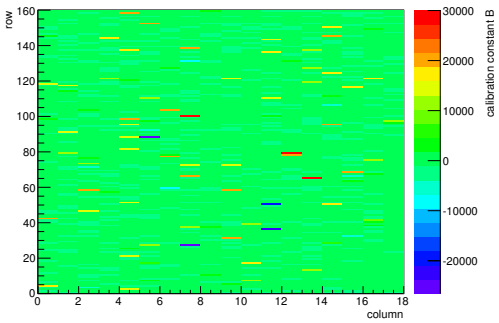

(g) Calibration constant B.

Figure C.83: Detailed plots for test beam measurement of DO-I-7 (description see section 6.1) sample (running as DUT0) during runs 61257 in the September 2011 test beam period at CERN SPS in area H6B. Summary of the data in chapter 9. *(cont.)*

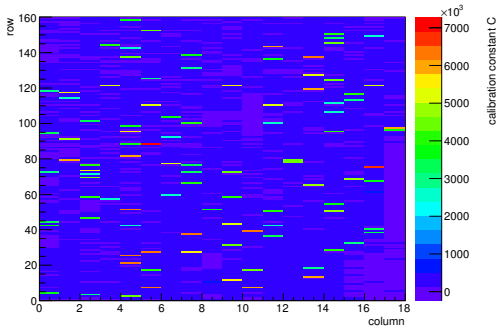

(h) Calibration constant C.

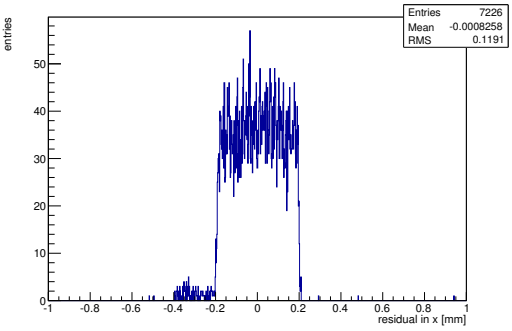

(i) Track residual in x.

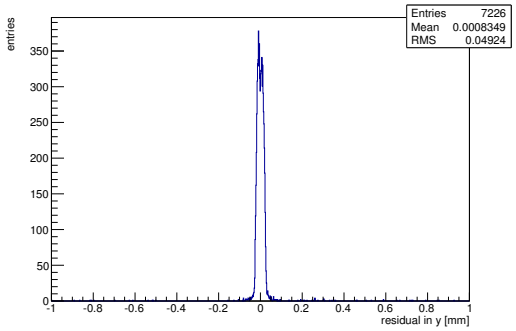

(j) Track residual in y.

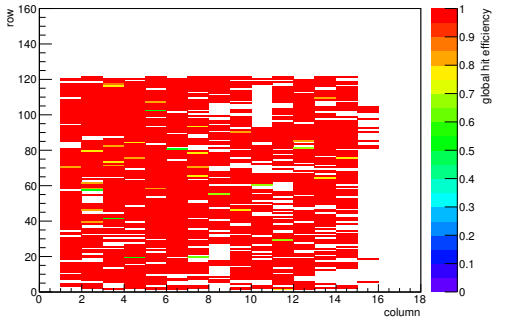

(k) Hit efficiency map.

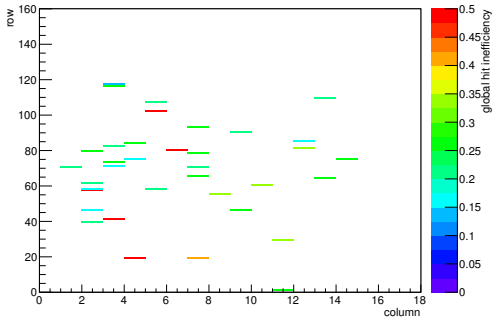

(l) Hit inefficiency map.

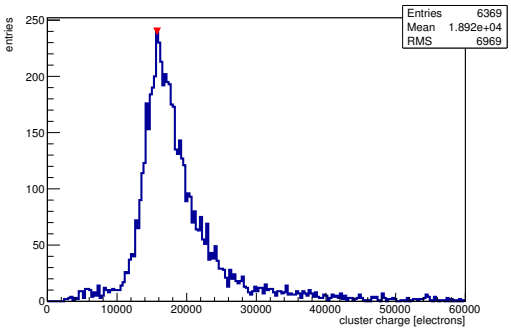

(m) Charge distribution (all cluster sizes included).

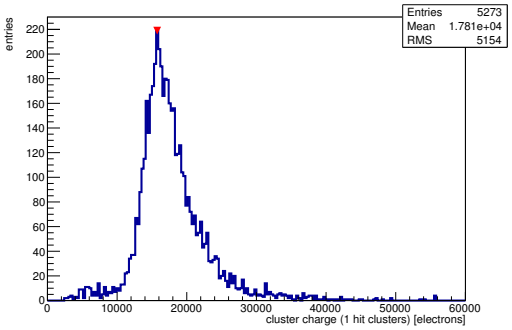

(n) Charge distribution (1 hit cluster).

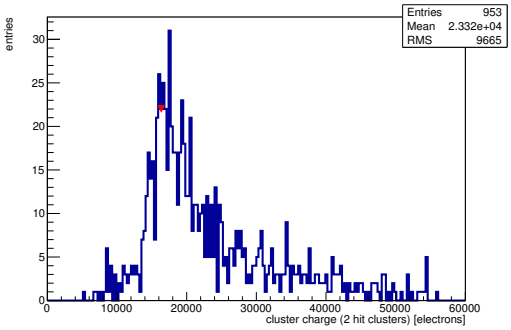

(o) Charge distribution (2 hit cluster).

Figure C.83: Detailed plots for test beam measurement of DO-I-7 (description see section 6.1) sample (running as DUT0) during runs 61257 in the September 2011 test beam period at CERN SPS in area H6B. Summary of the data in chapter 9. *(cont.)*

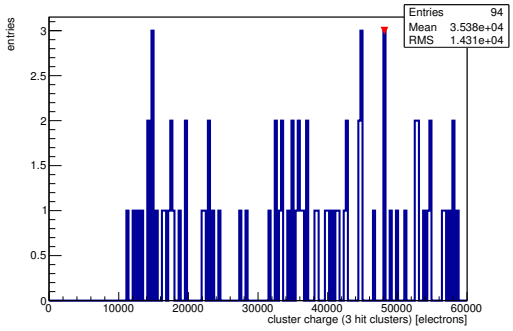

(p) Charge distribution (3 hit cluster).

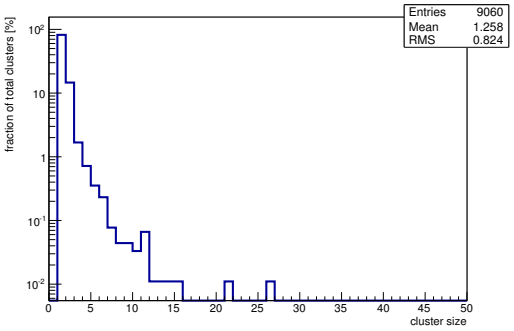

(q) Cluster size distribution.

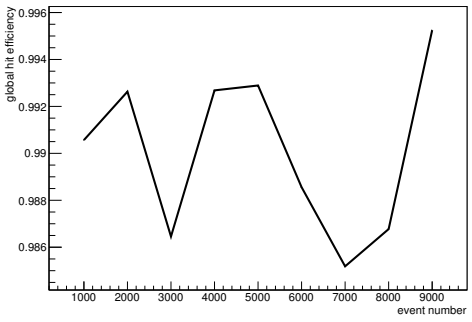

(r) Hit efficiency vs event number.

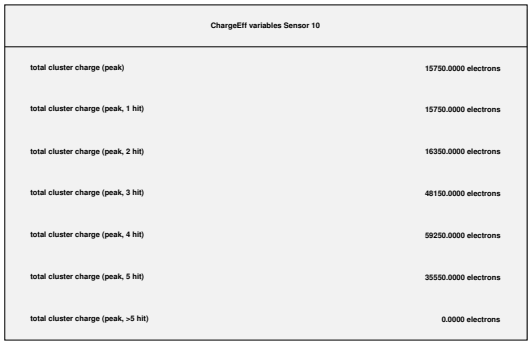

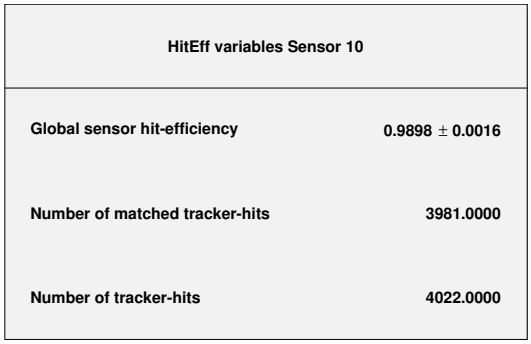

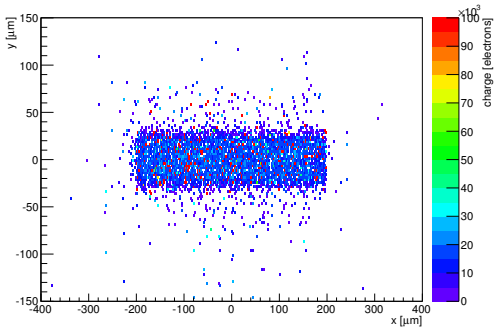

(s) Single pixel mean charge.

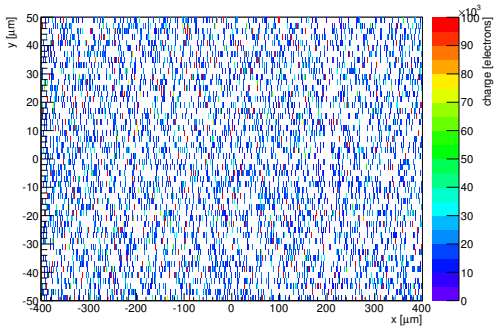

(t) Single pixel mean charge.

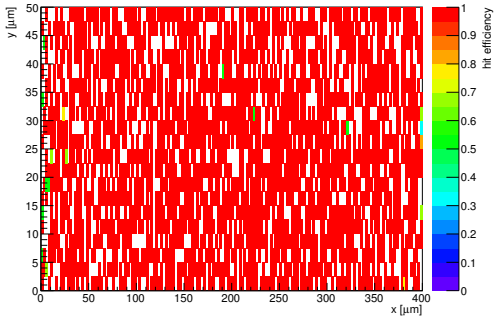

(u) Single pixel hit efficiency.

Figure C.83: Detailed plots for test beam measurement of DO-I-7 (description see section 6.1) sample (running as DUT0) during runs 61257 in the September 2011 test beam period at CERN SPS in area H6B. Summary of the data in chapter 9.

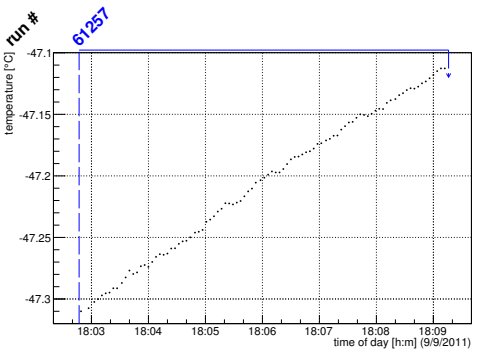

(a) Temperature vs time.

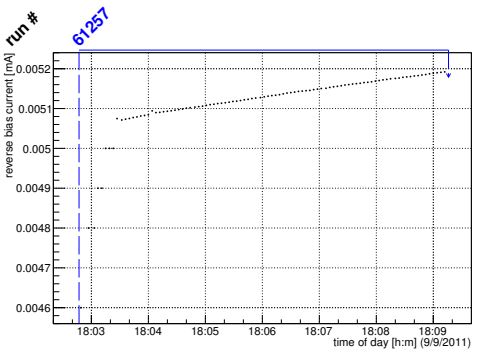

(b) Bias current vs time.

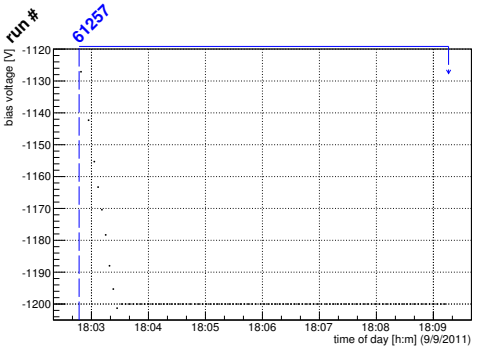

(c) Currently applied bias voltage vs time.

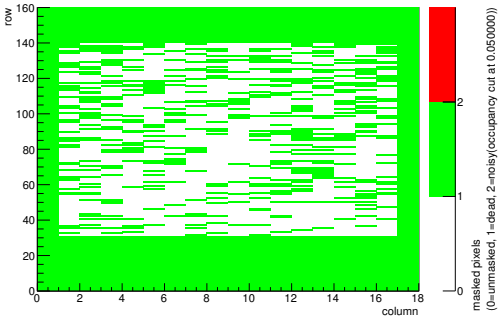

(d) Map of masked pixels.

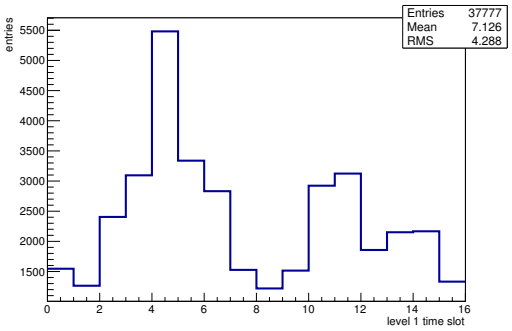

(e) Lvl1 distribution.

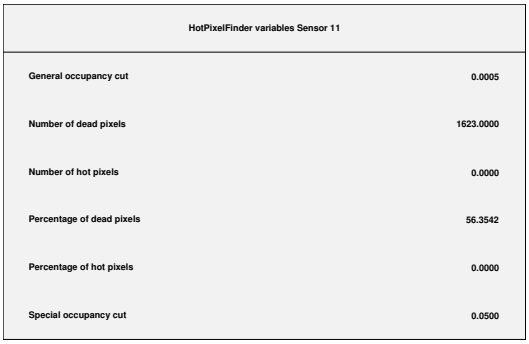

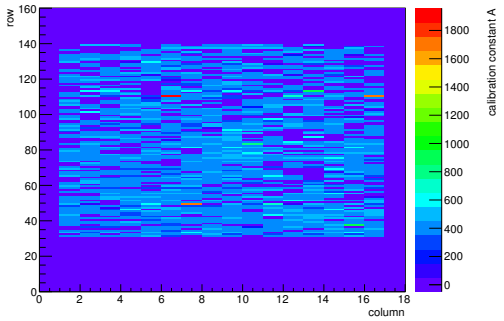

(f) Calibration constant A.

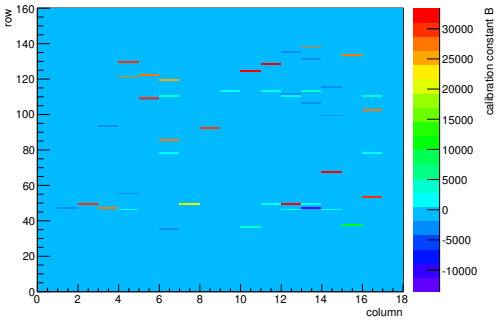

(g) Calibration constant B.

Figure C.84: Detailed plots for test beam measurement of DO-I-11 (description see section 6.1) sample (running as DUT1) during runs 61257 in the September 2011 test beam period at CERN SPS in area H6B. Summary of the data in chapter 9. *(cont.)*

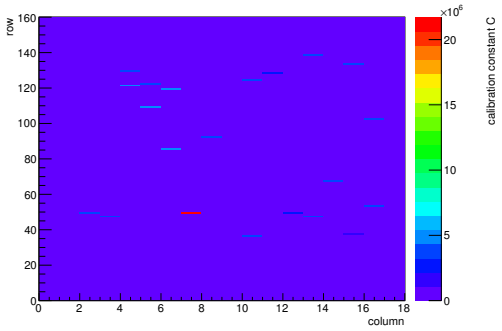

(h) Calibration constant C.

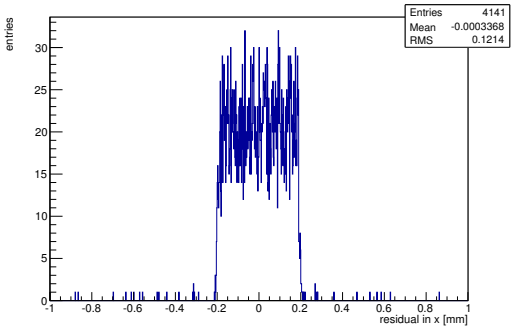

(i) Track residual in x.

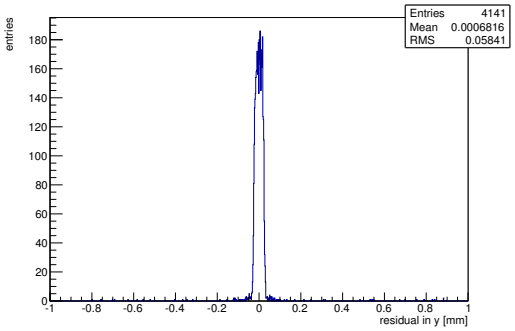

(j) Track residual in y.

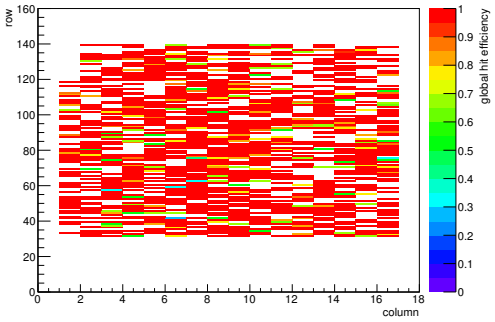

(k) Hit efficiency map.

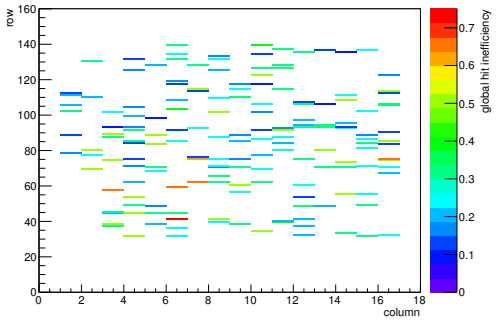

(l) Hit inefficiency map.

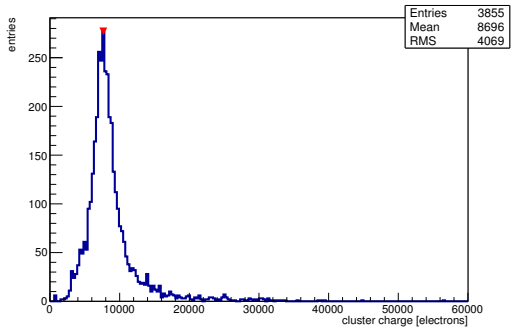

(m) Charge distribution (all cluster sizes included).

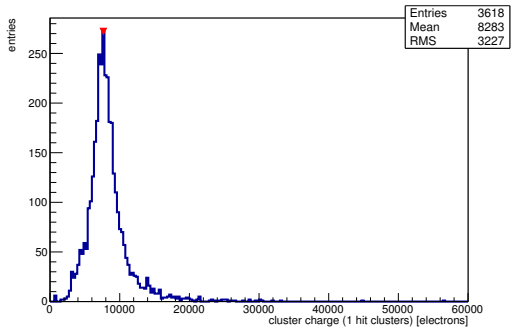

(n) Charge distribution (1 hit cluster).

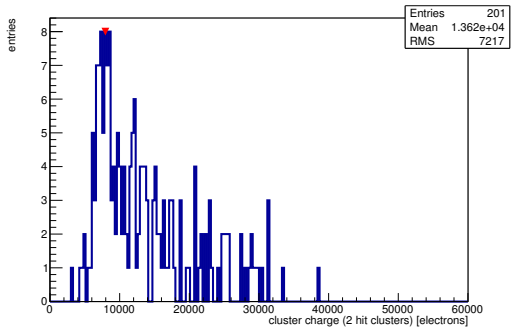

(o) Charge distribution (2 hit cluster).

Figure C.84: Detailed plots for test beam measurement of DO-I-11 (description see section 6.1) sample (running as DUT1) during runs 61257 in the September 2011 test beam period at CERN SPS in area H6B. Summary of the data in chapter 9. *(cont.)*

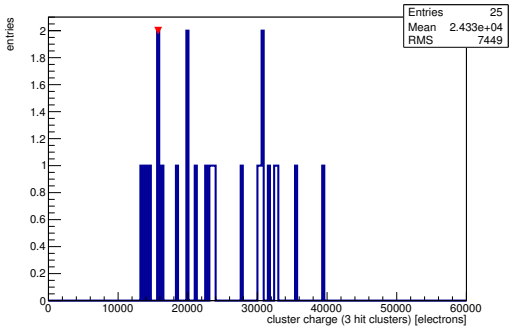

(p) Charge distribution (3 hit cluster).

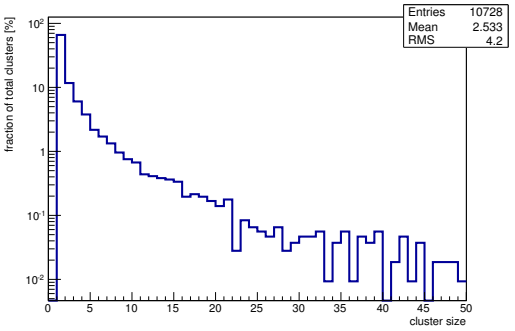

(q) Cluster size distribution.

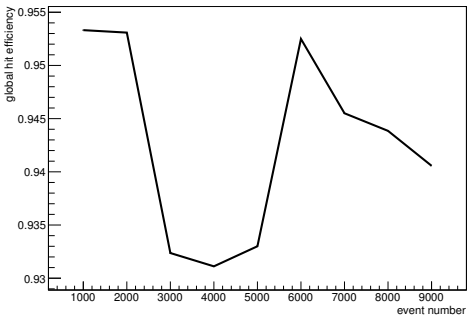

(r) Hit efficiency vs event number.

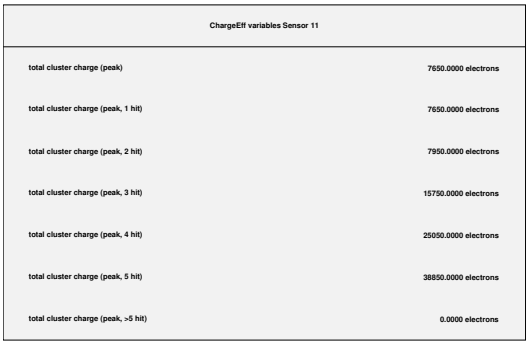

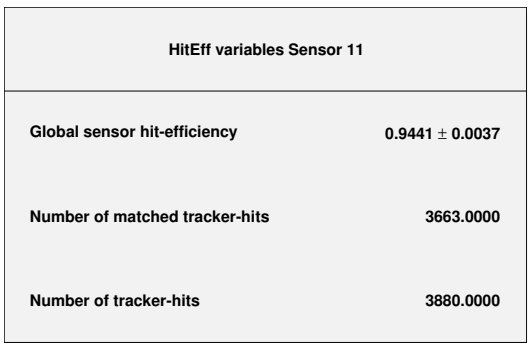

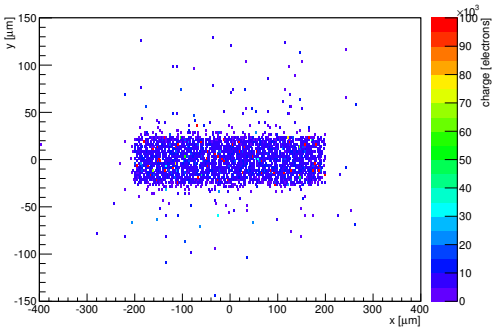

(s) Single pixel mean charge.

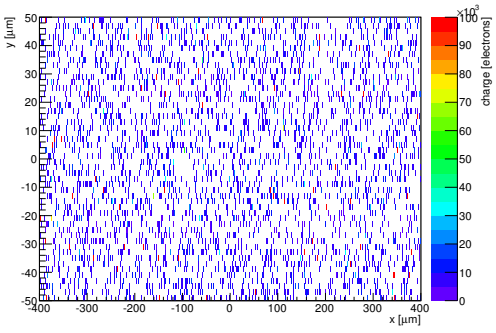

(t) Single pixel mean charge.

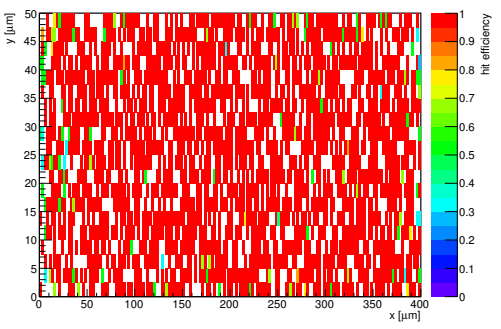

(u) Single pixel hit efficiency.

Figure C.84: Detailed plots for test beam measurement of DO-I-11 (description see section 6.1) sample (running as DUT1) during runs 61257 in the September 2011 test beam period at CERN SPS in area H6B. Summary of the data in chapter 9.

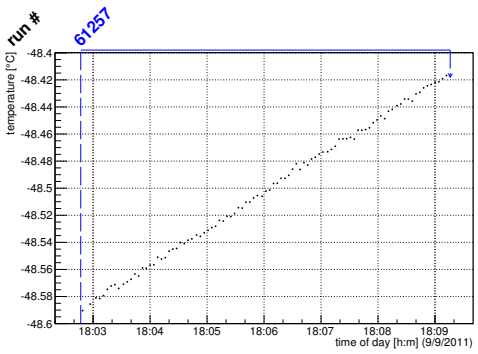

(a) Temperature vs time.

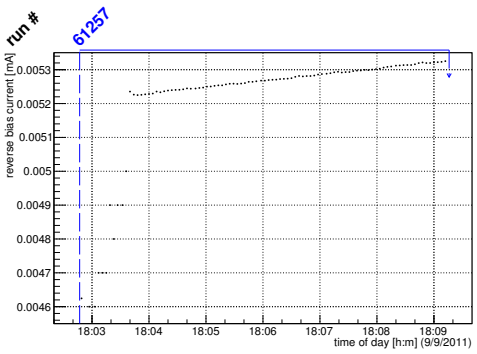

(b) Bias current vs time.

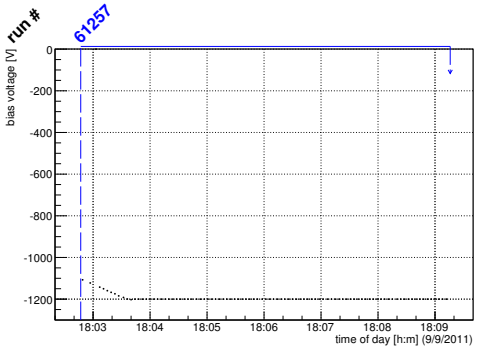

(c) Currently applied bias voltage vs time.

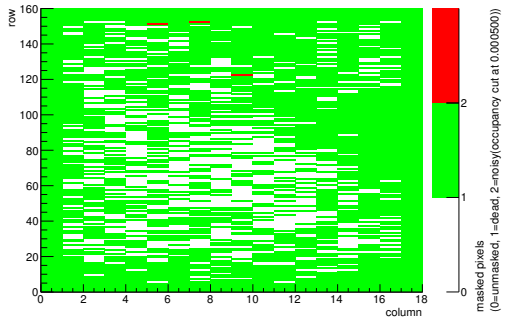

(d) Map of masked pixels.

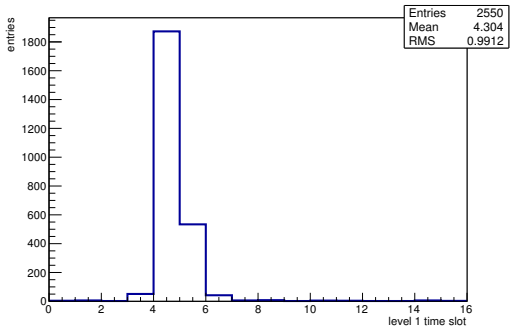

(e) Lvl1 distribution.

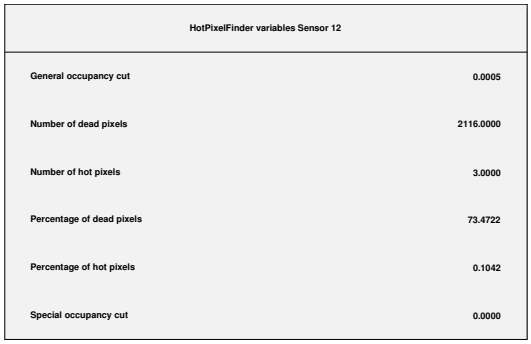

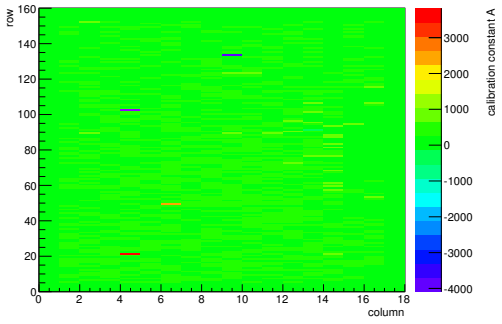

(f) Calibration constant A.

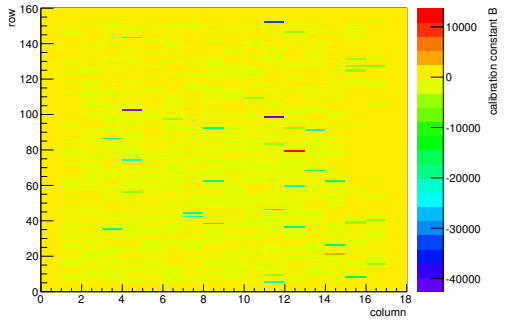

(g) Calibration constant B.

Figure C.85: Detailed plots for test beam measurement of DO-I-5 (description see section 6.1) sample (running as DUT2) during runs 61257 in the September 2011 test beam period at CERN SPS in area H6B. Summary of the data in chapter 9. *(cont.)*

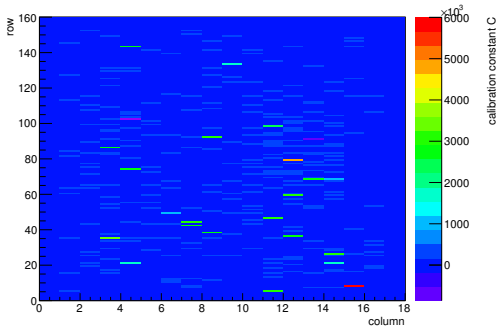

(h) Calibration constant C.

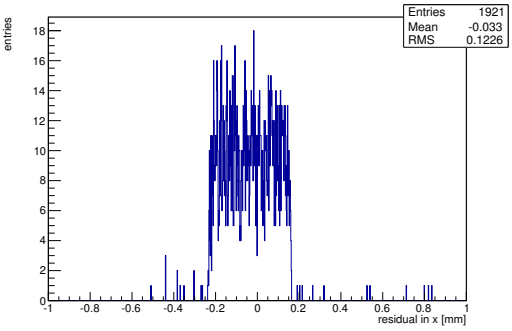

(i) Track residual in x.

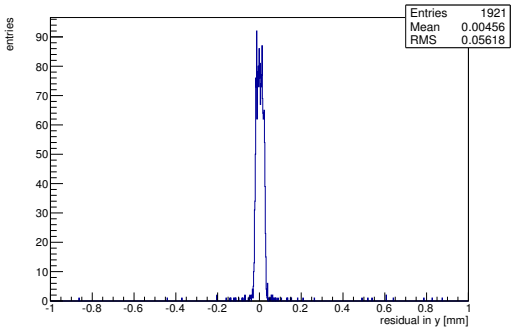

(j) Track residual in y.

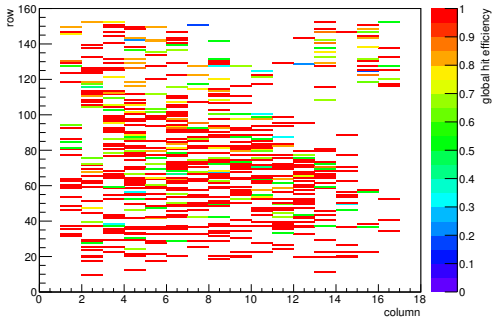

(k) Hit efficiency map.

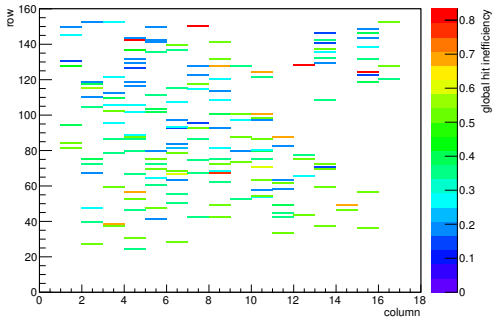

(l) Hit inefficiency map.

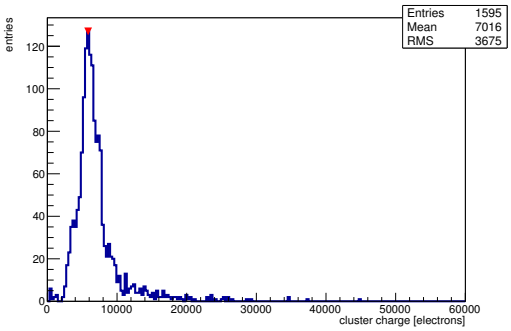

(m) Charge distribution (all cluster sizes included).

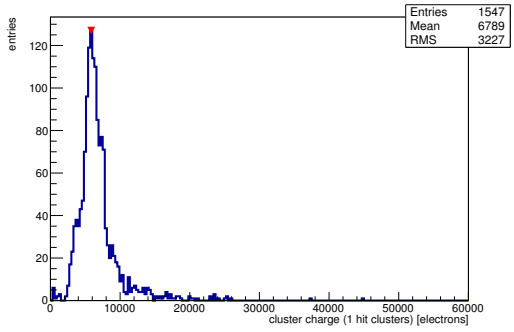

(n) Charge distribution (1 hit cluster).

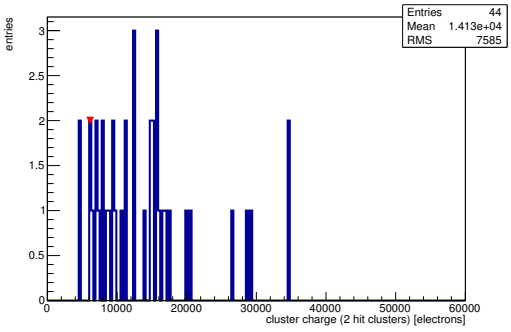

(o) Charge distribution (2 hit cluster).

Figure C.85: Detailed plots for test beam measurement of DO-I-5 (description see section 6.1) sample (running as DUT2) during runs 61257 in the September 2011 test beam period at CERN SPS in area H6B. Summary of the data in chapter 9. *(cont.)*

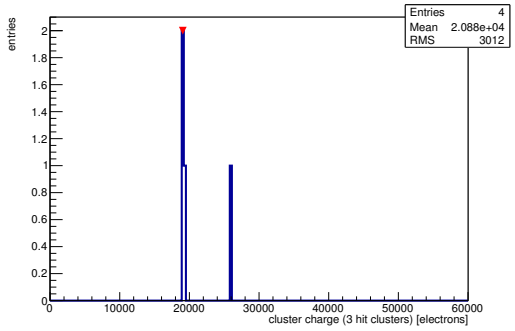

(p) Charge distribution (3 hit cluster).

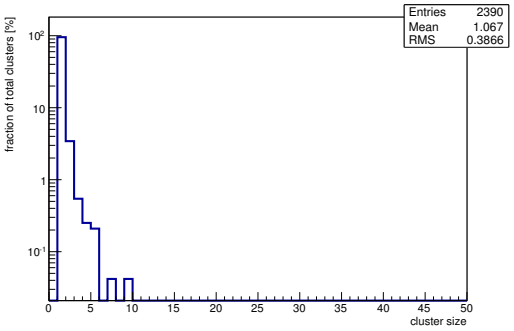

(q) Cluster size distribution.

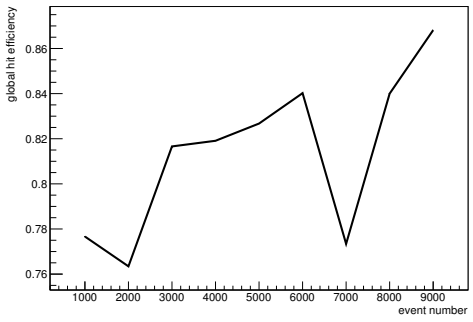

(r) Hit efficiency vs event number.

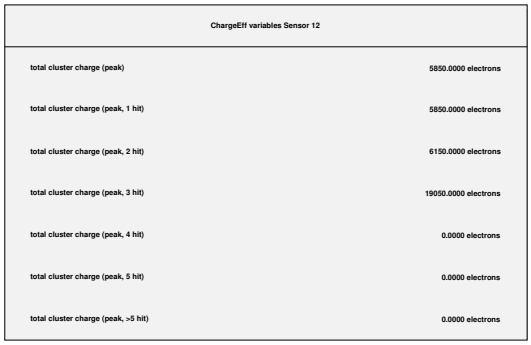

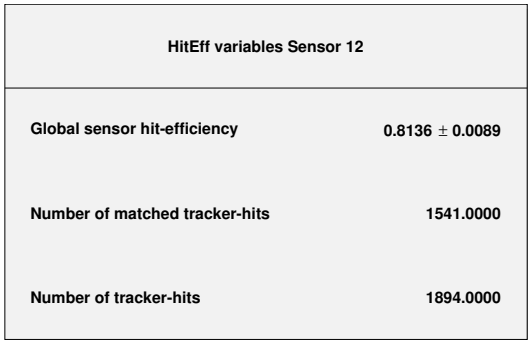

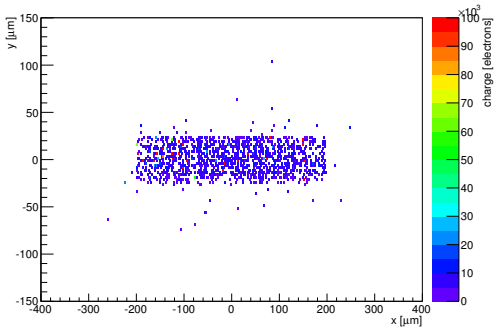

(s) Single pixel mean charge.

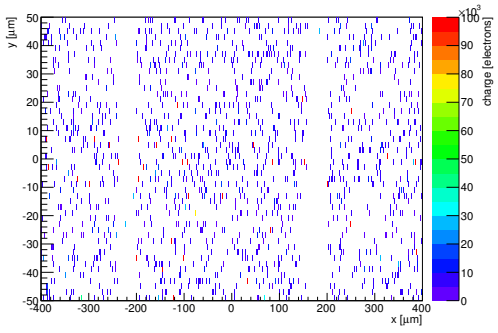

(t) Single pixel mean charge.

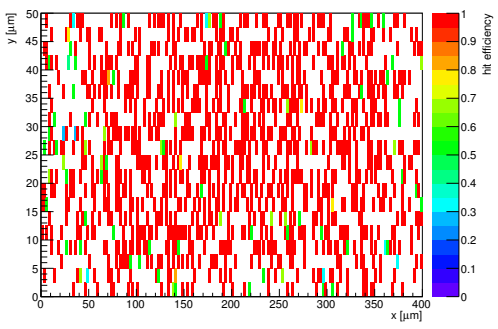

(u) Single pixel hit efficiency.

Figure C.85: Detailed plots for test beam measurement of DO-I-5 (description see section 6.1) sample (running as DUT2) during runs 61257 in the September 2011 test beam period at CERN SPS in area H6B. Summary of the data in chapter 9.

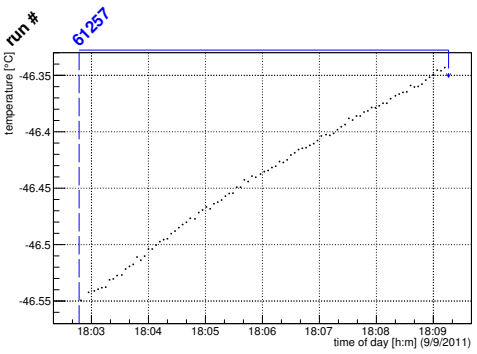

(a) Temperature vs time.

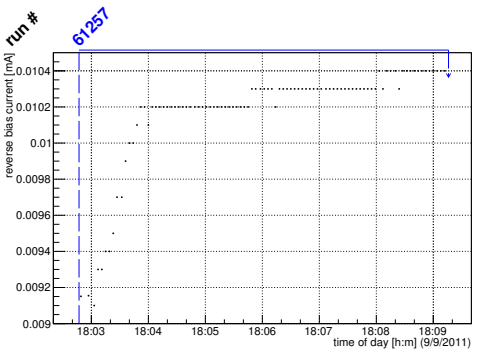

(b) Bias current vs time.

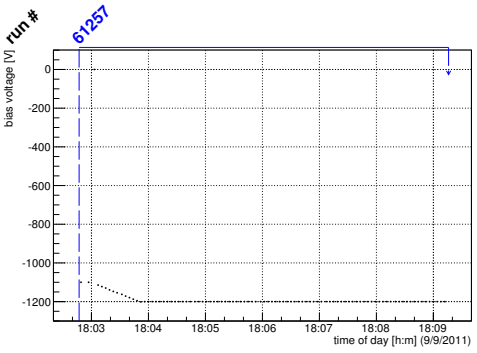

(c) Currently applied bias voltage vs time.

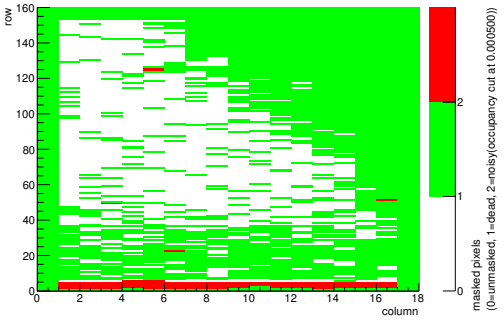

(d) Map of masked pixels.

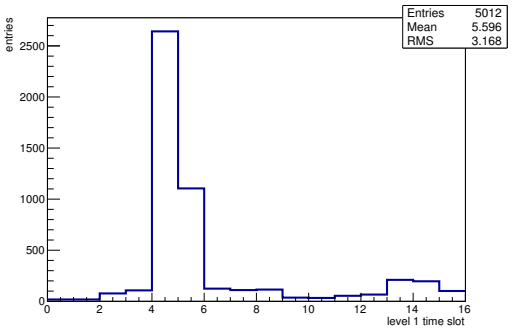

(e) Lvl1 distribution.

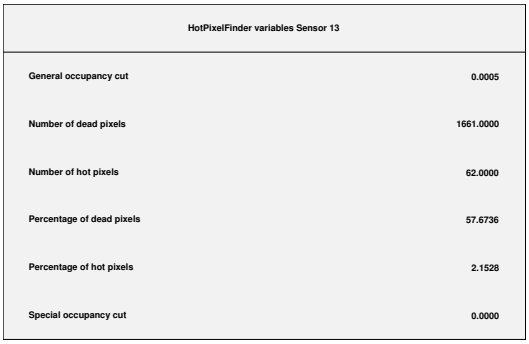

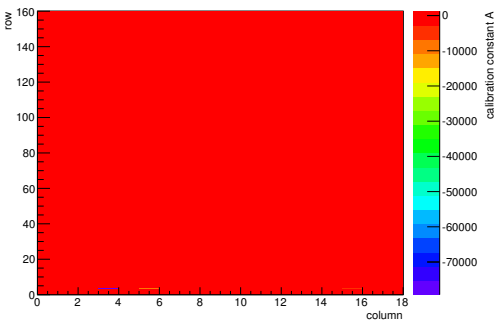

(f) Calibration constant A.

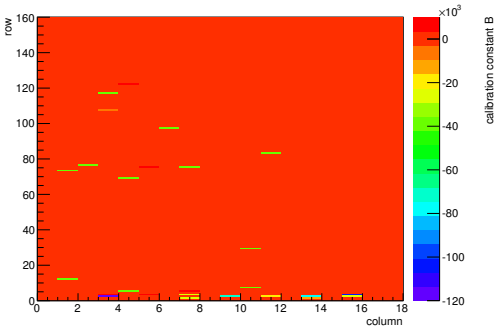

(g) Calibration constant B.

Figure C.86: Detailed plots for test beam measurement of DO-I-12 (description see section 6.1) sample (running as DUT3) during runs 61257 in the September 2011 test beam period at CERN SPS in area H6B. Summary of the data in chapter 9. *(cont.)*

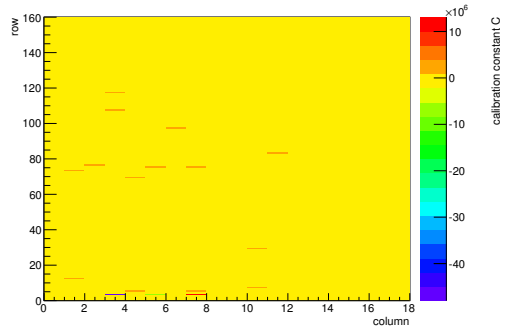

(h) Calibration constant C.

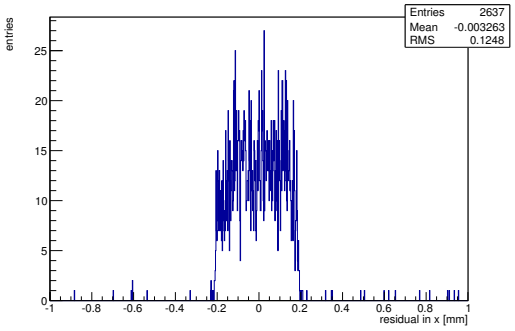

(i) Track residual in x.

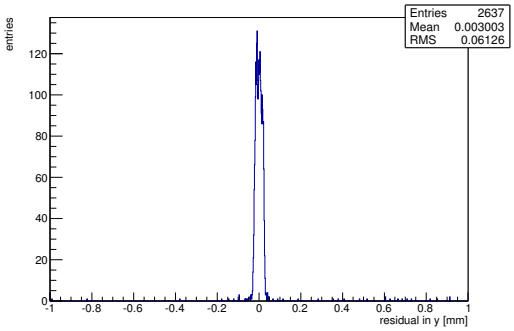

(j) Track residual in y.

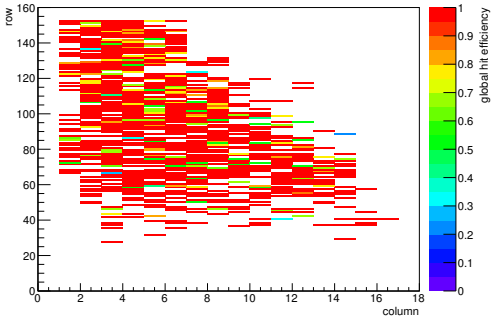

(k) Hit efficiency map.

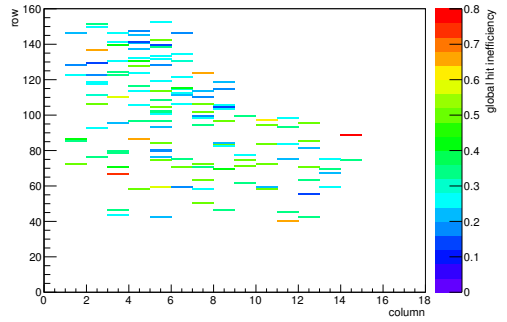

(l) Hit inefficiency map.

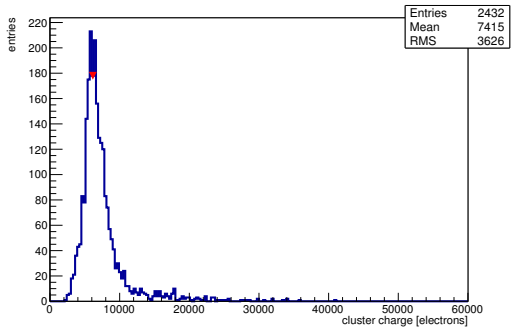

(m) Charge distribution (all cluster sizes included).

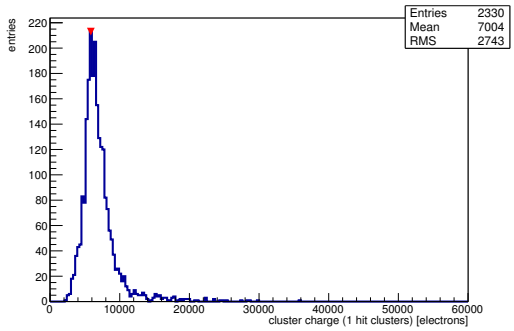

(n) Charge distribution (1 hit cluster).

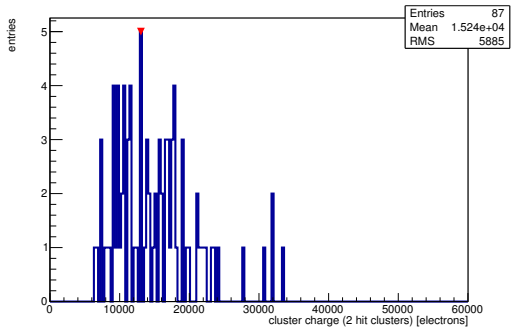

(o) Charge distribution (2 hit cluster).

Figure C.86: Detailed plots for test beam measurement of DO-I-12 (description see section 6.1) sample (running as DUT3) during runs 61257 in the September 2011 test beam period at CERN SPS in area H6B. Summary of the data in chapter 9. *(cont.)*

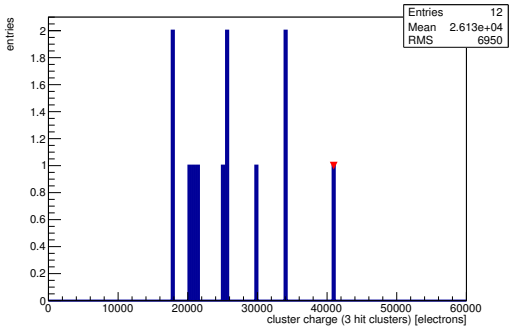

(p) Charge distribution (3 hit cluster).

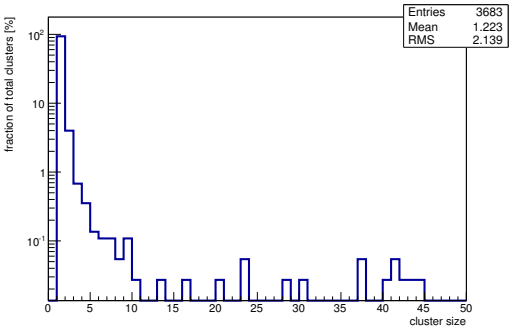

(q) Cluster size distribution.

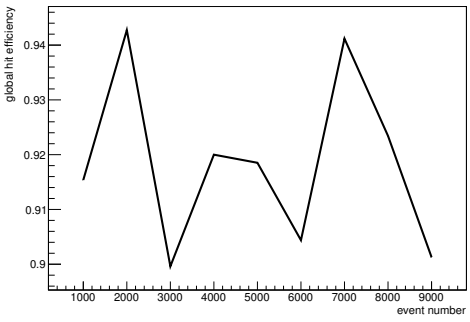

(r) Hit efficiency vs event number.

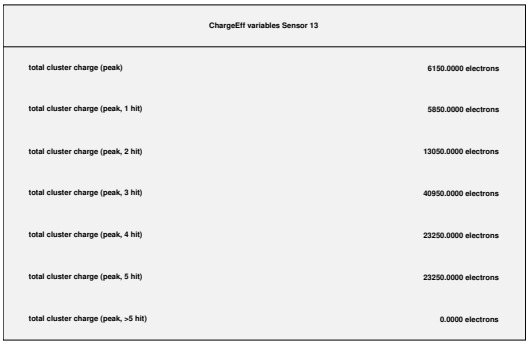

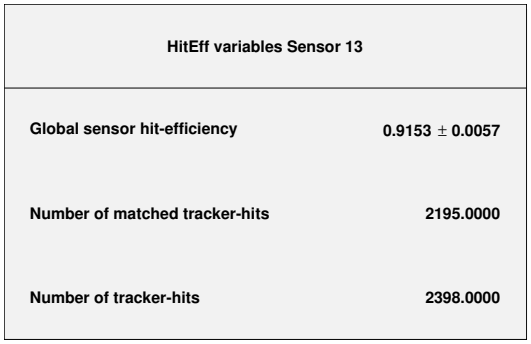

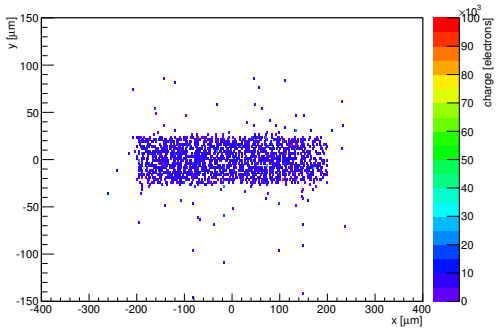

(s) Single pixel mean charge.

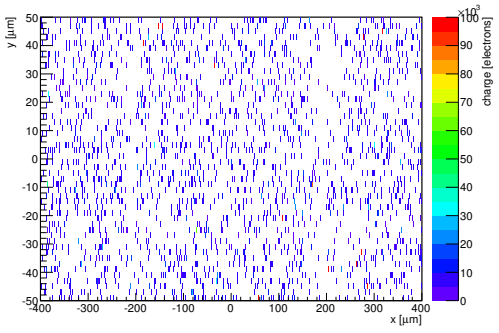

(t) Single pixel mean charge.

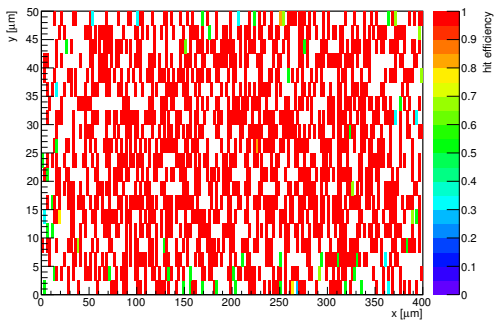

(u) Single pixel hit efficiency.

Figure C.86: Detailed plots for test beam measurement of DO-I-12 (description see section 6.1) sample (running as DUT3) during runs 61257 in the September 2011 test beam period at CERN SPS in area H6B. Summary of the data in chapter 9.

C.3.12 Runs 61258-61259

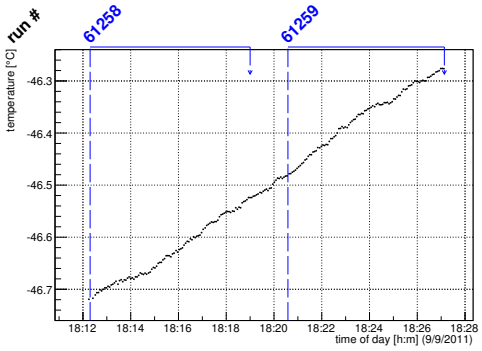

(a) Temperature vs time.

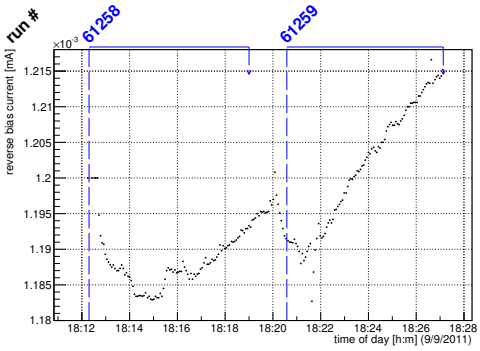

(b) Bias current vs time.

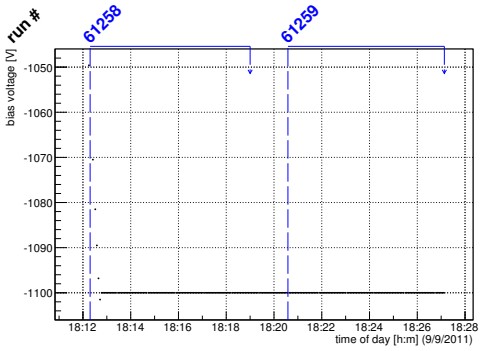

(c) Currently applied bias voltage vs time.

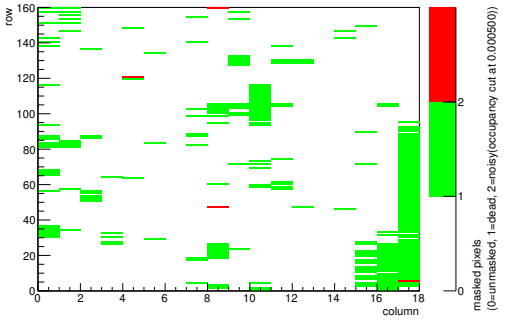

(d) Map of masked pixels.

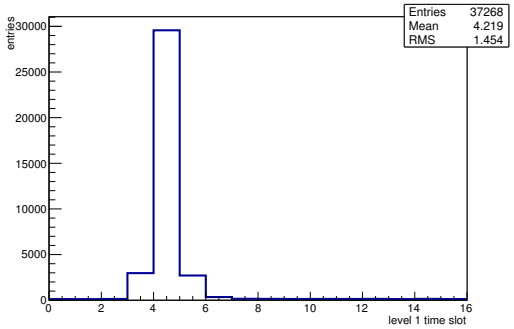

(e) Lvl1 distribution.

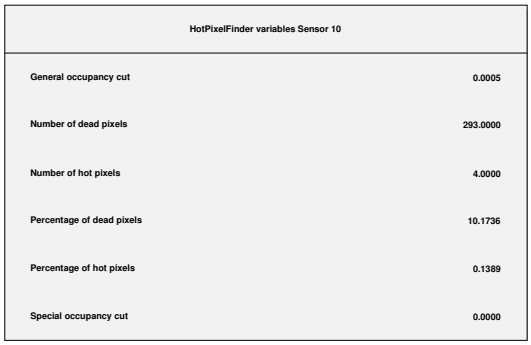

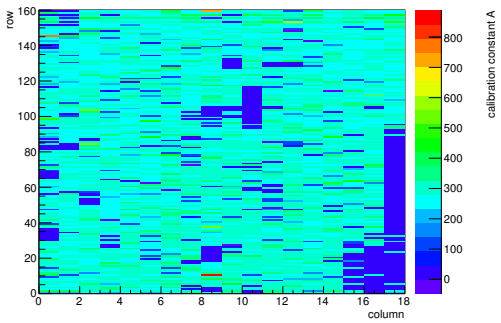

(f) Calibration constant A.

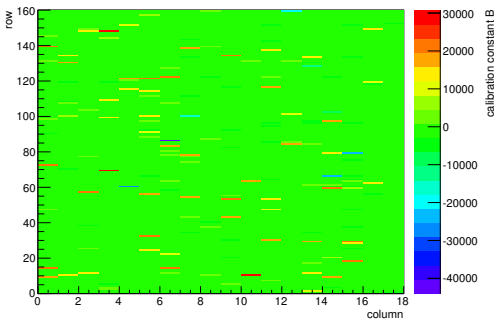

(g) Calibration constant B.

Figure C.87: Detailed plots for test beam measurement of DO-I-7 (description see section 6.1) sample (running as DUT0) during runs 61258-61259 in the September 2011 test beam period at CERN SPS in area H6B. Summary of the data in chapter 9. *(cont.)*

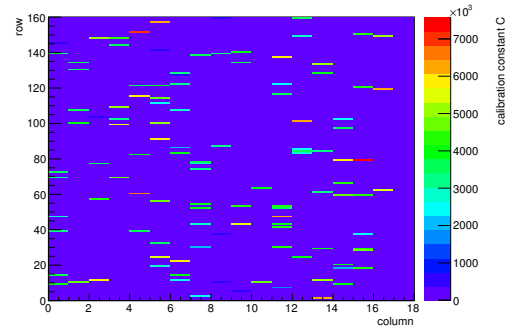

(h) Calibration constant C.

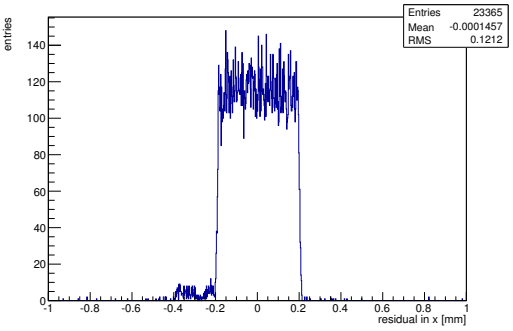

(i) Track residual in x.

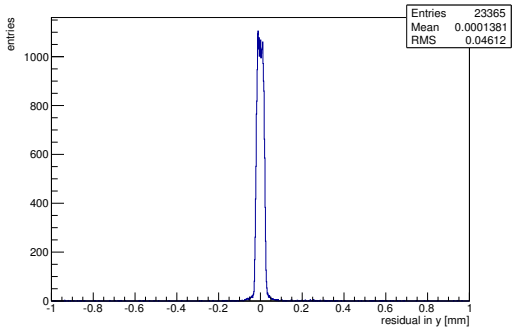

(j) Track residual in y.

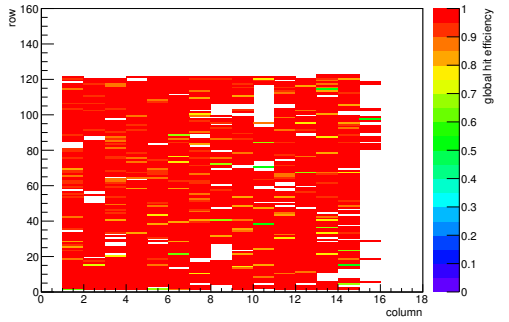

(k) Hit efficiency map.

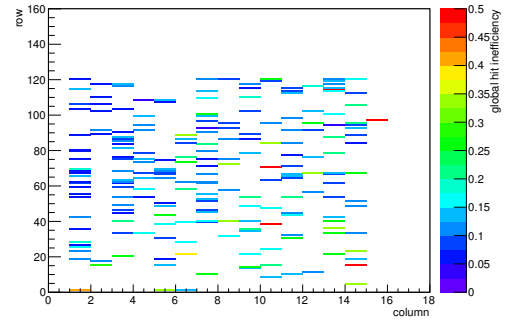

(l) Hit inefficiency map.

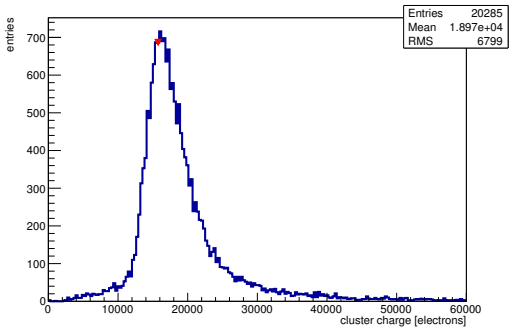

(m) Charge distribution (all cluster sizes included).

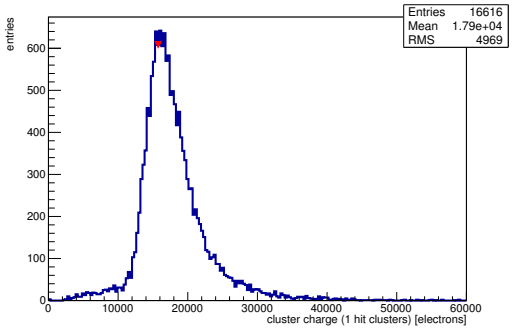

(n) Charge distribution (1 hit cluster).

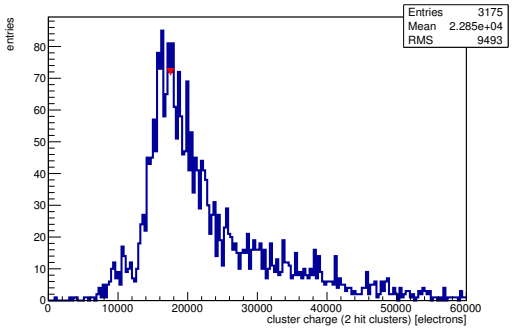

(o) Charge distribution (2 hit cluster).

Figure C.87: Detailed plots for test beam measurement of DO-I-7 (description see section 6.1) sample (running as DUT0) during runs 61258-61259 in the September 2011 test beam period at CERN SPS in area H6B. Summary of the data in chapter 9. *(cont.)*

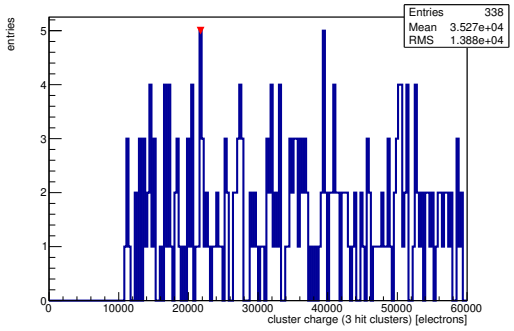

(p) Charge distribution (3 hit cluster).

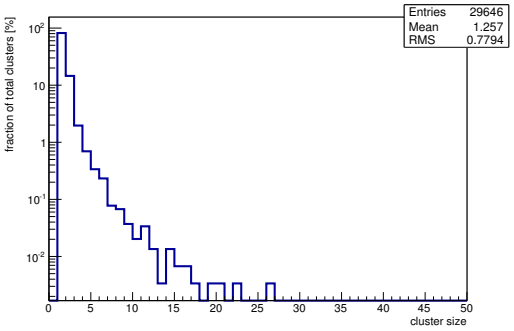

(q) Cluster size distribution.

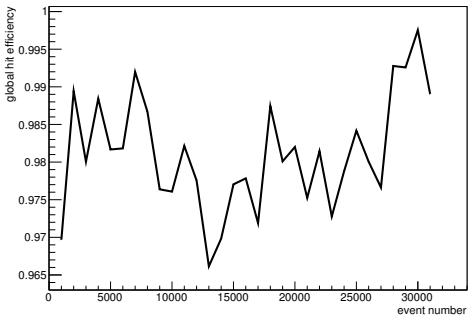

(r) Hit efficiency vs event number.

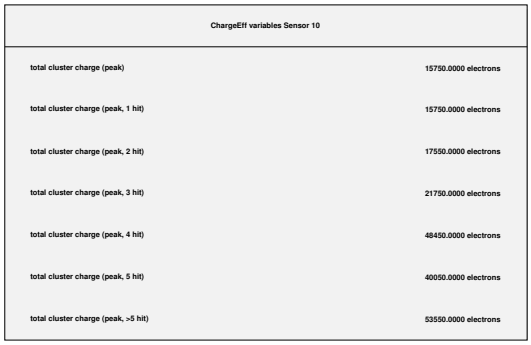

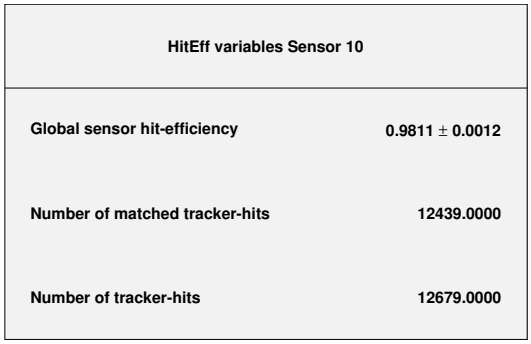

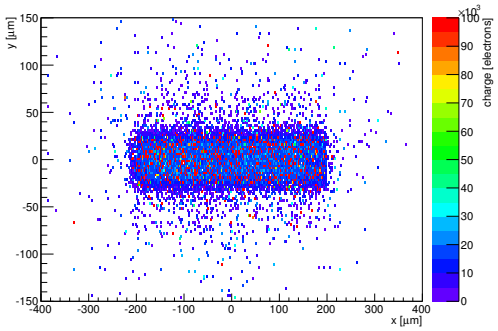

(s) Single pixel mean charge.

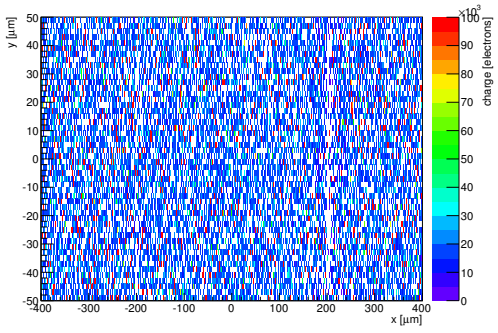

(t) Single pixel mean charge.

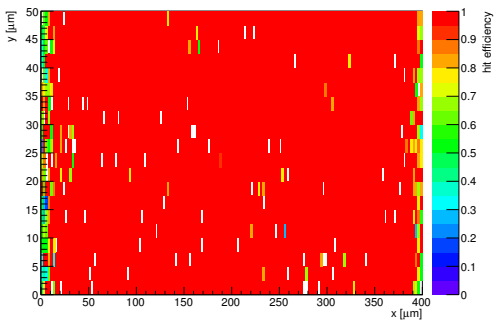

(u) Single pixel hit efficiency.

Figure C.87: Detailed plots for test beam measurement of DO-I-7 (description see section 6.1) sample (running as DUT0) during runs 61258-61259 in the September 2011 test beam period at CERN SPS in area H6B. Summary of the data in chapter 9.

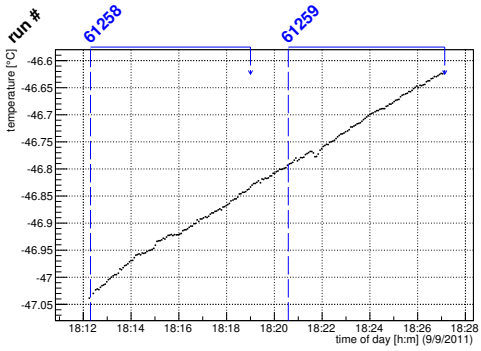

(a) Temperature vs time.

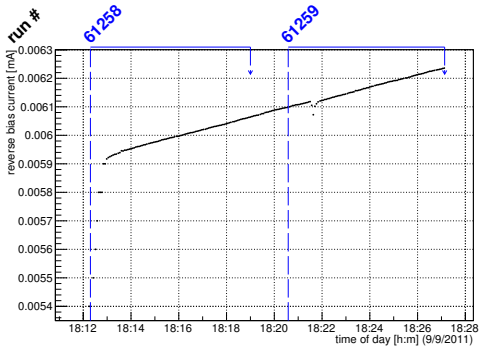

(b) Bias current vs time.

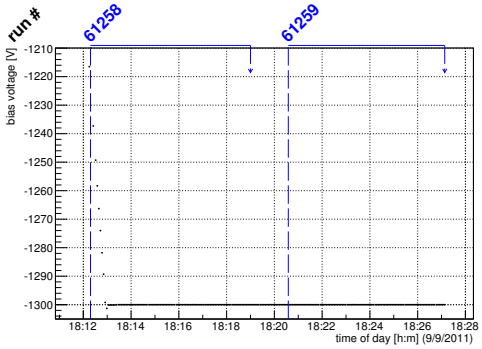

(c) Currently applied bias voltage vs time.

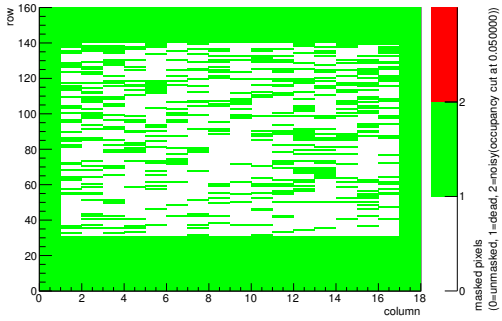

(d) Map of masked pixels.

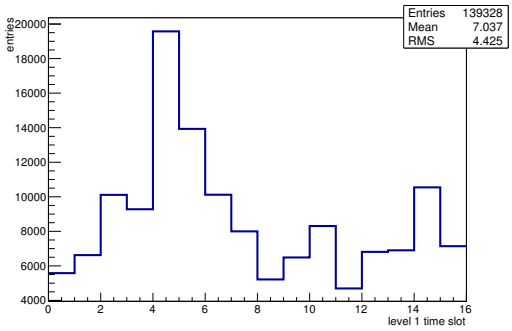

(e) Lvl1 distribution.

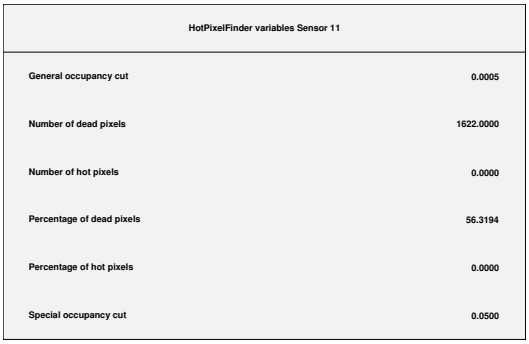

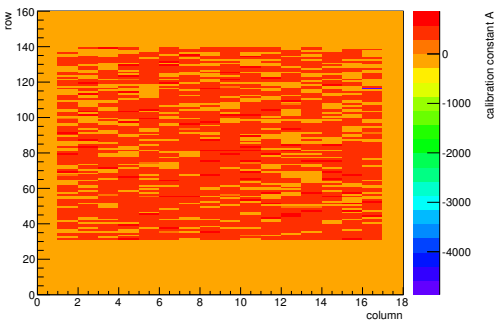

(f) Calibration constant A.

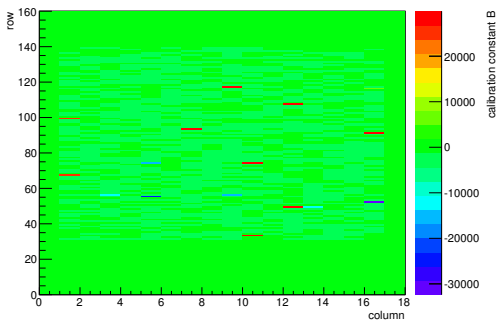

(g) Calibration constant B.

Figure C.88: Detailed plots for test beam measurement of DO-I-11 (description see section 6.1) sample (running as DUT1) during runs 61258-61259 in the September 2011 test beam period at CERN SPS in area H6B. Summary of the data in chapter 9. *(cont.)*

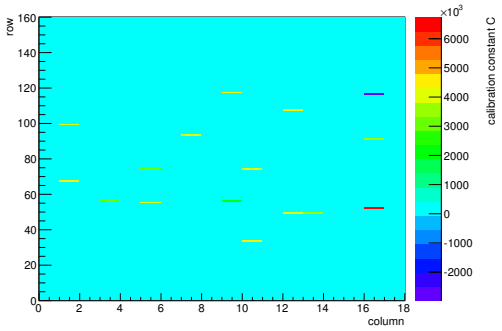

(h) Calibration constant C.

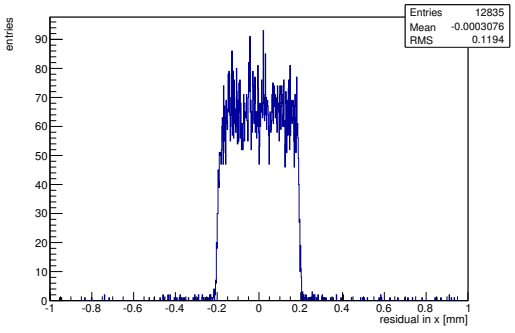

(i) Track residual in x.

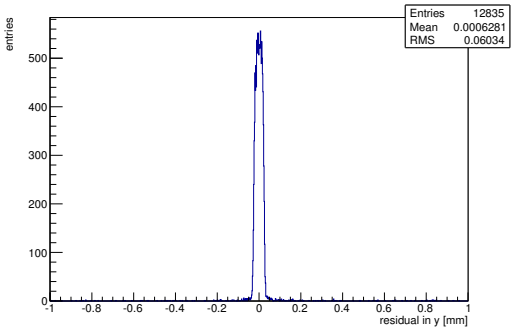

(j) Track residual in y.

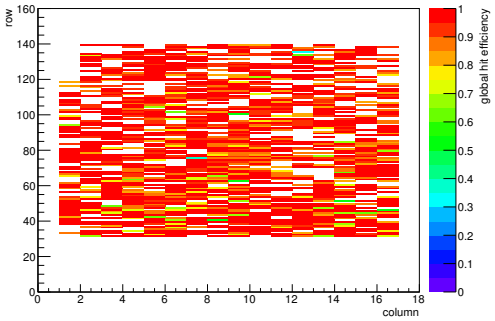

(k) Hit efficiency map.

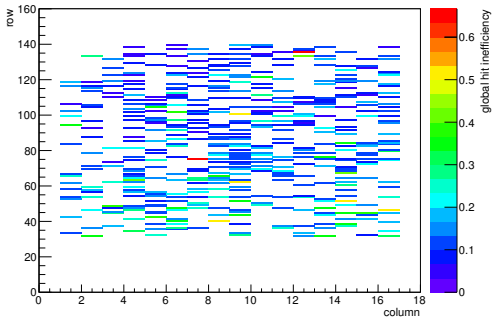

(l) Hit inefficiency map.

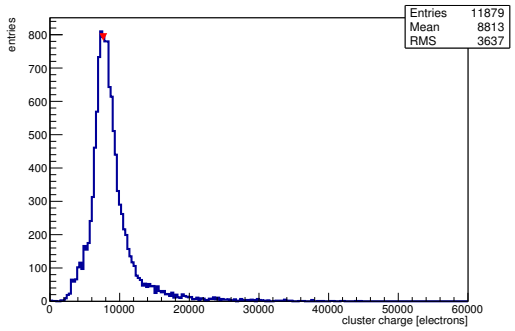

(m) Charge distribution (all cluster sizes included).

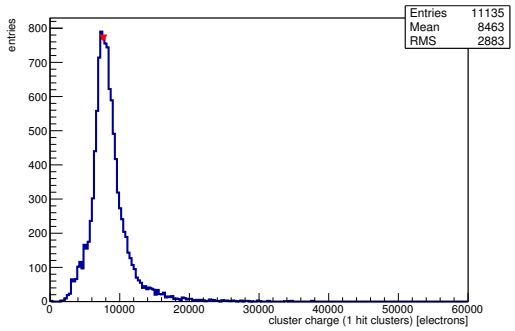

(n) Charge distribution (1 hit cluster).

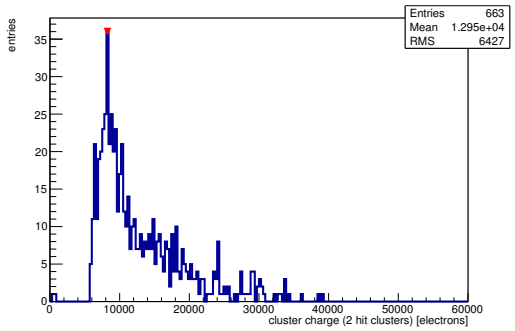

(o) Charge distribution (2 hit cluster).

Figure C.88: Detailed plots for test beam measurement of DO-I-11 (description see section 6.1) sample (running as DUT1) during runs 61258-61259 in the September 2011 test beam period at CERN SPS in area H6B. Summary of the data in chapter 9. *(cont.)*

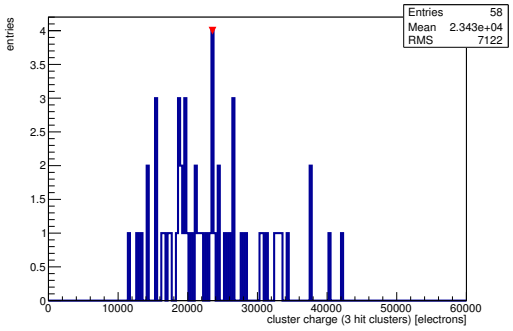

(p) Charge distribution (3 hit cluster).

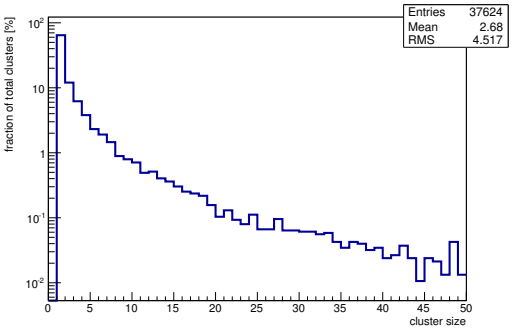

(q) Cluster size distribution.

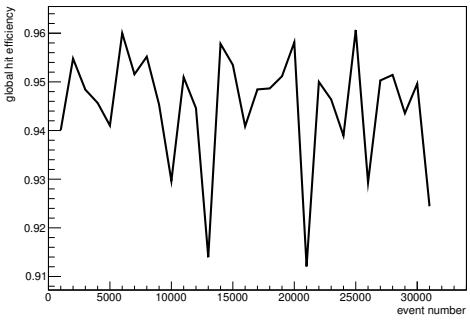

(r) Hit efficiency vs event number.

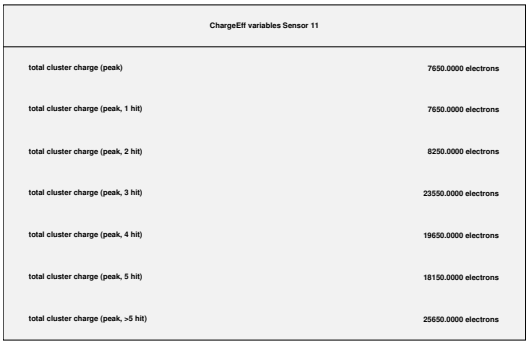

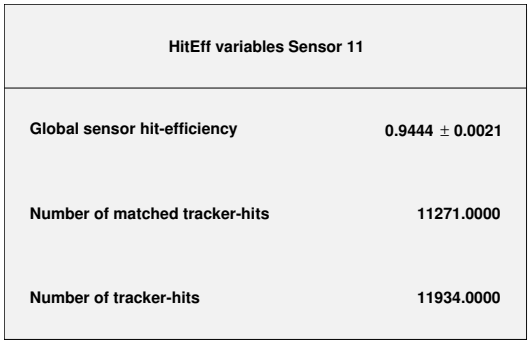

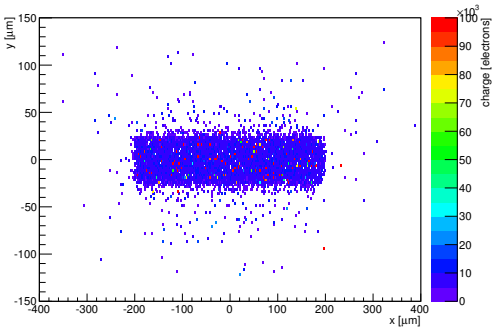

(s) Single pixel mean charge.

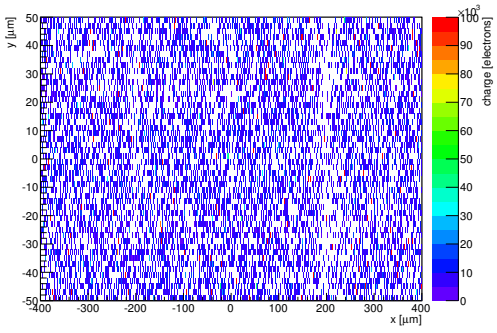

(t) Single pixel mean charge.

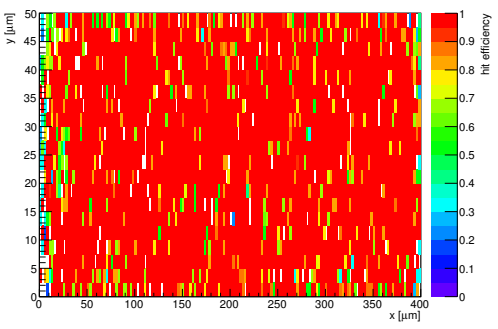

(u) Single pixel hit efficiency.

Figure C.88: Detailed plots for test beam measurement of DO-I-11 (description see section 6.1) sample (running as DUT1) during runs 61258-61259 in the September 2011 test beam period at CERN SPS in area H6B. Summary of the data in chapter 9.

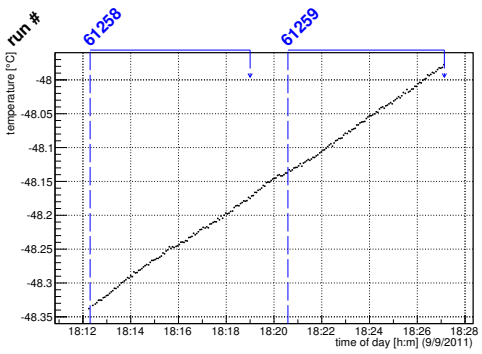

(a) Temperature vs time.

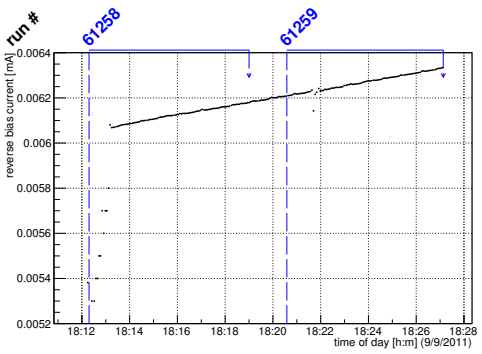

(b) Bias current vs time.

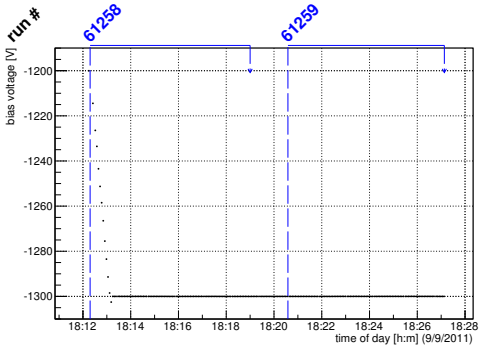

(c) Currently applied bias voltage vs time.

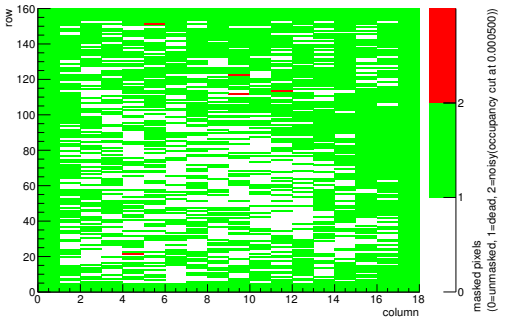

(d) Map of masked pixels.

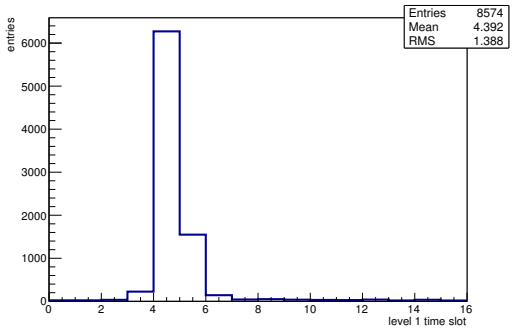

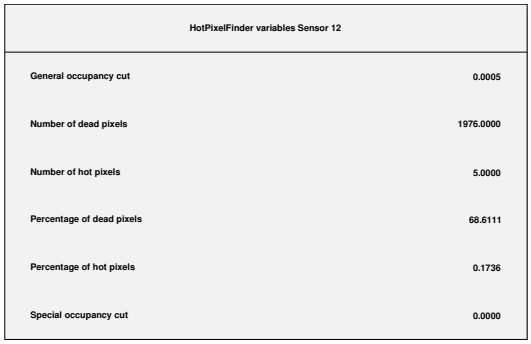

(e) Lvl1 distribution.

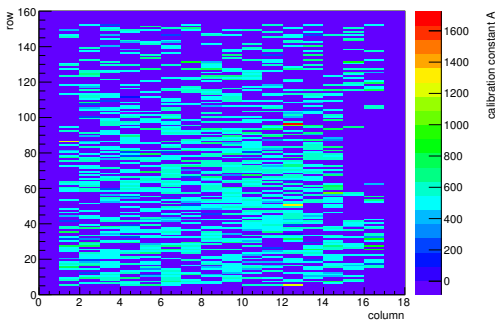

(f) Calibration constant A.

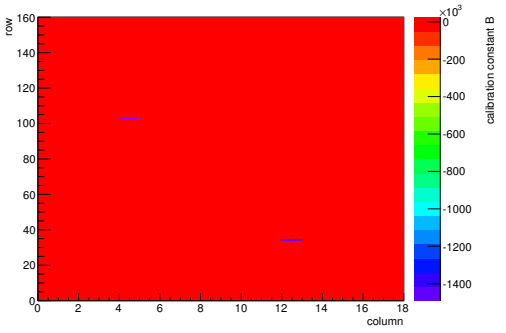

(g) Calibration constant B.

Figure C.89: Detailed plots for test beam measurement of DO-I-5 (description see section 6.1) sample (running as DUT2) during runs 61258-61259 in the September 2011 test beam period at CERN SPS in area H6B. Summary of the data in chapter 9. *(cont.)*

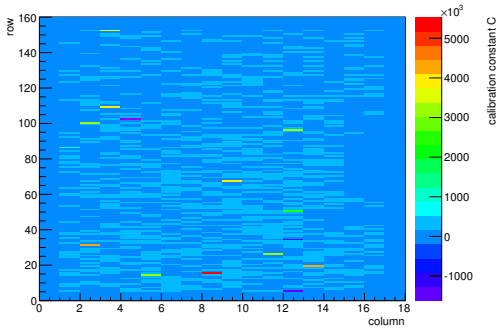

(h) Calibration constant C.

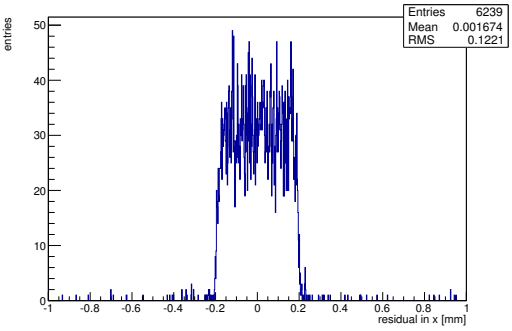

(i) Track residual in x.

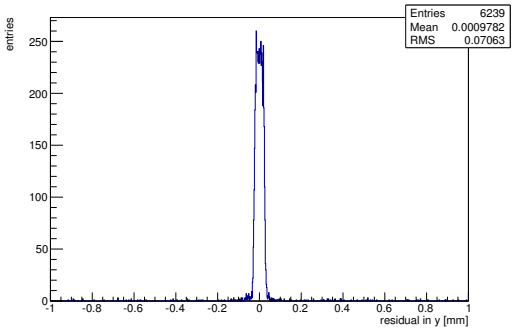

(j) Track residual in y.

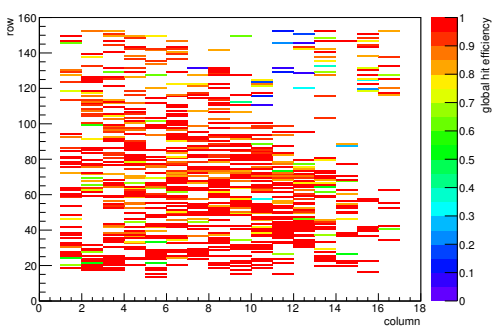

(k) Hit efficiency map.

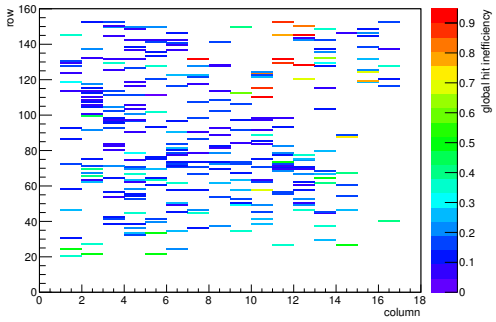

(l) Hit inefficiency map.

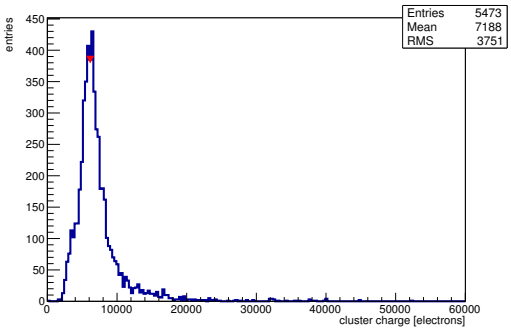

(m) Charge distribution (all cluster sizes included).

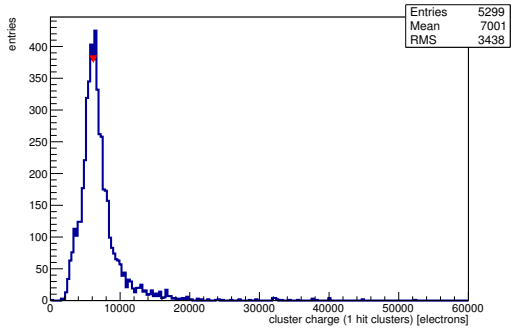

(n) Charge distribution (1 hit cluster).

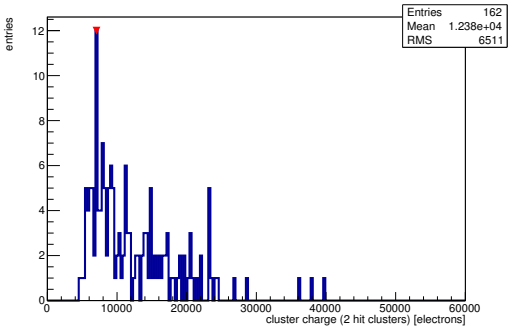

(o) Charge distribution (2 hit cluster).

Figure C.89: Detailed plots for test beam measurement of DO-I-5 (description see section 6.1) sample (running as DUT2) during runs 61258-61259 in the September 2011 test beam period at CERN SPS in area H6B. Summary of the data in chapter 9. *(cont.)*

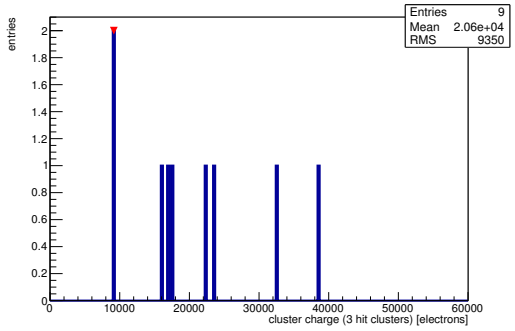

(p) Charge distribution (3 hit cluster).

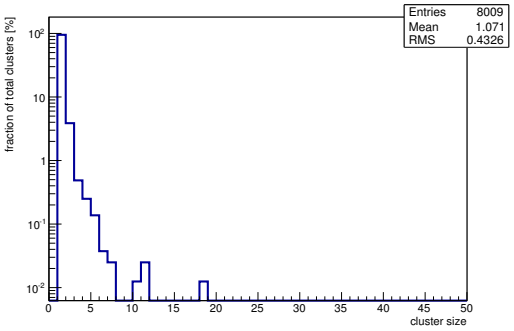

(q) Cluster size distribution.

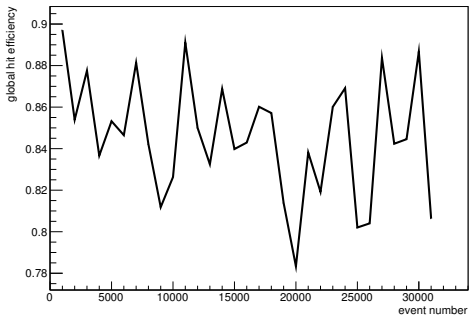

(r) Hit efficiency vs event number.

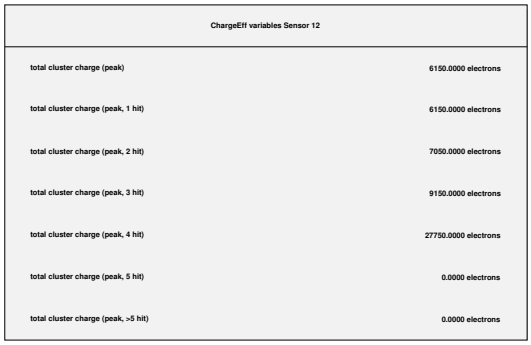

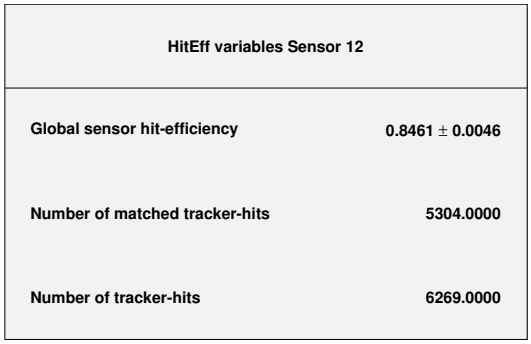

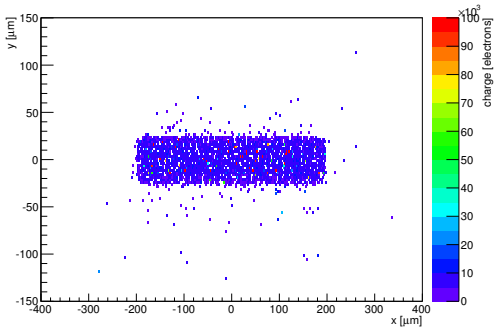

(s) Single pixel mean charge.

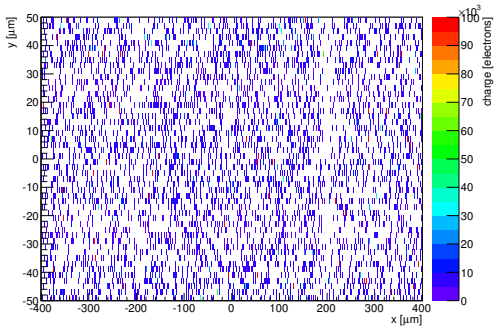

(t) Single pixel mean charge.

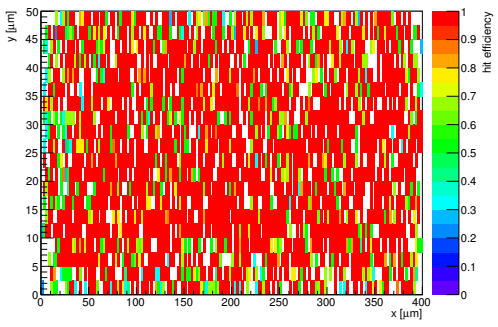

(u) Single pixel hit efficiency.

Figure C.89: Detailed plots for test beam measurement of DO-I-5 (description see section 6.1) sample (running as DUT2) during runs 61258-61259 in the September 2011 test beam period at CERN SPS in area H6B. Summary of the data in chapter 9.

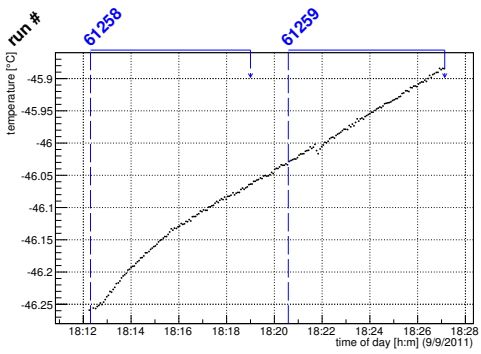

(a) Temperature vs time.

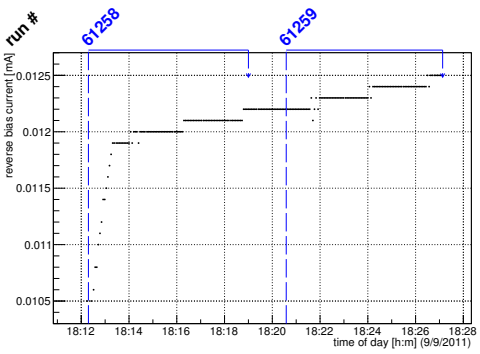

(b) Bias current vs time.

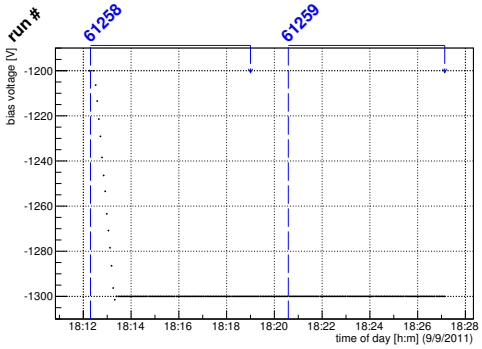

(c) Currently applied bias voltage vs time.

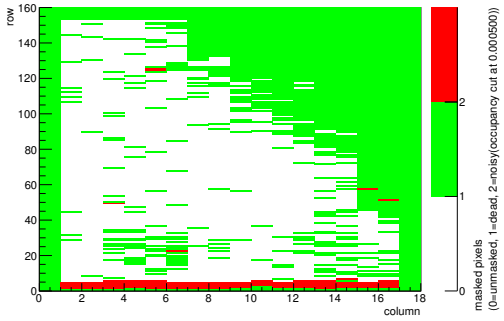

(d) Map of masked pixels.

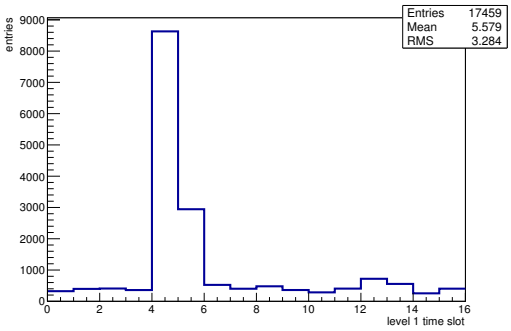

(e) Lvl1 distribution.

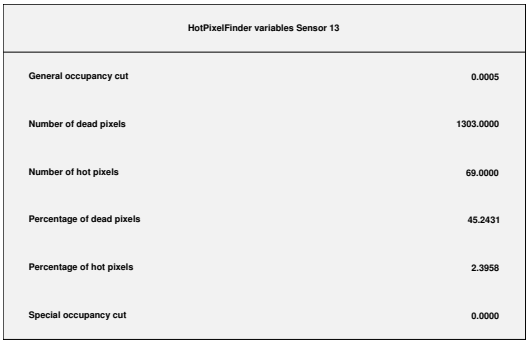

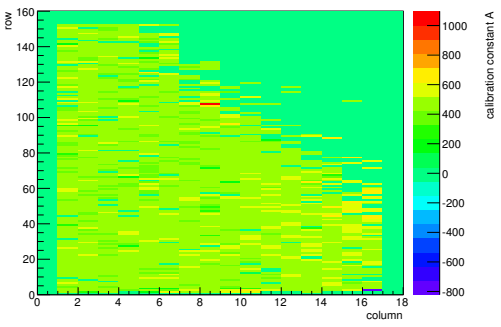

(f) Calibration constant A.

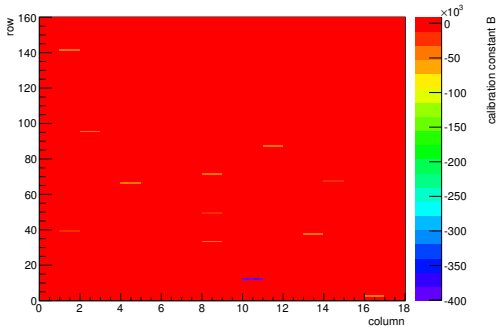

(g) Calibration constant B.

Figure C.90: Detailed plots for test beam measurement of DO-I-12 (description see section 6.1) sample (running as DUT3) during runs 61258-61259 in the September 2011 test beam period at CERN SPS in area H6B. Summary of the data in chapter 9. *(cont.)*

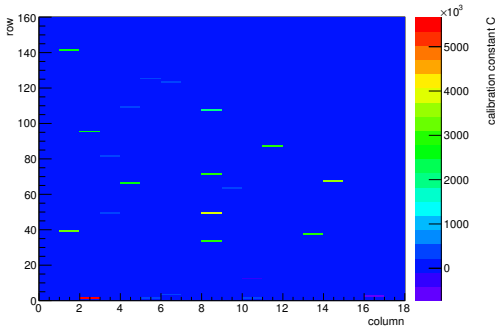

(h) Calibration constant C.

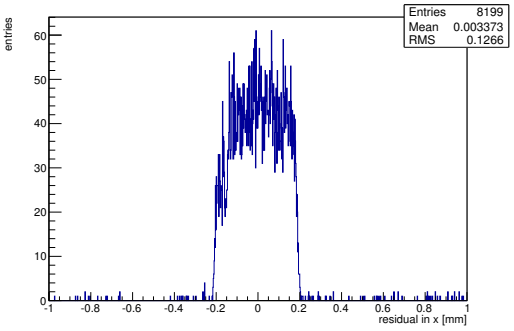

(i) Track residual in x.

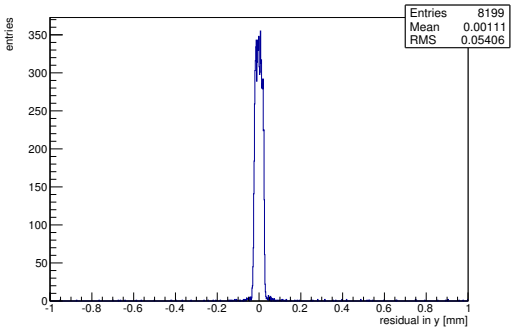

(j) Track residual in y.

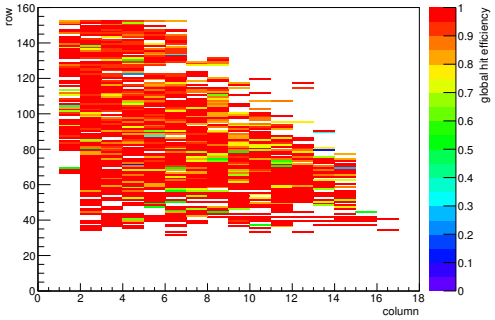

(k) Hit efficiency map.

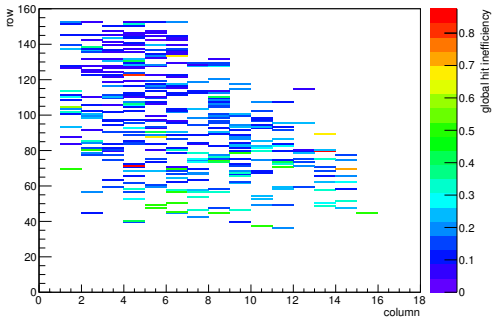

(l) Hit inefficiency map.

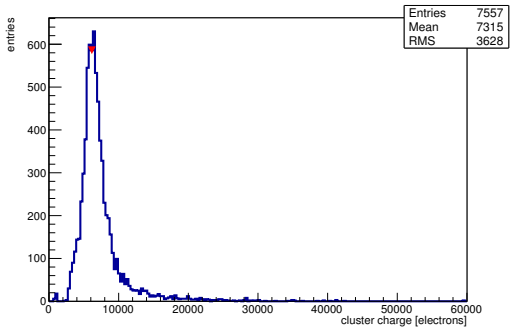

(m) Charge distribution (all cluster sizes included).

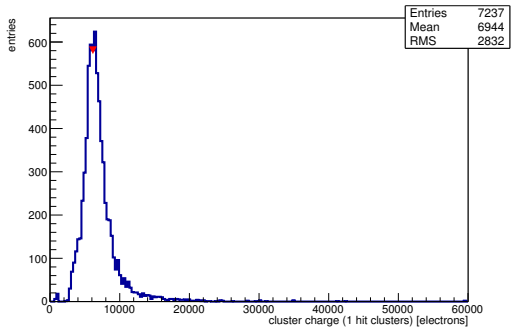

(n) Charge distribution (1 hit cluster).

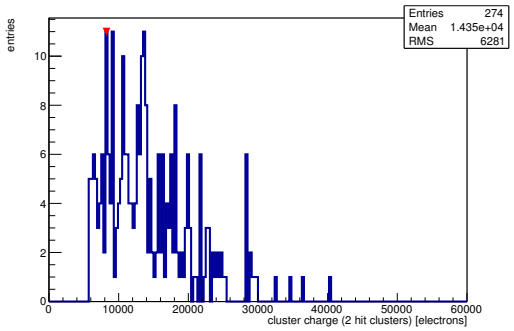

(o) Charge distribution (2 hit cluster).

Figure C.90: Detailed plots for test beam measurement of DO-I-12 (description see section 6.1) sample (running as DUT3) during runs 61258-61259 in the September 2011 test beam period at CERN SPS in area H6B. Summary of the data in chapter 9. *(cont.)*

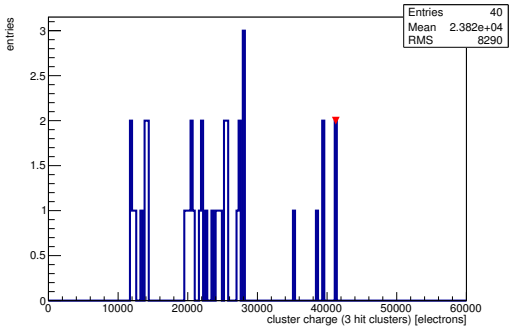

(p) Charge distribution (3 hit cluster).

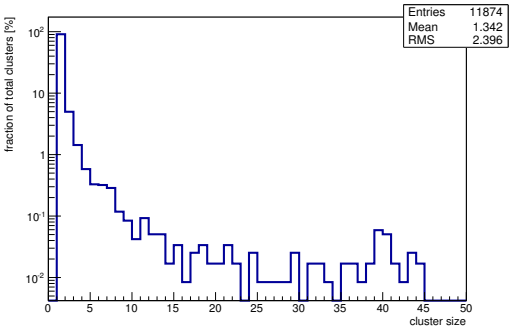

(q) Cluster size distribution.

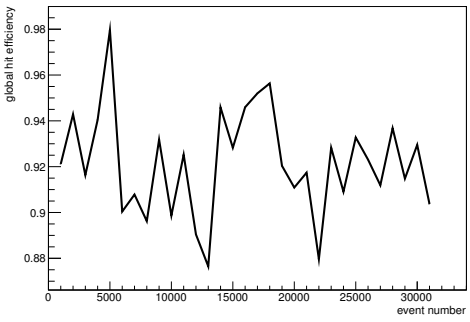

(r) Hit efficiency vs event number.

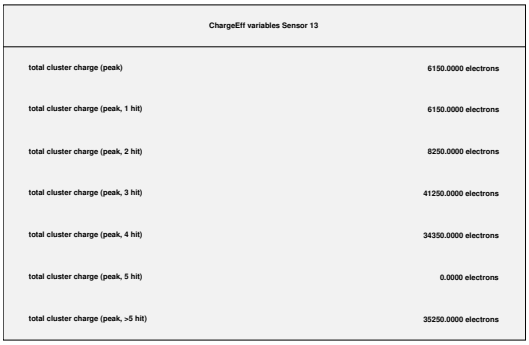

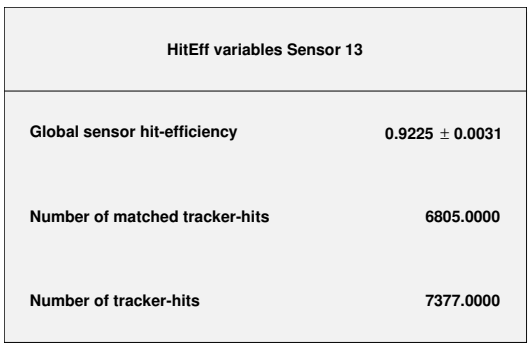

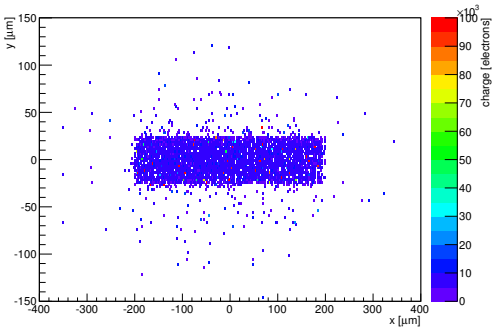

(s) Single pixel mean charge.

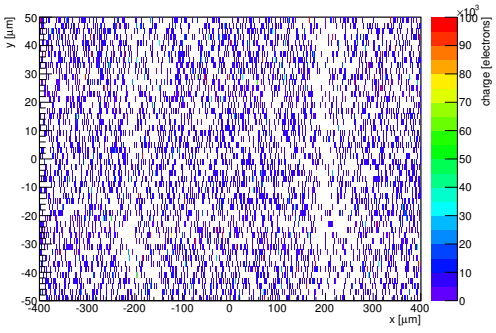

(t) Single pixel mean charge.

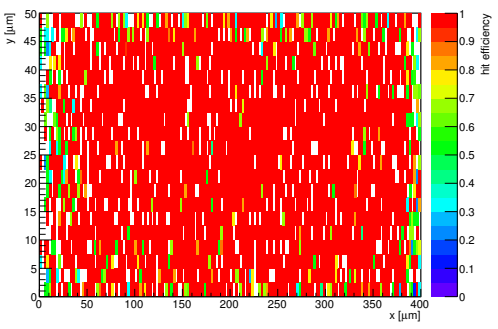

(u) Single pixel hit efficiency.

Figure C.90: Detailed plots for test beam measurement of DO-I-12 (description see section 6.1) sample (running as DUT3) during runs 61258-61259 in the September 2011 test beam period at CERN SPS in area H6B. Summary of the data in chapter 9.

C.3.13 Run 61260

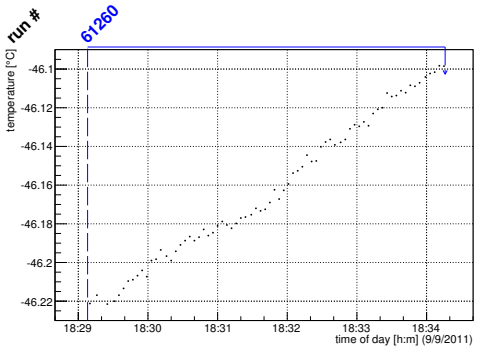

(a) Temperature vs time.

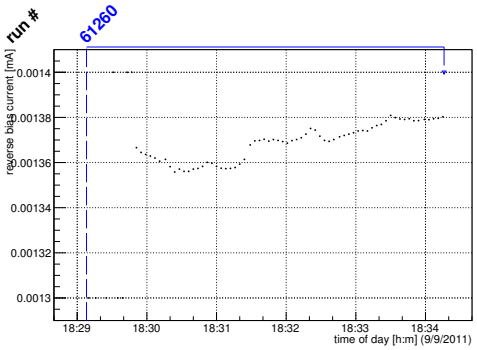

(b) Bias current vs time.

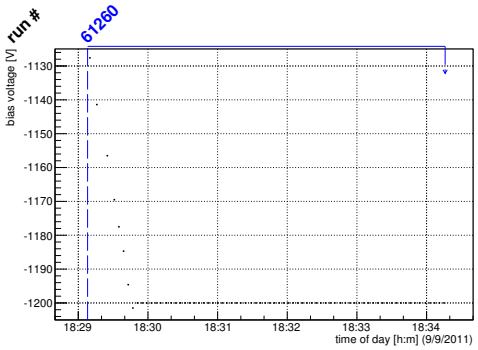

(c) Currently applied bias voltage vs time.

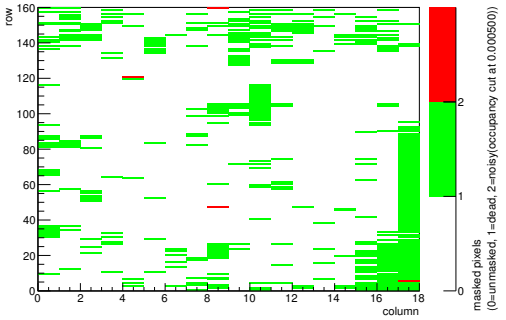

(d) Map of masked pixels.

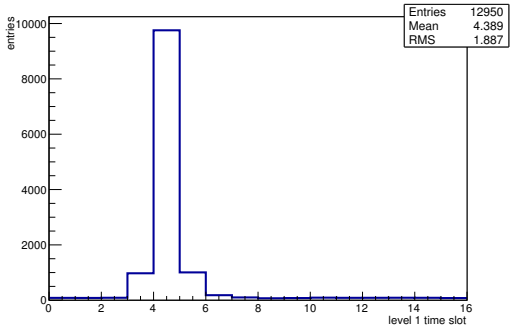

(e) Lvl1 distribution.

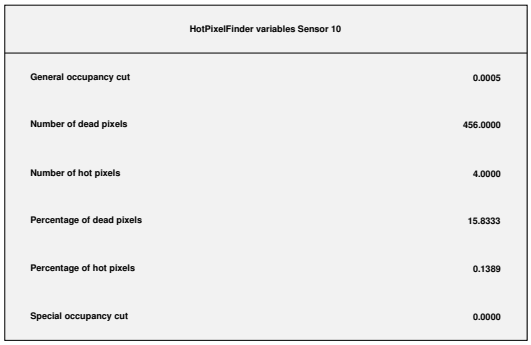

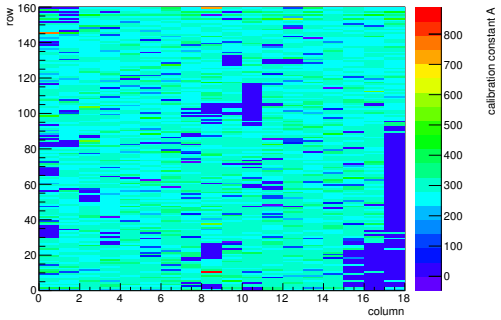

(f) Calibration constant A.

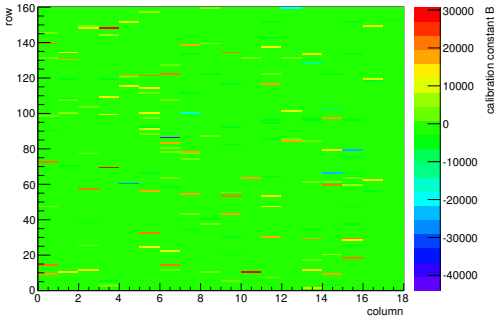

(g) Calibration constant B.

Figure C.91: Detailed plots for test beam measurement of DO-I-7 (description see section 6.1) sample (running as DUT0) during runs 61260 in the September 2011 test beam period at CERN SPS in area H6B. Summary of the data in chapter 9. *(cont.)*

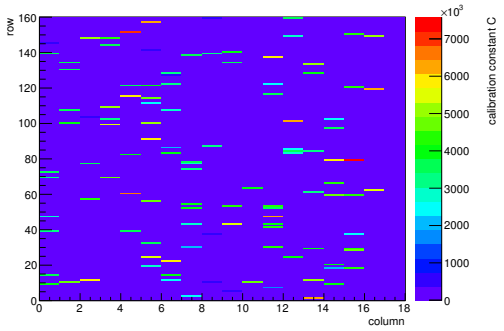

(h) Calibration constant C.

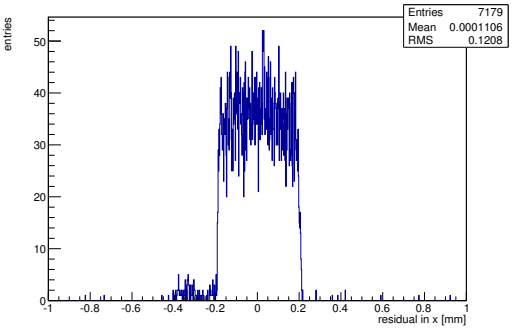

(i) Track residual in x.

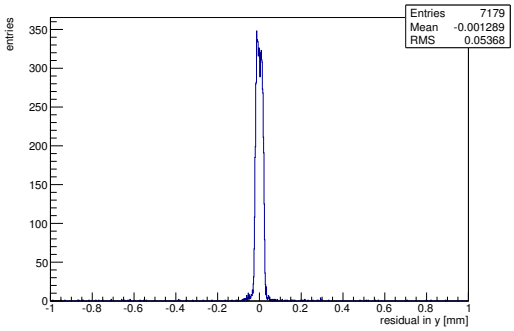

(j) Track residual in y.

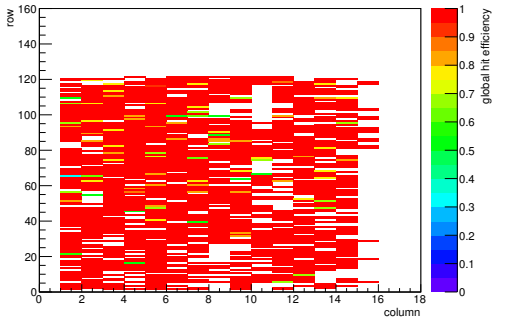

(k) Hit efficiency map.

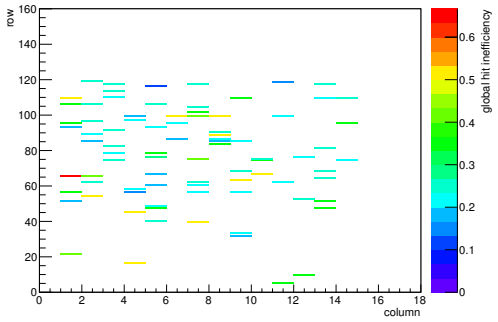

(l) Hit inefficiency map.

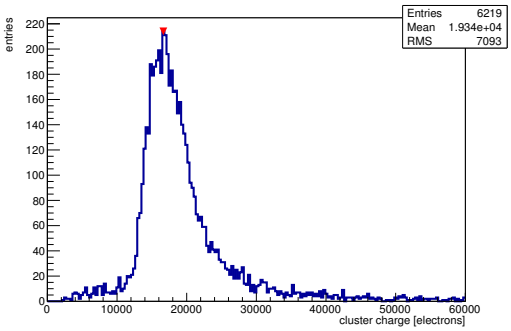

(m) Charge distribution (all cluster sizes included).

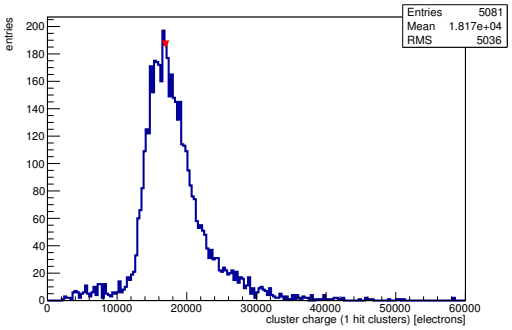

(n) Charge distribution (1 hit cluster).

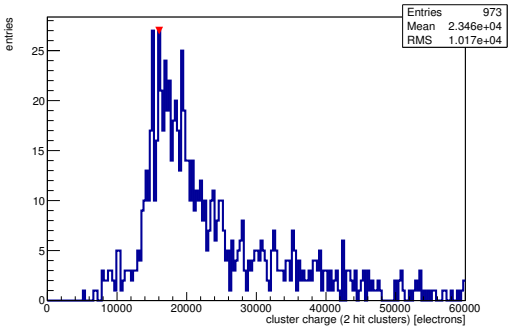

(o) Charge distribution (2 hit cluster).

Figure C.91: Detailed plots for test beam measurement of DO-I-7 (description see section 6.1) sample (running as DUT0) during runs 61260 in the September 2011 test beam period at CERN SPS in area H6B. Summary of the data in chapter 9. *(cont.)*

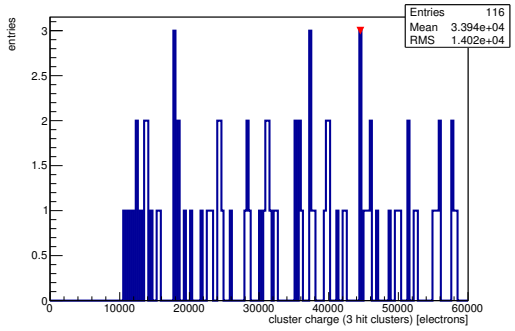

(p) Charge distribution (3 hit cluster).

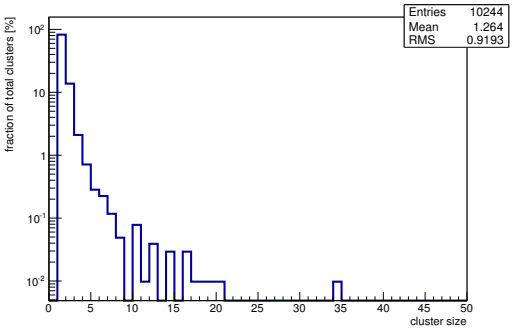

(q) Cluster size distribution.

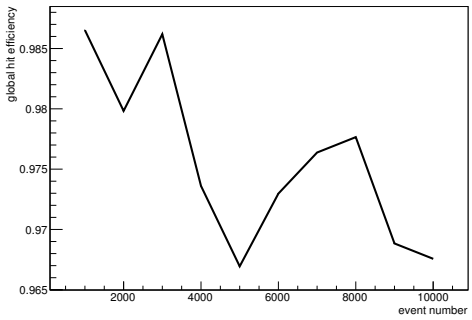

(r) Hit efficiency vs event number.

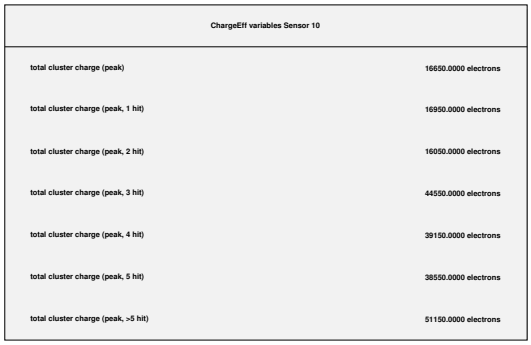

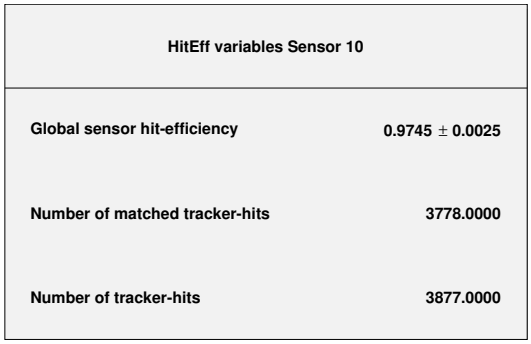

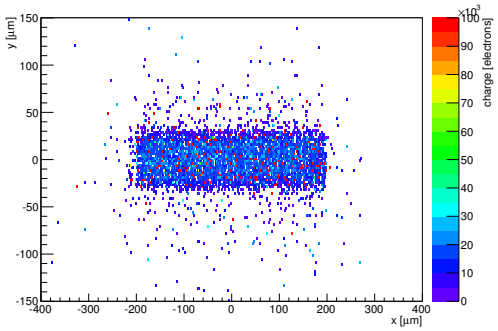

(s) Single pixel mean charge.

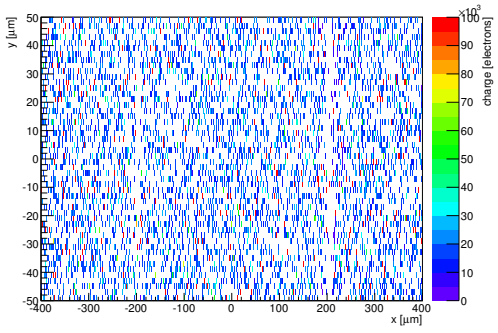

(t) Single pixel mean charge.

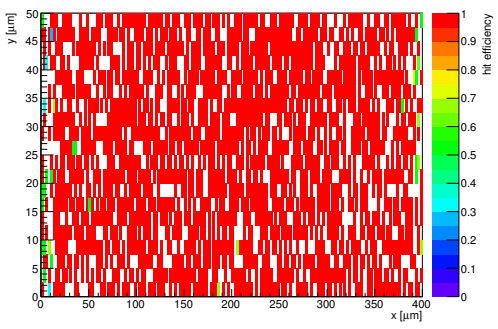

(u) Single pixel hit efficiency.

Figure C.91: Detailed plots for test beam measurement of DO-I-7 (description see section 6.1) sample (running as DUT0) during runs 61260 in the September 2011 test beam period at CERN SPS in area H6B. Summary of the data in chapter 9.

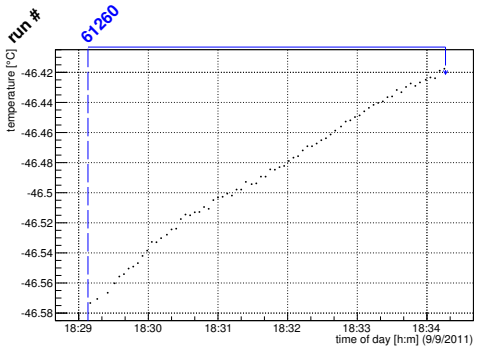

(a) Temperature vs time.

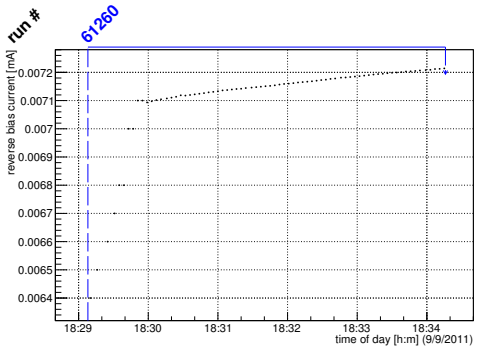

(b) Bias current vs time.

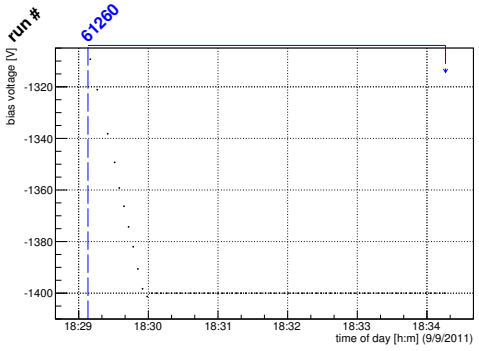

(c) Currently applied bias voltage vs time.

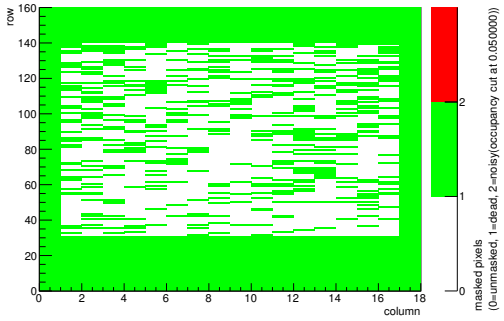

(d) Map of masked pixels.

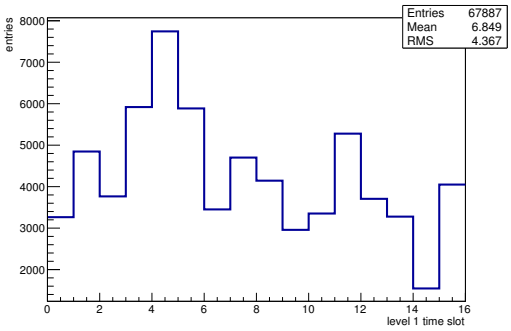

(e) Lvl1 distribution.

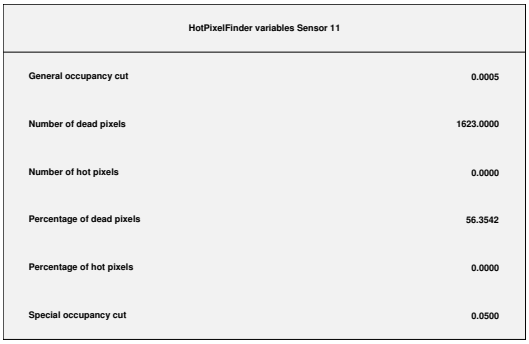

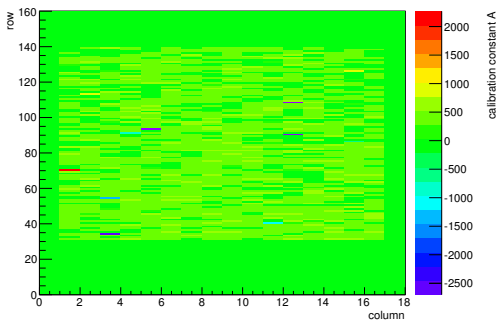

(f) Calibration constant A.

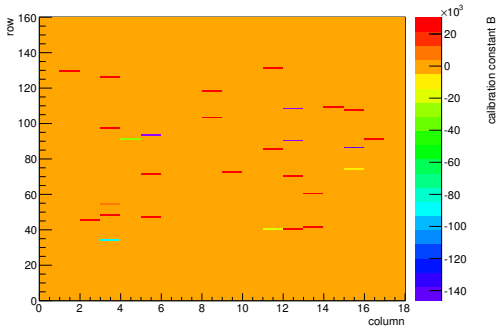

(g) Calibration constant B.

Figure C.92: Detailed plots for test beam measurement of DO-I-11 (description see section 6.1) sample (running as DUT1) during runs 61260 in the September 2011 test beam period at CERN SPS in area H6B. Summary of the data in chapter 9. *(cont.)*

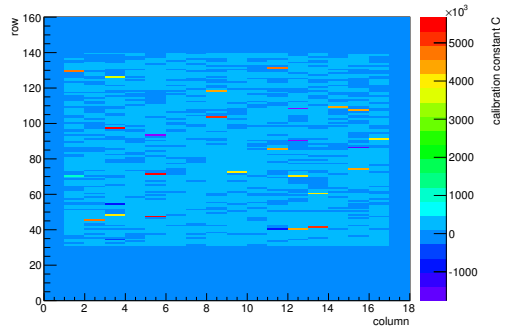

(h) Calibration constant C.

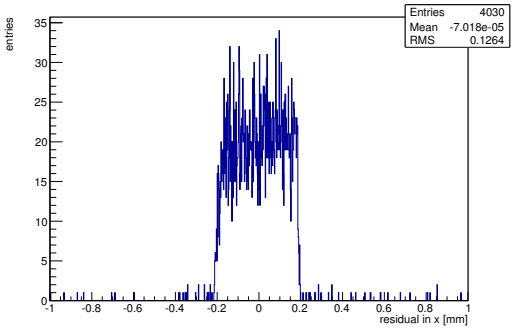

(i) Track residual in x.

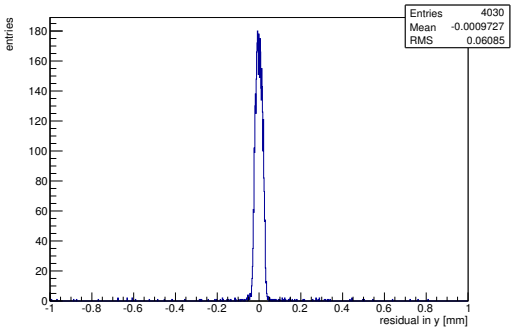

(j) Track residual in y.

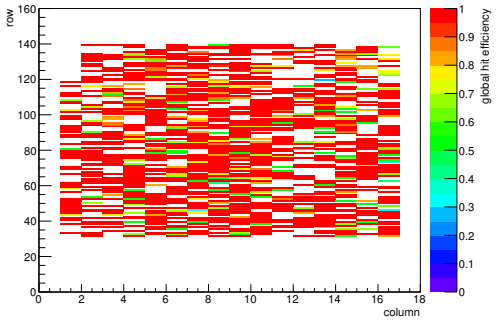

(k) Hit efficiency map.

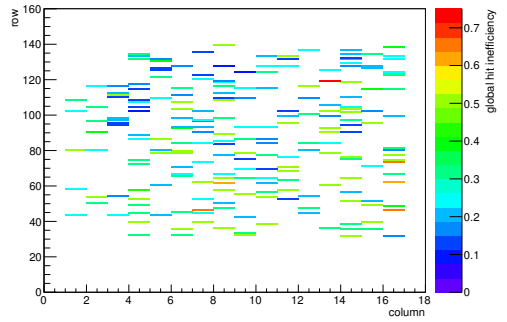

(l) Hit inefficiency map.

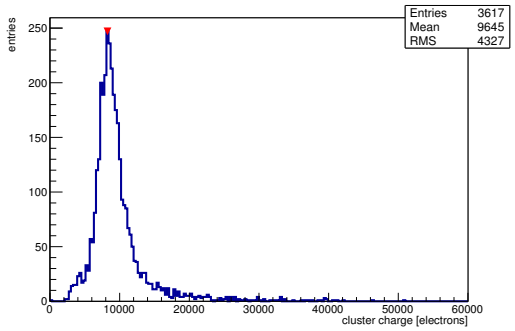

(m) Charge distribution (all cluster sizes included).

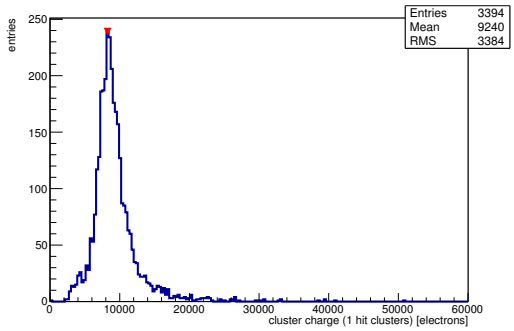

(n) Charge distribution (1 hit cluster).

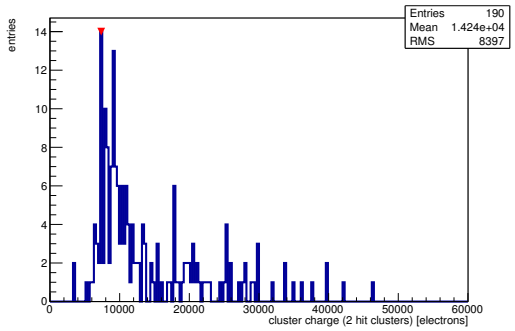

(o) Charge distribution (2 hit cluster).

Figure C.92: Detailed plots for test beam measurement of DO-I-11 (description see section 6.1) sample (running as DUT1) during runs 61260 in the September 2011 test beam period at CERN SPS in area H6B. Summary of the data in chapter 9. *(cont.)*

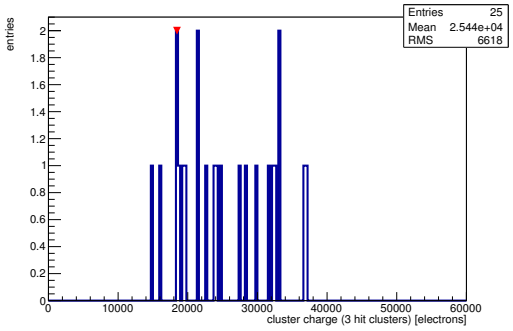

(p) Charge distribution (3 hit cluster).

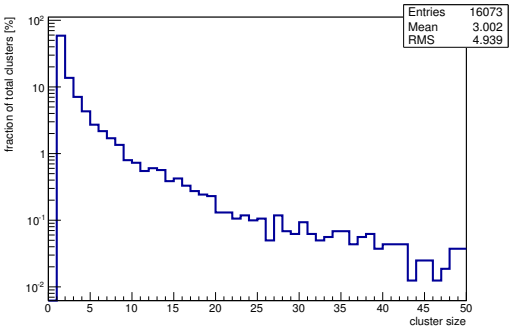

(q) Cluster size distribution.

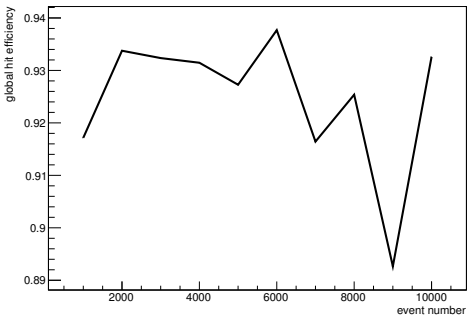

(r) Hit efficiency vs event number.

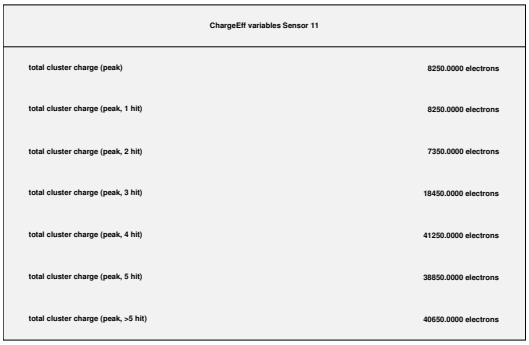

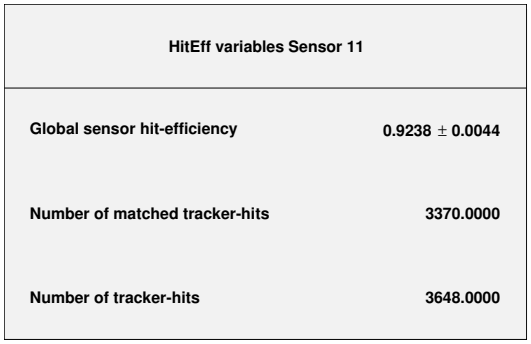

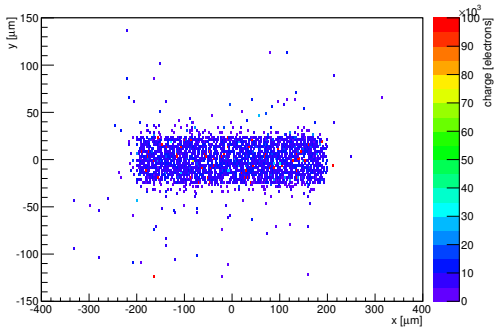

(s) Single pixel mean charge.

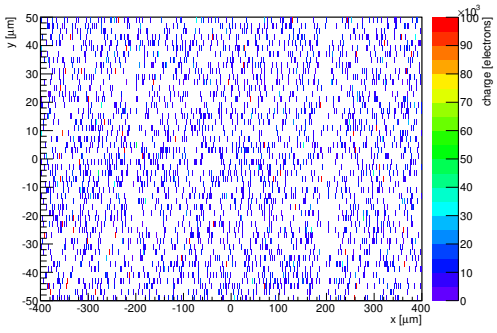

(t) Single pixel mean charge.

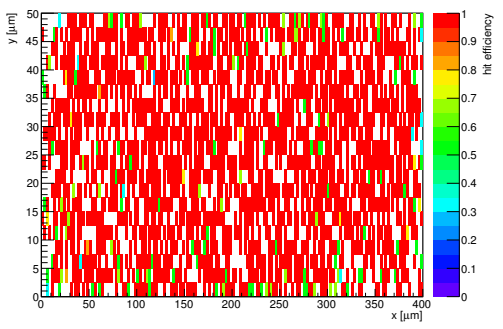

(u) Single pixel hit efficiency.

Figure C.92: Detailed plots for test beam measurement of DO-I-11 (description see section 6.1) sample (running as DUT1) during runs 61260 in the September 2011 test beam period at CERN SPS in area H6B. Summary of the data in chapter 9.

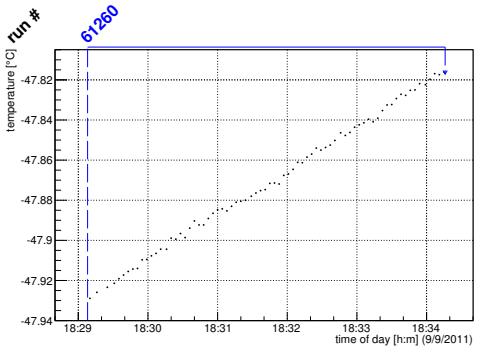

(a) Temperature vs time.

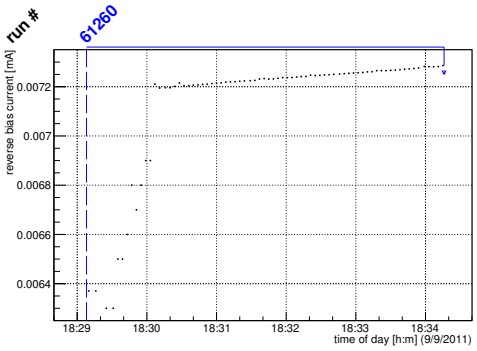

(b) Bias current vs time.

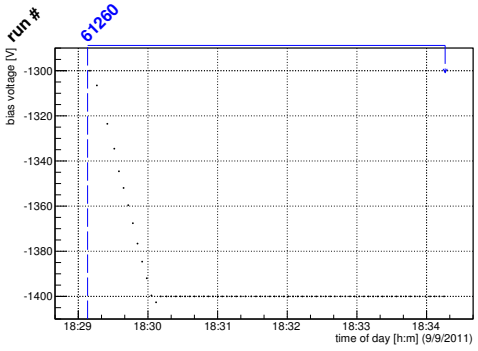

(c) Currently applied bias voltage vs time.

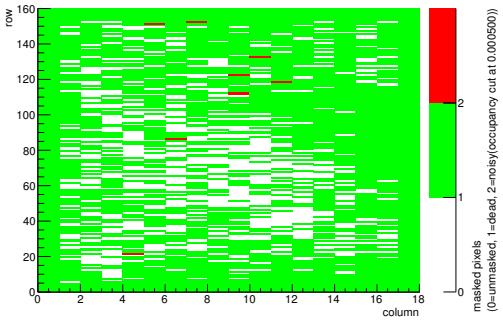

(d) Map of masked pixels.

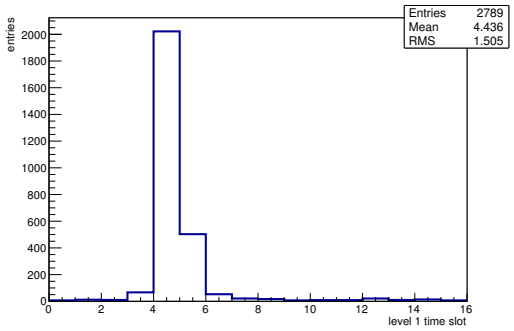

(e) Lvl1 distribution.

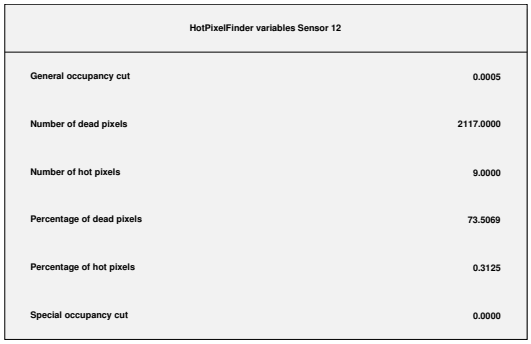

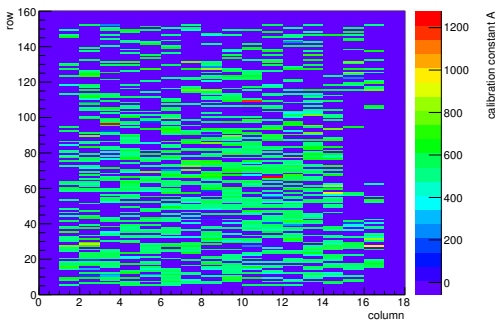

(f) Calibration constant A.

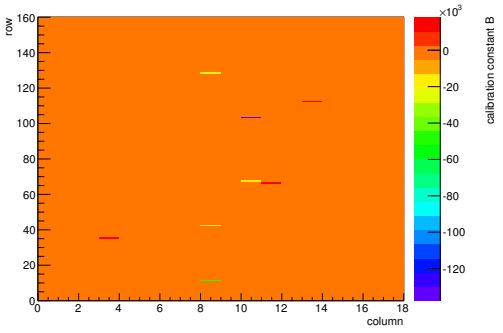

(g) Calibration constant B.

Figure C.93: Detailed plots for test beam measurement of DO-I-5 (description see section 6.1) sample (running as DUT2) during runs 61260 in the September 2011 test beam period at CERN SPS in area H6B. Summary of the data in chapter 9. *(cont.)*

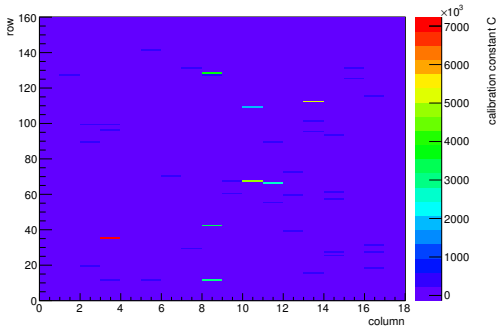

(h) Calibration constant C.

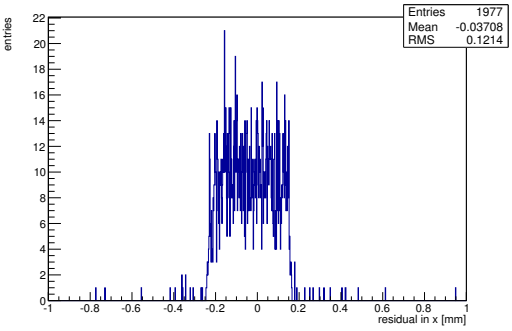

(i) Track residual in x.

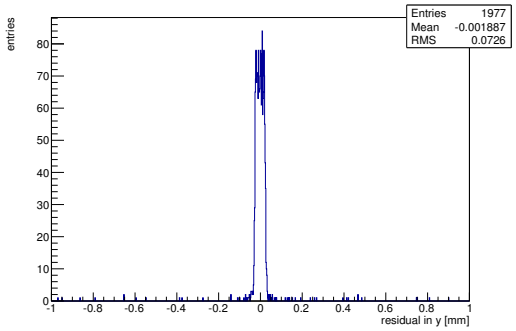

(j) Track residual in y.

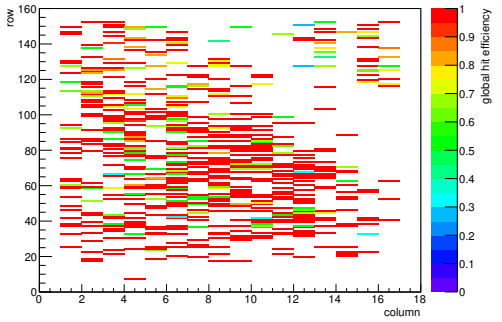

(k) Hit efficiency map.

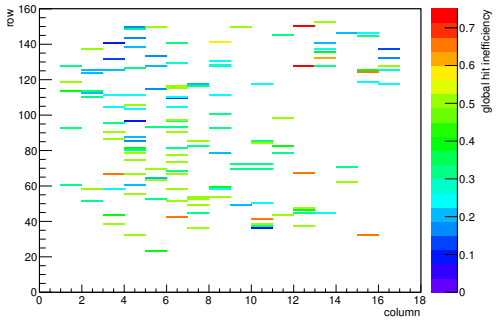

(l) Hit inefficiency map.

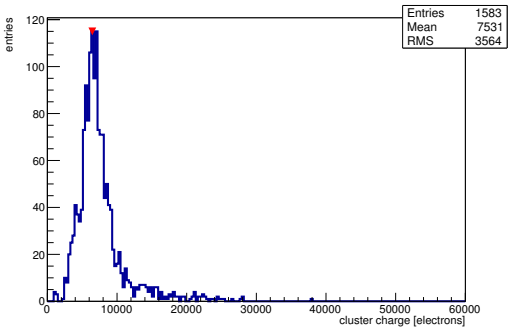

(m) Charge distribution (all cluster sizes included).

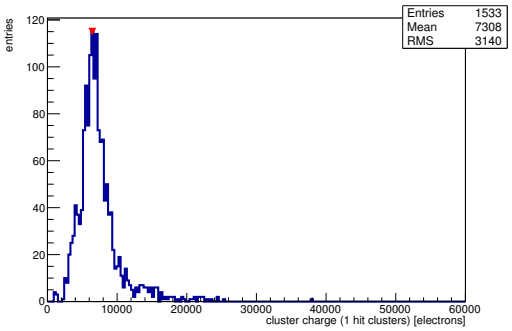

(n) Charge distribution (1 hit cluster).

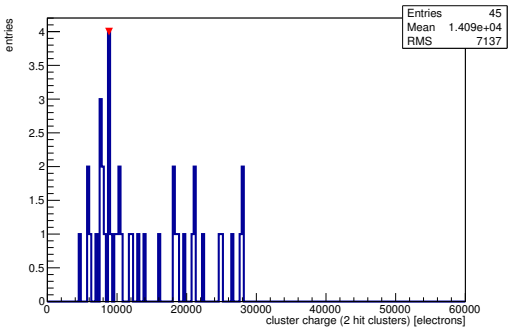

(o) Charge distribution (2 hit cluster).

Figure C.93: Detailed plots for test beam measurement of DO-I-5 (description see section 6.1) sample (running as DUT2) during runs 61260 in the September 2011 test beam period at CERN SPS in area H6B. Summary of the data in chapter 9. *(cont.)*

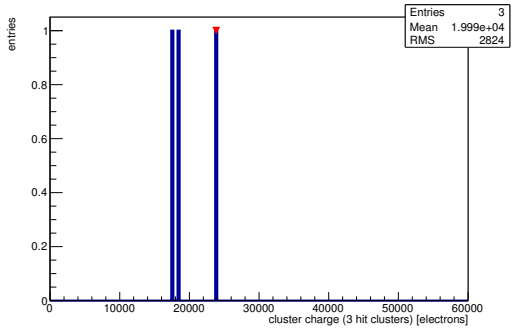

(p) Charge distribution (3 hit cluster).

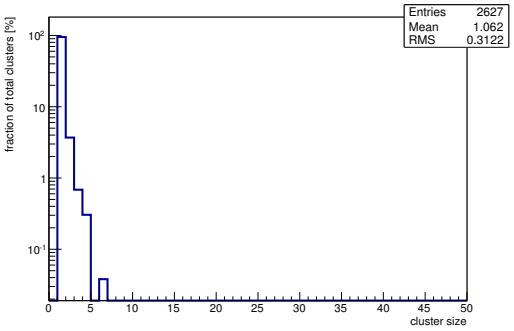

(q) Cluster size distribution.

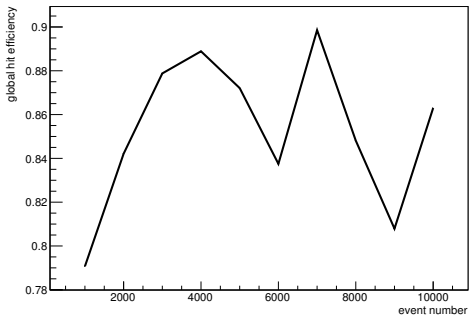

(r) Hit efficiency vs event number.

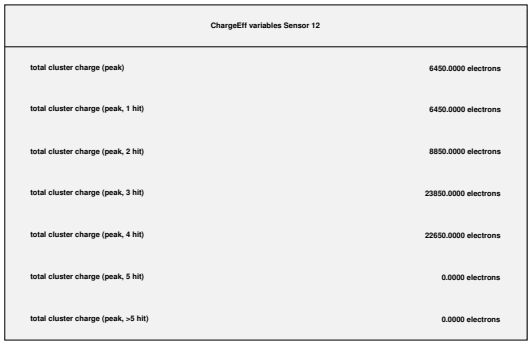

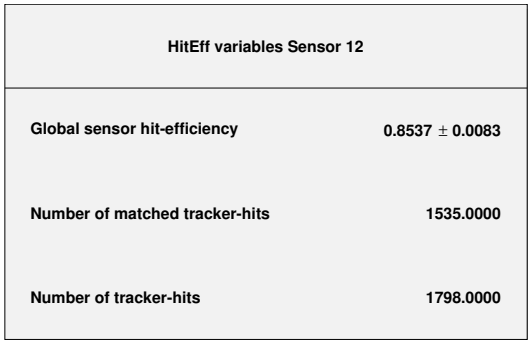

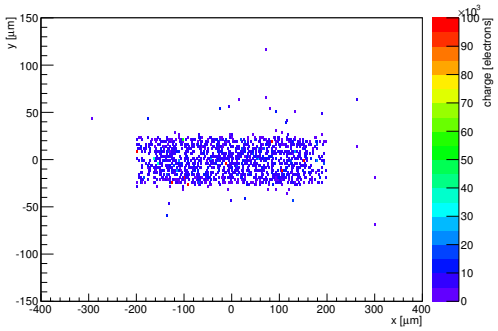

(s) Single pixel mean charge.

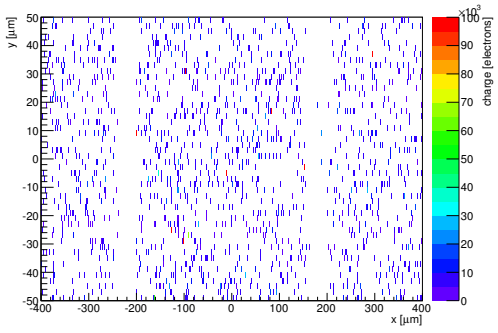

(t) Single pixel mean charge.

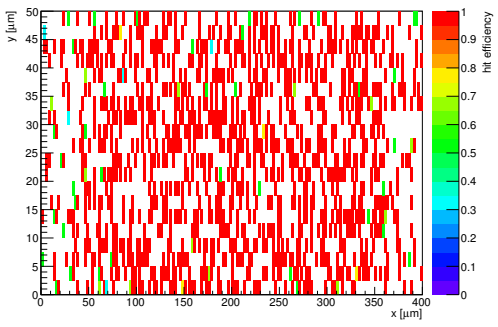

(u) Single pixel hit efficiency.

Figure C.93: Detailed plots for test beam measurement of DO-I-5 (description see section 6.1) sample (running as DUT2) during runs 61260 in the September 2011 test beam period at CERN SPS in area H6B. Summary of the data in chapter 9.

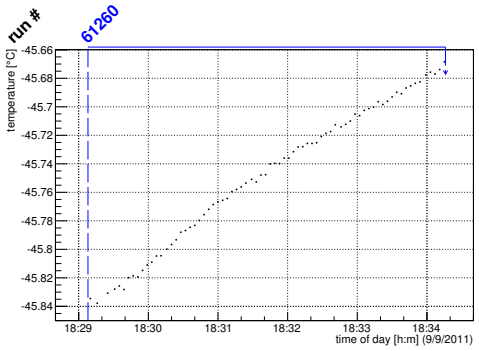

(a) Temperature vs time.

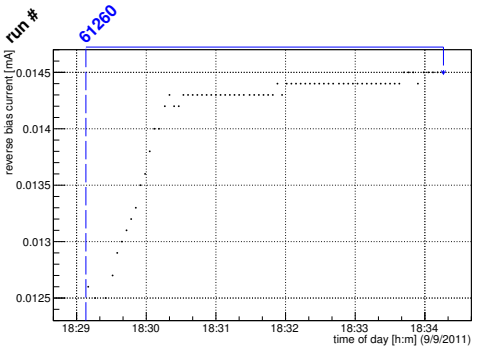

(b) Bias current vs time.

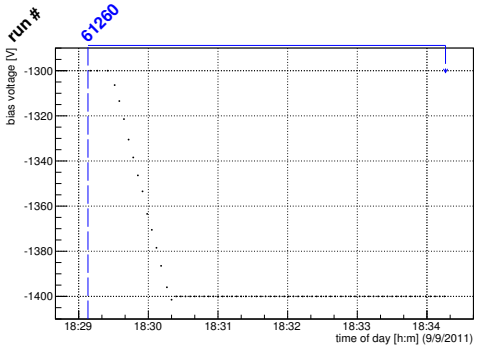

(c) Currently applied bias voltage vs time.

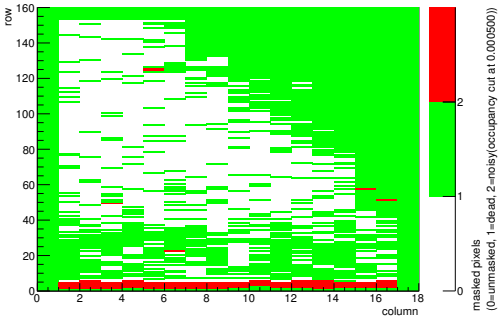

(d) Map of masked pixels.

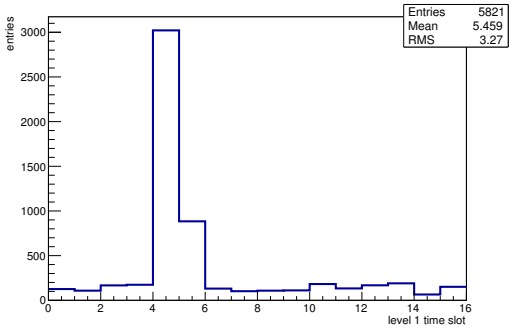

(e) Lvl1 distribution.

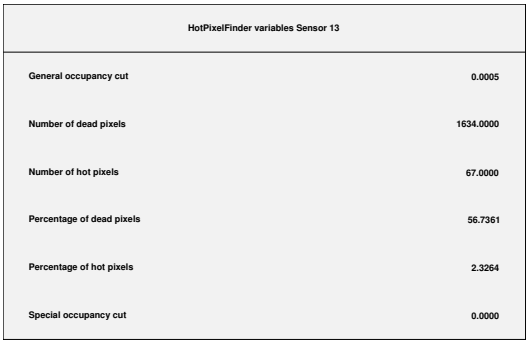

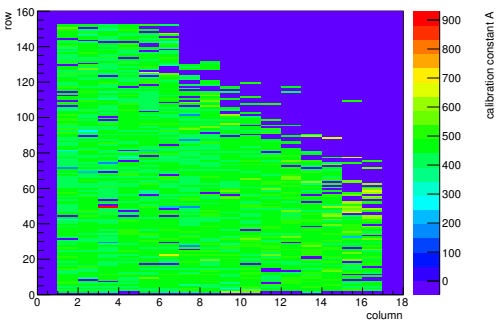

(f) Calibration constant A.

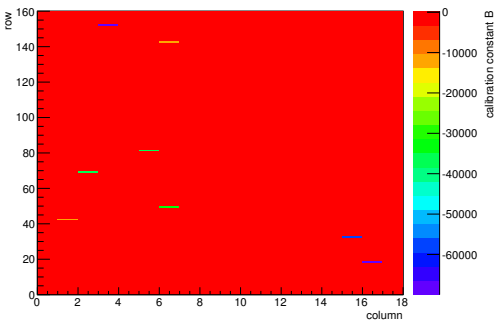

(g) Calibration constant B.

Figure C.94: Detailed plots for test beam measurement of DO-I-12 (description see section 6.1) sample (running as DUT3) during runs 61260 in the September 2011 test beam period at CERN SPS in area H6B. Summary of the data in chapter 9. *(cont.)*

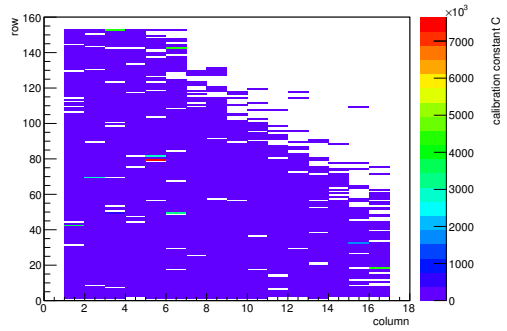

(h) Calibration constant C.

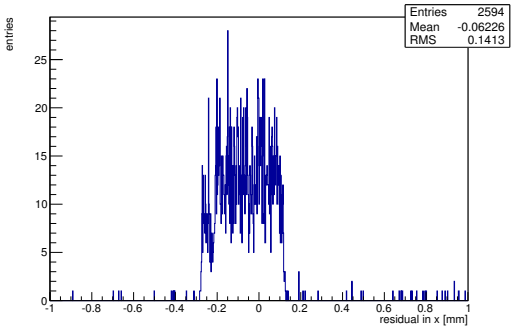

(i) Track residual in x.

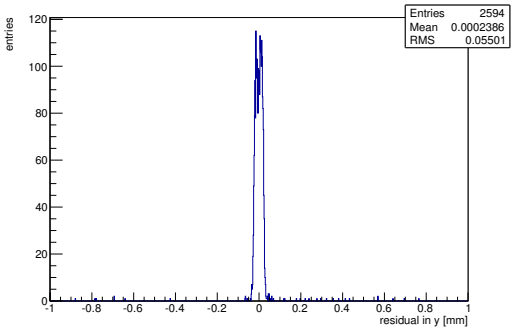

(j) Track residual in y.

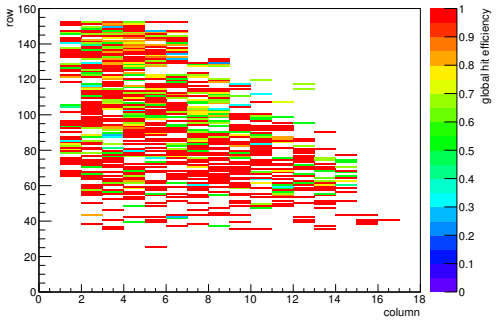

(k) Hit efficiency map.

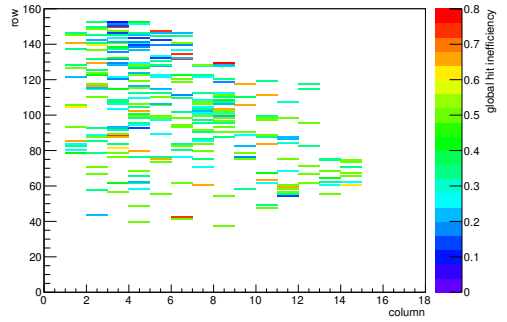

(l) Hit inefficiency map.

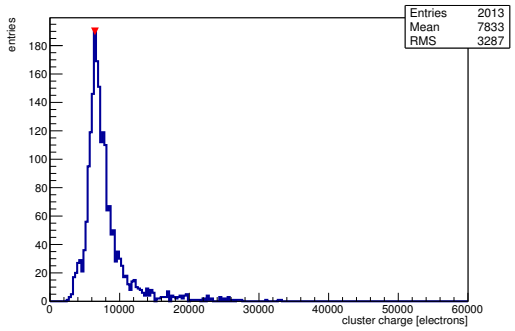

(m) Charge distribution (all cluster sizes included).

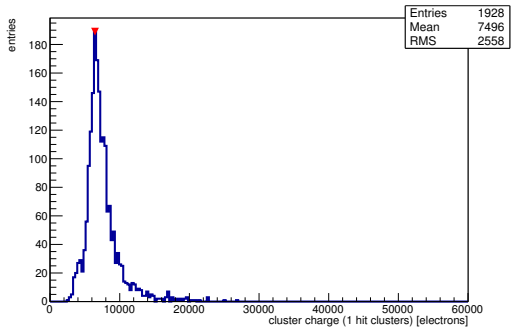

(n) Charge distribution (1 hit cluster).

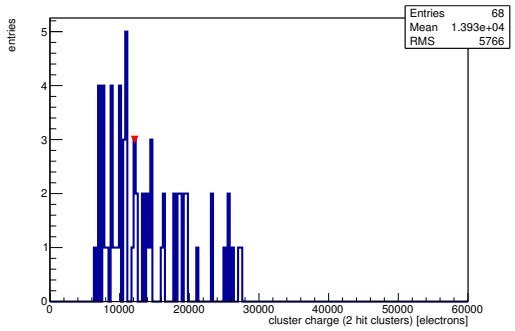

(o) Charge distribution (2 hit cluster).

Figure C.94: Detailed plots for test beam measurement of DO-I-12 (description see section 6.1) sample (running as DUT3) during runs 61260 in the September 2011 test beam period at CERN SPS in area H6B. Summary of the data in chapter 9. *(cont.)*

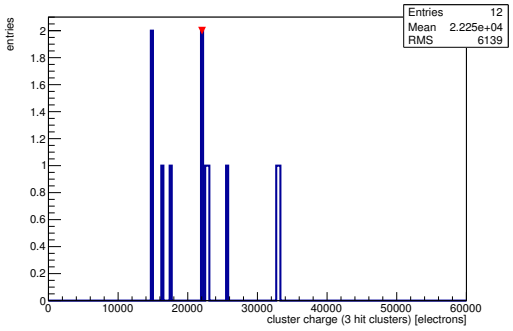

(p) Charge distribution (3 hit cluster).

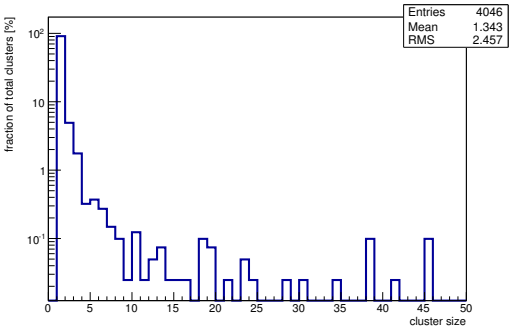

(q) Cluster size distribution.

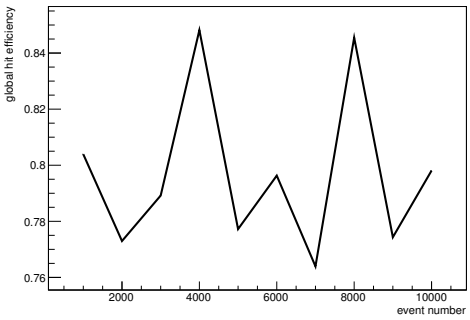

(r) Hit efficiency vs event number.

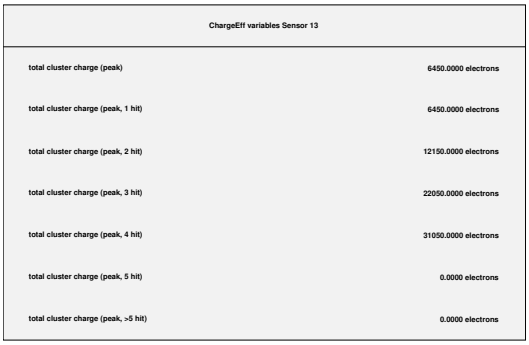

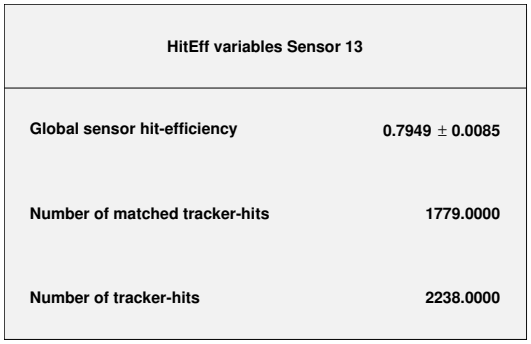

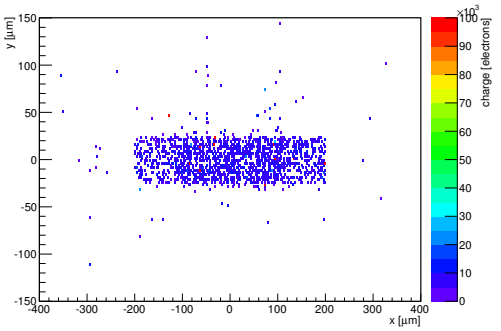

(s) Single pixel mean charge.

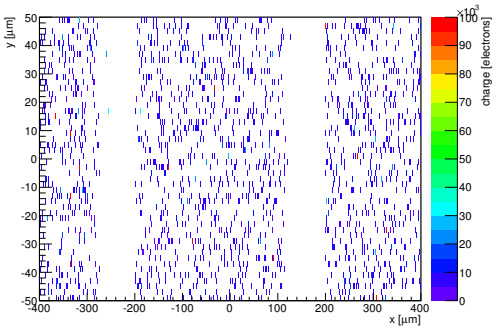

(t) Single pixel mean charge.

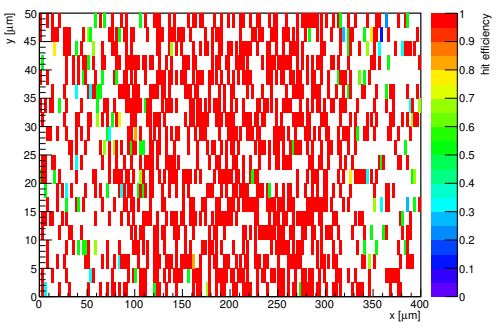

(u) Single pixel hit efficiency.

Figure C.94: Detailed plots for test beam measurement of DO-I-12 (description see section 6.1) sample (running as DUT3) during runs 61260 in the September 2011 test beam period at CERN SPS in area H6B. Summary of the data in chapter 9.

C.3.14 Run 61261

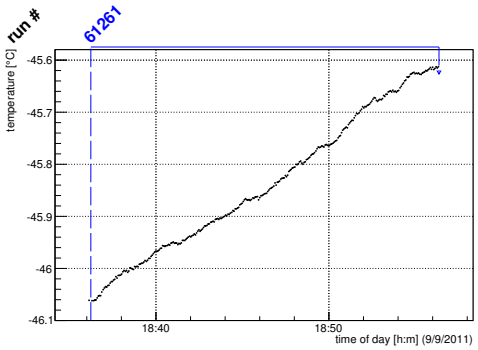

(a) Temperature vs time.

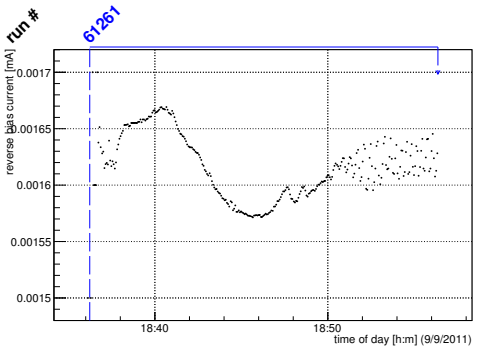

(b) Bias current vs time.

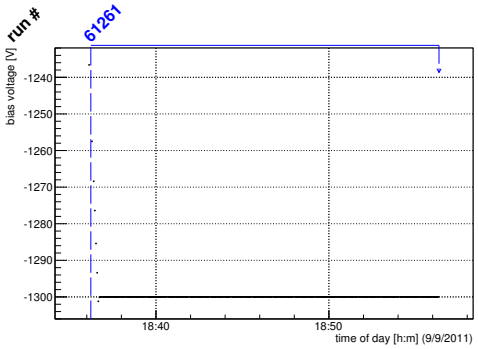

(c) Currently applied bias voltage vs time.

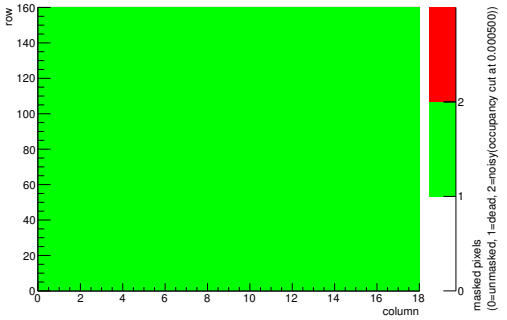

(d) Map of masked pixels.

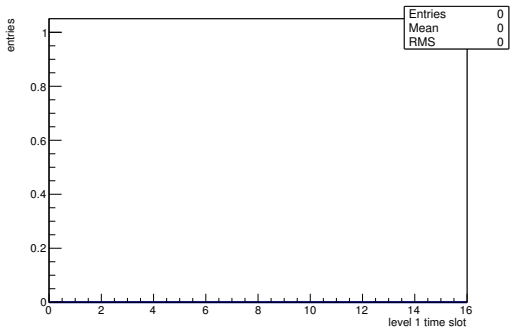

(e) Lvl1 distribution.

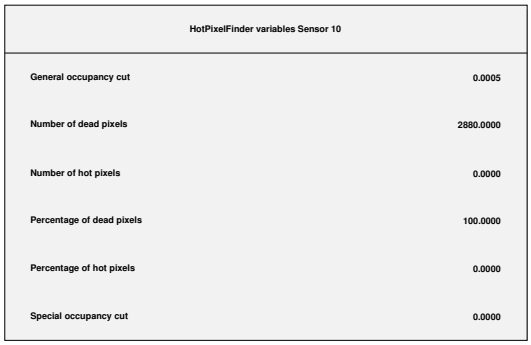

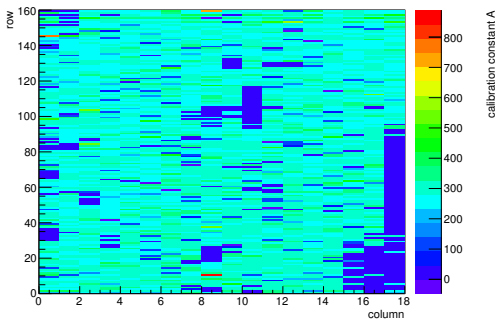

(f) Calibration constant A.

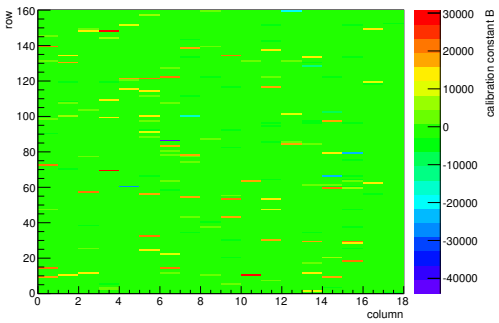

(g) Calibration constant B.

Figure C.95: Detailed plots for test beam measurement of DO-I-7 (description see section 6.1) sample (running as DUT0) during runs 61261 in the September 2011 test beam period at CERN SPS in area H6B. Summary of the data in chapter 9. *(cont.)*

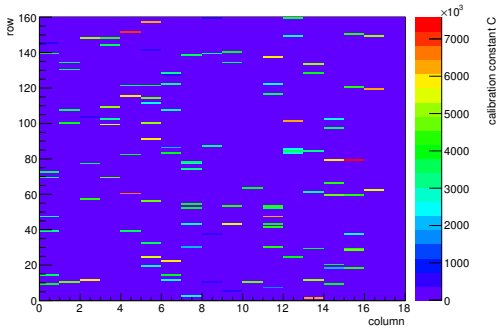

(h) Calibration constant C.

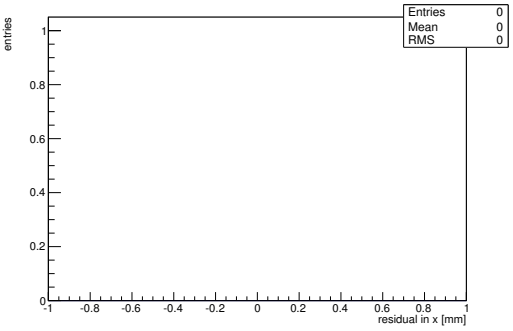

(i) Track residual in x.

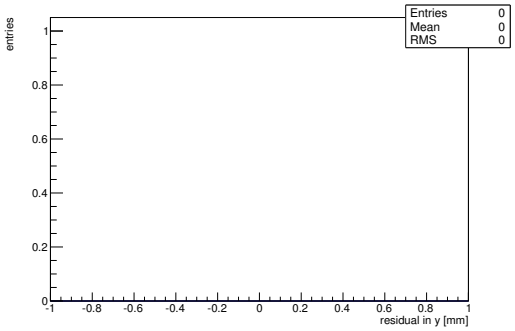

(j) Track residual in y.

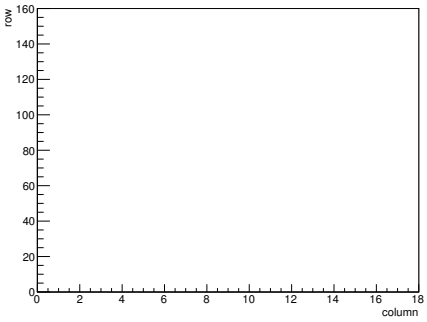

(k) Hit efficiency map.

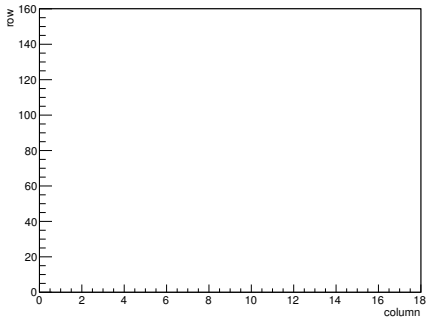

(l) Hit inefficiency map.

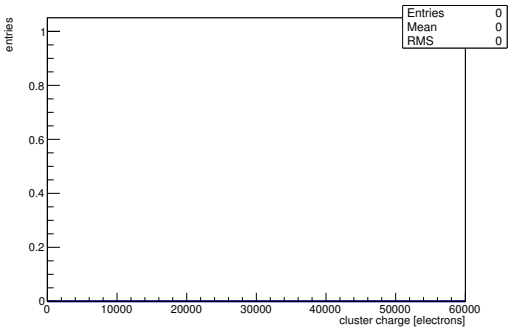

(m) Charge distribution (all cluster sizes included).

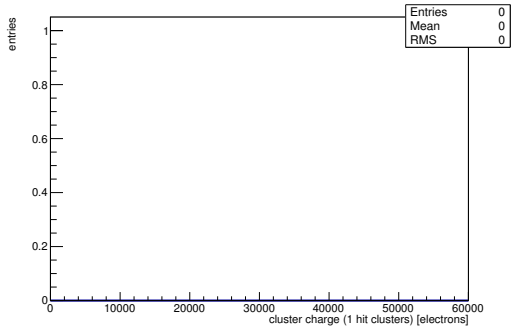

(n) Charge distribution (1 hit cluster).

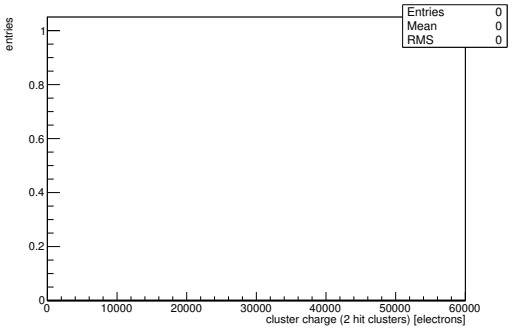

(o) Charge distribution (2 hit cluster).

Figure C.95: Detailed plots for test beam measurement of DO-I-7 (description see section 6.1) sample (running as DUT0) during runs 61261 in the September 2011 test beam period at CERN SPS in area H6B. Summary of the data in chapter 9. *(cont.)*

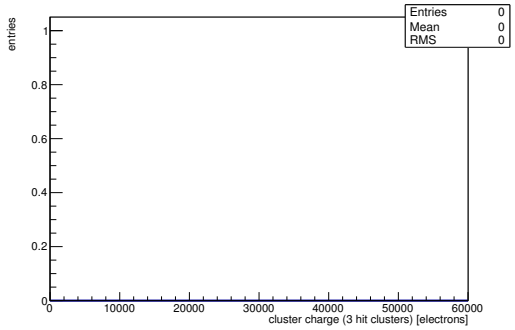

(p) Charge distribution (3 hit cluster).

(q) Cluster size distribution.

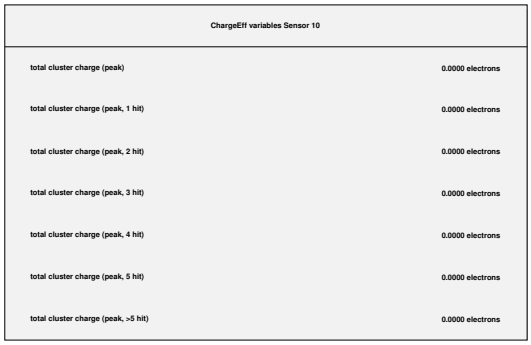

(r) Hit efficiency vs event number.

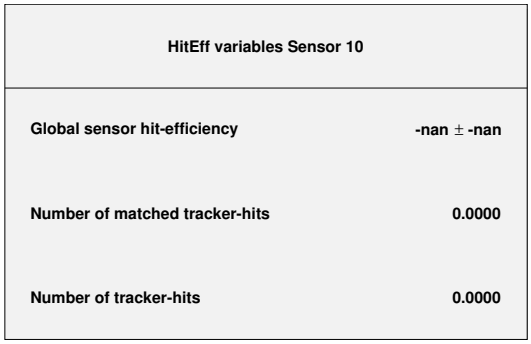

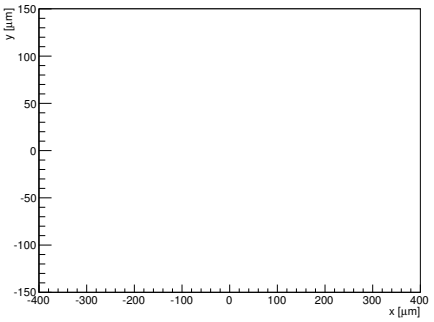

(s) Single pixel mean charge.

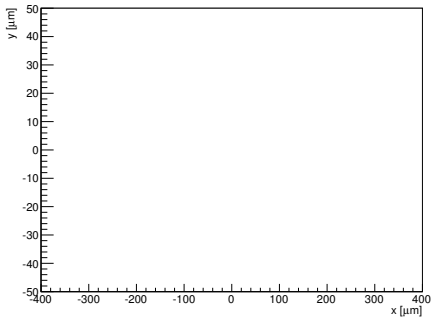

(t) Single pixel mean charge.

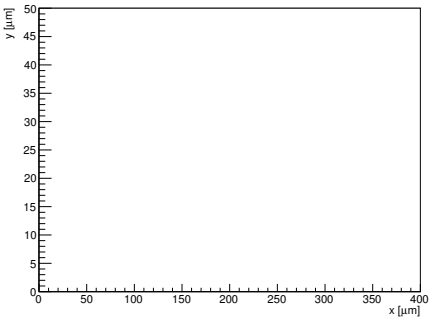

(u) Single pixel hit efficiency.

Figure C.95: Detailed plots for test beam measurement of DO-I-7 (description see section 6.1) sample (running as DUT0) during runs 61261 in the September 2011 test beam period at CERN SPS in area H6B. Summary of the data in chapter 9.

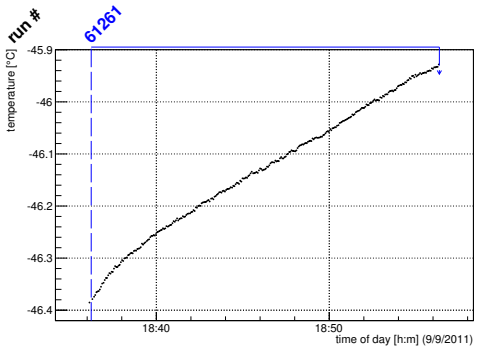

(a) Temperature vs time.

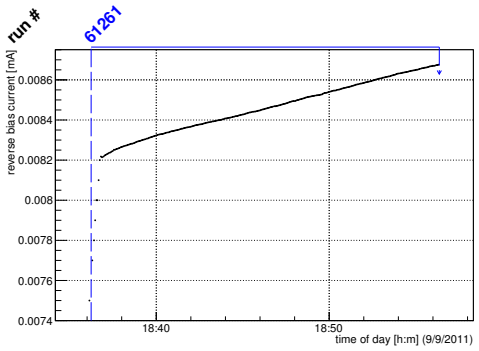

(b) Bias current vs time.

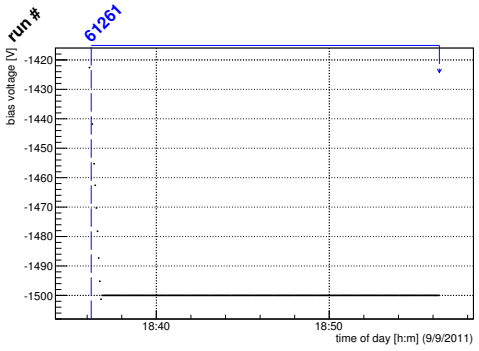

(c) Currently applied bias voltage vs time.

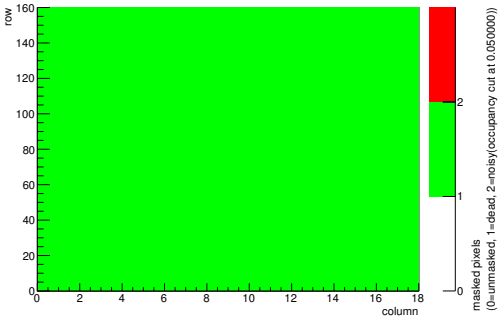

(d) Map of masked pixels.

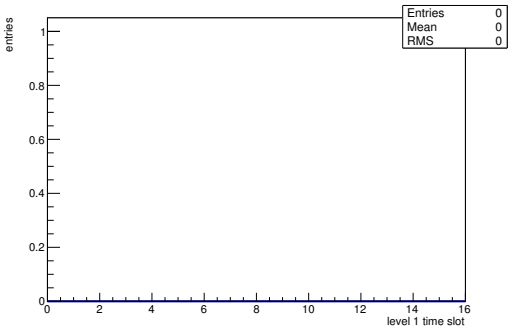

(e) Lvl1 distribution.

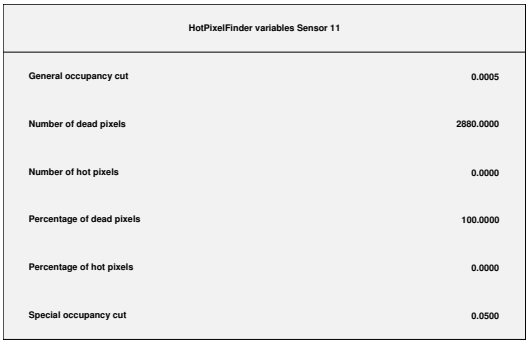

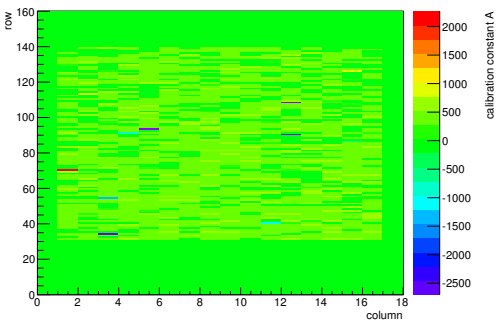

(f) Calibration constant A.

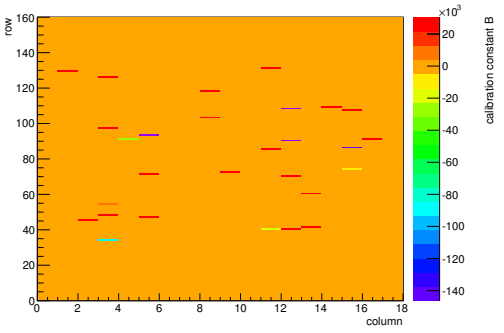

(g) Calibration constant B.

Figure C.96: Detailed plots for test beam measurement of DO-I-11 (description see section 6.1) sample (running as DUT1) during runs 61261 in the September 2011 test beam period at CERN SPS in area H6B. Summary of the data in chapter 9. *(cont.)*

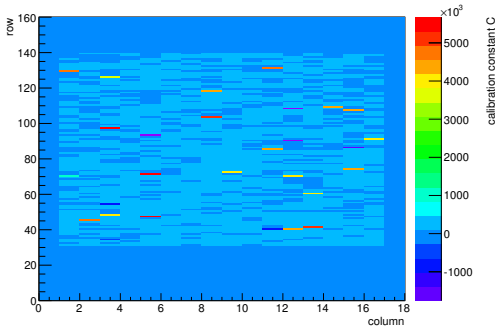

(h) Calibration constant C.

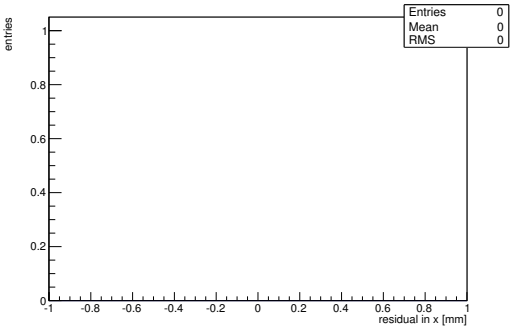

(i) Track residual in x.

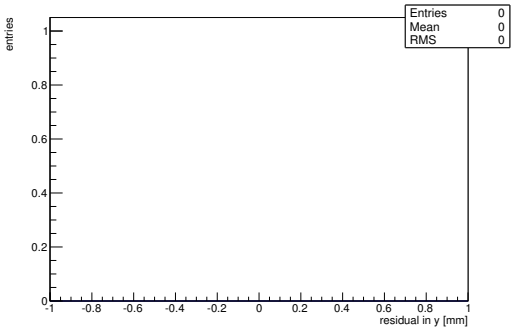

(j) Track residual in y.

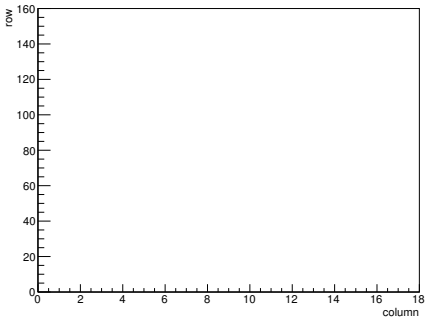

(k) Hit efficiency map.

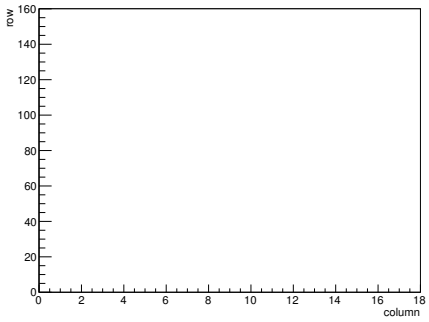

(l) Hit inefficiency map.

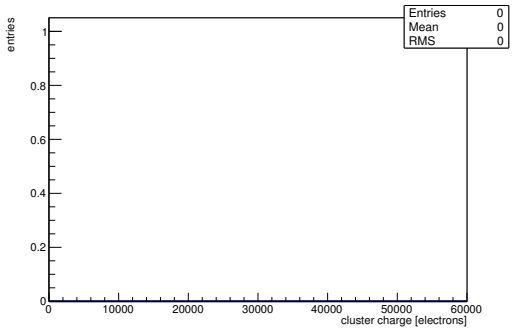

(m) Charge distribution (all cluster sizes included).

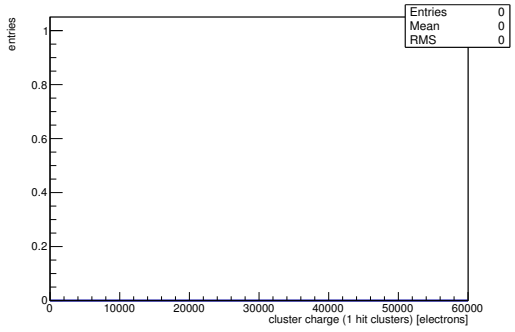

(n) Charge distribution (1 hit cluster).

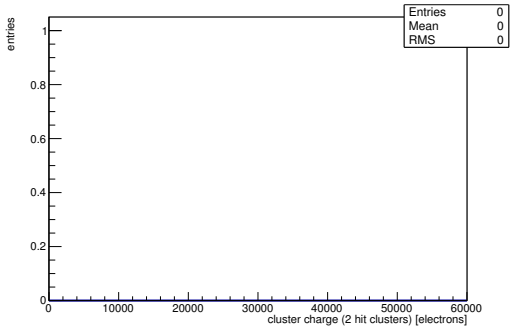

(o) Charge distribution (2 hit cluster).

Figure C.96: Detailed plots for test beam measurement of DO-I-11 (description see section 6.1) sample (running as DUT1) during runs 61261 in the September 2011 test beam period at CERN SPS in area H6B. Summary of the data in chapter 9. *(cont.)*

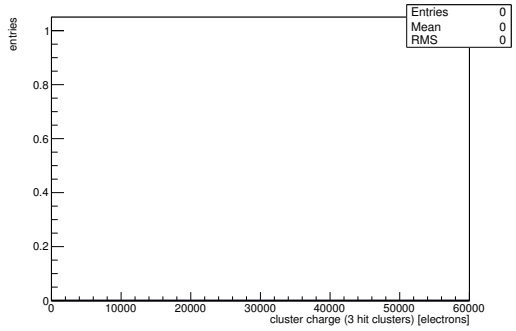

(p) Charge distribution (3 hit cluster).

(q) Cluster size distribution.

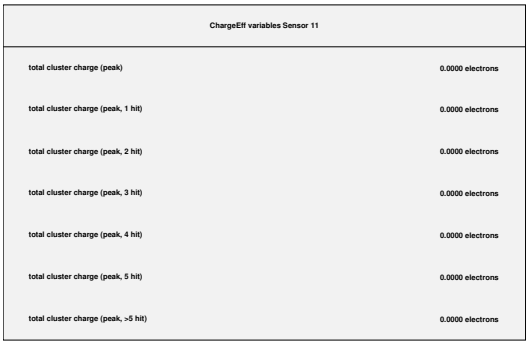

(r) Hit efficiency vs event number.

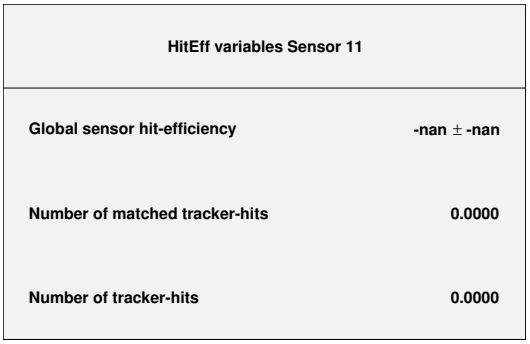

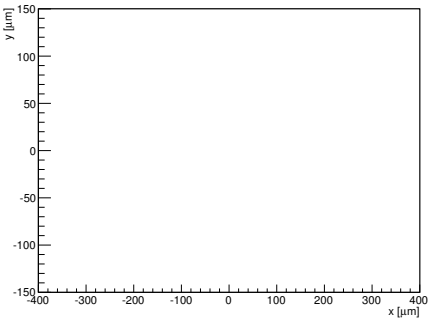

(s) Single pixel mean charge.

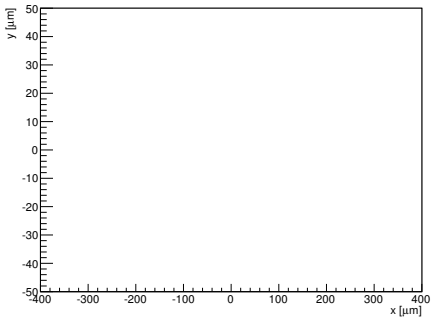

(t) Single pixel mean charge.

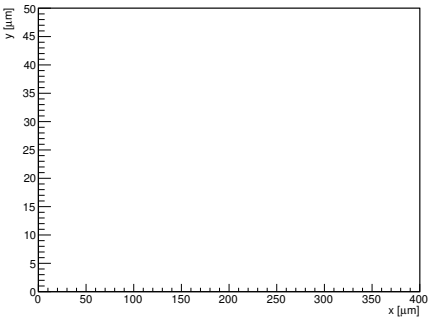

(u) Single pixel hit efficiency.

Figure C.96: Detailed plots for test beam measurement of DO-I-11 (description see section 6.1) sample (running as DUT1) during runs 61261 in the September 2011 test beam period at CERN SPS in area H6B. Summary of the data in chapter 9.

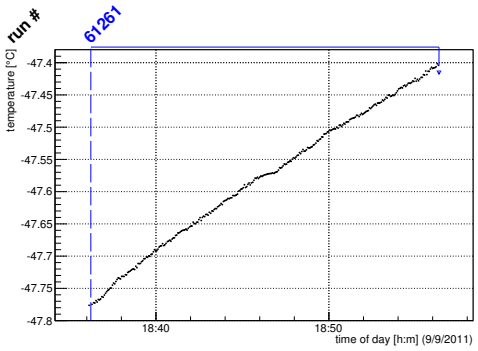

(a) Temperature vs time.

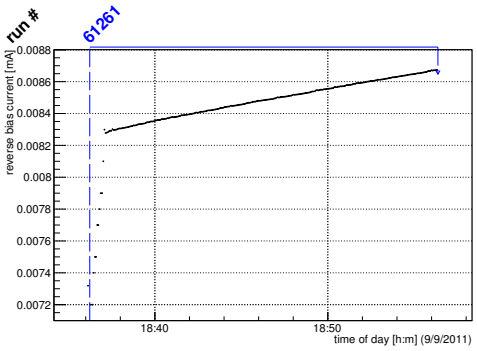

(b) Bias current vs time.

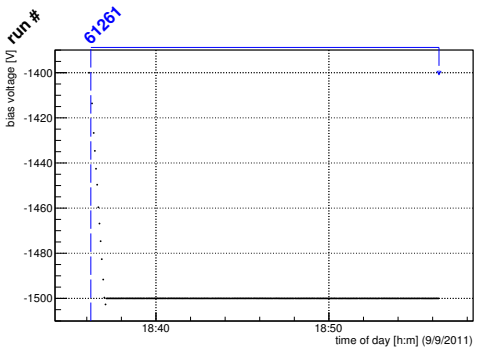

(c) Currently applied bias voltage vs time.

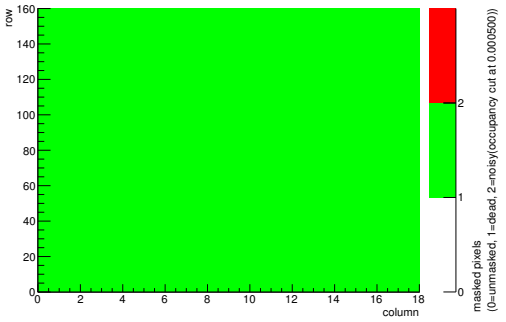

(d) Map of masked pixels.

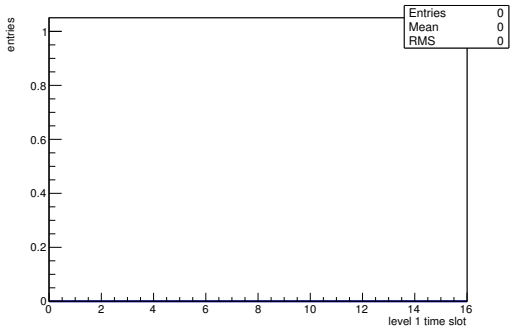

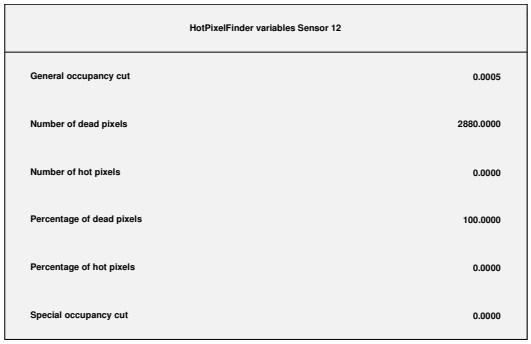

(e) Lvl1 distribution.

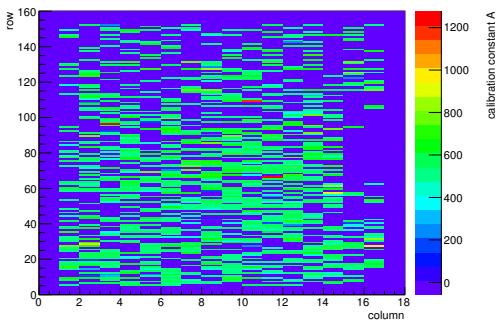

(f) Calibration constant A.

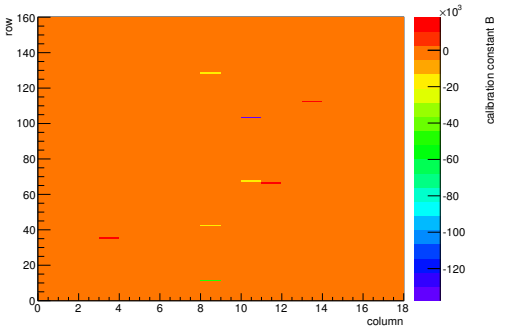

(g) Calibration constant B.

Figure C.97: Detailed plots for test beam measurement of DO-I-5 (description see section 6.1) sample (running as DUT2) during runs 61261 in the September 2011 test beam period at CERN SPS in area H6B. Summary of the data in chapter 9. *(cont.)*

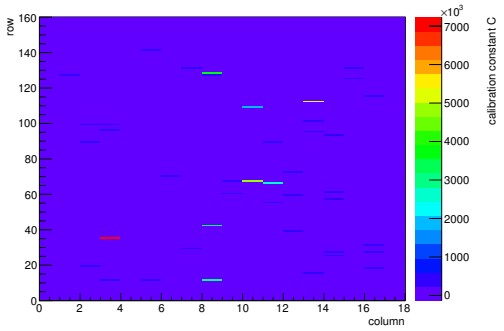

(h) Calibration constant C.

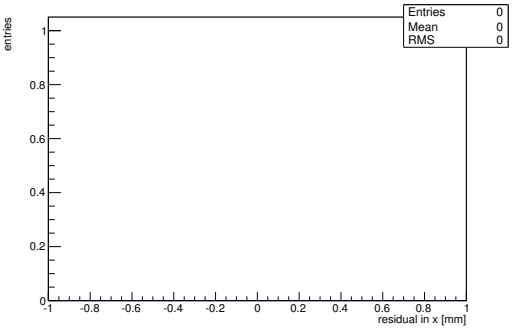

(i) Track residual in x.

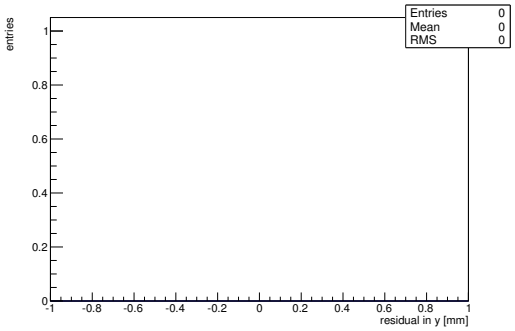

(j) Track residual in y.

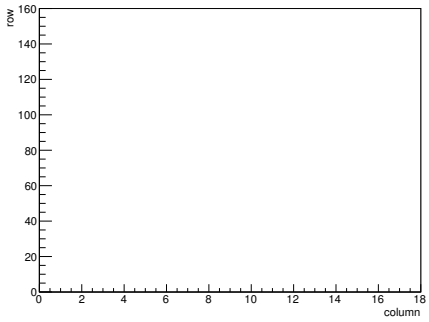

(k) Hit efficiency map.

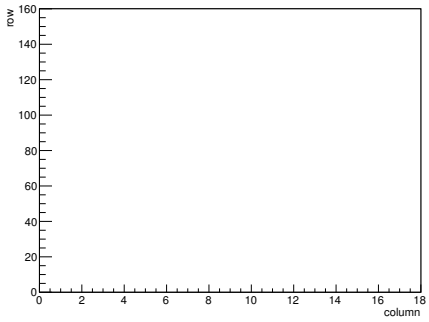

(l) Hit inefficiency map.

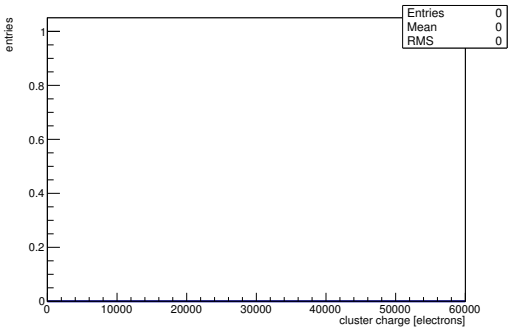

(m) Charge distribution (all cluster sizes included).

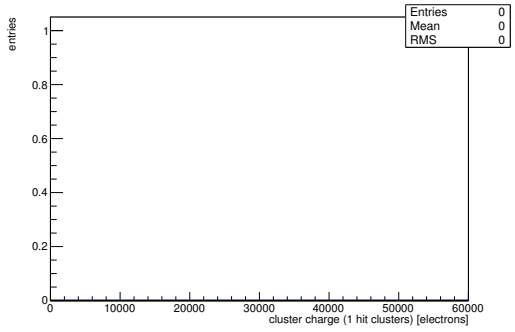

(n) Charge distribution (1 hit cluster).

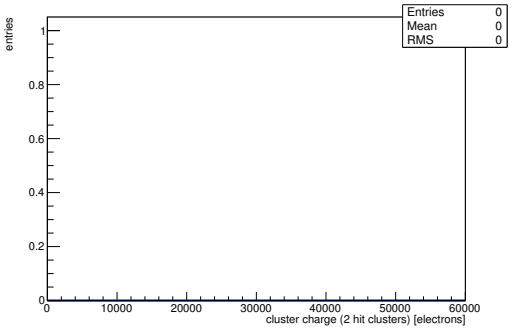

(o) Charge distribution (2 hit cluster).

Figure C.97: Detailed plots for test beam measurement of DO-I-5 (description see section 6.1) sample (running as DUT2) during runs 61261 in the September 2011 test beam period at CERN SPS in area H6B. Summary of the data in chapter 9. *(cont.)*

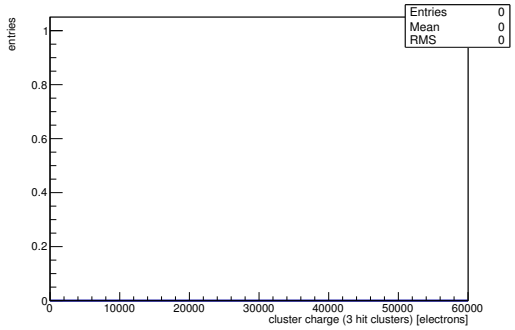

(p) Charge distribution (3 hit cluster).

(q) Cluster size distribution.

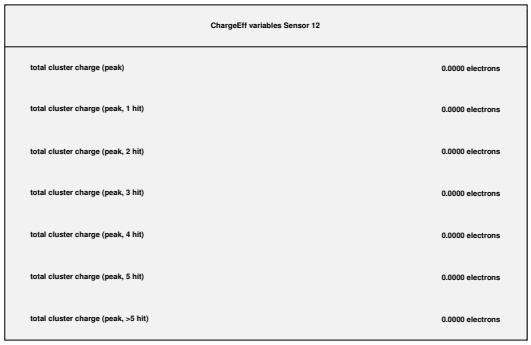

(r) Hit efficiency vs event number.

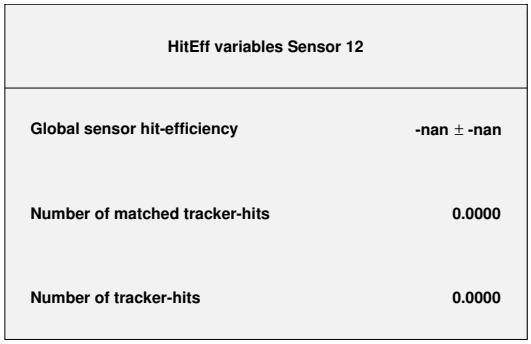

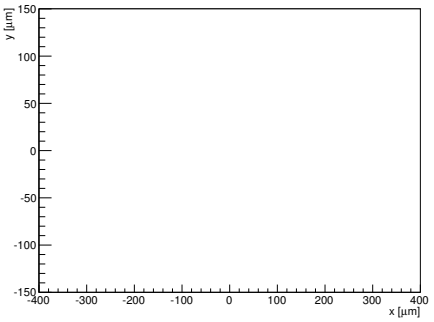

(s) Single pixel mean charge.

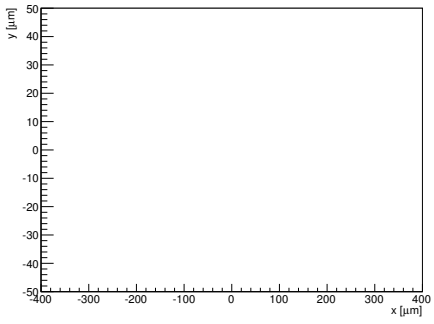

(t) Single pixel mean charge.

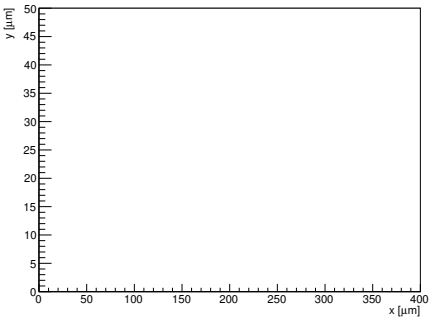

(u) Single pixel hit efficiency.

Figure C.97: Detailed plots for test beam measurement of DO-I-5 (description see section 6.1) sample (running as DUT2) during runs 61261 in the September 2011 test beam period at CERN SPS in area H6B. Summary of the data in chapter 9.

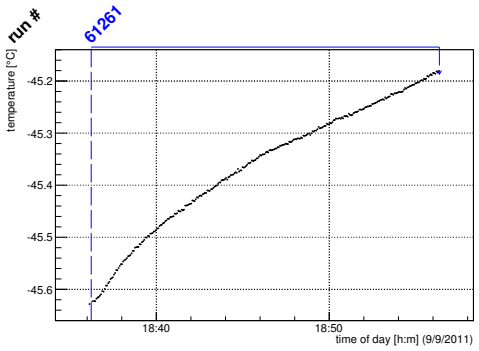

(a) Temperature vs time.

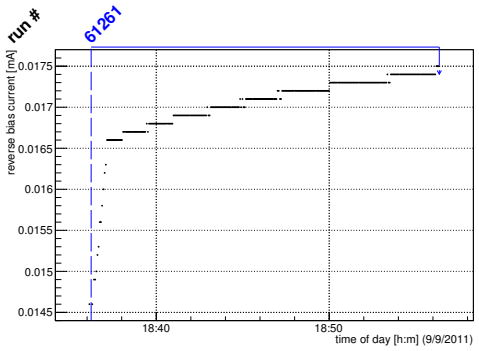

(b) Bias current vs time.

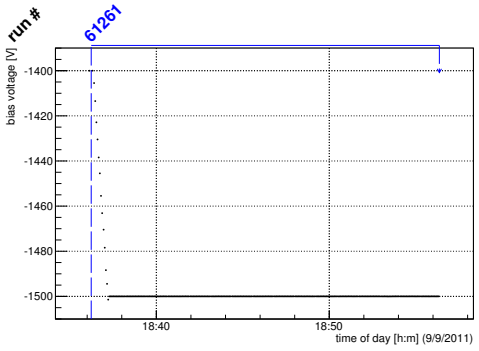

(c) Currently applied bias voltage vs time.

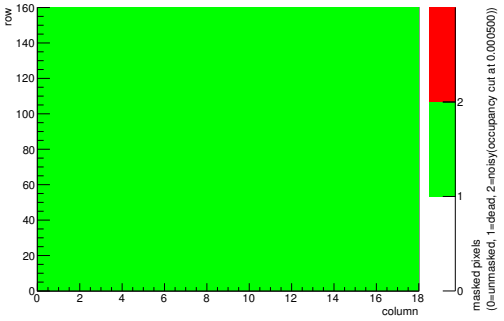

(d) Map of masked pixels.

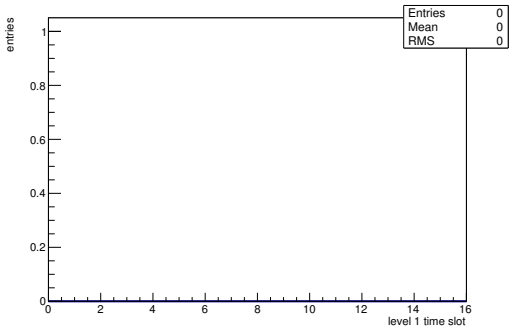

(e) Lvl1 distribution.

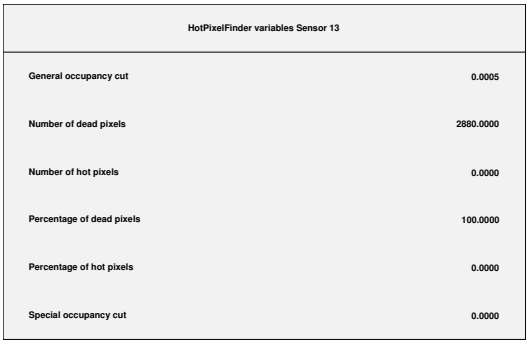

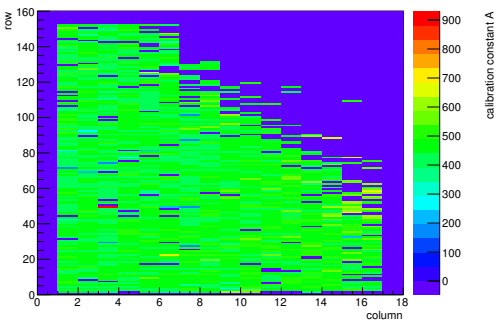

(f) Calibration constant A.

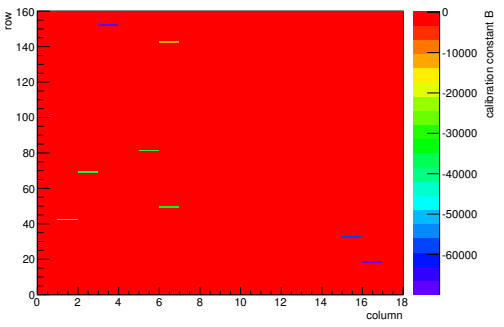

(g) Calibration constant B.

Figure C.98: Detailed plots for test beam measurement of DO-I-12 (description see section 6.1) sample (running as DUT3) during runs 61261 in the September 2011 test beam period at CERN SPS in area H6B. Summary of the data in chapter 9. *(cont.)*

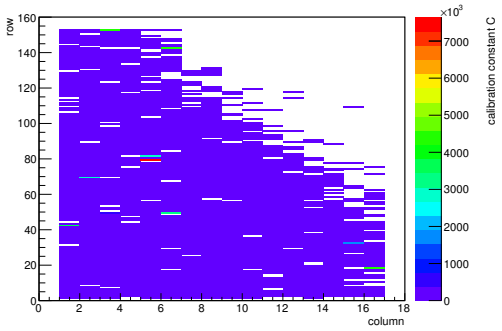

(h) Calibration constant C.

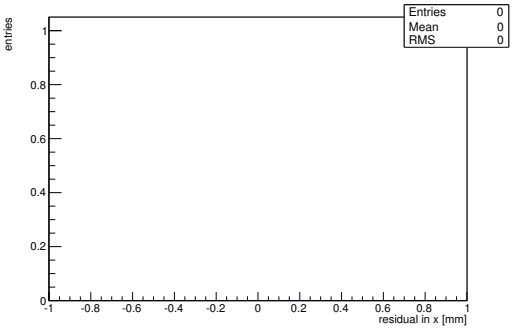

(i) Track residual in x.

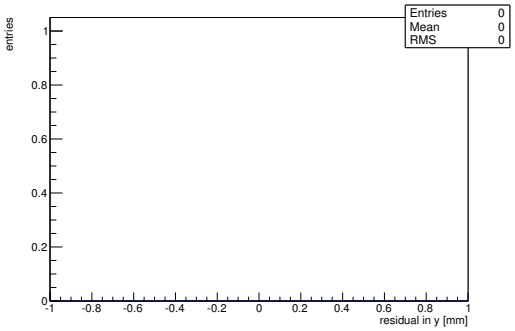

(j) Track residual in y.

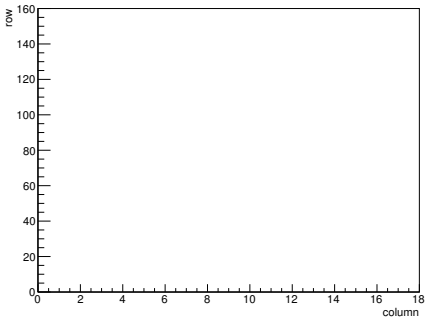

(k) Hit efficiency map.

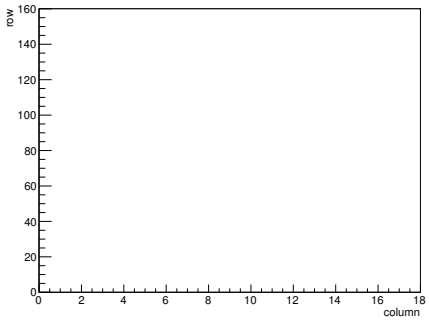

(l) Hit inefficiency map.

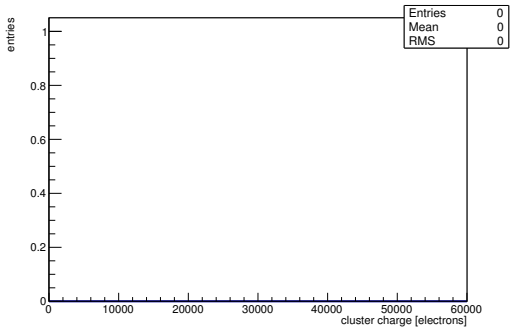

(m) Charge distribution (all cluster sizes included).

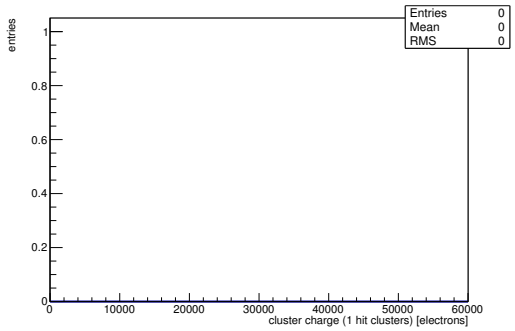

(n) Charge distribution (1 hit cluster).

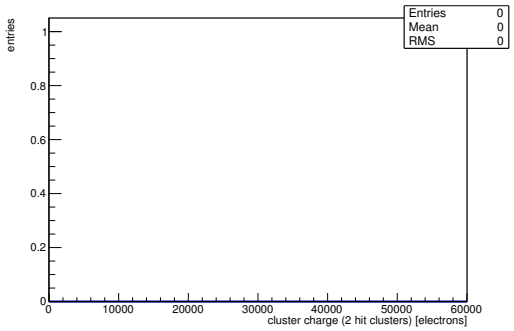

(o) Charge distribution (2 hit cluster).

Figure C.98: Detailed plots for test beam measurement of DO-I-12 (description see section 6.1) sample (running as DUT3) during runs 61261 in the September 2011 test beam period at CERN SPS in area H6B. Summary of the data in chapter 9. *(cont.)*

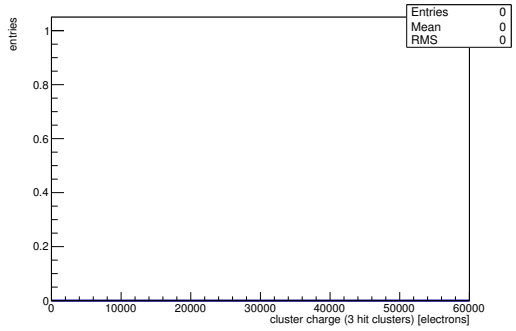

(p) Charge distribution (3 hit cluster).

(q) Cluster size distribution.

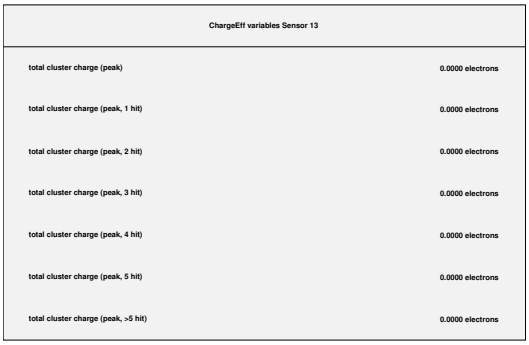

(r) Hit efficiency vs event number.

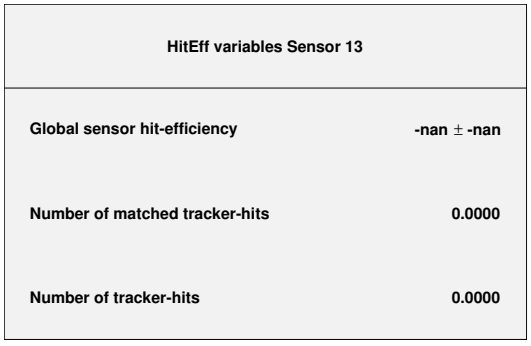

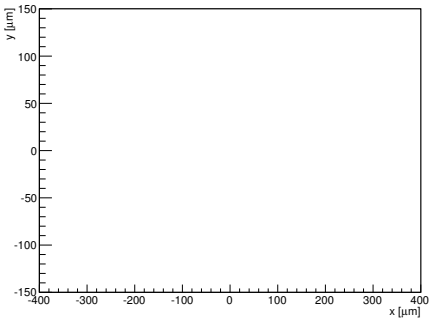

(s) Single pixel mean charge.

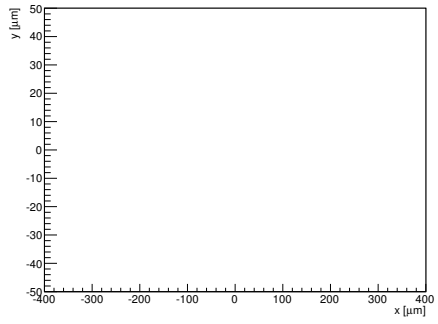

(t) Single pixel mean charge.

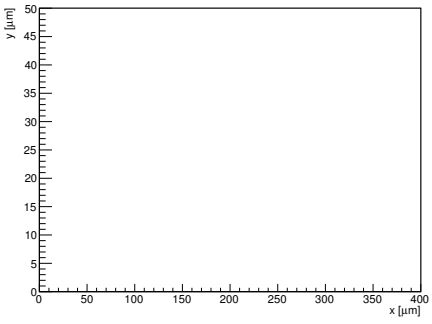

(u) Single pixel hit efficiency.

Figure C.98: Detailed plots for test beam measurement of DO-I-12 (description see section 6.1) sample (running as DUT3) during runs 61261 in the September 2011 test beam period at CERN SPS in area H6B. Summary of the data in chapter 9.

C.3.15 Run 61262

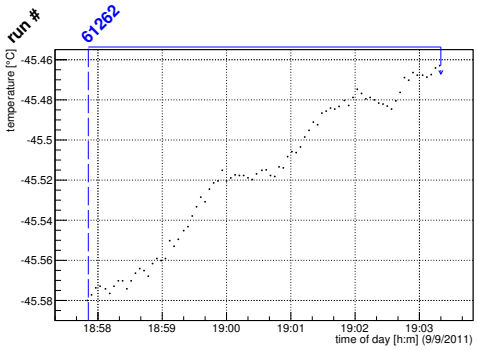

(a) Temperature vs time.

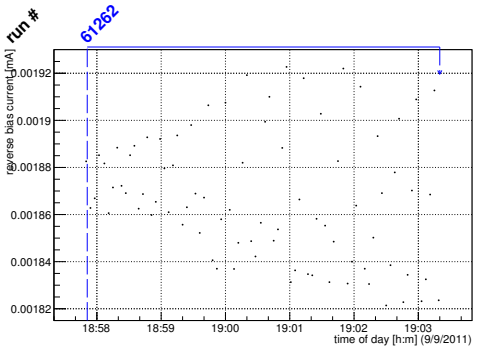

(b) Bias current vs time.

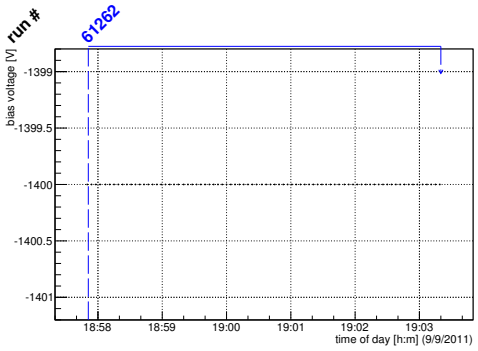

(c) Currently applied bias voltage vs time.

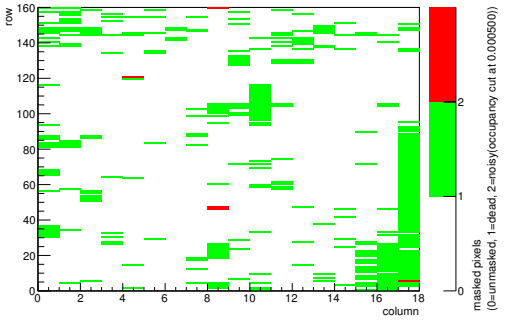

(d) Map of masked pixels.

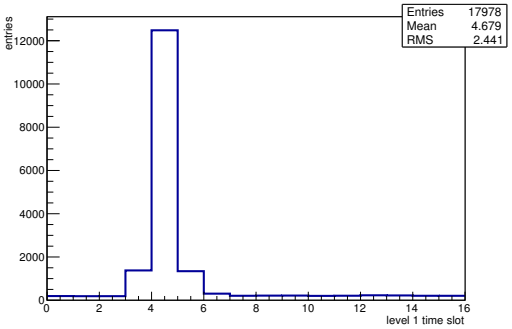

(e) Lvl1 distribution.

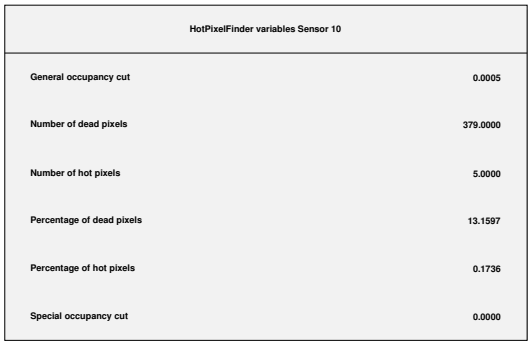

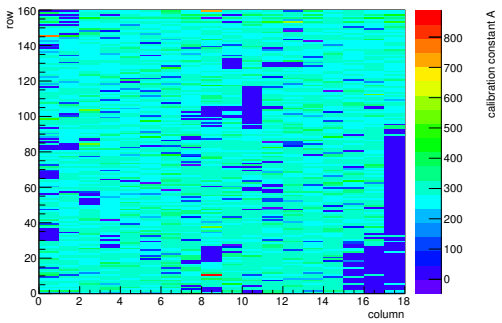

(f) Calibration constant A.

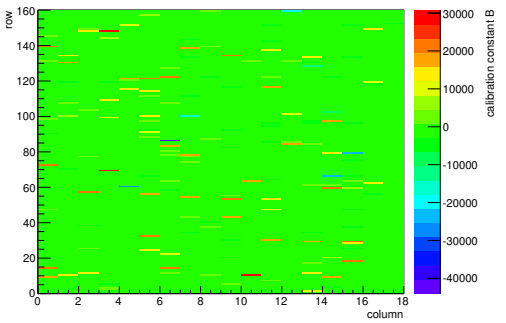

(g) Calibration constant B.

Figure C.99: Detailed plots for test beam measurement of DO-I-7 (description see section 6.1) sample (running as DUT0) during runs 61262 in the September 2011 test beam period at CERN SPS in area H6B. Summary of the data in chapter 9. *(cont.)*

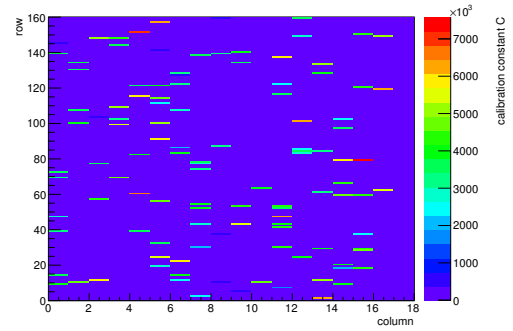

(h) Calibration constant C.

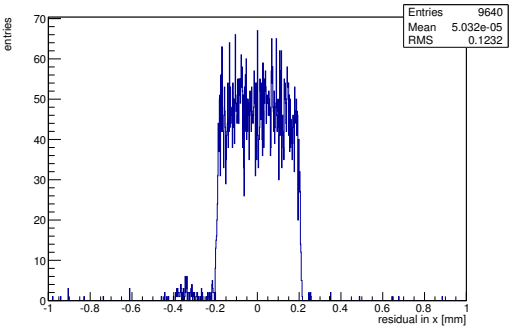

(i) Track residual in x.

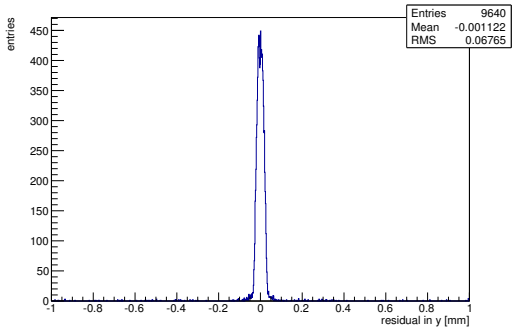

(j) Track residual in y.

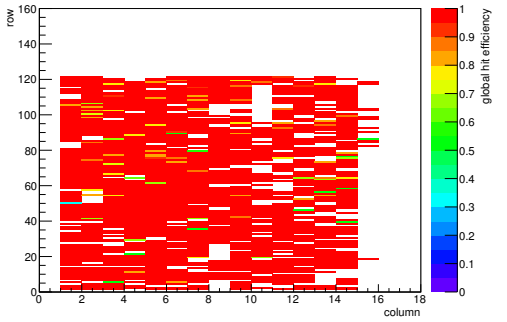

(k) Hit efficiency map.

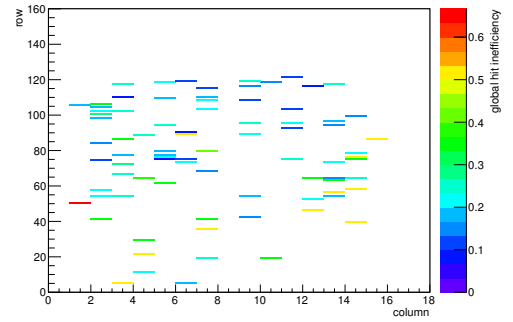

(l) Hit inefficiency map.

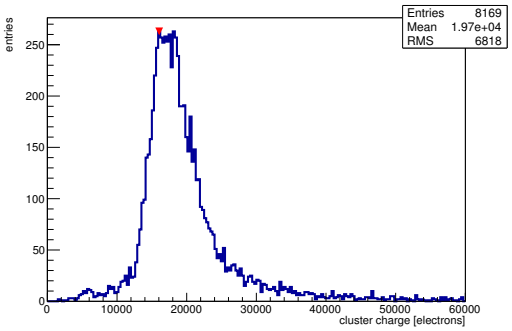

(m) Charge distribution (all cluster sizes included).

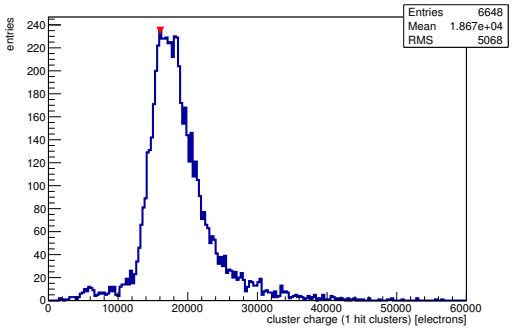

(n) Charge distribution (1 hit cluster).

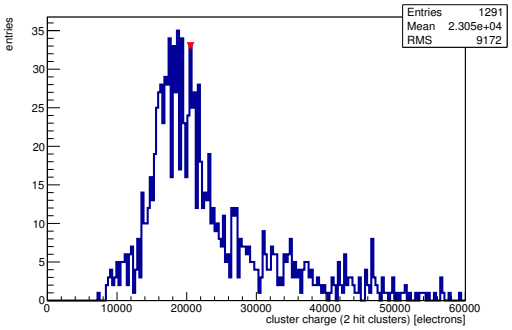

(o) Charge distribution (2 hit cluster).

Figure C.99: Detailed plots for test beam measurement of DO-I-7 (description see section 6.1) sample (running as DUT0) during runs 61262 in the September 2011 test beam period at CERN SPS in area H6B. Summary of the data in chapter 9. *(cont.)*

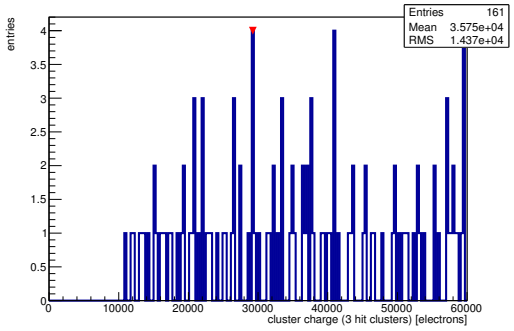

(p) Charge distribution (3 hit cluster).

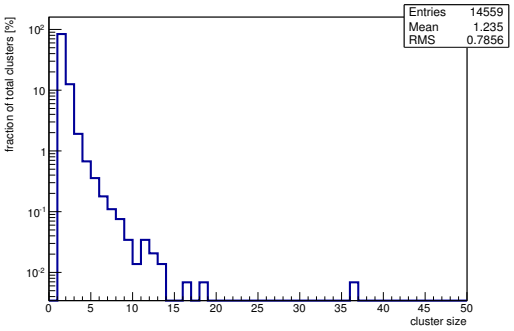

(q) Cluster size distribution.

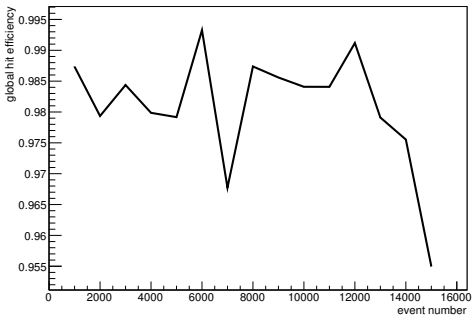

(r) Hit efficiency vs event number.

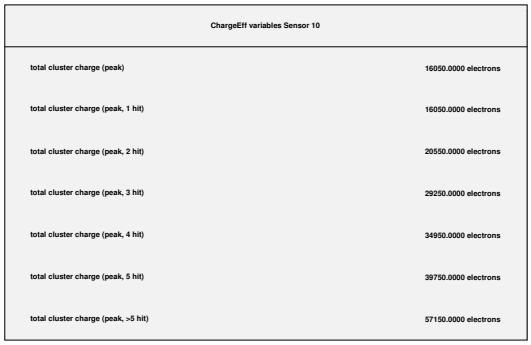

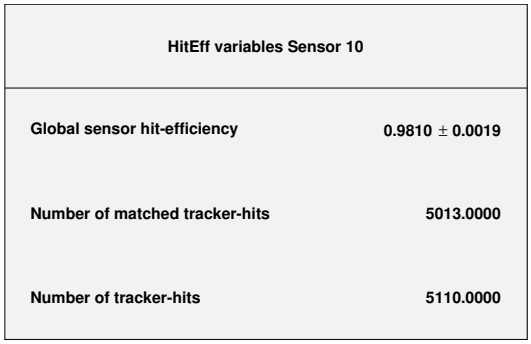

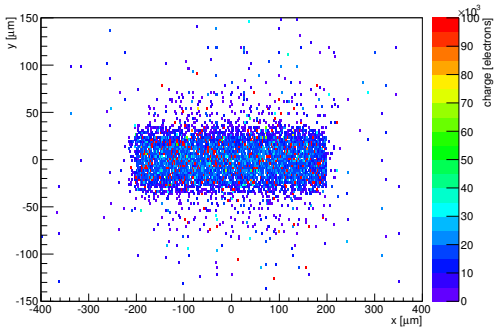

(s) Single pixel mean charge.

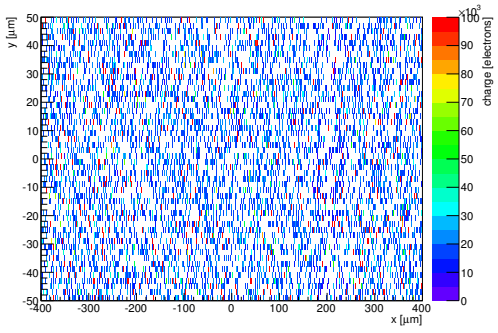

(t) Single pixel mean charge.

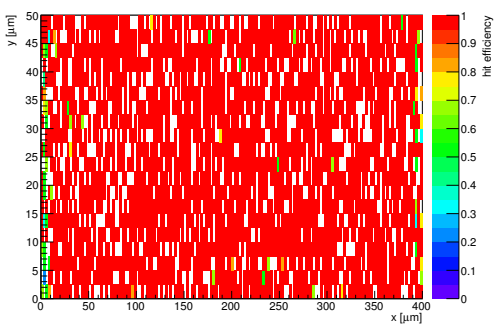

(u) Single pixel hit efficiency.

Figure C.99: Detailed plots for test beam measurement of DO-I-7 (description see section 6.1) sample (running as DUT0) during runs 61262 in the September 2011 test beam period at CERN SPS in area H6B. Summary of the data in chapter 9.

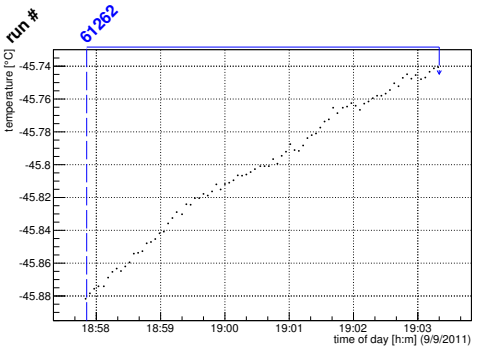

(a) Temperature vs time.

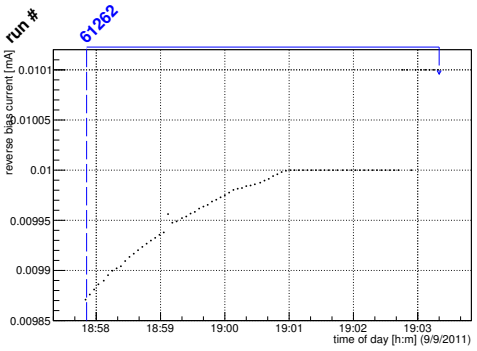

(b) Bias current vs time.

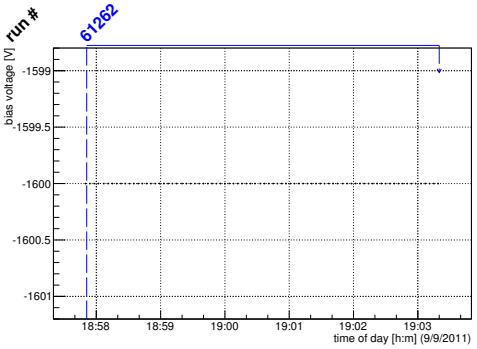

(c) Currently applied bias voltage vs time.

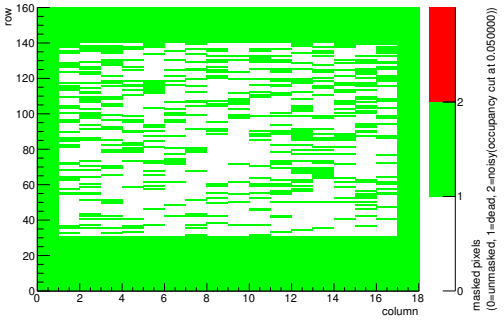

(d) Map of masked pixels.

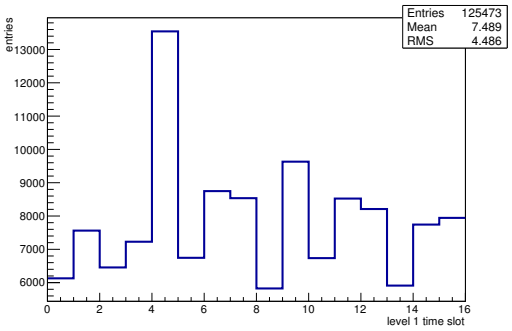

(e) Lvl1 distribution.

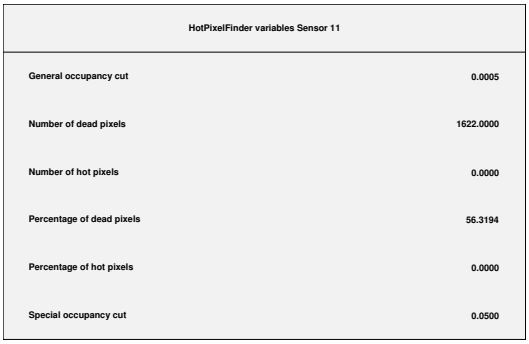

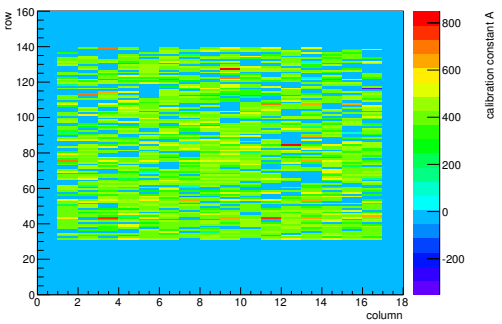

(f) Calibration constant A.

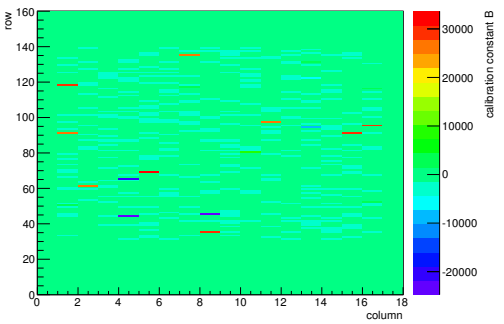

(g) Calibration constant B.

Figure C.100: Detailed plots for test beam measurement of DO-I-11 (description see section 6.1) sample (running as DUT1) during runs 61262 in the September 2011 test beam period at CERN SPS in area H6B. Summary of the data in chapter 9. *(cont.)*

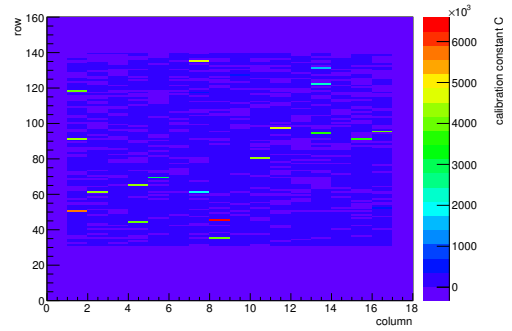

(h) Calibration constant C.

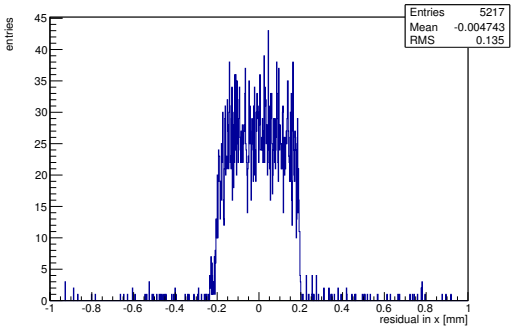

(i) Track residual in x.

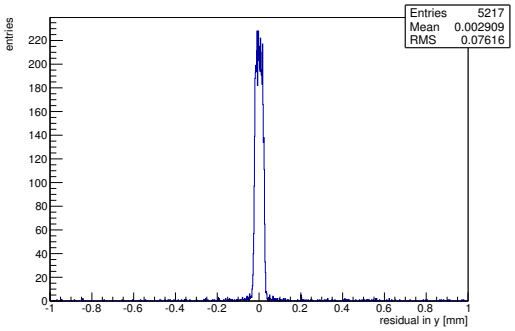

(j) Track residual in y.

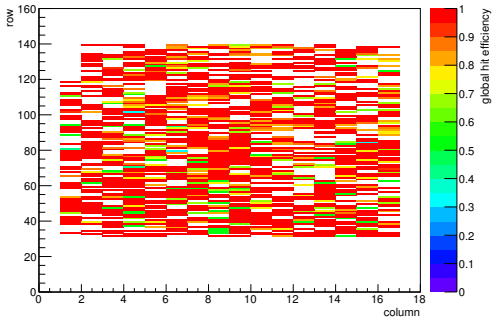

(k) Hit efficiency map.

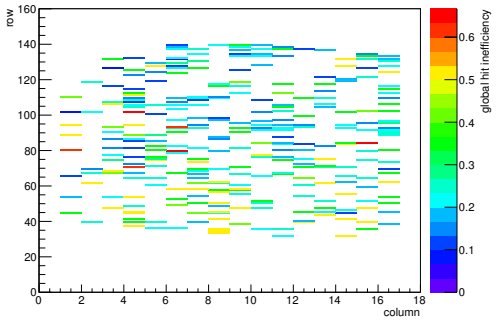

(l) Hit inefficiency map.

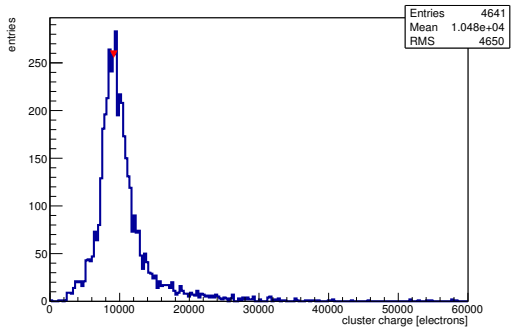

(m) Charge distribution (all cluster sizes included).

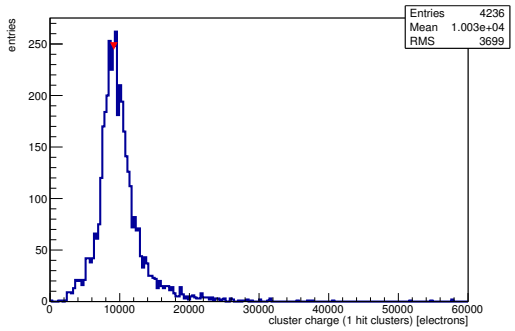

(n) Charge distribution (1 hit cluster).

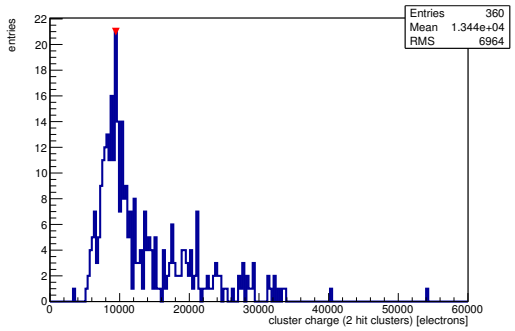

(o) Charge distribution (2 hit cluster).

Figure C.100: Detailed plots for test beam measurement of DO-I-11 (description see section 6.1) sample (running as DUT1) during runs 61262 in the September 2011 test beam period at CERN SPS in area H6B. Summary of the data in chapter 9. *(cont.)*

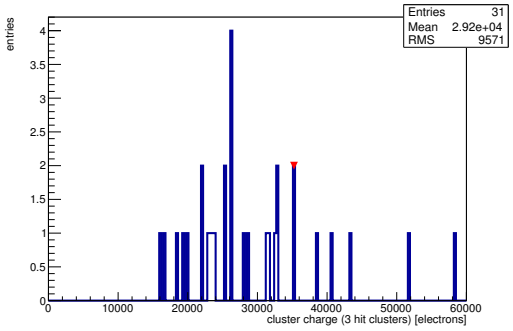

(p) Charge distribution (3 hit cluster).

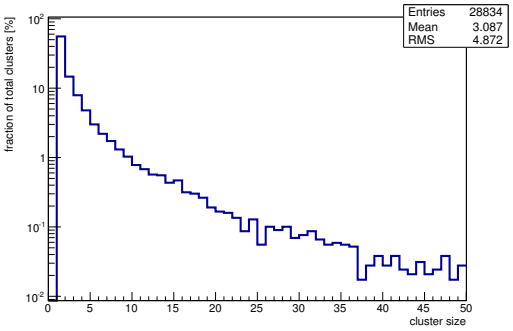

(q) Cluster size distribution.

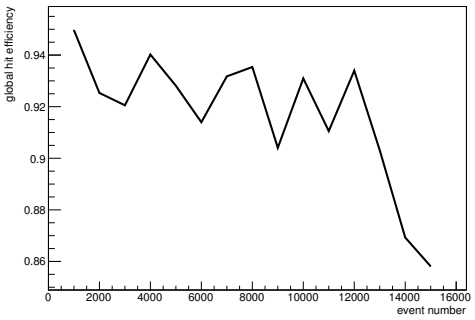

(r) Hit efficiency vs event number.

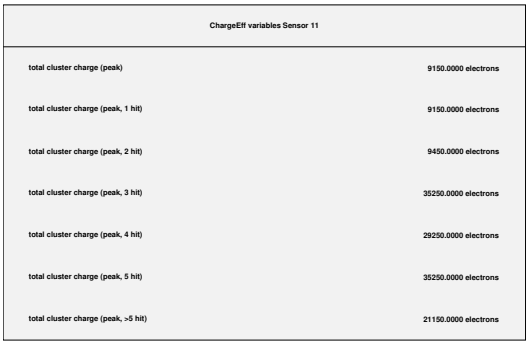

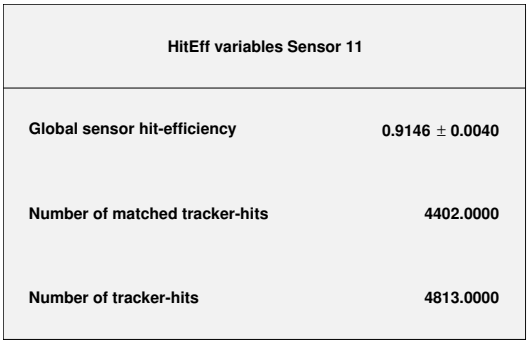

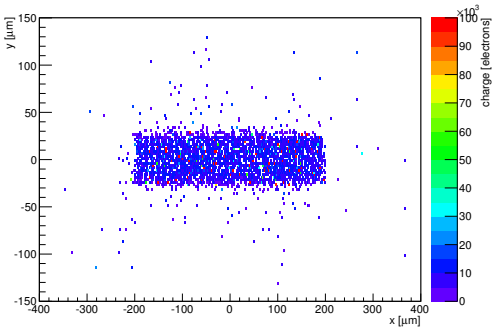

(s) Single pixel mean charge.

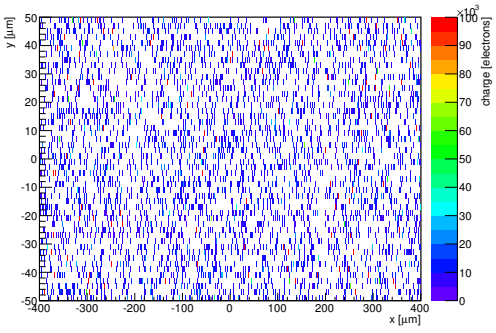

(t) Single pixel mean charge.

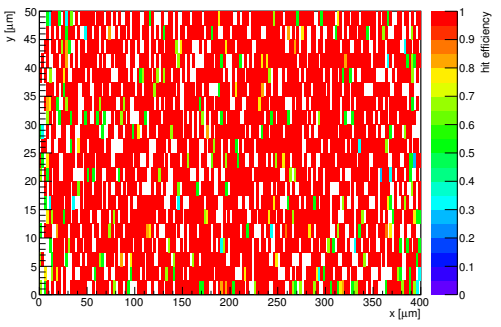

(u) Single pixel hit efficiency.

Figure C.100: Detailed plots for test beam measurement of DO-I-11 (description see section 6.1) sample (running as DUT1) during runs 61262 in the September 2011 test beam period at CERN SPS in area H6B. Summary of the data in chapter 9.

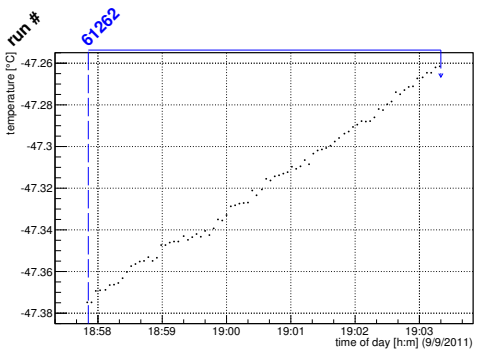

(a) Temperature vs time.

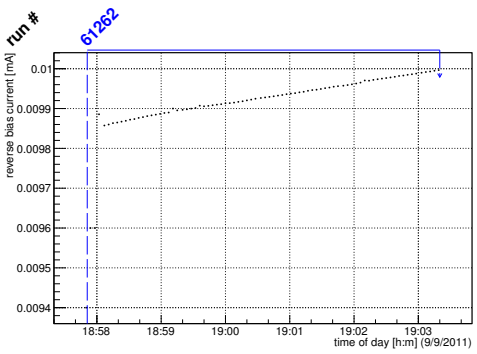

(b) Bias current vs time.

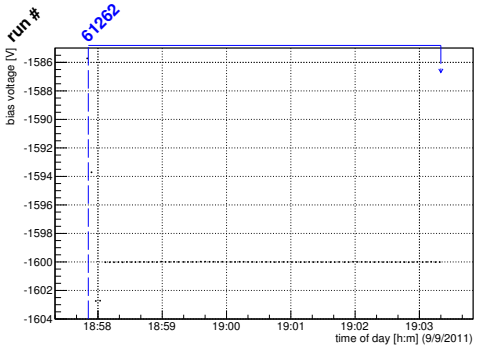

(c) Currently applied bias voltage vs time.

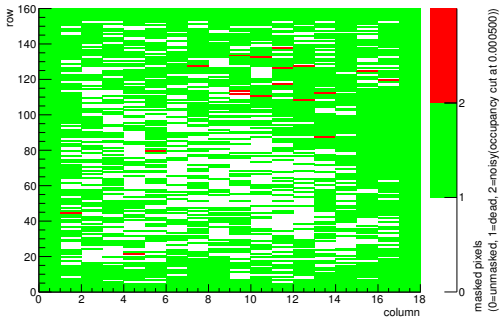

(d) Map of masked pixels.

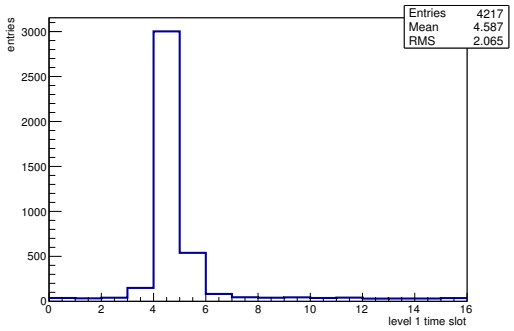

(e) Lvl1 distribution.

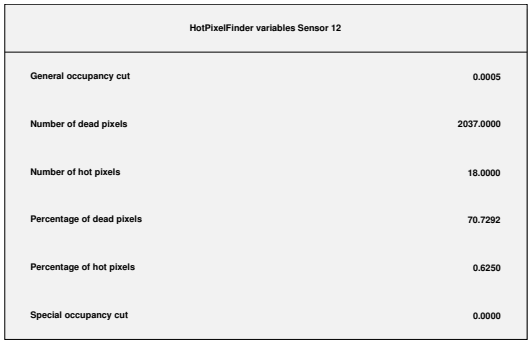

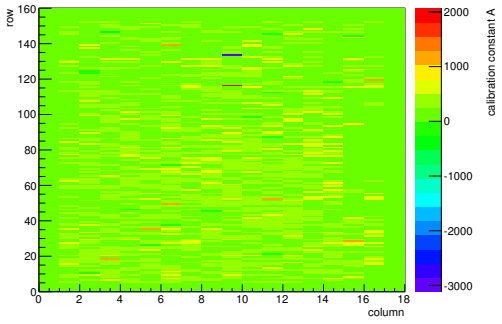

(f) Calibration constant A.

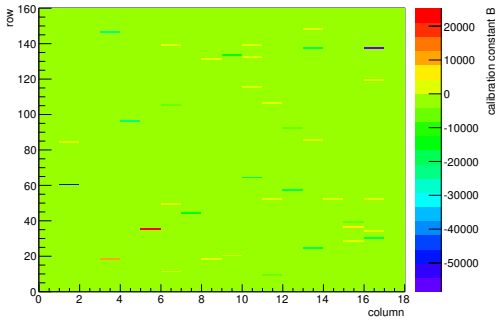

(g) Calibration constant B.

Figure C.101: Detailed plots for test beam measurement of DO-I-5 (description see section 6.1) sample (running as DUT2) during runs 61262 in the September 2011 test beam period at CERN SPS in area H6B. Summary of the data in chapter 9. *(cont.)*

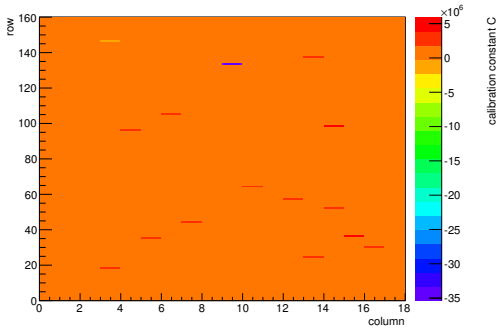

(h) Calibration constant C.

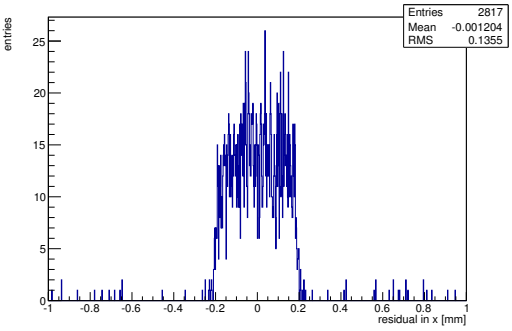

(i) Track residual in x.

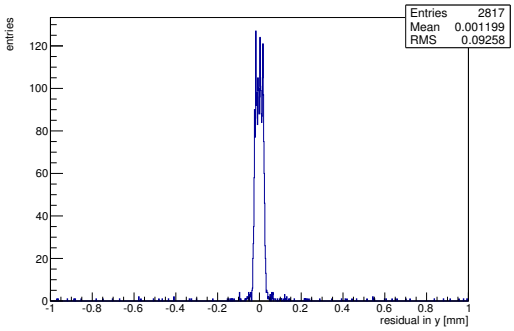

(j) Track residual in y.

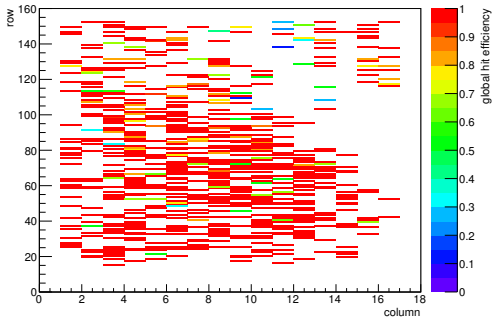

(k) Hit efficiency map.

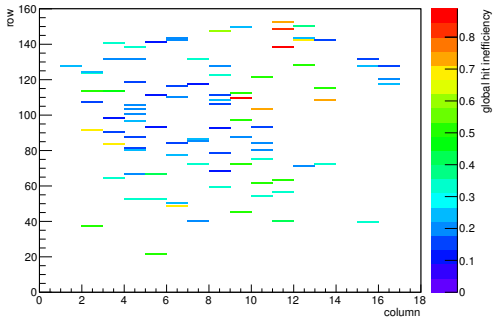

(l) Hit inefficiency map.

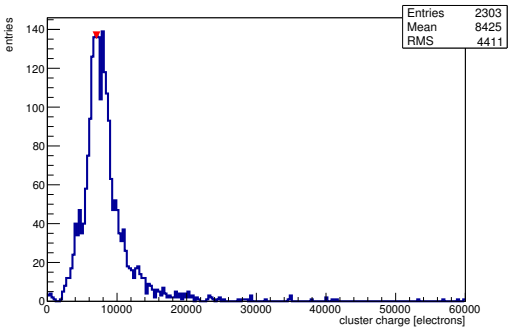

(m) Charge distribution (all cluster sizes included).

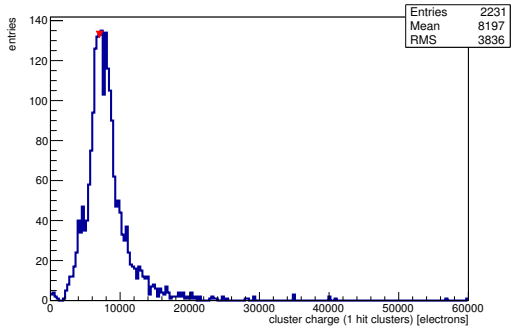

(n) Charge distribution (1 hit cluster).

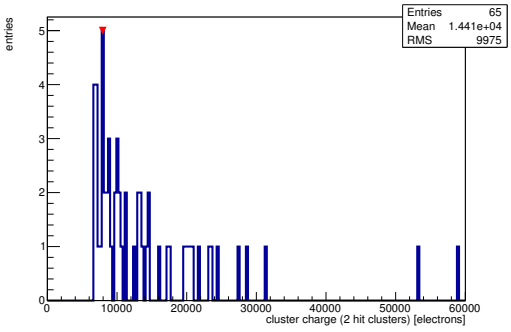

(o) Charge distribution (2 hit cluster).

Figure C.101: Detailed plots for test beam measurement of DO-I-5 (description see section 6.1) sample (running as DUT2) during runs 61262 in the September 2011 test beam period at CERN SPS in area H6B. Summary of the data in chapter 9. *(cont.)*

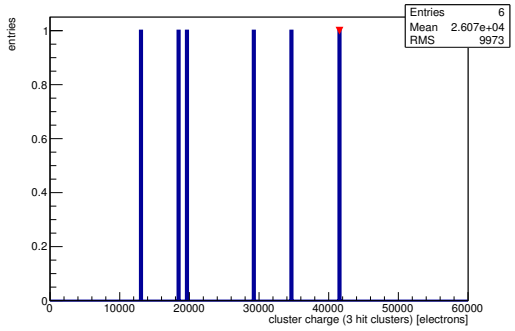

(p) Charge distribution (3 hit cluster).

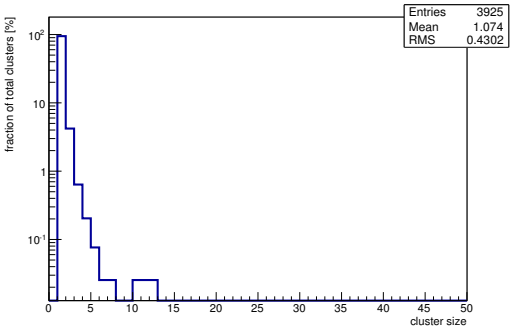

(q) Cluster size distribution.

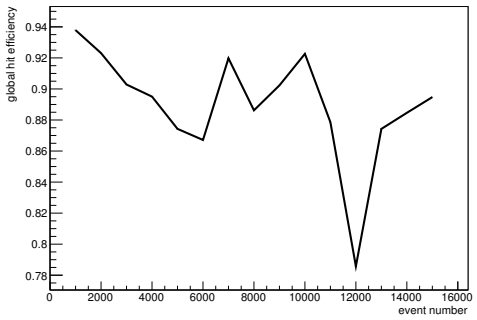

(r) Hit efficiency vs event number.

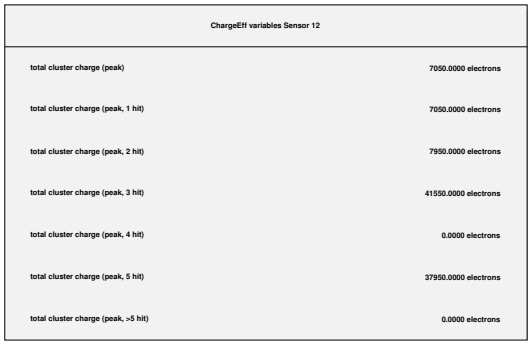

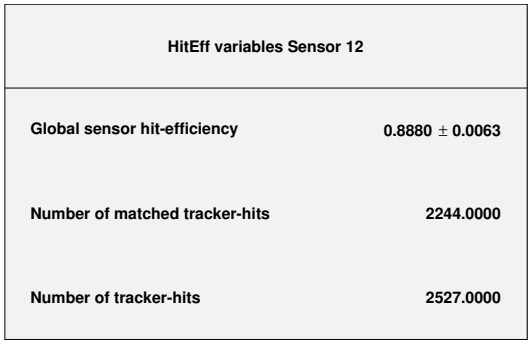

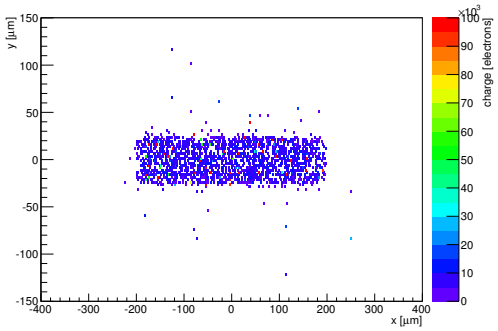

(s) Single pixel mean charge.

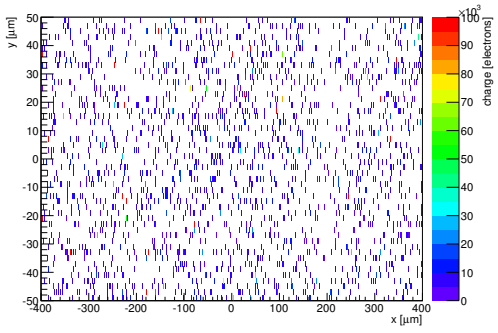

(t) Single pixel mean charge.

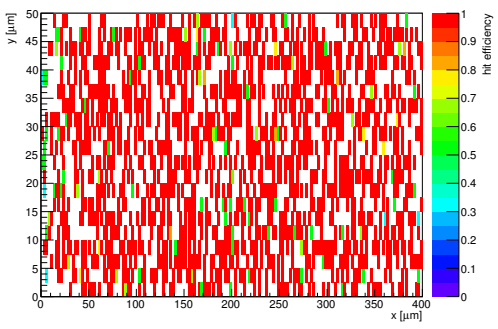

(u) Single pixel hit efficiency.

Figure C.101: Detailed plots for test beam measurement of DO-I-5 (description see section 6.1) sample (running as DUT2) during runs 61262 in the September 2011 test beam period at CERN SPS in area H6B. Summary of the data in chapter 9.

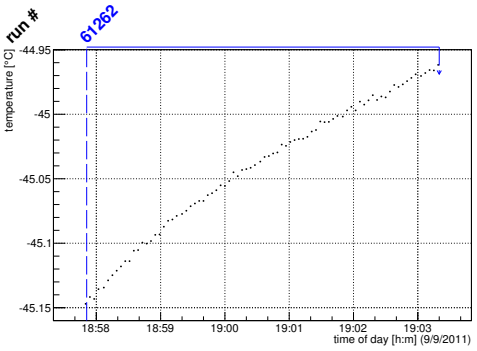

(a) Temperature vs time.

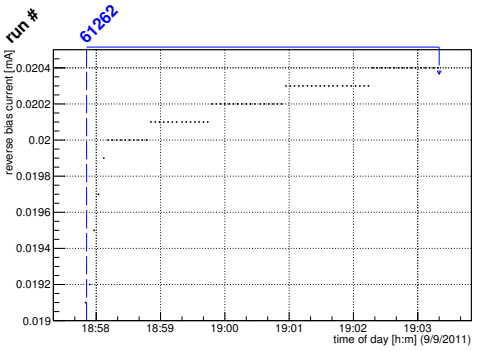

(b) Bias current vs time.

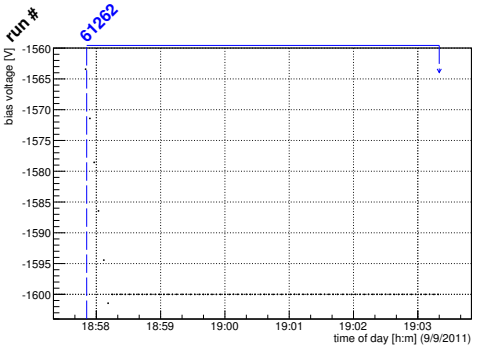

(c) Currently applied bias voltage vs time.

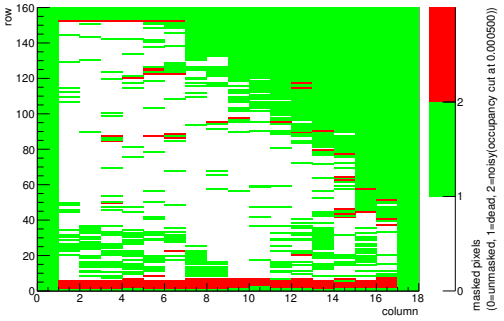

(d) Map of masked pixels.

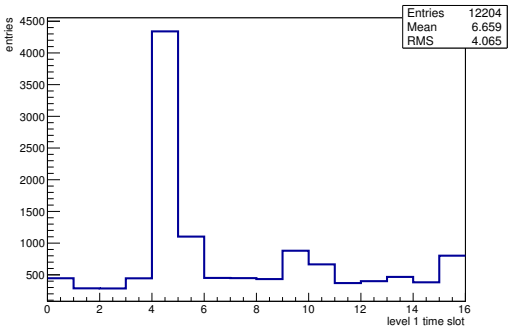

(e) Lvl1 distribution.

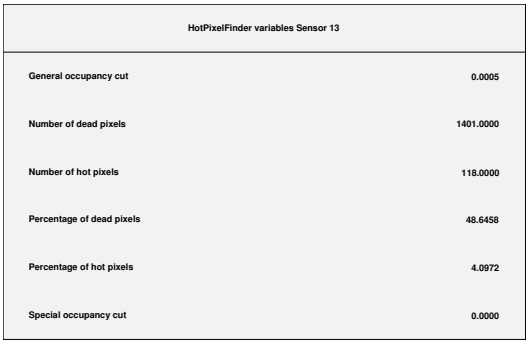

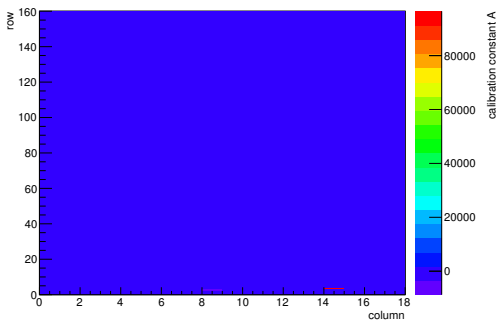

(f) Calibration constant A.

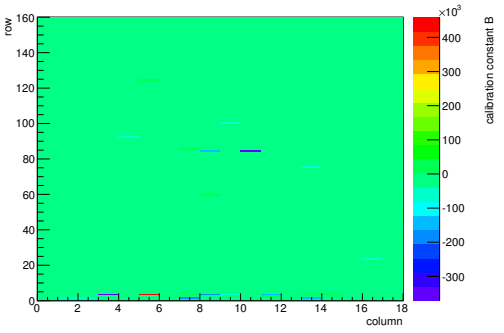

(g) Calibration constant B.

Figure C.102: Detailed plots for test beam measurement of DO-I-12 (description see section 6.1) sample (running as DUT3) during runs 61262 in the September 2011 test beam period at CERN SPS in area H6B. Summary of the data in chapter 9. *(cont.)*

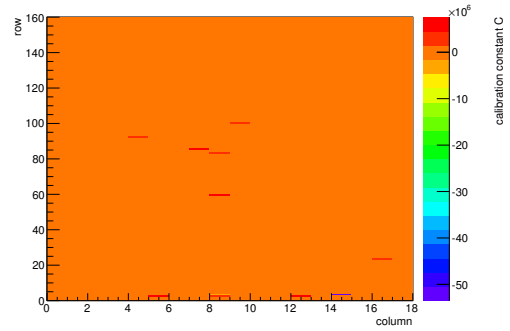

(h) Calibration constant C.

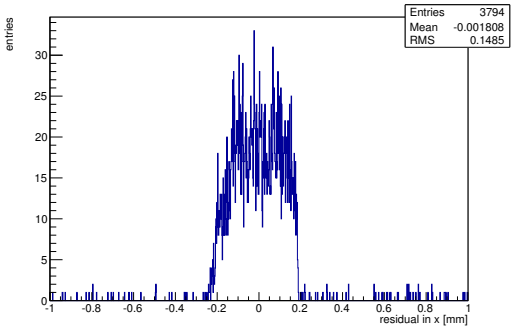

(i) Track residual in x.

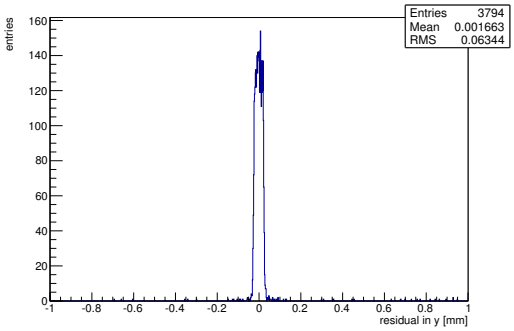

(j) Track residual in y.

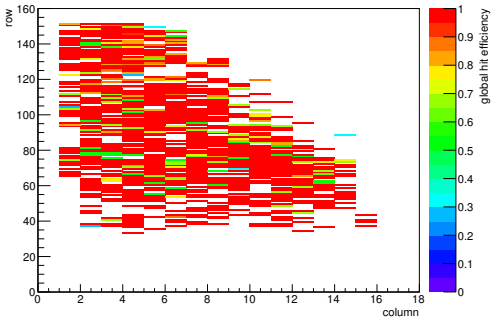

(k) Hit efficiency map.

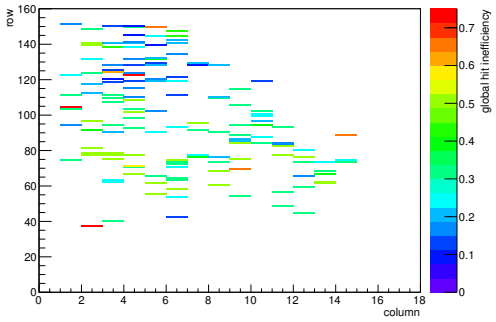

(l) Hit inefficiency map.

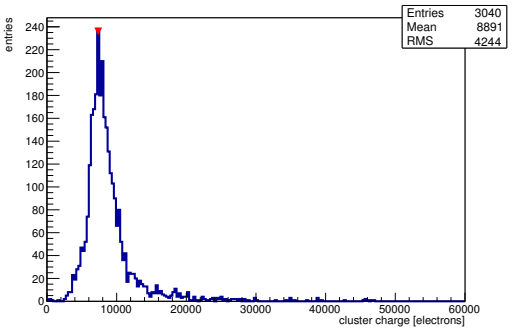

(m) Charge distribution (all cluster sizes included).

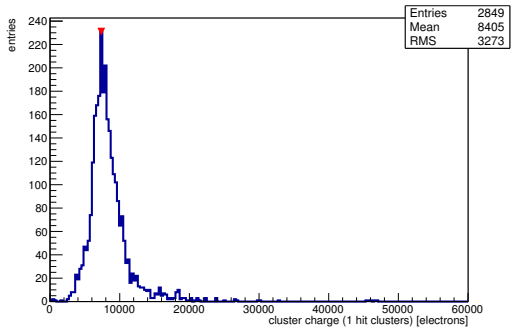

(n) Charge distribution (1 hit cluster).

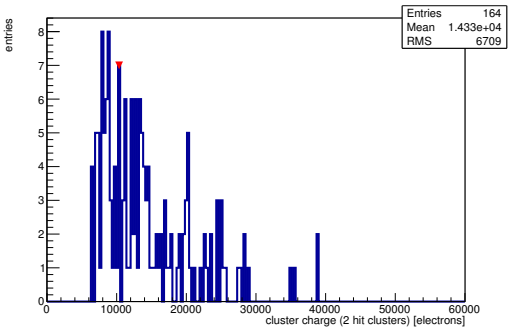

(o) Charge distribution (2 hit cluster).

Figure C.102: Detailed plots for test beam measurement of DO-I-12 (description see section 6.1) sample (running as DUT3) during runs 61262 in the September 2011 test beam period at CERN SPS in area H6B. Summary of the data in chapter 9. *(cont.)*

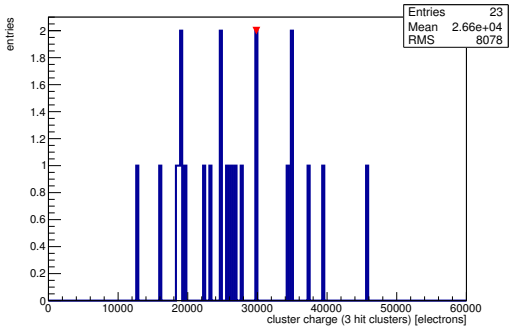

(p) Charge distribution (3 hit cluster).

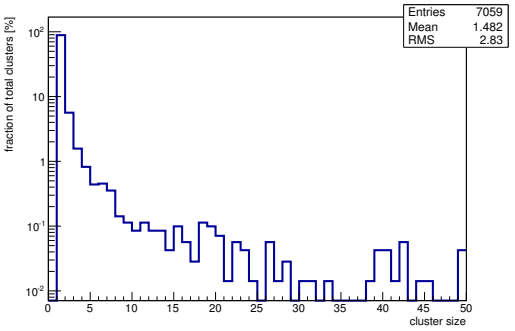

(q) Cluster size distribution.

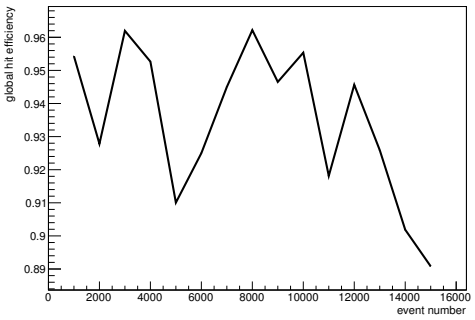

(r) Hit efficiency vs event number.

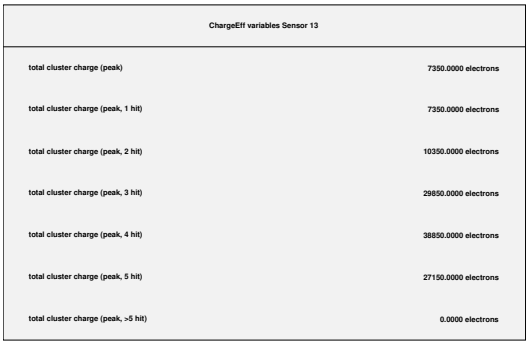

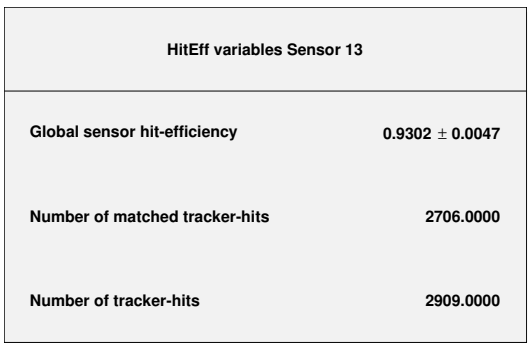

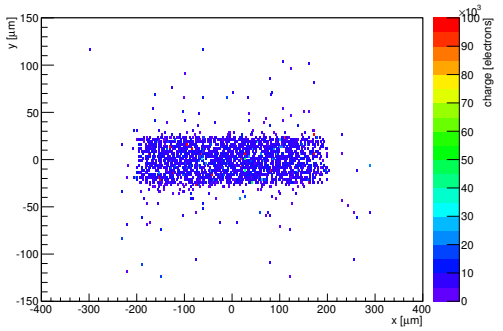

(s) Single pixel mean charge.

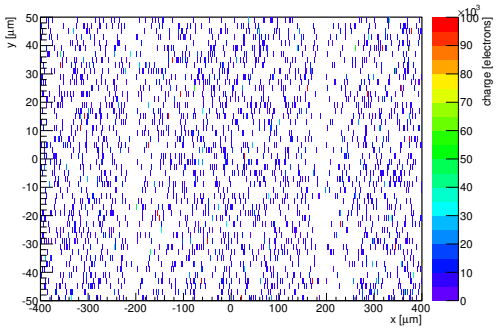

(t) Single pixel mean charge.

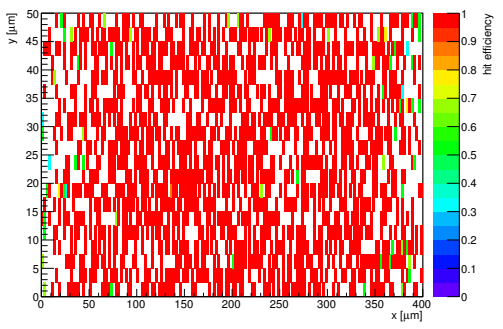

(u) Single pixel hit efficiency.

Figure C.102: Detailed plots for test beam measurement of DO-I-12 (description see section 6.1) sample (running as DUT3) during runs 61262 in the September 2011 test beam period at CERN SPS in area H6B. Summary of the data in chapter 9.

C.3.16 Run 61263

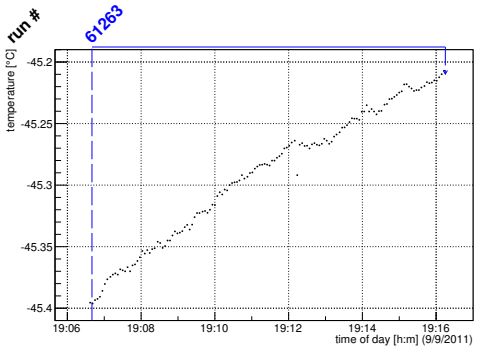

(a) Temperature vs time.

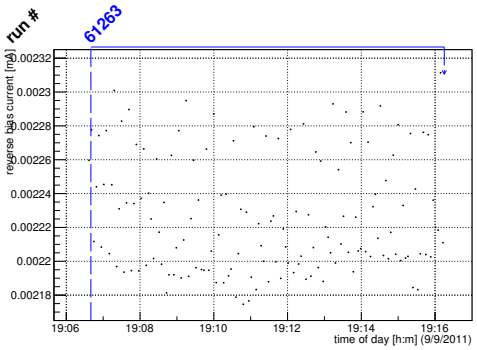

(b) Bias current vs time.

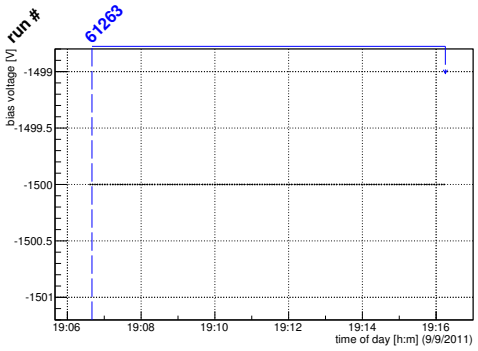

(c) Currently applied bias voltage vs time.

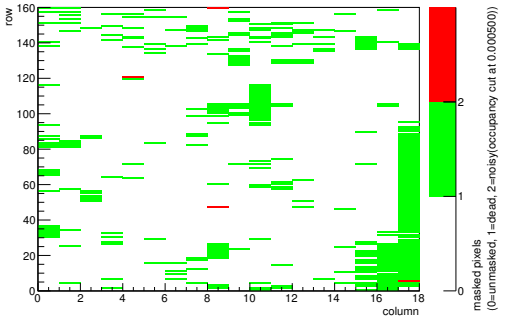

(d) Map of masked pixels.

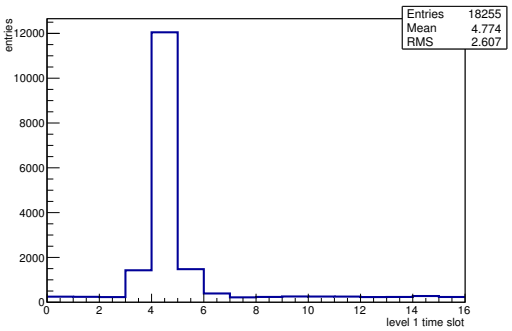

(e) Lvl1 distribution.

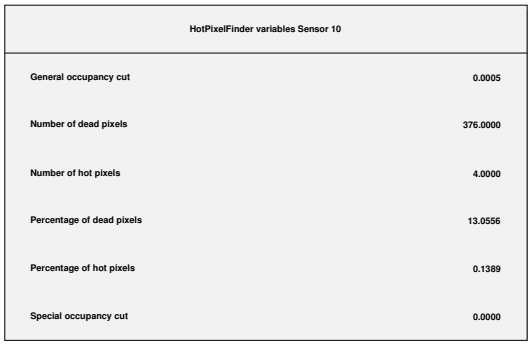

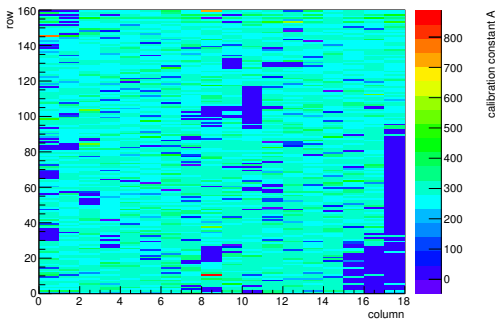

(f) Calibration constant A.

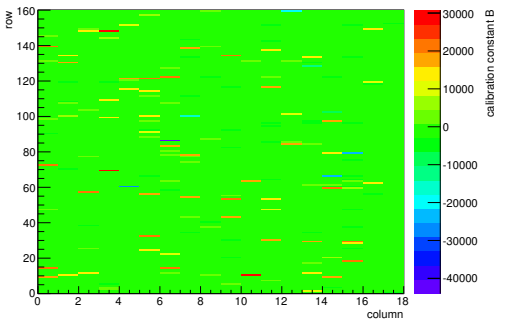

(g) Calibration constant B.

Figure C.103: Detailed plots for test beam measurement of DO-I-7 (description see section 6.1) sample (running as DUT0) during runs 61263 in the September 2011 test beam period at CERN SPS in area H6B. Summary of the data in chapter 9. *(cont.)*

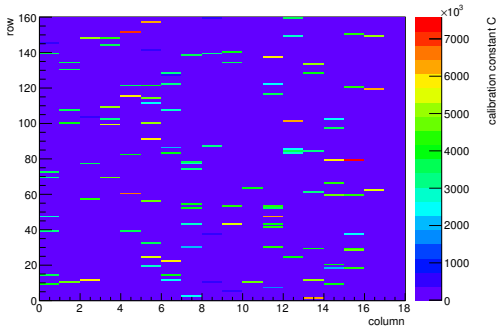

(h) Calibration constant C.

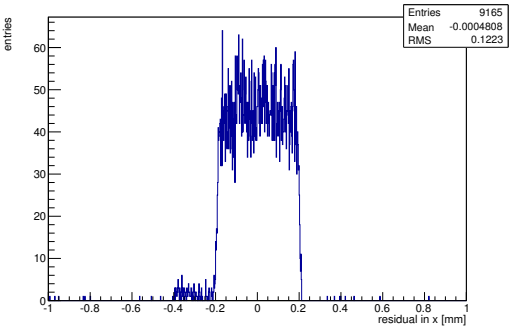

(i) Track residual in x.

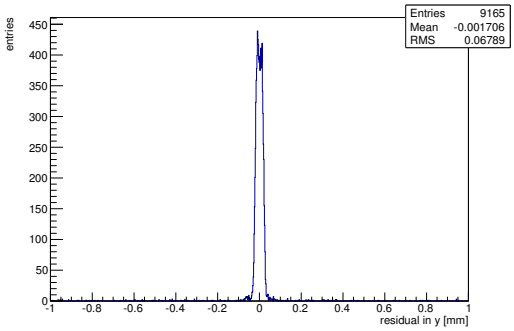

(j) Track residual in y.

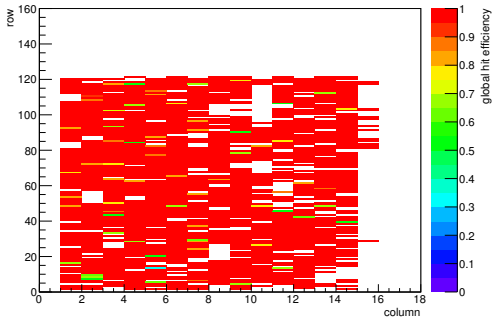

(k) Hit efficiency map.

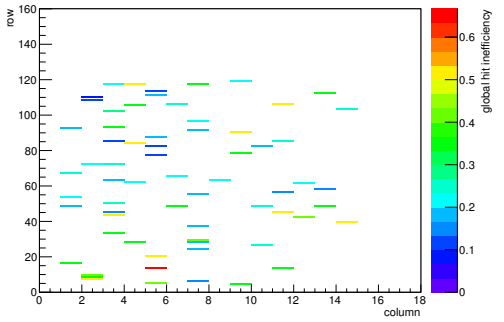

(l) Hit inefficiency map.

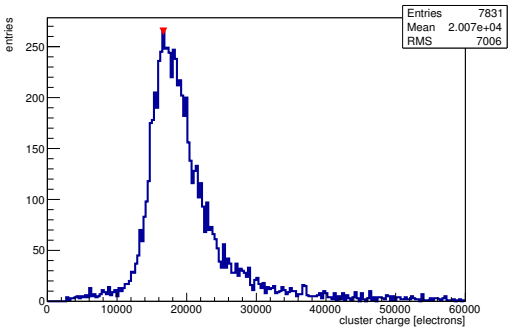

(m) Charge distribution (all cluster sizes included).

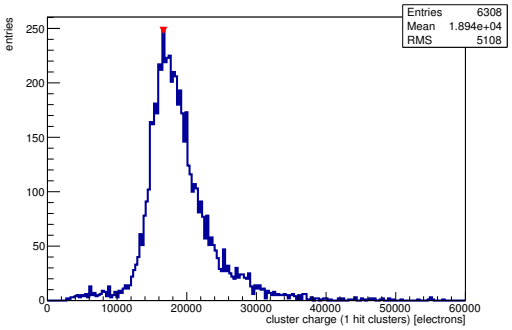

(n) Charge distribution (1 hit cluster).

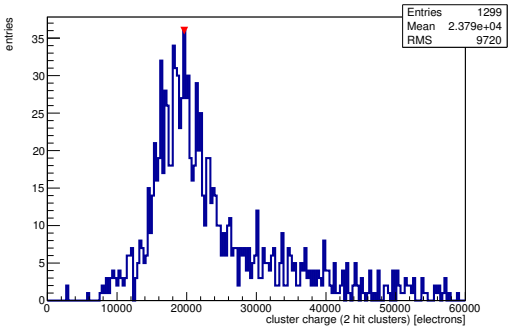

(o) Charge distribution (2 hit cluster).

Figure C.103: Detailed plots for test beam measurement of DO-I-7 (description see section 6.1) sample (running as DUT0) during runs 61263 in the September 2011 test beam period at CERN SPS in area H6B. Summary of the data in chapter 9. *(cont.)*

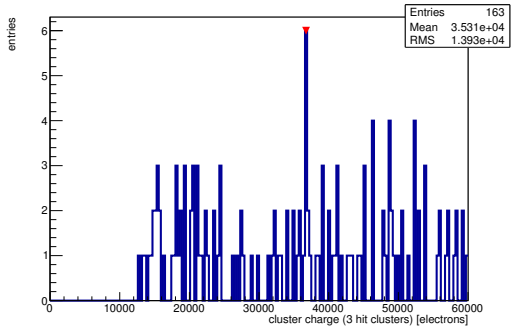

(p) Charge distribution (3 hit cluster).

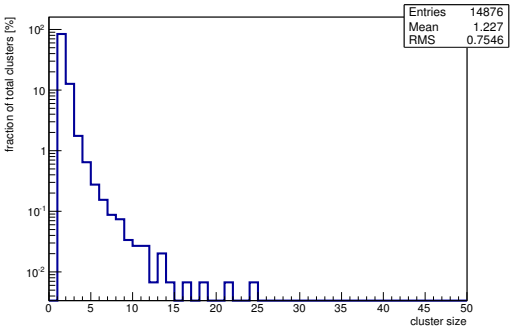

(q) Cluster size distribution.

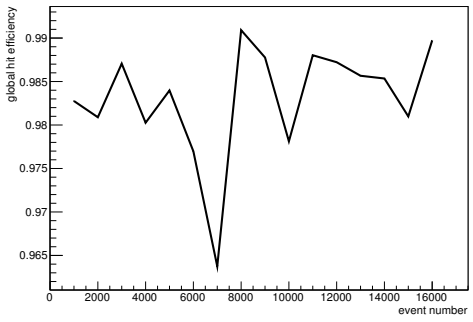

(r) Hit efficiency vs event number.

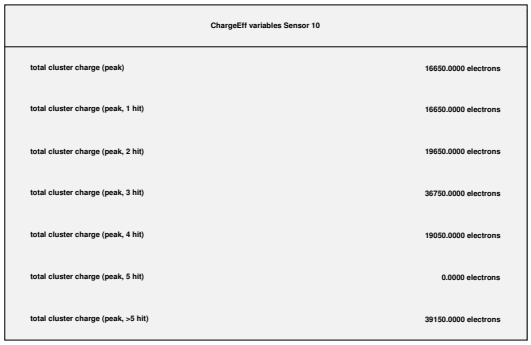

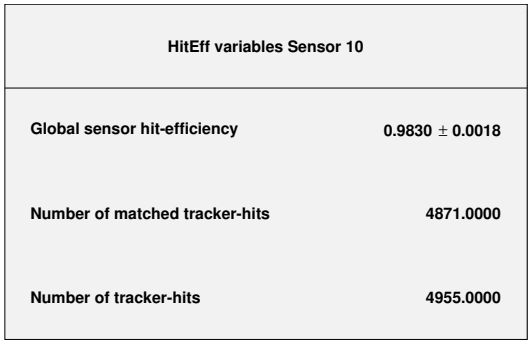

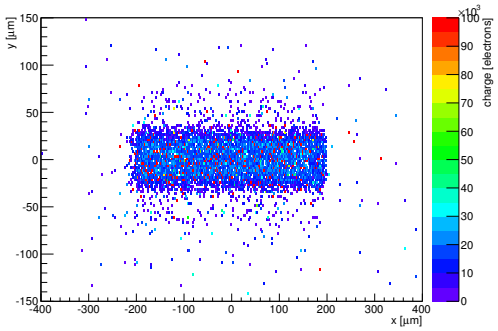

(s) Single pixel mean charge.

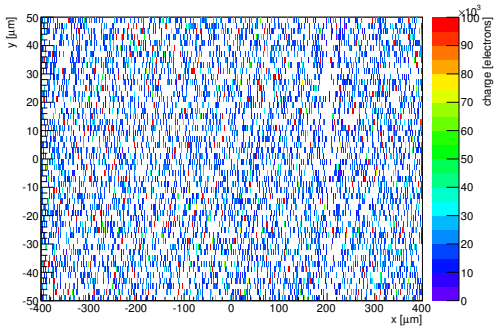

(t) Single pixel mean charge.

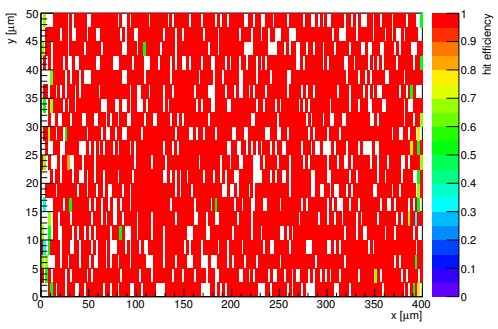

(u) Single pixel hit efficiency.

Figure C.103: Detailed plots for test beam measurement of DO-I-7 (description see section 6.1) sample (running as DUT0) during runs 61263 in the September 2011 test beam period at CERN SPS in area H6B. Summary of the data in chapter 9.

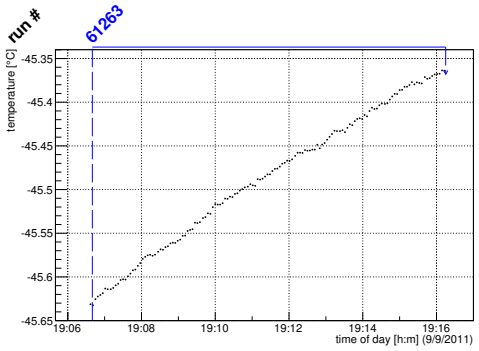

(a) Temperature vs time.

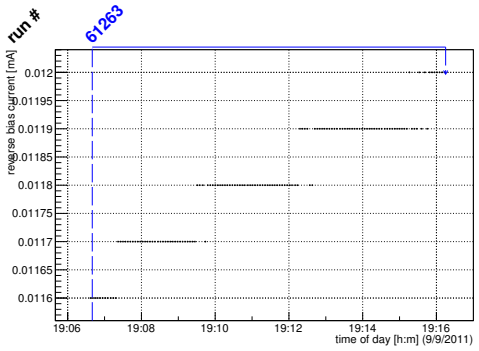

(b) Bias current vs time.

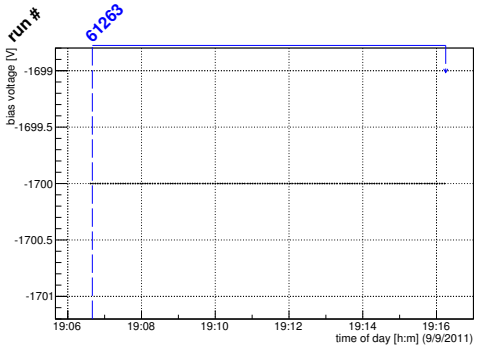

(c) Currently applied bias voltage vs time.

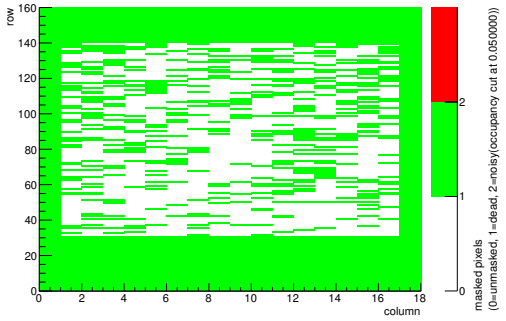

(d) Map of masked pixels.

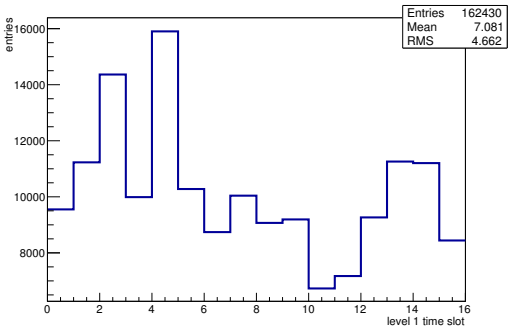

(e) Lvl1 distribution.

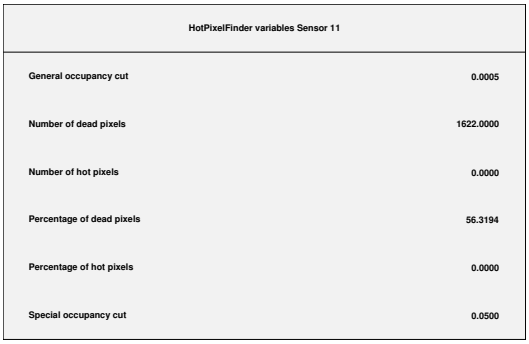

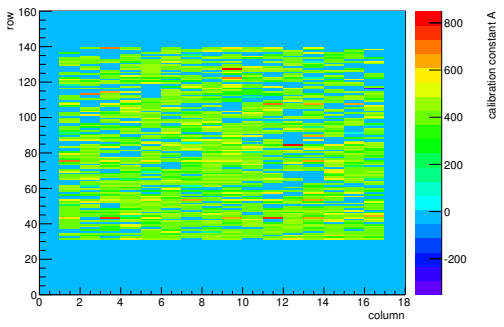

(f) Calibration constant A.

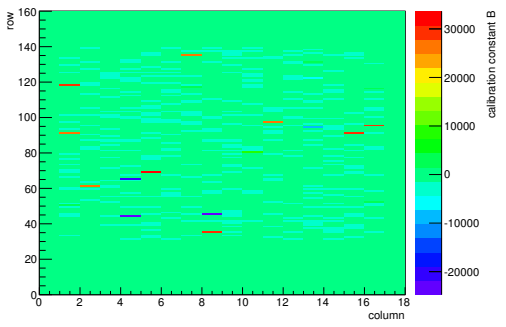

(g) Calibration constant B.

Figure C.104: Detailed plots for test beam measurement of DO-I-11 (description see section 6.1) sample (running as DUT1) during runs 61263 in the September 2011 test beam period at CERN SPS in area H6B. Summary of the data in chapter 9. *(cont.)*

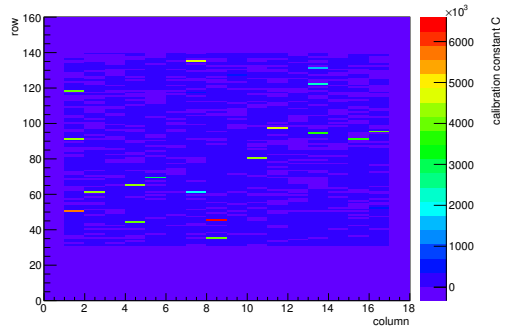

(h) Calibration constant C.

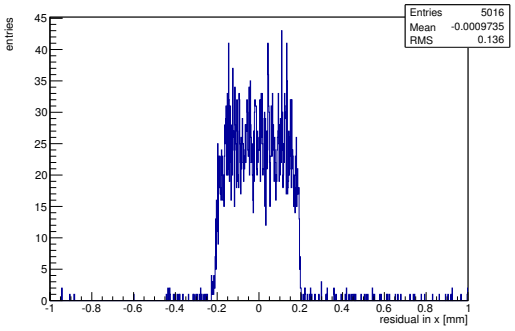

(i) Track residual in x.

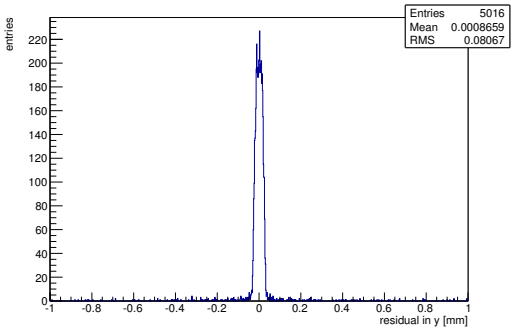

(j) Track residual in y.

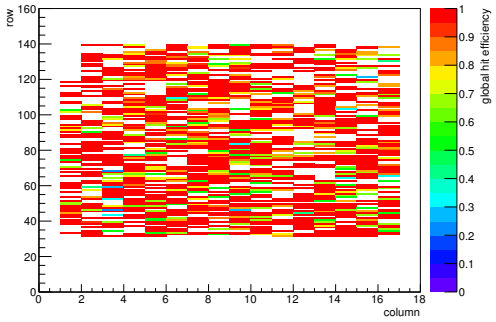

(k) Hit efficiency map.

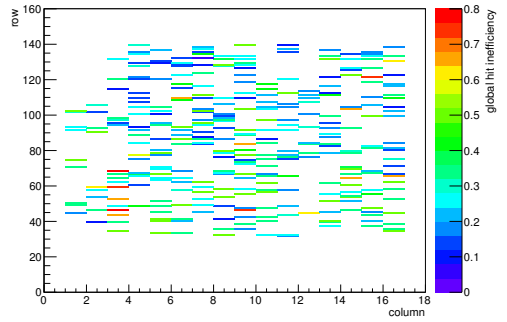

(l) Hit inefficiency map.

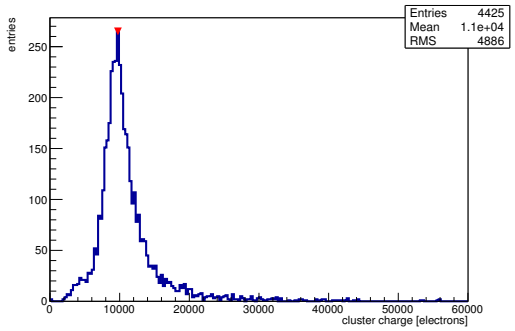

(m) Charge distribution (all cluster sizes included).

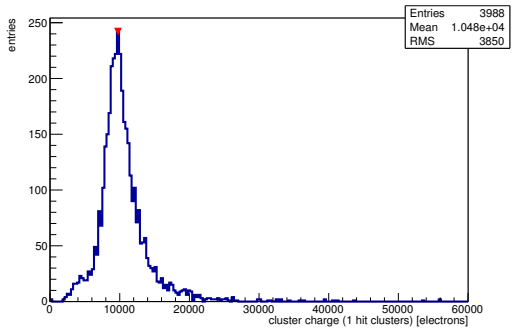

(n) Charge distribution (1 hit cluster).

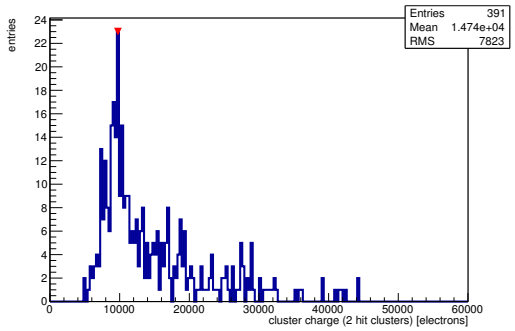

(o) Charge distribution (2 hit cluster).

Figure C.104: Detailed plots for test beam measurement of DO-I-11 (description see section 6.1) sample (running as DUT1) during runs 61263 in the September 2011 test beam period at CERN SPS in area H6B. Summary of the data in chapter 9. *(cont.)*

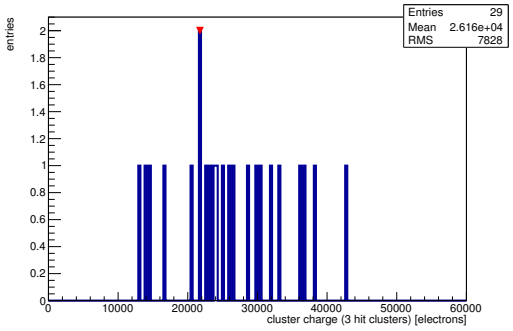

(p) Charge distribution (3 hit cluster).

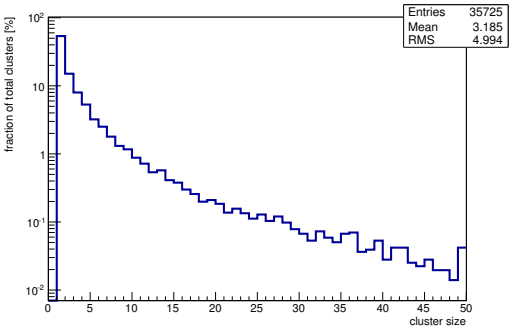

(q) Cluster size distribution.

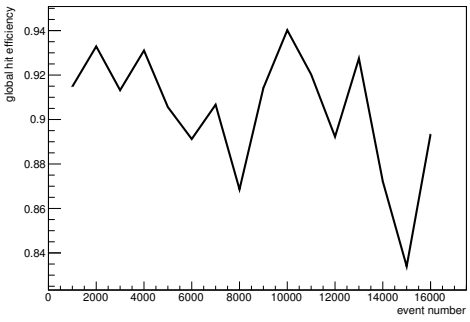

(r) Hit efficiency vs event number.

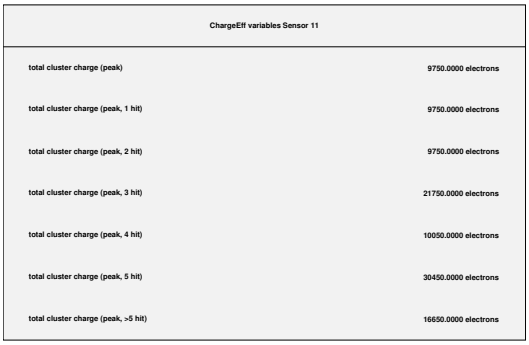

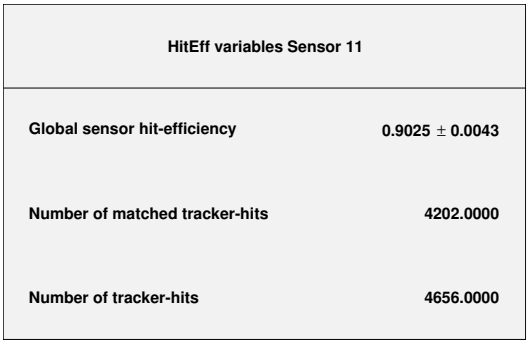

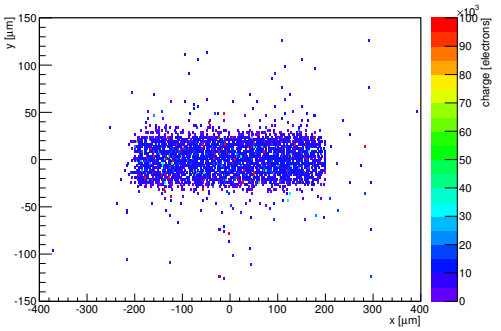

(s) Single pixel mean charge.

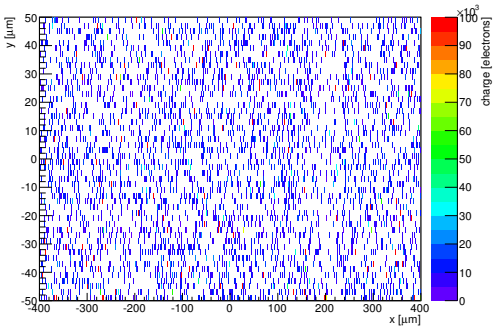

(t) Single pixel mean charge.

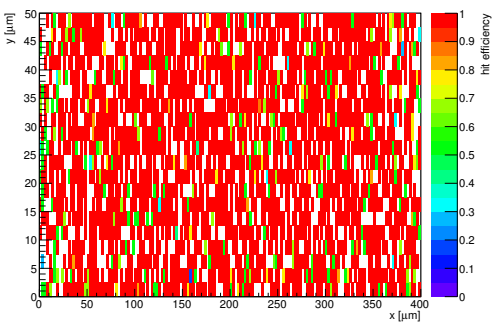

(u) Single pixel hit efficiency.

Figure C.104: Detailed plots for test beam measurement of DO-I-11 (description see section 6.1) sample (running as DUT1) during runs 61263 in the September 2011 test beam period at CERN SPS in area H6B. Summary of the data in chapter 9.

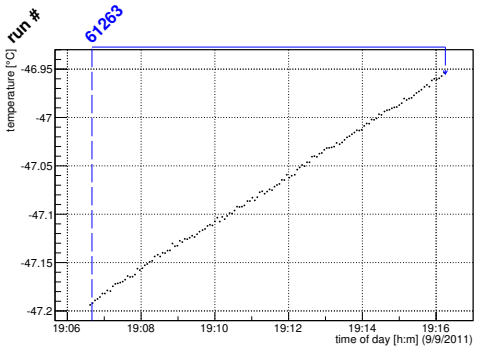

(a) Temperature vs time.

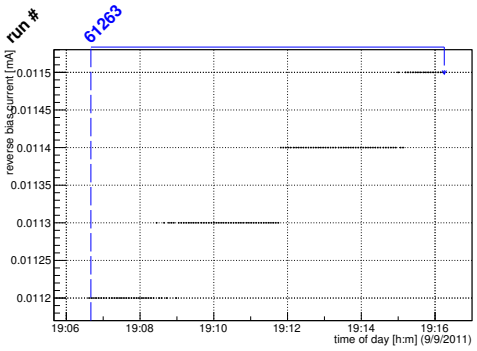

(b) Bias current vs time.

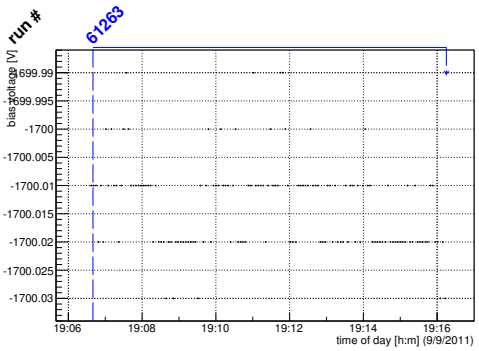

(c) Currently applied bias voltage vs time.

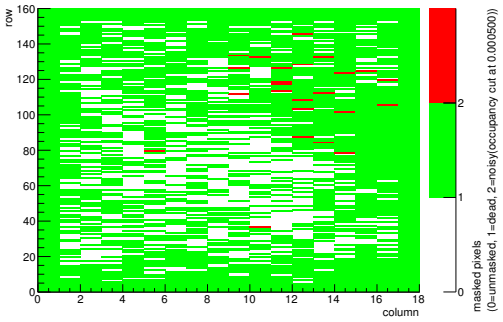

(d) Map of masked pixels.

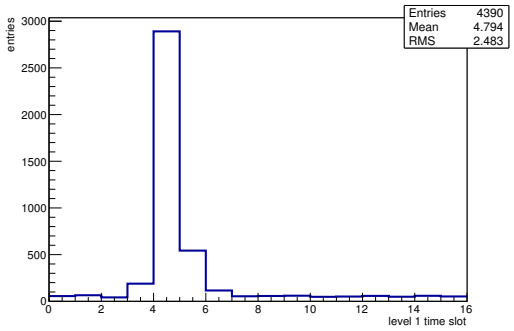

(e) Lvl1 distribution.

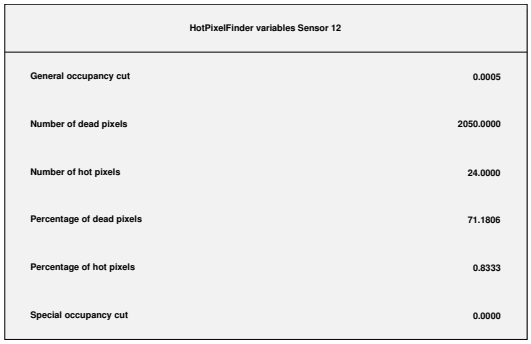

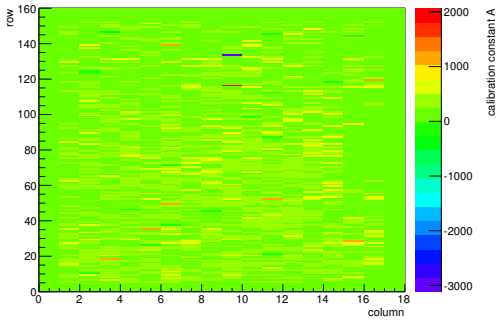

(f) Calibration constant A.

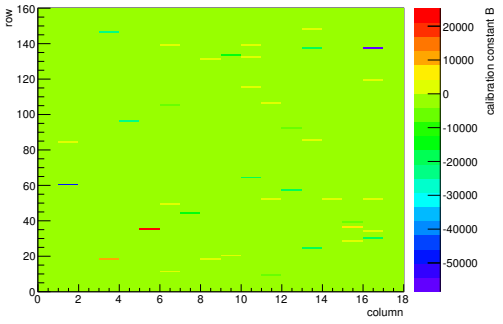

(g) Calibration constant B.

Figure C.105: Detailed plots for test beam measurement of DO-I-5 (description see section 6.1) sample (running as DUT2) during runs 61263 in the September 2011 test beam period at CERN SPS in area H6B. Summary of the data in chapter 9. *(cont.)*

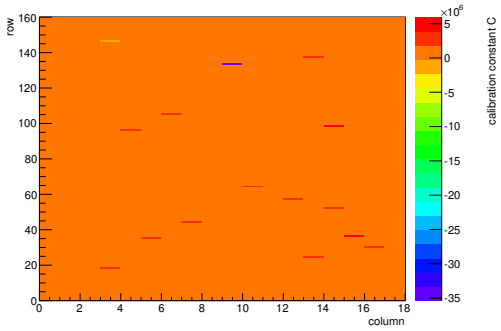

(h) Calibration constant C.

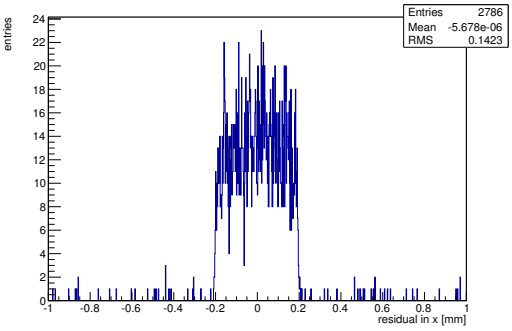

(i) Track residual in x.

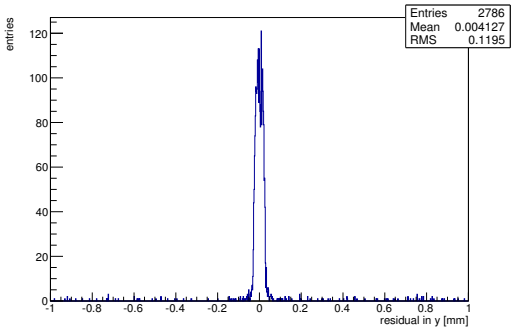

(j) Track residual in y.

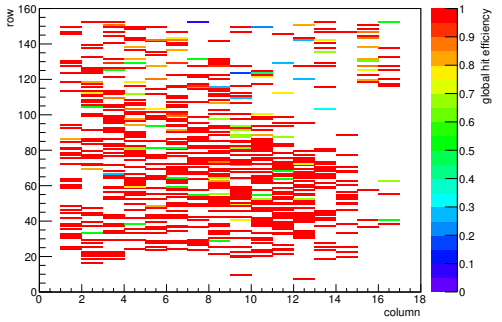

(k) Hit efficiency map.

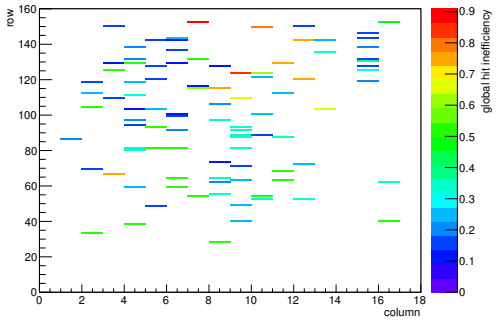

(l) Hit inefficiency map.

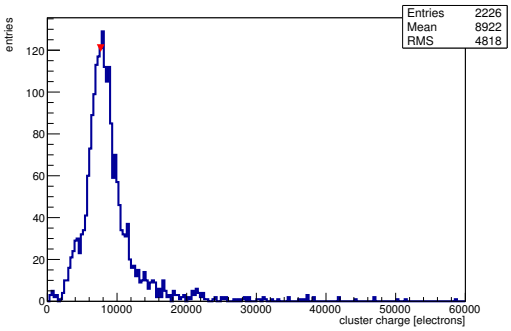

(m) Charge distribution (all cluster sizes included).

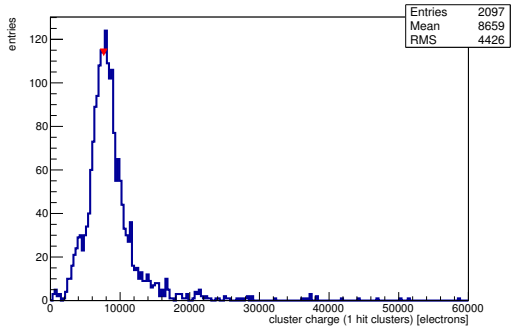

(n) Charge distribution (1 hit cluster).

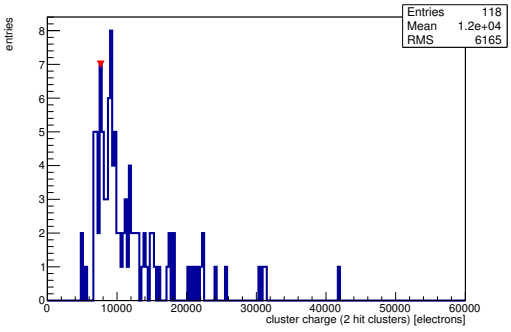

(o) Charge distribution (2 hit cluster).

Figure C.105: Detailed plots for test beam measurement of DO-I-5 (description see section 6.1) sample (running as DUT2) during runs 61263 in the September 2011 test beam period at CERN SPS in area H6B. Summary of the data in chapter 9. *(cont.)*

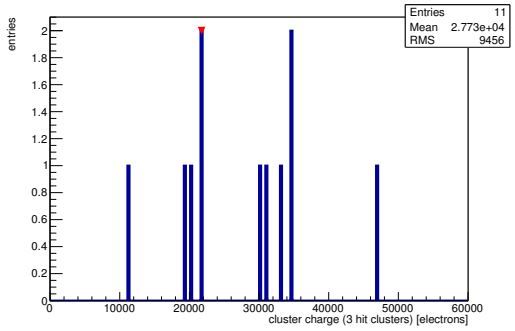

(p) Charge distribution (3 hit cluster).

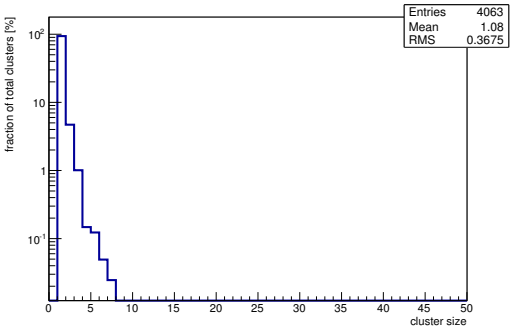

(q) Cluster size distribution.

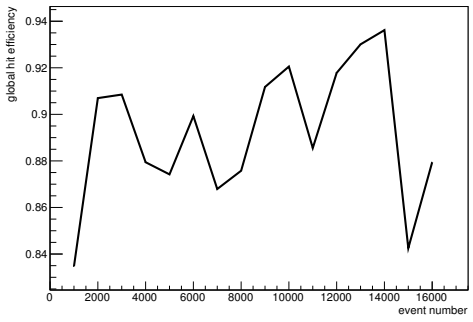

(r) Hit efficiency vs event number.

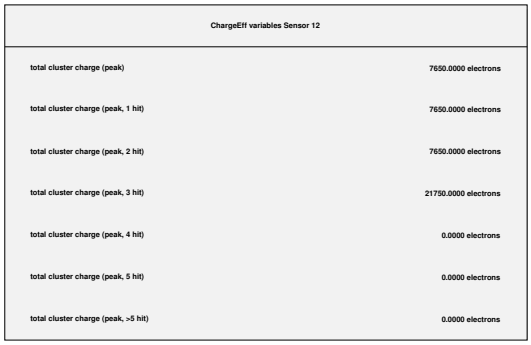

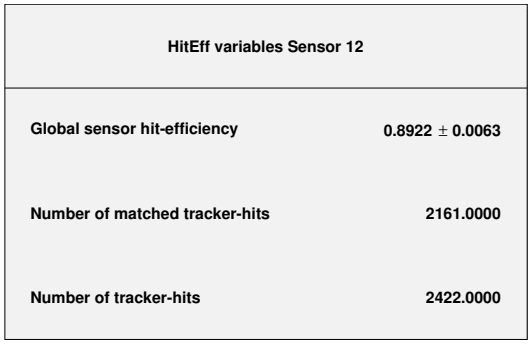

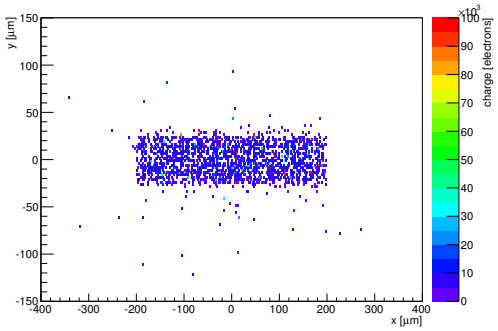

(s) Single pixel mean charge.

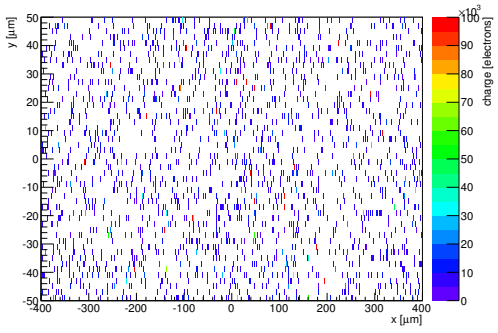

(t) Single pixel mean charge.

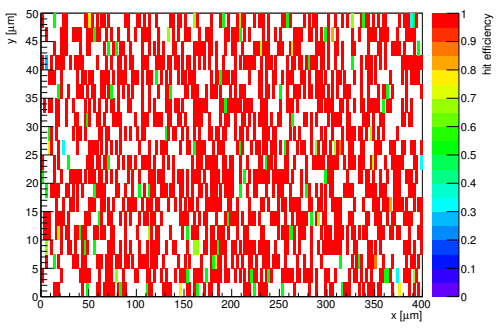

(u) Single pixel hit efficiency.

Figure C.105: Detailed plots for test beam measurement of DO-I-5 (description see section 6.1) sample (running as DUT2) during runs 61263 in the September 2011 test beam period at CERN SPS in area H6B. Summary of the data in chapter 9.

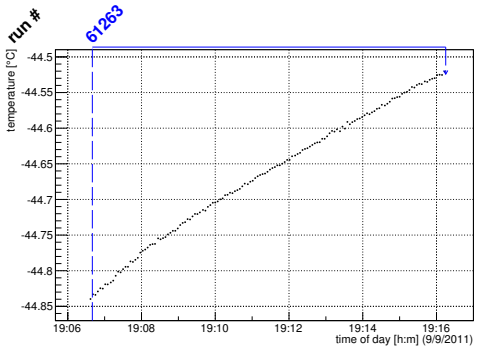

(a) Temperature vs time.

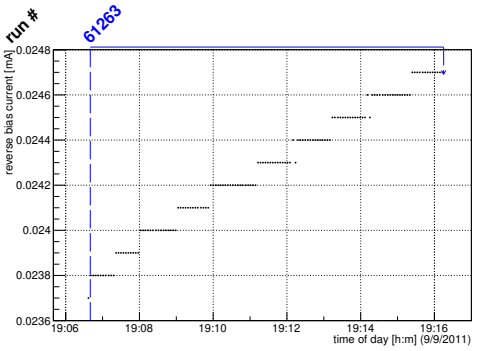

(b) Bias current vs time.

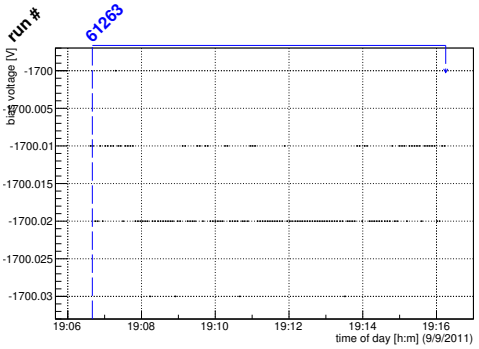

(c) Currently applied bias voltage vs time.

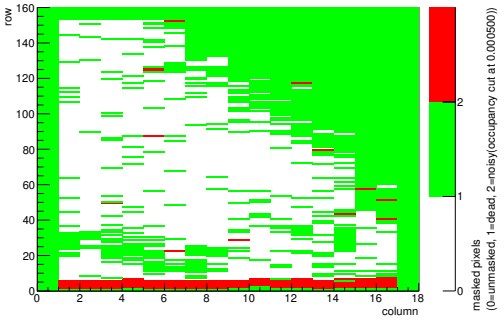

(d) Map of masked pixels.

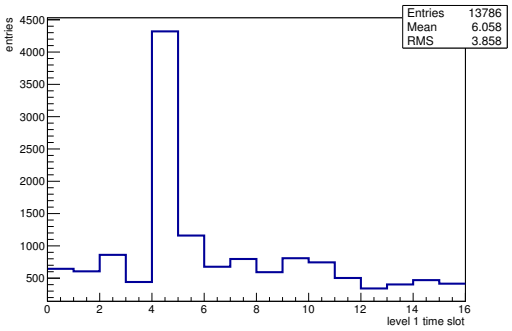

(e) Lvl1 distribution.

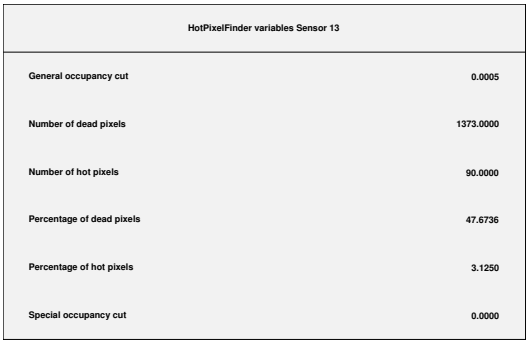

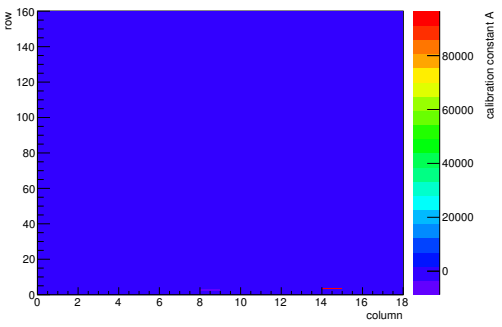

(f) Calibration constant A.

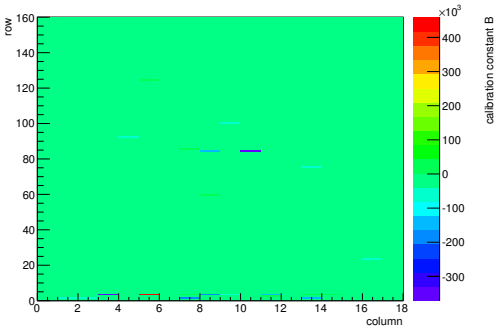

(g) Calibration constant B.

Figure C.106: Detailed plots for test beam measurement of DO-I-12 (description see section 6.1) sample (running as DUT3) during runs 61263 in the September 2011 test beam period at CERN SPS in area H6B. Summary of the data in chapter 9. *(cont.)*

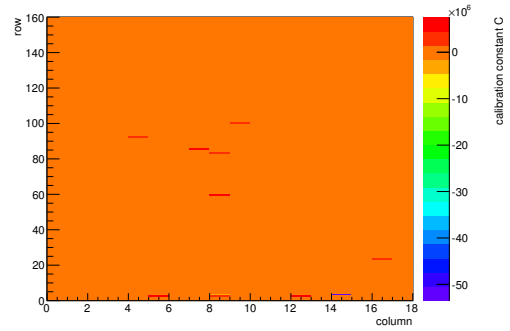

(h) Calibration constant C.

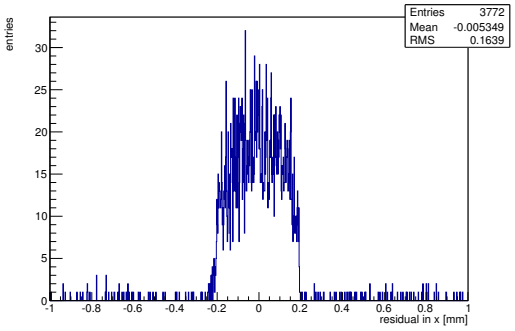

(i) Track residual in x.

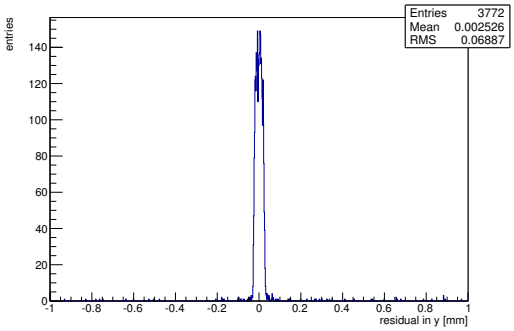

(j) Track residual in y.

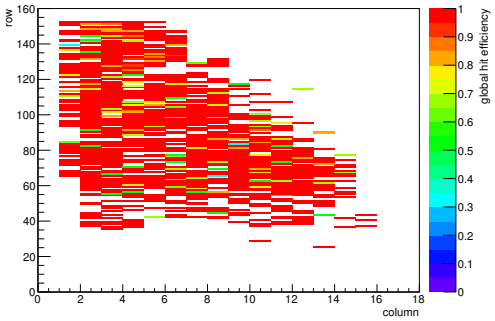

(k) Hit efficiency map.

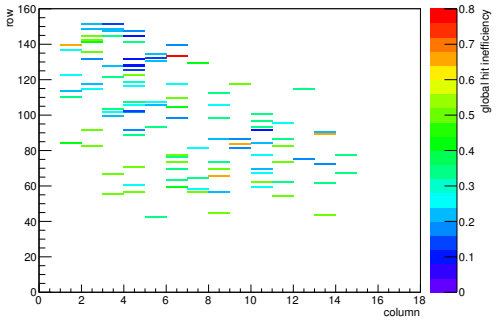

(l) Hit inefficiency map.

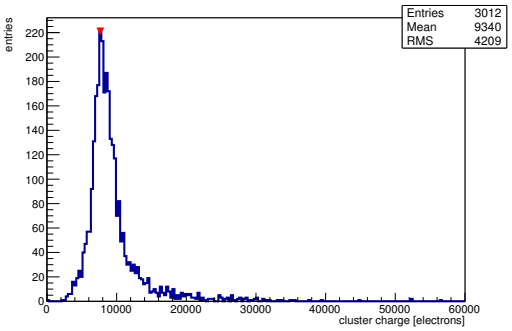

(m) Charge distribution (all cluster sizes included).

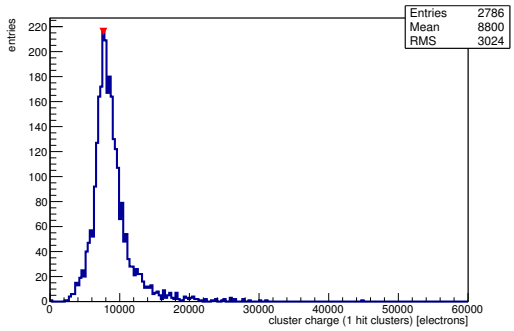

(n) Charge distribution (1 hit cluster).

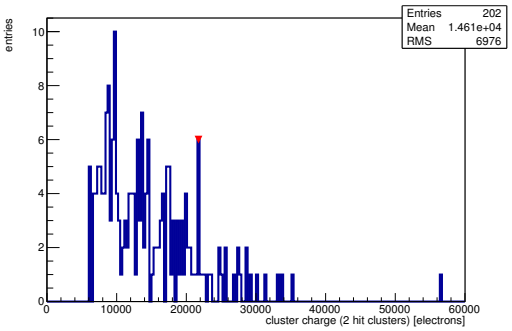

(o) Charge distribution (2 hit cluster).

Figure C.106: Detailed plots for test beam measurement of DO-I-12 (description see section 6.1) sample (running as DUT3) during runs 61263 in the September 2011 test beam period at CERN SPS in area H6B. Summary of the data in chapter 9. *(cont.)*

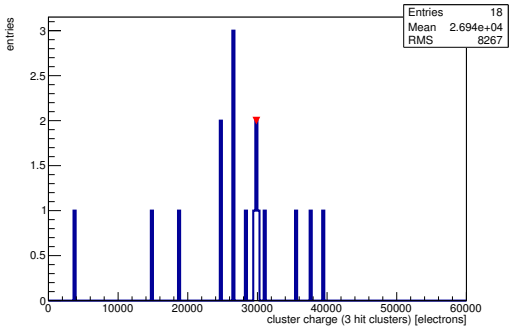

(p) Charge distribution (3 hit cluster).

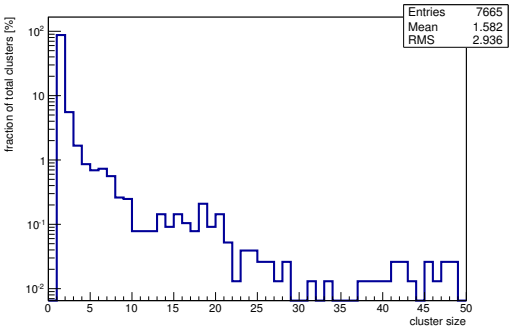

(q) Cluster size distribution.

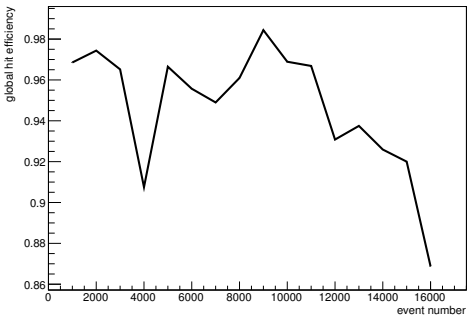

(r) Hit efficiency vs event number.

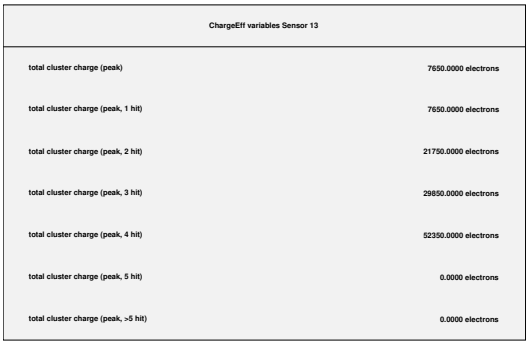

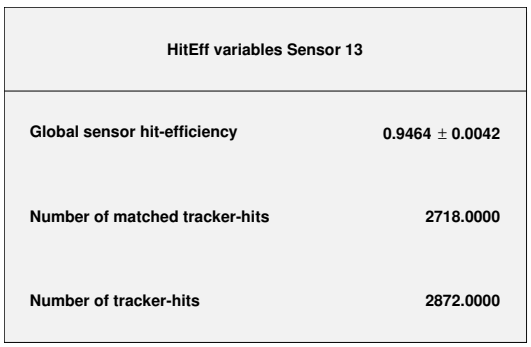

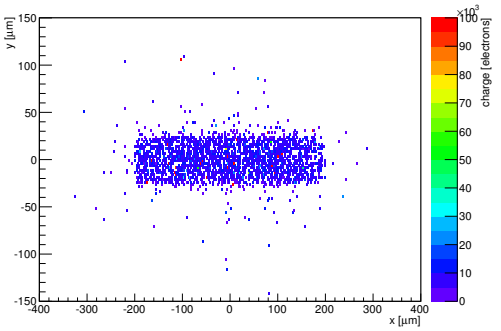

(s) Single pixel mean charge.

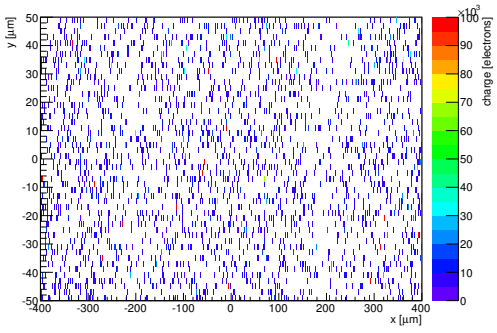

(t) Single pixel mean charge.

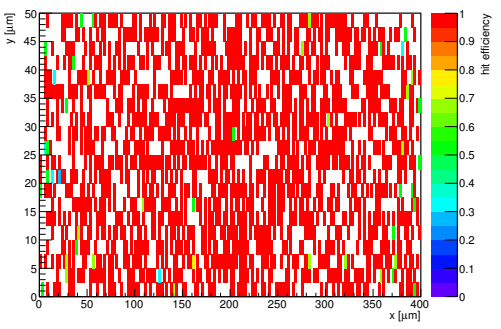

(u) Single pixel hit efficiency.

Figure C.106: Detailed plots for test beam measurement of DO-I-12 (description see section 6.1) sample (running as DUT3) during runs 61263 in the September 2011 test beam period at CERN SPS in area H6B. Summary of the data in chapter 9.

C.3.17 Runs 61264-61273

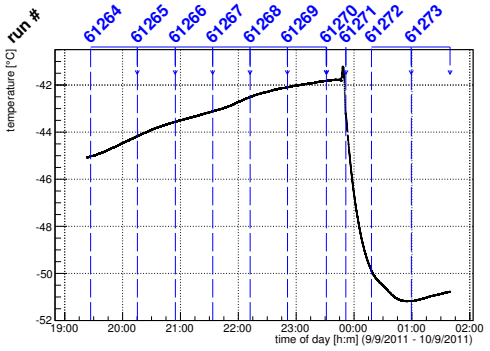

(a) Temperature vs time.

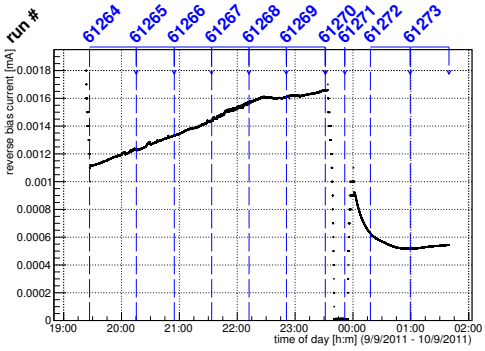

(b) Bias current vs time.

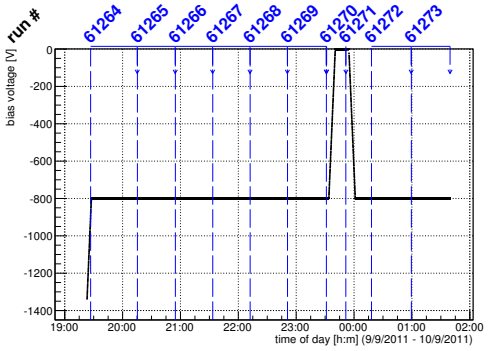

(c) Currently applied bias voltage vs time.

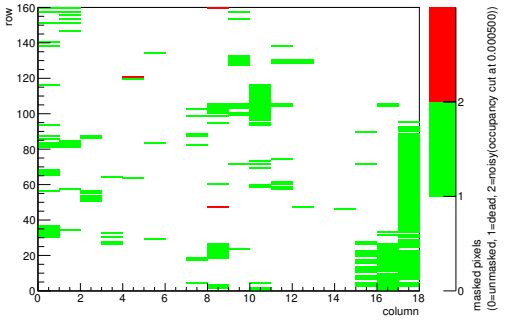

(d) Map of masked pixels.

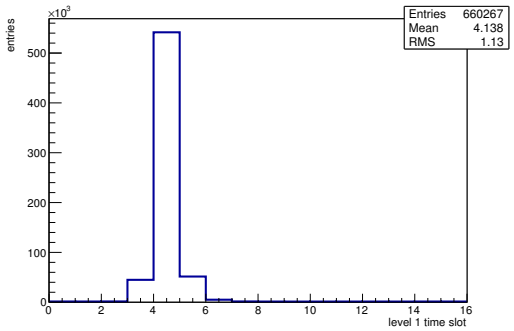

(e) Lvl1 distribution.

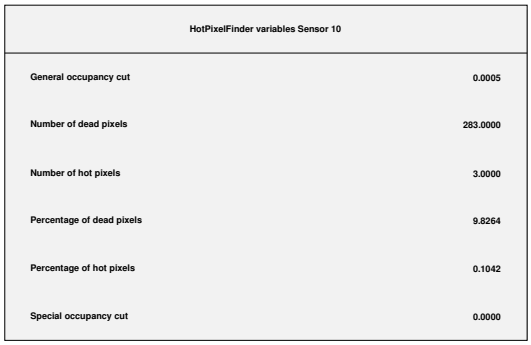

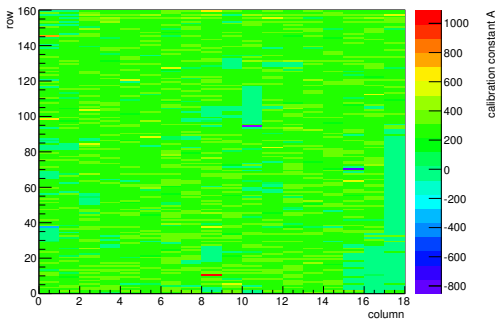

(f) Calibration constant A.

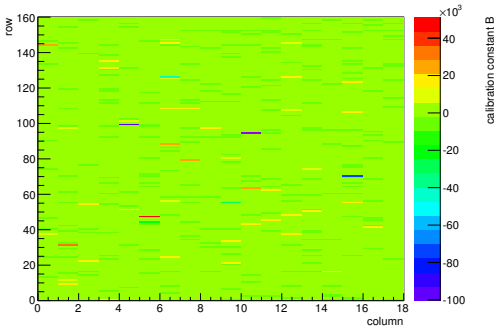

(g) Calibration constant B.

Figure C.107: Detailed plots for test beam measurement of DO-I-7 (description see section 6.1) sample (running as DUT0) during runs 61264-61273 in the September 2011 test beam period at CERN SPS in area H6B. Summary of the data in chapter 9. *(cont.)*

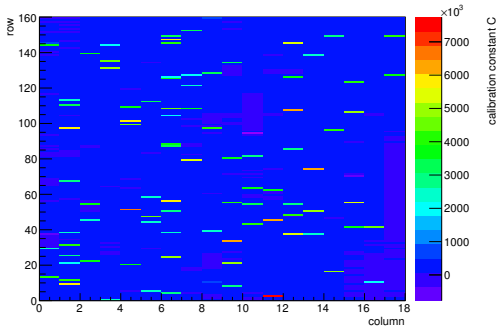

(h) Calibration constant C.

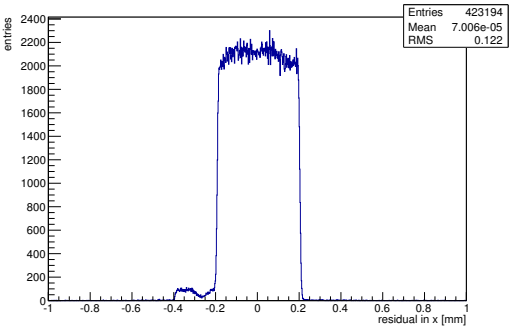

(i) Track residual in x.

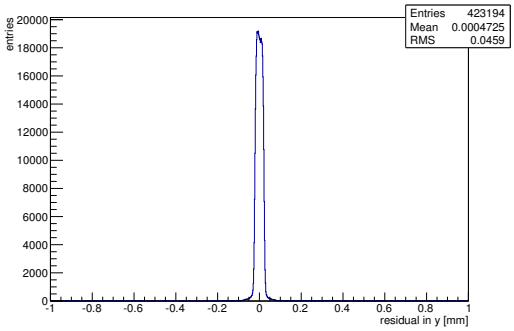

(j) Track residual in y.

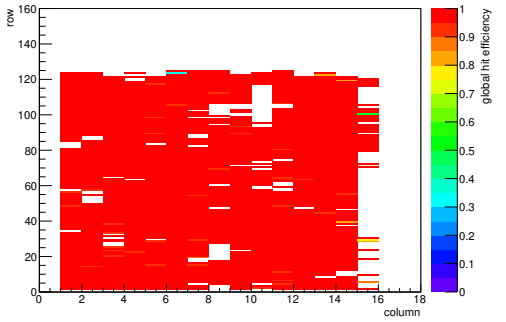

(k) Hit efficiency map.

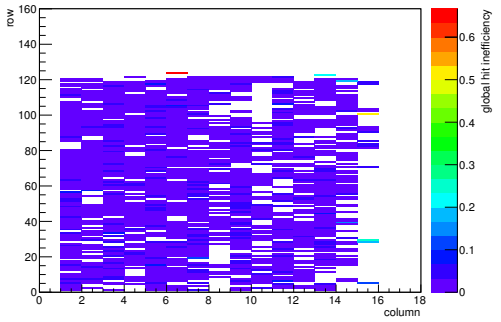

(l) Hit inefficiency map.

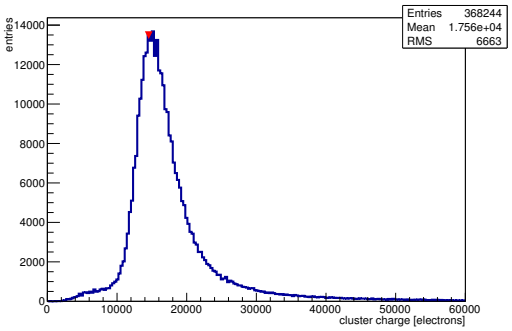

(m) Charge distribution (all cluster sizes included).

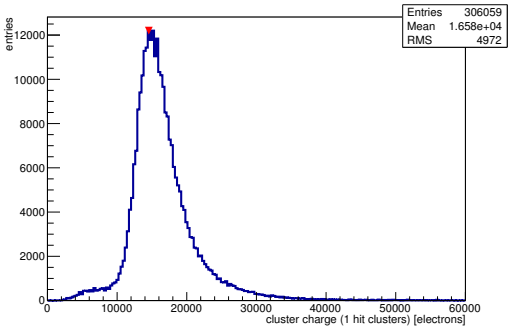

(n) Charge distribution (1 hit cluster).

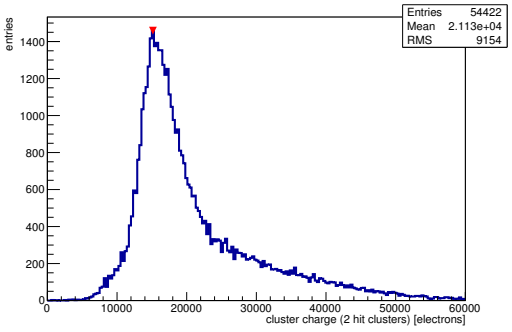

(o) Charge distribution (2 hit cluster).

Figure C.107: Detailed plots for test beam measurement of DO-I-7 (description see section 6.1) sample (running as DUT0) during runs 61264-61273 in the September 2011 test beam period at CERN SPS in area H6B. Summary of the data in chapter 9. *(cont.)*

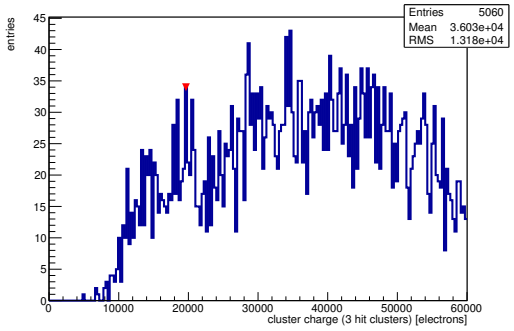

(p) Charge distribution (3 hit cluster).

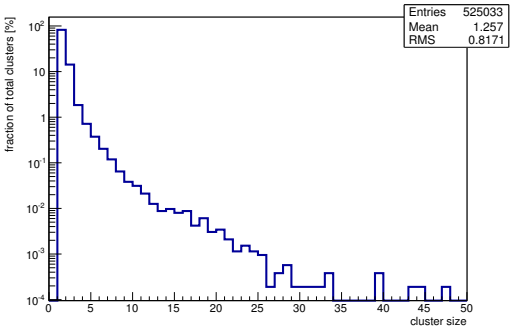

(q) Cluster size distribution.

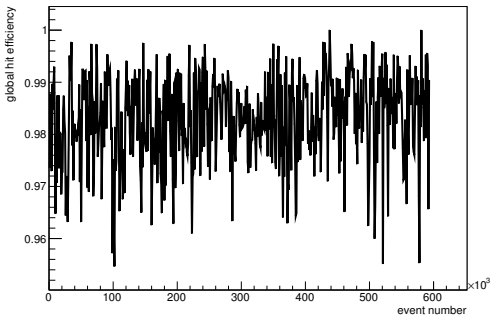

(r) Hit efficiency vs event number.

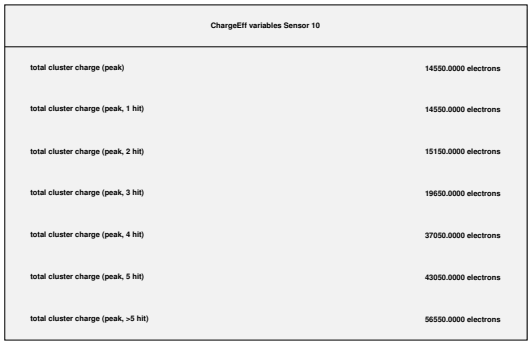

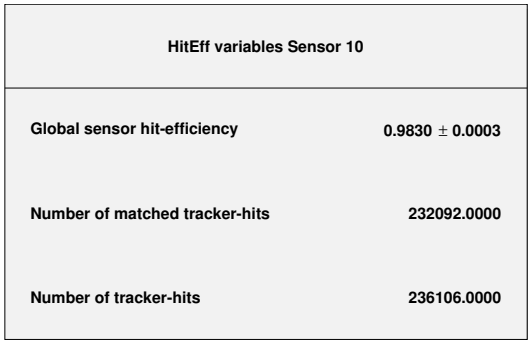

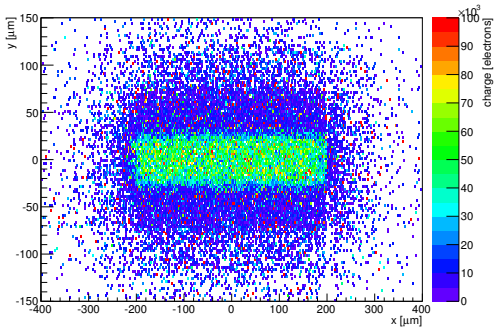

(s) Single pixel mean charge.

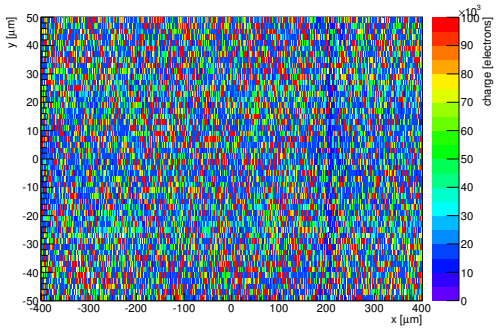

(t) Single pixel mean charge.

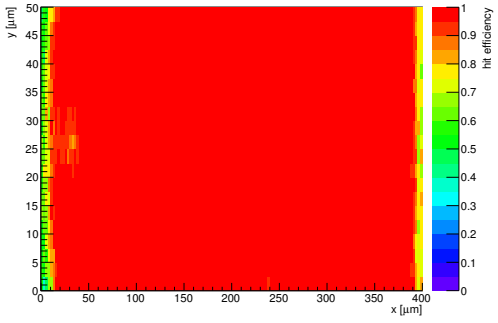

(u) Single pixel hit efficiency.

Figure C.107: Detailed plots for test beam measurement of DO-I-7 (description see section 6.1) sample (running as DUT0) during runs 61264-61273 in the September 2011 test beam period at CERN SPS in area H6B. Summary of the data in chapter 9.

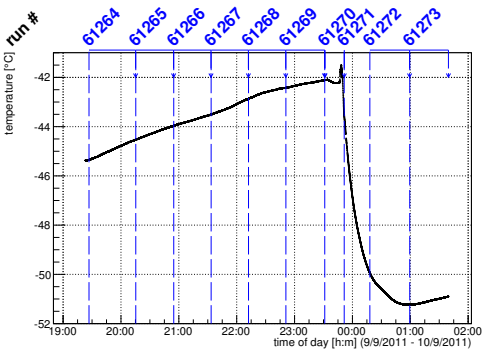

(a) Temperature vs time.

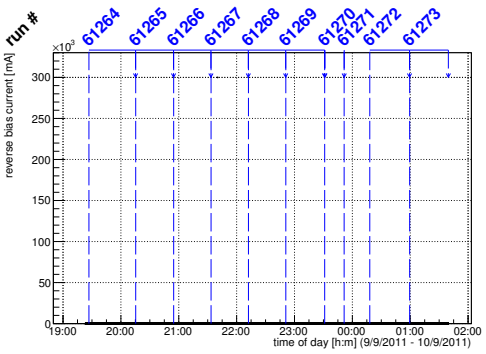

(b) Bias current vs time.

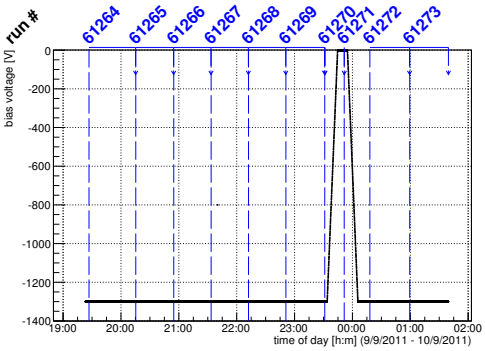

(c) Currently applied bias voltage vs time.

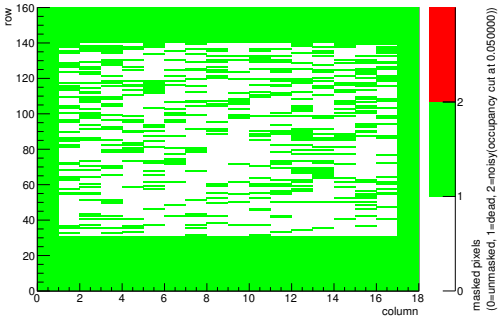

(d) Map of masked pixels.

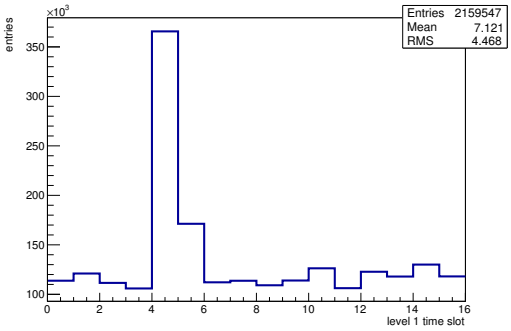

(e) Lvl1 distribution.

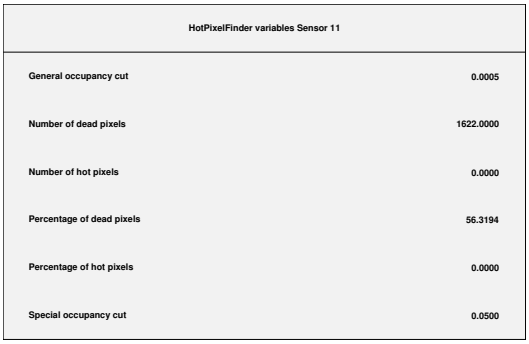

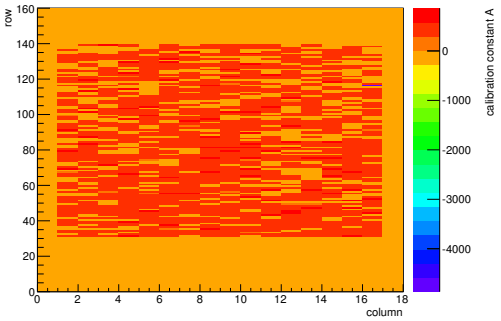

(f) Calibration constant A.

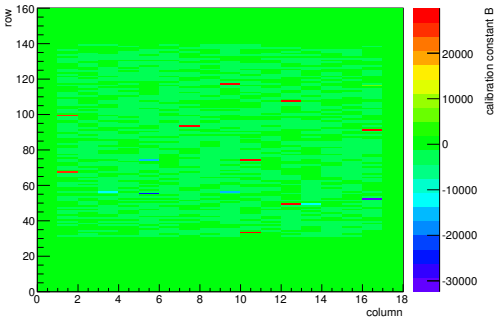

(g) Calibration constant B.

Figure C.108: Detailed plots for test beam measurement of DO-I-11 (description see section 6.1) sample (running as DUT1) during runs 61264-61273 in the September 2011 test beam period at CERN SPS in area H6B. Summary of the data in chapter 9. *(cont.)*

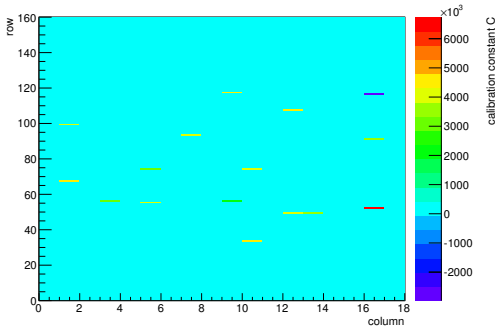

(h) Calibration constant C.

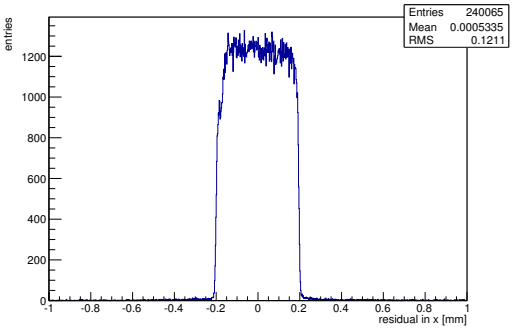

(i) Track residual in x.

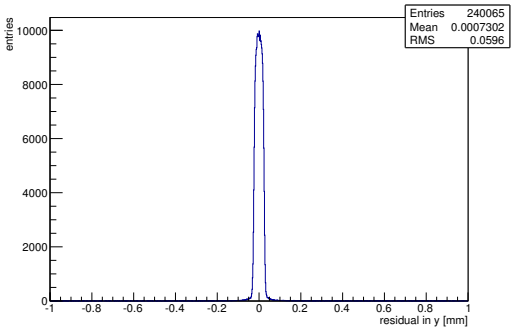

(j) Track residual in y.

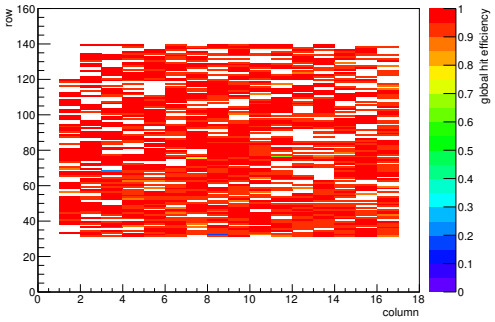

(k) Hit efficiency map.

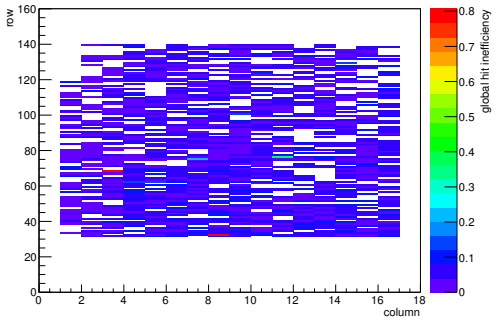

(l) Hit inefficiency map.

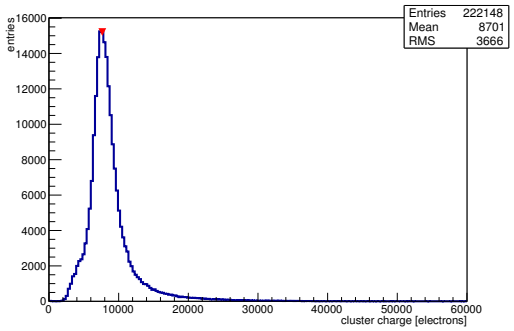

(m) Charge distribution (all cluster sizes included).

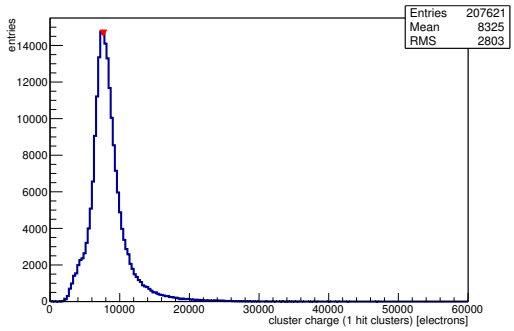

(n) Charge distribution (1 hit cluster).

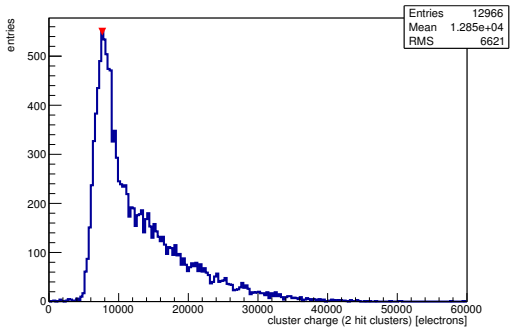

(o) Charge distribution (2 hit cluster).

Figure C.108: Detailed plots for test beam measurement of DO-I-11 (description see section 6.1) sample (running as DUT1) during runs 61264-61273 in the September 2011 test beam period at CERN SPS in area H6B. Summary of the data in chapter 9. *(cont.)*

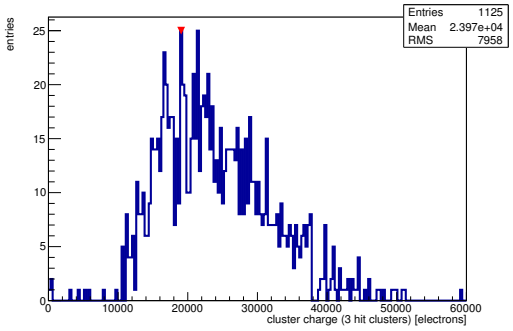

(p) Charge distribution (3 hit cluster).

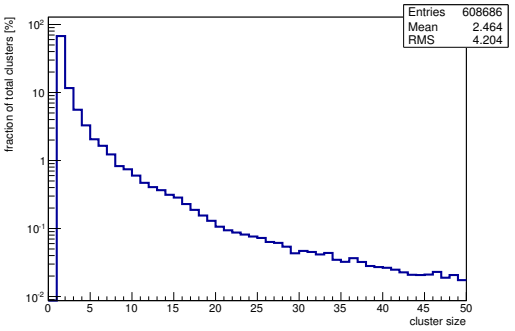

(q) Cluster size distribution.

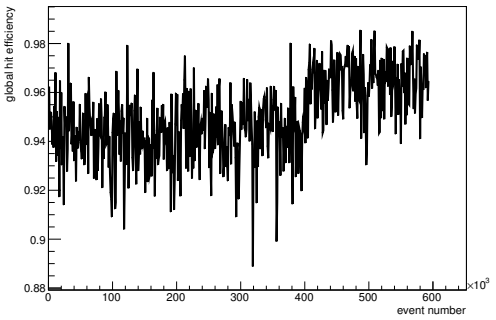

(r) Hit efficiency vs event number.

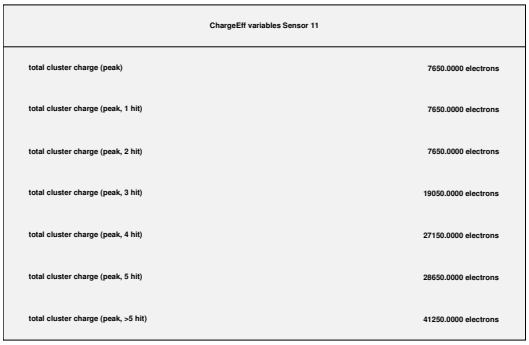

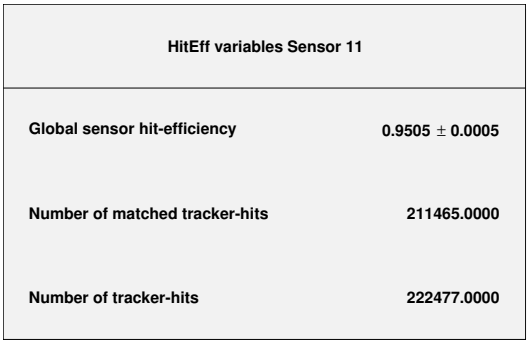

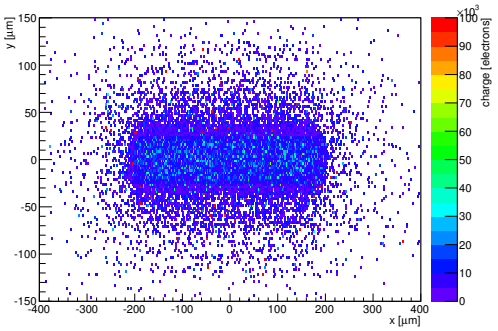

(s) Single pixel mean charge.

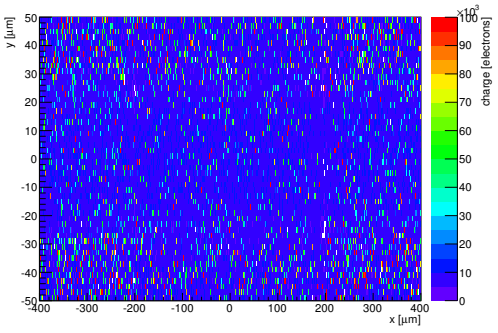

(t) Single pixel mean charge.

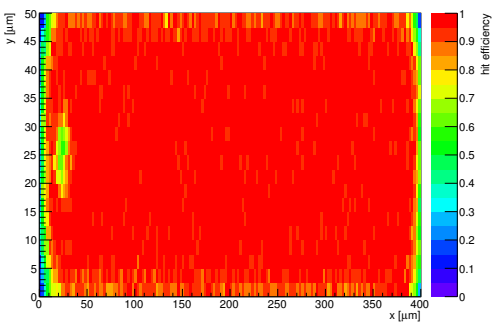

(u) Single pixel hit efficiency.

Figure C.108: Detailed plots for test beam measurement of DO-I-11 (description see section 6.1) sample (running as DUT1) during runs 61264-61273 in the September 2011 test beam period at CERN SPS in area H6B. Summary of the data in chapter 9.

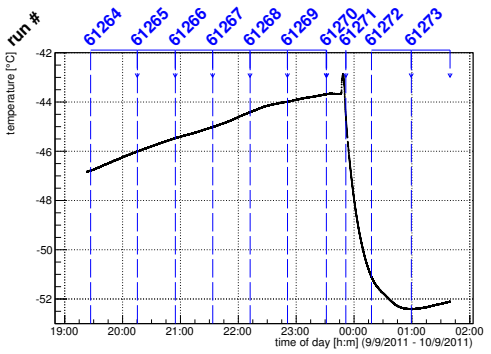

(a) Temperature vs time.

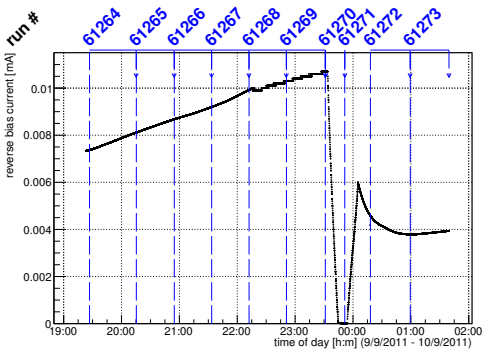

(b) Bias current vs time.

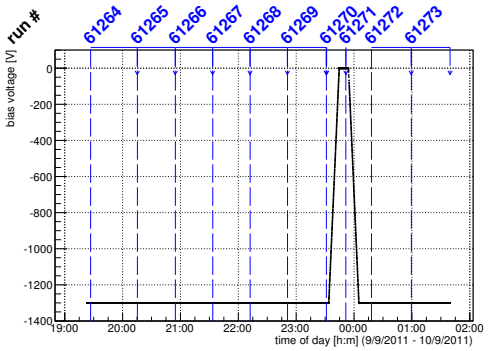

(c) Currently applied bias voltage vs time.

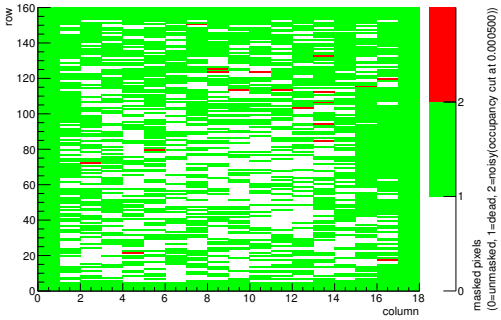

(d) Map of masked pixels.

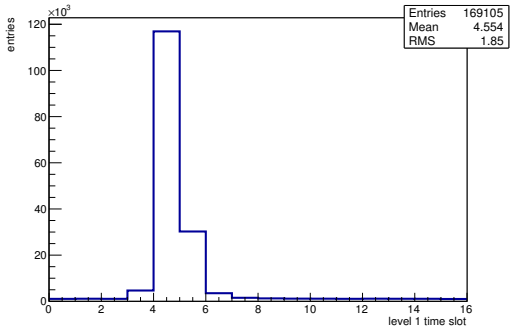

(e) Lvl1 distribution.

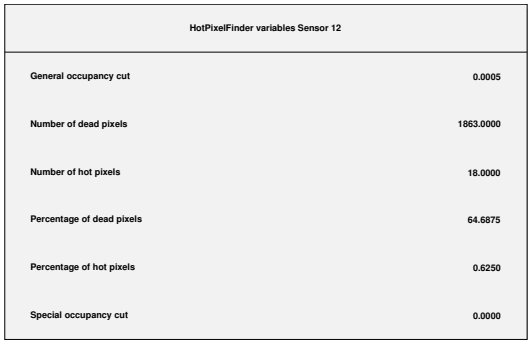

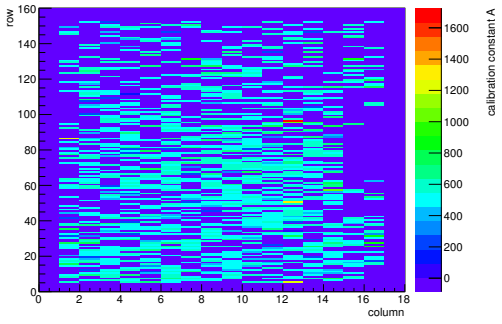

(f) Calibration constant A.

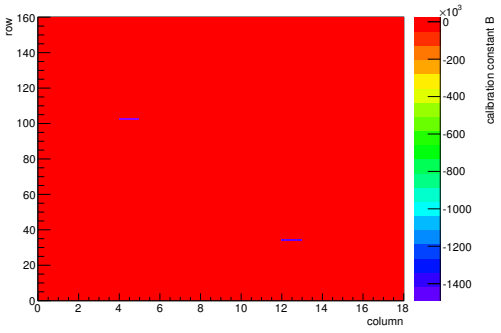

(g) Calibration constant B.

Figure C.109: Detailed plots for test beam measurement of DO-I-5 (description see section 6.1) sample (running as DUT2) during runs 61264-61273 in the September 2011 test beam period at CERN SPS in area H6B. Summary of the data in chapter 9. *(cont.)*

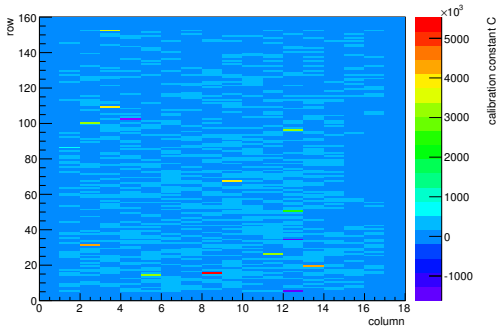

(h) Calibration constant C.

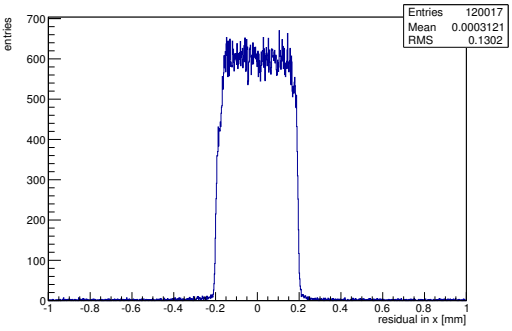

(i) Track residual in x.

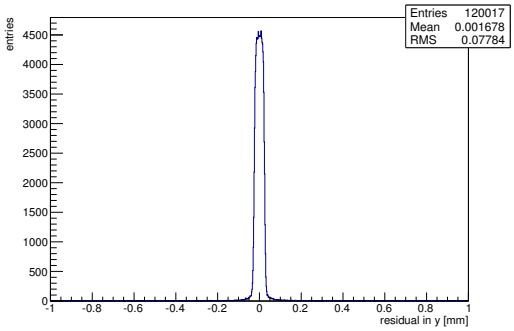

(j) Track residual in y.

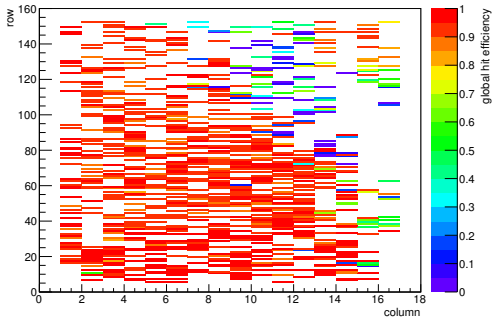

(k) Hit efficiency map.

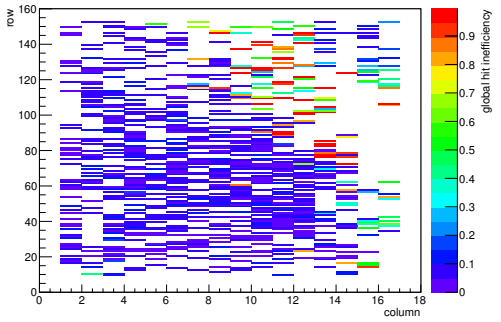

(l) Hit inefficiency map.

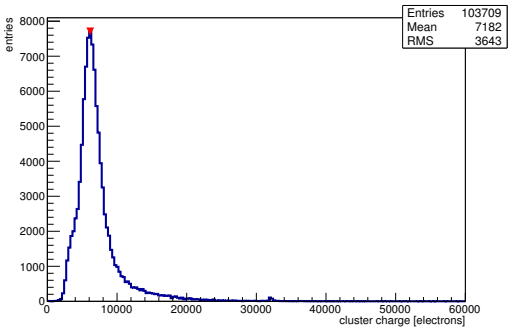

(m) Charge distribution (all cluster sizes included).

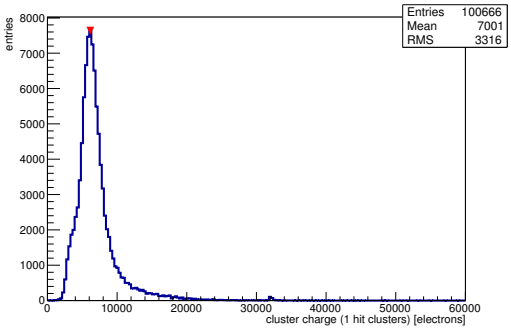

(n) Charge distribution (1 hit cluster).

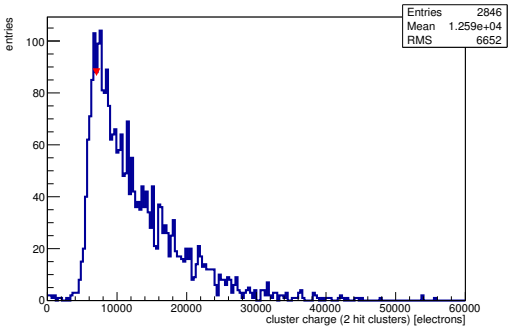

(o) Charge distribution (2 hit cluster).

Figure C.109: Detailed plots for test beam measurement of DO-I-5 (description see section 6.1) sample (running as DUT2) during runs 61264-61273 in the September 2011 test beam period at CERN SPS in area H6B. Summary of the data in chapter 9. *(cont.)*

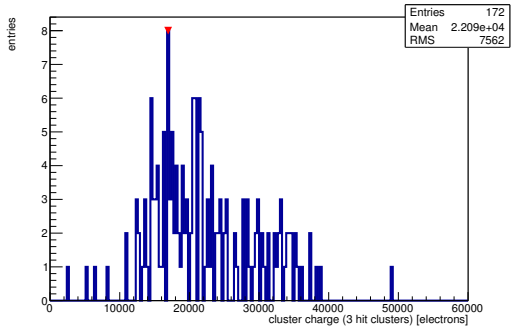

(p) Charge distribution (3 hit cluster).

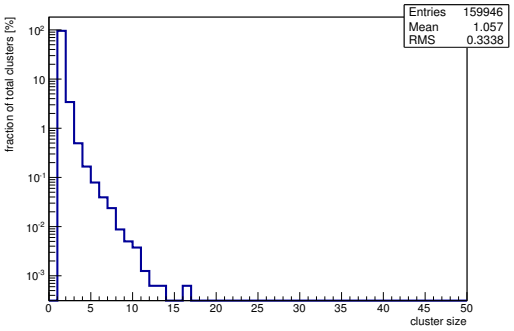

(q) Cluster size distribution.

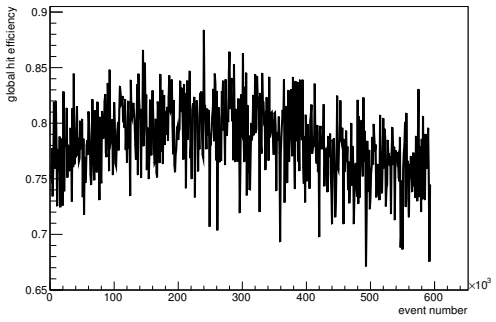

(r) Hit efficiency vs event number.

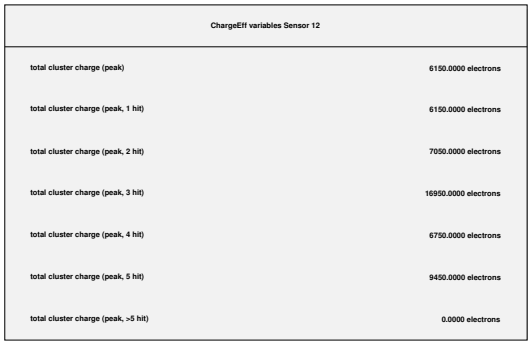

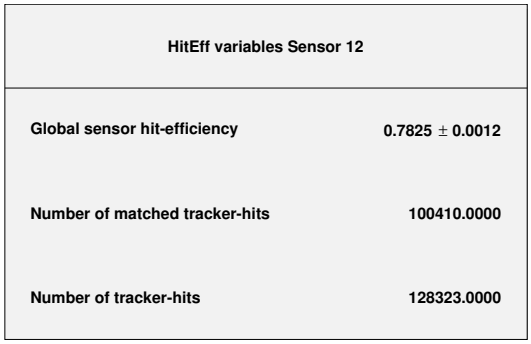

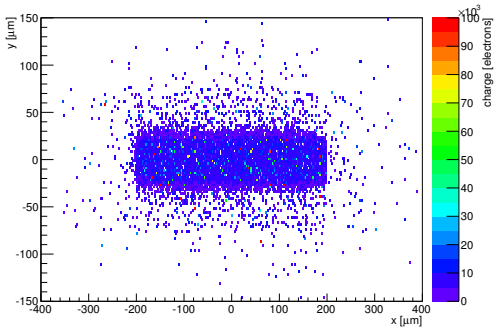

(s) Single pixel mean charge.

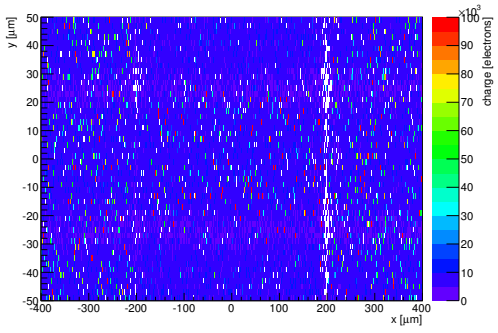

(t) Single pixel mean charge.

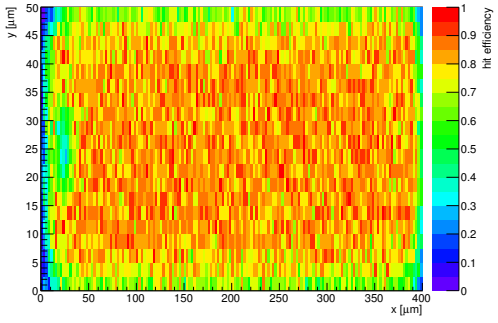

(u) Single pixel hit efficiency.

Figure C.109: Detailed plots for test beam measurement of DO-I-5 (description see section 6.1) sample (running as DUT2) during runs 61264-61273 in the September 2011 test beam period at CERN SPS in area H6B. Summary of the data in chapter 9.

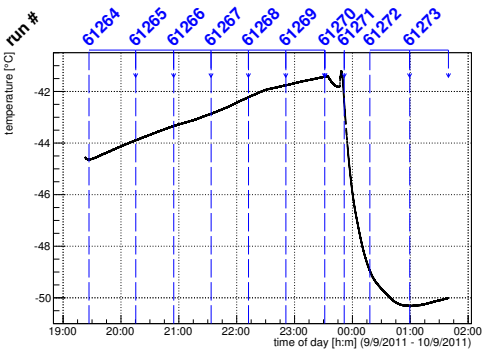

(a) Temperature vs time.

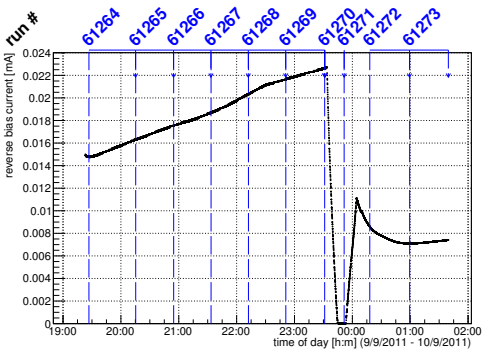

(b) Bias current vs time.

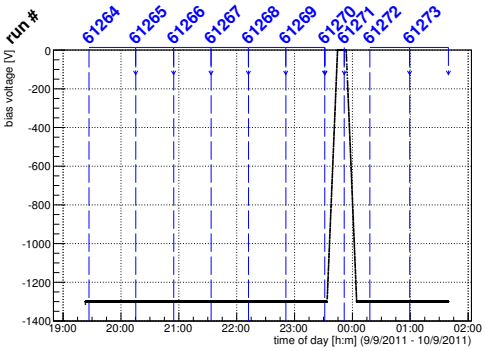

(c) Currently applied bias voltage vs time.

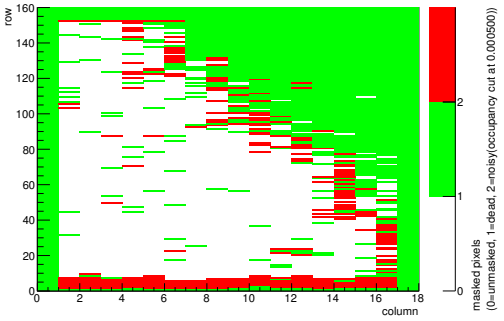

(d) Map of masked pixels.

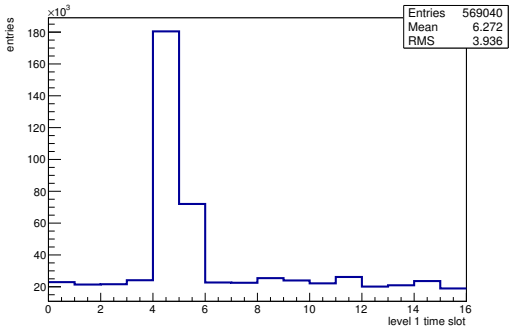

(e) Lvl1 distribution.

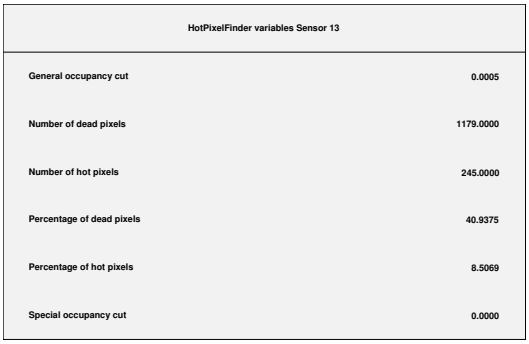

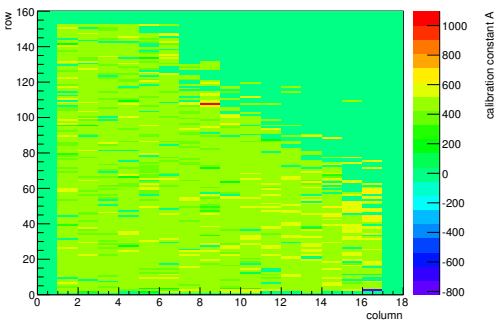

(f) Calibration constant A.

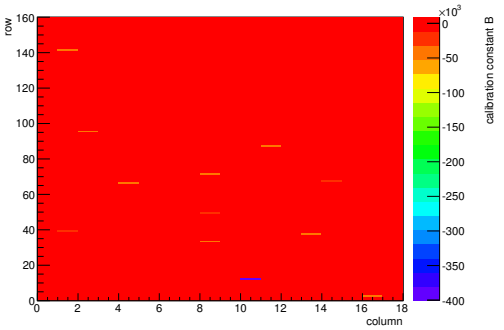

(g) Calibration constant B.

Figure C.110: Detailed plots for test beam measurement of DO-I-12 (description see section 6.1) sample (running as DUT3) during runs 61264-61273 in the September 2011 test beam period at CERN SPS in area H6B. Summary of the data in chapter 9. *(cont.)*

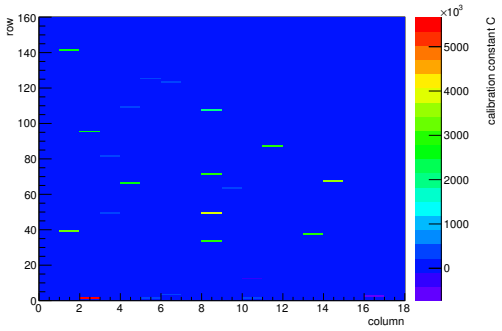

(h) Calibration constant C.

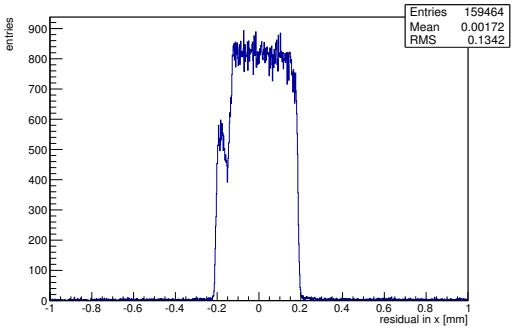

(i) Track residual in x.

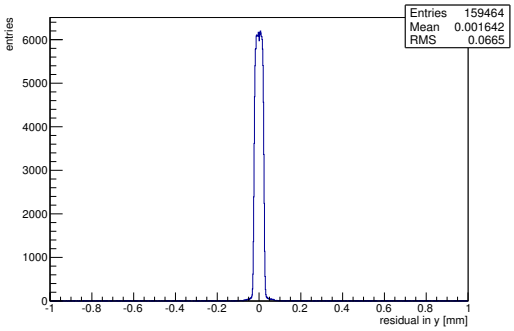

(j) Track residual in y.

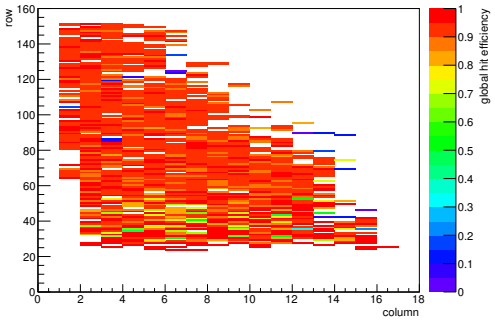

(k) Hit efficiency map.

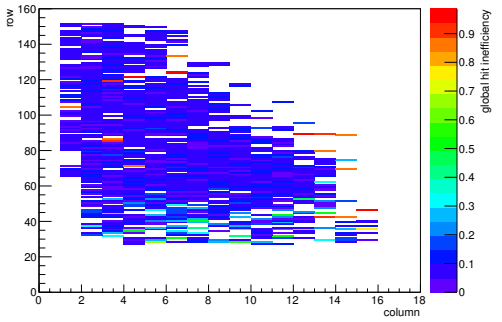

(l) Hit inefficiency map.

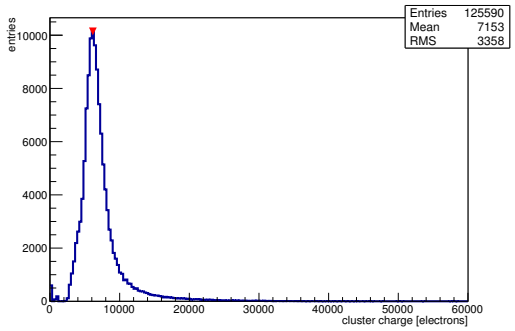

(m) Charge distribution (all cluster sizes included).

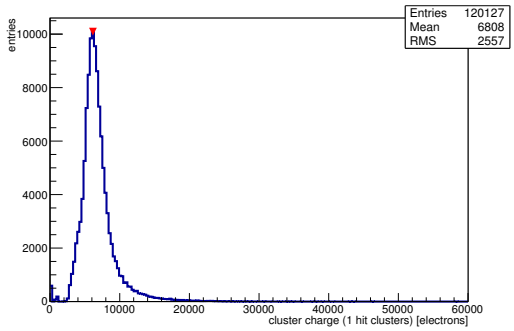

(n) Charge distribution (1 hit cluster).

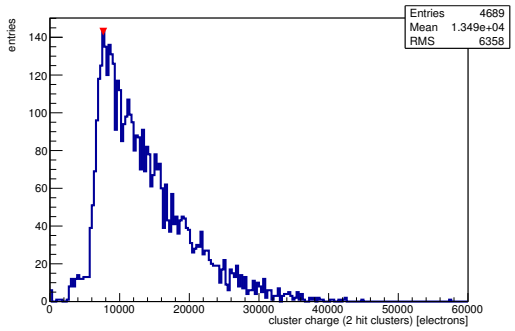

(o) Charge distribution (2 hit cluster).

Figure C.110: Detailed plots for test beam measurement of DO-I-12 (description see section 6.1) sample (running as DUT3) during runs 61264-61273 in the September 2011 test beam period at CERN SPS in area H6B. Summary of the data in chapter 9. *(cont.)*

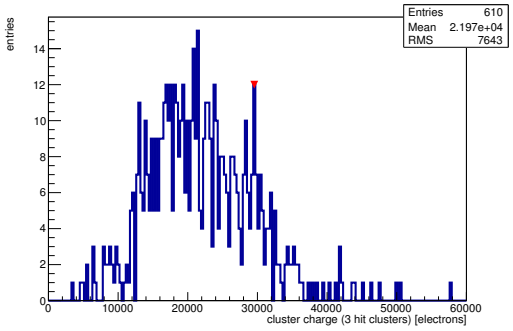

(p) Charge distribution (3 hit cluster).

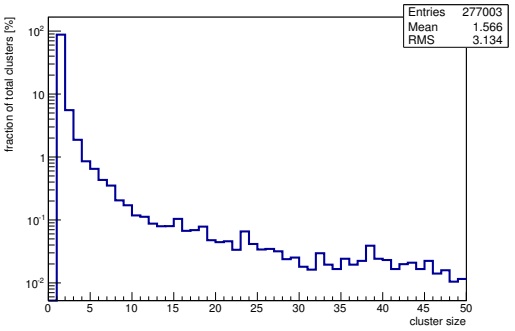

(q) Cluster size distribution.

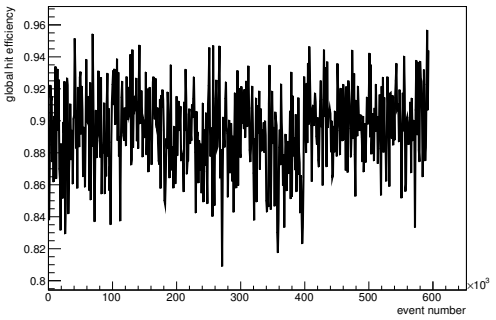

(r) Hit efficiency vs event number.

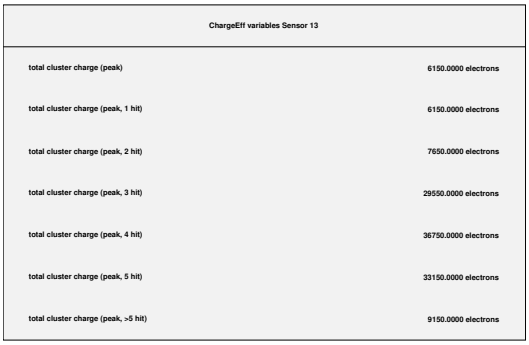

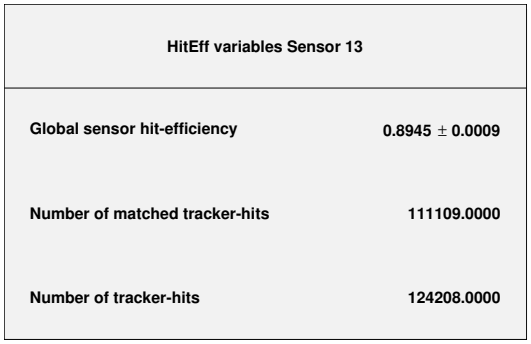

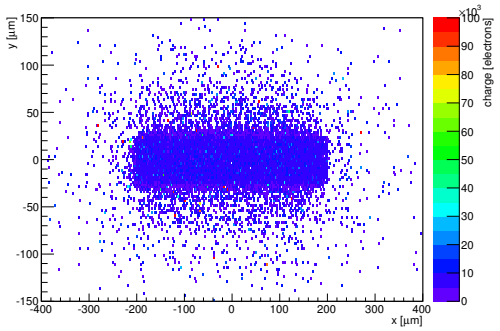

(s) Single pixel mean charge.

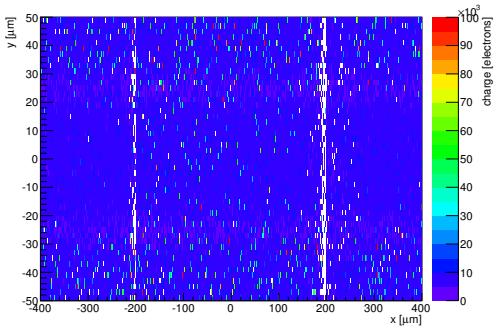

(t) Single pixel mean charge.

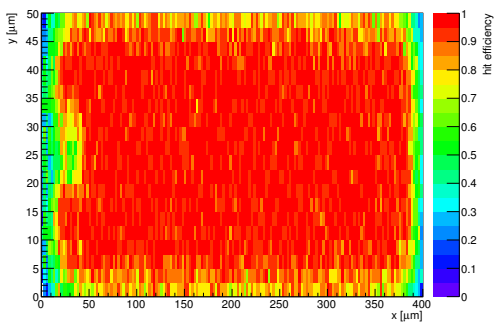

(u) Single pixel hit efficiency.

Figure C.110: Detailed plots for test beam measurement of DO-I-12 (description see section 6.1) sample (running as DUT3) during runs 61264-61273 in the September 2011 test beam period at CERN SPS in area H6B. Summary of the data in chapter 9.

C.3.18 Runs 61281-61289

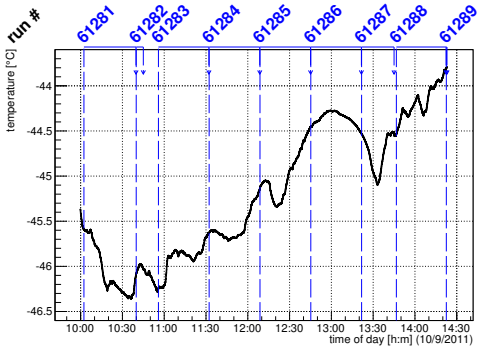

(a) Temperature vs time.

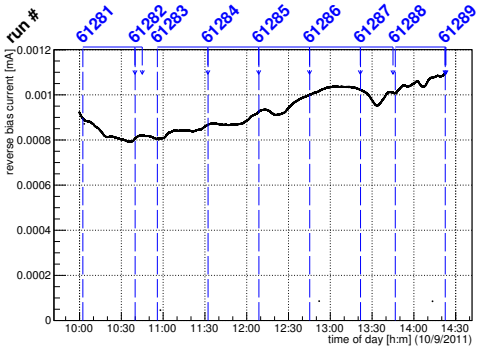

(b) Bias current vs time.

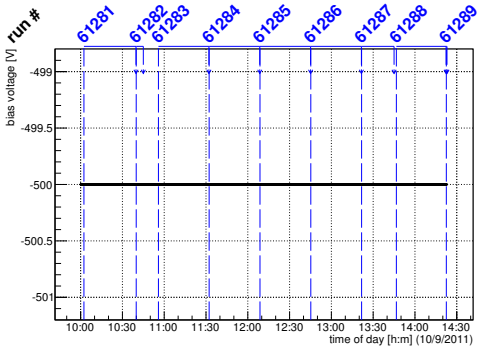

(c) Currently applied bias voltage vs time.

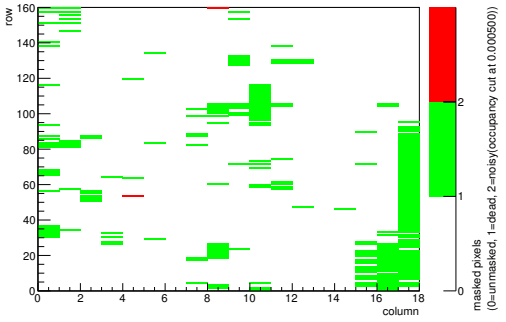

(d) Map of masked pixels.

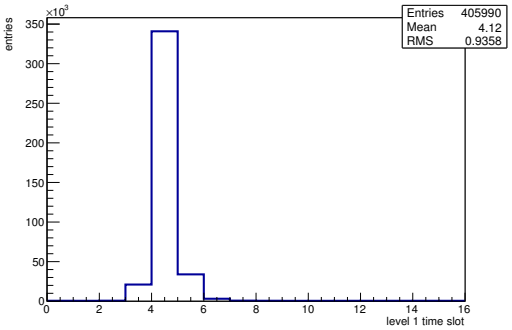

(e) Lvl1 distribution.

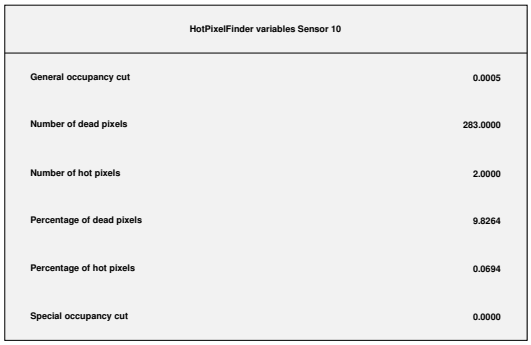

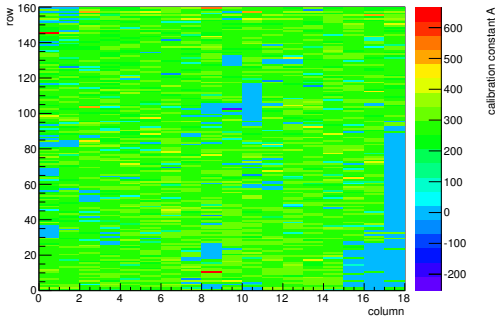

(f) Calibration constant A.

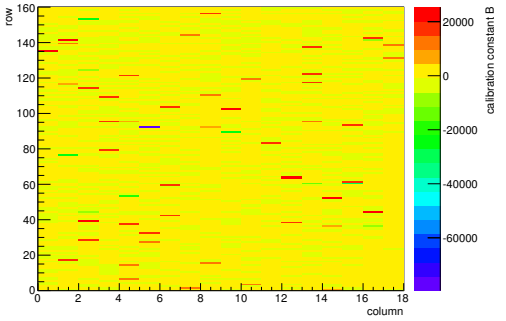

(g) Calibration constant B.

Figure C.111: Detailed plots for test beam measurement of DO-I-7 (description see section 6.1) sample (running as DUT0) during runs 61281-61289 in the September 2011 test beam period at CERN SPS in area H6B. Summary of the data in chapter 9. *(cont.)*

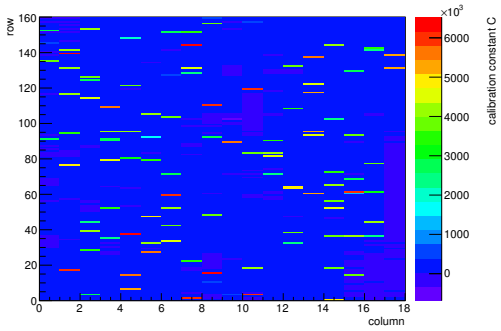

(h) Calibration constant C.

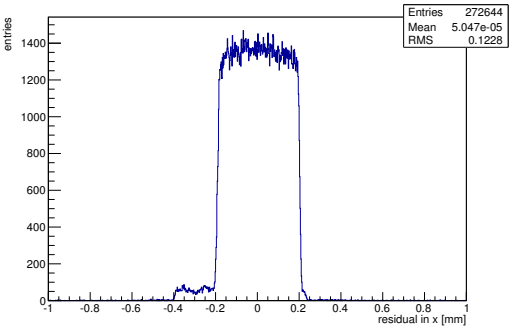

(i) Track residual in x.

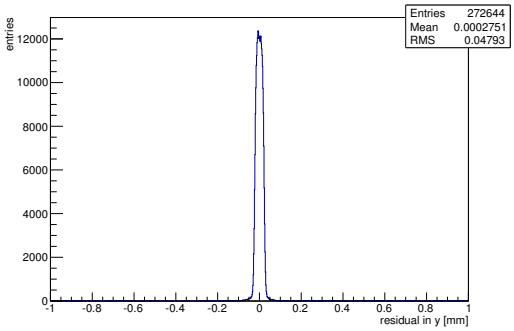

(j) Track residual in y.

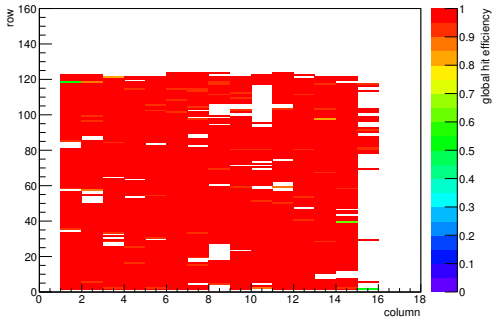

(k) Hit efficiency map.

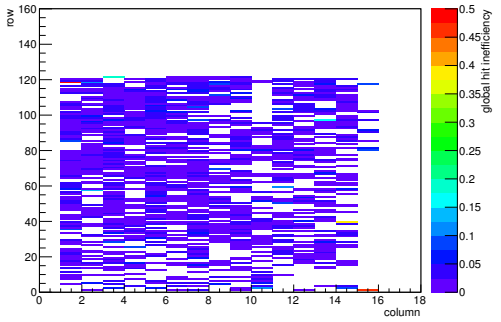

(l) Hit inefficiency map.

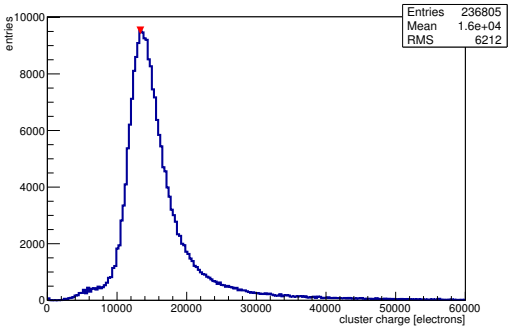

(m) Charge distribution (all cluster sizes included).

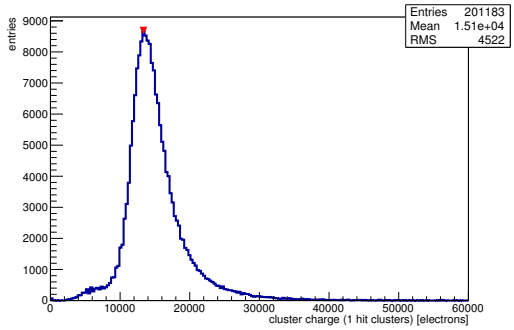

(n) Charge distribution (1 hit cluster).

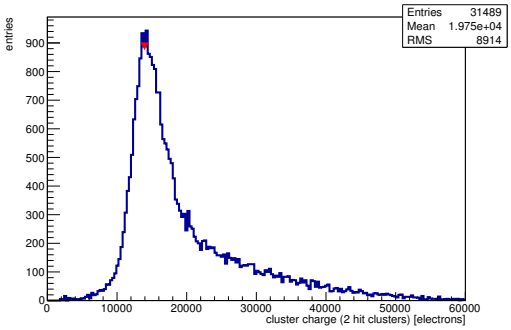

(o) Charge distribution (2 hit cluster).

Figure C.111: Detailed plots for test beam measurement of DO-I-7 (description see section 6.1) sample (running as DUT0) during runs 61281-61289 in the September 2011 test beam period at CERN SPS in area H6B. Summary of the data in chapter 9. *(cont.)*

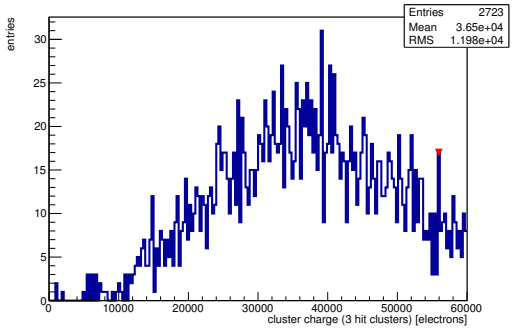

(p) Charge distribution (3 hit cluster).

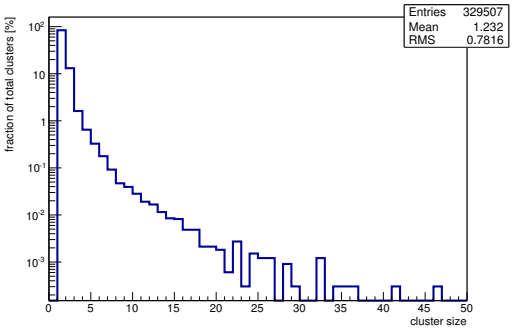

(q) Cluster size distribution.

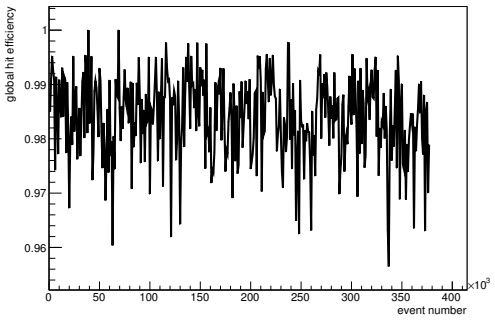

(r) Hit efficiency vs event number.

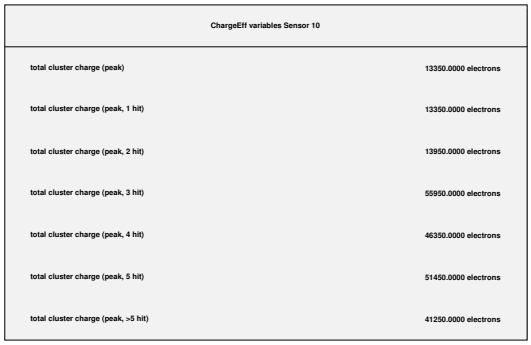

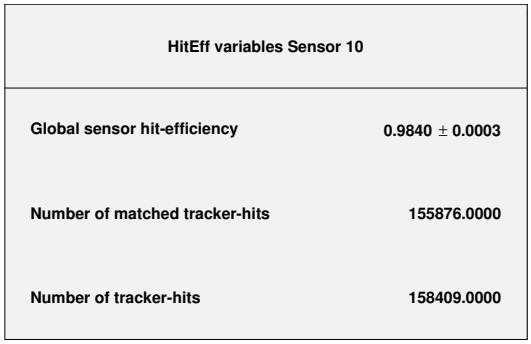

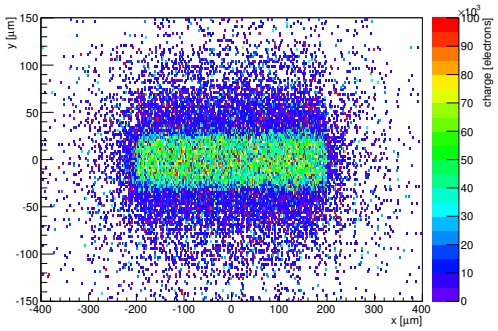

(s) Single pixel mean charge.

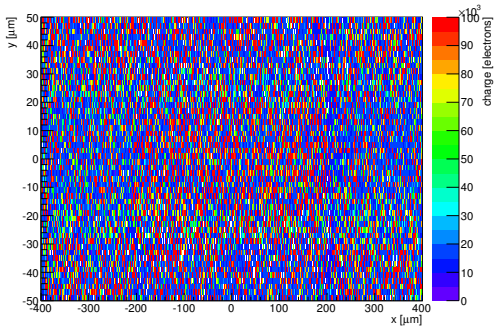

(t) Single pixel mean charge.

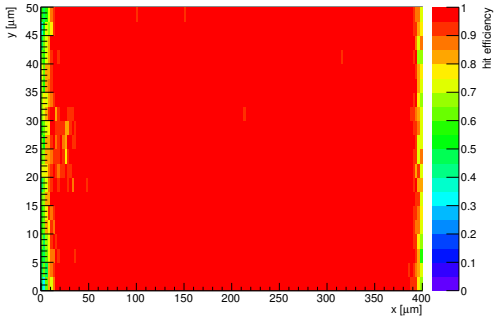

(u) Single pixel hit efficiency.

Figure C.111: Detailed plots for test beam measurement of DO-I-7 (description see section 6.1) sample (running as DUT0) during runs 61281-61289 in the September 2011 test beam period at CERN SPS in area H6B. Summary of the data in chapter 9.

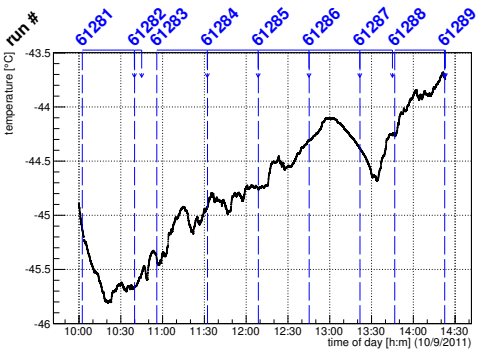

(a) Temperature vs time.

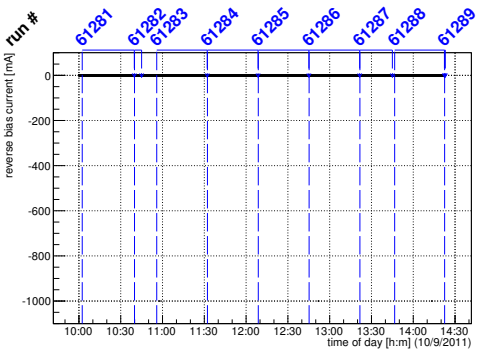

(b) Bias current vs time.

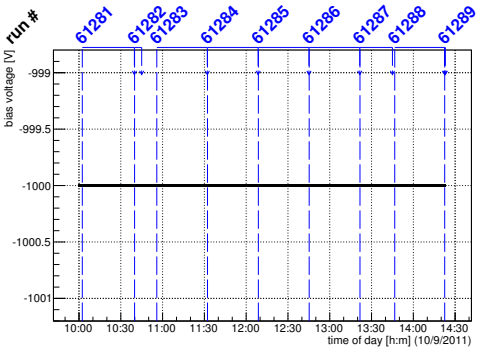

(c) Currently applied bias voltage vs time.

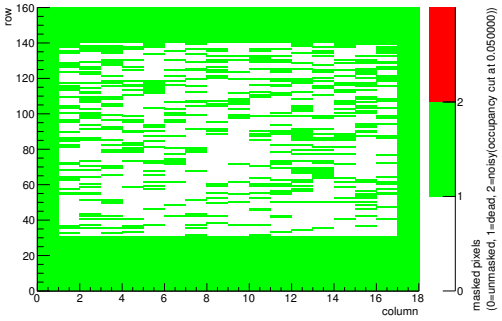

(d) Map of masked pixels.

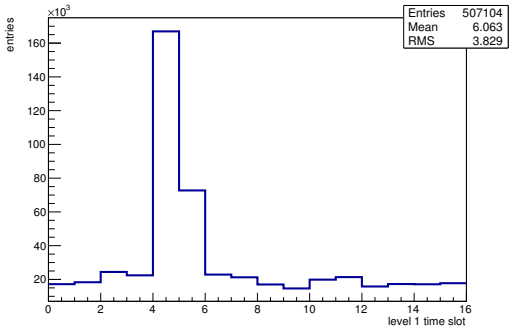

(e) Lvl1 distribution.

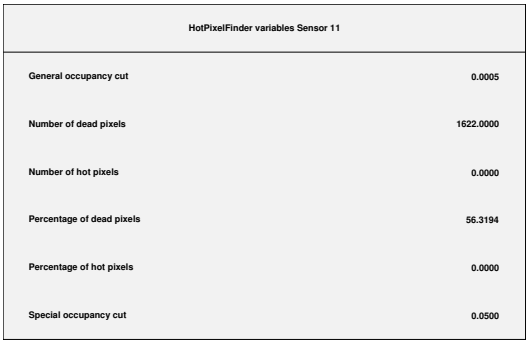

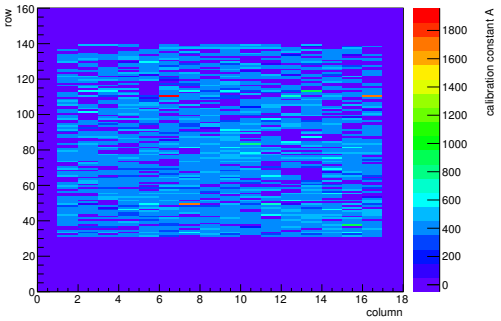

(f) Calibration constant A.

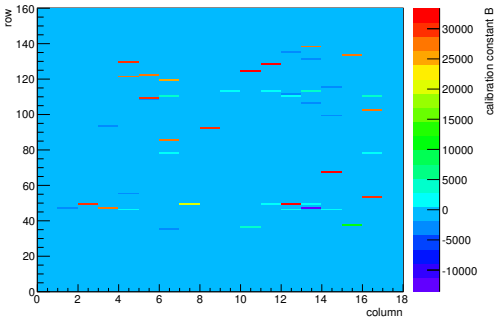

(g) Calibration constant B.

Figure C.112: Detailed plots for test beam measurement of DO-I-11 (description see section 6.1) sample (running as DUT1) during runs 61281-61289 in the September 2011 test beam period at CERN SPS in area H6B. Summary of the data in chapter 9. *(cont.)*

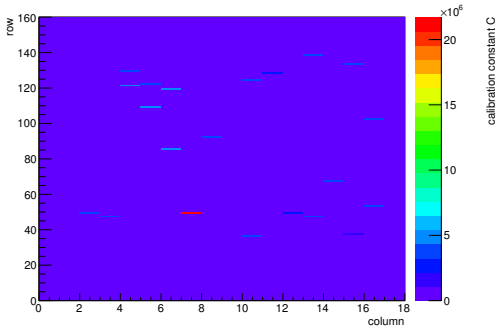

(h) Calibration constant C.

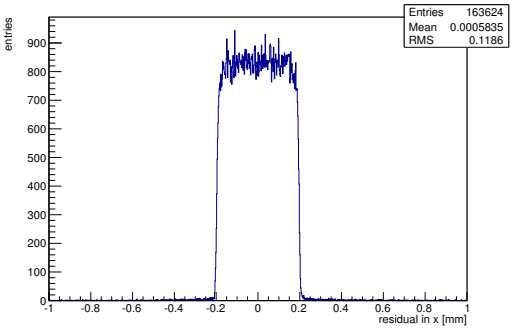

(i) Track residual in x.

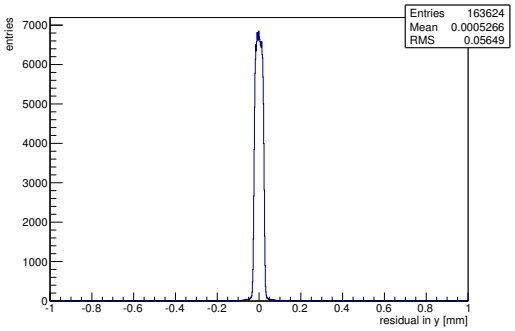

(j) Track residual in y.

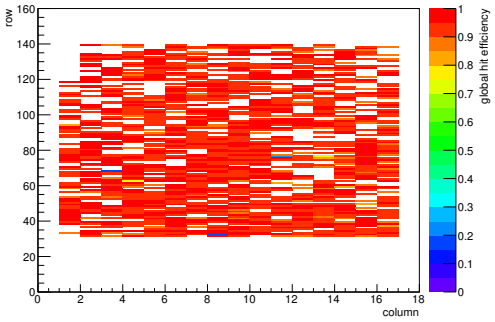

(k) Hit efficiency map.

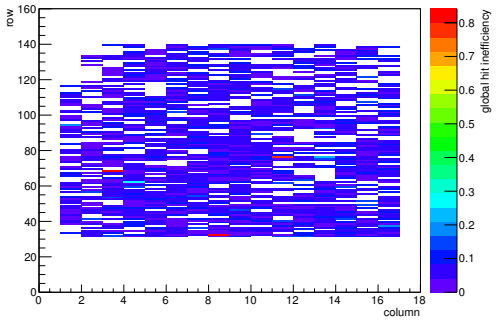

(l) Hit inefficiency map.

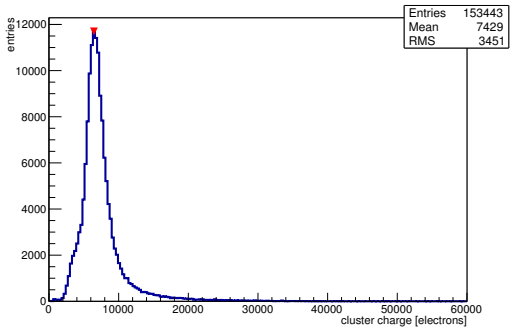

(m) Charge distribution (all cluster sizes included).

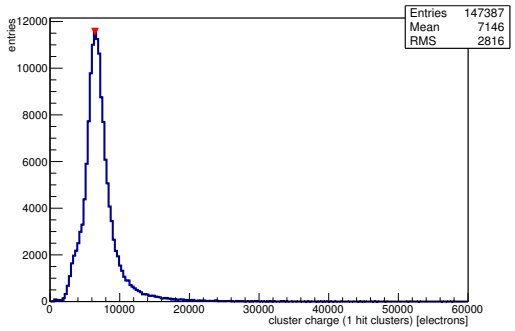

(n) Charge distribution (1 hit cluster).

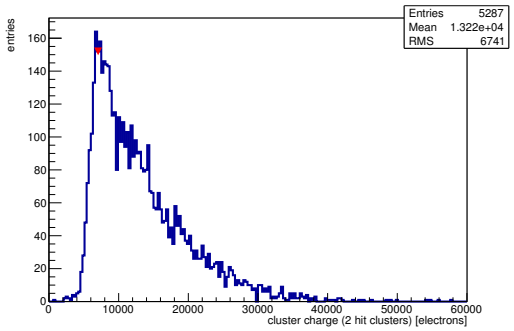

(o) Charge distribution (2 hit cluster).

Figure C.112: Detailed plots for test beam measurement of DO-I-11 (description see section 6.1) sample (running as DUT1) during runs 61281-61289 in the September 2011 test beam period at CERN SPS in area H6B. Summary of the data in chapter 9. *(cont.)*

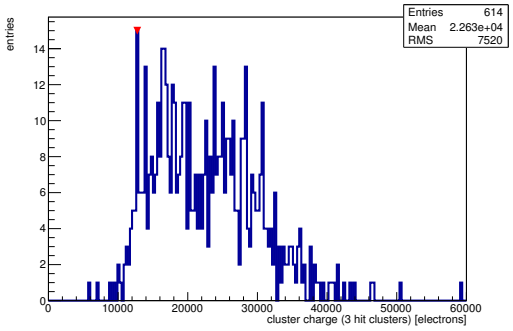

(p) Charge distribution (3 hit cluster).

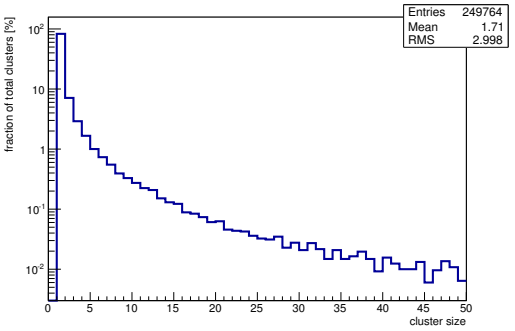

(q) Cluster size distribution.

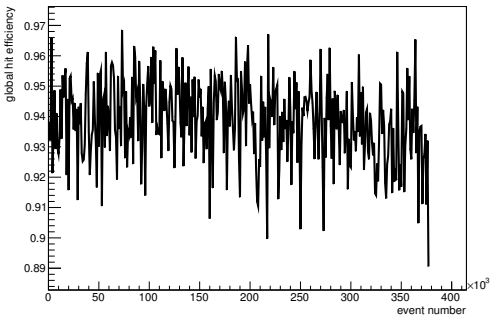

(r) Hit efficiency vs event number.

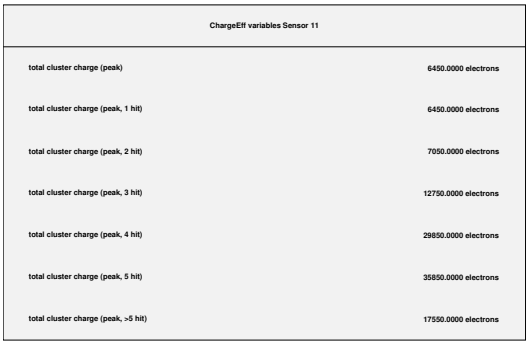

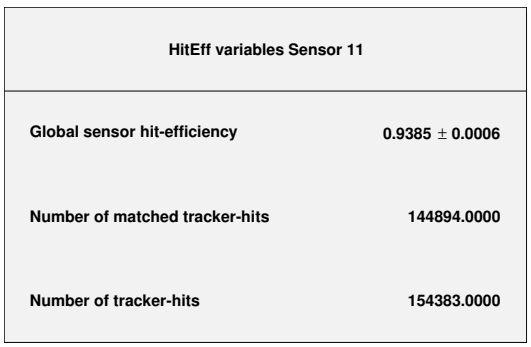

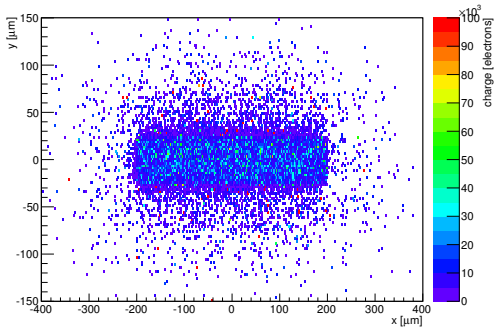

(s) Single pixel mean charge.

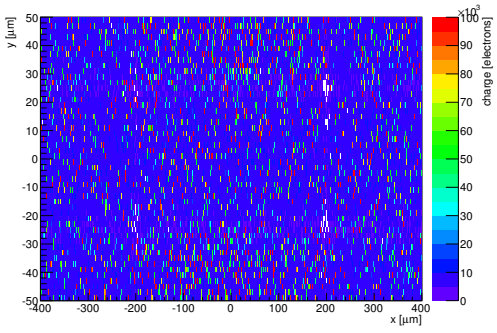

(t) Single pixel mean charge.

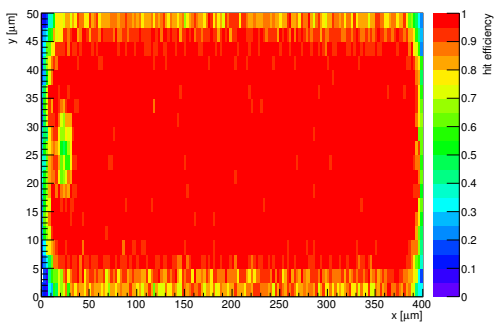

(u) Single pixel hit efficiency.

Figure C.112: Detailed plots for test beam measurement of DO-I-11 (description see section 6.1) sample (running as DUT1) during runs 61281-61289 in the September 2011 test beam period at CERN SPS in area H6B. Summary of the data in chapter 9.

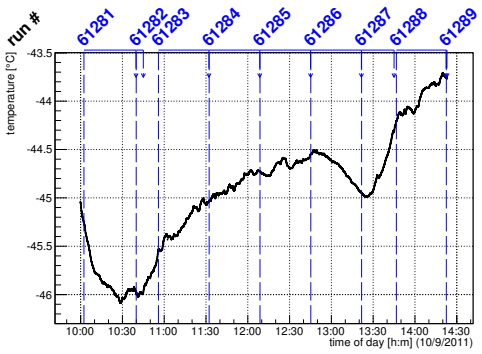

(a) Temperature vs time.

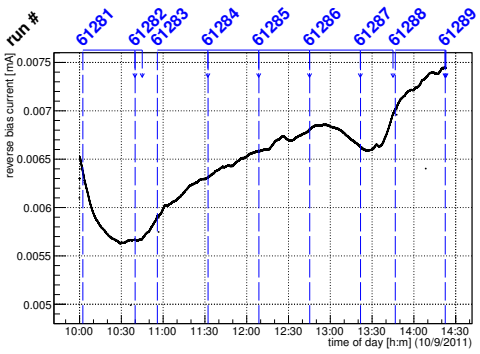

(b) Bias current vs time.

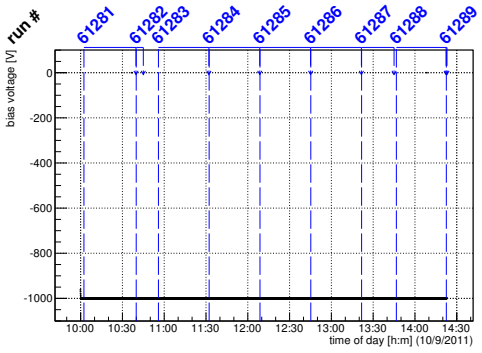

(c) Currently applied bias voltage vs time.

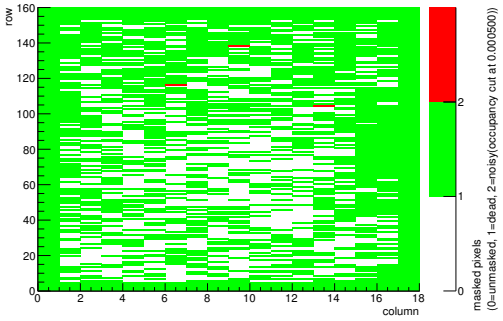

(d) Map of masked pixels.

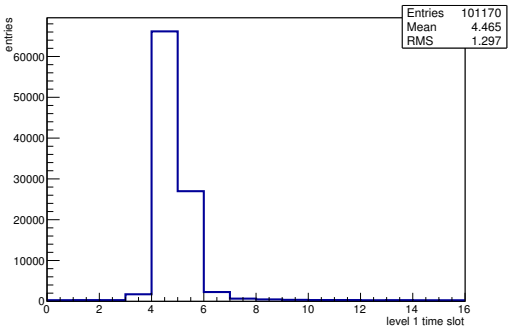

(e) Lvl1 distribution.

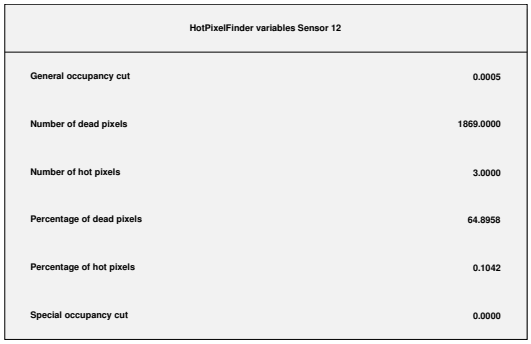

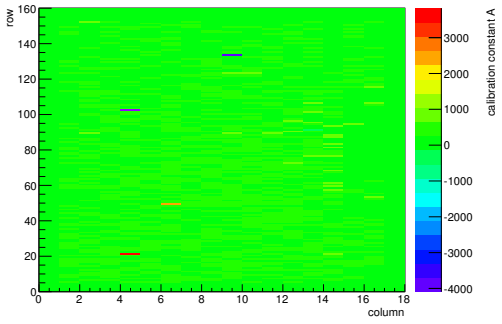

(f) Calibration constant A.

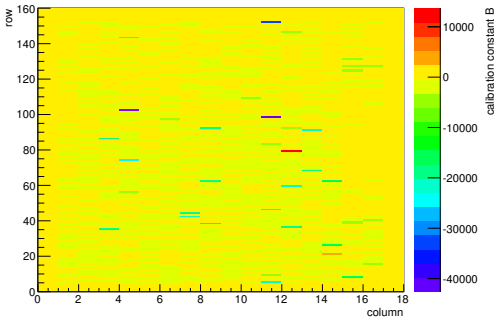

(g) Calibration constant B.

Figure C.113: Detailed plots for test beam measurement of DO-I-5 (description see section 6.1) sample (running as DUT2) during runs 61281-61289 in the September 2011 test beam period at CERN SPS in area H6B. Summary of the data in chapter 9. *(cont.)*

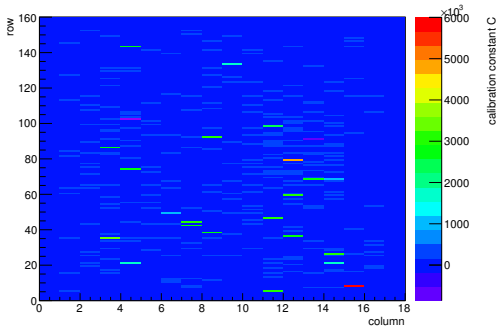

(h) Calibration constant C.

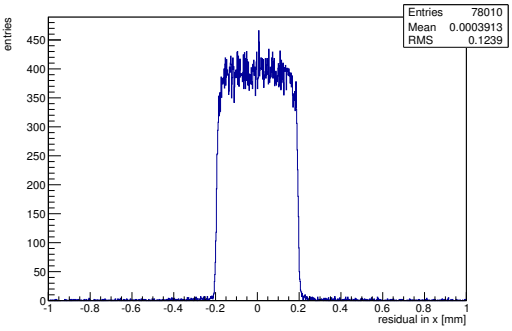

(i) Track residual in x.

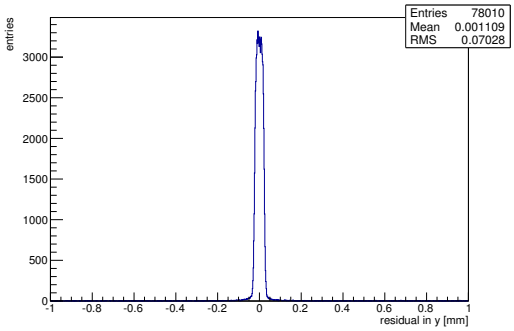

(j) Track residual in y.

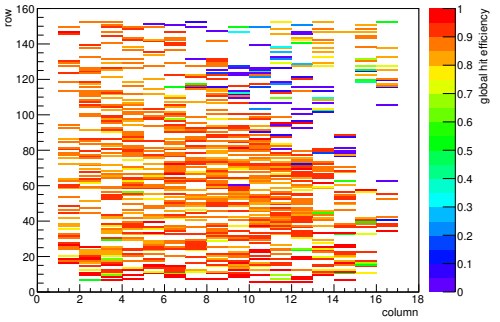

(k) Hit efficiency map.

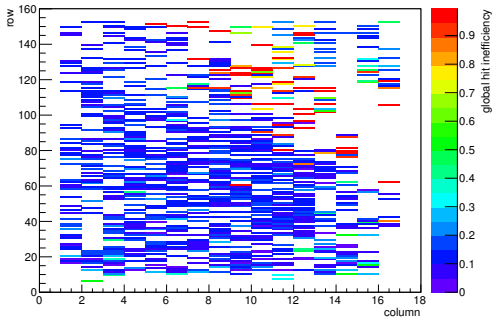

(l) Hit inefficiency map.

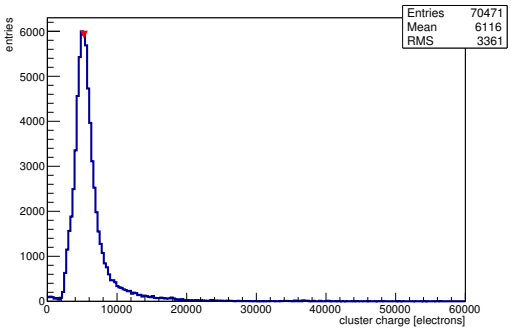

(m) Charge distribution (all cluster sizes included).

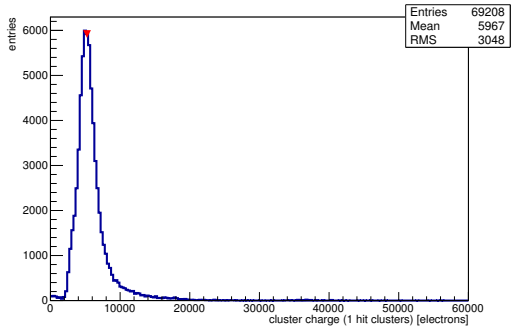

(n) Charge distribution (1 hit cluster).

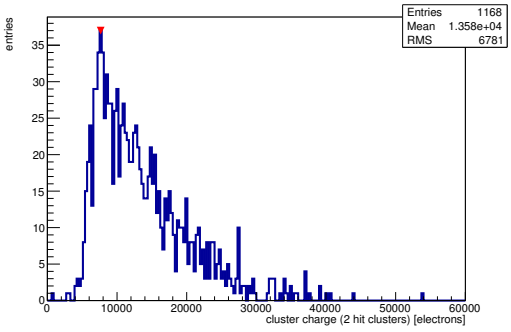

(o) Charge distribution (2 hit cluster).

Figure C.113: Detailed plots for test beam measurement of DO-I-5 (description see section 6.1) sample (running as DUT2) during runs 61281-61289 in the September 2011 test beam period at CERN SPS in area H6B. Summary of the data in chapter 9. *(cont.)*

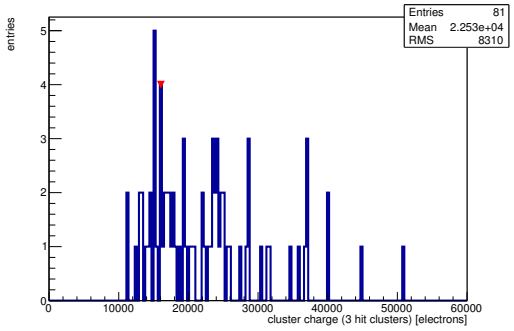

(p) Charge distribution (3 hit cluster).

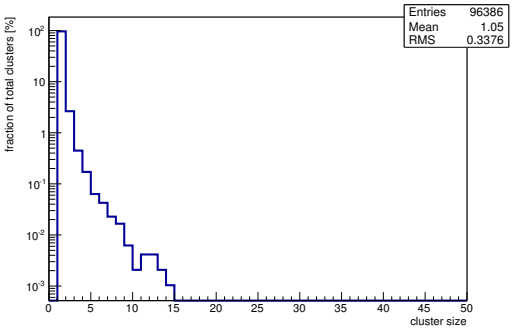

(q) Cluster size distribution.

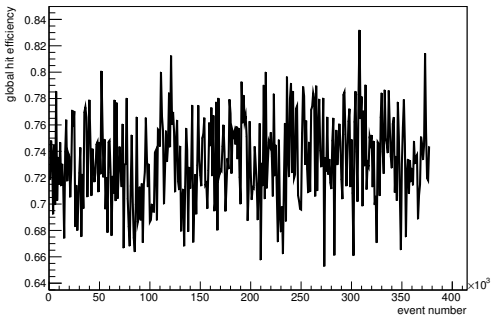

(r) Hit efficiency vs event number.

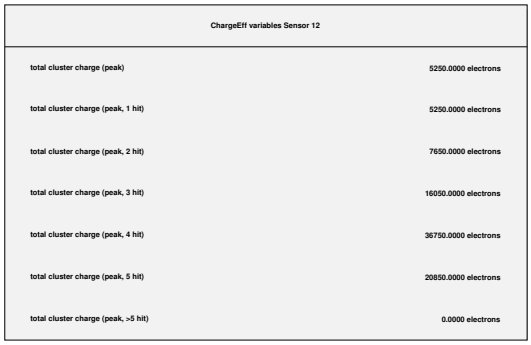

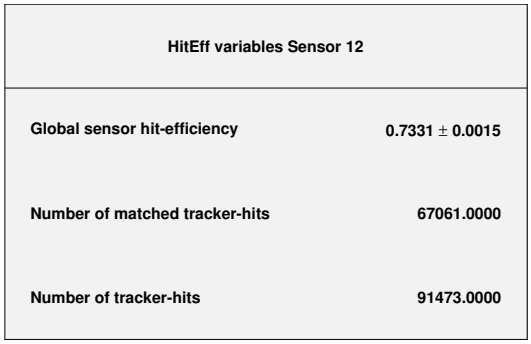

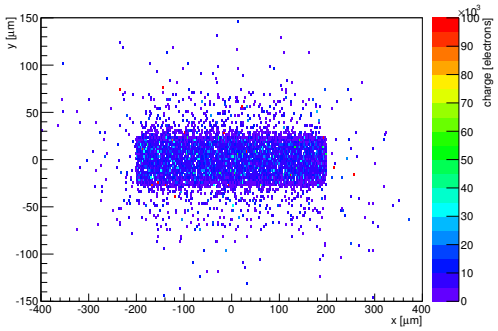

(s) Single pixel mean charge.

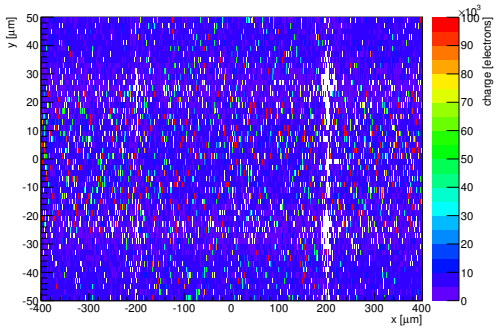

(t) Single pixel mean charge.

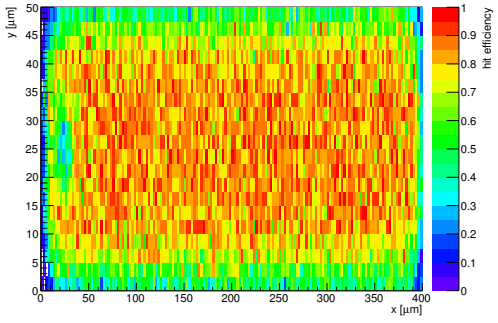

(u) Single pixel hit efficiency.

Figure C.113: Detailed plots for test beam measurement of DO-I-5 (description see section 6.1) sample (running as DUT2) during runs 61281-61289 in the September 2011 test beam period at CERN SPS in area H6B. Summary of the data in chapter 9.

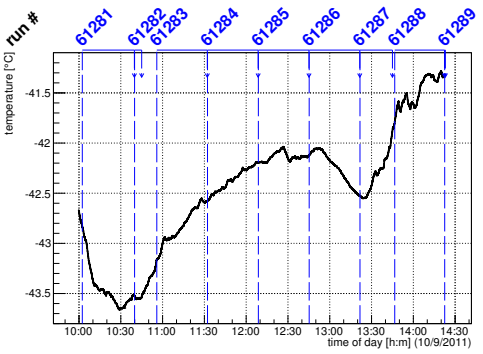

(a) Temperature vs time.

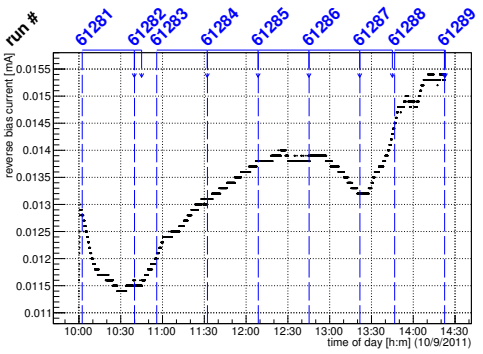

(b) Bias current vs time.

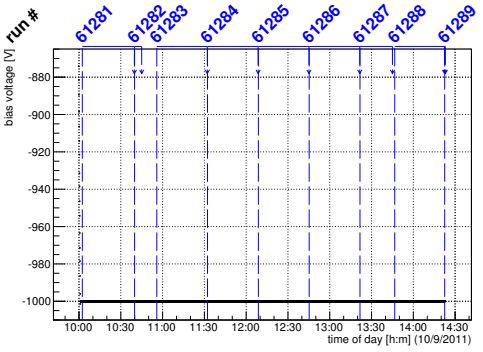

(c) Currently applied bias voltage vs time.

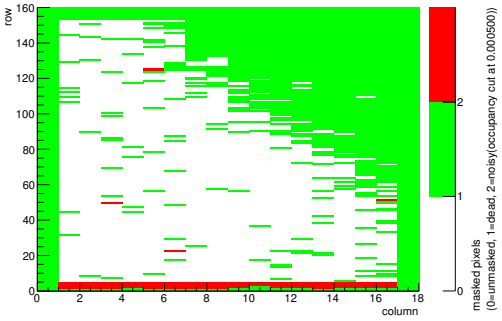

(d) Map of masked pixels.

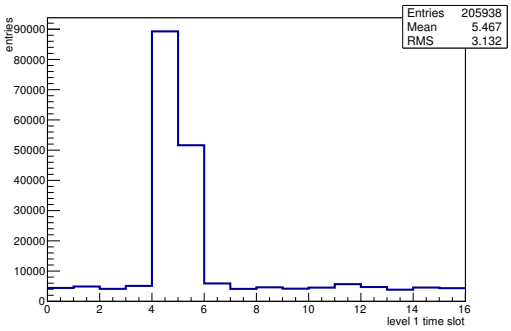

(e) Lvl1 distribution.

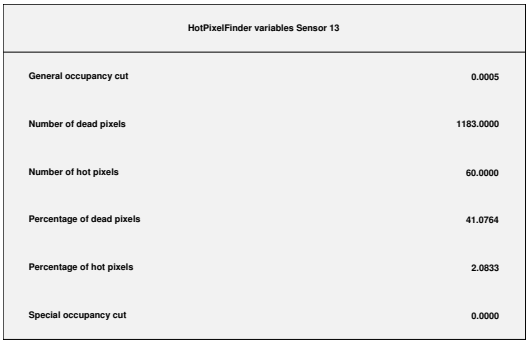

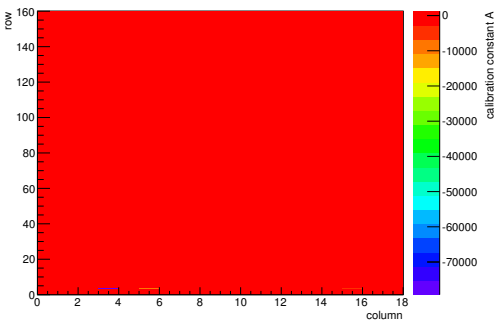

(f) Calibration constant A.

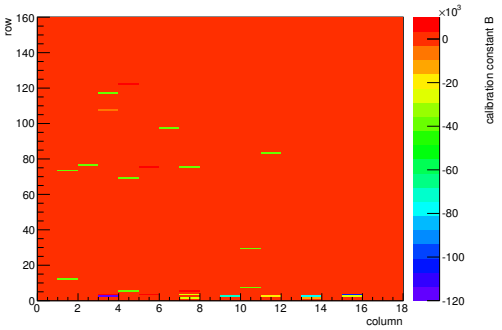

(g) Calibration constant B.

Figure C.114: Detailed plots for test beam measurement of DO-I-12 (description see section 6.1) sample (running as DUT3) during runs 61281-61289 in the September 2011 test beam period at CERN SPS in area H6B. Summary of the data in chapter 9. *(cont.)*

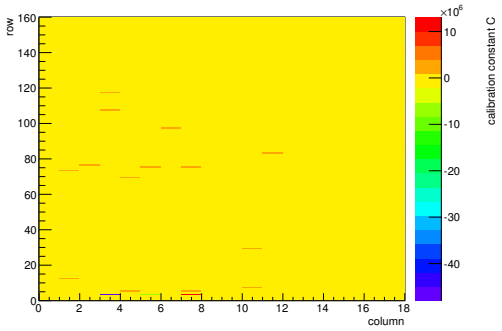

(h) Calibration constant C.

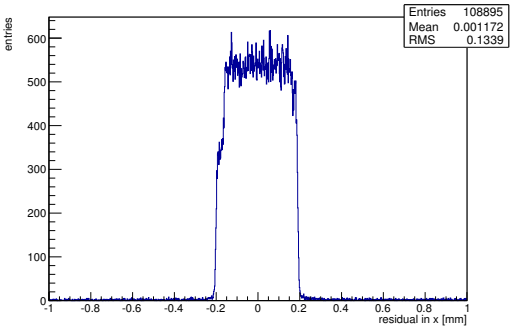

(i) Track residual in x.

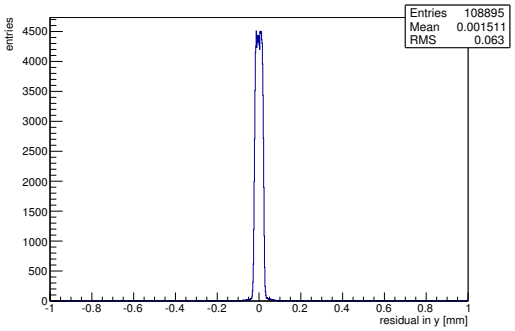

(j) Track residual in y.

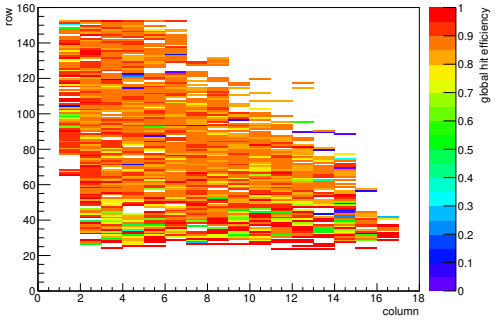

(k) Hit efficiency map.

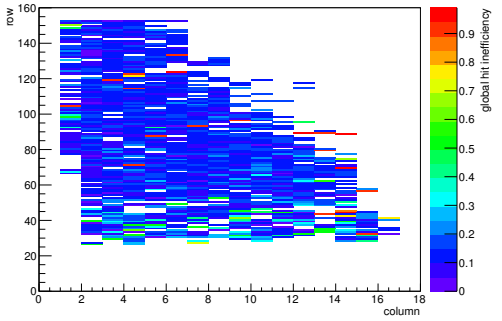

(l) Hit inefficiency map.

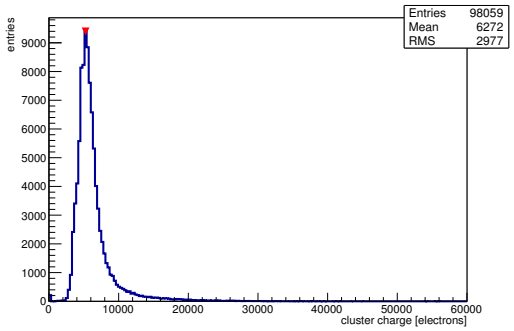

(m) Charge distribution (all cluster sizes included).

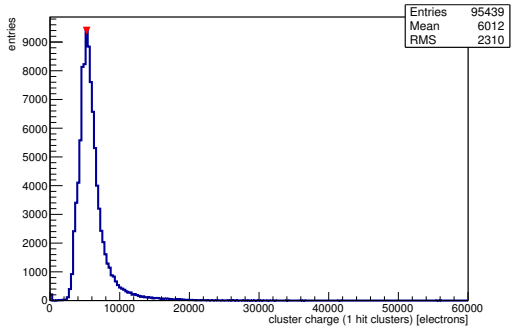

(n) Charge distribution (1 hit cluster).

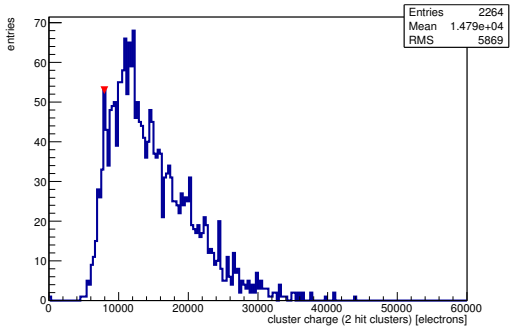

(o) Charge distribution (2 hit cluster).

Figure C.114: Detailed plots for test beam measurement of DO-I-12 (description see section 6.1) sample (running as DUT3) during runs 61281-61289 in the September 2011 test beam period at CERN SPS in area H6B. Summary of the data in chapter 9. *(cont.)*

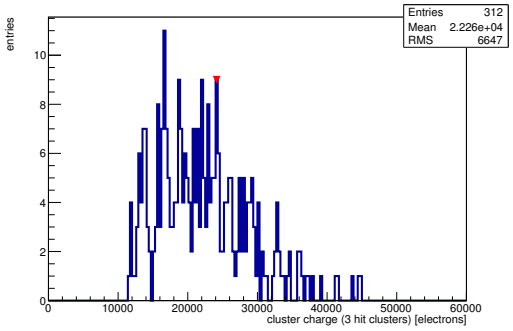

(p) Charge distribution (3 hit cluster).

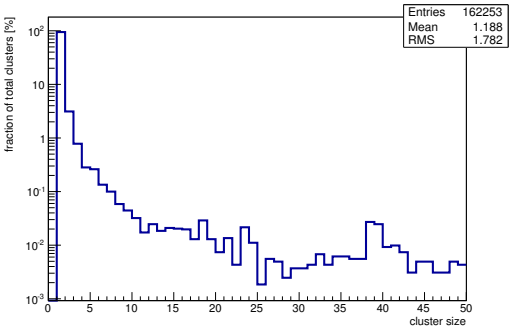

(q) Cluster size distribution.

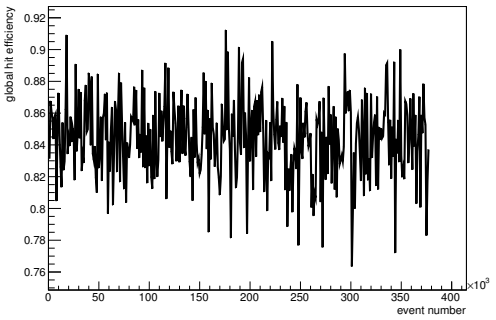

(r) Hit efficiency vs event number.

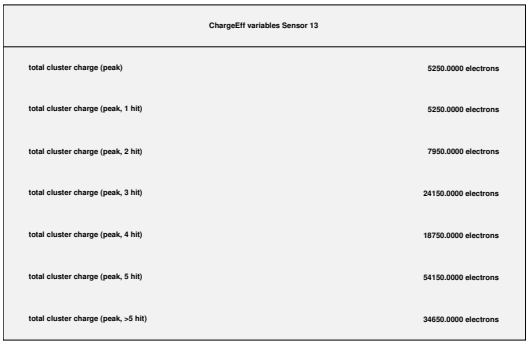

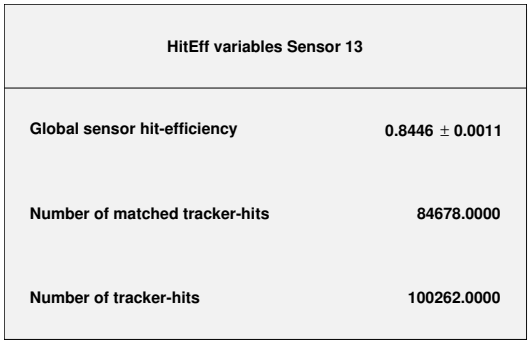

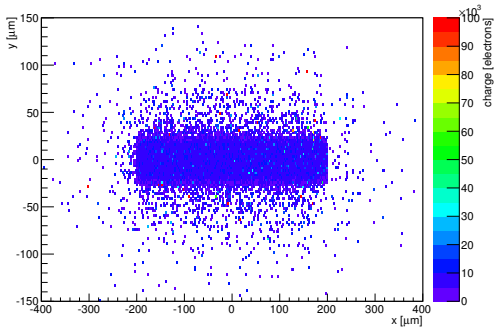

(s) Single pixel mean charge.

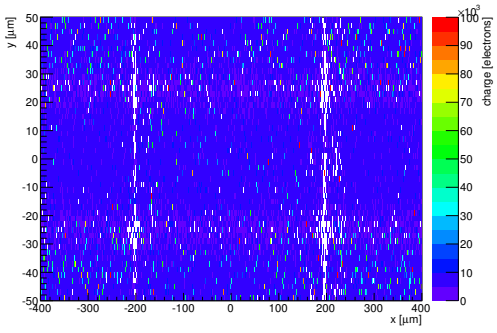

(t) Single pixel mean charge.

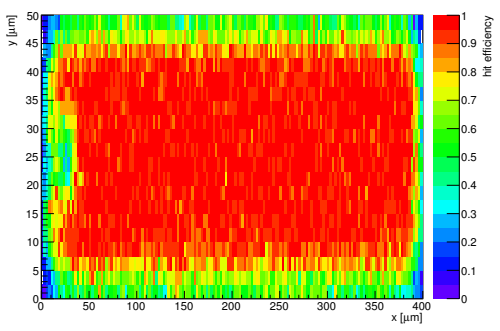

(u) Single pixel hit efficiency.

Figure C.114: Detailed plots for test beam measurement of DO-I-12 (description see section 6.1) sample (running as DUT3) during runs 61281-61289 in the September 2011 test beam period at CERN SPS in area H6B. Summary of the data in chapter 9.

C.3.19 Runs 61290-61296

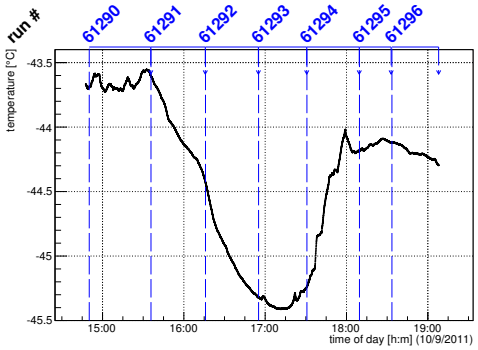

(a) Temperature vs time.

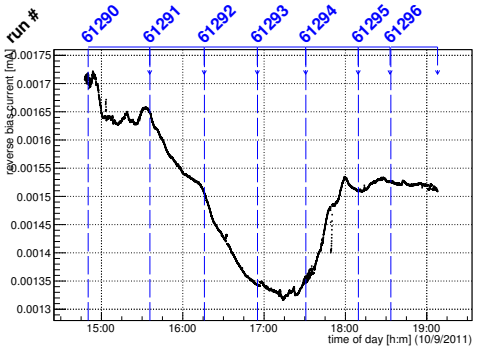

(b) Bias current vs time.

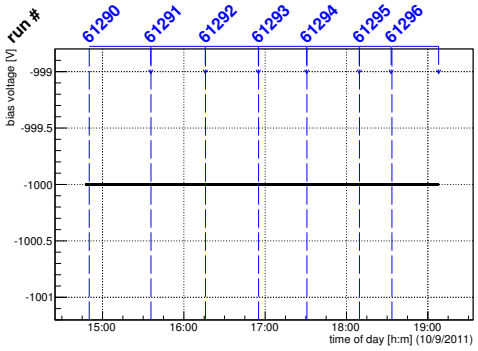

(c) Currently applied bias voltage vs time.

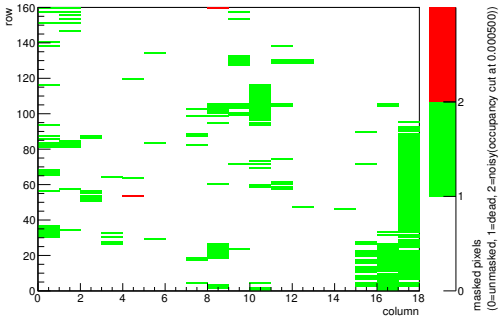

(d) Map of masked pixels.

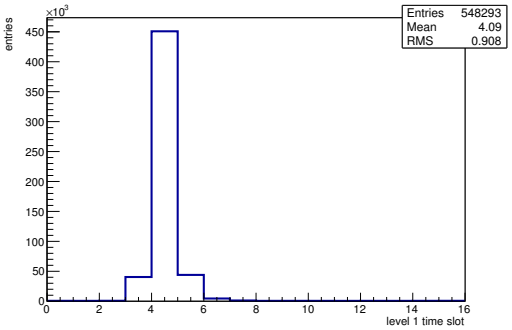

(e) Lvl1 distribution.

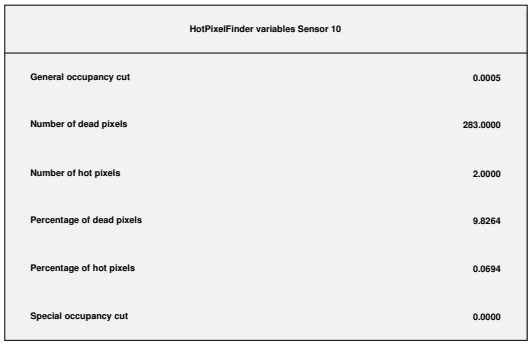

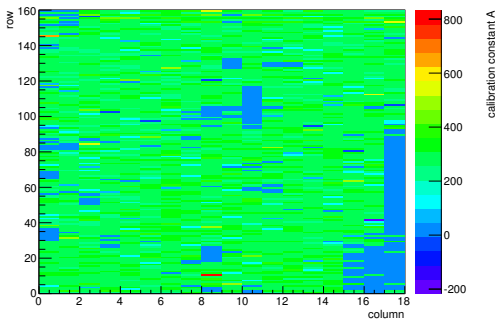

(f) Calibration constant A.

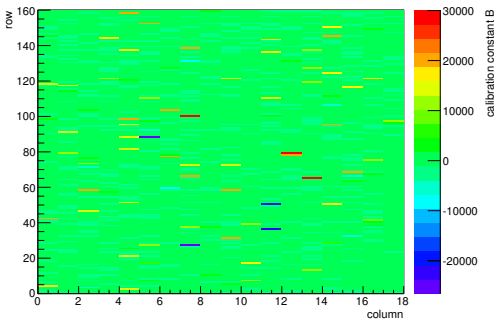

(g) Calibration constant B.

Figure C.115: Detailed plots for test beam measurement of DO-I-7 (description see section 6.1) sample (running as DUT0) during runs 61290-61296 in the September 2011 test beam period at CERN SPS in area H6B. Summary of the data in chapter 9. *(cont.)*

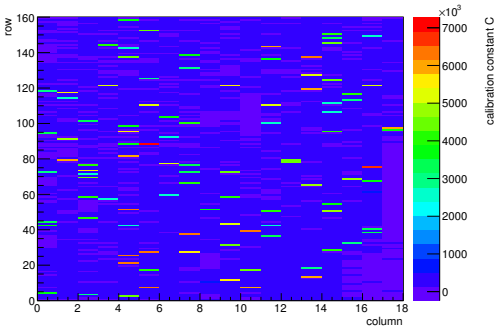

(h) Calibration constant C.

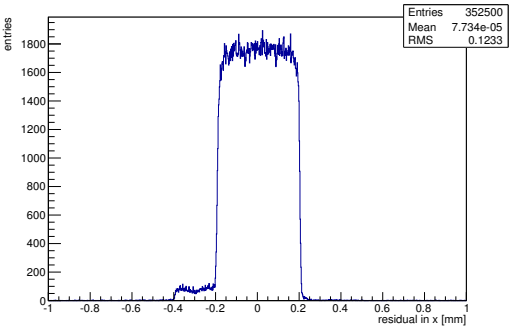

(i) Track residual in x.

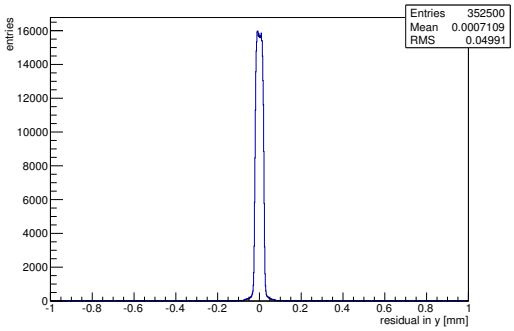

(j) Track residual in y.

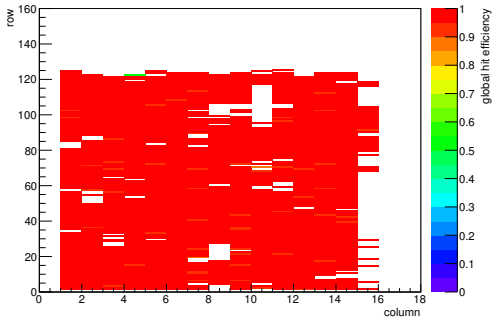

(k) Hit efficiency map.

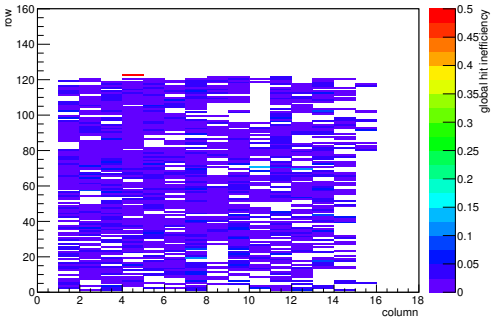

(l) Hit inefficiency map.

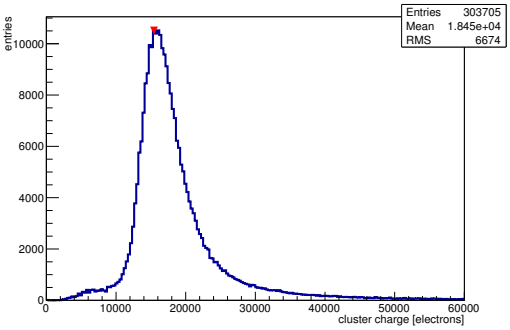

(m) Charge distribution (all cluster sizes included).

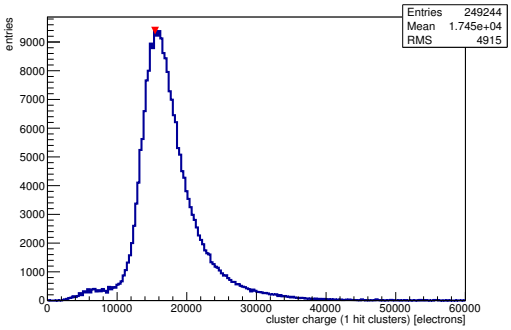

(n) Charge distribution (1 hit cluster).

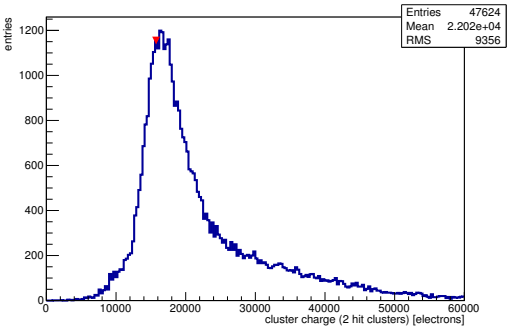

(o) Charge distribution (2 hit cluster).

Figure C.115: Detailed plots for test beam measurement of DO-I-7 (description see section 6.1) sample (running as DUT0) during runs 61290-61296 in the September 2011 test beam period at CERN SPS in area H6B. Summary of the data in chapter 9. *(cont.)*

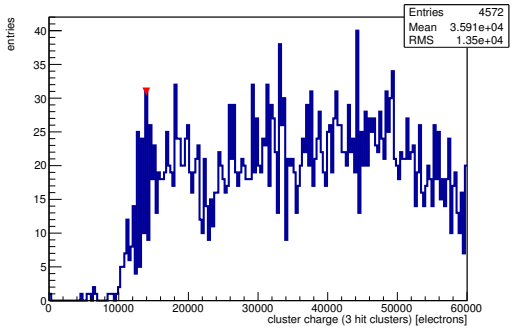

(p) Charge distribution (3 hit cluster).

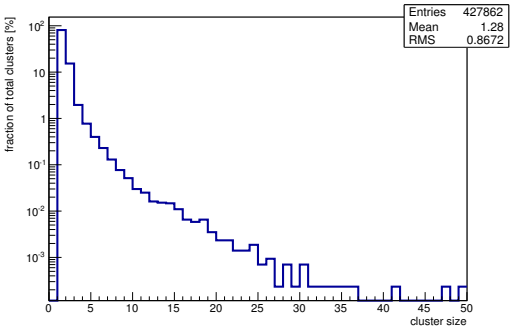

(q) Cluster size distribution.

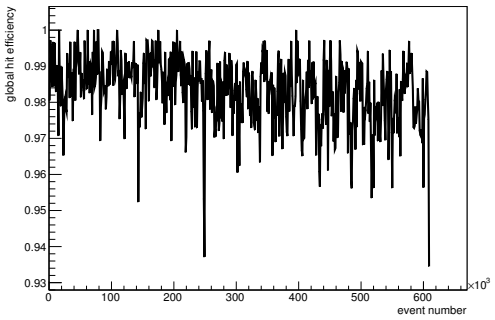

(r) Hit efficiency vs event number.

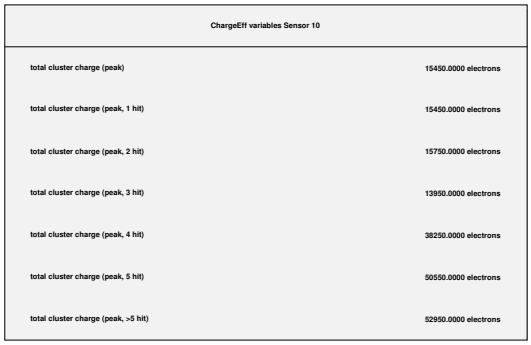

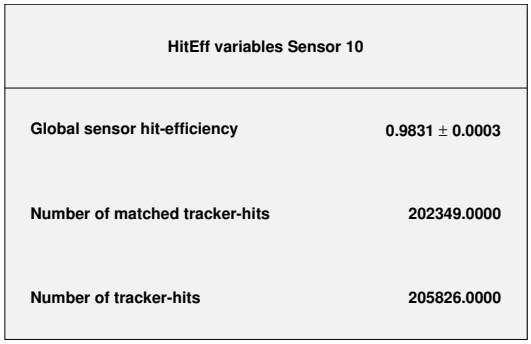

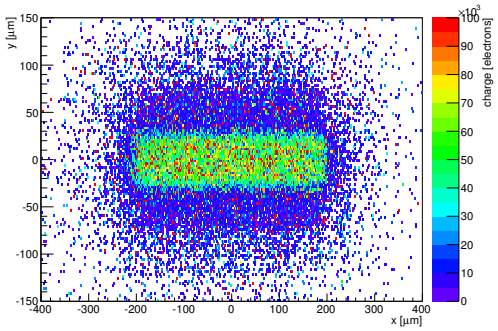

(s) Single pixel mean charge.

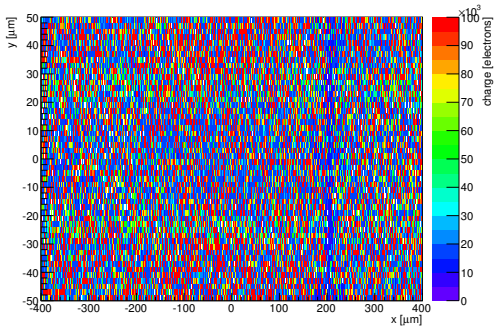

(t) Single pixel mean charge.

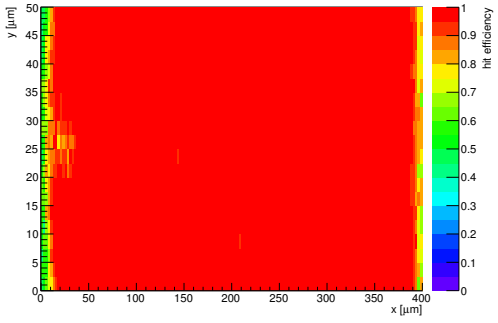

(u) Single pixel hit efficiency.

Figure C.115: Detailed plots for test beam measurement of DO-I-7 (description see section 6.1) sample (running as DUT0) during runs 61290-61296 in the September 2011 test beam period at CERN SPS in area H6B. Summary of the data in chapter 9.

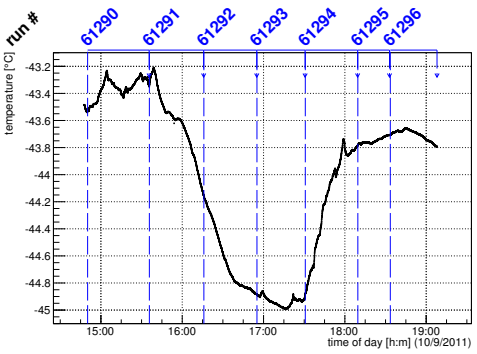

(a) Temperature vs time.

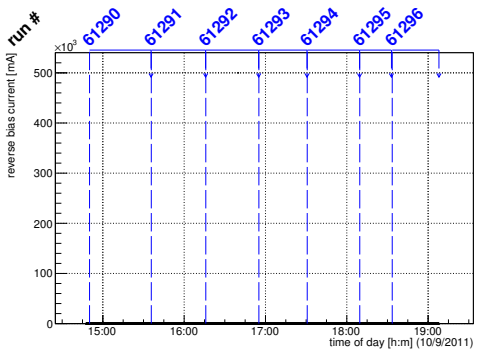

(b) Bias current vs time.

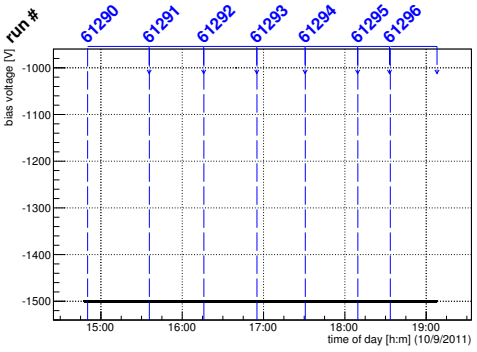

(c) Currently applied bias voltage vs time.

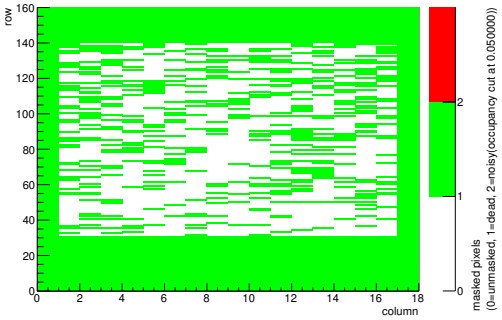

(d) Map of masked pixels.

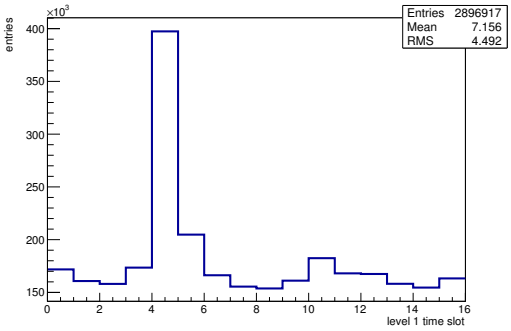

(e) Lvl1 distribution.

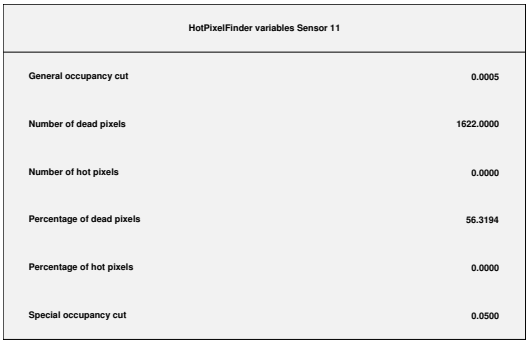

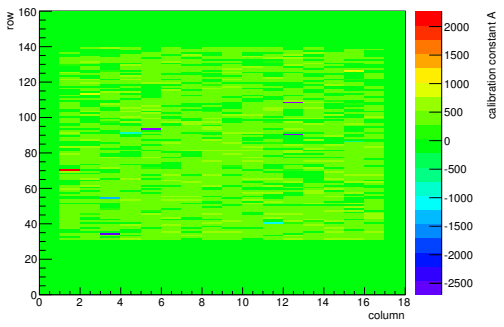

(f) Calibration constant A.

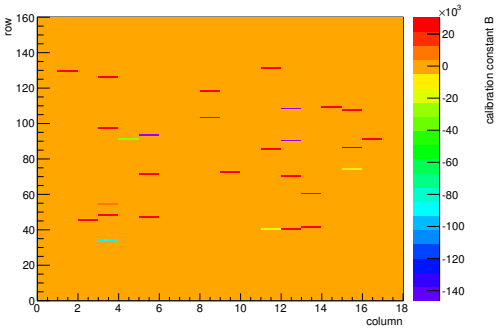

(g) Calibration constant B.

Figure C.116: Detailed plots for test beam measurement of DO-I-11 (description see section 6.1) sample (running as DUT1) during runs 61290-61296 in the September 2011 test beam period at CERN SPS in area H6B. Summary of the data in chapter 9. *(cont.)*

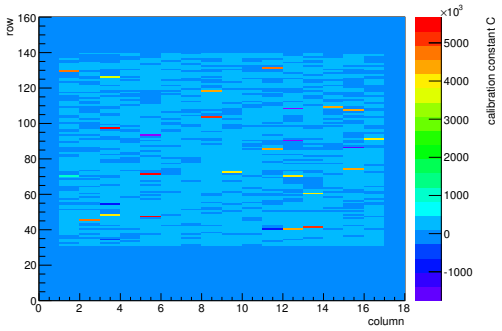

(h) Calibration constant C.

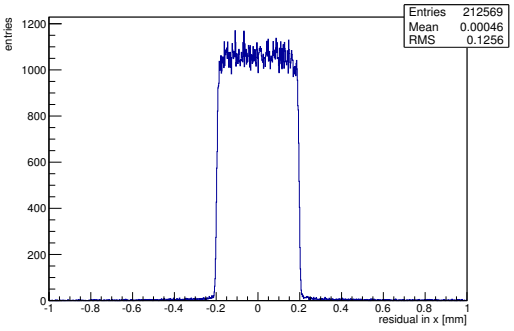

(i) Track residual in x.

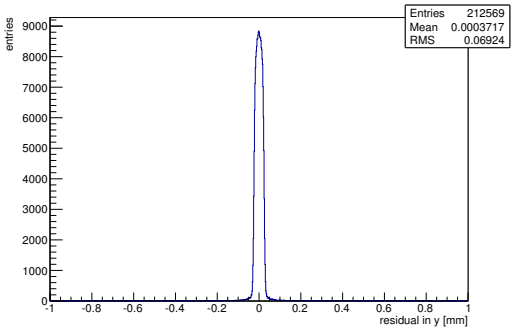

(j) Track residual in y.

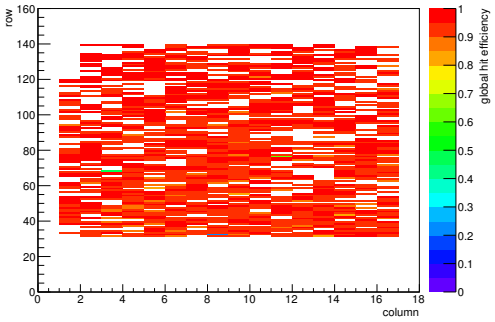

(k) Hit efficiency map.

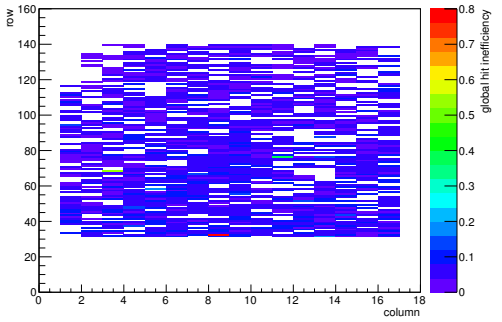

(l) Hit inefficiency map.

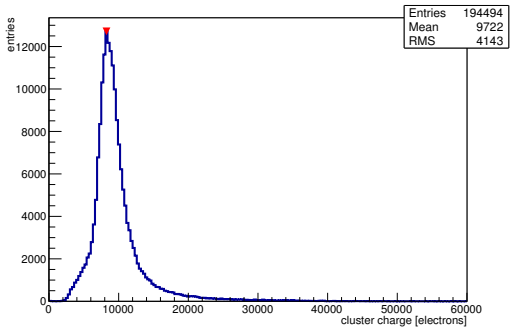

(m) Charge distribution (all cluster sizes included).

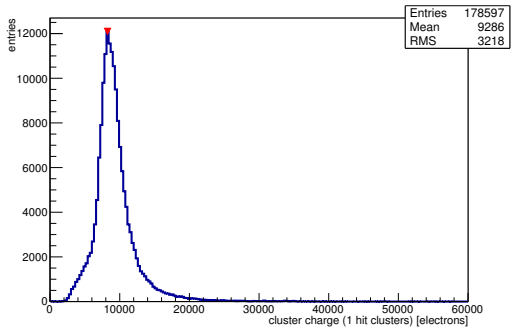

(n) Charge distribution (1 hit cluster).

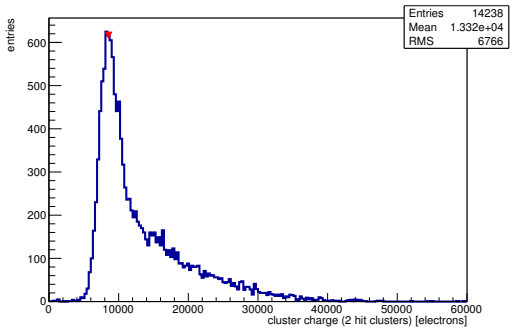

(o) Charge distribution (2 hit cluster).

Figure C.116: Detailed plots for test beam measurement of DO-I-11 (description see section 6.1) sample (running as DUT1) during runs 61290-61296 in the September 2011 test beam period at CERN SPS in area H6B. Summary of the data in chapter 9. *(cont.)*

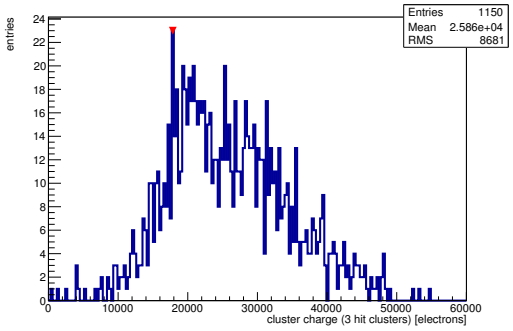

(p) Charge distribution (3 hit cluster).

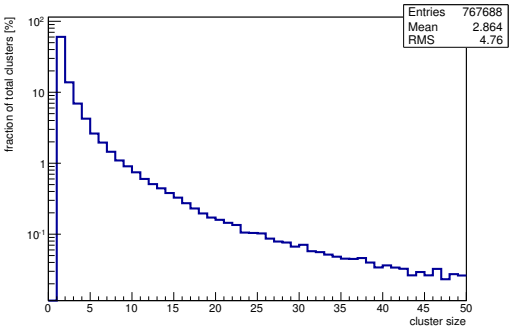

(q) Cluster size distribution.

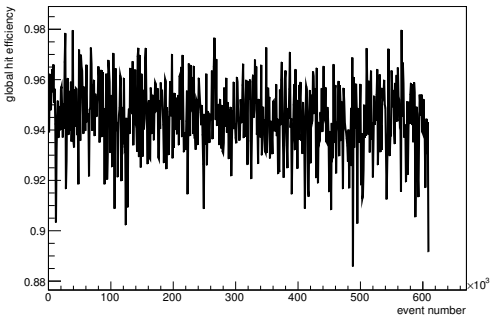

(r) Hit efficiency vs event number.

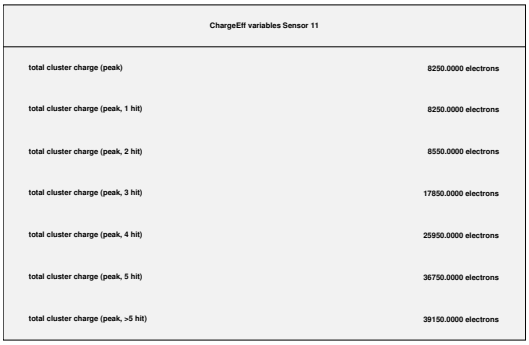

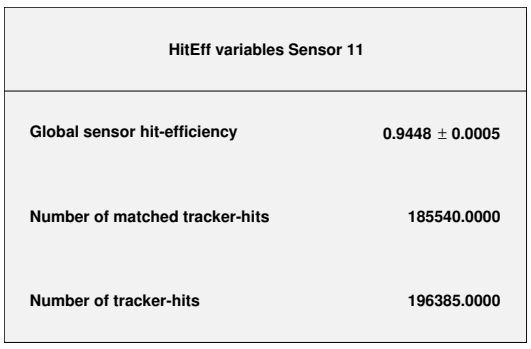

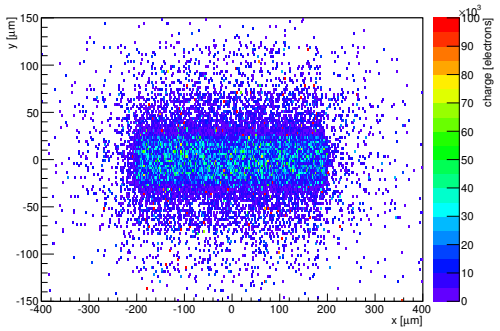

(s) Single pixel mean charge.

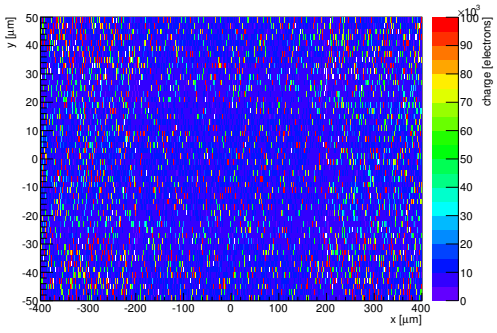

(t) Single pixel mean charge.

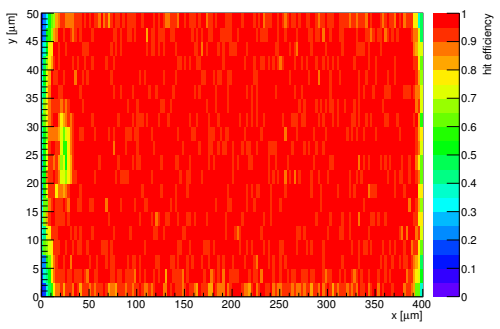

(u) Single pixel hit efficiency.

Figure C.116: Detailed plots for test beam measurement of DO-I-11 (description see section 6.1) sample (running as DUT1) during runs 61290-61296 in the September 2011 test beam period at CERN SPS in area H6B. Summary of the data in chapter 9.

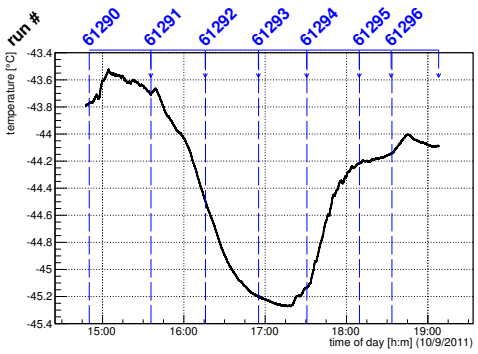

(a) Temperature vs time.

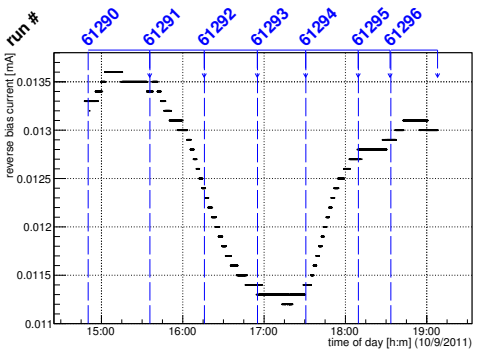

(b) Bias current vs time.

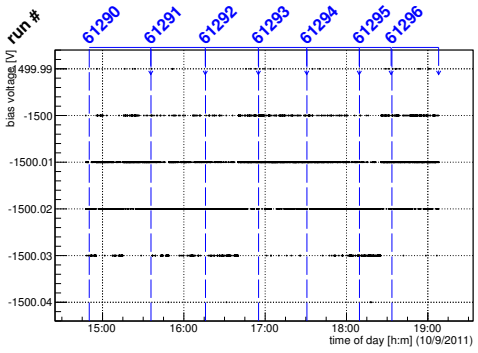

(c) Currently applied bias voltage vs time.

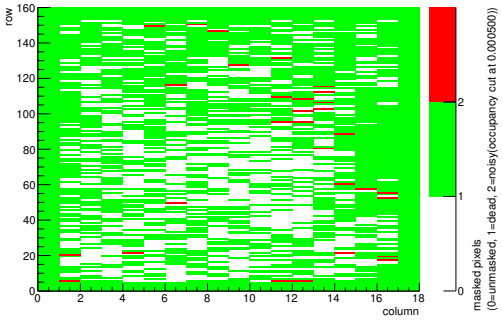

(d) Map of masked pixels.

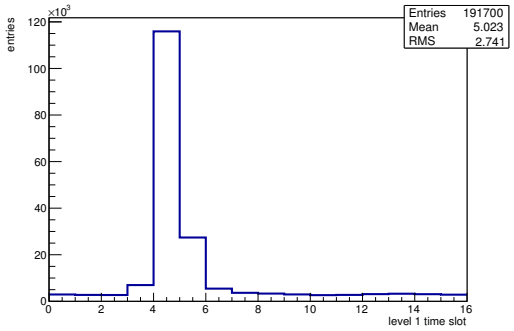

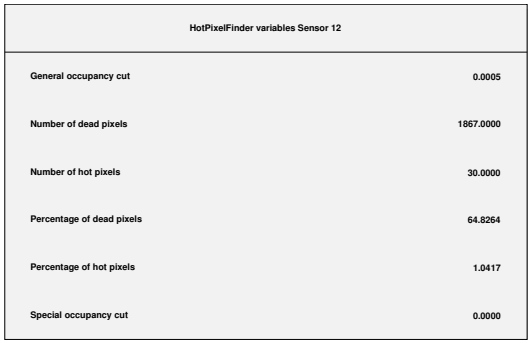

(e) Lvl1 distribution.

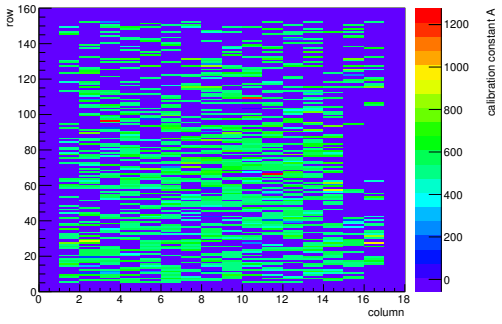

(f) Calibration constant A.

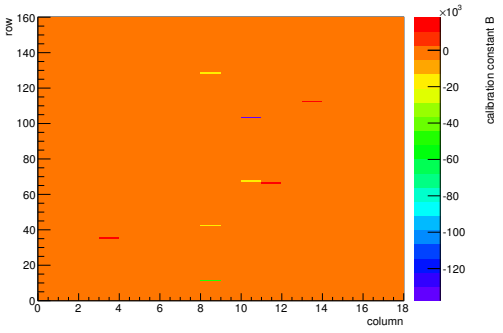

(g) Calibration constant B.

Figure C.117: Detailed plots for test beam measurement of DO-I-5 (description see section 6.1) sample (running as DUT2) during runs 61290-61296 in the September 2011 test beam period at CERN SPS in area H6B. Summary of the data in chapter 9. *(cont.)*

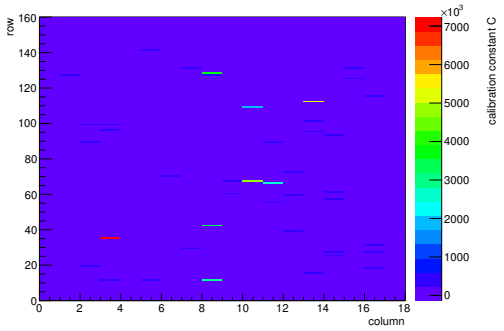

(h) Calibration constant C.

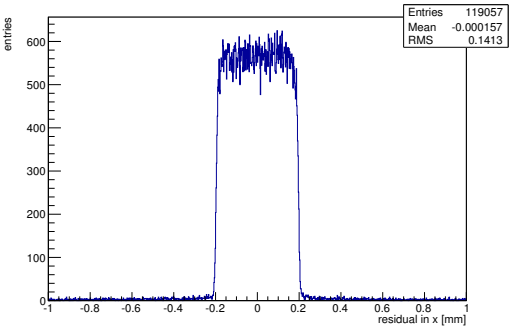

(i) Track residual in x.

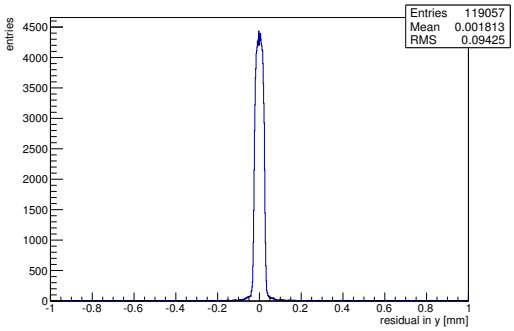

(j) Track residual in y.

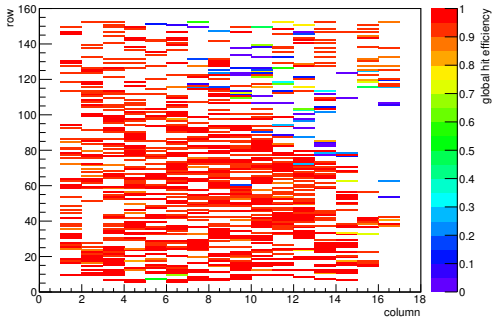

(k) Hit efficiency map.

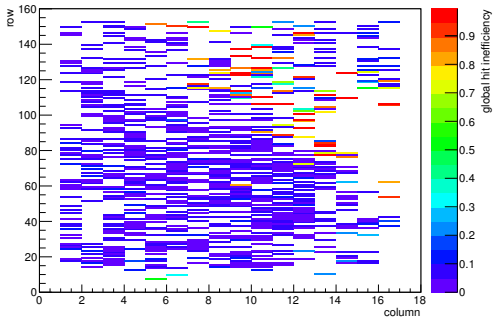

(l) Hit inefficiency map.

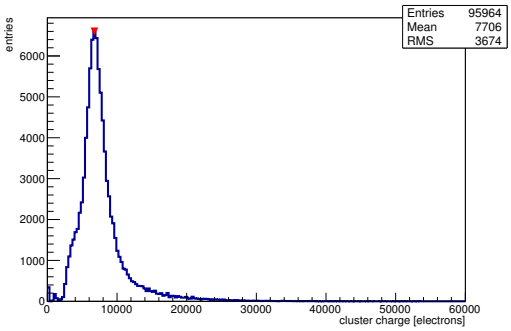

(m) Charge distribution (all cluster sizes included).

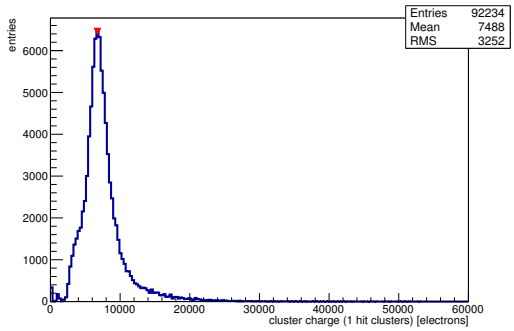

(n) Charge distribution (1 hit cluster).

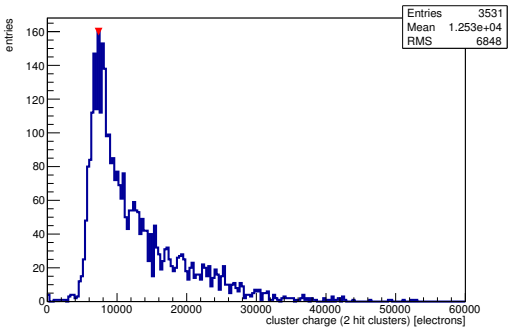

(o) Charge distribution (2 hit cluster).

Figure C.117: Detailed plots for test beam measurement of DO-I-5 (description see section 6.1) sample (running as DUT2) during runs 61290-61296 in the September 2011 test beam period at CERN SPS in area H6B. Summary of the data in chapter 9. *(cont.)*

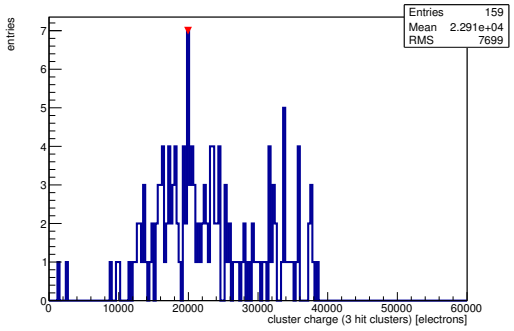

(p) Charge distribution (3 hit cluster).

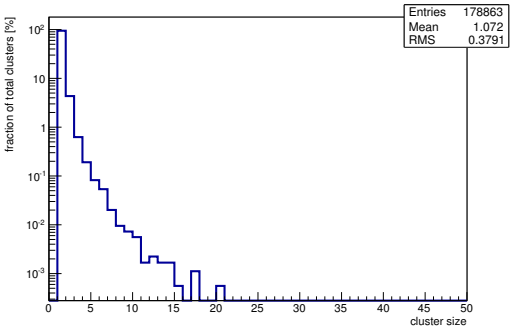

(q) Cluster size distribution.

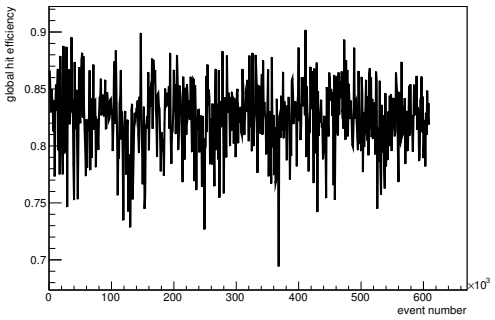

(r) Hit efficiency vs event number.

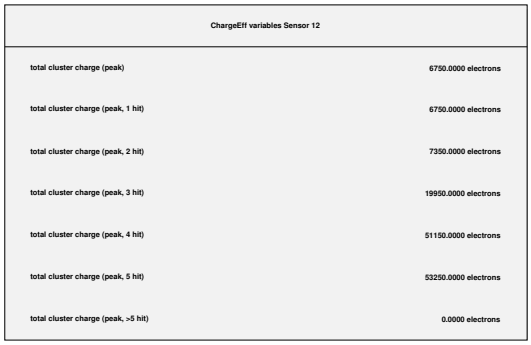

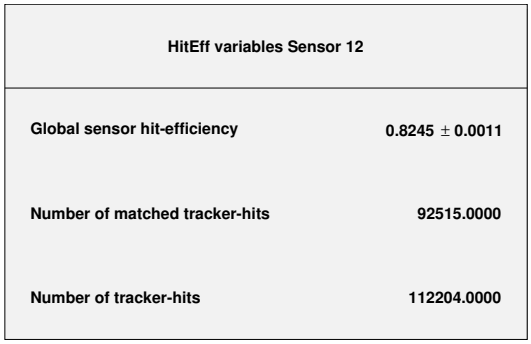

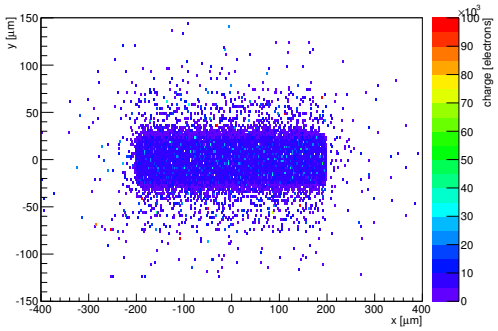

(s) Single pixel mean charge.

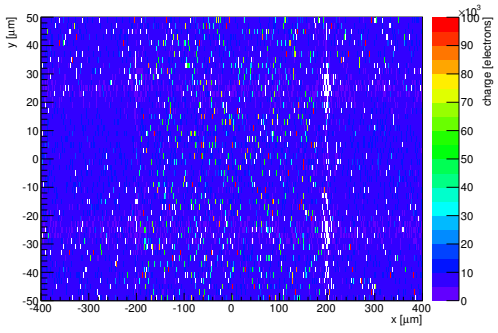

(t) Single pixel mean charge.

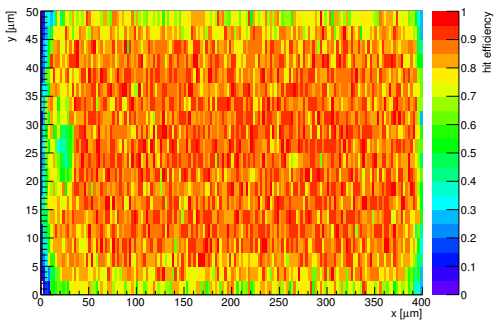

(u) Single pixel hit efficiency.

Figure C.117: Detailed plots for test beam measurement of DO-I-5 (description see section 6.1) sample (running as DUT2) during runs 61290-61296 in the September 2011 test beam period at CERN SPS in area H6B. Summary of the data in chapter 9.

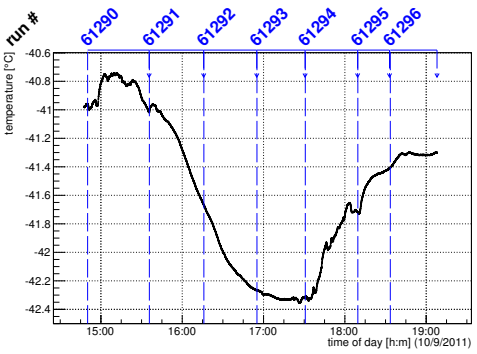

(a) Temperature vs time.

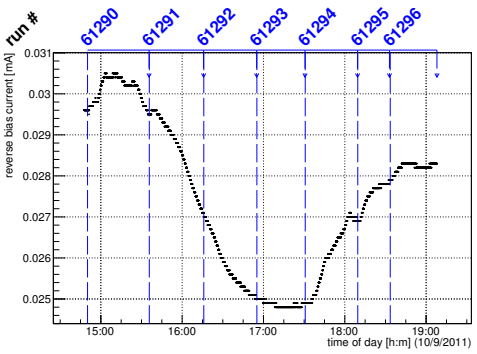

(b) Bias current vs time.

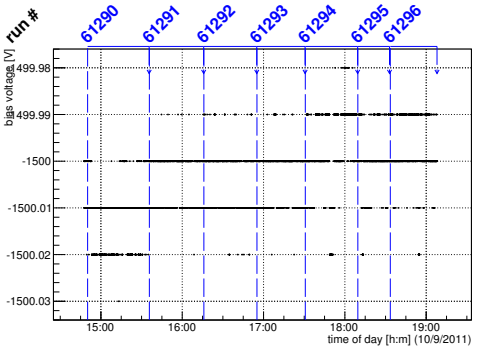

(c) Currently applied bias voltage vs time.

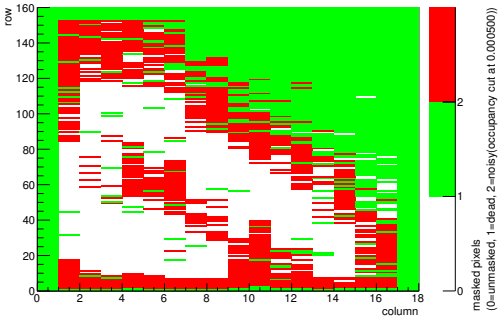

(d) Map of masked pixels.

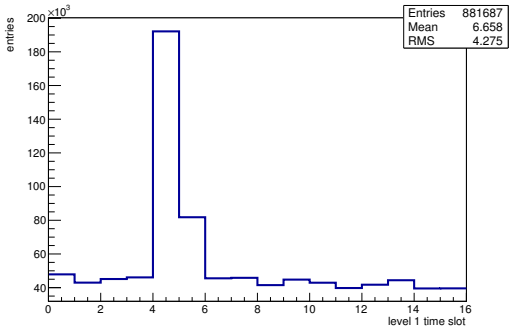

(e) Lvl1 distribution.

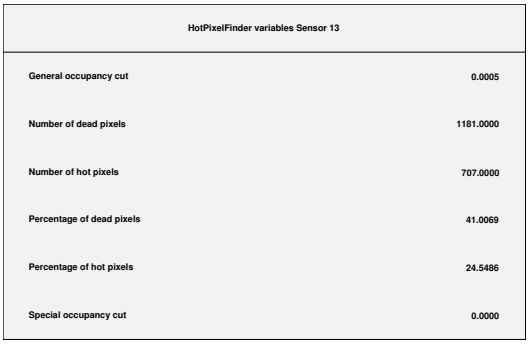

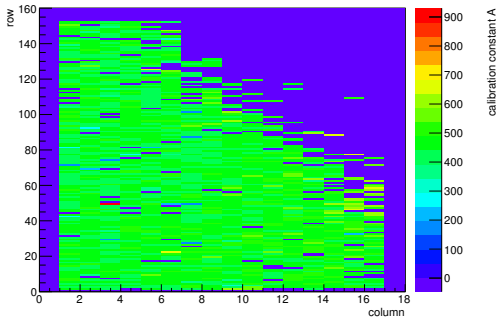

(f) Calibration constant A.

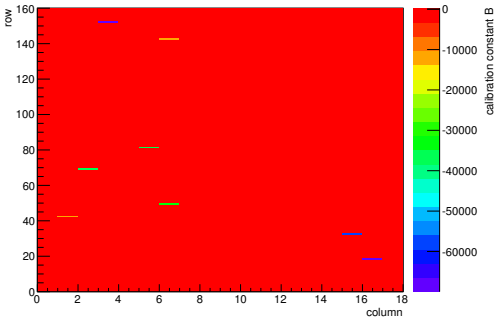

(g) Calibration constant B.

Figure C.118: Detailed plots for test beam measurement of DO-I-12 (description see section 6.1) sample (running as DUT3) during runs 61290-61296 in the September 2011 test beam period at CERN SPS in area H6B. Summary of the data in chapter 9. *(cont.)*

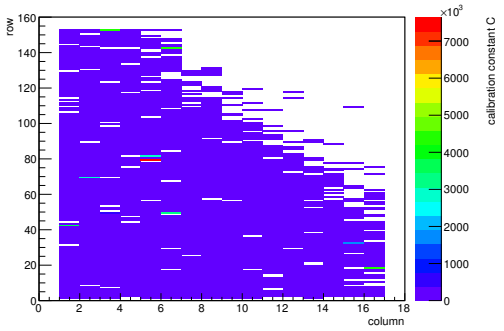

(h) Calibration constant C.

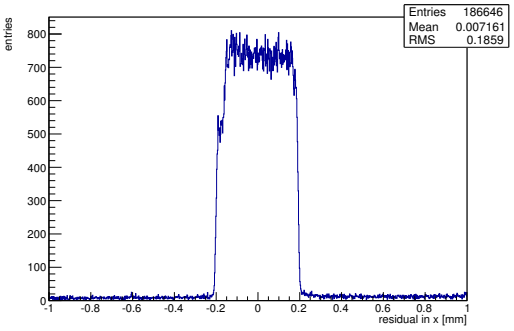

(i) Track residual in x.

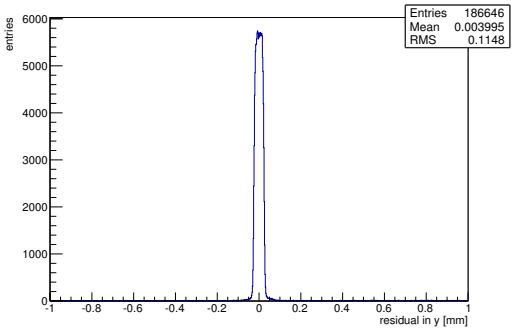

(j) Track residual in y.

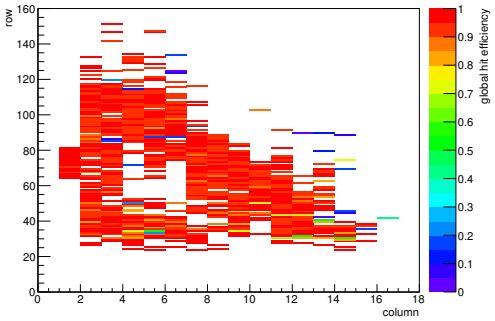

(k) Hit efficiency map.

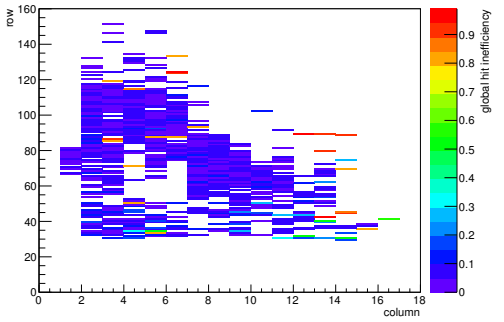

(l) Hit inefficiency map.

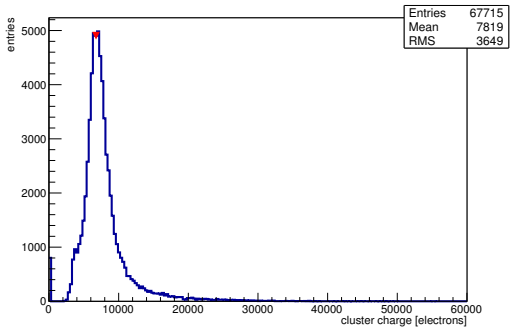

(m) Charge distribution (all cluster sizes included).

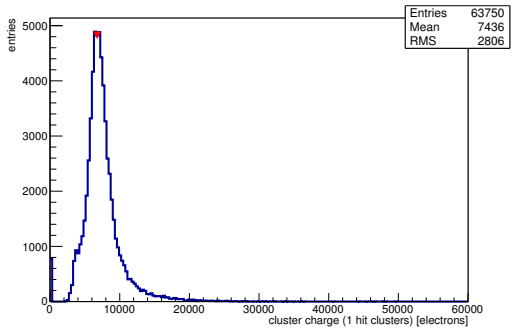

(n) Charge distribution (1 hit cluster).

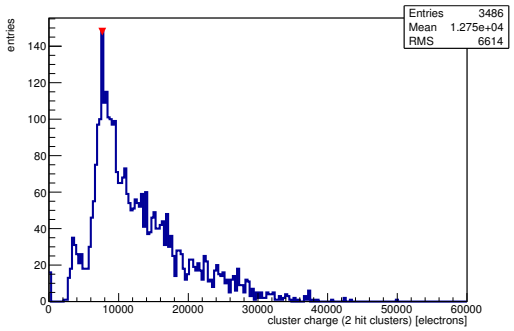

(o) Charge distribution (2 hit cluster).

Figure C.118: Detailed plots for test beam measurement of DO-I-12 (description see section 6.1) sample (running as DUT3) during runs 61290-61296 in the September 2011 test beam period at CERN SPS in area H6B. Summary of the data in chapter 9. *(cont.)*

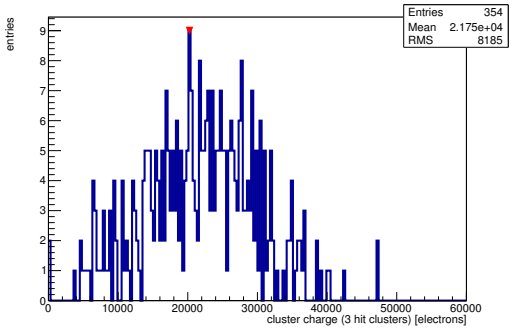

(p) Charge distribution (3 hit cluster).

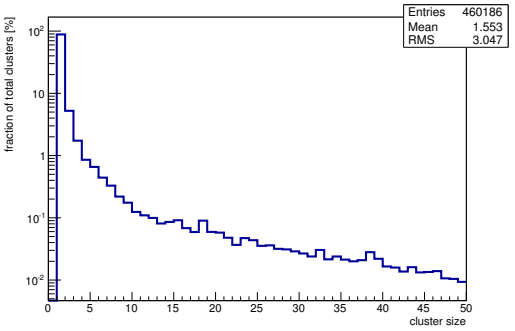

(q) Cluster size distribution.

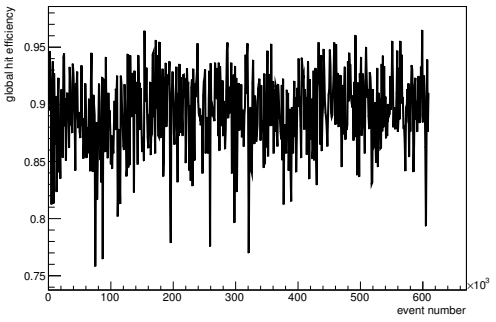

(r) Hit efficiency vs event number.

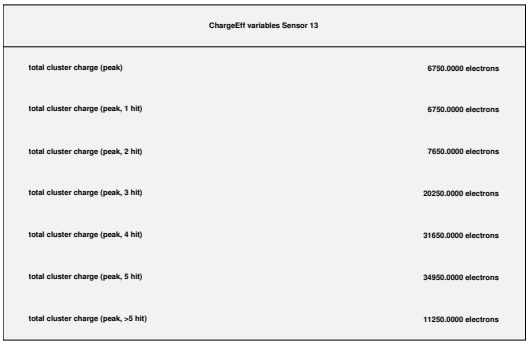

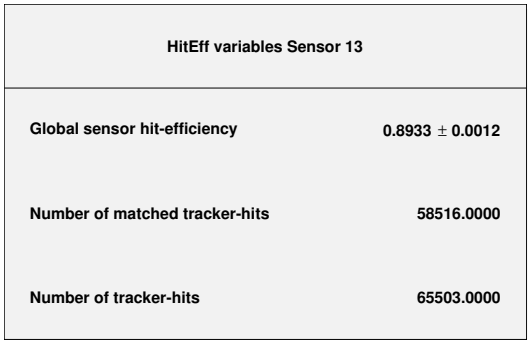

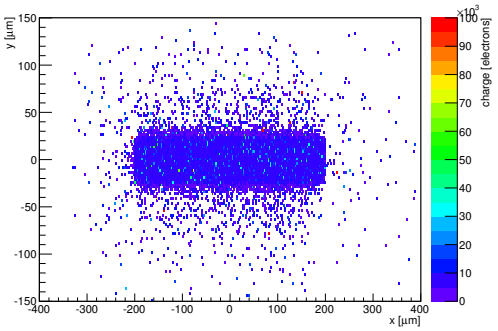

(s) Single pixel mean charge.

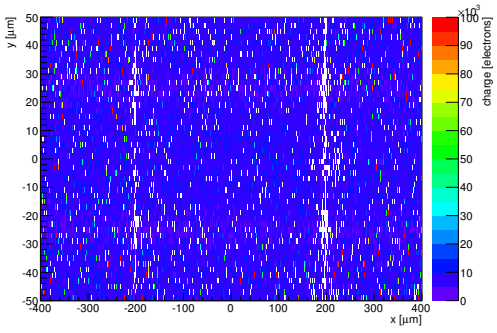

(t) Single pixel mean charge.

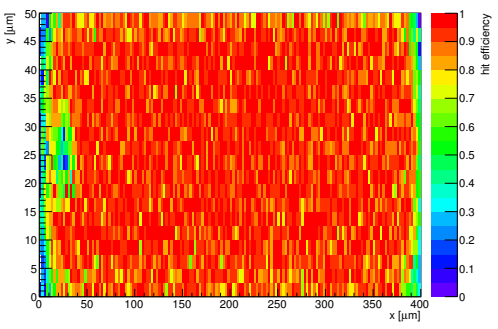

(u) Single pixel hit efficiency.

Figure C.118: Detailed plots for test beam measurement of DO-I-12 (description see section 6.1) sample (running as DUT3) during runs 61290-61296 in the September 2011 test beam period at CERN SPS in area H6B. Summary of the data in chapter 9.

C.3.20 Runs 61298-61303

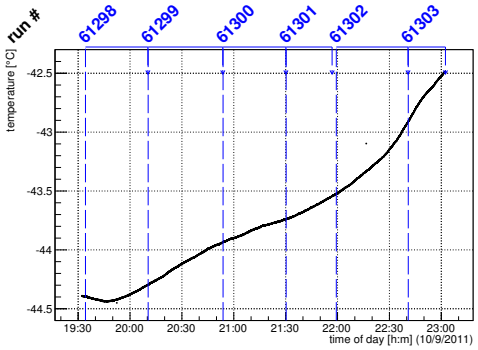

(a) Temperature vs time.

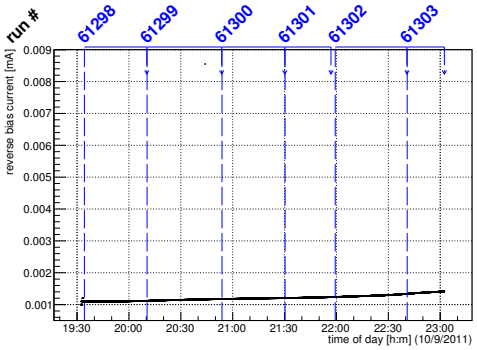

(b) Bias current vs time.

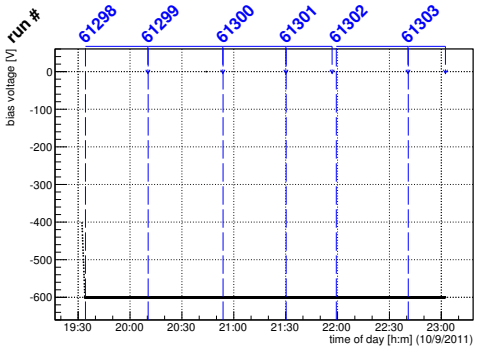

(c) Currently applied bias voltage vs time.

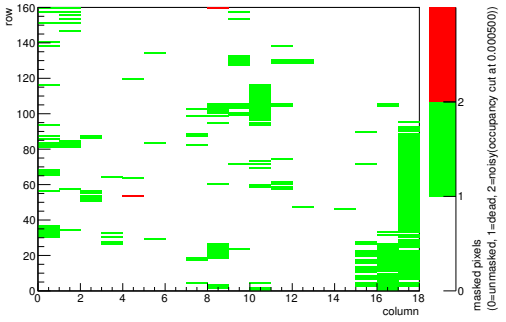

(d) Map of masked pixels.

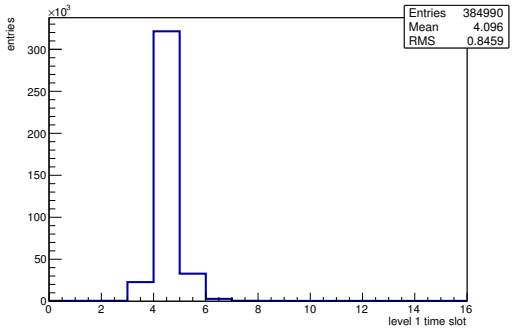

(e) Lvl1 distribution.

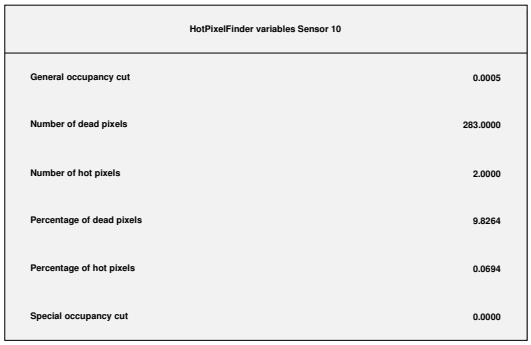

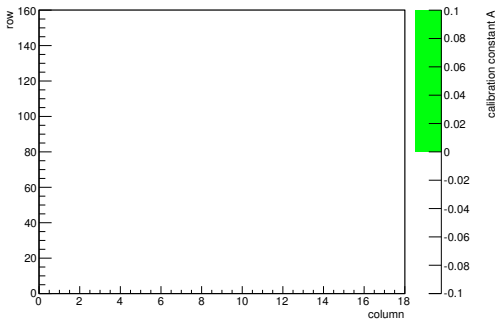

(f) Calibration constant A.

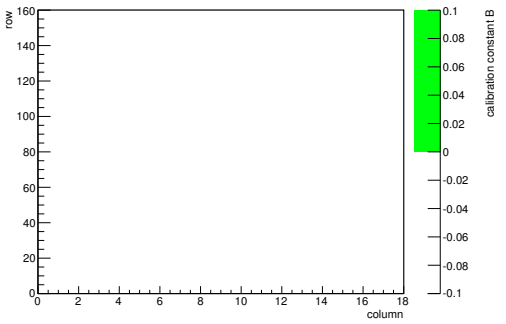

(g) Calibration constant B.

Figure C.119: Detailed plots for test beam measurement of DO-I-7 (description see section 6.1) sample (running as DUT0) during runs 61298-61303 in the September 2011 test beam period at CERN SPS in area H6B. Summary of the data in chapter 9. *(cont.)*

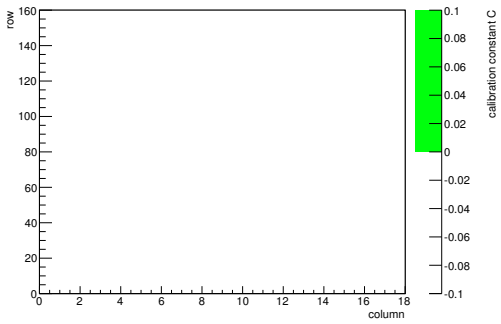

(h) Calibration constant C.

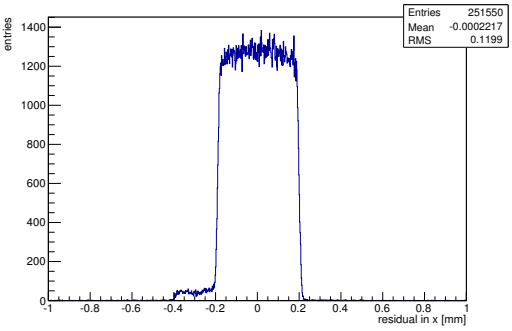

(i) Track residual in x.

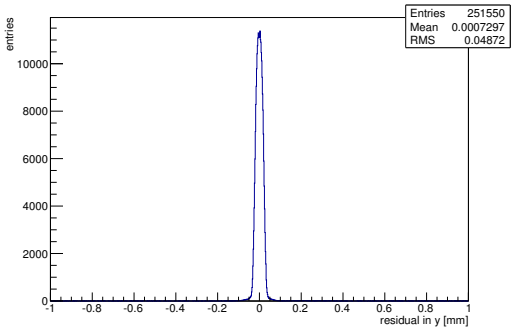

(j) Track residual in y.

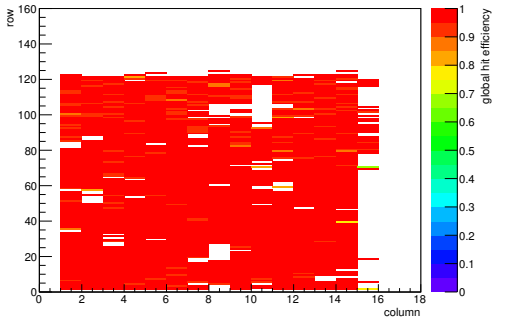

(k) Hit efficiency map.

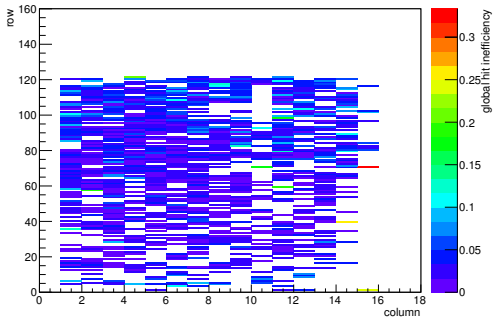

(l) Hit inefficiency map.

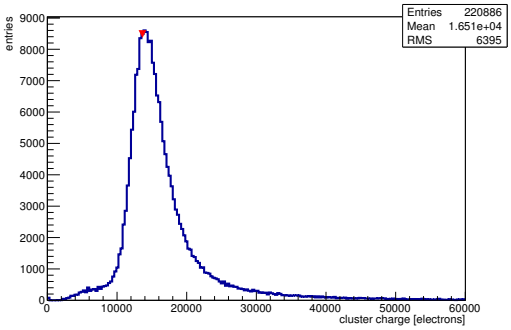

(m) Charge distribution (all cluster sizes included).

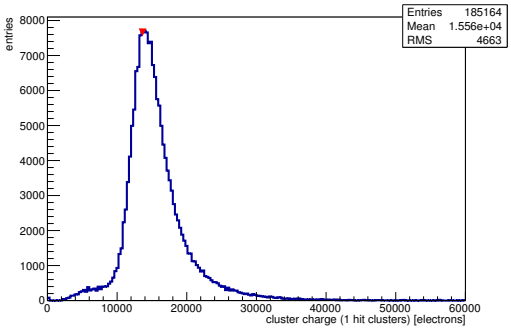

(n) Charge distribution (1 hit cluster).

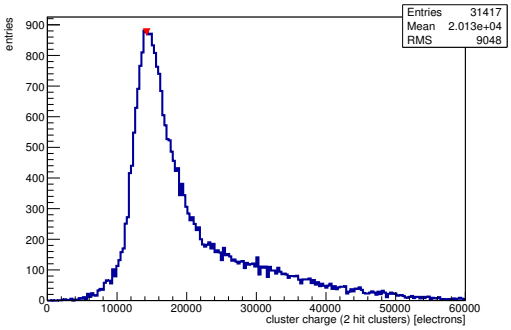

(o) Charge distribution (2 hit cluster).

Figure C.119: Detailed plots for test beam measurement of DO-I-7 (description see section 6.1) sample (running as DUT0) during runs 61298-61303 in the September 2011 test beam period at CERN SPS in area H6B. Summary of the data in chapter 9. *(cont.)*

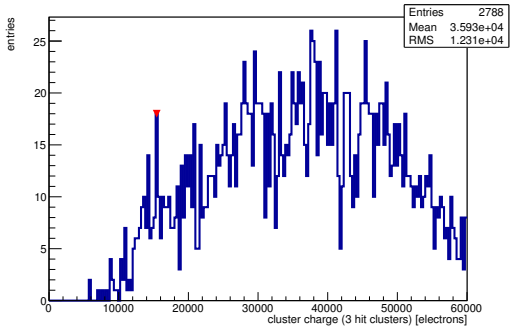

(p) Charge distribution (3 hit cluster).

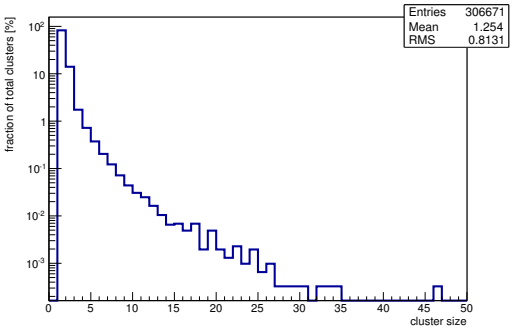

(q) Cluster size distribution.

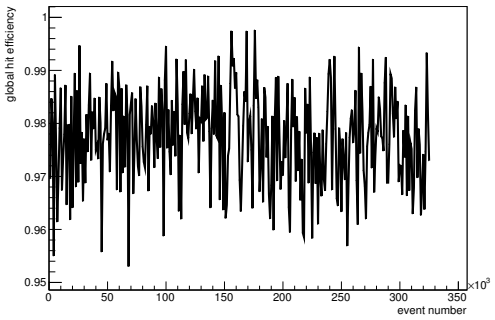

(r) Hit efficiency vs event number.

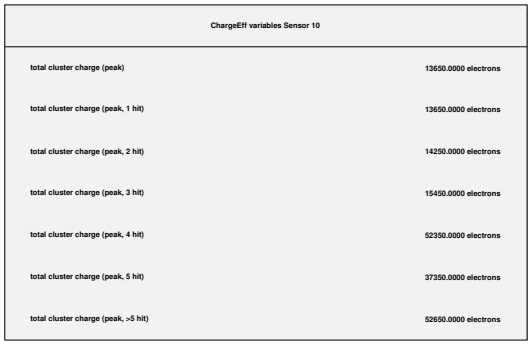

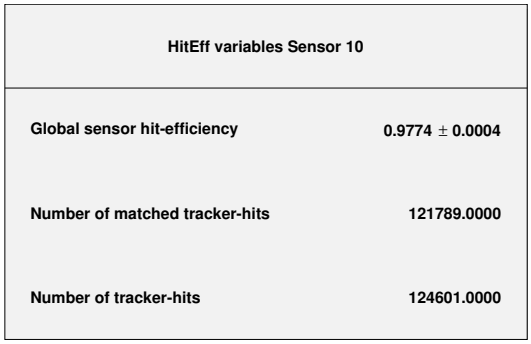

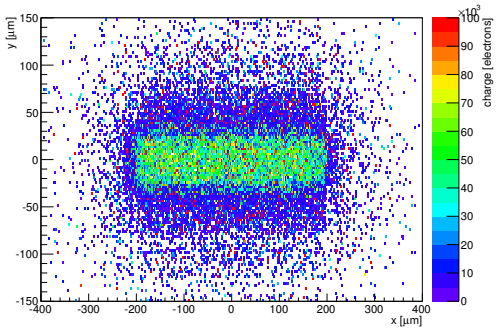

(s) Single pixel mean charge.

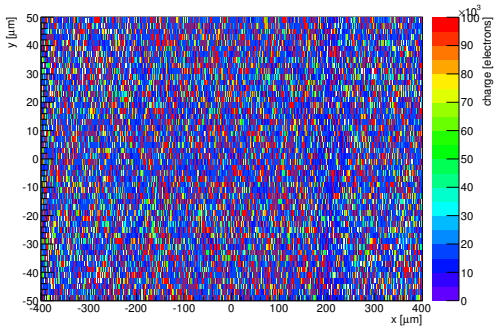

(t) Single pixel mean charge.

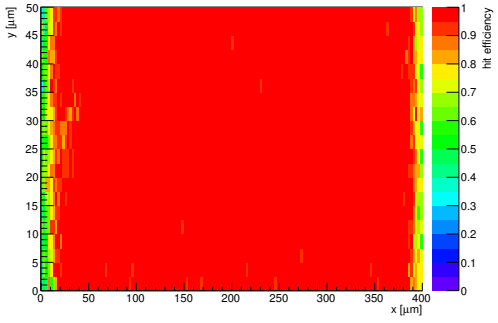

(u) Single pixel hit efficiency.

Figure C.119: Detailed plots for test beam measurement of DO-I-7 (description see section 6.1) sample (running as DUT0) during runs 61298-61303 in the September 2011 test beam period at CERN SPS in area H6B. Summary of the data in chapter 9.

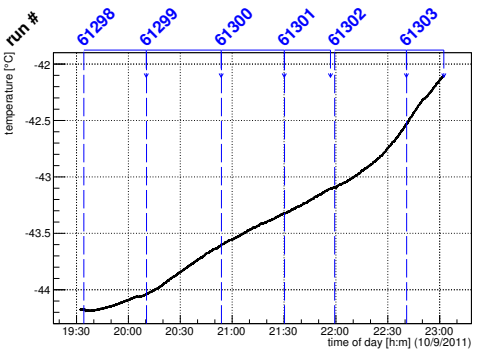

(a) Temperature vs time.

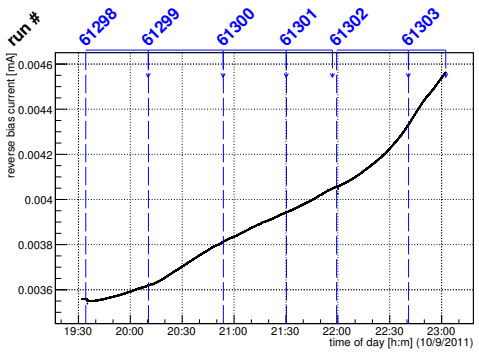

(b) Bias current vs time.

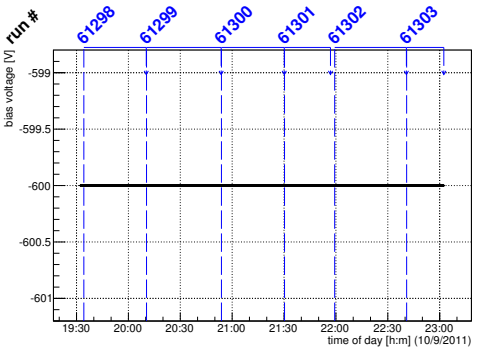

(c) Currently applied bias voltage vs time.

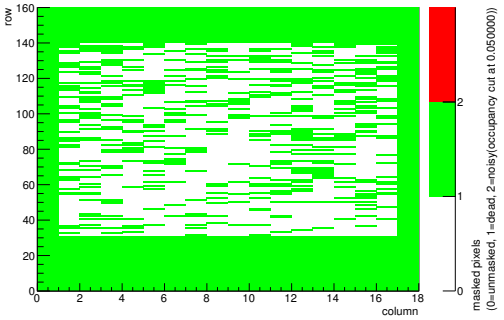

(d) Map of masked pixels.

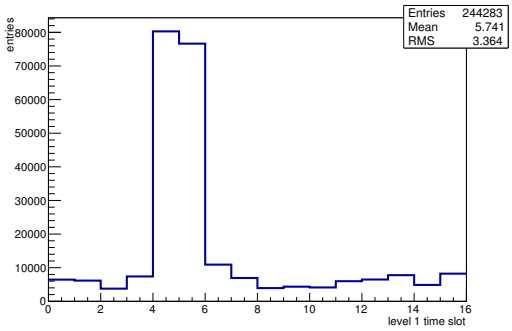

(e) Lvl1 distribution.

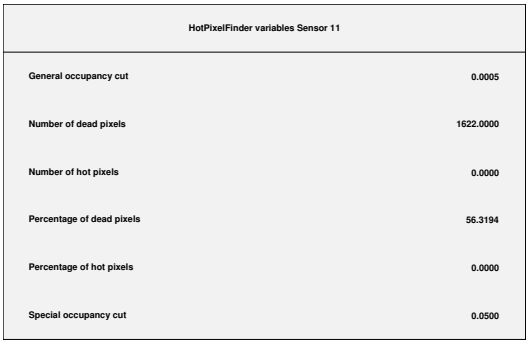

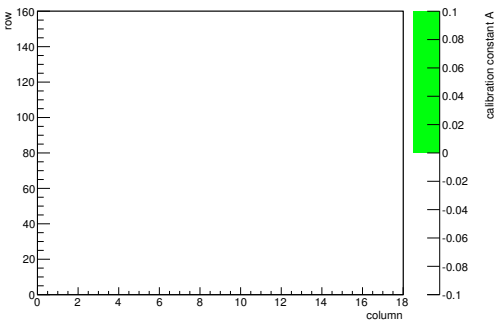

(f) Calibration constant A.

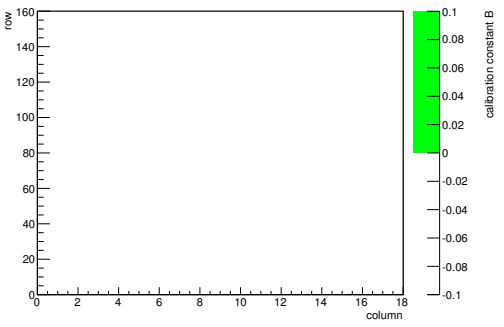

(g) Calibration constant B.

Figure C.120: Detailed plots for test beam measurement of DO-I-11 (description see section 6.1) sample (running as DUT1) during runs 61298-61303 in the September 2011 test beam period at CERN SPS in area H6B. Summary of the data in chapter 9. *(cont.)*

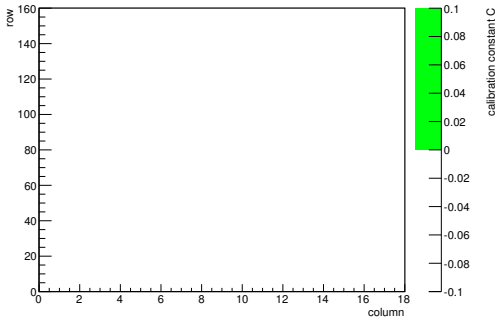

(h) Calibration constant C.

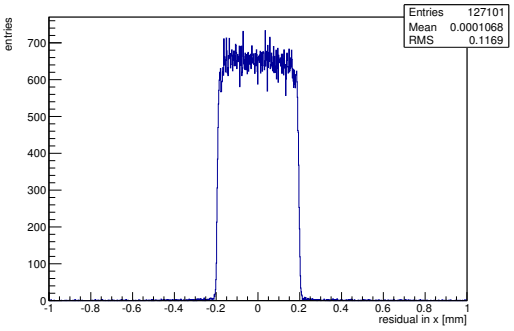

(i) Track residual in x.

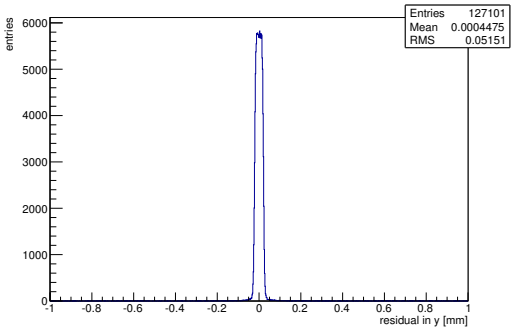

(j) Track residual in y.

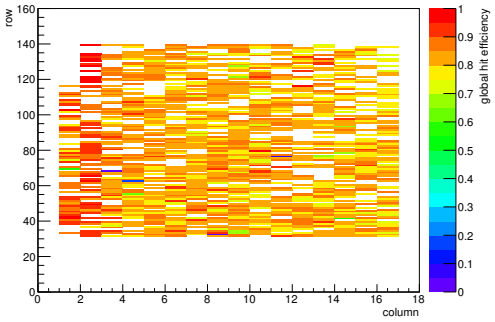

(k) Hit efficiency map.

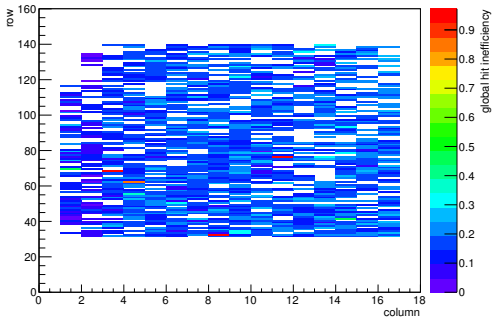

(l) Hit inefficiency map.

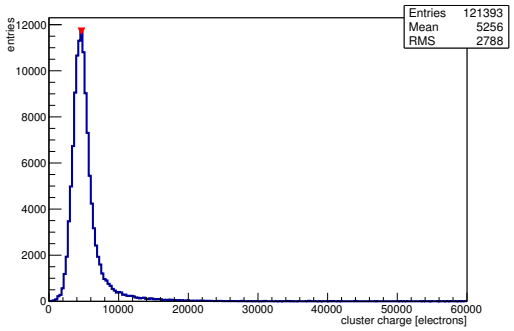

(m) Charge distribution (all cluster sizes included).

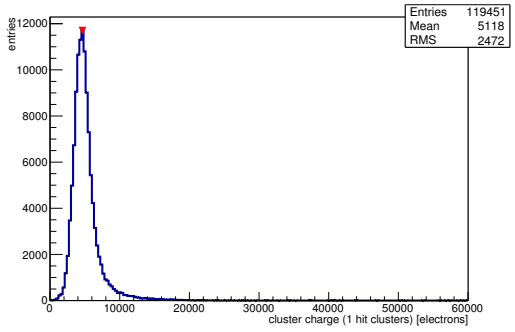

(n) Charge distribution (1 hit cluster).

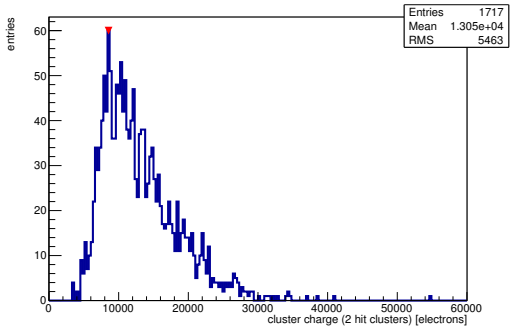

(o) Charge distribution (2 hit cluster).

Figure C.120: Detailed plots for test beam measurement of DO-I-11 (description see section 6.1) sample (running as DUT1) during runs 61298-61303 in the September 2011 test beam period at CERN SPS in area H6B. Summary of the data in chapter 9. *(cont.)*

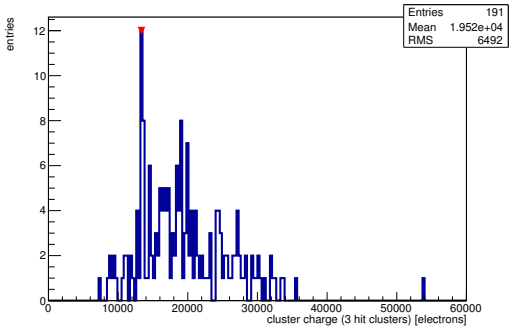

(p) Charge distribution (3 hit cluster).

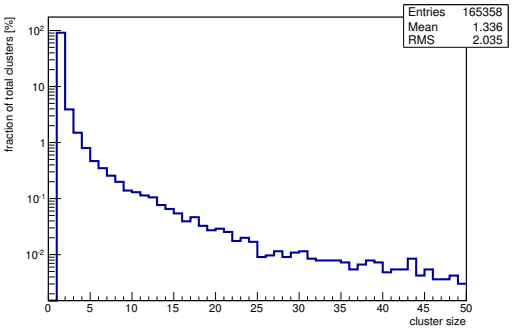

(q) Cluster size distribution.

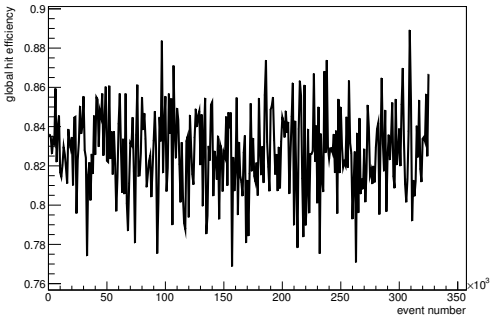

(r) Hit efficiency vs event number.

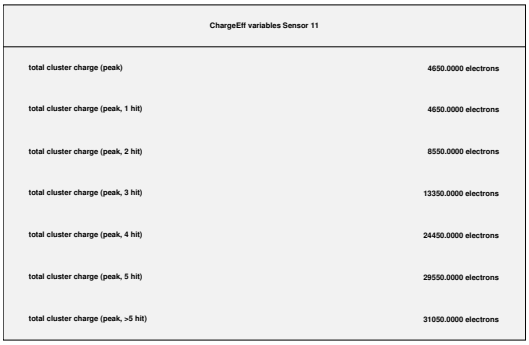

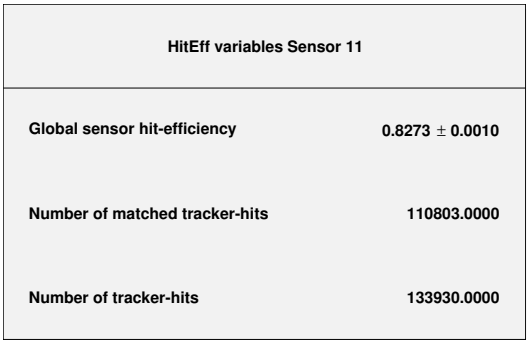

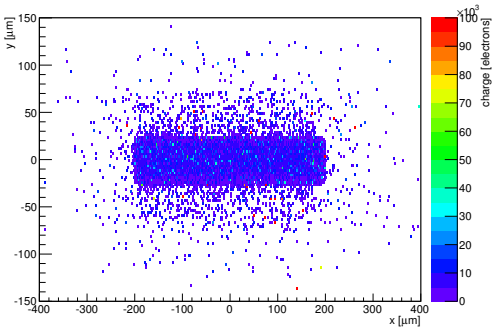

(s) Single pixel mean charge.

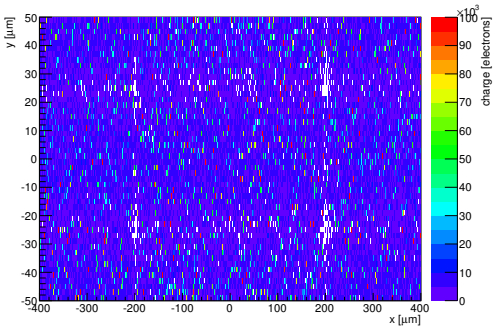

(t) Single pixel mean charge.

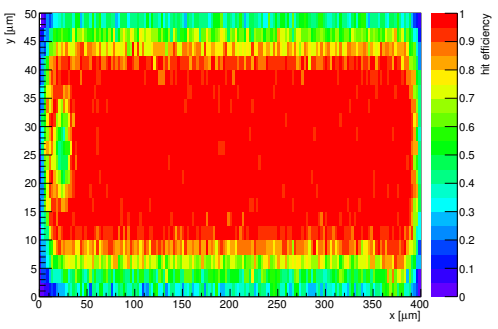

(u) Single pixel hit efficiency.

Figure C.120: Detailed plots for test beam measurement of DO-I-11 (description see section 6.1) sample (running as DUT1) during runs 61298-61303 in the September 2011 test beam period at CERN SPS in area H6B. Summary of the data in chapter 9.

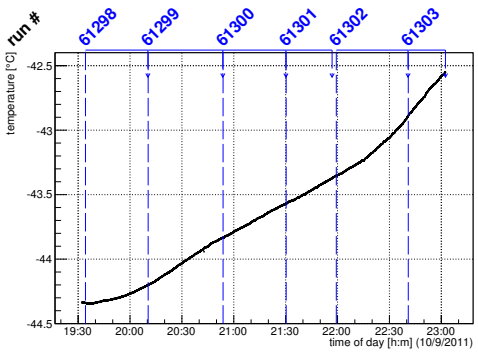

(a) Temperature vs time.

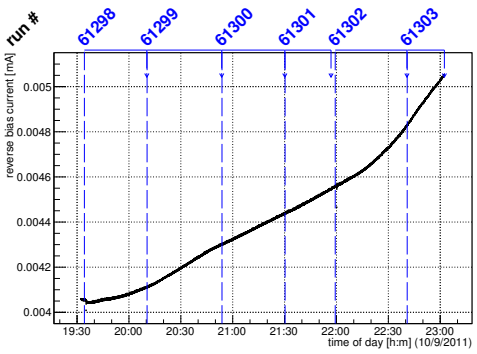

(b) Bias current vs time.

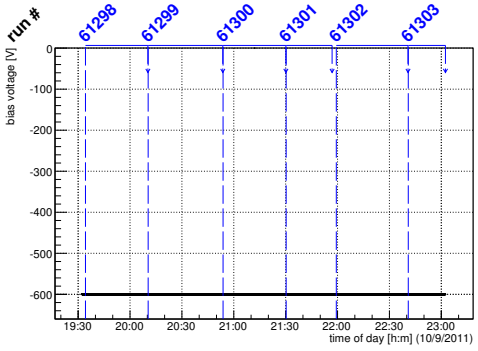

(c) Currently applied bias voltage vs time.

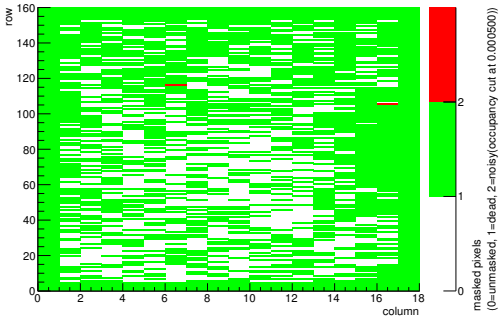

(d) Map of masked pixels.

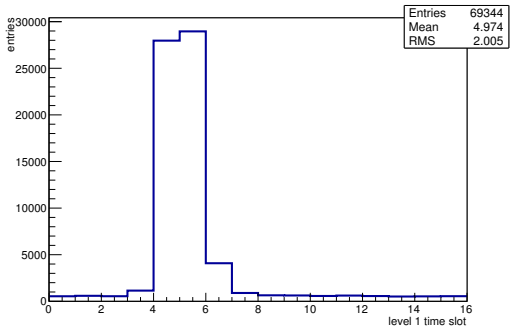

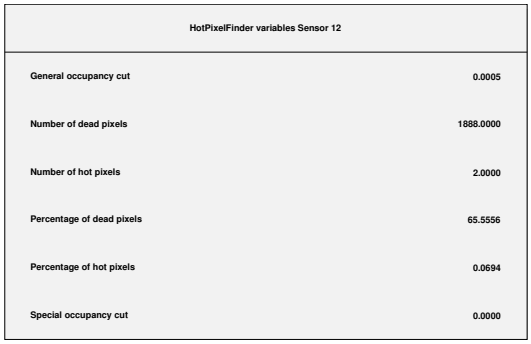

(e) Lvl1 distribution.

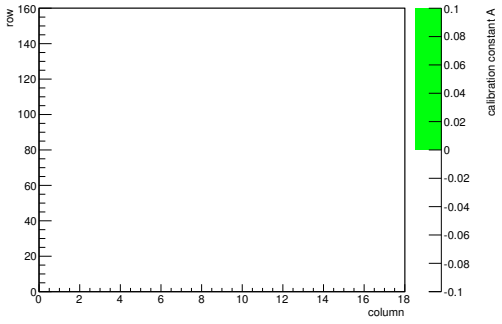

(f) Calibration constant A.

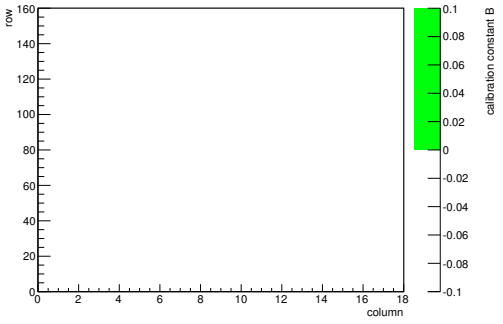

(g) Calibration constant B.

Figure C.121: Detailed plots for test beam measurement of DO-I-5 (description see section 6.1) sample (running as DUT2) during runs 61298-61303 in the September 2011 test beam period at CERN SPS in area H6B. Summary of the data in chapter 9. *(cont.)*

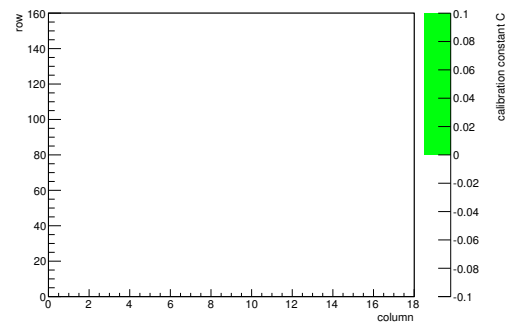

(h) Calibration constant C.

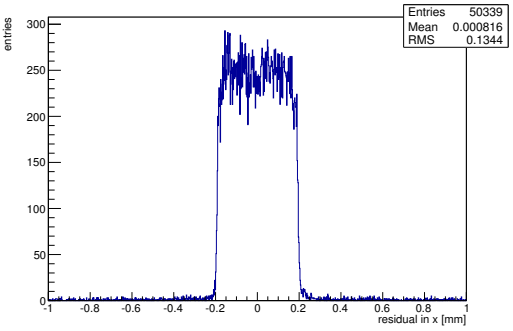

(i) Track residual in x.

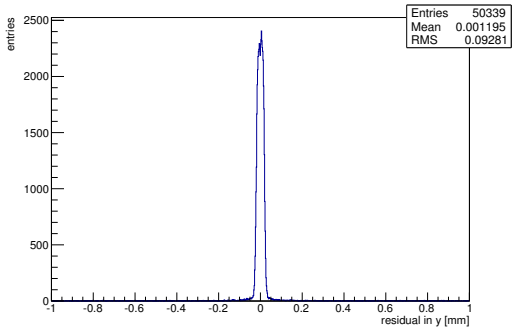

(j) Track residual in y.

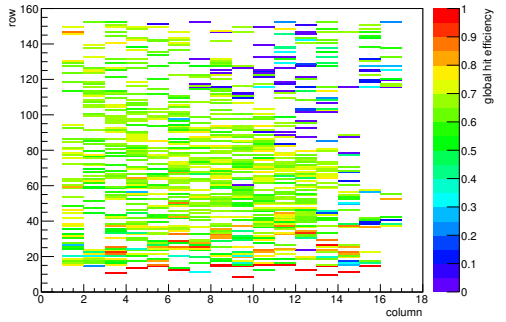

(k) Hit efficiency map.

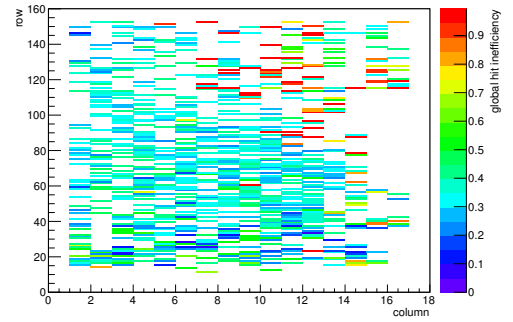

(l) Hit inefficiency map.

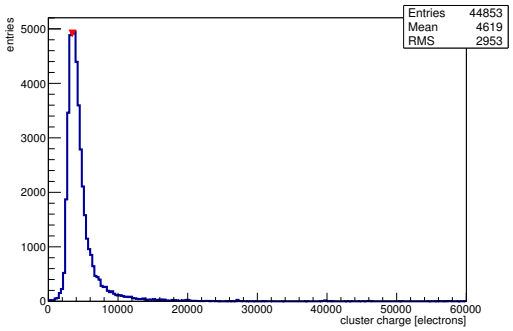

(m) Charge distribution (all cluster sizes included).

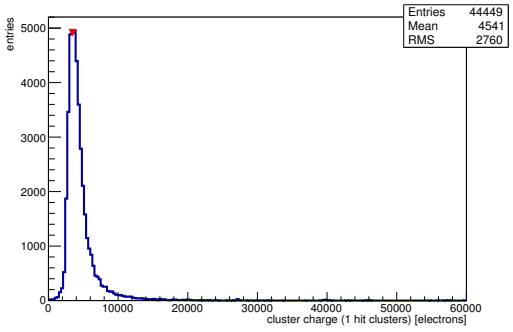

(n) Charge distribution (1 hit cluster).

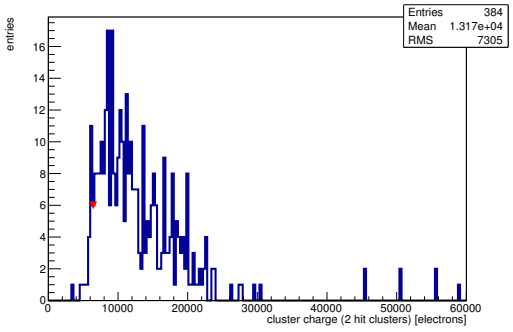

(o) Charge distribution (2 hit cluster).

Figure C.121: Detailed plots for test beam measurement of DO-I-5 (description see section 6.1) sample (running as DUT2) during runs 61298-61303 in the September 2011 test beam period at CERN SPS in area H6B. Summary of the data in chapter 9. *(cont.)*

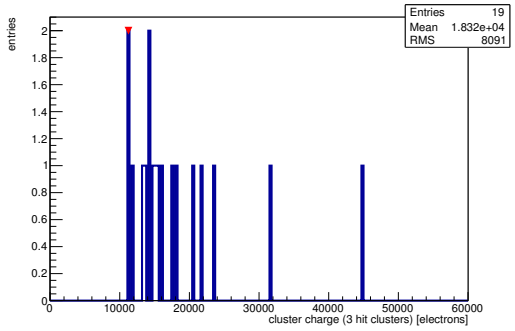

(p) Charge distribution (3 hit cluster).

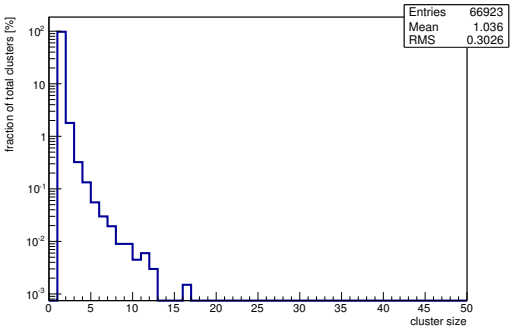

(q) Cluster size distribution.

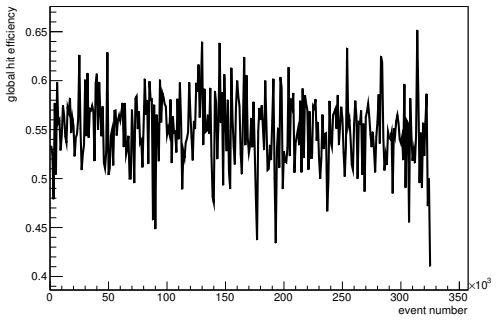

(r) Hit efficiency vs event number.

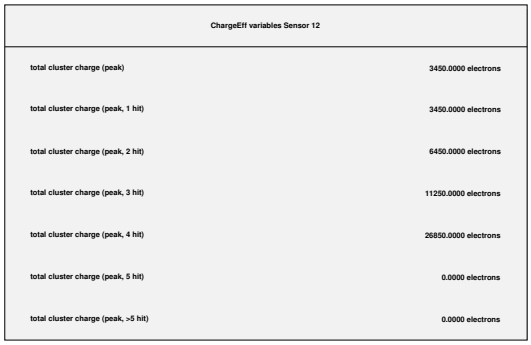

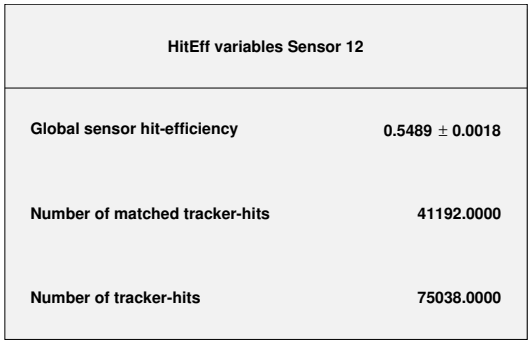

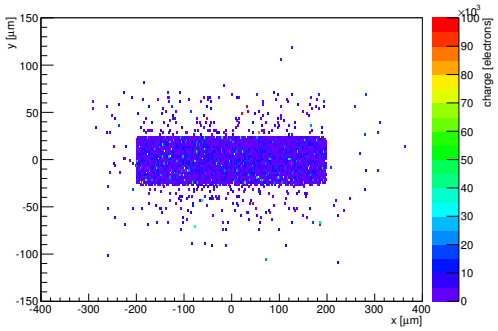

(s) Single pixel mean charge.

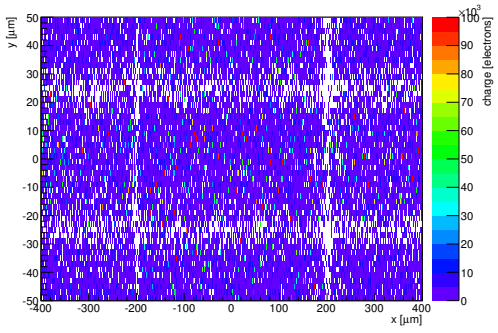

(t) Single pixel mean charge.

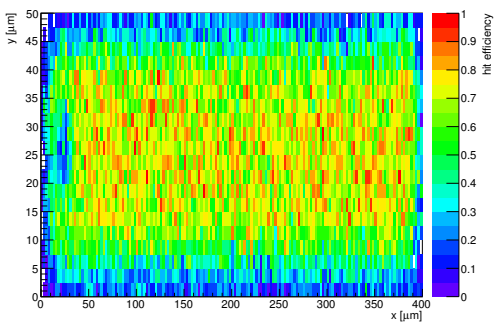

(u) Single pixel hit efficiency.

Figure C.121: Detailed plots for test beam measurement of DO-I-5 (description see section 6.1) sample (running as DUT2) during runs 61298-61303 in the September 2011 test beam period at CERN SPS in area H6B. Summary of the data in chapter 9.

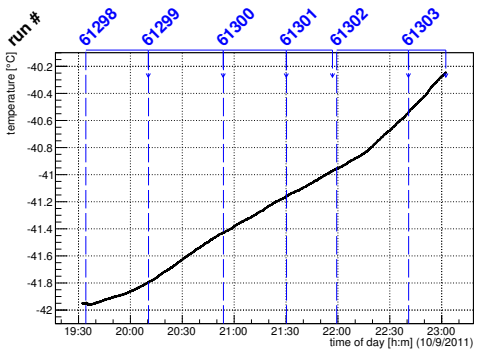

(a) Temperature vs time.

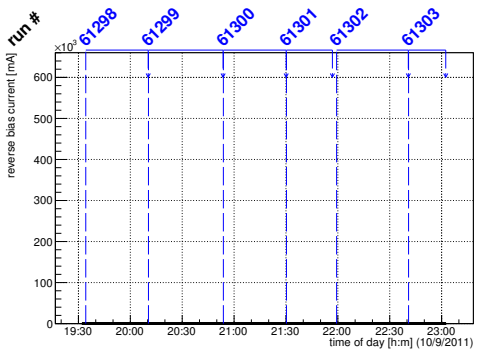

(b) Bias current vs time.

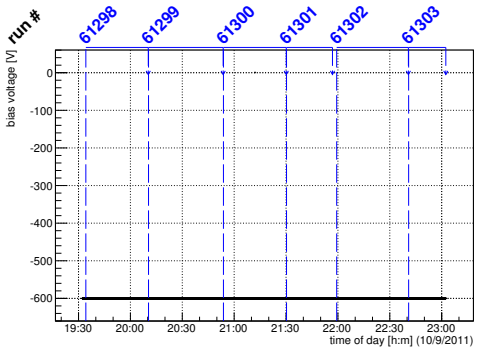

(c) Currently applied bias voltage vs time.

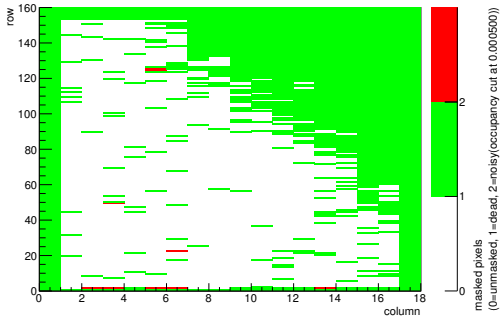

(d) Map of masked pixels.

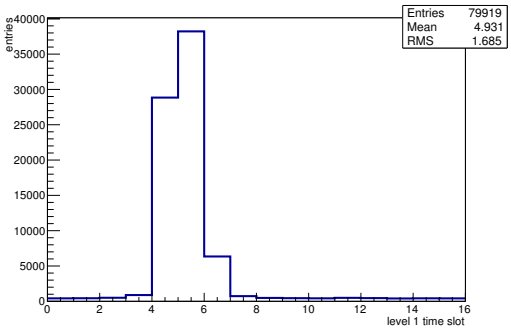

(e) Lvl1 distribution.

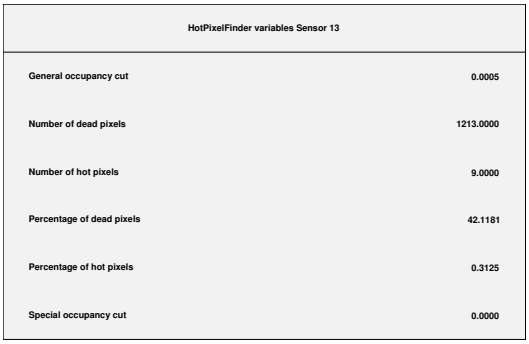

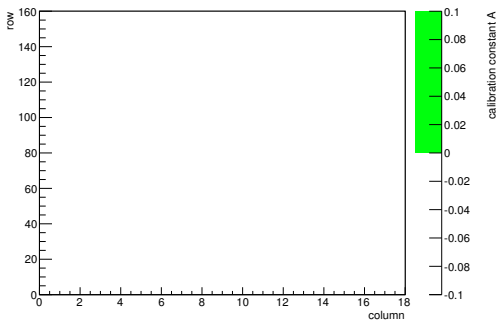

(f) Calibration constant A.

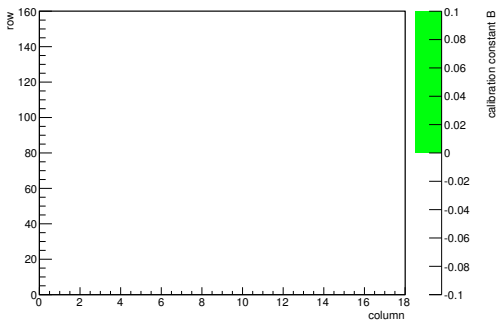

(g) Calibration constant B.

Figure C.122: Detailed plots for test beam measurement of DO-I-12 (description see section 6.1) sample (running as DUT3) during runs 61298-61303 in the September 2011 test beam period at CERN SPS in area H6B. Summary of the data in chapter 9. *(cont.)*

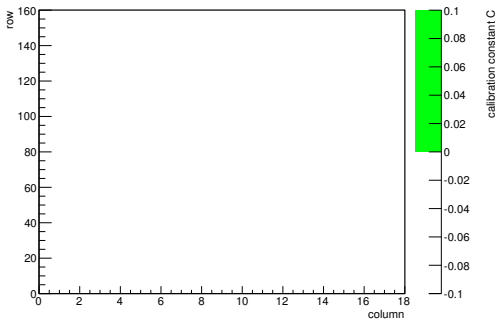

(h) Calibration constant C.

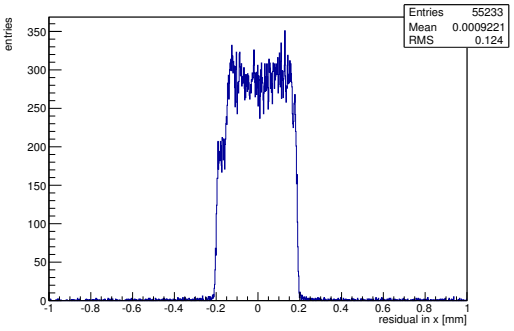

(i) Track residual in x.

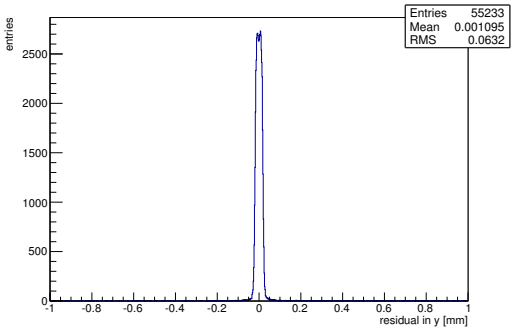

(j) Track residual in y.

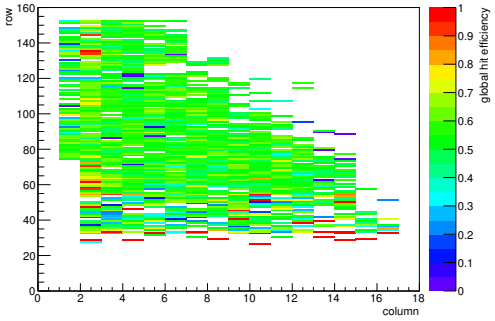

(k) Hit efficiency map.

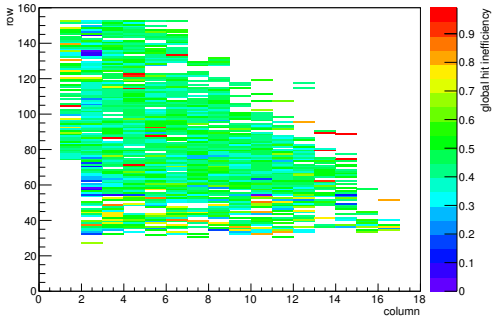

(l) Hit inefficiency map.

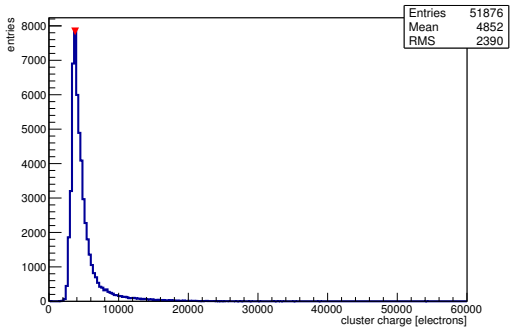

(m) Charge distribution (all cluster sizes included).

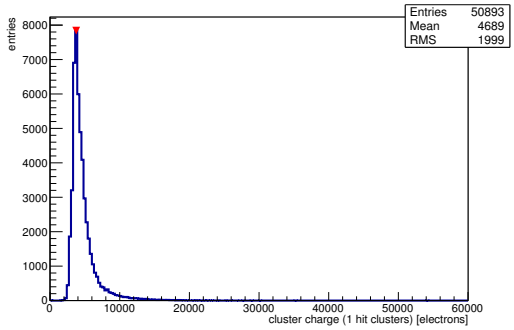

(n) Charge distribution (1 hit cluster).

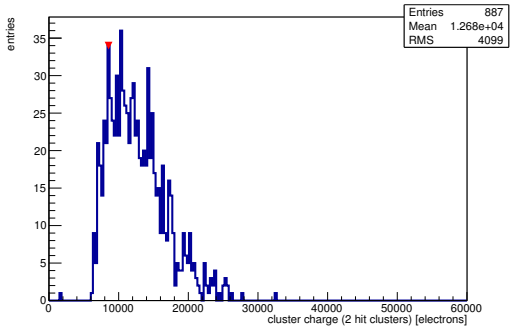

(o) Charge distribution (2 hit cluster).

Figure C.122: Detailed plots for test beam measurement of DO-I-12 (description see section 6.1) sample (running as DUT3) during runs 61298-61303 in the September 2011 test beam period at CERN SPS in area H6B. Summary of the data in chapter 9. *(cont.)*

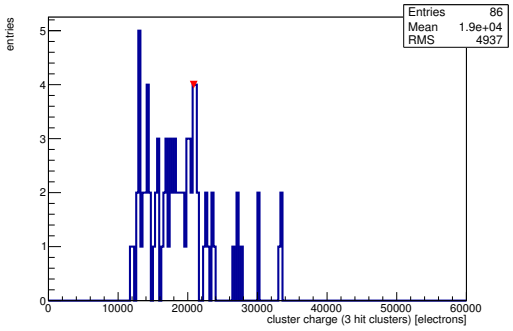

(p) Charge distribution (3 hit cluster).

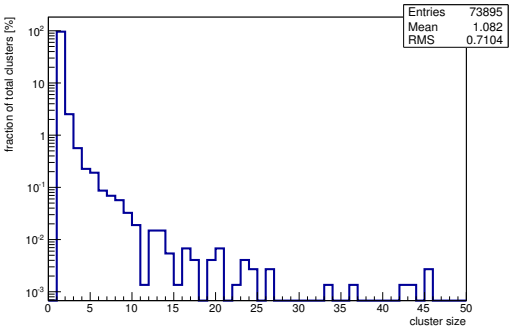

(q) Cluster size distribution.

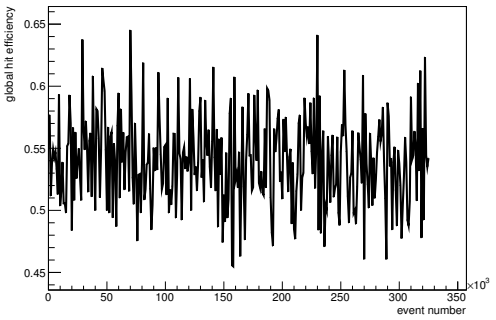

(r) Hit efficiency vs event number.

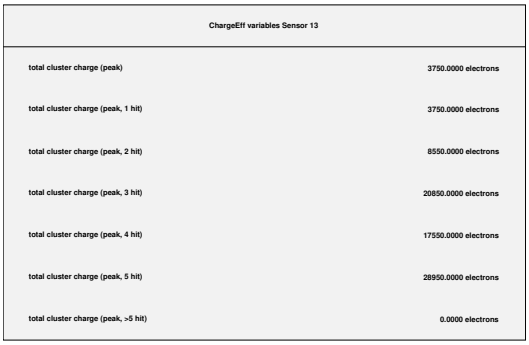

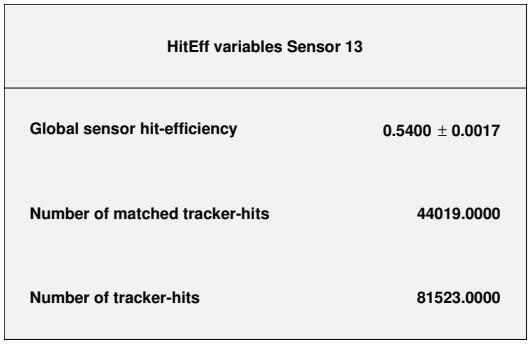

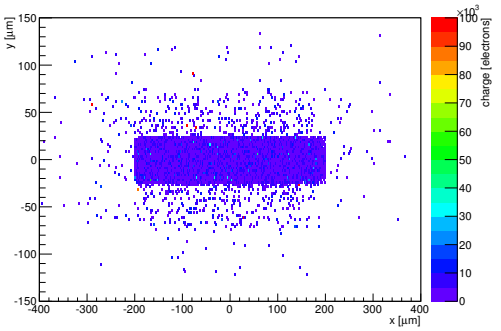

(s) Single pixel mean charge.

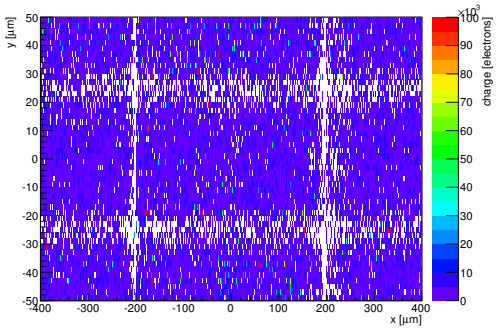

(t) Single pixel mean charge.

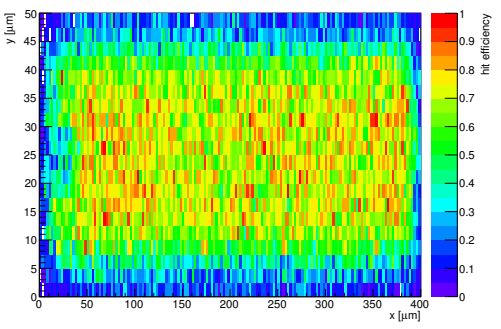

(u) Single pixel hit efficiency.

Figure C.122: Detailed plots for test beam measurement of DO-I-12 (description see section 6.1) sample (running as DUT3) during runs 61298-61303 in the September 2011 test beam period at CERN SPS in area H6B. Summary of the data in chapter 9.

C.3.21 Runs 61304-61315

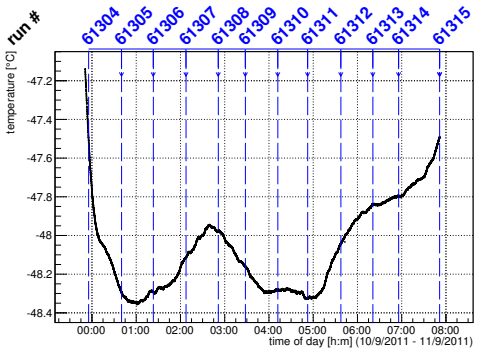

(a) Temperature vs time.

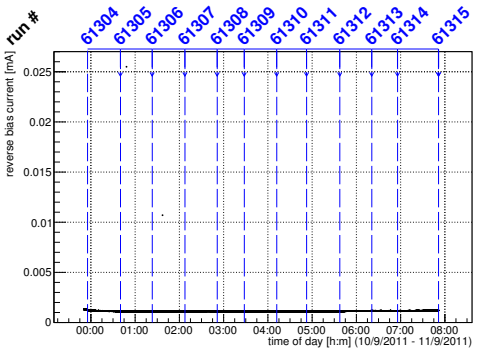

(b) Bias current vs time.

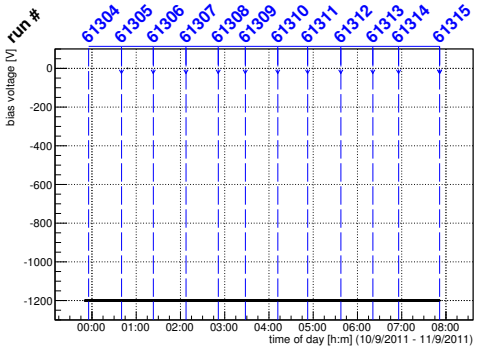

(c) Currently applied bias voltage vs time.

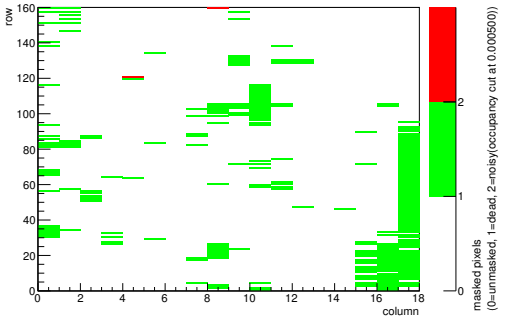

(d) Map of masked pixels.

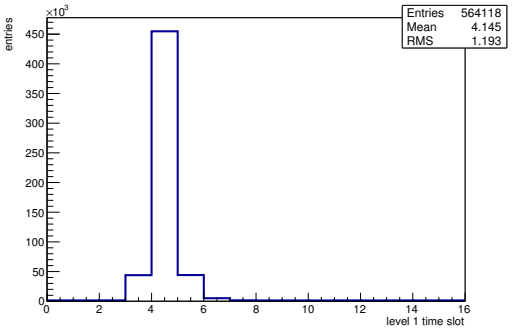

(e) Lvl1 distribution.

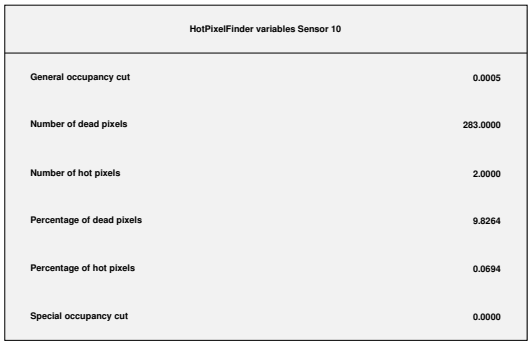

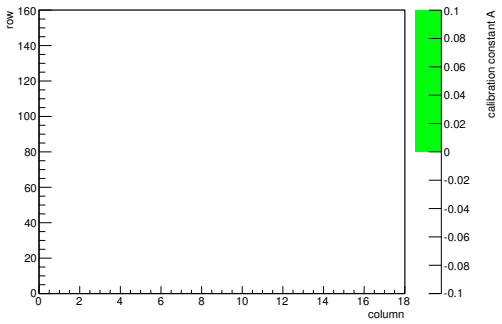

(f) Calibration constant A.

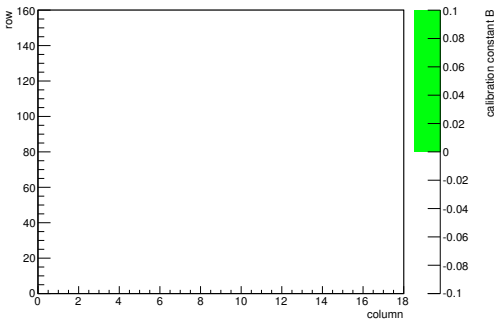

(g) Calibration constant B.

Figure C.123: Detailed plots for test beam measurement of DO-I-7 (description see section 6.1) sample (running as DUT0) during runs 61304-61315 in the September 2011 test beam period at CERN SPS in area H6B. Summary of the data in chapter 9. *(cont.)*

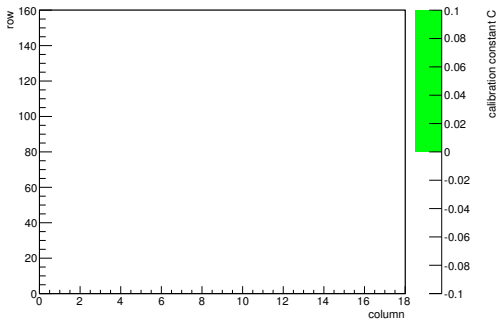

(h) Calibration constant C.

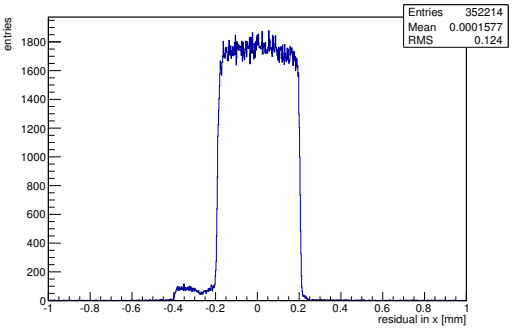

(i) Track residual in x.

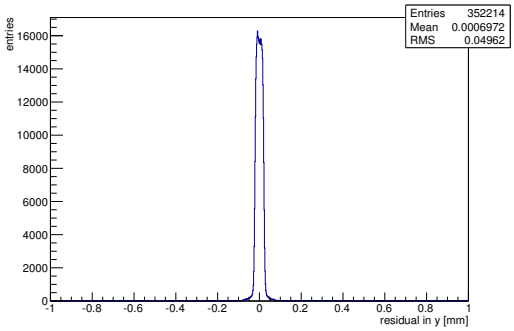

(j) Track residual in y.

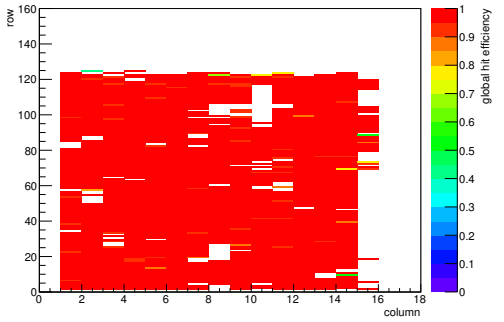

(k) Hit efficiency map.

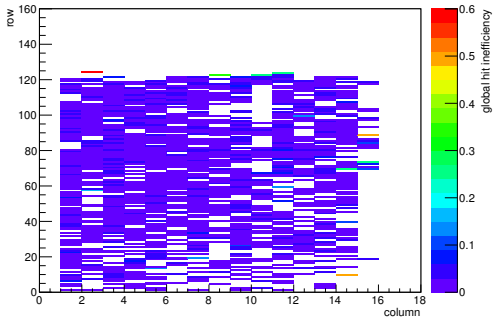

(l) Hit inefficiency map.

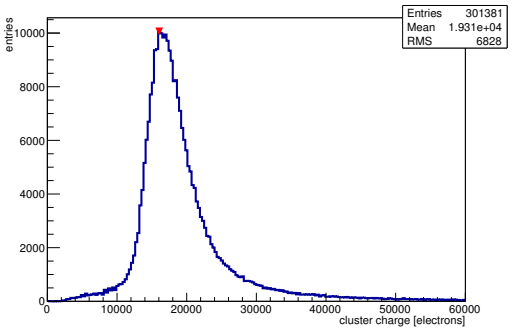

(m) Charge distribution (all cluster sizes included).

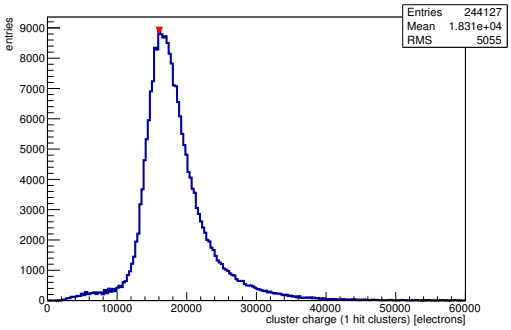

(n) Charge distribution (1 hit cluster).

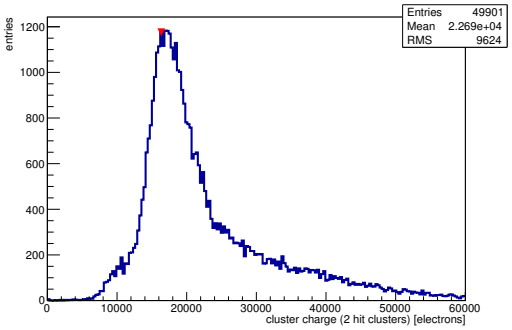

(o) Charge distribution (2 hit cluster).

Figure C.123: Detailed plots for test beam measurement of DO-I-7 (description see section 6.1) sample (running as DUT0) during runs 61304-61315 in the September 2011 test beam period at CERN SPS in area H6B. Summary of the data in chapter 9. *(cont.)*

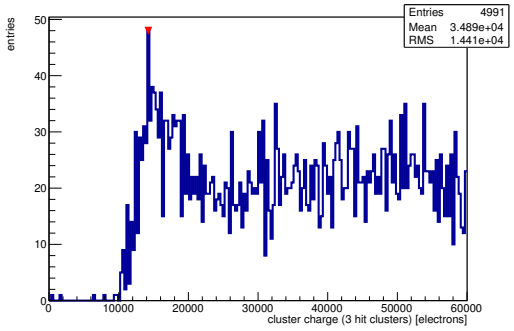

(p) Charge distribution (3 hit cluster).

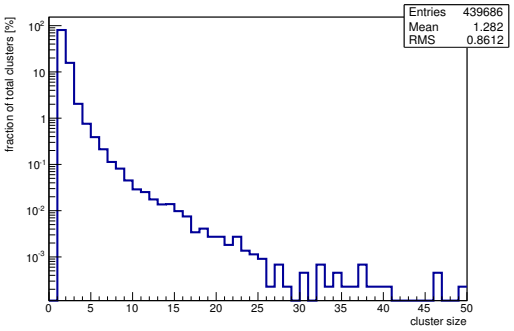

(q) Cluster size distribution.

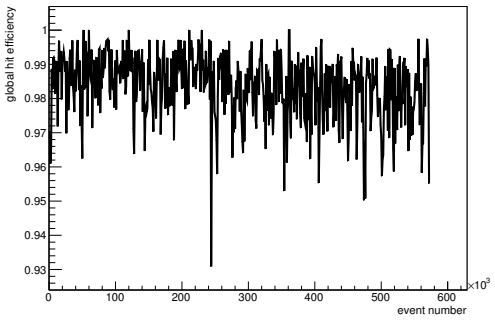

(r) Hit efficiency vs event number.

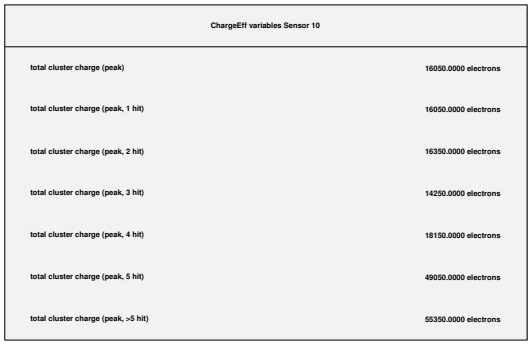

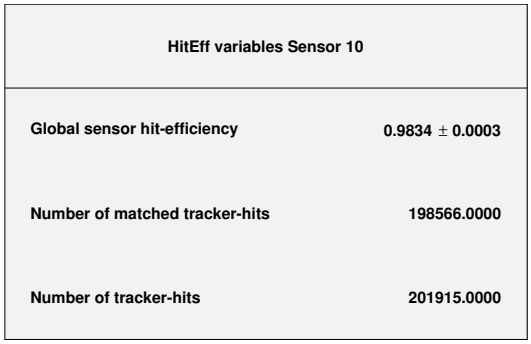

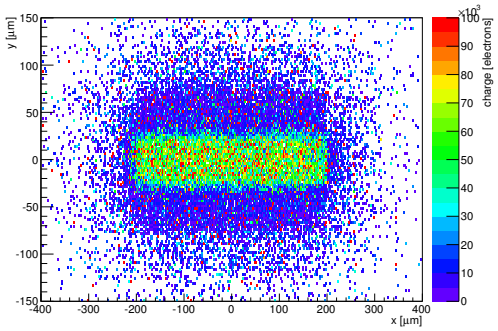

(s) Single pixel mean charge.

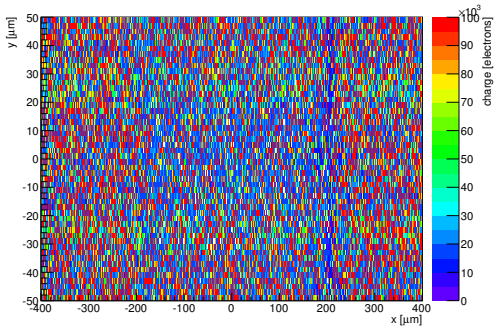

(t) Single pixel mean charge.

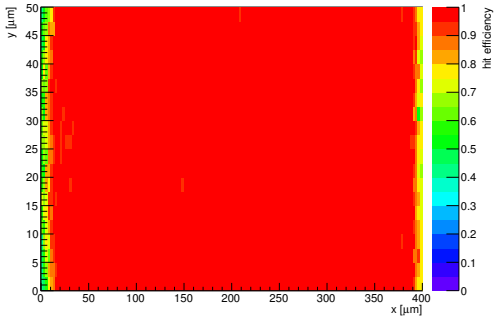

(u) Single pixel hit efficiency.

Figure C.123: Detailed plots for test beam measurement of DO-I-7 (description see section 6.1) sample (running as DUT0) during runs 61304-61315 in the September 2011 test beam period at CERN SPS in area H6B. Summary of the data in chapter 9.

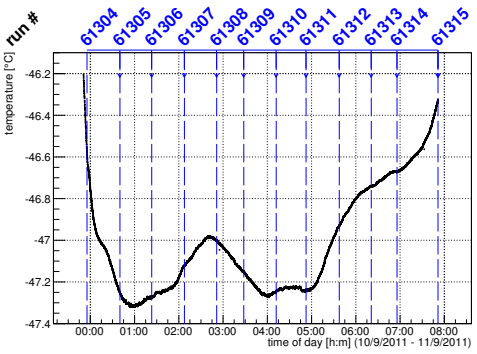

(a) Temperature vs time.

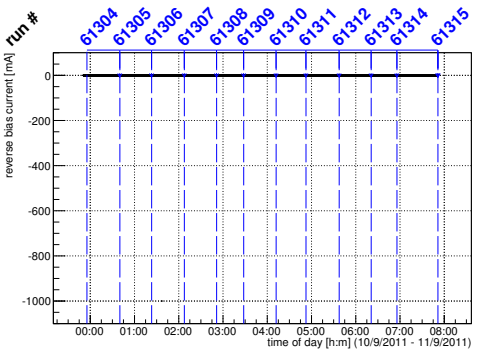

(b) Bias current vs time.

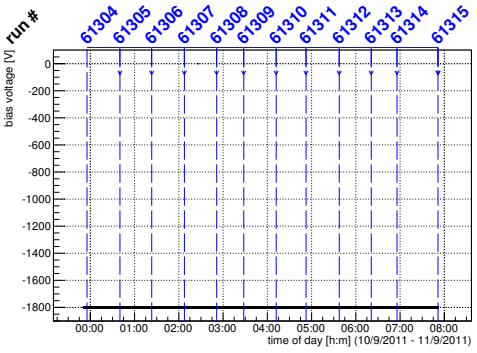

(c) Currently applied bias voltage vs time.

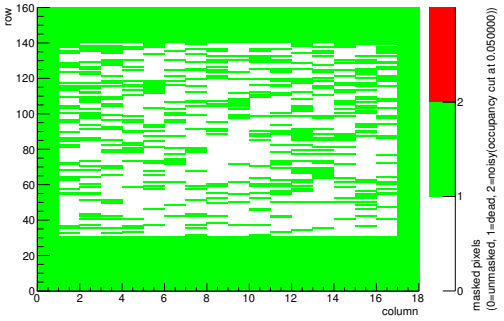

(d) Map of masked pixels.

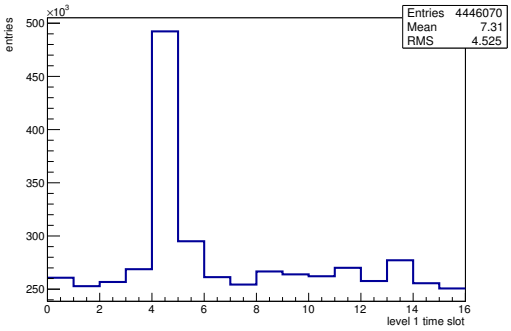

(e) Lvl1 distribution.

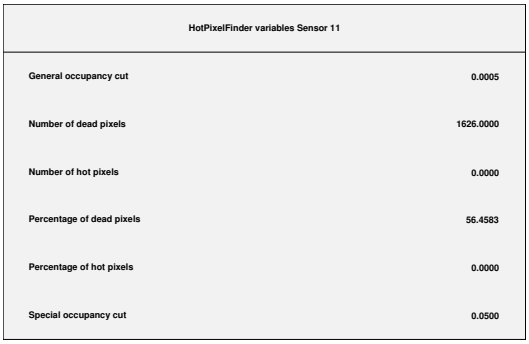

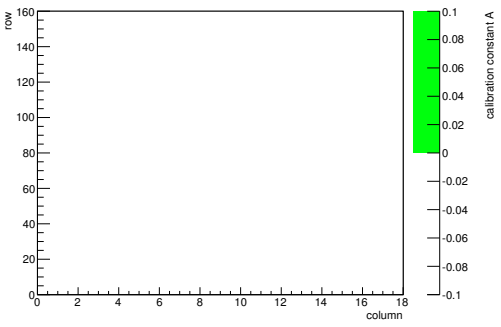

(f) Calibration constant A.

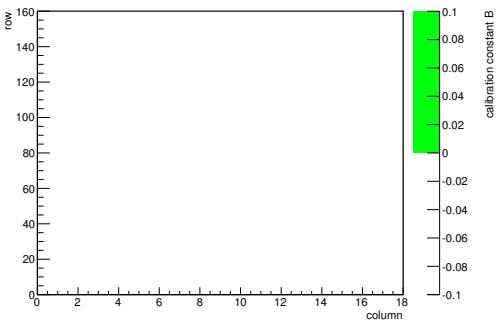

(g) Calibration constant B.

Figure C.124: Detailed plots for test beam measurement of DO-I-11 (description see section 6.1) sample (running as DUT1) during runs 61304-61315 in the September 2011 test beam period at CERN SPS in area H6B. Summary of the data in chapter 9. *(cont.)*

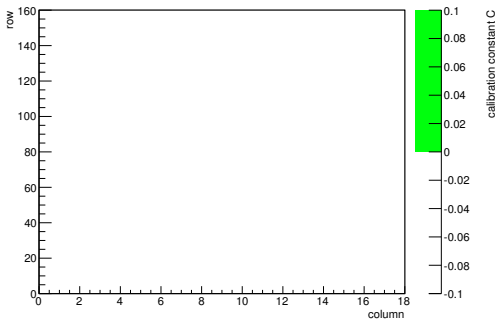

(h) Calibration constant C.

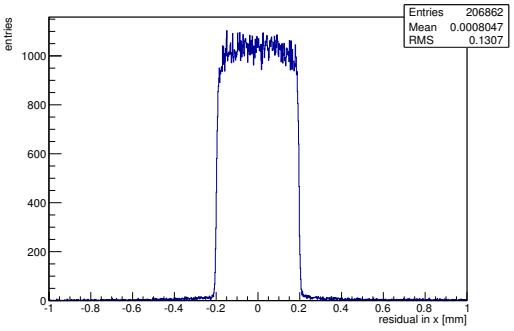

(i) Track residual in x.

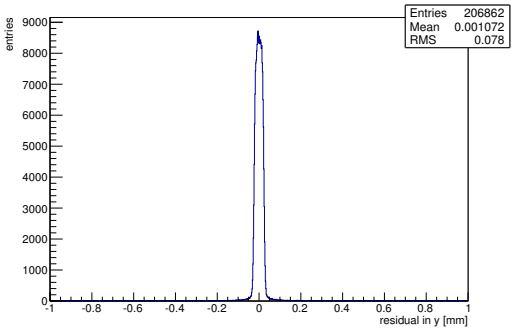

(j) Track residual in y.

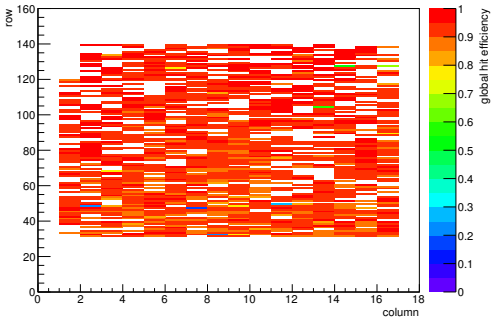

(k) Hit efficiency map.

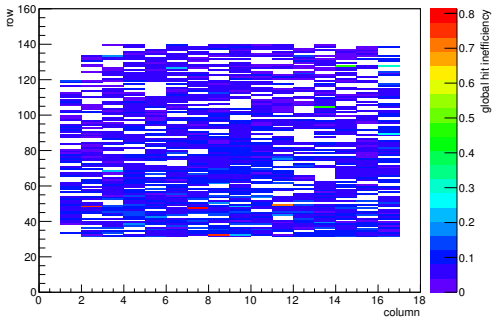

(l) Hit inefficiency map.

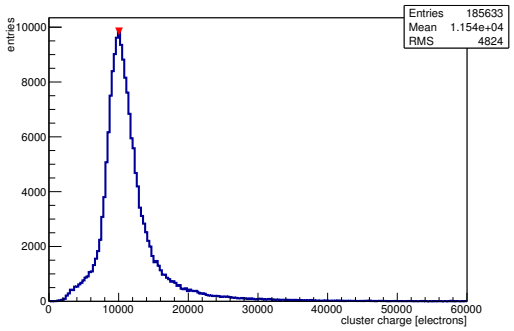

(m) Charge distribution (all cluster sizes included).

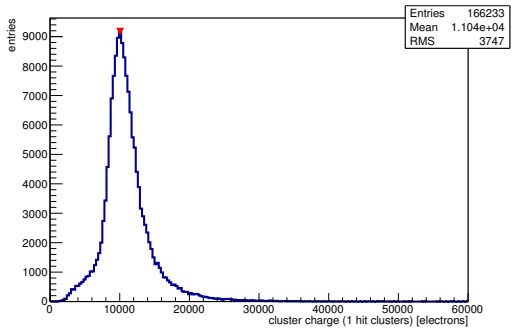

(n) Charge distribution (1 hit cluster).

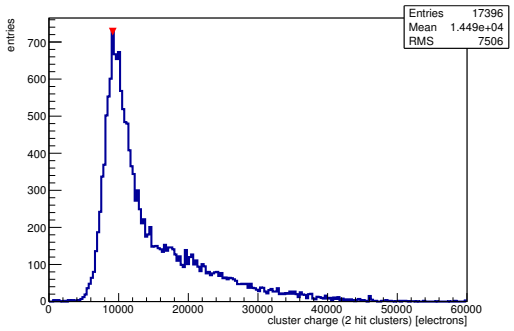

(o) Charge distribution (2 hit cluster).

Figure C.124: Detailed plots for test beam measurement of DO-I-11 (description see section 6.1) sample (running as DUT1) during runs 61304-61315 in the September 2011 test beam period at CERN SPS in area H6B. Summary of the data in chapter 9. *(cont.)*

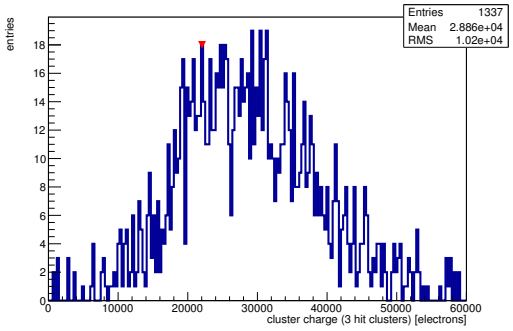

(p) Charge distribution (3 hit cluster).

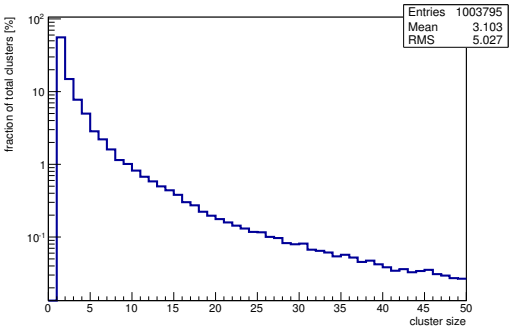

(q) Cluster size distribution.

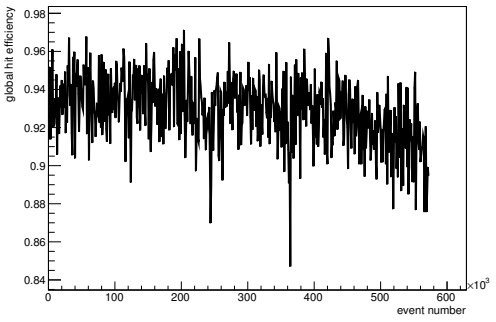

(r) Hit efficiency vs event number.

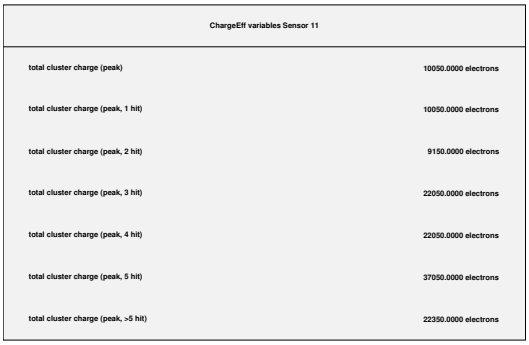

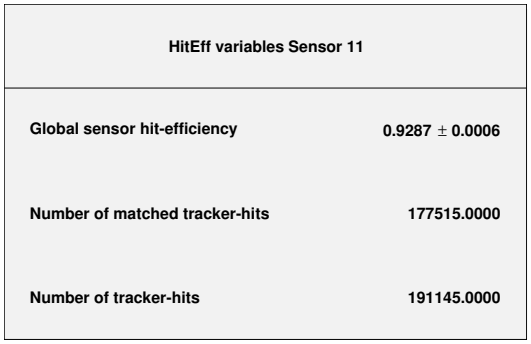

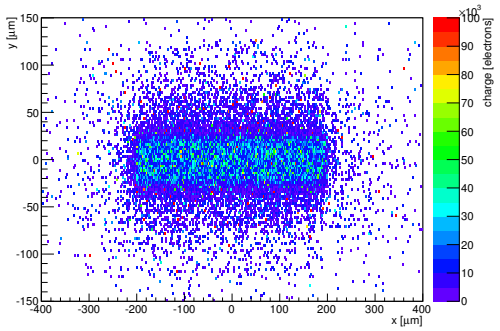

(s) Single pixel mean charge.

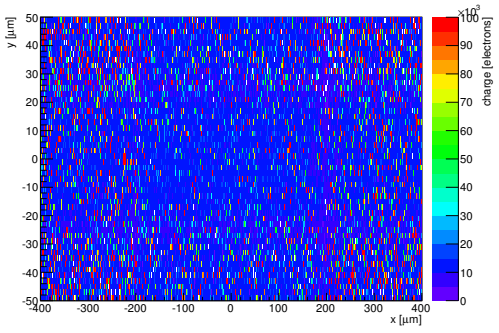

(t) Single pixel mean charge.

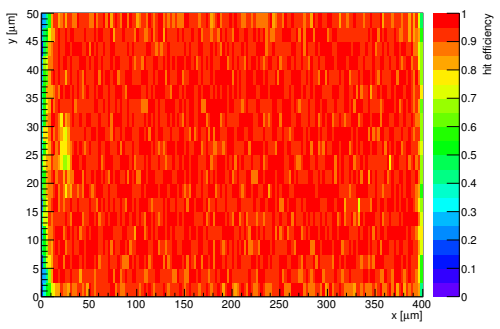

(u) Single pixel hit efficiency.

Figure C.124: Detailed plots for test beam measurement of DO-I-11 (description see section 6.1) sample (running as DUT1) during runs 61304-61315 in the September 2011 test beam period at CERN SPS in area H6B. Summary of the data in chapter 9.

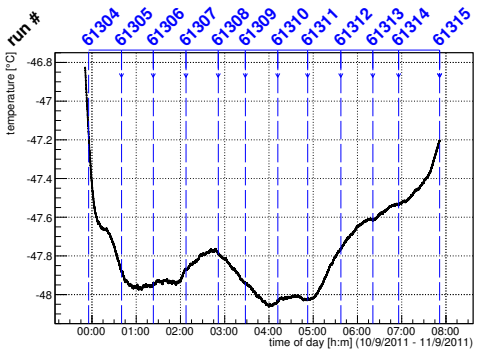

(a) Temperature vs time.

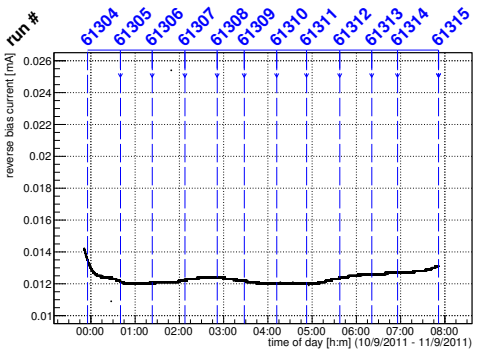

(b) Bias current vs time.

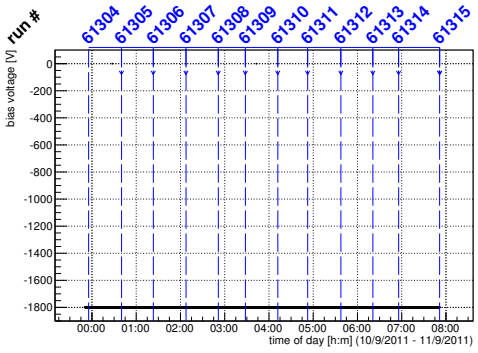

(c) Currently applied bias voltage vs time.

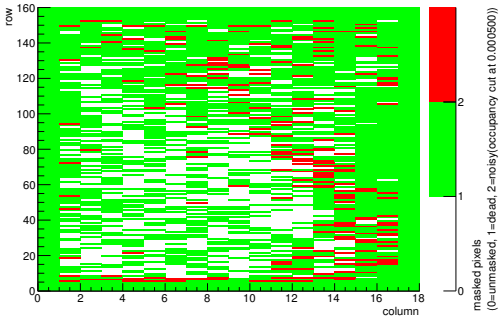

(d) Map of masked pixels.

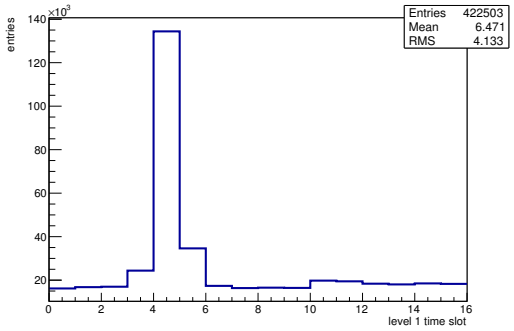

(e) Lvl1 distribution.

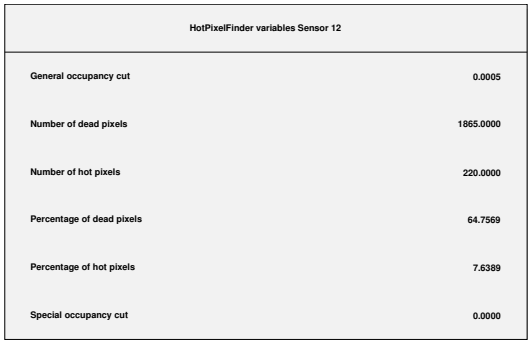

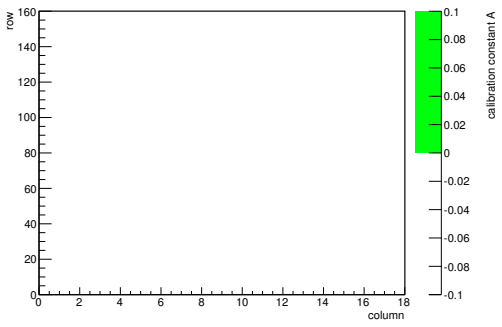

(f) Calibration constant A.

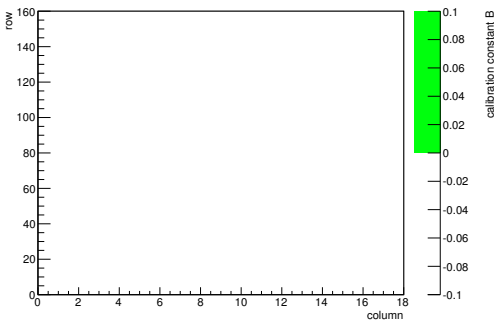

(g) Calibration constant B.

Figure C.125: Detailed plots for test beam measurement of DO-I-5 (description see section 6.1) sample (running as DUT2) during runs 61304-61315 in the September 2011 test beam period at CERN SPS in area H6B. Summary of the data in chapter 9. *(cont.)*

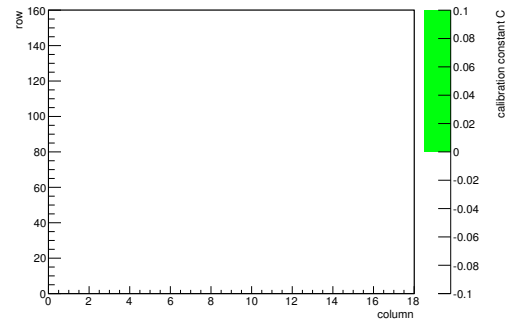

(h) Calibration constant C.

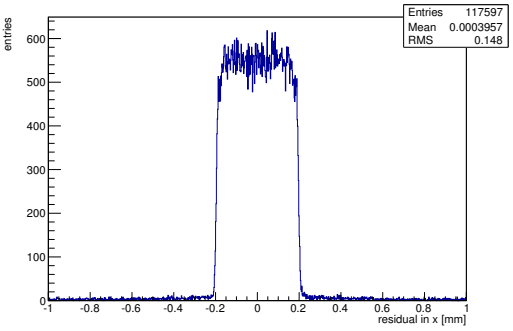

(i) Track residual in x.

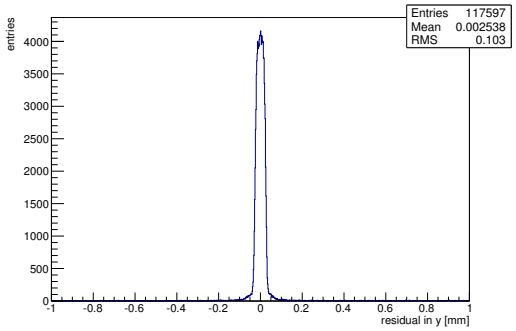

(j) Track residual in y.

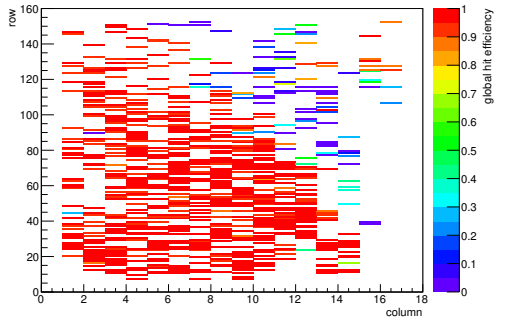

(k) Hit efficiency map.

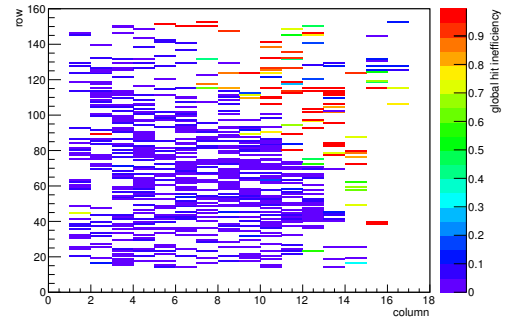

(l) Hit inefficiency map.

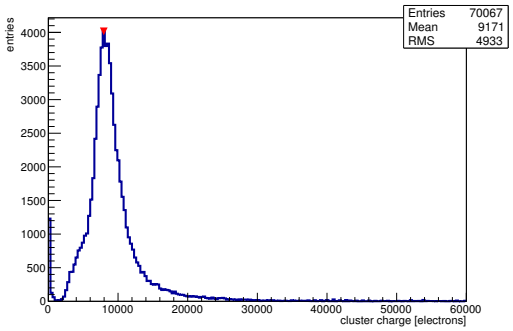

(m) Charge distribution (all cluster sizes included).

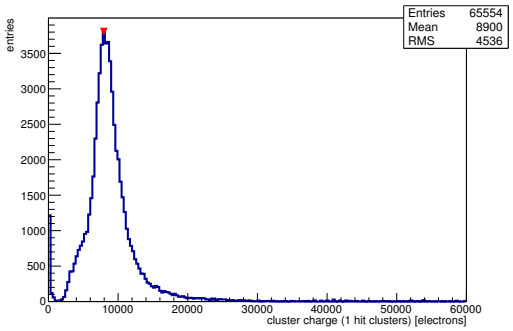

(n) Charge distribution (1 hit cluster).

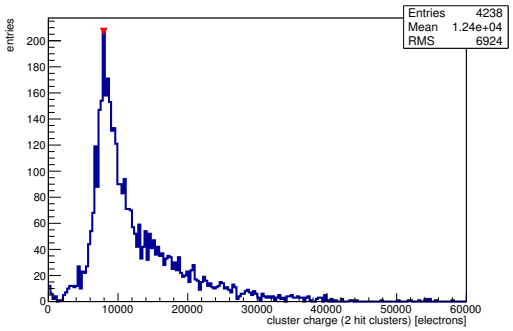

(o) Charge distribution (2 hit cluster).

Figure C.125: Detailed plots for test beam measurement of DO-I-5 (description see section 6.1) sample (running as DUT2) during runs 61304-61315 in the September 2011 test beam period at CERN SPS in area H6B. Summary of the data in chapter 9. *(cont.)*

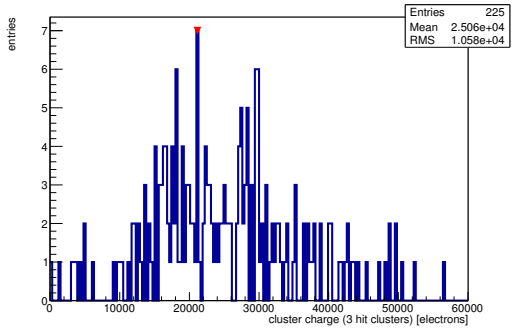

(p) Charge distribution (3 hit cluster).

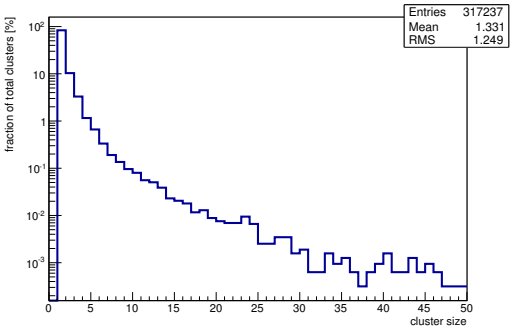

(q) Cluster size distribution.

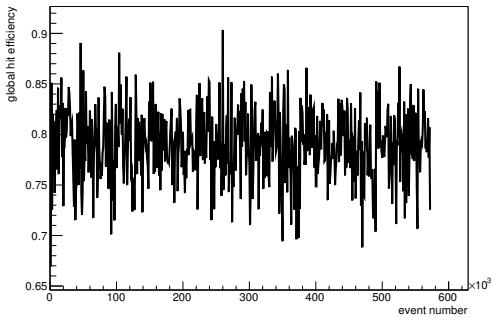

(r) Hit efficiency vs event number.

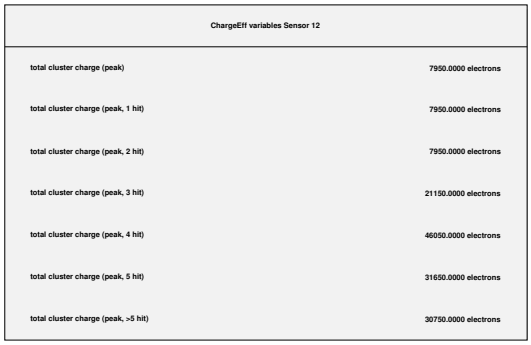

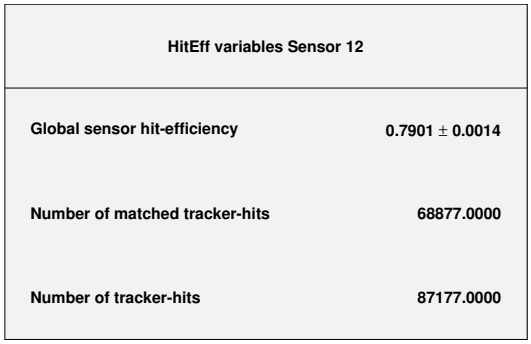

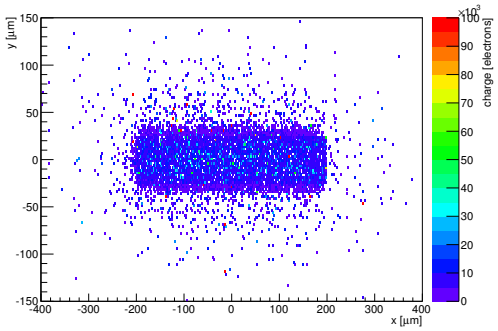

(s) Single pixel mean charge.

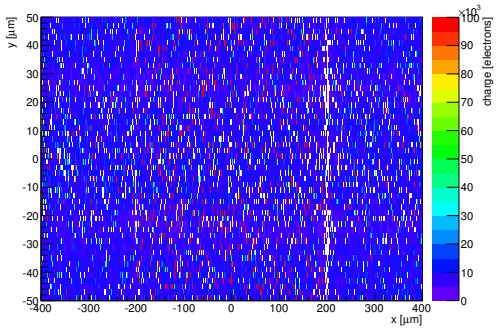

(t) Single pixel mean charge.

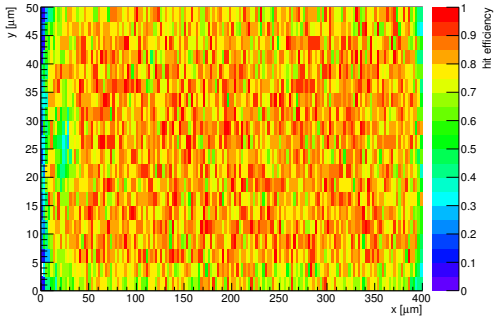

(u) Single pixel hit efficiency.

Figure C.125: Detailed plots for test beam measurement of DO-I-5 (description see section 6.1) sample (running as DUT2) during runs 61304-61315 in the September 2011 test beam period at CERN SPS in area H6B. Summary of the data in chapter 9.

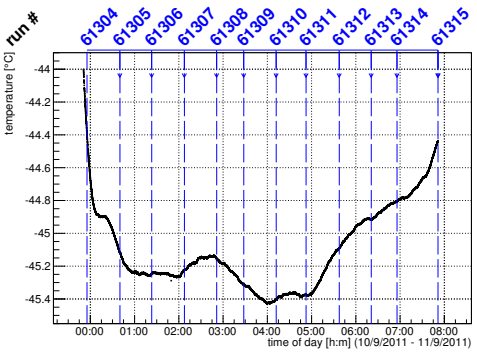

(a) Temperature vs time.

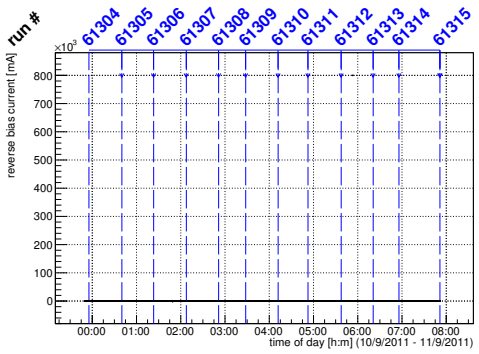

(b) Bias current vs time.

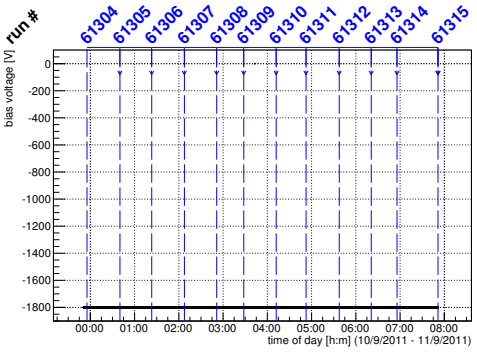

(c) Currently applied bias voltage vs time.

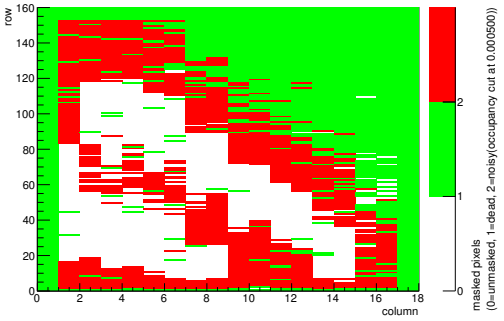

(d) Map of masked pixels.

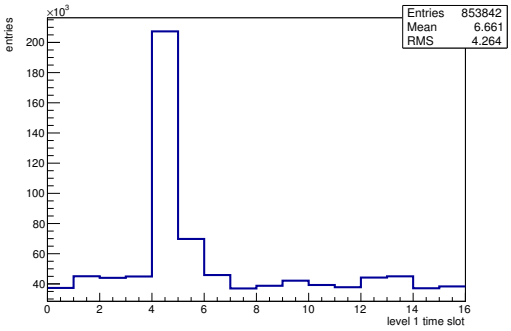

(e) Lvl1 distribution.

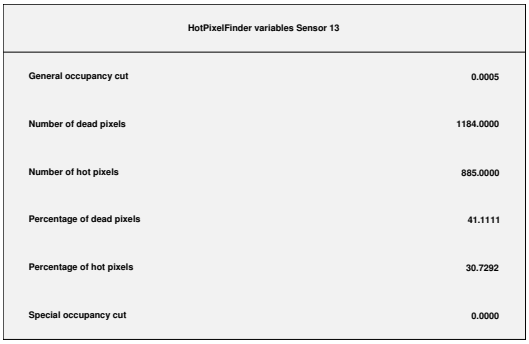

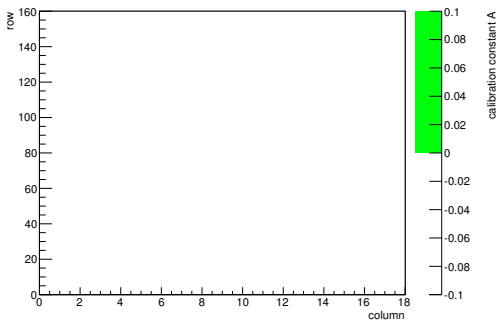

(f) Calibration constant A.

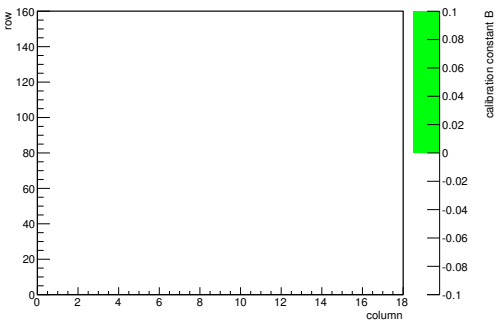

(g) Calibration constant B.

Figure C.126: Detailed plots for test beam measurement of DO-I-12 (description see section 6.1) sample (running as DUT3) during runs 61304-61315 in the September 2011 test beam period at CERN SPS in area H6B. Summary of the data in chapter 9. *(cont.)*

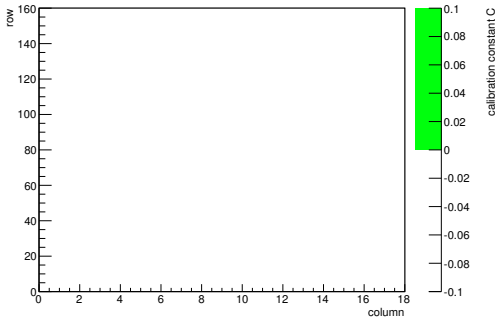

(h) Calibration constant C.

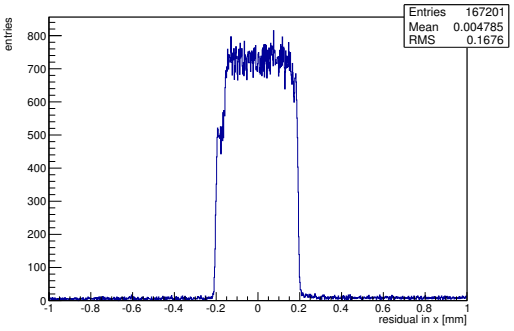

(i) Track residual in x.

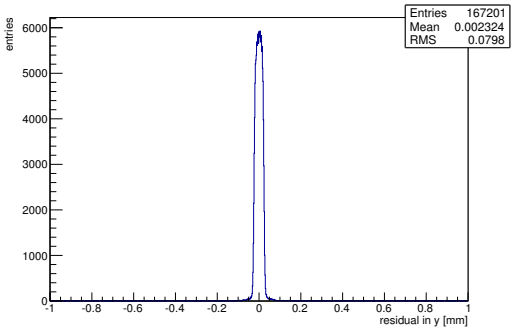

(j) Track residual in y.

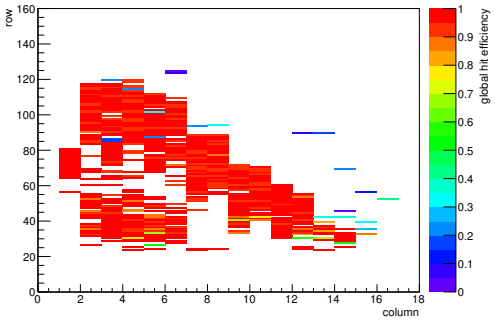

(k) Hit efficiency map.

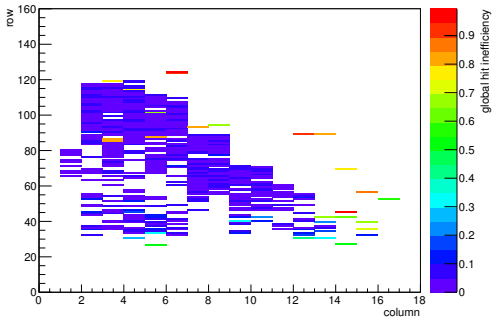

(l) Hit inefficiency map.

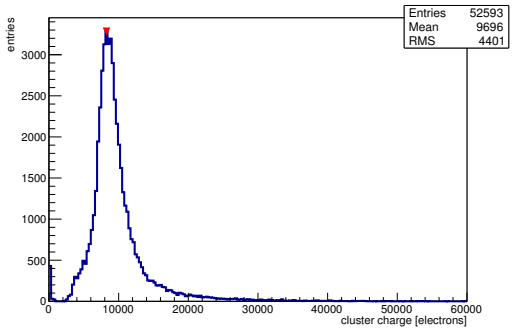

(m) Charge distribution (all cluster sizes included).

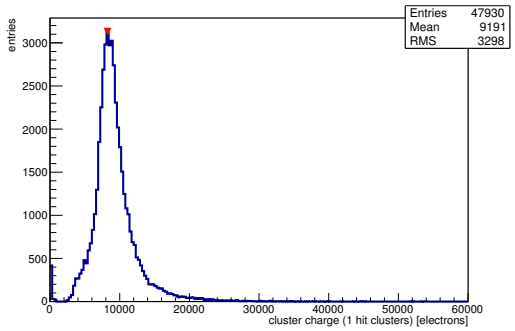

(n) Charge distribution (1 hit cluster).

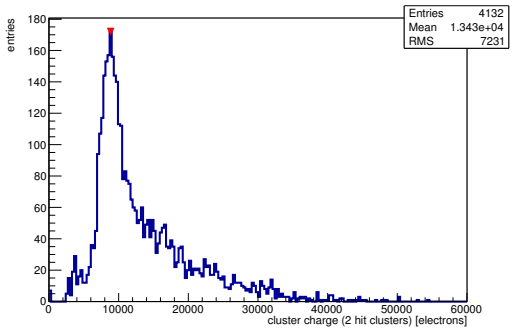

(o) Charge distribution (2 hit cluster).

Figure C.126: Detailed plots for test beam measurement of DO-I-12 (description see section 6.1) sample (running as DUT3) during runs 61304-61315 in the September 2011 test beam period at CERN SPS in area H6B. Summary of the data in chapter 9. *(cont.)*

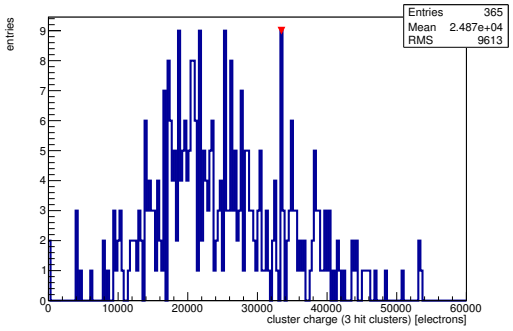

(p) Charge distribution (3 hit cluster).

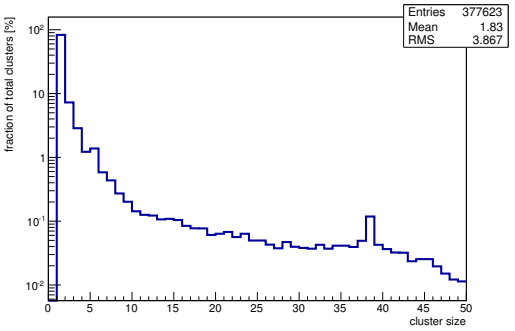

(q) Cluster size distribution.

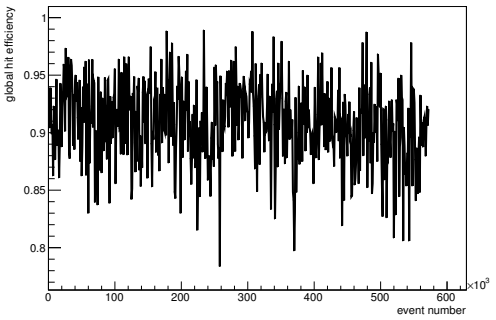

(r) Hit efficiency vs event number.

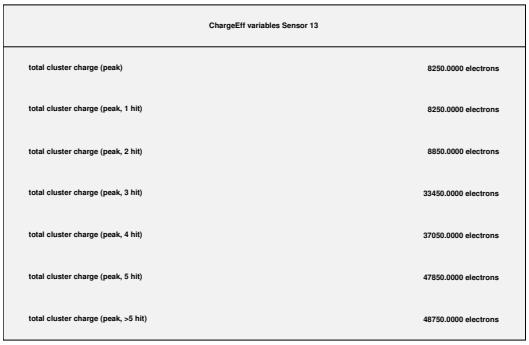

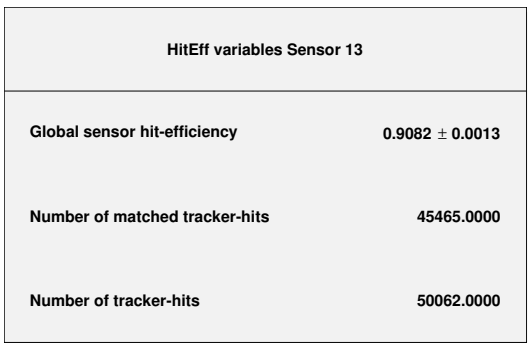

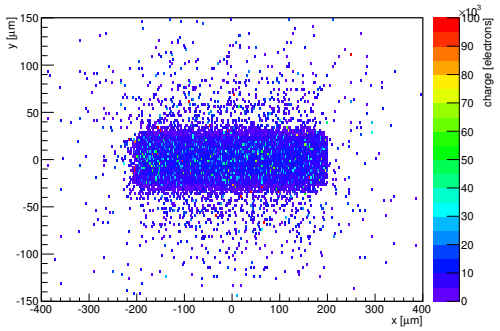

(s) Single pixel mean charge.

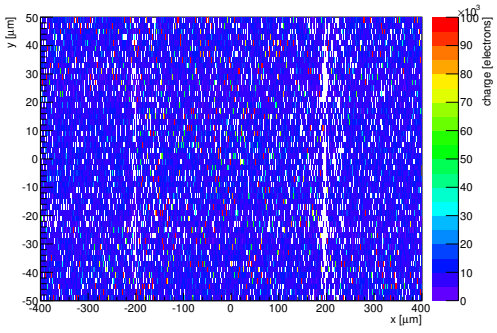

(t) Single pixel mean charge.

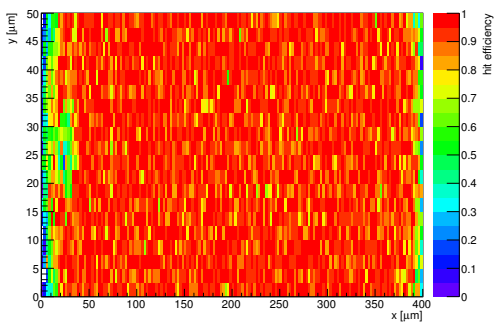

(u) Single pixel hit efficiency.

Figure C.126: Detailed plots for test beam measurement of DO-I-12 (description see section 6.1) sample (running as DUT3) during runs 61304-61315 in the September 2011 test beam period at CERN SPS in area H6B. Summary of the data in chapter 9.

C.4 DESY March 2012

C.4.1 Runs 125-129

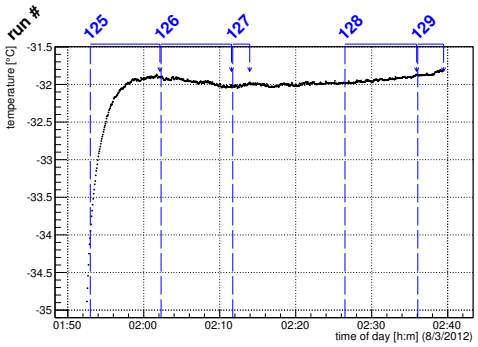

(a) Temperature vs time.

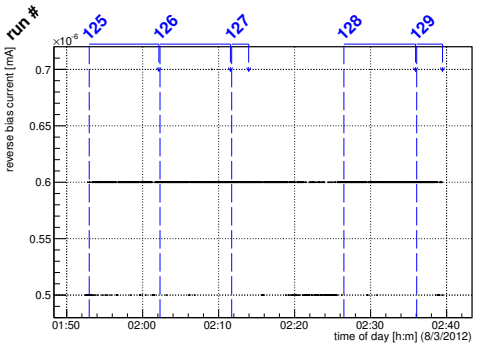

(b) Bias current vs time.

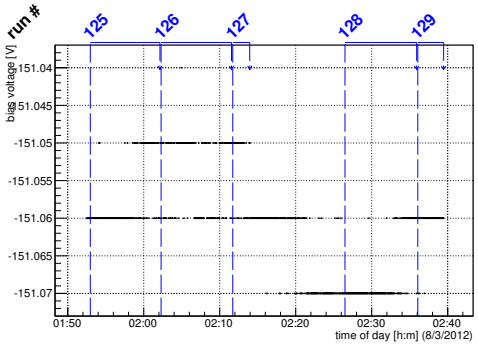

(c) Currently applied bias voltage vs time.

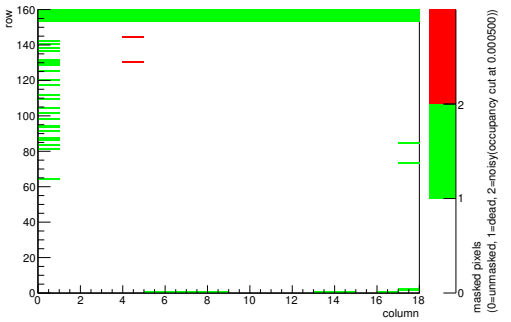

(d) Map of masked pixels.

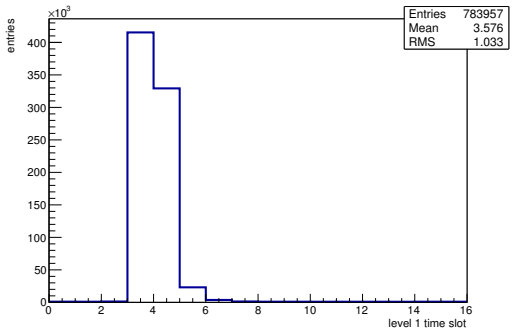

(e) Lvl1 distribution.

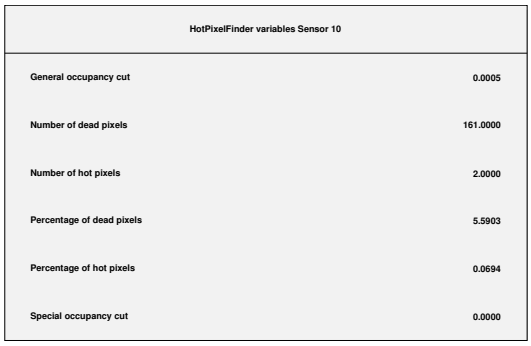

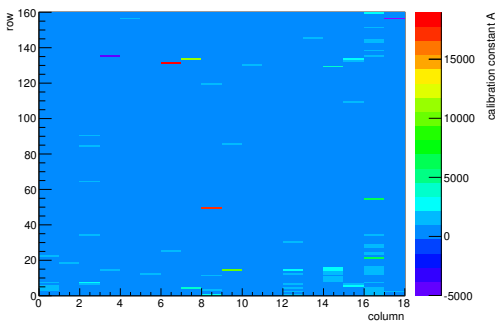

(f) Calibration constant A.

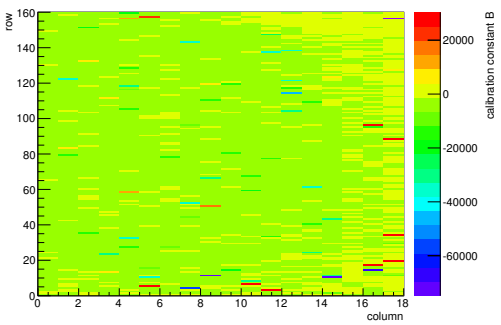

(g) Calibration constant B.

Figure C.127: Detailed plots for test beam measurement of SCC-31 (description see section 6.1) sample (running as DUT0) during runs 125-129 in the March 2012 test beam period at DESY. Summary of the data in chapter 9. *(cont.)*

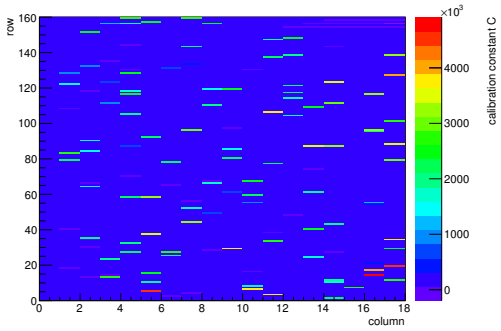

(h) Calibration constant C.

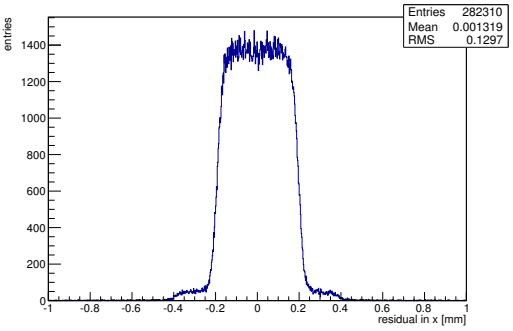

(i) Track residual in x.

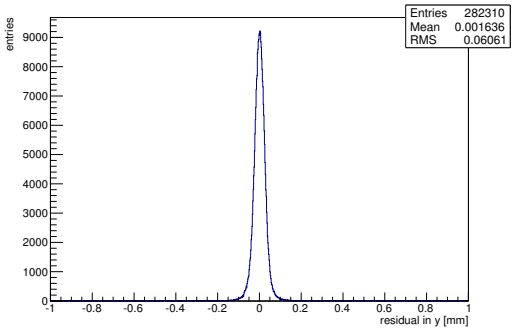

(j) Track residual in y.

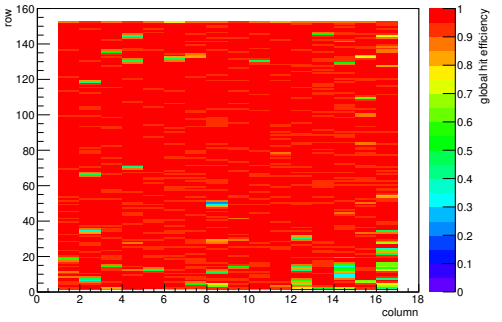

(k) Hit efficiency map.

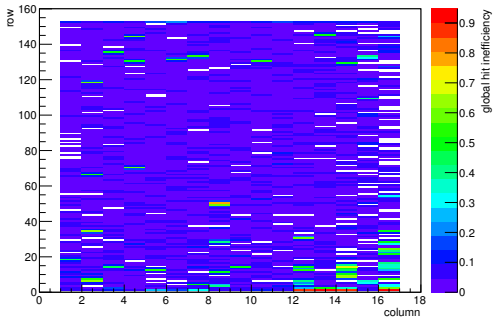

(l) Hit inefficiency map.

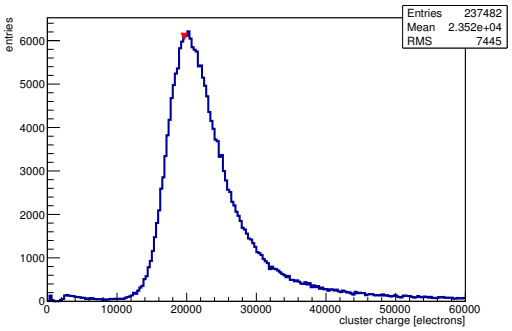

(m) Charge distribution (all cluster sizes included).

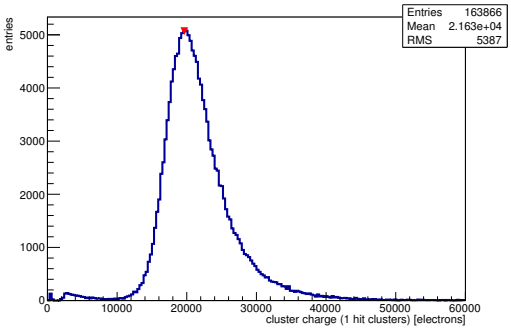

(n) Charge distribution (1 hit cluster).

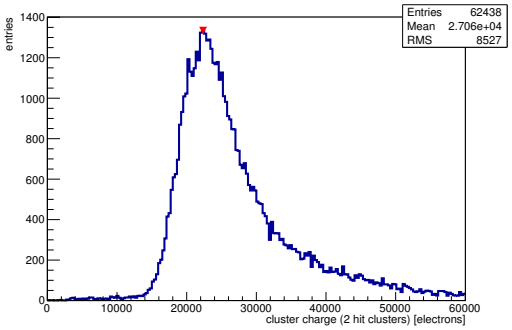

(o) Charge distribution (2 hit cluster).

Figure C.127: Detailed plots for test beam measurement of SCC-31 (description see section 6.1) sample (running as DUT0) during runs 125-129 in the March 2012 test beam period at DESY. Summary of the data in chapter 9. *(cont.)*

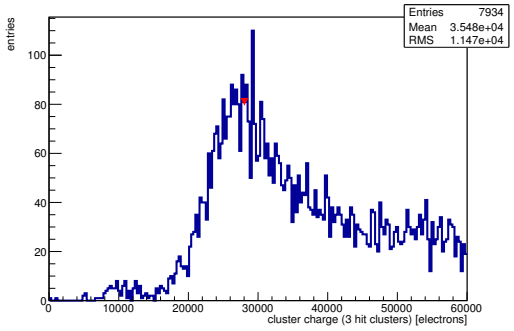

(p) Charge distribution (3 hit cluster).

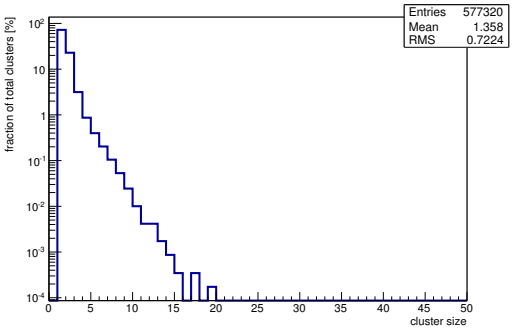

(q) Cluster size distribution.

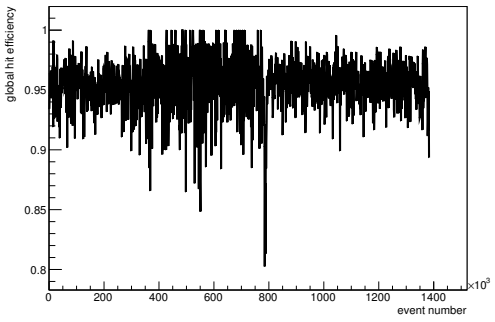

(r) Hit efficiency vs event number.

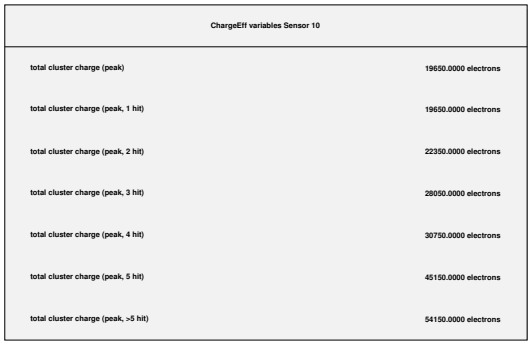

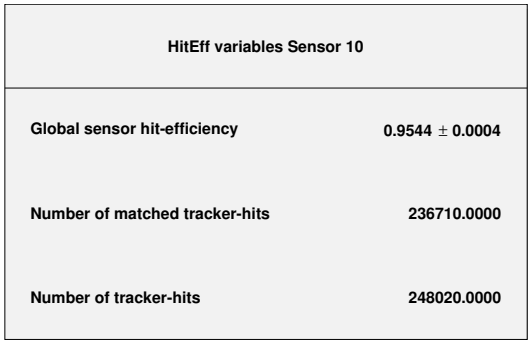

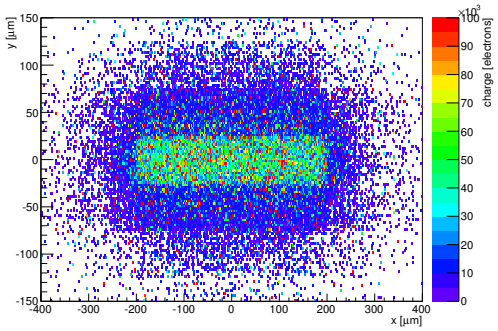

(s) Single pixel mean charge.

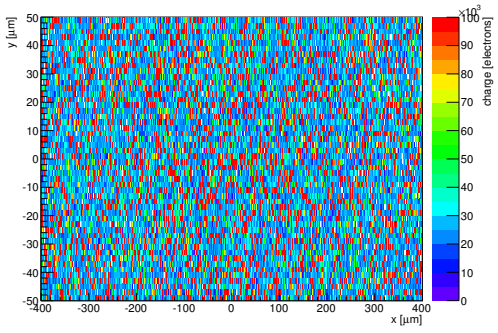

(t) Single pixel mean charge.

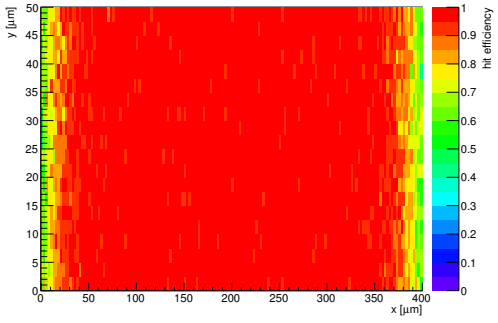

(u) Single pixel hit efficiency.

Figure C.127: Detailed plots for test beam measurement of SCC-31 (description see section 6.1) sample (running as DUT0) during runs 125-129 in the March 2012 test beam period at DESY. Summary of the data in chapter 9.

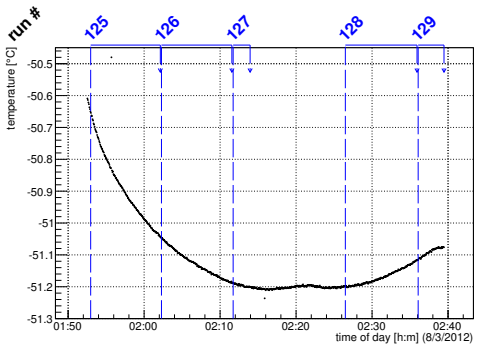

(a) Temperature vs time.

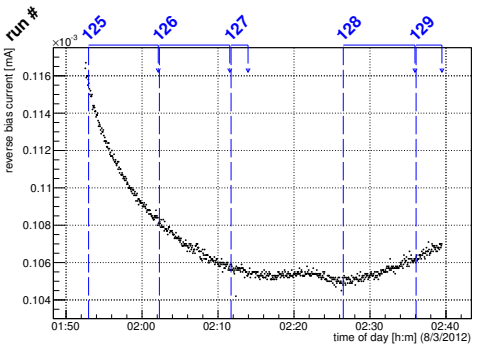

(b) Bias current vs time.

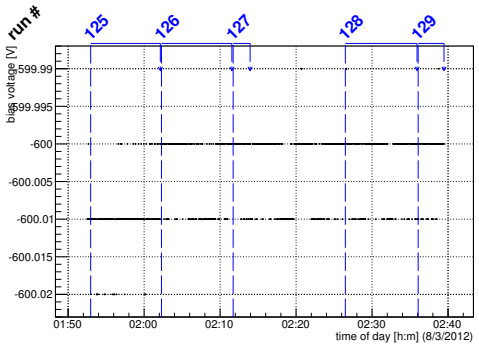

(c) Currently applied bias voltage vs time.

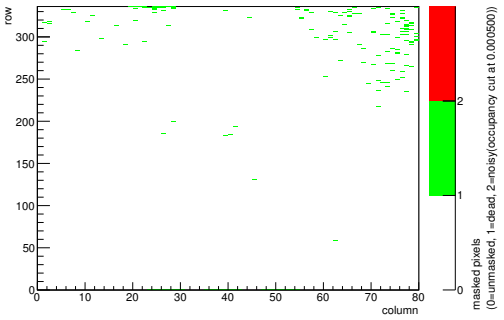

(d) Map of masked pixels.

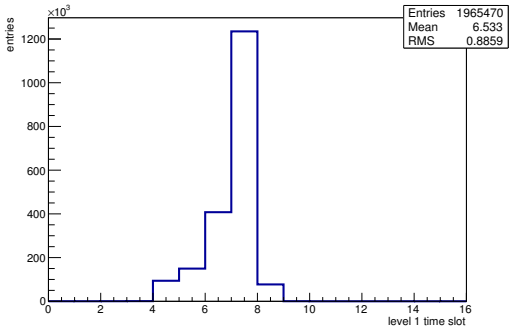

(e) Lvl1 distribution.

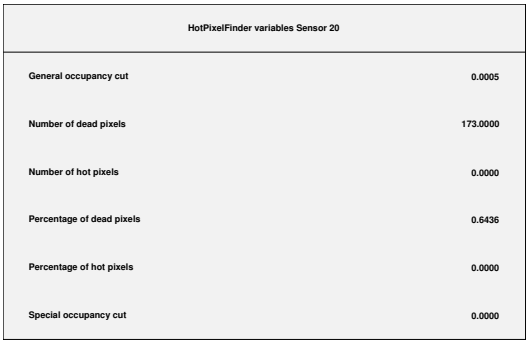

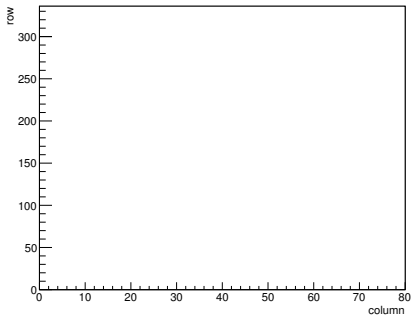

(f) Calibration constant A.

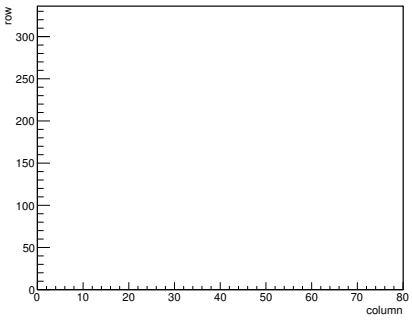

(g) Calibration constant B.

Figure C.128: Detailed plots for test beam measurement of DO-36 (description see section 6.1) sample (running as DUT1) during runs 125-129 in the March 2012 test beam period at DESY. Summary of the data in chapter 9. *(cont.)*

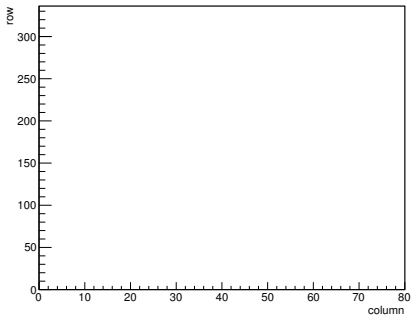

(h) Calibration constant C.

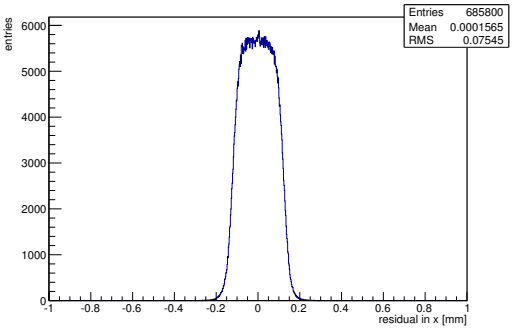

(i) Track residual in x.

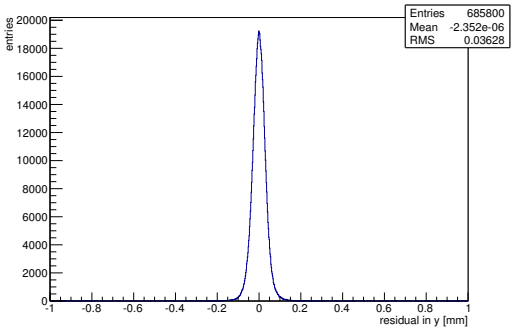

(j) Track residual in y.

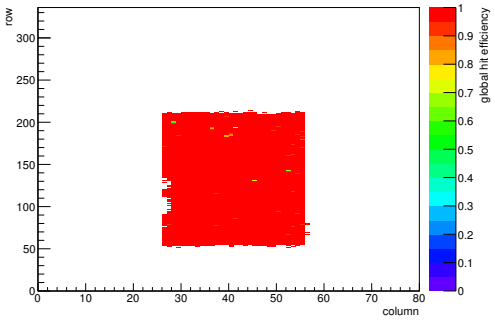

(k) Hit efficiency map.

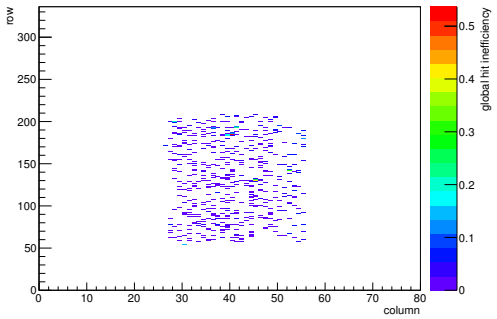

(l) Hit inefficiency map.

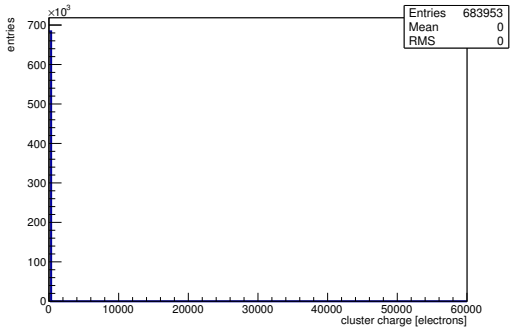

(m) Charge distribution (all cluster sizes included).

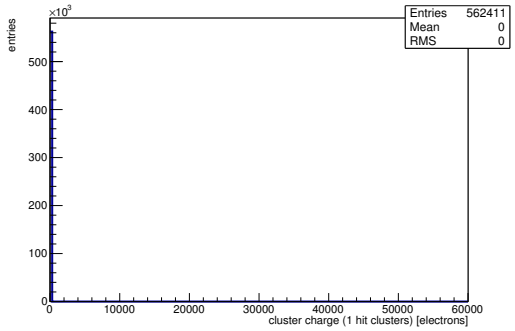

(n) Charge distribution (1 hit cluster).

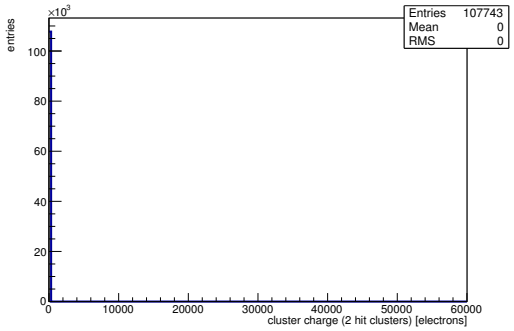

(o) Charge distribution (2 hit cluster).

Figure C.128: Detailed plots for test beam measurement of DO-36 (description see section 6.1) sample (running as DUT1) during runs 125-129 in the March 2012 test beam period at DESY. Summary of the data in chapter 9. *(cont.)*

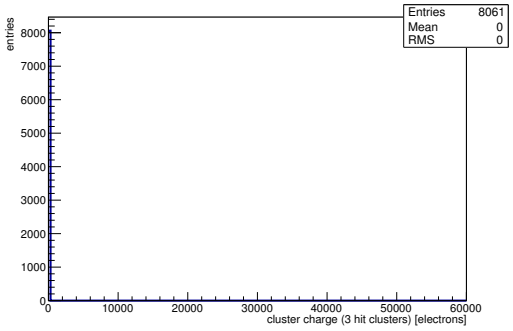

(p) Charge distribution (3 hit cluster).

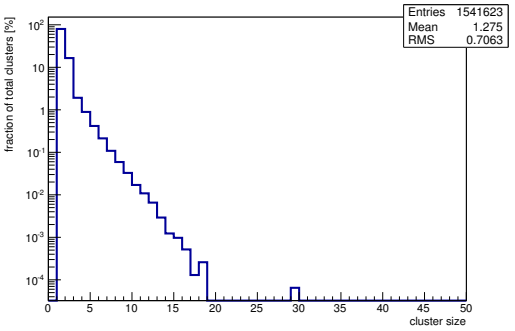

(q) Cluster size distribution.

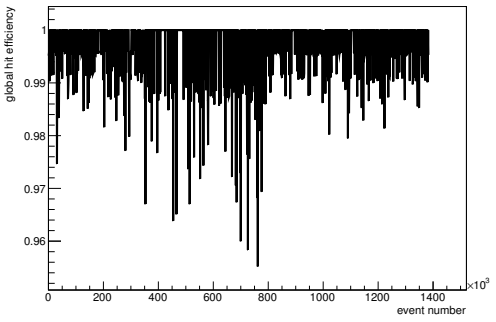

(r) Hit efficiency vs event number.

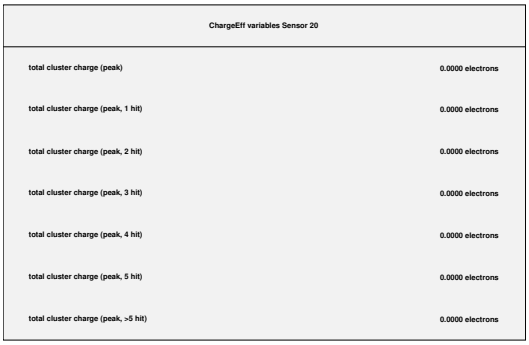

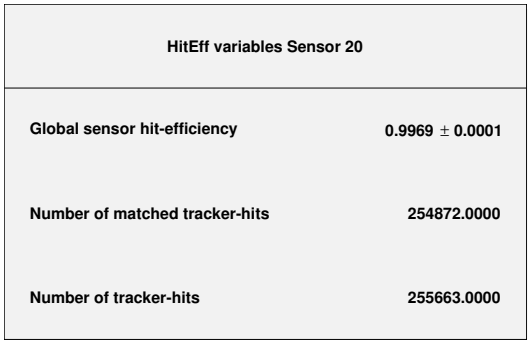

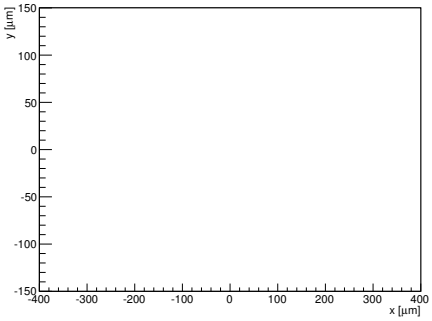

(s) Single pixel mean charge.

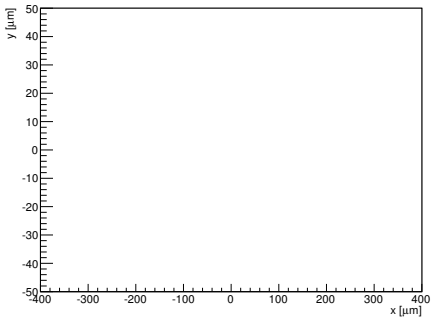

(t) Single pixel mean charge.

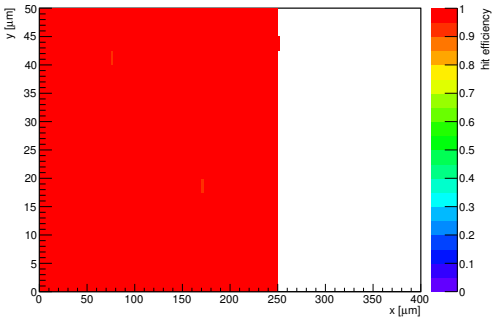

(u) Single pixel hit efficiency.

Figure C.128: Detailed plots for test beam measurement of DO-36 (description see section 6.1) sample (running as DUT1) during runs 125-129 in the March 2012 test beam period at DESY. Summary of the data in chapter 9.

C.4.2 Runs 130-135

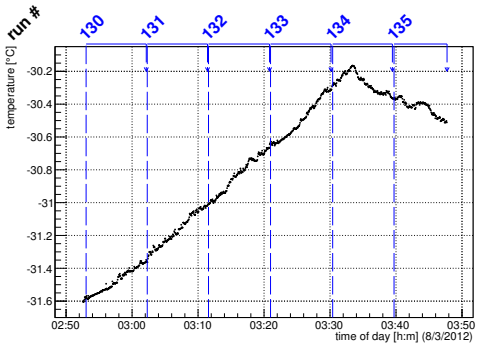

(a) Temperature vs time.

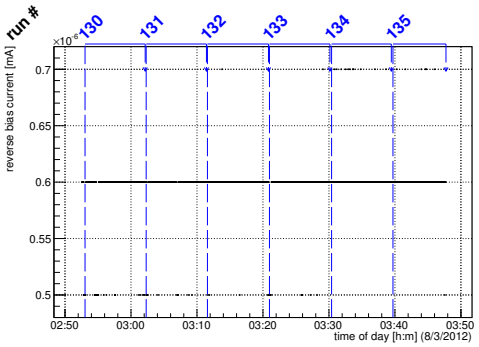

(b) Bias current vs time.

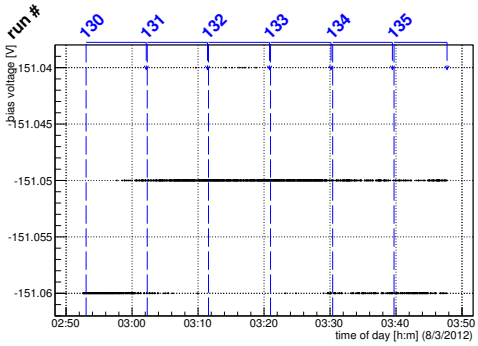

(c) Currently applied bias voltage vs time.

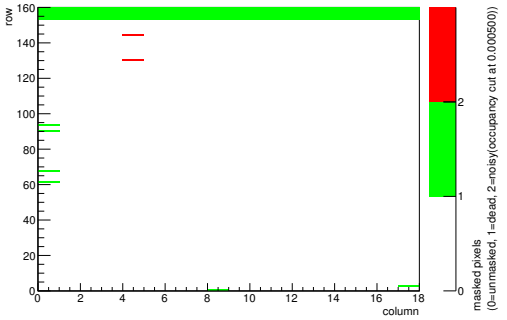

(d) Map of masked pixels.

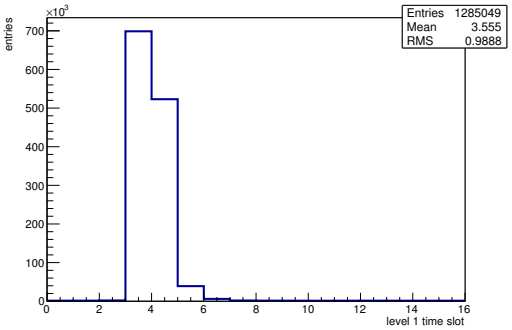

(e) Lvl1 distribution.

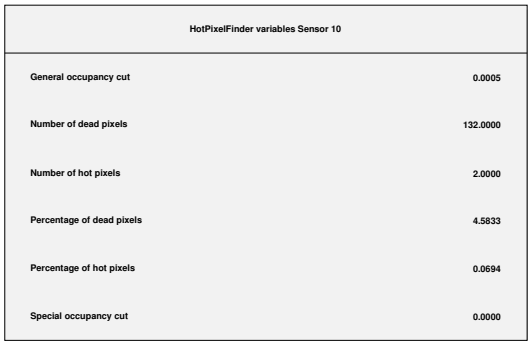

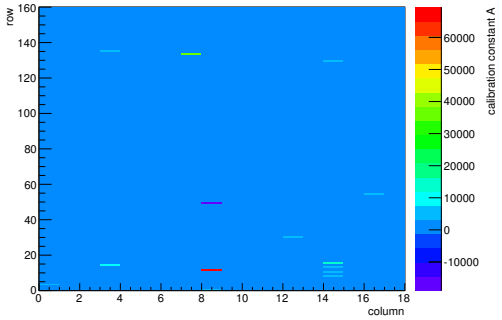

(f) Calibration constant A.

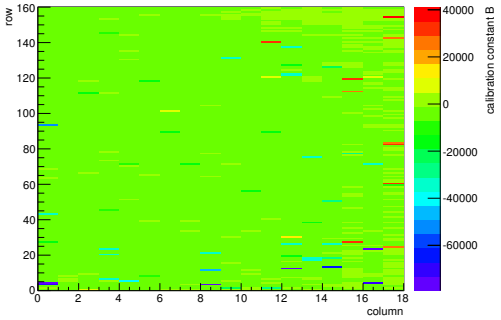

(g) Calibration constant B.

Figure C.129: Detailed plots for test beam measurement of SCC-31 (description see section 6.1) sample (running as DUT0) during runs 130-135 in the March 2012 test beam period at DESY. Summary of the data in chapter 9. *(cont.)*

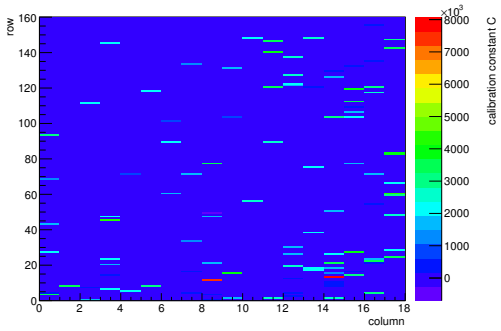

(h) Calibration constant C.

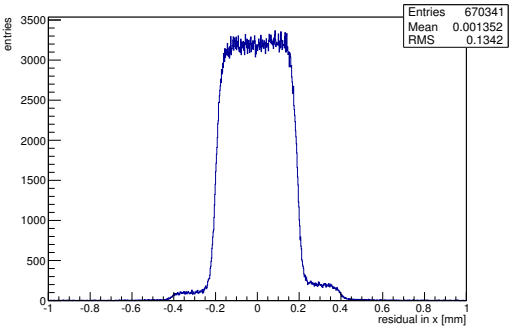

(i) Track residual in x.

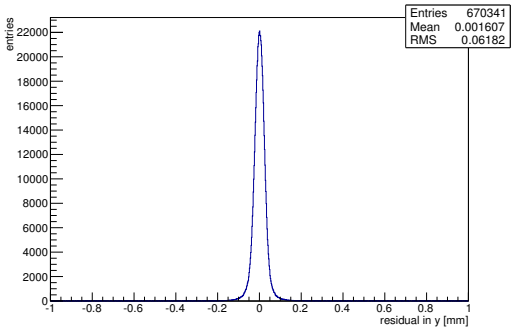

(j) Track residual in y.

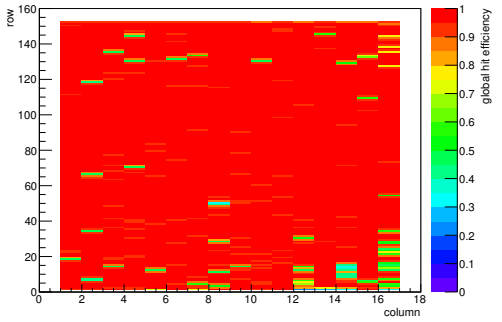

(k) Hit efficiency map.

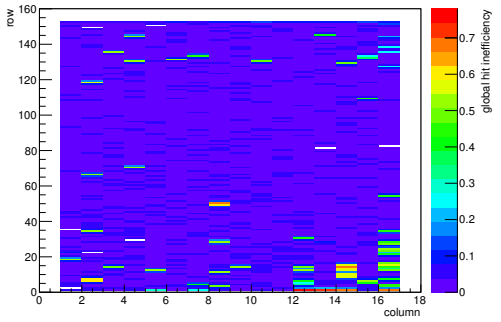

(l) Hit inefficiency map.

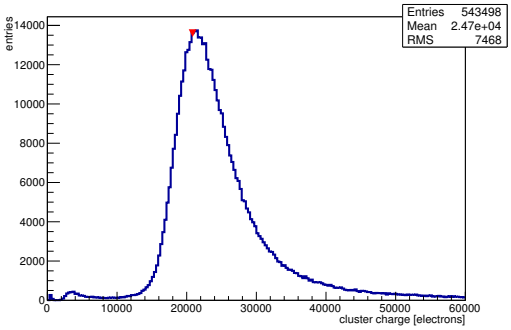

(m) Charge distribution (all cluster sizes included).

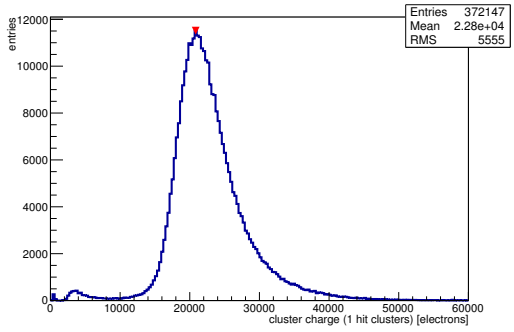

(n) Charge distribution (1 hit cluster).

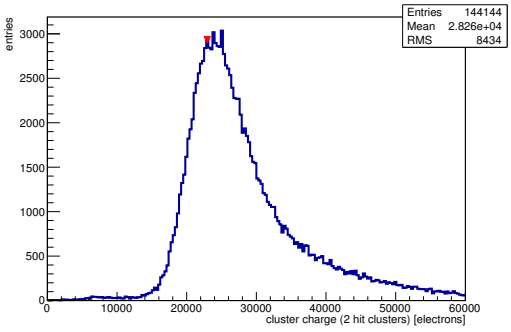

(o) Charge distribution (2 hit cluster).

Figure C.129: Detailed plots for test beam measurement of SCC-31 (description see section 6.1) sample (running as DUT0) during runs 130-135 in the March 2012 test beam period at DESY. Summary of the data in chapter 9. *(cont.)*

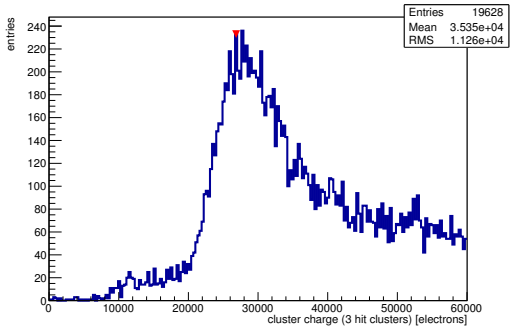

(p) Charge distribution (3 hit cluster).

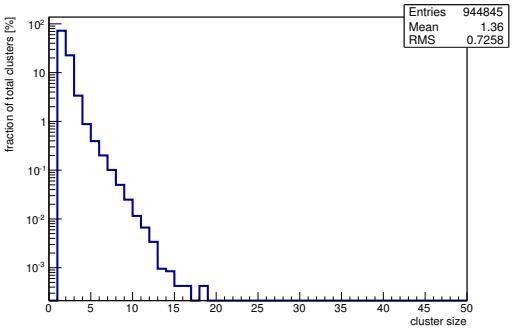

(q) Cluster size distribution.

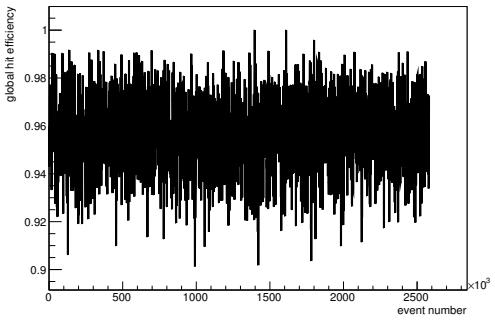

(r) Hit efficiency vs event number.

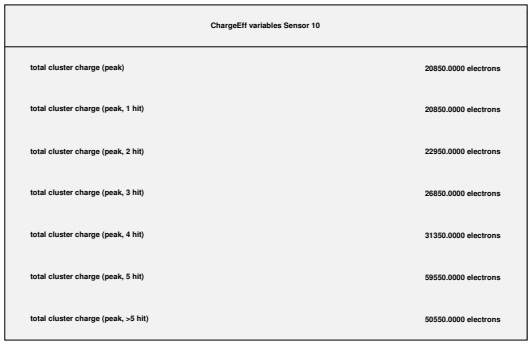

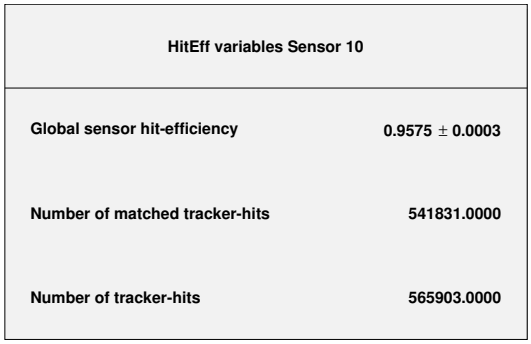

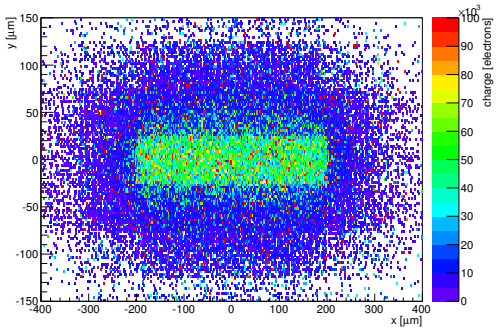

(s) Single pixel mean charge.

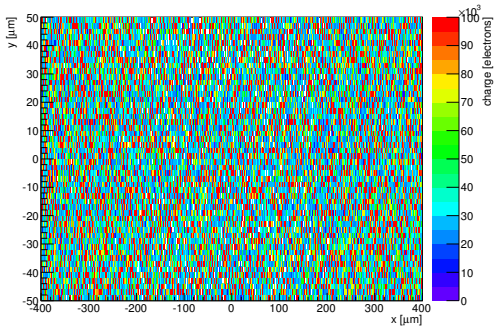

(t) Single pixel mean charge.

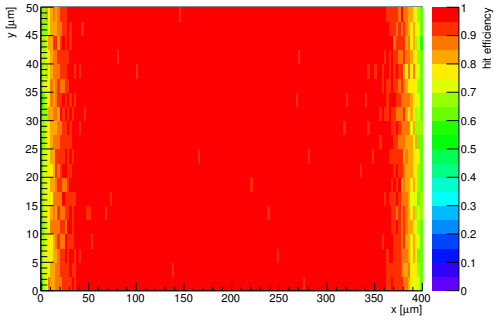

(u) Single pixel hit efficiency.

Figure C.129: Detailed plots for test beam measurement of SCC-31 (description see section 6.1) sample (running as DUT0) during runs 130-135 in the March 2012 test beam period at DESY. Summary of the data in chapter 9.

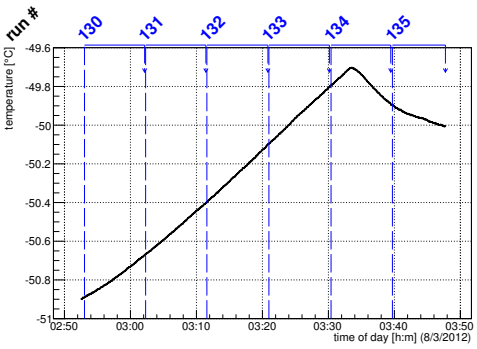

(a) Temperature vs time.

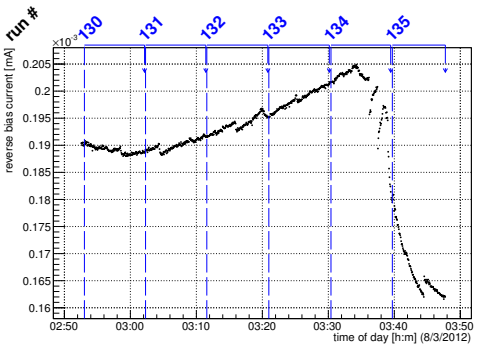

(b) Bias current vs time.

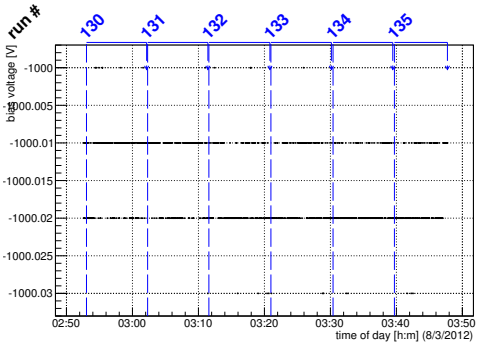

(c) Currently applied bias voltage vs time.

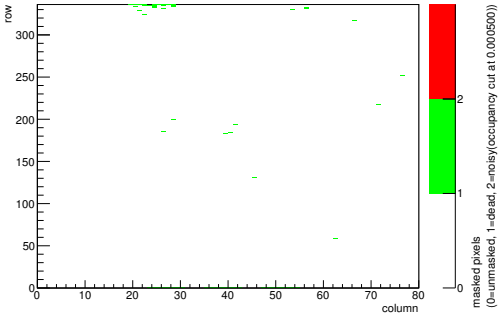

(d) Map of masked pixels.

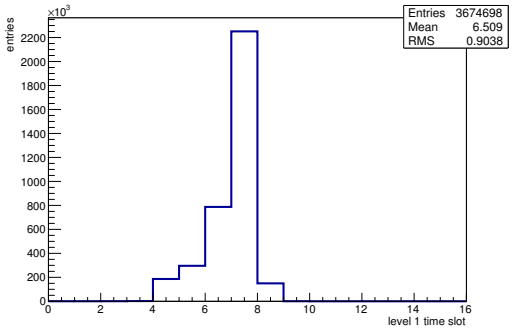

(e) Lvl1 distribution.

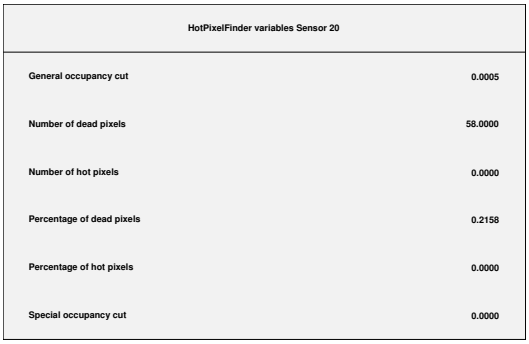

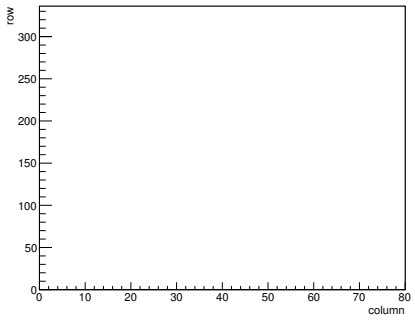

(f) Calibration constant A.

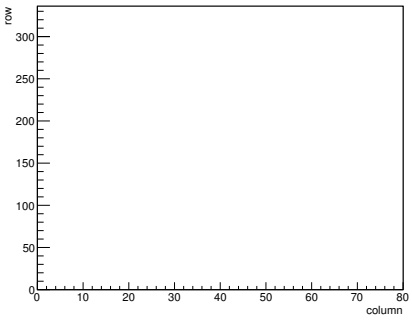

(g) Calibration constant B.

Figure C.130: Detailed plots for test beam measurement of DO-36 (description see section 6.1) sample (running as DUT1) during runs 130-135 in the March 2012 test beam period at DESY. Summary of the data in chapter 9. *(cont.)*

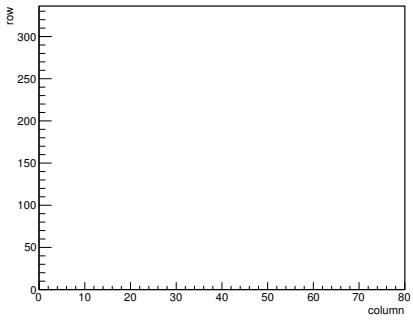

(h) Calibration constant C.

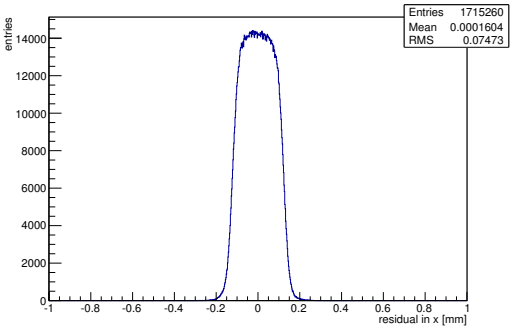

(i) Track residual in x.

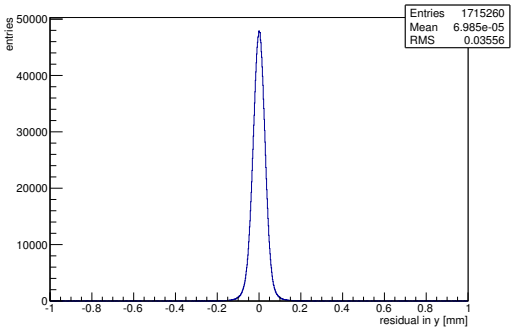

(j) Track residual in y.

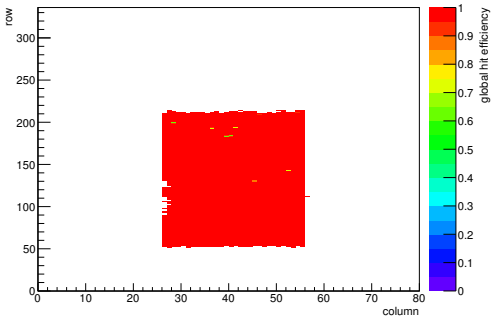

(k) Hit efficiency map.

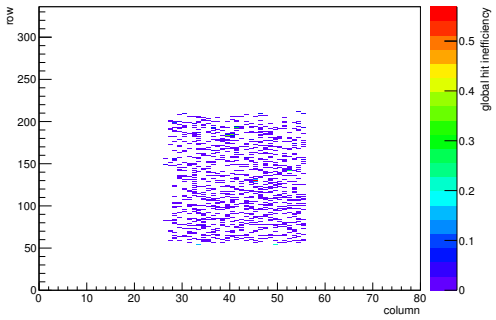

(l) Hit inefficiency map.

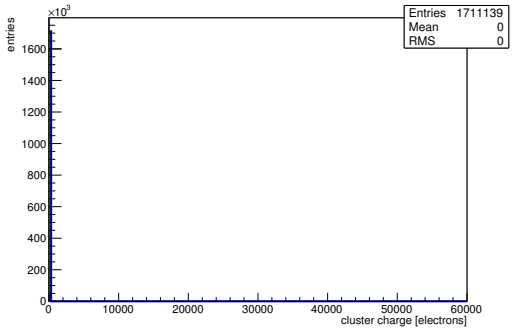

(m) Charge distribution (all cluster sizes included).

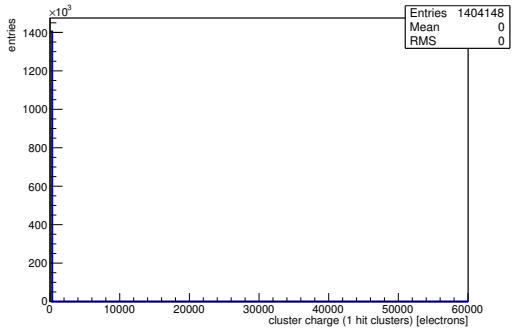

(n) Charge distribution (1 hit cluster).

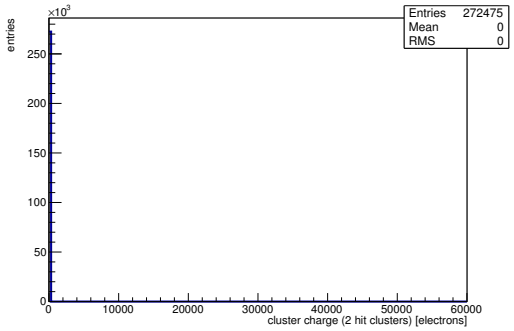

(o) Charge distribution (2 hit cluster).

Figure C.130: Detailed plots for test beam measurement of DO-36 (description see section 6.1) sample (running as DUT1) during runs 130-135 in the March 2012 test beam period at DESY. Summary of the data in chapter 9. *(cont.)*

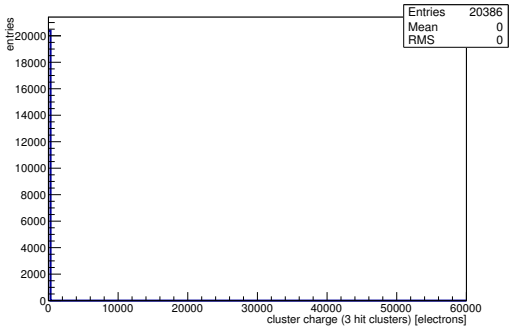

(p) Charge distribution (3 hit cluster).

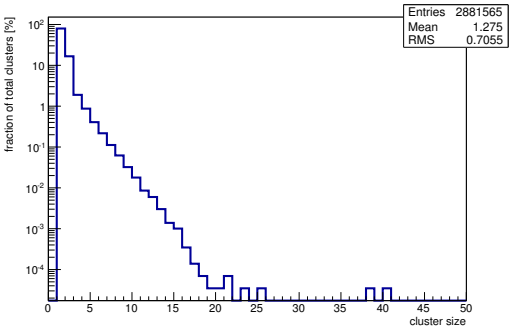

(q) Cluster size distribution.

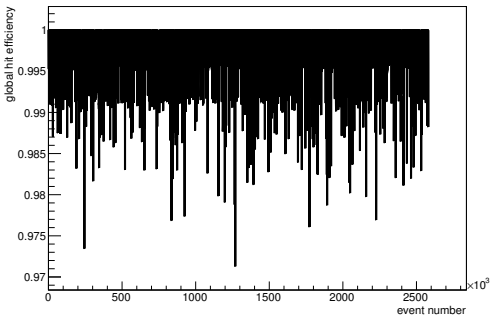

(r) Hit efficiency vs event number.

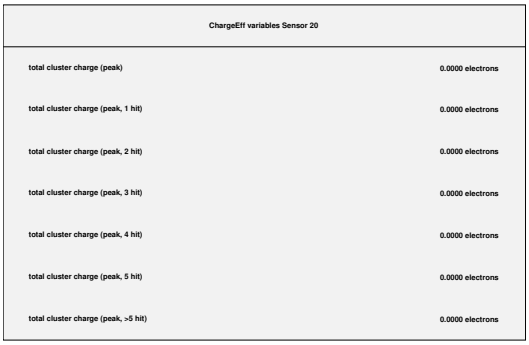

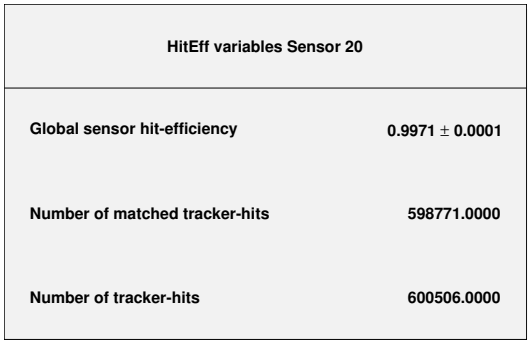

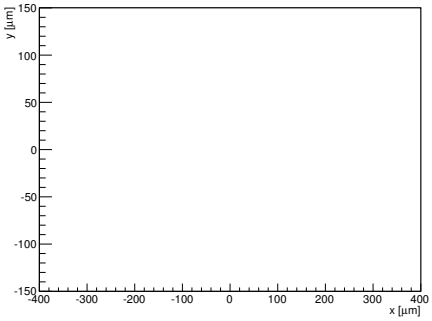

(s) Single pixel mean charge.

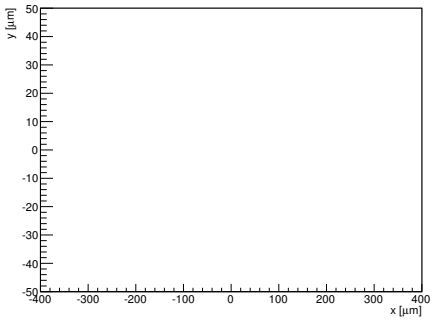

(t) Single pixel mean charge.

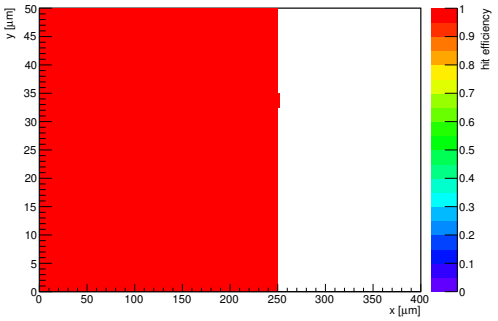

(u) Single pixel hit efficiency.

Figure C.130: Detailed plots for test beam measurement of DO-36 (description see section 6.1) sample (running as DUT1) during runs 130-135 in the March 2012 test beam period at DESY. Summary of the data in chapter 9.

C.4.3 Runs 143-147

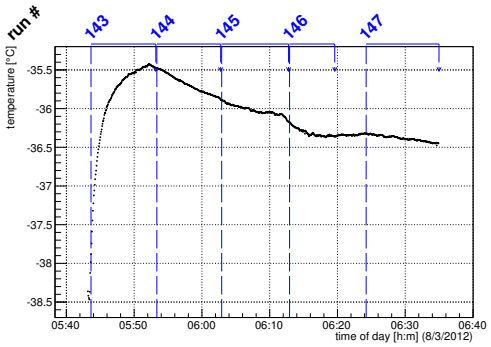

(a) Temperature vs time.

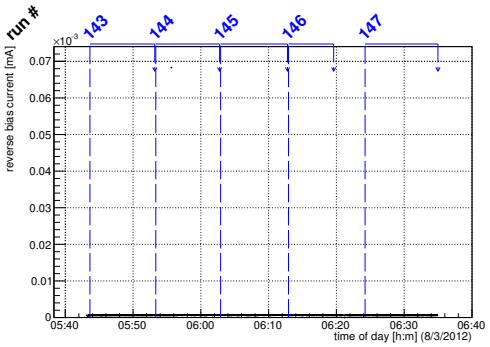

(b) Bias current vs time.

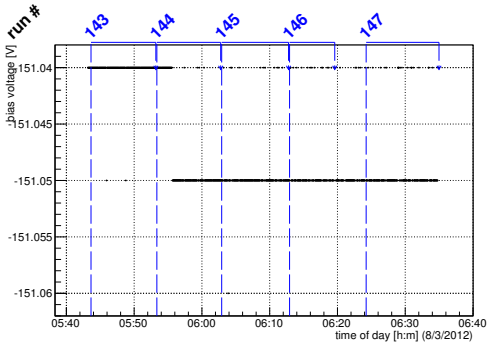

(c) Currently applied bias voltage vs time.

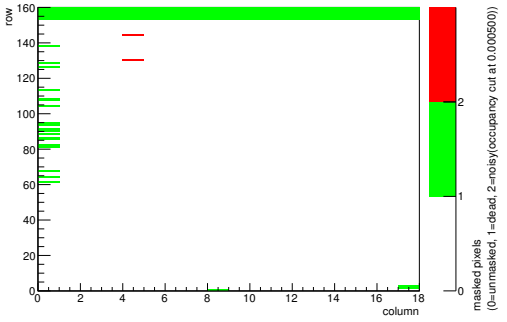

(d) Map of masked pixels.

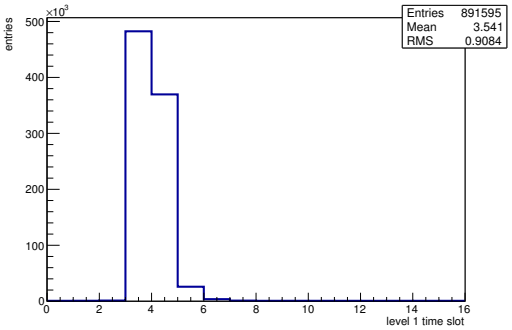

(e) Lvl1 distribution.

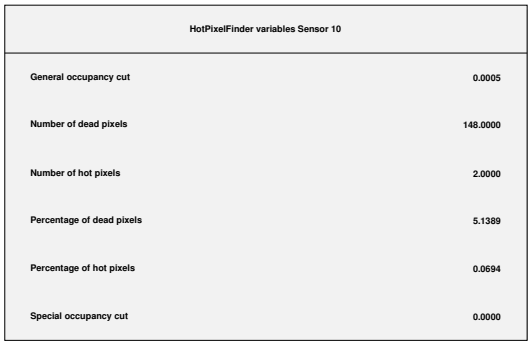

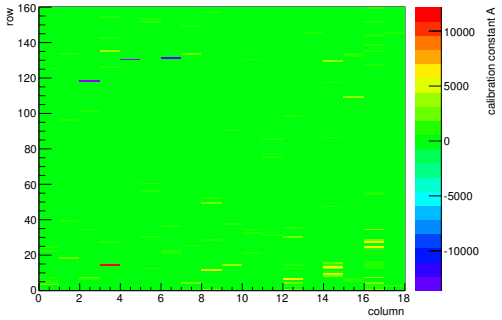

(f) Calibration constant A.

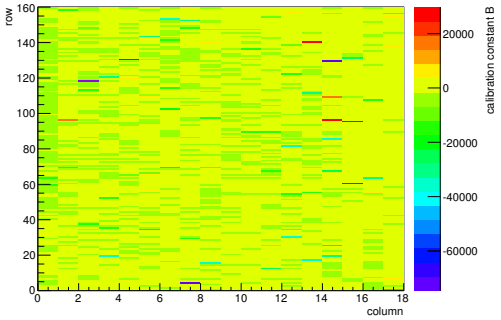

(g) Calibration constant B.

Figure C.131: Detailed plots for test beam measurement of SCC-31 (description see section 6.1) sample (running as DUT0) during runs 143-147 in the March 2012 test beam period at DESY. Summary of the data in chapter 9. *(cont.)*

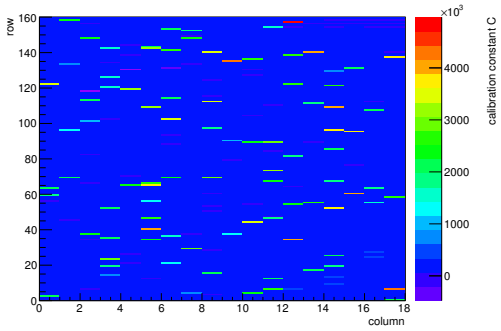

(h) Calibration constant C.

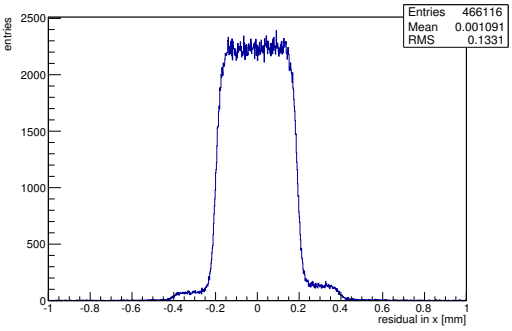

(i) Track residual in x.

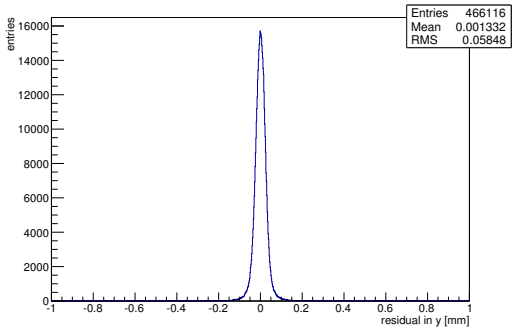

(j) Track residual in y.

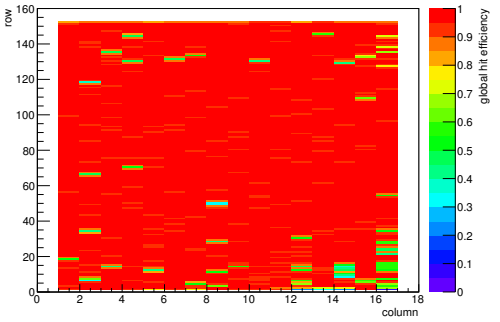

(k) Hit efficiency map.

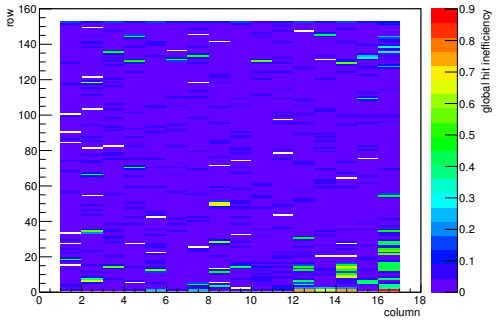

(l) Hit inefficiency map.

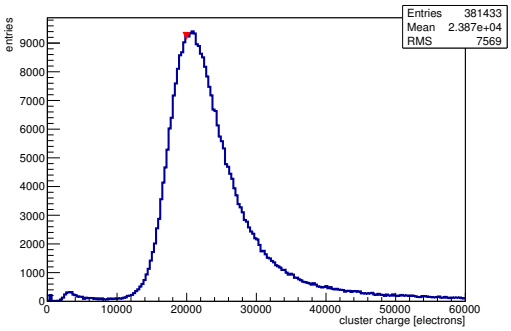

(m) Charge distribution (all cluster sizes included).

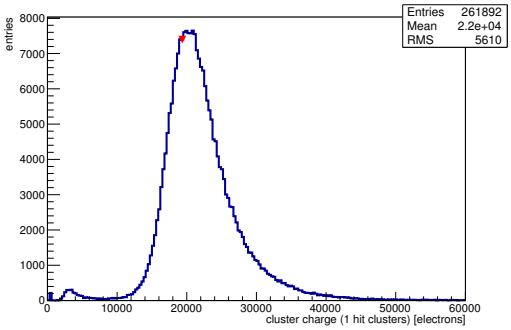

(n) Charge distribution (1 hit cluster).

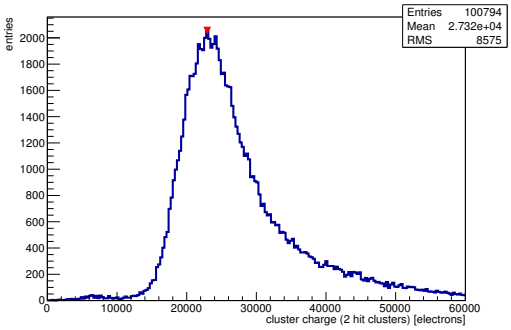

(o) Charge distribution (2 hit cluster).

Figure C.131: Detailed plots for test beam measurement of SCC-31 (description see section 6.1) sample (running as DUT0) during runs 143-147 in the March 2012 test beam period at DESY. Summary of the data in chapter 9. *(cont.)*

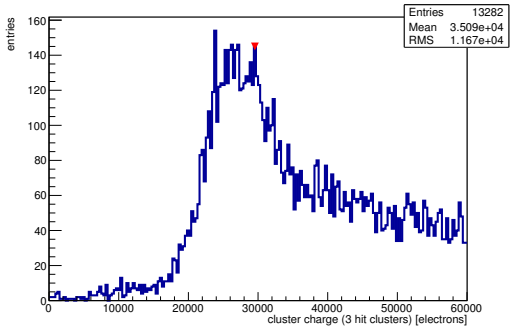

(p) Charge distribution (3 hit cluster).

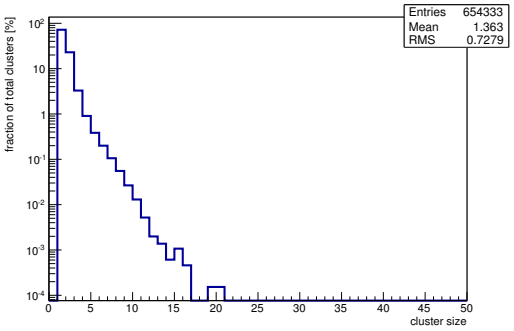

(q) Cluster size distribution.

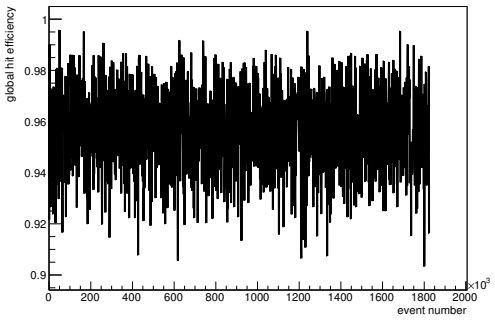

(r) Hit efficiency vs event number.

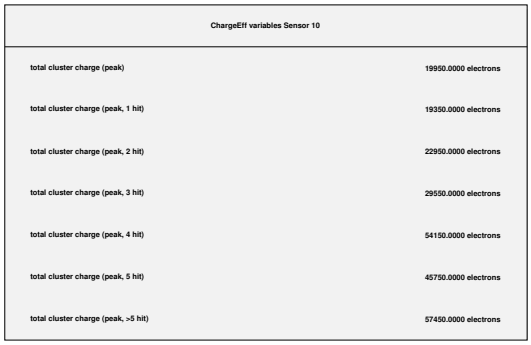

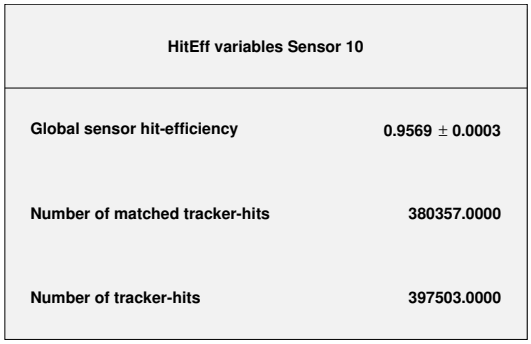

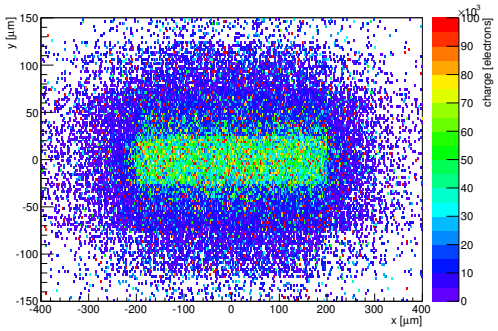

(s) Single pixel mean charge.

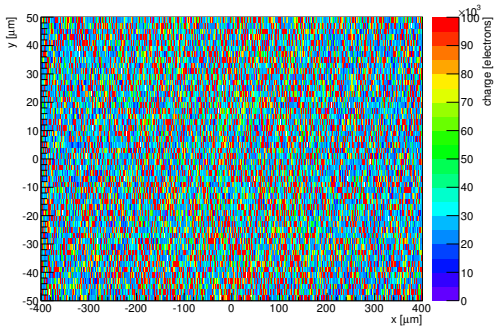

(t) Single pixel mean charge.

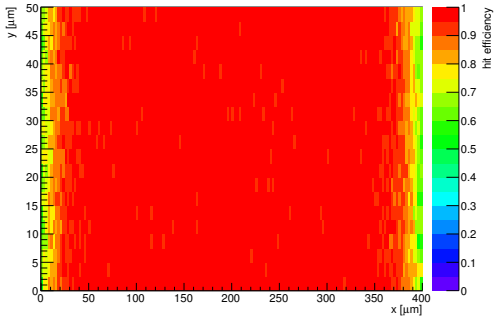

(u) Single pixel hit efficiency.

Figure C.131: Detailed plots for test beam measurement of SCC-31 (description see section 6.1) sample (running as DUT0) during runs 143-147 in the March 2012 test beam period at DESY. Summary of the data in chapter 9.

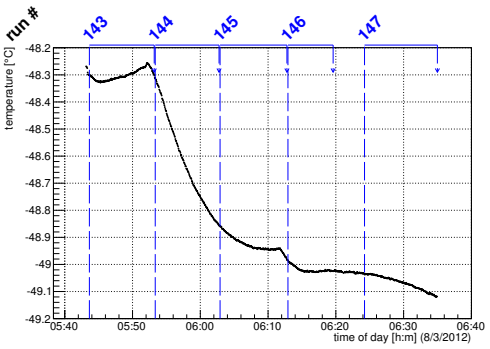

(a) Temperature vs time.

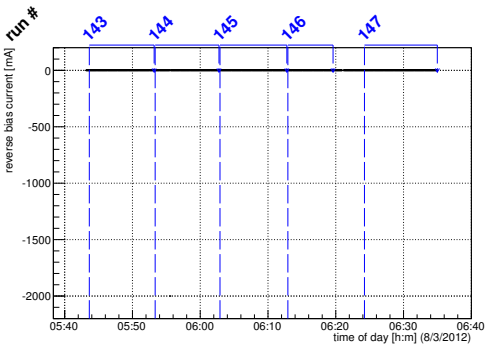

(b) Bias current vs time.

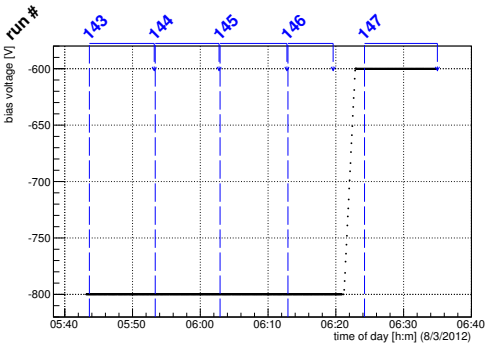

(c) Currently applied bias voltage vs time.

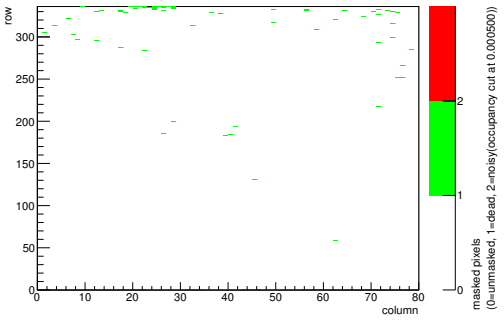

(d) Map of masked pixels.

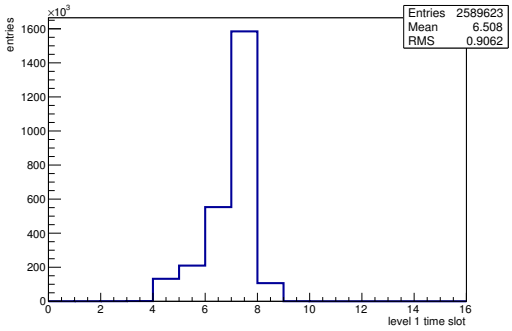

(e) Lvl1 distribution.

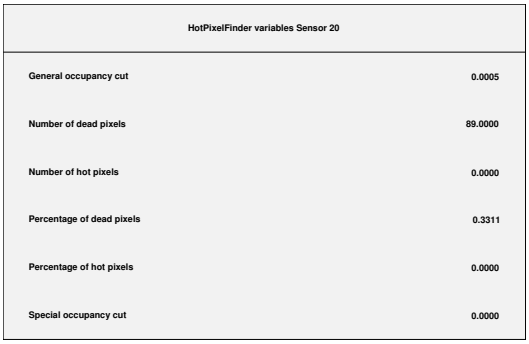

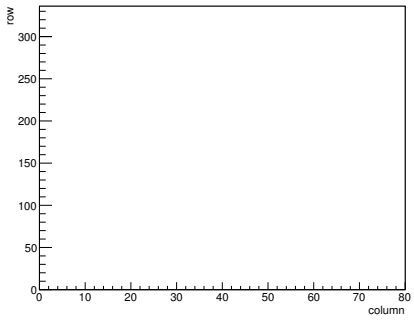

(f) Calibration constant A.

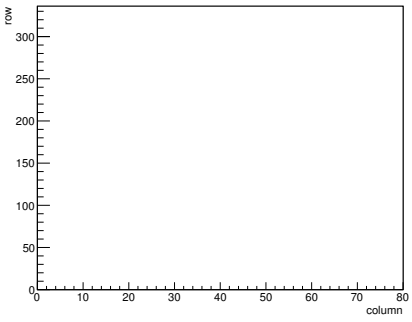

(g) Calibration constant B.

Figure C.132: Detailed plots for test beam measurement of DO-36 (description see section 6.1) sample (running as DUT1) during runs 143-147 in the March 2012 test beam period at DESY. Summary of the data in chapter 9. *(cont.)*

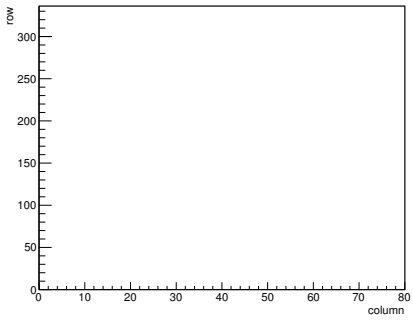

(h) Calibration constant C.

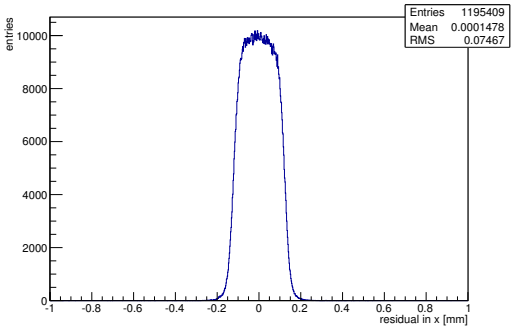

(i) Track residual in x.

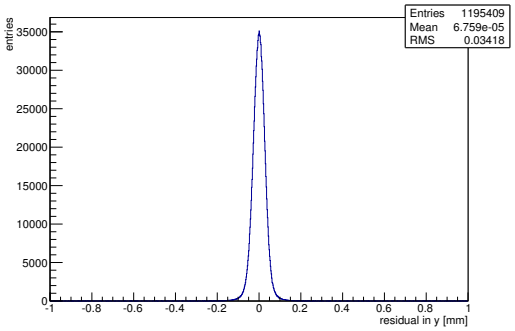

(j) Track residual in y.

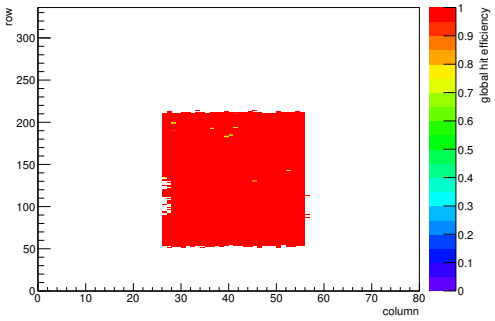

(k) Hit efficiency map.

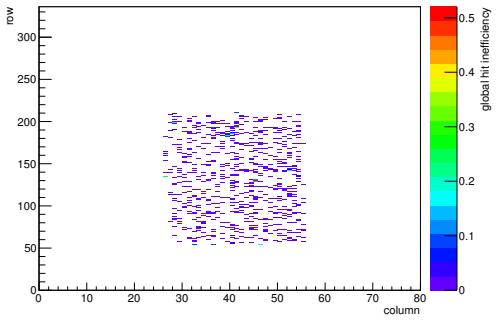

(l) Hit inefficiency map.

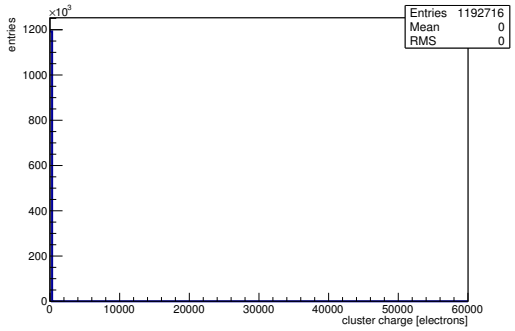

(m) Charge distribution (all cluster sizes included).

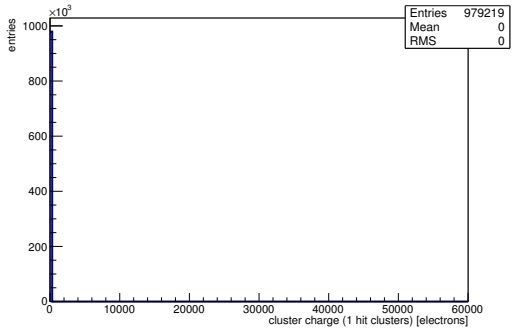

(n) Charge distribution (1 hit cluster).

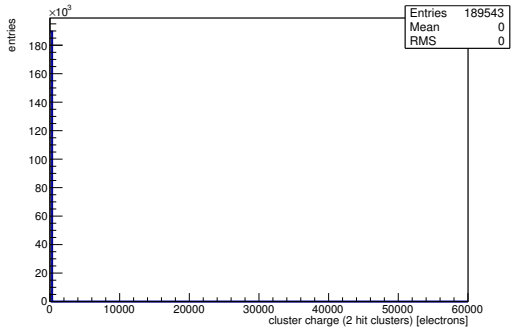

(o) Charge distribution (2 hit cluster).

Figure C.132: Detailed plots for test beam measurement of DO-36 (description see section 6.1) sample (running as DUT1) during runs 143-147 in the March 2012 test beam period at DESY. Summary of the data in chapter 9. *(cont.)*

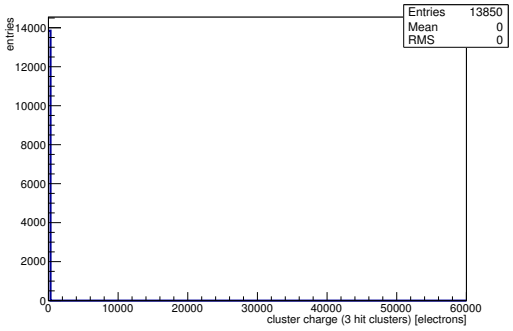

(p) Charge distribution (3 hit cluster).

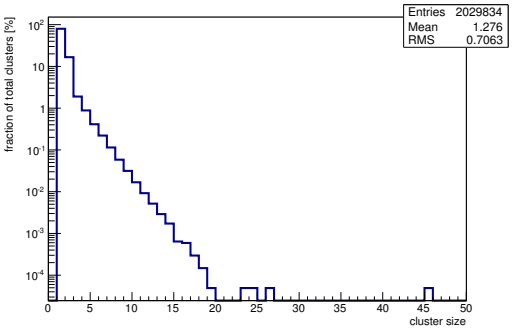

(q) Cluster size distribution.

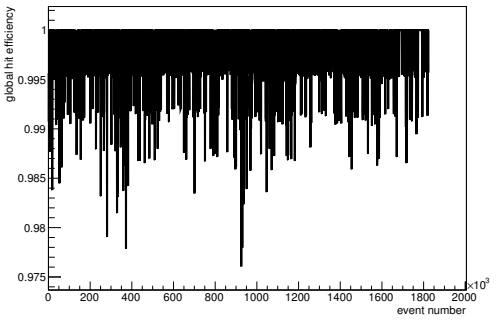

(r) Hit efficiency vs event number.

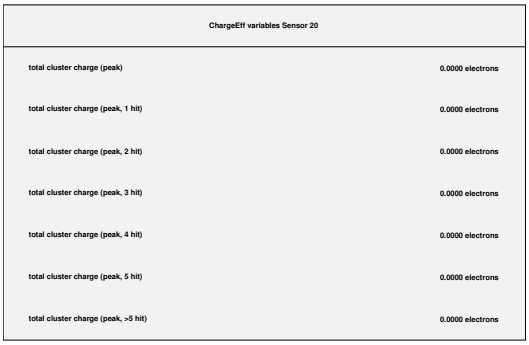

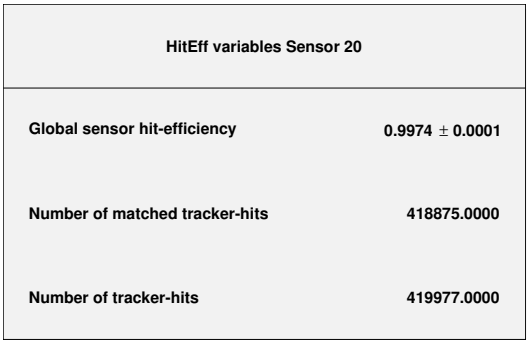

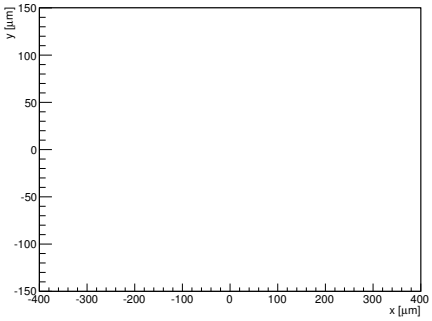

(s) Single pixel mean charge.

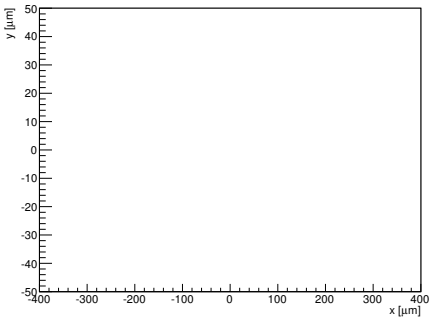

(t) Single pixel mean charge.

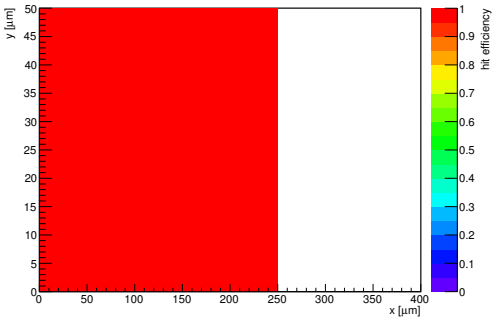

(u) Single pixel hit efficiency.

Figure C.132: Detailed plots for test beam measurement of DO-36 (description see section 6.1) sample (running as DUT1) during runs 143-147 in the March 2012 test beam period at DESY. Summary of the data in chapter 9.

C.4.4 Runs 149-154

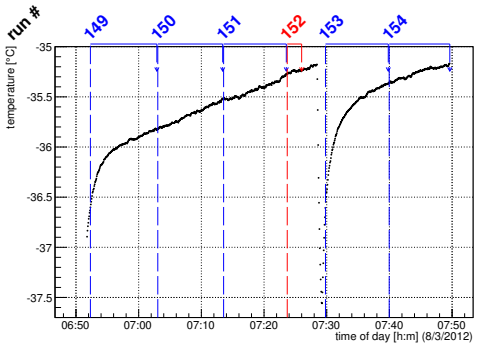

(a) Temperature vs time.

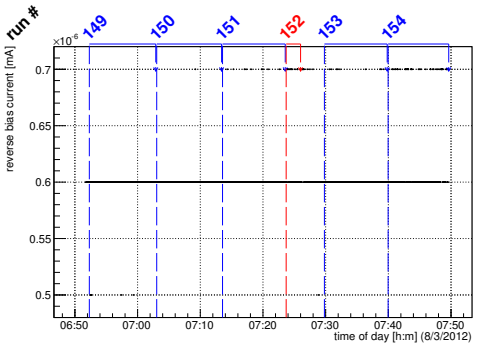

(b) Bias current vs time.

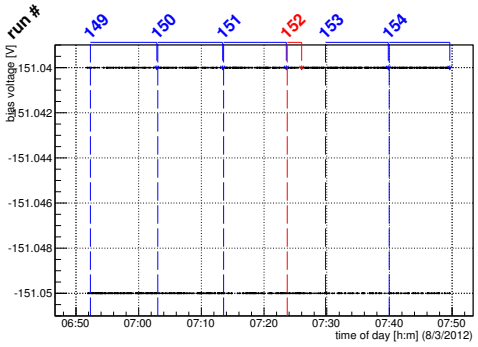

(c) Currently applied bias voltage vs time.

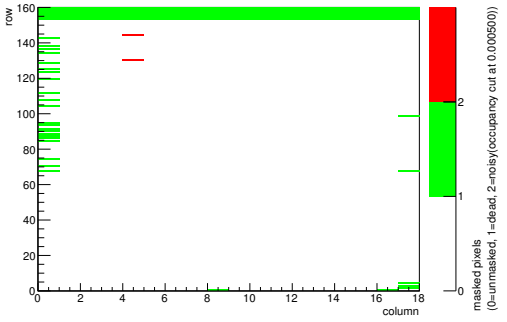

(d) Map of masked pixels.

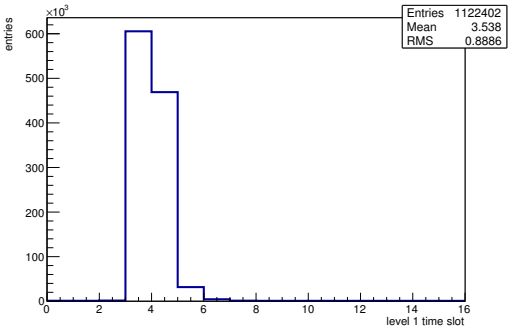

(e) Lvl1 distribution.

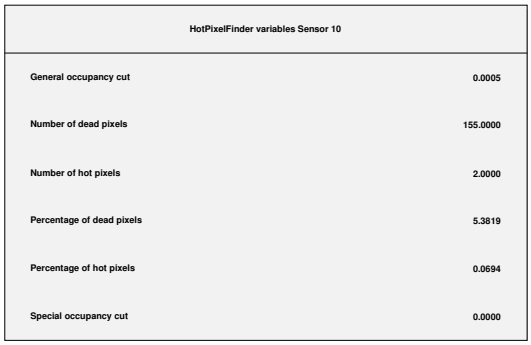

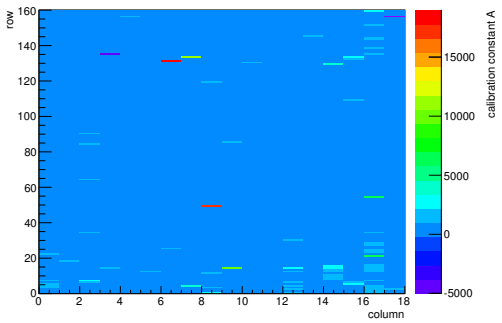

(f) Calibration constant A.

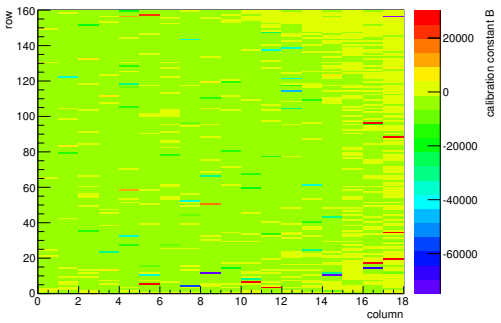

(g) Calibration constant B.

Figure C.133: Detailed plots for test beam measurement of SCC-31 (description see section 6.1) sample (running as DUT0) during runs 149-154 in the March 2012 test beam period at DESY. Summary of the data in chapter 9. *(cont.)*

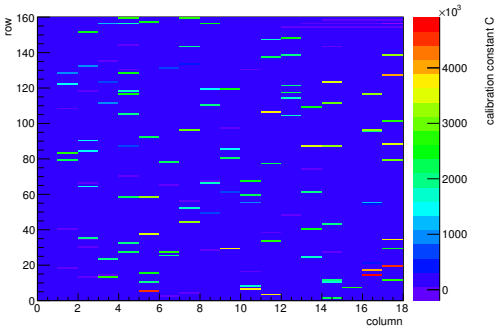

(h) Calibration constant C.

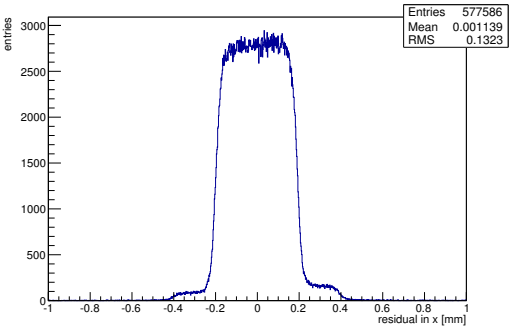

(i) Track residual in x.

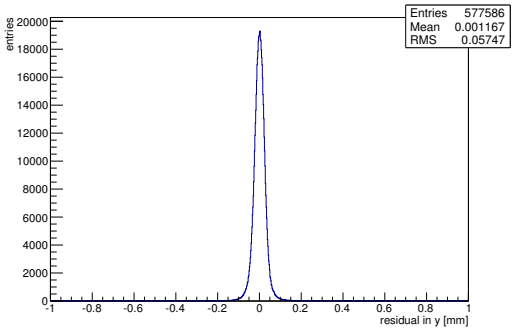

(j) Track residual in y.

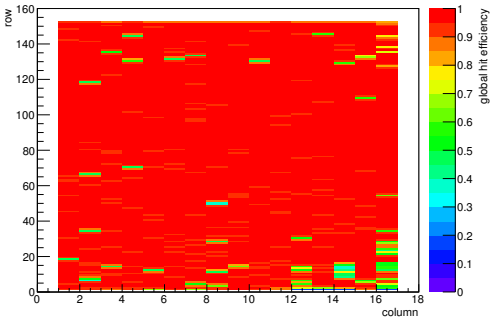

(k) Hit efficiency map.

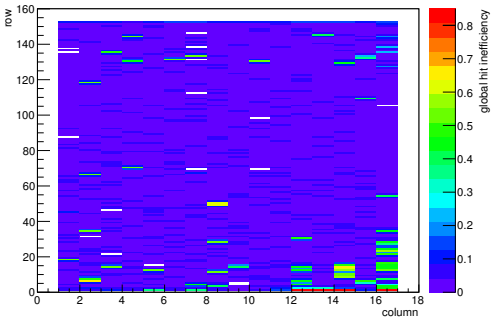

(l) Hit inefficiency map.

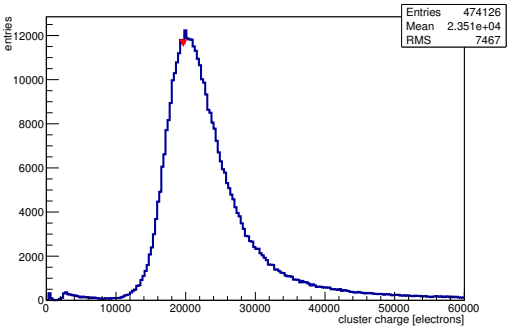

(m) Charge distribution (all cluster sizes included).

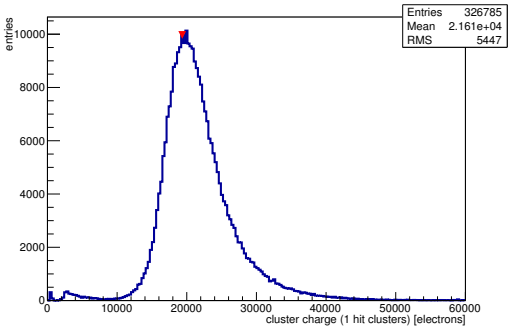

(n) Charge distribution (1 hit cluster).

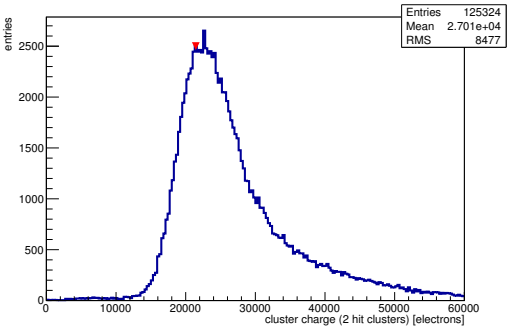

(o) Charge distribution (2 hit cluster).

Figure C.133: Detailed plots for test beam measurement of SCC-31 (description see section 6.1) sample (running as DUT0) during runs 149-154 in the March 2012 test beam period at DESY. Summary of the data in chapter 9. *(cont.)*

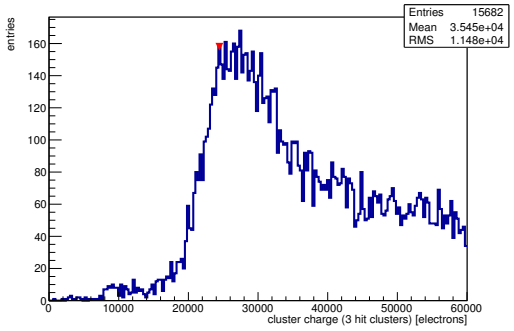

(p) Charge distribution (3 hit cluster).

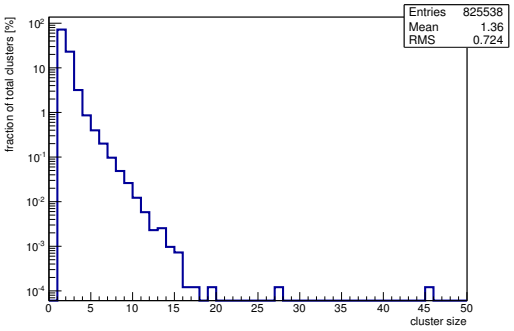

(q) Cluster size distribution.

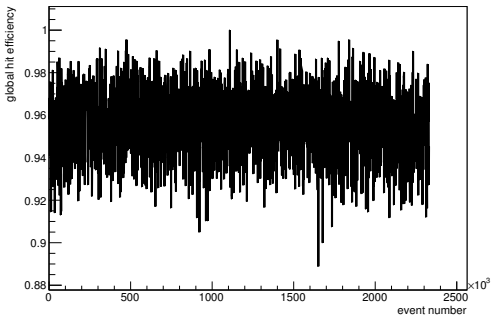

(r) Hit efficiency vs event number.

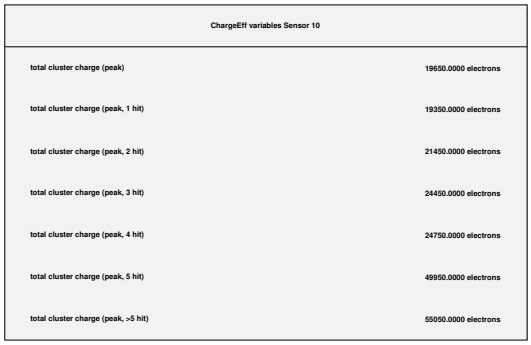

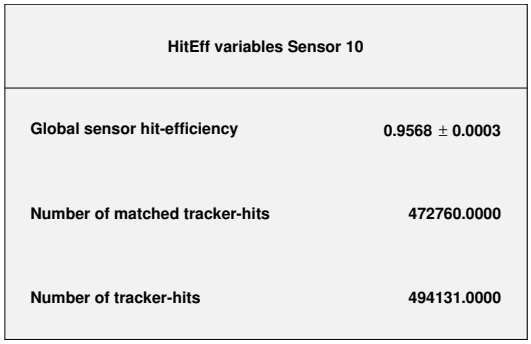

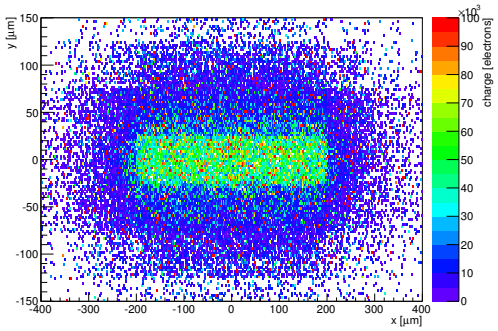

(s) Single pixel mean charge.

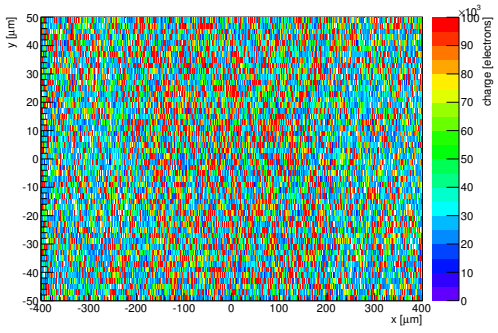

(t) Single pixel mean charge.

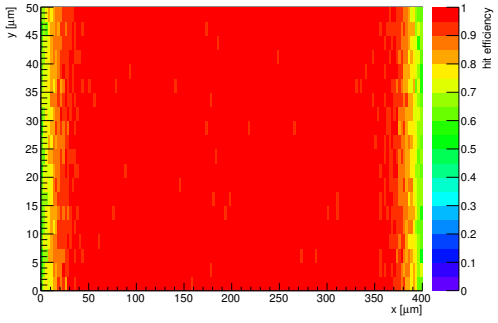

(u) Single pixel hit efficiency.

Figure C.133: Detailed plots for test beam measurement of SCC-31 (description see section 6.1) sample (running as DUT0) during runs 149-154 in the March 2012 test beam period at DESY. Summary of the data in chapter 9.

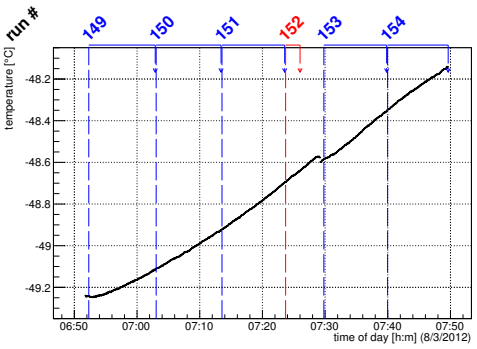

(a) Temperature vs time.

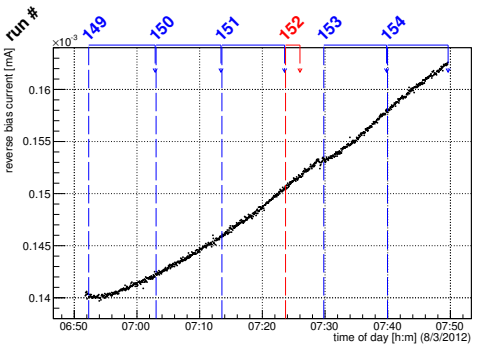

(b) Bias current vs time.

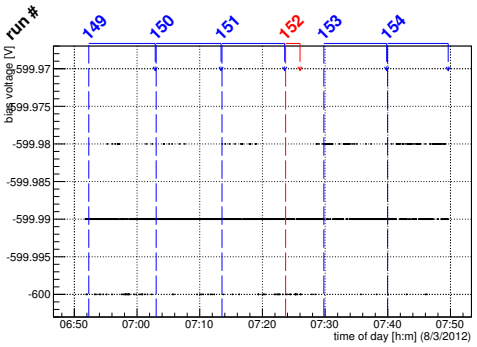

(c) Currently applied bias voltage vs time.

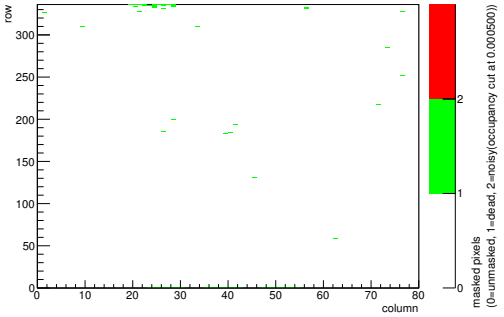

(d) Map of masked pixels.

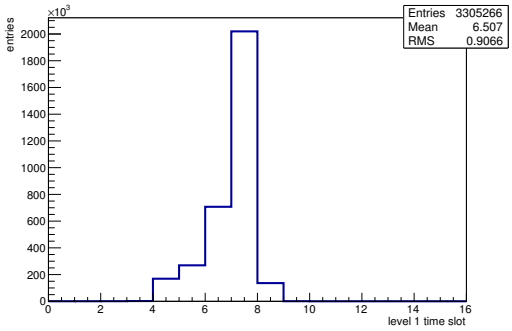

(e) Lvl1 distribution.

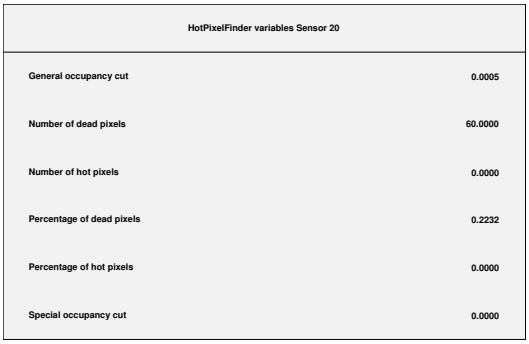

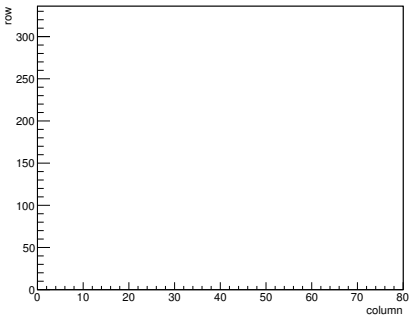

(f) Calibration constant A.

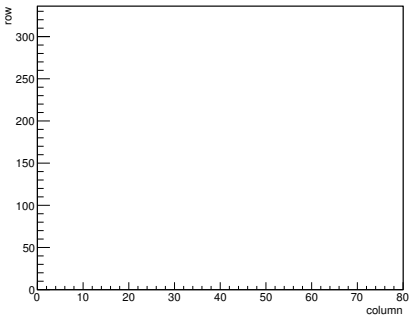

(g) Calibration constant B.

Figure C.134: Detailed plots for test beam measurement of DO-36 (description see section 6.1) sample (running as DUT1) during runs 149-154 in the March 2012 test beam period at DESY. Summary of the data in chapter 9. *(cont.)*

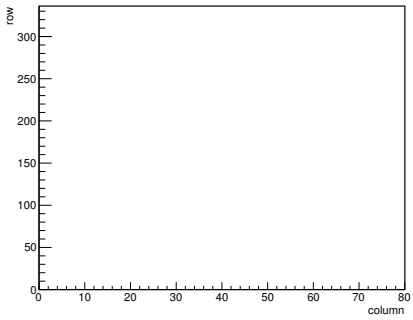

(h) Calibration constant C.

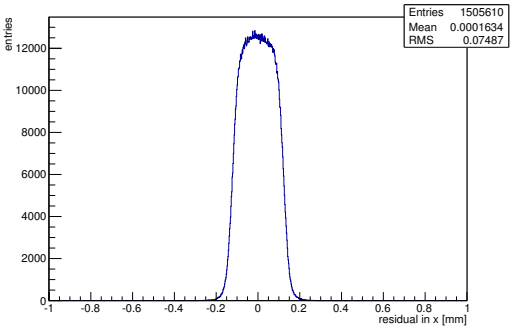

(i) Track residual in x.

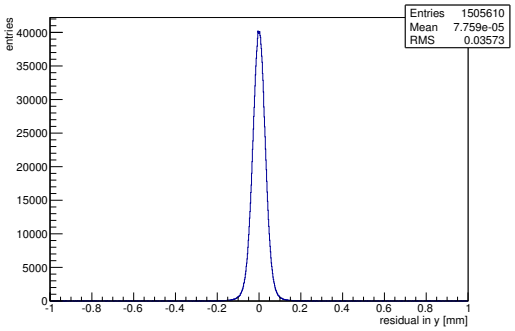

(j) Track residual in y.

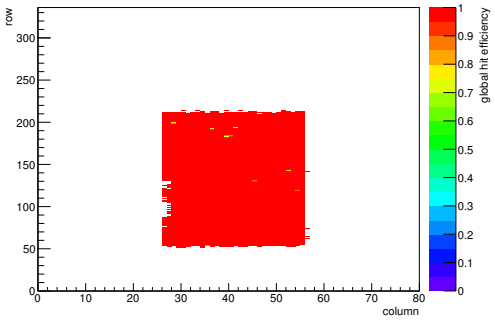

(k) Hit efficiency map.

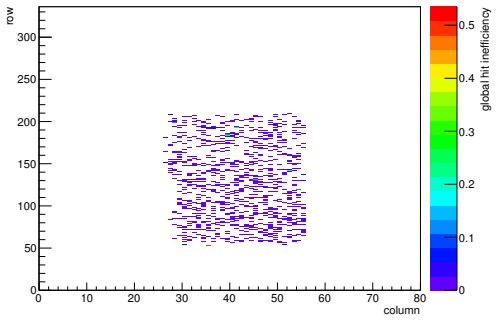

(l) Hit inefficiency map.

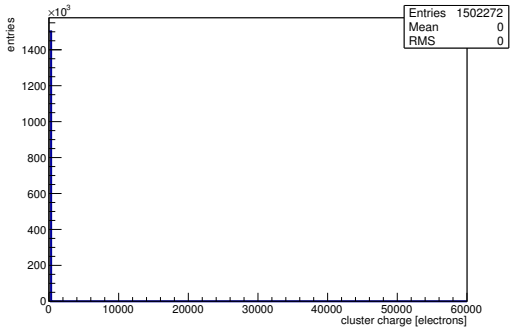

(m) Charge distribution (all cluster sizes included).

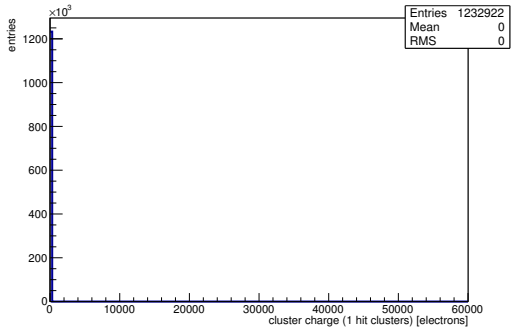

(n) Charge distribution (1 hit cluster).

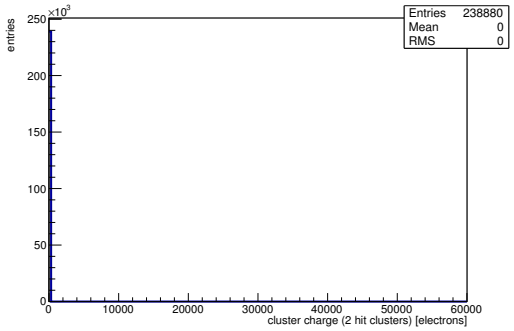

(o) Charge distribution (2 hit cluster).

Figure C.134: Detailed plots for test beam measurement of DO-36 (description see section 6.1) sample (running as DUT1) during runs 149-154 in the March 2012 test beam period at DESY. Summary of the data in chapter 9. *(cont.)*

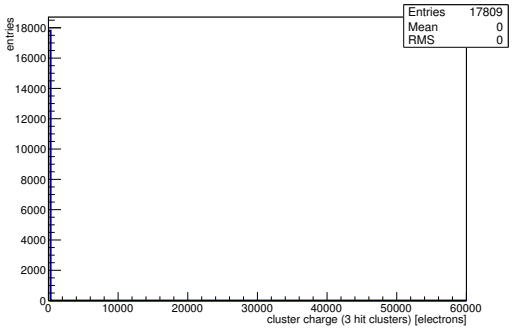

(p) Charge distribution (3 hit cluster).

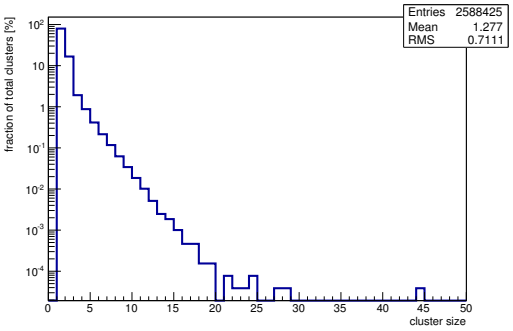

(q) Cluster size distribution.

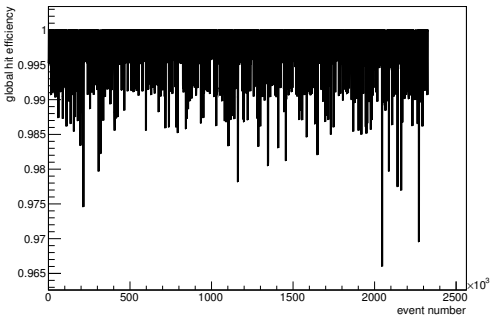

(r) Hit efficiency vs event number.

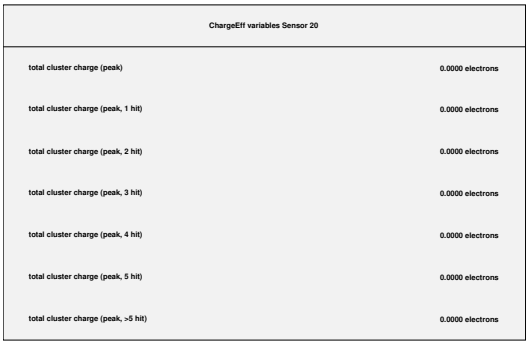

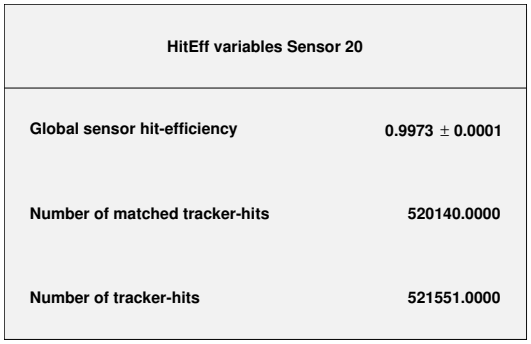

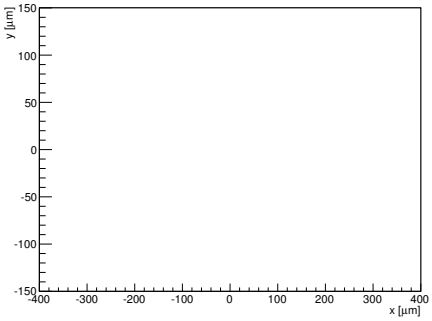

(s) Single pixel mean charge.

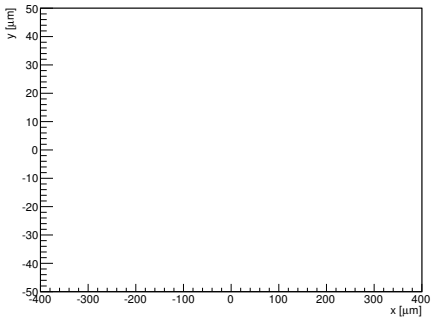

(t) Single pixel mean charge.

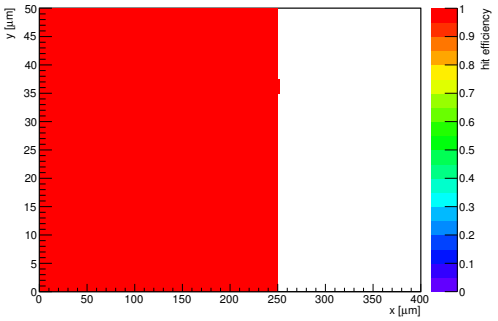

(u) Single pixel hit efficiency.

Figure C.134: Detailed plots for test beam measurement of DO-36 (description see section 6.1) sample (running as DUT1) during runs 149-154 in the March 2012 test beam period at DESY. Summary of the data in chapter 9.

C.4.5 Runs 160-165

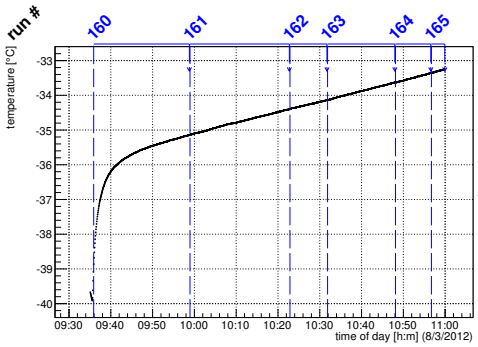

(a) Temperature vs time.

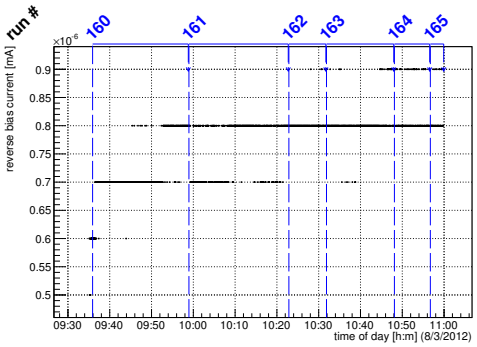

(b) Bias current vs time.

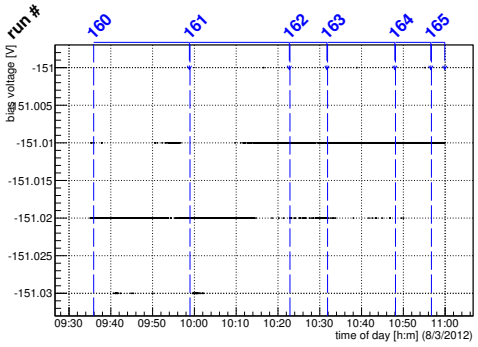

(c) Currently applied bias voltage vs time.

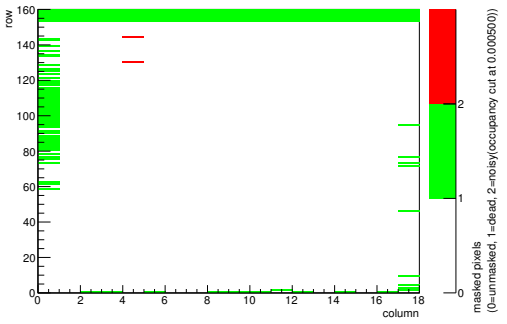

(d) Map of masked pixels.

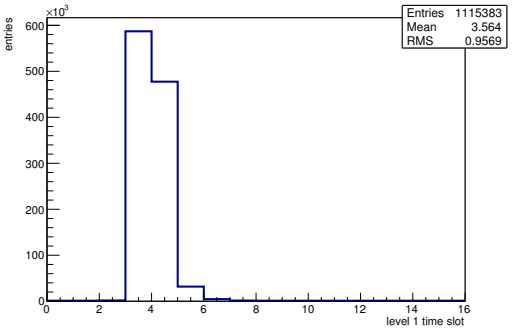

(e) Lvl1 distribution.

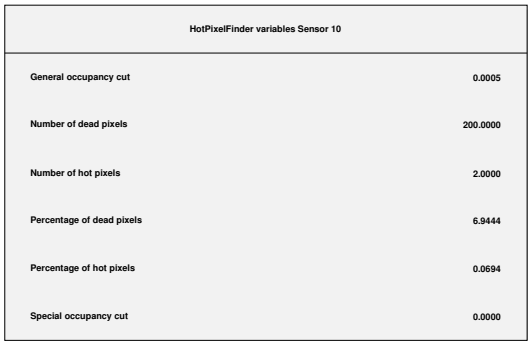

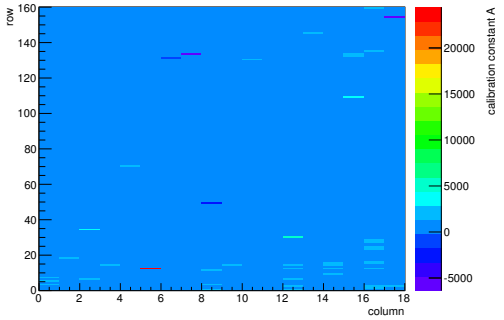

(f) Calibration constant A.

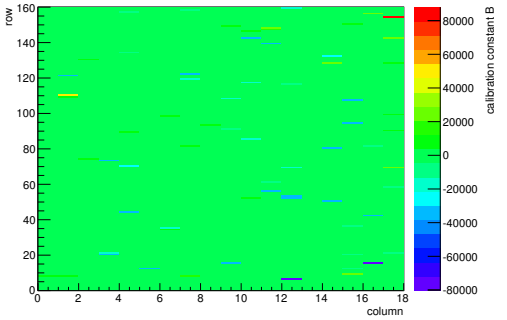

(g) Calibration constant B.

Figure C.135: Detailed plots for test beam measurement of SCC-31 (description see section 6.1) sample (running as DUT0) during runs 160-165 in the March 2012 test beam period at DESY. Summary of the data in chapter 9. *(cont.)*

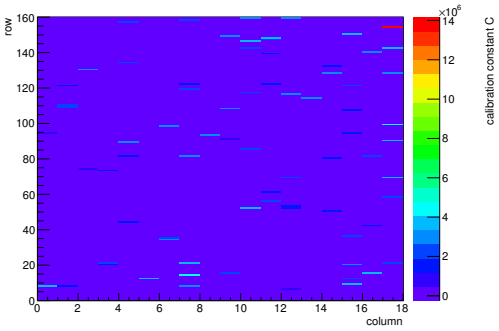

(h) Calibration constant C.

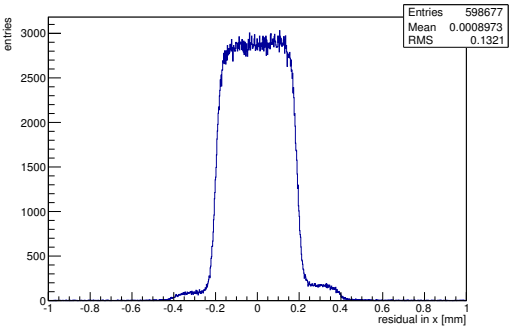

(i) Track residual in x.

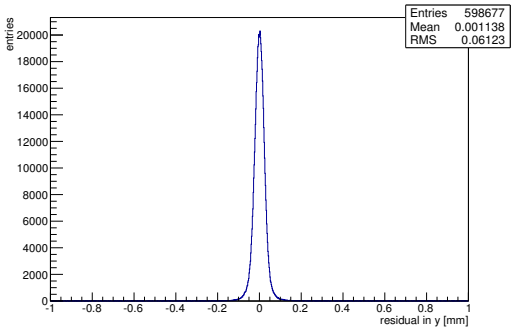

(j) Track residual in y.

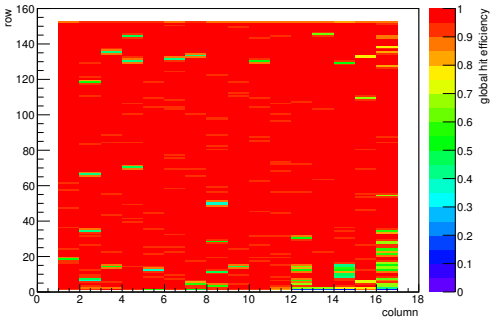

(k) Hit efficiency map.

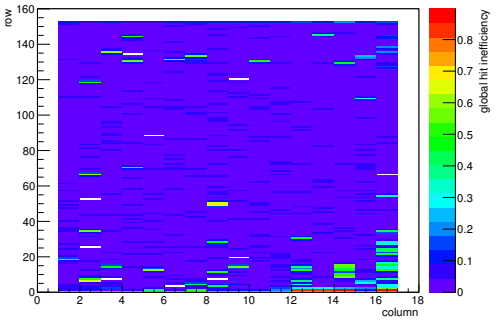

(l) Hit inefficiency map.

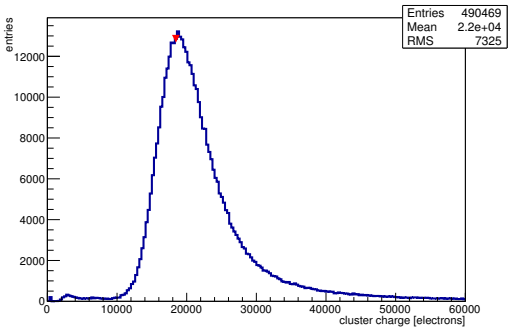

(m) Charge distribution (all cluster sizes included).

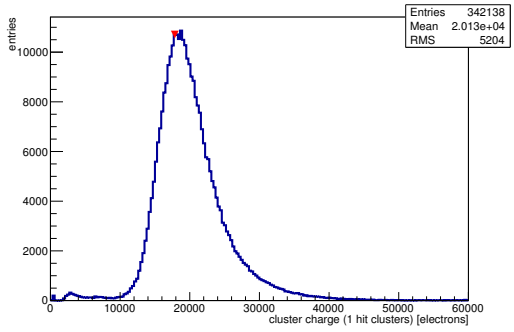

(n) Charge distribution (1 hit cluster).

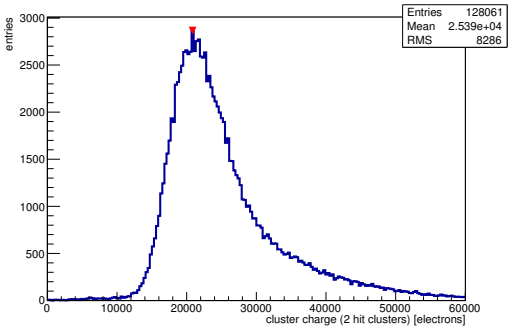

(o) Charge distribution (2 hit cluster).

Figure C.135: Detailed plots for test beam measurement of SCC-31 (description see section 6.1) sample (running as DUT0) during runs 160-165 in the March 2012 test beam period at DESY. Summary of the data in chapter 9. *(cont.)*

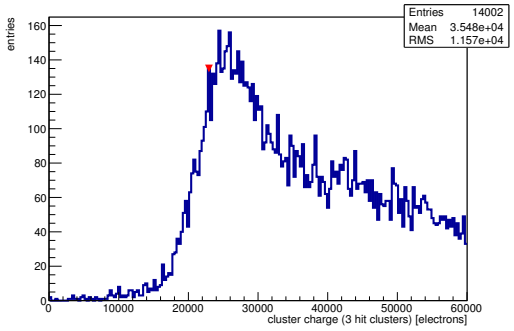

(p) Charge distribution (3 hit cluster).

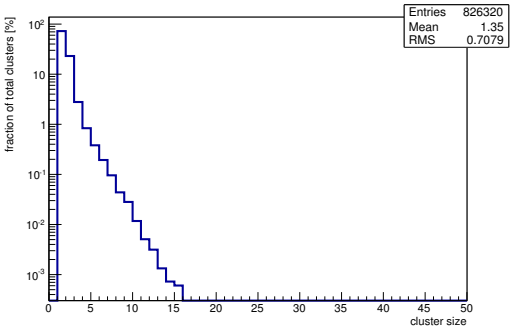

(q) Cluster size distribution.

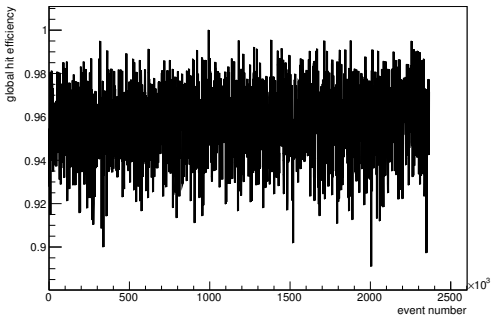

(r) Hit efficiency vs event number.

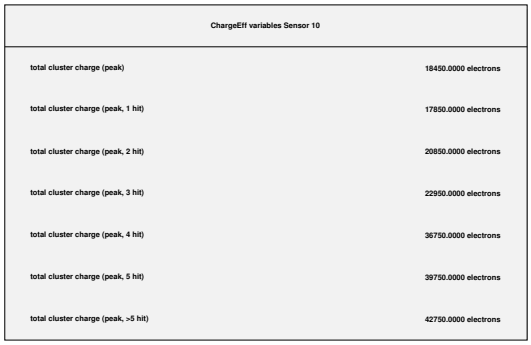

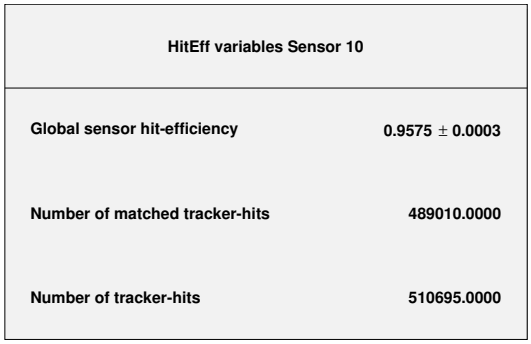

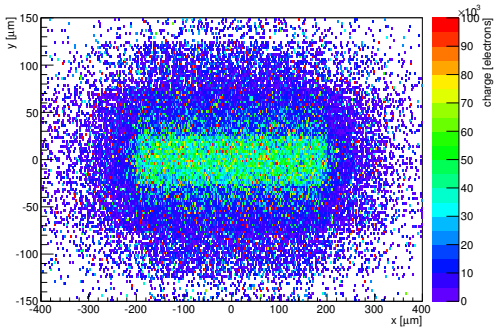

(s) Single pixel mean charge.

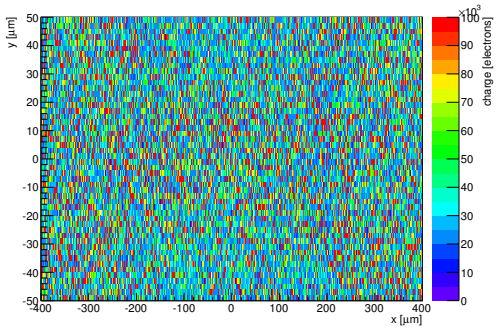

(t) Single pixel mean charge.

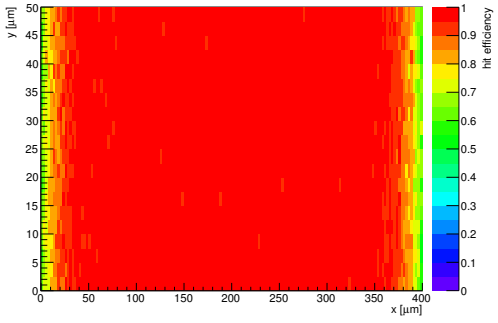

(u) Single pixel hit efficiency.

Figure C.135: Detailed plots for test beam measurement of SCC-31 (description see section 6.1) sample (running as DUT0) during runs 160-165 in the March 2012 test beam period at DESY. Summary of the data in chapter 9.

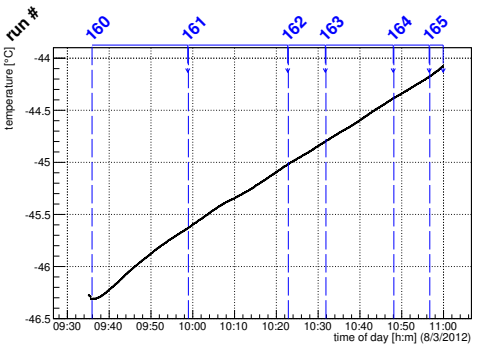

(a) Temperature vs time.

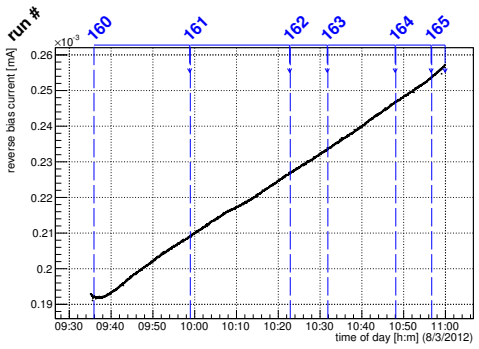

(b) Bias current vs time.

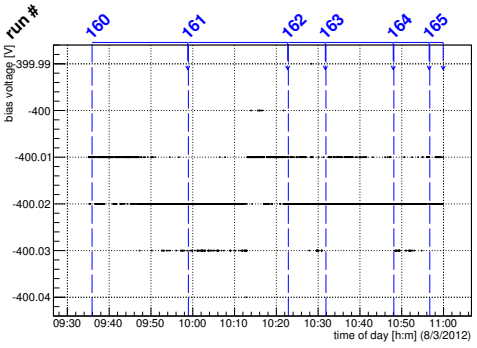

(c) Currently applied bias voltage vs time.

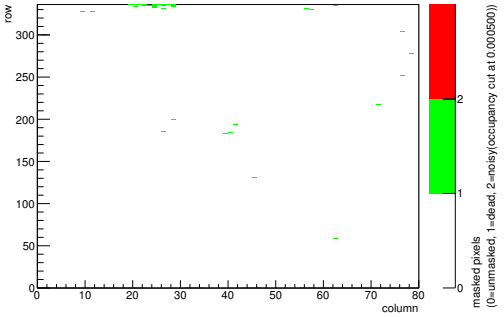

(d) Map of masked pixels.

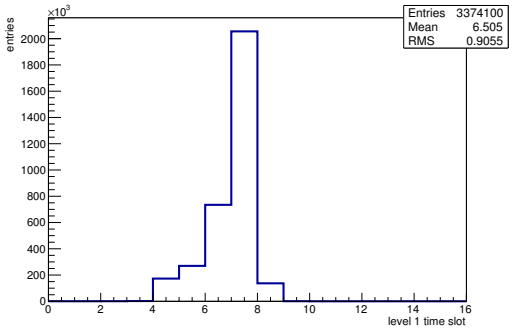

(e) Lvl1 distribution.

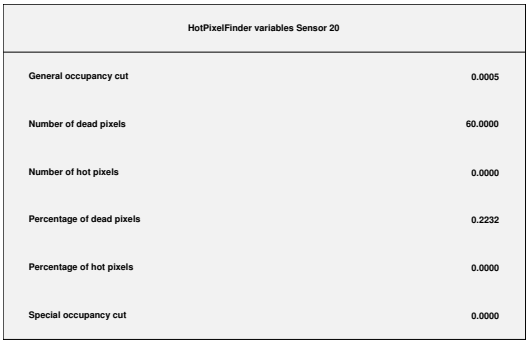

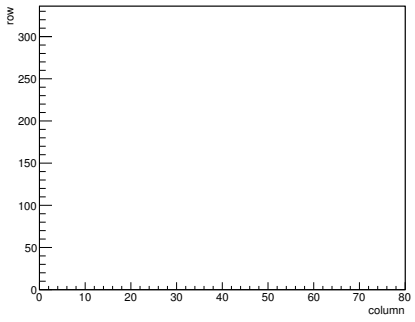

(f) Calibration constant A.

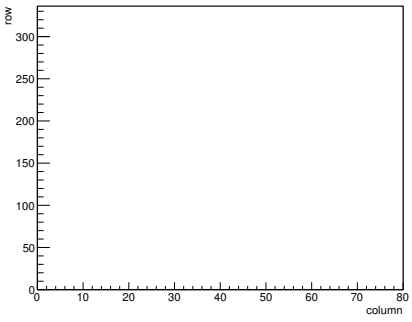

(g) Calibration constant B.

Figure C.136: Detailed plots for test beam measurement of DO-36 (description see section 6.1) sample (running as DUT1) during runs 160-165 in the March 2012 test beam period at DESY. Summary of the data in chapter 9. *(cont.)*

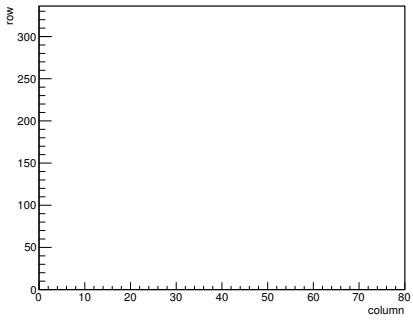

(h) Calibration constant C.

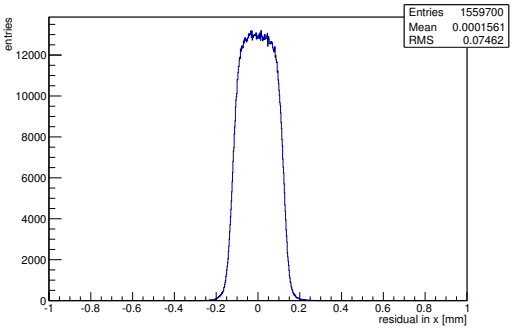

(i) Track residual in x.

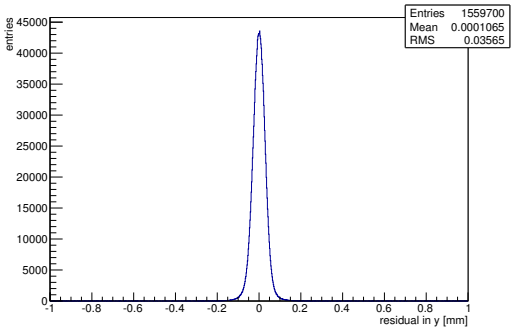

(j) Track residual in y.

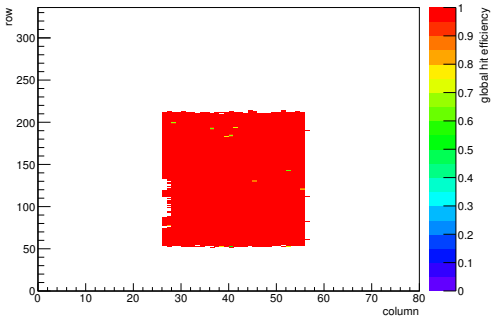

(k) Hit efficiency map.

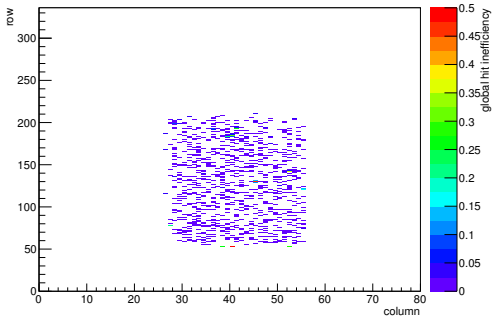

(l) Hit inefficiency map.

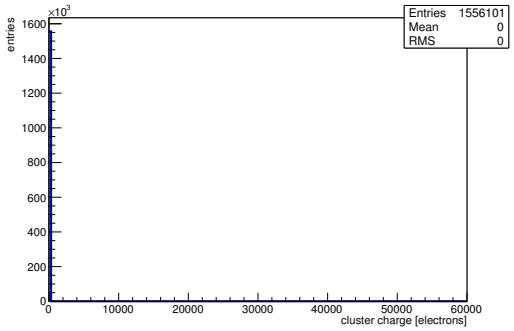

(m) Charge distribution (all cluster sizes included).

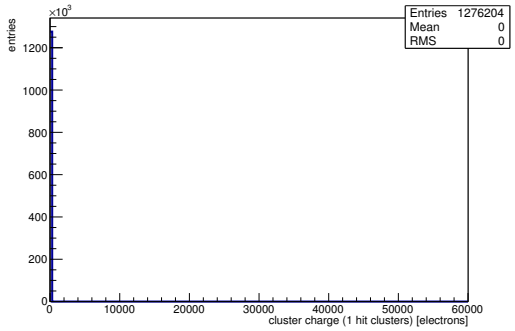

(n) Charge distribution (1 hit cluster).

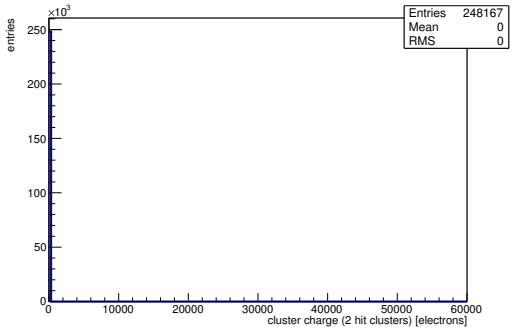

(o) Charge distribution (2 hit cluster).

Figure C.136: Detailed plots for test beam measurement of DO-36 (description see section 6.1) sample (running as DUT1) during runs 160-165 in the March 2012 test beam period at DESY. Summary of the data in chapter 9. *(cont.)*

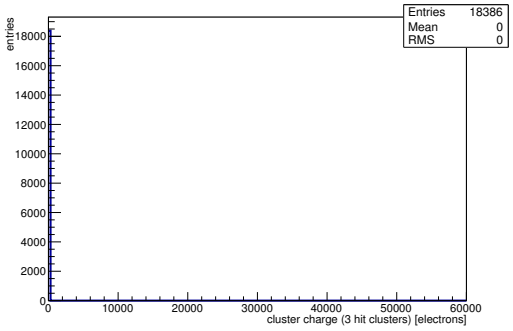

(p) Charge distribution (3 hit cluster).

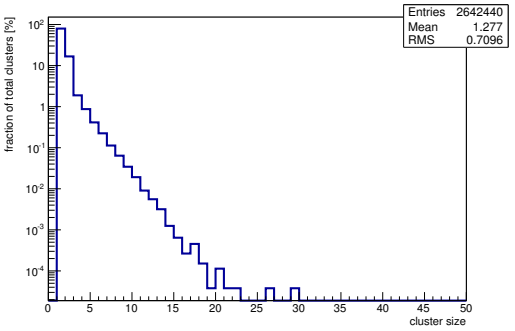

(q) Cluster size distribution.

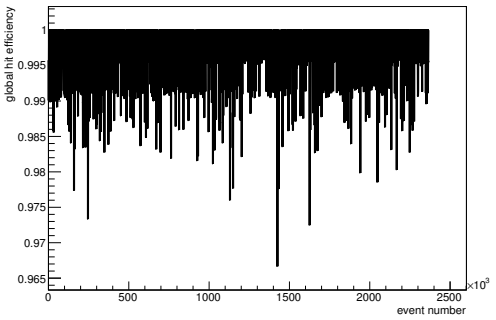

(r) Hit efficiency vs event number.

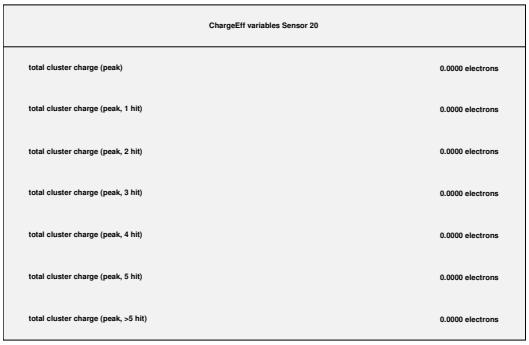

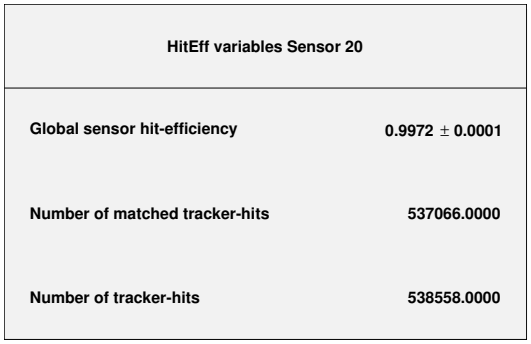

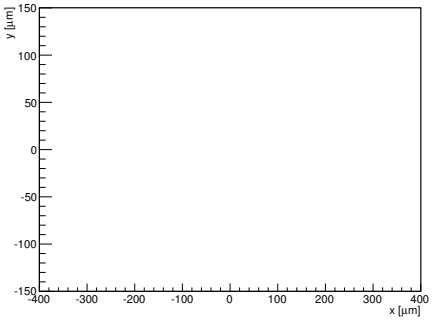

(s) Single pixel mean charge.

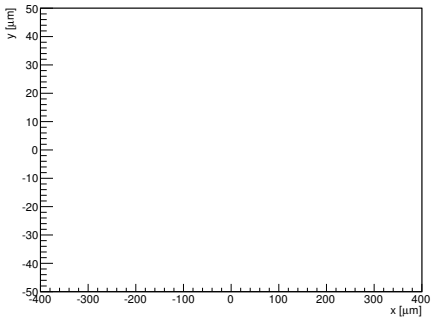

(t) Single pixel mean charge.

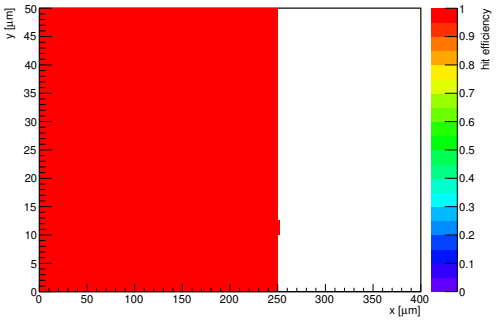

(u) Single pixel hit efficiency.

Figure C.136: Detailed plots for test beam measurement of DO-36 (description see section 6.1) sample (running as DUT1) during runs 160-165 in the March 2012 test beam period at DESY. Summary of the data in chapter 9.

C.4.6 Runs 166-172

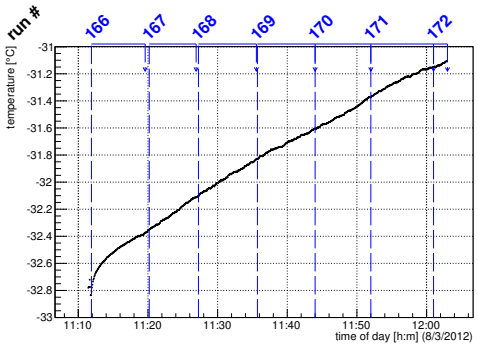

(a) Temperature vs time.

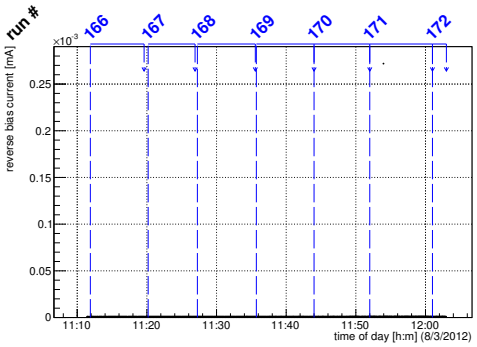

(b) Bias current vs time.

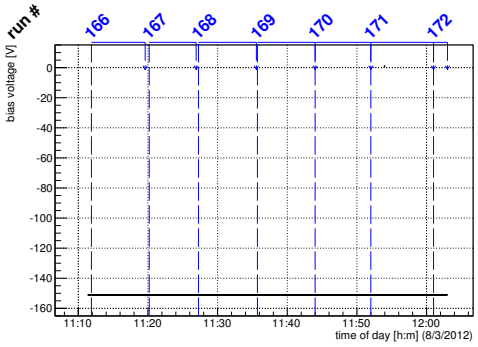

(c) Currently applied bias voltage vs time.

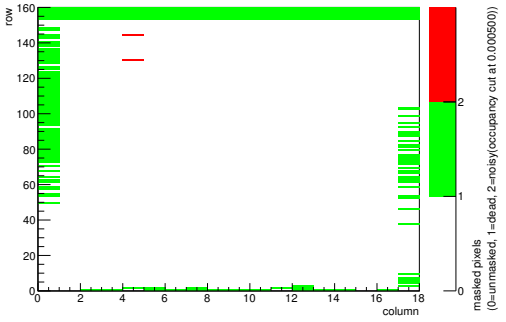

(d) Map of masked pixels.

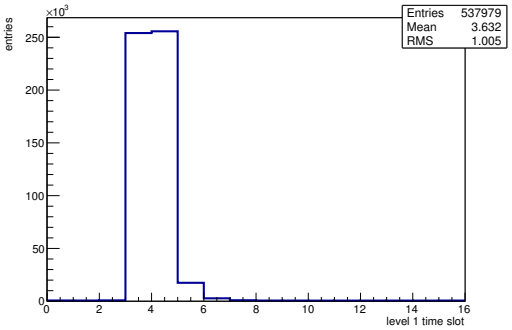

(e) Lvl1 distribution.

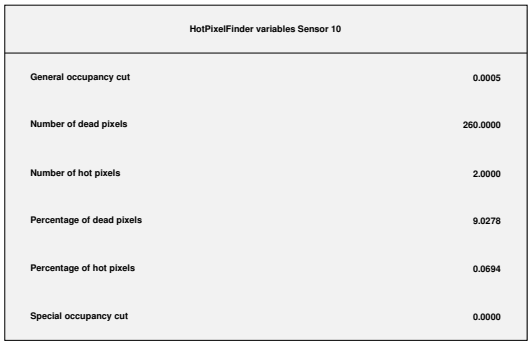

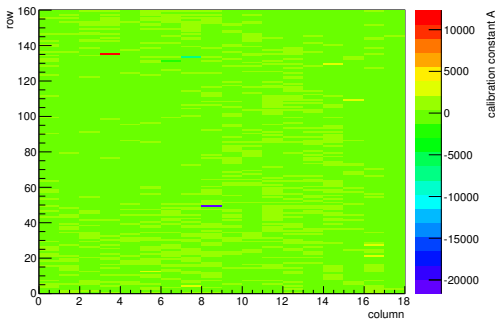

(f) Calibration constant A.

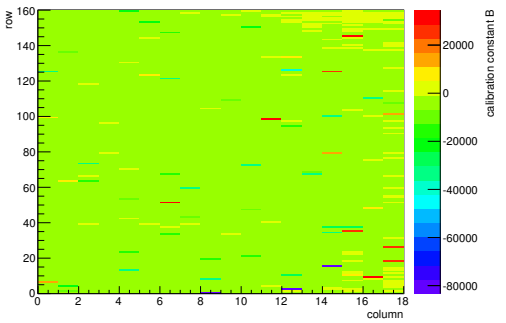

(g) Calibration constant B.

Figure C.137: Detailed plots for test beam measurement of SCC-31 (description see section 6.1) sample (running as DUT0) during runs 166-172 in the March 2012 test beam period at DESY. Summary of the data in chapter 9. *(cont.)*

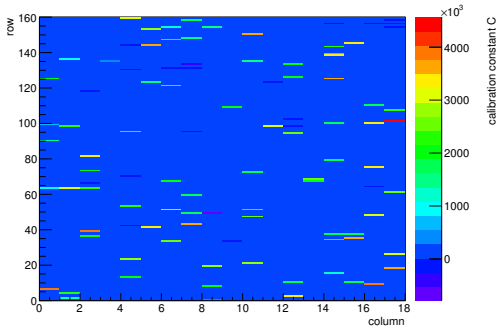

(h) Calibration constant C.

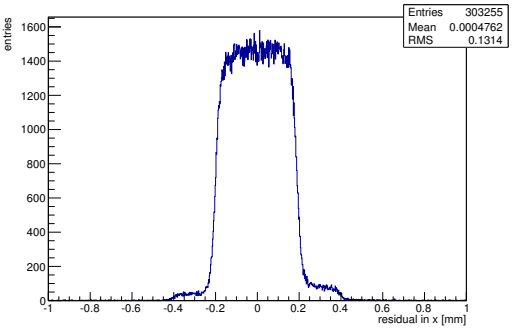

(i) Track residual in x.

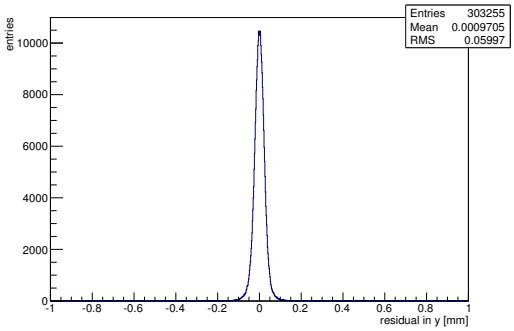

(j) Track residual in y.

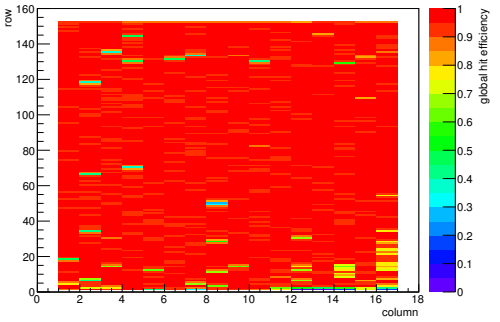

(k) Hit efficiency map.

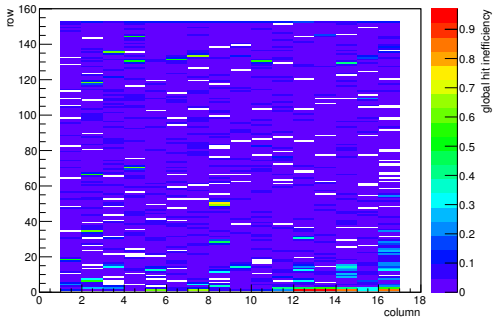

(l) Hit inefficiency map.

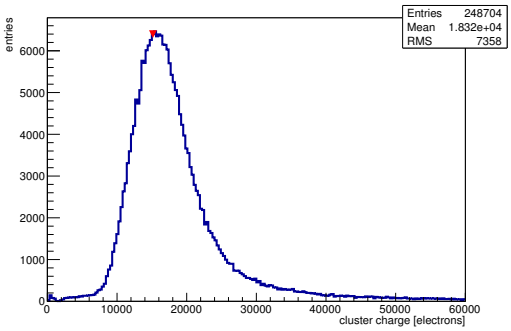

(m) Charge distribution (all cluster sizes included).

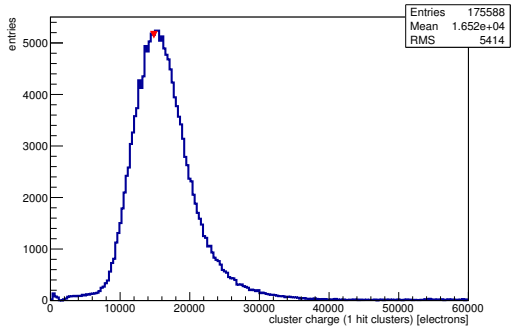

(n) Charge distribution (1 hit cluster).

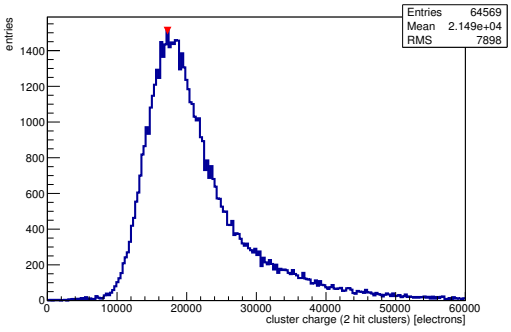

(o) Charge distribution (2 hit cluster).

Figure C.137: Detailed plots for test beam measurement of SCC-31 (description see section 6.1) sample (running as DUT0) during runs 166-172 in the March 2012 test beam period at DESY. Summary of the data in chapter 9. *(cont.)*

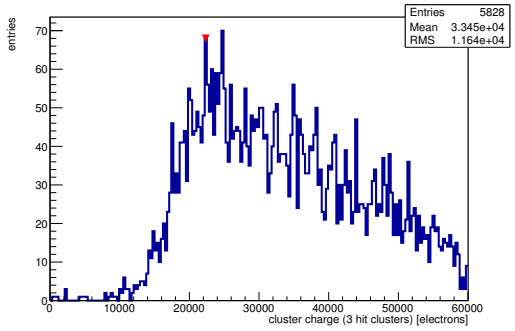

(p) Charge distribution (3 hit cluster).

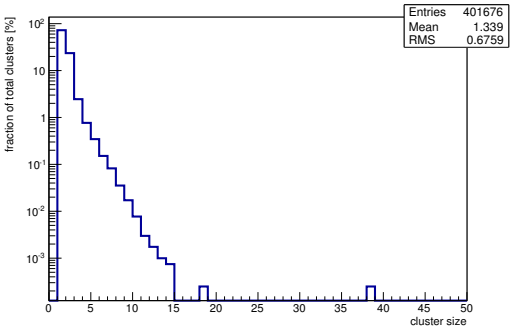

(q) Cluster size distribution.

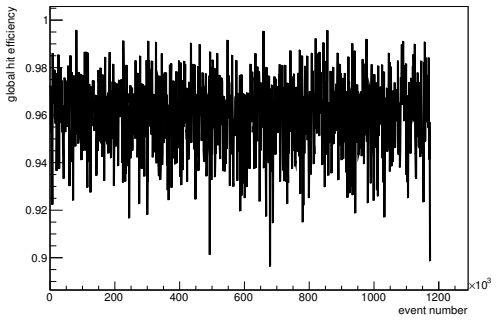

(r) Hit efficiency vs event number.

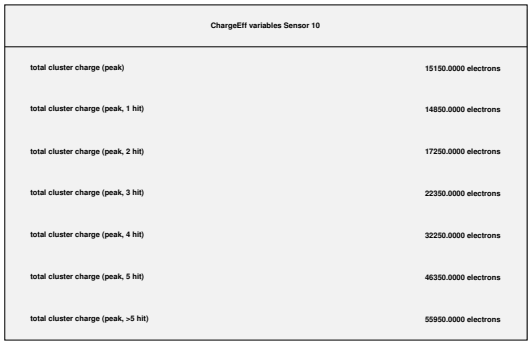

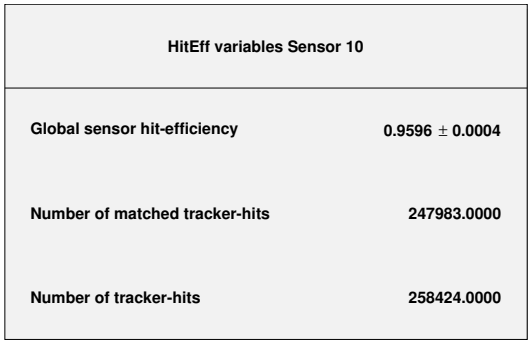

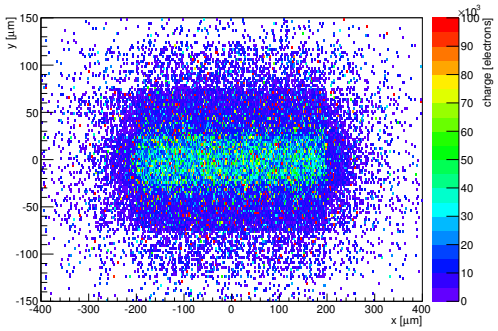

(s) Single pixel mean charge.

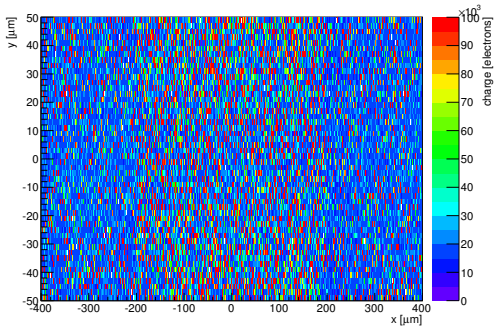

(t) Single pixel mean charge.

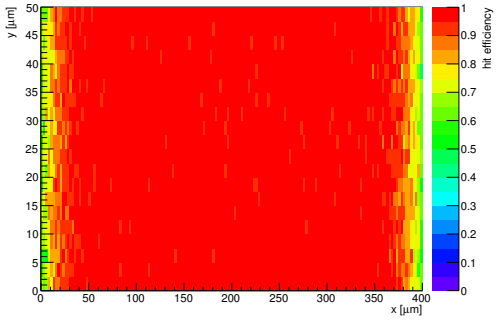

(u) Single pixel hit efficiency.

Figure C.137: Detailed plots for test beam measurement of SCC-31 (description see section 6.1) sample (running as DUT0) during runs 166-172 in the March 2012 test beam period at DESY. Summary of the data in chapter 9.

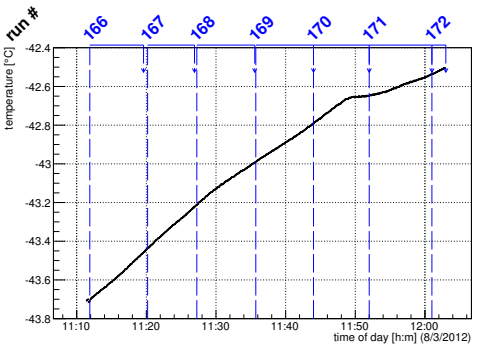

(a) Temperature vs time.

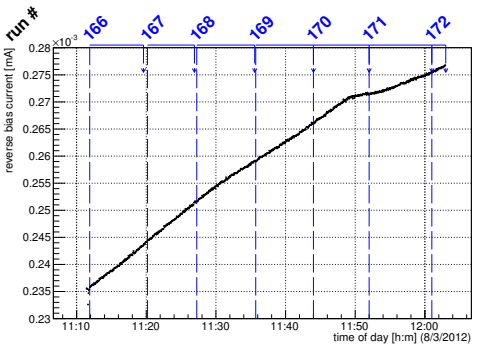

(b) Bias current vs time.

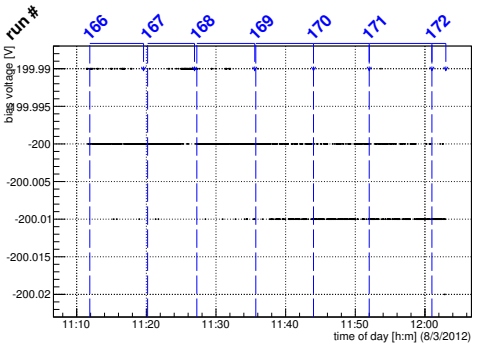

(c) Currently applied bias voltage vs time.

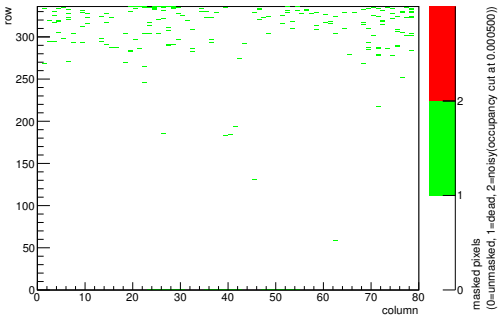

(d) Map of masked pixels.

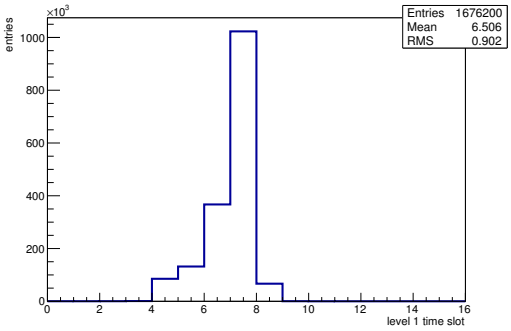

(e) Lvl1 distribution.

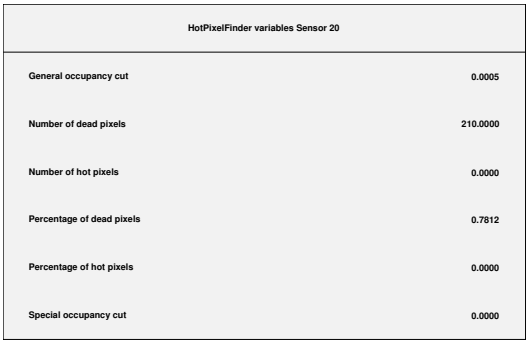

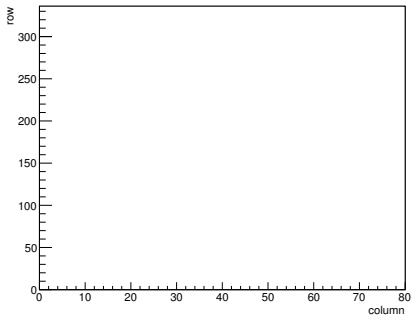

(f) Calibration constant A.

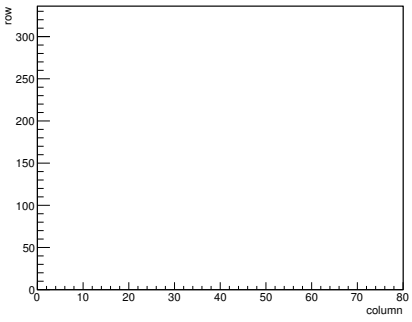

(g) Calibration constant B.

Figure C.138: Detailed plots for test beam measurement of DO-36 (description see section 6.1) sample (running as DUT1) during runs 166-172 in the March 2012 test beam period at DESY. Summary of the data in chapter 9. *(cont.)*

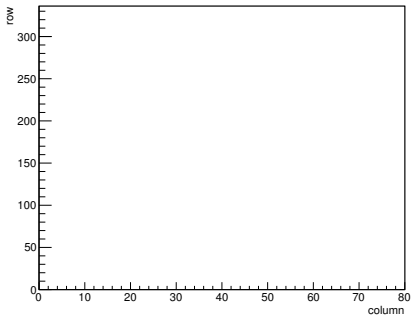

(h) Calibration constant C.

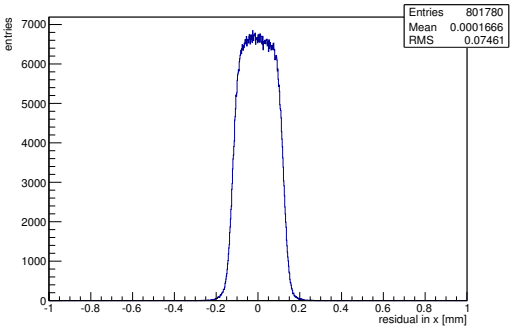

(i) Track residual in x.

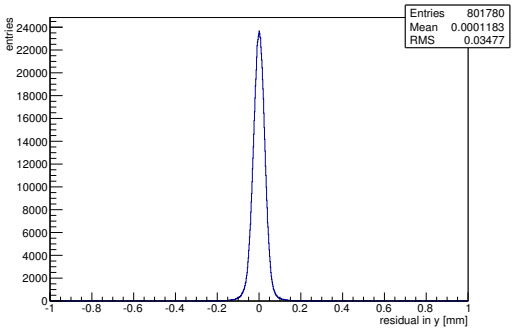

(j) Track residual in y.

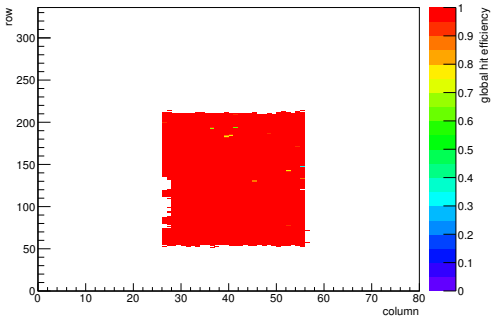

(k) Hit efficiency map.

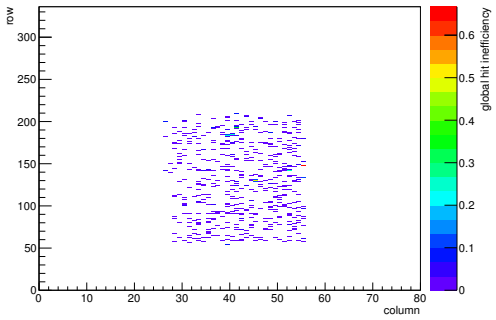

(l) Hit inefficiency map.

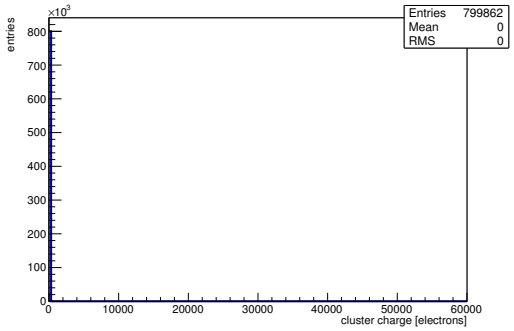

(m) Charge distribution (all cluster sizes included).

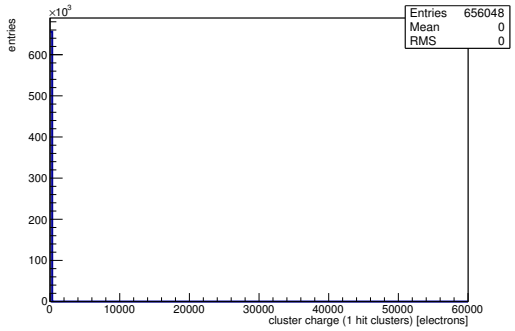

(n) Charge distribution (1 hit cluster).

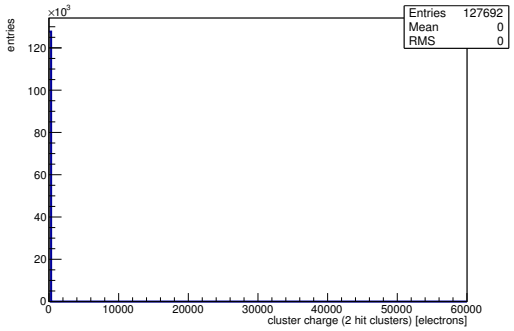

(o) Charge distribution (2 hit cluster).

Figure C.138: Detailed plots for test beam measurement of DO-36 (description see section 6.1) sample (running as DUT1) during runs 166-172 in the March 2012 test beam period at DESY. Summary of the data in chapter 9. *(cont.)*

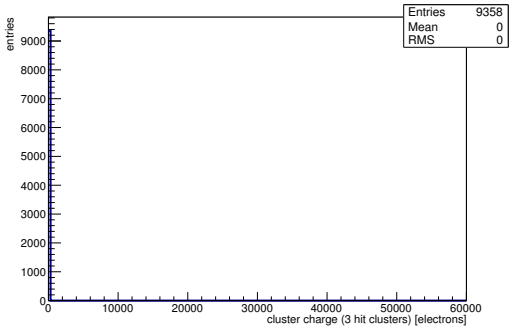

(p) Charge distribution (3 hit cluster).

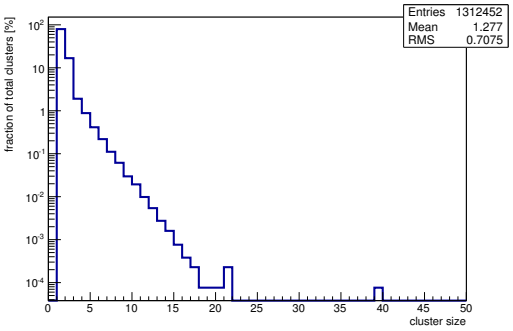

(q) Cluster size distribution.

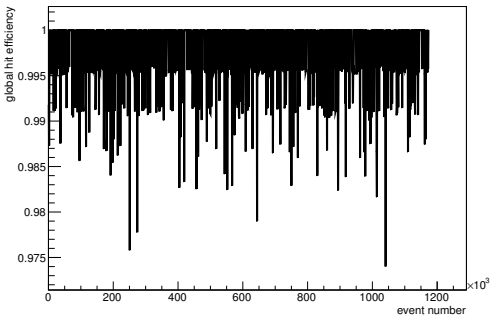

(r) Hit efficiency vs event number.

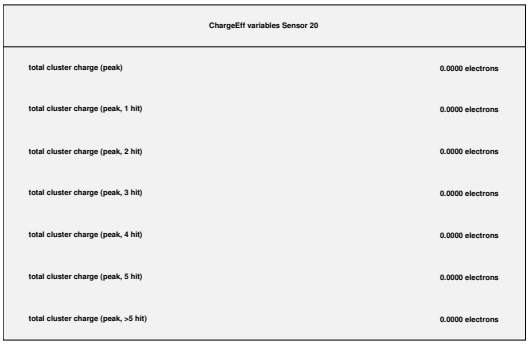

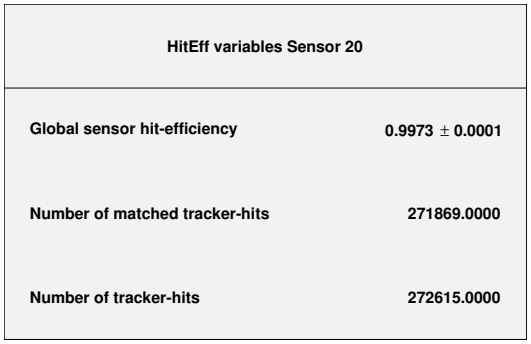

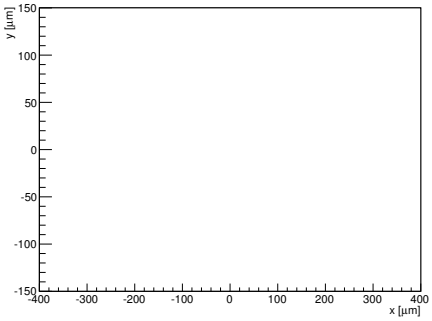

(s) Single pixel mean charge.

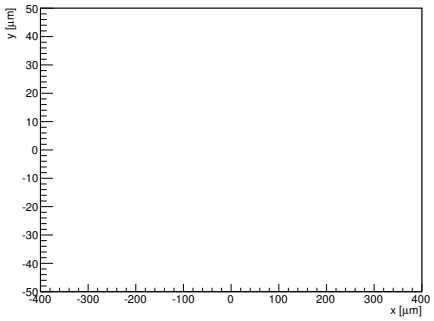

(t) Single pixel mean charge.

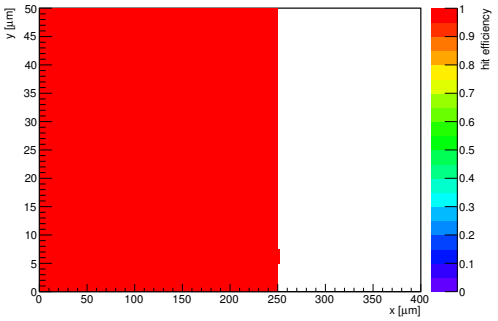

(u) Single pixel hit efficiency.

Figure C.138: Detailed plots for test beam measurement of DO-36 (description see section 6.1) sample (running as DUT1) during runs 166-172 in the March 2012 test beam period at DESY. Summary of the data in chapter 9.

C.4.7 Runs 210-249

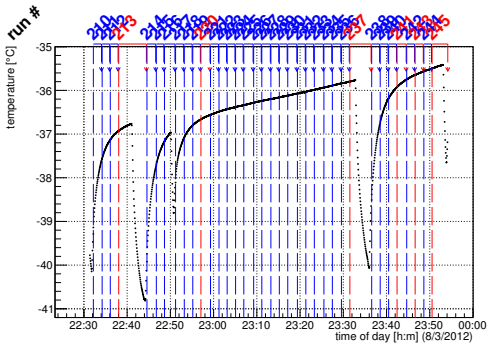

(a) Temperature vs time.

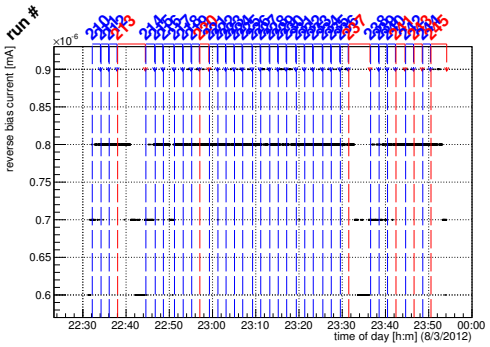

(b) Bias current vs time.

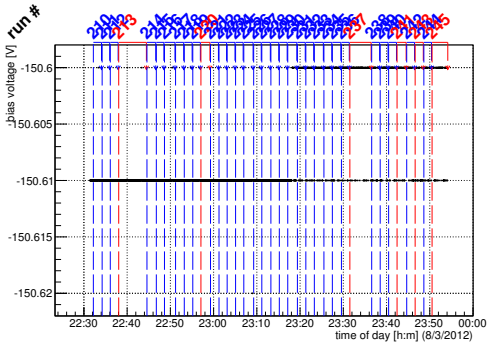

(c) Currently applied bias voltage vs time.

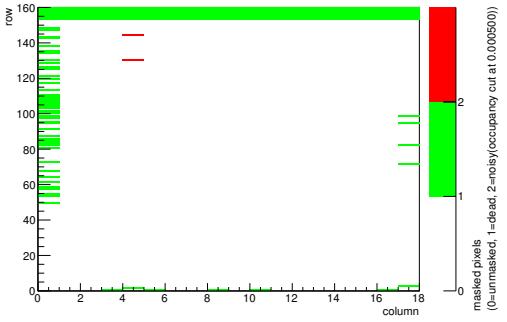

(d) Map of masked pixels.

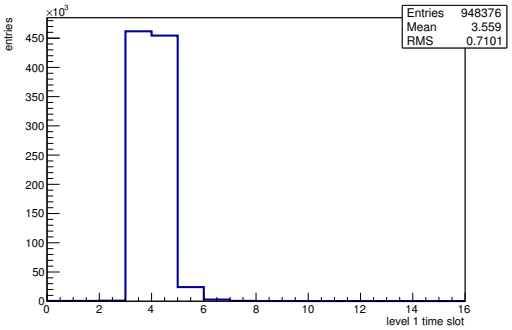

(e) Lvl1 distribution.

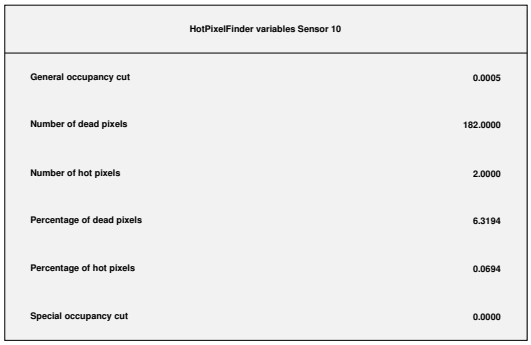

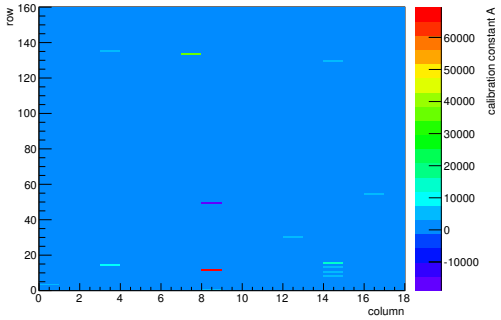

(f) Calibration constant A.

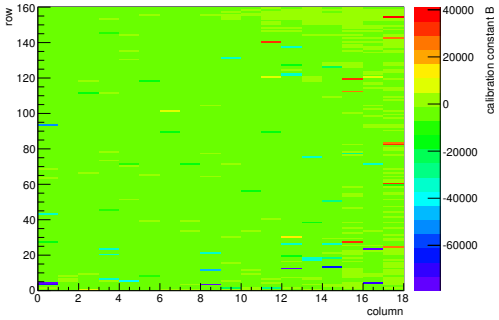

(g) Calibration constant B.

Figure C.139: Detailed plots for test beam measurement of SCC-31 (description see section 6.1) sample (running as DUT0) during runs 210-249 in the March 2012 test beam period at DESY. Summary of the data in chapter 9. *(cont.)*

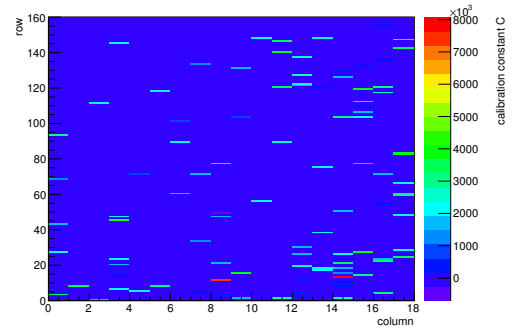

(h) Calibration constant C.

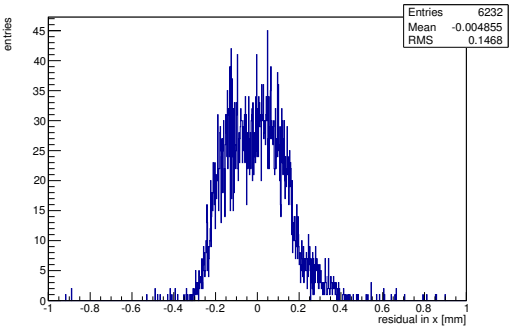

(i) Track residual in x.

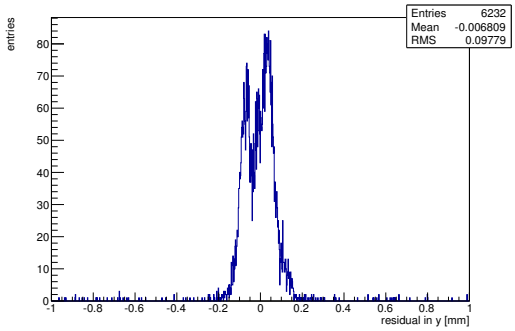

(j) Track residual in y.

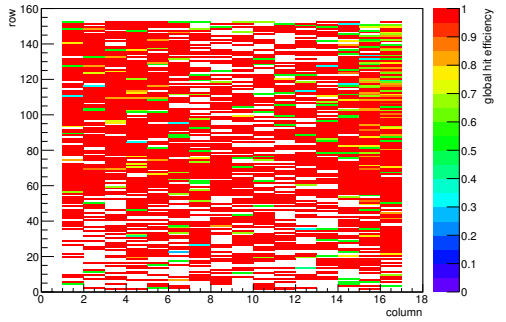

(k) Hit efficiency map.

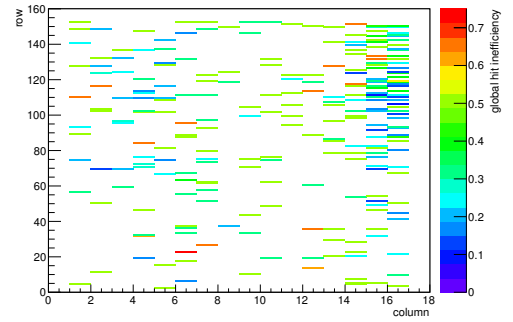

(l) Hit inefficiency map.

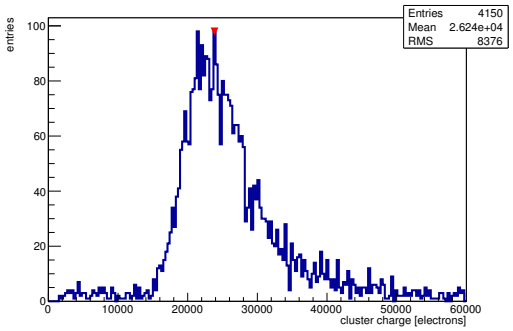

(m) Charge distribution (all cluster sizes included).

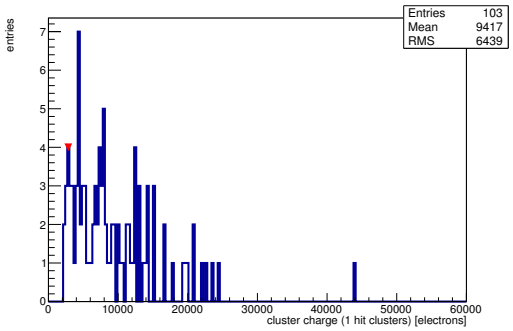

(n) Charge distribution (1 hit cluster).

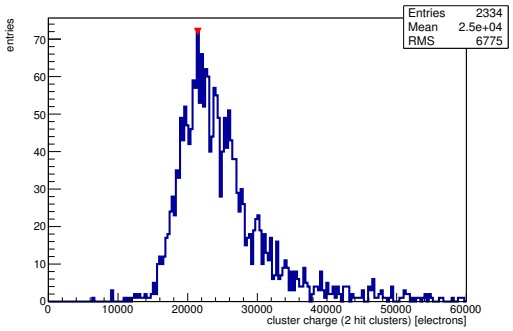

(o) Charge distribution (2 hit cluster).

Figure C.139: Detailed plots for test beam measurement of SCC-31 (description see section 6.1) sample (running as DUT0) during runs 210-249 in the March 2012 test beam period at DESY. Summary of the data in chapter 9. *(cont.)*

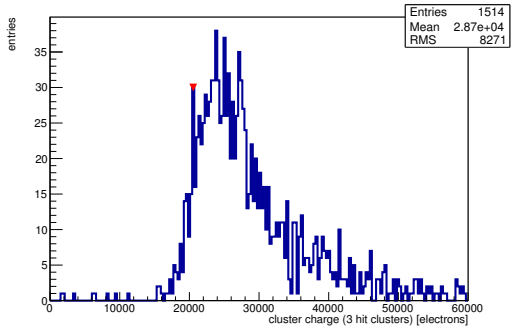

(p) Charge distribution (3 hit cluster).

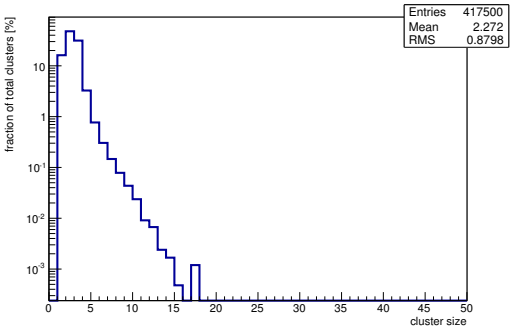

(q) Cluster size distribution.

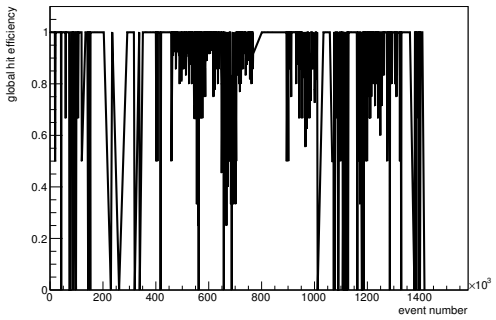

(r) Hit efficiency vs event number.

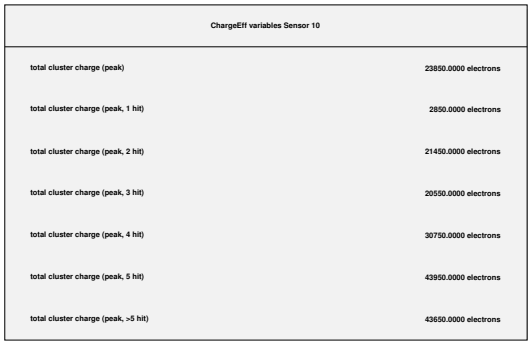

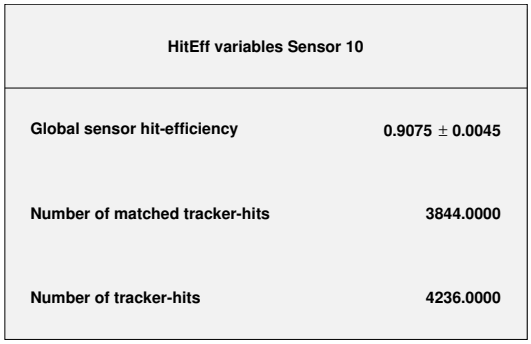

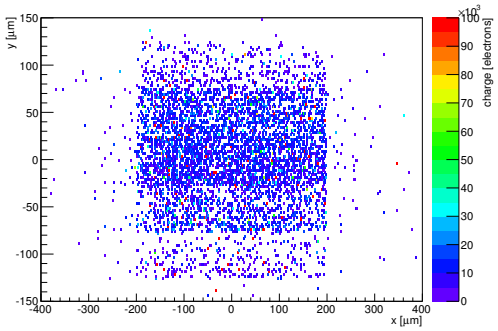

(s) Single pixel mean charge.

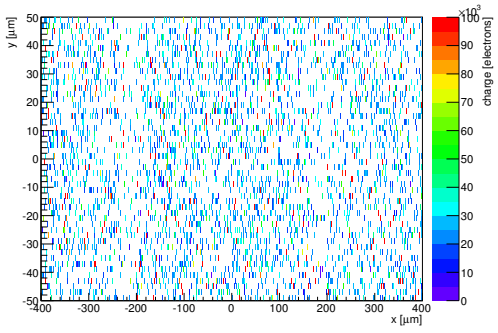

(t) Single pixel mean charge.

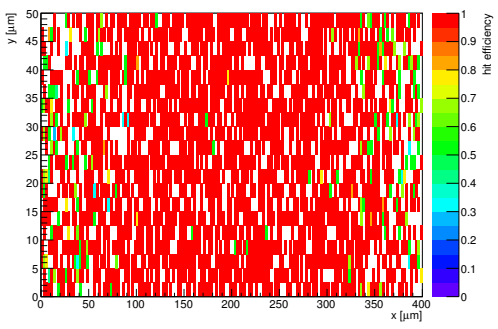

(u) Single pixel hit efficiency.

Figure C.139: Detailed plots for test beam measurement of SCC-31 (description see section 6.1) sample (running as DUT0) during runs 210-249 in the March 2012 test beam period at DESY. Summary of the data in chapter 9.

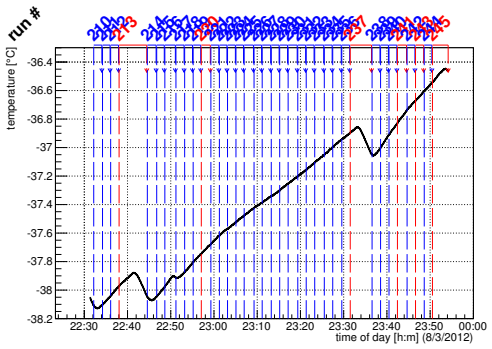

(a) Temperature vs time.

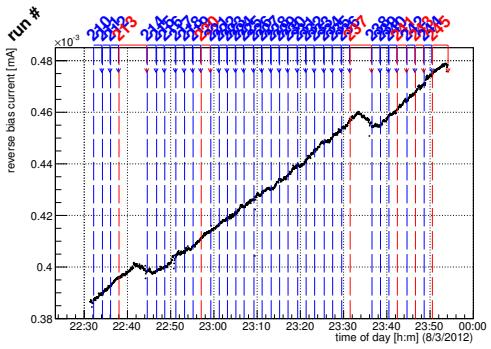

(b) Bias current vs time.

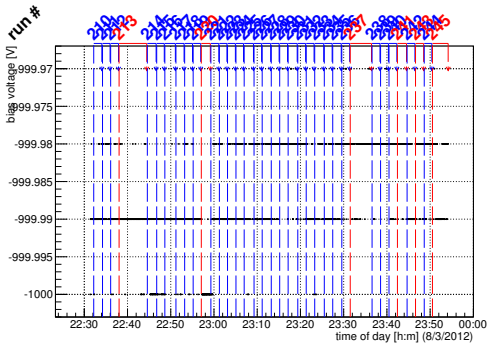

(c) Currently applied bias voltage vs time.

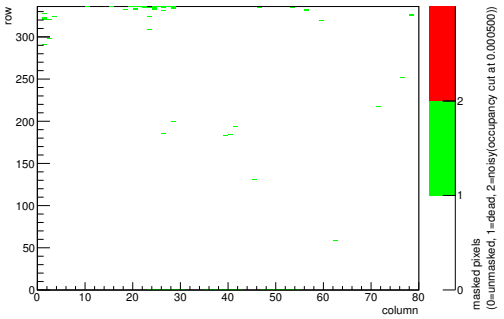

(d) Map of masked pixels.

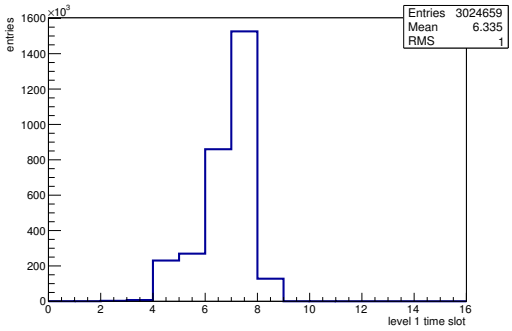

(e) Lvl1 distribution.

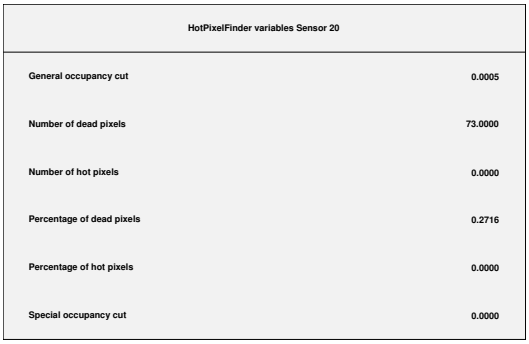

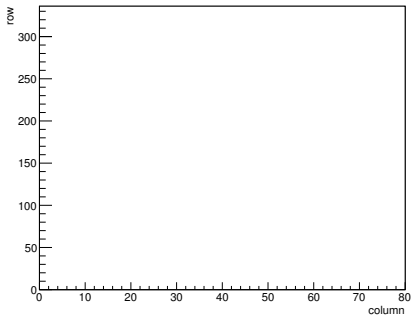

(f) Calibration constant A.

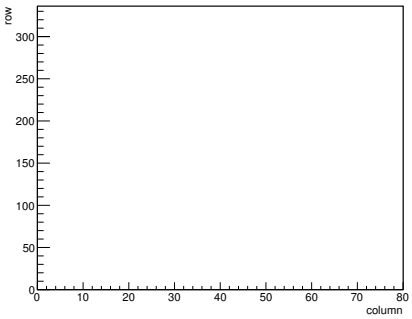

(g) Calibration constant B.

Figure C.140: Detailed plots for test beam measurement of DO-36 (description see section 6.1) sample (running as DUT1) during runs 210-249 in the March 2012 test beam period at DESY. Summary of the data in chapter 9. *(cont.)*

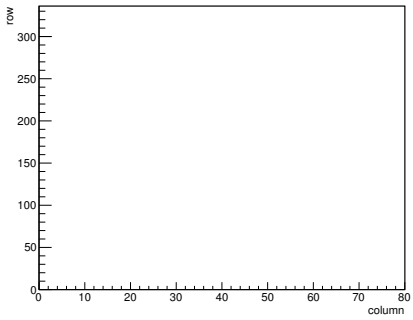

(h) Calibration constant C.

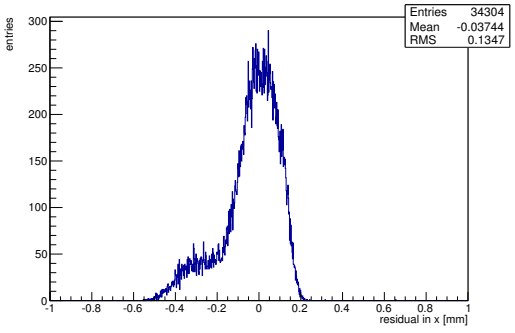

(i) Track residual in x.

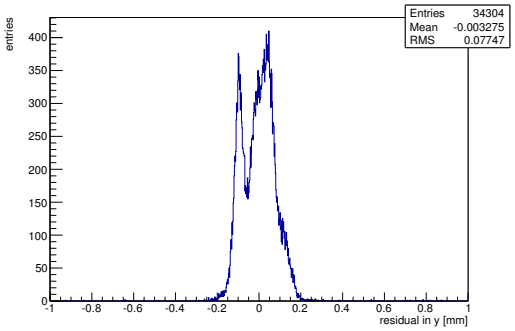

(j) Track residual in y.

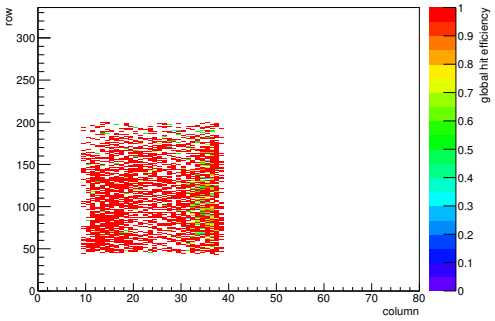

(k) Hit efficiency map.

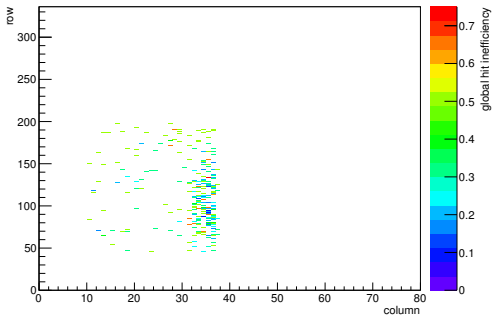

(l) Hit inefficiency map.

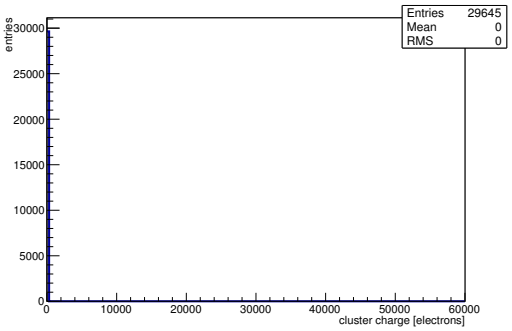

(m) Charge distribution (all cluster sizes included).

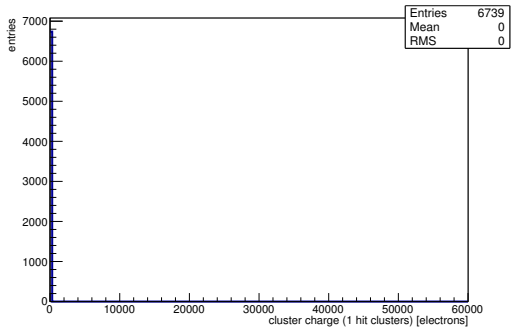

(n) Charge distribution (1 hit cluster).

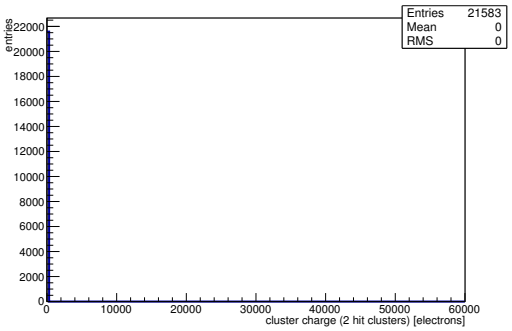

(o) Charge distribution (2 hit cluster).

Figure C.140: Detailed plots for test beam measurement of DO-36 (description see section 6.1) sample (running as DUT1) during runs 210-249 in the March 2012 test beam period at DESY. Summary of the data in chapter 9. *(cont.)*

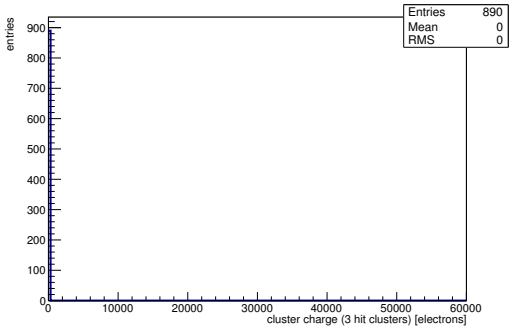

(p) Charge distribution (3 hit cluster).

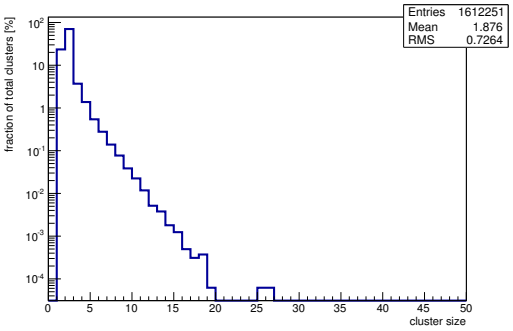

(q) Cluster size distribution.

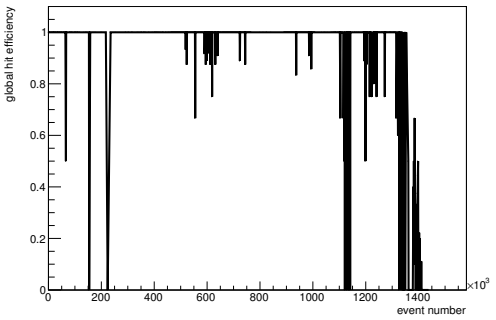

(r) Hit efficiency vs event number.

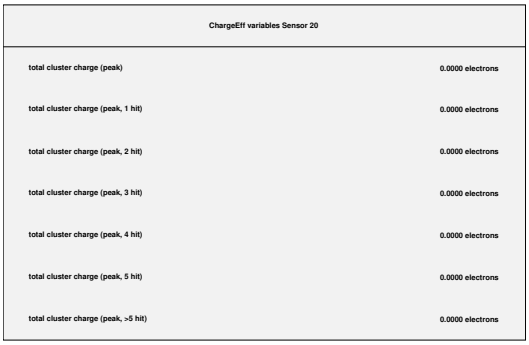

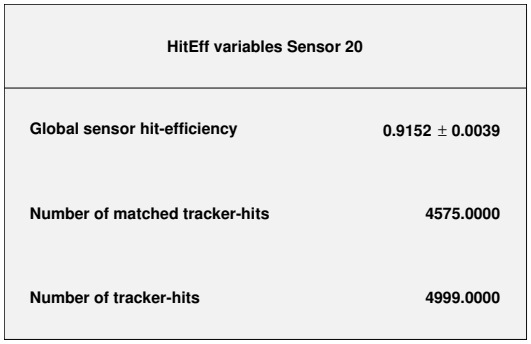

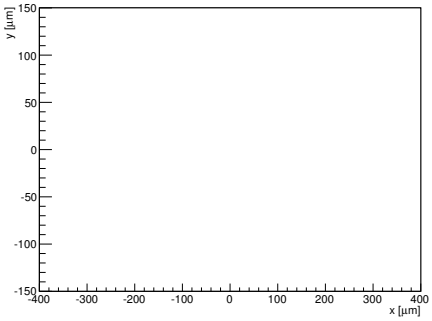

(s) Single pixel mean charge.

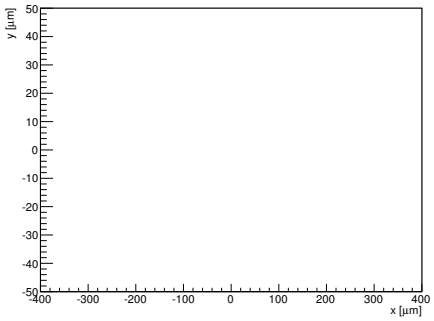

(t) Single pixel mean charge.

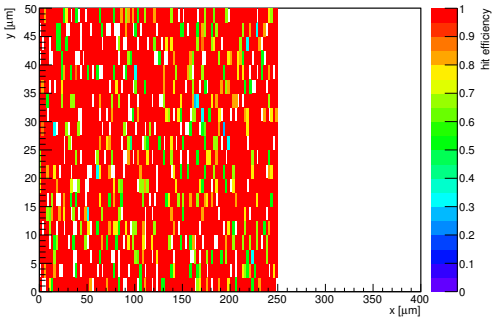

(u) Single pixel hit efficiency.

Figure C.140: Detailed plots for test beam measurement of DO-36 (description see section 6.1) sample (running as DUT1) during runs 210-249 in the March 2012 test beam period at DESY. Summary of the data in chapter 9.

C.4.8 Runs 251-303

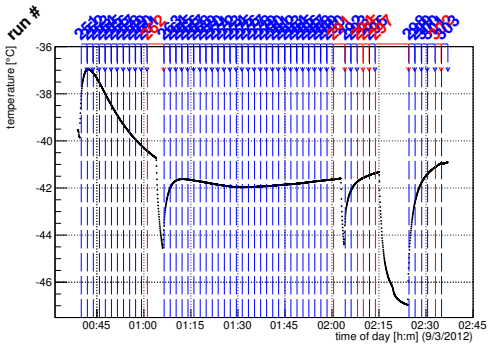

(a) Temperature vs time.

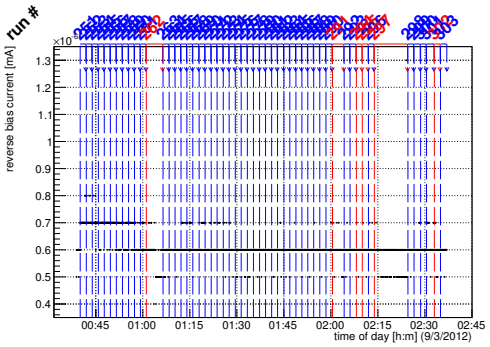

(b) Bias current vs time.

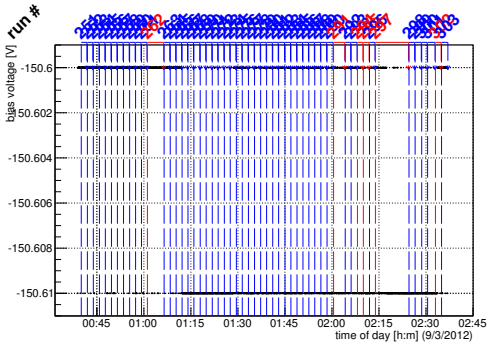

(c) Currently applied bias voltage vs time.

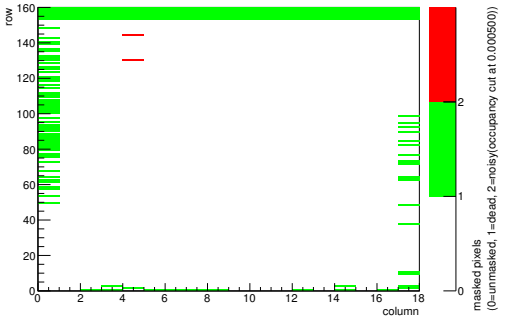

(d) Map of masked pixels.

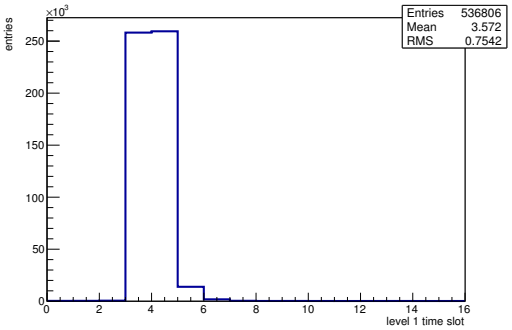

(e) Lvl1 distribution.

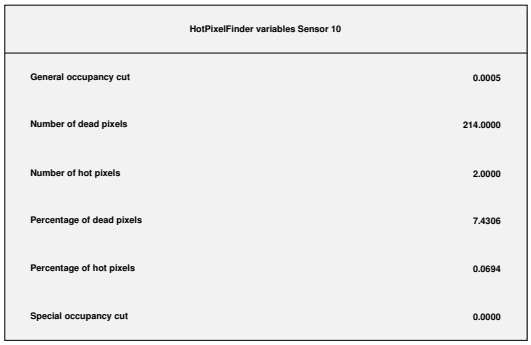

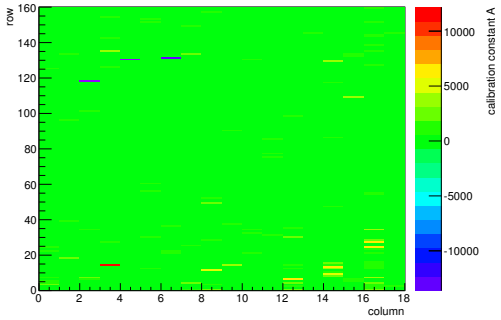

(f) Calibration constant A.

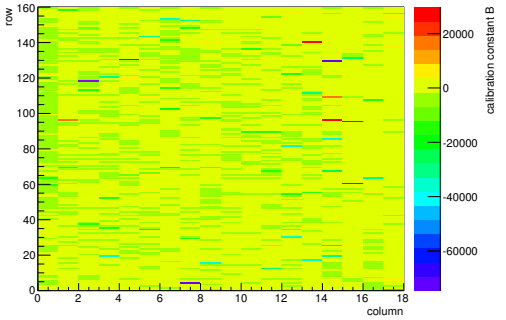

(g) Calibration constant B.

Figure C.141: Detailed plots for test beam measurement of SCC-31 (description see section 6.1) sample (running as DUT0) during runs 251-303 in the March 2012 test beam period at DESY. Summary of the data in chapter 9. *(cont.)*

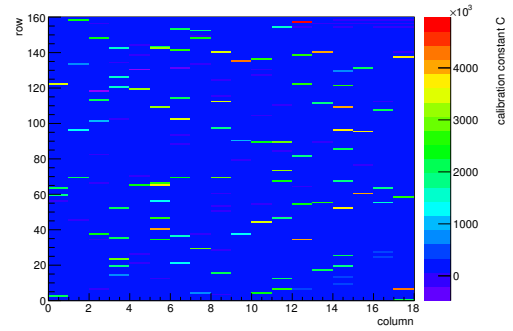

(h) Calibration constant C.

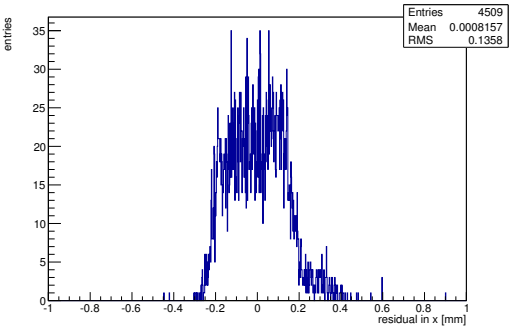

(i) Track residual in x.

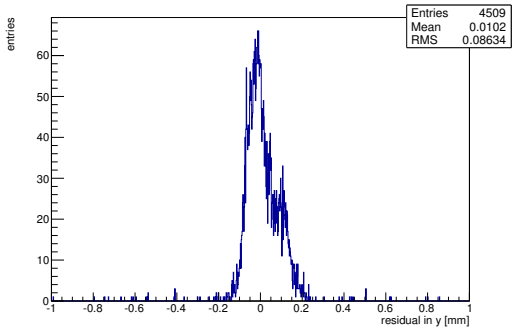

(j) Track residual in y.

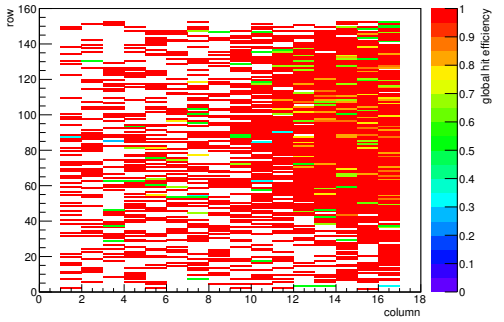

(k) Hit efficiency map.

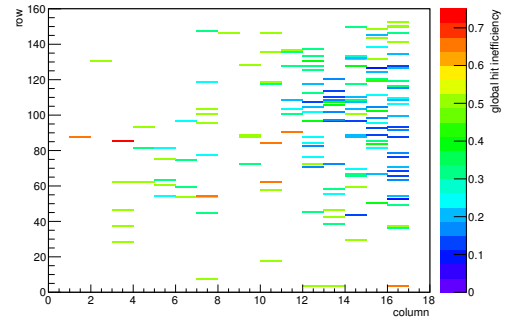

(l) Hit inefficiency map.

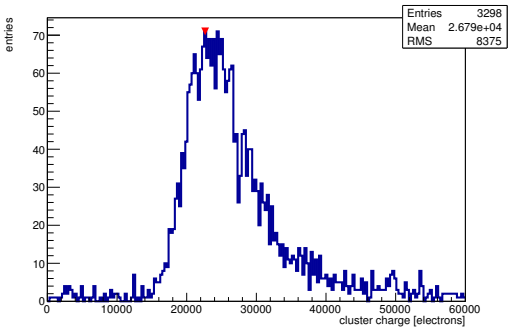

(m) Charge distribution (all cluster sizes included).

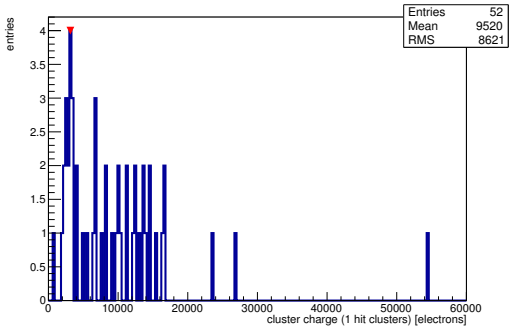

(n) Charge distribution (1 hit cluster).

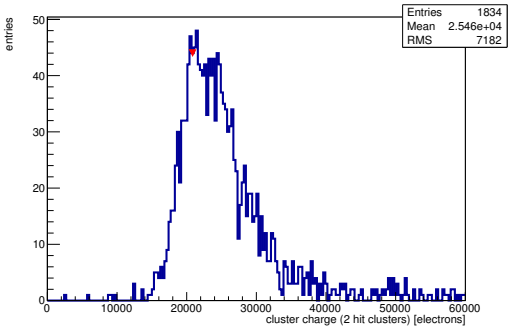

(o) Charge distribution (2 hit cluster).

Figure C.141: Detailed plots for test beam measurement of SCC-31 (description see section 6.1) sample (running as DUT0) during runs 251-303 in the March 2012 test beam period at DESY. Summary of the data in chapter 9. *(cont.)*

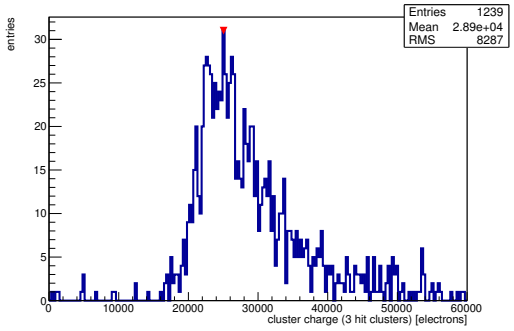

(p) Charge distribution (3 hit cluster).

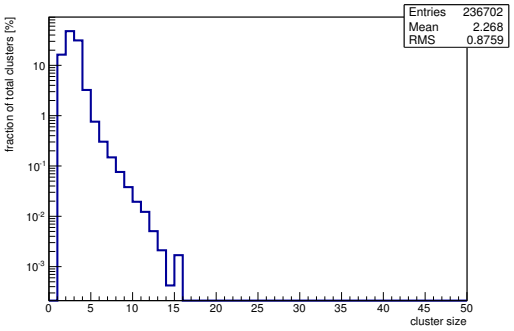

(q) Cluster size distribution.

not available

(r) Hit efficiency vs event number.

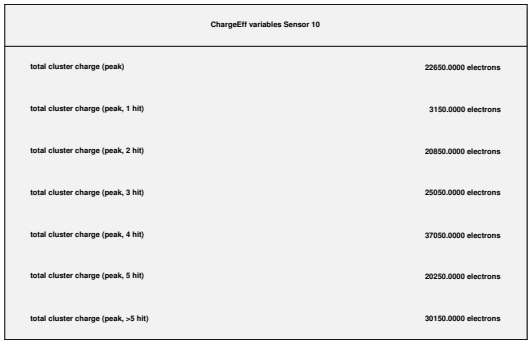

HitEff variables Sensor 10	
Global sensor hit-efficiency	0.9273 ± 0.0044
Number of matched tracker-hits	3289.0000
Number of tracker-hits	3547.0000

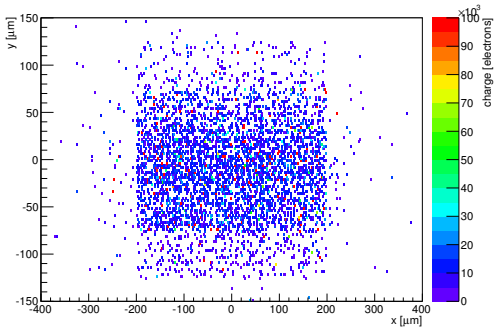

(s) Single pixel mean charge.

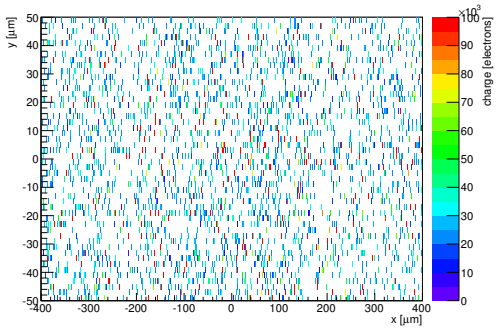

(t) Single pixel mean charge.

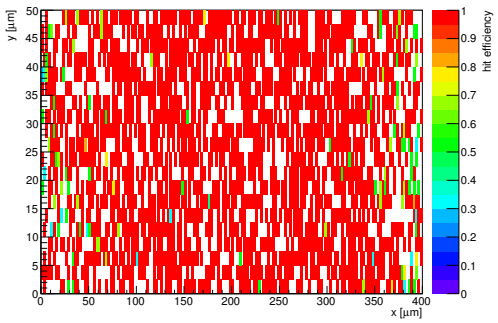

(u) Single pixel hit efficiency.

Figure C.141: Detailed plots for test beam measurement of SCC-31 (description see section 6.1) sample (running as DUT0) during runs 251-303 in the March 2012 test beam period at DESY. Summary of the data in chapter 9.

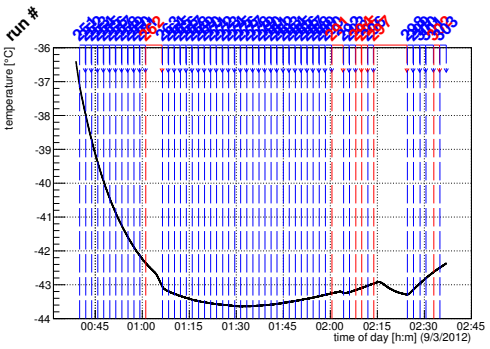

(a) Temperature vs time.

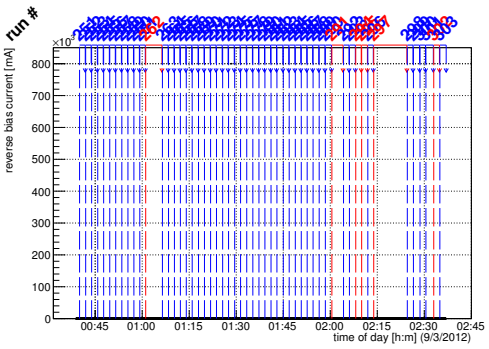

(b) Bias current vs time.

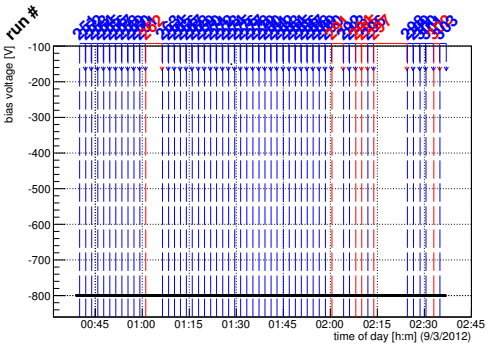

(c) Currently applied bias voltage vs time.

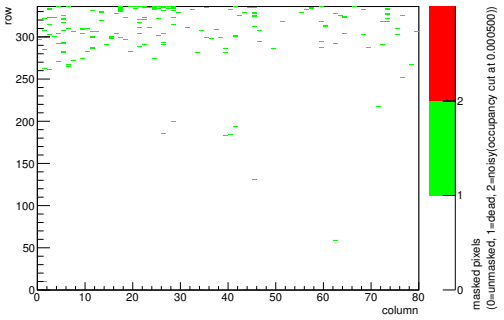

(d) Map of masked pixels.

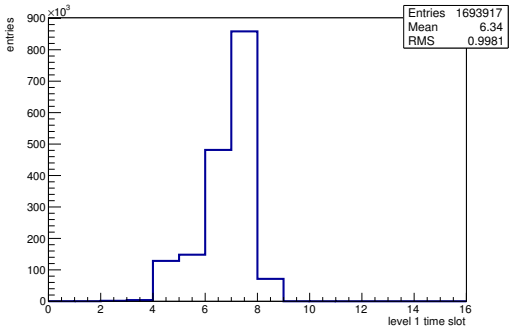

(e) Lvl1 distribution.

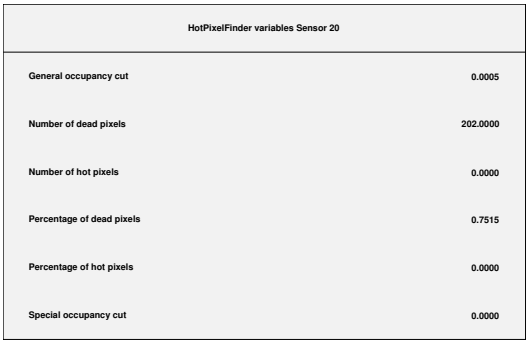

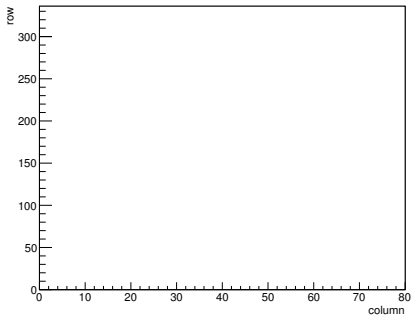

(f) Calibration constant A.

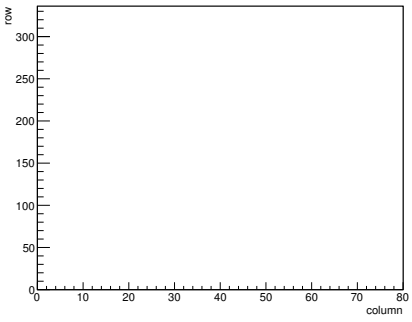

(g) Calibration constant B.

Figure C.142: Detailed plots for test beam measurement of DO-36 (description see section 6.1) sample (running as DUT1) during runs 251-303 in the March 2012 test beam period at DESY. Summary of the data in chapter 9. *(cont.)*

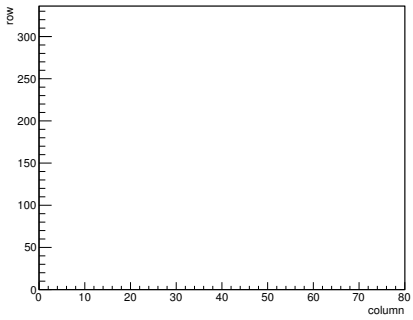

(h) Calibration constant C.

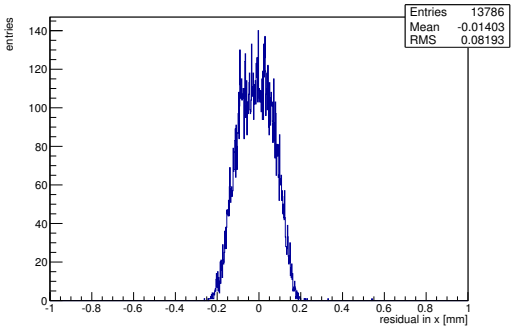

(i) Track residual in x.

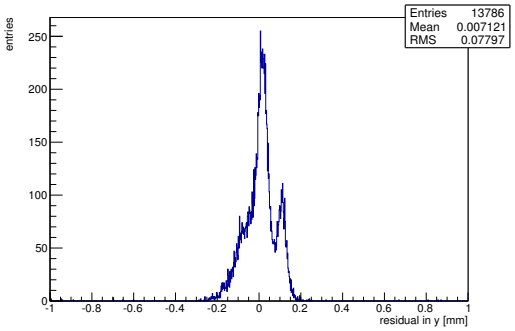

(j) Track residual in y.

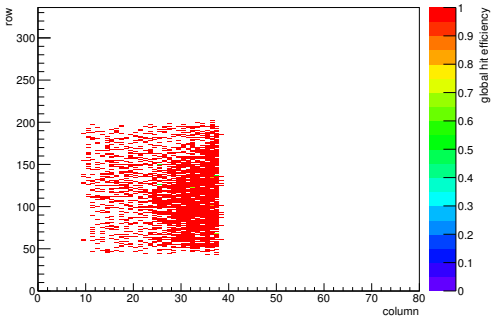

(k) Hit efficiency map.

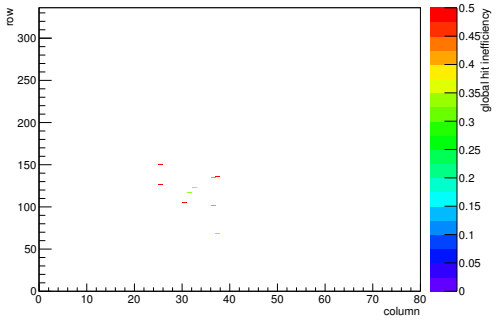

(l) Hit inefficiency map.

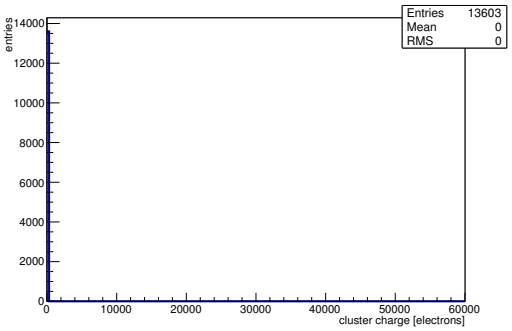

(m) Charge distribution (all cluster sizes included).

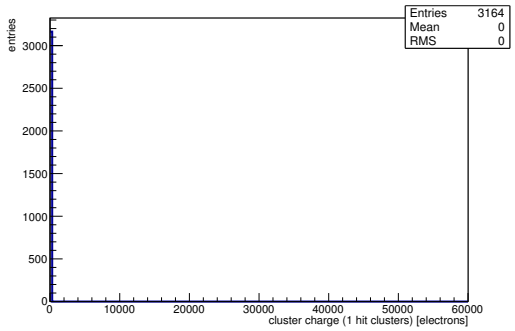

(n) Charge distribution (1 hit cluster).

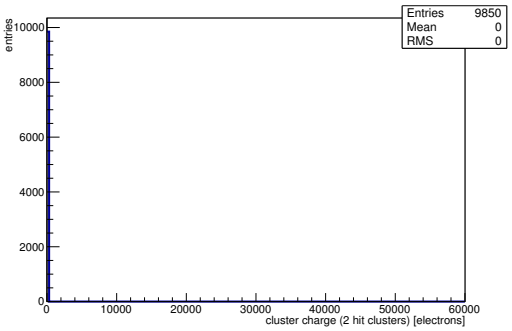

(o) Charge distribution (2 hit cluster).

Figure C.142: Detailed plots for test beam measurement of DO-36 (description see section 6.1) sample (running as DUT1) during runs 251-303 in the March 2012 test beam period at DESY. Summary of the data in chapter 9. *(cont.)*

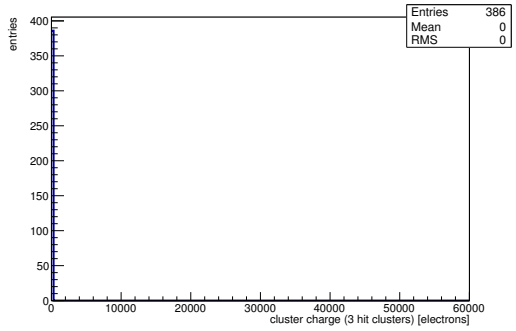

(p) Charge distribution (3 hit cluster).

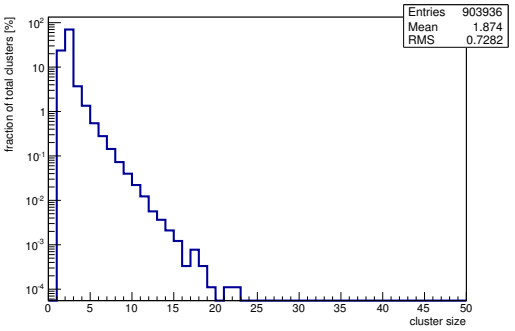

(q) Cluster size distribution.

not available

(r) Hit efficiency vs event number.

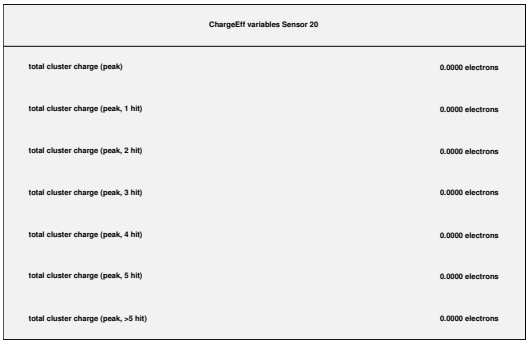

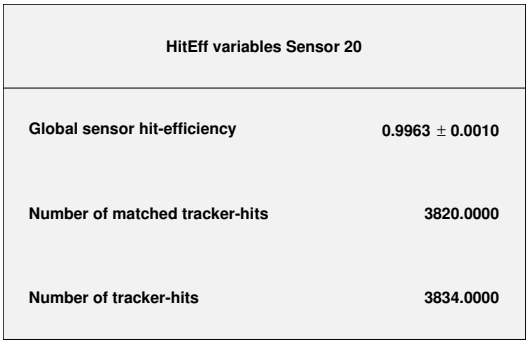

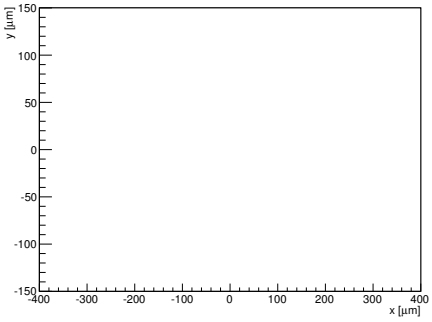

(s) Single pixel mean charge.

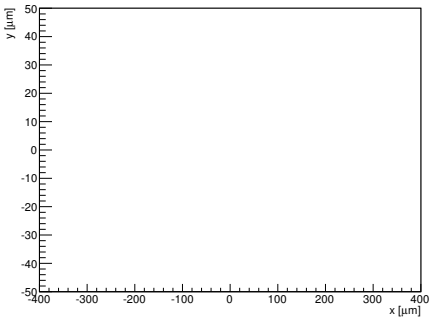

(t) Single pixel mean charge.

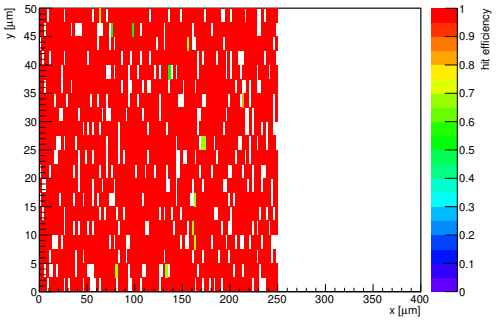

(u) Single pixel hit efficiency.

Figure C.142: Detailed plots for test beam measurement of DO-36 (description see section 6.1) sample (running as DUT1) during runs 251-303 in the March 2012 test beam period at DESY. Summary of the data in chapter 9.

C.4.9 Runs 305-356

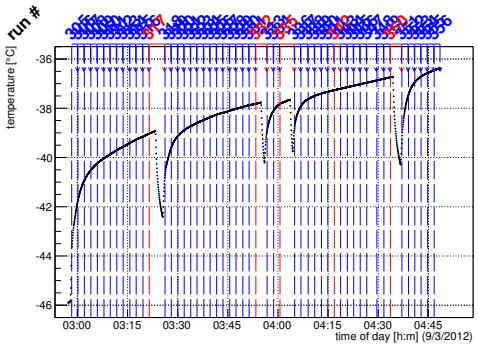

(a) Temperature vs time.

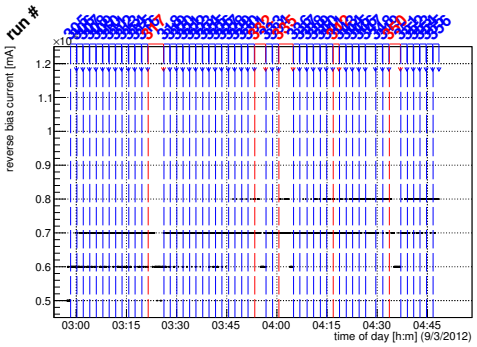

(b) Bias current vs time.

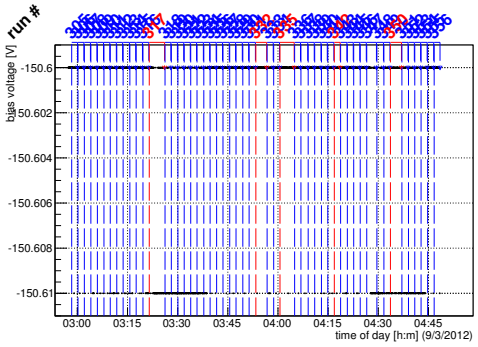

(c) Currently applied bias voltage vs time.

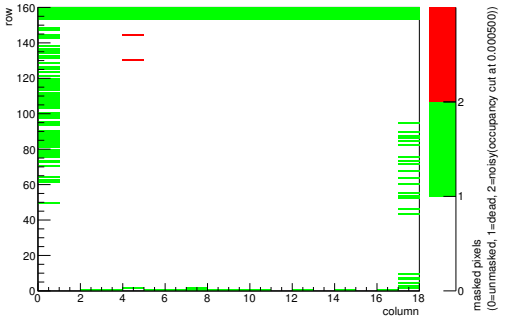

(d) Map of masked pixels.

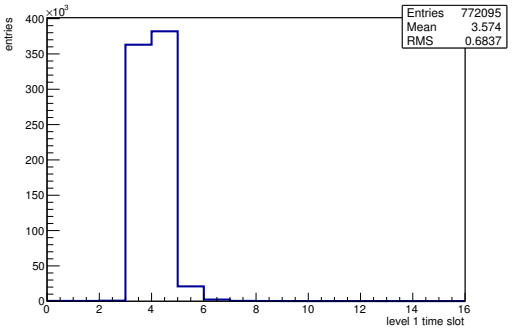

(e) Lvl1 distribution.

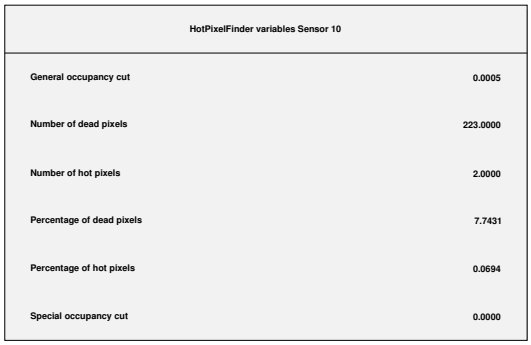

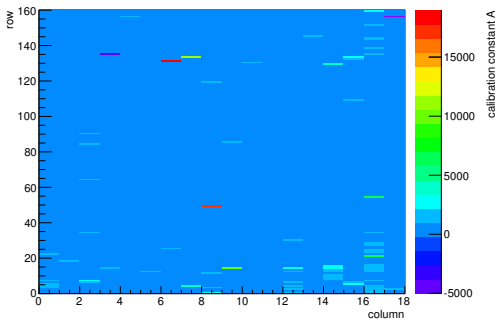

(f) Calibration constant A.

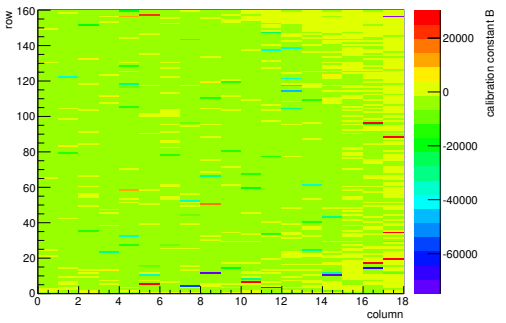

(g) Calibration constant B.

Figure C.143: Detailed plots for test beam measurement of SCC-31 (description see section 6.1) sample (running as DUT0) during runs 305-356 in the March 2012 test beam period at DESY. Summary of the data in chapter 9. *(cont.)*

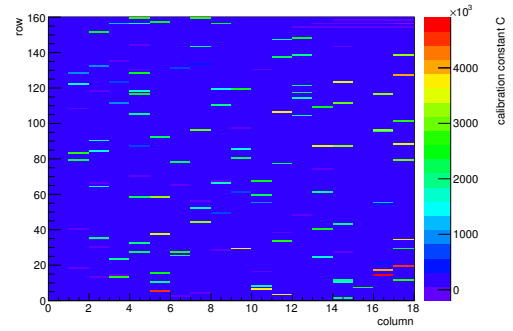

(h) Calibration constant C.

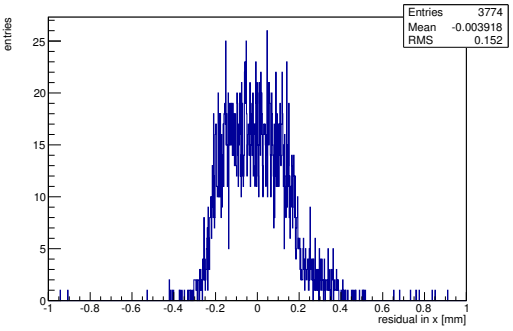

(i) Track residual in x.

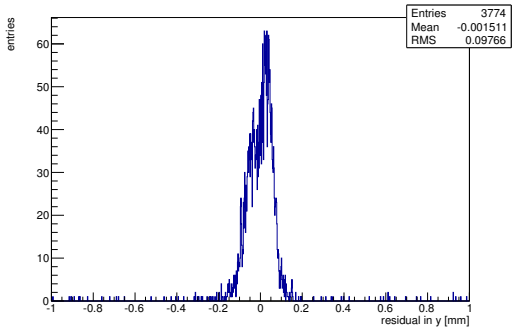

(j) Track residual in y.

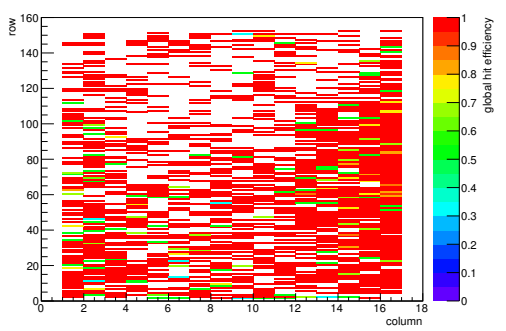

(k) Hit efficiency map.

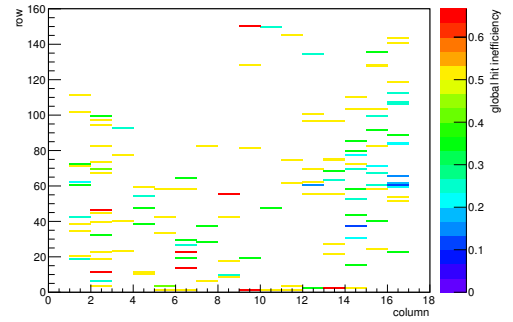

(l) Hit inefficiency map.

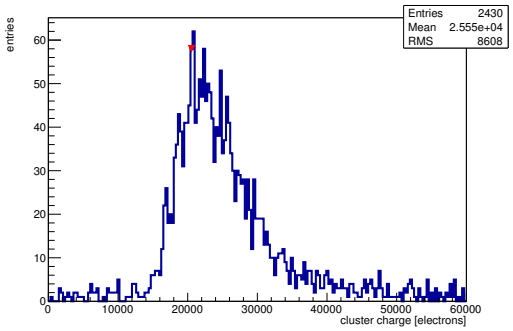

(m) Charge distribution (all cluster sizes included).

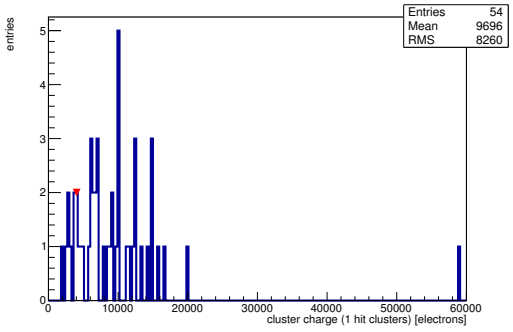

(n) Charge distribution (1 hit cluster).

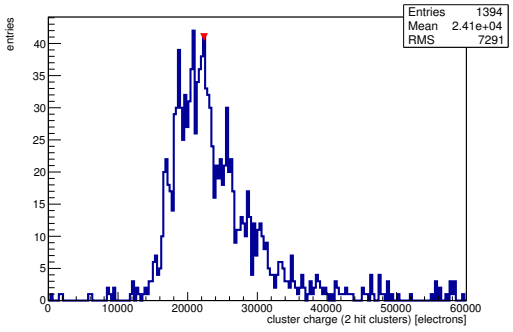

(o) Charge distribution (2 hit cluster).

Figure C.143: Detailed plots for test beam measurement of SCC-31 (description see section 6.1) sample (running as DUT0) during runs 305-356 in the March 2012 test beam period at DESY. Summary of the data in chapter 9. *(cont.)*

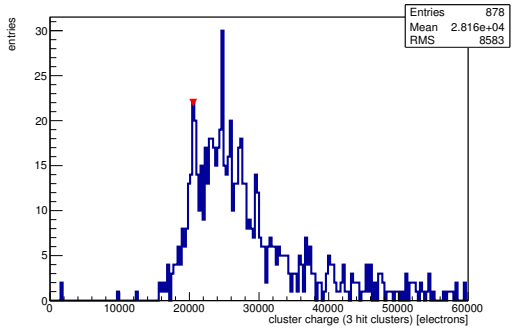

(p) Charge distribution (3 hit cluster).

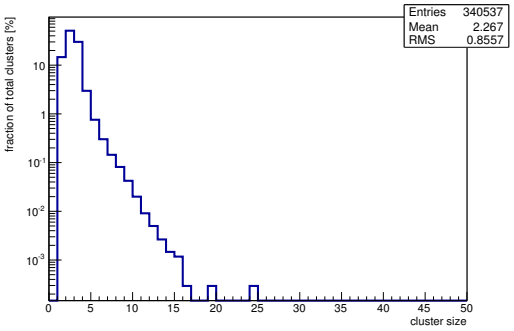

(q) Cluster size distribution.

not available

(r) Hit efficiency vs event number.

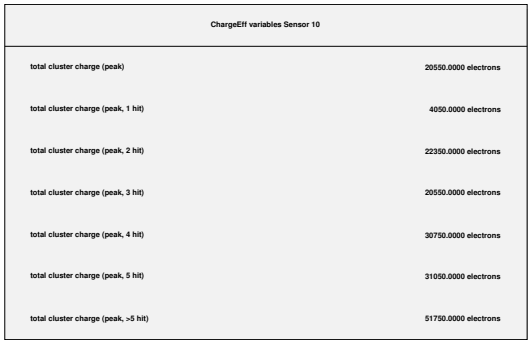

HitEff variables Sensor 10	
Global sensor hit-efficiency	0.9057 ± 0.0057
Number of matched tracker-hits	2412.0000
Number of tracker-hits	2663.0000

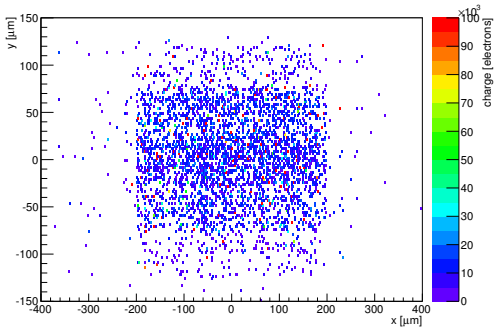

(s) Single pixel mean charge.

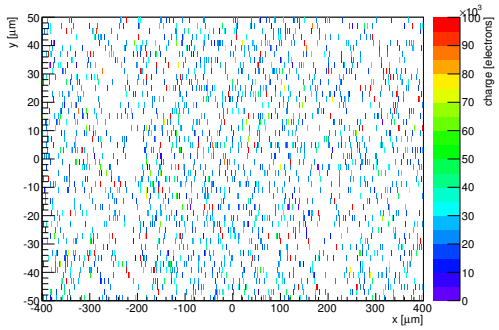

(t) Single pixel mean charge.

(u) Single pixel hit efficiency.

Figure C.143: Detailed plots for test beam measurement of SCC-31 (description see section 6.1) sample (running as DUT0) during runs 305-356 in the March 2012 test beam period at DESY. Summary of the data in chapter 9.

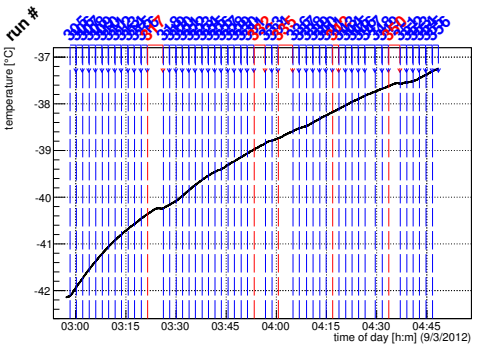

(a) Temperature vs time.

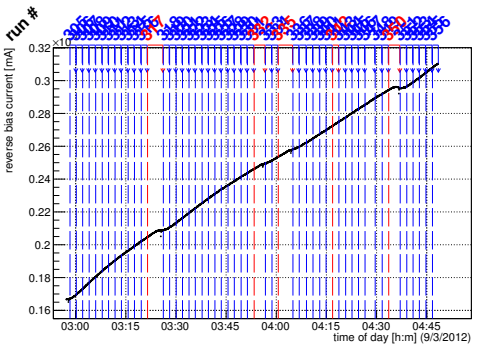

(b) Bias current vs time.

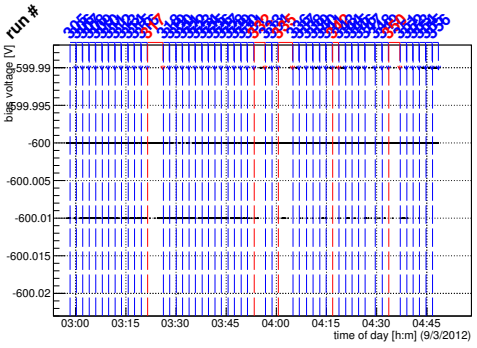

(c) Currently applied bias voltage vs time.

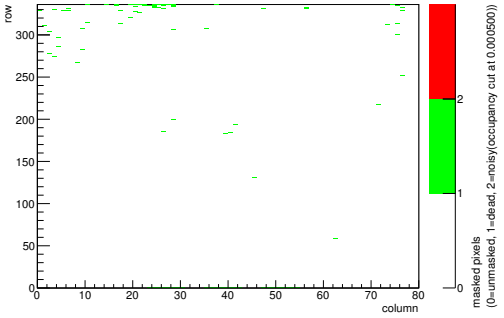

(d) Map of masked pixels.

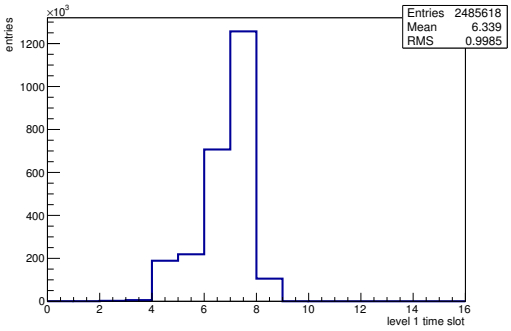

(e) Lvl1 distribution.

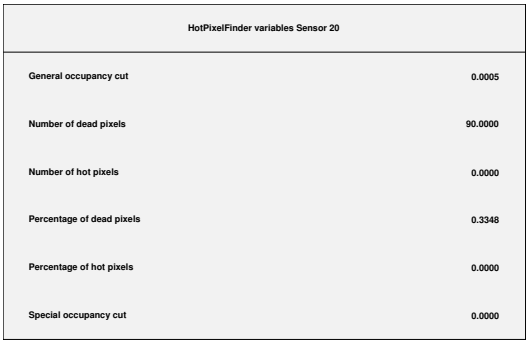

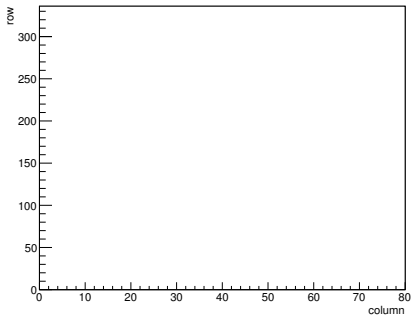

(f) Calibration constant A.

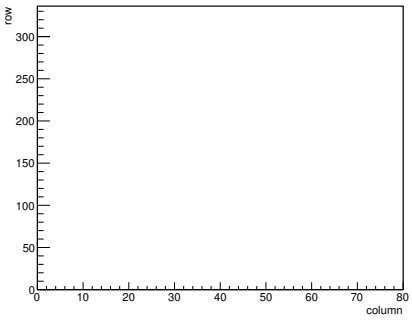

(g) Calibration constant B.

Figure C.144: Detailed plots for test beam measurement of DO-36 (description see section 6.1) sample (running as DUT1) during runs 305-356 in the March 2012 test beam period at DESY. Summary of the data in chapter 9. *(cont.)*

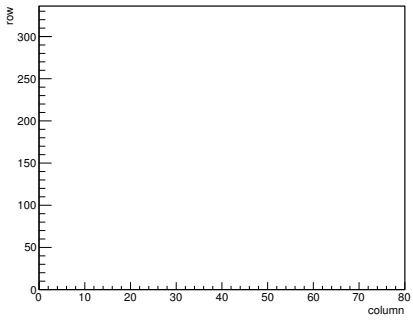

(h) Calibration constant C.

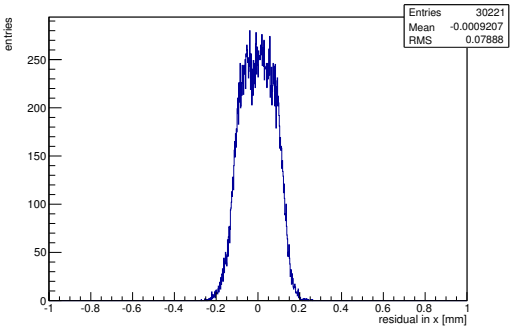

(i) Track residual in x.

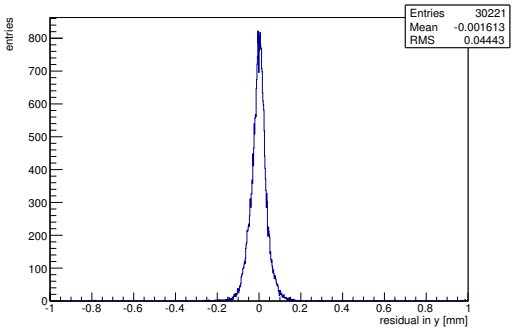

(j) Track residual in y.

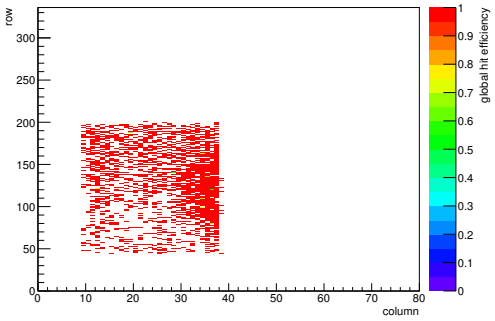

(k) Hit efficiency map.

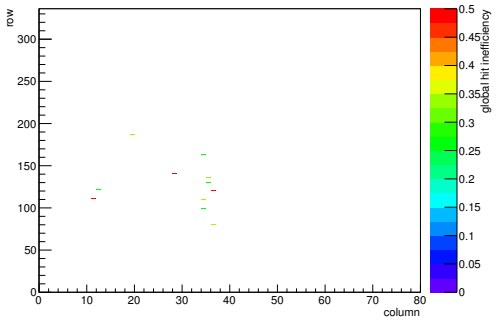

(l) Hit inefficiency map.

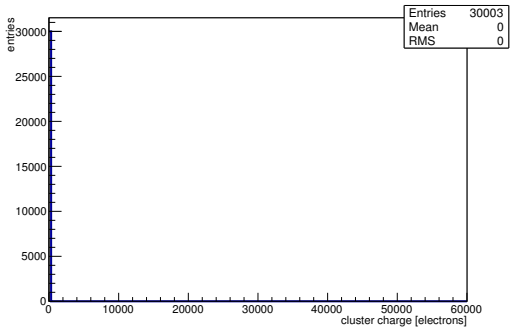

(m) Charge distribution (all cluster sizes included).

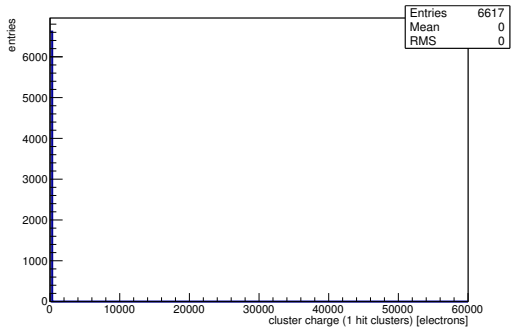

(n) Charge distribution (1 hit cluster).

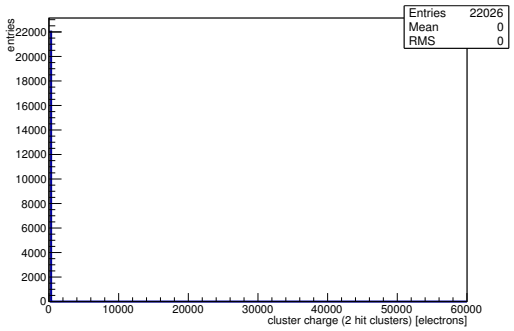

(o) Charge distribution (2 hit cluster).

Figure C.144: Detailed plots for test beam measurement of DO-36 (description see section 6.1) sample (running as DUT1) during runs 305-356 in the March 2012 test beam period at DESY. Summary of the data in chapter 9. *(cont.)*

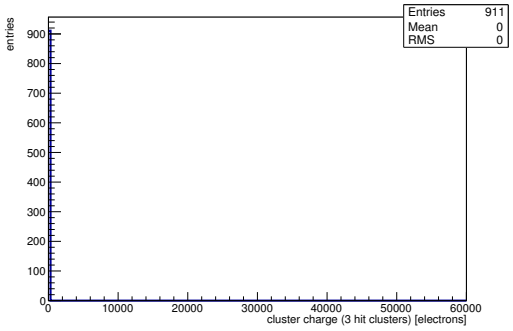

(p) Charge distribution (3 hit cluster).

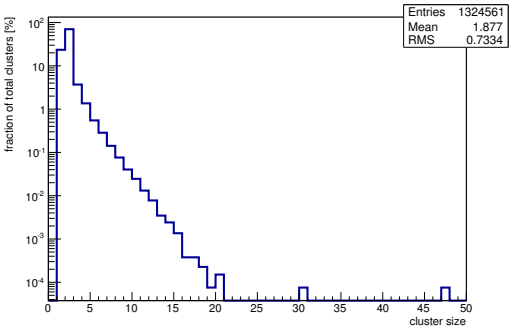

(q) Cluster size distribution.

not available

(r) Hit efficiency vs event number.

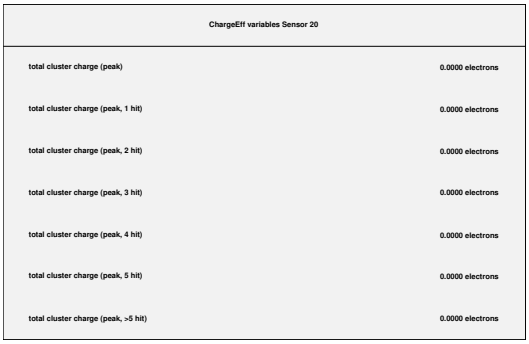

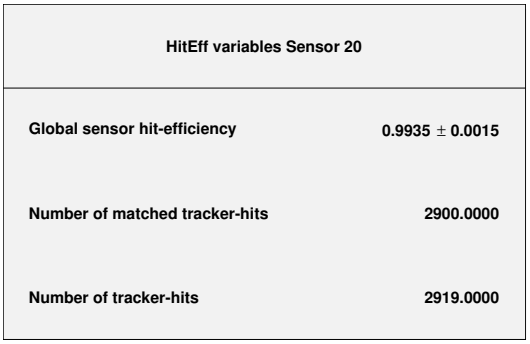

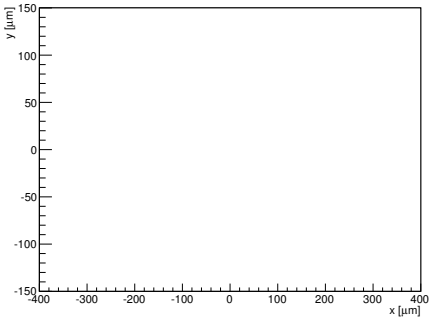

(s) Single pixel mean charge.

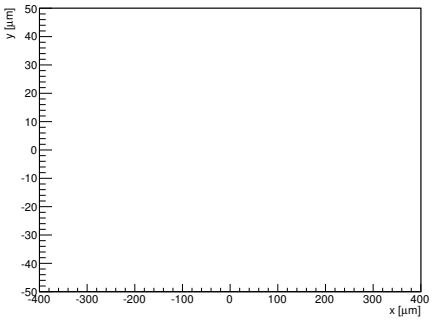

(t) Single pixel mean charge.

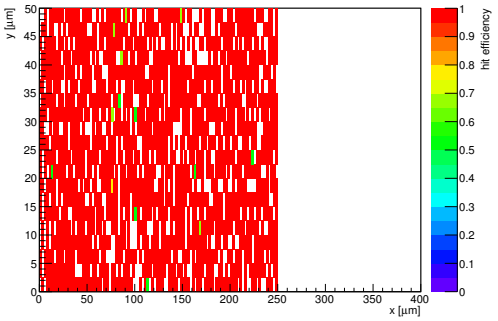

(u) Single pixel hit efficiency.

Figure C.144: Detailed plots for test beam measurement of DO-36 (description see section 6.1) sample (running as DUT1) during runs 305-356 in the March 2012 test beam period at DESY. Summary of the data in chapter 9.

C.4.10 Runs 358-405

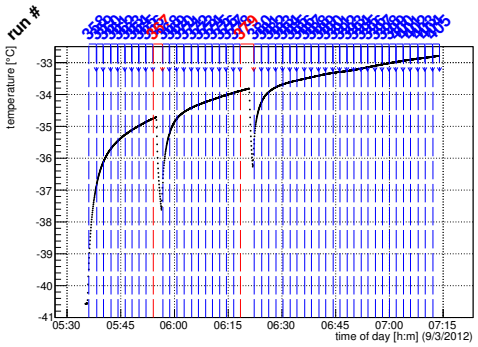

(a) Temperature vs time.

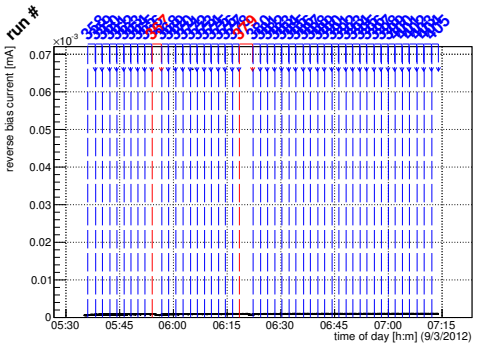

(b) Bias current vs time.

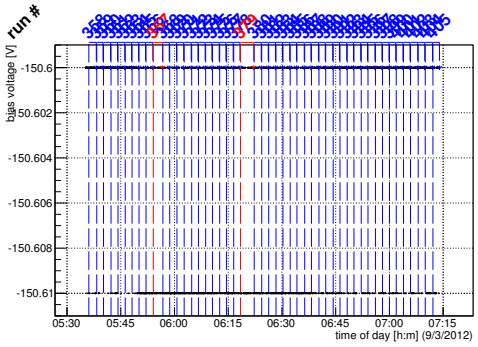

(c) Currently applied bias voltage vs time.

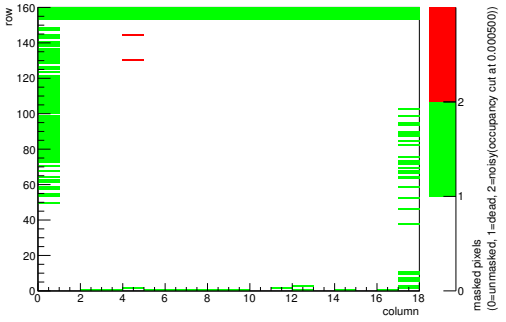

(d) Map of masked pixels.

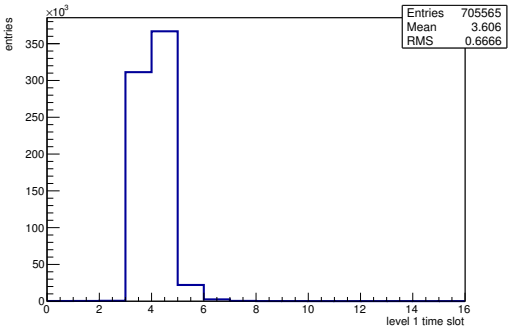

(e) Lvl1 distribution.

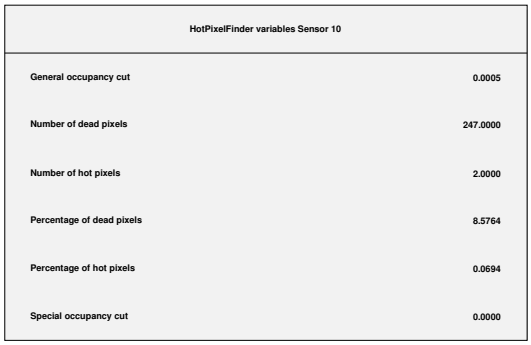

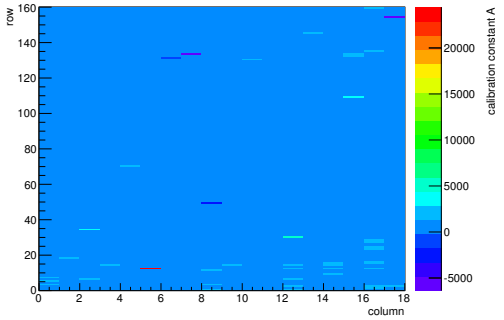

(f) Calibration constant A.

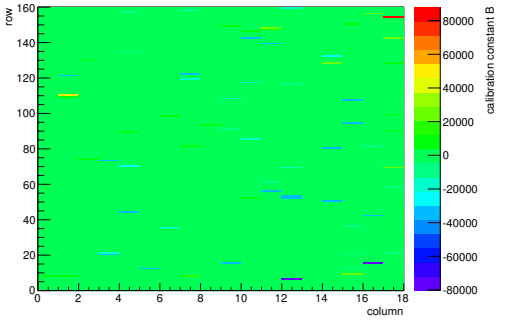

(g) Calibration constant B.

Figure C.145: Detailed plots for test beam measurement of SCC-31 (description see section 6.1) sample (running as DUT0) during runs 358-405 in the March 2012 test beam period at DESY. Summary of the data in chapter 9. *(cont.)*

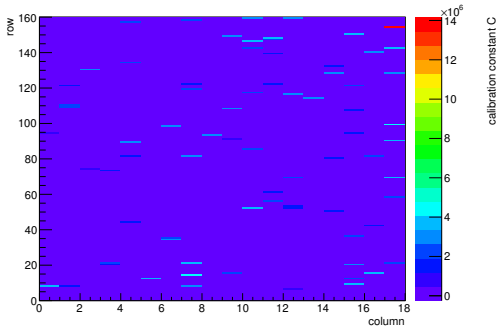

(h) Calibration constant C.

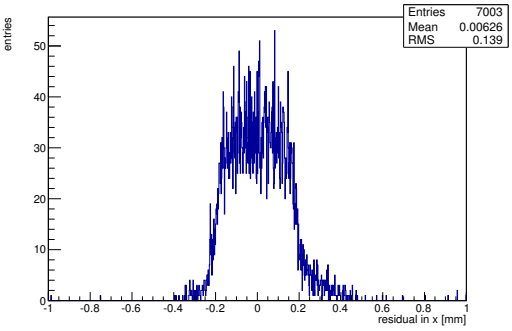

(i) Track residual in x.

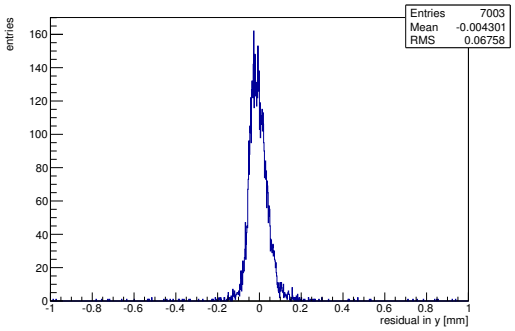

(j) Track residual in y.

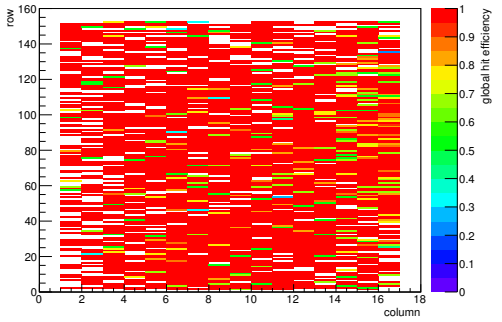

(k) Hit efficiency map.

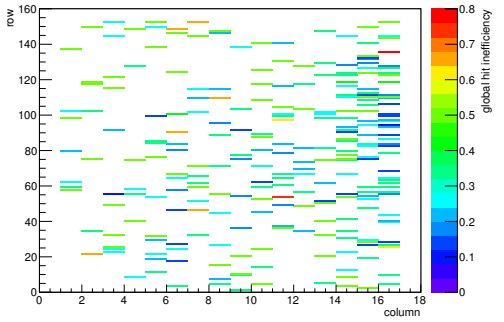

(l) Hit inefficiency map.

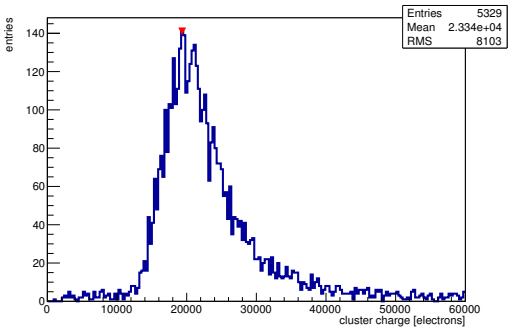

(m) Charge distribution (all cluster sizes included).

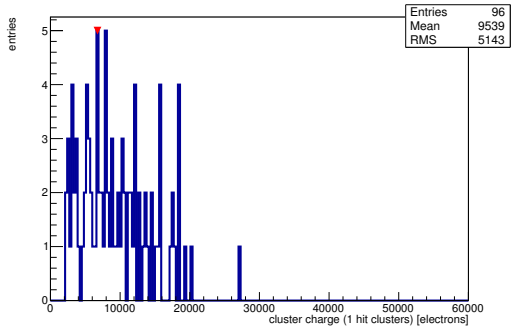

(n) Charge distribution (1 hit cluster).

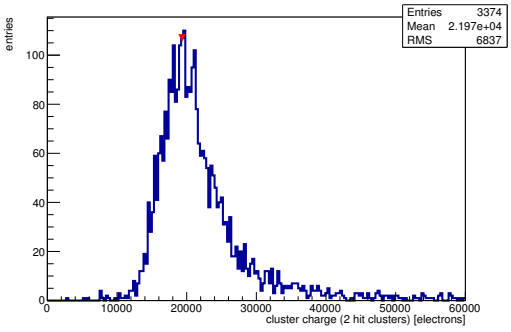

(o) Charge distribution (2 hit cluster).

Figure C.145: Detailed plots for test beam measurement of SCC-31 (description see section 6.1) sample (running as DUT0) during runs 358-405 in the March 2012 test beam period at DESY. Summary of the data in chapter 9. *(cont.)*

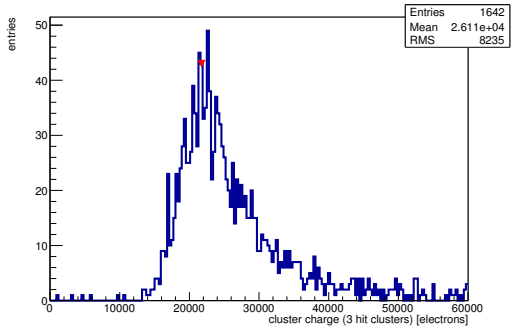

(p) Charge distribution (3 hit cluster).

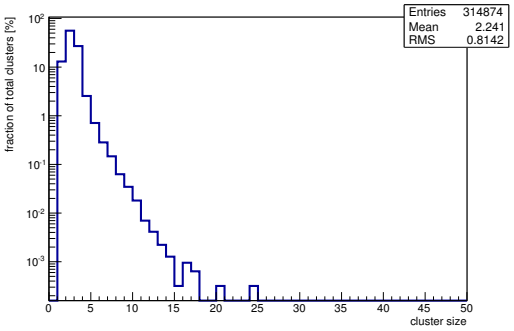

(q) Cluster size distribution.

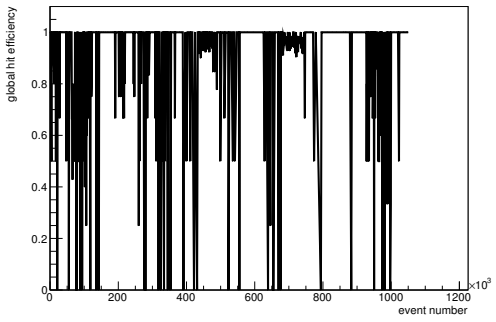

(r) Hit efficiency vs event number.

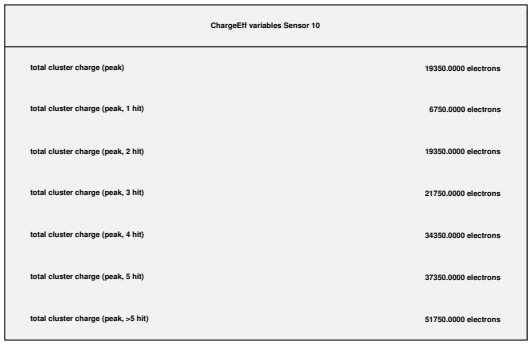

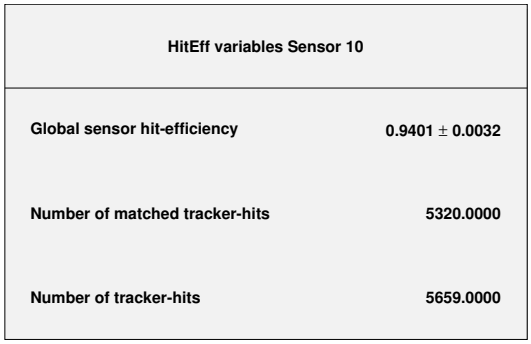

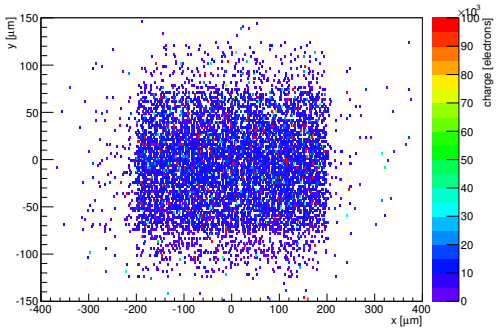

(s) Single pixel mean charge.

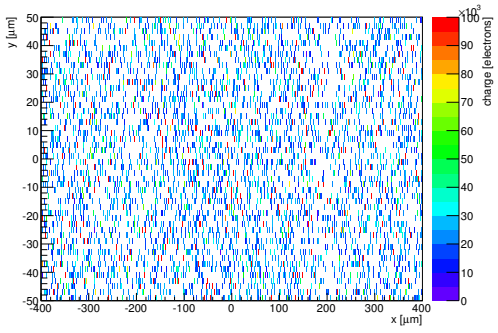

(t) Single pixel mean charge.

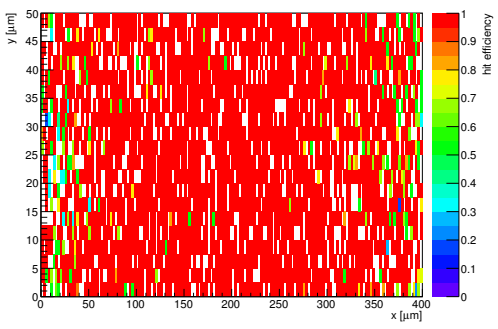

(u) Single pixel hit efficiency.

Figure C.145: Detailed plots for test beam measurement of SCC-31 (description see section 6.1) sample (running as DUT0) during runs 358-405 in the March 2012 test beam period at DESY. Summary of the data in chapter 9.

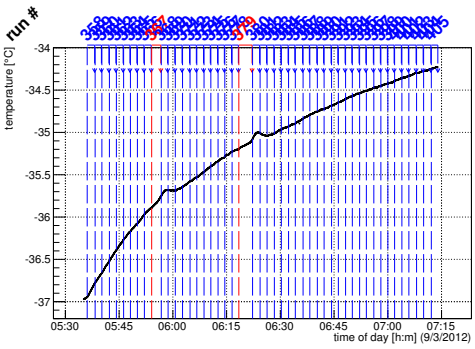

(a) Temperature vs time.

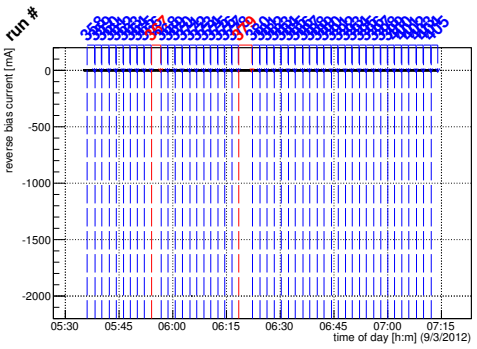

(b) Bias current vs time.

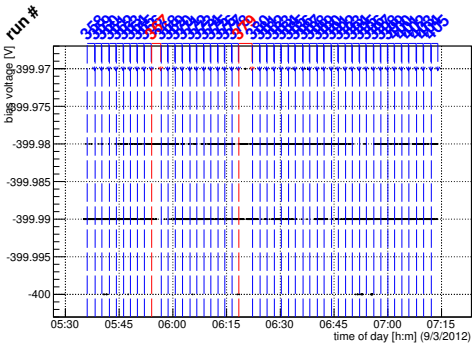

(c) Currently applied bias voltage vs time.

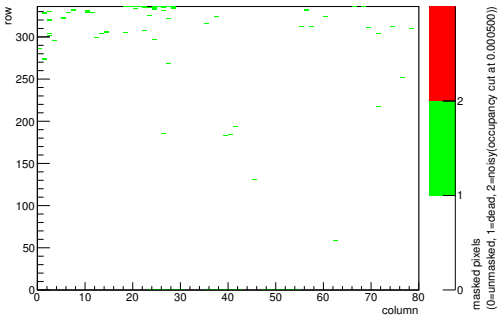

(d) Map of masked pixels.

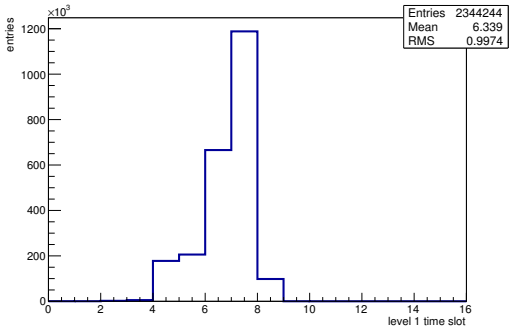

(e) Lvl1 distribution.

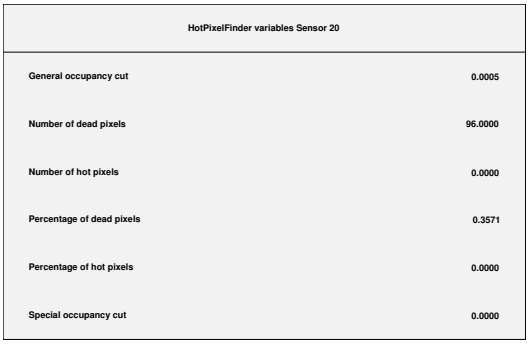

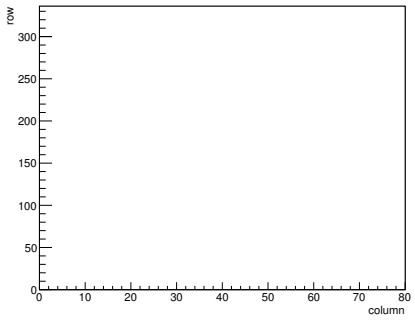

(f) Calibration constant A.

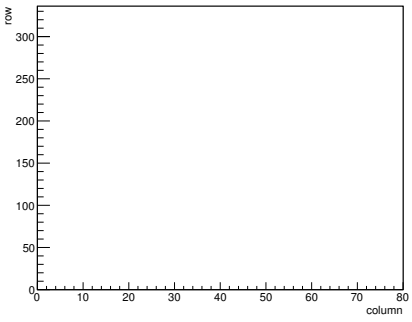

(g) Calibration constant B.

Figure C.146: Detailed plots for test beam measurement of DO-36 (description see section 6.1) sample (running as DUT1) during runs 358-405 in the March 2012 test beam period at DESY. Summary of the data in chapter 9. *(cont.)*

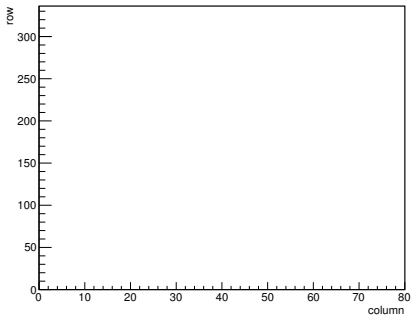

(h) Calibration constant C.

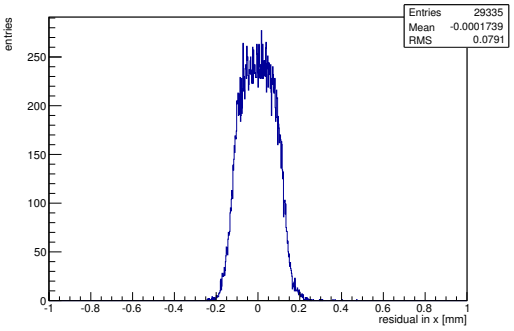

(i) Track residual in x.

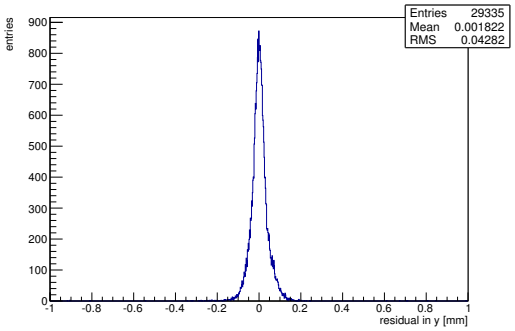

(j) Track residual in y.

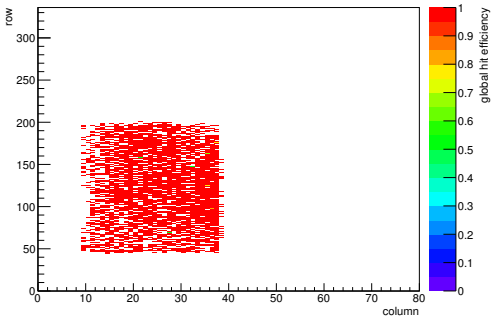

(k) Hit efficiency map.

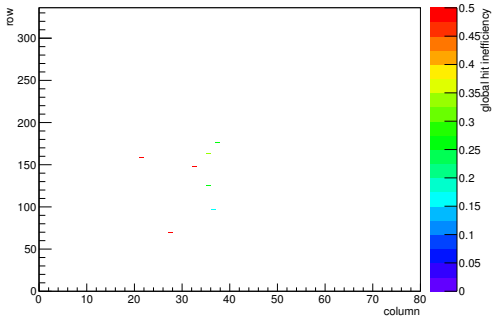

(l) Hit inefficiency map.

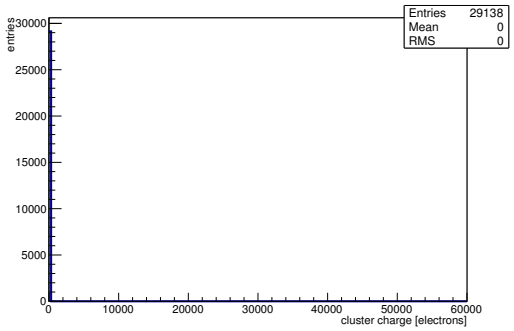

(m) Charge distribution (all cluster sizes included).

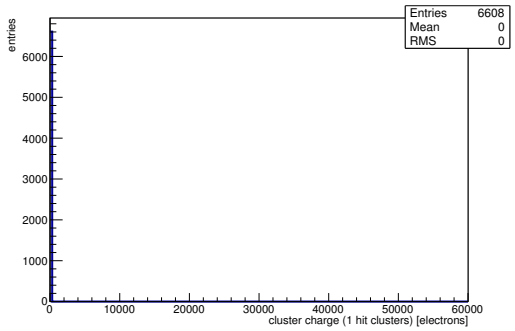

(n) Charge distribution (1 hit cluster).

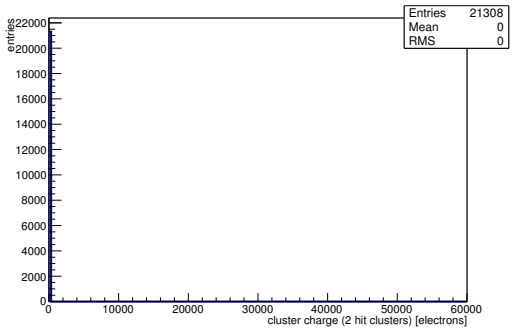

(o) Charge distribution (2 hit cluster).

Figure C.146: Detailed plots for test beam measurement of DO-36 (description see section 6.1) sample (running as DUT1) during runs 358-405 in the March 2012 test beam period at DESY. Summary of the data in chapter 9. *(cont.)*

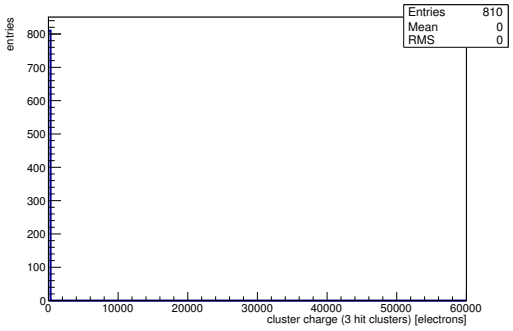

(p) Charge distribution (3 hit cluster).

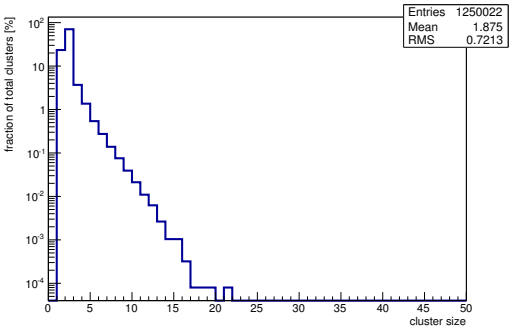

(q) Cluster size distribution.

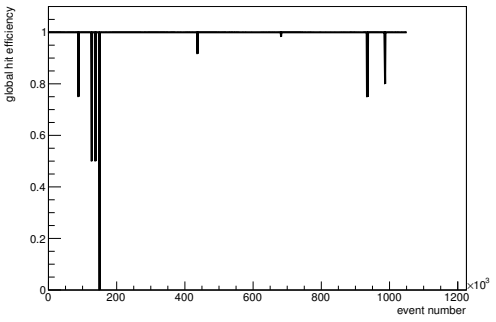

(r) Hit efficiency vs event number.

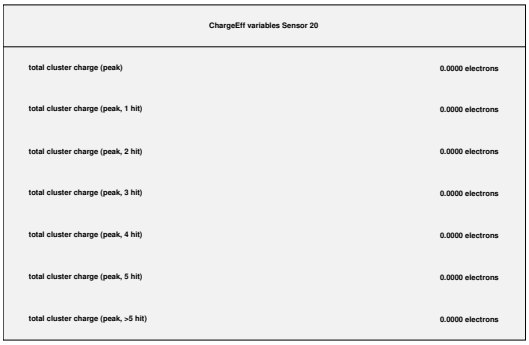

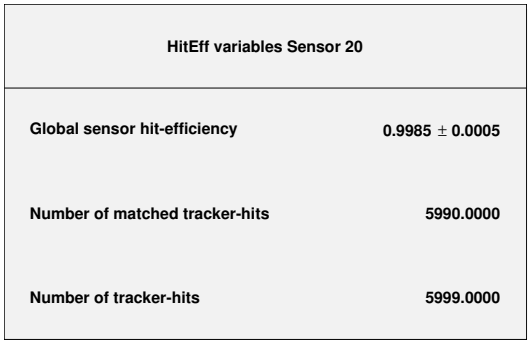

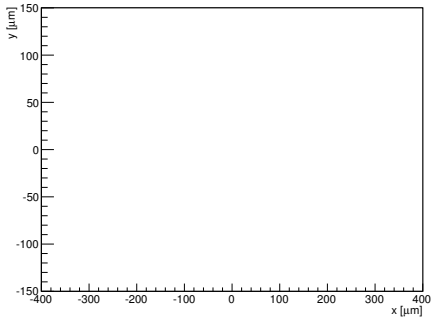

(s) Single pixel mean charge.

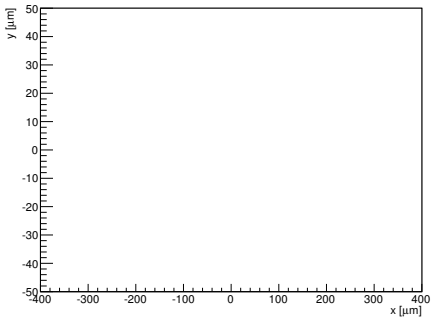

(t) Single pixel mean charge.

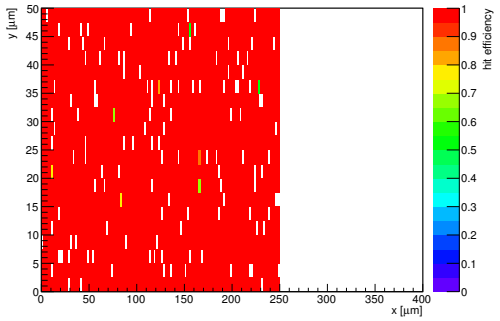

(u) Single pixel hit efficiency.

Figure C.146: Detailed plots for test beam measurement of DO-36 (description see section 6.1) sample (running as DUT1) during runs 358-405 in the March 2012 test beam period at DESY. Summary of the data in chapter 9.

C.4.11 Runs 408-452

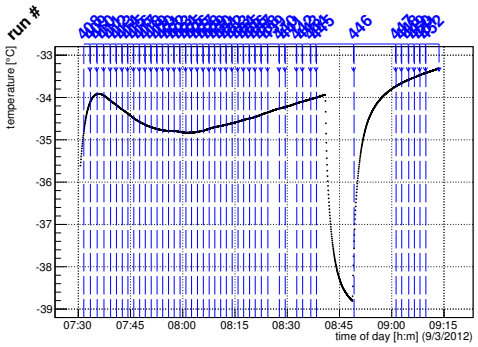

(a) Temperature vs time.

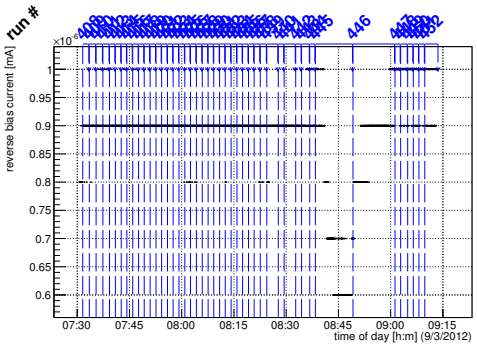

(b) Bias current vs time.

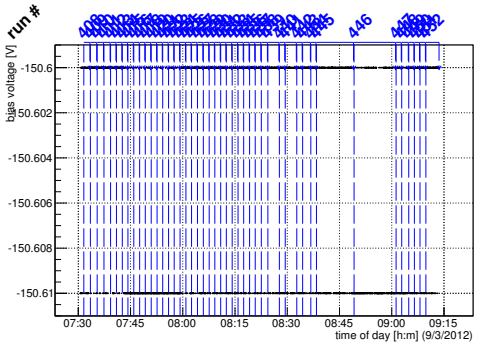

(c) Currently applied bias voltage vs time.

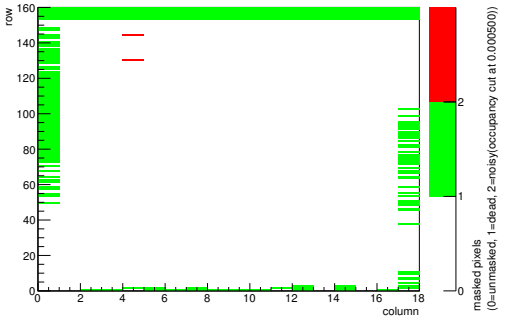

(d) Map of masked pixels.

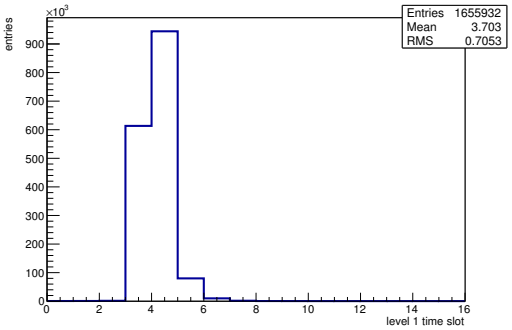

(e) Lvl1 distribution.

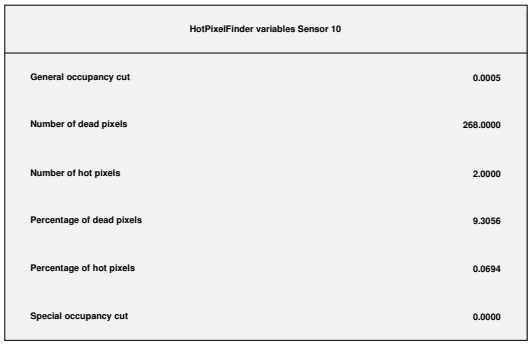

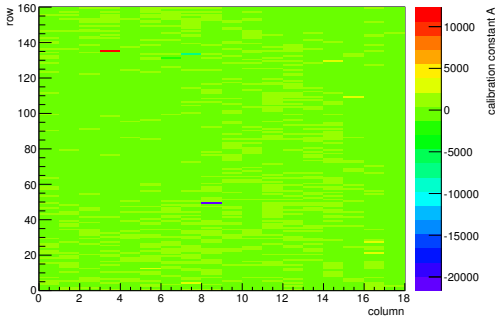

(f) Calibration constant A.

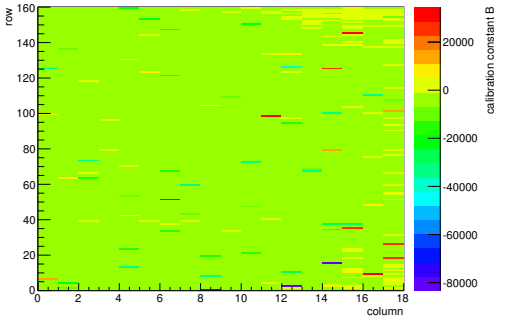

(g) Calibration constant B.

Figure C.147: Detailed plots for test beam measurement of SCC-31 (description see section 6.1) sample (running as DUT0) during runs 408-452 in the March 2012 test beam period at DESY. Summary of the data in chapter 9. *(cont.)*

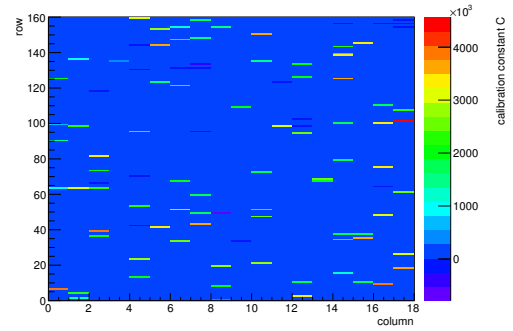

(h) Calibration constant C.

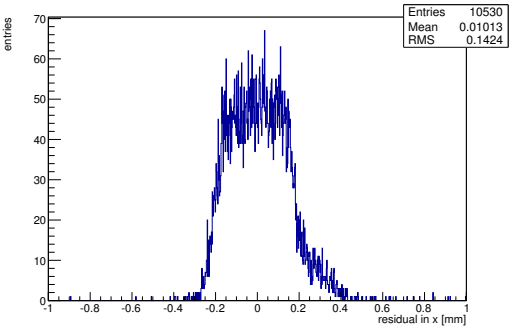

(i) Track residual in x.

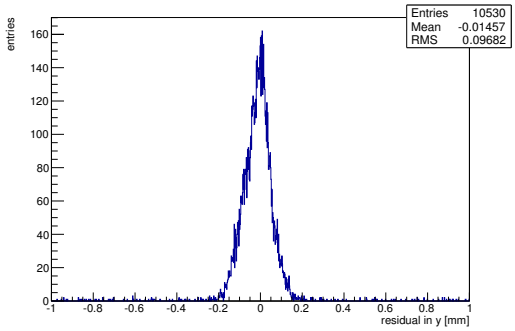

(j) Track residual in y.

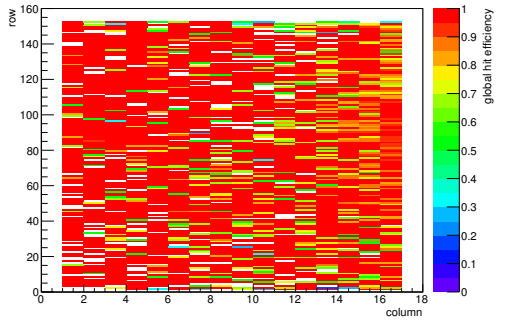

(k) Hit efficiency map.

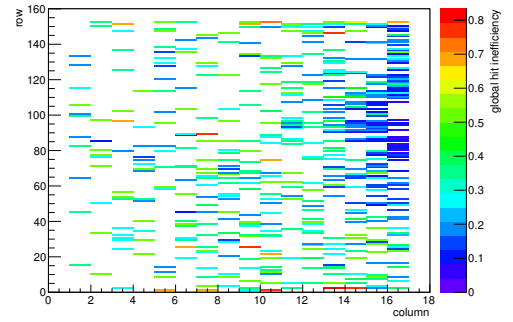

(l) Hit inefficiency map.

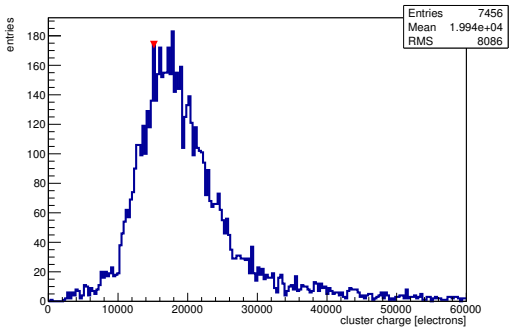

(m) Charge distribution (all cluster sizes included).

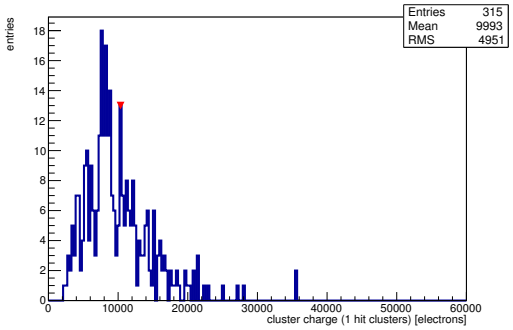

(n) Charge distribution (1 hit cluster).

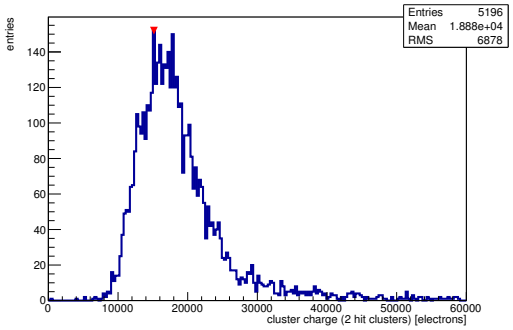

(o) Charge distribution (2 hit cluster).

Figure C.147: Detailed plots for test beam measurement of SCC-31 (description see section 6.1) sample (running as DUT0) during runs 408-452 in the March 2012 test beam period at DESY. Summary of the data in chapter 9. *(cont.)*

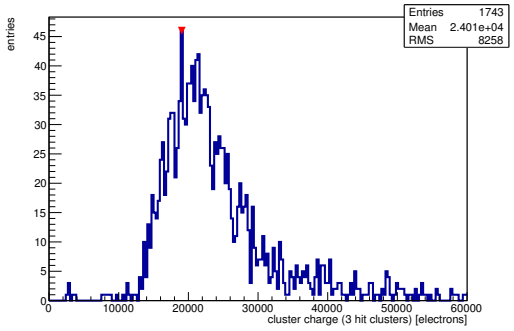

(p) Charge distribution (3 hit cluster).

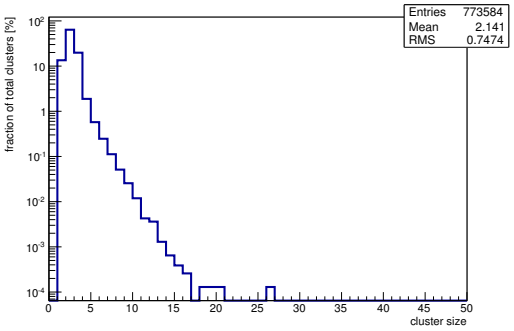

(q) Cluster size distribution.

not available

(r) Hit efficiency vs event number.

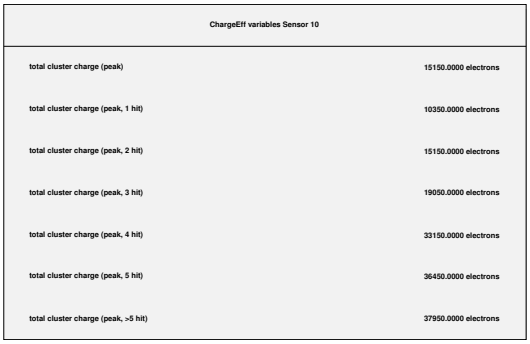

HitEff variables Sensor 10	
Global sensor hit-efficiency	0.9165 ± 0.0031
Number of matched tracker-hits	7411.0000
Number of tracker-hits	8086.0000

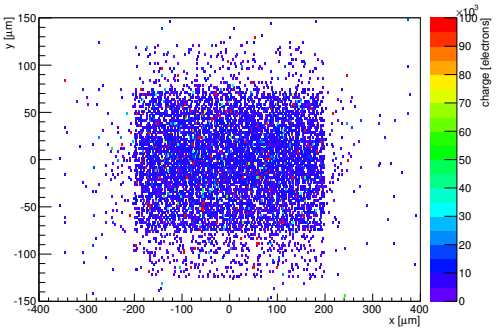

(s) Single pixel mean charge.

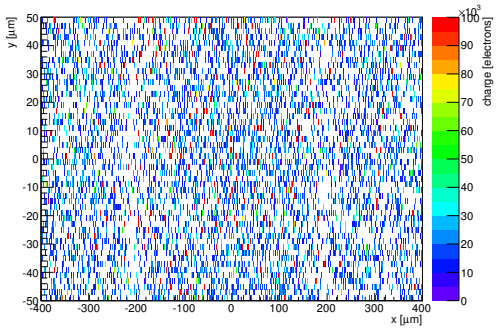

(t) Single pixel mean charge.

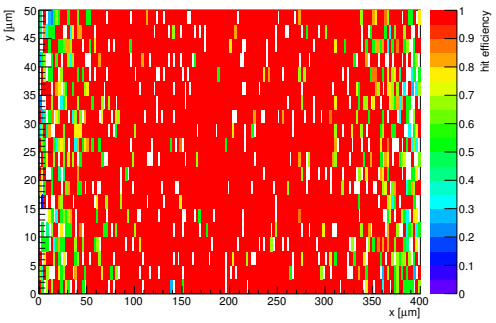

(u) Single pixel hit efficiency.

Figure C.147: Detailed plots for test beam measurement of SCC-31 (description see section 6.1) sample (running as DUT0) during runs 408-452 in the March 2012 test beam period at DESY. Summary of the data in chapter 9.

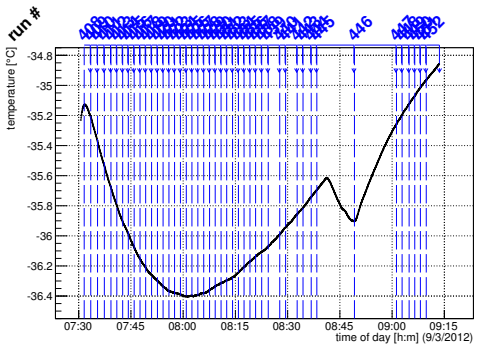

(a) Temperature vs time.

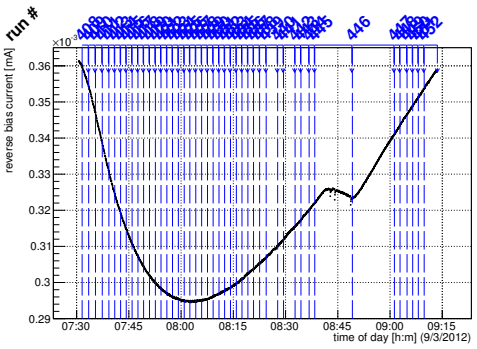

(b) Bias current vs time.

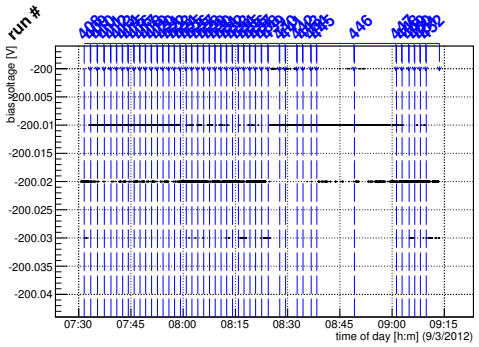

(c) Currently applied bias voltage vs time.

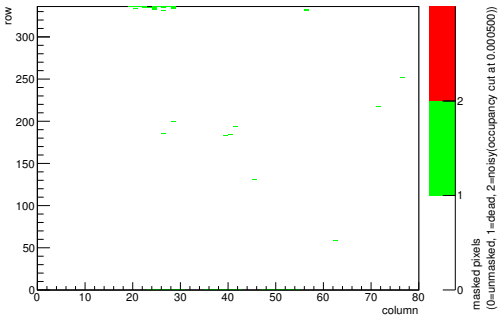

(d) Map of masked pixels.

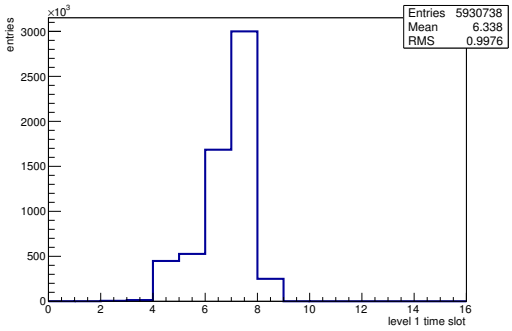

(e) Lvl1 distribution.

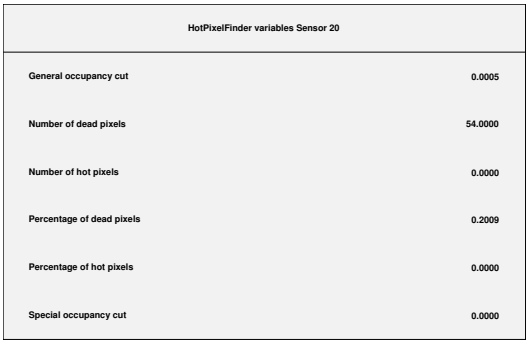

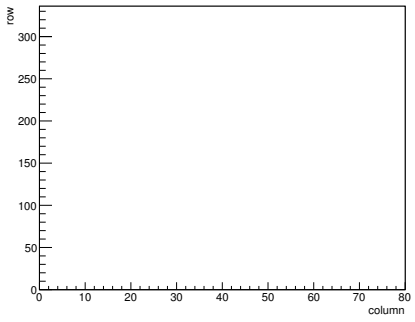

(f) Calibration constant A.

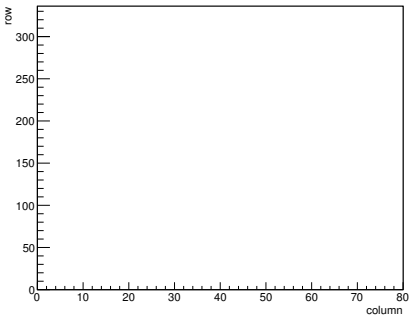

(g) Calibration constant B.

Figure C.148: Detailed plots for test beam measurement of DO-36 (description see section 6.1) sample (running as DUT1) during runs 408-452 in the March 2012 test beam period at DESY. Summary of the data in chapter 9. *(cont.)*

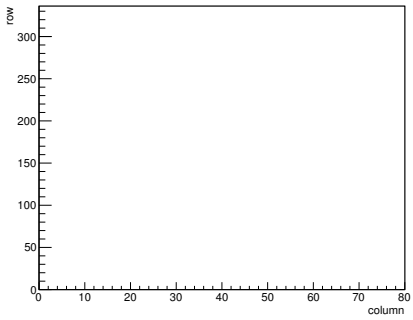

(h) Calibration constant C.

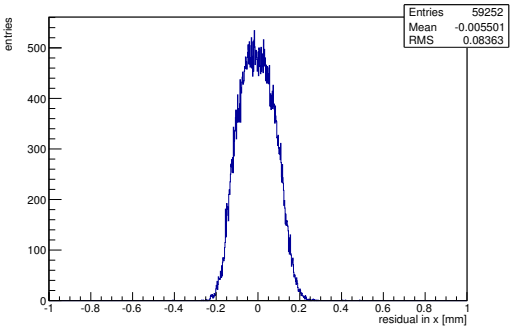

(i) Track residual in x.

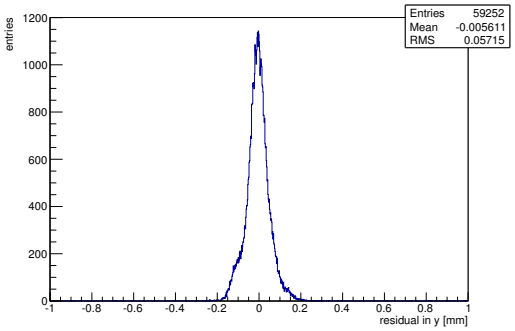

(j) Track residual in y.

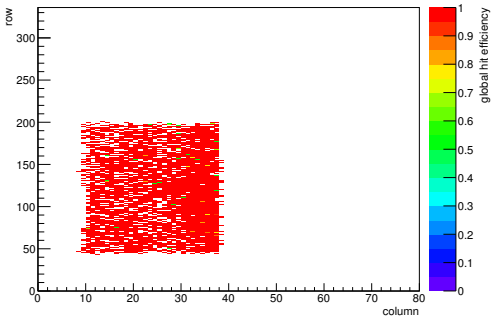

(k) Hit efficiency map.

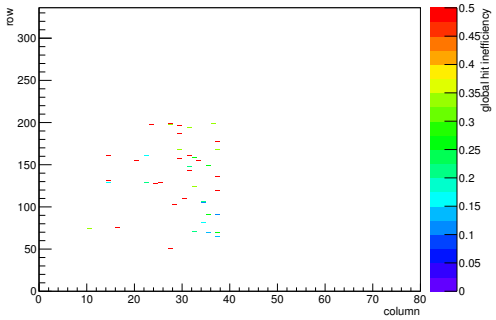

(l) Hit inefficiency map.

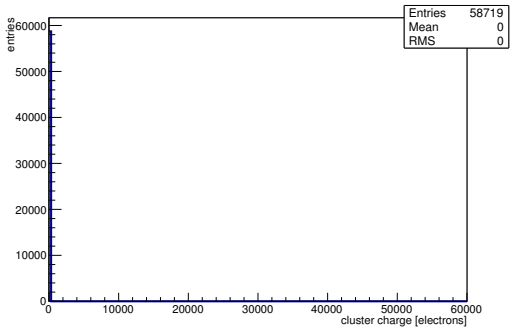

(m) Charge distribution (all cluster sizes included).

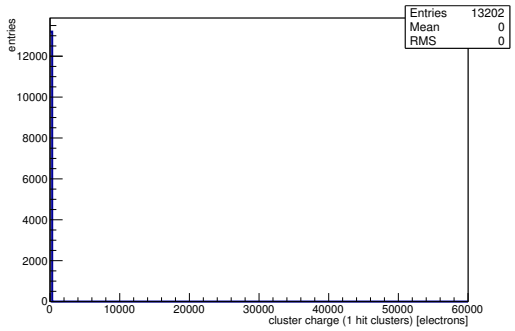

(n) Charge distribution (1 hit cluster).

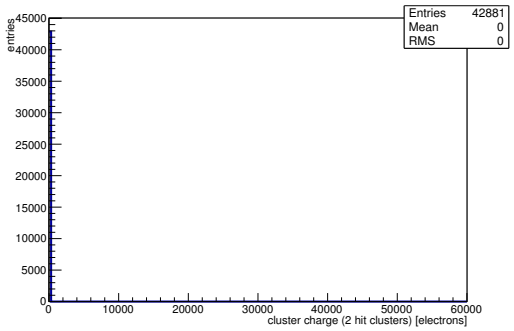

(o) Charge distribution (2 hit cluster).

Figure C.148: Detailed plots for test beam measurement of DO-36 (description see section 6.1) sample (running as DUT1) during runs 408-452 in the March 2012 test beam period at DESY. Summary of the data in chapter 9. *(cont.)*

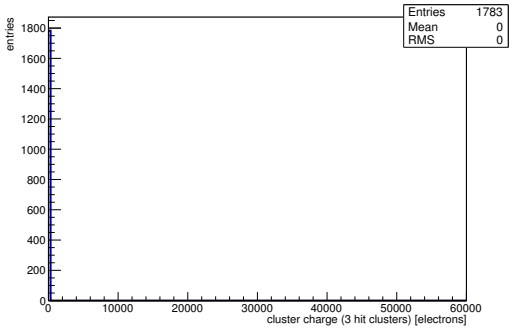

(p) Charge distribution (3 hit cluster).

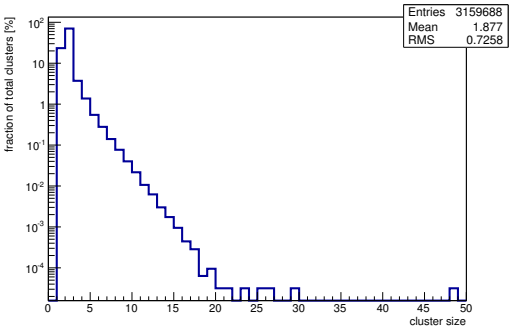

(q) Cluster size distribution.

not available

(r) Hit efficiency vs event number.

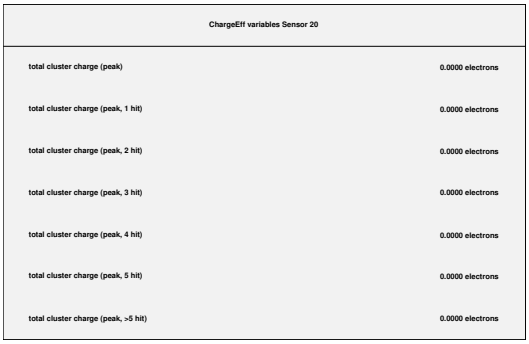

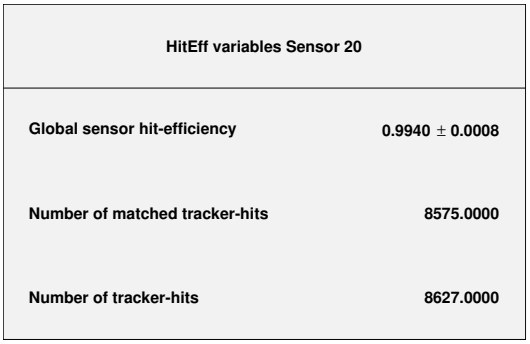

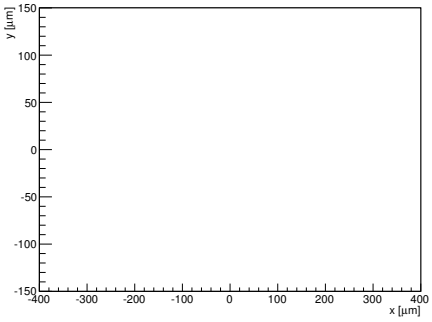

(s) Single pixel mean charge.

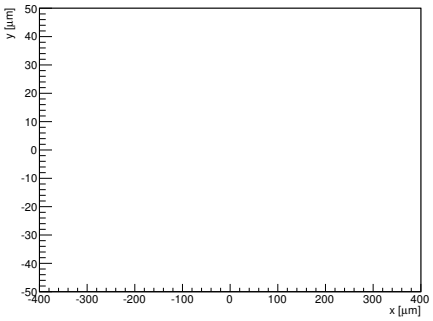

(t) Single pixel mean charge.

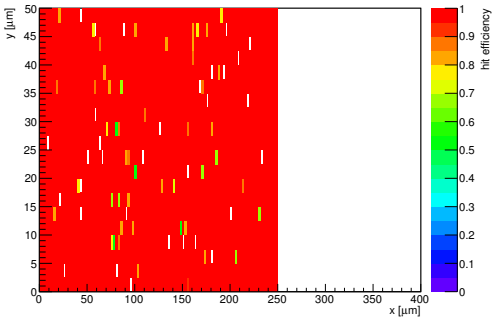

(u) Single pixel hit efficiency.

Figure C.148: Detailed plots for test beam measurement of DO-36 (description see section 6.1) sample (running as DUT1) during runs 408-452 in the March 2012 test beam period at DESY. Summary of the data in chapter 9.

C.4.12 Runs 464-519

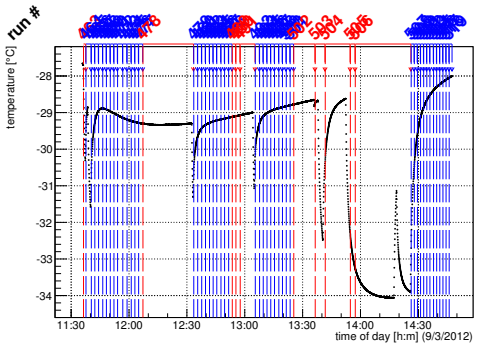

(a) Temperature vs time.

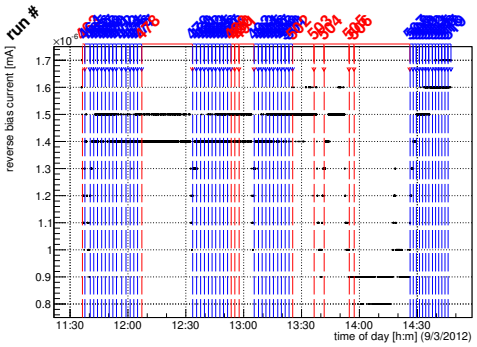

(b) Bias current vs time.

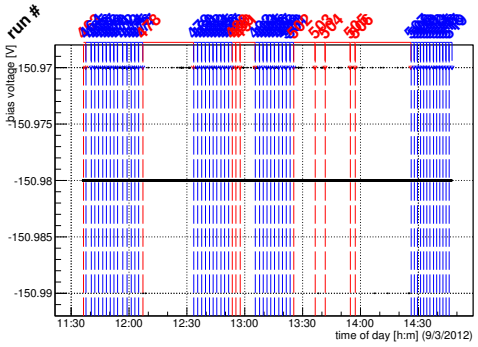

(c) Currently applied bias voltage vs time.

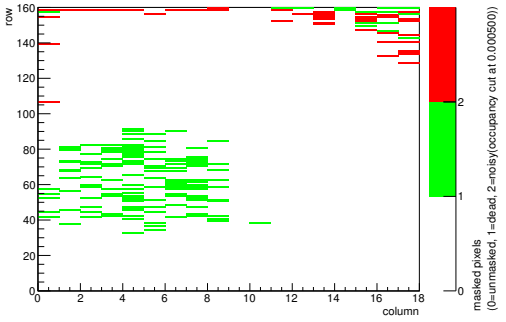

(d) Map of masked pixels.

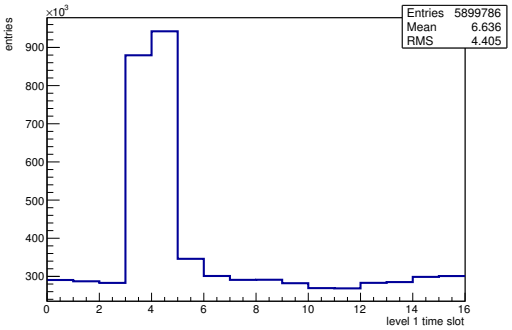

(e) Lvl1 distribution.

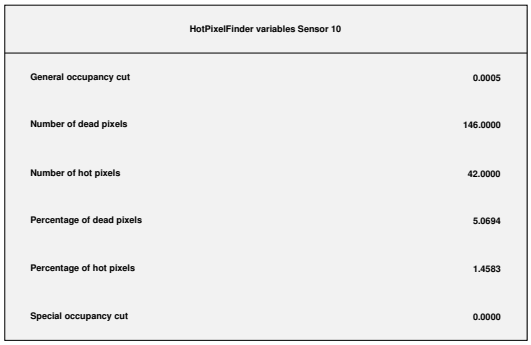

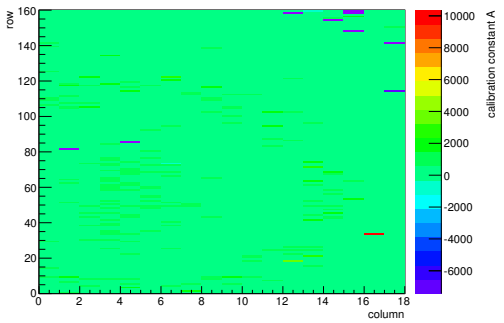

(f) Calibration constant A.

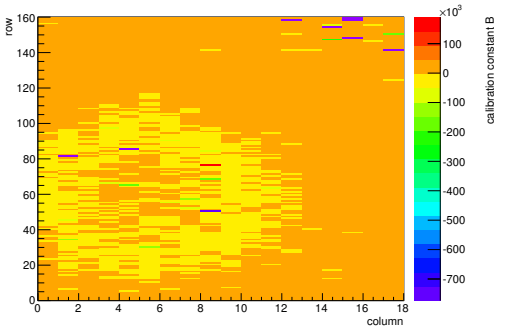

(g) Calibration constant B.

Figure C.149: Detailed plots for test beam measurement of SCC-31 (description see section 6.1) sample (running as DUT0) during runs 464-519 in the March 2012 test beam period at DESY. Summary of the data in chapter 9. *(cont.)*

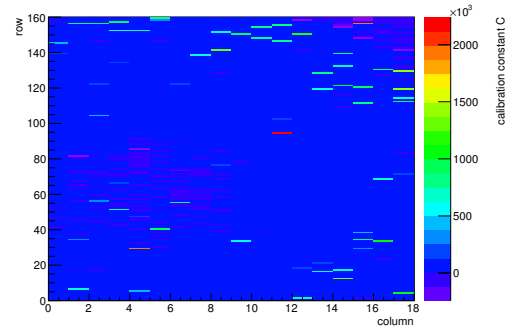

(h) Calibration constant C.

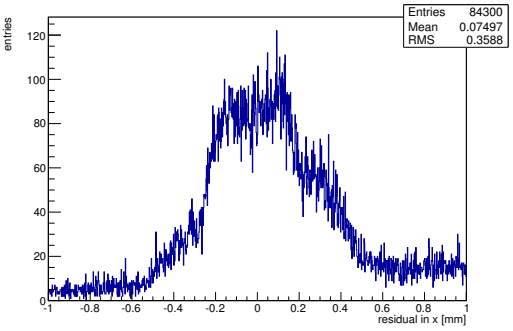

(i) Track residual in x.

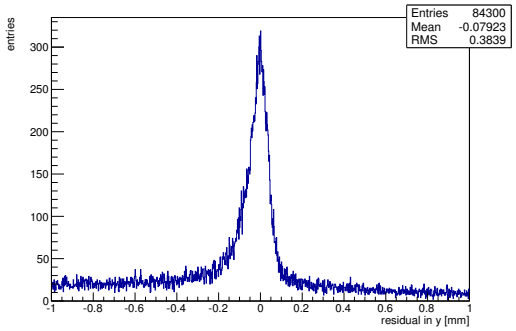

(j) Track residual in y.

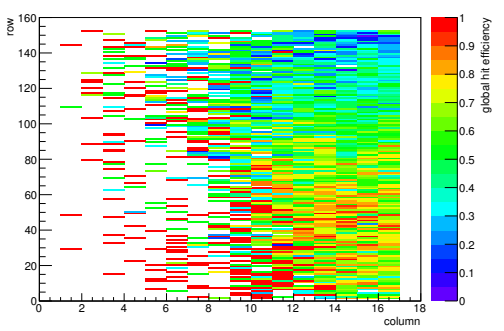

(k) Hit efficiency map.

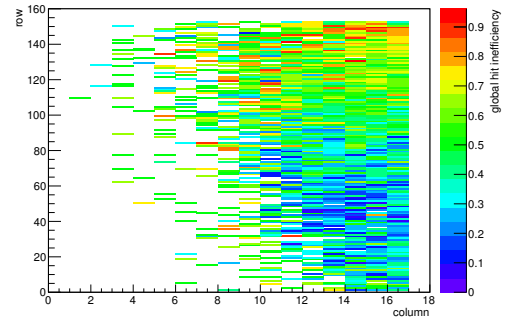

(l) Hit inefficiency map.

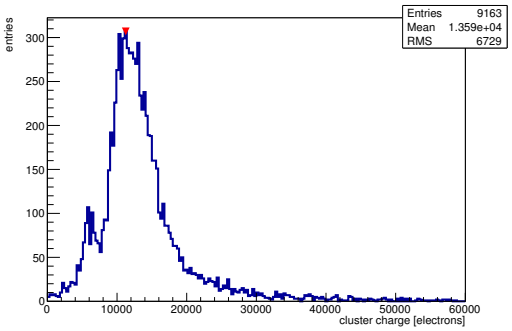

(m) Charge distribution (all cluster sizes included).

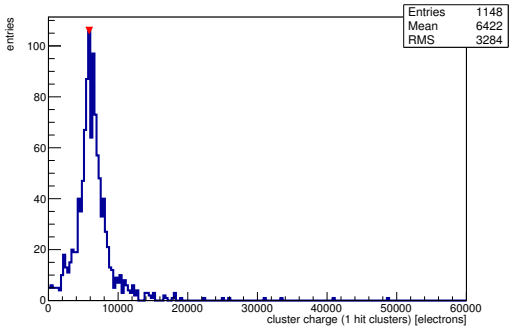

(n) Charge distribution (1 hit cluster).

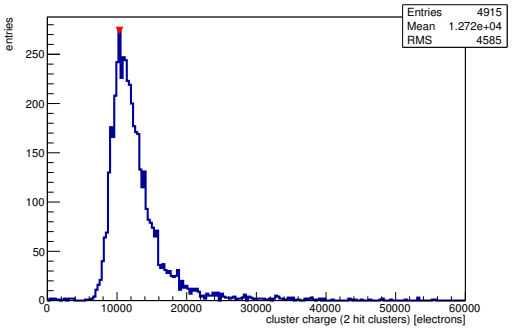

(o) Charge distribution (2 hit cluster).

Figure C.149: Detailed plots for test beam measurement of SCC-31 (description see section 6.1) sample (running as DUT0) during runs 464-519 in the March 2012 test beam period at DESY. Summary of the data in chapter 9. *(cont.)*

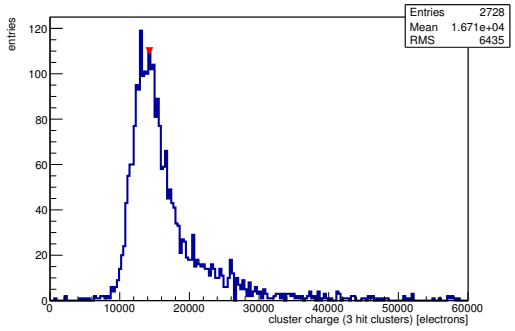

(p) Charge distribution (3 hit cluster).

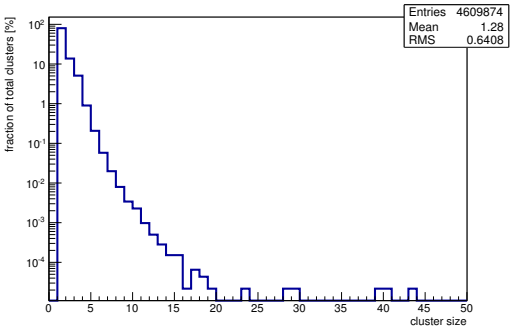

(q) Cluster size distribution.

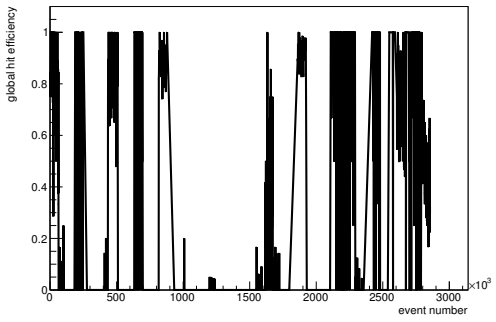

(r) Hit efficiency vs event number.

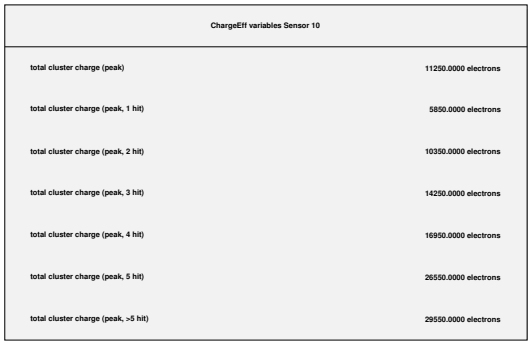

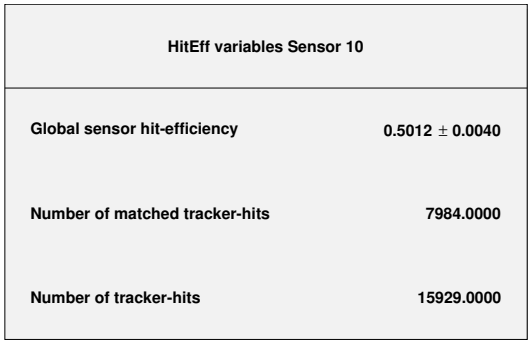

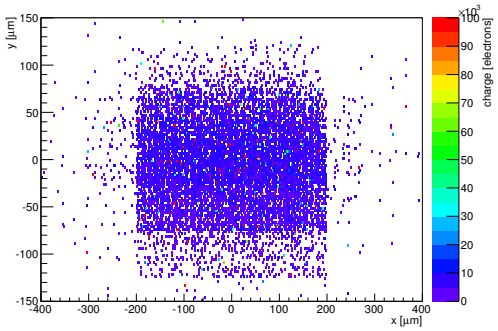

(s) Single pixel mean charge.

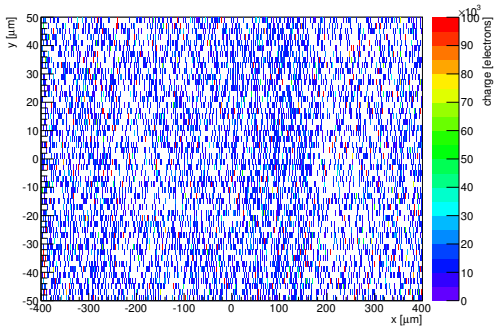

(t) Single pixel mean charge.

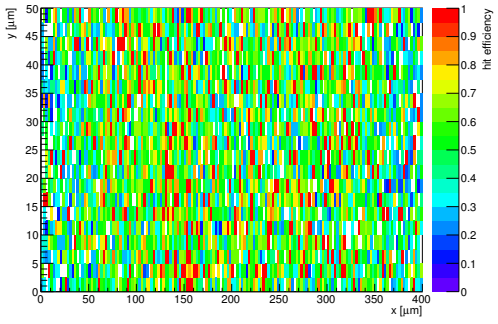

(u) Single pixel hit efficiency.

Figure C.149: Detailed plots for test beam measurement of SCC-31 (description see section 6.1) sample (running as DUT0) during runs 464-519 in the March 2012 test beam period at DESY. Summary of the data in chapter 9.

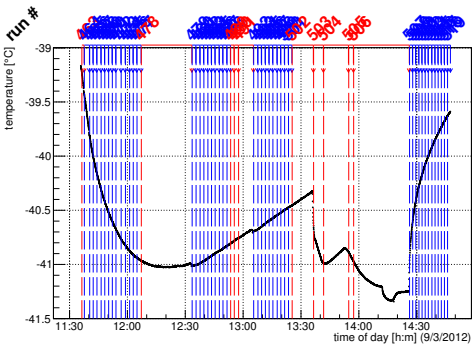

(a) Temperature vs time.

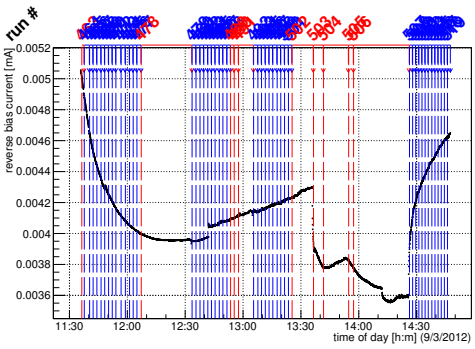

(b) Bias current vs time.

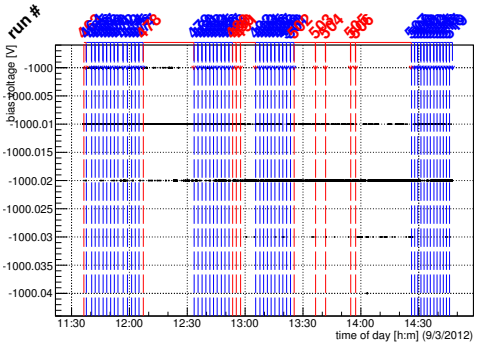

(c) Currently applied bias voltage vs time.

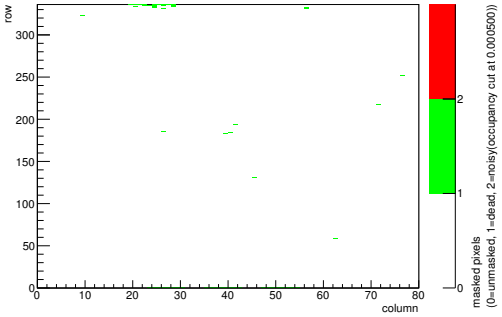

(d) Map of masked pixels.

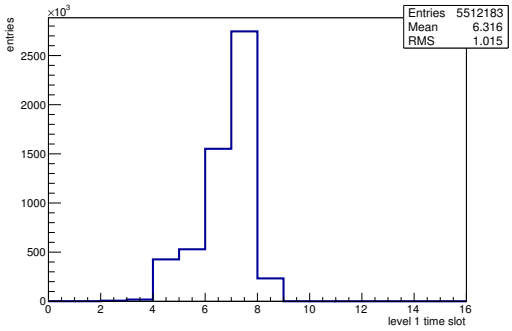

(e) Lvl1 distribution.

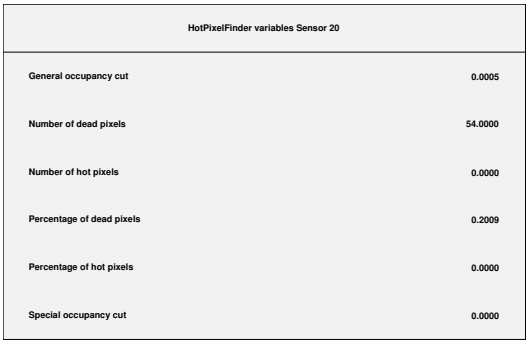

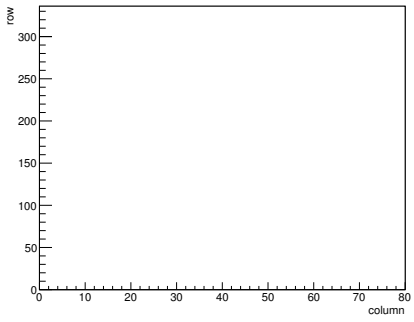

(f) Calibration constant A.

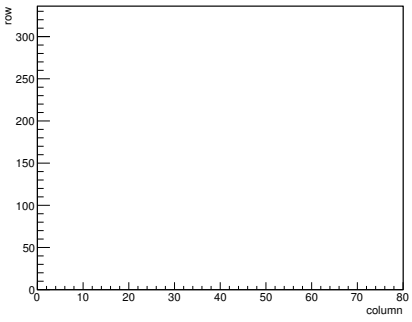

(g) Calibration constant B.

Figure C.150: Detailed plots for test beam measurement of DO-36 (description see section 6.1) sample (running as DUT1) during runs 464-519 in the March 2012 test beam period at DESY. Summary of the data in chapter 9. *(cont.)*

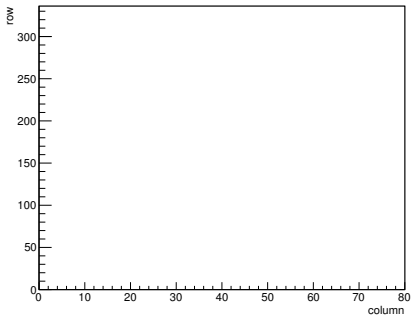

(h) Calibration constant C.

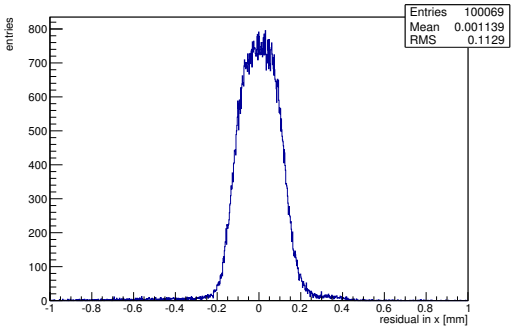

(i) Track residual in x.

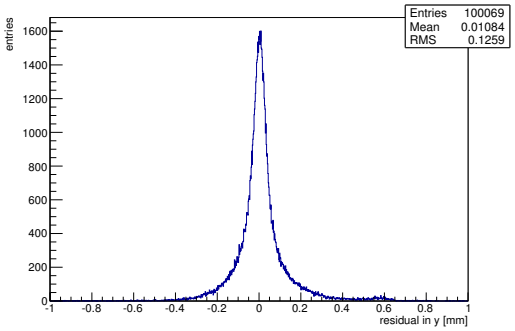

(j) Track residual in y.

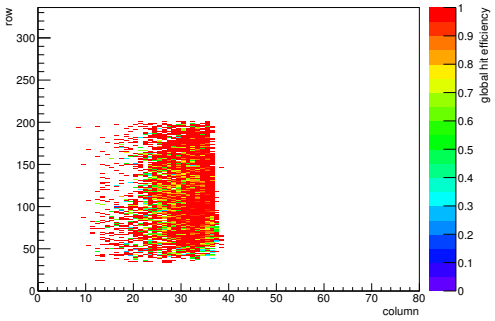

(k) Hit efficiency map.

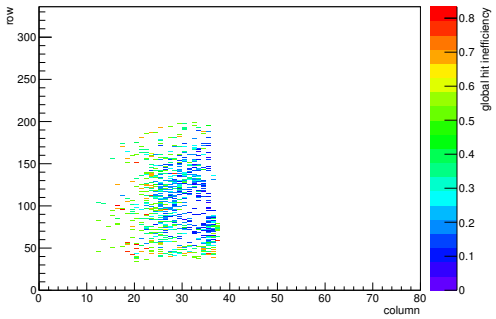

(l) Hit inefficiency map.

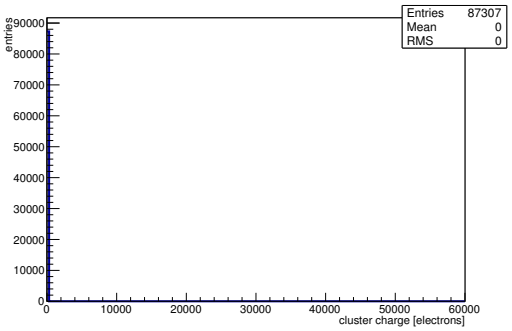

(m) Charge distribution (all cluster sizes included).

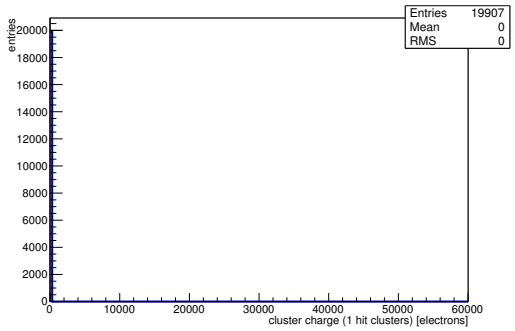

(n) Charge distribution (1 hit cluster).

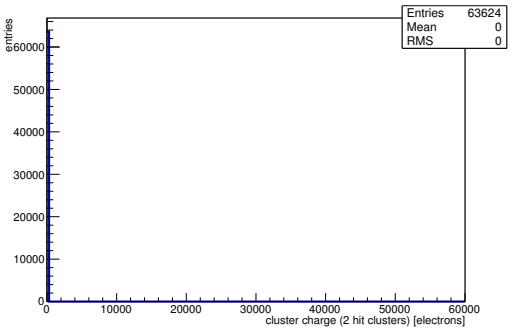

(o) Charge distribution (2 hit cluster).

Figure C.150: Detailed plots for test beam measurement of DO-36 (description see section 6.1) sample (running as DUT1) during runs 464-519 in the March 2012 test beam period at DESY. Summary of the data in chapter 9. *(cont.)*

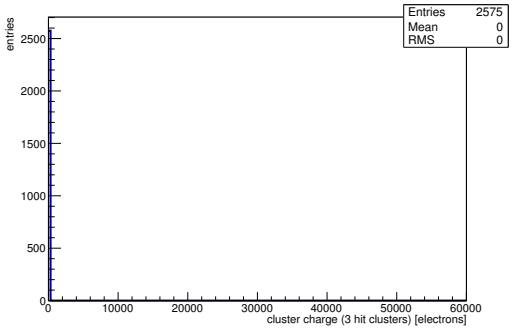

(p) Charge distribution (3 hit cluster).

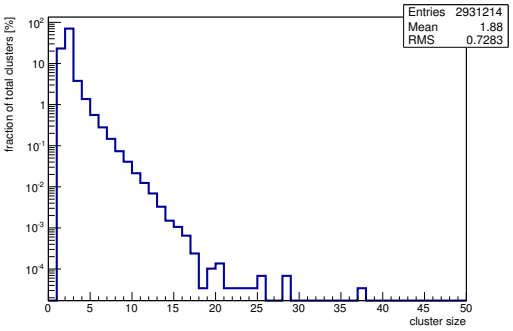

(q) Cluster size distribution.

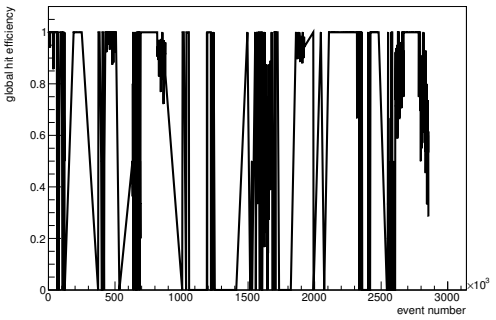

(r) Hit efficiency vs event number.

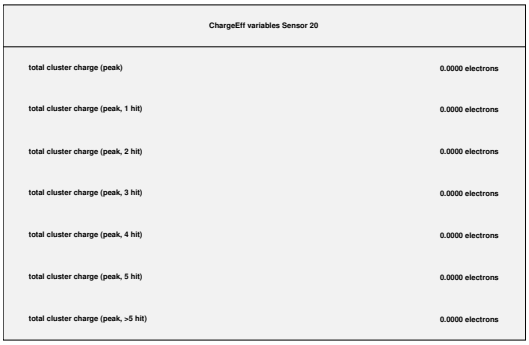

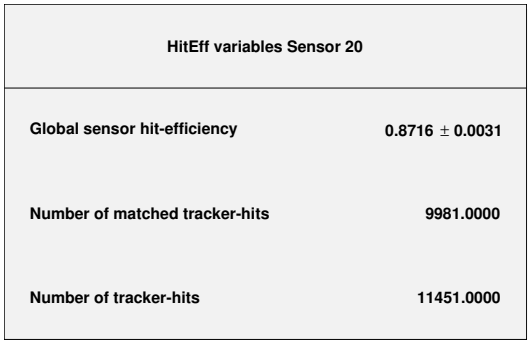

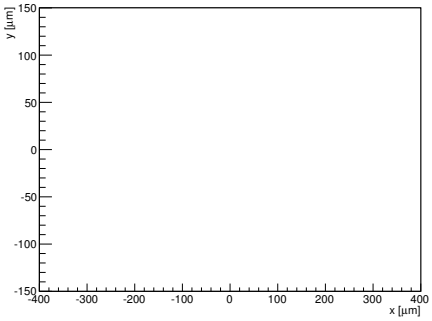

(s) Single pixel mean charge.

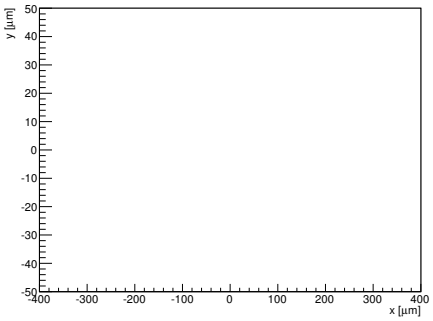

(t) Single pixel mean charge.

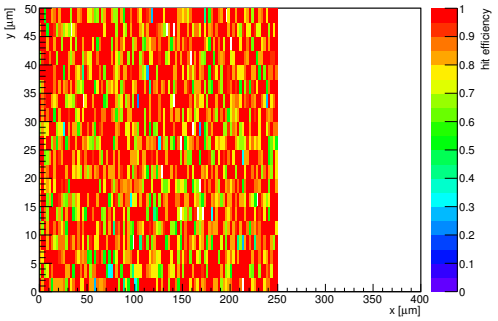

(u) Single pixel hit efficiency.

Figure C.150: Detailed plots for test beam measurement of DO-36 (description see section 6.1) sample (running as DUT1) during runs 464-519 in the March 2012 test beam period at DESY. Summary of the data in chapter 9.

C.4.13 Runs 521-572

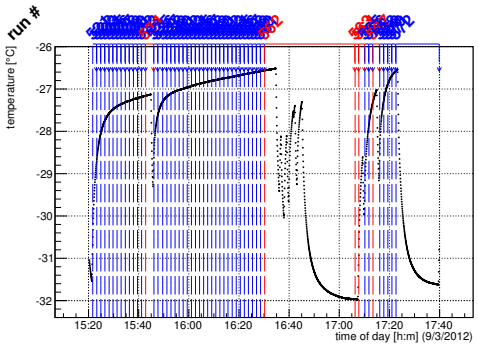

(a) Temperature vs time.

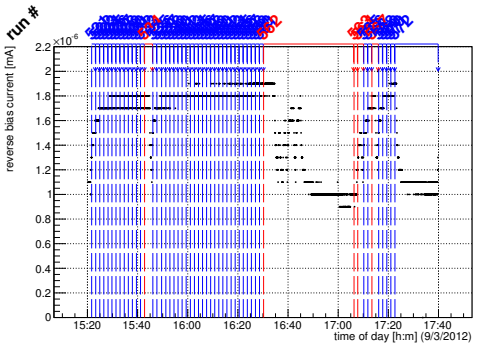

(b) Bias current vs time.

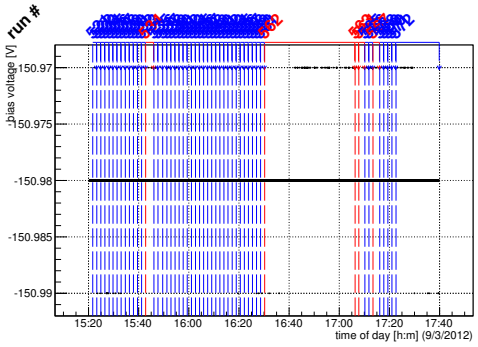

(c) Currently applied bias voltage vs time.

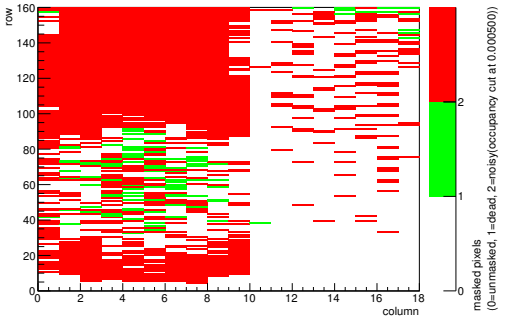

(d) Map of masked pixels.

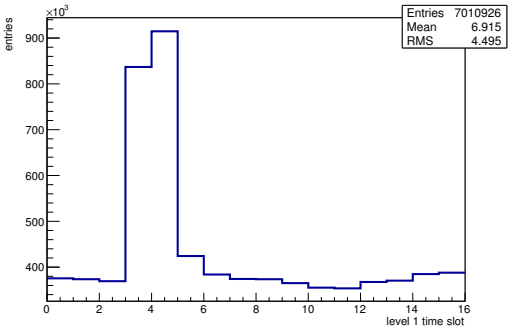

(e) Lvl1 distribution.

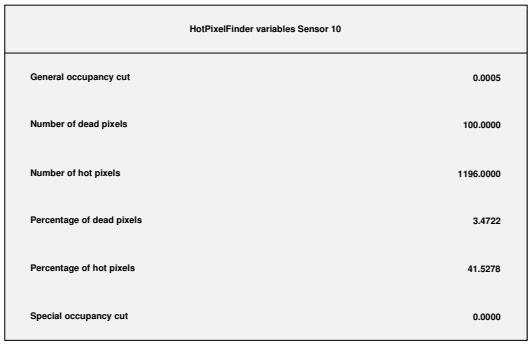

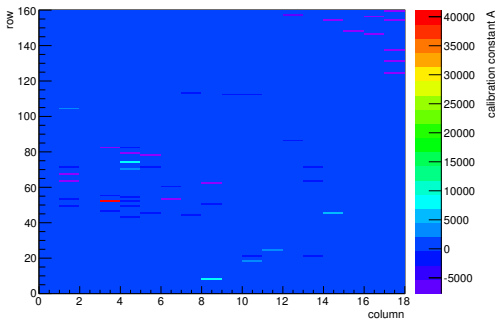

(f) Calibration constant A.

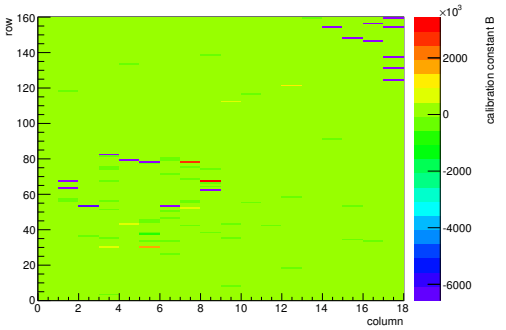

(g) Calibration constant B.

Figure C.151: Detailed plots for test beam measurement of SCC-31 (description see section 6.1) sample (running as DUT0) during runs 521-572 in the March 2012 test beam period at DESY. Summary of the data in chapter 9. *(cont.)*

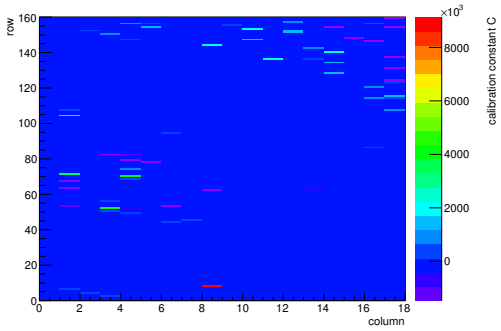

(h) Calibration constant C.

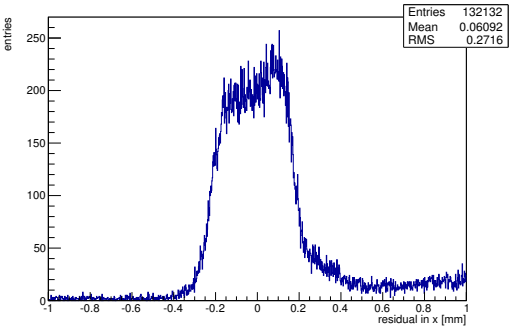

(i) Track residual in x.

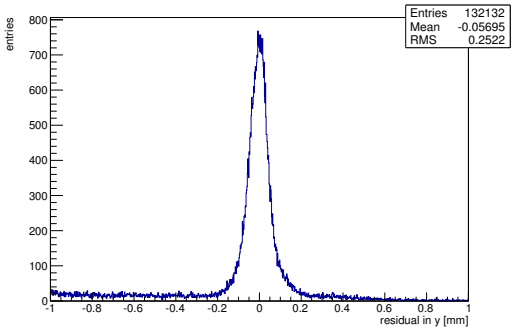

(j) Track residual in y.

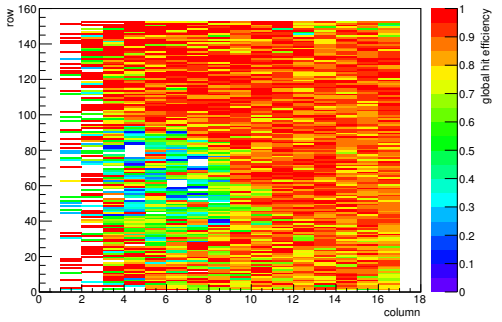

(k) Hit efficiency map.

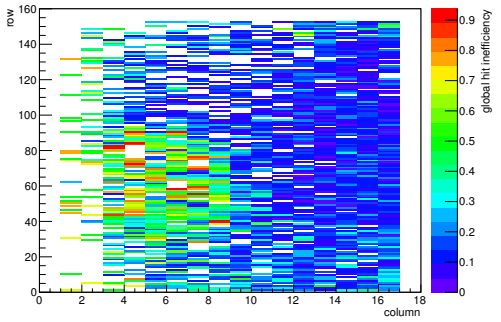

(l) Hit inefficiency map.

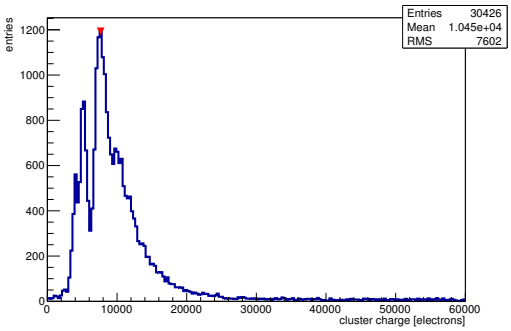

(m) Charge distribution (all cluster sizes included).

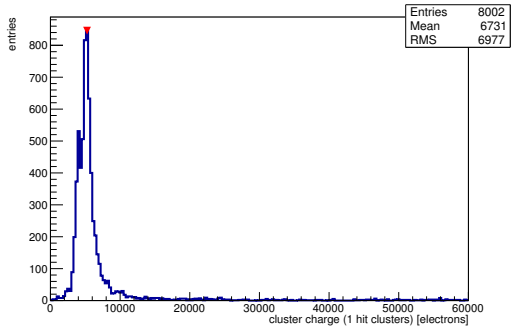

(n) Charge distribution (1 hit cluster).

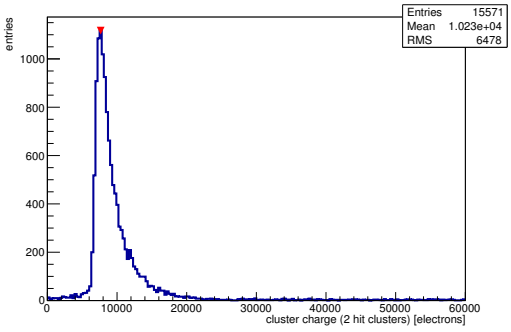

(o) Charge distribution (2 hit cluster).

Figure C.151: Detailed plots for test beam measurement of SCC-31 (description see section 6.1) sample (running as DUT0) during runs 521-572 in the March 2012 test beam period at DESY. Summary of the data in chapter 9. *(cont.)*

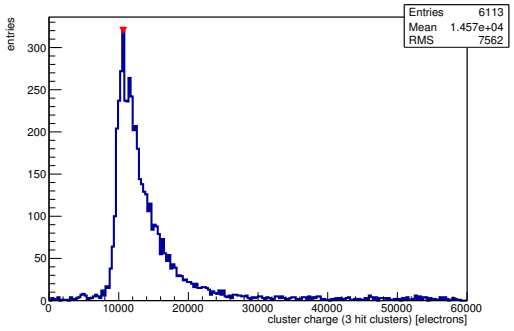

(p) Charge distribution (3 hit cluster).

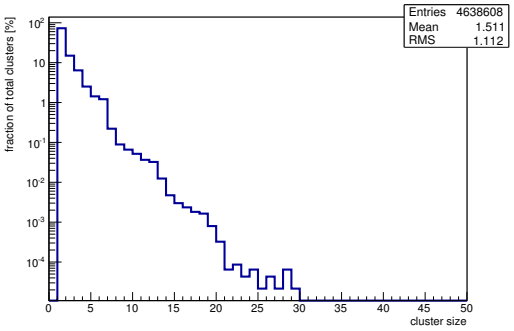

(q) Cluster size distribution.

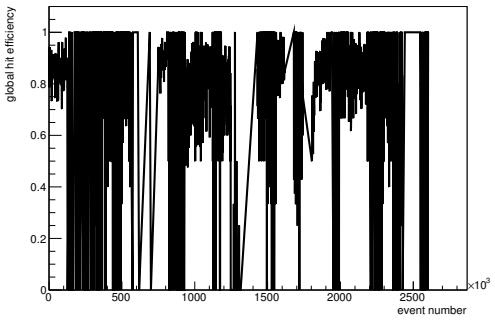

(r) Hit efficiency vs event number.

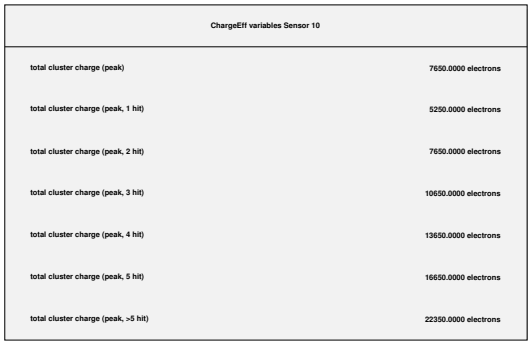

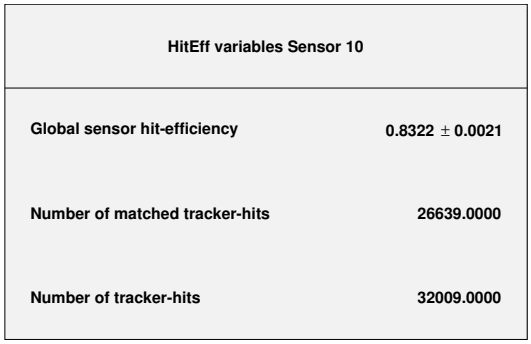

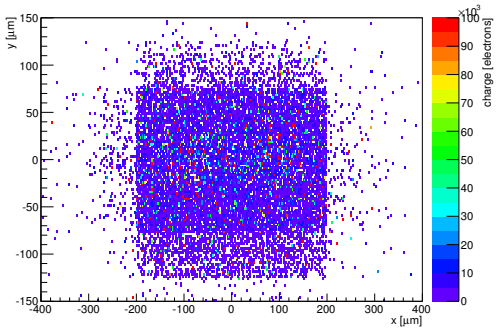

(s) Single pixel mean charge.

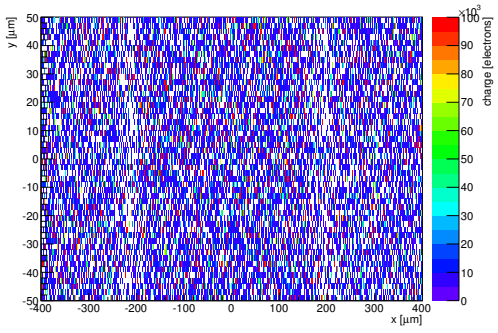

(t) Single pixel mean charge.

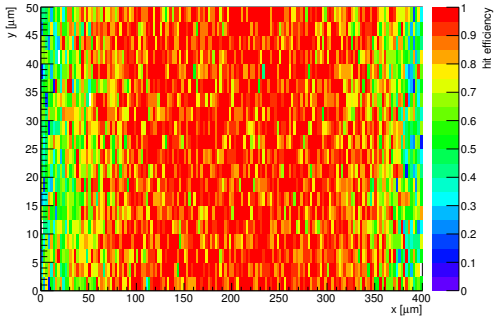

(u) Single pixel hit efficiency.

Figure C.151: Detailed plots for test beam measurement of SCC-31 (description see section 6.1) sample (running as DUT0) during runs 521-572 in the March 2012 test beam period at DESY. Summary of the data in chapter 9.

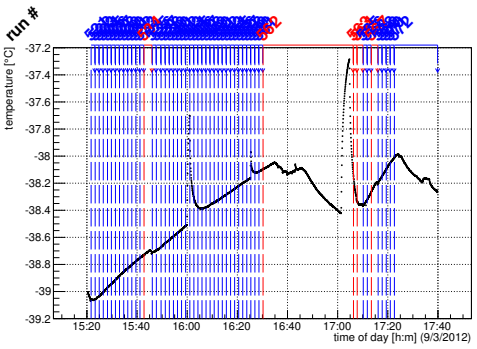

(a) Temperature vs time.

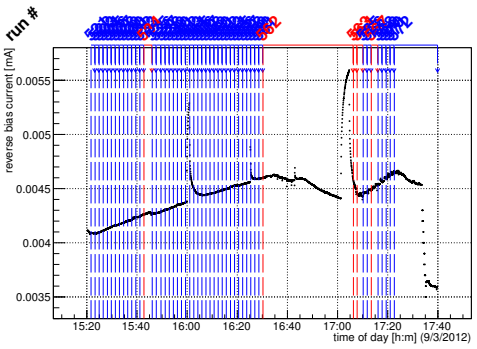

(b) Bias current vs time.

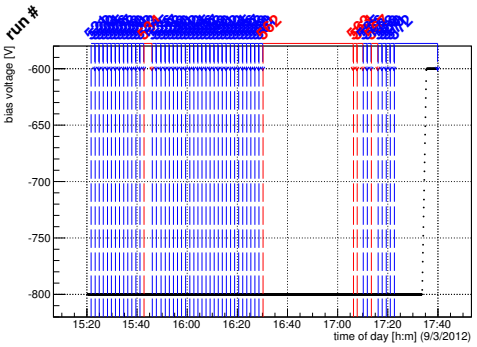

(c) Currently applied bias voltage vs time.

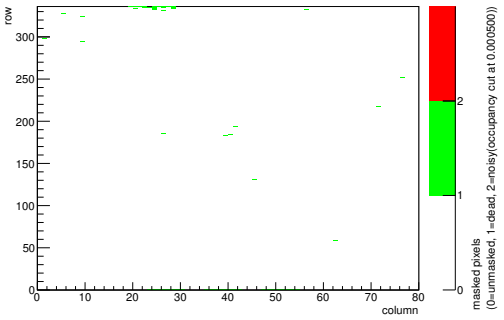

(d) Map of masked pixels.

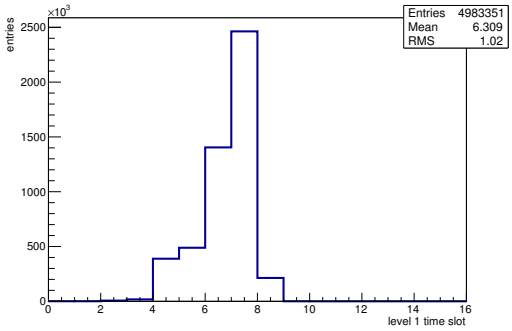

(e) Lvl1 distribution.

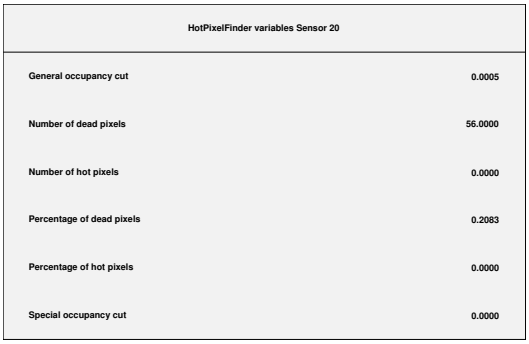

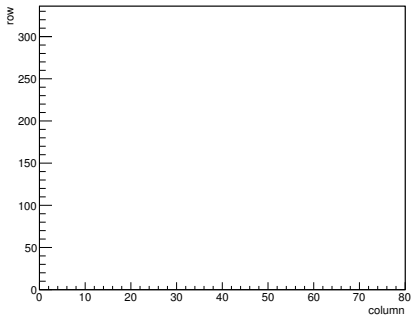

(f) Calibration constant A.

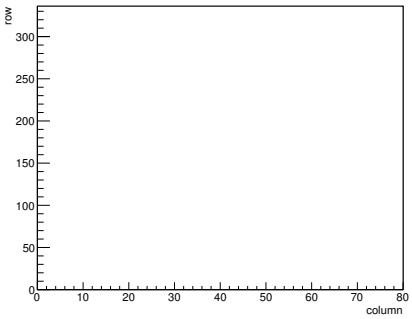

(g) Calibration constant B.

Figure C.152: Detailed plots for test beam measurement of DO-36 (description see section 6.1) sample (running as DUT1) during runs 521-572 in the March 2012 test beam period at DESY. Summary of the data in chapter 9. *(cont.)*

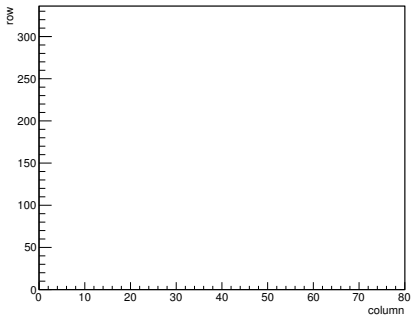

(h) Calibration constant C.

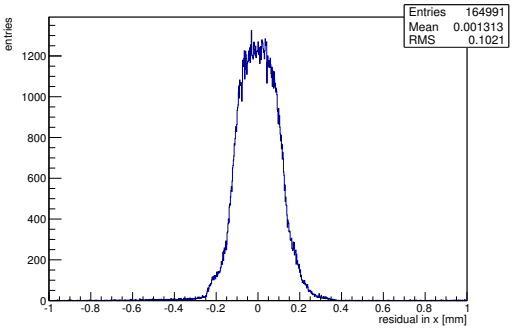

(i) Track residual in x.

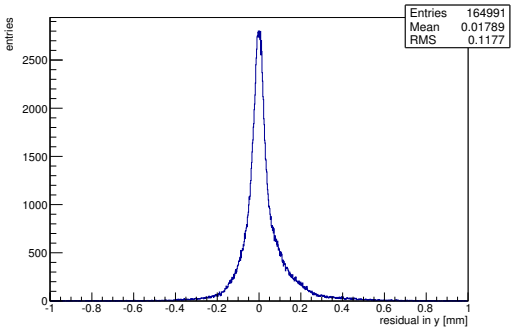

(j) Track residual in y.

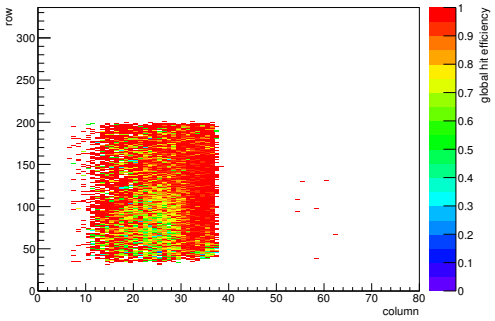

(k) Hit efficiency map.

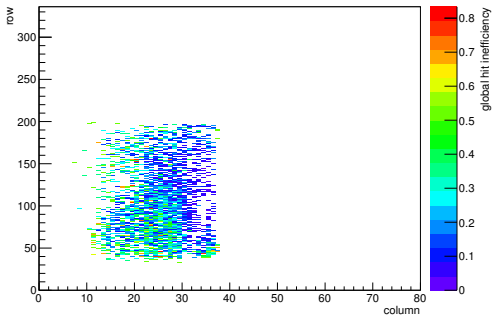

(l) Hit inefficiency map.

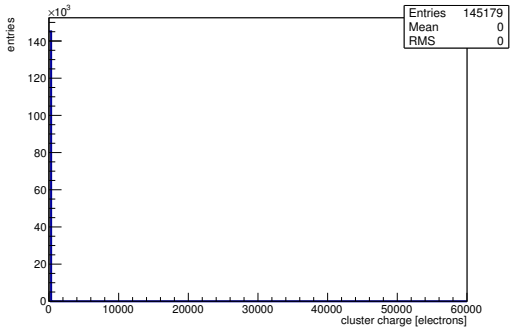

(m) Charge distribution (all cluster sizes included).

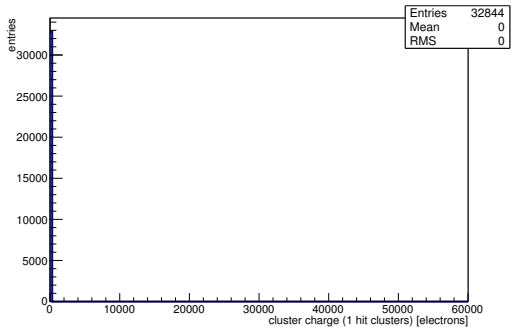

(n) Charge distribution (1 hit cluster).

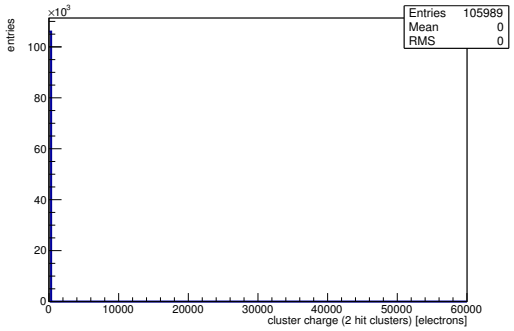

(o) Charge distribution (2 hit cluster).

Figure C.152: Detailed plots for test beam measurement of DO-36 (description see section 6.1) sample (running as DUT1) during runs 521-572 in the March 2012 test beam period at DESY. Summary of the data in chapter 9. *(cont.)*

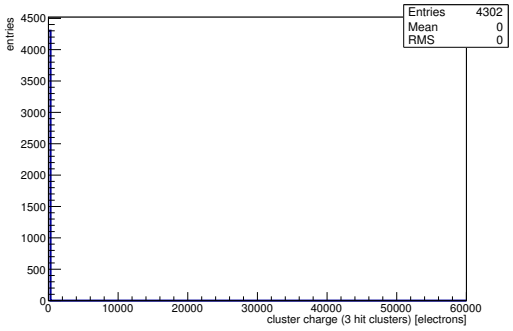

(p) Charge distribution (3 hit cluster).

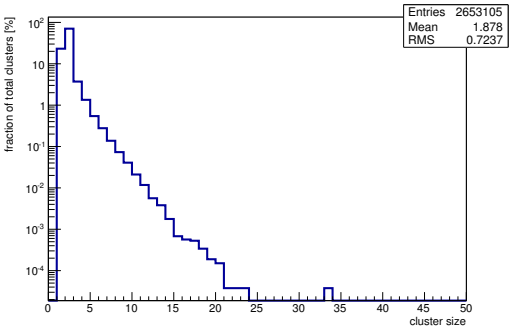

(q) Cluster size distribution.

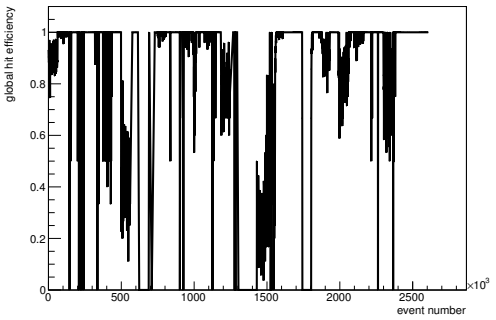

(r) Hit efficiency vs event number.

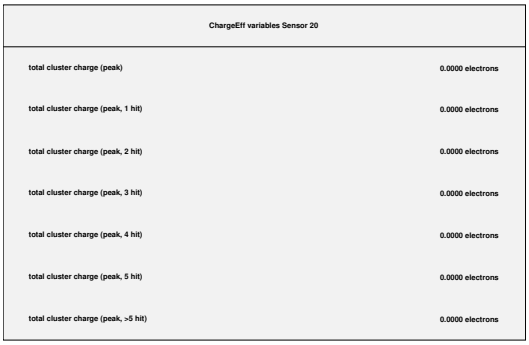

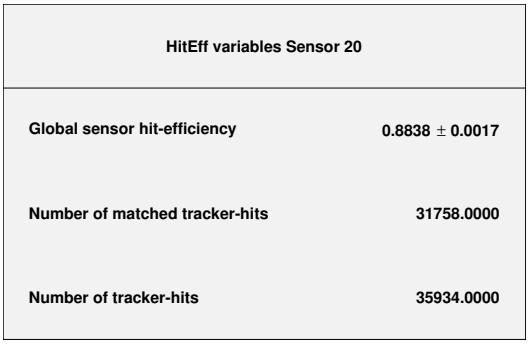

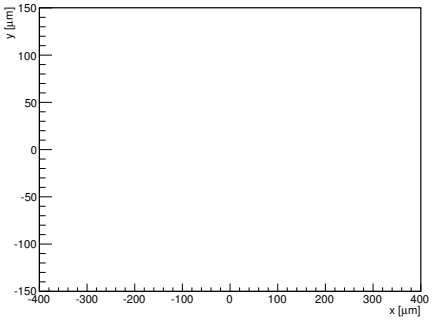

(s) Single pixel mean charge.

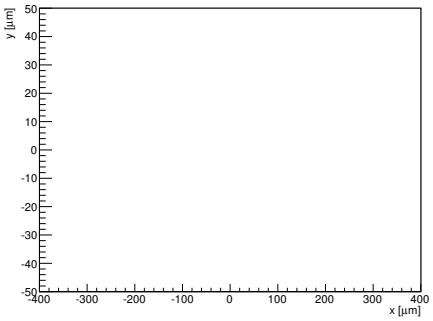

(t) Single pixel mean charge.

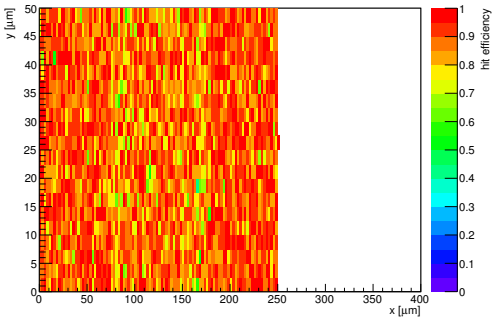

(u) Single pixel hit efficiency.

Figure C.152: Detailed plots for test beam measurement of DO-36 (description see section 6.1) sample (running as DUT1) during runs 521-572 in the March 2012 test beam period at DESY. Summary of the data in chapter 9.

C.4.14 Runs 573-624

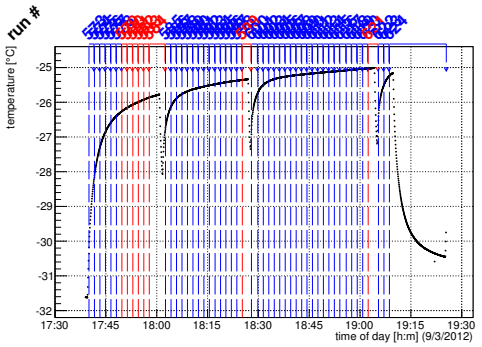

(a) Temperature vs time.

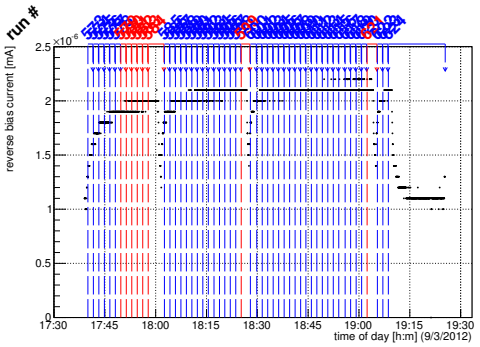

(b) Bias current vs time.

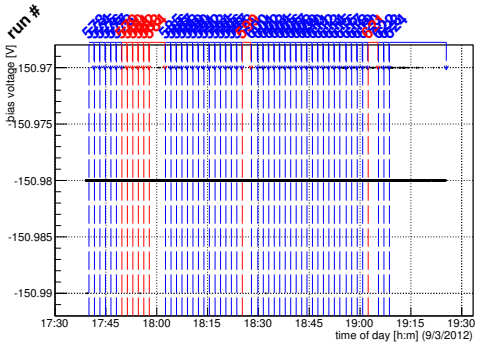

(c) Currently applied bias voltage vs time.

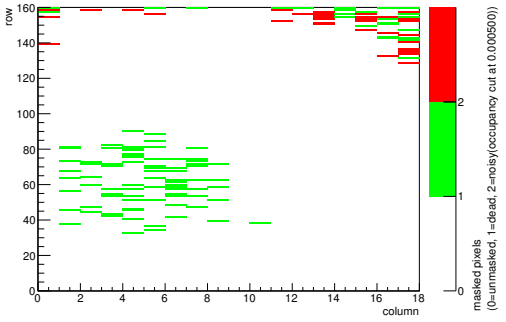

(d) Map of masked pixels.

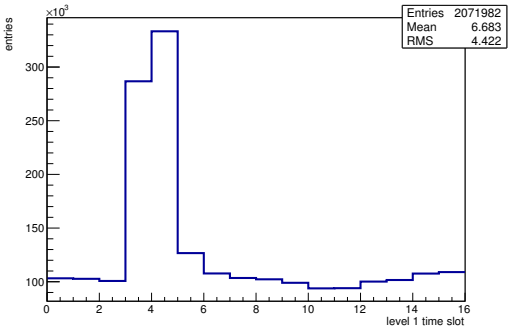

(e) Lvl1 distribution.

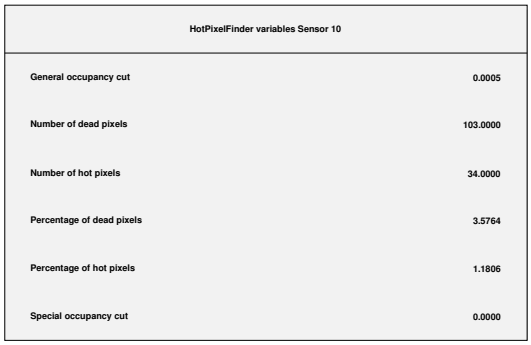

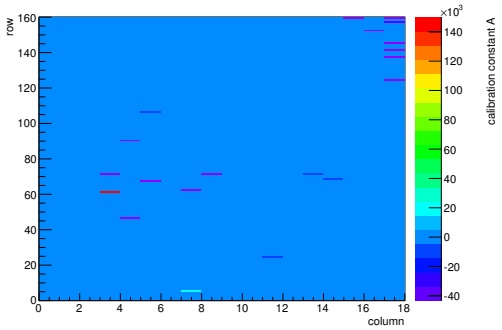

(f) Calibration constant A.

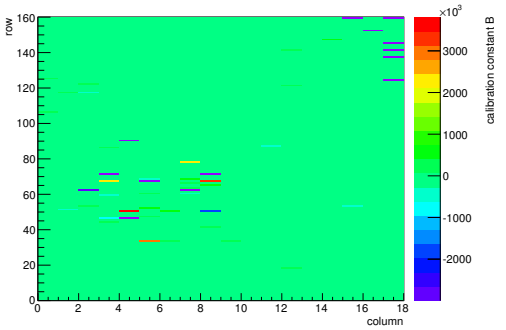

(g) Calibration constant B.

Figure C.153: Detailed plots for test beam measurement of SCC-31 (description see section 6.1) sample (running as DUT0) during runs 573-624 in the March 2012 test beam period at DESY. Summary of the data in chapter 9. *(cont.)*

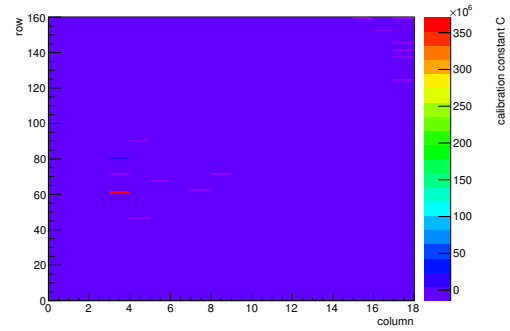

(h) Calibration constant C.

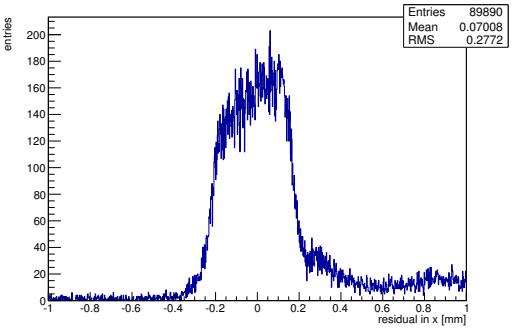

(i) Track residual in x.

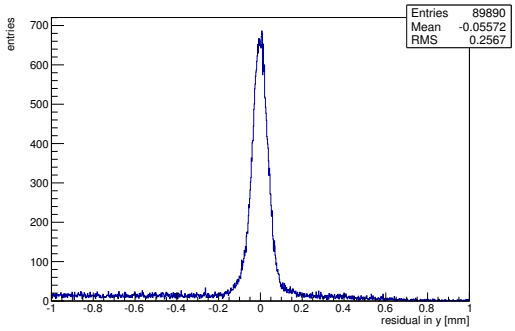

(j) Track residual in y.

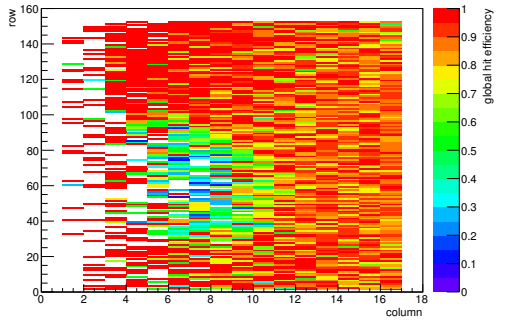

(k) Hit efficiency map.

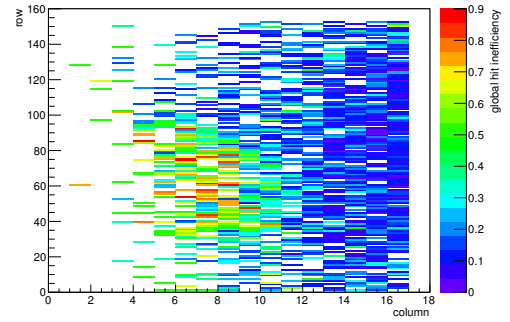

(l) Hit inefficiency map.

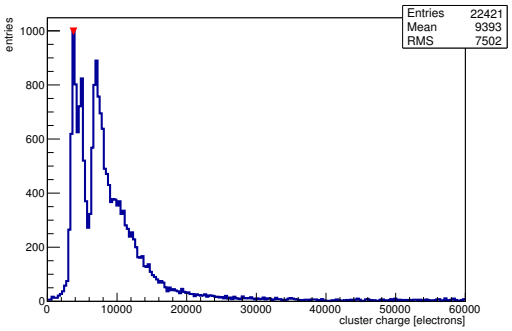

(m) Charge distribution (all cluster sizes included).

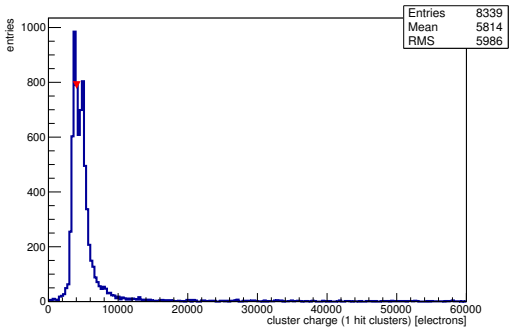

(n) Charge distribution (1 hit cluster).

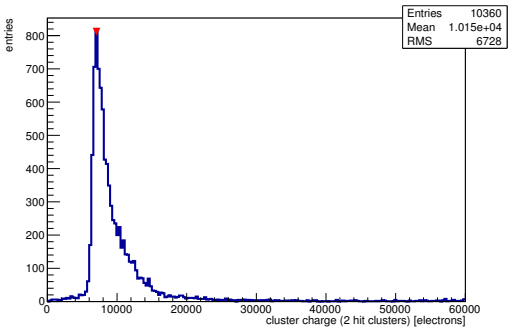

(o) Charge distribution (2 hit cluster).

Figure C.153: Detailed plots for test beam measurement of SCC-31 (description see section 6.1) sample (running as DUT0) during runs 573-624 in the March 2012 test beam period at DESY. Summary of the data in chapter 9. *(cont.)*

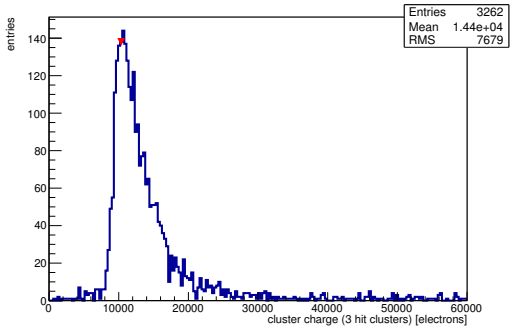

(p) Charge distribution (3 hit cluster).

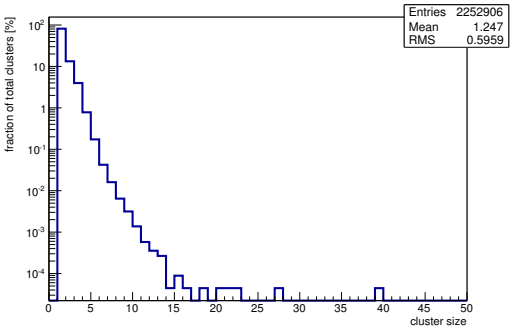

(q) Cluster size distribution.

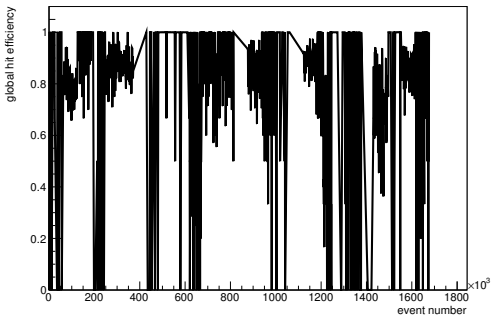

(r) Hit efficiency vs event number.

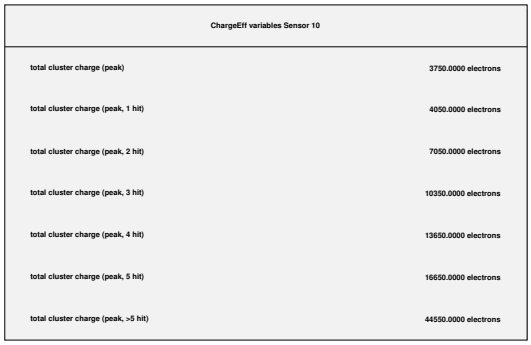

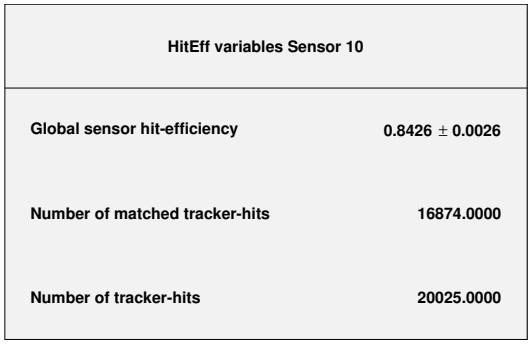

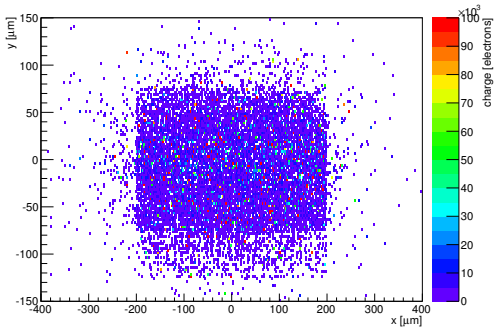

(s) Single pixel mean charge.

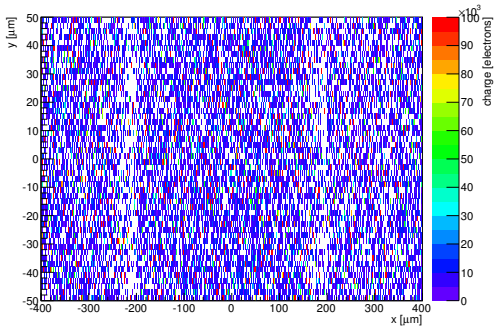

(t) Single pixel mean charge.

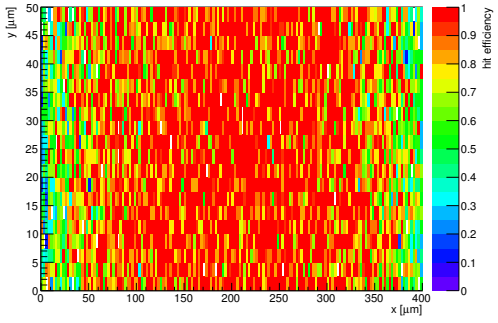

(u) Single pixel hit efficiency.

Figure C.153: Detailed plots for test beam measurement of SCC-31 (description see section 6.1) sample (running as DUT0) during runs 573-624 in the March 2012 test beam period at DESY. Summary of the data in chapter 9.

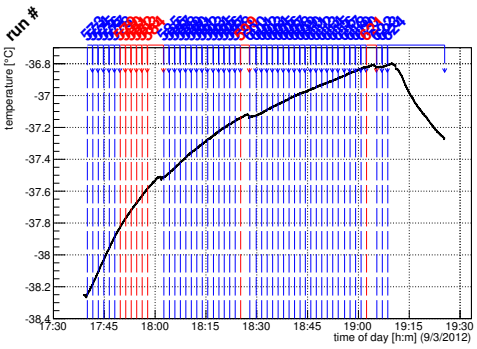

(a) Temperature vs time.

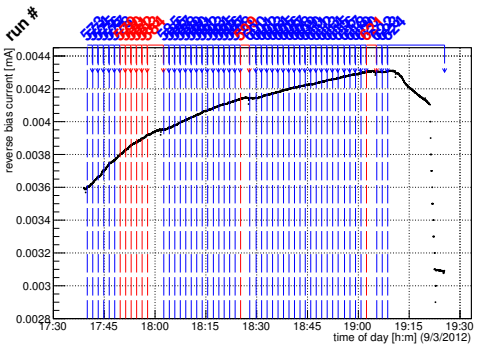

(b) Bias current vs time.

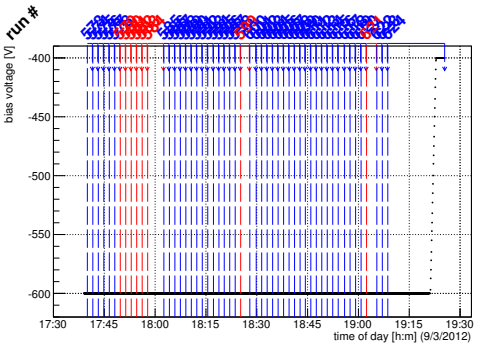

(c) Currently applied bias voltage vs time.

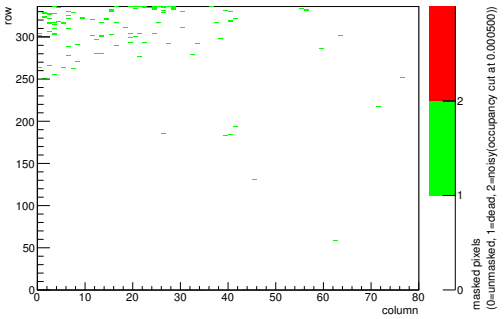

(d) Map of masked pixels.

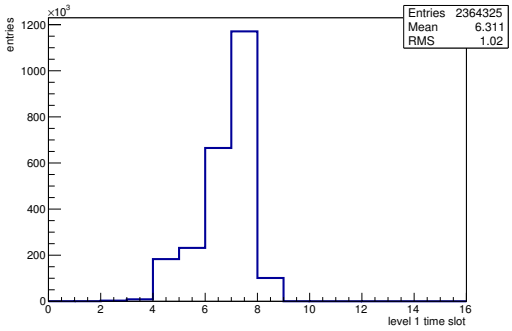

(e) Lvl1 distribution.

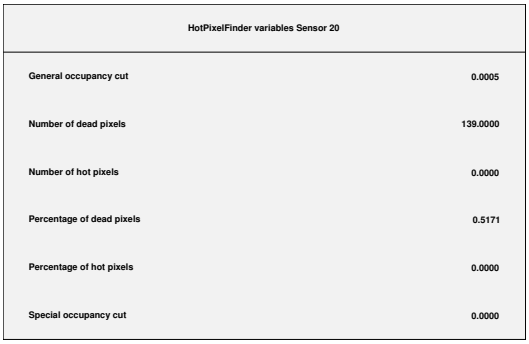

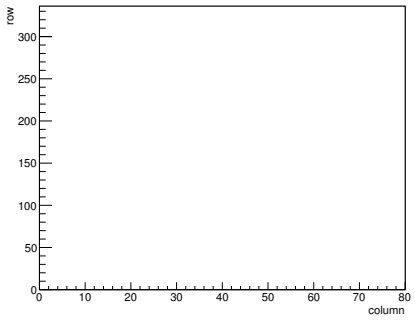

(f) Calibration constant A.

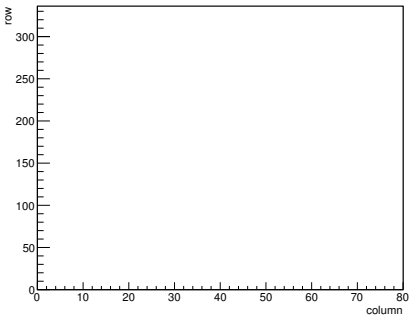

(g) Calibration constant B.

Figure C.154: Detailed plots for test beam measurement of DO-36 (description see section 6.1) sample (running as DUT1) during runs 573-624 in the March 2012 test beam period at DESY. Summary of the data in chapter 9. *(cont.)*

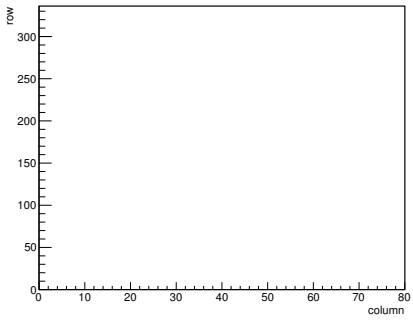

(h) Calibration constant C.

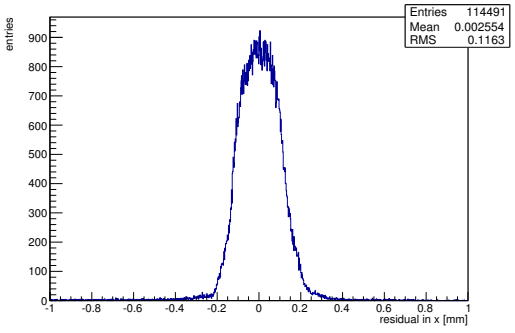

(i) Track residual in x.

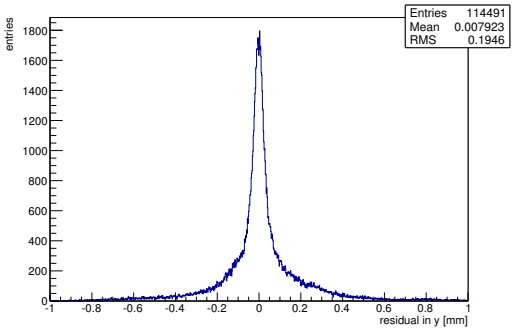

(j) Track residual in y.

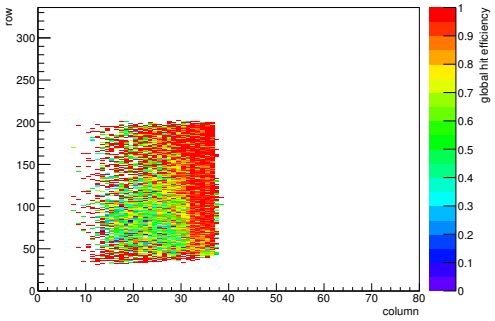

(k) Hit efficiency map.

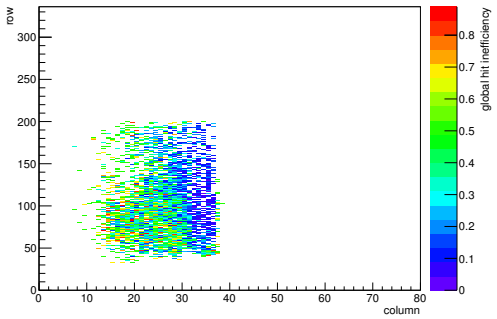

(l) Hit inefficiency map.

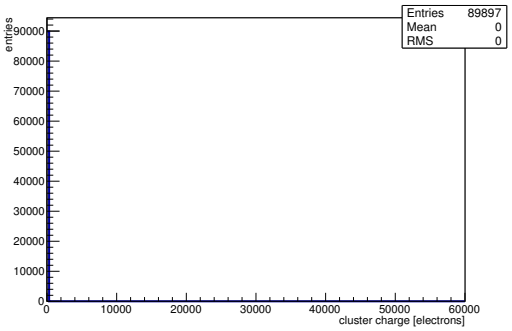

(m) Charge distribution (all cluster sizes included).

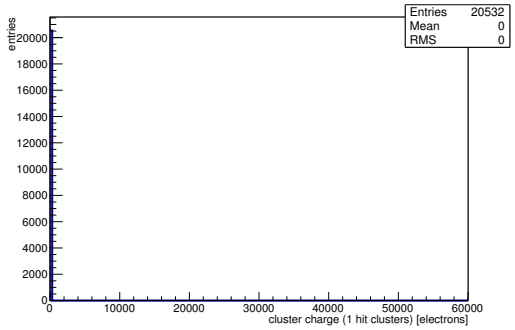

(n) Charge distribution (1 hit cluster).

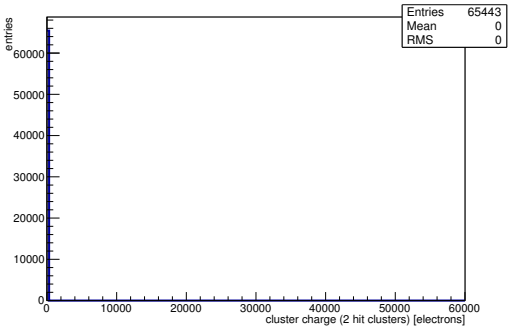

(o) Charge distribution (2 hit cluster).

Figure C.154: Detailed plots for test beam measurement of DO-36 (description see section 6.1) sample (running as DUT1) during runs 573-624 in the March 2012 test beam period at DESY. Summary of the data in chapter 9. *(cont.)*

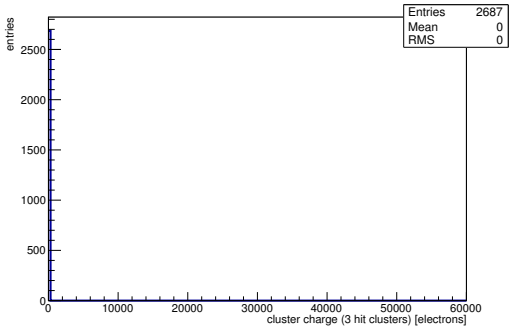

(p) Charge distribution (3 hit cluster).

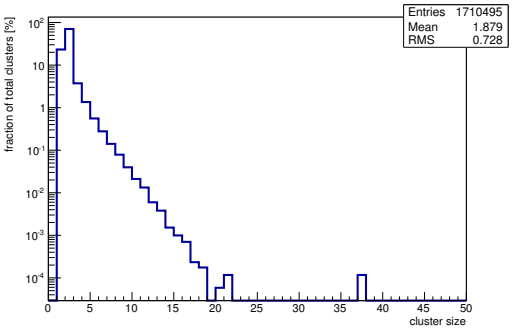

(q) Cluster size distribution.

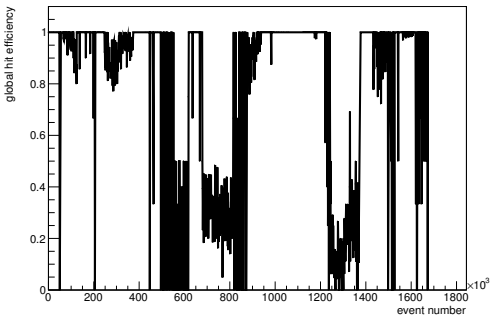

(r) Hit efficiency vs event number.

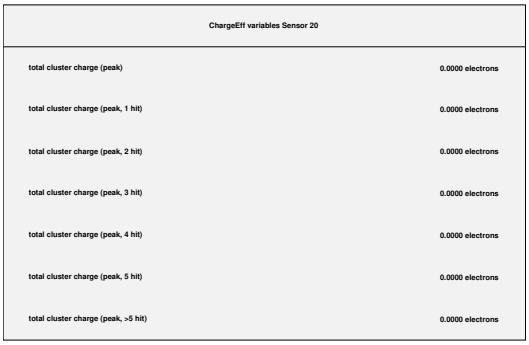

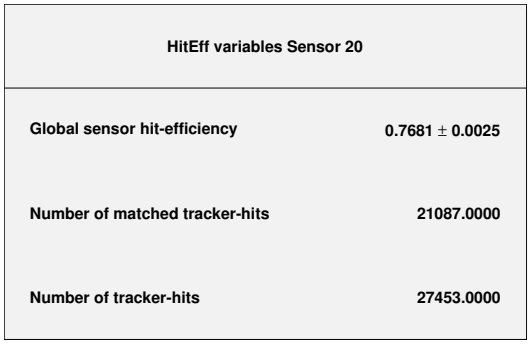

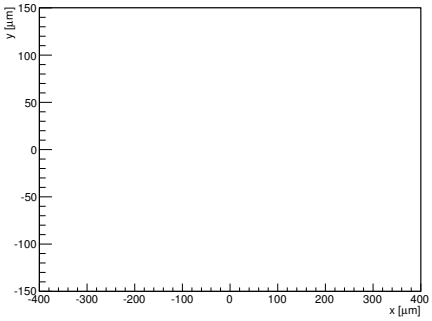

(s) Single pixel mean charge.

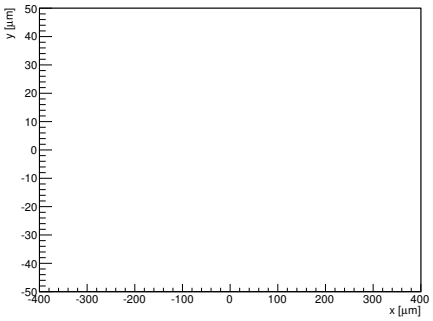

(t) Single pixel mean charge.

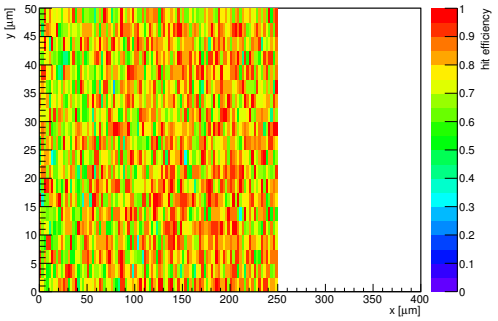

(u) Single pixel hit efficiency.

Figure C.154: Detailed plots for test beam measurement of DO-36 (description see section 6.1) sample (running as DUT1) during runs 573-624 in the March 2012 test beam period at DESY. Summary of the data in chapter 9.

C.5 CERN SPS May 2012

C.5.1 Runs 739-765

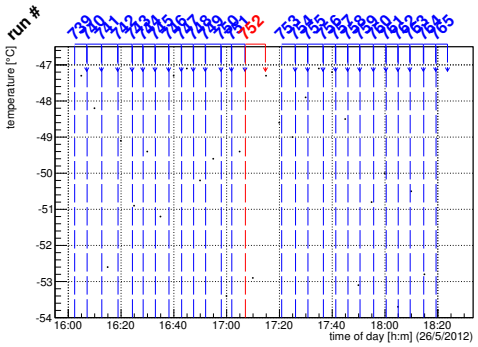

(a) Temperature vs time.

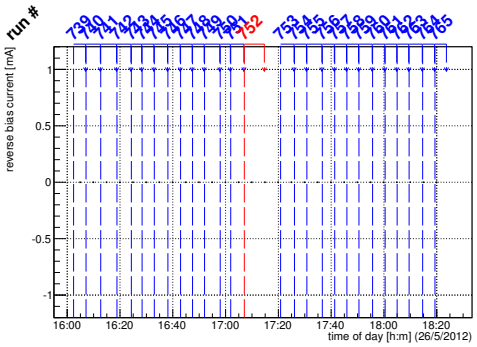

(b) Bias current vs time.

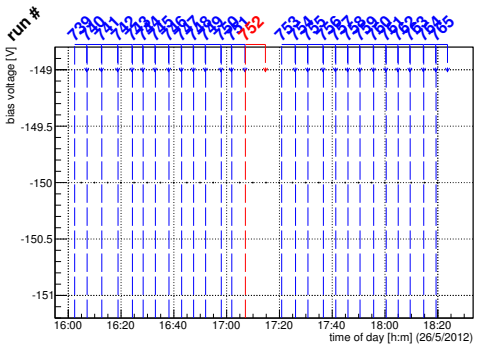

(c) Currently applied bias voltage vs time.

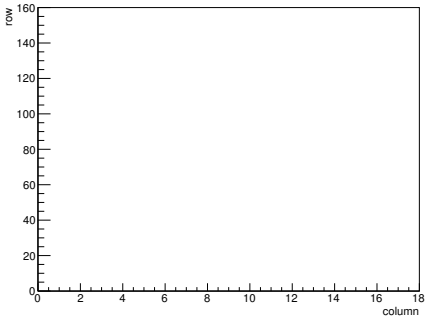

(d) Map of masked pixels.

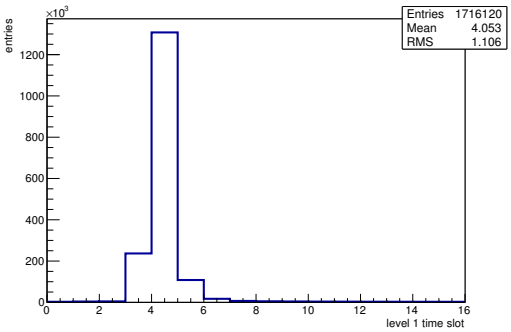

(e) Lvl1 distribution.

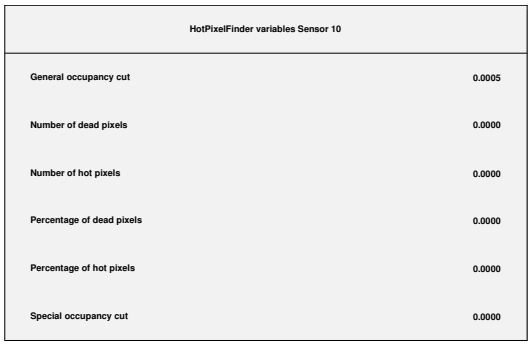

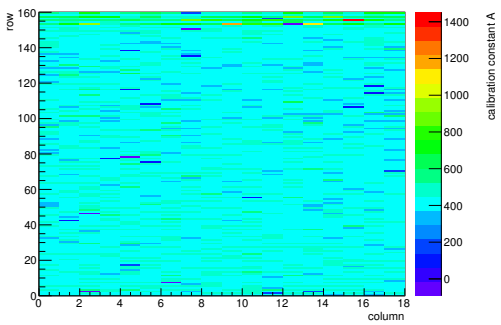

(f) Calibration constant A.

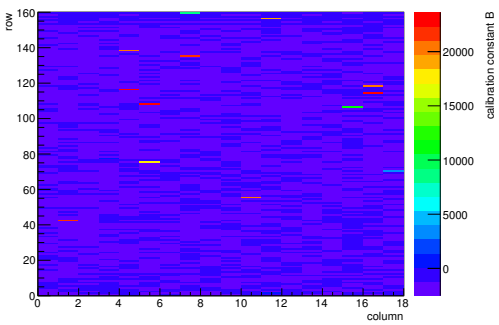

(g) Calibration constant B.

Figure C.155: Detailed plots for test beam measurement of DO-1 (description see section 6.1) sample (running as DUT0) during runs 739-765 in the May 2012 test beam period at CERN SPS in area H6B. Summary of the data in chapter 9. *(cont.)*

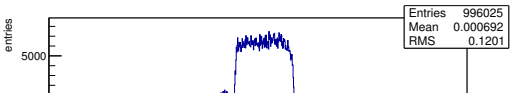

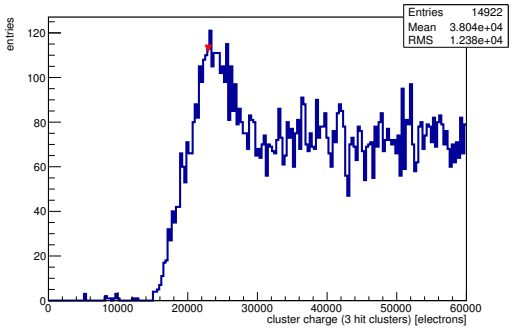

(p) Charge distribution (3 hit cluster).

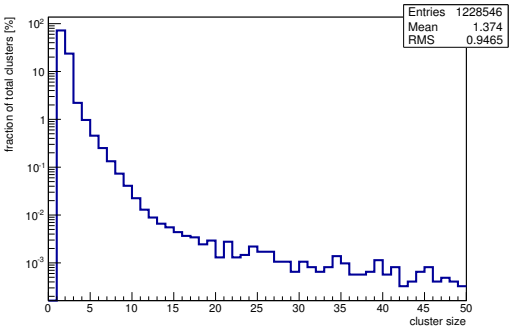

(q) Cluster size distribution.

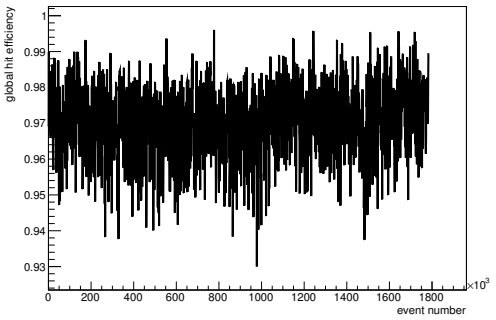

(r) Hit efficiency vs event number.

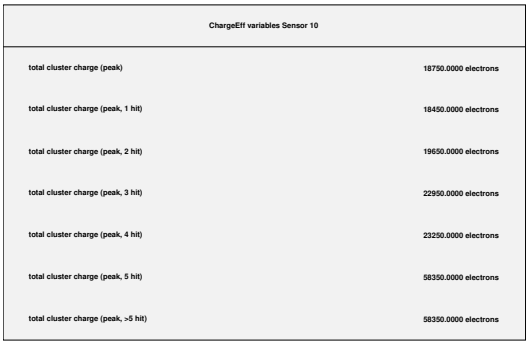

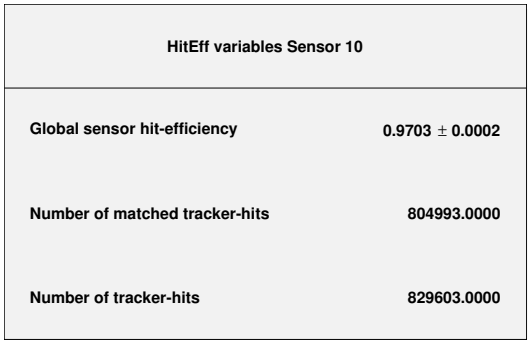

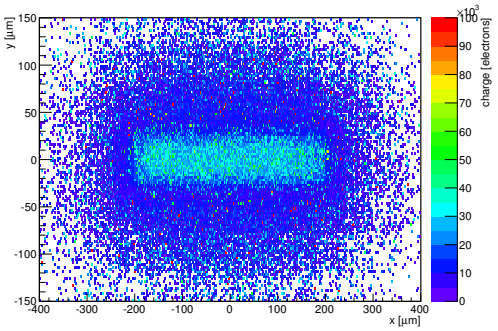

(s) Single pixel mean charge.

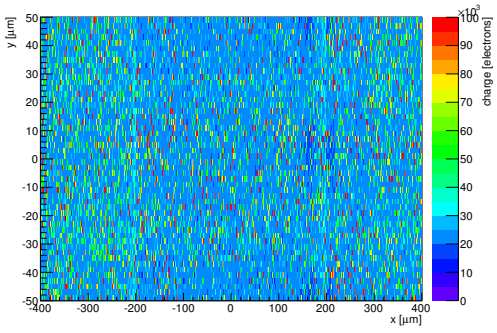

(t) Single pixel mean charge.

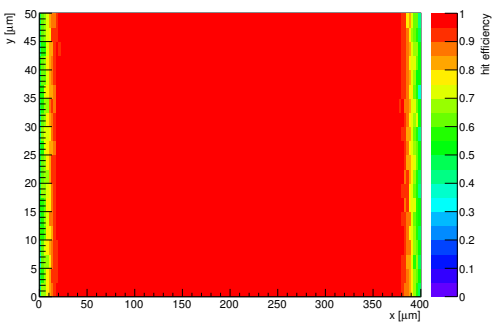

(u) Single pixel hit efficiency.

Figure C.155: Detailed plots for test beam measurement of DO-1 (description see section 6.1) sample (running as DUT0) during runs 739-765 in the May 2012 test beam period at CERN SPS in area H6B. Summary of the data in chapter 9.

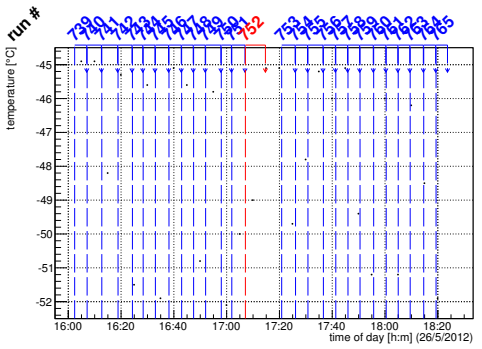

(a) Temperature vs time.

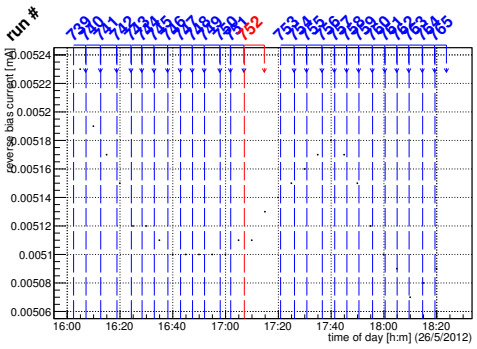

(b) Bias current vs time.

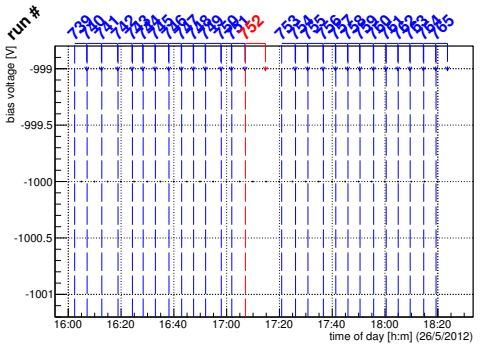

(c) Currently applied bias voltage vs time.

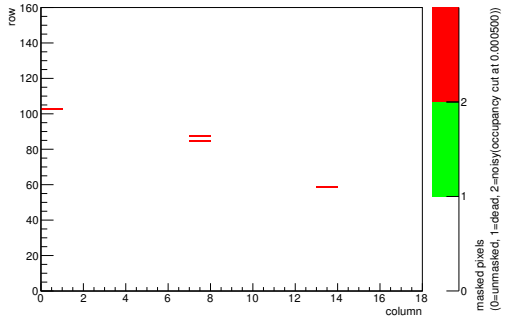

(d) Map of masked pixels.

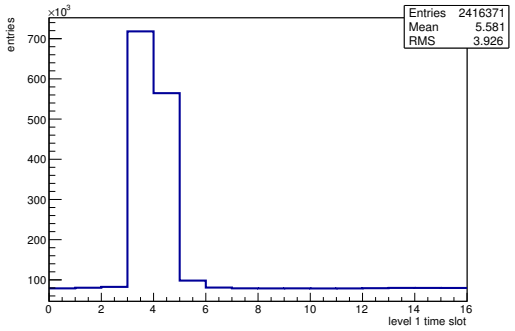

(e) Lvl1 distribution.

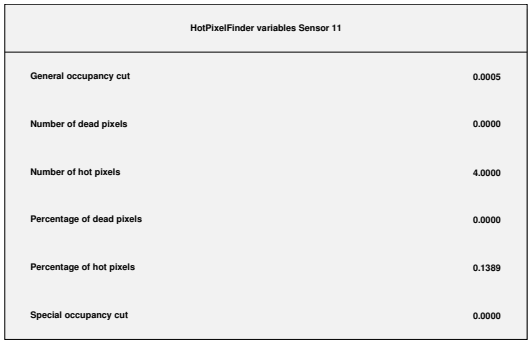

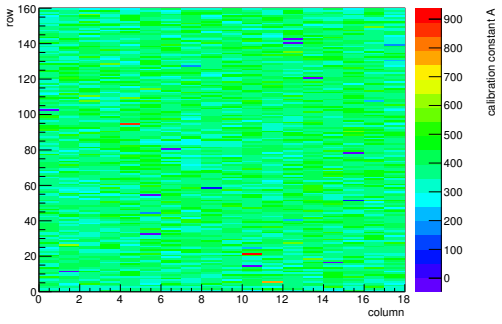

(f) Calibration constant A.

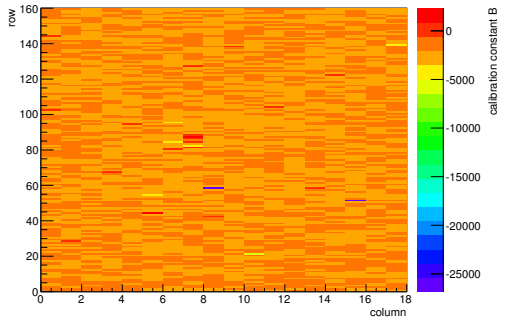

(g) Calibration constant B.

Figure C.156: Detailed plots for test beam measurement of DO-10 (description see section 6.1) sample (running as DUT1) during runs 739-765 in the May 2012 test beam period at CERN SPS in area H6B. Summary of the data in chapter 9. *(cont.)*

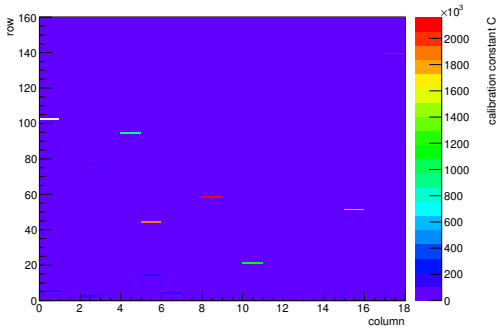

(h) Calibration constant C.

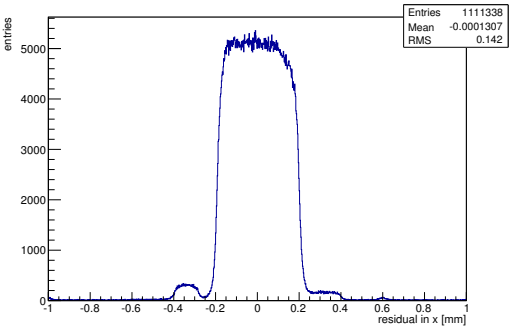

(i) Track residual in x.

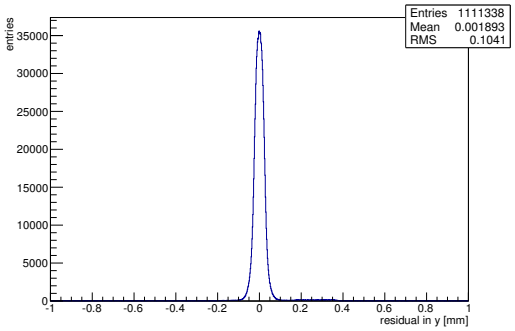

(j) Track residual in y.

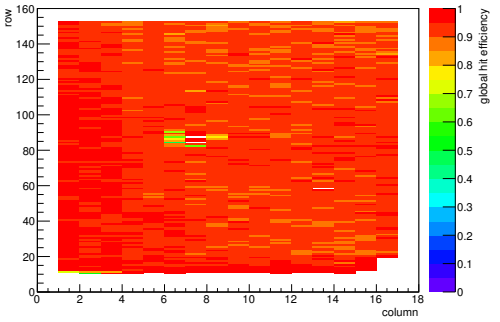

(k) Hit efficiency map.

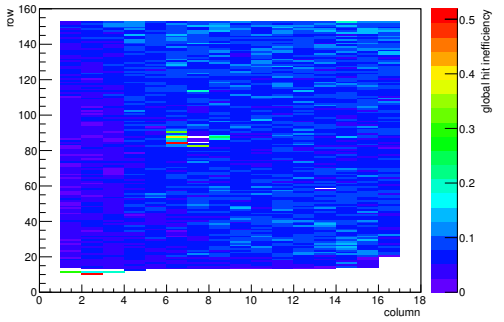

(l) Hit inefficiency map.

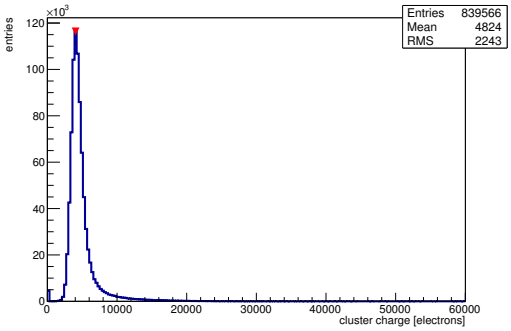

(m) Charge distribution (all cluster sizes included).

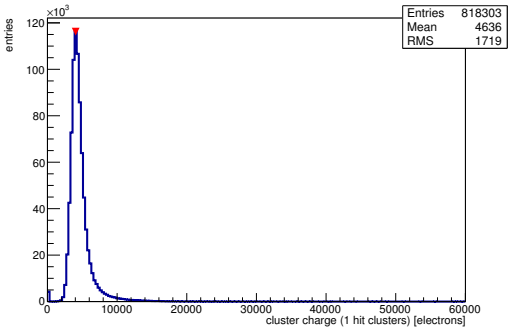

(n) Charge distribution (1 hit cluster).

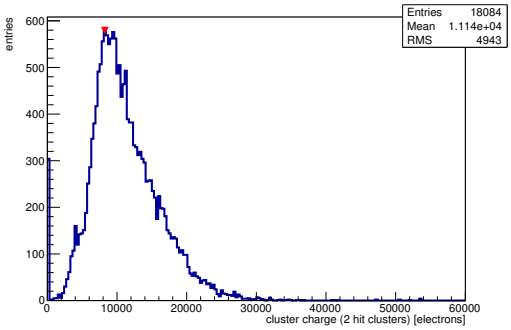

(o) Charge distribution (2 hit cluster).

Figure C.156: Detailed plots for test beam measurement of DO-10 (description see section 6.1) sample (running as DUT1) during runs 739-765 in the May 2012 test beam period at CERN SPS in area H6B. Summary of the data in chapter 9. *(cont.)*

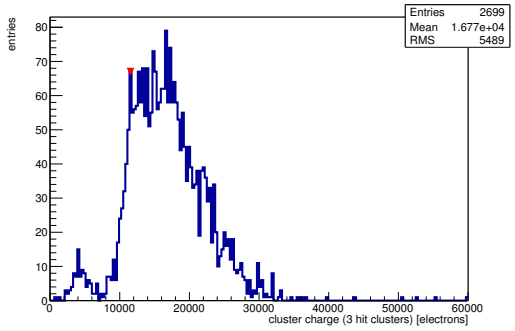

(p) Charge distribution (3 hit cluster).

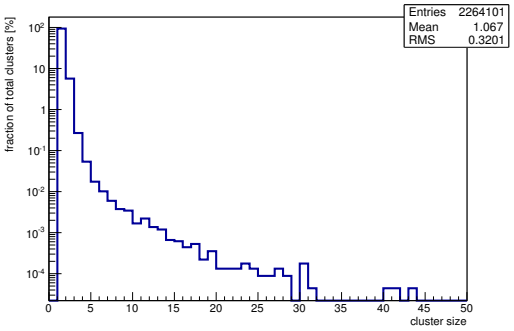

(q) Cluster size distribution.

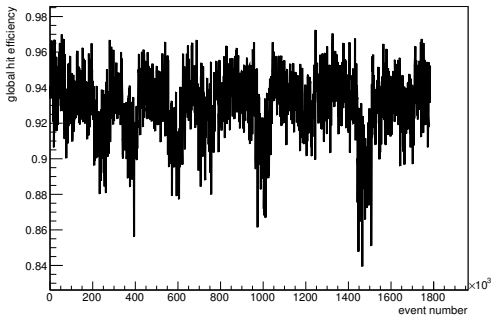

(r) Hit efficiency vs event number.

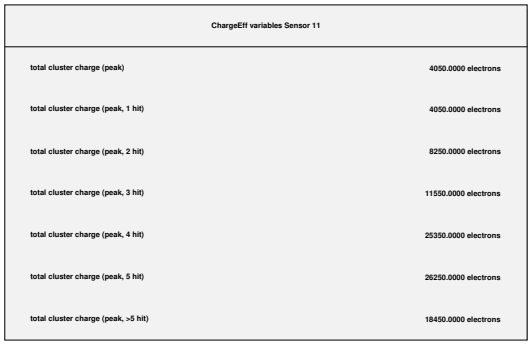

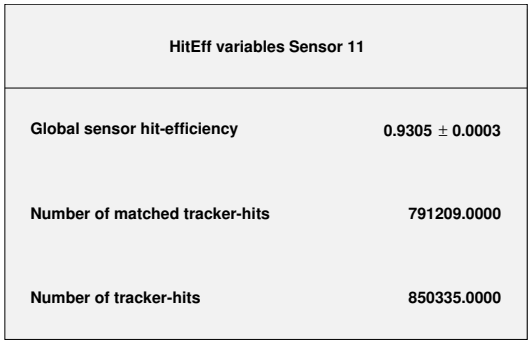

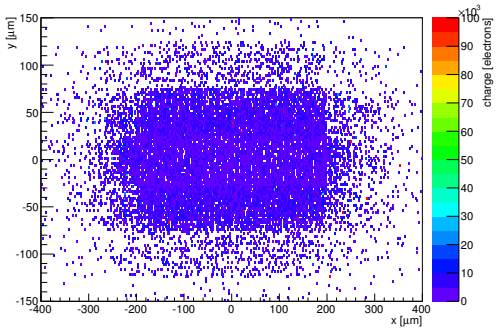

(s) Single pixel mean charge.

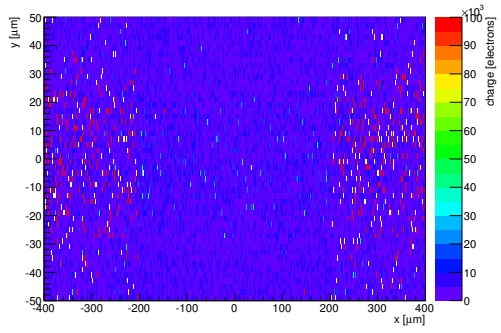

(t) Single pixel mean charge.

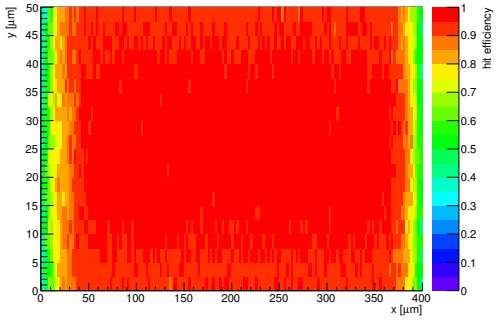

(u) Single pixel hit efficiency.

Figure C.156: Detailed plots for test beam measurement of DO-10 (description see section 6.1) sample (running as DUT1) during runs 739-765 in the May 2012 test beam period at CERN SPS in area H6B. Summary of the data in chapter 9.

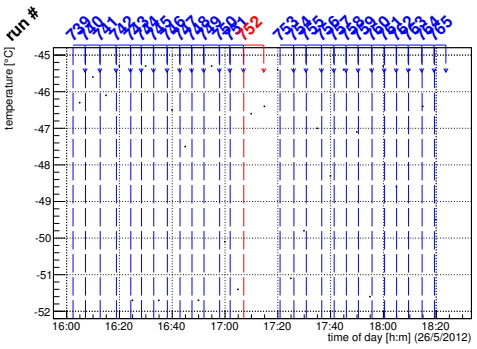

(a) Temperature vs time.

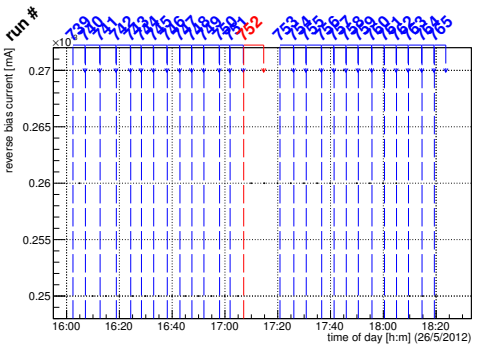

(b) Bias current vs time.

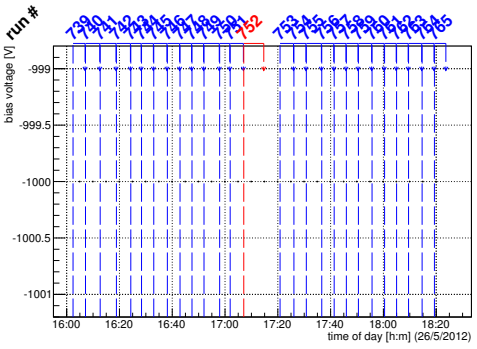

(c) Currently applied bias voltage vs time.

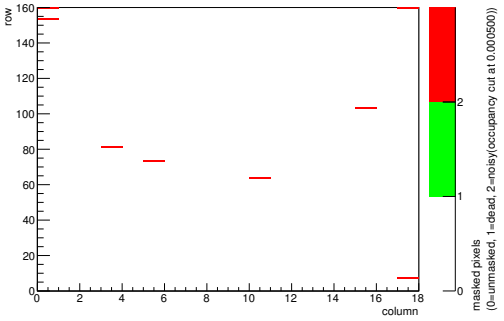

(d) Map of masked pixels.

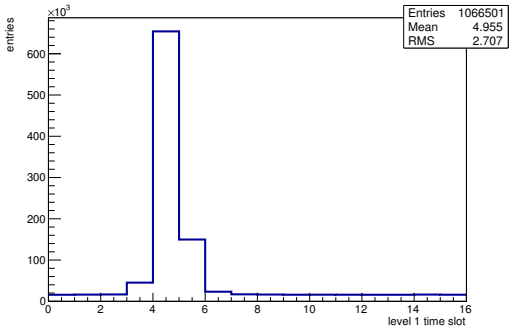

(e) Lvl1 distribution.

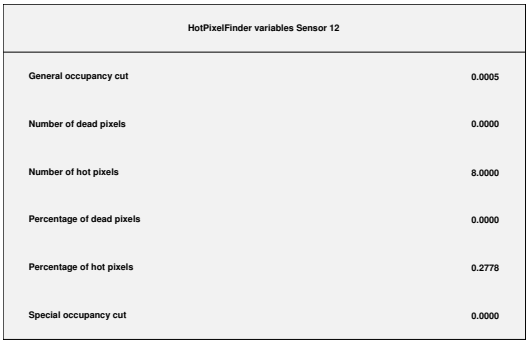

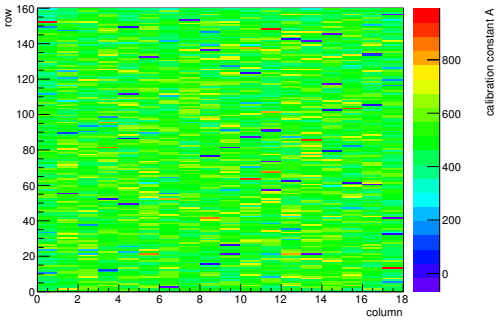

(f) Calibration constant A.

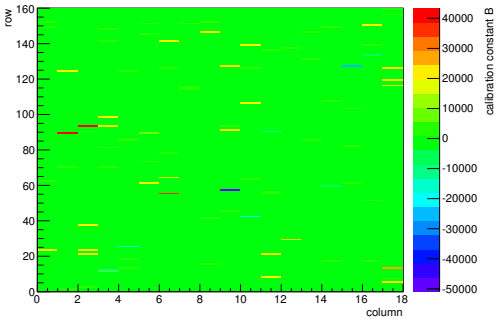

(g) Calibration constant B.

Figure C.157: Detailed plots for test beam measurement of DO-24 (description see section 6.1) sample (running as DUT2) during runs 739-765 in the May 2012 test beam period at CERN SPS in area H6B. Summary of the data in chapter 9. *(cont.)*

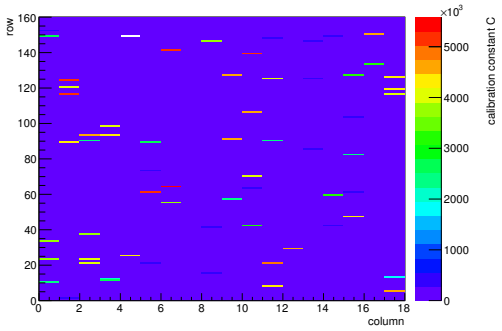

(h) Calibration constant C.

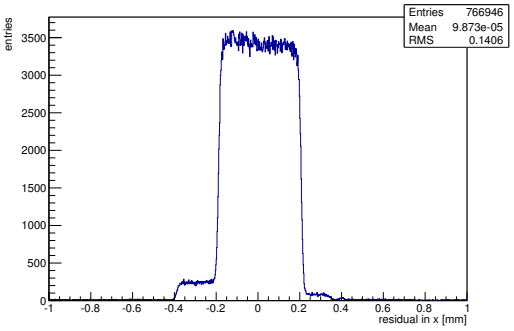

(i) Track residual in x.

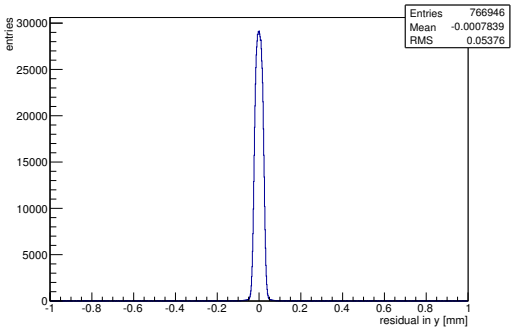

(j) Track residual in y.

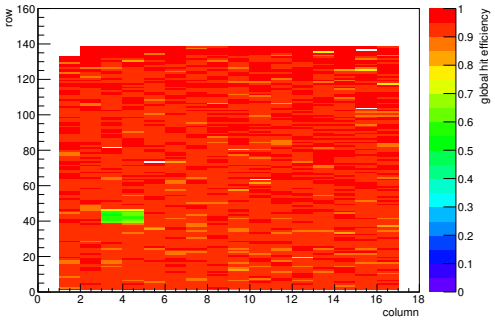

(k) Hit efficiency map.

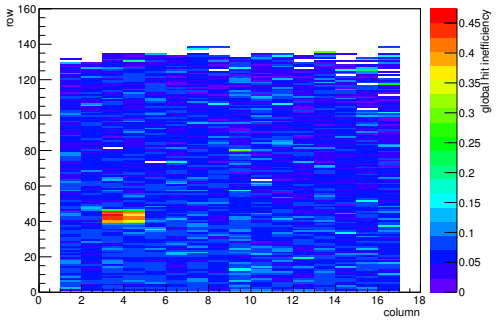

(l) Hit inefficiency map.

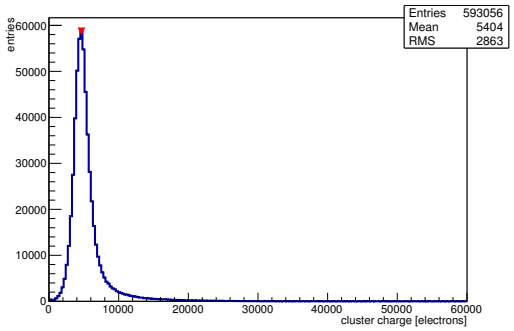

(m) Charge distribution (all cluster sizes included).

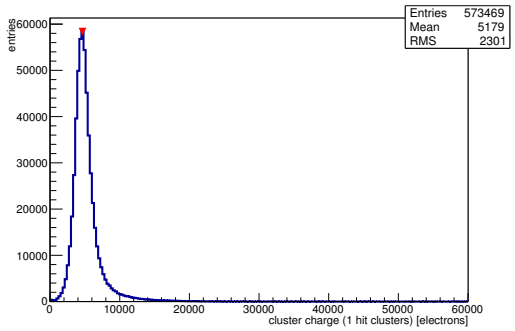

(n) Charge distribution (1 hit cluster).

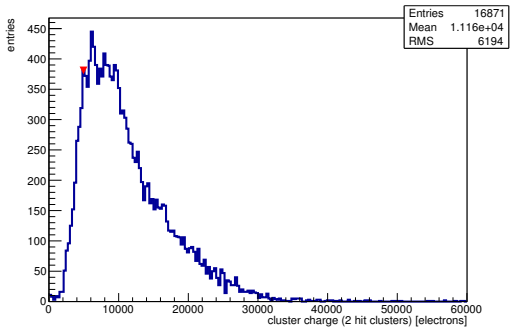

(o) Charge distribution (2 hit cluster).

Figure C.157: Detailed plots for test beam measurement of DO-24 (description see section 6.1) sample (running as DUT2) during runs 739-765 in the May 2012 test beam period at CERN SPS in area H6B. Summary of the data in chapter 9. *(cont.)*

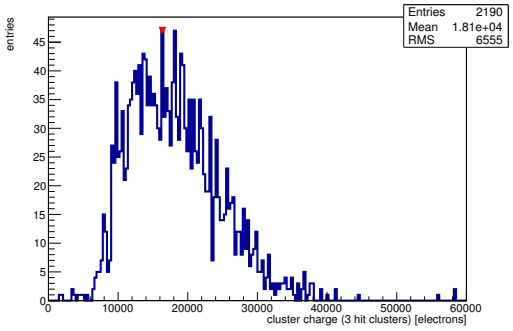

(p) Charge distribution (3 hit cluster).

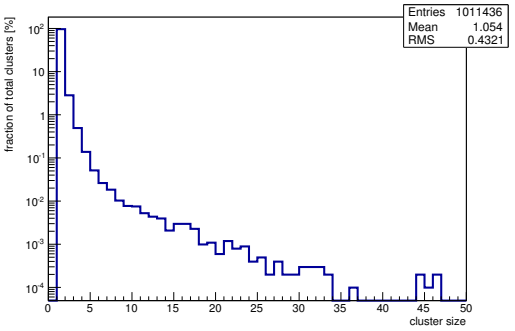

(q) Cluster size distribution.

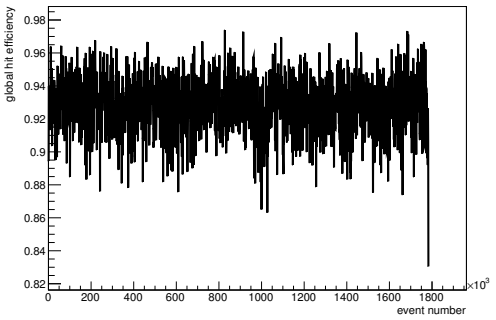

(r) Hit efficiency vs event number.

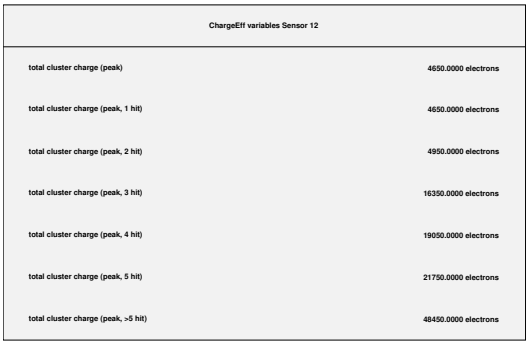

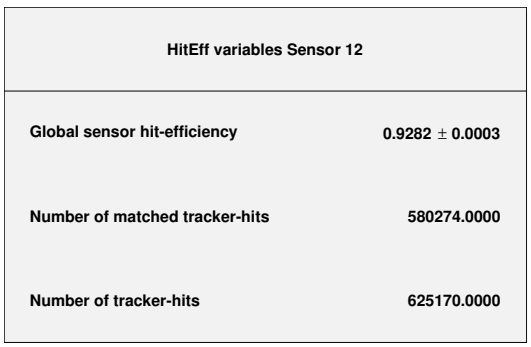

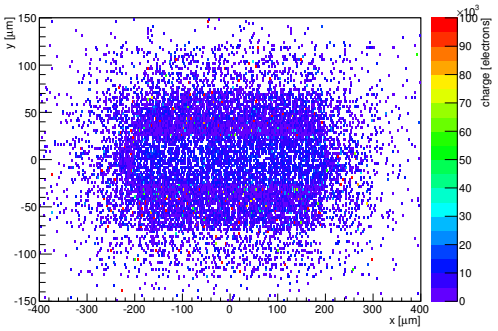

(s) Single pixel mean charge.

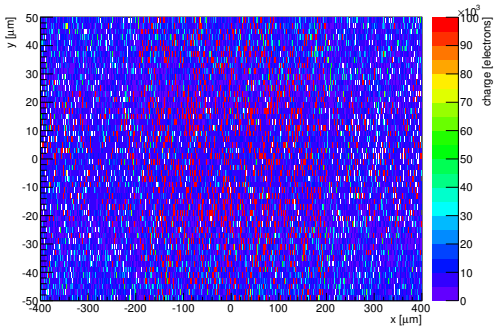

(t) Single pixel mean charge.

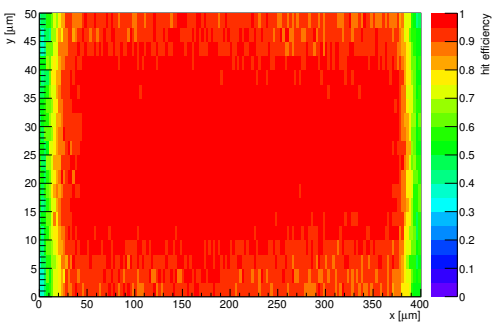

(u) Single pixel hit efficiency.

Figure C.157: Detailed plots for test beam measurement of DO-24 (description see section 6.1) sample (running as DUT2) during runs 739-765 in the May 2012 test beam period at CERN SPS in area H6B. Summary of the data in chapter 9.

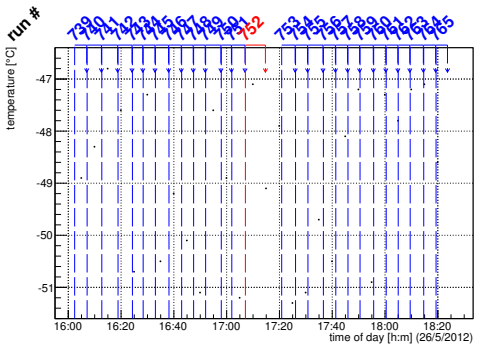

(a) Temperature vs time.

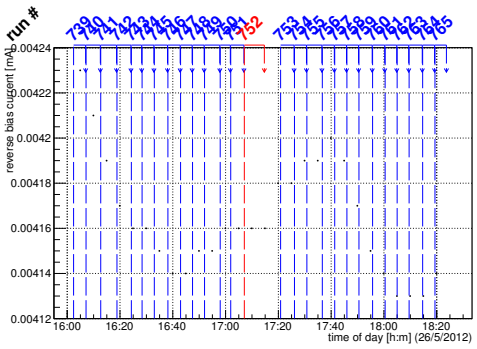

(b) Bias current vs time.

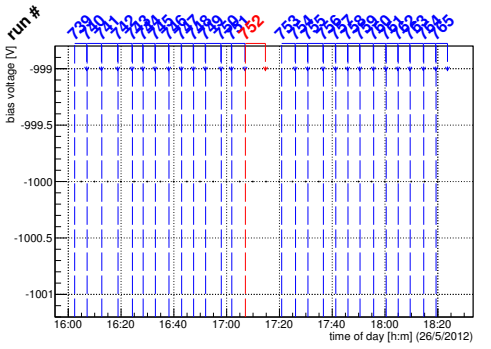

(c) Currently applied bias voltage vs time.

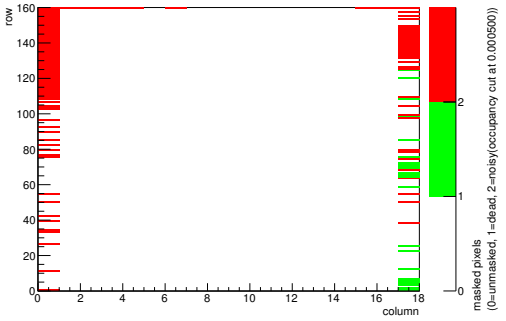

(d) Map of masked pixels.

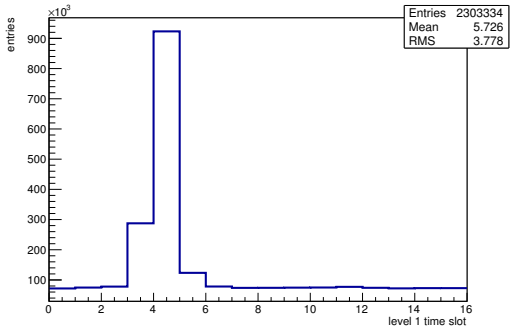

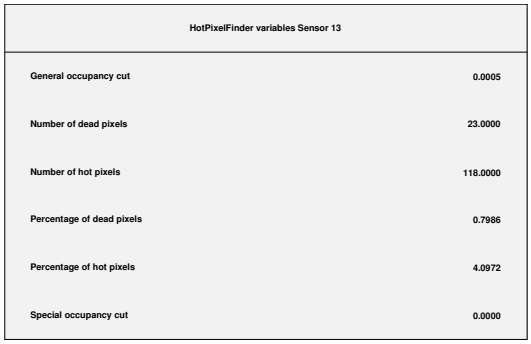

(e) Lvl1 distribution.

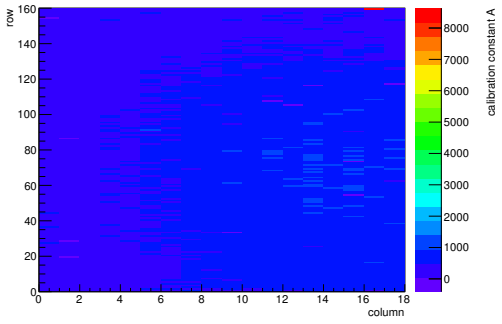

(f) Calibration constant A.

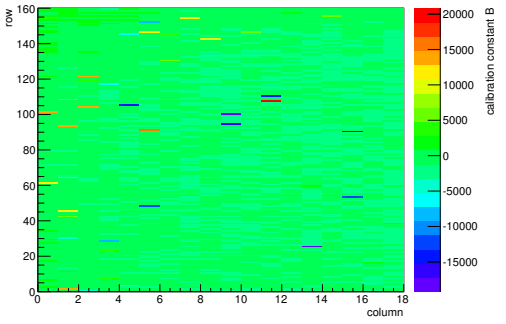

(g) Calibration constant B.

Figure C.158: Detailed plots for test beam measurement of DO-38 (description see section 6.1) sample (running as DUT3) during runs 739-765 in the May 2012 test beam period at CERN SPS in area H6B. Summary of the data in chapter 9. *(cont.)*

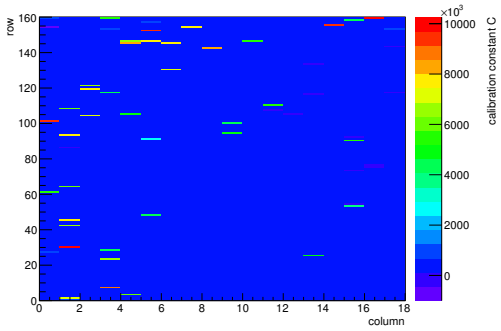

(h) Calibration constant C.

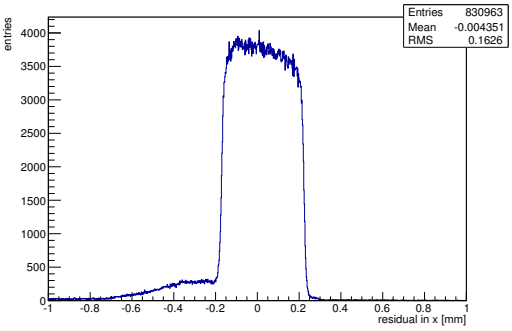

(i) Track residual in x.

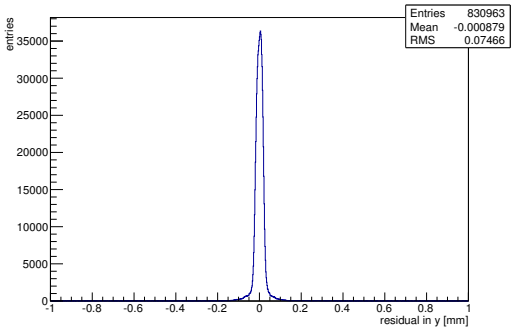

(j) Track residual in y.

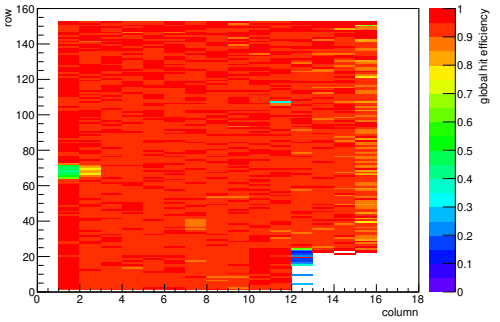

(k) Hit efficiency map.

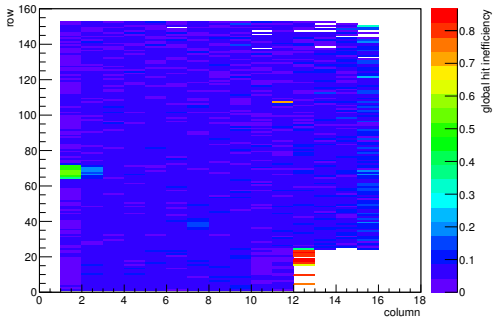

(l) Hit inefficiency map.

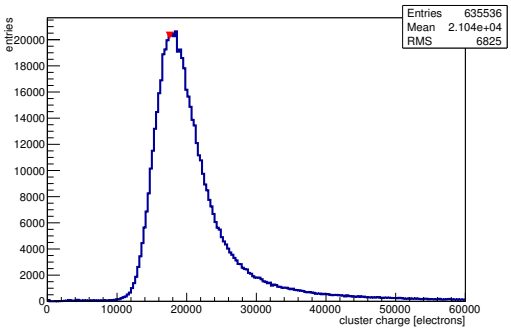

(m) Charge distribution (all cluster sizes included).

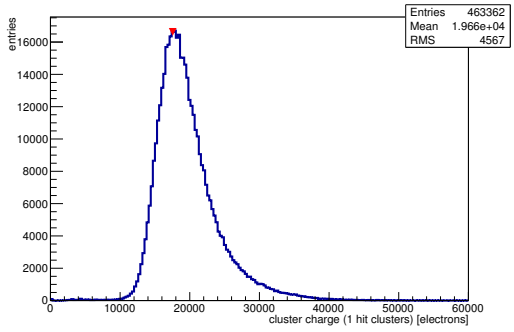

(n) Charge distribution (1 hit cluster).

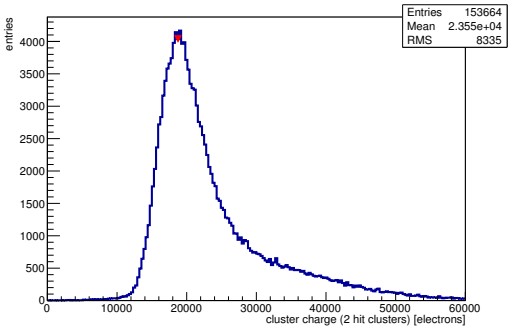

(o) Charge distribution (2 hit cluster).

Figure C.158: Detailed plots for test beam measurement of DO-38 (description see section 6.1) sample (running as DUT3) during runs 739-765 in the May 2012 test beam period at CERN SPS in area H6B. Summary of the data in chapter 9. *(cont.)*

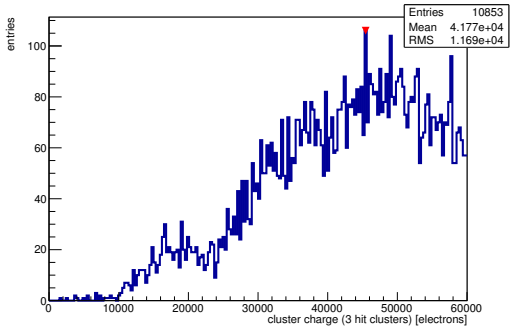

(p) Charge distribution (3 hit cluster).

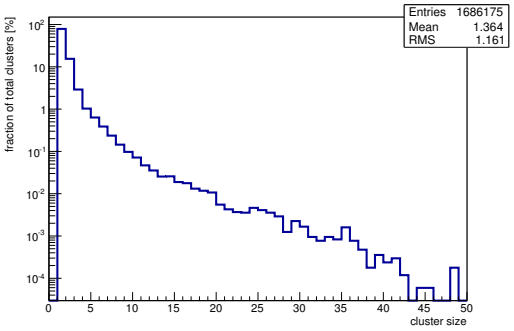

(q) Cluster size distribution.

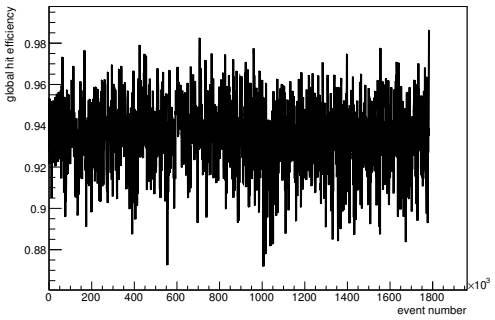

(r) Hit efficiency vs event number.

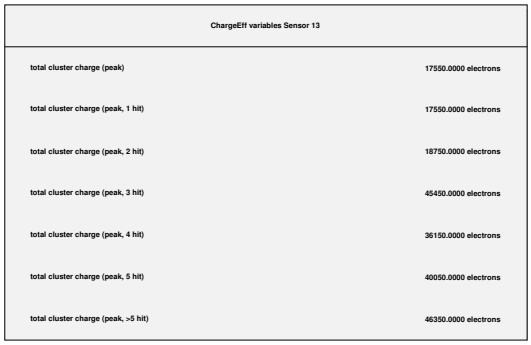

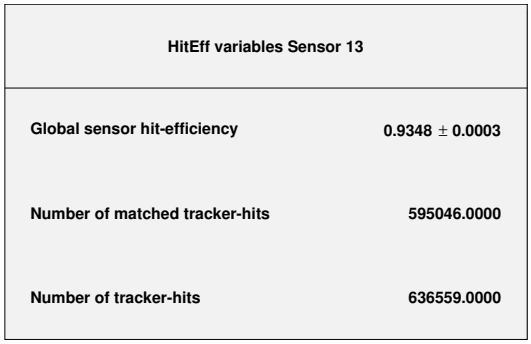

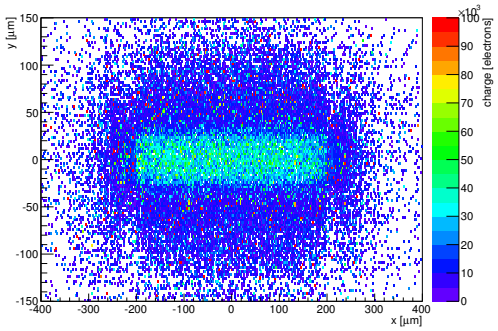

(s) Single pixel mean charge.

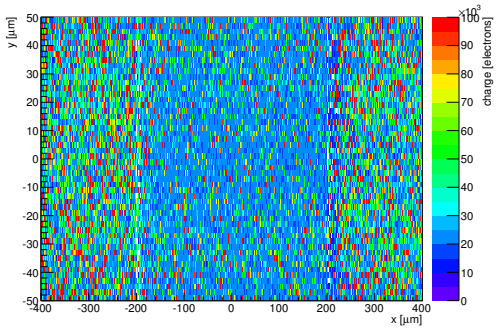

(t) Single pixel mean charge.

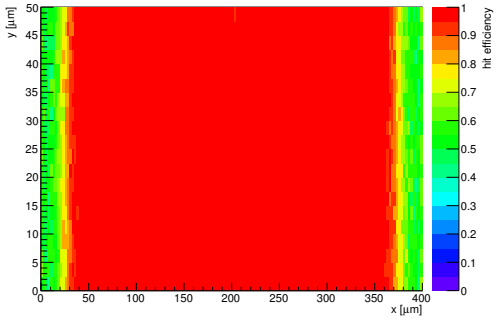

(u) Single pixel hit efficiency.

Figure C.158: Detailed plots for test beam measurement of DO-38 (description see section 6.1) sample (running as DUT3) during runs 739-765 in the May 2012 test beam period at CERN SPS in area H6B. Summary of the data in chapter 9.

C.5.2 Runs 767-795

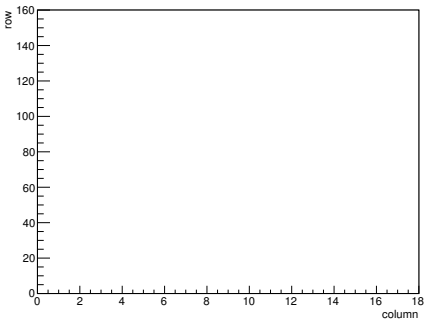

(a) Map of masked pixels.

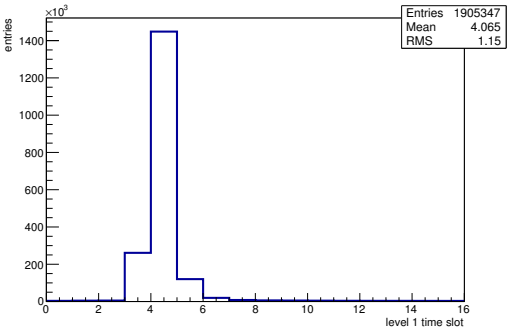

(b) Lvl1 distribution.

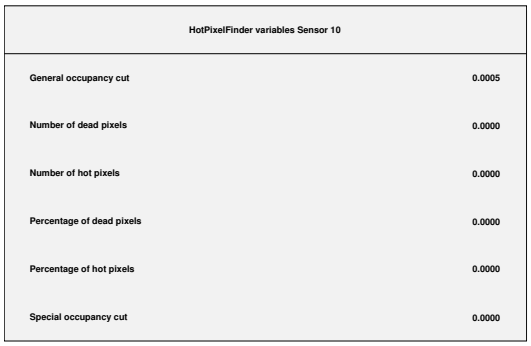

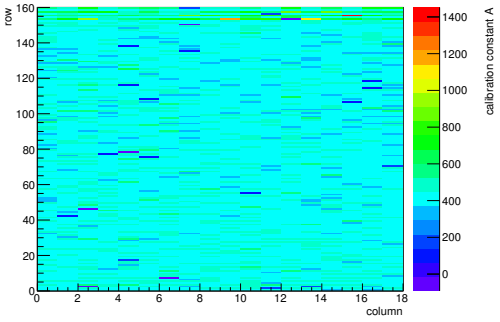

(c) Calibration constant A.

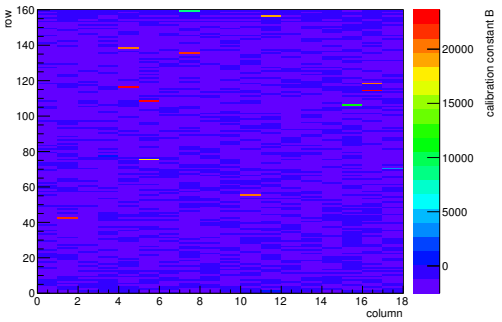

(d) Calibration constant B.

Figure C.159: Detailed plots for test beam measurement of DO-1 (description see section 6.1) sample (running as DUT0) during runs 767-795 in the May 2012 test beam period at CERN SPS in area H6B. Summary of the data in chapter 9. *(cont.)*

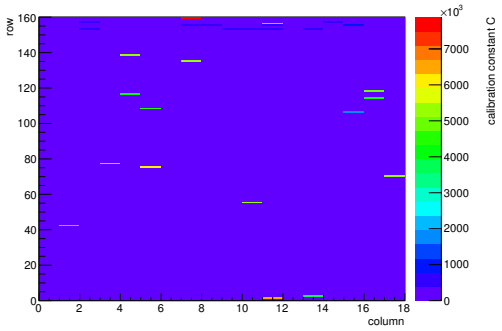

(e) Calibration constant C.

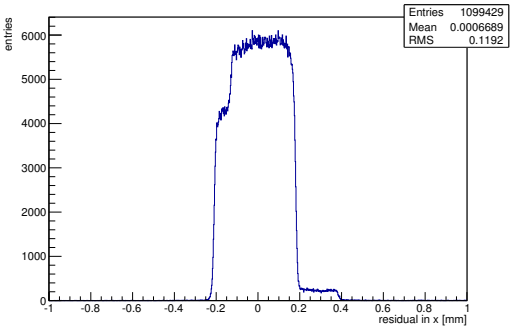

(f) Track residual in x.

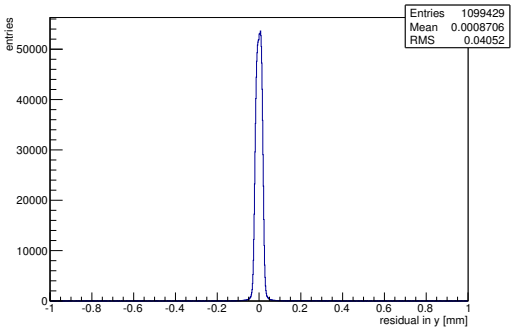

(g) Track residual in y.

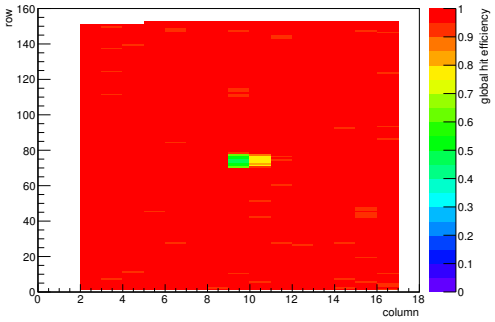

(h) Hit efficiency map.

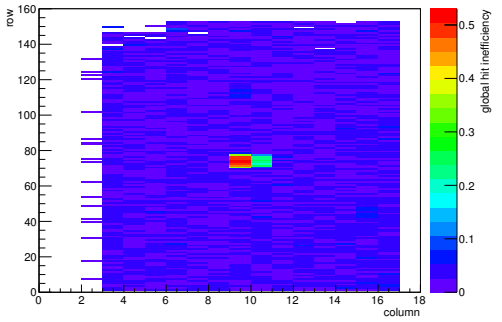

(i) Hit inefficiency map.

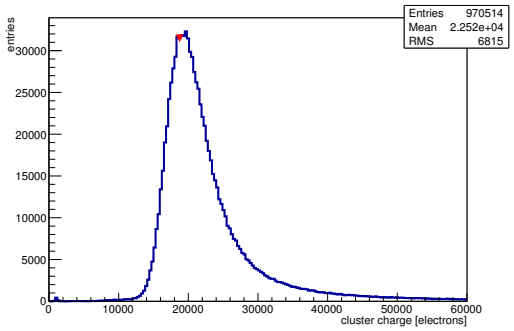

(j) Charge distribution (all cluster sizes included).

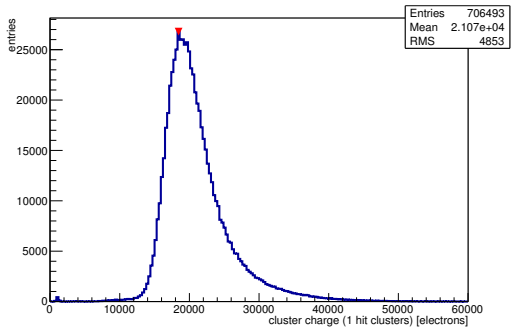

(k) Charge distribution (1 hit cluster).

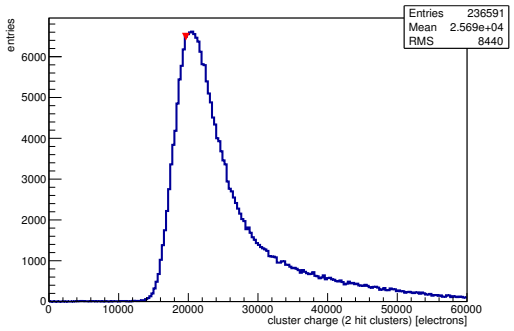

(l) Charge distribution (2 hit cluster).

Figure C.159: Detailed plots for test beam measurement of DO-1 (description see section 6.1) sample (running as DUT0) during runs 767-795 in the May 2012 test beam period at CERN SPS in area H6B. Summary of the data in chapter 9. *(cont.)*

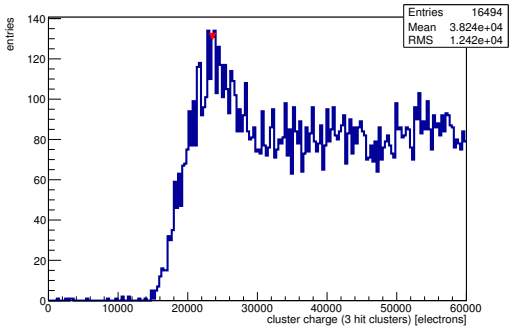

(m) Charge distribution (3 hit cluster).

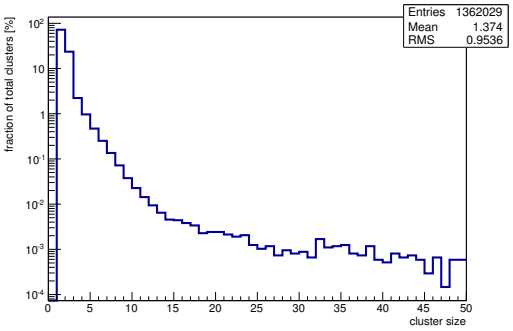

(n) Cluster size distribution.

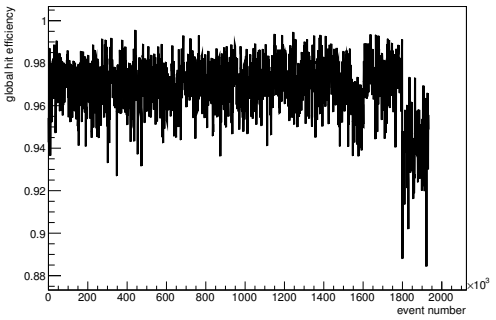

(o) Hit efficiency vs event number.

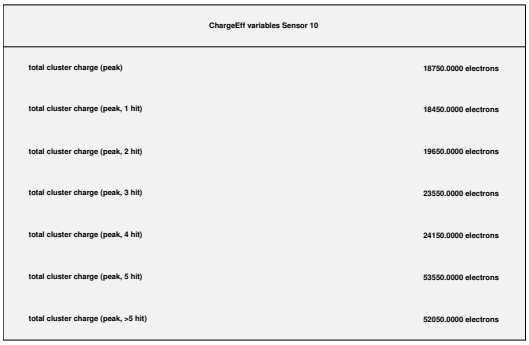

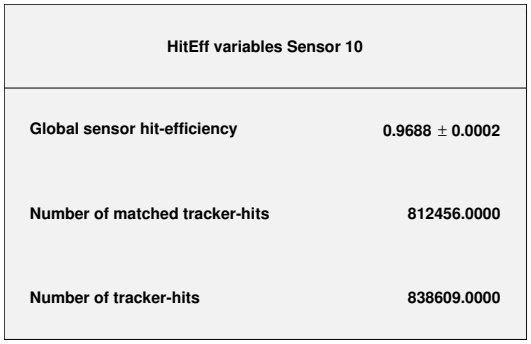

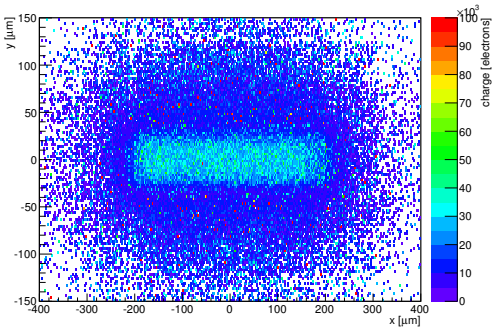

(p) Single pixel mean charge.

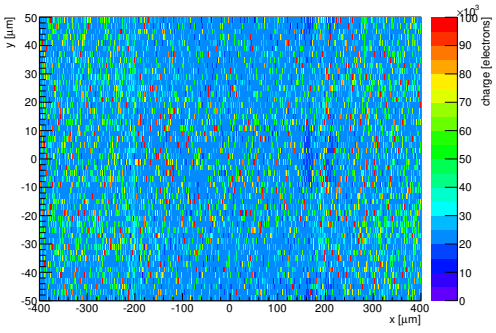

(q) Single pixel mean charge.

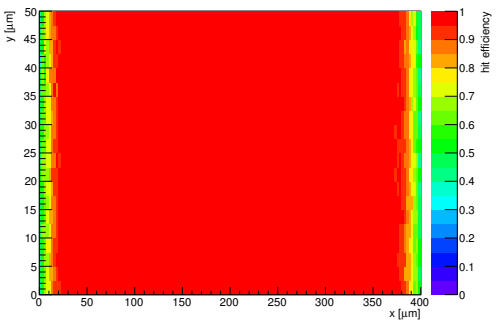

(r) Single pixel hit efficiency.

Figure C.159: Detailed plots for test beam measurement of DO-1 (description see section 6.1) sample (running as DUT0) during runs 767-795 in the May 2012 test beam period at CERN SPS in area H6B. Summary of the data in chapter 9.

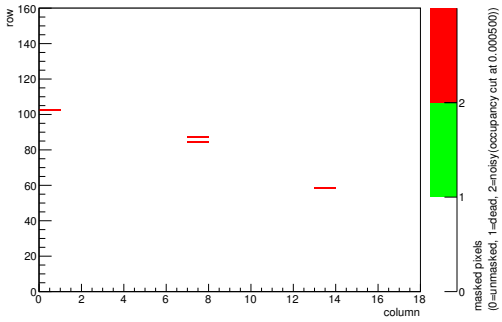

(a) Map of masked pixels.

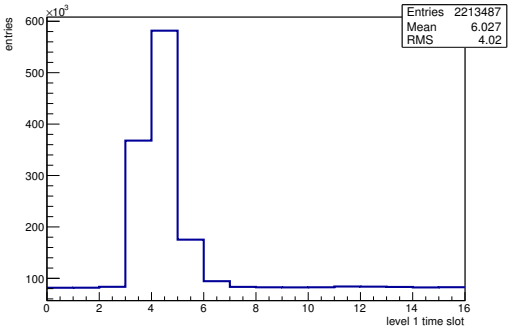

(b) Lvl1 distribution.

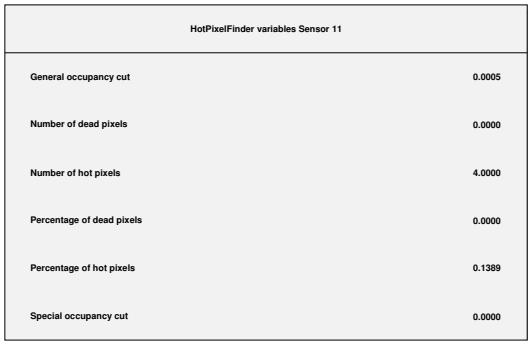

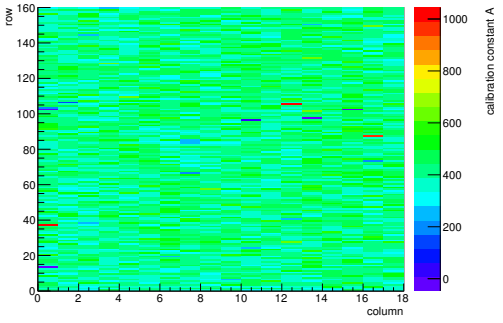

(c) Calibration constant A.

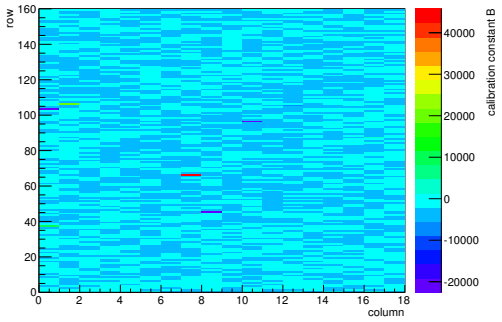

(d) Calibration constant B.

Figure C.160: Detailed plots for test beam measurement of DO-10 (description see section 6.1) sample (running as DUT1) during runs 767-795 in the May 2012 test beam period at CERN SPS in area H6B. Summary of the data in chapter 9. *(cont.)*

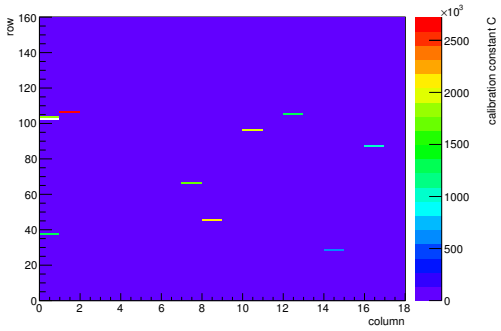

(e) Calibration constant C.

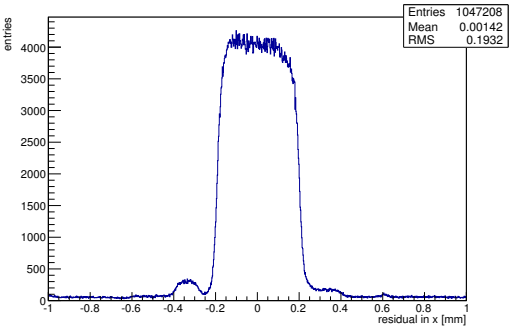

(f) Track residual in x.

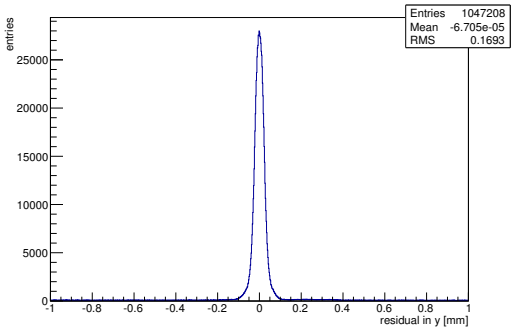

(g) Track residual in y.

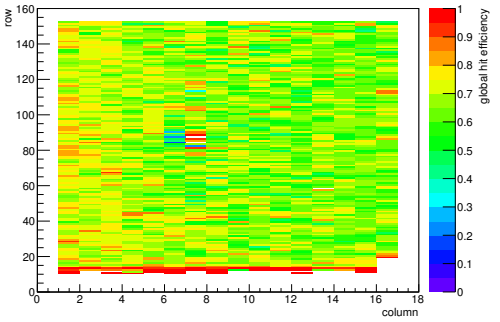

(h) Hit efficiency map.

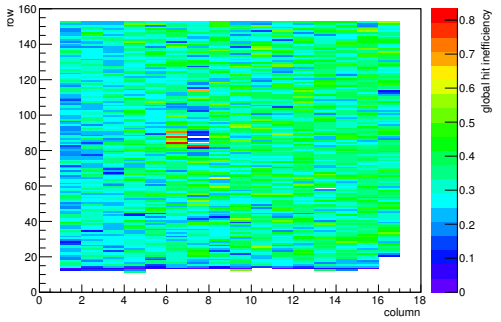

(i) Hit inefficiency map.

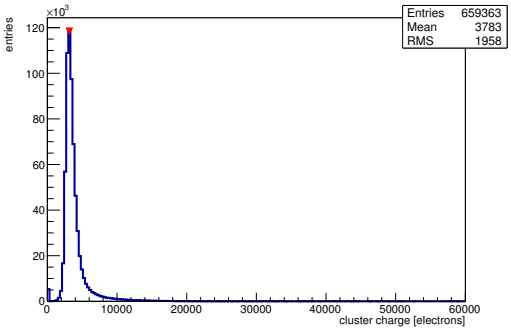

(j) Charge distribution (all cluster sizes included).

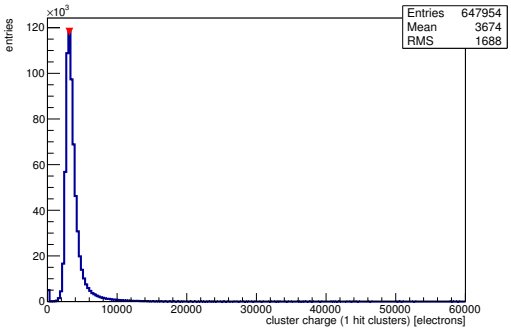

(k) Charge distribution (1 hit cluster).

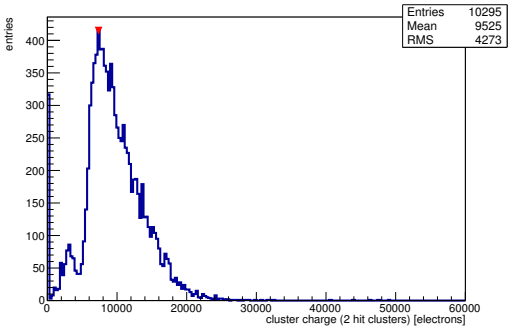

(l) Charge distribution (2 hit cluster).

Figure C.160: Detailed plots for test beam measurement of DO-10 (description see section 6.1) sample (running as DUT1) during runs 767-795 in the May 2012 test beam period at CERN SPS in area H6B. Summary of the data in chapter 9. *(cont.)*

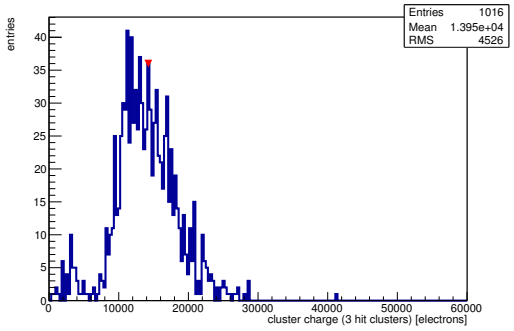

(m) Charge distribution (3 hit cluster).

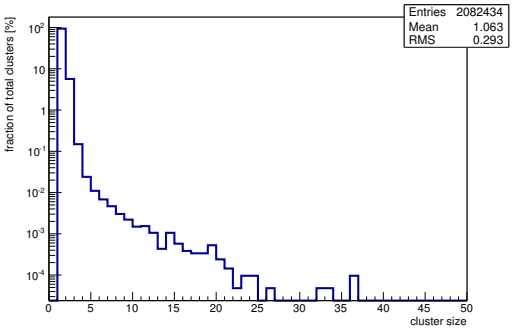

(n) Cluster size distribution.

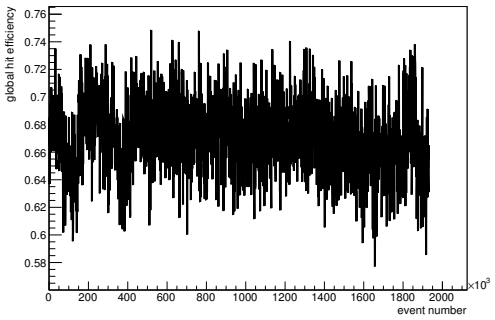

(o) Hit efficiency vs event number.

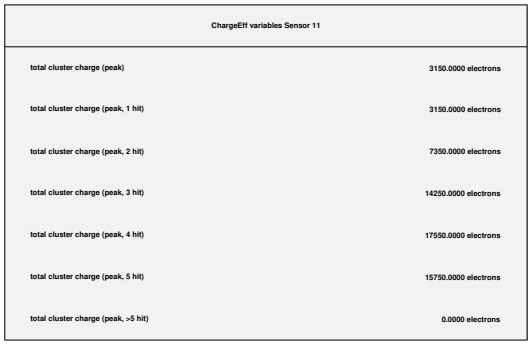

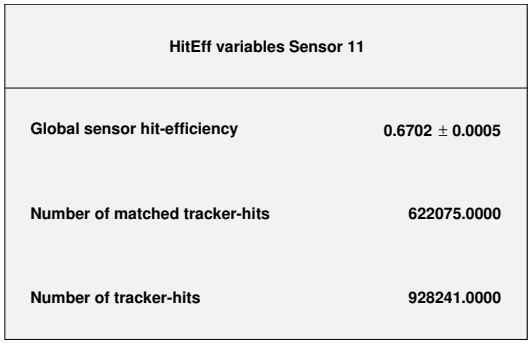

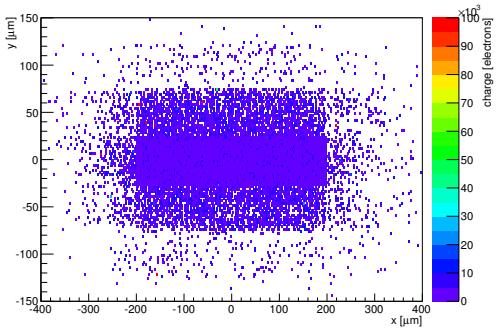

(p) Single pixel mean charge.

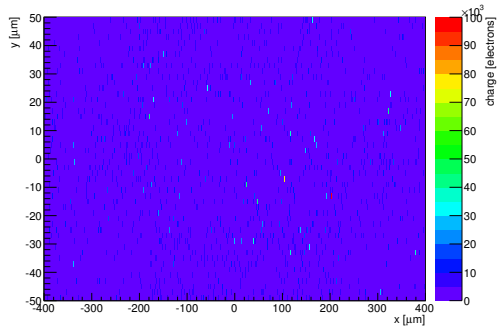

(q) Single pixel mean charge.

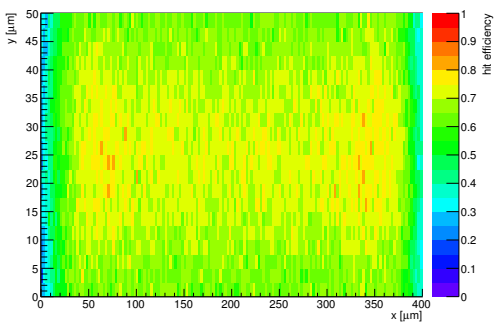

(r) Single pixel hit efficiency.

Figure C.160: Detailed plots for test beam measurement of DO-10 (description see section 6.1) sample (running as DUT1) during runs 767-795 in the May 2012 test beam period at CERN SPS in area H6B. Summary of the data in chapter 9.

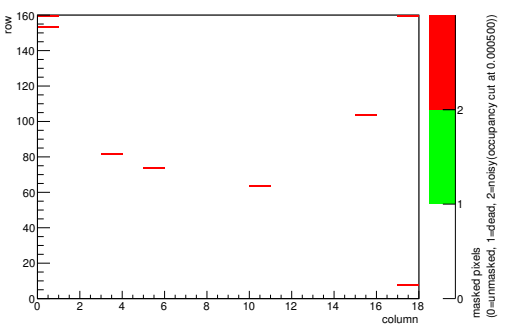

(a) Map of masked pixels.

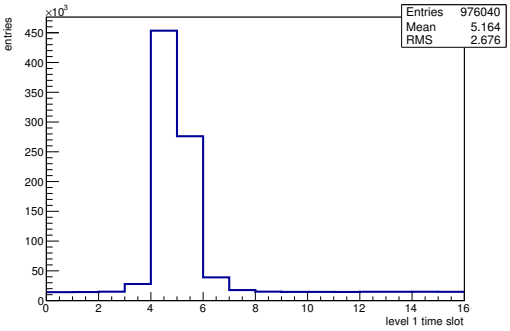

(b) Lvl1 distribution.

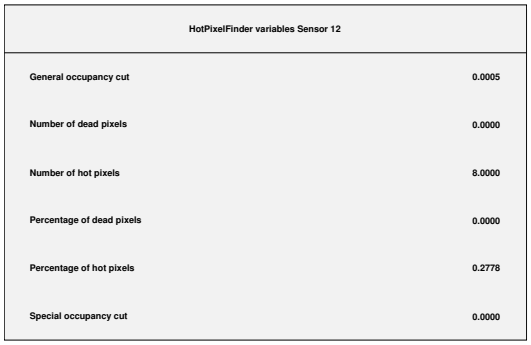

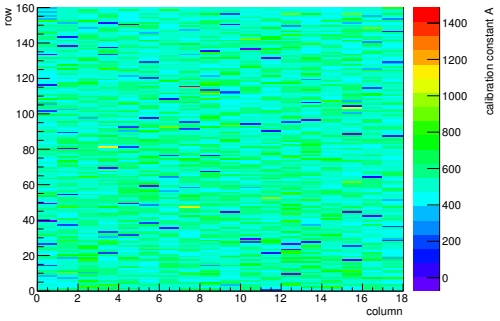

(c) Calibration constant A.

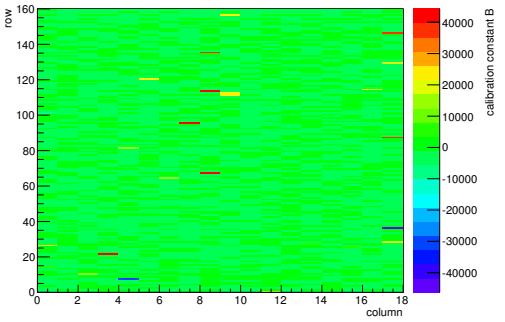

(d) Calibration constant B.

Figure C.161: Detailed plots for test beam measurement of DO-24 (description see section 6.1) sample (running as DUT2) during runs 767-795 in the May 2012 test beam period at CERN SPS in area H6B. Summary of the data in chapter 9. *(cont.)*

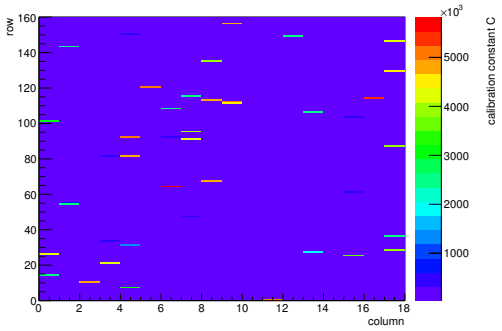

(e) Calibration constant C.

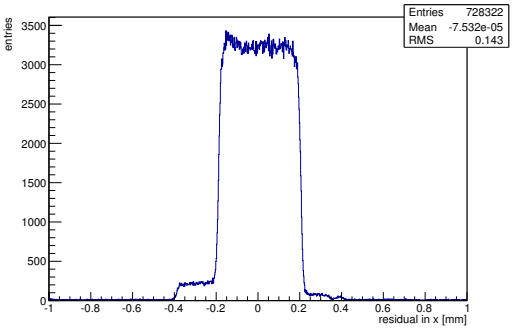

(f) Track residual in x.

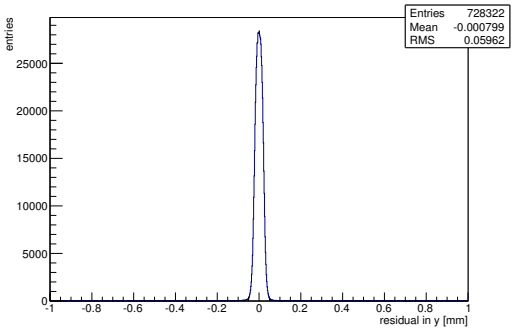

(g) Track residual in y.

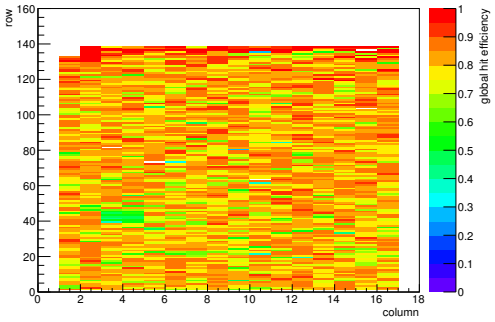

(h) Hit efficiency map.

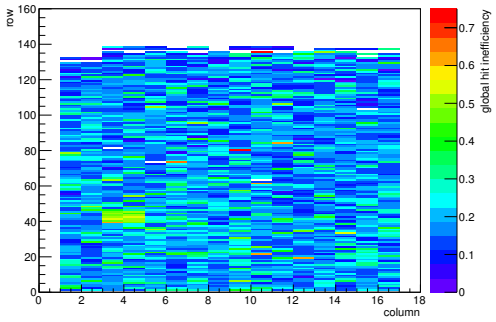

(i) Hit inefficiency map.

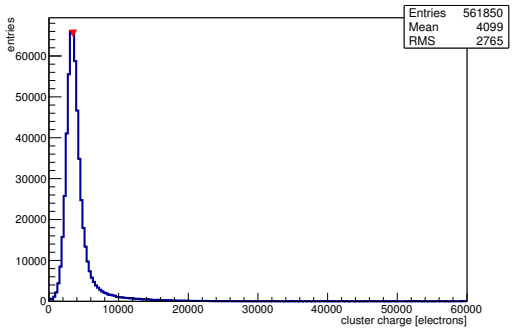

(j) Charge distribution (all cluster sizes included).

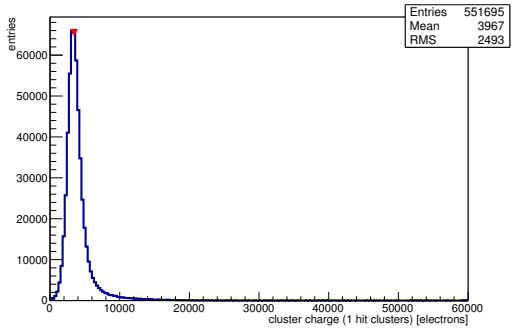

(k) Charge distribution (1 hit cluster).

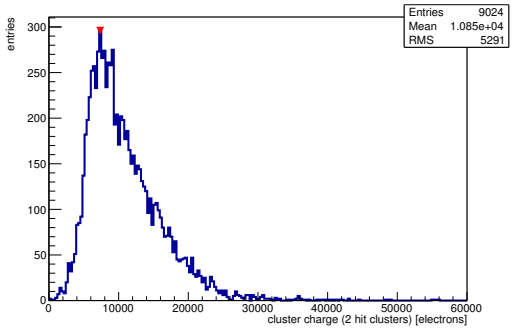

(l) Charge distribution (2 hit cluster).

Figure C.161: Detailed plots for test beam measurement of DO-24 (description see section 6.1) sample (running as DUT2) during runs 767-795 in the May 2012 test beam period at CERN SPS in area H6B. Summary of the data in chapter 9. *(cont.)*

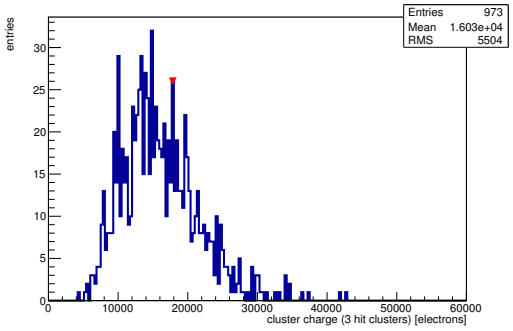

(m) Charge distribution (3 hit cluster).

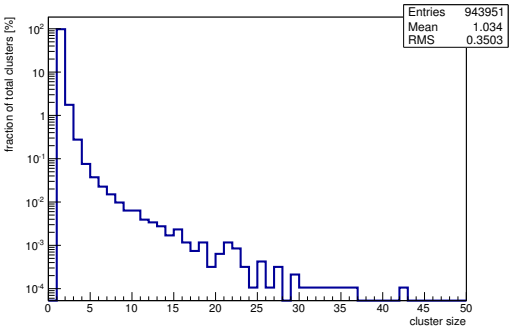

(n) Cluster size distribution.

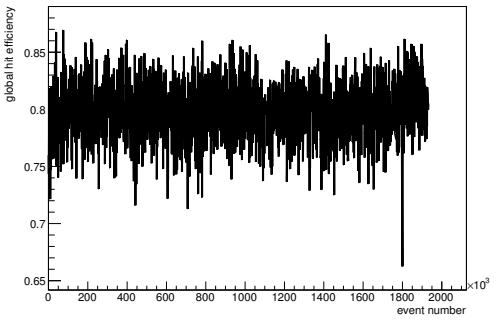

(o) Hit efficiency vs event number.

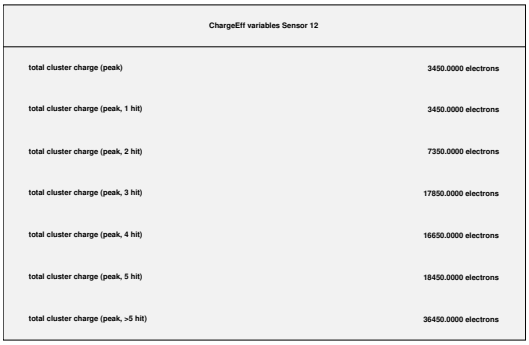

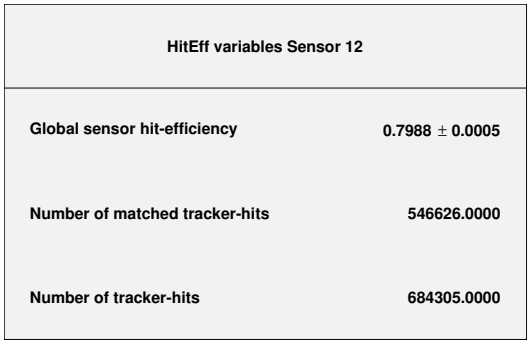

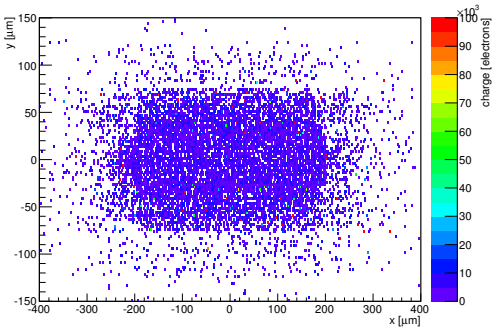

(p) Single pixel mean charge.

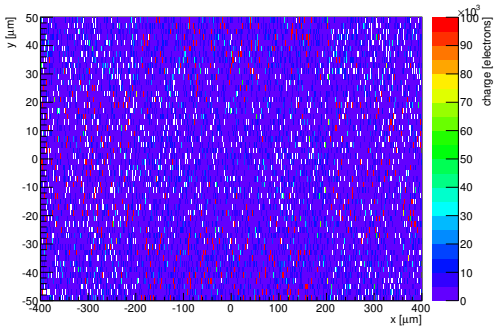

(q) Single pixel mean charge.

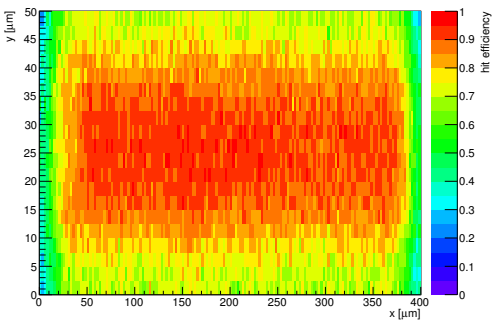

(r) Single pixel hit efficiency.

Figure C.161: Detailed plots for test beam measurement of DO-24 (description see section 6.1) sample (running as DUT2) during runs 767-795 in the May 2012 test beam period at CERN SPS in area H6B. Summary of the data in chapter 9.

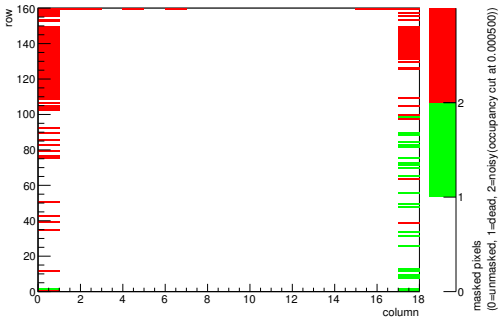

(a) Map of masked pixels.

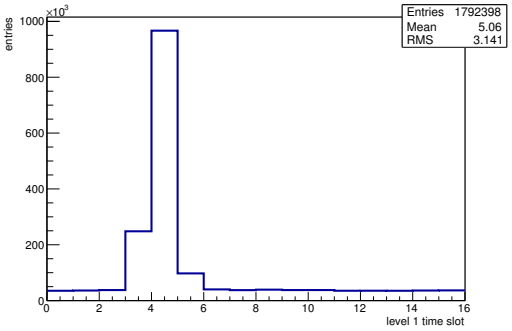

(b) Lvl1 distribution.

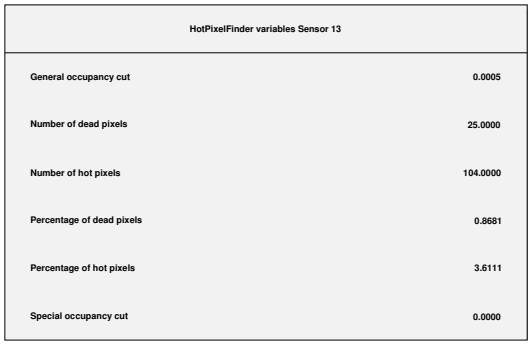

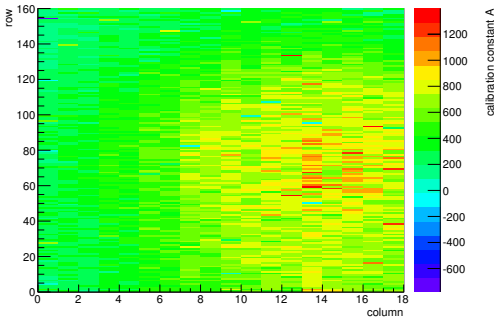

(c) Calibration constant A.

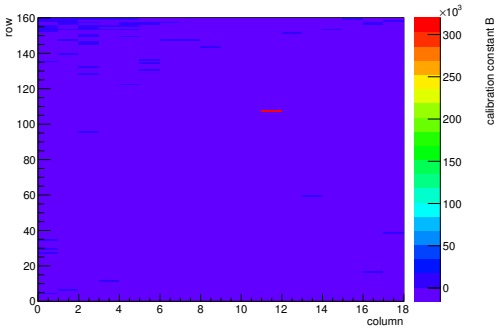

(d) Calibration constant B.

Figure C.162: Detailed plots for test beam measurement of DO-38 (description see section 6.1) sample (running as DUT3) during runs 767-795 in the May 2012 test beam period at CERN SPS in area H6B. Summary of the data in chapter 9. *(cont.)*

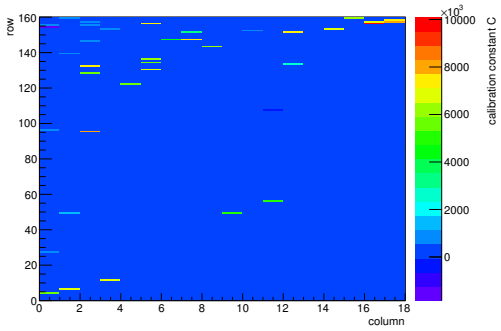

(e) Calibration constant C.

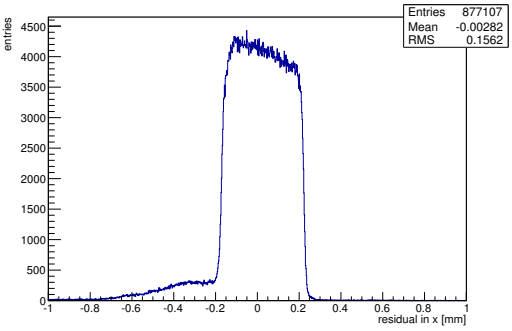

(f) Track residual in x.

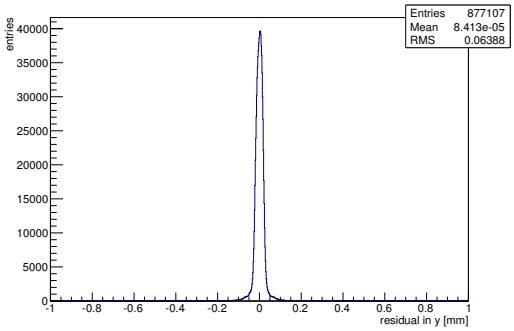

(g) Track residual in y.

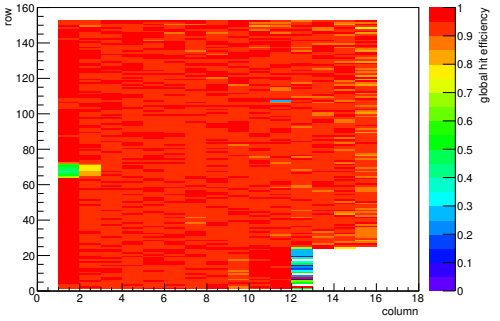

(h) Hit efficiency map.

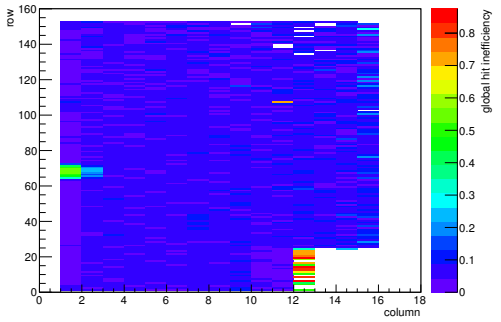

(i) Hit inefficiency map.

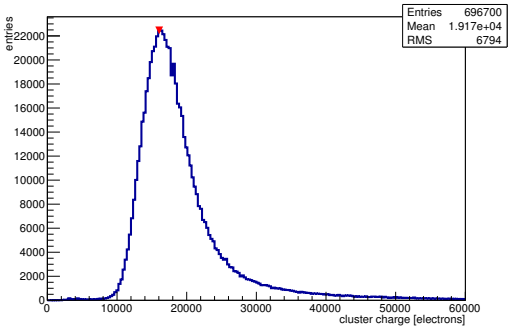

(j) Charge distribution (all cluster sizes included).

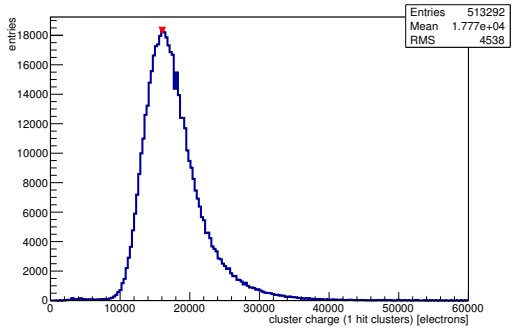

(k) Charge distribution (1 hit cluster).

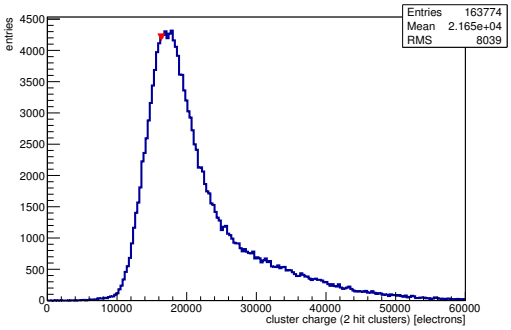

(l) Charge distribution (2 hit cluster).

Figure C.162: Detailed plots for test beam measurement of DO-38 (description see section 6.1) sample (running as DUT3) during runs 767-795 in the May 2012 test beam period at CERN SPS in area H6B. Summary of the data in chapter 9. *(cont.)*

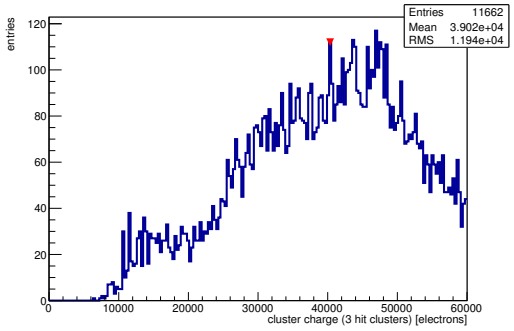

(m) Charge distribution (3 hit cluster).

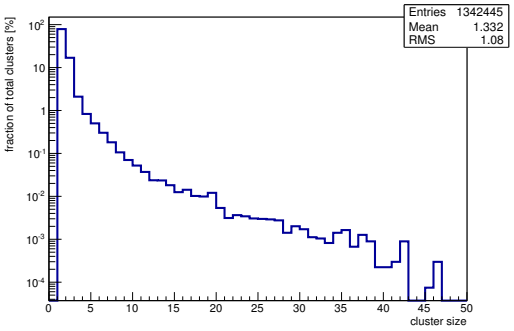

(n) Cluster size distribution.

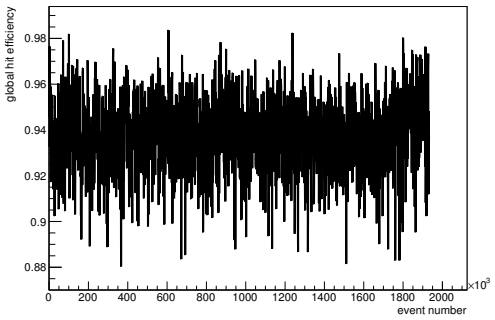

(o) Hit efficiency vs event number.

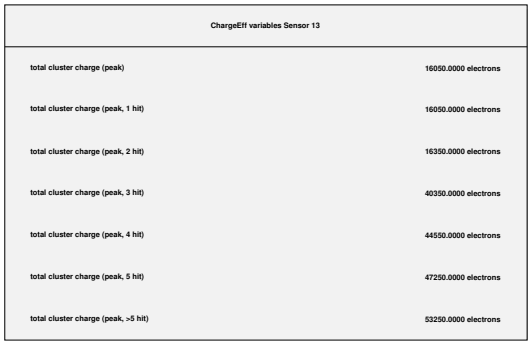

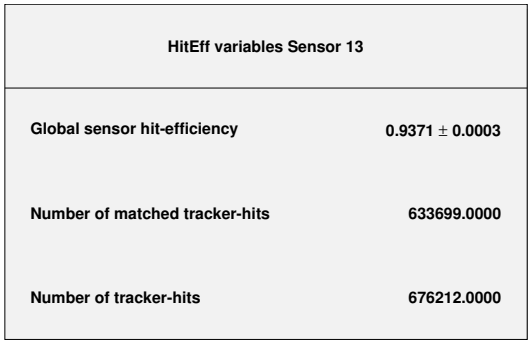

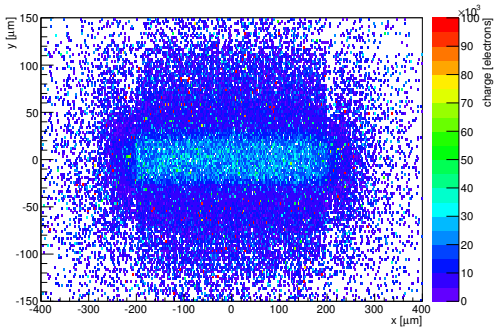

(p) Single pixel mean charge.

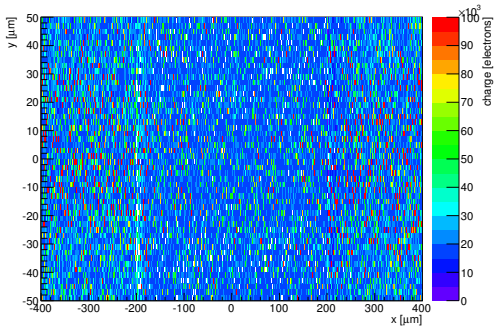

(q) Single pixel mean charge.

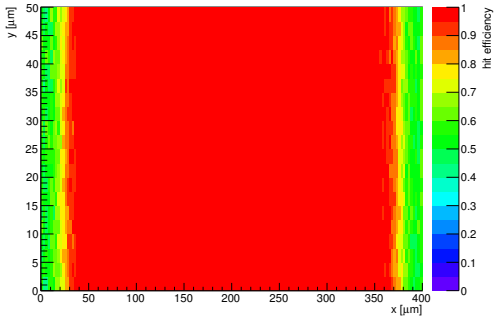

(r) Single pixel hit efficiency.

Figure C.162: Detailed plots for test beam measurement of DO-38 (description see section 6.1) sample (running as DUT3) during runs 767-795 in the May 2012 test beam period at CERN SPS in area H6B. Summary of the data in chapter 9.

C.5.3 Runs 797-833

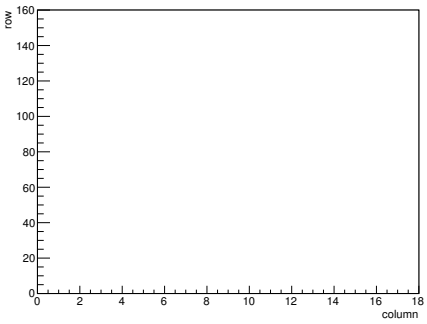

(a) Map of masked pixels.

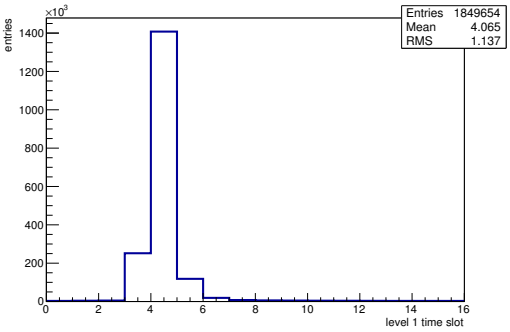

(b) Lvl1 distribution.

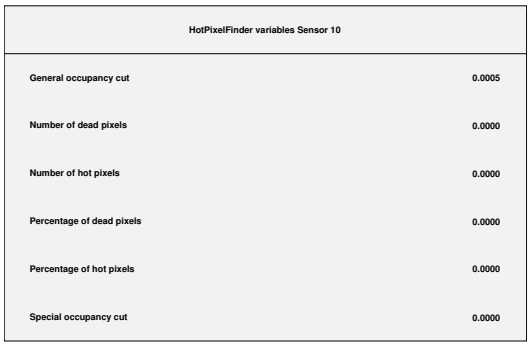

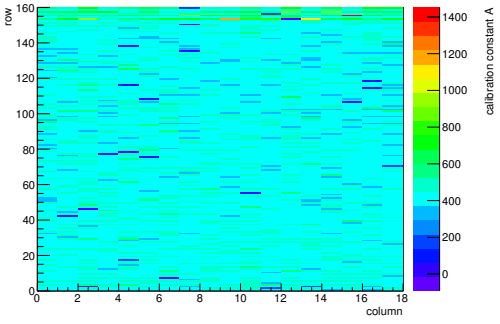

(c) Calibration constant A.

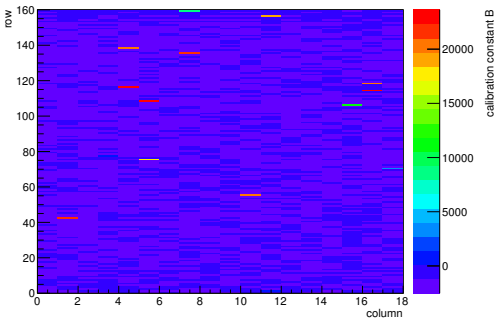

(d) Calibration constant B.

Figure C.163: Detailed plots for test beam measurement of DO-1 (description see section 6.1) sample (running as DUT0) during runs 797-833 in the May 2012 test beam period at CERN SPS in area H6B. Summary of the data in chapter 9. *(cont.)*

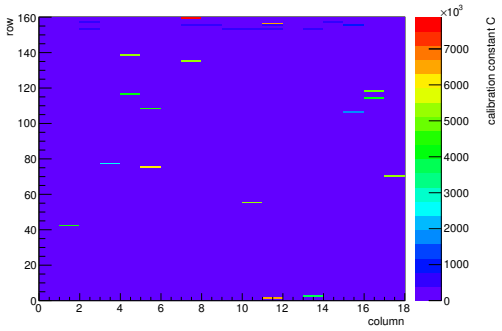

(e) Calibration constant C.

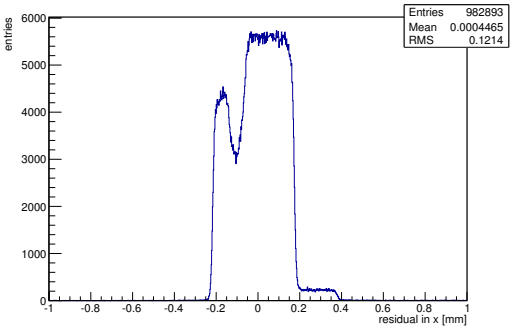

(f) Track residual in x.

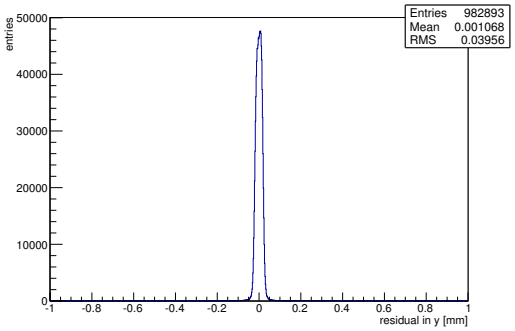

(g) Track residual in y.

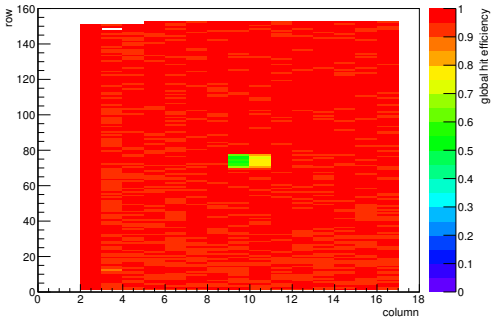

(h) Hit efficiency map.

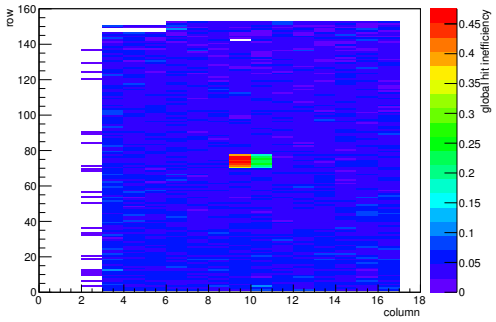

(i) Hit inefficiency map.

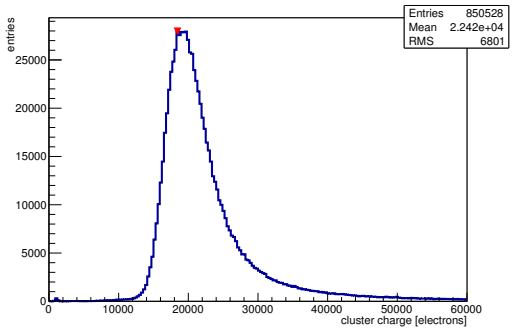

(j) Charge distribution (all cluster sizes included).

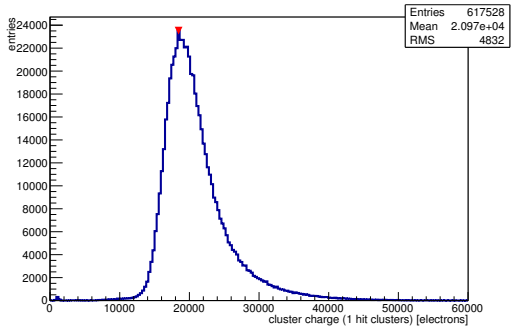

(k) Charge distribution (1 hit cluster).

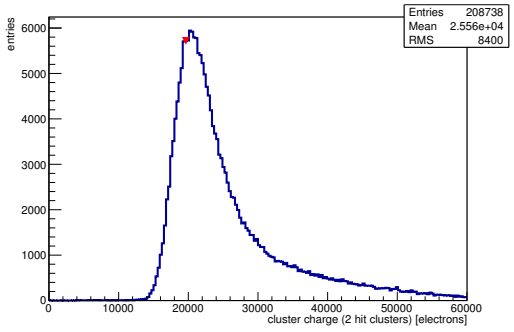

(l) Charge distribution (2 hit cluster).

Figure C.163: Detailed plots for test beam measurement of DO-1 (description see section 6.1) sample (running as DUT0) during runs 797-833 in the May 2012 test beam period at CERN SPS in area H6B. Summary of the data in chapter 9. *(cont.)*

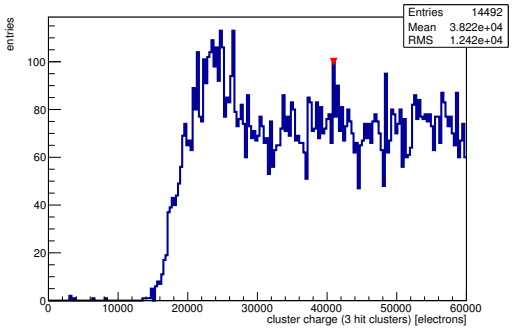

(m) Charge distribution (3 hit cluster).

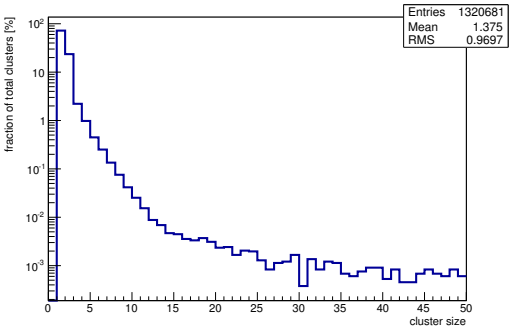

(n) Cluster size distribution.

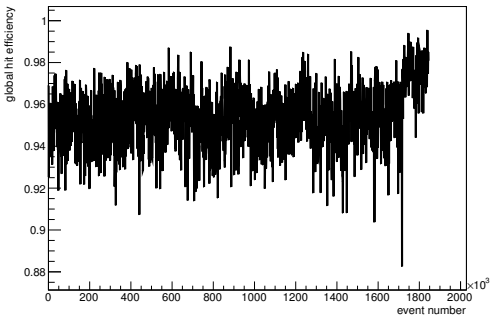

(o) Hit efficiency vs event number.

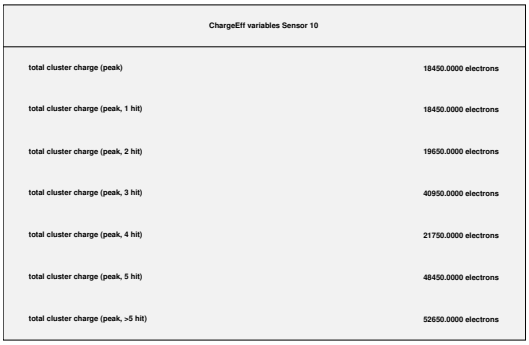

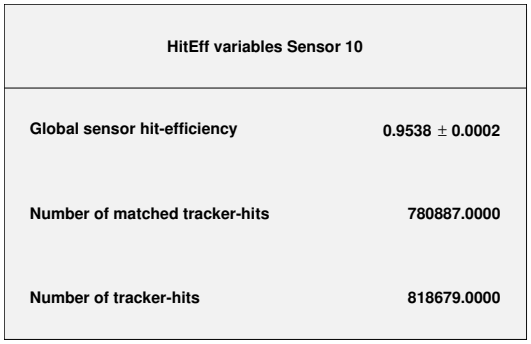

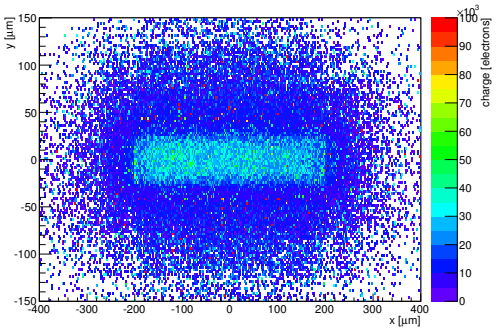

(p) Single pixel mean charge.

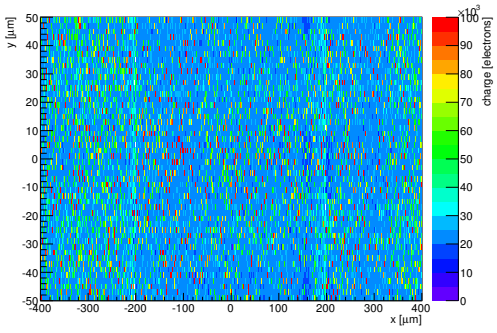

(q) Single pixel mean charge.

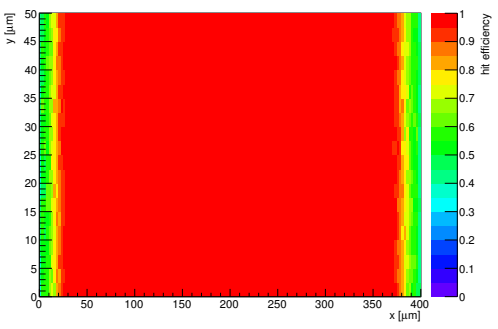

(r) Single pixel hit efficiency.

Figure C.163: Detailed plots for test beam measurement of DO-1 (description see section 6.1) sample (running as DUT0) during runs 797-833 in the May 2012 test beam period at CERN SPS in area H6B. Summary of the data in chapter 9.

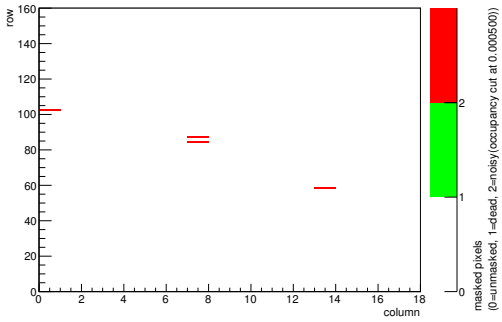

(a) Map of masked pixels.

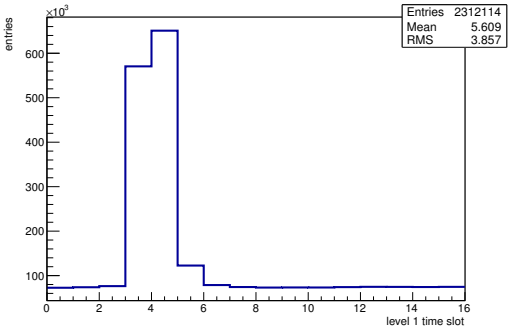

(b) Lvl1 distribution.

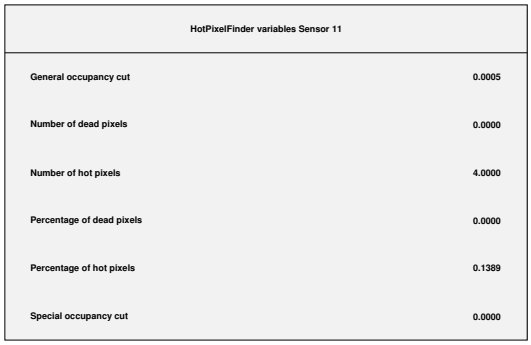

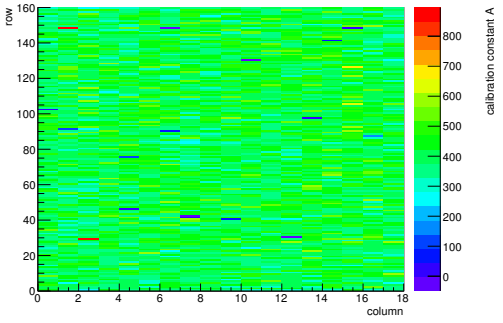

(c) Calibration constant A.

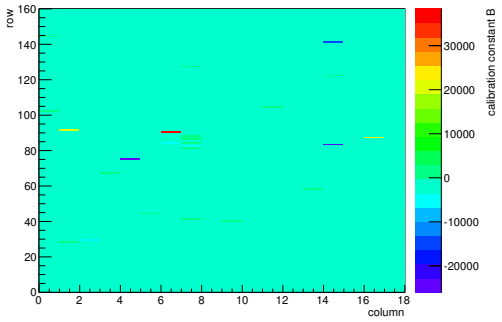

(d) Calibration constant B.

Figure C.164: Detailed plots for test beam measurement of DO-10 (description see section 6.1) sample (running as DUT1) during runs 797-833 in the May 2012 test beam period at CERN SPS in area H6B. Summary of the data in chapter 9. *(cont.)*

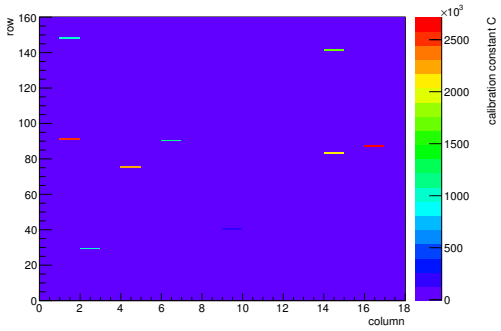

(e) Calibration constant C.

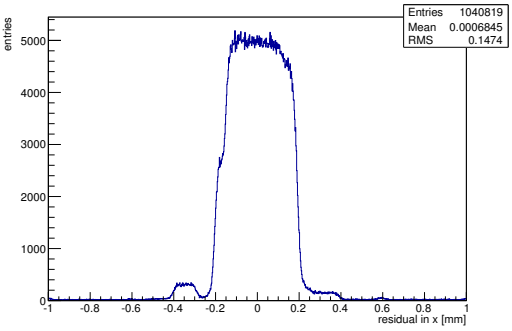

(f) Track residual in x.

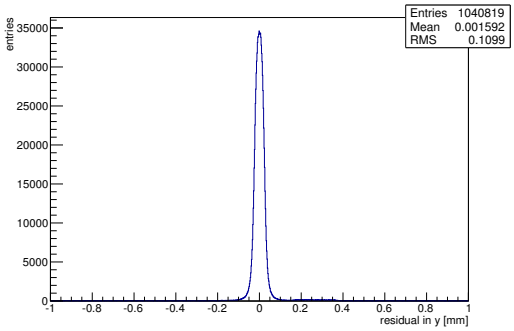

(g) Track residual in y.

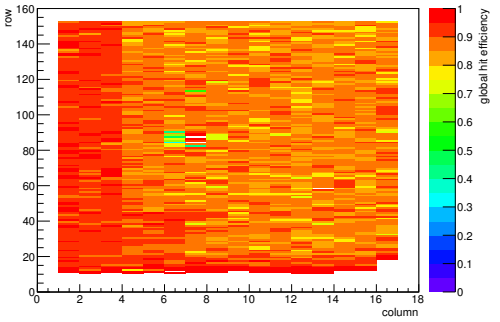

(h) Hit efficiency map.

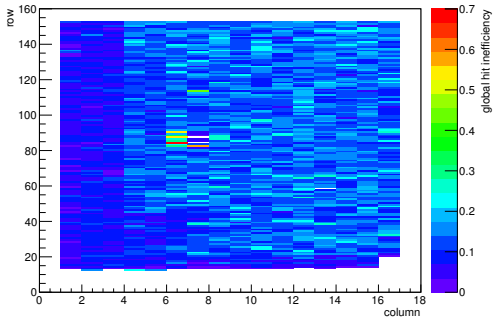

(i) Hit inefficiency map.

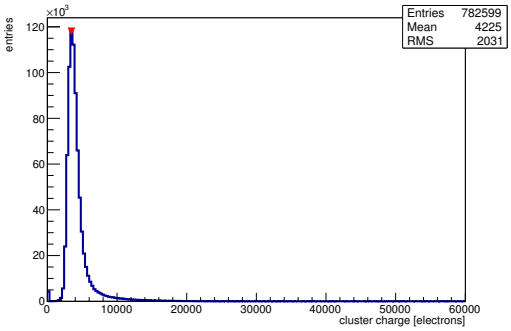

(j) Charge distribution (all cluster sizes included).

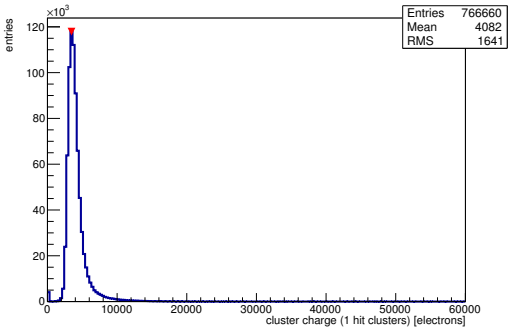

(k) Charge distribution (1 hit cluster).

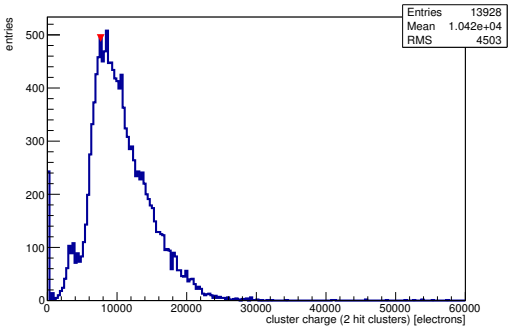

(l) Charge distribution (2 hit cluster).

Figure C.164: Detailed plots for test beam measurement of DO-10 (description see section 6.1) sample (running as DUT1) during runs 797-833 in the May 2012 test beam period at CERN SPS in area H6B. Summary of the data in chapter 9. *(cont.)*

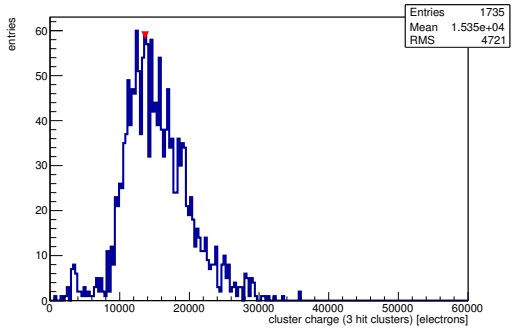

(m) Charge distribution (3 hit cluster).

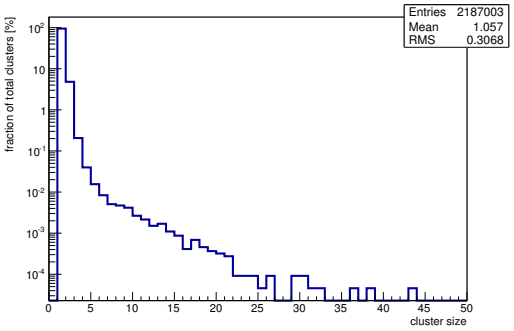

(n) Cluster size distribution.

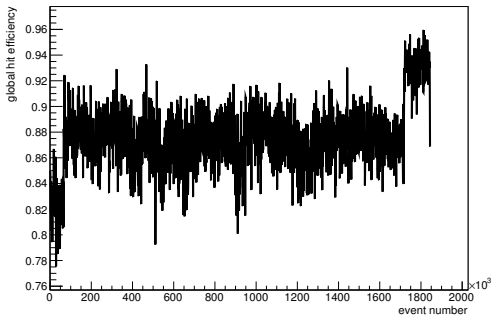

(o) Hit efficiency vs event number.

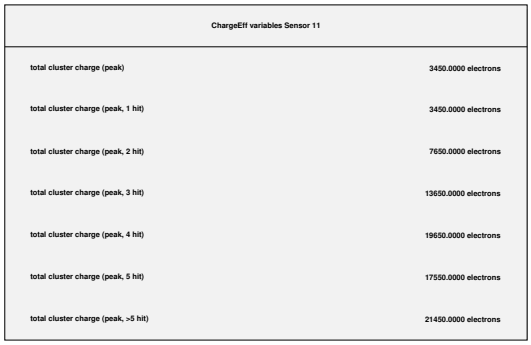

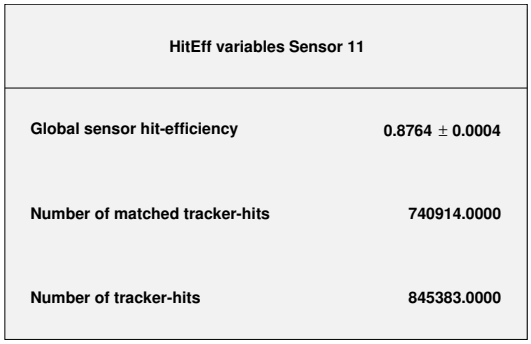

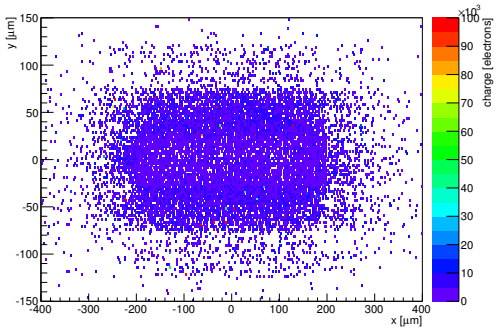

(p) Single pixel mean charge.

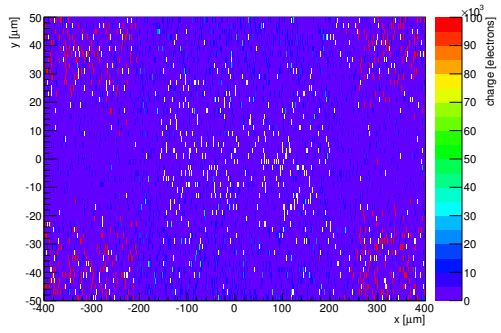

(q) Single pixel mean charge.

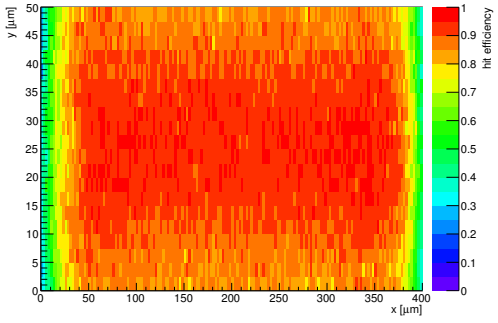

(r) Single pixel hit efficiency.

Figure C.164: Detailed plots for test beam measurement of DO-10 (description see section 6.1) sample (running as DUT1) during runs 797-833 in the May 2012 test beam period at CERN SPS in area H6B. Summary of the data in chapter 9.

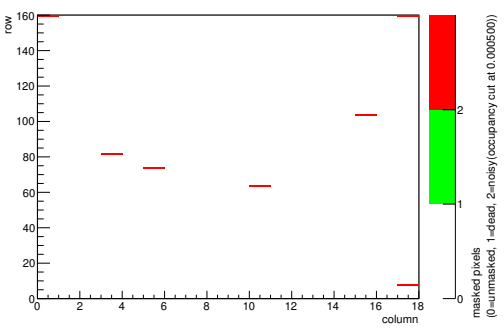

(a) Map of masked pixels.

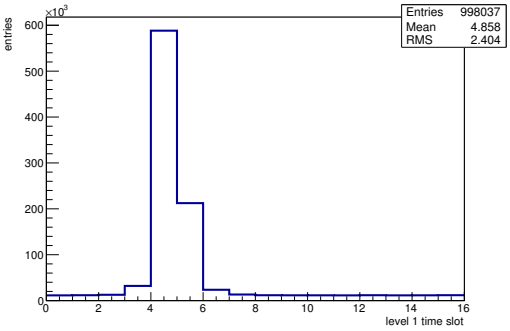

(b) Lvl1 distribution.

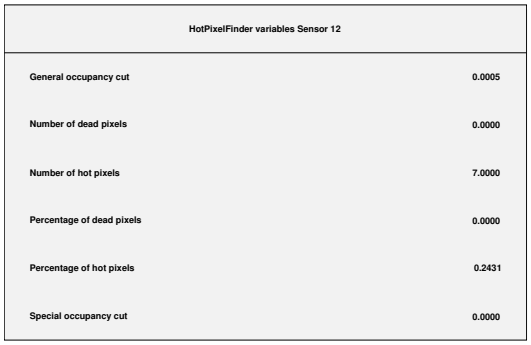

HotPixelFinder variables Sensor 12	
General occupancy cut	0.0005
Number of dead pixels	0.0000
Number of hot pixels	7.0000
Percentage of dead pixels	0.0000
Percentage of hot pixels	0.2431
Special occupancy cut	0.0000

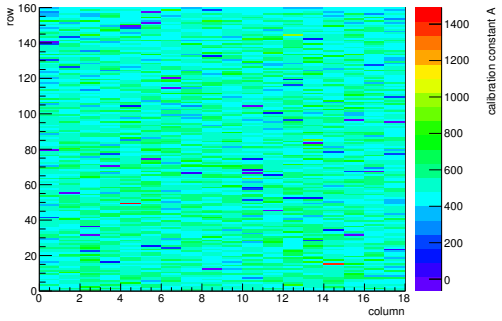

(c) Calibration constant A.

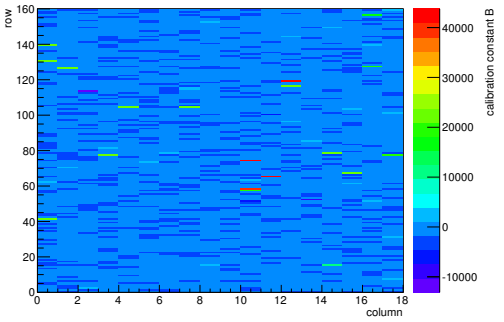

(d) Calibration constant B.

Figure C.165: Detailed plots for test beam measurement of DO-24 (description see section 6.1) sample (running as DUT2) during runs 797-833 in the May 2012 test beam period at CERN SPS in area H6B. Summary of the data in chapter 9. *(cont.)*

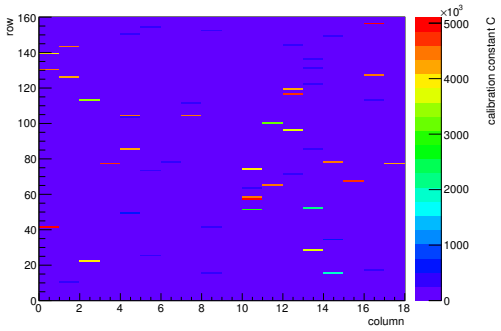

(e) Calibration constant C.

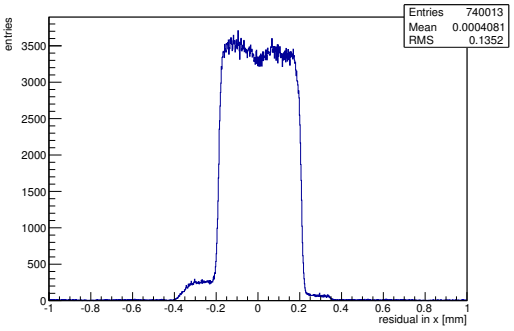

(f) Track residual in x.

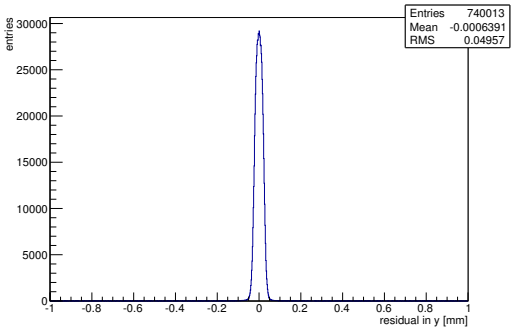

(g) Track residual in y.

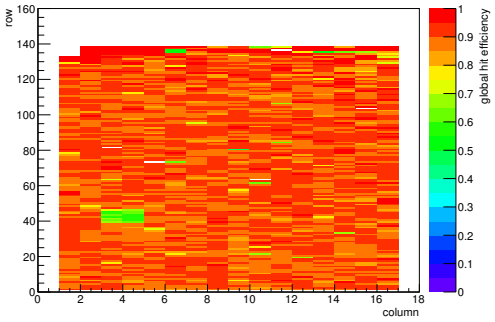

(h) Hit efficiency map.

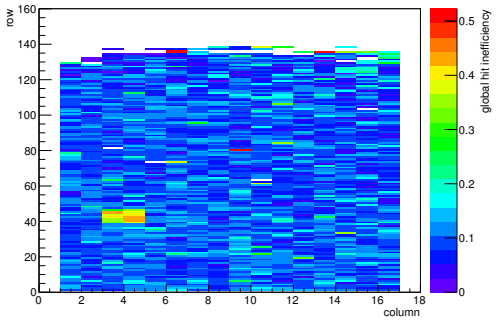

(i) Hit inefficiency map.

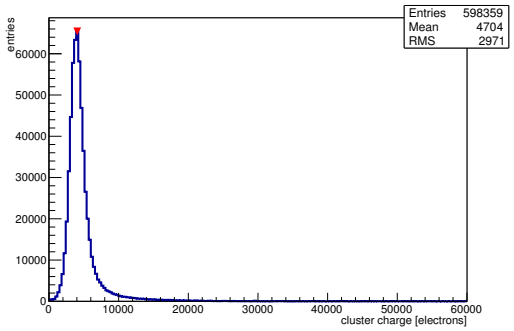

(j) Charge distribution (all cluster sizes included).

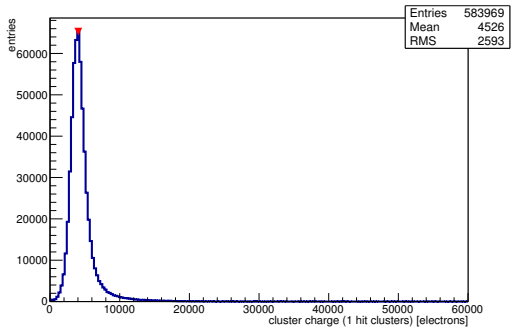

(k) Charge distribution (1 hit cluster).

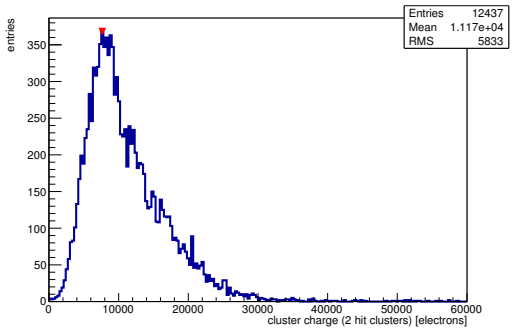

(l) Charge distribution (2 hit cluster).

Figure C.165: Detailed plots for test beam measurement of DO-24 (description see section 6.1) sample (running as DUT2) during runs 797-833 in the May 2012 test beam period at CERN SPS in area H6B. Summary of the data in chapter 9. *(cont.)*

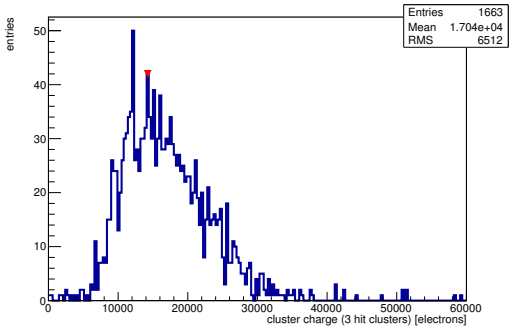

(m) Charge distribution (3 hit cluster).

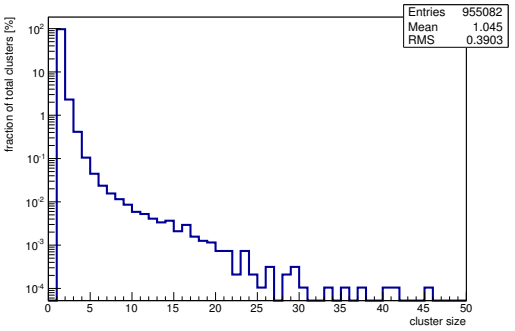

(n) Cluster size distribution.

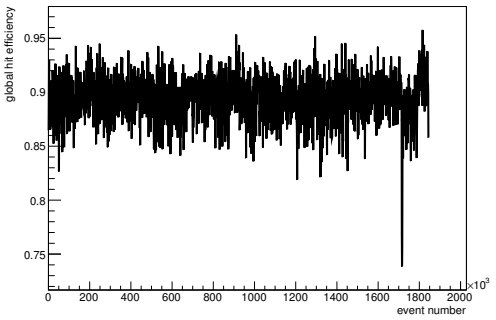

(o) Hit efficiency vs event number.

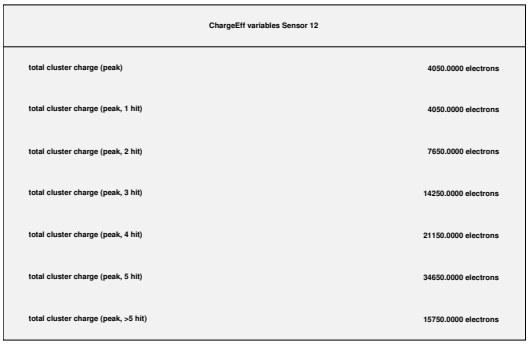

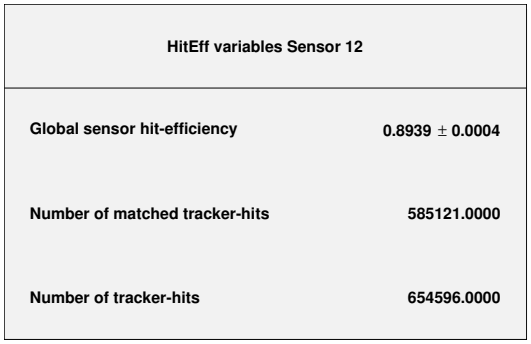

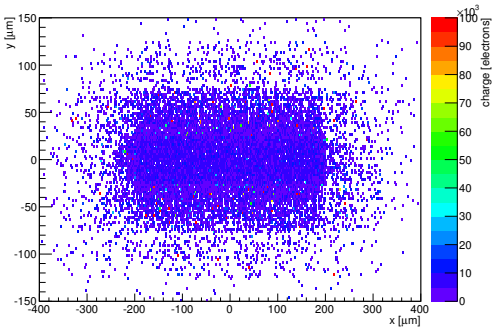

(p) Single pixel mean charge.

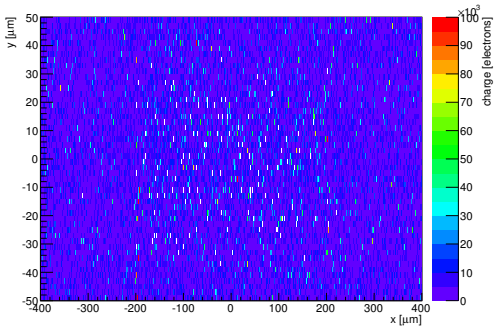

(q) Single pixel mean charge.

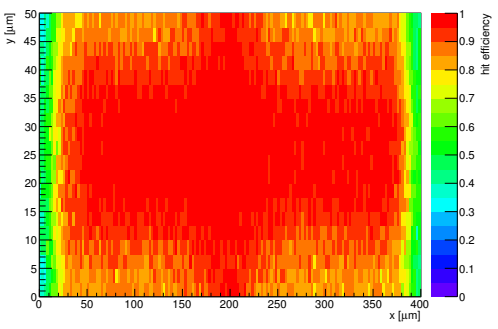

(r) Single pixel hit efficiency.

Figure C.165: Detailed plots for test beam measurement of DO-24 (description see section 6.1) sample (running as DUT2) during runs 797-833 in the May 2012 test beam period at CERN SPS in area H6B. Summary of the data in chapter 9.

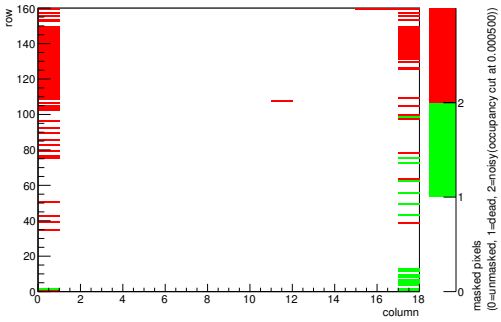

(a) Map of masked pixels.

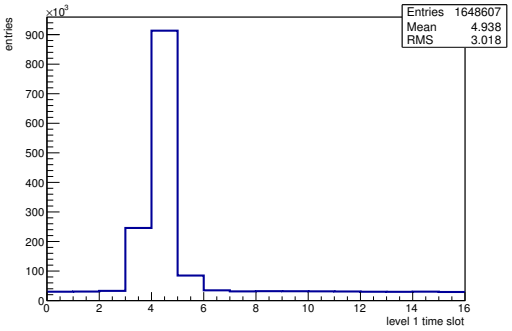

(b) Lvl1 distribution.

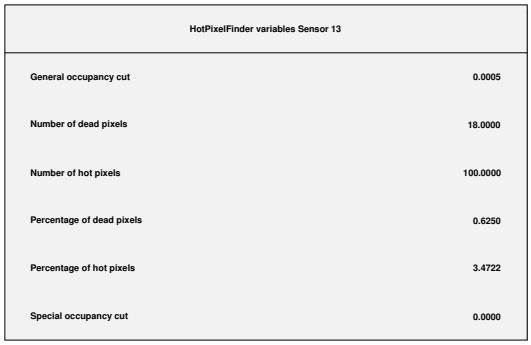

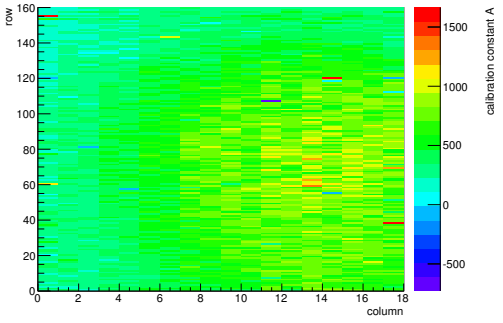

(c) Calibration constant A.

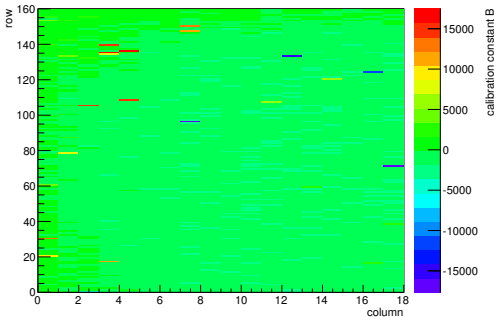

(d) Calibration constant B.

Figure C.166: Detailed plots for test beam measurement of DO-38 (description see section 6.1) sample (running as DUT3) during runs 797-833 in the May 2012 test beam period at CERN SPS in area H6B. Summary of the data in chapter 9. *(cont.)*

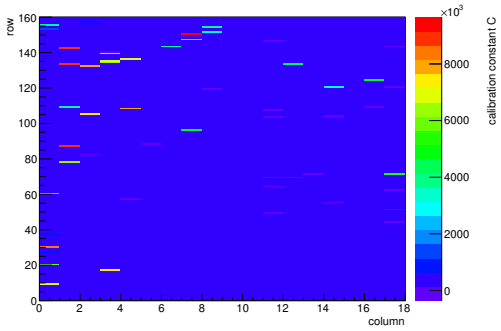

(e) Calibration constant C.

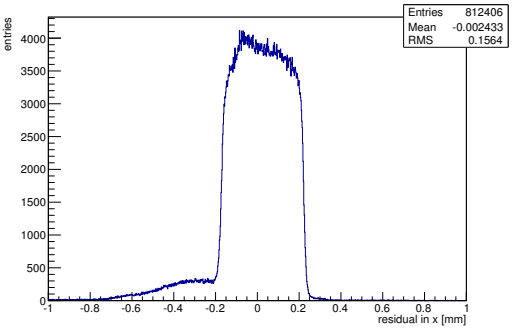

(f) Track residual in x.

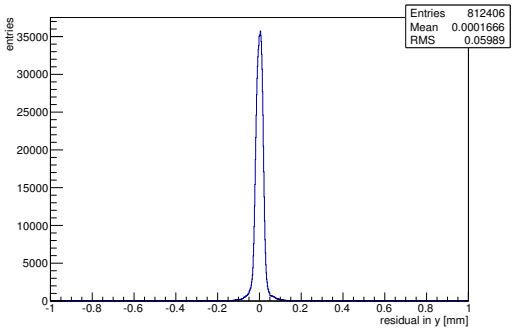

(g) Track residual in y.

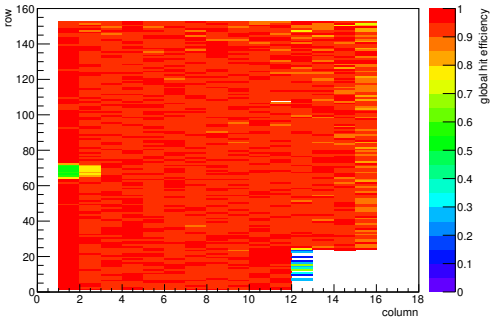

(h) Hit efficiency map.

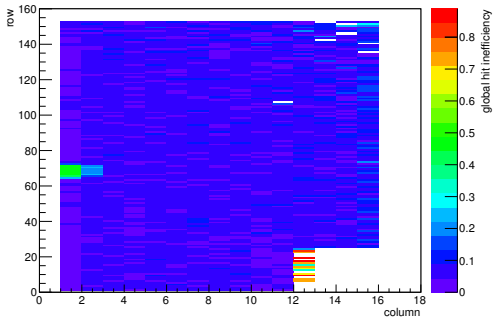

(i) Hit inefficiency map.

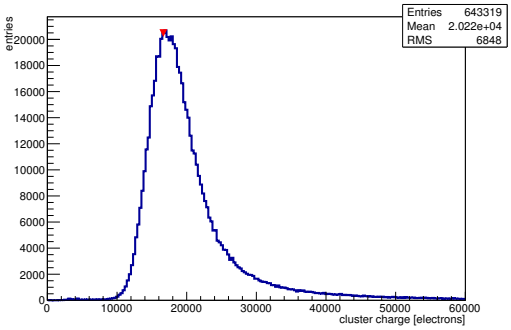

(j) Charge distribution (all cluster sizes included).

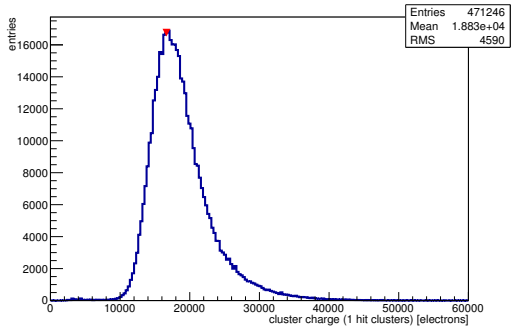

(k) Charge distribution (1 hit cluster).

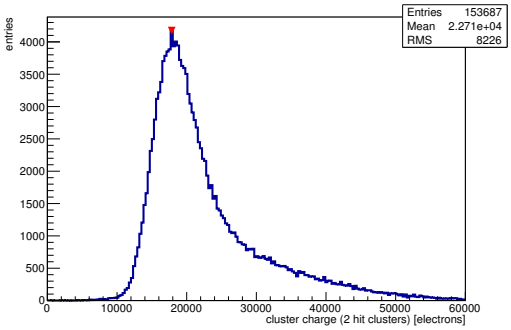

(l) Charge distribution (2 hit cluster).

Figure C.166: Detailed plots for test beam measurement of DO-38 (description see section 6.1) sample (running as DUT3) during runs 797-833 in the May 2012 test beam period at CERN SPS in area H6B. Summary of the data in chapter 9. *(cont.)*

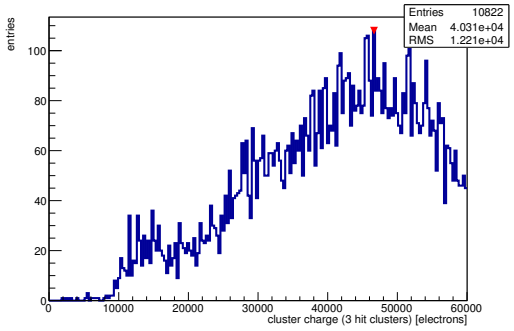

(m) Charge distribution (3 hit cluster).

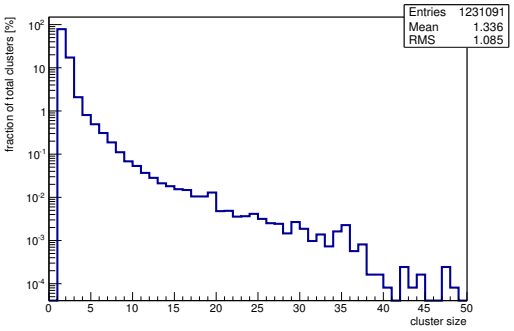

(n) Cluster size distribution.

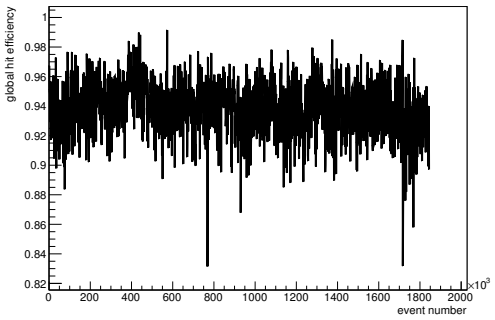

(o) Hit efficiency vs event number.

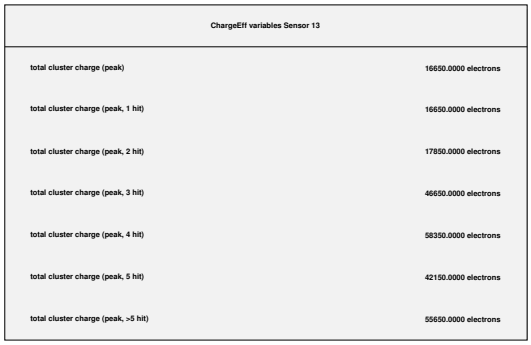

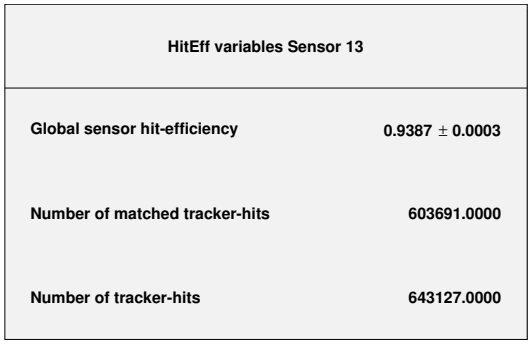

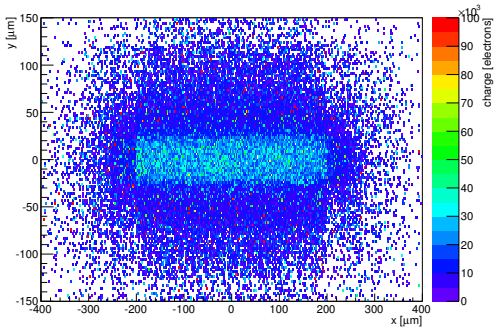

(p) Single pixel mean charge.

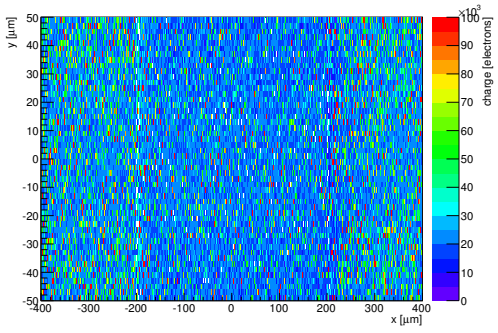

(q) Single pixel mean charge.

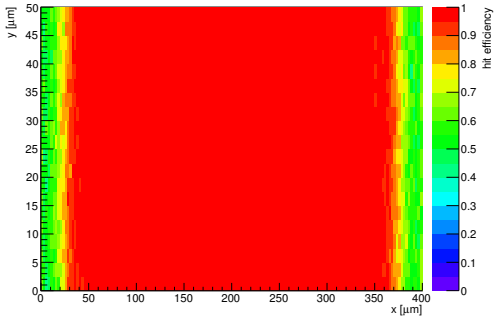

(r) Single pixel hit efficiency.

Figure C.166: Detailed plots for test beam measurement of DO-38 (description see section 6.1) sample (running as DUT3) during runs 797-833 in the May 2012 test beam period at CERN SPS in area H6B. Summary of the data in chapter 9.

C.5.4 Runs 835-882

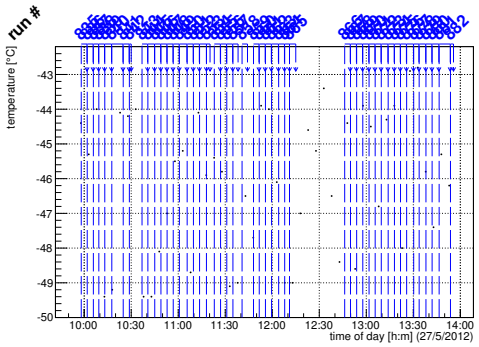

(a) Temperature vs time.

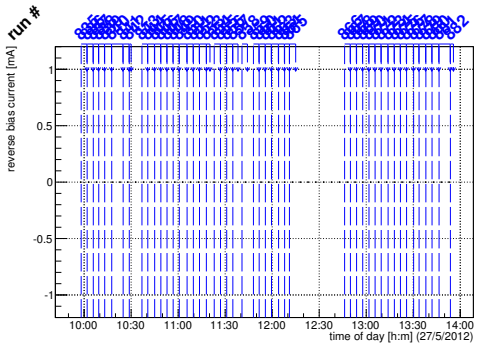

(b) Bias current vs time.

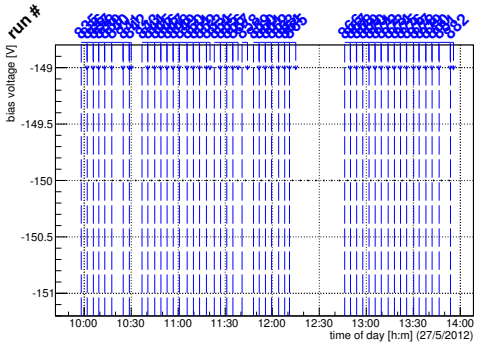

(c) Currently applied bias voltage vs time.

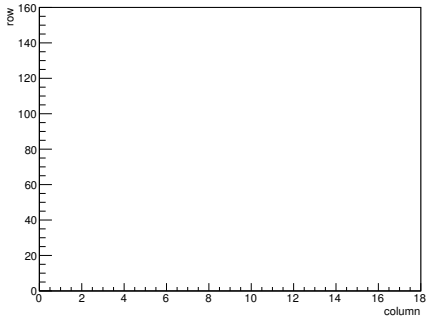

(d) Map of masked pixels.

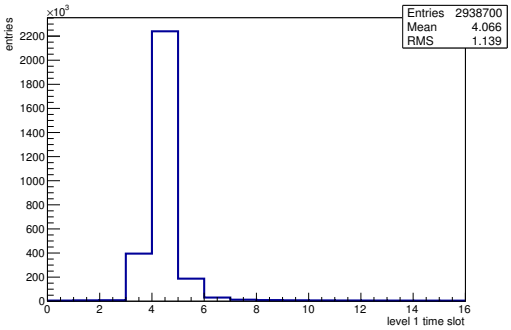

(e) Lvl1 distribution.

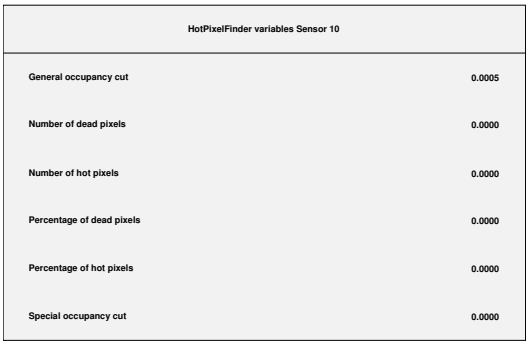

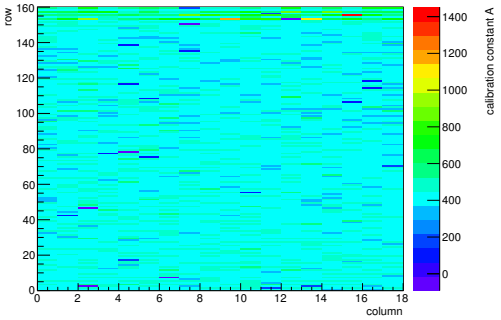

(f) Calibration constant A.

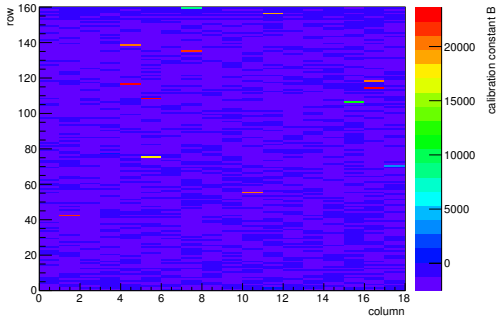

(g) Calibration constant B.

Figure C.167: Detailed plots for test beam measurement of DO-1 (description see section 6.1) sample (running as DUT0) during runs 835-882 in the May 2012 test beam period at CERN SPS in area H6B. Summary of the data in chapter 9. *(cont.)*

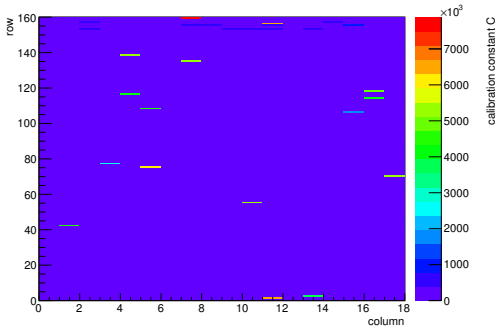

(h) Calibration constant C.

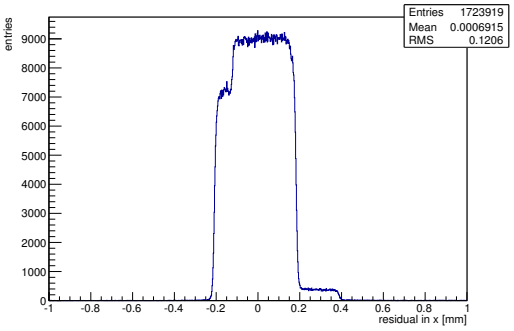

(i) Track residual in x.

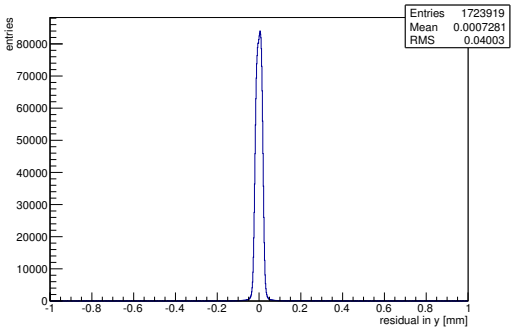

(j) Track residual in y.

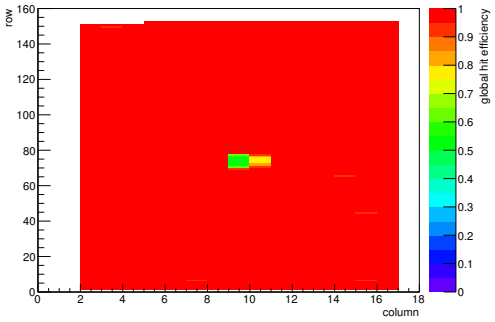

(k) Hit efficiency map.

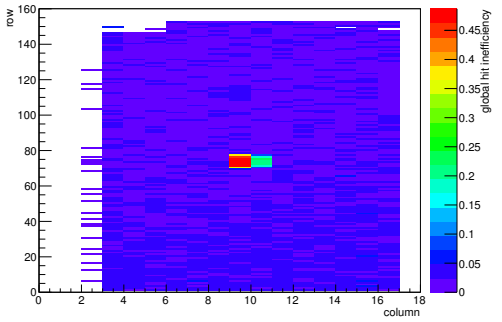

(l) Hit inefficiency map.

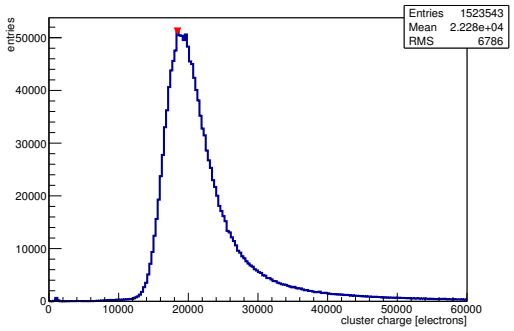

(m) Charge distribution (all cluster sizes included).

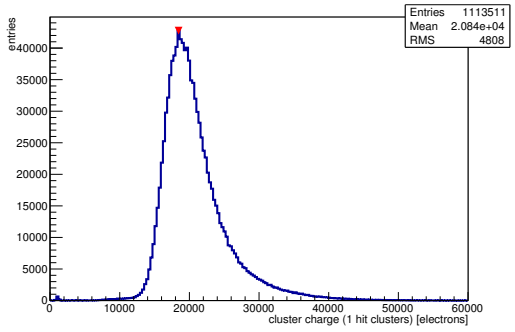

(n) Charge distribution (1 hit cluster).

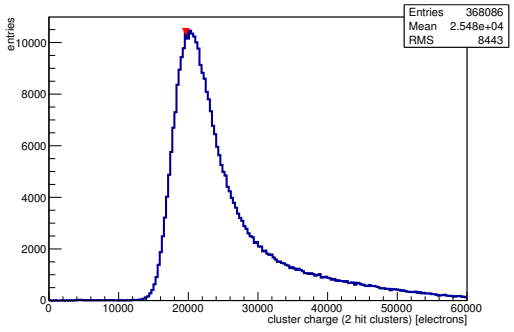

(o) Charge distribution (2 hit cluster).

Figure C.167: Detailed plots for test beam measurement of DO-1 (description see section 6.1) sample (running as DUT0) during runs 835-882 in the May 2012 test beam period at CERN SPS in area H6B. Summary of the data in chapter 9. *(cont.)*

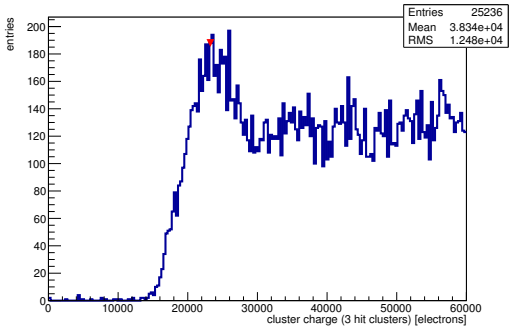

(p) Charge distribution (3 hit cluster).

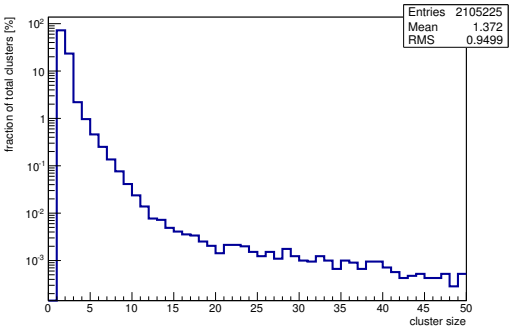

(q) Cluster size distribution.

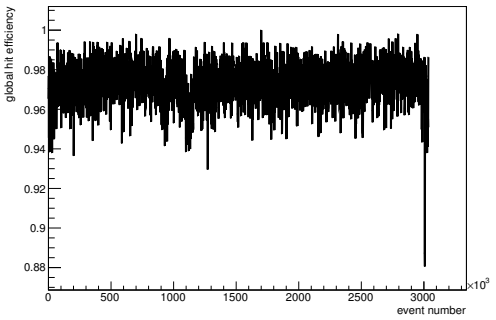

(r) Hit efficiency vs event number.

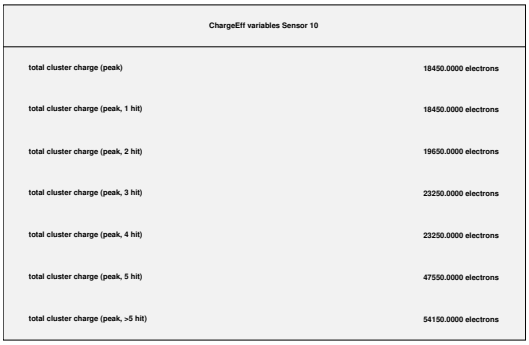

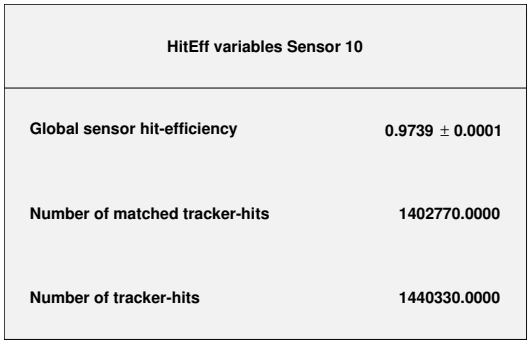

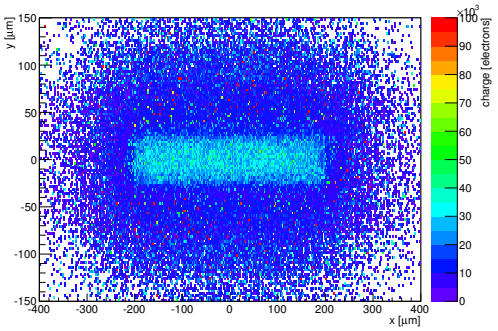

(s) Single pixel mean charge.

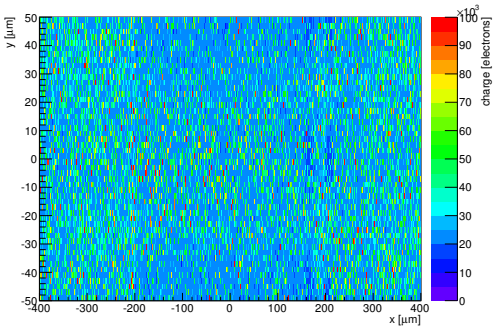

(t) Single pixel mean charge.

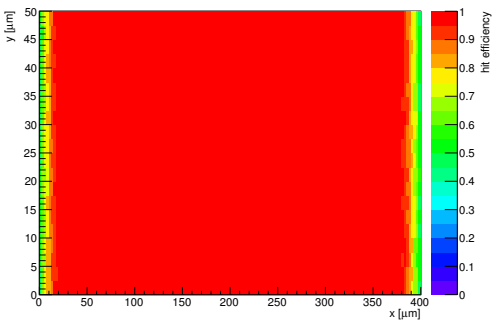

(u) Single pixel hit efficiency.

Figure C.167: Detailed plots for test beam measurement of DO-1 (description see section 6.1) sample (running as DUT0) during runs 835-882 in the May 2012 test beam period at CERN SPS in area H6B. Summary of the data in chapter 9.

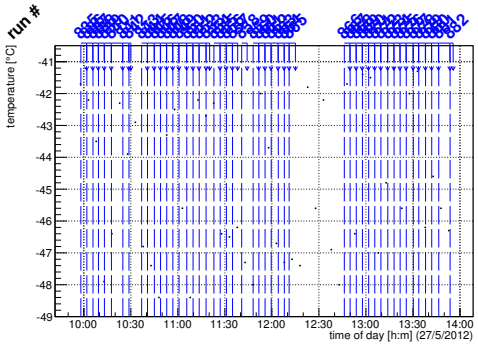

(a) Temperature vs time.

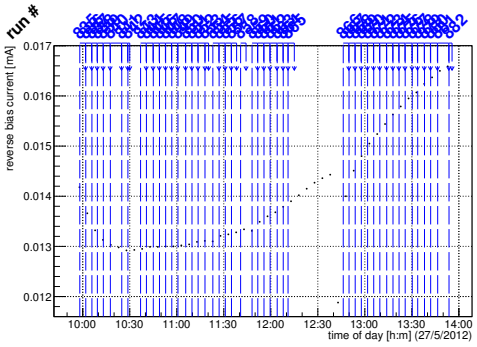

(b) Bias current vs time.

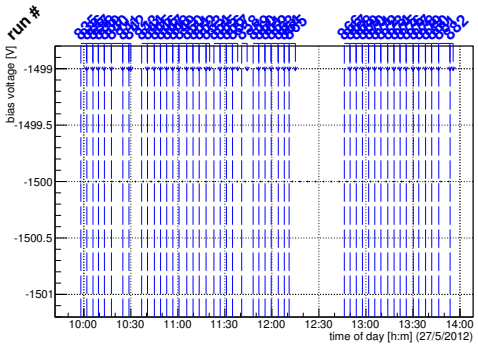

(c) Currently applied bias voltage vs time.

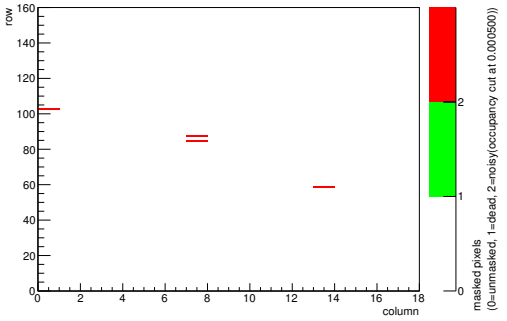

(d) Map of masked pixels.

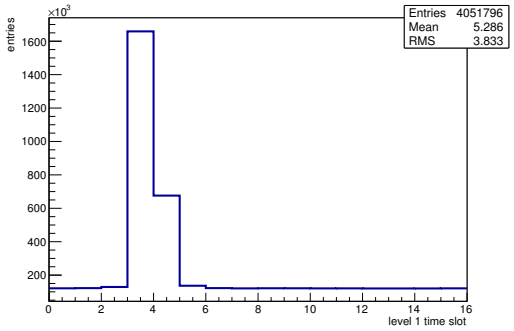

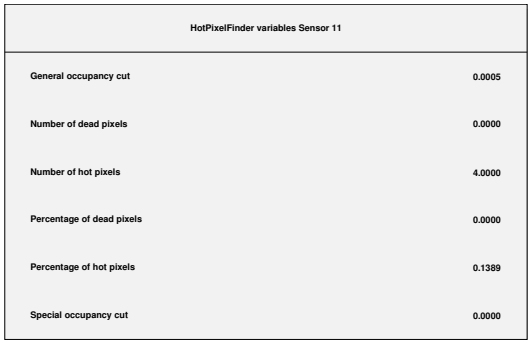

(e) Lvl1 distribution.

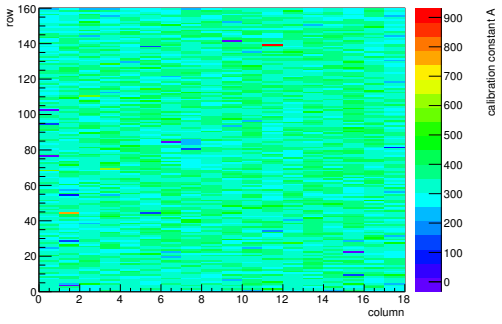

(f) Calibration constant A.

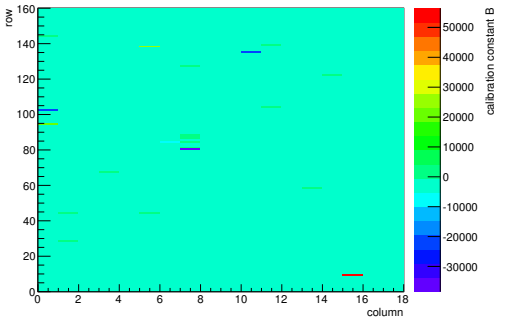

(g) Calibration constant B.

Figure C.168: Detailed plots for test beam measurement of DO-10 (description see section 6.1) sample (running as DUT1) during runs 835-882 in the May 2012 test beam period at CERN SPS in area H6B. Summary of the data in chapter 9. *(cont.)*

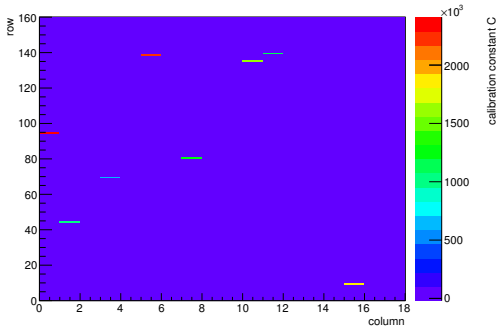

(h) Calibration constant C.

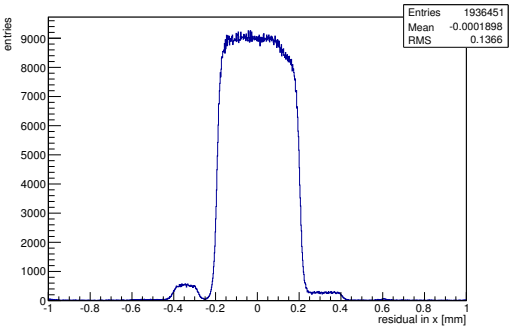

(i) Track residual in x.

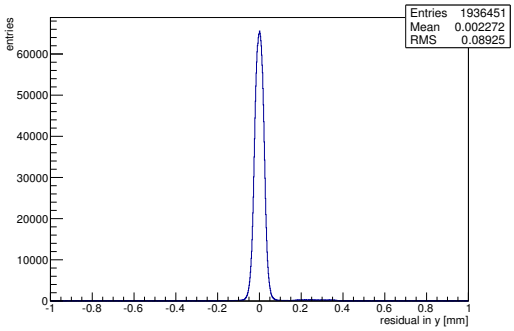

(j) Track residual in y.

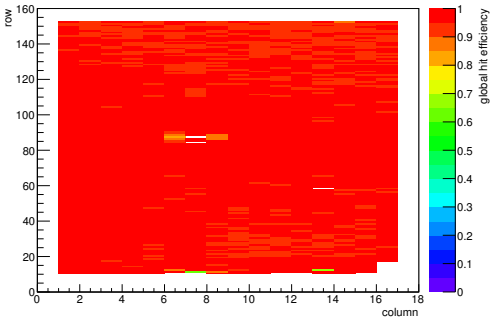

(k) Hit efficiency map.

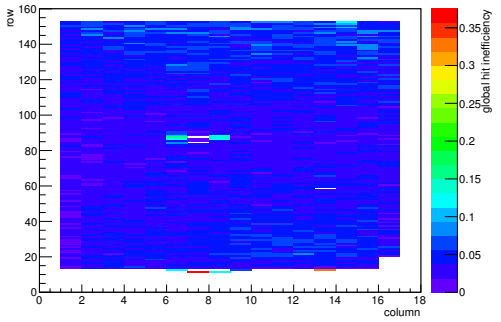

(l) Hit inefficiency map.

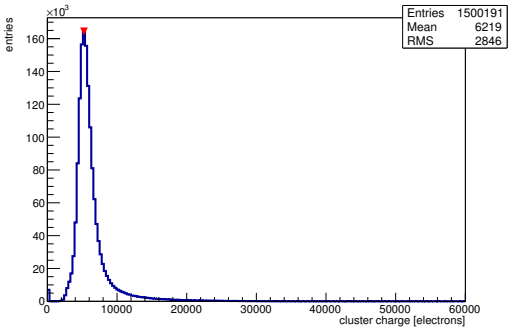

(m) Charge distribution (all cluster sizes included).

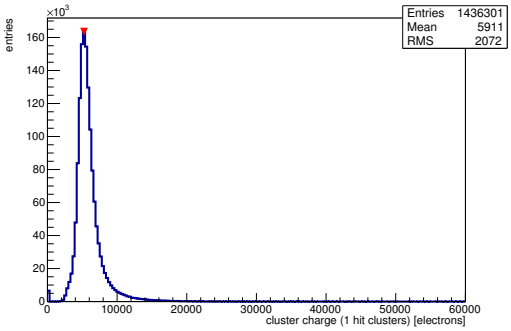

(n) Charge distribution (1 hit cluster).

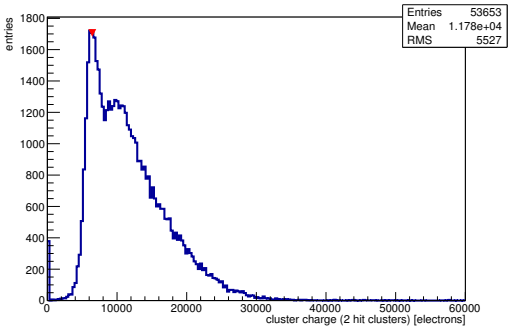

(o) Charge distribution (2 hit cluster).

Figure C.168: Detailed plots for test beam measurement of DO-10 (description see section 6.1) sample (running as DUT1) during runs 835-882 in the May 2012 test beam period at CERN SPS in area H6B. Summary of the data in chapter 9. *(cont.)*

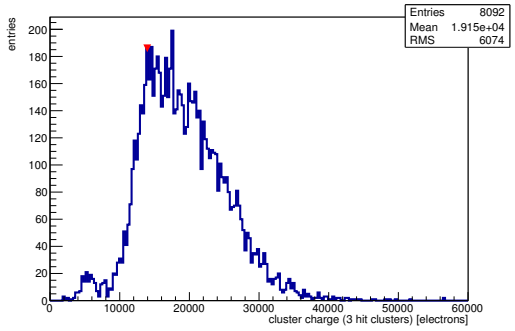

(p) Charge distribution (3 hit cluster).

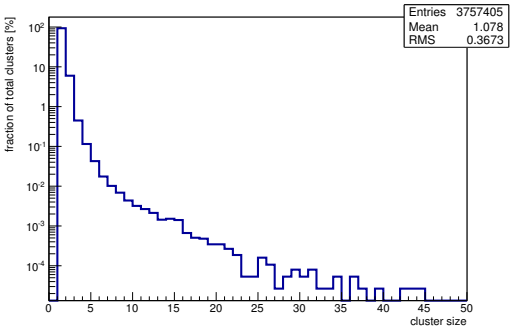

(q) Cluster size distribution.

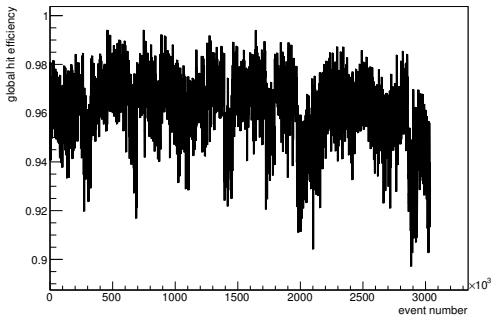

(r) Hit efficiency vs event number.

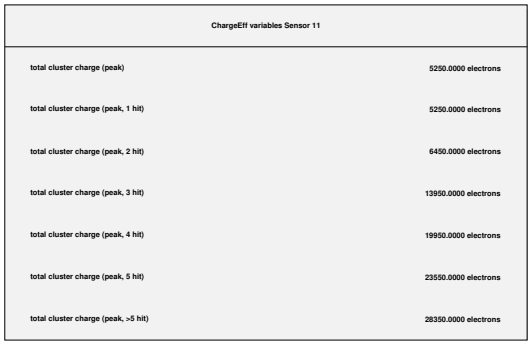

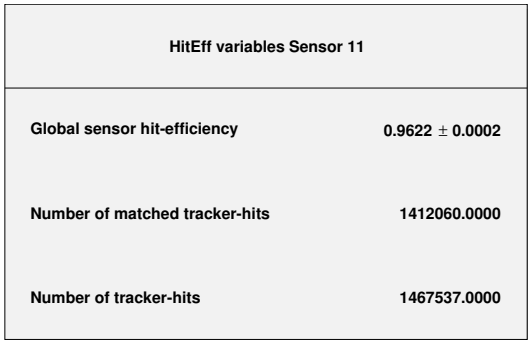

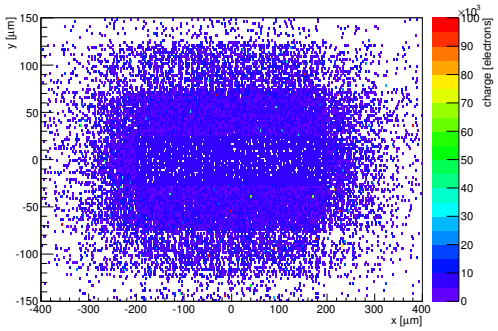

(s) Single pixel mean charge.

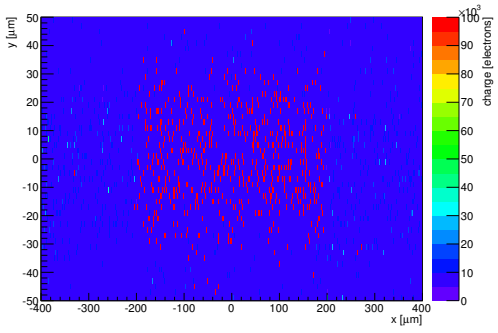

(t) Single pixel mean charge.

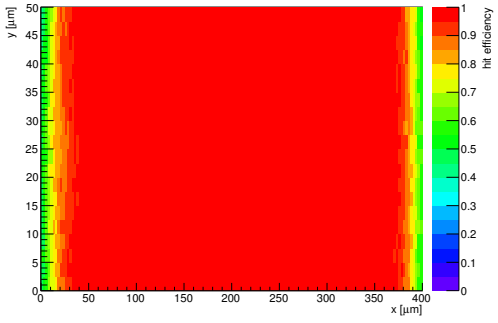

(u) Single pixel hit efficiency.

Figure C.168: Detailed plots for test beam measurement of DO-10 (description see section 6.1) sample (running as DUT1) during runs 835-882 in the May 2012 test beam period at CERN SPS in area H6B. Summary of the data in chapter 9.

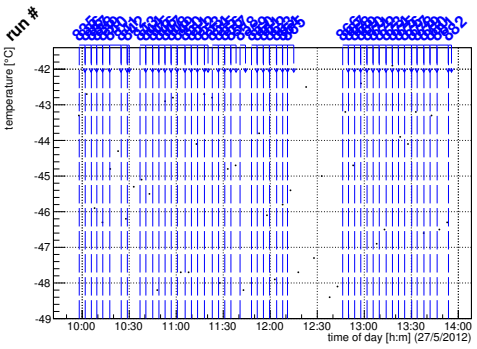

(a) Temperature vs time.

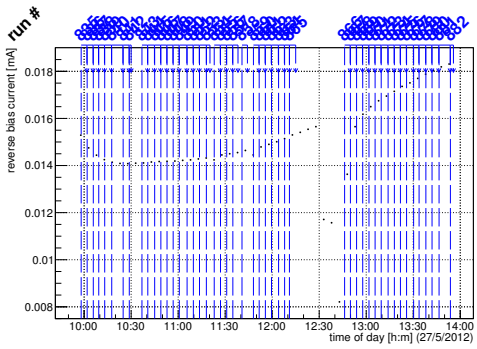

(b) Bias current vs time.

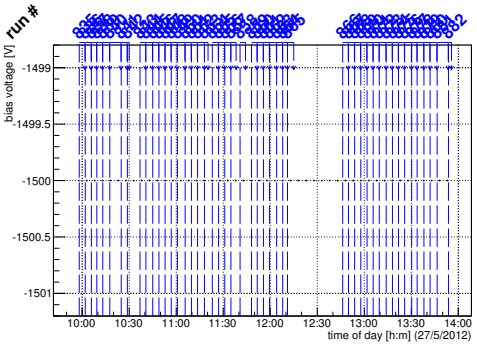

(c) Currently applied bias voltage vs time.

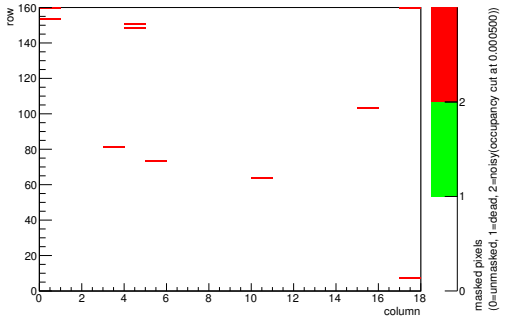

(d) Map of masked pixels.

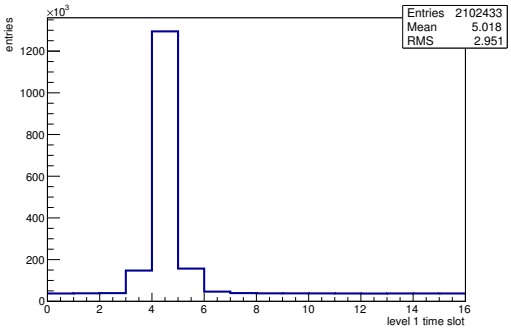

(e) Lvl1 distribution.

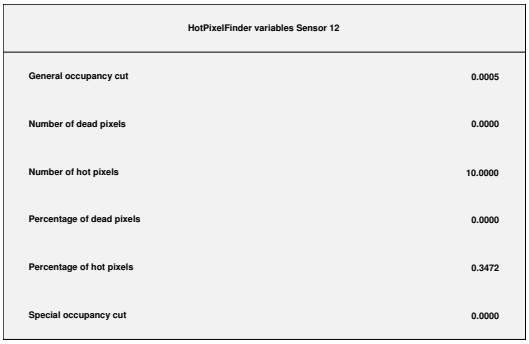

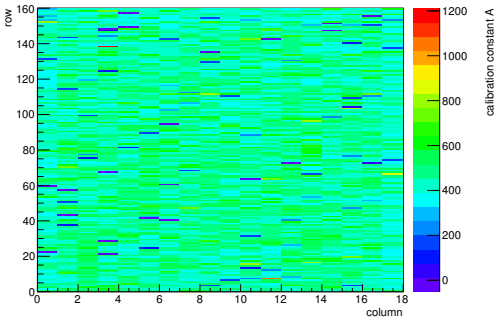

(f) Calibration constant A.

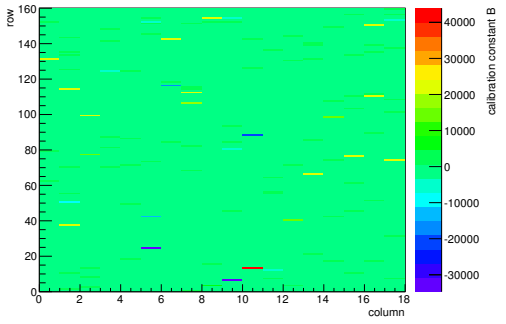

(g) Calibration constant B.

Figure C.169: Detailed plots for test beam measurement of DO-24 (description see section 6.1) sample (running as DUT2) during runs 835-882 in the May 2012 test beam period at CERN SPS in area H6B. Summary of the data in chapter 9. *(cont.)*

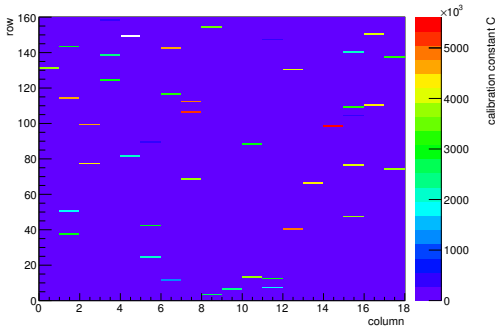

(h) Calibration constant C.

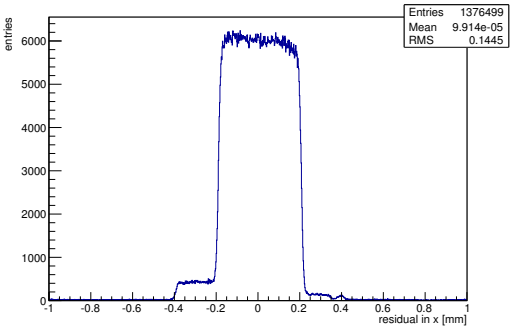

(i) Track residual in x.

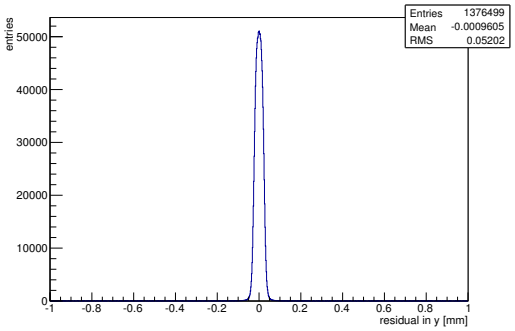

(j) Track residual in y.

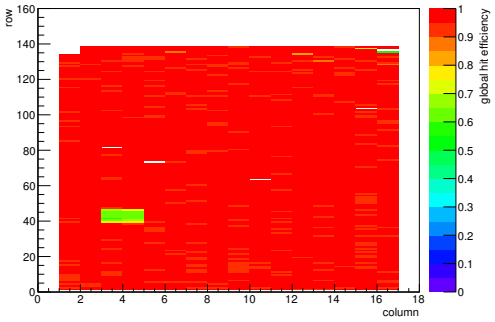

(k) Hit efficiency map.

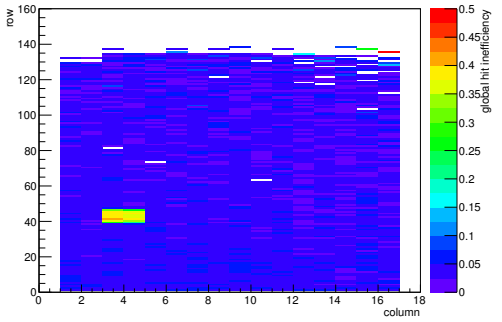

(l) Hit inefficiency map.

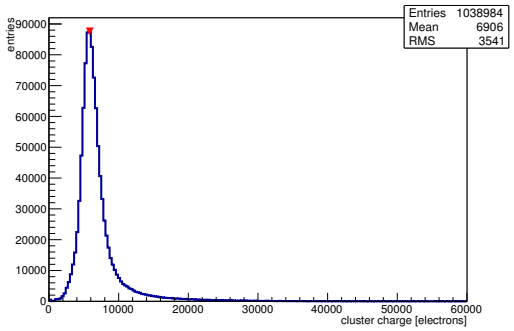

(m) Charge distribution (all cluster sizes included).

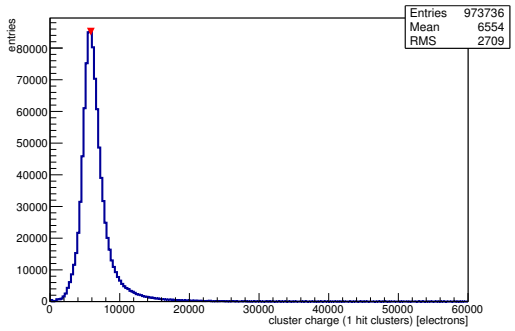

(n) Charge distribution (1 hit cluster).

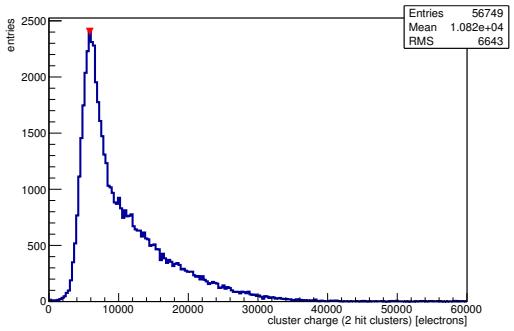

(o) Charge distribution (2 hit cluster).

Figure C.169: Detailed plots for test beam measurement of DO-24 (description see section 6.1) sample (running as DUT2) during runs 835-882 in the May 2012 test beam period at CERN SPS in area H6B. Summary of the data in chapter 9. *(cont.)*

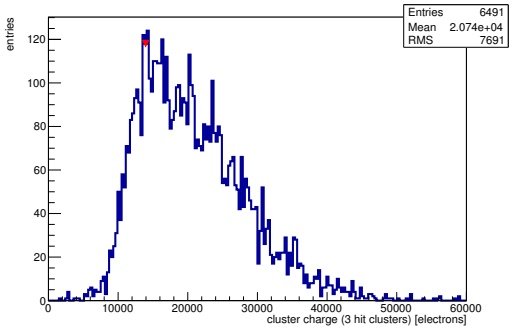

(p) Charge distribution (3 hit cluster).

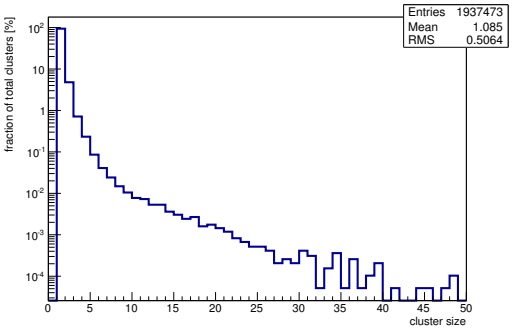

(q) Cluster size distribution.

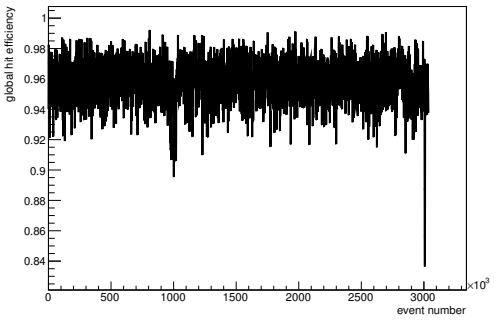

(r) Hit efficiency vs event number.

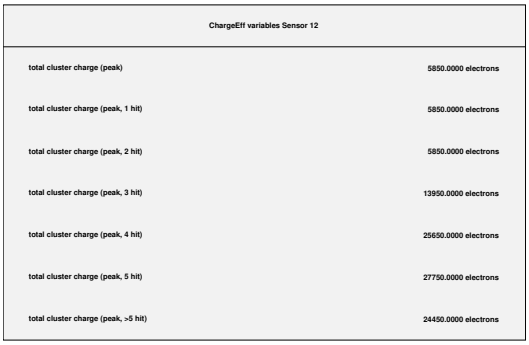

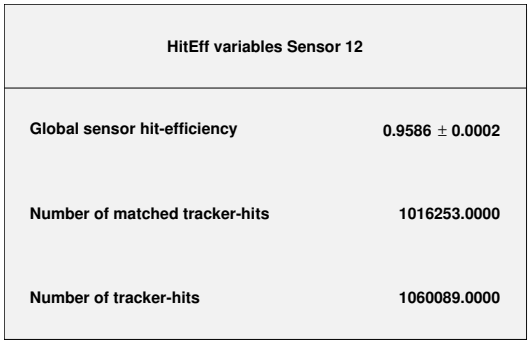

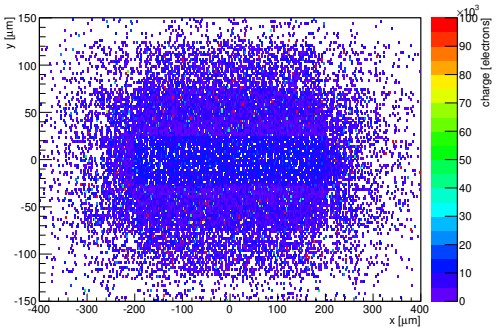

(s) Single pixel mean charge.

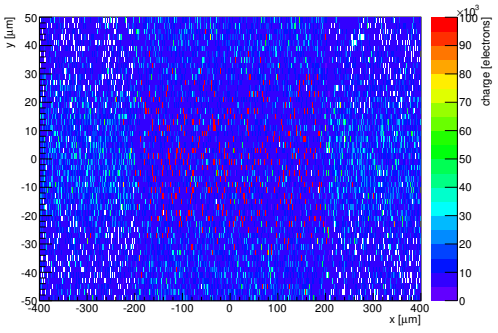

(t) Single pixel mean charge.

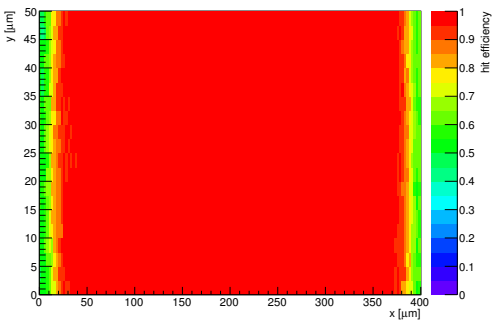

(u) Single pixel hit efficiency.

Figure C.169: Detailed plots for test beam measurement of DO-24 (description see section 6.1) sample (running as DUT2) during runs 835-882 in the May 2012 test beam period at CERN SPS in area H6B. Summary of the data in chapter 9.

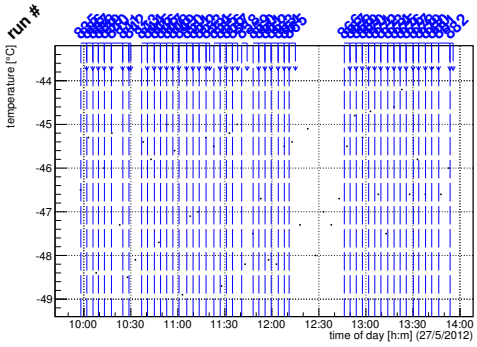

(a) Temperature vs time.

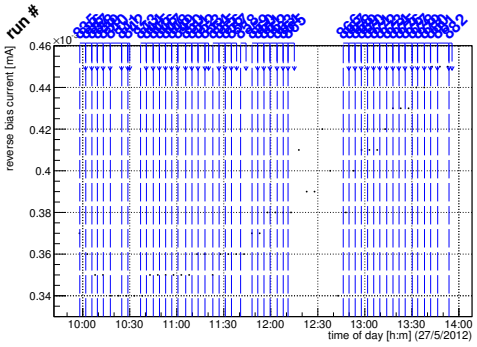

(b) Bias current vs time.

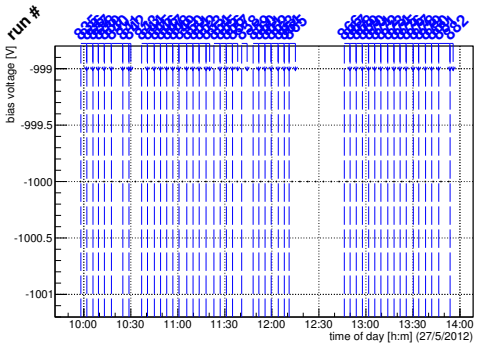

(c) Currently applied bias voltage vs time.

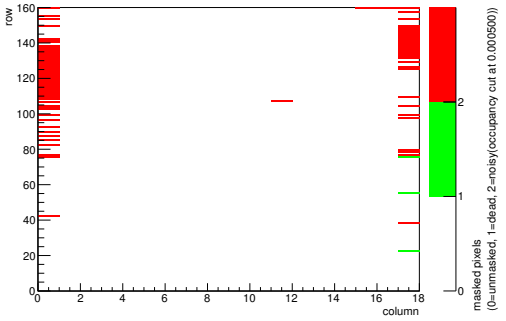

(d) Map of masked pixels.

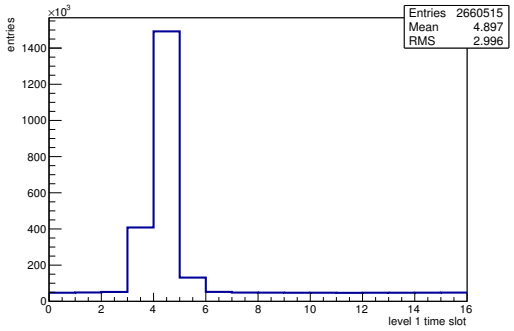

(e) Lvl1 distribution.

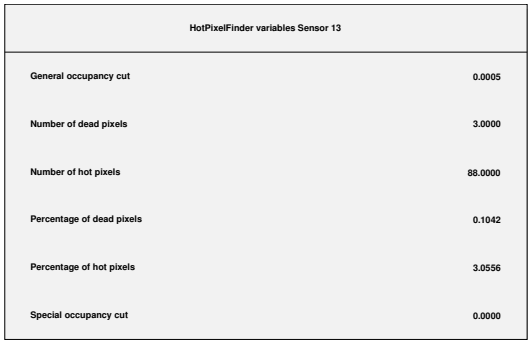

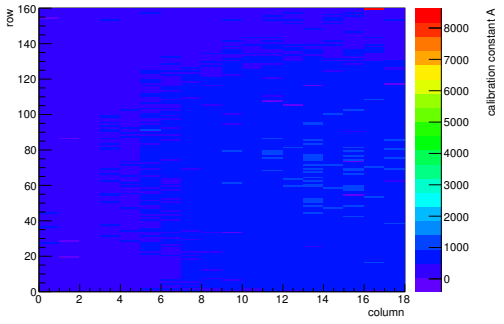

(f) Calibration constant A.

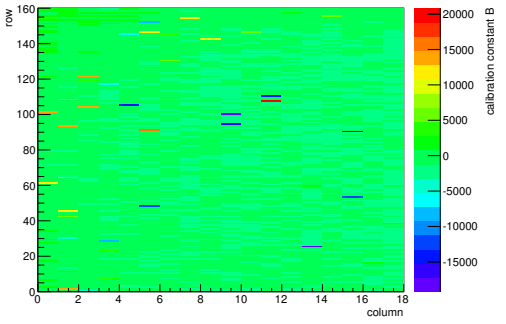

(g) Calibration constant B.

Figure C.170: Detailed plots for test beam measurement of DO-38 (description see section 6.1) sample (running as DUT3) during runs 835-882 in the May 2012 test beam period at CERN SPS in area H6B. Summary of the data in chapter 9. *(cont.)*

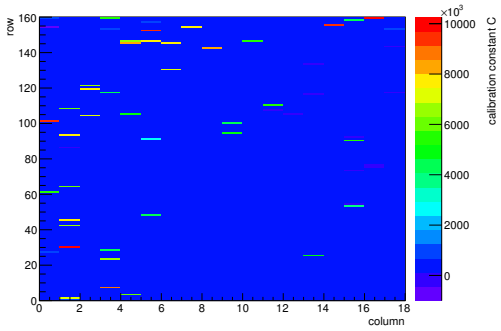

(h) Calibration constant C.

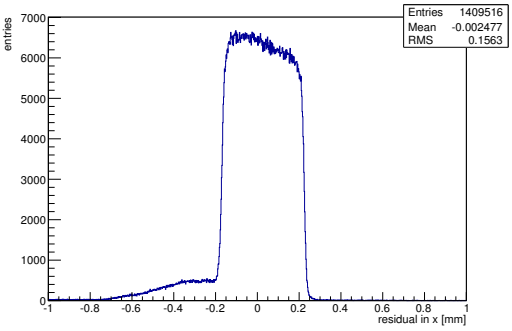

(i) Track residual in x.

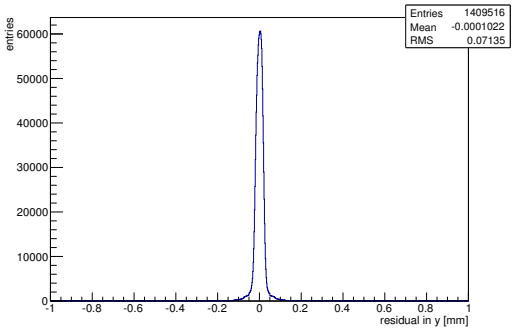

(j) Track residual in y.

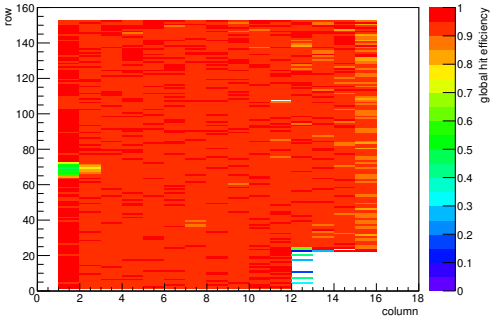

(k) Hit efficiency map.

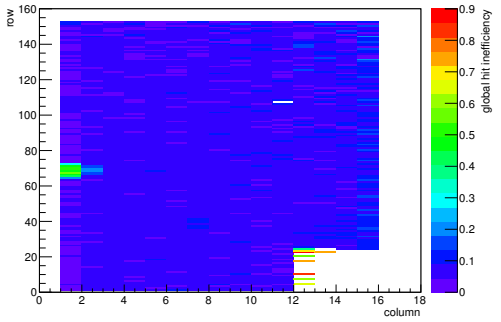

(l) Hit inefficiency map.

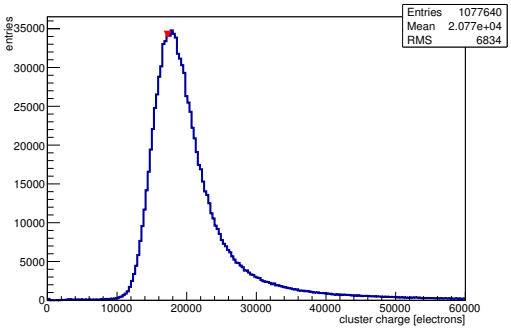

(m) Charge distribution (all cluster sizes included).

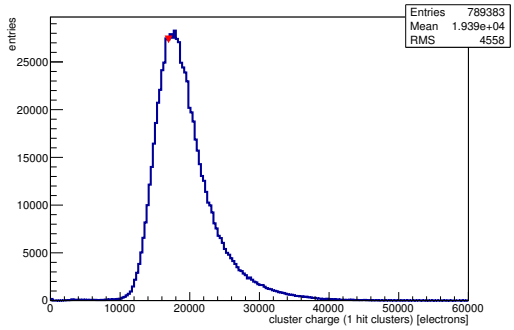

(n) Charge distribution (1 hit cluster).

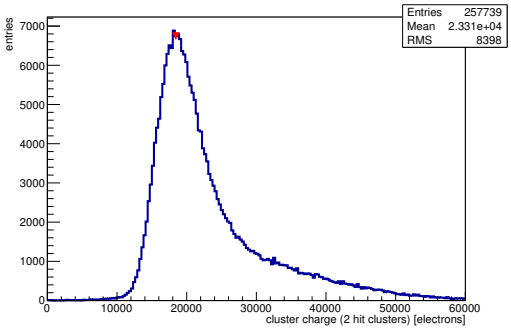

(o) Charge distribution (2 hit cluster).

Figure C.170: Detailed plots for test beam measurement of DO-38 (description see section 6.1) sample (running as DUT3) during runs 835-882 in the May 2012 test beam period at CERN SPS in area H6B. Summary of the data in chapter 9. *(cont.)*

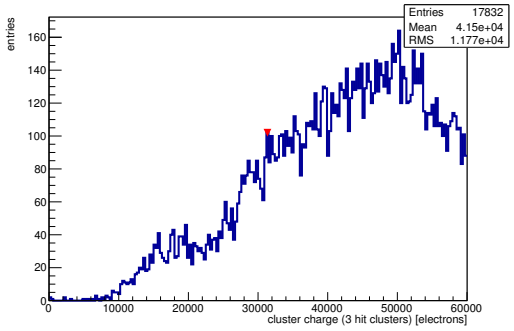

(p) Charge distribution (3 hit cluster).

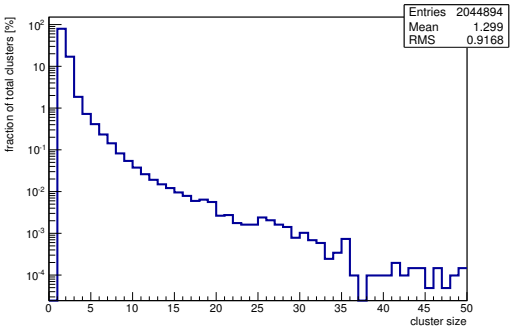

(q) Cluster size distribution.

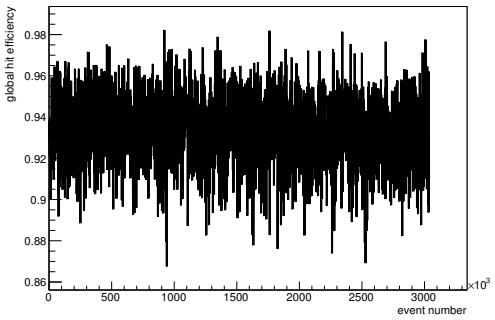

(r) Hit efficiency vs event number.

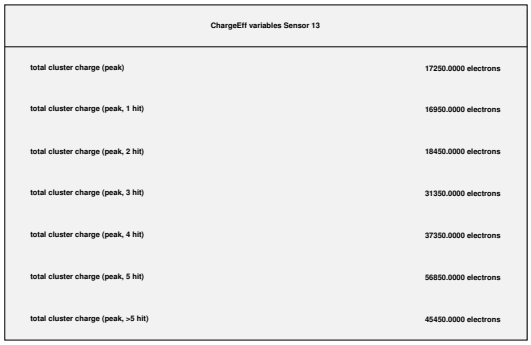

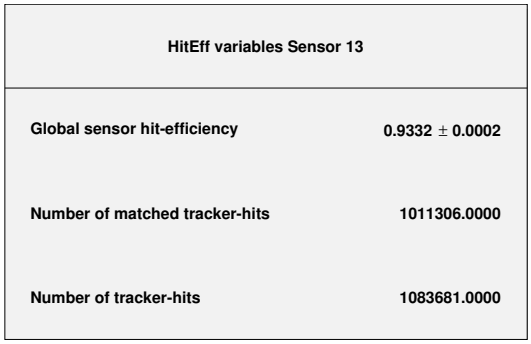

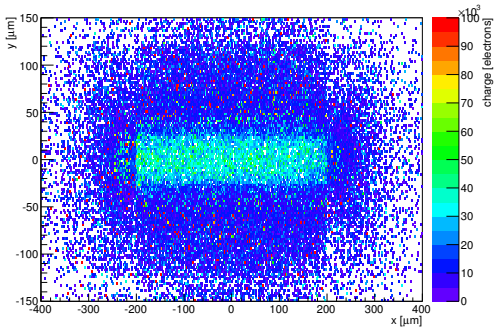

(s) Single pixel mean charge.

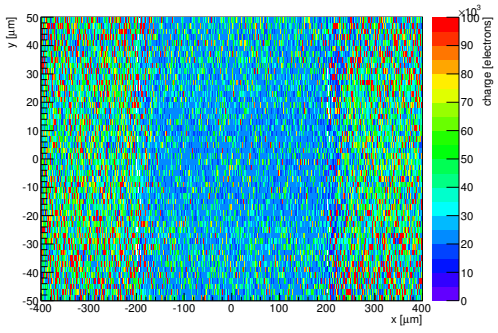

(t) Single pixel mean charge.

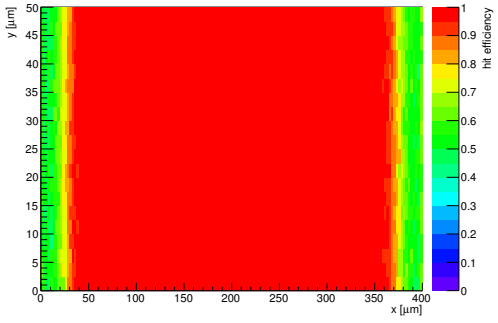

(u) Single pixel hit efficiency.

Figure C.170: Detailed plots for test beam measurement of DO-38 (description see section 6.1) sample (running as DUT3) during runs 835-882 in the May 2012 test beam period at CERN SPS in area H6B. Summary of the data in chapter 9.

C.5.5 Runs 883-907

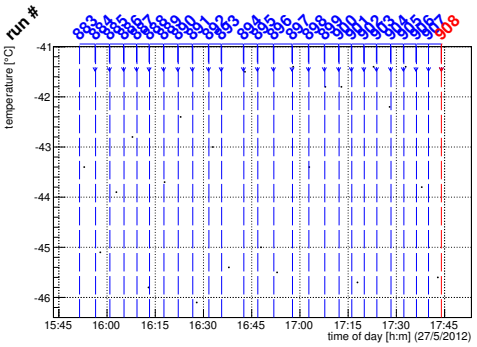

(a) Temperature vs time.

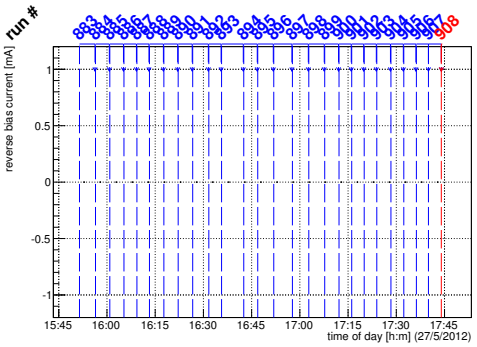

(b) Bias current vs time.

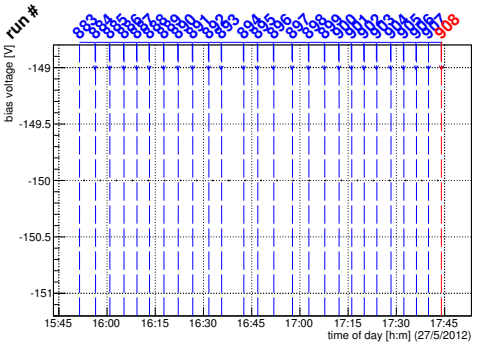

(c) Currently applied bias voltage vs time.

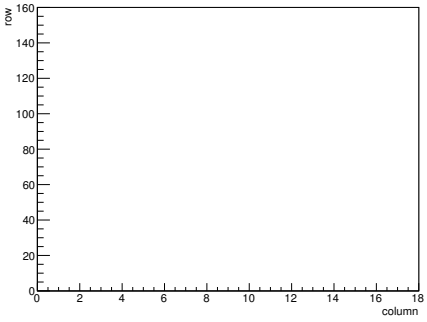

(d) Map of masked pixels.

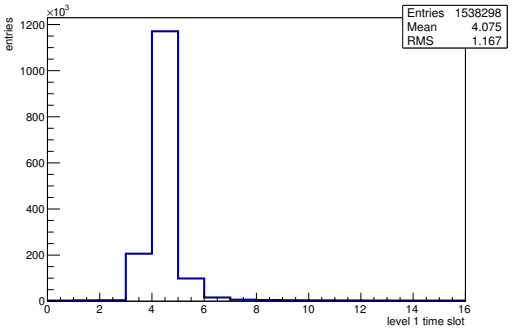

(e) Lvl1 distribution.

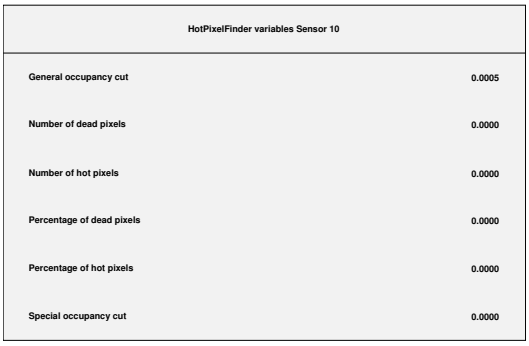

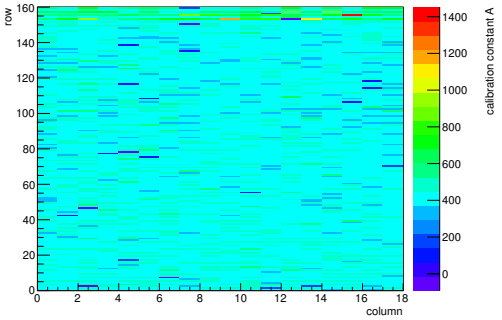

(f) Calibration constant A.

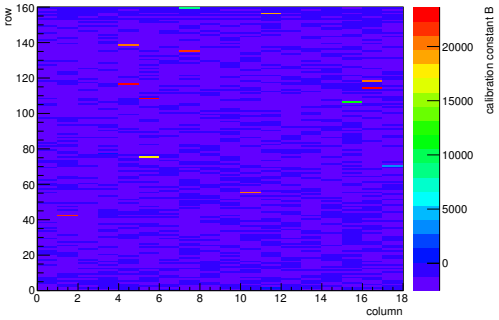

(g) Calibration constant B.

Figure C.171: Detailed plots for test beam measurement of DO-1 (description see section 6.1) sample (running as DUT0) during runs 883-907 in the May 2012 test beam period at CERN SPS in area H6B. Summary of the data in chapter 9. *(cont.)*

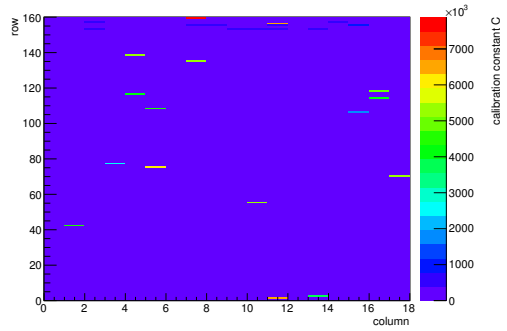

(h) Calibration constant C.

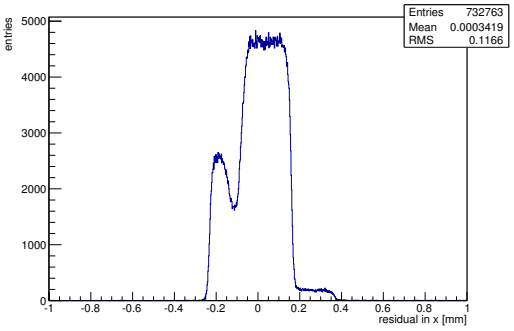

(i) Track residual in x.

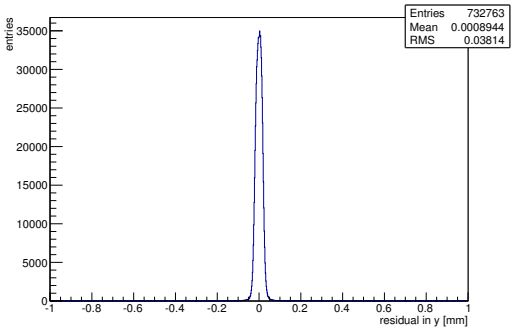

(j) Track residual in y.

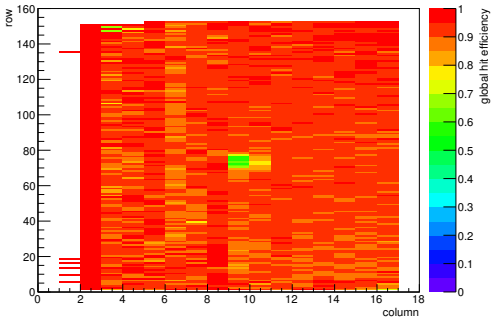

(k) Hit efficiency map.

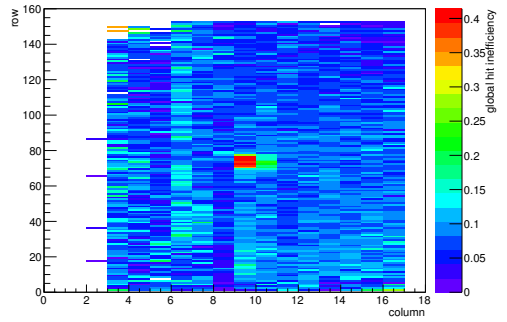

(l) Hit inefficiency map.

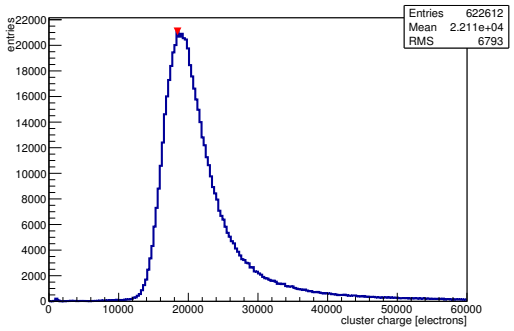

(m) Charge distribution (all cluster sizes included).

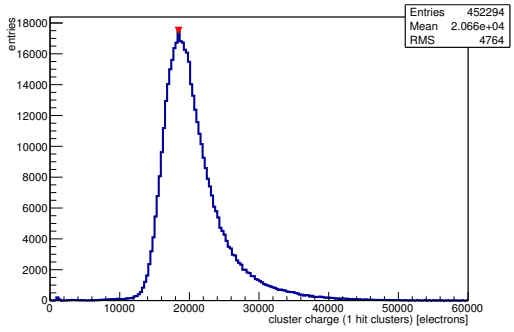

(n) Charge distribution (1 hit cluster).

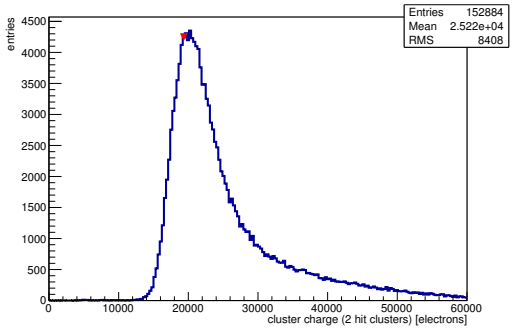

(o) Charge distribution (2 hit cluster).

Figure C.171: Detailed plots for test beam measurement of DO-1 (description see section 6.1) sample (running as DUT0) during runs 883-907 in the May 2012 test beam period at CERN SPS in area H6B. Summary of the data in chapter 9. *(cont.)*

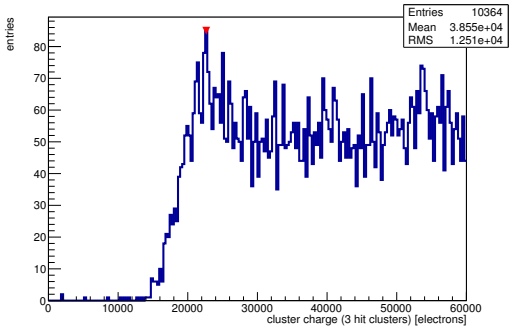

(p) Charge distribution (3 hit cluster).

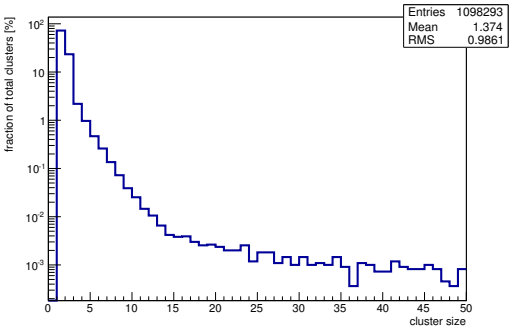

(q) Cluster size distribution.

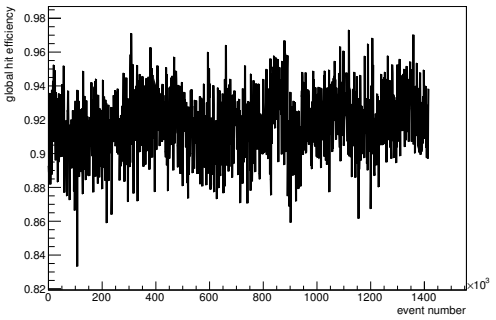

(r) Hit efficiency vs event number.

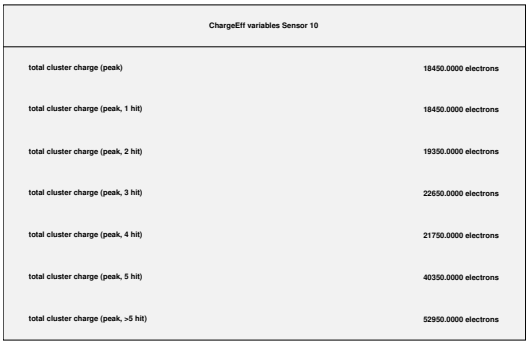

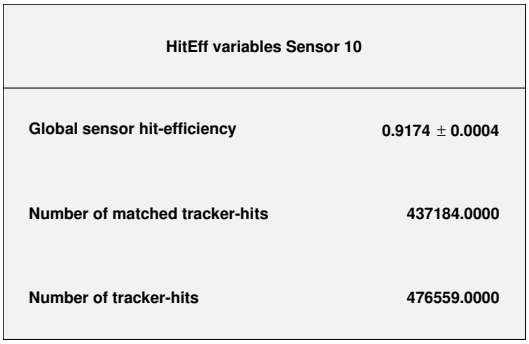

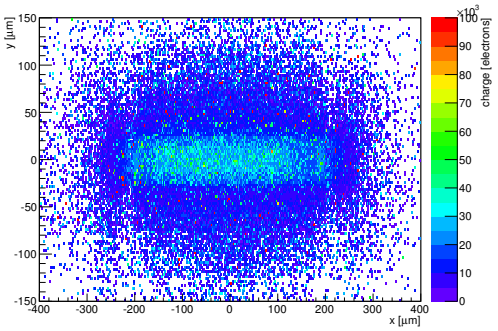

(s) Single pixel mean charge.

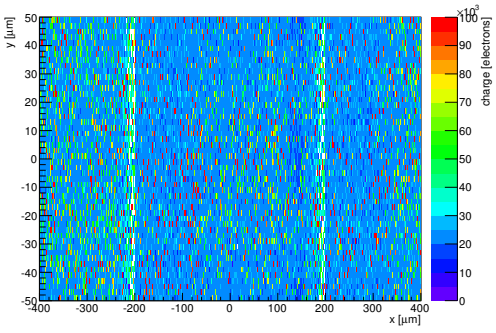

(t) Single pixel mean charge.

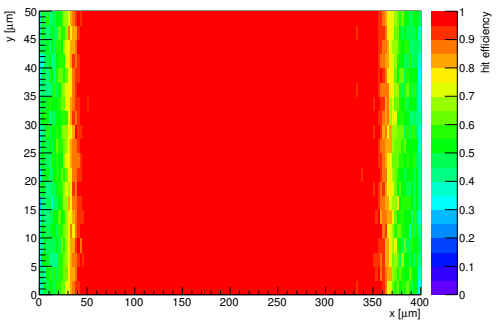

(u) Single pixel hit efficiency.

Figure C.171: Detailed plots for test beam measurement of DO-1 (description see section 6.1) sample (running as DUT0) during runs 883-907 in the May 2012 test beam period at CERN SPS in area H6B. Summary of the data in chapter 9.

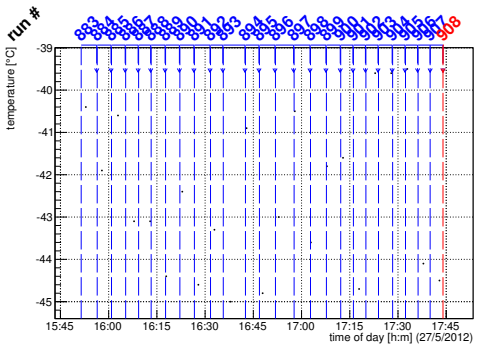

(a) Temperature vs time.

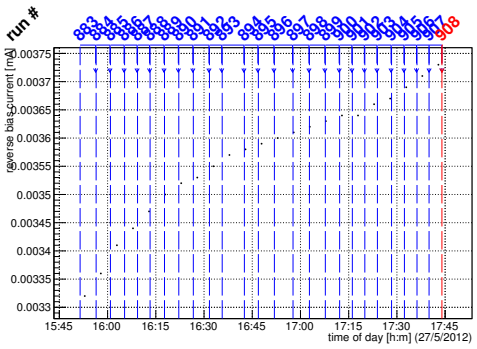

(b) Bias current vs time.

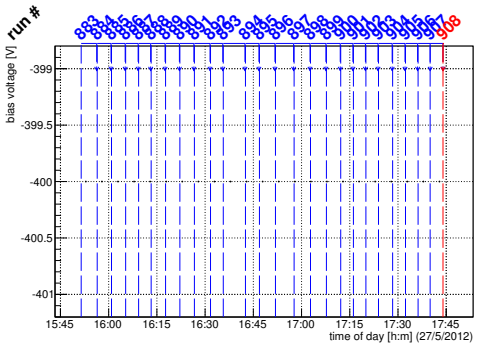

(c) Currently applied bias voltage vs time.

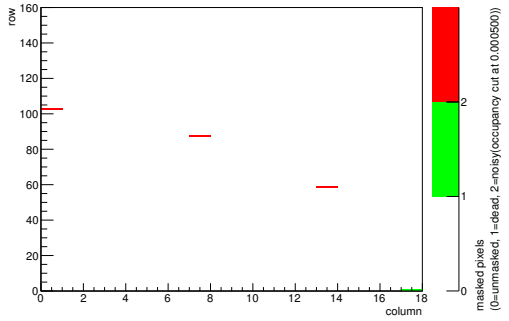

(d) Map of masked pixels.

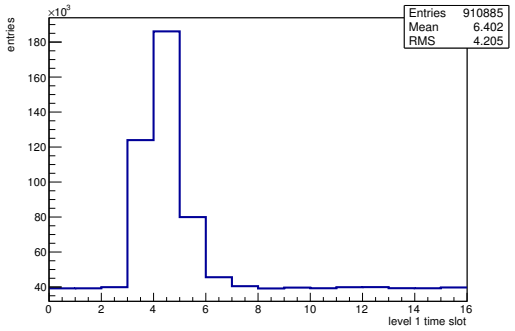

(e) Lvl1 distribution.

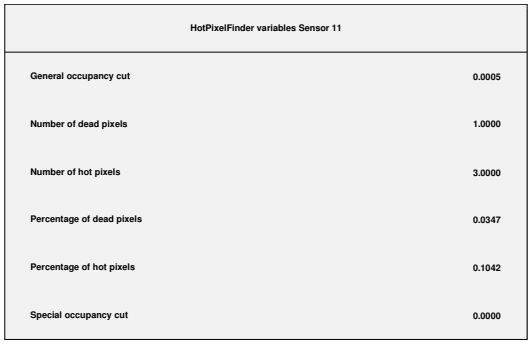

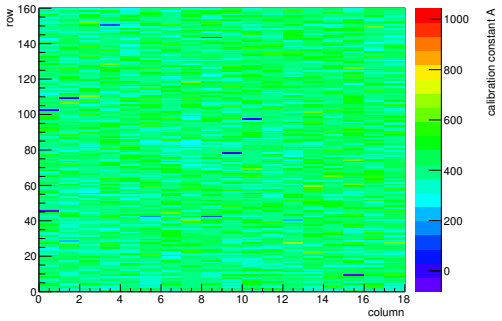

(f) Calibration constant A.

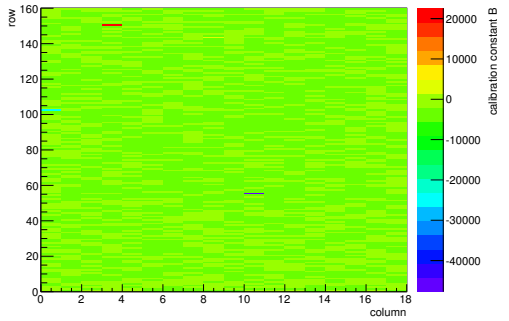

(g) Calibration constant B.

Figure C.172: Detailed plots for test beam measurement of DO-10 (description see section 6.1) sample (running as DUT1) during runs 883-907 in the May 2012 test beam period at CERN SPS in area H6B. Summary of the data in chapter 9. *(cont.)*

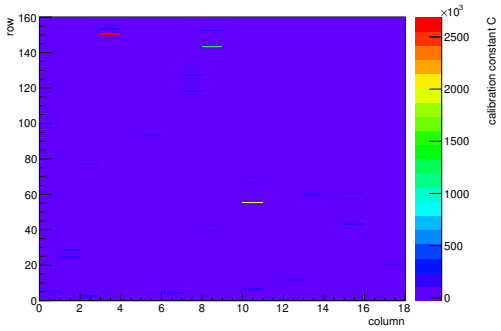

(h) Calibration constant C.

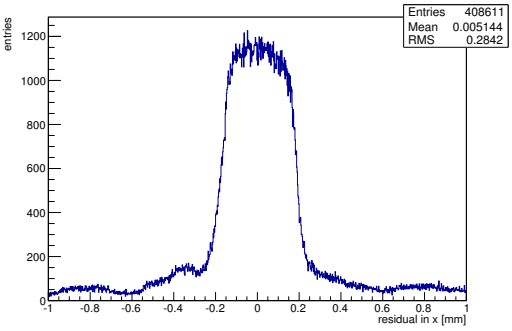

(i) Track residual in x.

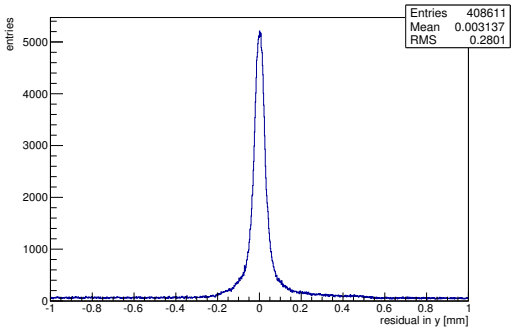

(j) Track residual in y.

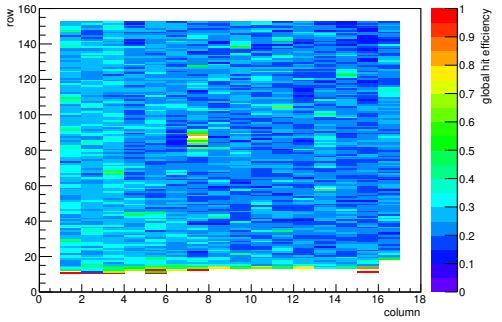

(k) Hit efficiency map.

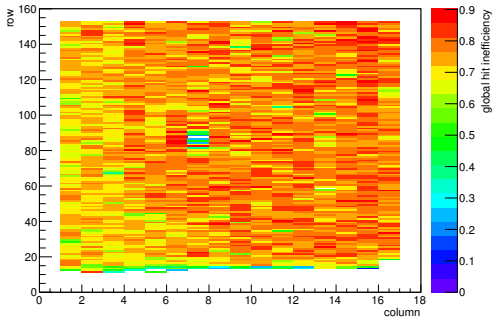

(l) Hit inefficiency map.

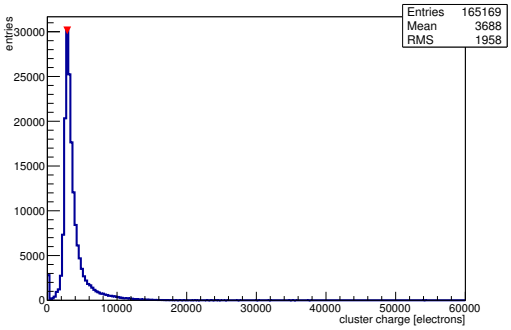

(m) Charge distribution (all cluster sizes included).

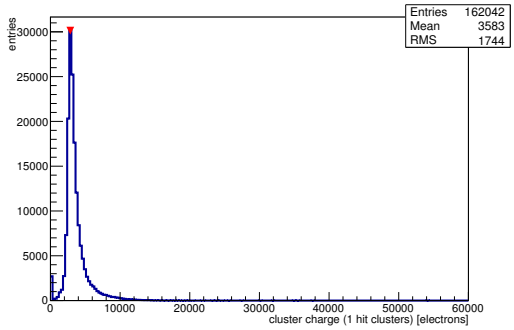

(n) Charge distribution (1 hit cluster).

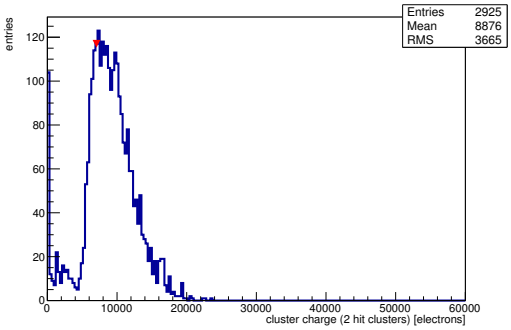

(o) Charge distribution (2 hit cluster).

Figure C.172: Detailed plots for test beam measurement of DO-10 (description see section 6.1) sample (running as DUT1) during runs 883-907 in the May 2012 test beam period at CERN SPS in area H6B. Summary of the data in chapter 9. *(cont.)*

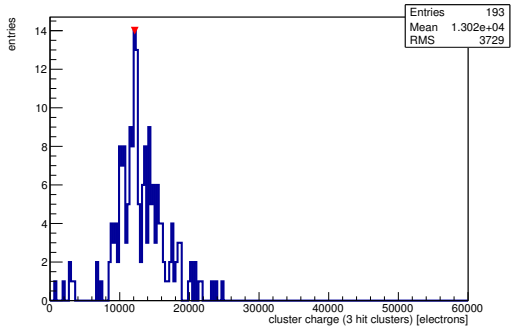

(p) Charge distribution (3 hit cluster).

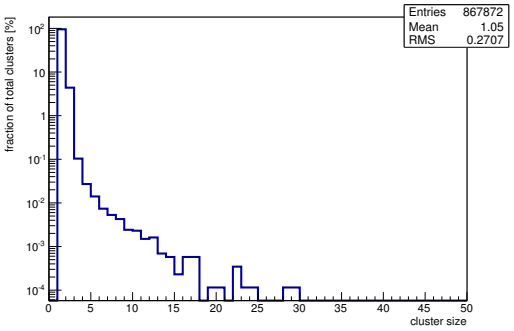

(q) Cluster size distribution.

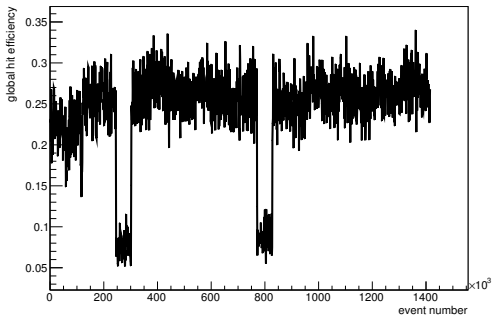

(r) Hit efficiency vs event number.

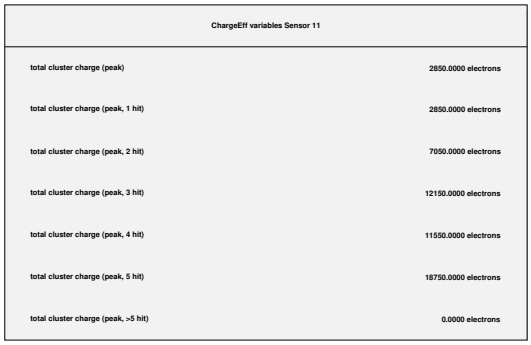

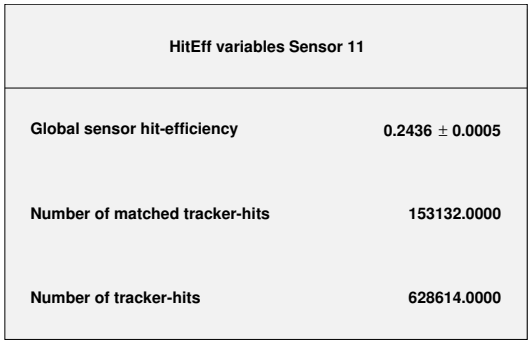

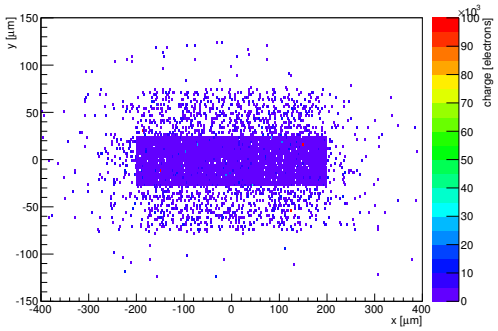

(s) Single pixel mean charge.

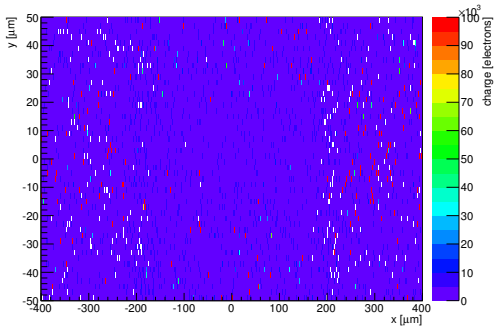

(t) Single pixel mean charge.

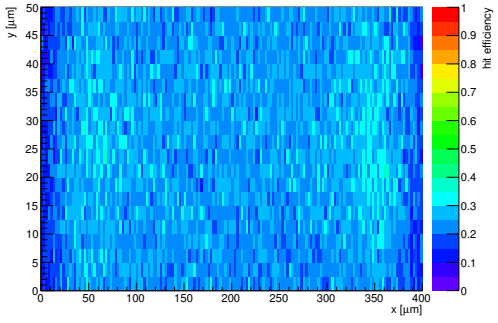

(u) Single pixel hit efficiency.

Figure C.172: Detailed plots for test beam measurement of DO-10 (description see section 6.1) sample (running as DUT1) during runs 883-907 in the May 2012 test beam period at CERN SPS in area H6B. Summary of the data in chapter 9.

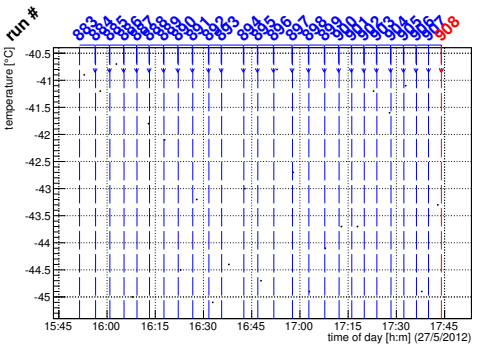

(a) Temperature vs time.

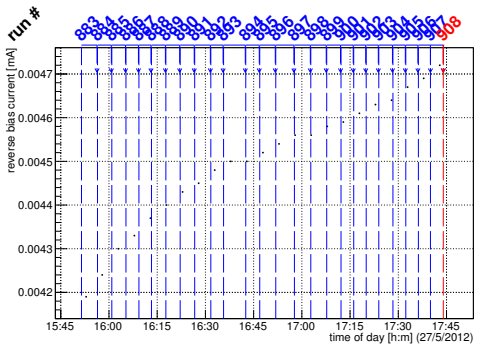

(b) Bias current vs time.

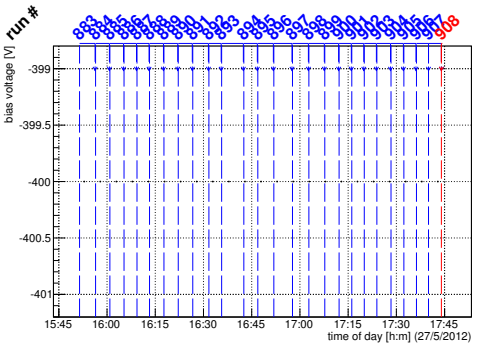

(c) Currently applied bias voltage vs time.

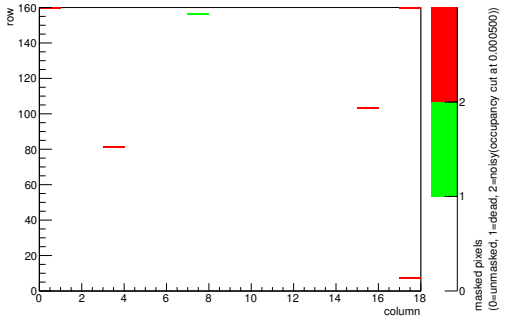

(d) Map of masked pixels.

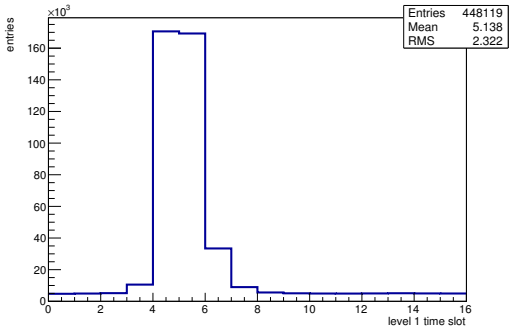

(e) Lvl1 distribution.

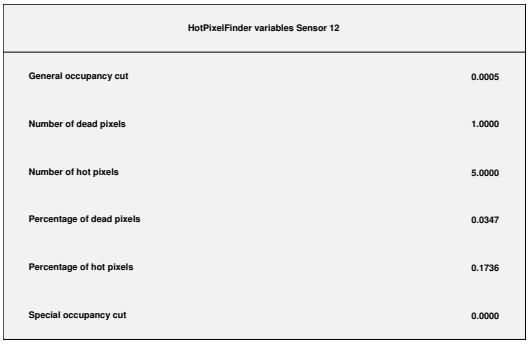

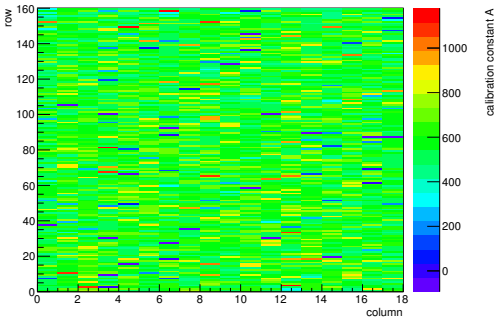

(f) Calibration constant A.

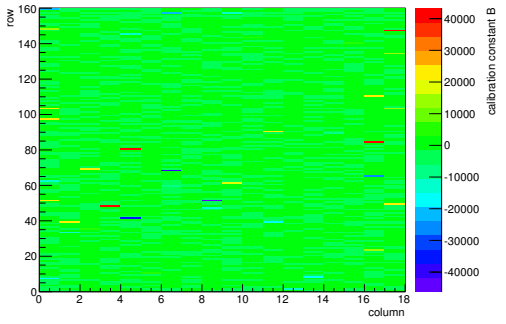

(g) Calibration constant B.

Figure C.173: Detailed plots for test beam measurement of DO-24 (description see section 6.1) sample (running as DUT2) during runs 883-907 in the May 2012 test beam period at CERN SPS in area H6B. Summary of the data in chapter 9. *(cont.)*

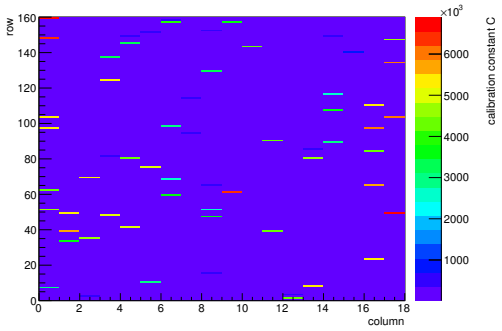

(h) Calibration constant C.

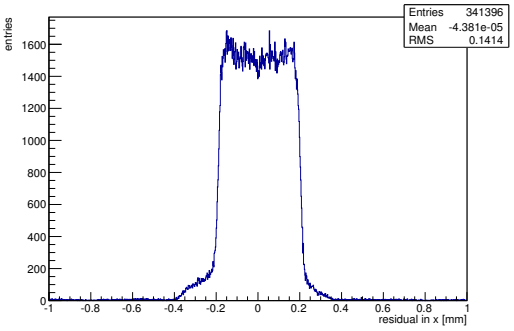

(i) Track residual in x.

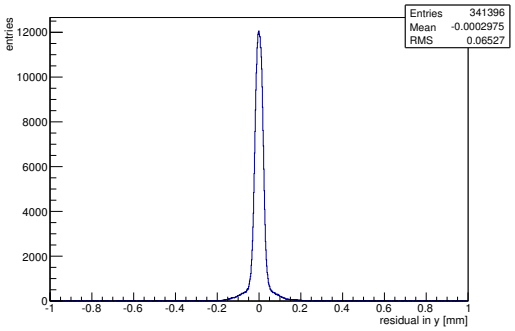

(j) Track residual in y.

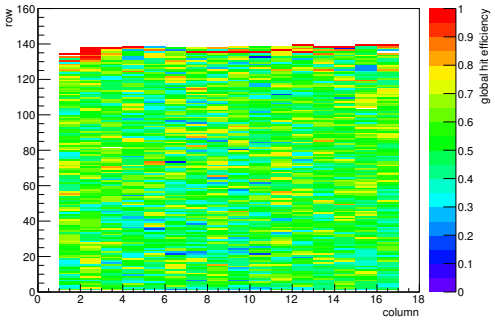

(k) Hit efficiency map.

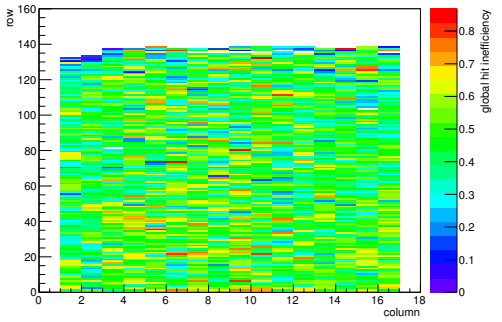

(l) Hit inefficiency map.

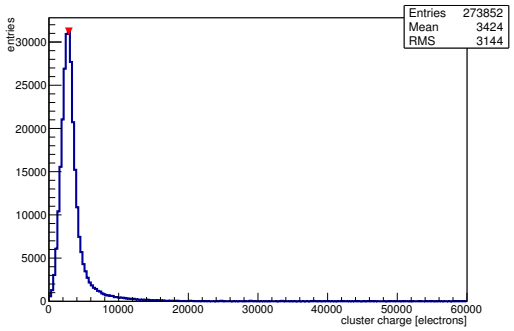

(m) Charge distribution (all cluster sizes included).

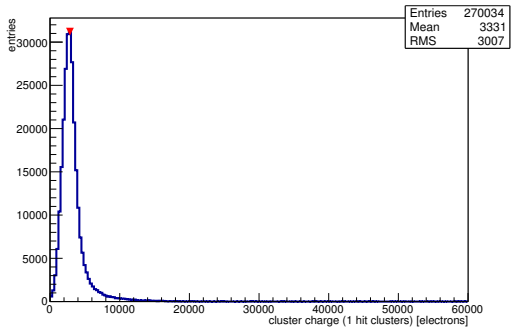

(n) Charge distribution (1 hit cluster).

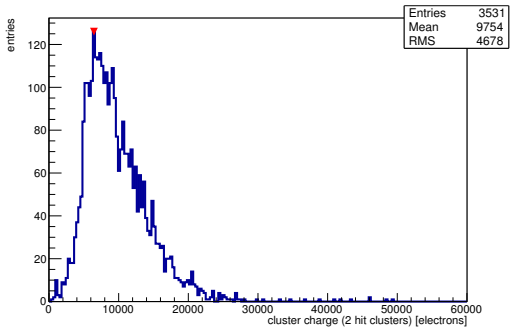

(o) Charge distribution (2 hit cluster).

Figure C.173: Detailed plots for test beam measurement of DO-24 (description see section 6.1) sample (running as DUT2) during runs 883-907 in the May 2012 test beam period at CERN SPS in area H6B. Summary of the data in chapter 9. *(cont.)*

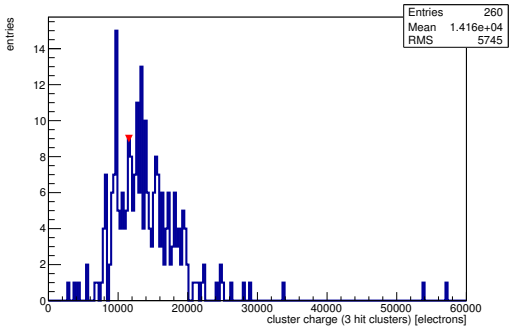

(p) Charge distribution (3 hit cluster).

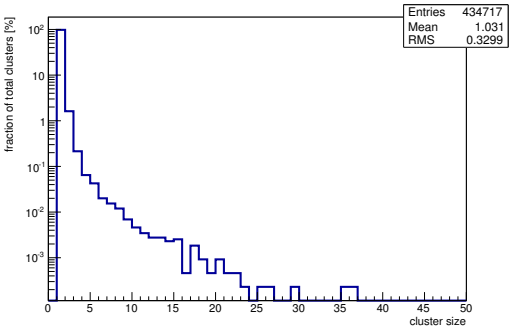

(q) Cluster size distribution.

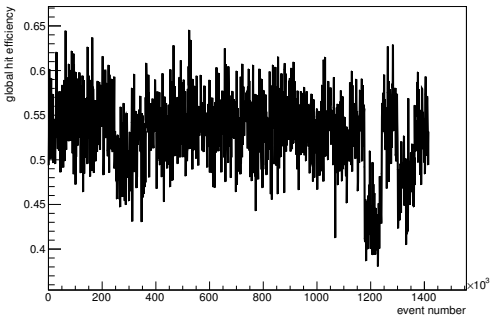

(r) Hit efficiency vs event number.

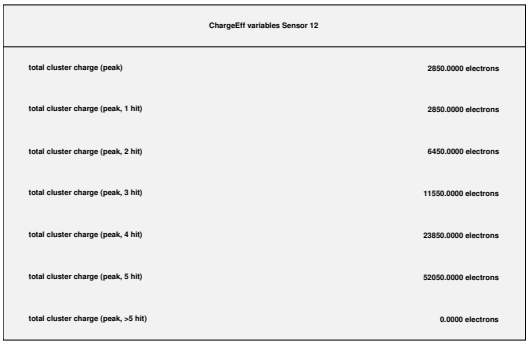

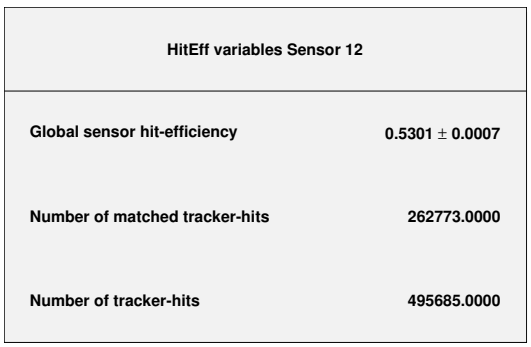

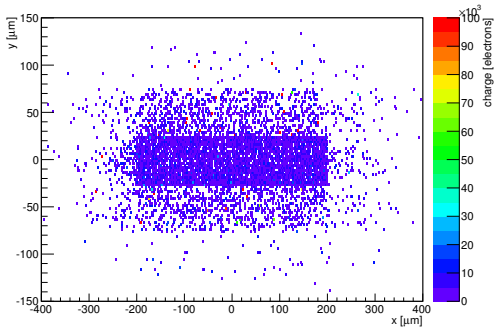

(s) Single pixel mean charge.

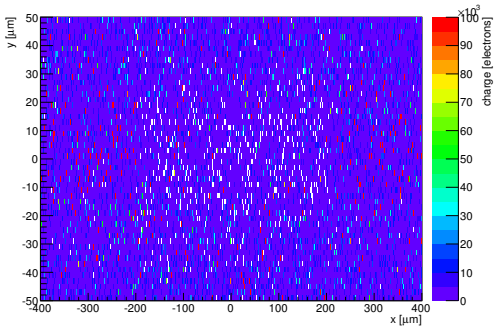

(t) Single pixel mean charge.

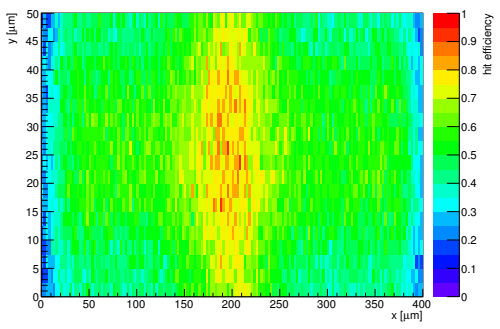

(u) Single pixel hit efficiency.

Figure C.173: Detailed plots for test beam measurement of DO-24 (description see section 6.1) sample (running as DUT2) during runs 883-907 in the May 2012 test beam period at CERN SPS in area H6B. Summary of the data in chapter 9.

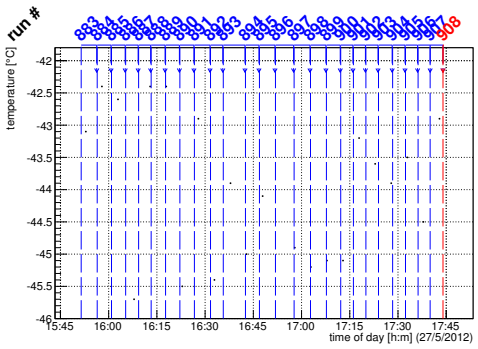

(a) Temperature vs time.

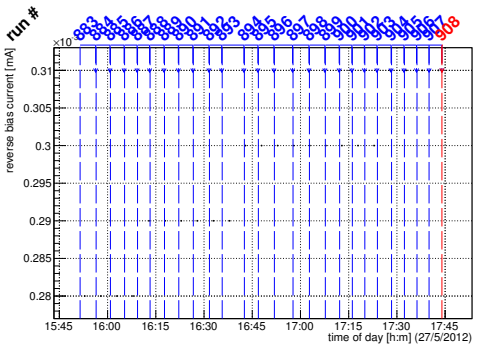

(b) Bias current vs time.

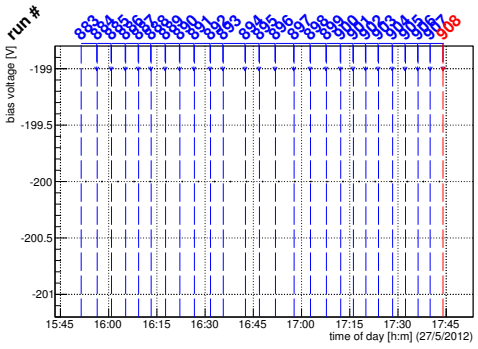

(c) Currently applied bias voltage vs time.

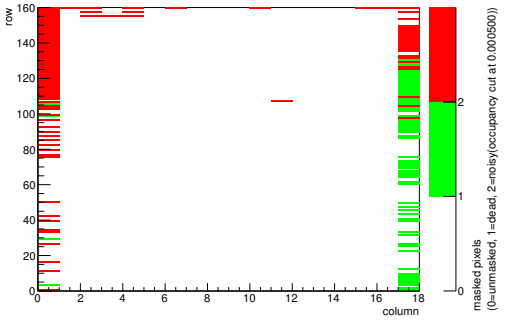

(d) Map of masked pixels.

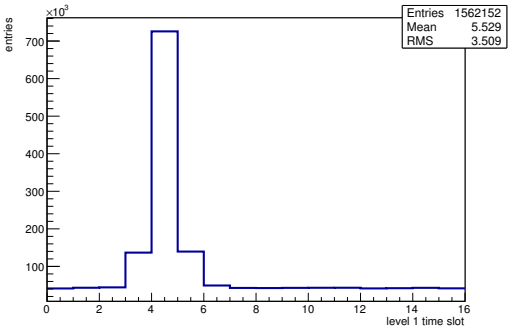

(e) Lvl1 distribution.

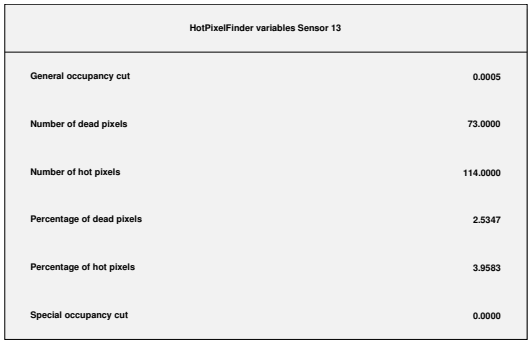

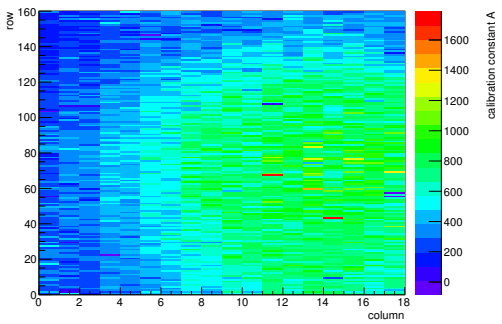

(f) Calibration constant A.

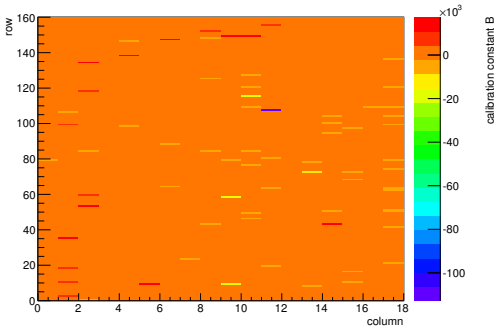

(g) Calibration constant B.

Figure C.174: Detailed plots for test beam measurement of DO-38 (description see section 6.1) sample (running as DUT3) during runs 883-907 in the May 2012 test beam period at CERN SPS in area H6B. Summary of the data in chapter 9. *(cont.)*

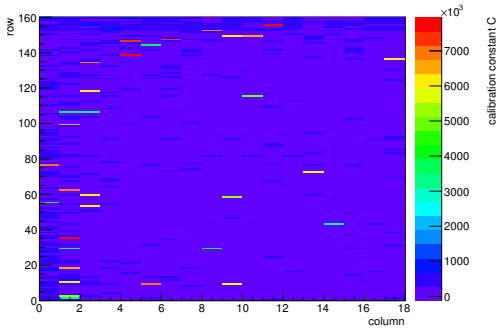

(h) Calibration constant C.

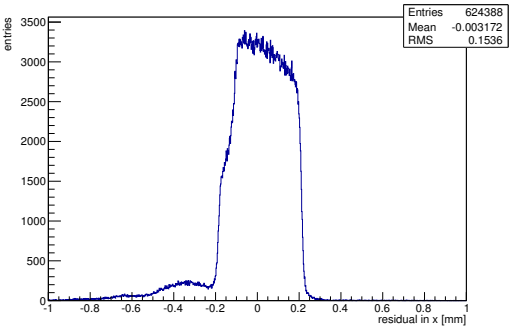

(i) Track residual in x.

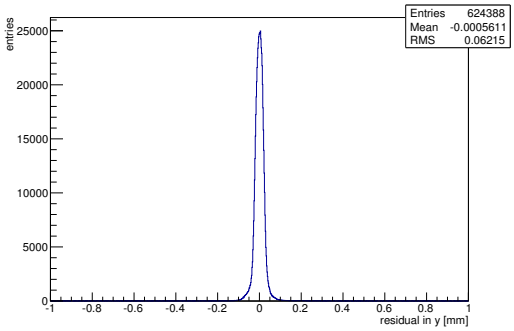

(j) Track residual in y.

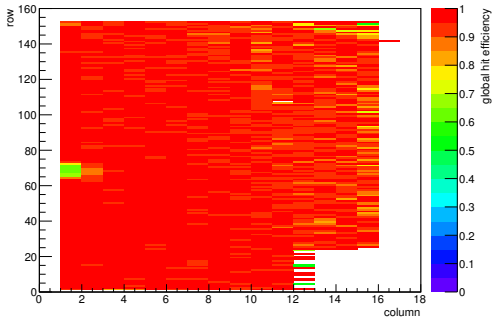

(k) Hit efficiency map.

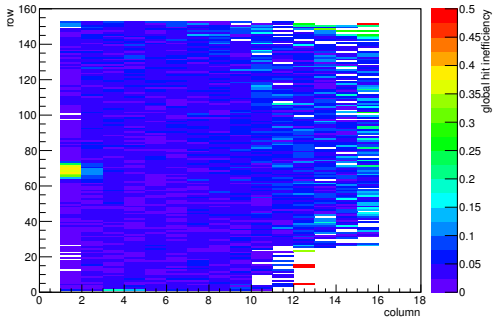

(l) Hit inefficiency map.

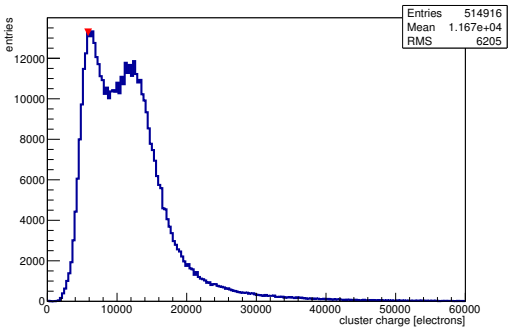

(m) Charge distribution (all cluster sizes included).

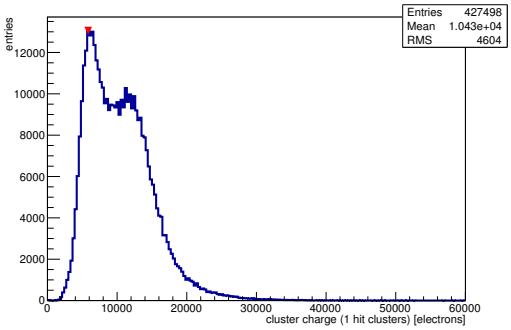

(n) Charge distribution (1 hit cluster).

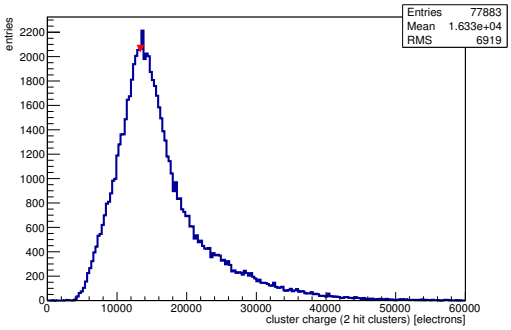

(o) Charge distribution (2 hit cluster).

Figure C.174: Detailed plots for test beam measurement of DO-38 (description see section 6.1) sample (running as DUT3) during runs 883-907 in the May 2012 test beam period at CERN SPS in area H6B. Summary of the data in chapter 9. *(cont.)*

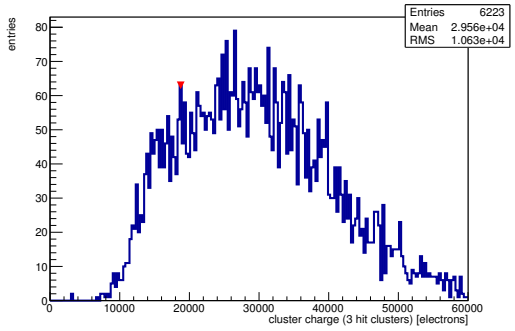

(p) Charge distribution (3 hit cluster).

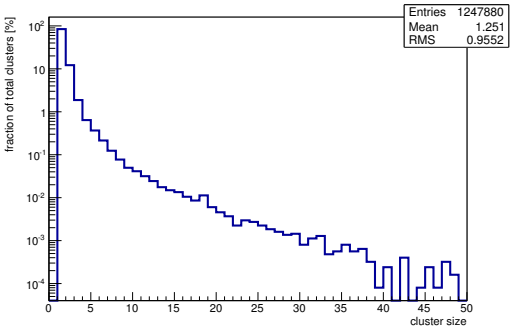

(q) Cluster size distribution.

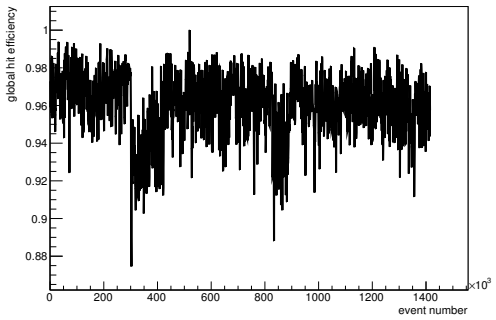

(r) Hit efficiency vs event number.

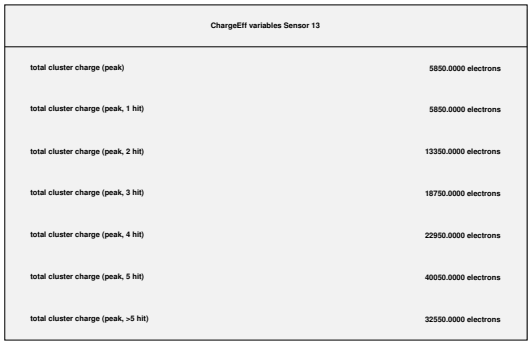

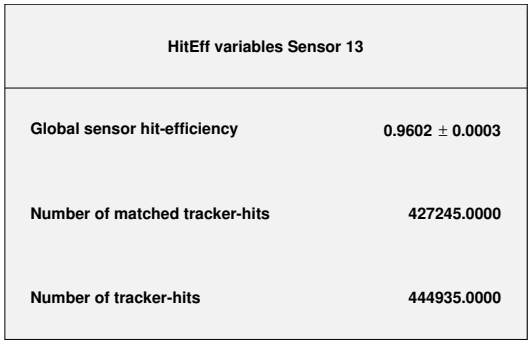

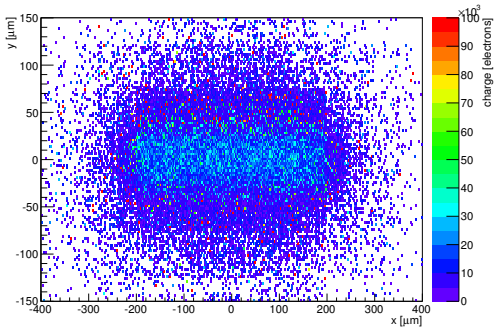

(s) Single pixel mean charge.

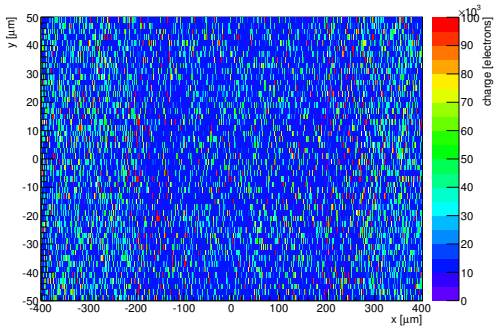

(t) Single pixel mean charge.

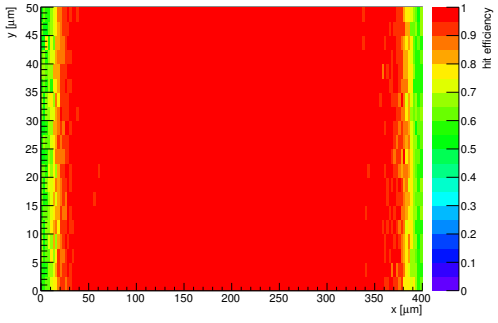

(u) Single pixel hit efficiency.

Figure C.174: Detailed plots for test beam measurement of DO-38 (description see section 6.1) sample (running as DUT3) during runs 883-907 in the May 2012 test beam period at CERN SPS in area H6B. Summary of the data in chapter 9.

C.5.6 Runs 918-945

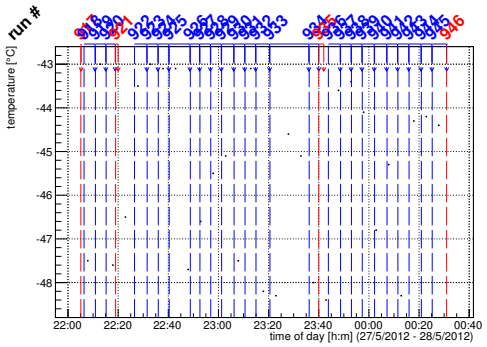

(a) Temperature vs time.

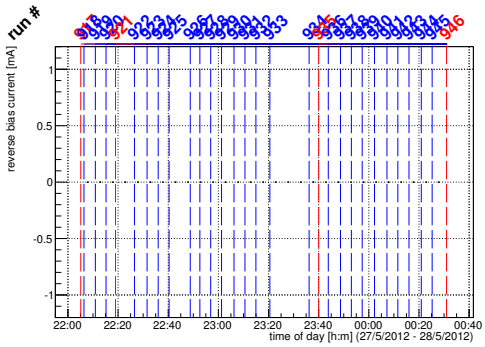

(b) Bias current vs time.

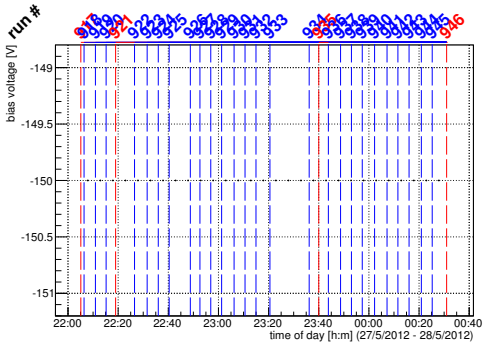

(c) Currently applied bias voltage vs time.

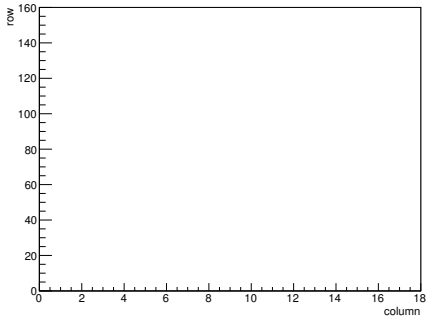

(d) Map of masked pixels.

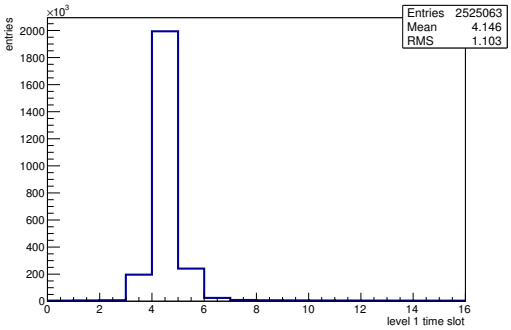

(e) Lvl1 distribution.

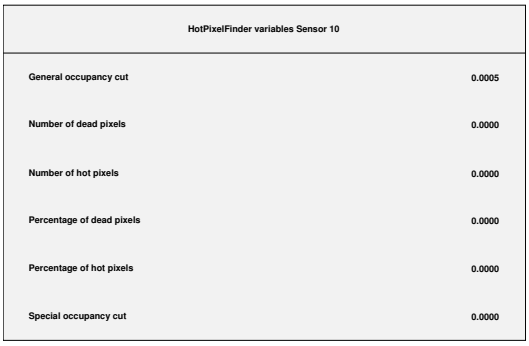

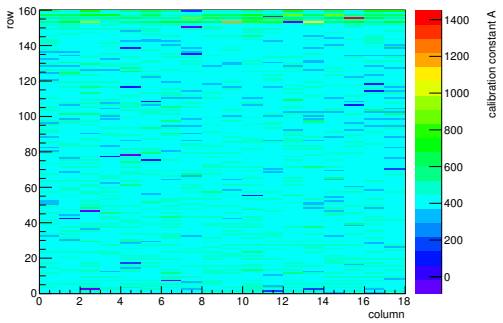

(f) Calibration constant A.

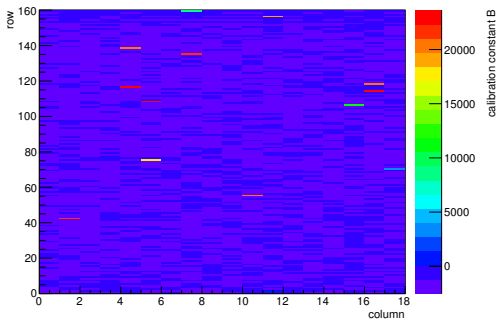

(g) Calibration constant B.

Figure C.175: Detailed plots for test beam measurement of DO-1 (description see section 6.1) sample (running as DUT0) during runs 918-945 in the May 2012 test beam period at CERN SPS in area H6B. Summary of the data in chapter 9. *(cont.)*

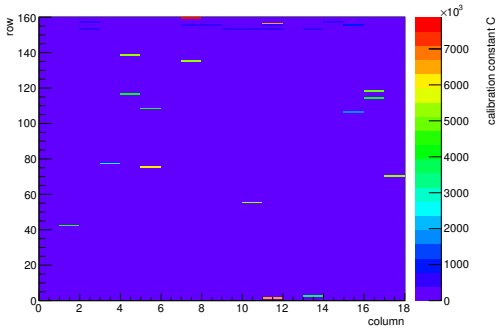

(h) Calibration constant C.

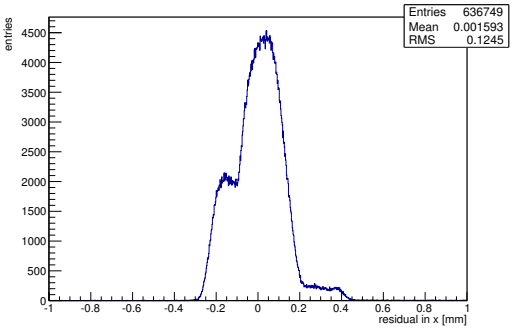

(i) Track residual in x.

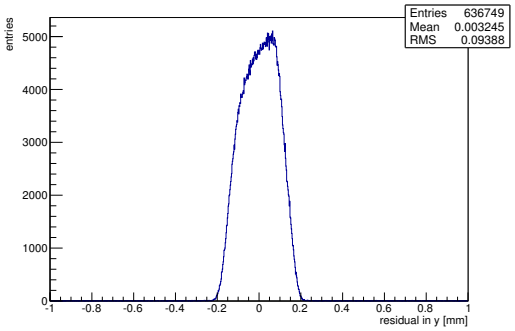

(j) Track residual in y.

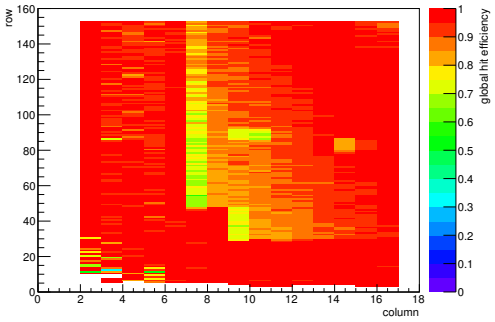

(k) Hit efficiency map.

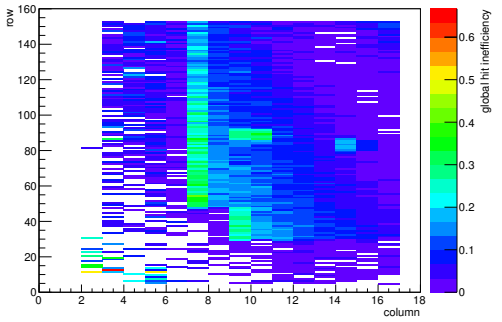

(l) Hit inefficiency map.

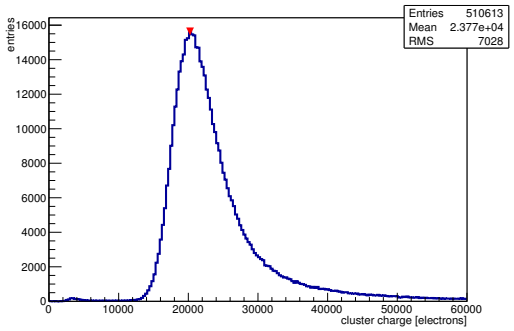

(m) Charge distribution (all cluster sizes included).

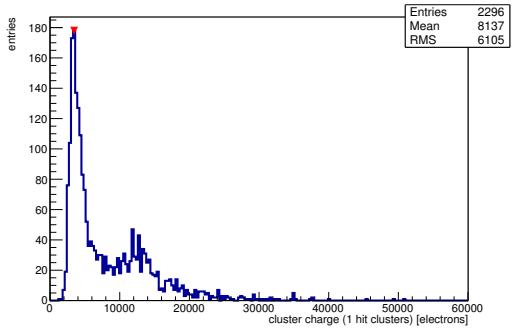

(n) Charge distribution (1 hit cluster).

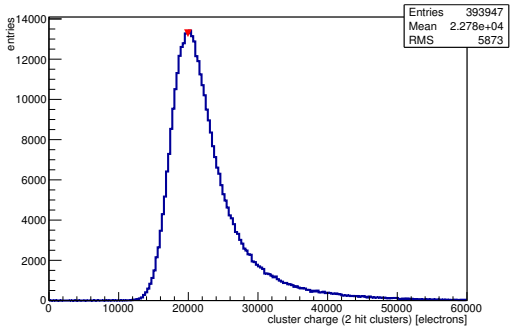

(o) Charge distribution (2 hit cluster).

Figure C.175: Detailed plots for test beam measurement of DO-1 (description see section 6.1) sample (running as DUT0) during runs 918-945 in the May 2012 test beam period at CERN SPS in area H6B. Summary of the data in chapter 9. *(cont.)*

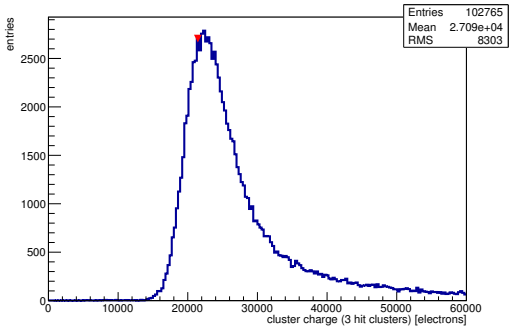

(p) Charge distribution (3 hit cluster).

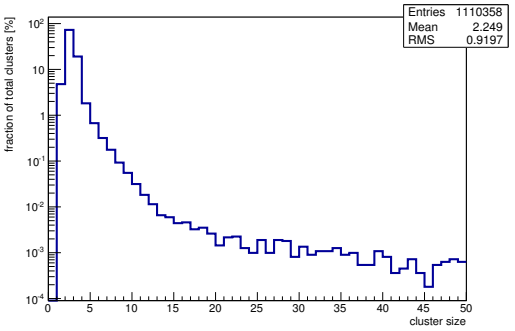

(q) Cluster size distribution.

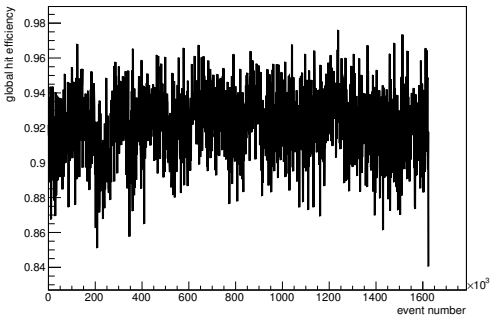

(r) Hit efficiency vs event number.

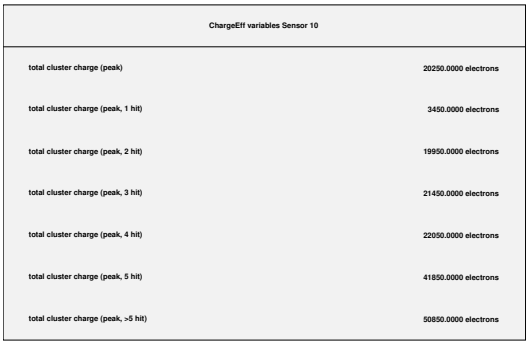

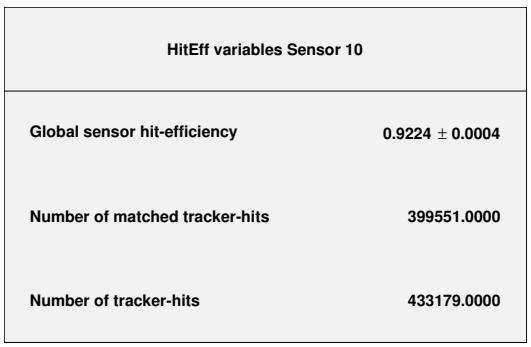

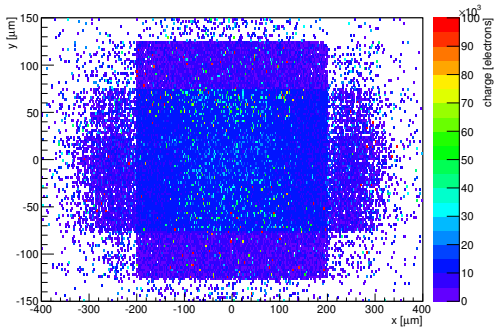

(s) Single pixel mean charge.

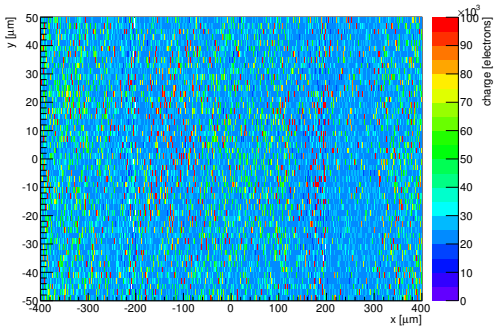

(t) Single pixel mean charge.

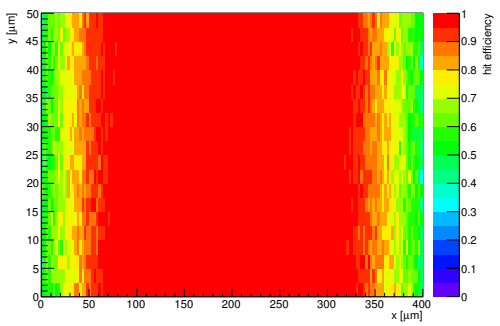

(u) Single pixel hit efficiency.

Figure C.175: Detailed plots for test beam measurement of DO-1 (description see section 6.1) sample (running as DUT0) during runs 918-945 in the May 2012 test beam period at CERN SPS in area H6B. Summary of the data in chapter 9.

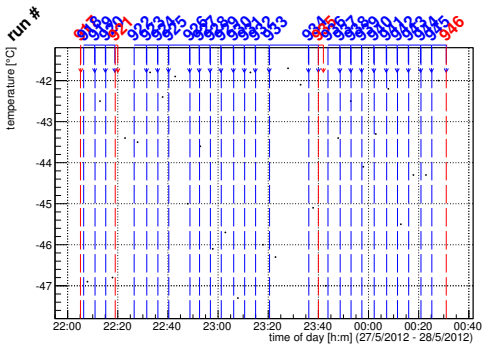

(a) Temperature vs time.

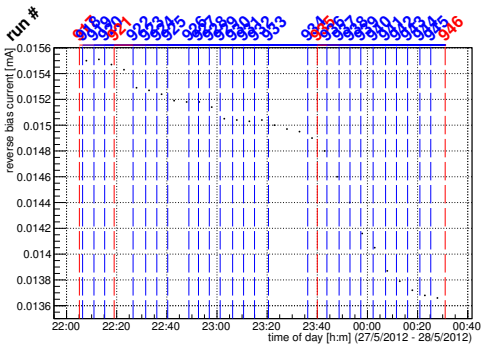

(b) Bias current vs time.

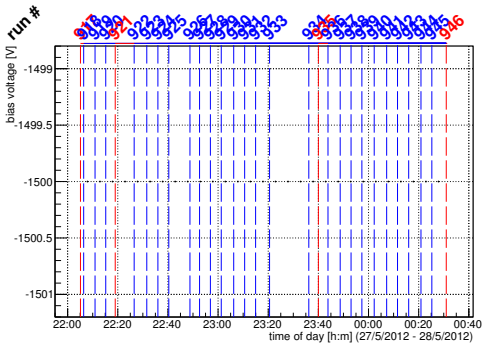

(c) Currently applied bias voltage vs time.

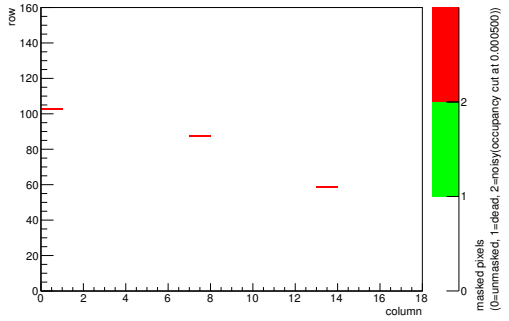

(d) Map of masked pixels.

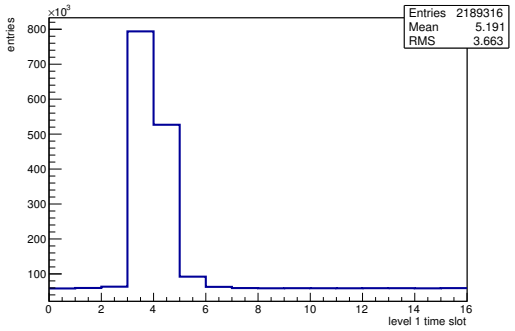

(e) Lvl1 distribution.

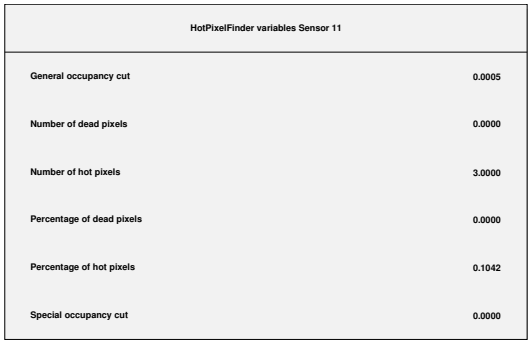

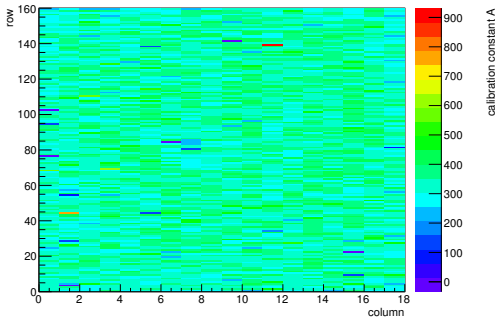

(f) Calibration constant A.

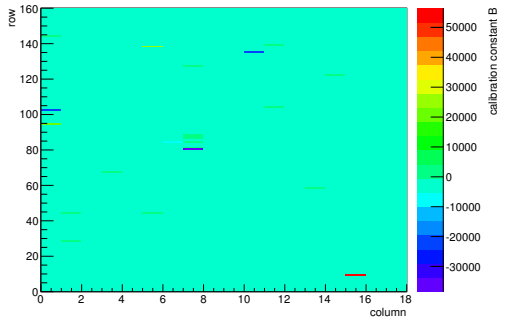

(g) Calibration constant B.

Figure C.176: Detailed plots for test beam measurement of DO-10 (description see section 6.1) sample (running as DUT1) during runs 918-945 in the May 2012 test beam period at CERN SPS in area H6B. Summary of the data in chapter 9. *(cont.)*

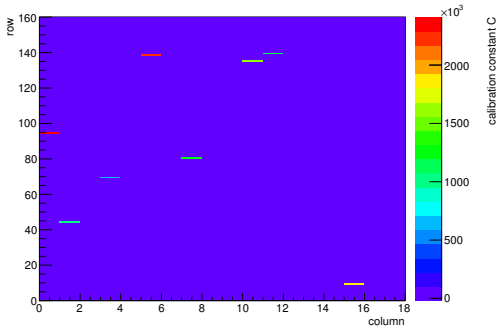

(h) Calibration constant C.

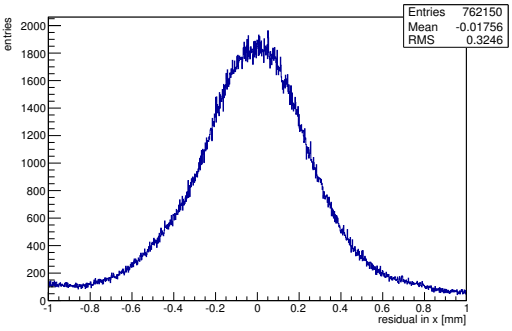

(i) Track residual in x.

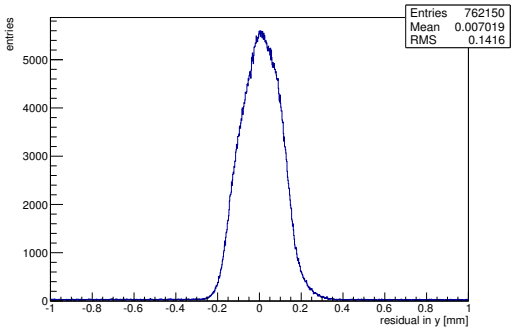

(j) Track residual in y.

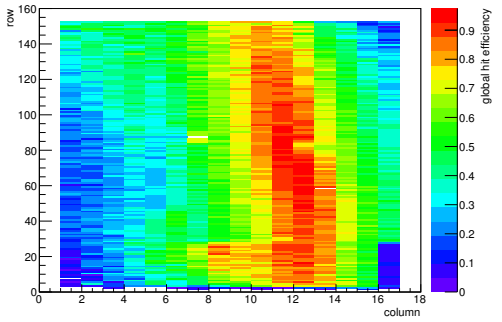

(k) Hit efficiency map.

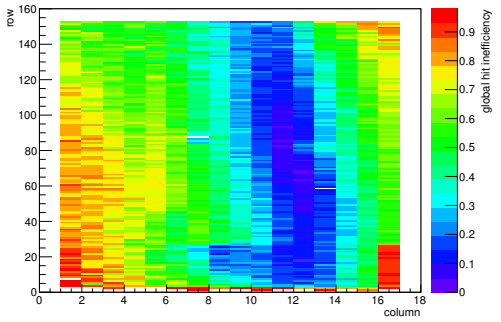

(l) Hit inefficiency map.

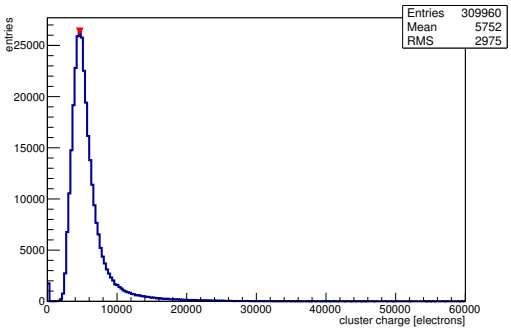

(m) Charge distribution (all cluster sizes included).

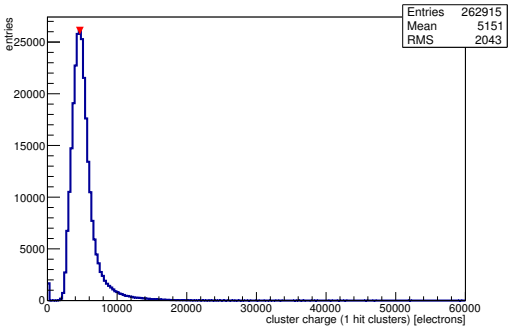

(n) Charge distribution (1 hit cluster).

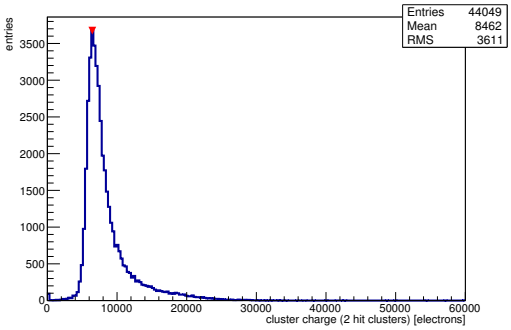

(o) Charge distribution (2 hit cluster).

Figure C.176: Detailed plots for test beam measurement of DO-10 (description see section 6.1) sample (running as DUT1) during runs 918-945 in the May 2012 test beam period at CERN SPS in area H6B. Summary of the data in chapter 9. *(cont.)*

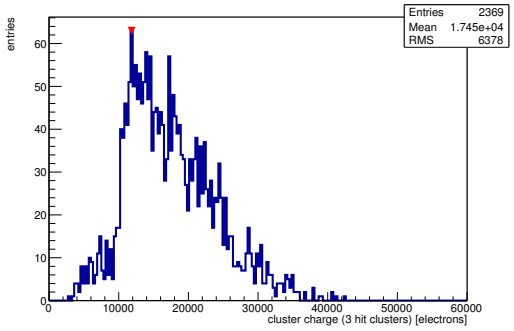

(p) Charge distribution (3 hit cluster).

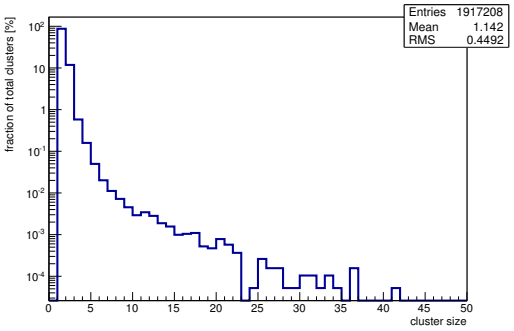

(q) Cluster size distribution.

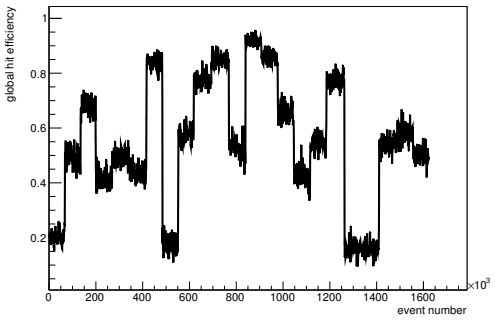

(r) Hit efficiency vs event number.

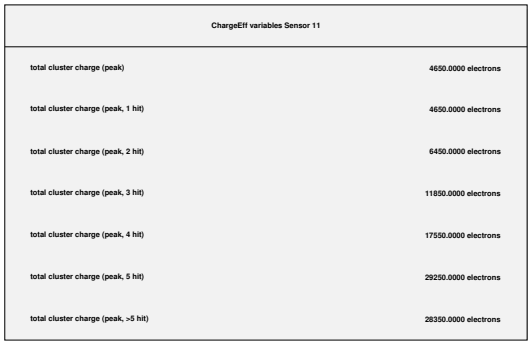

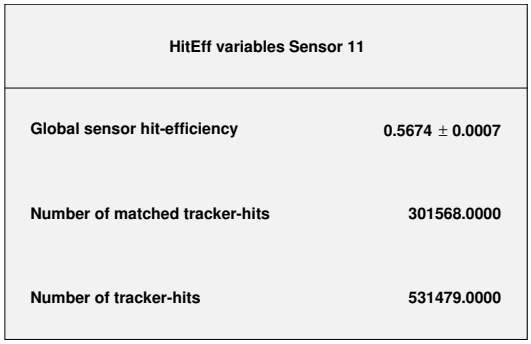

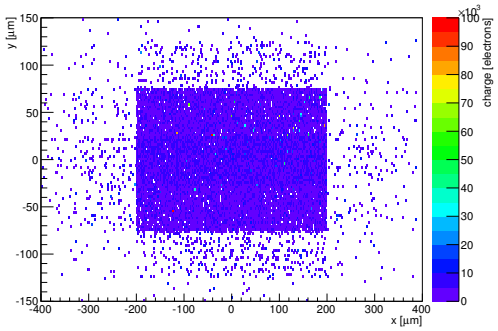

(s) Single pixel mean charge.

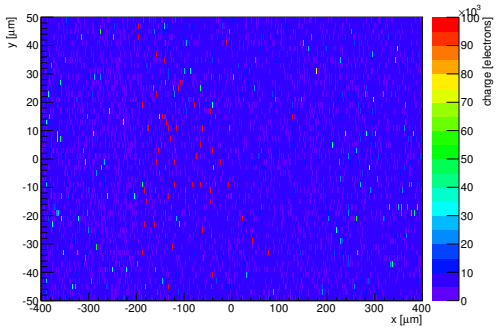

(t) Single pixel mean charge.

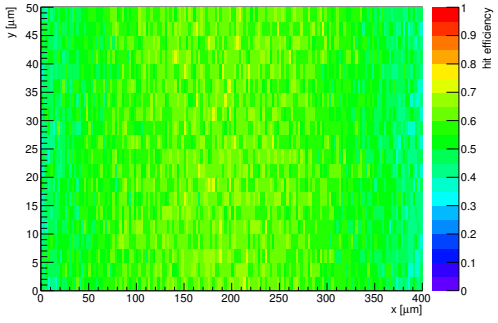

(u) Single pixel hit efficiency.

Figure C.176: Detailed plots for test beam measurement of DO-10 (description see section 6.1) sample (running as DUT1) during runs 918-945 in the May 2012 test beam period at CERN SPS in area H6B. Summary of the data in chapter 9.

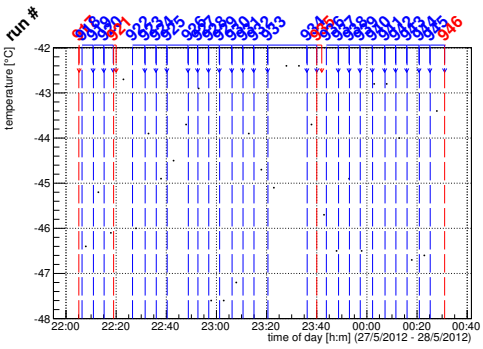

(a) Temperature vs time.

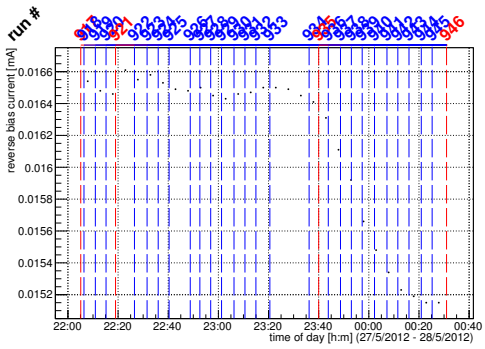

(b) Bias current vs time.

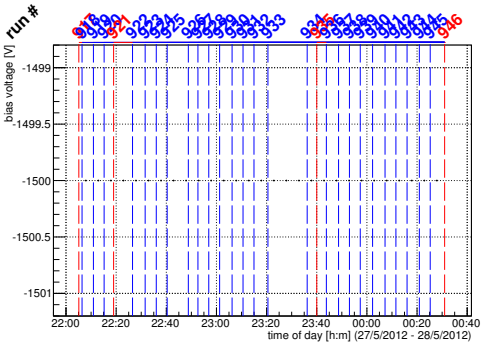

(c) Currently applied bias voltage vs time.

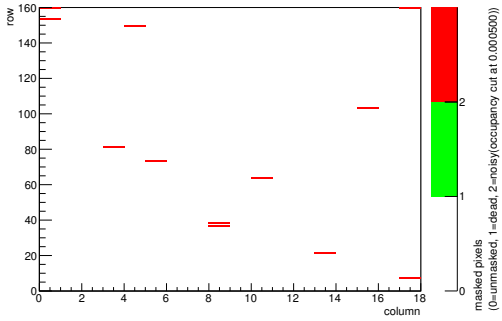

(d) Map of masked pixels.

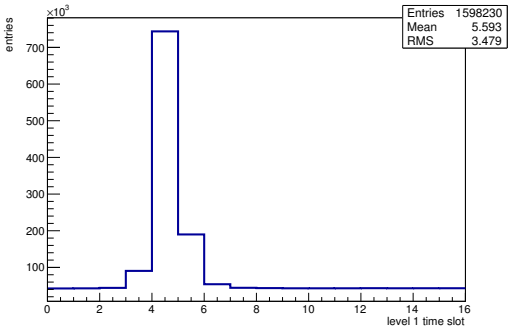

(e) Lvl1 distribution.

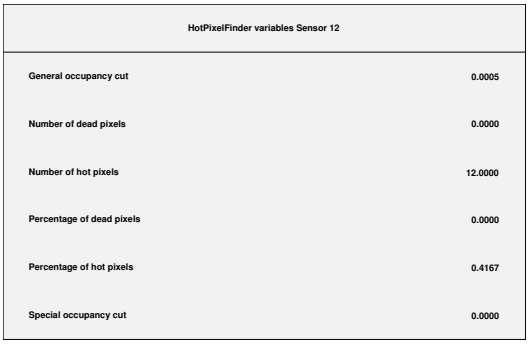

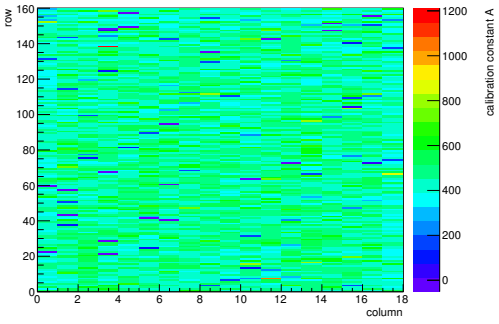

(f) Calibration constant A.

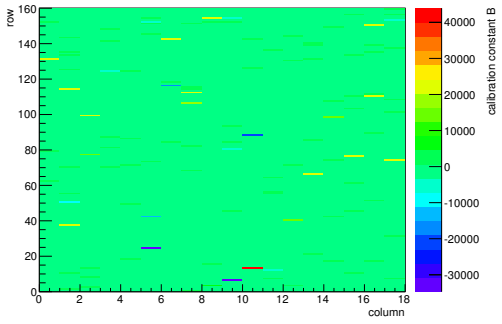

(g) Calibration constant B.

Figure C.177: Detailed plots for test beam measurement of DO-24 (description see section 6.1) sample (running as DUT2) during runs 918-945 in the May 2012 test beam period at CERN SPS in area H6B. Summary of the data in chapter 9. *(cont.)*

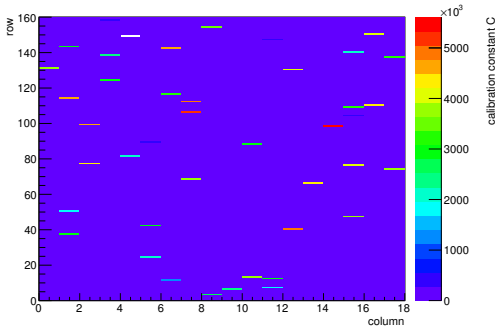

(h) Calibration constant C.

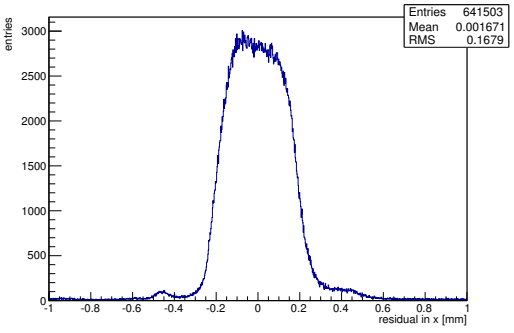

(i) Track residual in x.

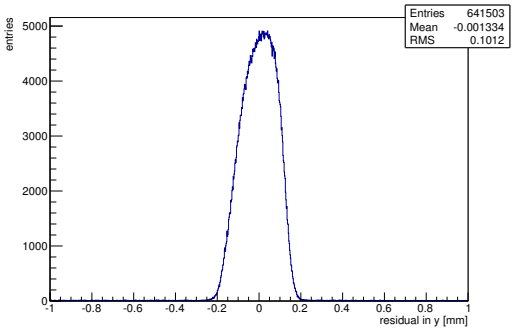

(j) Track residual in y.

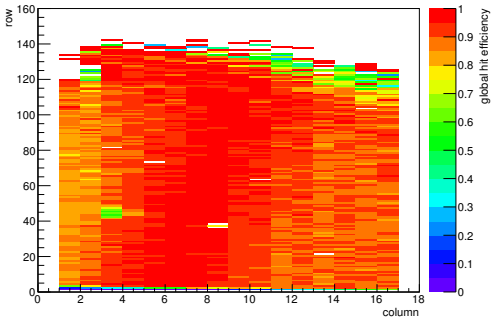

(k) Hit efficiency map.

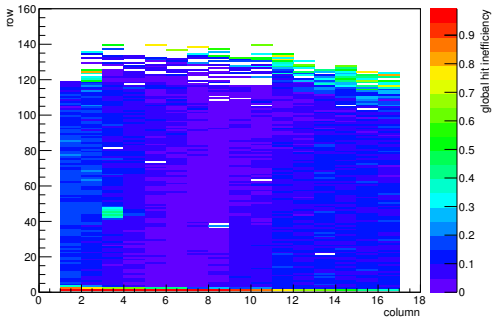

(l) Hit inefficiency map.

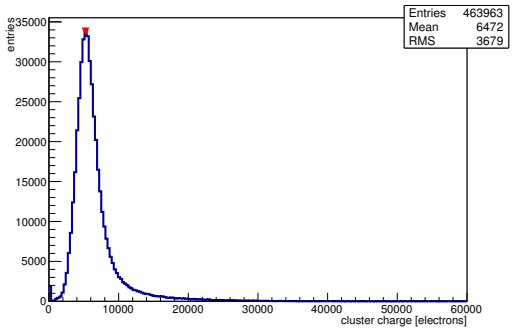

(m) Charge distribution (all cluster sizes included).

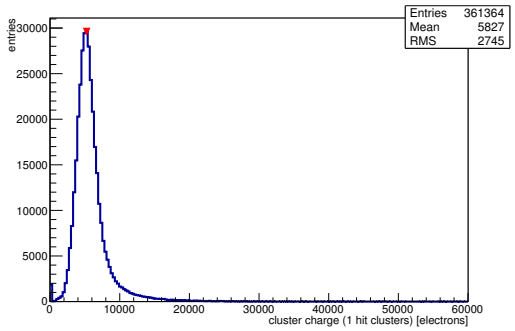

(n) Charge distribution (1 hit cluster).

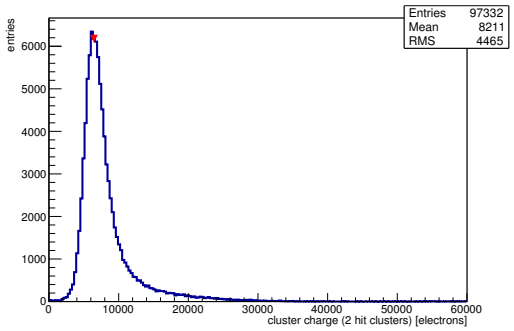

(o) Charge distribution (2 hit cluster).

Figure C.177: Detailed plots for test beam measurement of DO-24 (description see section 6.1) sample (running as DUT2) during runs 918-945 in the May 2012 test beam period at CERN SPS in area H6B. Summary of the data in chapter 9. *(cont.)*

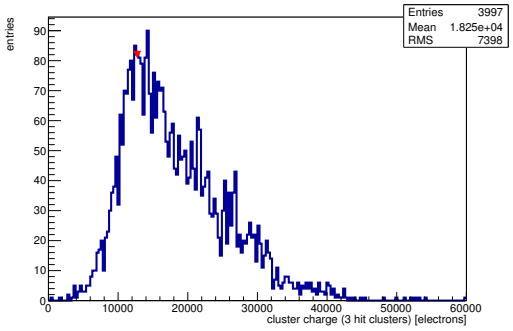

(p) Charge distribution (3 hit cluster).

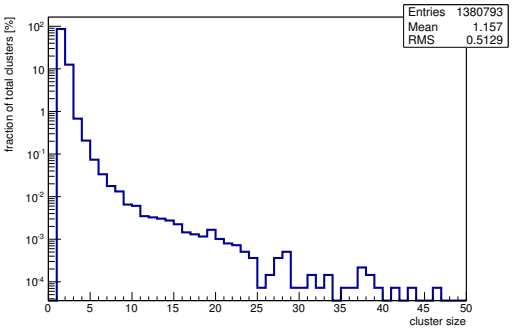

(q) Cluster size distribution.

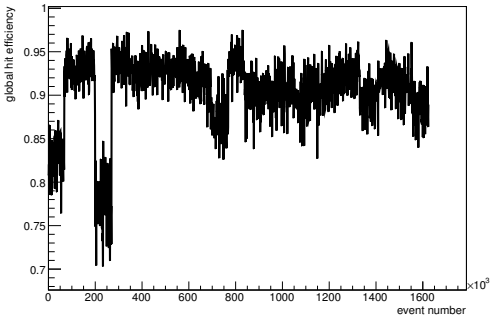

(r) Hit efficiency vs event number.

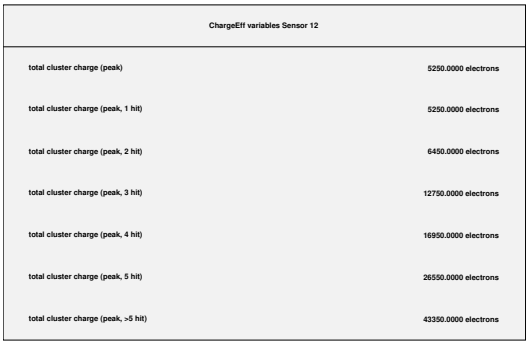

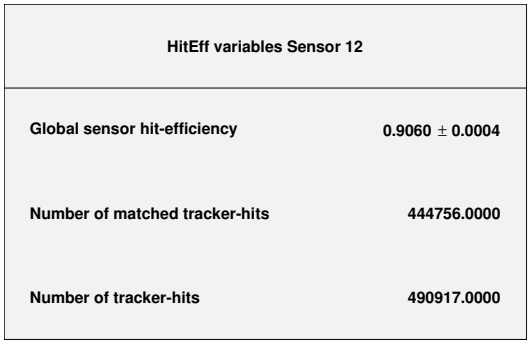

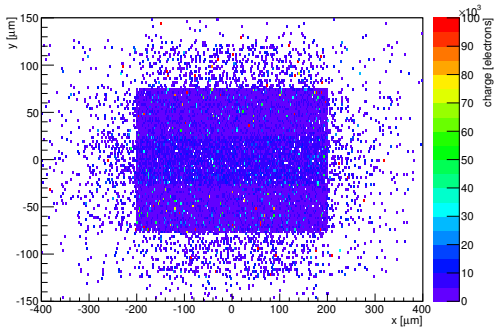

(s) Single pixel mean charge.

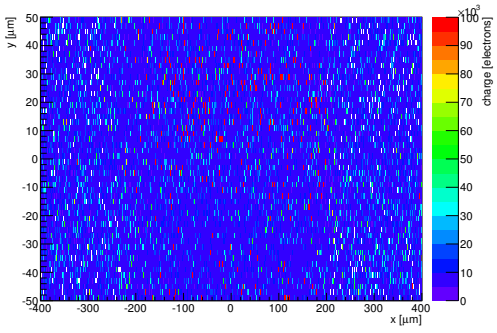

(t) Single pixel mean charge.

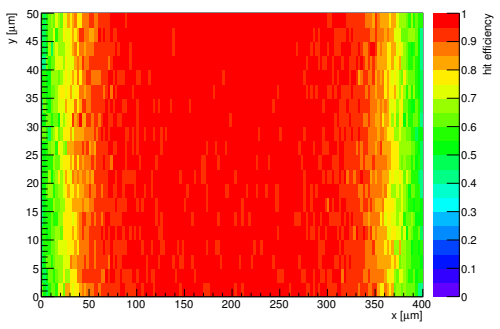

(u) Single pixel hit efficiency.

Figure C.177: Detailed plots for test beam measurement of DO-24 (description see section 6.1) sample (running as DUT2) during runs 918-945 in the May 2012 test beam period at CERN SPS in area H6B. Summary of the data in chapter 9.

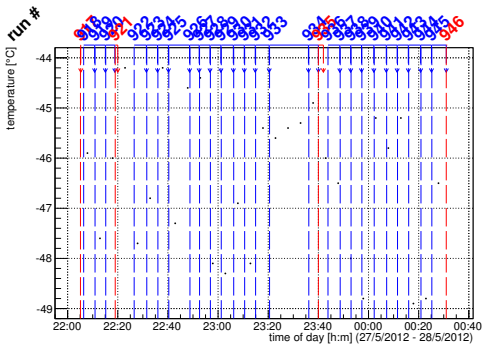

(a) Temperature vs time.

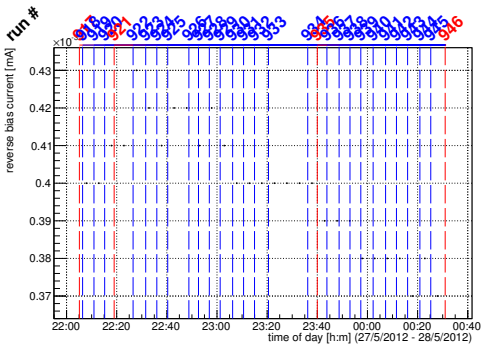

(b) Bias current vs time.

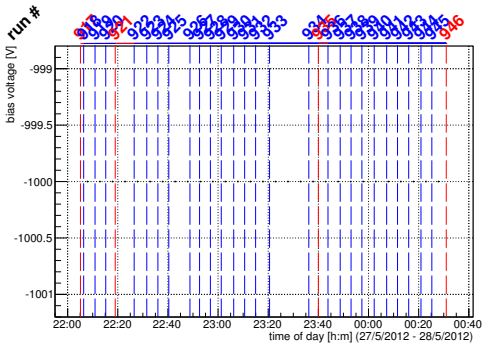

(c) Currently applied bias voltage vs time.

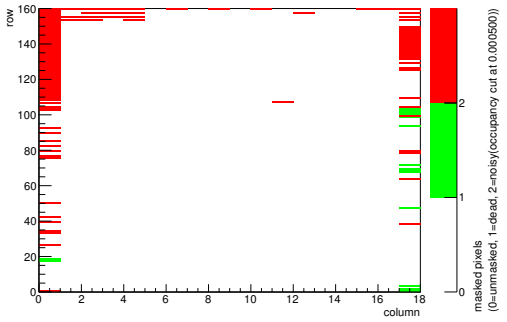

(d) Map of masked pixels.

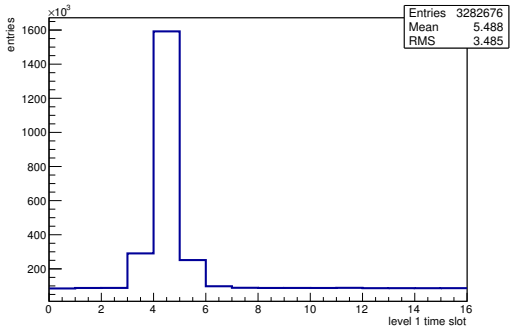

(e) Lvl1 distribution.

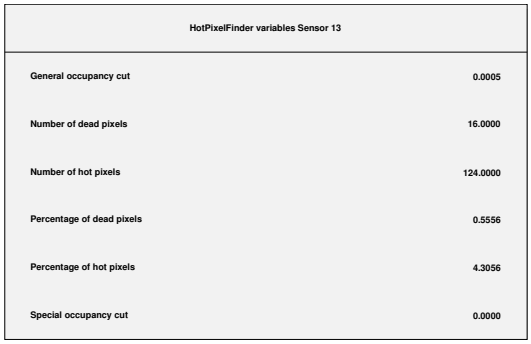

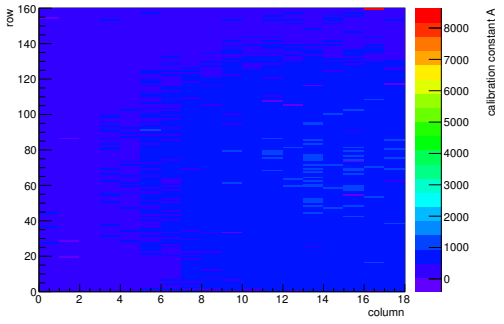

(f) Calibration constant A.

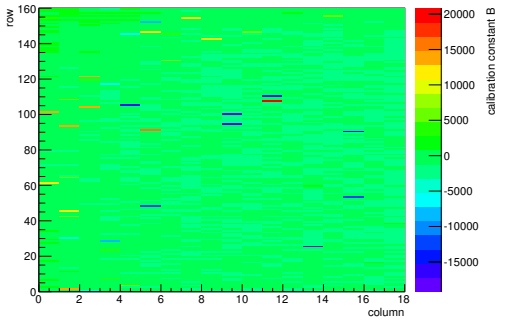

(g) Calibration constant B.

Figure C.178: Detailed plots for test beam measurement of DO-38 (description see section 6.1) sample (running as DUT3) during runs 918-945 in the May 2012 test beam period at CERN SPS in area H6B. Summary of the data in chapter 9. *(cont.)*

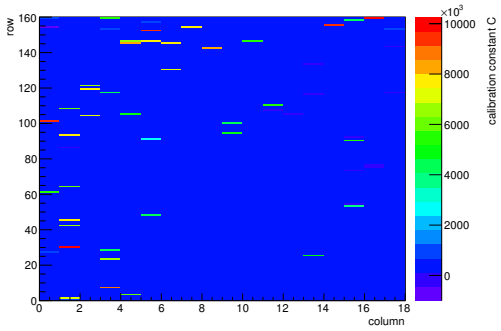

(h) Calibration constant C.

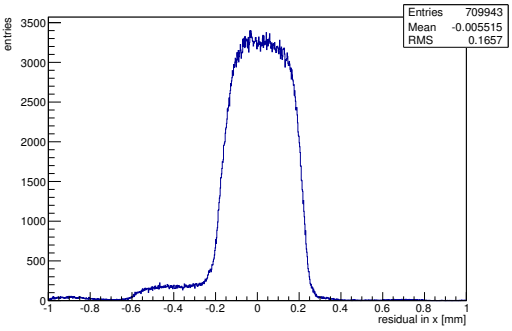

(i) Track residual in x.

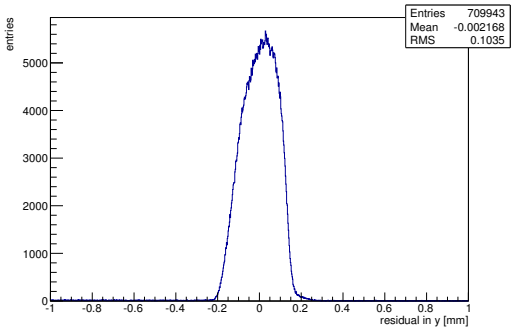

(j) Track residual in y.

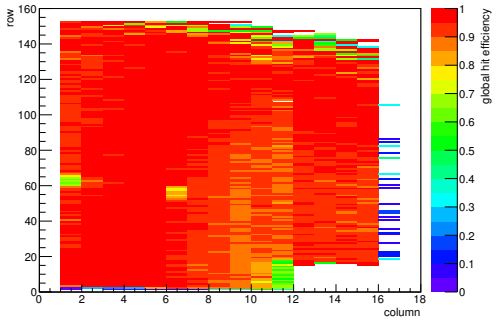

(k) Hit efficiency map.

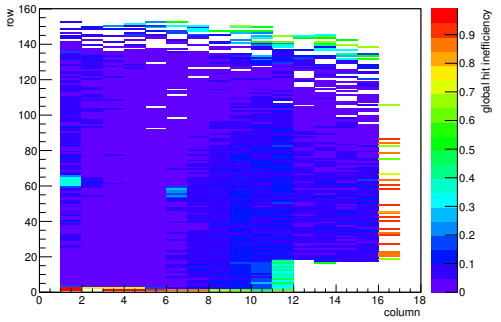

(l) Hit inefficiency map.

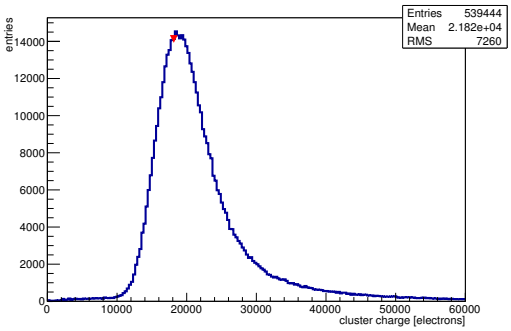

(m) Charge distribution (all cluster sizes included).

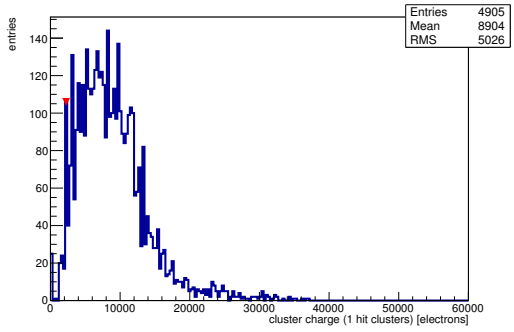

(n) Charge distribution (1 hit cluster).

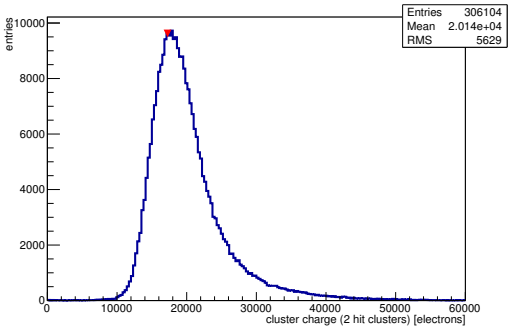

(o) Charge distribution (2 hit cluster).

Figure C.178: Detailed plots for test beam measurement of DO-38 (description see section 6.1) sample (running as DUT3) during runs 918-945 in the May 2012 test beam period at CERN SPS in area H6B. Summary of the data in chapter 9. *(cont.)*

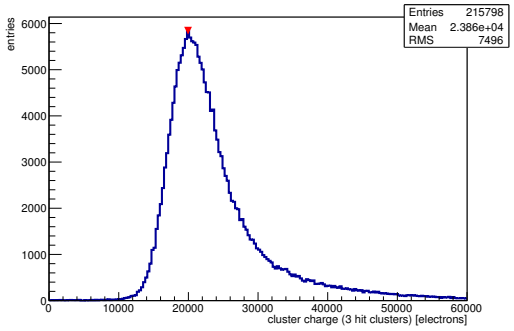

(p) Charge distribution (3 hit cluster).

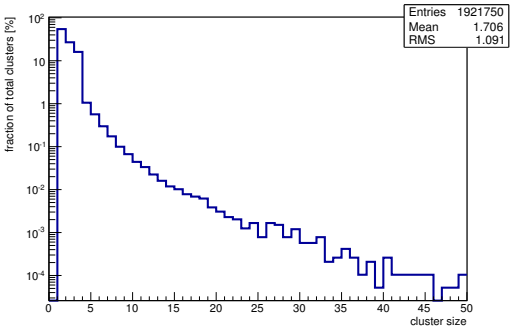

(q) Cluster size distribution.

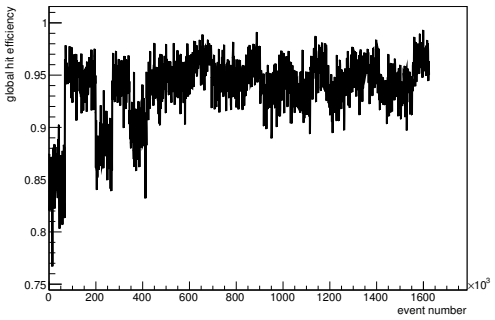

(r) Hit efficiency vs event number.

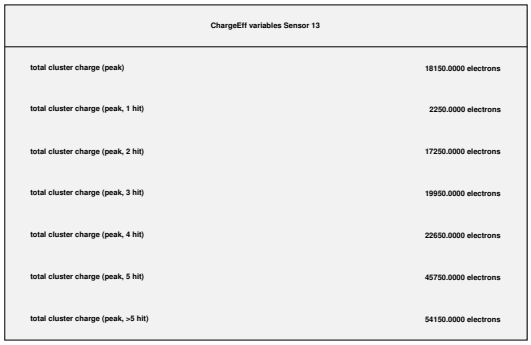

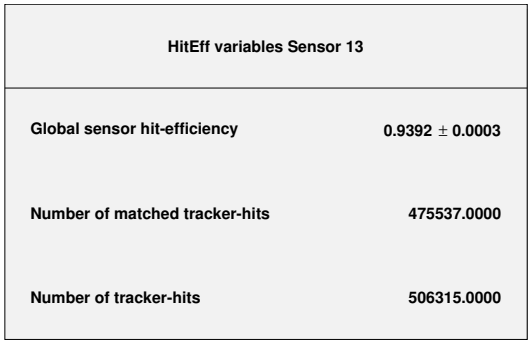

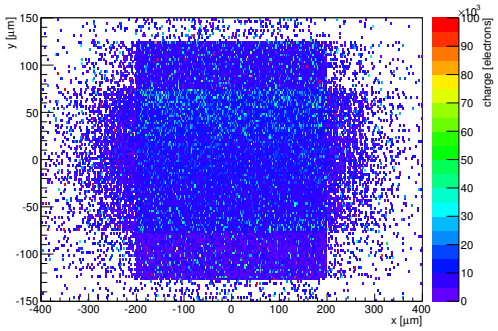

(s) Single pixel mean charge.

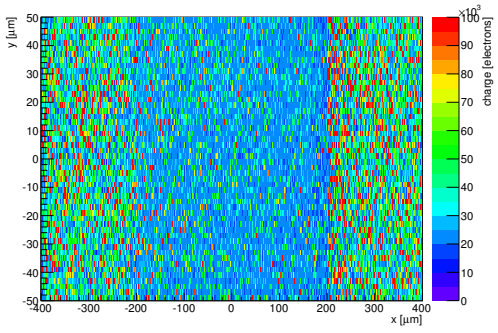

(t) Single pixel mean charge.

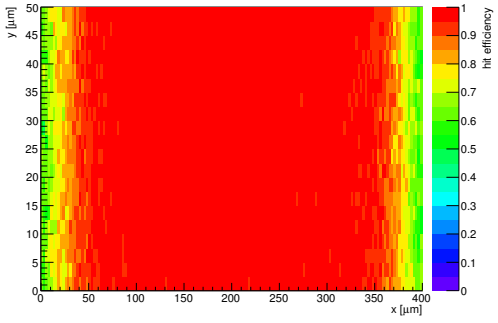

(u) Single pixel hit efficiency.

Figure C.178: Detailed plots for test beam measurement of DO-38 (description see section 6.1) sample (running as DUT3) during runs 918-945 in the May 2012 test beam period at CERN SPS in area H6B. Summary of the data in chapter 9.

C.5.7 Runs 947-980

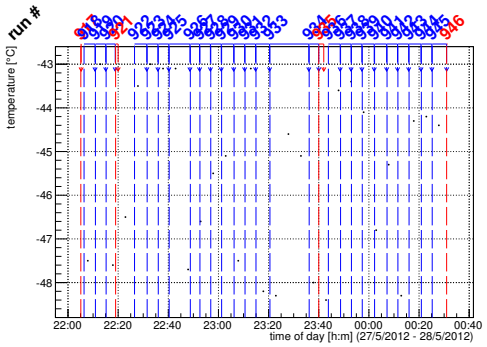

(a) Temperature vs time.

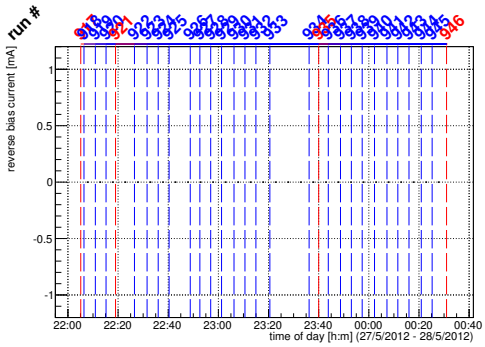

(b) Bias current vs time.

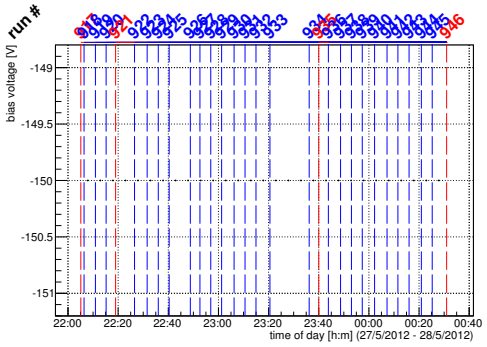

(c) Currently applied bias voltage vs time.

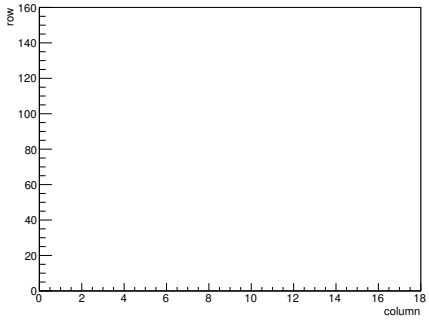

(d) Map of masked pixels.

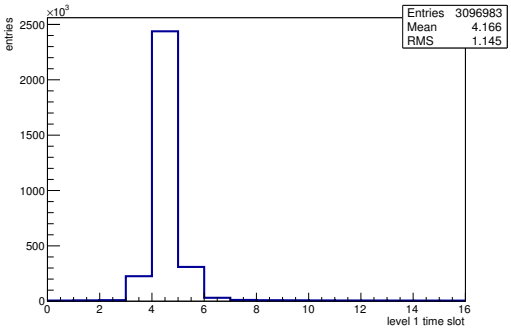

(e) Lvl1 distribution.

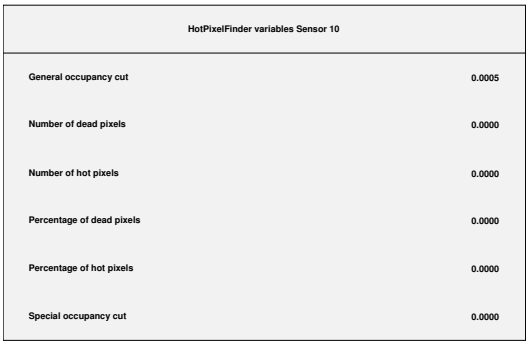

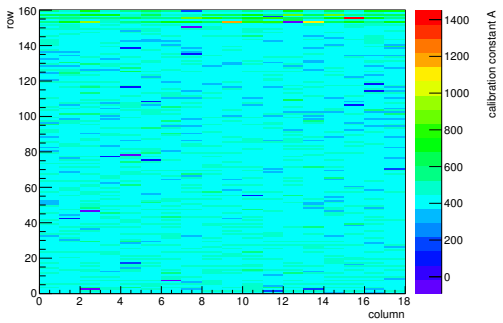

(f) Calibration constant A.

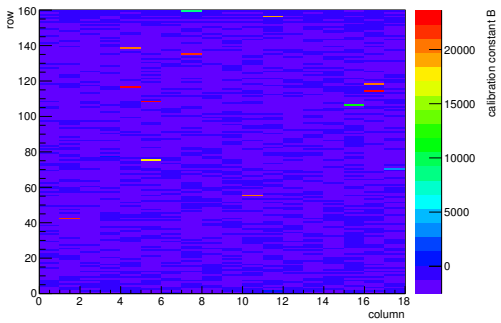

(g) Calibration constant B.

Figure C.179: Detailed plots for test beam measurement of DO-1 (description see section 6.1) sample (running as DUT0) during runs 947-980 in the May 2012 test beam period at CERN SPS in area H6B. Summary of the data in chapter 9. *(cont.)*

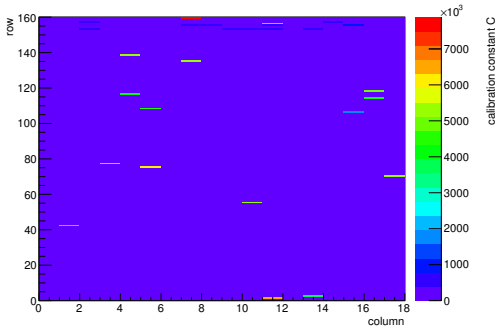

(h) Calibration constant C.

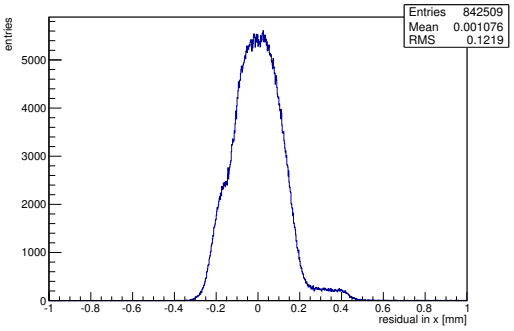

(i) Track residual in x.

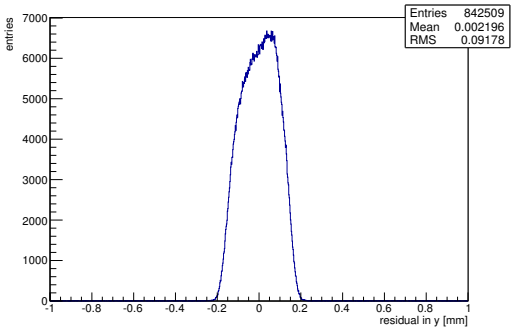

(j) Track residual in y.

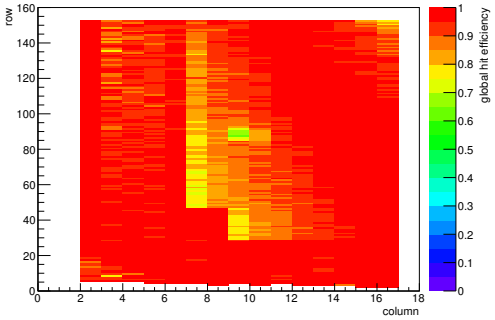

(k) Hit efficiency map.

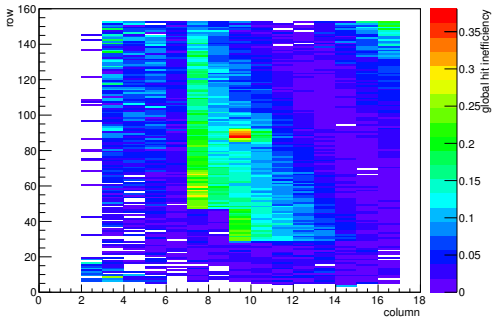

(l) Hit inefficiency map.

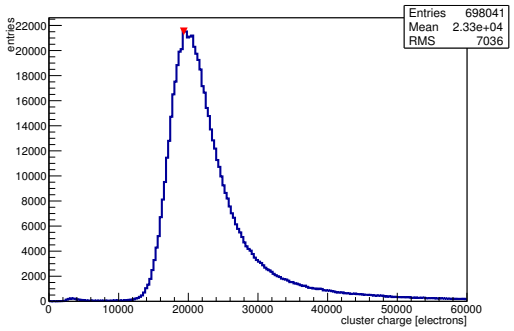

(m) Charge distribution (all cluster sizes included).

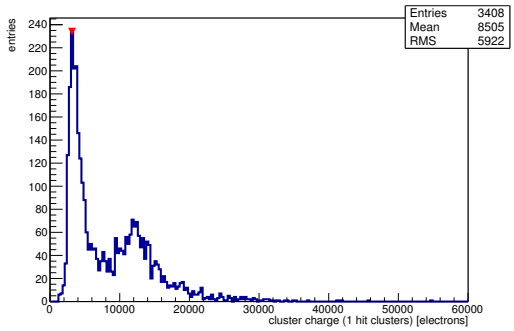

(n) Charge distribution (1 hit cluster).

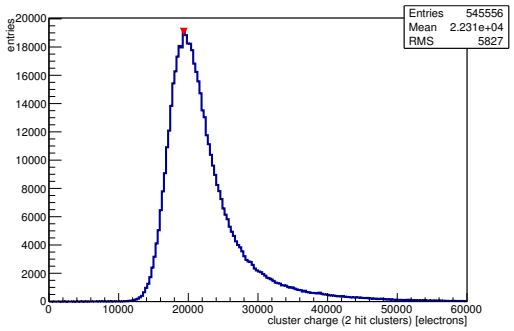

(o) Charge distribution (2 hit cluster).

Figure C.179: Detailed plots for test beam measurement of DO-1 (description see section 6.1) sample (running as DUT0) during runs 947-980 in the May 2012 test beam period at CERN SPS in area H6B. Summary of the data in chapter 9. *(cont.)*

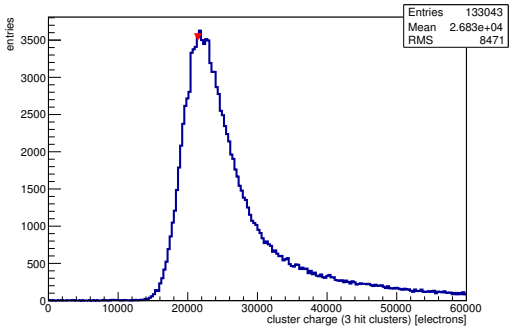

(p) Charge distribution (3 hit cluster).

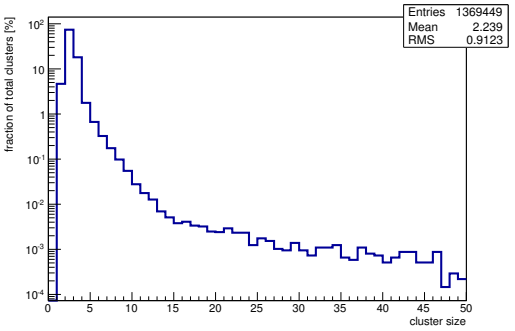

(q) Cluster size distribution.

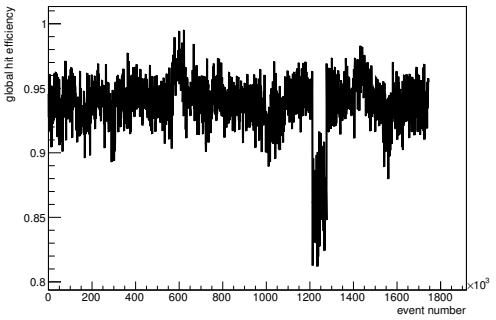

(r) Hit efficiency vs event number.

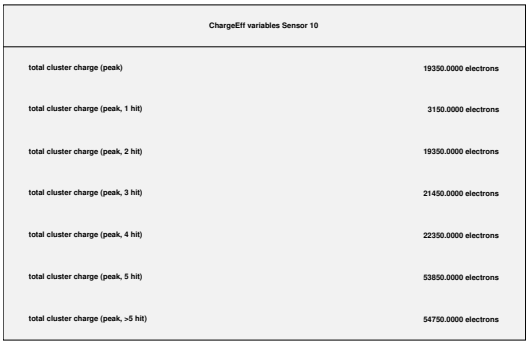

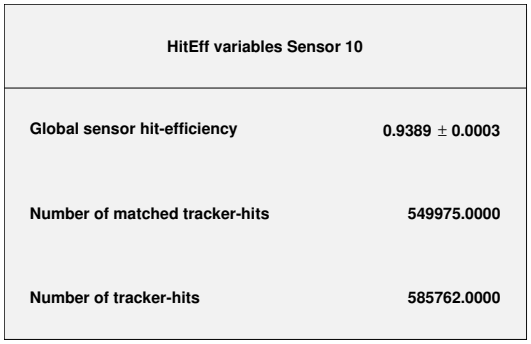

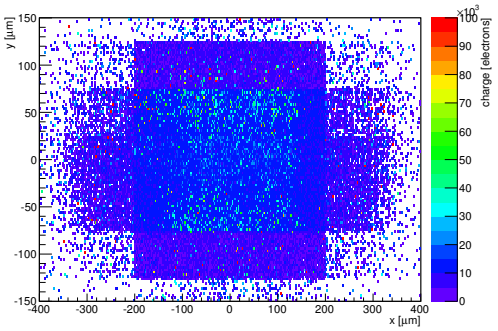

(s) Single pixel mean charge.

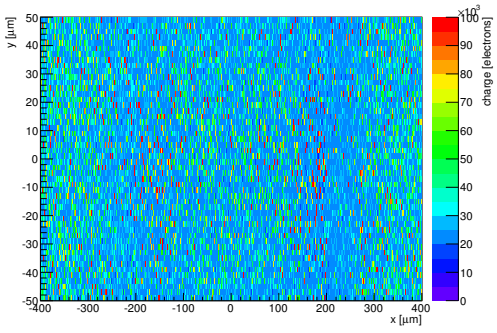

(t) Single pixel mean charge.

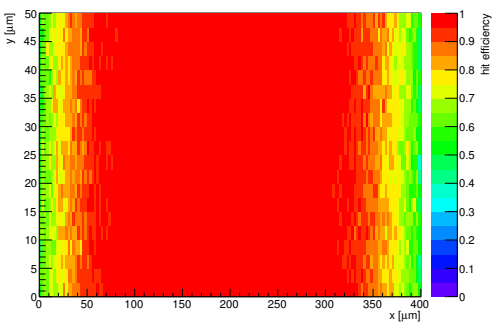

(u) Single pixel hit efficiency.

Figure C.179: Detailed plots for test beam measurement of DO-1 (description see section 6.1) sample (running as DUT0) during runs 947-980 in the May 2012 test beam period at CERN SPS in area H6B. Summary of the data in chapter 9.

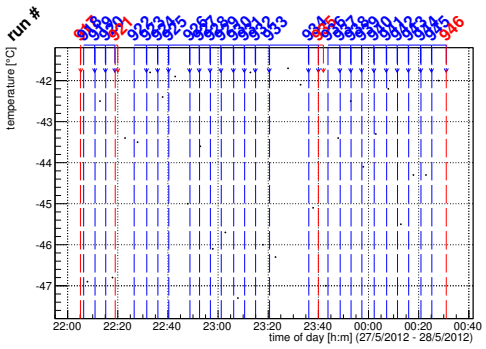

(a) Temperature vs time.

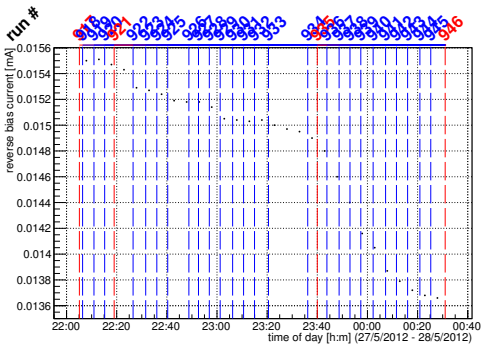

(b) Bias current vs time.

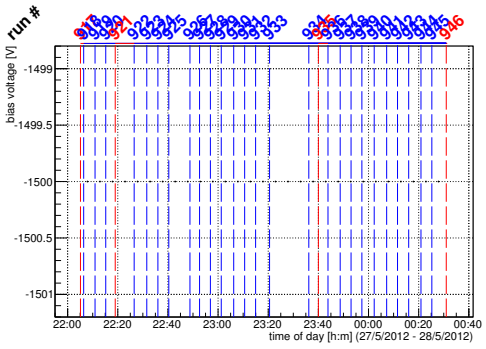

(c) Currently applied bias voltage vs time.

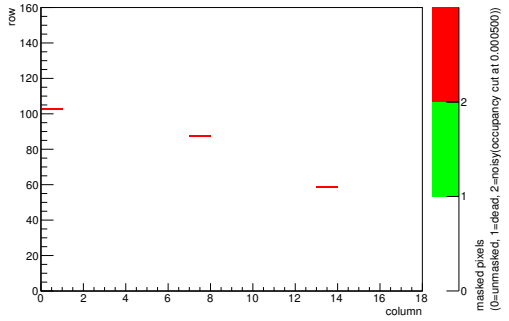

(d) Map of masked pixels.

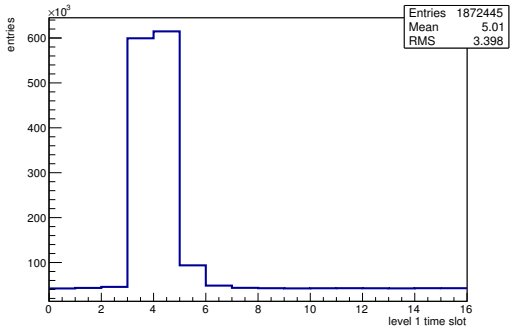

(e) Lvl1 distribution.

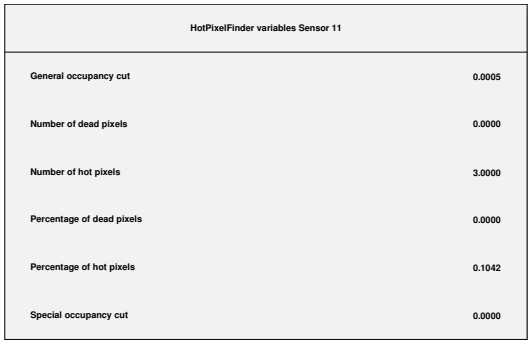

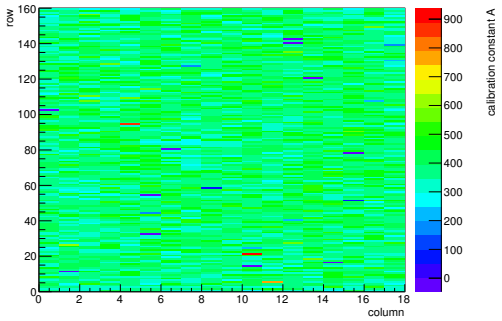

(f) Calibration constant A.

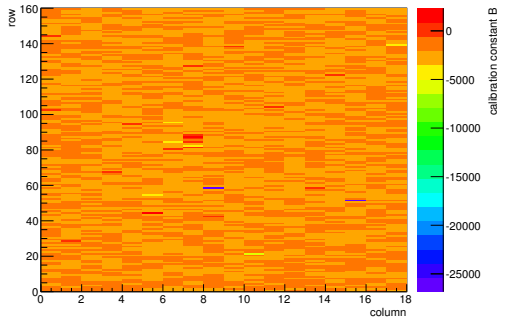

(g) Calibration constant B.

Figure C.180: Detailed plots for test beam measurement of DO-10 (description see section 6.1) sample (running as DUT1) during runs 947-980 in the May 2012 test beam period at CERN SPS in area H6B. Summary of the data in chapter 9. *(cont.)*

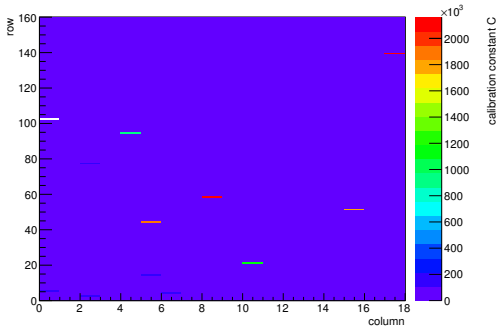

(h) Calibration constant C.

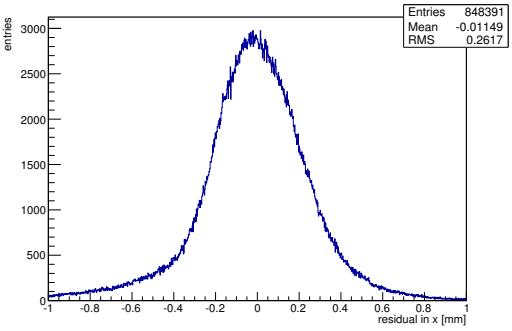

(i) Track residual in x.

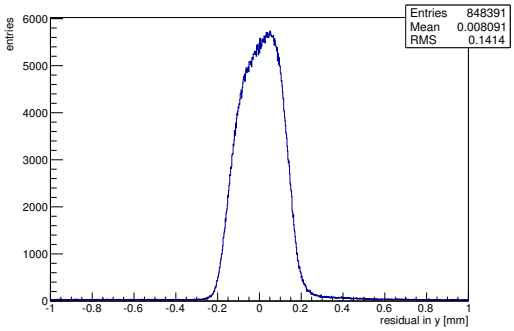

(j) Track residual in y.

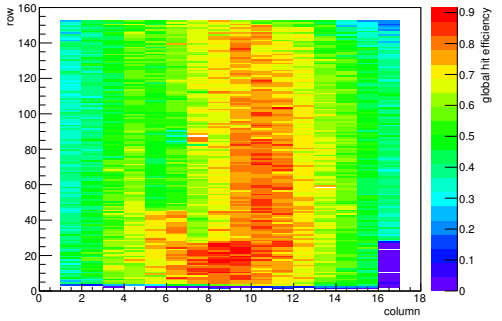

(k) Hit efficiency map.

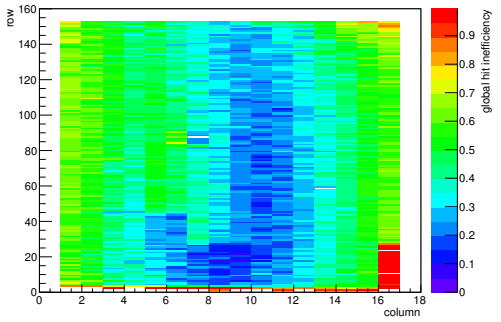

(l) Hit inefficiency map.

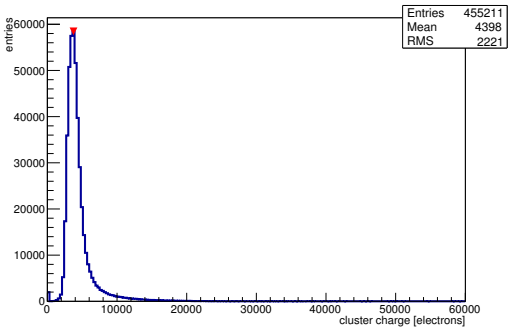

(m) Charge distribution (all cluster sizes included).

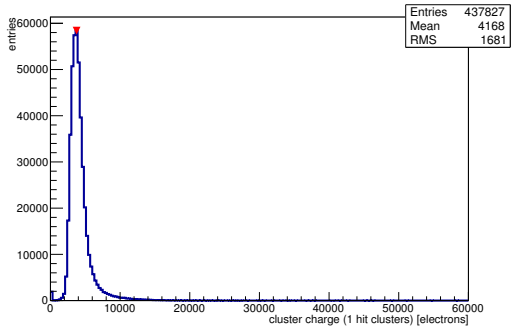

(n) Charge distribution (1 hit cluster).

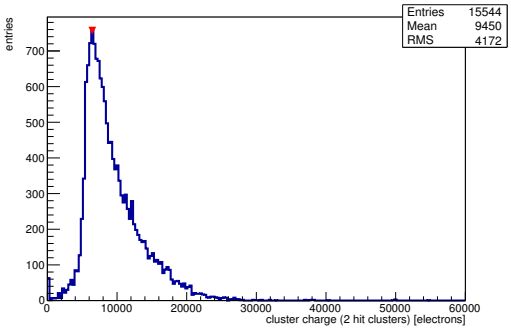

(o) Charge distribution (2 hit cluster).

Figure C.180: Detailed plots for test beam measurement of DO-10 (description see section 6.1) sample (running as DUT1) during runs 947-980 in the May 2012 test beam period at CERN SPS in area H6B. Summary of the data in chapter 9. *(cont.)*

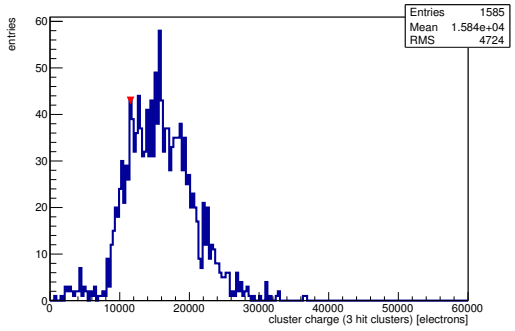

(p) Charge distribution (3 hit cluster).

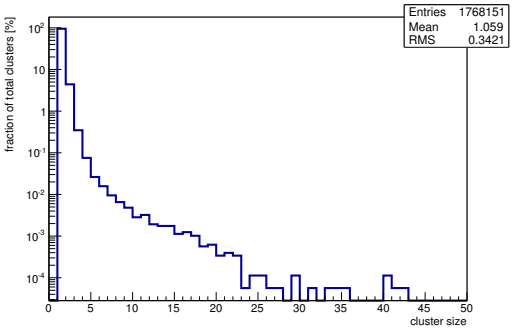

(q) Cluster size distribution.

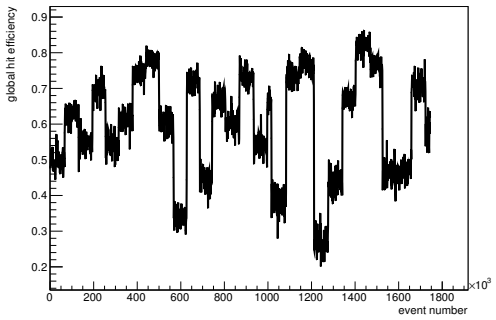

(r) Hit efficiency vs event number.

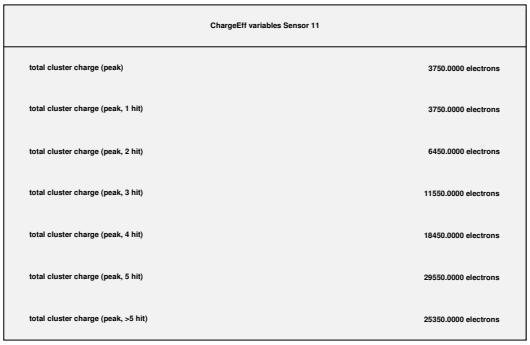

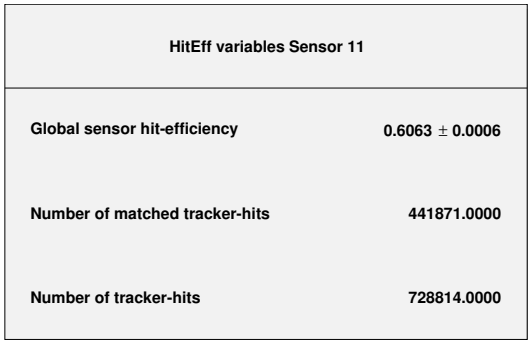

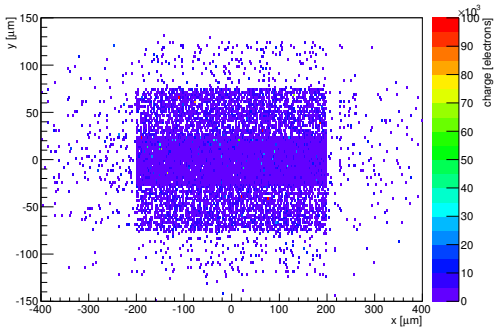

(s) Single pixel mean charge.

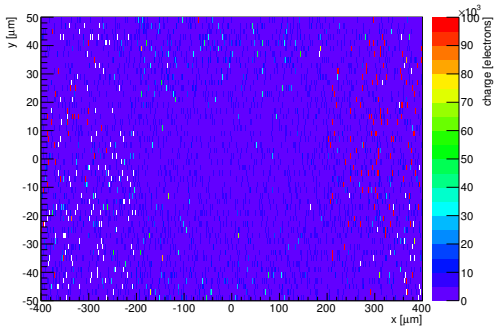

(t) Single pixel mean charge.

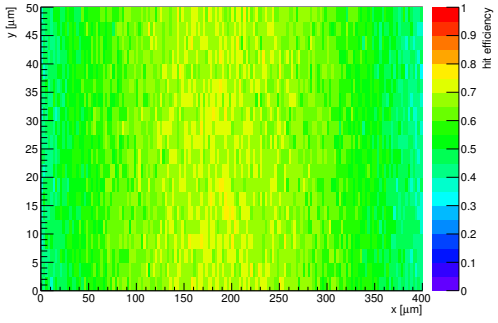

(u) Single pixel hit efficiency.

Figure C.180: Detailed plots for test beam measurement of DO-10 (description see section 6.1) sample (running as DUT1) during runs 947-980 in the May 2012 test beam period at CERN SPS in area H6B. Summary of the data in chapter 9.

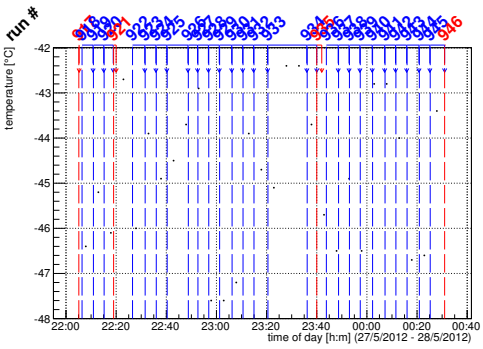

(a) Temperature vs time.

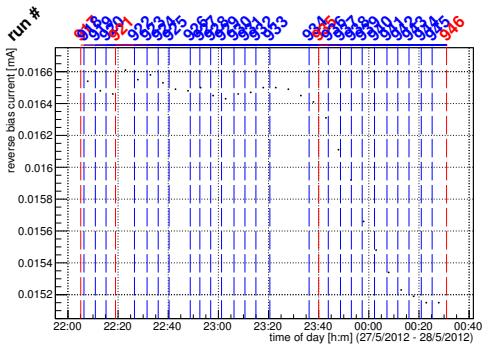

(b) Bias current vs time.

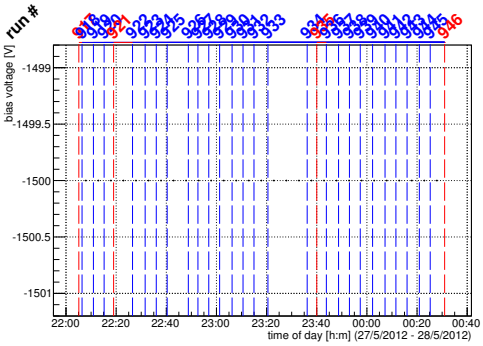

(c) Currently applied bias voltage vs time.

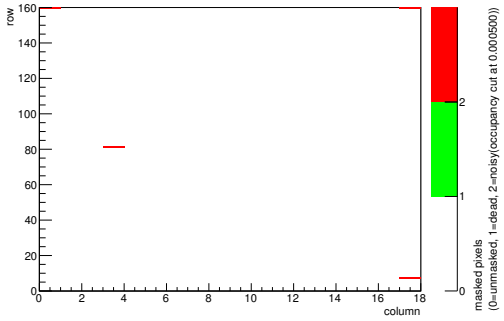

(d) Map of masked pixels.

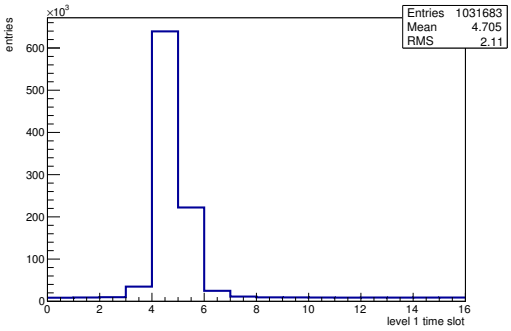

(e) Lvl1 distribution.

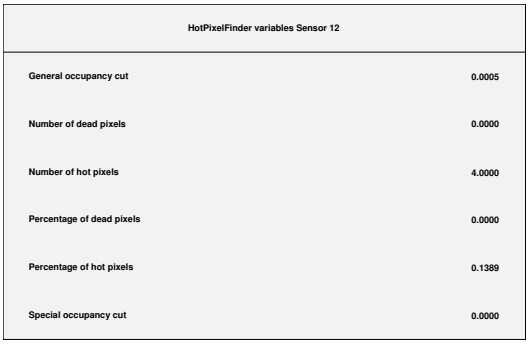

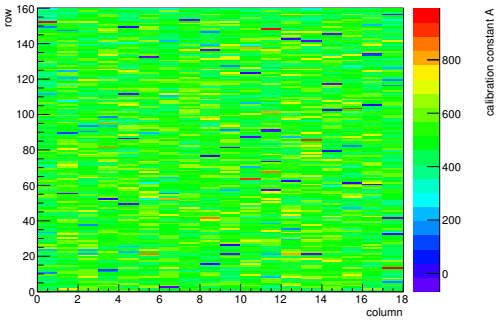

(f) Calibration constant A.

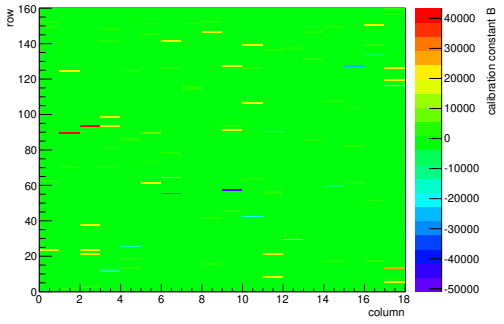

(g) Calibration constant B.

Figure C.181: Detailed plots for test beam measurement of DO-24 (description see section 6.1) sample (running as DUT2) during runs 947-980 in the May 2012 test beam period at CERN SPS in area H6B. Summary of the data in chapter 9. *(cont.)*

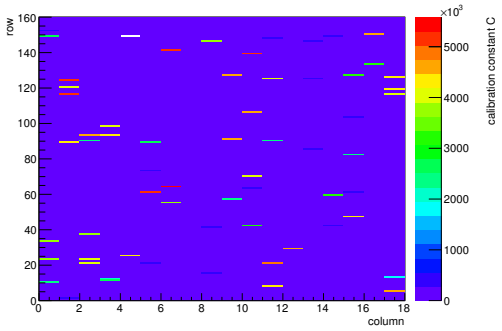

(h) Calibration constant C.

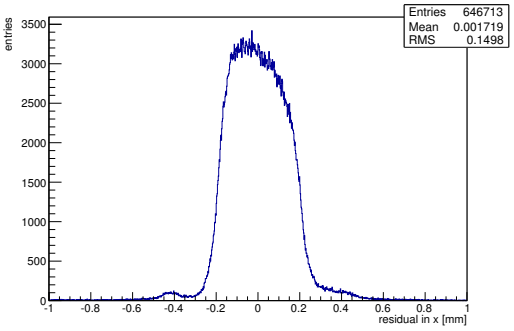

(i) Track residual in x.

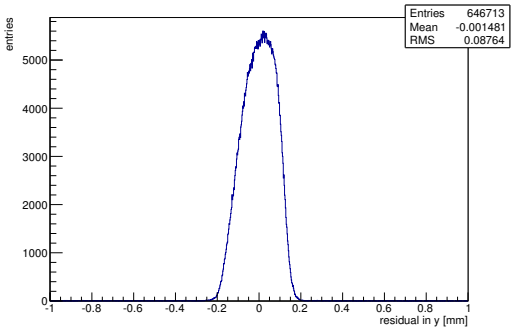

(j) Track residual in y.

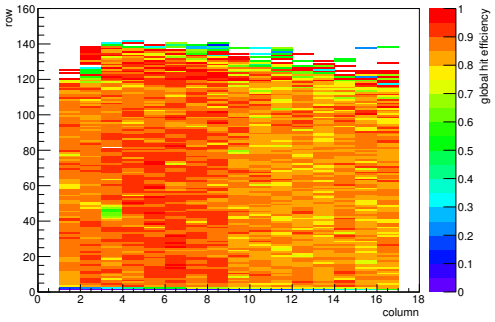

(k) Hit efficiency map.

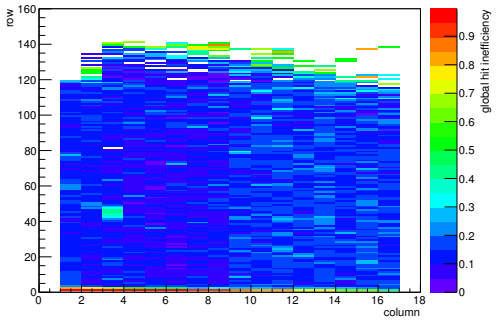

(l) Hit inefficiency map.

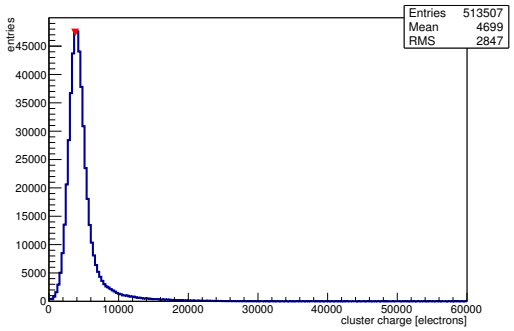

(m) Charge distribution (all cluster sizes included).

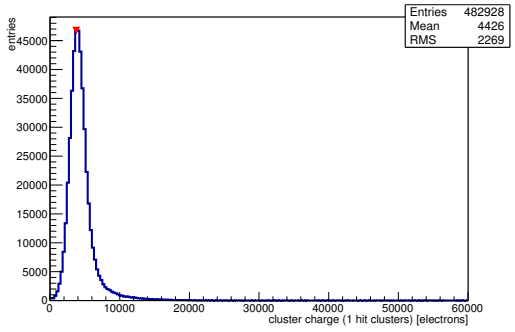

(n) Charge distribution (1 hit cluster).

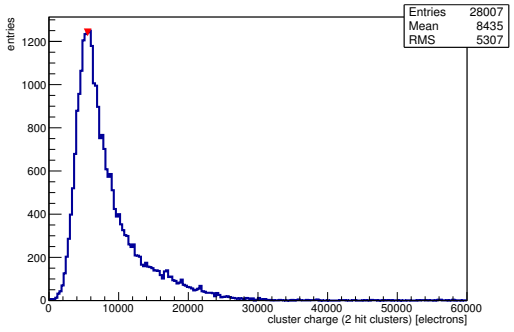

(o) Charge distribution (2 hit cluster).

Figure C.181: Detailed plots for test beam measurement of DO-24 (description see section 6.1) sample (running as DUT2) during runs 947-980 in the May 2012 test beam period at CERN SPS in area H6B. Summary of the data in chapter 9. *(cont.)*

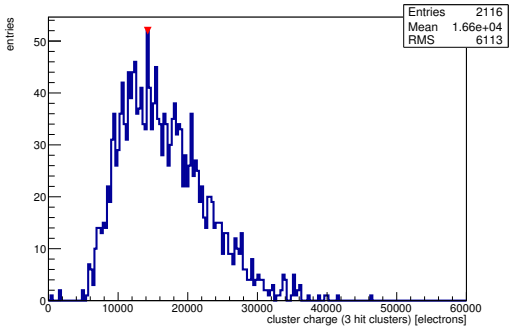

(p) Charge distribution (3 hit cluster).

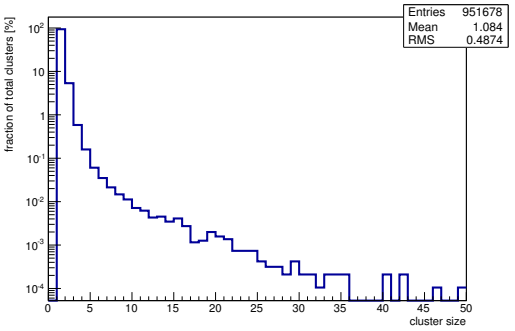

(q) Cluster size distribution.

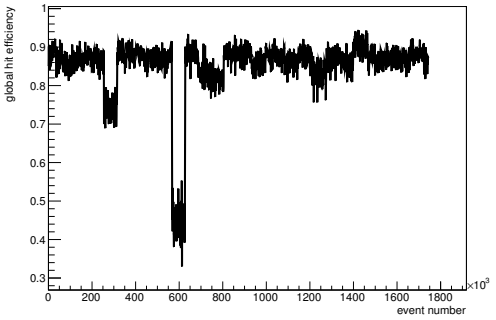

(r) Hit efficiency vs event number.

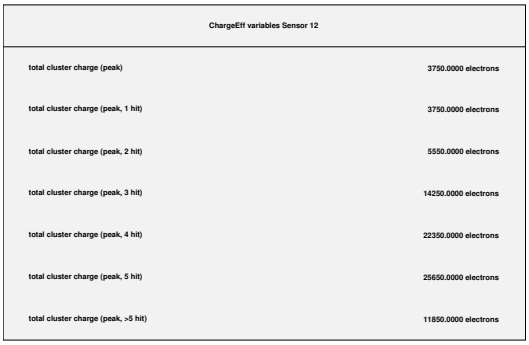

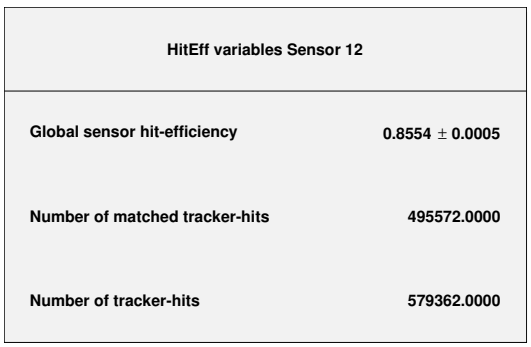

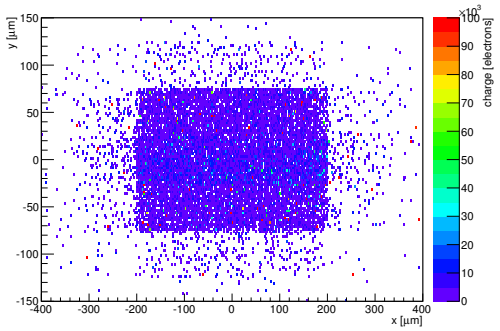

(s) Single pixel mean charge.

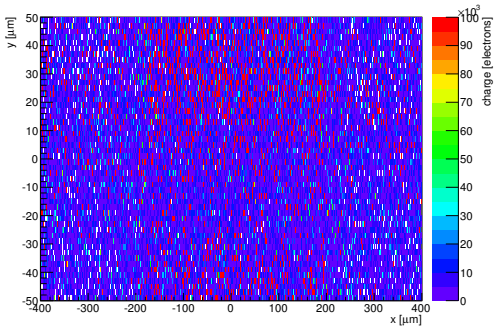

(t) Single pixel mean charge.

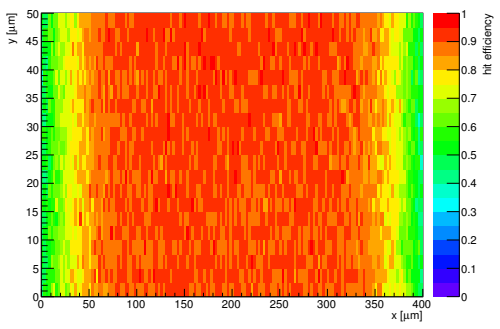

(u) Single pixel hit efficiency.

Figure C.181: Detailed plots for test beam measurement of DO-24 (description see section 6.1) sample (running as DUT2) during runs 947-980 in the May 2012 test beam period at CERN SPS in area H6B. Summary of the data in chapter 9.

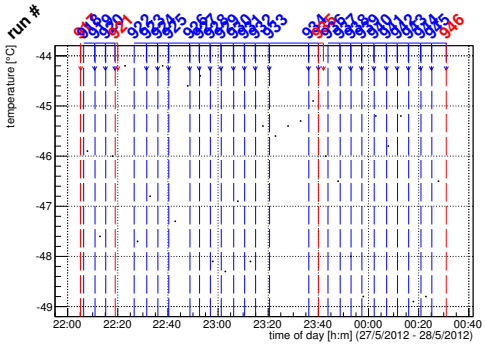

(a) Temperature vs time.

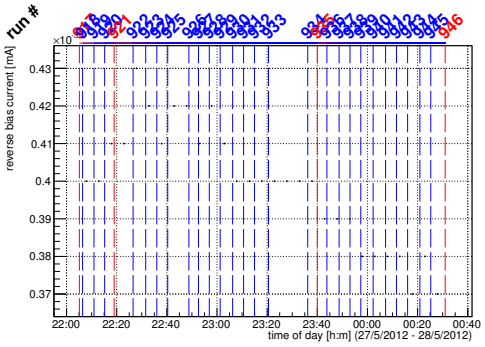

(b) Bias current vs time.

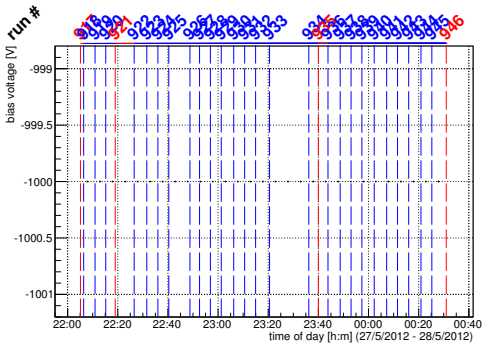

(c) Currently applied bias voltage vs time.

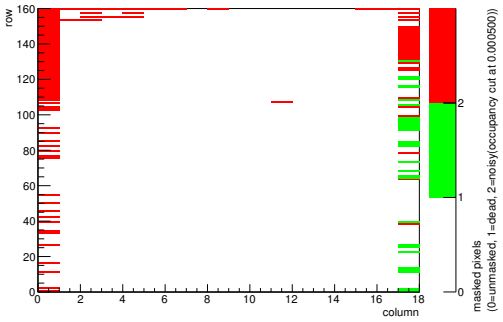

(d) Map of masked pixels.

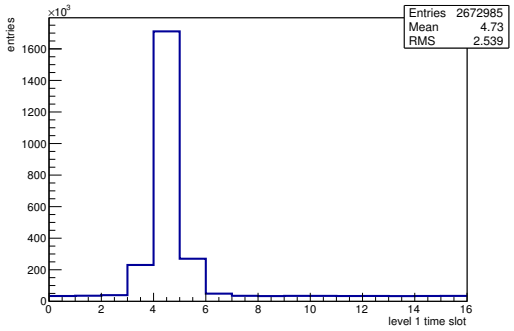

(e) Lvl1 distribution.

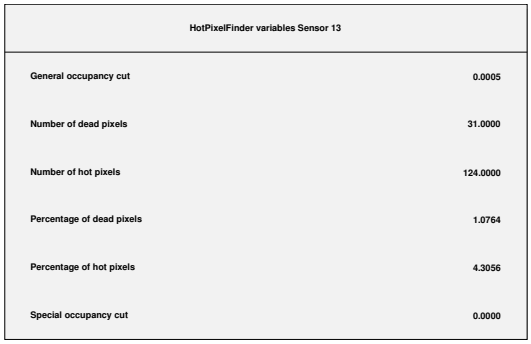

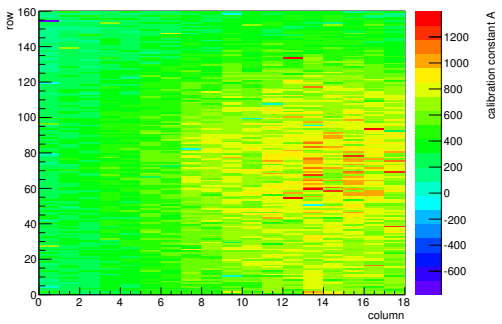

(f) Calibration constant A.

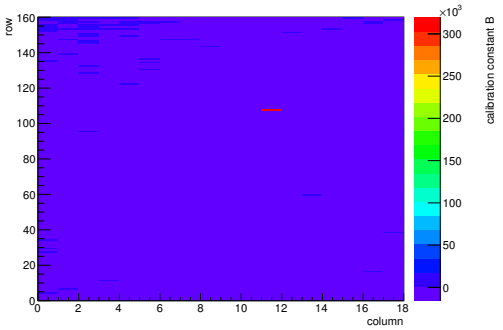

(g) Calibration constant B.

Figure C.182: Detailed plots for test beam measurement of DO-38 (description see section 6.1) sample (running as DUT3) during runs 947-980 in the May 2012 test beam period at CERN SPS in area H6B. Summary of the data in chapter 9. *(cont.)*

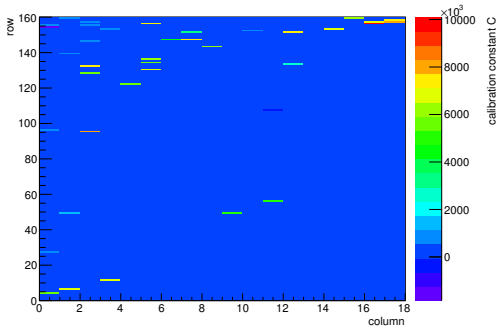

(h) Calibration constant C.

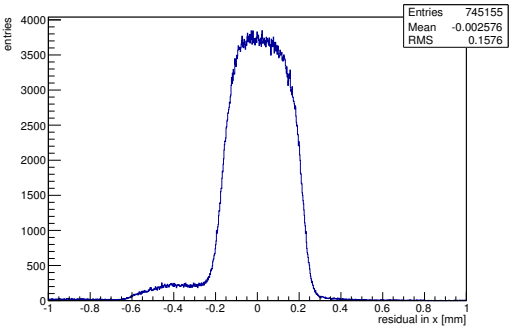

(i) Track residual in x.

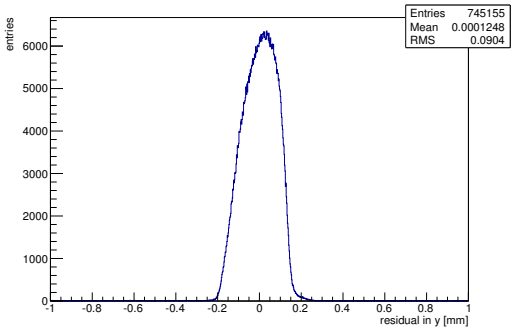

(j) Track residual in y.

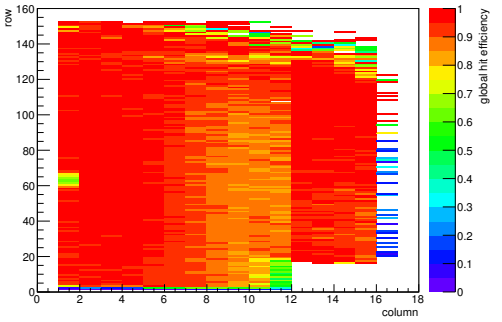

(k) Hit efficiency map.

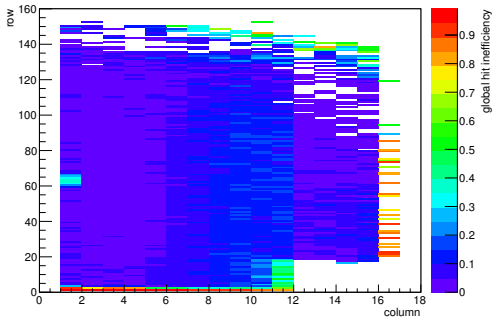

(l) Hit inefficiency map.

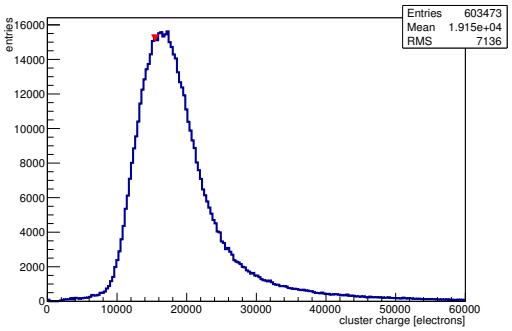

(m) Charge distribution (all cluster sizes included).

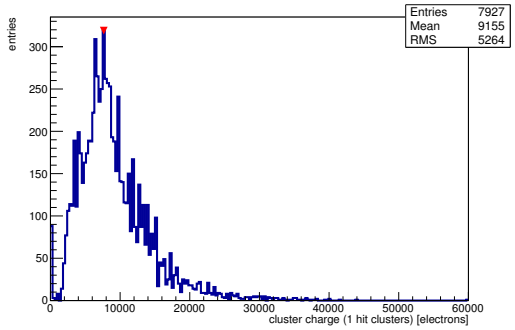

(n) Charge distribution (1 hit cluster).

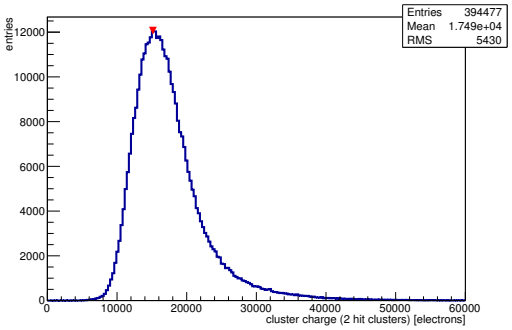

(o) Charge distribution (2 hit cluster).

Figure C.182: Detailed plots for test beam measurement of DO-38 (description see section 6.1) sample (running as DUT3) during runs 947-980 in the May 2012 test beam period at CERN SPS in area H6B. Summary of the data in chapter 9. *(cont.)*

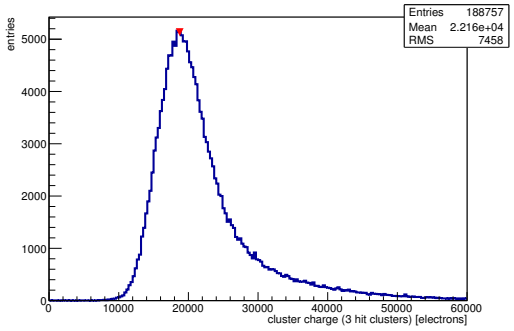

(p) Charge distribution (3 hit cluster).

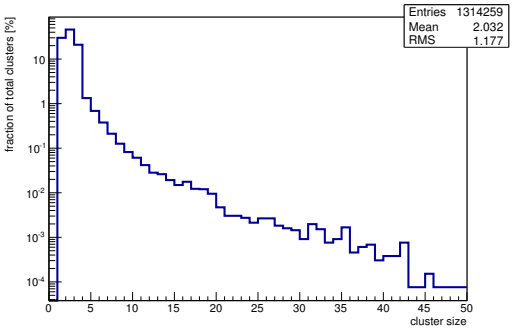

(q) Cluster size distribution.

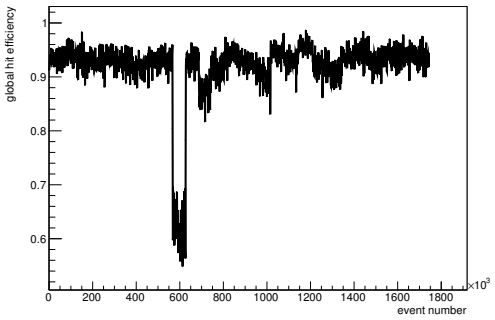

(r) Hit efficiency vs event number.

ChargeEff variables Sensor 13	
total cluster charge (peak)	15450.0000 electrons
total cluster charge (peak, 1 hit)	7650.0000 electrons
total cluster charge (peak, 2 hit)	15150.0000 electrons
total cluster charge (peak, 3 hit)	18750.0000 electrons
total cluster charge (peak, 4 hit)	15450.0000 electrons
total cluster charge (peak, 5 hit)	29550.0000 electrons
total cluster charge (peak, >5 hit)	43050.0000 electrons

HitEff variables Sensor 13	
Global sensor hit-efficiency	0.9220 ± 0.0004
Number of matched tracker-hits	536816.0000
Number of tracker-hits	582232.0000

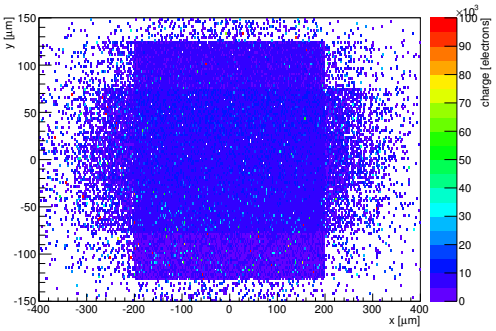

(s) Single pixel mean charge.

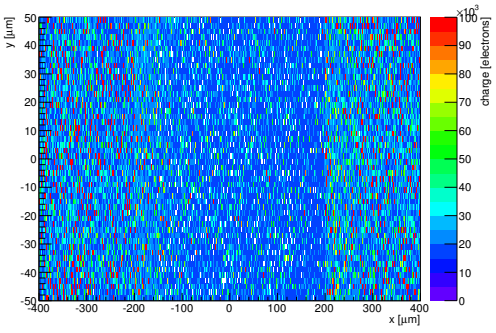

(t) Single pixel mean charge.

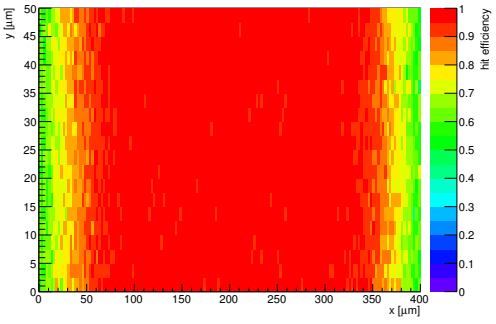

(u) Single pixel hit efficiency.

Figure C.182: Detailed plots for test beam measurement of DO-38 (description see section 6.1) sample (running as DUT3) during runs 947-980 in the May 2012 test beam period at CERN SPS in area H6B. Summary of the data in chapter 9.

C.6 CERN SPS August 2012

C.6.1 Runs 71579-71628

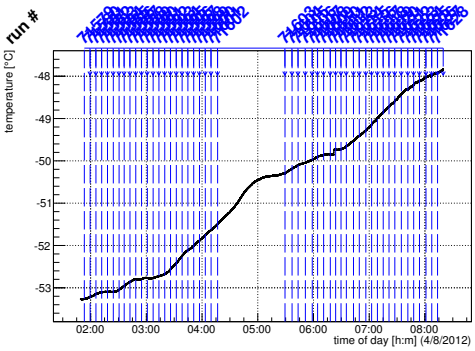

(a) Temperature vs time.

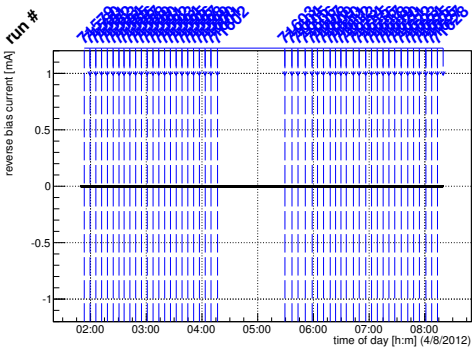

(b) Bias current vs time.

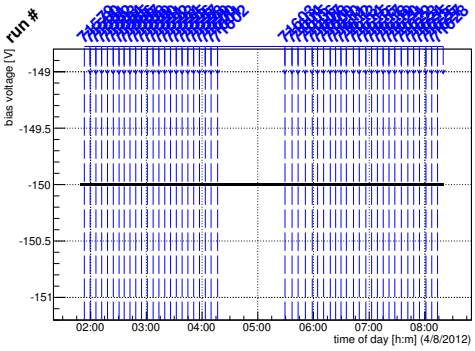

(c) Currently applied bias voltage vs time.

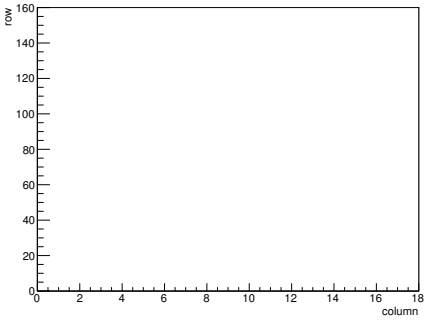

(d) Map of masked pixels.

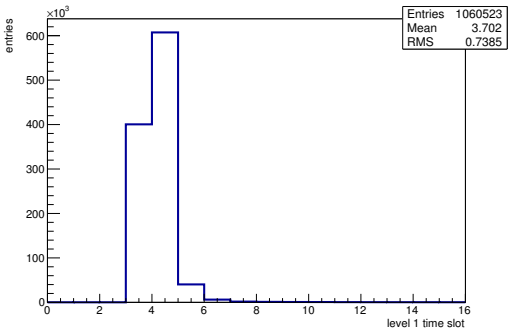

(e) Lvl1 distribution.

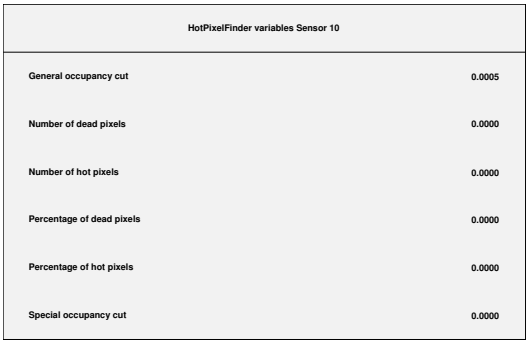

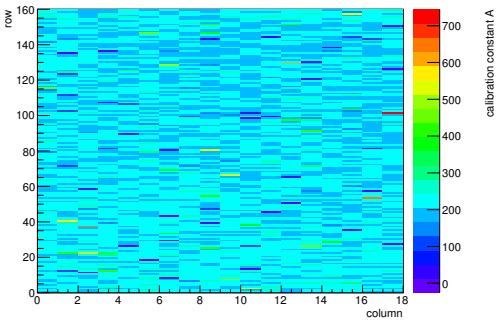

(f) Calibration constant A.

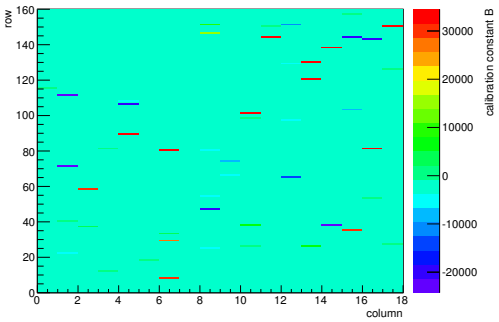

(g) Calibration constant B.

Figure C.183: Detailed plots for test beam measurement of DO-1 (description see section 6.1) sample (running as DUT0) during runs 71579-71628 in the August 2012 test beam period at CERN SPS in area H6B. Summary of the data in chapter 9. *(cont.)*

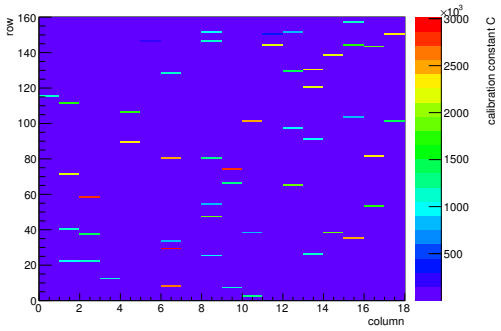

(h) Calibration constant C.

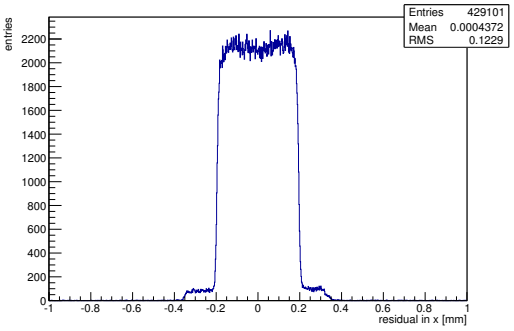

(i) Track residual in x.

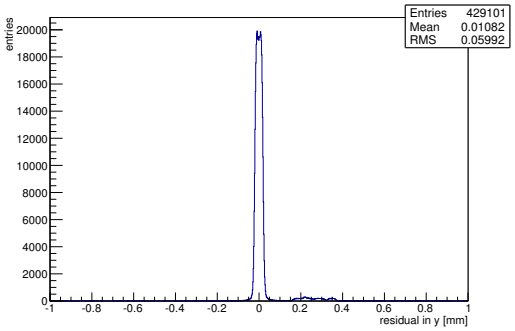

(j) Track residual in y.

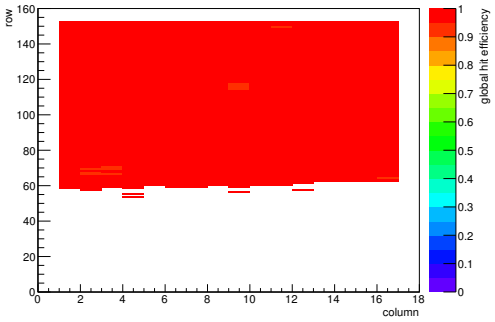

(k) Hit efficiency map.

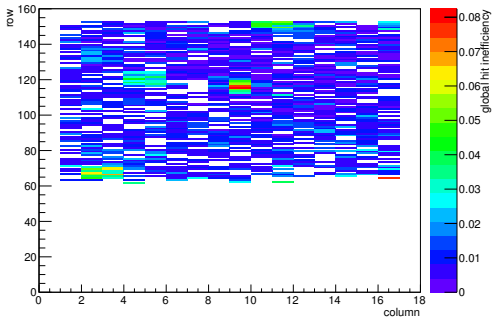

(l) Hit inefficiency map.

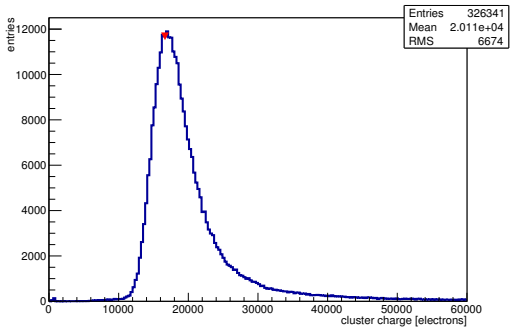

(m) Charge distribution (all cluster sizes included).

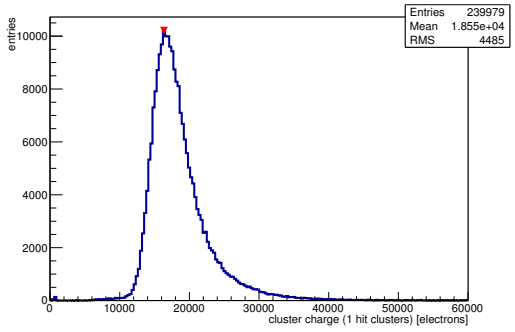

(n) Charge distribution (1 hit cluster).

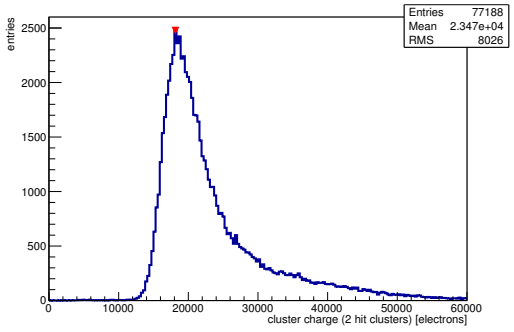

(o) Charge distribution (2 hit cluster).

Figure C.183: Detailed plots for test beam measurement of DO-1 (description see section 6.1) sample (running as DUT0) during runs 71579-71628 in the August 2012 test beam period at CERN SPS in area H6B. Summary of the data in chapter 9. *(cont.)*

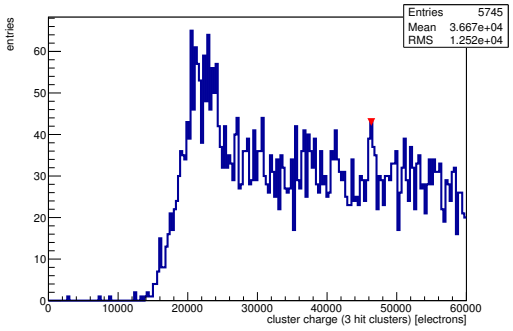

(p) Charge distribution (3 hit cluster).

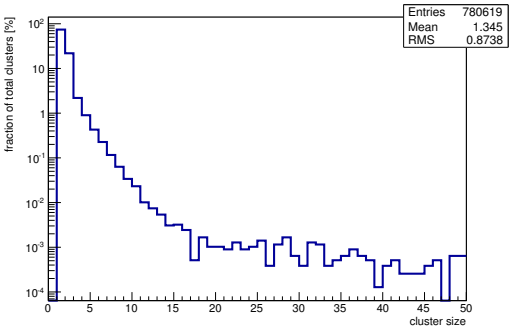

(q) Cluster size distribution.

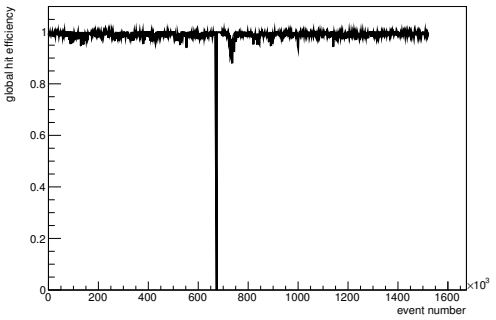

(r) Hit efficiency vs event number.

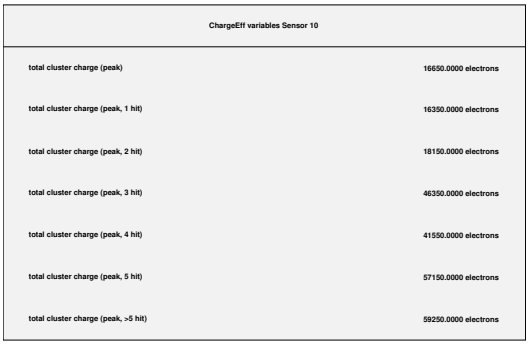

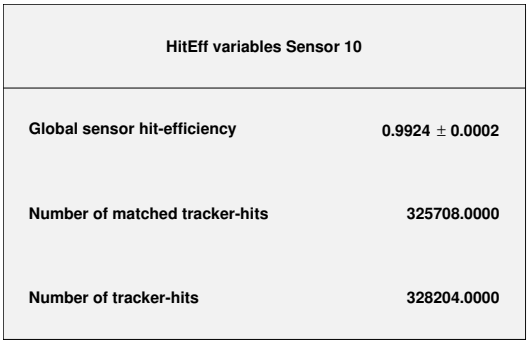

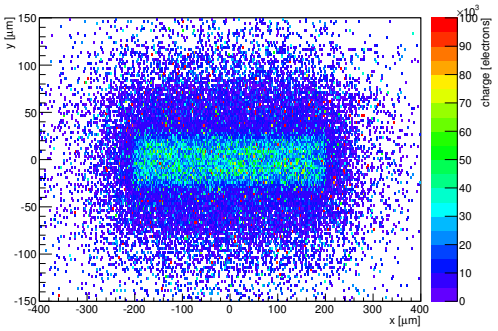

(s) Single pixel mean charge.

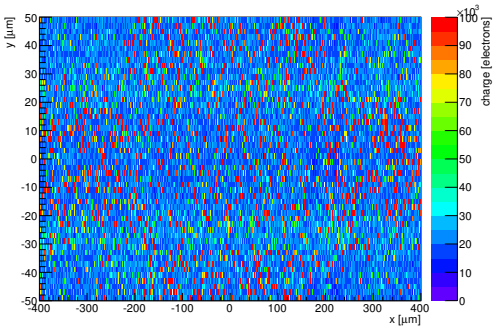

(t) Single pixel mean charge.

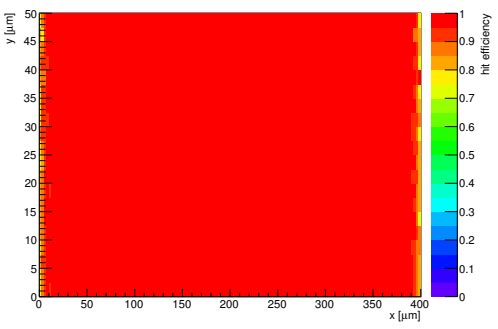

(u) Single pixel hit efficiency.

Figure C.183: Detailed plots for test beam measurement of DO-1 (description see section 6.1) sample (running as DUT0) during runs 71579-71628 in the August 2012 test beam period at CERN SPS in area H6B. Summary of the data in chapter 9.

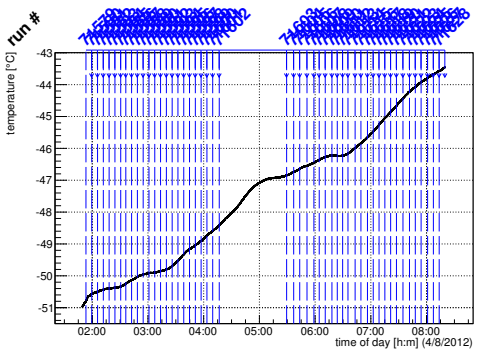

(a) Temperature vs time.

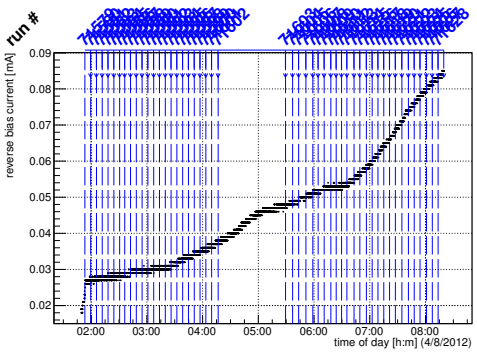

(b) Bias current vs time.

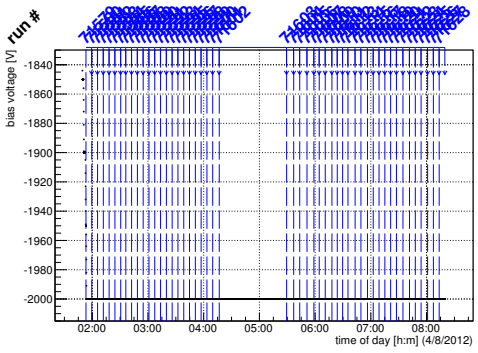

(c) Currently applied bias voltage vs time.

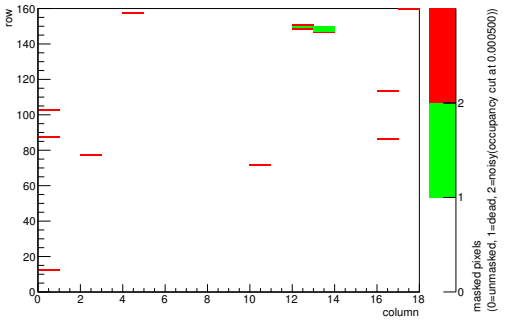

(d) Map of masked pixels.

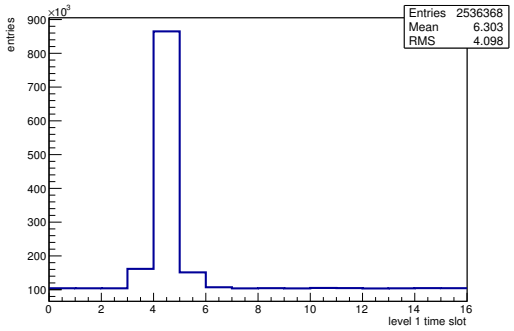

(e) Lvl1 distribution.

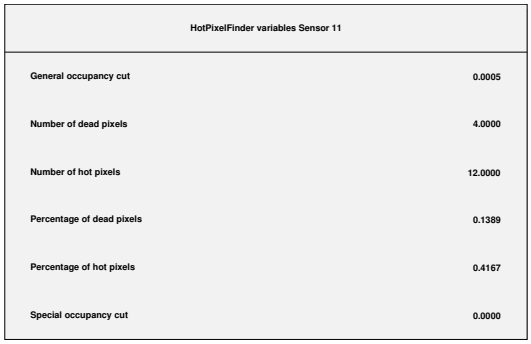

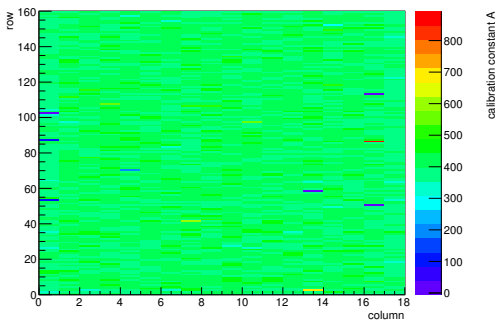

(f) Calibration constant A.

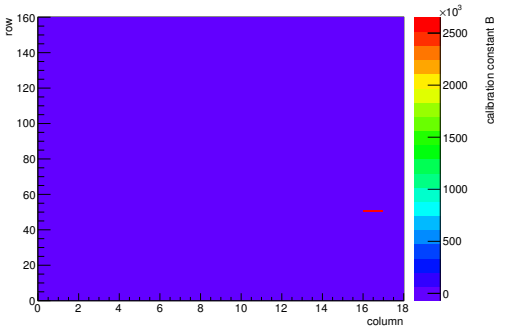

(g) Calibration constant B.

Figure C.184: Detailed plots for test beam measurement of DO-10 (description see section 6.1) sample (running as DUT1) during runs 71579-71628 in the August 2012 test beam period at CERN SPS in area H6B. Summary of the data in chapter 9. *(cont.)*

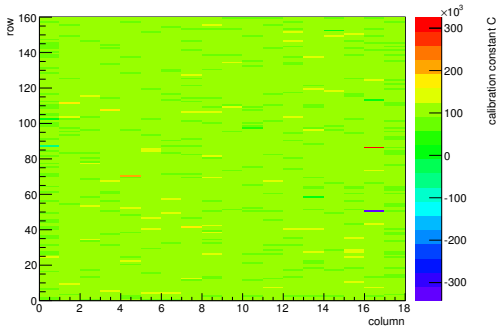

(h) Calibration constant C.

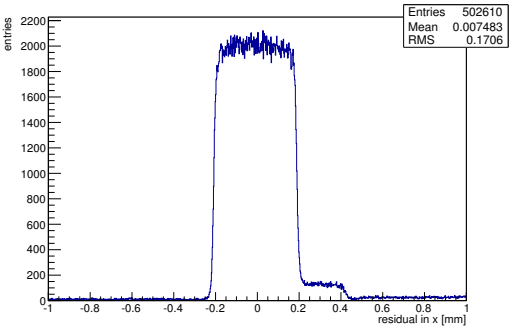

(i) Track residual in x.

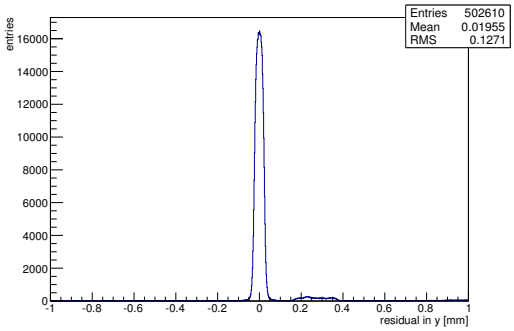

(j) Track residual in y.

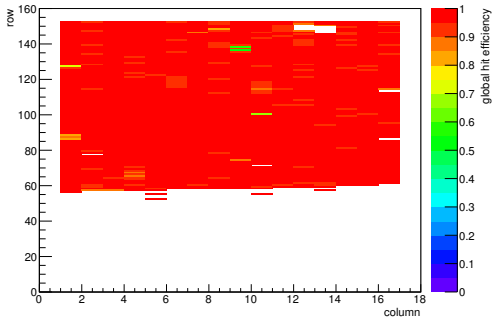

(k) Hit efficiency map.

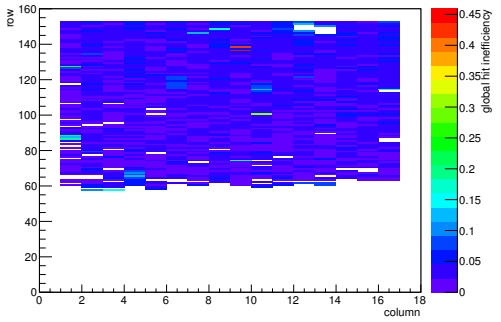

(l) Hit inefficiency map.

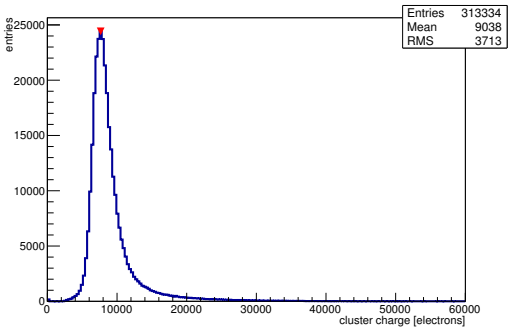

(m) Charge distribution (all cluster sizes included).

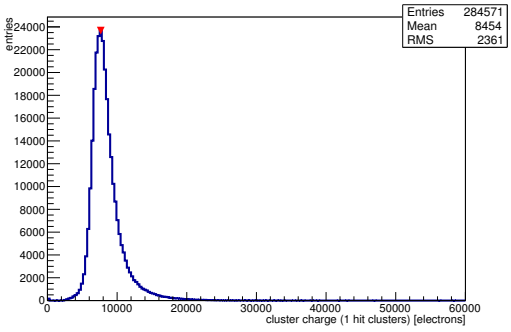

(n) Charge distribution (1 hit cluster).

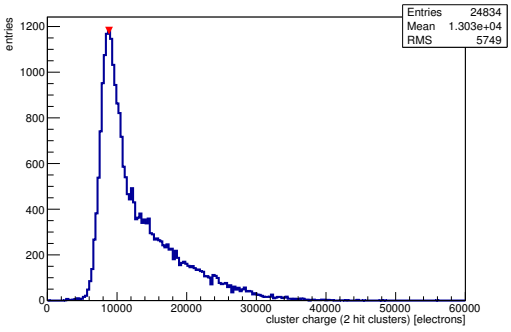

(o) Charge distribution (2 hit cluster).

Figure C.184: Detailed plots for test beam measurement of DO-10 (description see section 6.1) sample (running as DUT1) during runs 71579-71628 in the August 2012 test beam period at CERN SPS in area H6B. Summary of the data in chapter 9. *(cont.)*

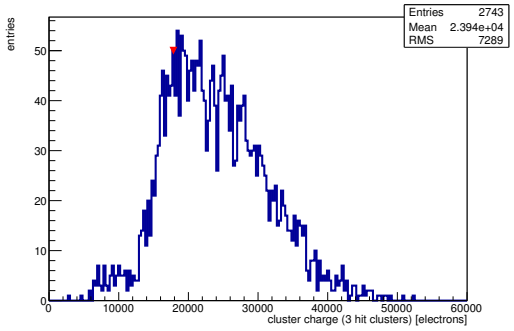

(p) Charge distribution (3 hit cluster).

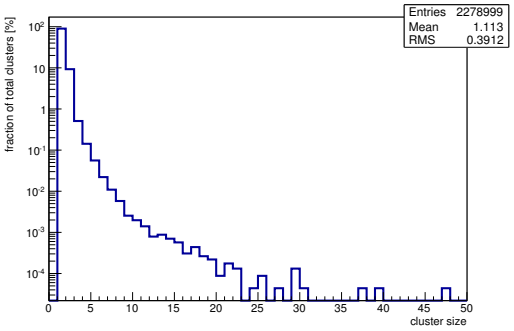

(q) Cluster size distribution.

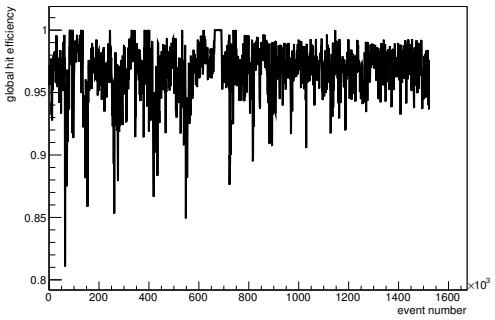

(r) Hit efficiency vs event number.

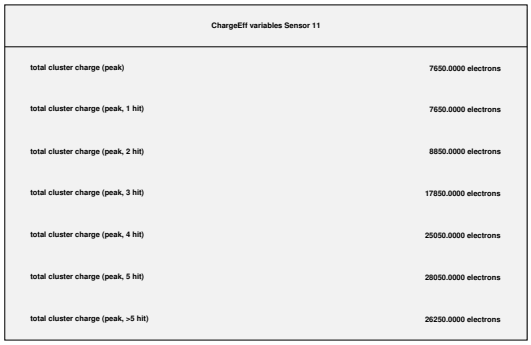

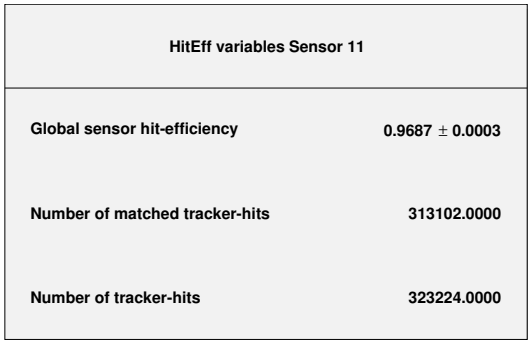

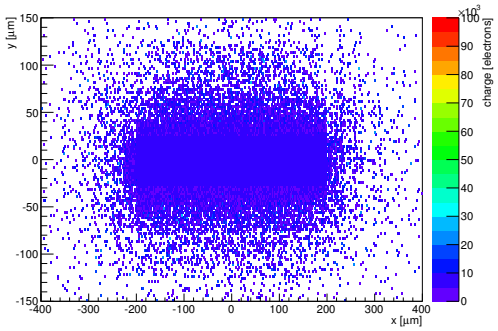

(s) Single pixel mean charge.

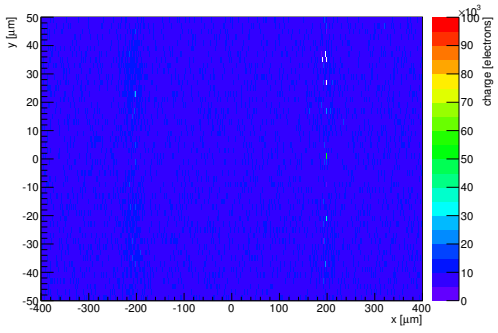

(t) Single pixel mean charge.

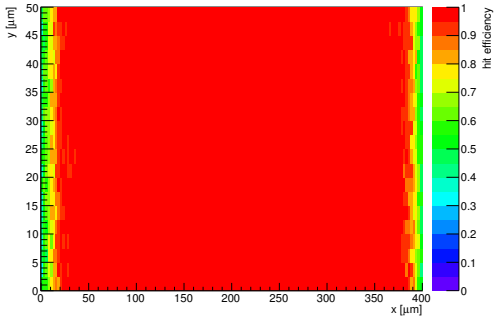

(u) Single pixel hit efficiency.

Figure C.184: Detailed plots for test beam measurement of DO-10 (description see section 6.1) sample (running as DUT1) during runs 71579-71628 in the August 2012 test beam period at CERN SPS in area H6B. Summary of the data in chapter 9.

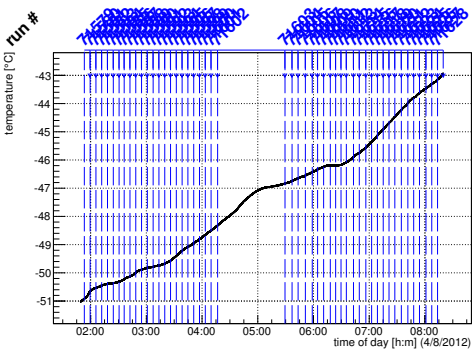

(a) Temperature vs time.

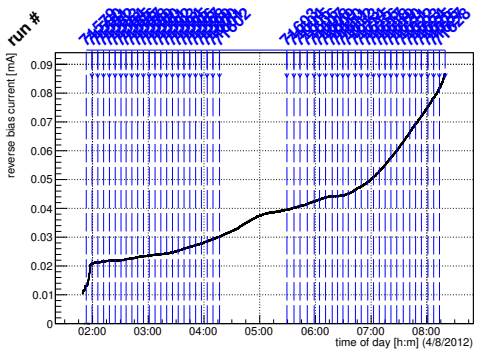

(b) Bias current vs time.

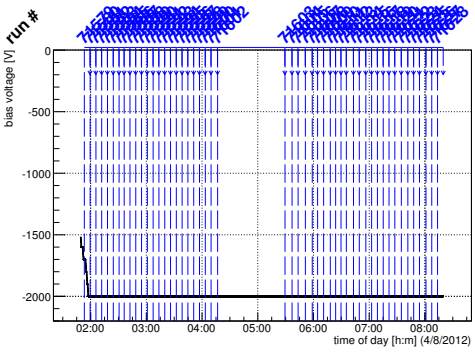

(c) Currently applied bias voltage vs time.

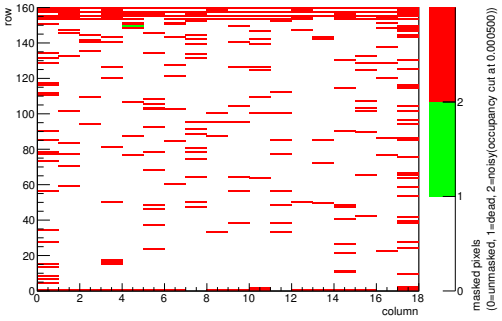

(d) Map of masked pixels.

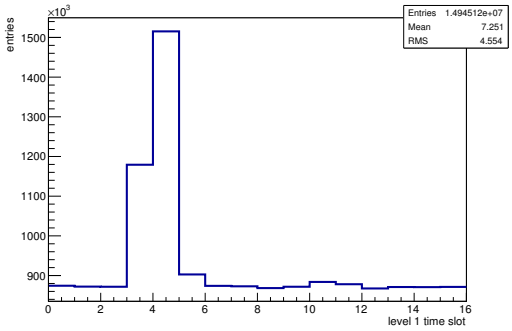

(e) Lvl1 distribution.

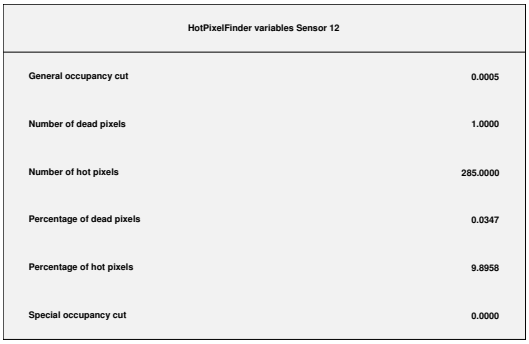

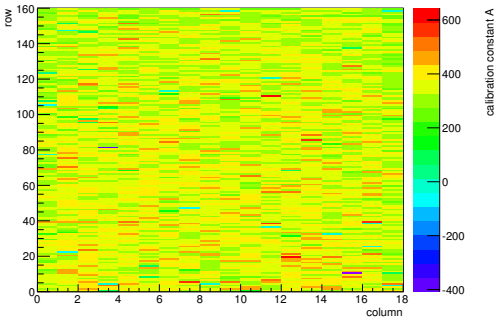

(f) Calibration constant A.

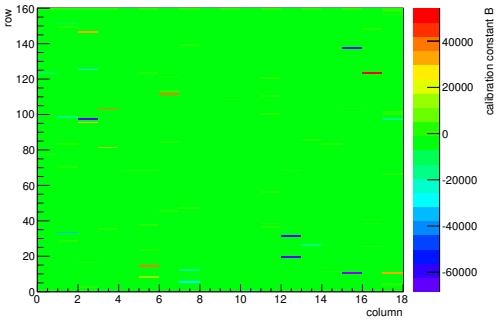

(g) Calibration constant B.

Figure C.185: Detailed plots for test beam measurement of DO-24 (description see section 6.1) sample (running as DUT2) during runs 71579-71628 in the August 2012 test beam period at CERN SPS in area H6B. Summary of the data in chapter 9. *(cont.)*

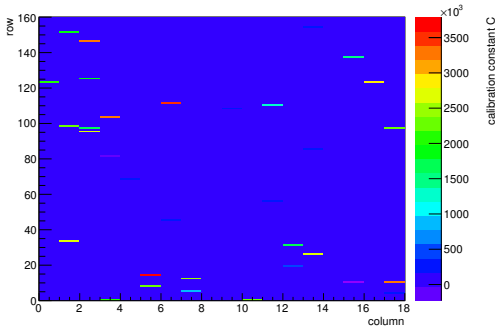

(h) Calibration constant C.

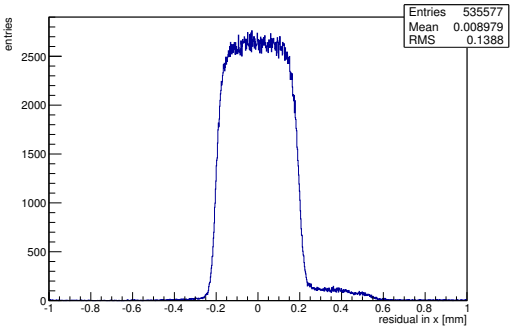

(i) Track residual in x.

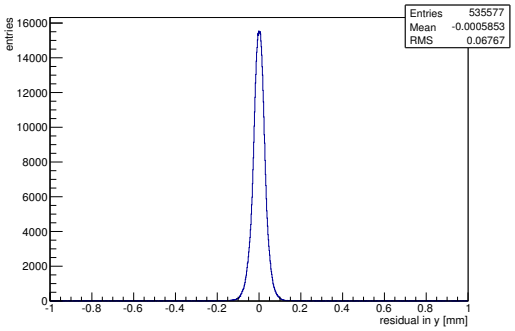

(j) Track residual in y.

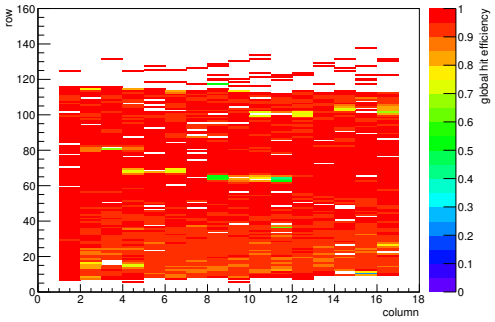

(k) Hit efficiency map.

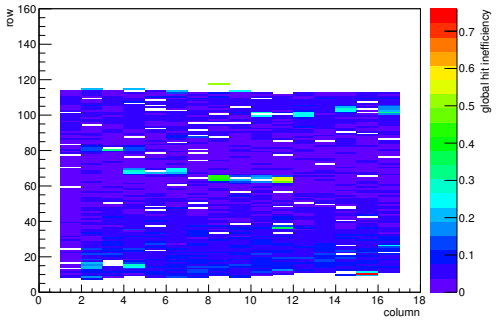

(l) Hit inefficiency map.

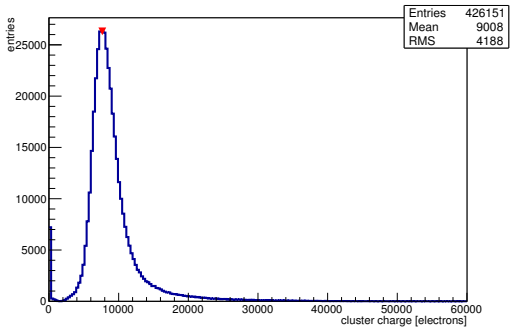

(m) Charge distribution (all cluster sizes included).

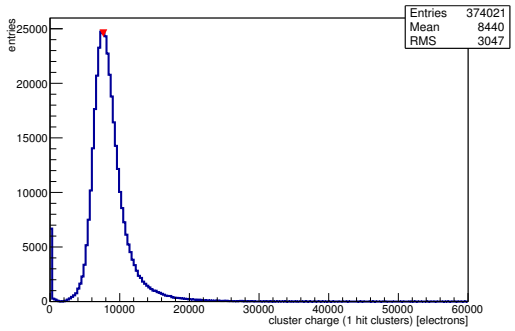

(n) Charge distribution (1 hit cluster).

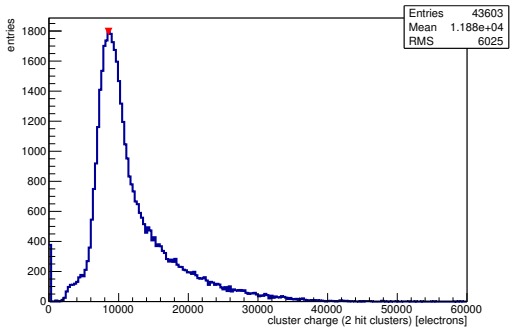

(o) Charge distribution (2 hit cluster).

Figure C.185: Detailed plots for test beam measurement of DO-24 (description see section 6.1) sample (running as DUT2) during runs 71579-71628 in the August 2012 test beam period at CERN SPS in area H6B. Summary of the data in chapter 9. *(cont.)*

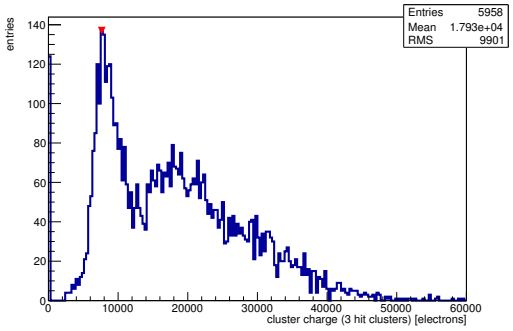

(p) Charge distribution (3 hit cluster).

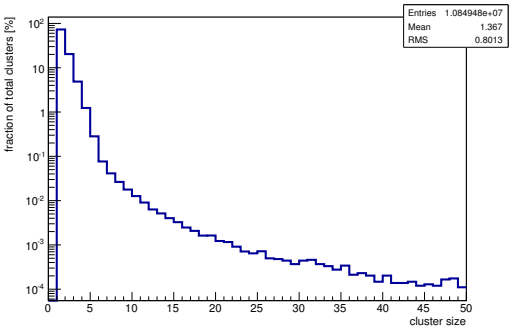

(q) Cluster size distribution.

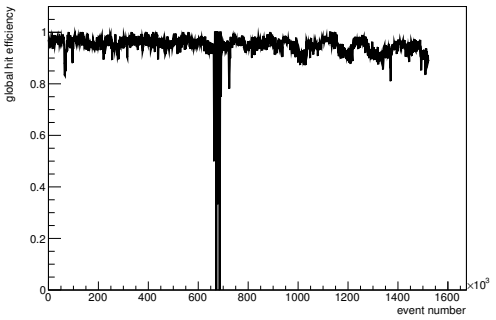

(r) Hit efficiency vs event number.

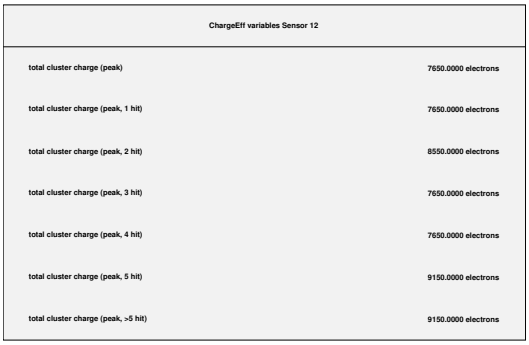

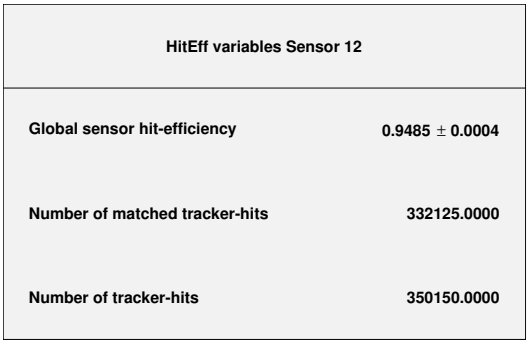

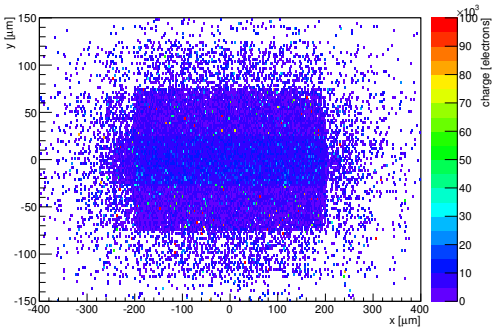

(s) Single pixel mean charge.

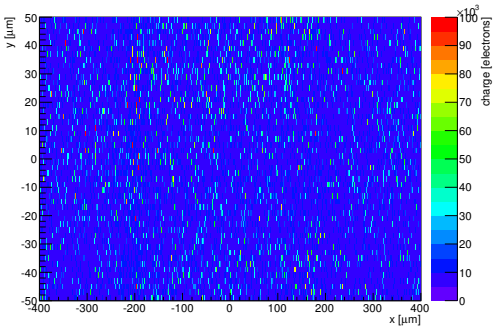

(t) Single pixel mean charge.

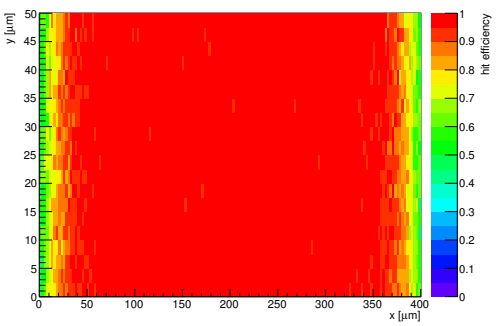

(u) Single pixel hit efficiency.

Figure C.185: Detailed plots for test beam measurement of DO-24 (description see section 6.1) sample (running as DUT2) during runs 71579-71628 in the August 2012 test beam period at CERN SPS in area H6B. Summary of the data in chapter 9.

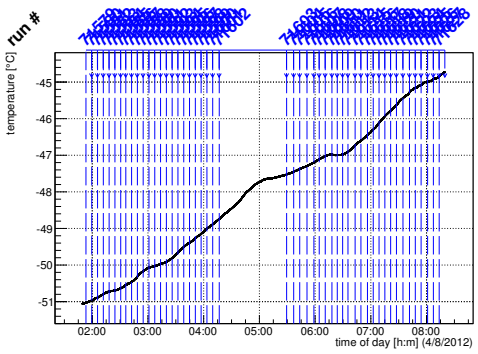

(a) Temperature vs time.

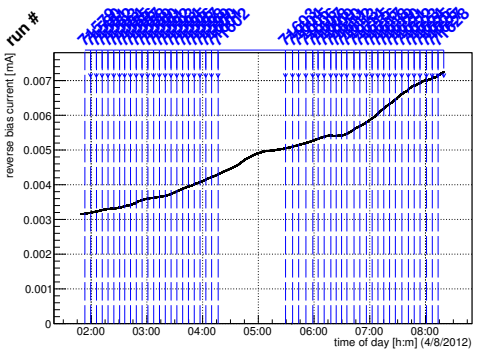

(b) Bias current vs time.

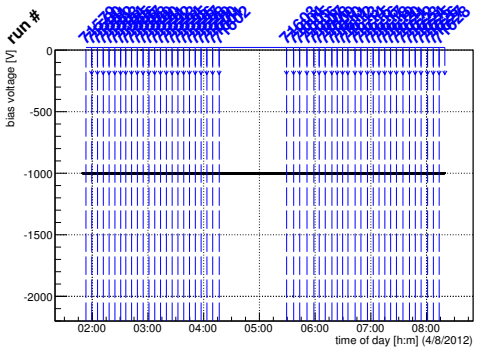

(c) Currently applied bias voltage vs time.

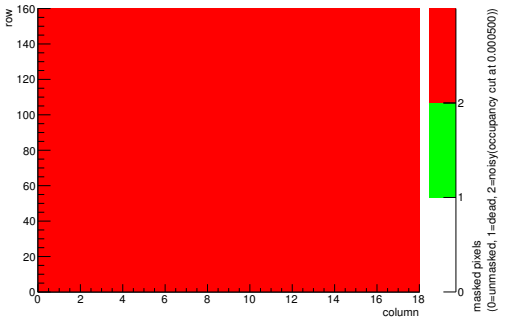

(d) Map of masked pixels.

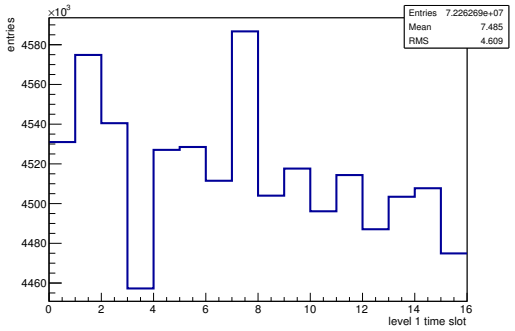

(e) Lvl1 distribution.

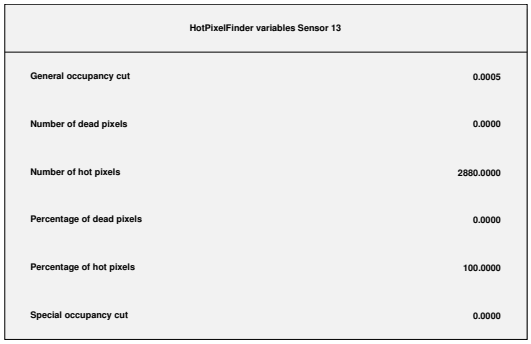

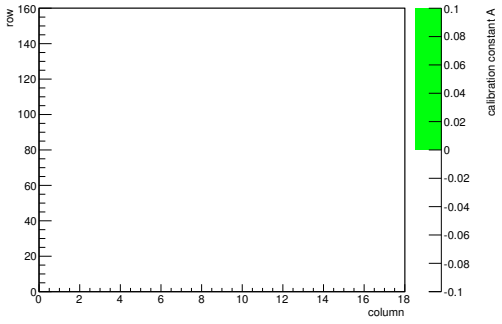

(f) Calibration constant A.

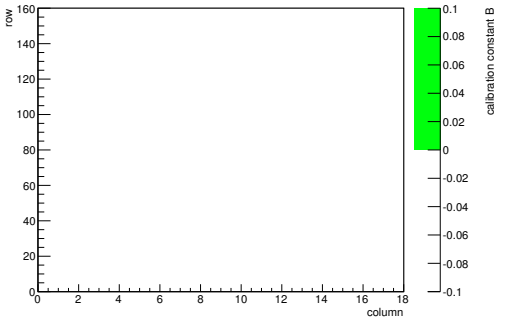

(g) Calibration constant B.

Figure C.186: Detailed plots for test beam measurement of DO-23 (description see section 6.1) sample (running as DUT3) during runs 71579-71628 in the August 2012 test beam period at CERN SPS in area H6B. Summary of the data in chapter 9. *(cont.)*

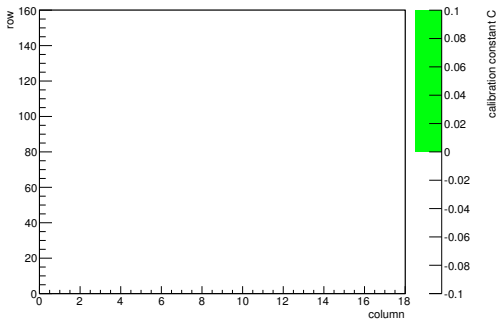

(h) Calibration constant C.

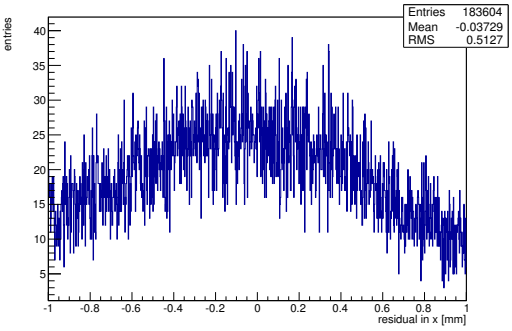

(i) Track residual in x.

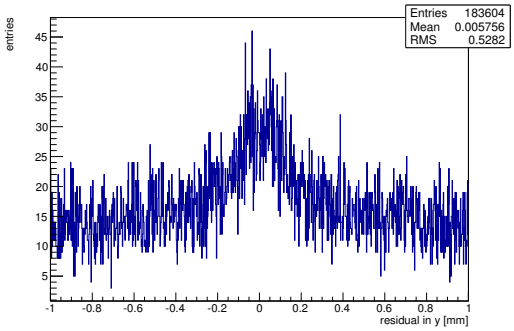

(j) Track residual in y.

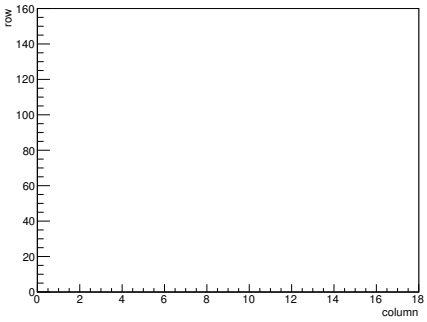

(k) Hit efficiency map.

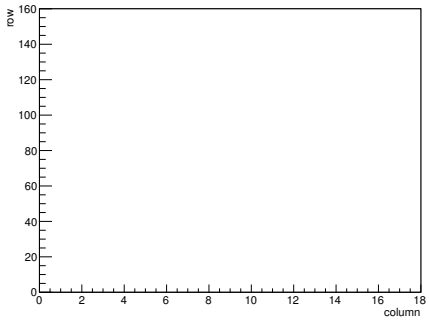

(l) Hit inefficiency map.

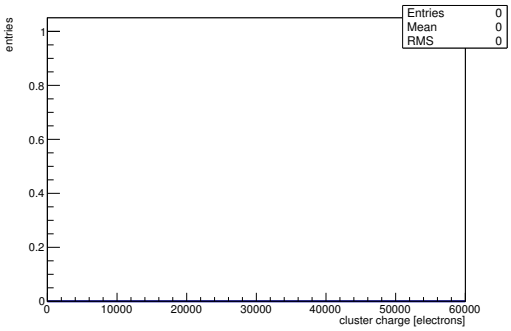

(m) Charge distribution (all cluster sizes included).

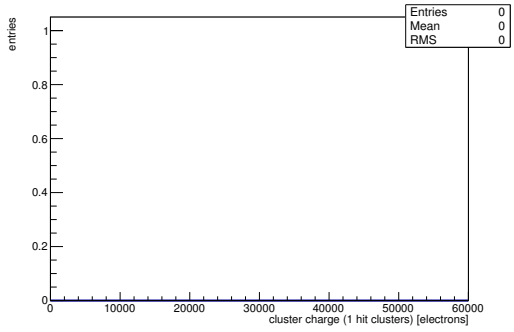

(n) Charge distribution (1 hit cluster).

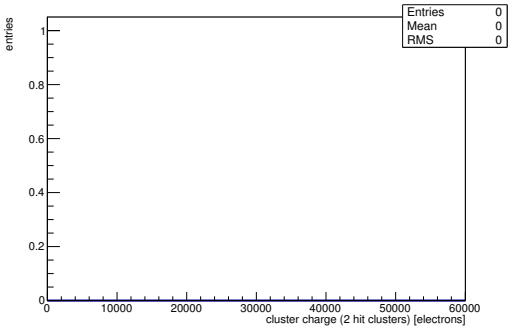

(o) Charge distribution (2 hit cluster).

Figure C.186: Detailed plots for test beam measurement of DO-23 (description see section 6.1) sample (running as DUT3) during runs 71579-71628 in the August 2012 test beam period at CERN SPS in area H6B. Summary of the data in chapter 9. *(cont.)*

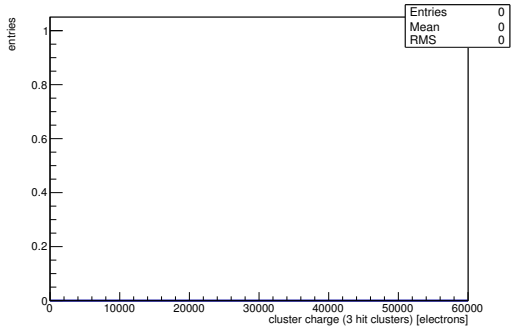

(p) Charge distribution (3 hit cluster).

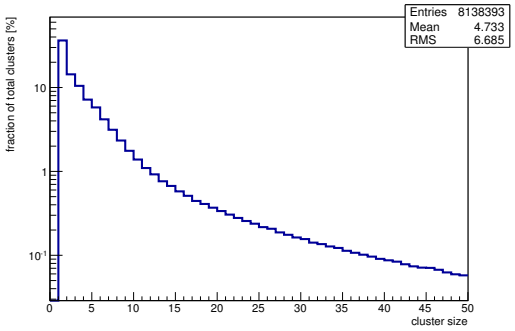

(q) Cluster size distribution.

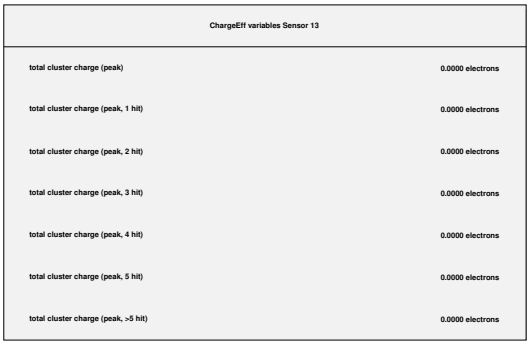

(r) Hit efficiency vs event number.

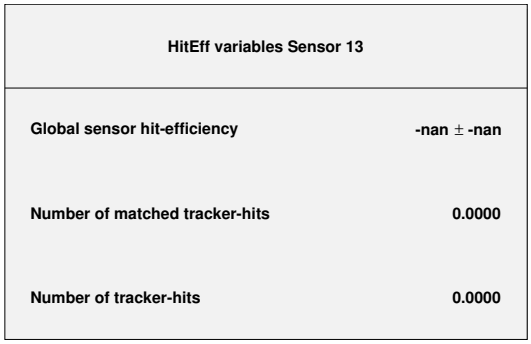

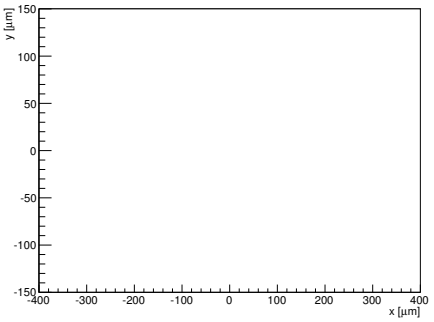

(s) Single pixel mean charge.

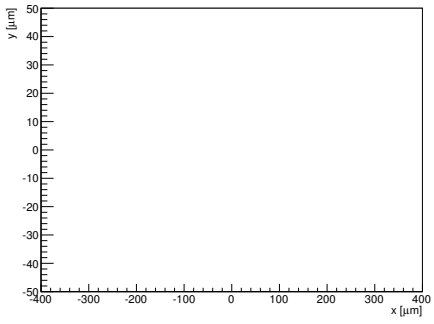

(t) Single pixel mean charge.

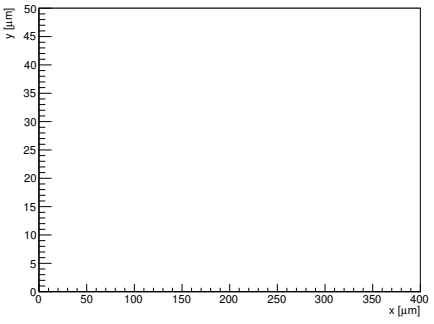

(u) Single pixel hit efficiency.

Figure C.186: Detailed plots for test beam measurement of DO-23 (description see section 6.1) sample (running as DUT3) during runs 71579-71628 in the August 2012 test beam period at CERN SPS in area H6B. Summary of the data in chapter 9.

APPENDIX D

Publications

D.1 Articles

A. Affolder, A. Aleev, P.P. Allport, L. Andricek, M. Artuso, **A. Rummler**, et al. Silicon detectors for the sLHC. *Nuclear Instruments and Methods in Physics Research Section A*, A658:11–16, 2011.

S. Altenheiner, C. Gossling, J. Jentzsch, R. Klingenberg, D. Muenstermann, **A. Rummler**, et al. Radiation hardness studies of n^+-in-n planar pixel sensors for the ATLAS upgrades. *Nuclear Instruments and Methods in Physics Research Section A*, A658:25–29, 2011.

C. Goessling, R. Klingenberg, D. Muenstermann, **A. Rummler**, G. Troska, and T. Wittig. Planar n^+-in-n silicon pixel sensors for the ATLAS IBL upgrade. *Nuclear Instruments and Methods in Physics Research Section A*, 650(1):198–201, 2011.

S. Altenheiner, C. Goessling, J. Jentzsch, R. Klingenberg, T. Lapsien, D. Muenstermann, **A. Rummler**, G. Troska, and T. Wittig. Planar slim-edge pixel sensors for the ATLAS upgrades. *Journal of Instrumentation*, 7(02):C02051, 2012.

J. Weingarten, S. Altenheiner, M. Beimforde, M. Benoit, M. Bomben, **A. Rummler**, et al. Planar Pixel Sensors for the ATLAS Upgrade: Beam Tests results. *Journal of Instrumentation*, 7:P10028, 2012.

R. Nagai, J. Idarraga, C. Gallrapp, Y. Unno, **A. Rummler**, et al. Evaluation of novel KEK/HPK n-in-p pixel sensors for ATLAS upgrade with testbeam. *Nuclear Instruments and Methods in Physics Research Section A*, A699:78–83, 2013.

R. Klingenberg, S. Altenheiner, M. Andrzejewski, K. Dette, C. Gößling, **A. Rummler**, and F. Wizemann. Temperature-Dependent Characterisations of Irradiated Planar n^+-in-n Pixel Assemblies. *Nuclear Instruments and Methods in Physics Research Section A*, doi:10.1016/j.nima.2014.04.059, 2014, in press

D.2 Conference Talks

A. Rummler. Ideas for n-in-n slim edges. 1st Planar Pixel Sensor Upgrade Meeting, June 2008.

A. Rummler. Sensor design, irradiation results and wafer submissions: n-in-n activities at dortmund. 2nd Planar Pixel Sensor Upgrade Meeting, October 9th-10th 2008.

A. Rummler. Evaluation of radiation tolerant ATLAS pixel sensors under SuperLHC conditions. Particle Physics DPG Spring Meeting 2009, March 2009.

A. Rummler. DOBOX - a coldbox for multiple angle studies á la 3D-CCE. 5th Planar Pixel Sensor Upgrade Meeting, November 2009.

A. Rummler. Evaluation of ATLAS pixel sensors at SuperLHC conditions. Particle Physics DPG Spring Meeting 2010, March 2010.

A. Rummler. A look at FE-I3 SingleChipAssemblies with up to 2×10^{16} n_{eq}/cm^2. 6th Planar Pixel Sensor Upgrade Meeting, April 2010.

A. Rummler. Status of the n-in-n CiS pixel production. 16th RD50 workshop, June 2010.

A. Rummler. Outlook on the 2010 n-in-n CiS pixel production on thinned silicon. 16th RD50 workshop, June 2010.

A. Rummler. Results from n-irradiated n-in-n FE-I3 SCAs. 7th Planar Pixel Sensor Upgrade Meeting, September 2010.

A. Rummler. Radiation hardness studies of n^+-in-n planar pixel sensors for the ATLAS upgrades. RESMDD2010, October 2010.

A. Rummler. Cooling measurements with SC-adapter cards. 8th Planar Pixel Sensor Upgrade Meeting, February 2011.

A. Rummler. Silicon n-in-n pixel detectors: Sensor productions for the ATLAS upgrades, first slim-edge measurements and experiences with detectors irradiated up to SLHC fluences. 6th Trento Workshop on Advanced Radiation Detectors, March 2011.

A. Rummler. Lab measurements and testbeam results of irradiated n^+-in-n planar pixel sensors for IBL and beyond. 18th RD50 Workshop, May 2011.

A. Rummler. Results for n^+-in-n neutron irradiated planar pixel sensors from the february 2011 test beam campaign. 9th Planar Pixel Sensor Upgrade Meeting, May 2011.

A. Rummler on behalf of the RD50 collaboration. Radiation-hard silicon for HL-LHC trackers. IEEE NSS 2011, October 2011.

A. Rummler. Measurements of highly irradiated ATLAS n^+-in-n planar pixel sensors with unirradiated readout electronics. 19^{th} RD50 Workshop, November 2011.

A. Rummler. Introduction in TBmon - a testbeam data analysis software. ATLAS pixel upgrade testbeam analysis workshop, February 2012.

A. Rummler. Measurements of highly irradiated ATLAS n^+-in-n planar pixel sensors. 7^{th} Trento Workshop on Advanced Radiation Detectors, March 2012.

A. Rummler. n^+-in-n planar pixel sensors for the ATLAS upgrades. ATLAS Upgrade Week, March 2012.

A. Rummler. Introduction in TBmon - a testbeam data analysis software. EU-Telescope Workshop 2013, March 2013.

D.3 Conference Posters

A. Rummler and T. Wittig. Evaluation and development for a radiation hard pixel sensor in the ATLAS experiment under SuperLHC conditions. IEEE NSS 2008, October 2008.

A. Rummler. Investigation of n^+-in-n pixel sensors up to HLLHC fluences for the ATLAS upgrades using unirradiated readout electronics. PSD09 - 9^{th} International Conference on Position Sensitive Devices, September 2011.

D.4 Co-supervised Theses

Andreas Gisen. Ladungssammlung in bestrahlten planaren n^+-in-n Siliziumsensoren. Bachelor thesis, TU Dortmund, November 2012.

Tobias Lapsien. Messungen an hochbestrahlten ATLAS Silizium Pixel Sensoren mit unbestrahlter Ausleseelektronik. Diploma thesis, TU Dortmund, 2012.

Till Plümer. Fanout enabled charge collection measurements of planar n^+-in-n ATLAS silicon pixel sensors. Diploma thesis, TU Dortmund, 2012. In the course of this thesis the first unirradiated fanout assembly, which had been prepared before, was put into operation.

Mona Abt. Aufbau eines Messplatzes zur automatischen IV-Charakterisierung von Fanout-basierten n^+-in-n planaren Siliziumpixelsensoren. Bachelor thesis, TU Dortmund, September 2013.

Rouven Heikenfeld. Charakterisierung von Silizium-Pixelsensoren und Auswirkungen von harten Spannungsabfällen. Bachelor thesis, TU Dortmund, 2013.

Branislav Ristic. Characterization of Planar Pixel Sensors in Test Beam Experiments with Shallow Incidence Angle. Master thesis, TU Dortmund, 2013.

Felix Wizemann. Annealing abhängige Messungen an einem hochbestrahlten planaren n^+-in-n Slilzium-Pixelsensor-FE-I3-Assembly. Bachelor thesis, TU Dortmund, July 2013.

Patrik Hermanns. SiPM-Auslese für Trigger-Szintillatoren. Bachelor thesis, TU Dortmund, April 2014.

Julia Rietenbach. Further Development on a read-out system for the Fanout. Master thesis, TU Dortmund, April 2014.

Acknowledgements

Zuerst möchte ich mich sehr herzlich bei Herrn Professor Dr. Gößling bedanken, sowohl für die Betreuung und Korrektur meiner Arbeit, als auch für die Möglichkeit sie unter optimalen Bedingungen an seinem Lehrstuhl erstellen zu können. Innerhalb so kurzer Zeit, derart viele Teststrahl-Kampagnen durchführen und auf so vielen internationalen Konferenzen vortragen zu dürfen, ist nicht selbstverständlich und ich bin dankbar für die gewährten Mittel.

Ein besonderer Dank an PD Dr. Reiner Klingenberg für die vielen Diskussionen, die guten Ratschläge und die Erfahrung, wenn es mal nicht weiterging, und die im Labor als auch beim Teststrahl gewährte Hilfe. Danke auch für die Bereitschaft die Zweitkorrektur dieser Arbeit zu übernehmen.

Frau Dr. Siegmann möchte ich für die spontane Zustimmung danken in meiner Prüfung Beisitzerin zu sein.

Vielen Dank an Daniel Münstermann für all die Unterstützung in allen Lebenslagen, ob am CERN oder anderswo und vor allem für all die guten Ideen, welche aus seinem großartigen Überblick über alles, was gerade aktuell ist und interessant sein könnte, resultieren.

Allen am Lehrstuhl E4, insbesondere auch denen, die ich im weiteren nicht namentlich erwähne, da es sonst den Rahmen sprengen würde und ich hier ohnehin keinen Anspruch auf Vollständigkeit habe, möchte ich für die wirklich einzigartige, geradezu legendäre, Atmosphäre am Lehrstuhl und den kollegialen Zusammenhalt danken.

Allen momentanen, ehemaligen und zukünftigen Mitgliedern der E4-Upgrade Gruppe kann ich nur sagen: Wir haben in den letzten 5 Jahren zusammen unglaublich viel erreicht — weiter so.

Vielen Dank an Tobias Wittig, meinen ehemaligen Schreibtischnachbar zur rechten Seite, mit dem ich viele Jahre, seit der Formierung der Upgrade-Gruppe bei E4, zusammen gearbeitet habe. Es war eine sehr schöne Zeit und echt vielen Dank für das Mitmachen bei jeder noch so verrückten Aktion am Teststrahl zu den unmöglichsten Uhrzeiten...ich sage nur: Umbau um 2 Uhr morgens.

Großer Dank an Silke Altenheiner für die netten Gespräche, die viele Arbeit am Teststrahl und fürs Stellunghalten, wenn ich mal wieder endlos lange nicht in Dortmund war (und natürlich für die gute Stimmung und die aufmunternden Worte).

Meinem Büronachbar Christian Jung möchte ich nicht nur für die gute Nachbarschaft, sondern auch für das kurzfristige Korrekturlesen dieser Arbeit danken.

Danke auch an Georg Troska für die Zusammenarbeit von Studienbeginn an, in Praktika und Übungsgruppen, bis hin zur Doktorarbeit bei derselben Gruppe. Von ihm stammt auch einiges an Teststrahlinfrastruktur, welche auch dieser Arbeit zugrundelag und sicherlich auch in Zukunft Verwendung finden wird.

Insbesondere auch Danke an alle, deren Arbeiten ich mitbetreuen durfte, für die gute und erfolgreiche Zusammenarbeit: Andreas Gisen, Branislav “Bane” Ristic, Felix Wizemann, Julia Rietenbach, Patrik Hermanns, Mona Abt, Rouven Heikenfeld, Till Plümer und Tobias Lapsien.

Ohne unsere Mechanik- und Elektronik-Werkstatt wäre eine experimentelle Arbeit wie diese kaum denkbar. Für die Erfüllung der unmöglichsten Anforderungen auf kürzester Zeitbasis möchte ich allen Beteiligten danken, insbesondere Frau Krallemann und Herrn Koch. In diesem Zusammenhang auch vielen Dank an Markus Alex und seinen Vorgänger, Theo Villett, für all die Koordination.

Wolfgang Dietsche und allen anderen Beteiligten am Silizium Pixel Lab in Bonn vielen Dank für das Wirebonden von fast allen in dieser Arbeit verwendeten Assemblies. Insbesondere gilt mein Dank auch Fabian Hügging, welcher dies immer auf kurzer Zeitskala ermöglicht hat.

All members of the PPS and IBL collaboration, I would like to thank for the good cooperation at various test beams and particularly for all the nice collaboration meetings, which were not only instructive, but also a lot of fun. Mathieu Benoit for using his language skills to help out with the radiation protection service at CERN. Matthias George and Stefano Terzo for reconstructing a lot of our data. Marco Bomben and Jens Weingarten who served exemplary as our test beam coordinators under conditions that sometimes probably resembled the experience of herding cats. Philipp Weigel for meeting him at every conference and also for all the test beam shifts where we worked together.

I would like to express gratitude to Simonetta Di Gioia from SELEX Sistemi Integrati S.p.A (now Selex ES, formerly AMS) for flip-chipping the irradiated sensors with indium stubs for free and for accomodating my unusual request for cooling of the sensors and assemblies before and after the flip-chip process.

A crucial step required for the research in this thesis was naturally the irradiation of the assemblies. Here I would like to thank both the institutions as well as the

persons directly involved in the irradiation effort: Maurice Glaser who conducted the irradiations with protons at CERN-PS, Alexander Dierlamm who managed the proton irradiation at Karlsruhe and special thanks go to Gregor Kramberger for organising the neutron irradiation at the reactor of the Jožef Stefan Institute, who also helped to expediate the process immensely, when the time grew short before upcoming test beam campaigns.

I am grateful to the whole EUDET team at DESY who made our test beam measurements possible in the first place. Particularly, Ingrid-Maria Gregor for accomodating our wishes and Igor Rubinsky for being always present and helping with the telescope. Vladislav "Slava" Libov for a lot of fun finding common languages during one of those infamous test beam dinners.

Many thanks to Henric Wilkens for all his help with the test beam at CERN and especially for organizing a quick solution for the broken shutter, which threatened to shut down our data taking, before it could have started.

I would like to thank Daniel Hynds for all his help with the TimePix telescope and Martin Kocian for the FE-I3 implementation in the RCE software, including the remote last-minute debugging from across the pond.

An experimental thesis, such as the present one, requires substantial financial support as well. At this opportunity, I would like to give the following organizations credit for either funding part of this thesis directly or providing some of the necessary means. This work was supported by the German Federal Ministry of Education and Research (BMBF) with grant 05 HA9PEA. The research leading to these results has received funding for test beam access and irradiations from the European Commission under the FP7 Research Infrastructures project AIDA, grant agreement no. 262025. Part of the irradiations were financed by the Initiative and Networking Fund of the Helmholtz Association, contract HA-101 ("Physics at the Terascale").

Děkuju meiner Mutter für die Unterstützung und immense Geduld während meines ganzen Studiums und insbesondere auch während der Erstellung dieser Arbeit.

,